An accept-and-reject algorithm to determine performance objectives that comply with a food safety objective

Laurent Guillier, J.C. Augustin, Jean-Baptiste Denis, Marie-Laure Delignette-Muller

7th International Conference on Predictive Modelling of Food Quality and Safety

7ICPMF, September 12 — 15th, 2011, Dublin, Ireland

Radisson Blu Royal Hotel, Golden Lane, Dublin 8, Ireland

Conference Proceedings

www.icpmf.org/2011

E. Cummins, J.M. Frías and V.P. Valdramidis (Eds.),
Predictive Modelling of Food Quality and Safety – Conference Proceedings,
UCD, DIT, Teagasc, Dublin, Ireland

E. Cummins, J.M. Frías and V.P. Valdramidis (Eds.),
Predictive Modelling of Food Quality and Safety – Conference Proceedings,
UCD, DIT, Teagasc, Dublin, Ireland

ISBN 1 900454 46 7

Preface

This book contains the proceedings of the Seventh International Conference on Predictive Modelling of Food Quality and Safety (7ICPMF). Following a decision by the Committee of the PMF society the name of the conference, originally Predictive Modelling in Foods, has been altered in order to accommodate research activities in the wider area of modelling in Food Science. The conference is hosted in Dublin, Ireland (September 12-15, 2011) and has been co-organised by three major Irish Institutes: University College Dublin, Dublin Institute of Technology and Teagasc Food Research Centre, all having pioneer research activities in the area of predictive modelling and food science and being involved in the organisation of other major events, e.g., European Symposia — International Association for Food Protection (2010), ProSafeBeef Safety Conference (2009), FOODSIM (2008).

Over 130 contributions from 23 nationalities have been received for presentation. These are presented as oral lectures or as posters. The oral presentations have been organised in a single session to ensure that all attendees will have the chance to actively participate in all the presented works.

The current state of new outbreaks (e.g., Shiga toxin-producing *E. coli*) requires the application of modern quantitative risk assessment techniques that can help food authorities on the tasks of risk management and communication. Additionally, unraveling the mechanism of chemical, microbial and physical changes require studies at a microscopic level. All these, and more issues, are addressed in the presented works of this conference based on either bottom up or top down modelling approaches. The topics are showcased including modelling at single cell levels, quantitative (microbial) risk assessment, predictive modelling in the food chain, quality and safety management, modelling of food processes, predictive mycology, and sampling and experimental designs/plans. Most of the sessions start with a more elaborated keynote lecture from experienced and distinguished international scientists.

At this point we would like to thank Tom McMeekin for accepting to be the Honorary President of 7ICPMF and all members of the International Scientific Committee for their active contribution to the review procedure and session planning. Many thanks also to the companies and institutes who support this event in different ways.

We hope that the UNESCO city of literature will inspire you to continue contributing in the PMF community with your research findings and finally, wish you a pleasant, enjoyable and fruitful time in Dublin at 7ICPMF.

Vasilis P. Valdramidis

Chair of 7ICPMF & the National Organising Committee
Dublin, September 2011

Organisation

The Seventh International Conference on Predictive Modelling of Food Quality and Safety is organised by:

University College Dublin **Dublin Institute of Technology** **Teagasc Food Research Centre**

And proudly sponsored by:

Science Foundation Ireland
(www.sfi.ie)

Food Safety Authority of Ireland
(www.fsai.ie)

Creme Software Ltd
(www.cremeglobal.com)

The International Committee on Food Microbiology and Hygiene of the IUMS
(http://icfmh.org/)

Society for Applied Microbiology
(www.sfam.org.uk)

Innovative Science
(www. innovative-science.com)

Fáilte Ireland
(www.failteireland.ie)

Meet in Ireland
(www.meetinireland.com)

Commitees

Honorary President
T.A. McMeekin

Chair
V.P. Valdramidis

International Scientific Committee

Vice-chair
F. Butler

Members

J.-C. Augustin (FR)
J. Baranyi (UK)
S. Brul (NL)
K. Cronin (IE)
P. Dalgaard (DE)
F. Devlieghere (BE)
R.M. García-Gimeno (ES)
A.H. Geeraerd (BE)
L.G.M. Gorris (NL)
J. Grant (IE)
V.K. Juneja (US)
S. Koseki (JP)
K.P. Koutsoumanis (GR)
A.M. Lammerding (CA)
I. Leguérinel (FR)
P. Mafart (FR)
T.A. McMeekin (AU)
J.-M. Membré (FR)
G.-J.E. Nychas (GR)
J. Oliveira (IE)
T.P. Oscar (US)
C. Prats (ES)
C. Pin (UK)
T. Ross (AU)
D. Schaffner (US)
P.N. Skandamis (GR)
I. Souchon (FR)
M.L. Tamplin (AU)
P.S. Taoukis (GR)
D. Thuault (FR)
J.F.M. Van Impe (BE)
M.H. Zwietering (NL)

National Organising Committee

Vice-chair
G. Duffy*

Members

N. Abu-Ghannam*
P. Bourke
J. Cahill
P.J. Cullen*
E. Cummins*
S. Fanning
J.M. Frías*
U. Gonzales-Barron
C.P. O' Donnell*
L. Rivas
B.K. Tiwari*

**also members of the International Scientific Committee*

Committee of PMF Society

J. Baranyi
P. Dalgaard
G.-J.E. Nychas
T. Ross
D. Schaffner
V.P. Valdramidis
J.F.M. Van Impe
M.H. Zwietering

General Information

Registration Desk

The registration/information desk will remain open throughout the conference and will be staffed at the following times:

Monday, 12th September	7.00pm-9.00pm
Tuesday, 13th September	8.00am-5.00pm
Wednesday, 14th September	9.00am-4.00pm
Thursday, 15th September	9.00am-5.30pm

Badges

For security reasons and catering purposes please make sure your wear your conference badge.

Meetings Room Locations

Oral presentations will be given in the Main Hall
Poster presentations will be given in Hall 1

Messages

Messages for delegates received at the registration desk will be posted on the message board at registration. You are welcome to use the message board to contact fellow delegates.

Poster Session

Posters will be displayed for the duration of the Congress in Hall 1. Presenters should refer to the program to check which of the three viewing sessions their posters are assigned.

Speaker Technical Area

Please upload your presentation at the beginning of the day on which you are presenting.

Conference Meals

The following are included in the registration fee for all delegates:

- Drinks Reception – Monday 12th September 7.00pm — 9.00pm in Main Hall of the venue.
- A lunch will be served for all delegates in Radisson Blu restaurant.
  Please make sure that you wear your conference badge to obtain lunch.
- Mid-session coffee/tea breaks will be served as mentioned in the conference program

Certificates of Attendance

Certificates of Attendance will be available upon request from the registration desk.

Conference Secretariat

For post-conference enquiries, please contact 7icpmf@dit.ie

Plan of Conference Venue

GROUND FLOOR

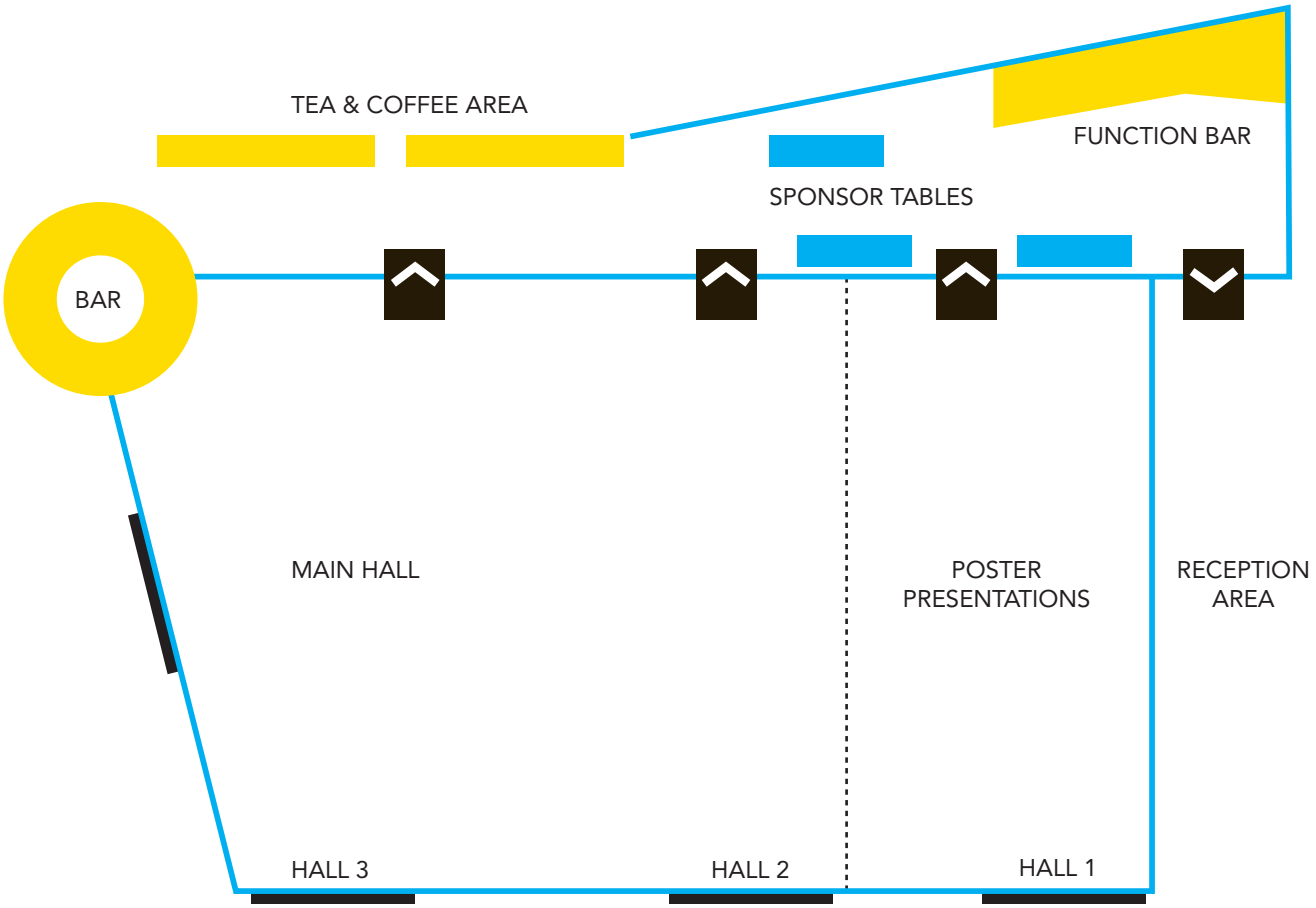

Program Overview

Monday September 12

19.00-21.00	Reception

Tuesday September 13

08.30-09.00	Opening lectures
09.00-09.30	Plenary lecture
09.30-10.45	Technical Sessions
10.45-11.30	**Tea/coffee break and poster sessions**
11.30-12.45	Technical Sessions
12.45-14.00	**Lunches**
14.00-14.30	Keynote lecture
14.30-15.45	Technical Sessions
15.45-16.30	**Tea/coffee break and poster sessions**
16.30-17.15	Technical Sessions

Wednesday September 14

09.00-09.30	Keynote lecture
09.30-10.45	Technical Sessions
10.45-11.30	**Tea/coffee break and poster sessions**
11.30-12.45	Technical Sessions
12.45-14.00	**Lunches**
14.00-14.30	Keynote lecture
14.30-16.00	Technical Sessions
	Free afternoon
19.00	Gala dinner

Thursday September 15

09.00-09.30	Keynote lecture
09.30-10.45	Technical Sessions
10.45-11.30	**Tea/coffee break and poster sessions**
11.30-12.45	Technical Sessions
12.45-14.00	**Lunches**
14.00-15.30	Technical Sessions
15.30-16.00	**Tea/coffee break and poster sessions**
16.00-17.00	Technical Sessions
17.00-17.15	Closing remarks

Contents

Advances in quantitative risk assessment

Predictive modelling in the food chain

Quality and safety management

Quantitative food quality assessment

Predictive models and tools for food processing

Modelling of thermal processes

Predictive mycology

Sampling and experimental designs/plans

Systems biology

A Bird's Eye View on Predictive Modelling in Foods (presented as posters)

272 Sublethal heating of *Cronobacter* spp. followed by determination of individual lag times during recovery
Y. Xu, JP Sutherland

273 Modelling the effect of sublethal injury on variability of individual lag times of *Cronobacter turicensis* cells compared with undamaged cells
Y. Xu, D. Stasinopoulos, JP Sutherland

274 Effect of low inoculum size on the *Listeria innocua* lag phase at refrigeration temperatures
J. Aguirre, M. R. Rodríguez, M. Gañán, A. González, G. G. De Fernando

275 Modelling the inhibitory effects of ZnCl2 on *Saccharomyces cerevisiae* TOMC Y4
J. Bautista-Gallego, V. Romero-Gil, A. Garrido-Fernández, F.N. Arroyo-López

279 Impact of texture on *Listeria monocytogenes* growth in gel models
T. De Broucker, M. El Jabri, F. Postollec, D. Thuault

280 Assessing the effect of a gelified environment on the heterogeneous heat response of *E. coli* K12 at temperatures close to T*max*
K. Boons, E. Van Derlinden, L. Mertens, J.F. Van Impe

284 Modelling the growth of *E.coli* under the effect of *Rhus coriaria L.* essential oil, temperature and pH
G. Karim, B. Radmehr, R. Khaksar, M. Sadatmosavi

288 Modelling growth of *Escherichia coli* 0157:H7 in extract of different leafy vegetables
G. Posada-Izquierdo, S. Del Rosal, F. Perez-Rodriguez, M. Rodríguez, A. Morales, E. Todd, A. Valero, E. Carrasco, G. Zurera

292 Modelling the effect of an abrupt temperature shift on the lag phase and the growth curve
W.S. Robazza, J.T. Teleken, G.A. Gomes

296 Modelling the effects of temperature and osmotic shifts on the growth kinetics of *Bacillus weihenstephanensis* in broth and food products
V. Antolinos, M. Muñoz-Cuevas, M. Ros-Chumillas, P.M. Periago, P. S. Fernández, Y. Le Marc

300 Modelling the growth of *Escherichia coli* under the effects of *Carum copticum* essential oil, pH, temperature, and NaCl using response surface methodology
M. Shahnia, A. Khanlarkhani, F. Shahraz, B. Radmehr, R. Khaksar

304 Performance evaluation of models describing the growth rate as a function of temperature: focus on the suboptimal temperature range
E. Van Derlinden, B. Herckens, J.F. Van Impe

308 Growth response and modelling the effects of *Carum copticum* essential oil, pH, temperature, and NaCl on *Escherichia coli, Listeria monocytogenes* and *Staphylococcus aureus* by an optimized computational neural networks (OCNN)
M. Shahnia, A. Khanlarkhani, S. Shojaee, F. Shahraz, R. Khaksar, H. Hosseini

309 Effect of temperature and inoculum level on the maximum population (Rg) of *Lactobacillus fermentum* grown in co-culture with *Saccharomyces cerevisiae* using sugar cane must as substrate
V.O. Alvarenga, P.R. Massaguer

Modelling at a single cell level (presented as posters)

313 Microbial individual-based models and sensitivity analyses: local and global methods
M. Ginovart, C. Prats, X. Portell

317 Upgrading the uptake and metabolism sub-models of the Individual-based Model INDISIM-YEAST to tackle the behaviour of *Saccharomyces cerevisiae* in different culture conditions
X. Portell, A. Gras, R. Carbó, M. Ginovart

321 How does the average number of cells per sample influence the lag phase distribution of single cells?
J. Aguirre, M. Ganan, M.R. Rodriguez, A. Gonzalez, G.D. Garcia de Fernando

322 Live-cell imaging of aerobic bacteria; a tool to assess and model heterogeneous germination & outgrowth of *Bacillus subtilis* spores
R. Pandey, A. Ter Beek, N.O. Vischer, E.M.M. Manders, S. Brul

Quantitative (microbial) risk assessment and applications (presented as posters)

327 Quantitative risk assessment of *Listeria monocytogenes* in cold-smoked salmon in the Republic of Ireland
S. Chitlapilly Dass, N. Abu-Ghannam, E. J. Cummins

328 Probabilistic exposure assessment of coagulase + staphylococci, *Clostridium perfringens* and *Listeria monocytogenes* in large wild game meats in Europe
J.-M. Membré, M. Laroche, C. Magras

332 Development of a quantitative risk assessment for cheese made from raw goat milk contaminated by *Listeria monocytogenes*
L. Delhalle, M. Ellouze; A. Clinquart, G. Daube, M. Yde, N. Korsak

336 The paradox of validating a Monte Carlo model that predicts non-testable microbial contamination risks
B.M. de Roode, J. Meeuwisse, E. Wemmenhove, M.H.J. Wells Bennik

340 Risk assessments of *Listeria monocytogenes* in Dutch-type semihard cheese: incorporating variability in both product parameters and microbial growth parameters
E. Wemmenhove, M.H. Zwietering, A.C.M. van Hooijdonk, M.H.J. Wells-Bennik

344 *Listeria monocytogenes* – process risk modelling of lightly preserved and ready-to-eat seafood
A.C.J. Grønlund, O. Mejlholm, P. Dalgaard

345 A quantitative microbial risk assessment model for *Campylobacter* and *Listeria monocytogenes* contamination of boxed beef trimmings from Irish abattoirs
C. Shanahan, G. Duffy, F. Butler

346 Quantitative risk assessment of chemical decontamination on *Campylobacter* on chicken skin
H. Meredith, E. Cummins, D. McDowell, D. Bolton

347 A predictive model for *Escherichia coli* O157:H7 in Salami: quantitative risk assessment
E. Cosciani Cunico, J. Baranyi, G. Maccabiani, G. Finazzi, P. Boni

348 Probabilistic modelling of dioxins and dioxin-like PCBs consumed in dairy products
A.O. Adekunte, B.K. Tiwari, C.P. O'Donnell

352 A semi-quantitative risk assessment methodology to prioritise microbial hazards in reconstituted powdered infant formula
A.O. Adekunte, B.K. Tiwari, C.P. O'Donnell, A.G.M. Scannell

Predictive modelling in the food chain (presented as posters)

356 Dynamic modelling of *L. monocytogenes* growth in vacuum packed cold-smoked salmon under typical retail and consumer storage conditions
S. Chitlapilly Dass, N. Abu-Ghannam, E.J. Cummins

357 Predictive modelling as a tool for Performance Objectives (PO) achievement and Performance Criteria (PC) and Process/Product Criteria (PcC/PdC) calculation for the mycotoxin hazard
D. García, A.J. Ramos, V. Sanchis, S. Marín

361 Development of predictive model to predict the outgrowth of *Listeria monocytogenes* in Ready-To-Eat food products
S. Kumar, T. Wijtzes, G. Lommerse, D. Visser, E. Bontenbal

362 Application of predictive microbiology in food and drink SMEs: assessment based on 20 years of experience
M. El Jabri, F. Postollec, D. Sohier, C. Travaille, D. Thuault

363 Accurate assessment of microbial safety in food industry: adapting predictive models for specific food products
A.M. Cappuyns, A. Vermeulen, H. Paelinck, F. Devlieghere, J.F. Van Impe

Quality and Safety Management (presented as posters)

Quantitative Food Quality Assessment (presented as posters)

Predictive models and tools for food processing (presented as posters)

412 Modelling the effect of a_W and fat content on the high pressure resistance of *Listeria monocytogenes*
S. Bover-Cid, N. Belletti, M. Garriga, T. Aymerich

416 Effect of nisin and citral on the heat resistance and recovery of *Alicyclobacillus acidoterrestris* spores
J.P. Huertas, M.D Esteban, A. Palop

420 Antimicrobial activity of melt blended and Layer by Layer (LBL) self assembled Low Density Polyethylene (LDPE) – Silver Nanocomposite
M. Jokar, R. Abdul Rahman

423 Comparison of the kinetic data of spores obtained in different heating systems
Z. Atamer, S. Bachmann, M. Witthuhn, J. Hinrichs

427 From laboratory inactivation experiments in static conditions to spore reduction at ultra-high temperature processing
M. Witthuhn, O. Couvert, Z. Atamer, J. Hinrichs, L. Coroller

431 Effect of heat treatment and recovery conditions on the inactivation of Salmonella Enteritidis
M. Munoz-Cuevas, A. Metris, J. Baranyi

435 Modelling the thermochemical non-isothermal *Bacillus coagulans* spores inactivation in nutrient broth added with oregano essential oil
L.U. Haberbeck, C. Dannenhauer, B.C. Salomão, G.M.F. Aragão

439 Kinetic characterisation of *Bacillus sporothermodurans* in liquid food under static and dynamic heating regimes
F. Cattani, S. D. Oliveira, C.A.S. Ferreira, P.M. Periago, M. Muñoz, V.P. Valdramidis, P. S. Fernandez

443 Modelling the survival and growth of *Salmonella* spp. in vacuum-packaged slices of RTE stuffed chicken breast as a function of temperature
A. Morales-Rueda, E. Carrasco, A. Valero, F. Pérez-Rodríguez, M.Y Rodríguez- Caturla, G.D Posadas-Izquierdo, R.M García-Gimeno and G. Zurera

447 Modelling the influence of the starter culture on proto-cooperation
W.S. Robazza, D.A. Longhi, G.A. Gomes, D.O. Stolf

451 Modelling the effect of high pressure on the activity of orange limonoid glucosultransferase and limonin degradation
E. Gogou, M. Strofyllas, L. Goga, P. S. Taoukis

452 Monte Carlo simulation to predict the shelf-life of high pressure and thermally processed orange juice
B. Tiwari, T. Norton, C.Brennan, PJ Cullen, C. O'Donnell

Modelling of thermal processes (presented as posters)

453 Modelling the heat resistance of *Bacillus* spores as a function of sporulation temperature and pH
E. Baril, L. Coroller, O. Couvert, I. Leguerinel, F. Postollec, C. Boulais, F. Carlin, P. Mafart

457 Effect of thymol in heating and recovery media on the heat resistance of *Bacillus* species
M.D. Esteban, J.P. Huertas, and A. Palop

461 Modelling inactivation of *Leuconostoc mesenteroides* in dextran added to dairy ingredients
C.P. Pacheco, A.R. Silva, P.R. Massaguer

465 Calorimetric assessment of *Listeria innocua* relevant to thermal processes
T. Skåra, A.M. Cappuyns, D. Skipnes, E. Van Derlinden, J.T. Rosnes, J.F.M. Van Impe, V.P. Valdramidis

469 Effect of a gelified matrix on the heat inactivation of *E. coli* and *Salmonella* Typhimurium
E.G. Velliou, E. Van Derlinden, L. Mertens, A. Cappuyns, A.H. Geeraerd, F. Devlieghere, J. Van Impe

473 A theoretical assessment of microbial inactivation in thermally processed fruits in syrup in still cans
A. Dimou, N. G. Stoforos, S. Yanniotis

Predictive Mycology (presented as posters)

474 An asymmetric model dedicated to germination of fungi
P. Dantigny

478 Influence of humidity, time of storage and temperature on the germination time of *Penicillium chrysogenum*
S. Nanguy, P. Dantigny

482 Modelling the effect of temperature on the germination and mycelium formation dynamics of fungal spores
M. Gougouli, K.P. Koutsoumanis

486 From single spores to mycelium: variability of *Aspergillus westerdijkiae, Aspergillus carbonarius* and *Penicillium verrucosum* growth and ochratoxin A production
A.E. Kapetanakou, E.H. Drosinos, M. Mataragas and P.N. Skandamis

490 Predictive modelling to describe the effect of water activity and temperature on the radial growth of heat resistant molds
A. Tremarin, B.C.M. Salomão, S. Zandonai, G.M.F. Aragao

Sampling and experimental designs/plans (presented as posters)

494 Optimal sequential sampling design for improving parametric identification of complex microbiological dynamic systems by nonlinear filtering
J.-P. Gauchi, J.-P. Vila

498 A novel class of statistical process control for microbial counts in foods
U. Gonzales-Barron, F. Butler

499 Proposal of operating characteristic curves developed for *Cronobacter* in powder infant formula
A. Moussida, F. Butler

500 Tracing the contamination levels of acid curd cheese implicated in an outbreak of listeriosis in Austria, 2009/2010
P. Skandamis, M. Wagner, D. Schoder

Predictive microbiology, theory and application: is it all about rates?

T.A. McMeekin, J. Olley, D.A. Ratkowsky, T. Ross

School of Agricultural Science and Tasmanian Institute of Agricultural Research, University of Tasmania, Hobart, Tasmania 7001, Australia.

Keywords: growth rates, Copenhagen School, balanced growth, stringent response and persister cells, temperature models, integrating ecology, physiology and genomics

Rates: all pervasive and all persuasive?

Time scales range in microbiology from milliseconds for enzyme catalysed reactions to doubling times of seven minutes for *Clostridium perfringens*, to days, weeks or months for psychrophiles growing under their optimum conditions, to 3.5 billion years to reach the current stage of adaptive evolution. In microbial ecology and physiology we tend to focus on the rates at which population and intracellular events occur with time as the universal denominator. A very readable account of early work on bacterial growth rates was given by Schaechter (2006) indicating the major contribution of Monod. In 1958 Schaechter had also introduced the concept of "balanced growth" during which all cell constituents increased in proportion in the same time interval. From that realisation it became clear that growth rate was the primary factor determining the physiological state of cells. Schaechter (2006) also argued strongly for precision in design and execution of experiments to ensure balanced growth. Prerequisites included exact media composition, inoculum size and time/temperature conditions to prepare starter cultures. Cooper (1993) is a "must read" paper to understand the origins and meaning of the Schaechter – Maaløe – Kjeldgaard experiments and the excitement generated by the pioneering research of the Copenhagen School. The balanced growth condition also provided a physiological explanation for transition from the lag phase to the exponential phase and then to the stationary phase of growth, respectively as a nutritional up-shift and a series of nutritional down-shifts. While the lag and stationary phases are regions of zero growth rates, it is important not to lose sight that zero rates have important physiological and practical implications. Another member of the Copenhagen School (Neidhardt 1999) wrote about the obsession with *dN/dt* but did not subscribe to the view that emphasis on growth had delayed work on the stationary phase.

The stringent response (SR) – paradigm lost in food microbiology?

Earlier we briefly considered the gamut of time spans in microbiology and here note that even major changes, involving a large part of cellular physiological capacity, can occur in seconds. A good example is the transition from the relaxed response (RR) state to that of the SR and the converse switch which occur in 20-30 seconds (Cashel 1975). Thus, in a few seconds the purpose of cellular metabolism is totally reversed from a focus on growth (RR) to a focus on survival (SR). The SR may provide an explanation for the Jameson Effect which describes a non-specific interaction where the component of a mixed culture first approaching its maximum population density (MPD) produces sufficient levels of the alarmone, guanosine tetraphosphate (ppGpp) signalling its entry into the SR state as well as that of competing organisms that cease growth before reaching their MPD. Relief from the SR condition is achieved by inoculation into a fresh batch culture or is prevented by growth in continuous cultures in which the alarmone is continually diluted and nutrients are continually added. However, if a continuous culture is set up in a retentostat (a chemostat with 100% feedback of biomass) very slow or zero growth rates ensue. The phenomenon can be attributed to the programmed objective of the SR physiological state: survival at any cost. Cell density and quorum sensing compounds have been proposed to have a role in the mechanism of transition from the exponential to the stationary phase. However, as other factors also change, quorum sensing alone is insufficient to explain the transition. An alternative conclusion, based on both batch and continuous culture experiments, is that specific growth rate plays a prominent role

and that ppGpp is an intracellular signal linking general stress responses and specific growth rate. From an ecological standpoint this strategy of self determination by individual cells is preferable to the more risky option of depending on signals from other cells.

Persister cells: stealth bombers in the microbial survival armoury?

Cells with slow or zero growth rates confer a very distinct advantage on microbial populations in that, as a result of minimal metabolism, they are extremely difficult to inactivate. This trait is well described by the term "persisters" which represent a distinct physiological state in *E.coli* (Shah et al., 2006) and other organisms such as *Pseudomonas aeruginosa*, *Mycobacterium tuberculosis* and *Candida albicans* (Silver, 2011).

Categorising models in predictive microbiology

The title for this section does not require a question mark as the scheme of Whiting and Buchanan (1993) classifying predictive models as primary, secondary and tertiary is entirely logical. Commonly used primary models describing sigmoidal bacterial growth curves include the Logistic, Gompertz and Baranyi models. Secondary growth models describe the effect of environmental factors on growth rate. A paper by Mejholm et al. (2010) describing the combined effects of up to nine environmental factors on the growth of *L. monocytogenes* is in the "must read" category. Tertiary models are algorithms incorporated into devices that record and integrate the effect of environmental variables. Microbial Resources Viewer (MRV: http://mrv.nfri.affrc.go.jp) was developed at the National Food Research Institute, Japan (Koseki 2009). MRV provides growth/no growth data sets with growth rate contour plots allowing users to identify conditions at the growth/no growth boundary visually as well as quantitatively. Koseki (2009) is another "must read" publication.

Temperature dependence models – a never ending source of scientific debate?

Temperature is the primary target for measurement as it is the factor likely to fluctuate, to the greatest extent and most often. The major "competitors" for this purpose are Arrhenius-type and Bělehrádek-type models. Whilst the goodness fit of these models have been compared in many studies differences are often minimal. The conclusion is that both logarithmic and square root transformations of data are very effective in homogenising variance. Subsequent arguments may arise about the relative merits of a model on the basis of other criteria e.g. does the model have a mechanistic basis? Arrhenius type models have their origin in chemical reaction kinetics which has been sufficient to give them a "mechanistic aura" despite not adequately describing biological reaction kinetics. But this is a non-issue if the primary objective of homogenising variance is achieved. Differences of opinion on the goodness of fit within a particular model type also arise e.g. what is the best exponent to select for a Bělehrádek-type model. Normally an exponent of 2 is used giving rise to square root models but Huang (2010) suggested that a better fit was obtained with an exponent of 1.5. Much of this discussion arose from failure to recognise that Tmin is the theoretical minimum growth temperature. It is not the actual minimum growth temperature which is several degrees higher than Tmin. The widely accepted concept of absolute zero, proposed by Lord Kelvin as a basis for chemical reaction kinetics, suggests that a theoretical Tmin has a credible precedent in science.

Can we effectively integrate knowledge of quantitative microbial ecology with knowledge of microbial physiology and genomics?

Food industries are faced with a complex series of drivers that interact with each other changing with time in relative importance. One of the drivers, food safety, is a *sine qua non* and has considerable influence on the approach adopted by industry and regulators to other drivers including political, economic, social, technological, environmental and regulatory and trade drivers (Quested et al. 2010).

Above we suggest that the quantitative microbial ecology of foods is now underpinned by enormous databases that have been synthesised into knowledge capsules termed predictive models. The need to link this ecological resource with knowledge of microbial physiology is not new. However, it seems that in food microbiology we may have squandered the benefits of cementing this connection by forgetting the basic experiments of the Paris and Copenhagen Schools in the 1940's and 50's.

As world population increases food security and increasing food prices are now front of mind for government policy makers and food industry strategists in developed countries. At the same time hunger, malnutrition, famine and poverty continue unabated in the developing world, often exacerbated by environmental degradation and natural disasters. This brings into stark relief the imperative to preserve and store foods post-harvest to prevent major loss of food resources after successful growing and harvesting. Properly controlled storage conditions will maintain nutritional qualities, and ensure safety.

This is where food scientists and technologists have a pivotal role and responsibility and where food microbiologists can contribute greatly to global goals. The principles of microbial eco-physiology are the same whether the target is safe and nutritious food and clean water for underprivileged communities or minimal processing to produce "as fresh" food for wealthy consumers with apparently sophisticated palates. It follows that the answer to the last question posed must be yes! We are encouraged by studies such as that by Vieira-Silva and Rocha (2010) which the authors summarised as follows:

"Microbial minimal generation times vary from a few minutes to several weeks. The reasons for this disparity have been thought to lie on different life-history strategies…. Prokaryotes have evolved a set of genomic traits to grow fast, including biased codon usage and/or… gene multiplication for dosage effects. Here, we studied the relative role of these traits and show they can be used to predict minimal generation times from the genomic data of the vast majority of microbes that cannot be cultivated. …this inference can also be made within complete genomes and thus be applied to metagenomic data…. Our results also allow a better understanding of the co-evolution between growth rates and genomic traits and how they can be manipulated in synthetic biology. ***Growth rates have been a key variable in microbial physiology in the last century…and they are linked with genome organization and prokaryotic ecology."***

Conclusions

We conclude that the Copenhagen School struck a rich research vein in the late 1950's and that the "mother lode" continues to provide excellent scope for returns in significance and impact. Growth rates are, indeed, all pervasive and all persuasive!

Acknowledgements

We acknowledge stimulating discussions and correspondence with Stanley Brul, University of Amsterdam, The Netherlands, Erwin Galinski, University of Bonn, Germany and Shigenobu Koseki, National Food Research Institute, Japan. We gratefully acknowledge financial support from the Geoffrey Gardiner Dairy Research (www.gardinerfoundation.com.au), Victoria, Australia.

References

Cashel, M. (1975) Regulation of bacterial ppGpp and pppGpp. *Annual Reviews in Microbiology* 29. 301-318.

Cooper, S. (1993) The origins and meaning of the Schaechter-Maaløe-Kjellgaard experiments. *Journal of General Microbiology* 139, 1117-1124.

Huang, L. (2010) Growth kinetics of *Escherichia coli* 0157:H7 in mechanically tenderized beef. *International Journal of Food Microbiology* 140, 40-48.

Koseki, S. (2009) Microbial responses viewer (MRV): A new ComBase-derived database of microbial responses to food environments *International Journal of Food Microbiology* 134, 75-82.

Mejholm, O., Grundvig, A., Borggaard, C., Blom-Hanssen, J., Mellefont, L., Ross, T., Leroi, F., Else, T., Visser, D. and Dalgaard, P. (2010) Predicting growth rates and growth boundary of *Listeria monocytogenes* – an

international validation study focusing on processed and ready to eat meat and seafood. *International Journal of Food Microbiology* 137-150.
Neidhardt, F.C. (1999) Bacterial growth: constant obsession with dN/dt. *Journal of Bacteriology* 181, 7405-7408.
Quested, T.E., Cook, P.E., Gorris, L.G.M. and Cole, M.B. (2010) Trends in technology trade and consumption likely to impact on microbial food safety. *International Journal of Food Microbiology* 139, S29-S42.
Schaechter, M. (2006). From growth physiology to systems biology. *International Microbiology* 9, 157-161.
Shah, D., Zhang, Z., Khordursky, A.B., Niilo, Kaldalu, Kurd, K. and Lewis, K. (2006) Persisters: a distinct physiological state of *E.coli*. *BMC Microbiology* 6:53.
Silver, L.L. (2011) A persistent problem. *Journal of Medical Microbiology* 60, 267-268.
Vieira- Silver, S. and Rocha, E.P.C. (2010) The systematic imprint of growth and its uses in ecological (meta) genetics. PLoS Genetics 6, e1000808 (15pp).
Whiting, R.C. and Buchanan, R.L.B. (1993) A classification of models in food microbiology. *Food Microbiology* 10, 175-177.

Extension of the Gamma concept for modelling non-thermal inactivation of *Escherichia coli* O157:H7 in model acidic dressings

Y. Le Marc[1], D. Kan-King-Yu[1] A. Amézquita[1]

[1] Unilever, Safety & Environmental Assurance Centre, Colworth Science Park, Sharnbrook, Befordshire, MK44 1LQ, United Kingdom. (yvan.le-marc@unilever.com, denis.kan-king-yu@unilever.com, alejandro.amezquita@unilever.com)

Abstract

The objective of this study was to evaluate the combined effects of temperature, pH, NaCl, potassium sorbate and acetic acid on the inactivation of *Escherichia coli* O157:H7. Seventy five experimental conditions were tested and the organisms enumerated for up to 28 days. The survival kinetics were described by the Weibull model (defined by a scale parameter δ and a shape parameter p).The secondary model for δ was developed based on the Gamma concept extended to bacterial survival. Based on experimental observations, the parameter p was modelled as a function of temperature and NaCl concentration. A one-step fitting procedure was performed to identify directly the secondary model parameters from the survival curves. The model describes accurately the observed kinetics (R^2_{adj}=0.87). Model validation was performed by comparison against ComBase and literature data. Results are promising for further application of the Gamma concept for non-thermal inactivation and the model developed will aid in supporting the safe design of dressing formulations ensuring rapid inactivation of *E. coli* O157:H7 at ambient and chilled temperatures. The approach taken may also be applied to other infectious agents that are relevant to this type of product formulation.

Keywords: *Escherichia coli* O157:H7, *non-thermal inactivation, weibull model, Gamma concept*

Introduction

Salad dressings rely on low pH combined with acetic acid and to a lesser degree, citric and lactic acids (in the aqueous phase), natural antimicrobials and preservatives such as sorbic or benzoic acid, to control pathogenic and spoilage microorganisms. The objective of this work was to develop a model for the effects of temperature (5, 10 and 23°C), pH (3.5-4.7), NaCl (2-10%), potassium sorbate (0-0.1%) and acetic acid (0-0.5%) on the inactivation of *Escherichia coli* O157:H7. The ability of the Gamma concept (successfully applied to model bacterial growth, see e.g. Rosso *et al.* 1995) to model non-thermal bacterial inactivation was investigated.

Materials and Methods

Microorganism and media preparation

A cocktail of five strains of *E. coli* O157:H7 was used. Experiments were conducted in Tryptone Soya Broth (TSB) and seventy five experimental conditions (with two independent replicates) were studied. The different media compositions were prepared by the addition of sodium chloride, acetic acid and potassium sorbate to TSB and were pre-incubated at the appropriate temperatures (23°C for the ambient experiments and 5°C and 10°C for the experiments at chill) for 24 hours prior to inoculation.

Each composition was inoculated with 100 µl of the pathogen cocktail to give an inoculum of ca. 10^6 cfu/ml. Compositions were incubated at the appropriate temperatures. *E. coli* O157:H7 was enumerated at various time-points for up to 21 days (23°C) or 28 days (5 and 10°C) by spread plating onto Tryptone Soya Agar supplemented with 0.1% pyruvate (TSAP). Each inactivation curve consists at least of 6 time/ log counts points.

Mathematical model

The Weibull model reparametrized by Mafart *et al.* (2002) was used as a primary model. It is defined by a scale parameter δ and a shape parameter p. The secondary model is based on the

Gamma concept which assumed that the combined effects of the environmental factors on the bacterial growth rate can be obtained by multiplying their separates effects. The concept has been extended to bacterial resistance by Mafart (2000):

$$\frac{1}{\delta} = \frac{1}{\delta^*} \prod \lambda_i(X_i) \quad (1)$$

where λ_i (X_i) is the effect of the environmental factor X_i and δ^* is the value of δ when $\prod \lambda_i(X_i) = 1$. When taking the logarithm of both sides of Eq. (1), it becomes:

$$\log(\delta) = \log(\delta^*) - \sum \lambda_i(X_i) \quad (2)$$

Assuming that the effect of each factor can be described by $\lambda_i(X_i) = a_i X_i$, Eq. (2) can be rearranged into:

$$\log(\delta) = a_0 + a_1 T + a_2[H^+] + a_3 b_w + a_4[AceticU] + a_5[SorbicU] \quad (3)$$

Where T is the temperature, $[H^+]$ is the proton concentration ($x10^{-3}$ mM), b_w=sqrt(1-a_w), [*AceticU*] and [*SorbicU*] are the concentrations of undissociated acetic and sorbic acid (mM), respectively.

Based on experimental observations the shape parameter p was modelled as a function of temperature and b_w by the following equation:

$$p = b_0 + b_1 * T + b_2 * b_w \quad (4)$$

To minimize the effects of the structural correlation between p and δ in the Weibull model, a one-step fitting procedure (implemented in Matlab R2009a, The Mathworks, Natick, MA, USA) was performed to identify directly the secondary model parameters from the survival curves. The interpolation region of the model was defined by the MCP (Minimum Convex Polyhedron) which encompasses all the conditions used to develop the model (Baranyi *et al.* 1996).

Model validation

There are limited literature data in the model region; validation was performed with the aim of studying the model performance beyond the interpolation region. Model outputs were compared against ComBase data (30 curves, temperature range: 5-20°C, pH range: 3.5-5.0, NaCl range: 0-10%) and observations from Chapman *et al.* (2006) (ambient temperature, pH range 3.5-4; NaCl range: 1-8%; acetic acid range: 0.7-2.1%). Predictive ability of the model was assessed by comparing: (i) whether or not a 3-log reduction was achieved within 28 days (maximum length of experiment), and (ii) the time to 3-log reduction observed and predicted by the model.

Results and Discussion

Effects of environmental factors

At chilled temperatures (5°C and 10°C), only a few conditions gave an inactivation greater than a 3-log reduction within the sampling period of 28 days. As expected, faster inactivation was observed at ambient temperature. Compositions with potassium sorbate appeared to be the most effective at causing rapid inactivation. For example, at pH 3.8, 6% NaCl, 0.2% acetic acid, cells of *E. coli* O157:H7 were able to survive for 21 days whereas the microorganism was not detected after 7 days when 0.05% potassium sorbate was added to the formulation.

Modelling

The model described accurately the observed kinetics (R^2_{adj}=0.87). Examples of fitted curves are shown in Fig. 1.Estimated parameters and standard errors are indicated in Table 1.

A strong structural correlation between the parameters p and δ has been highlighted by other researchers (Couvert *et al.* 2005). To overcome this problem, instead of modelling separately two parameters mutually dependent on each other, we have therefore used a single-step fitting procedure. Attempts to follow the usual two-step procedure (primary modelling and development of secondary models of δ and p) led to a poor description of the inactivation curves (data not shown). An additional advantage of the one-step fitting approach used in this study was that it also allowed for inclusion of curves exhibiting only small log reductions (and therefore for which the parameters of the Weibull model could have not been identified otherwise).

The parameter p was not fixed to a single value as in other studies (e.g. Couvert *et al.* 2005) as the survival curves exhibited different shapes (linear, upward and downward curvatures) depending on the experimental conditions. A linear relationship between p and the temperature and b_w was assumed, which was found sufficient to describe the data accurately. Attempts to introduce the effects of pH, sorbic and acetic acids in Equation 4 did not improve significantly the quality of fit (at p=0.05).

Table 1: Estimates of the model parameters and their 95% confidence intervals.

Model	Parameter	Estimate	95% Confidence Interval
$\ln(\delta)$	a_0	2.98	[2.89 3.07]
	a_1	-0.034	[-0.036 -0.032]
	a_2	-1.75	[-1.85 -1.65]
	a_3	0.22	[0.18 0.25]
	a_4	-0.022	[-0.026 -0.019]
	a_5	-6.58	[-6.81 -6.34]
	a_6	-0.31	[-0.36 -0.26]
p	c_0	1.94	[1.67 2.21]
	c_1	0.052	[0.044 0.062]
	c_2	-0.20	[-0.23 -0.17]

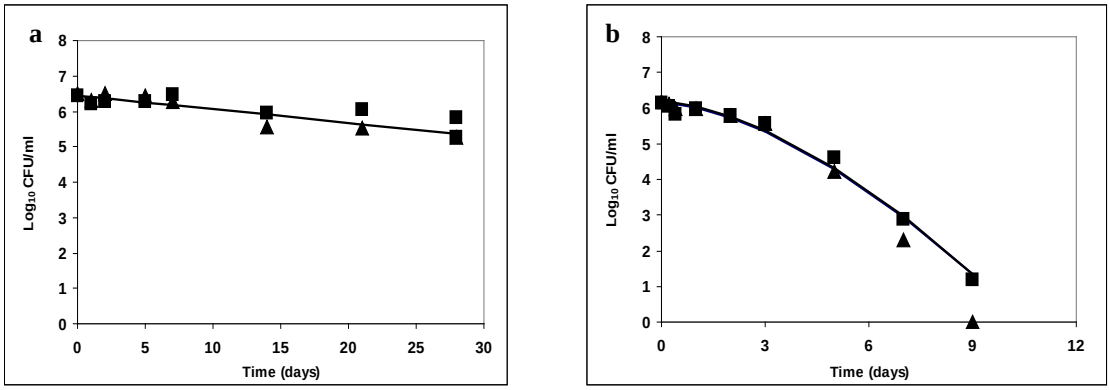

Figure 1: Examples of comparison between observed (replicate 1: ▲; replicate 2: ■) and fitted inactivation curves (solid line). a) T=5°C, pH=4.6, NaCl=6%, %potassium sorbate=0.1, %acetic acid=0.5%; b) T=23°C, pH=3.8, NaCl=9%, %potassium sorbate=0.05, %acetic acid=0.2.

The main purpose of the model is to provide predictions either at chilled (5-10°C) or at ambient temperature (23°C). In their model on inactivation of *L. monocytogenes*, Coroller *et al.* (2011) used two functions for the effect of temperature on $\ln(\delta)$: a linear effect for $T \leq 12$°C and a quadratic effect (for T>12°C). Using a quadratic model did not improve the description

of our data but it could be due to the lack of data between 10 and 23°C. Consequently, the model should be used with caution for temperatures values ranging between 10 and 23°C.

Model validation

Out of 30 survival curves selected in ComBase, only 8 fell within the model MCP. For 7 conditions, the model predicted correctly that a 3-log reduction in the concentration of *E. coli* O157:H7 was not achieved within 28 days. For the remaining condition, the model provided fail-safe predictions (3-log reduction not achieved whereas observations showed a reduction >3-log). Fig. 2 shows comparison between observed and predicted time to 3-log reduction for conditions outside the model region. Although, the model would need to be improved for predictions in an expanded region, results are promising for further application in a wider experimental range.

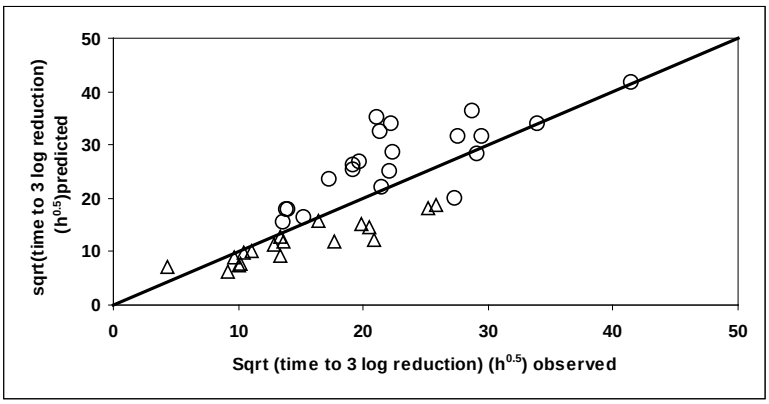

Figure 2: Observed vs. predicted time to achieve a 3-log reduction of *E. coli* O157:H7 (data outside the model interpolation region, o: Combase data, △: Chapman et *al*. 2006).

Conclusions

The Gamma concept was successfully applied for the non-thermal inactivation of *E. coli* O157:H7 at ambient and chilled temperatures. The methods used in this work include a one step fitting procedure to minimize the effects of the structural correlation between the Weibull model parameters and the description of the shape parameter *p* as a function of temperature and water activity. Future work will focus on extending the model to a wider range of formulations and on applying the same methodology for other infectious pathogens, such as *L. monocytogenes* or *Salmonella* spp.

References

Baranyi J., Ross T., McMeekin T. and Roberts T.A. (1996) The effect of parameterisation on the performance of empirical models used in Predictive Microbiology. *International Journal of Food Microbiology* 13, 83-91.

Chapman B., Jensen N., Ross T. and Cole M. (2006) Salt, alone or in combination with sucrose, can improve the survival of *Escherichia coli* O157 (SERL 2) in model acidic sauces. *Applied and Environmental Microbiology* 72, 5165-5172.

Coroller L., Kan-King-Yu D., Leguerinel I., Mafart P. and Membré J-M. (2011) Modelling of growth, growth/no-growth interface and inactivation areas of *Listeria in* foods. *International Journal of Food Microbiology* (submitted to publication).

Couvert O., Gaillard S., Savy N., Mafart P. and Leguérinel I. (2005) Survival curves of heated bacterial spores: effect of environmental factors on Weibull parameters. *International Journal of Food Microbiology* 101, 73-81.

Mafart P. (2000) Taking injuries of surviving bacteria into account for optimising heat treatments. *International Journal of Food Microbiology* 55, 175-179.

Mafart P., Couvert O., Gaillard S., and Leguerinel I. (2002) On calculating sterility in thermal preservation methods : application of the Weibull frequency distribution model. *International Journal of Food Microbiology* 72, 107-113.

Rosso L., Lobry J.R., Bajard S. and Flandrois J.P. (1995) Convenient model to describe the combined effects of temperature and pH on microbial growth. *Applied and Environmental Microbiology* 61, 610-616.

On the evaluation of the gamma hypothesis: the effect of pH on the cardinal temperatures

M. Baka, E. Van Derlinden, K. Boons, J. F. Van Impe

CPMF2 – Flemish Cluster Predictive Microbiology in Foods – www.cpmf2.be
Chemical and Biochemical Process Technology and Control (BioTeC), Department of Chemical Engineering, Katholieke Universiteit Leuven, Leuven, Belgium, [maria.baka, jan.vanimpe]@cit.kuleuven.be

Abstract

Prediction of the microbial specific growth rate and cardinal temperatures for growth are important issues in food industry. The Cardinal Temperature Model with Inflection (CTMI), which describes the influence of temperature on the specific growth rate from the minimum (T_{min}) to the maximum growth temperature (T_{max}), is a suitable model to incorporate the temperature effect. Following the so-called gamma hypothesis, the cardinal temperatures are only determined by the microbial temperature response and not influenced by other environmental conditions. The purpose of this research is to examine if pH influences the values of the cardinal temperatures. CTMI parameters were derived based on experimental data. T_{min}, T_{max} and μ_{opt} as a function of pH follow a parabolic trend. For T_{opt}, however, no obvious trend could be observed.

Keywords: *E. coli, cardinal temperatures, pH, gamma concept*

Introduction

In recent years, it is widely accepted that temperature, pH and water activity are among the major environmental factors that affect growth. In several articles, predictive models have been developed that describe microbial growth rate as a function of different environmental factors (see, e.g., McMeekin *et al.* (1987), Wijtzes *et al.* (1993; 1995), and Zwietering *et al.* (1993)). These models are based on the gamma concept where the effects of controlling variables can be multiplied, and cardinal parameters are not a function of other variables (temperature, pH, and water activity). By the combination of the previous models, Wijtzes *et al.* (2001) validated the gamma concept over a wide range of controlling variables. In the current work, the effect of different pH values (between the limits that permit growth) on the cardinal temperatures of *E. coli* K12 is examined. As such, the gamma hypothesis is evaluated. In addition, cardinal temperatures and cardinal pH values are estimated.

Materials and Methods

Bacterial strain and inoculum preparation

E. coli K12 MG1655 (CGSC#6300) was acquired from the *E. coli* Genetic Stock Center from Yale University. For the inoculum, a loopful of *E. coli* stock culture was transferred into 20 mL BHI incubated at 37 ºC. The refresh of the inoculum took place after 9 h, when 20 μL were transferred into 20 mL fresh BHI and again incubated at 37 ºC for 15h.

Bioreactor experiments

Dynamic experiments were performed in a bench top bioreactor (BioFlo 3000, New Brunswick Scientific Inc.). The reactor vessel, filled with 3.5 L BHI was aerated at 2 L/min and the stirrer speed was set at 400 rpm. To avoid foam accumulation, 1 mL of anti-foam agent (Sigma) was added at the start of the experiment. Time–temperature profiles were implemented via the AFS-biocommand Software (New Brunswick Scientific Inc.). The bioreactor unit was connected to a circulation cooler (CFT-33, Neslab Instruments Inc.) enabling temperature control. The pH value was kept constant by the addition of base (1 N KOH) or acid (1 N H2SO4) (Acros Organics). At regular time intervals, a sample was taken

aseptically to determine the cell density via plate counting. The appropriate dilutions were plated on BHI agar (i.e., BHI + 14 g/L agar) using a spiral plater (Eddy Jet, IUL Instruments s.a.). Plates were counted after 18 hours of incubation at 37 °C.

Cardinal temperature model with inflection (CTMI)

The Cardinal Temperature Model (CTMI) with inflection point relates the maximum specific growth rate with temperature (T [ºC]) (Rosso *et al.* (1995))

$$\mu_{\max}(T) = \mu_{opt}\left[\frac{(T - T_{\max})(T - T_{\min})^2}{(T_{opt} - T_{\min})\left[(T_{opt} - T_{\min})(T - T_{opt}) - (T_{opt} - T_{\max})(T_{opt} + T_{\min} - 2T)\right]}\right] = \mu_{opt}\gamma(T)$$

(1)

with T_{min}, T_{max}, T_{opt} [ºC] the minimum, optimum and maximum temperatures for growth. At $T>T_{max}$ and $T<T_{min}$, the growth rate is zero.

Cardinal pH Model (CPM)

The CPM model describes the effect of pH on the maximum specific growth rate, i.e,

$$\mu_{\max}(pH) = \mu_{opt}\frac{(pH - pH_{\max})(pH - pH_{\min})}{(pH - pH_{\min})(pH - pH_{\max}) - (pH - pH_{opt})^2} = \mu_{opt}\ \gamma(pH)$$

(2)

with pH_{min}, pH_{opt}, pH_{max} [-] the minimum, optimum, maximum pH values for growth. At $pH>pH_{max}$ and $pH<pH_{min}$, the growth rate is zero.

Gamma concept

The gamma-concept is based on the assumption that the effect of various factors affecting the growth rate of microorganisms can be combined by multiplying the separate effects (Zwietering *et al.* (1996))

$$\mu_{\max}(T, pH) = \mu_{opt}\gamma(T)\gamma(pH)$$

(3)

For this research $\gamma(T)$ and $\gamma(pH)$ are corresponding to Equations (1) and (2) respectively.

Results and Discussion

To study the relation between temperature and pH, dynamic T-profiles are implemented at different pH values. In Table 1, the temperature profiles applied for each pH value are given. For stressing pH values, more than one temperature profile was applied. A single experiment was designed using OED/PE to optimize the estimation of the four CTMI parameters (Van Derlinden *et al*. 2008). This optimal experiment, (see the second column in Table 1), was used as a starting point for the experiments implemented at non-stressing pH-values. At pH values close to the minimum and maximum growth pH, performing this single optimal experiment was shown insufficient: either the lag phase was too long or the duration of the exponential phase was too short. Previous experiments have shown that temperature changes up to 5 ºC/h do not induce an intermediate adaptation phase.

The combination of the growth model of Baranyi and Roberts (1994) and the CTMI model was fitted to all data for a single pH value. For pH values where more than one temperature profiles was applied, data were combined in a global fitting. The resulting T_{min}, T_{opt}, T_{max} and μ_{opt} values are represented in Figure 1 as a function of pH.

These results indicate that the factor pH affects the cardinal temperatures. T_{min}, T_{max} and μ_{opt} versus pH follow a parabolic relation, in contrast to T_{opt} versus pH for which the relation is inconclusive. The T_{opt} cannot be considered statistically constant, but it is not following any other relationship with a biological meaning. In Figure 1, it can be seen that in stressing pH values T_{min}, T_{max} and μ_{opt} are lower than for pH values close to optimum values. This

observation can be of high importance for the food industry, as two factors that affect growth seem to interact.

Table 1: Temperature profiles applied for each pH value [T1, Tf]-ΔT/Δt. T1: the initial T, Tf: the final T and -ΔT/Δt the slope of temperature decrease in ºC/h.

pH	Temperature profiles		
4.5	[45ºC, 15.1ºC] -4.1916		
5	[45ºC, 15.1ºC] -4.1916	[43ºC, 27ºC] -1.729	[35ºC, 12.5ºC] -2.75
5.5	[45ºC, 15.1ºC] -4.1916	[43ºC, 27ºC] -1.729	[35ºC, 12.3ºC] -2.75
6	[45ºC, 15.1ºC] -4.1916		
6.5	[45ºC, 15.1ºC] -4.1916	[43ºC, 27ºC] -1.75	
7	[45ºC, 15.1ºC] -4.1916		
7.55	[45ºC, 15.1ºC] -4.1916		
8	[45ºC, 15.1ºC] -4.1916		
8.5	[45ºC, 15.1ºC] -4.1916	[43ºC, 27ºC] -1.75	[35ºC, 17.2ºC] -1.729
9	[45ºC, 15.1ºC] -4.1916	[43ºC, 27ºC] -1.75	[35ºC, 14.9ºC] -2
9.5	[45ºC, 15.1ºC] -4.1916		

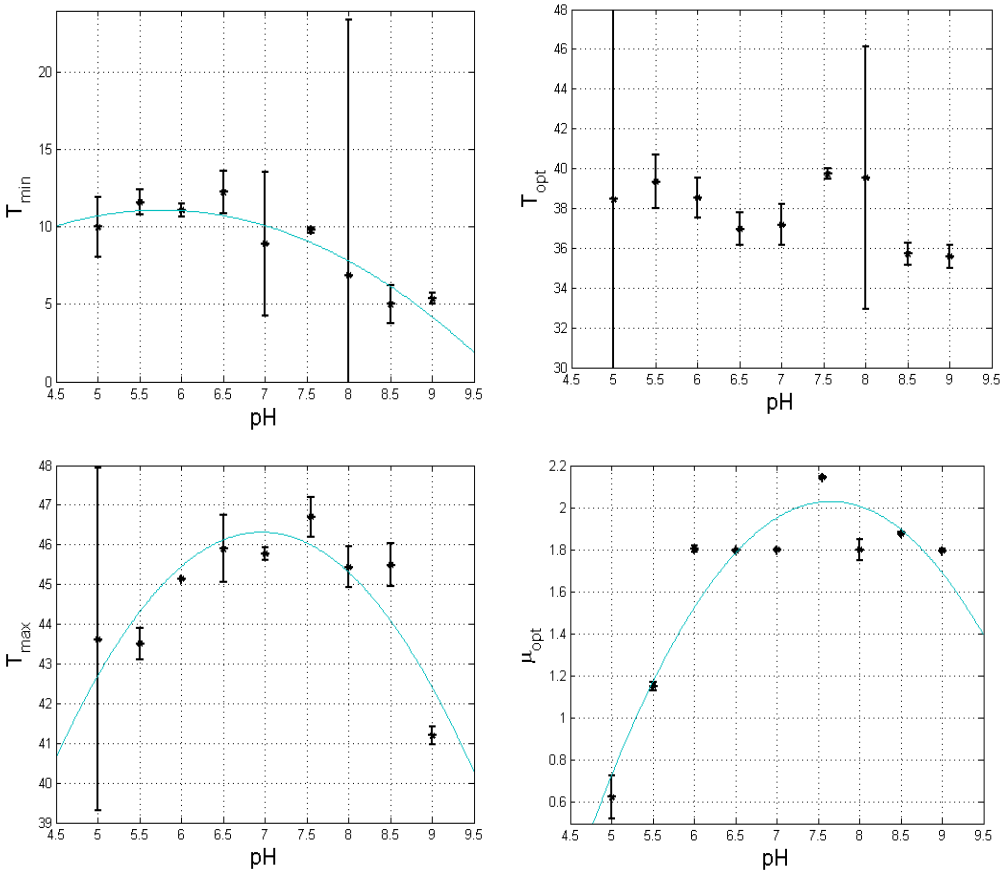

Figure 1: Cardinal temperatures and μ_{opt} as a function of pH with 95% confidence intervals.

The relations are in contrast to what Ratkowsky *et al.* (1982), McMeekin *et al.* (1987) and Wijtzes *et al.* (1995) observed, i.e., independence of T_{min}, pH_{min} and pH_{max} to other environmental factors. Results of Ratkowsky *et al.* (1982) indicated that T_{min} is independent of medium and aeration, and is an intrinsic property of the organism when growth conditions other than temperature are nonlimiting. In accordance to that research, McMeekin *et al.* (1987), using the square root model and Arrhenius equations, found that T_{min} remains constant with changing water activity, as well as T_{opt} and T_{max}, for which they suggested that more data are required. These data were collected by optical density measurements, in contrast to plate counting method of our research. Wijtzes *et al.* (1995) found that T_{min} could be assumed constant and around zero for *Lactobacillus curvatus* using the square root model

of Ratkowsky *et al.* (1982). Data from that research were coming from constant temperature experiments concluded in the same way as in the previous researchers

Conclusions

This research based on dynamic temperature profiles implemented for different constant pH values resulted in a parabolic relation between T_{min}, T_{max} and μ_{max} versus pH and a non-determined relation between T_{opt} and pH. These observations are in contrast to other results coming from different experimental conditions (basically from constant temperature profiles) and the use of different models. For that reason, the gamma concept still demands further validation, as these results are contradicting results already published and consequently to gamma hypothesis, as cardinal temperatures seem dependent to pH. Further experimental data are required for the validation of the gamma hypothesis. The use of different temperature profiles, a more wide range of pH values (more close to pH_{min} and pH_{max}), dynamic pH profiles in constant temperatures and combination of dynamic temperature and pH profiles could give more reliable results for the evaluation of the gamma concept. In addition, experiments including the factor of water activity in combination to the other factors would contribute in a conclusion about the gamma concept.

Acknowledgements

This work was supported by project PFV/10/002 (Center of Excellence OPTEC-Optimization in Engineering) of the Research Council of the K.U.Leuven, Knowledge Platform KP/09/005 (www.scores4chem.be) of the Industrial Research Fund, and the Belgian Program on Interuniversity Poles of Attraction, initiated by the Belgian Federal Science Policy Office. E. Van Derlinden is supported by postdoctoral grant PDMK/10/122 of the K.U.Leuven Research Fund. J. Van Impe holds the chair Safety Engineering sponsored by the Belgian chemistry and life sciences federation essenscia.

References

Baranyi J. and Roberts T.A (1994) A dynamic approach to predicting bacterial growth in food. *International Journal Food Microbiology* 23, 277–294.

McMeekin T.A., Chandler R.E., Doe P.E., Garland C.D., Olley J., Putro S. and Ratkowsky D.A. (1987) Model for combined effect of temperature and salt concentration/water activity on the growth rate of *Staphylococcus xylosus*. *Journal of Applied Bacteriology* 62, 1-5.

Ratkowsky D.A., Olley J., McMeekin T.A. and Ball A. (1982) Relationship between temperature and growth rate of bacterial cultures. *Journal of Bacteriology* 149, 1-5.

Rosso L., Lobry J.R., Bajard S. and Flandrois J.P. (1995) Convenient model to describe the combined effects of temperature and pH on microbial growth. *Applied and Environmental Microbiology* 61, 610-616.

Van Derlinden E., Bernaerts K. and Van Impe J.F. (2008) Accurate estimation of cardinal growth temperatures of *Escherichia coli* from optimal experiments. *International Journal of Food Microbiology* 128, 89-100.

Witzes T., Rombouts F.M., Kant-Muermans M.L.T, van't Riet K. and Zwietering M. H. (2001) Development and validation of a combined temperature, water activity, pH model for bacterial growth rate of *Lactobacillus curvatus*. International *Journal of Food Microbiology* 63, 57-64.

Wijtzes T., de Wit J.C., Huis in't Veld J.H.J., van't Riet K. and Zwietering M.H. (1995) Modelling bacterial growth of *Lactobacillus curvatus* as a function of acidity and temperature. *Applied and Environmental Microbiology* 61, 2533-2539.

Wijtzes T., McClure P.J., Zwietering M.H. and Roberts T.A. (1993) Modelling bacterial growth of Listeria monocytogenes as a function of water activity, pH and temperature. *International Journal of Food Microbiology* 18, 139-149.

Zwietering M. H., de Wit J.C. and Notermans S. (1996) Application of predictive microbiology to estimate the number of *Bacillus cereus* in pasteurised milk at the point of consumption. *International Journal of Food Microbiology* 30, 55-70.

Zwietering M. H., Wijtzes J. C., De Wit and Van't Riet K. (1993) A decision support system for prediction of microbial spoilage in foods. *Journal of Food Protection* 55, 973-979.

Methodology for modelling the effects of hurdle technology in presence of disparate data sets.

L. Pujol[1,2], D. Kan-King-Yu[3], Y. Le Marc[3], M. D. Johnston[3], F. Rama-Heuzard[1,2], S. Guillou[1,2], J.M. Membré[2,1]

[1] LUNAM Université, Oniris, UMR1014 Secalim, Nantes, F-44307, France. (jeanne-marie.membre@oniris-nantes.fr)
[2] INRA, Nantes, F-44307, France. (jeanne-marie.membre@oniris-nantes.fr)
[3] Unilever Safety & Environmental Assurance Centre, Sharnbrook, MK44 1LQ, UK. (Denis.Kan-King-Yu@unilever.com)

Abstract

Gamma models describe the combined effect of preservative factors on growth inhibition in a modular way, i.e. by estimating independently the effect γ_i of each single factor and then multiplying these together ($\mu = \mu_{opt} \times \Pi\gamma_i$). Such models are known to mimic the concept of hurdle technology. This paper presents a methodology for modelling the effects of hurdle technology in the presence of disparate data sets. It includes i) data selection, ii) the procedure for estimating the parameters of the Gamma-type model, and iii) generation of experimental data for model validation. Data from industry, public database and literature were used in the study. Model development was carried out using R (nls function and nlstools package). Statistical criteria and graphical inspections were used to assess the goodness-of-fit. The validation procedure combined targeted generation of new data with the use of performance indicators. The methodology was illustrated with *Listeria monocytogenes*. The effects of temperature (1 to 40 °C), pH (4.5 to 8.2), a_w (0.911 to 0.997), acetic (0.05 to 1%), lactic (0.05 to 2 %) and sorbic (0.025 to 0.3 %) acids on the bacterial growth rate were assessed. A Gamma-type model was successfully validated against the generated data. In a last step, the possibility of testing equivalences between inhibitory factors ('iso-hurdle rules') was explored. The iso-hurdle rule 'replacement of salt by combination of organic acids' was successfully tested. This is promising for supporting the food industry in developing milder safe and stable preservation systems with limited data.

Keywords: growth modelling, Gamma model, hurdle effect, Listeria monocytogenes, organic acids

Introduction

Preservatives act as hurdles against microbial proliferation by inhibiting microbial growth. The safety and stability of a food product often rely on the concentration of each preservative present in the food preservation system. Modular models such as Gamma-type models (Zwietering *et al.* 1991) allow the quantification of individual and combined hurdle effects. Different combinations of hurdles can be then compared to each other to derive inhibitory effect equivalences (namely 'iso-hurdle rules').

It is not uncommon for food companies to generate and accumulate data on microbiological contaminants associated with their food production (e.g. for safety and quality purposes). However, such data are often disparate. For example, one data set may have been generated to describe the interaction effects of temperature, pH and water activity on microbial growth, and a separate one generated for describing the interaction effects of pH and organic acids. Should additional data be generated for investigating the interaction effects of temperature, pH, water activity and organic acids together? This paper presents a methodology for developing microbiological models based upon re-analyses of existing data, and validating them by generating very few new data.

The objective of the study was to demonstrate the feasibility of establishing iso-hurdle rules based on the modelling of disparate existing data sets.

The methodology and the iso-hurdle concept are illustrated with *Listeria monocytogenes* and the factors temperature, pH, a_w, acetic, lactic and sorbic acids.

Materials and Methods

Selection of the existing experimental data

A total of 1778 growth curves obtained from the literature, Combase or industrial trials were collected for this study. Several data selection criteria were applied to ensure the relevance and the quality of the final data to be used. 652 growth rates of *Listeria monocytogenes* were kept in the analysis, corresponding to 25 sub-datasets from different sources. The factors studied were temperature (1 to 40°C), pH (4.5 to 8.2), water activity (0.911 to 0.997), sorbic (0.025 to 0.3% of potassium sorbate), acetic (0.05 to 1% of sodium acetate), and lactic (0.05 to 2% of sodium lactate) acids.

Predictive models

Maximum specific growth rates, μ_{max} (h^{-1}) were obtained by fitting the kinetic data with the logistic model with delay used by Zuliani *et al.* (2007) . The secondary model is based on a Gamma-type model (Rosso *et al.* 1995) with or without a synergistic term (Le Marc *et al.* 2002). The effects of acids (possibly in combination) are included in the model as proposed by Coroller *et al.* (2005). The model can be written as:

$$\mu_{\max} = \mu_{opt}\gamma(T)\gamma(pH)\gamma(a_w)\gamma(sorbic)\gamma(acetic)\gamma(lactic)\xi \quad (1)$$

where μ_{opt} is the specific growth rate at optimum growth conditions, γ(T), γ(pH), $\gamma(a_w)$, γ(sorbic), γ(acetic), γ(lactic) are the effects of temperature, pH, a_w, sorbic, acetic and lactic acids, respectively. ξ is a term for the synergistic effects of factors at the growth limits.

Statistical Methods and software

Two fitting procedures were used: a 'sequential' method, consisting of estimating the effect of each Gamma term successively, using its associated subset of data; and a 'simultaneous' method, for which all model parameters were estimated simultaneously using the whole data set. Fitting was carried out using R (http://www.r-project.org/).

Experimental design for model validation

To validate the model, a total of 64 experiments (each duplicated) were carried out at 23°C. The experimental design was built to verify the inhibition equivalence (iso-hurdles rules) of various preservative formulations. Three iso-hurdle rules were tested: i) replacement of acetic acid by lactic acid, ii) partial replacement of NaCl by a combination of organic acids, and iii) replacement of sorbic acid with a combination of salt and acetic or lactic acids (clean label).
For example, the iso-hurdle rule (ii) was tested at four different pH levels. For each pH level, salt and acid concentrations were set to achieve an equivalent inhibitory effect of salt ($(\gamma(a_w)=k$, $k<1$) and acids (γ(acetic)×γ(lactic)×γ(sorbic)=k).

Experimental procedure

A cocktail of 11 strains of *Listeria monocytogenes* was used throughout the study. One hundred milliliters of Tryptone Soya Broth (TSB) were inoculated at a level of ca 500 cfu/ml. The growth of *L. monocytogenes* was followed by plate counts (5 days at 30°C).

Model validation

The Bias factor (B_f) and the Accuracy factor (A_f) as defined by Ross (1996) and the discrepancy factor by Baranyi *et al.* (1999) were used along to assess model performance. An ANOVA was performed to compare specific growth rates obtained for the same iso-hurdle rules.

Results and Discussion

Building the model on the existing dataset, validating it with new experimental data

The inhibitory effect of each hurdle (i.e. each Gamma term) was estimated by using two models (with or without synergistic term ξ) and two fitting procedures (sequential or simultaneous). Parameter estimates (for the non-synergistic model fitted using the simultaneous method) are presented in Table 1.

Table 1: Estimated parameters and their confidence interval obtained for the simultaneous method without including the interaction term ξ.

	Estimated parameters	Confidence interval	
		2.5%	97.5%
T_{min}(°C)	-0.904	-1.19	-0.613
pH_{min}	4.19	4.12	4.26
aw_{min}	0.921	0.919	0.924
MIC_{sorbic}(mM)	6.35	5.50	7.20
MIC_{lactic}(mM)	9.87	6.82	12.9
MIC_{acetic}(mM)	10.9	9.42	12.4

T_{min}, pH_{min}, aw_{min} were estimated from the cardinal model (Rosso *et al.* (1995)).
MICs were determined using equations cited by Zuliani *et al.* (2007)

Once the model was built, the observed growth rates from the new experimental data were compared with the predictions (Figure 1) and Bias factor (B_f) were calculated.

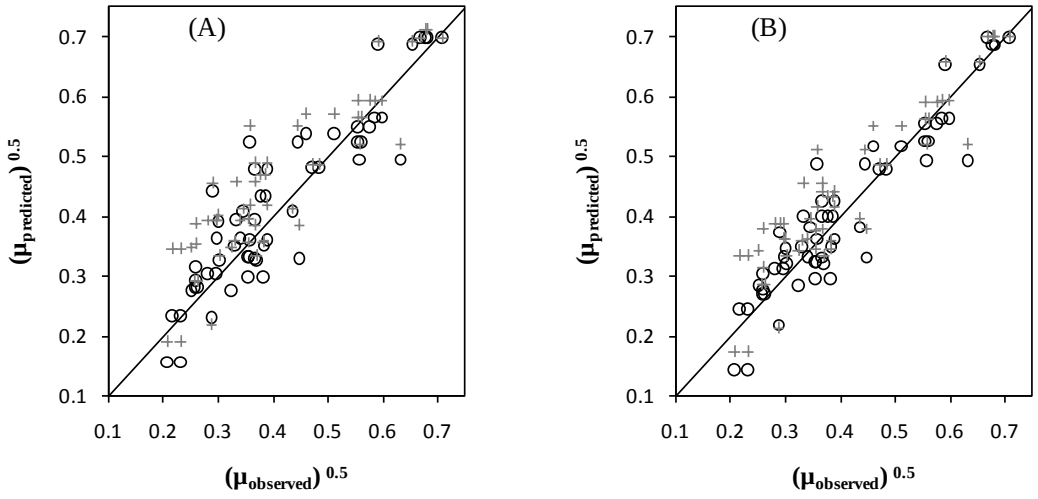

Figure 1: Comparison of observed and predicted growth rates (square root transformation), for sequential method (A), without ξ (○), B_f =1.03, and with ξ (+), B_f=*1.25;* for simultaneous method (B), without ξ (○), B_f =1.03, and with ξ (+), B_f=*1.17*.

Regarding bias factors, the best fit was obtained with the simultaneous method with a slight difference in terms of prediction ability whether ξ is integrated or not in the model. As the addition of the interaction term generates more complexity in estimation, it should only be chosen in particular applications, e.g. near the growth/no growth interface. That is to say, if the objective is to predict growth under mild stress conditions ($\prod \gamma \geq 0.2$) (e.g. where limited growth is tolerated) a model without interaction might be sufficient.

Applying the predictive model to derive iso-hurdle rules

Once the Gamma-type model was built, the inhibitory effect of one environmental factor could be quantified independently of the level of the other inhibitory factors. This mathematical characteristic was used to deduce iso-hurdle rules. For example, in theory, the

inhibitory effect of salt (hurdle effect $\gamma(a_w)$) is equivalent to a combination of inhibitory effects due to acids (hurdle effect $\gamma(\text{acetic})\times\gamma(\text{lactic})\times\gamma(\text{sorbic})$). This leads directly to an iso-hurdle rule which might be formulated as 'replacement of salt by combination of organic acids'. To validate whether the mathematical characteristics derived from Gamma-type models might be explored further, kinetics obtained in broth, with or without salt ($(\gamma(a_w)=k$, $0<k<1$) were compared against kinetics obtained with combination of acids ($\gamma(\text{acetic})\times\gamma(\text{lactic})\times\gamma(\text{sorbic})=k$), at various pH values (Figure 2).

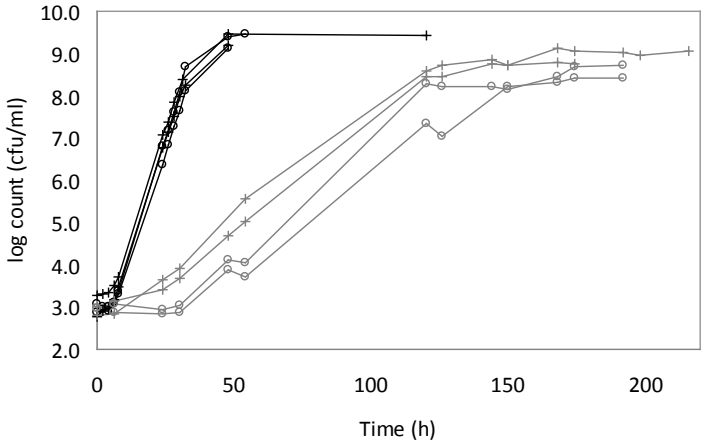

Figure 2: Kinetics of *L. monocytogenes* at pH 6.5 (black symbols and lines) and pH 5.7 (grey symbols and lines). Culture in presence of salt (o) or acids (+).

There was no difference ($p>0.05$) between growth rates from *L. monocytogenes* kinetics obtained in presence of salt or acids. This confirms the model outputs and emphasizes the possibility of using Gamma-type models to aid in new product formulation development.

Conclusions

A methodology for using disparate data to assess the effects of preservative factors on microbial growth has been developed. The Gamma model structure is appropriate to perform this analysis. The methodology has been successfully applied to *L. monocytogenes* for temperature, pH, a_w, sorbic, acetic and lactic acids. Iso-hurdle rules such as 'replacement of salt by combination of organic acids' were successfully tested. This is promising for supporting the food industry in developing milder safe and stable preservation systems with limited data.

References

Baranyi J., Pin C. and Ross T. (1999) Validating and comparing predictive models. *International Journal of Food Microbiology* 48 (3), 159-166.

Coroller L., Guerrot V., Huchet V., Le Marc Y., Mafart P., Sohier D. and Thuault D. (2005) Modelling the influence of single acid and mixture on bacterial growth. *International Journal of Food Microbiology* 100 (1-3), 167-178.

Le Marc Y., Huchet V., Bourgeois C.M., Guyonnet J.P., Mafart P. and Thuault D. (2002) Modelling the growth kinetics of Listeria as a function of temperature, pH and organic acid concentration. *International Journal of Food Microbiology* 73 (2-3), 219-237.

Ross T. (1996) Indices for performance evaluation of predictive models in food microbiology. *Journal of Applied Bacteriology* 81 501-508.

Rosso L., Lobry J.R., Bajard S. and Flandrois J.P. (1995) Convenient Model To Describe the Combined Effects of Temperature and pH on Microbial Growth. *Applied and Environmental Microbiology* 61 (2), 610-616.

Zuliani V., Lebert I., Augustin J.C., Garry P., Vendeuvre J.L. and Lebert A. (2007) Modelling the behaviour of *Listeria monocytogenes* in ground pork as a function of pH, water activity, nature and concentration of organic acid salts. *Journal of Applied Microbiology* 103 (3), 536-550.

Zwietering M.H., de Koos J.T., Hasenack B.E., de Witt J.C. and van't Riet K. (1991) Modeling of bacterial growth as a function of temperature. *Applied and Environmental Microbiology* 57 (4), 1094-1101.

A stochastic modelling approach integrating strain variability of *Salmonella enterica* growth kinetic behavior

A. Lianou, K.P. Koutsoumanis

Laboratory of Food Microbiology and Hygiene, Department of Food Science and Technology, School of Agriculture, Aristotle University of Thessaloniki, Thessaloniki 54124, Greece. (alianou@agro.auth.gr; kkoutsou@agro.auth.gr)

Abstract

A stochastic model integrating intra-species variability data, and predicting the maximum specific growth rate (μ_{max}) of *Salmonella enterica* as a function of pH and water activity (a_w), was developed in the present study. The growth kinetic data utilized for this purpose were μ_{max} values of 60 *S. enterica* isolates, estimated during monitoring of growth in tryptone soy broth of different pH (4.0-7.0) and a_w (0.964-0.992) values. The effects of the environmental parameters on μ_{max} were modelled for each tested strain using cardinal type and gamma concept models for pH and a_w, respectively. A multiplicative without interaction-type model, combining the models for pH and a_w, was used to describe the combined effect of these two parameters on μ_{max}. The strain variability of the growth behavior of *S. enterica* was incorporated in the modelling procedure by using the cumulative probability distributions of the values of pH_{min}, pH_{opt} and a_{wmin} as inputs to the growth model, while the cumulative probability distribution of the observed μ_{max} values corresponding to growth at pH 7.0-a_w 0.992 was introduced in the place of the model's parameter μ_{opt}. The introduction of the above distributions into the growth model resulted, using Monte Carlo simulation, in a stochastic model with its predictions being distributions of μ_{max} characterizing the strain variability. The developed model was validated using independent growth kinetic data (μ_{max} values) generated for the 60 strains of the pathogen at pH 5.0-a_w 0.977, and exhibited a satisfactory performance.

Keywords: *Salmonella enterica, strain variability, stochastic growth model*

Introduction

Strain variability of the growth behavior of foodborne pathogens has been recognized as an important issue in food safety management. It has been acknowledged that such intra-species variability may have a great impact on quantitative microbial risk assessment, and, thus, should be systematically assessed and accounted for (Delignette-Muller and Rosso 2000). Although microbial growth variability among strains of a single bacterial species has been observed for several foodborne pathogens, only a limited number of studies have attempted to characterize this variability (Lianou and Koutsoumanis 2010), while stochastic approaches explicitly taking into account strain variability have been described mainly during the last decade (Delignette-Muller and Rosso 2000). Furthermore, in contrast to what is the case for other bacterial foodborne pathogens, the available research data on the variability of the growth behavior among strains of *Salmonella enterica* are relatively few. Therefore, the objective of the present study was the development and validation of a stochastic model for integrating strain variability in modelling *S. enterica* growth.

Materials and Methods

Growth data of S. enterica strains

The growth kinetic data used in this work were maximum specific growth rate (μ_{max}) values corresponding to 60 *S. enterica* isolates, and were generated in a previous study undertaken in our laboratory (Lianou and Koutsoumanis 2010). The tested strains were primarily isolates of human or animal (almost exclusively bovine) origin belonging to various serotypes, and their growth kinetic behavior was assessed at 37°C in culture broth (tryptone soy broth) of different

pH (4.3, 4.5, 5.0, 5.5 and 7.0) and a_w (0.964, 0.977, 0.983 and 0.992) values. The μ_{max} values corresponding to each strain and growth condition were estimated by means of absorbance detection times of serially decimally diluted cultures using an automated turbidimetric system (Lianou and Koutsoumanis 2010). In order for the μ_{max} modelling as a function of pH to be facilitated, additional experiments assessing the growth kinetic behavior of the 60 *S. enterica* strains in tryptone soy broth (TSB; Lab M Limited, Lancashire, United Kingdom) of pH 4.0 (and 0.5% NaCl as part of its basal composition) were undertaken in the present study. The pH of TSB was adjusted to this value using HCl (min. 37%; Sigma-Aldrich, Seelze, Germany), and the growth experiments were carried out following, overall, previously described procedures (Lianou and Koutsoumanis, 2010).

Growth rate modelling

The effect of pH on μ_{max} was modelled for each *S. enterica* strain using the cardinal type model of Rosso (Rosso *et al*. 1995):

$$\mu_{max} = \mu_{opt} \cdot \rho(pH)$$

$$\rho(pH) = \begin{cases} 0, & pH \le pH_{min} \\ \dfrac{(pH - pH_{min}) \cdot (pH - pH_{max})}{(pH - pH_{min}) \cdot (pH - pH_{max}) - (pH - pH_{opt})^2}, & pH_{min} < pH < pH_{max} \\ 0, & pH \ge pH_{max} \end{cases} \quad (1)$$

where pH_{min}, pH_{opt} and pH_{max} are the corresponding cardinal values, and μ_{opt} is the optimum value of the maximum specific growth rate (when $pH=pH_{opt}$). The effect of a_w on μ_{max} was modelled using the gamma concept model of Zwietering *et al.* (1996), with the gamma factor for a_w being slightly modified:

$$\mu_{max} = \mu_{opt} \cdot \gamma(a_w)$$

$$\gamma(a_w) = \left(\frac{a_w - a_{w\min}}{a_{w\,opt} - a_{w\min}} \right)^2 \quad (2)$$

where $a_{w\min}$ is the a_w value below which growth is not possible, and $a_{w\,opt}$ is the a_w value at which the maximum specific growth rate is equal to its optimum value.

The values of pH_{min}, pH_{opt}, pH_{max} and $a_{w\min}$ were determined by fitting the estimated μ_{max} values for each tested strain to the above models using the Excel v4 format of the curve-fitting program TableCurve 2D (Systat Software Inc., San Jose, CA, USA). The $a_{w\,opt}$ was set at 1 when the μ_{max} data were fitted to the gamma concept model. A multiplicative without interaction-type model, combining the above models for pH and a_w, was used to describe the combined effect of these two environmental parameters on μ_{max}:

$$\mu_{max} = \mu_{opt} \cdot \rho(pH) \cdot \gamma(a_w) \quad (3)$$

where μ_{opt} is the maximum specific growth rate corresponding to optimum growth conditions.

Stochastic modelling approach

The intra-species variability of the growth behavior of *S. enterica* was incorporated in the modelling procedure by using the cumulative probability distributions of the values of pH_{min}, pH_{opt} and $a_{w\min}$ as inputs to the growth model described above. The cumulative probability distribution of the estimated μ_{max} values corresponding to growth at pH 7.0-a_w 0.992 (regarded as optimum growth conditions) was introduced in the place of the model's parameter μ_{opt}. The introduction of the above probability distributions into the growth model was carried out using the custom cumulative function of the @RISK 4.5 for Excel software (Palisade Corporation, Newfield, NY, USA), and resulted in a stochastic model with its predictions, using Monte Carlo simulation (10000 iterations), being distributions of μ_{max} values.

Model validation

The stochastic growth model was validated against independent data generated for the 60 strains of the pathogen at pH 5.0 and a_w 0.977. The latter growth kinetic data were μ_{max} values corresponding to growth at 37°C in TSB of the above characteristics, and were estimated as

described previously (Lianou and Koutsoumanis, 2010). The pH of TSB was adjusted to 5.0 with HCl as previously practiced, while the a_w value of 0.977 corresponded to a NaCl (Merck, Darmstadt, Germany) concentration of 4.5% (w/v). Model validation was undertaken utilizing the Monte Carlo simulation technique with 10000 iterations, performed with the @RISK 4.5 for Excel software, and was based on the comparative evaluation of the predicted and observed distributions of μ_{max}. The latter comparison was made graphically and quantitatively using the percent relative error (%RE) values for the mean, standard deviation and percentiles of the μ_{max} distributions based on the following equation:

$$\%RE = [(x_o - x_p)/x_o]*100 \quad (2)$$

where x_o and x_p are the values of the above statistics for the observed and predicted distributions, respectively.

Results and Discussion

The μ_{max} data exploited in this study were overall well-fitted to the secondary models used, with the mean (± standard deviation) coefficient of determination (r^2) for all the fitting trials (n=60) being 0.934 (± 0.034) and 0.983 (± 0.009) for pH and a_w, respectively. The mean and the 5th and 95th percentiles of the estimated pH_{min} for the 60 *S. enterica* strains were 3.84 and 3.75 and 3.99, respectively, while the corresponding values for the a_{wmin} were 0.939 and 0.934 and 0.947. The mean and the 5th and 95th percentiles of the estimated pH_{opt} were 6.47 and 6.17 and 6.72, respectively. No considerable association was observed between the values of pH_{min}, pH_{opt} and a_{wmin}. For pH_{max}, the mean and the 5th and 95th percentiles were 14.10 and 13.99 and 14.99, respectively. For the latter parameter, however, a high uncertainty was observed from the fitting of the μ_{max} data to the model due to the absence of data at superoptimal conditions. Thus, the distribution of pH_{max} was chosen not to be used in the stochastic model development, and, alternatively, pH_{max} was set at 14.0. Moreover, since the distribution of the estimated μ_{max} values corresponding to growth at a_w 0.992 was used as μ_{opt} in the stochastic model, the a_{wopt} was set at 0.992.

Via the introduction of the cumulative probability distributions of the values of pH_{min}, pH_{opt} and a_{wmin} into the growth model and the use of Monte Carlo simulation, the model is converted into a stochastic one, which, by integrating strain variability, provides μ_{max} predictions in the form of distributions. As demonstrated in Fig. 1, where the single effects of pH and a_w on the predicted μ_{max} are presented, the growth environment affected both the position and the shape of the predicted μ_{max} distributions. Furthermore, these stochastic predictions obtained with simulations at various pH (assuming a_w=a_{wopt}) and a_w (assuming pH=pH_{opt}) values, were, overall, in good agreement with the observed μ_{max} values (i.e. dependent data), with most of the observed data being satisfactorily allocated within the predicted distributions (Fig. 1).

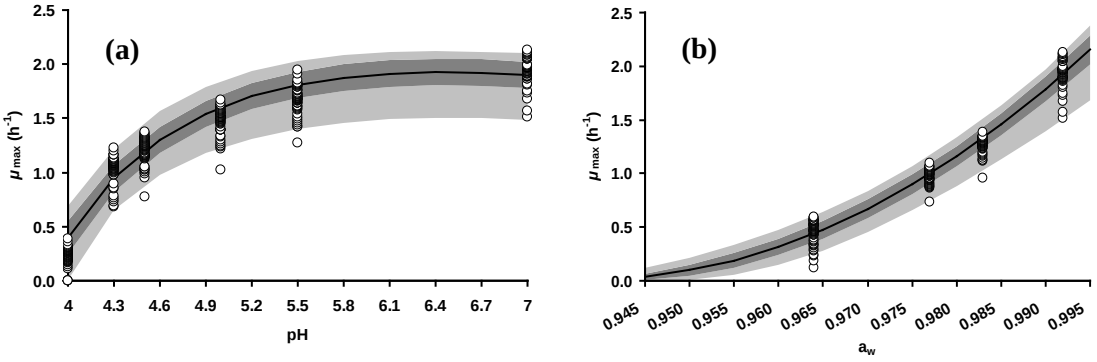

Figure 1: Single effects of pH (a) and a_w (b) on the maximum specific growth rate (μ_{max}) of *Salmonella enterica*, as predicted by the developed growth model. Points (o) represent the observed values of μ_{max}.

The performance of the stochastic model was evaluated by comparing its predictions with independent data obtained at pH 5.0-a_w 0.977. The predicted probability distribution of μ_{max}

obtained with Monte Carlo simulation was fairly close to the probability distribution of the observed values. The mean, standard deviation, and the 5th and 95th percentiles of the predicted μ_{max} distribution were 0.83, 0.08, and 0.69 and 0.96 h^{-1}, respectively, while the corresponding values of the observed distribution were 0.73, 0.09, and 0.61 and 0.85 h^{-1}. The mean (± standard deviation, n=100) %RE for all the percentiles of the μ_{max} distributions was -13.8 (± 2.1) %. It has been suggested that %RE values in the range of -30% (fail-safe) to 15% (fail-dangerous) delimit an "acceptable prediction zone" for model evaluation purposes (Oscar, 2005). The stochastic growth model described here meets the above criterion, with its predictions being exclusively localized in the fail-safe area. When the stochasticity provided by a modelling approach, such as the one described in the present study, is embedded in a primary model, then more realistic predictions of microbial growth than those resulting from deterministic models are expected to be generated. For instance, incorporation of the developed stochastic model in the place of μ_{max} in a three-phase linear model (Buchanan *et al.*, 1997), and assuming for all the tested *S. enterica* strains an initial population N_0=2 log CFU/ml and a physiological state h_0=1, resulted, using Monte Carlo simulation (5000 iterations), in the stochastic growth prediction at pH 5.0-a_w 0.977 illustrated in Fig. 2.

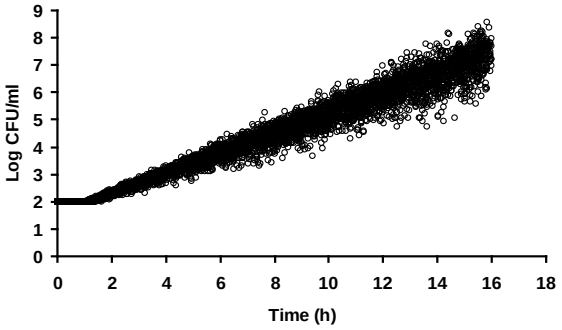

Figure 2: Growth of *Salmonella enterica* at pH 5.0-a_w 0.977 as predicted using a three-phase linear model combined with the developed stochastic model for integration of growth rate variability among strains of the pathogen.

Conclusions

The stochastic approach developed in this study described adequately the μ_{max} variability among strains of *S. enterica* while modelling its growth as a function of pH and a_w, and can be useful in integrating this variability in quantitative microbiology and microbial risk assessment.

Acknowledgements

This study has been carried out with the financial support of the Commission of the European Communities, Project ProSafeBeef "Food-CT-2006-36241".

References

Buchanan R.L., Whiting R.C. and Damert W.C. (1997) When is simple good enough: a comparison of the Gompertz, Baranyi, and three-phase linear models for fitting bacterial growth curves. *Food Microbiology* 14, 313-326.

Delignette-Muller M.L. and Rosso L. (2000) Biological variability and exposure assessment. *International Journal of Food Microbiology* 58, 203-212.

Lianou A. and Koutsoumanis K.P. (2011) Effect of the growth environment on the strain variability of *Salmonella enterica* kinetic behavior. *Food Microbiology* 28, 827-837.

Oscar T.P. (2005) Validation of lag time and growth rate models for *Salmonella* Typhimurium: acceptable prediction zone method. *Journal of Food Science* 70, M129-137.

Rosso L., Lobry J.R., Bajard S. and Flandrois J.P. (1995) Convenient model to describe the combined effects of temperature and pH on microbial growth. *Applied and Environmental Microbiology* 61, 610-616.

Zwietering M.H., de Wit J.C. and Notermans S. (1996) Application of predictive microbiology to estimate the number of *Bacillus cereus* in pasteurised milk at the point of consumption. *International Journal of Food Microbiology* 30, 55-70.

Modelling transfer of *Salmonella* Typhimurium DT104 during the grinding of pork

C.O.A. Møller[1], M.J. Nauta[1], B.B. Christensen[2], P. Dalgaard[3], T.B. Hansen[1]

[1] Technical University of Denmark (DTU), National Food Institute, Mørkhøj Bygade 19, DK-2860, Søborg, Denmark. (clemo@food.dtu.dk)
[2] University of Copenhagen (KU), Faculty of Life Sciences, Department of Food Science, Rolighedsvej 30, DK-1958, Frederiksberg C, Denmark. (bbc@life.ku.dk)
[3] Technical University of Denmark (DTU), National Food Institute, Søltofts Plads, Bygning 221, DK-2800, Kgs. Lyngby, Denmark. (pada@food.dtu.dk)

Abstract

During grinding of pork, *Salmonella* present on a single slice of meat may be transferred to many portions of minced meat due to cross contamination. In order to develop a mathematical model describing this process, transfer rates of *Salmonella* were measured in three experiments, where between 10 and 20 kg meat was ground into 200-g-portions. In each experiment, 5 pork slices (ca. 200 g/slice) were inoculated with 8-9 log-units of *Salmonella* Typhimurium DT104 and used for building up the contamination in the grinder. Subsequently, *Salmonella* free slices were ground and collected as samples of *approx*. 200 g minced pork. Throughout the process, representative samples were analyzed quantitatively for *Salmonella*. In minced pork, *Salmonella* counts decreased quickly and reached 5 log-units in the 13-16th portion but after observing up to 100 portions it was still possible to detect *Salmonella* at levels around 4 log-units. A model suggested by Nauta *et al.* (2005) predicting cross contamination of *Campylobacter* in poultry-processing could efficiently describe the observed transfer of *Salmonella* during grinding of the first 20 slices but could not explain the 'tail' of low contaminated portions. Therefore, it was hypothesized that the input of *Salmonella* is organized in two different matrices inside the grinder. One matrix, where *Salmonella* is loosely attached, is responsible for the fast transfer to the minced meat and from a second matrix *Salmonella*'s transfer occurs at a slower rate. Based on this hypothesis a modified model was implemented and challenged. This model satisfactorily predicted the observed behaviour of *Salmonella* during its cross contamination in the grinding of up to 110 pork slices. The proposed model may be an important tool to examine the effect of cross contamination in quantitative microbial risk assessments.

Keywords: *pork, Salmonella, cross contamination, modelling*

Introduction

Salmonella has been linked to many foodborne illness cases across the world, and it is considered to be one of the main agents causing human gastroenteritis. In Denmark, the locally produced pork was estimated as an important source of salmonellosis in 2009. Investigations showed that *S*. Typhimurium was the predominant serotype in retail pork cuttings in Denmark. Surface cross contamination of foodborne pathogens during processing or preparation is a major concern to consumers and food manufactures. The aim of this study was to develop a model to predict cross contamination of *Salmonella* in pork processing.

Materials and Methods

Salmonella culture and inoculation of meat

A strain of *Salmonella* Typhimurium DT104 isolated from pigs was grown in LB-broth with shaking (200 rpm) overnight at 37°C. The culture was then kept at 5°C/24 h and then diluted to *approx*. 10^9 CFU ml^{-1} or 10^7 CFU ml^{-1}. A whole piece of meat was surface inoculated with 10 drops of 10 µl of the *Salmonella* culture. The inoculum was spread on the whole surface of the selected side of the meat that subsequently was kept for 40 min to allow attachment of cells. The inoculated piece of pork was then divided into five 200-g-slices.

Transfer experiment

A semi-industrial grinder (la Minerva®, Italy) was used to process *Salmonella* free pieces of vacuum packaged boneless skinless fresh pork leg (6-8% fat) measuring about 7 x 10 x 15 cm and weighing *approx*. 1 kg. Five 200g-slices of non-inoculated meat were processed to create a matrix inside the grinder. The five inoculated samples were then ground and 40 to 90 200-g-slices of non-inoculated pork were processed. Individual portions corresponding to each processed slice were collected in separate sterile stomacher bags and mixed two-times during 1 min to ensure a homogeneous distribution of *Salmonella*. Subsequently, 25 g samples were diluted in 225 ml of Brain Heart Infusion broth and mixed in a stomacher for 2 min. Further dilutions were made in Maximum Recovery Diluent and drop-plated (3 x 10 µl) or spread-plated (1 x 100µl or 3 x 333µl) onto XLD agar (37°C, 16-24 h).

Model development

A model from Nauta *et al*. (2005) predicting cross contamination of *Campylobacter* in poultry-processing could efficiently describe the transfer of *Salmonella* during grinding of the first 20 slices, but not explain the 'tail' of low contaminated portions. It was hypothesized that input of *Salmonella* is organized in two different matrices inside the grinder as shown in Figure 1. One matrix, with *Salmonella* relatively loosely attached, is responsible for the fast transfer to the minced meat, while in the second matrix the transfer occurs at a slower rate.

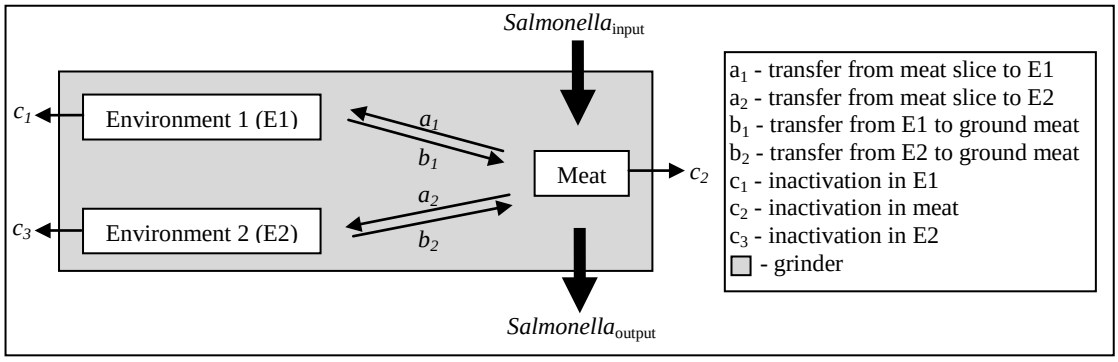

Figure 1: Diagram of the transfer hypothesis of *Salmonella* during grinding of pork.

Based on this hypothesis a modified version of Nauta *et al*. (2005) model was implemented. Modifications of the parameters and addition of an extra parameter to the model in order to describe the whole transfer were tested as shown in the following model equations:

$$\begin{cases} M_i = (1-a_1)(1-a_2)(1-c_2)\, S_i + (b_1\, gr_{1,i-1}) + (b_2\, gr_{2,i-1}) \\ gr_{1,i} = a_1\, S_i + (1-b_1)(1-c_1)\, gr_{1,i-1} \\ gr_{2,i} = a_2\, S_i + (1-b_2)(1-c_3)\, gr_{2,i-1} \end{cases} \qquad \text{Equation 1}$$

This model has seven parameters but two of them have their values assumed as zero since no inactivation in meat (c_2) or environment 1 (c_1) is expected. Therefore, it is considered as a five parameters model (all with values between 0 and 1) and considers k portions of sliced meat that are processed in a grinder to minced meat (i = 1, 2,... k). The i^{th} slice carries S_i *Salmonella*. Minced portion of meat *i*, is the same slice of meat after grinding and carries M_i *Salmonella*. The 'contamination status' of the grinder is gr_i. The probability of transfer per cell from meat to grinder (environment 1) and to grinder (environment 2) is represented by a_1 and a_2, respectively. The backward transfer probabilities from the grinder (environments 1 and 2) to ground meat are given by b_1, and b_2. The survival in grinder (environment 2) is represented by $(1-c_3)$. The equations were applied to the *Salmonella* counts (CFU/slice or portion) for S_i and M_i. For estimation of parameters, the Residual Sum of Squares (RSS) of the difference between observed and predicted log counts was minimized using the Solver function in MS Excel. Three experiments, studying levels of 10^9 CFU of *Salmonella* per contaminated slice, were used for fitting of parameter values and three different models were applied to those datasets.

Statistical analysis and validation of models

A four-parameter model (4p-1ge) that considers one grinder environment (Nauta *et al*. 2005), a modified version of this model (4p-2ge) also with four parameters but taking into account two grinder environments (Equation 1 with c_3=0), and a version of the last model with 5 parameters (5p-2ge) (Equation 1) were used to fit the data and to calculate the Residual Sum of Squares (RSS). Fitting of the three studied models were compared by F-tests. Considering the RSS of the model, the number of observations and the number of model parameters the Root Mean sum of Squared Errors (RMSE) and the bias-corrected version of Akaike Information Criterion (AICc) were used as measures for goodness of fit (Ratkowsky 2004; Hurvich & Tsai 1989). In order to validate the best-fit model, two challenge tests were performed. The first challenge test (100 processed slices) was conducted by adding slices contaminated with 10^9 CFU of *Salmonella* per slice processed as 1st, 2nd and 3rd, 29th and 55th slices. A second challenge test processed 110 portions where 1st, 2nd and 3rd slices were contaminated with 10^7 CFU of *Salmonella* per slice, and the 19th and 35th slices had 10^9 CFU and 10^7 CFU of *Salmonella*, respectively. In addition to the visual inspection of the data, bias and accuracy factors (Ross 1996) with $\log_{10}$CFU/slice as the response variable, were used to evaluate the performance of the fitted model (Equation 1).

Results and Discussion

The fitted models and evaluation of goodness of fit

As shown in Table 1, three different models were fitted to datasets from three transfer experiments. The suggested 5p-2ge model was evaluated as the best choice as it resulted in the lowest RMSE- and AICc-values for all three datasets (Table 1). Pair wise comparisons of the models using F-tests supported this conclusion (results not shown).

Table 1: Evaluation criteria for each model performed – Number of parameters, Root Mean sum of Squared Error (RMSE) and Akaike Information Criterion (AICc).

Model	Dataset 1		Dataset 2		Dataset 3	
	RMSE	*AICc*	*RMSE*	*AICc*	*RMSE*	*AICc*
5p-2ge	1.2029	2.608	1.1345	0.856	1.1378	1.563
4p-2ge	1.2612	5.383	1.2364	5.512	1.2291	7.184
4p-1ge	1.4534	16.172	1.2862	8.382	1.3596	18.073

Figure 2 is an example of fitting the three models to dataset 2. It clearly shows why the 5p-2ge was the superior model. For parameter estimation, dataset 3, which included the highest number of processed slices, was applied. The following parameter estimates were obtained: a_1 (0.0010), b_1 (0.0275), a_2 (0.8909), b_2 (0.0558) and 1-c_3 (0.4887).

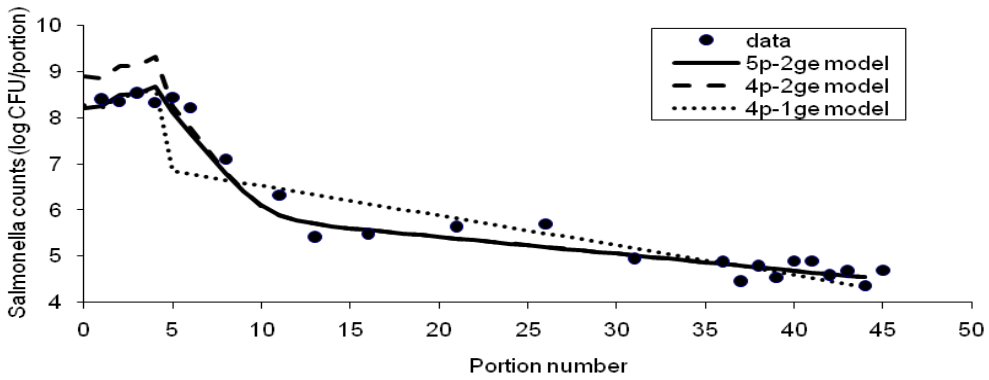

Figure 2: Transfer of *Salmonella* Typhimurium DT104 during grinding of 45 slices of 200-g boneless skinless pork leg (dataset 2) fitted to the three proposed models.

Validation of the new model

Levels of 10^9 and 10^7 CFU per 200 g were used in order to follow the decrease of *Salmonella* quantitatively for validation of the model describing transfer during the grinding process. Bias factors between 0.88 and 1.04, and accuracy factors between 1.03 and 1.15, were obtained using the parameter estimates from the three different datasets, indicating good performance in all cases. However, Figure 3 shows that only the parameter estimates from fitting of dataset 3 could predict the observed tailing phenomenon.

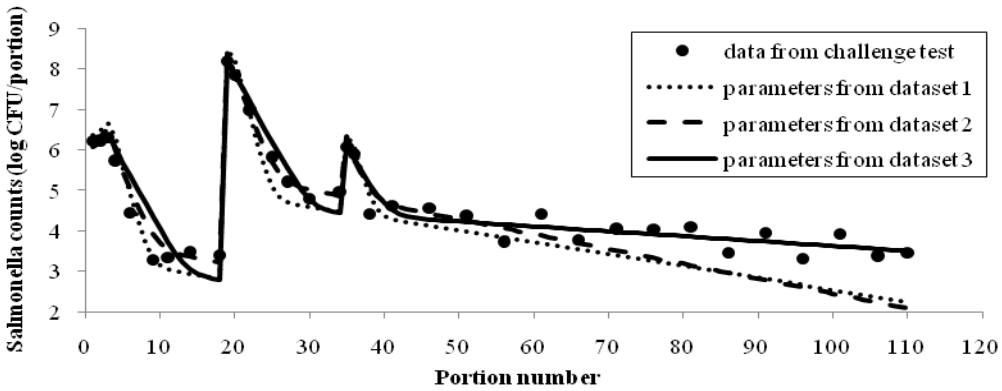

Figure 3: Observed and predicted transfer of *Salmonella* Typhimurium DT104 during grinding of 110 slices of 200-g boneless skinless pork leg (validation dataset 3).

The fitted model obtained (Figure 2) is specific to the studied grinding process including the evaluated grinder. However, the structure of the model, and particularly its ability to predict the tailing phenomenon, seems relevant for different cross contamination processes. The tailing corresponds to transfer of low concentrations of a pathogen to numerous portions of food, and it has been observed in several studies of slicing and food contact processes (Vorst *et al*. 2006; Aarnisalo *et al*. 2007; Sheen 2008; Sheen & Hwang 2010).

Conclusions

The present study observed a tailing phenomenon of transfer of *Salmonella* during a small-scale grinding process. It was, therefore, hypothesized that transfer occurred from two environmental matrices inside the grinder and a model was developed. The developed model satisfactorily predicted the observed behaviour of *Salmonella* during its cross contamination in the grinding of up to 110 pork slices. The proposed model is an important tool to examine the effect of cross contamination in quantitative microbial risk assessment investigations and might also be applied to various other food processes where cross contamination is involved.

References

Aarnisalo K., Sheen S., Raaska L. and Tamplin M. (2007) Modelling transfer of *Listeria monocytogenes* during slicing of 'gravad' salmon. *International Journal of Food Microbiology* 118, 69-78.

Hurvich C.M. and Tsai C. (1989) Regression and time series model selection in small samples. *Biometrika* 76 (2), 297-307.

Nauta M., van der Fels-Klerx I. and Havelaar A. (2005) A poultry-processing model for quantitative microbiological risk assessment. *Risk Analysis* 25 (1), 85-98.

Ratkowsky D.A. (2004) Model fitting and uncertainty. In: Mckellar R.C., Lu X. (Eds.), *Modelling Microbial Responses in food*, Chapter 4, 156-179, CRC Press, Boca Raton, Fl, USA, 343 pp. (ISBN 0-8493-1237-X).

Ross T. (1996) Indices for performance evaluation of predictive models in food microbiology. *Journal of Applied Bacteriology* 81, 501-508.

Sheen, S. (2008) Modeling surface transfer of *Listeria monocytogenes* on salami during slicing. *Journal of Food Science* 73 (6), E304-E311.

Sheen S. and Hwang C. (2010) Mathematical modelling the cross-contamination of *Escherichia coli* O157:H7 on the surface of ready-to-eat meat product while slicing. Food Microbiology 27, 37-43.

Vorst, K.L., Todd E.C.D. and Ryser E.T. (2006) Transfer of *Listeria monocytogenes* during slicing of turkey breast, bologna, and salami with simulated kitchen knives. *Journal of Food Protection* 69 (12), 2939-2946.

Effect of abrupt temperature shifts on the kinetic behavior of very small populations (2-10 cells) of *Salmonella* Typhimurium

P. Danias, A. Lianou, K. Koutsoumanis

Laboratory of Food Microbiology and Hygiene, Department of Food Science and Technology, School of Agriculture, Aristotle University of Thessaloniki, Thessaloniki 54124, Greece. (alianou@agro.auth.gr; kkoutsou@agro.auth.gr)

Abstract

A time-lapse microscopy method was applied to study the effect of abrupt temperature shifts on the kinetic behavior of very small populations (2-10 cells) of *Salmonella* Typhimurium on tryptone soy agar. The temperature was initially set at 25 ^{o}C and decreased to 15 ^{o}C after a few cell divisions (one to five). Images were taken at 5-min intervals for 20 h after inoculation. In total, the behaviour of 81 single cells was monitored. After counting, the numbers of cells vs. time for each colony, after the temperature shift, were fitted to the primary model of Baranyi and Roberts for the estimation of the maximum specific growth rate and the "additional lag" caused by the shift. The results showed a significant variability in the kinetic behaviour after the temperature downshift. The "additional lag" ranged from 0 to 1.26 h (mean=0.291 h) with a coefficient of variation (CV) of 116.7%. The maximum specific growth rate (mean=0.326 h^{-1}) after the shift showed less but still significant variability with CV=36.1%. The above distributions of the kinetic parameters were used to simulate the effect of abrupt temperature shifts on the kinetic behavior of the pathogen at various population levels.

Keywords: *Salmonella, single cell, temperature shifts*

Introduction

Predictive microbiology deals with the development of deterministic models based on studies with large microbial populations. Most available mathematical models describe the growth of microbial populations as a whole, without considering individual cells. In practice, however, contamination of foods with pathogens usually occurs at levels of few or even one cell. Recently, the importance of single-cell microbiology and the interest in stochastic models capable of predicting the effects of more "realistic" contamination events (low microbial numbers) in food safety has been stressed. Thus, predictive microbiology studies have focused on monitoring microbial kinetics at a single-cell level.

Recently, several studies have focused on monitoring the kinetics of single microbial cells. Elfwing *et al.* (2004) and Wakamoto *et al*. (2001) developed novel automated microscopic methods that enabled the user to monitor the division times of individual cells. Both of the above methods, however, allow for monitoring of only one cell with the daughter cell being removed after division. This approach does not take into account the "community effect". Indeed, in "real life", interactions among cells of a forming colony may occur during growth of an initially single cell on a solid food. In addition, all available studies on single-cell behavior have been performed at constant temperature conditions without taking into account temperature fluctuations which are common during distribution and storage of foods. The objective of the present study was to apply a time-lapse microscopy method for monitoring colonial growth of single cells, and to study the effect of abrupt temperature shifts on the kinetic behavior of very small populations (2-10 cells) of *Salmonella* Typhimurium. Beyond the scientific interest in understanding single-cell growth dynamics at fluctuating temperature conditions, the data provided are valuable for the development of stochastic models and for quantitative microbial risk assessment purposes.

Materials and Methods

The bacterial strain used in the study was *Salmonella enterica* serotype Typhimyrium FSL S5-520 (bovine isolate), kindly provided by Dr. Martin Wiedmann (Cornell University, Ithaca, New York). Ten microliters of a 24-h culture of the isolate, after the latter was diluted in quarter-strength Ringer's solution (Lab M Limited, Lancashire, United Kingdom) to a concentration of ~7.5 log cfu/ml, were added to 150 µl of tryptone soy agar (TSA; Lab M Limited) solidified on a glass slide, and were left to dry in a biological safety cabinet for 5 min. A z-motorized microscope (Olympus BX61) equipped with a ×100 objective (Olympus) and a high-resolution device camera (Olympus DP71) was used for monitoring growth of single cells. The temperature was initially set at 25 ^{o}C and decreased to 15 ^{o}C after a few cell divisions (one to five). Images were taken at 5-min intervals for 20 h after inoculation. The quality of the images was improved using the ScopePro module of the ImageProPlus software and an auto-focus procedure with an Extended Depth of Focus (EDF) system developed in our laboratory. The auto-focus procedure in conjunction with the EDF system allow for multiple serial images in different z-axis planes to be taken, and then combine the best focal areas of the serial images into a single in-focus image (z-stack). The latter procedure provided high quality images of bacterial colonies in which cells could be counted either manually or by the image analysis software. After counting, the numbers of cells vs. time for each colony, after the temperature shift, were fitted to the primary model of Baranyi and Roberts (1994) for the estimation of the maximum specific growth rate and the "additional lag" caused by the shift. In this study the colonial growth of 81 *Salmonella* Typhimurium single cells was monitored. Experiments are still in progress in order to increase the number of cells tested.

Results and Discussion

Fig. 1 shows a representative colonial growth of a *S.* Typhimurium single cell and the formation of a colony on TSA during a temperature shift at 195 min from 25 to 15 ^{o}C.

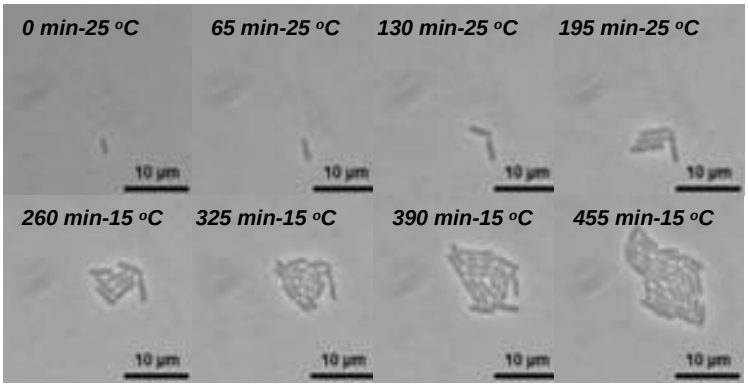

Figure 1: Representative colonial growth of a *S.* Typhimurium single cell and the formation of a colony on TSA during a temperature shift at 195 min from 25 to 15^{o}C.

Representative growth curves of *S.* Typhimurium during the above temperature conditions are shown in Fig. 2. After counting, the numbers of cells vs. time for each colony, after the temperature shift, were fitted to the primary model of Baranyi and Roberts (1994) for the estimation of the maximum specific growth rate and the "additional lag" caused by the shift.

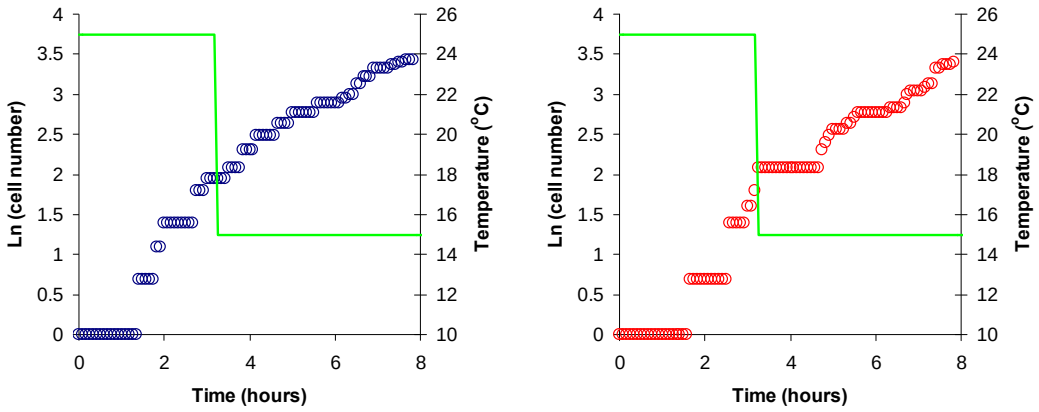

Figure 2: Representative growth curves of *S.* Typhimurium single cells during a temperature shift at 195 min from 25 to 15°C.

The data showed that the temperature shift may result in an "additional lag phase". However, a significant variability in the kinetic behaviour after the temperature downshift was observed. The "additional lag" ranged from 0 to 1.26 h (mean=0.291 h) with a coefficient of variation (CV) of 116.7%. The maximum specific growth rate (mean=0.326 h^{-1}) after the shift showed less but still significant variability with CV=36.1%. The distributions of the maximum specific growth rate and the "additional lag" after the temperature shift are presented in Fig. 3.

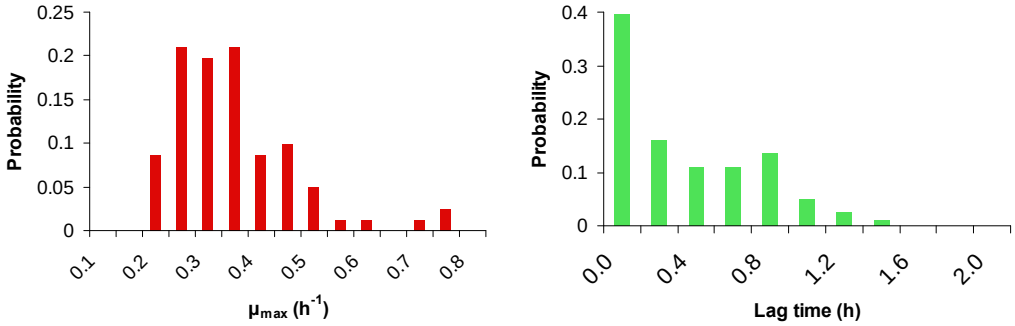

Figure 3: Distributions of the maximum specific growth rate (μ_{max}) and the "additional lag" after the temperature shift from 25 to 15°C.

Conclusions

The data showed that the temperature shift may result in an "additional lag phase" of *S.* Typhimurium growth. However, a significant variability in the kinetic behaviour after the temperature downshift was observed. The distributions of the kinetic parameters were used to simulate the effect of abrupt temperature shifts on the kinetic behavior of the pathogen at various population levels. The Monte Carlo simulations showed that the variability is masked at high population levels. The results of the present study provide useful information for understanding the colonial growth of single cells under changing temperature conditions.

Acknowledgements

This study has been carried out with the financial support of the Commission of the European Communities, Project ProSafeBeef "Food-CT-2006-36241".

References

Baranyi J. and Roberts T. A. (1994) A dynamic approach to predicting bacterial growth in food. *International Journal of Food Microbiology* 23, 277-294.

Elfwing A., LeMarc Y., Baranyi J. and Ballagi A. (2004) Observing growth and division of large numbers of individual bacteria by Image Analysis. *Applied Environmental Microbiology* 70, 675-678.

Wakamoto Y., Inoue I., Morguchi H. and Yasuda K. (2001) Analysis of single-cell differences by use of an on-chip microculture system and optical trapping. *Fresenius' Journal of Analytical Chemistry* 371, 276-281.

Individual-based modelling combined with micro-scale modelling of foods

R. Ferrier[1,2], A. Czarnecka[1], M. Ecosse[2], B. Hezard[2], F. Kuntz[2], A. Lintz[2], S. Oppici[1], V. Stahl[2], J.-C. Augustin[1]

[1] Université Paris-Est, Ecole Nationale Vétérinaire d'Alfort, Unité MASQ, 7 Avenue du Général de Gaulle, F-94704 Maisons-Alfort Cedex, France (jcaugustin@vet-alfort.fr)
[2] Aérial, Parc d'Innovation, F-67412 Illkirch, France (r.ferrier@aerial-crt.com)

Abstract

It is now well established that the growth prediction of pathogenic microorganisms in foods often requires a probabilistic approach taking into account the individual cell behaviour of contaminating cells. In this Individual-based Modelling (IbM) approach, we also have to deal with the description of the microenvironment surrounding the bacterial cells. The aim of this study was then to characterize the physico-chemical environment of bacterial cells contaminating the surface of a smear soft cheese and to assess the impact of the heterogeneity of the microenvironment on the bacterial behaviour. We used microelectrodes for pH measurements and freeze-drying to measure the water activity of micro-samples. Models were then established to describe the spatial and temporal variability for the pH and water activity at the surface of a smear soft cheese during ripening. The individual cell growth probability of *Listeria monocytogenes* according to the pH and the water activity was also determined. Probabilistic individual-based growth models were then combined with the micro-environmental models to predict the behaviour of *L. monocytogenes* cells contaminating the surface of the cheese during the ripening and the IbM approach was compared to growth predictions obtained with a population and macroscopic approach.

Keywords: *Individual-based Modelling, Listeria monocytogenes, cheese, micro-environment*

Introduction

The importance of variability of biological and natural phenomena is widely recognized in the context of risk analysis framework (WHO 2008). The major sources of variability affecting microbial responses in foods are the initial contamination level, the variability in processing factors, the variability in the food characteristics, in the storage conditions and the biological variability, i.e., the variability of microbial behaviour. This biological variability encompasses the strain variability in growth rates and limits, in physiological state, and in individual cell behaviour (Koutsoumanis 2008; Pin and Baranyi 2006). Although the significance to study individual cell behaviour to assess the risks linked to natural contaminations by few stressed cells of foodborne pathogenic microorganisms is well established, this approach was, to our knowledge, never combined with a description of the microenvironment surrounding the bacterial cells. The aim of our study was then to characterize the physico-chemical properties of a smear soft cheese at a microscopic scale and to compare a classical population macroscopic modelling approach with a fully Individual-based Modelling (IbM) approach.

Materials and Methods

Characterization of the physico-chemical properties of smear soft cheese

The pH and water activity (a_w) of the surface of smear soft cheese were measured during ripening at 14°C. For the macroscopic approach, the surface of cheese was sampled and mixed and the pH was measured with a conventional pH-meter (Hanna instruments). The surface a_w was measured with a GBX FA-st/1 water activity meter. The within-batch (or between cheeses) variability of pH and a_w was characterized by examining several cheese surfaces. For the micro-scale characterization of the surface pH of cheese, we used a pH microelectrode with a 50 μm tip diameter (Unisense). The micro-a_w of 30 mg surface cheese

samples was deduced from the water content sublimated during a freeze-drying cycle with a Telstar LyoBeta 25.

Characterization of the individual L. monocytogenes *cell growth probability*

Individual *L. monocytogenes* (strain LM14) cell growth probability according to the pH adjusted with HCl and a_w adjusted with NaCl was assessed with MPN estimates using the microwell plates method and pH 7 TSBYE at 37°C as the reference medium allowing the growth of every cells present in the bacterial suspensions (Dupont and Augustin 2009).

Prediction of the fate of L. monocytogenes *cells contaminating the cheese surface*

Individual-based growth models were combined with the micro-environmental pH and a_w models to predict the behaviour of *L. monocytogenes* cells contaminating the surface of the cheese during ripening at 14°C for 20 days. The individual growth probability models were combined with secondary cardinal and square root models and with the differential form of the primary Baranyi and Roberts model to take into account the pH profile. The differential form was solved numerically with the Runge-Kutta method using the Matlab software.
Growth predictions were also performed with a population and macroscopic approach by assuming a between-cheese variability of pH and a_w.
Three initial contamination levels (10, 100, and 1 000 cells) and three initial physiological states were considered. The three initial physiological states corresponded to cells with no lag phase (product μ_{max}•*lag* equal to 0), intermediate stressed cells (product μ_{max}•*lag* equal to 4.5, Couvert *et al.* 2010) and severely stressed cells (product μ_{max}•*lag* equal to 8, Couvert *et al.* 2010). The parameters of individual-based microscopic-scale and population macroscopic-scale approaches are reported in Table 1.

Table 1: Identification of parameters used in the population and individual-based modelling approaches.

Parameters		Population approach	Individual-based modelling
Cheese characteristics	Initial pH	N(4.83, 0.054)[a]	N(4.83, 0.039)
	Final pH	N(6.91, 0.064)	N(6.91, 0.235)
	pH increase rate (day^{-1})	N(0.298, 0.015)	N(0.298, 0.055)
	aw	N(0.961, 0.006)	U(0.916, 0.998)
Individual cell growth probability	*pH*	_	[exp(-4.32)-exp(-*pH*)]/[exp(-4.32)-exp(-6.33)]
	aw	_	(0.925-aw)/(0.925-0.998)
Listeria monocytogenes growth characteristics	Initial physiological state μ_{max}•*lag*	0, 4.5, 8	Extreme values distribution
	μ_{opt} (h^{-1})	0.212	0.212
	T_{min} (°C)	-1.08	-1.08
	T_{opt} (°C)	38.2	38.2
	T_{max} (°C)	43.3	43.3
	pH_{min}	4.32	4.32
	pH_{opt}	7	7
	pH_{max}	9.68	9.68
	aw_{min}	0.925	0.925
	aw_{opt}	0.998	0.998
	Initial contamination n_0	10, 100, 1000	10, 100, 1000
	Growth yield	$\log(n_0)+6$	$\log(n_0)+6$

[a] N(*a*,*b*) is the normal distribution with expected value *a* and standard deviation *b*, U(*a*,*b*) is the uniform distribution with minimal value *a* and maximum value *b*.

Results and Discussion

Micro-scale physico-chemical properties of smear soft cheese

An increase of surface pH was observed during the ripening of cheese at 14°C and a logistic type model was used to model it (Figure 1a). The micro-scale variability of initial and final pH and pH increase rate was estimated assuming a nonlinear mixed effects model and fitting was performed with the Monolix 2.4 software. No significant evolution of the a_w was observed during ripening and a uniform distribution adequately described the micro-scale variability of a_w (Figure 1b).

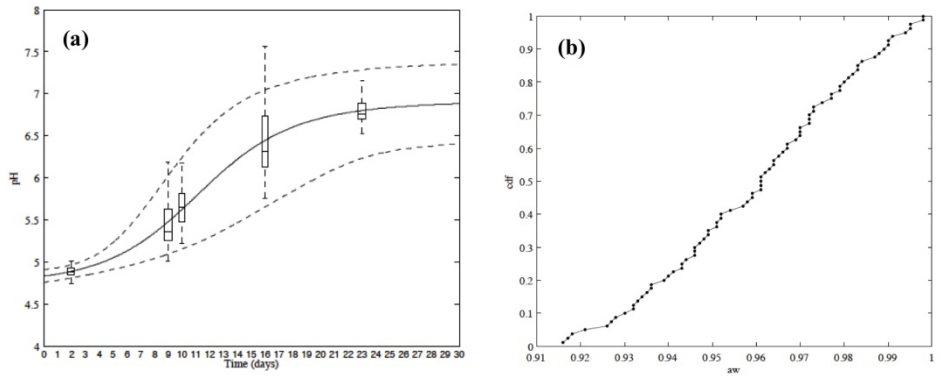

Figure 1: (a) Evolution of the micro-scale pH at the surface of smear soft cheese during ripening at 14°C (boxplots are observed values, the solid line is the median pH evolution and dashed lines represent the 95% confidence envelope of the model predictions) and (b) cumulative distribution of micro-scale water activity values at the surface of cheese.

Individual L. monocytogenes *cell growth probability*

The individual cell growth probability logarithmically increased with pH between 4.32 and 6.33 (Figure 2a) and linearly increased with a_w between 0.925 and 0.998 (Figure 2b).

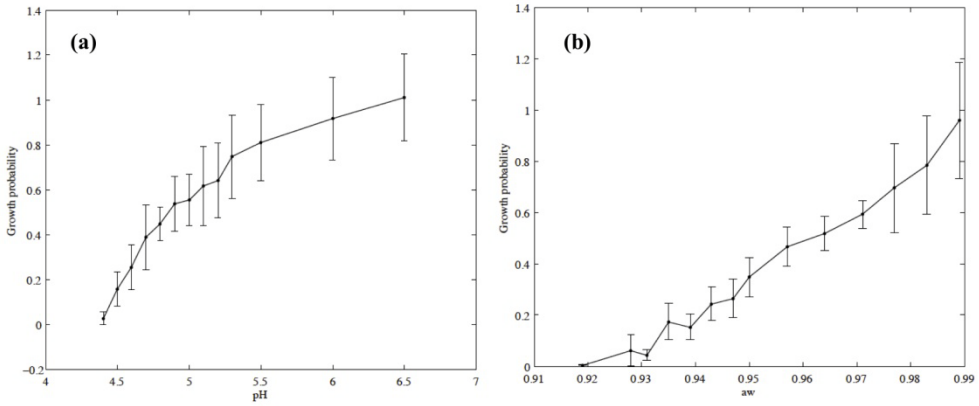

Figure 2: Individual cell growth probability of *L. monocytogenes* according to (a) the pH and (b) the water activity. Circles represent the mean values and vertical bars represent standard deviations of replicated experiments.

Prediction of the fate of L. monocytogenes *cells contaminating the cheese surface*

The distributions describing the variability of the final contamination of cheese are shown in Figure 3. With the population modelling approach, the variability of the final contamination was approximately constant whatever the initial contamination level and physiological state. Distributions were essentially the same, only the scale was disturbed depending on the initial parameters. Conversely, the distributions obtained with the IbM approach were very dependent on the initial contamination level and physiological state. For low initial contamination level, i.e. 10 cells, as it can be expected for natural contaminations, the final contamination exhibited a very large variability with no growth in 10 to 80% of cases depending on initial physiological state and a maximum contamination sometimes exceeding 10^6 cells (Figure 3d). When the number of initial cells increased, the growth yield was significantly increased and the variability of the final contamination was decreased. For instance, most of the final contamination levels were in a 0.5 log range for an initial contamination of 1 000 unstressed cells (Figure 3f). In these cases, the variability of the contamination was even lower than with the population modelling approach. This could be explained by an increasing probability to find cells surrounded by a particularly favourable microenvironment leading to a substantial growth. This phenomenon could be observed when challenge tests are performed in heterogeneous foods and these results highlight the risk to

overestimate the growth when using these experiments and average macroscopic food characteristics.

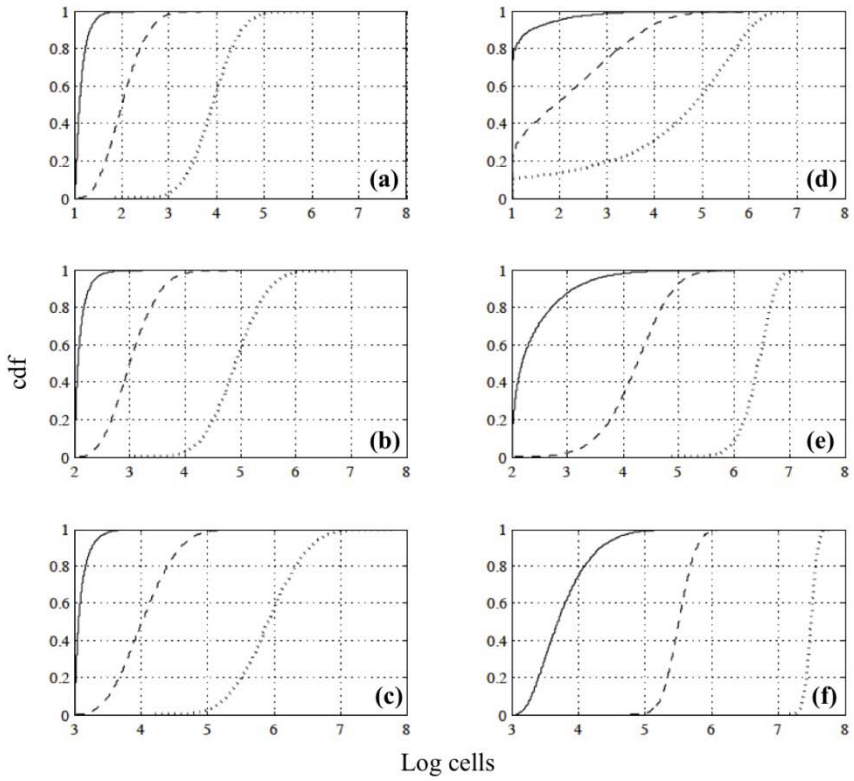

Figure 3: Cumulative distributions of *L. monocytogenes* contamination on the surface of smear soft cheese after 20 days at 14°C. Cumulative distributions obtained for a population modelling approach / IbM approach with initial contamination levels of (a/d) 10, (b/e) 100, (c/f) 1 000 cells. Solid, dashed and dotted lines are cumulative distributions obtained with a physiological parameter equal to 8, 4.5 and 0, respectively.

Conclusions

This study clearly shows the large discrepancies in the growth predictions performed when using a population approach associated with a macroscopic description of food environment in comparison to an IbM approach of the bacterial growth in foods.

Acknowledgements

R. Ferrier is the recipient of a doctoral fellowship from the French ANRT. Studies on the micro-scale description of foods were supported by CNIEL and CITPPM and studies on the individual cell growth probability were supported by a grant from INRIA.

References

Couvert O., Pinon A., Bergis H., Bourdichon F. Carlin F., Cornu M., Denis C., Gnanou Besse N., Guillier L., Jamet E., Mettler E., Stahl V., Thuault D., Zuliani V. and Augustin J.-C. (2010) Validation of a stochastic modelling approach for *Listeria monocytogenes* growth in refrigerated foods. *International Journal of Food Microbiology* 144, 236-242.

Dupont C. and Augustin J.-C. (2009) Influence of stress on single-cell lag time and growth probability for *Listeria monocytogenes* in half Fraser broth. *Applied and Environmental Microbiology* 75, 3069-3076.

Koutsoumanis K. (2008) A study on the variability in the growth limits of individual cells and its effect on the behavior of microbial populations. *International Journal of Food Microbiology* 128, 116-121.

Pin C. and Baranyi J. (2006) Kinetics of single cells: observation and modelling of a stochastic process. *Applied and Environmental Microbiology* 72, 2163-2169.

WHO (2008) Exposure assessment of microbiological hazards in food. Microbiological risk assessment series No 7. World Health Organization / Food and Agriculture Organization of the United Nations.

Single cell variability and population dynamics of *Listeria monocytogenes* and *Salmonella* Typhimurium in fresh-cut salads and their sterile liquid or solidified extracts

S.G. Manios, N. Konstantinidis, A.S. Gounadaki, P.N. Skandamis

Laboratory of Food Quality Control & Hygiene, Department of Food Science & Technology, Agricultural University of Athens (pskan@aua.gr)

Abstract

We aimed to evaluate the growth variability of *Listeria monocytogenes* and *Salmonella* Typhimurium single cells in leafy-vegetable salads, identifying potential uncertainty sources in broth-based simulations. Freshly cut lettuce and cabbage samples were inoculated with 1-4 or 1000 cells and stored at 8^{o}C. Their liquid or solidified sterile extracts were also inoculated with the above cell numbers to evaluate the behaviour of pathogens in the presence or absence of indigenous flora. Storage at 8-10^{o}C was tested to simulate marginal temperature fluctuations. A minimum of 30 independent samples were analyzed per sampling day. Population of 1000 cells increased with limited variation (SD <1 log CFU/g), as opposed to the great variability (<0.5-3 log CFU/g increase) in the growth of single cells, especially in different batches and in liquid extracts. The percentage of lettuce samples exceeding the microbiological criterion of 100 CFU/g for *L. monocytogenes* varied from 5 to 70%, depending on storage time. Cabbage did not support growth of *Salmonella*. Conversely, *L. monocytogenes* single cells did not increase in sterile cabbage extracts, whereas they increased from 1 to 3.5 logs in cabbage salad, probably due to the stimulatory effect of indigenous flora. Notably, this was not evident with high inocula. *Salmonella* showed no growth at 8°C but increased 4 logs at 10°C, illustrating the impact of boundary conditions on food safety. Results of Monte Carlo simulation of bacterial growth based on broth data overestimated growth of *L. monocytogenes* on lettuce, while it underestimated the actual increase in cabbage. The above suggest that growth simulations in risk assessment should consider the interactions of pathogens with background flora.

Keywords: *stochastic, individual, single cells modelling, variability, vegetables*

Introduction

It is well known that great variability exists in lag time and probability of growth among individual cells. This biological variability markedly impacts the dynamics of low populations, such as 1-50 cells and increases with the intensity of environmental stresses (Francois *et al*. 2006). However, the majority of challenge tests are performed with high inoculation levels, e.g. 1000 cells, in order to obtain the average behaviour of the population derived from the fastest growing cells and hence, the worst case scenario for risk assessment. Thus, in order to extrapolate the results to realistic conditions of low contamination, the variability of population numbers due to the variance of individual cell lag times also needs to be evaluated. Contrary to the extended research on individual-based modelling in laboratory media, limited information is available for the assessment of individual cell variability in foods. Considering the implication of fresh-cut salads, made of leafy greens, in various outbreaks and that the intrinsic factors of these products favour bacterial growth, we aimed: (i) to determine the variability in the growth of 2 pathogens in lettuce and cabbage at 8°C; (ii) to compare the response of individual cells with that of higher populations; (iii) to identify the contribution of the commensal flora, temperature abuse and food structure in the above variability; and (iv) to evaluate whether broth-based growth simulations may approximate the average outgrowth of a population from single cells in foods.

Materials and Methods

Bacterial strains and single cell isolation

Listeria monocytogenes Scott A (serotype 4b; epidemic strain) and *Salmonella* enterica subsp. enterica Le Minor and Poppof serovar Typhimurium (calf bowel isolate) were used. The isolation of single cells was conducted according to a modified protocol of Francois *et al*. (2003) involving 2-fold dilutions in a 8 x 12 microtitre plate, starting from an OD-counts standardized 10^3 CFU ml^{-1} suspension in the first column. The whole content of the wells of the appropriate column was used for the inoculation of the samples.

Inoculation and microbiological analysis of vegetables

Whole heads of Romaine lettuce and white cabbage were always purchased from a local retailer on the day of the study. Following removal of 4-5 outer leaves from each head, both vegetables were treated with 200 ppm chlorine for 15 min and washed with sterile water for 5 min. The dry leaves of lettuce were evenly cut into strips (*approx*. 1 cm width), while cabbage was cut using a household cabbage cutter. Portions (10 g) of each vegetable were transferred into sterile 100-ml containers, spot-inoculated with single (*approx*. 1-4) or 1000 cells of *L. monocytogenes* or *S.* Typhimurium and aerobically stored at 8^{o}C. Periodically, the pathogens were enumerated on ALOA (*L. monocytogenes*) or XLD (*S.* Typhimurium) plates. In addition, the indigenous microflora of the samples was enumerated on TSA (total viable counts), CFC (*Pseudomonas* sp.) and VRBG (Enterobacteriaceae).

Preparation and inoculation of sterile extracts

Portions of lettuce or cabbage were blended for 1 min with distilled water (1:1 ratio) and the pulp was heated for 2 hours at 80^{o}C, in order to denature the enzymes and proteins of the vegetables. The homogenate was filtered and autoclaved in 5 ml tubes (liquid extract) or after the addition of 1.5% agar (solidified extract). Both prepared media were inoculated with single or 1000 cells of *L. monocytogenes* or *S.* Typhimurium and were stored at 8 or 10^{o}C. Bacteria were enumerated on TSA plates.

Results and Discussion

Growth of single or 1000 cells on lettuce and cabbage salad

Fitting a Poisson distribution (λ=1.932) to actual measurements of cells numbers in each well of the target 2-fold dilution, we estimated that 27% of samples were inoculated with a single cell (0.1 CFU/g), whereas 95% of samples were inoculated with 1-4 cells (0.4 CFU/g) of each pathogen. Growth of 'single' cells of *Salmonella* occurred in lettuce but not in cabbage, whereas 'single' cells of *L. monocytogenes* grew in both foods. Recorded increase from single cells ranged from 1-3 log CFU/g and was always halted when the psychrotrophic background flora reached the maximum level of 10^8 and 10^9 CFU/g in cabbage and lettuce, respectively (Fig. 1). This phenomenon may be associated with the so-called 'Jameson' effect (Mellefont *et al*. 2008). Growth of the 1000 cells inoculum also ceased under the same constraints, but notably, the total log-increase was limited to 2 log CFU/g, compared to that observed for 'single' cells (Fig. 1). Competition between adjacent colonies within a population density of 1000 cells may possibly explain the latter observation. Growth of 1000 cells was less variable than growth of single cells. These results suggest that if log increase was judged only by a challenge test with high initial population, the actual risk would have been underestimated. Overall, cabbage seemed a more stressful environment than lettuce and this likely explains the higher variability in log numbers during storage (death also occurred; Figs 2 & 3).

Contribution of background flora, structure, batch and temperature to the variability of microbial responses

In general, factors which inhibited growth of pathogens, such as the type of salad, the substrate structure and the storage temperature caused marked variability in the log-increase. Such variability was more pronounce between different batches (Figs 2 & 3).

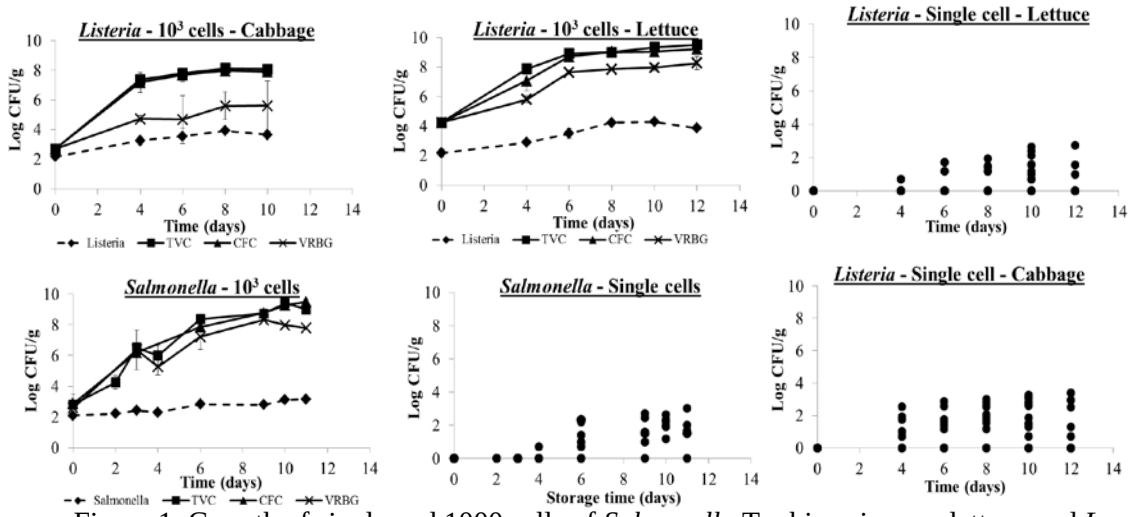

Figure 1: Growth of single and 1000 cells of *Salmonella* Typhimurium on lettuce and *L. monocytogenes* on lettuce and cabbage at 8°C.

The role of background flora was crucial for both pathogens. In particular, although *Salmonella* did not grow on cabbage, remarkable growth from single cells was observed on solidified cabbage extract (Fig.2). Notable is also the observation that growth of *L. monocytogenes* occurred only on cabbage, contrary to the complete inhibition of the bacterium in product extracts, suggesting that the increase of background flora on the surface of cut-tissue enhanced growth of the pathogen. This is a potential result of *metabiosis* (Marshal and Schmidt 1991), either due to the local increase of pH around *L. monocytogenes* cells, or due to the conversion of macro-molecules by psychrotrophs to readily available nutrients for *L. monocytogenes*. The stimulatory effects of background flora on pathogens introduce variability in microbial responses and are hardly accounted for by broth-based models. Moreover, the fact that this was evident only in growth from single cells suggests that challenge tests with high inocula would have indicated fail-dangerous trends. The structure (i.e., solid *vs.* liquid) of product extracts also influenced growth of pathogens with liquid extracts being on average more inhibitory than solid ones. A single cell of *Salmonella* could initiate growth on the surface of solid cabbage extract, but not in the corresponding juice, in which only the high inocula of 1000 cells was capable of growth initiation. It is likely that the intensity of stress factors, e.g., non-fermentable nutrients, or phenolic and acid compounds, possibly extracted from the plant tissues, is perceived by bacteria more in juices than on agar surfaces (Skandamis *et al.* 2000).

In many cases, increase in temperature from 8 to 10°C had such a pronounce effect on pathogen response that could shift cells from no growth to a growth status. If that was not the case, then marked variability was observed between batches, as some batches did support growth and some did not (Figs 2 & 3). This was more evident for *Salmonella*, due to the range of 8-10°C being close to the growth boundaries. For instance, depending on the batch, the 1000 cells inocula had 50% probability of growth at 8°C contrary to the single cells which could not initiate growth.

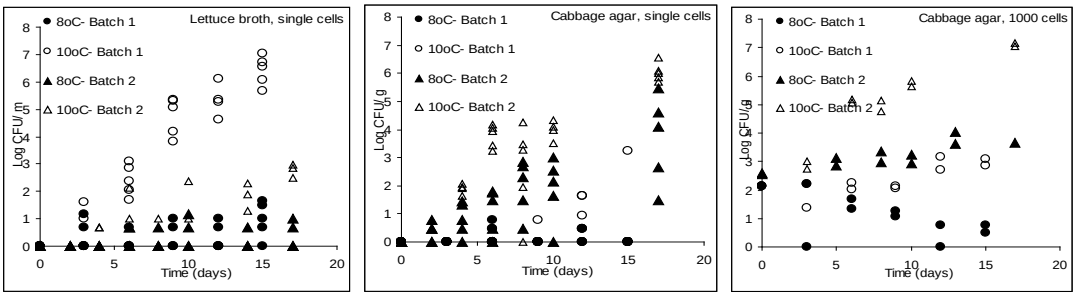

Figure 2: Growth of *Salmonella* Typhimurium on lettuce and cabbage extracts at 8 and 10°C.

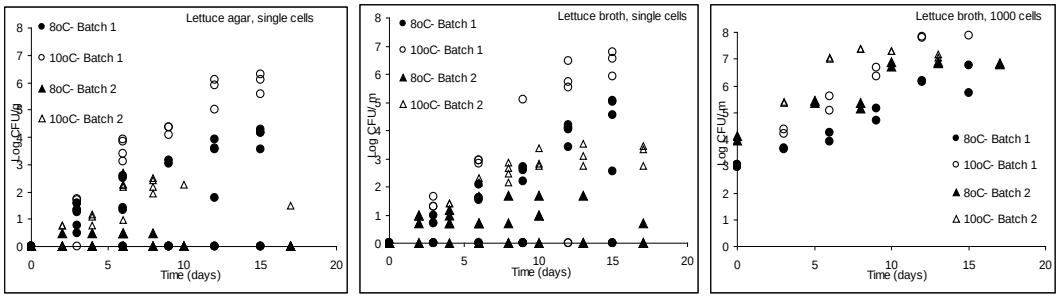

Figure 3: Growth of *L. monocytogenes* on lettuce and cabbage extracts at 8 and 10°C.

Broth-based simulation of growth on lettuce and cabbage

Considering the pH and a_w of the salads (i.e., 6.0±0.2 - 0.978±0.002 for lettuce and 5.8±0.2-0.970±0.002 for cabbage), the Weibull distributions of broth-based individual lag times by Francois *et al*. (2006), corresponding to the approximate levels of the above intrinsic factors, were used to simulate growth of *L. monocytogenes* from 'single' cells in salads. The μ_{max} estimated by the experiments with the high inoculum was used as 0.016 and 0.011 h^{-1} for growth in lettuce and cabbage, respectively. Simulations for 6 and 12 days of storage over predicted growth on lettuce but significantly under-estimated growth in cabbage (Fig. 4). This deviation is associated with the fact that growth on lettuce occurred more slowly than that predicted based on broth data due to the competitive effect of background flora, whereas on cabbage, the stimulatory effect of background flora on growth of *L. monocytogenes* was an uncertainty factor of the broth-based lag distributions, leading to fail-dangerous predictions.

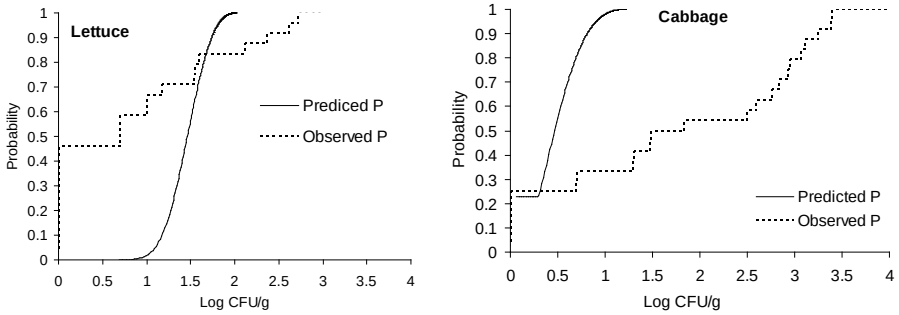

Figure 4: Predicted and observed cumulative distribution of *L. monocytogenes* on lettuce and cabbage after 12 days of storage

Conclusions

High uncertainty is expected when extrapolating broth-based simulations from single cells in foods. The stimulatory or competitive effect of background flora is more pronounce and evident only at low inocula, compared to higher levels, suggesting that challenge tests in fresh produce based on high initial bacterial numbers may underestimate the actual growth risk.

References

Francois K., Devlieghere F., Stadaert A.R., Geeraerd A.H., Van Impe J.F. and Debevere J. (2003) Modelling the individual cell lag phase. Isolating single cells: protocol development. *Letters in Applied Microbiology* 37, 26-30.

Francois K., Devlieghere, F. Standaert A.R., Geeraerd, A.H., Van Impe, J.F. and Debevere J. (2006). Effect of environmental parameters (temperature, pH and a_w) on the individual cell lag phase and generation time. *International Journal of Food Microbiology* 108, 326-335.

Marshall D.L. and Schmidt R.H. (1991) Physiological evaluation of stimulated growth of *Listeria monocytogenes* by *Pseudomonas* species in milk. *Can. J. Microbiol*. 37, 594-599.

Mellefont L.A., McMeekin T.A. and Ross T. (2008) Effect of relative inoculum concentration on *Listeria monocytogenes* growth in co-culture. *International Journal of Food Microbiology* 121, 157-168.

Skandamis P., Tsigarida I. and Nychas G-J.E. (2000) Ecophysiological attributes of *Salmonella typhimurium* in liquid culture and within gelatin gel with or without the addition of oregano essential oil. *World Journal of Microbiology and Biotechnology* 16, 31-35.

A simple individual-based model to explore the spatial competition between *Listeria monocytogenes* and *Lactococcus lactis* in mixed-species biofilms with constant renewal of nutrients

L. Guillier[1], O. Habimana[2], R. Briandet[2]

[1] Agence nationale de sécurité sanitaire (Anses), Laboratoire de sécurité des aliments, 23 avenue du Général de Gaulle, F-94700 Maisons-Alfort, France (laurent.guillier@anses.fr)
[2] INRA/AgroParisTech, UMR 1319 MICALIS, 25 avenue de la République, F-91300 Massy, France (romain.briandet@jouy.inra.fr)

Abstract

The objective of this work was to reconstruct spatial heterogeneities based on observations made from growth and spatial localisation of *Listeria monocytogenes* and *Lactococcus lactis*, in dual-species biofilms under constant nutrient renewal, using an individual-based model (IBM). The dynamics of biofilm formation of *L. monocytogenes* and *L. lactis*, in mono- and dual-species biofilms was first studied by performing cell counts at different growth intervals in mono-species as well as mixed-species biofilms. Then, for localization inside mixed biofilms, *L. monocytogenes* cells were tagged with green fluorescent protein and the dynamics of biofilm growth in mixed biofilms in the presence of *L. lactis* were investigated by the use of confocal laser scanning microscopy (CLSM). The proposed IBM simulates bacterial cell growth in a three dimensional space. It uses few parameters that can be easily estimated from broth experiments and for which variability is taken into account. It also uses a small number of properties compared to other IBMs. Experimental data obtained from cell-count enumeration and *in-situ* time course CLSM observations in mono- and dual-species flow- cell grown biofilms, were compared with simulated data. We successfully reconstructed the spatial competition heterogeneities of individual cells constituting a dual-species biofilms and predicted cell counts results. *Listeria* cells at the bottom layers of the biofilm are literally "smothered" by their competitor and are forced into a survival lifestyle, rather than into a proliferation or colonization lifestyles. This competition takes place at the initial phases of biofilm formation. *L. lactis* had shorter generation time and lag time compared to *L. monocytogenes*. These parameters lead to the competitive advantage of *L. lactis* towards *L. monocytogenes* in our experimental setup.

Keywords: *biofilm, spatial competition, individual based model, dynamic flow conditions*

Introduction

L. monocytogenes cells are well equipped to adhere, form biofilms and persist on food processing surfaces. Surfaces of industrial settings host resident biofilms that likely interact with *L. monocytogenes* attachment, growth and survival (Carpentier and Cerf 2011). In fermented food processing, resident biofilms can host technological flora such as lactic acid bacteria. Biofilms of *Lactococcus lactis* have been shown to be efficient in controlling the development of *L. monocytogenes* through competitive exclusion, synthesis of bacteriocins, as well as inhibition of initial settlement (Habimana *et al.* 2009). All these studies, describing *L. monocytogenes* biofilms interactions, were conducted under static conditions, and little is known about the behaviour of *L. monocytogenes* in mixed-species communities under flow conditions, where fresh medium is constantly renewed above the biofilm.

The use of modelling tools has helped to better understand bacterial interactions inside biofilms. In recent years, individual based models (IBM) have proven invaluable for studying the behaviour of single bacterial cells in mixed-species communities (e.g. Ferrer *et al.* 2008). Besides predicting biofilm structure, data provided by IBM can be rendered as a three dimensional spatial representation of a given biofilm population and can also simulate emerging patterns from interactions between individuals from two to several other populations.

The present study aims to investigate the interactions between *L. monocytogenes* and a competitive host resident model strain, *L. lactis*, during the initial stages of biofilm formation under constant renewal of nutrients.

Materials and Methods

Continuous flow-biofilm experiments

The *L. lactis* MG1363, *L. monocytogenes* EGDe and LO28 strains were used in this study. Biofilms were cultivated at 25°C in disposable three-channel flowcells (Stovall®) with individual channel dimensions of 1 x 4 x 40 mm and a glass coverslip substratum. BHI broth medium supplemented with glucose (0.5%) was continuously pumped through flowcell channels at a rate of 1.5 ml/hour. To initiate biofilm growth, the flow of medium was stopped and the flow-chambers were inoculated by injecting lactococcal and/or *L. monocytogenes* cells into each flow channel using a small syringe. No flow conditions were maintained for 1h after inoculation to allow bacteria to attach. After this time, the flow was resumed and the bacteria were cultivated in the flow cell at 25°C. Biofilms were subsequently analyzed after 0h, 24h, 48h, and 72 h.

In-situ time course Confocal Laser Microscopy (CLSM)

Biofilm growth development was visualized *in-situ* by means of confocal microscopy laser-scanning microscopy. Stacks of horizontal plane images were acquired using a Leica SP2 AOBS CLSM (Leica Microsystems, France) equipped with a 488-nm argon laser and a 633-nm He-Ne laser at the MIMA2 microscopy platform (http://voxel.jouy.inra.fr/mima2). For localization inside mono- and dual-species biofilms, GFP-tagged *L. monocytogenes* strains carrying pNF8 plasmid were employed during experiments.

A new simplified spatial individual-based model (IBM)

The proposed spatial IBM simulates the behaviour of bacterial cells in a three dimensional space. This space has the following size (length, width, height): 1000 by 1000 by 50µm. We assumed that *L. monocytogenes* and *L. lactis* cells are of the same size. They were both represented as cubes of 1 μm^3 in this model. At time *t*, each cell was characterized by two state variables: the first being its position in the three dimensional area, and the second, its generation time. We considered that bacterial cells were immotile and that there was no passive attachment and reattachment of cells onto the substratum. Time was discretized in constant 5 minutes steps. At t_0, N_0 cells were randomly positioned on the bottom plane of the x-y-z space. For each time step, sequential processes were performed based on the generation time for each individual cell. When generation time was reached, the 'mother' cell kept its position while the 'daughter' cell was randomly placed at any of the eight possible available positions on the same x-y plane next to the 'mother' cell. In the event of no available positions on the x-y plane, the 'daughter' cell was then randomly placed at any of the nine possible available positions on the upper x-y plane. An individual cell was considered as non-growing, when found to be unable to divide onto an upper x-y plane.

Doubling times (DT) of cells were considered to be variable within a population and were derived from values of lag time and growth rate obtained for planktonic cells in BHI. For the first generation (DT_0, i.e. lag time), DT_0 of *L. monocytogenes* cells were estimated from lag time in broth according to models of Guillier and Augustin (Guillier and Augustin 2006). For the following generations, the DT of both populations were derived from growth rate values obtained in broth. We considered that DT followed of normal distribution of mean $\ln(2)/\mu_{max}$ and a standard deviation of 10% of the mean as previous studies observed a coefficient of variation of DT close to 10% (e.g. Pin *et al.* 2006). The same parameters were used for the two *L. monocytogenes* strains.

The results of the spatial IBM can be presented either as a classical kinetic growth curve, obtained by summing the cells of each population present at different times or as a three dimensional representation of a biofilm at a chosen time point. This model was implemented in Matlab 6.5 (The MathWorks Inc., Natick, MA, USA).

Table 1: Parameters used in the spatial individual based model.

Parameters	*Listeria monocytogenes*	*Lactococcus lactis*	Units
First doubling time	Extreme ValueIIb (-4.75,7.98)	Uniform (0,74)	minutes
Doubling times	Normal (114,11.4)	Normal (74, 7.4)	minutes
N0	3000	5000	cells

Results and Discussion

Observed and predicted spatial development of biofilms

Mixed inoculation of auto-fluorescent *Listeria* strains and non-fluorescent *L. lactis* strains allowed the visualization of the spatial localization of the pathogen inside mixed-species biofilms. *L. monocytogenes* in mixed-species biofilms was spatialized exclusively at the base of the biofilm, in contact with the substratum (Figure 1).

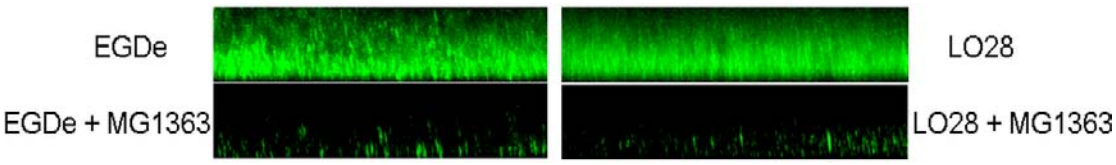

Figure 1. Spatial distribution of GFP tagged *L. monocytogenes* in the absence or presence of *L. lactis* MG 1363 after 72 hours growth represented by vertical sections in the xz- plane (the lower side of the section corresponds to the substratum).

The spatial development of *L. monocytogenes* in the presence of *L. lactis* in dual-species biofilms predicted by the IBM is presented on Figure 2. The competitive nature between *L. monocytogenes* and *L. lactis* best fits a 'spatial' competition type of interaction, governed mainly by the access of available nutrients. *Listeria* cells that find themselves at the bottom layers of the biofilm are literally 'smothered' by their competitor and are forced into a survival lifestyle. This type of competition takes place at the initial phases of biofilm formation, where growth parameters of the different strains in competition will determine which strain will have the upper hand.

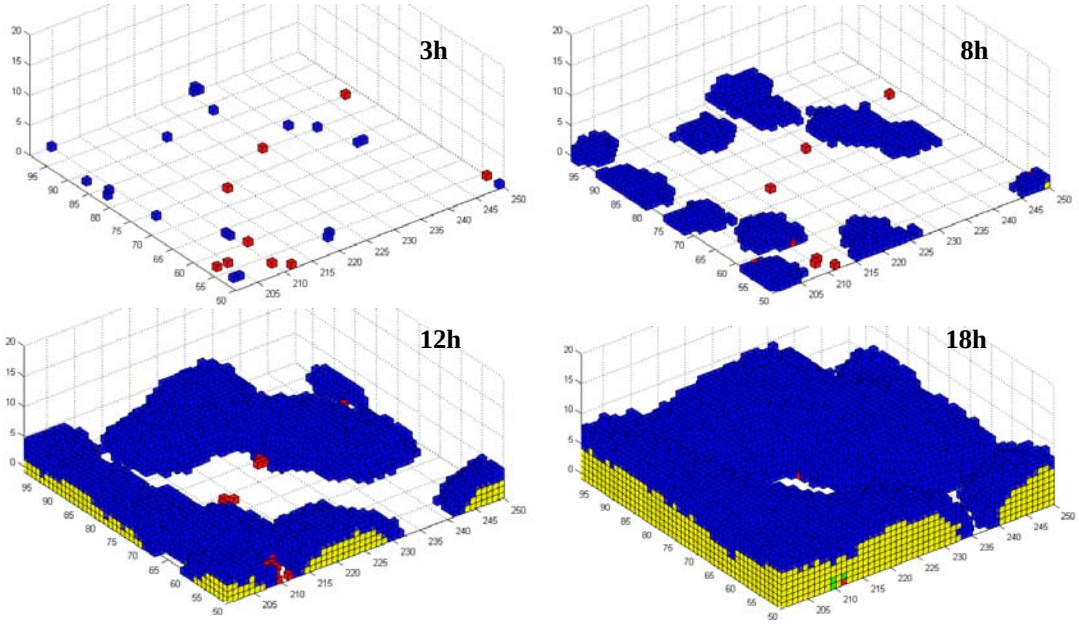

Figure 2: Fragment of spatial biofilm simulated with IBM. Growing and non-growing L. *monocytogenes* cells are represented as ■ and ■ cubes respectfully, while growing and non-growing L. lactis cells are represented as ■ and ■ cubes respectfully.

Observed and predicted growth developments

The predicted and measured growth counts of *L. monocytogenes* strains in mono-species biofilms or, in the presence of *L. lactis* are presented in Figure 3. In mixed-species biofilms, *L. monocytogenes* cells were greatly inhibited by the presence of *L. lactis*. For both strains observed cell counts were lower or equal to inoculum levels (Figure 3). Compared to measured values of *L. monocytogenes*, the spatial IBM predicted a population increase of about 1 $\log_{10}$. Probable reasons could be that our model did not take into account bacterial death that can occur inside microbial colonies (Theys *et al.* 2009).

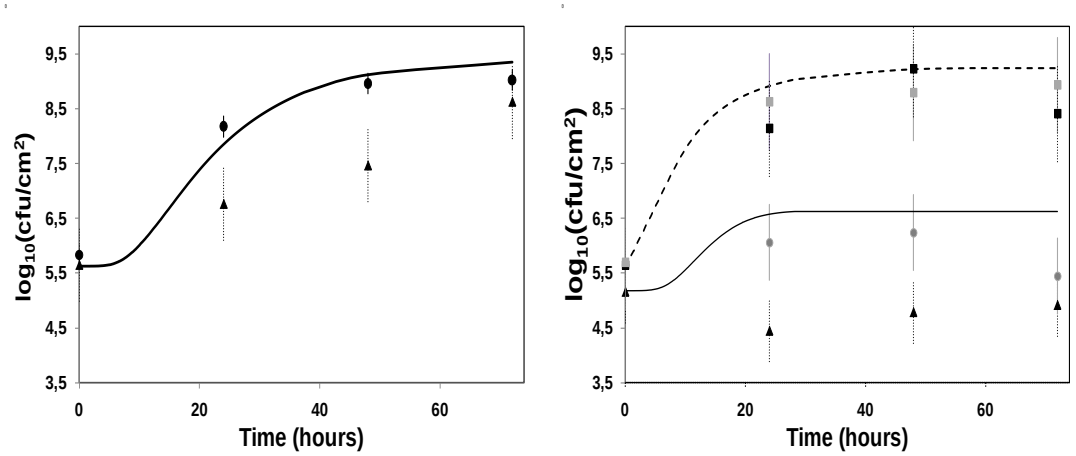

Figure 3: (A) Measured growth of *L. monocytogenes* EGDe (▲) and LO28 (●) in mono-species biofilms. (B) Mixed-species biofilms composed of *L. lactis* (■) with EGDe (▲) or of *L. lactis* (■) with LO28 (●). Error bars represent 95% CI of bacterial counts. (–) *L. monocytogenes* and (--) *L. lactis* growth as predicted by the spatial individual based model.

Conclusions

By using a very simple IBM, we were able to demonstrate that the initial disparity in generation times between *L. monocytogenes* and *L. lactis* most likely explains the observed species spatialization inside dual-species biofilms, and hence the growth inhibition of the pathogen.

Acknowledgements

Olivier Habimana was the recipient of a fellowship from LABHEALTH, under the Marie Curie contract MEST-CT-2004-514428. We also thank the 'Département de l'Essonnes' for its financial support for the CLSM microscope (ASTRE n°A02137).

References

Carpentier B. and Cerf O. (2011) Review — Persistence of *Listeria monocytogenes* in food industry equipment and premises. *International Journal of Food Microbiology* 145, 1-8.

Ferrer J., Prats C. and Lopez D. (2008) Individual-based modelling: an essential tool for microbiology. *Journal of Biological Physics* 34, 19-37.

Guillier L. and Augustin J.-C. (2006) Modelling the individual cell lag time distributions of *Listeria monocytogenes* as a function of the physiological state and the growth conditions. *International Journal of Food Microbiology* 111, 241-251.

Habimana O., Meyrand M., Meylheuc T., Kulakauskas S. and Briandet R. (2009) Genetic features of resident biofilms determine attachment of *Listeria monocytogenes*. *Applied and Environmental Microbiology* 75, 7814-7821.

Pin C. and Baranyi J. (2006) Kinetics of single cells: observation and modeling of a stochastic process. *Applied and Environmental Microbiology* 72, 2163-2169.

Theys T.E., Geeraerd A.H., Devlieghere F. and Van Impe J.F. (2009) Extracting information on the evolution of living- and dead-cell fractions of *Salmonella* Typhimurium colonies in gelatin gels based on microscopic images and plate-count data. *Letters in Applied Microbiology* 49, 39-45.

Effect of the variability in the growth limits of individual cells on the lag phase of microbial populations

J. Aguirre, K. Koutsoumanis

Laboratory of Food Microbiology and Hygiene, Department of Food Science and Technology, School of Agriculture, Aristotle University of Thessaloniki, Thessaloniki 54124, Greece. (juaguirr@vet.ucm.es; kkoutsou@agro.auth.gr)

Abstract

The water activity (a_w) growth limits of *Listeria monocytogenes* individual cells were studied based on the method used by Koutsoumanis (2008). The results showed that the a_w limits are a distribution varying from 0.937 to 0.997. In addition, the growth kinetics of *L. monocytogenes* on tryptone soy agar with a_w adjusted to values ranging from 0.997 to 0.940 was monitored. The growth data were fitted to the model of Baranyi and Roberts for the estimation of the "apparent lag". In order to estimate the "physiological lag" of the growing fraction of the inoculum, the growth data were refitted to the model using as initial population level the number of cells that were able to grow and excluding the rest of the data during the lag. The results showed that for a_w values ranging from 0.997 to 0.970 there was no difference between apparent and physiological lag. As the a_w decreased from 0.970 to 0.940, however, the above difference increased significantly due to the increase of the ratio between non-growing and growing cells. For the lower a_w tested (0.940), the apparent and physiological lag were 23.2 and 10.1 h, respectively. In contrast to the apparent lag, a linear relation between physiological lag and a_w was observed. Furthermore, the physiological state (h_0) of the growing fraction of the inoculum was found to be independent by the growth environment (i.e a_w). The data presented in this work show that the variability in the growth limits of individual cells can lead to a better understanding of the microbial behavior at conditions close to the boundary of growth, and stress the need for stochastic approaches in predictive microbiology.

Keywords: Listeria monocytogenes, growth limits, individual cells

Introduction

Since the 1980s predictive microbiology has focused on the development of deterministic primary models to predict microbial behavior in foods as a function of storage time (growth and survival) and treatment time (inactivation). However, deterministic models are not effective in describing the behavior of small microbial populations since they ignore the variability among individual cells (Baranyi 1998). Considering that, in practice, contamination of foods with pathogens occurs at very low levels, it is becoming clear that the behavior of single cells should be taken into account through stochastic modelling approaches (Pin and Baranyi 2006). The importance of stochastic models which are able to deal with more "realistic" contamination events has been further increased after the recognition of risk assessment as the main tool in food safety management.

In contrast to the increased number of studies on the lag and generation time of individual microbial cells, not many data are available on the growth limits of single cells. In recent years, however, the need for studying and modelling microbial growth limits has been increasingly recognized. Prediction of limits for pathogen growth can lead to accurate description of the conditions which can be applied to control a process or specify the product formulation for safer food production. Thus, data and information on the growth limits of pathogens at a single-cell level would be of great importance.

Based on the observed variability of single-cell lag, and considering that the limit of growth for a microbial cell can be identified to a certain level of an environmental factor where lag becomes infinite, variability of the growth limits of individual cells would also be expected. The latter is supported by the findings of several studies which demonstrated that an increase

in the inoculum size of microbial populations results to a shift in the position of the growth boundary to more extreme inhibitory conditions. Koutsoumanis and Sofos (2005), attempting to explain the effect of inoculum size on the growth limits of *Listeria monocytogenes* populations, stated that as in the case of lag times, growth limits of individual cells in microbial populations should be better described by distributions rather than being uniform. This was confirmed by Koutsoumanis (2008) who described quantitatively the a_w limits of Salmonella.

The aim of this work was to study the a_w growth limits of individual *L. monocytogenes* cells and to evaluate the effect of growth limit variability on the lag phase of microbial populations.

Materials and Methods

A *L. monocytogenes* strain, serotype 1/2a, was used in this study, kindly provided by Dr. Martin Wiedmann (Cornell University, Ithaca, NY, USA). The water activity (a_w) growth limits of individual *L. monocytogenes* cells at 30 ^oC and pH 7.3 were studied based on the method used by Koutsoumanis (2008). About 200 cells of the pathogen were inoculated on tryptone soy agar plates with a_w adjusted to values ranging from 0.997 to 0.937 After inoculation plates were covered with Parafilm to avoid dehydration and stored at 30 ^oC in high-precision temperature incubators. The distribution of a_w growth limits of individual cells was estimated from the ratio between the average number of colonies formed at each a_w increment and the average number of cells initially inoculated, based on the assumption that each colony was derived from a single cell. The inoculum size was estimated based on the number of colonies formed on agar plates with optimum conditions (a_w=0.997). In addition, the growth kinetics of the pathogen on tryptone soy agar with a_w adjusted to values ranging from 0.997 to 0.940 was monitored at 30 ^oC. The growth data were fitted to the model of Baranyi and Roberts (1994) for the estimation of the kinetic parameters. The growth curves in combination with the identification of the growing fraction of the population at each a_w condition allowed for the calculation of the apparent and the physiological lag. Additional replicate experiments are still in progress.

Results and Discussion

The cumulative distribution of the water activity (a_w) growth limits of individual *L. monocytogenes* cells is presented in Fig. 1. As it is shown, the a_w limits varied from 0.937 to 0.997. The observed variability in the growth limits of individual cells indicates that as the a_w conditions approach the boundary of growth an increasing number of cells in the population are not able to grow. The presence of this non-growing fraction results in an additional lag of the population, which we have called “pseudo-lag” (Koutsoumanis 2008). Consequently, at conditions close to the boundary of growth the total apparent lag of the population is the sum of the pseudo-lag and the physiological lag of the growing cells.

The objective of the present study was to estimate the apparent lag, the physiological lag and the pseudo-lag as affected by the growth environment. For this, the growth kinetics of *L. monocytogenes* on tryptone soy agar with a_w adjusted to values ranging from 0.997 to 0.940 was monitored.

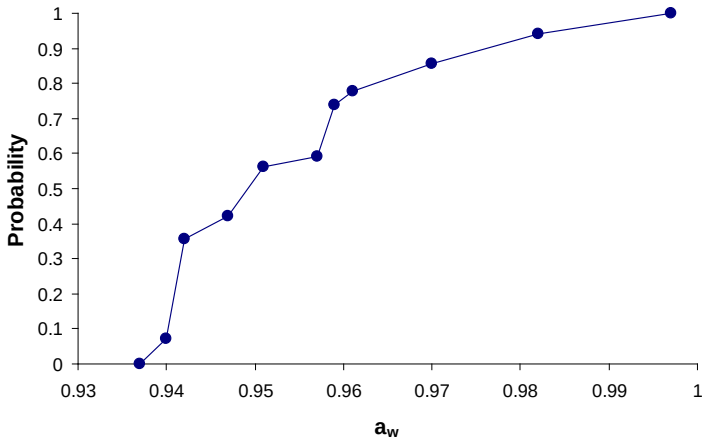

Figure 1: Cumulative distribution of the water activity (a_w) growth limits of *L. monocytogenes* individual cells

The growth data were fitted to the model of Baranyi and Roberts (1994) for the estimation of the apparent lag. In order to estimate the physiological lag of the growing fraction of the inoculum, the growth data were refitted to the model using as initial population level the number of cells that were able to grow and excluding the rest of the data during the lag (Fig. 2). The number of cells that were able to grow was estimated based on the colonies formed on the agar plates at the end of storage period. The pseudo-lag was estimated from the difference between the apparent and physiological lag.

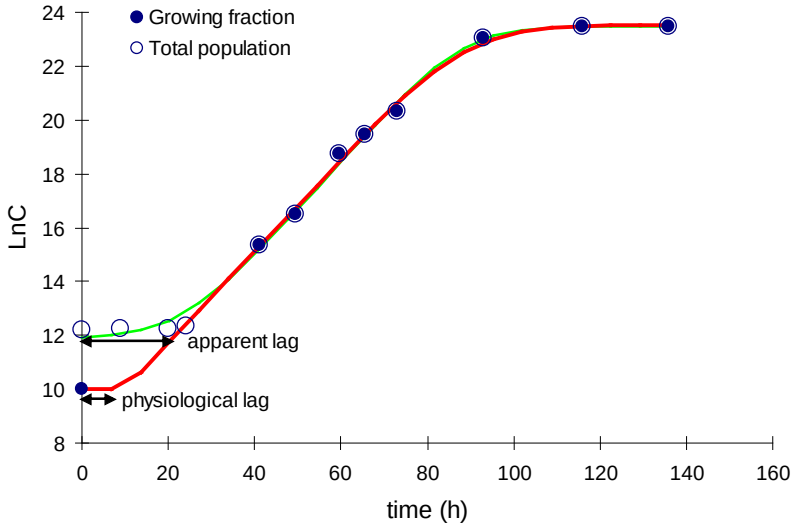

Figure 2: Fitting of the total population and the growing fraction of *L. monocytogenes* to the Baranyi and Roberts model and calculation of the apparent and physiological lag.

The effect of a_w on the apparent lag, the physiological lag and the pseudo-lag is presented in Fig. 3. The results showed that for a_w values ranging from 0.997 to 0.970 there was no difference between apparent and physiological lag. As the a_w decreased from 0.970 to 0.940, however, the above difference increased significantly. For example, for the lower a_w tested (0.940) the apparent and physiological lag was 23.2 and 10.1 h, respectively. In contrast to the apparent lag, a linear relation between physiological lag and a_w was observed. As shown in Fig. 3, the non-linearity of the apparent lag can be attributed to the increasing pseudo-lag as the a_w approaches the boundary of growth which is a result of the increasing number of cells that are not able to grow. Furthermore, the physiological state (h_0) of the growing fraction of

the inoculum was found to be independent of the growth environment (i.e a_w). The above results indicate that the use of models for the apparent lag developed using high inoculum levels can lead to significant underpredictions of the lag and be fail-dangerous when applied for low inoculum levels.

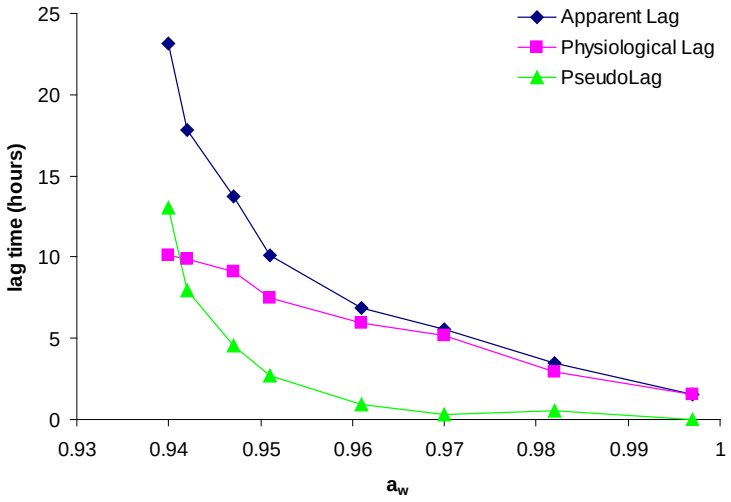

Figure 3: Effect of aw on the apparent lag, physiological lag and pseudo-lag of *L. monocytogenes*

Conclusions

The water activity growth limits of individual *L. monocytogenes* individual cells vary significantly. This variability results in an increasing number of cells in the population which are not able to grow as the a_w conditions approach the boundary of growth. At conditions close to the boundary of growth the total apparent lag of the population is the sum of the pseudo-lag and the physiological lag of the growing cells. For a_w values ranging from 0.997 to 0.970 there was no difference between apparent and physiological lag but as the a_w decreased from 0.970 to 0.940 the above difference increased significantly. The data presented in this work show that the variability in the growth limits of individual cells can lead to a better understanding of the microbial behavior at conditions close to the boundary of growth, and stress the need for stochastic approaches in predictive microbiology.

Acknowledgements

This research was in part supported by the General Secretarial for Research and Technology, Greek Ministry of Education (Synergasia, 09ΣΥΝ-22-977) and by the EU Framework VI programme on Food Quality and Safety, ProSafeBeef "Food-CT-2006-36241".

References

Baranyi J. (1998) Comparison of stochastic and deterministic concepts of bacterial lag. *Journal of Theoretical Biology* 192, 403-408.

Baranyi J. and Roberts T.A. (1994) A dynamic approach to predicting bacterial growth in food. *International Journal of Food Microbiology* 23, 277-294.

Koutsoumanis K. and Sofos J.N. (2005) Effect of inoculum size on the combined temperature, pH and a_w limits for growth of *Listeria monocytogenes*. *International Journal of Food Microbiology* 104, 83-91.

Koutsoumanis K. (2008) A study on the variability in the growth limits of individual cells and its effect on the behavior of microbial populations. *International Journal of Food Microbiology*, 128, 116-121.

Pin C. and Baranyi J. (2006) Kinetics of single cells: observation and modeling of a stochastic process. *Applied and Environmental Microbiology* 72, 2163-2169.

How can we make the best use of predictive microbiology (PM) data and models in food safety risk assessments?

David Vose

Vose Software BVBA, Iepenstraat 98, 9000 Gent, Belgium

Food safety risk assessment

Food safety risk assessment is the analytical component of food safety risk management. It attempts to quantify the risk and uncertainty in a food safety-related problem to give managers a better understanding of the impact of the different decision options they have available. In order to provide a quantitative risk assessment we need a mathematical model that will be a *simplified* representation of how the system is *assumed* to behave both now and after any interventions under consideration. *Simplified* implies that our probability values are approximate, and *assumed* implies that the numbers generated would only be true if the list of assumptions all turned out to be correct. The more numerous and tentative the assumptions are, the less useful the numerical results will be, and often we have no good way of estimating the level of inaccuracy we are introducing by making assumptions. Then we have to add statistical uncertainty of the parameter estimates. From a risk assessor's perspective, data quality translates into how few assumptions one has to make in using a data set, and how little statistical uncertainty it adds to the assessment.

Designing a risk assessment and selecting PM data and models

The design of a risk assessment model is, or at least should be, quite a creative process. The risk assessor should look at the questions being asked by the risk managers, the scope of a model that might be able to answer those questions, the data available that would populate the model, how robust the assumptions would be, what could be put together within the timeframe and budget, whether there are sufficient in-house skills to be able to write the model, and whether it will be mathematically tractable.

I describe below two variations of the most common type of population-based food safety risk assessment model, the difficulties we face as modellers in using PM data is these models, and how the PM community could help make our models better. I acknowledge that there are plenty of other food safety-related areas in which PM can be used, for example in evaluating detection sampling plans or determining shelf-life.

Simulation farm-to-fork models

These models focus on a particular food animal species and a specific pathogen. The models attempt to represent the microbial load on a unit and the prevalence of contamination in a continuum beginning with the production of the animal at the farm, through slaughtering, processing of the meat, storage and handling in the retail, commercial restaurant and domestic settings, leading to an estimate of how often people in a population are exposed to the pathogen from this food type and how much they ingest. If we have some estimate of the dose-response relationship (the probability of infection or illness given a specific number of organisms ingested) we can end with an estimate the risk to the consuming population. A schematic of a typical model for Campylobacter in chicken is shown in Figure 1. Models for other food types that tend to remain as a single unit from production to consumption, like whole eggs or shellfish, have fewer components.

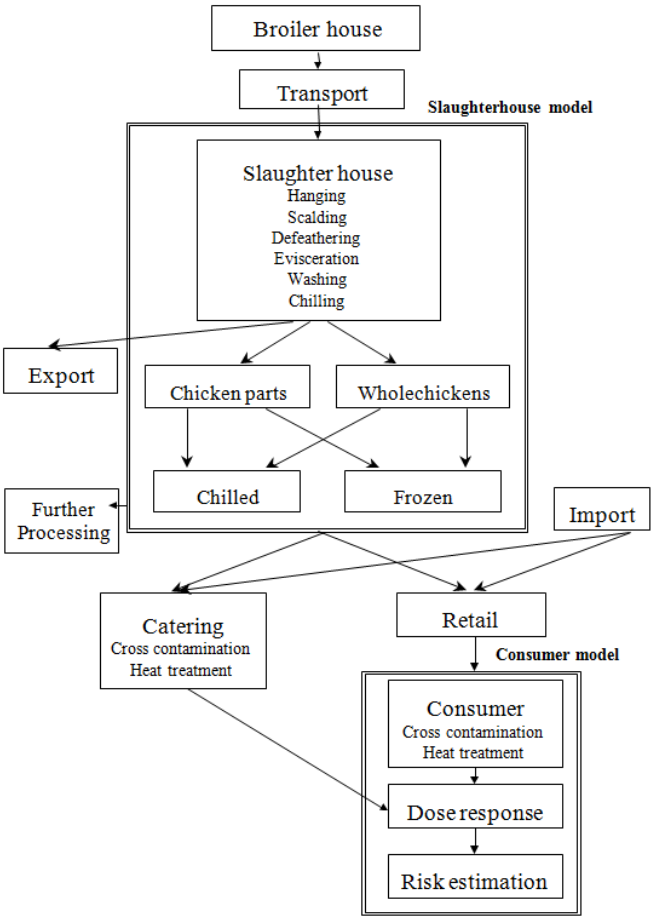

Figure 1: Schematic of a typical farm-to-fork risk assessment model (from Christensen *et al.*2001).

In order to make such a model one has to pare it down to the most essential components, which means trying to constrain the model to those pathogen strains and exposure routes that represent the greatest risk, including at a minimum those processes for which risk management decisions need to be made and modelling only the most common types of systems. The biggest problem a farm-to-fork model faces is the heterogeneity of the system. In reality, a system like that depicted in Figure 1 will vary greatly in size and style of operating between farms, slaughter and processing plants, food products and consumer behaviour. On top of it all is the heterogeneity of the bacterial populations.

Moment-based models

In 2010, we produced a *Campylobacter* food safety risk assessment model for EFSA that took a different mathematical approach to farm-to-fork risk assessment. The task was to develop a risk assessment model with a farm-to-fork scope that could be applied to any EU Member State provided there were data available for that Member State. The model was asked to address the effect of a wide number of interventions. The unique aspect of the problem was that the model needed to be anchored to the very large and harmonized EFSA baseline survey data related to microbial load and prevalence of *Campylobacter* at the post-chilling stage of poultry meat production, as well as anchoring to the observed illness rates in Member States. The usual Monte Carlo simulation methods used in farm-to-fork risk assessment simulate a

process from the farm onwards and are unable to anchor to observations further along the farm-to-fork continuum.

If a food item has a microbial log-load defined by some distribution A and an intervention is being considered that reduces the load by B logs, where B follows a distribution, then one can estimate the raw moments of the remaining load $Z = A - B$ using standard equations. The equation are also reversible so if we have data to estimate the log load Z after the intervention and we have data to estimate the log reduction effect of the intervention, then the moments of the original log load A before the intervention can be estimated.

Data limitations

Aside from essentially having to ignore heterogeneity, farm-to-fork models are hampered by lack of data. The data we have are usually at only a few points in the whole system. There are a number of areas that an improvement of reporting of PM models and data can be very helpful:

Log load reduction for interventions

For interventions that reduce the number of viable bacteria on a food product or carcass, experiments usually quote the mean and variance (or standard deviation) of log load before and after the intervention under a certain condition (temperature, pH, time, etc), so risk assessors have to interpret the information using a Normal distribution for the log load which could easily under- or over-estimate the tails of the distribution. The data are also often reported for pooled samples which are not useful for modelling load. Ideally, PM results would make the raw data readily available to the risk assessment community because this allows us to completely specify the distribution of change with attendant statistical uncertainty. At a minimum, quoting the skewness of the data would allow a more precise modelling of the load.

A common assumption is that the log reduction that would be achieved is independent of (i.e. not correlated with) the initial log load. A related assumption is that the load in samples is representative of the whole food item or carcass. This is equivalent to saying that every bacterium present on the food item has the same probability of being attenuated by the intervention (or detected). It would be helpful to have data that allow us to support or refute this assumption.

Changing prevalence

An intervention may have an impact on the between/within flock/herd/batch prevalence. PM can help us evaluate the impact of within batch prevalence, e.g. what the effect would be of a change in processing on the fraction of a food product that would be contaminated. In risk assessment we are interested in the fraction of food items that are contaminated (true prevalence), not the fraction of food items that test positive (apparent prevalence). We can *only* be reasonably comfortable about using apparent prevalence as a surrogate for true prevalence provided that:

- Statistically a lot more bacteria are required to cause infection than the test threshold ;
- Bacteria are quite homogeneously distributed in the food item being tested; *and*
- The bacteria are very unlikely to multiply between the point of testing and the exposure event that could cause human illness.

It is rare that all three conditions will be met, so we need to make a correction between apparent prevalence and true prevalence, which requires some statistical modelling that requires knowing the method of sampling, the distribution of microbial load in contaminated items and the performance of the test itself.

Summary

Precise PM data are of great value in manufacturing processes to optimise the quality and shelf-life of food products where the system is highly controllable and homogeneous. By contrast, food safety risk assessments attempt to model a highly variable and uncertain system so our PM data needs are different. We need:

- Access to raw data or, at least, more comprehensive statistical descriptions of PM studies;
- Corrections for detection thresholds and true prevalence estimates;
- Analysis of whether log load increase or reduction are functions of the initial load;
- Help with understanding how to translate the estimated load in a sample into the load on the food item as a whole, including sometimes the location of the pathogen;
- Help with being able to make simple models for mixed pathogenic populations;
- Help with rational arguments for determining how we can simplify our models without greatly reducing their accuracy.

References

Christensen B., Sommer H., Rosenquist H. and Nielsen N. (2001) Risk Assessment on *Campylobacter jejuni* : In Chicken Products First Edition. The Danish Veterinary and Food Administration, Institute Of Food Safety and Toxicology, Division of Microbiological Safety.

General risk assessment for *Salmonella* in formulated dry foods

D.W. Schaffner

Food Science Department, 65 Dudley Road, School of Environmental and Biological Sciences, Rutgers University, New Brunswick, NJ 08901 USA. (schaffner@aesop.rutgers.edu)

Abstract

Recent U.S. *Salmonella* outbreaks and recalls, including the Peanut Butter Corporation of America outbreak, the Plainview non-fat dry milk recall, and the Basic Food Flavors hydrolyzed vegetable protein recall have highlighted the importance of controlling *Salmonella* in Formulated Dry Foods. This risk assessment was undertaken to assist food companies in managing the risks associated with formulated dry food products that do not support the growth of *Salmonella*. Specific model components include: serving size, weight of contaminated ingredient per serving, *Salmonella* cells per gram, the effect of negative test results on *Salmonella* prevalence, the effect of thermal processing on *Salmonella* in the dry state and the effect on storage time on *Salmonella* survival. A component of the model was also created to use the effect of environmental sampling test results to predict finished product risk. Estimated number of illnesses resulting from contaminated servings was calculated using the FAO/WHO beta-Poisson dose-response model for *Salmonella*. The risk model was developed using the Microsoft Excel add-in, @Risk (Palisade Corporation, Ithaca, NY). Results show that even when foods are contaminated with very low levels of *Salmonella*, when millions of servings are simulated, hundreds or thousands of illnesses are predicted to result. Product manufactured with significantly (~1 year) older ingredients represent a measureable lower risk due to *Salmonella* die-off during storage. When hundreds of negative test results are obtained, the predicted risk is lower. Finally, when low water-activity foods are processed, *Salmonella* survival may present a significant risk unless very high temperatures and long times are used.

Keywords: Salmonella, *risk assessment, water activity, survival modeling*

Introduction

Recent U.S. *Salmonella* outbreaks and recalls, including the Peanut Butter Corporation of America outbreak, the Plainview non-fat dry milk recall, and the Basic Food Flavors hydrolyzed vegetable protein recall have highlighted the importance of controlling *Salmonella* in Formulated Dry Foods.

This paper was inspired by a series of risk assessments undertaken to assist food companies in managing the risks associated with formulated dry food products that do not support the growth of *Salmonella*.

Materials and Methods

Surface sanitation indicator data was provided in the form of a Microsoft Excel file. One years worth of data from a single food processing plant location, containing ~5700 data points was analysed. Data were extracted from Excel, and converted to a format suitable for import into Microsoft Access. Access was used to extract and query the dataset, with subsequent analysis done in Excel.

D-values for *Salmonella* were based on data provided in the "Annex to Control of *Salmonella* in Low-Moisture Foods", published by GMA on February 4, 2009, specifically the data from Dega *et al.* (1972) – Table A-4 of the GMA report and McDonough and Hargrove (1968) – Table A-5 of the GMA report. Data were extracted from these tables and used to construct a mathematical model.

These models were combined with other information including assumed *Salmonella* prevalence and concentration to construct a microbial risk assessment using the @risk add-in for Microsoft Excel.

Results and Discussion

Surface sanitation indicators

Table 1 below shows surface contamination data taken from a single food processing plant in one year. These data show the degree of correlation between indicator (Enterobacteriaceae) counts and *Salmonella* prevalence.

Table 1: Summary of surface sampling for pathogens and indicators.

	Enterobacteriaceae				
Salmonella	Absent	<100	>=100	TNTC	Total
Absent	4400	1000	40	200	5640
Present	10	15	2	25	52
Total	4410	1015	42	225	5692

Table 2 shows an example calculation that can be performed with this data, using the concept of odds-ratio, common in epidemiology. The first line shows the odds of *Salmonella* occurring (simply total *Salmonella* positives divided by the total samples tested). The next line shows a similar calculation where it's the odds of a very high Enterobacteriaceae (EB) count occurring. The third line combines these two probabilities to estimate the theoretical odds of the joint occurrence, while the last line shows the actual odds based on the table above. It's clear that the actual odds are much higher (by about 10 times).

Table 2: Odds ratios for pathogen and indicator occurrence.

Odds of *Salmonella* occurring	52/5692	0.90%
Odds of EB occurring at TNTC	225/5692	4.00%
Calculated odds together	0.9*4.0	0.04%
Actual odds together	24/5692	0.44%

Table 3 below shows the relative risk, ranging from double (when any EB are present) to four times higher (when EB exceed 100), to ten times higher when the EB are too numerous to count.

Table 3: Relative risk of pathogen occurrence depending on indicator level.

Countable EB	Double the risk
>=100 EB	Four times the risk
TNTC	Ten times the risk

Data on EB for food contact surfaces (where *Salmonella* tests are not typically performed) can be used in conjunction with the other risk calculations that follow, but only when two additional critical pieces of information are known: the concentration of *Salmonella* when they are present and the cross contamination rate from surface to food.

No information in the published literature for either of these two important data gaps were located, however levels are likely to be low when *Salmonella* are present (based on anecdotal information), and cross contamination rates very low (based on typical cross contamination rates of 1% when surfaces are wet – Chen *et al.* 2001) since moisture is known to facilitate transfer.

D-values for *Salmonella* were based on data provided in the "Annex to Control of *Salmonella* in Low-Moisture Foods", published by GMA on February 4, 2009, specifically the data from Dega *et al.* (1972) – Table A-4 of the GMA report and McDonough and Hargrove (1968) –

Table A-5 of the GMA report. These data were used to create a mathematical model used to interpolate between the highest moisture in the Dega report (49% moisture) and the moisture in the McDonough and Hargrove report (4%). This model is shown in the Figure below, where each colored line corresponds to a different solids/moisture ratio.

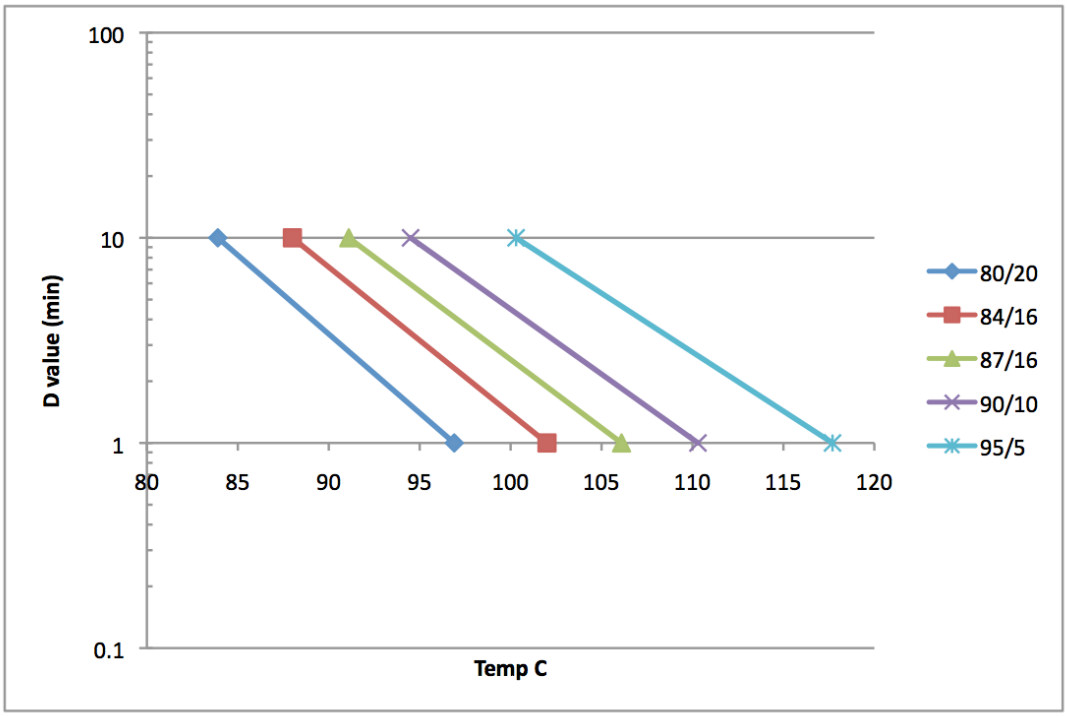

Table 4 below shows an excerpt from the @risk-based Excel spreadsheet. The first column is a description of the information found in each row. The next column shows an example of the value that might be found at any point in time in the simulation. The next column contains a cell number, which corresponds to the cell in the excel spreadsheet where the value can be found. This is important to understand how the formula, found in the next column works to perform the calculations. The formula column either contains the excel formula that shows how the contents of different cells are combined or indicated that the contents of the cell come from user input. Formulas can either be strictly mathematical (i.e. B7: =B6*B2*B5) or they can contain @risk functions. The two @risk functions currently implemented in the spreadsheet are the RiskBeta function, used the calculate the probability that a pathogen is present, or the RiskTriang function, used to calculate the expected log reduction due to the application of heat.

Table 4: Example results from risk assessment showing calculations.

Description	Value	Cell		Formula
Cells per gram	1	B	2	user input
Positive tests	0	B	3	user input
Negative tests	21	B	4	user input
Probability of positive	0.043478261	B	5	=RiskBeta(1+B3,1+B4)
Grams per serving	25	B	6	user input
Cells per serving (pre)	1.09	B	7	=B6*B2*B5
Log cells per serving (pre)	0.036212174	B	8	=LOG(B7)
Log reduction by process 1	0.63	B	9	=RiskTriang(C9,D9,E9)
Log reduction by process 2	0.34	B	10	=RiskTriang(C10,D10,E10)
Log cells per serving (post)	-0.93	B	11	=B8-B9-B10
Cells per serving (post)	0.1165	B	12	=10^B11
Risk per serving	0.0003	B	13	=1-(1+B12/51)^-0.13

Finally, in addition the analysis shown here, another factor which serves to mitigate *Salmonella* risk is dried products is the fact that *Salmonella* is known to die off slowly in such foods. One of the most comprehensive datasets on this topic can be found in Tamminga, *et al.* (1976) where the researchers studied the survival of *Salmonella* in chocolate. These data show that *Salmonella* dies at a rate of about 0.25 log CFU per month. While this may seem very low, considering many dried ingredients may be held for a year or more before use, the net effect on risk may be significant.

Conclusions

In summary, (a) indicator organisms can be useful in assessing risk, although significant data gaps are still needed to make a direct connection to risk. (b) When low water-activity foods are processed, *Salmonella* may survive unless high temperatures and long times are used. (c) When foods are contaminated with very low levels of *Salmonella* many illnesses may still result, when millions of servings are simulated. (d) Negative test results can be used in risk assessment to demonstrate lower risk. (e) Product manufactured with older ingredients represent a measurably lower risk. All of the above factors can be integrated into a comprehensive risk assessment to aid food processors in managing *Salmonella* risk in dried foods.

References

Chen Y., Jackson K.M., Chea F.P. and Schaffner D.W. (2001) Quantification and variability analysis of bacterial cross-contamination rates in the kitchen. *Journal of Food Protection* 64(1):72-80.

Grocery Manufacturers Association. (2009) *Annex to Control of Salmonella in Low-Moisture Food.*

Dega C. A., Goepfert J. M., and Amundson C. H. (1972) Heat resistance of *Salmonella*e in concentrated milk. *Applied Microbiology* 23:415-420.

McDonough F. E., and Hargrove R.E. (1968) Heat resistance of *Salmonella* in dried milk. Journal of Dairy Science 51:1587-1591.

Tamminga S.K., Beumer R.R., Kampelmacher E.H. and van Leusden F.M. (1976) Survival of *Salmonella* eastbourne and *Salmonella* typhimurium in chocolate. *The Journal of Hygiene (London)* 76:41-47.

Probabilistic modelling for the implementation of microbiological criteria within a farm-to-fork based-approach of *Salmonella* Enteritidis in shell and liquid pasteurized eggs

A. Valero[1], M. Rodríguez[1], F. Pérez-Rodríguez[1], E. Carrasco[1], G.D. Posada[1], A. Morales[1], R.M. García-Gimeno[1]

[1] Department of Food Science and Technology, Faculty of Veterinary, University of Cordoba, Campus Rabanales s/n Edif. Darwin C1 14014 Córdoba, Spain. (bt2vadia@uco.es)

Abstract

Contamination of egg products by *Salmonella* Enteritidis has emerged as a one of the main causes of salmonellosis in Europe. At the same time, the performance of microbiological criteria (MC) and risk-based metrics provides a substantial improvement in microbial assessment schemes. In the present work, the efficacy of the implementation of Performance Objectives (PO) at different contamination levels of *S.* Enteritidis in shell and liquid pasteurized egg products (before pasteurization) was studied. Growth/inactivation kinetics were estimated at various stages in the food chain to determine the exposure level of *S.* Enteritidis in the final products. Statistical techniques and distribution fitting was performed in ModelRisk v3.0. Log increase after storage in shell eggs and final concentration of *S.* Enteritidis after pasteurization in liquid egg products were evaluated as risk outputs. The results obtained in shell eggs showed that, under appropriate storage conditions, *S.* Enteritidis did not grow in 72.1% of the cases, while in 83% of the cases; growth increase was lower than 1 log cfu/g, since low temperatures delayed yolk membrane disruption. The developed MC in shell eggs (lot mean = 1.13 log cfu/g; s.d. = 0.56; n = 35; m = absence in 25g; c = 0 and PO = 0.35 log cfu/g) increased the percentage of no-growth cases up to 88.8% of cases, and reduced the extreme values of the log increase distribution from 9.23 to 6.93 log cfu/g. On the other hand, the establishment of POs in liquid eggs before pasteurization (PO = 0.22 log cfu/ml) produced a substantial reduction in the mean values of the concentration of *S.* Enteritidis after pasteurization (from -0.71 to -2.34 log cfu/ml). These results are of great importance for risk managers in order to set risk-based control strategies in shell eggs and egg products.

Keywords: *S.* Enteritidis, *Performance Objectives, Microbiological Criteria, Risk assessment, growth/inactivation models*

Introduction

Salmonella is a well-known foodborne pathogen which is present in a wide variety range of foods. Eggs and egg products are found as the food commodities where most of the outbreaks are reported in Europe (EFSA/ECDC 2011). Although the salmonellosis cases in humans have decreased by 17.4% compared to 2008 thanks in part to the implementation of national control programmes, additional measures are required since data regarding storage conditions and consumer practices are still scarce and highly variable. On the other hand, risk-based metrics (such as Performance Objectives [PO], Food Safety Objectives [FSO]) have emerged as risk management measures to be implemented throughout the food chain that can help to set public health goals. In this context, microbiological criteria (MC) based on within-lot testing are defined to provide a statistically-designed approach for determining POs and FSO (van Schothorst *et al.* 2009).

In this work, an exposure assessment model was built for determining as risks outputs: (i) the growth increase of *Salmonella* Enteritidis in shell eggs after processing and storage conditions, as well as (ii) the final concentration in liquid pasteurized eggs. Subsequently, different values of the prevalence distribution of contaminated eggs were taken to determine potential POs. Finally MC were implemented (assuming log-normal distributions for the *Salmonella* concentration) and their impact on risk outputs were evaluated in order to give an

example of potential risk management measures within the farm-to-fork chain of eggs and egg products.

Materials and Methods

An exposure assessment model was implemented in an Excel spreadsheet. The most representative variables in the model together with their corresponding distributions and values are represented in Table 1.

Prevalence and concentration data

Prevalence and concentration distributions in shell eggs were obtained from the studies of Chemaly *et al.* (2009) and from the risk assessment of *S.* Enteritidis performed by USDA/FSIS (2005). We considered contamination per individual shell egg coming from the same flock. Subsequently, during the cracking process of contaminated eggs, *S.* Enteritidis was assumed to be transferred from the shell to the egg yolk (being initially negative for *S.* Enteritidis) with a probability of 0.639, basing on the data obtained by Rivoal *et al.* (2009).

Modelling growth/inactivation of S. Enteritidis *in shell and liquid eggs*

The Baranyi model was used to determine growth of *Salmonella* at various steps in the food chain, while a secondary Gamma model was used to calculate maximum growth rate ($\mu_{max,}$ h^{-1}) as a function of temperature and pH conditions (μ_{opt} = 2.34 h^{-1}; T_{min} = 5.2ºC; T_{opt} = Uniform (35,43); T_{max} = 46.2; pH_{min} = 3.8; pH_{opt} = Uniform (7,7.5); pH_{max} = 8.8).
Time and temperature distributions of eggs in farm and during processing and storage conditions were obtained from Latimer *et al.* (2002). Growth of *S.* Enteritidis was assumed to occur once the pathogen has penetrated into the yolk. Therefore, the loss of membrane integrity (LI_{YM}) was considered in the growth model (USDA/FSIS 2005). The equation used was:

$$LI_{YM} = (2.087 - 0.043 \times T) \pm 0.313\{(1/32) + [(T - 21.6)^2 / 1382.4]^{0.5}\}$$

Eq.1, where T represents the internal egg temperature (ºC)

The inactivation model of Jordan et al. (2010) was used to calculate the number reductions (log) of *S.* Enteritidis in liquid eggs due to pasteurization treatment (61.5ºC-3 min).
A MonteCarlo simulation was run in ModelRisk v 3.0 (Vose Consulting, Belgium) with 10,000 iterations to characterize variability in the parameters. Additionally, a crude sensitivity analysis through the calculation of rank correlation coefficients was carried out in order to evaluate the effect of each input on final risk outputs. Finally, the log increase of *S.* Enteritidis in shell eggs and the final concentration after pasteurization in liquid eggs were calculated as model outputs.

Implementation of POs and MC

MC were established assuming log normal distributions for the concentration of *S.* Enteritidis in eggs. Knowledge of the mean value together with the standard deviation served to develop a MC. The safety limit required (maximum frequency of the hazard) and its relationship with the lot mean, was determined by taking different percentiles of the prevalence distributions of *S.* Enteritidis in shell eggs and unpasteurized liquid eggs. The acceptability of the food lot was described through a two-class sampling plan (n, c, m). A consumer acceptable level of safety (ALS) of 95% was assumed.

Results and Discussion

The exposure assessment model considered that all contaminated units belonged to shell eggs. Contamination to liquid eggs was assumed to be originated through penetration of *Salmonella* to the egg yolk because of the loss of integrity of yolk membrane (LI_{YM}). The disruption of the yolk membrane might be dependent on the internal egg temperature and the exposure (USDA/FSIS 05). Results obtained indicated that there was no growth of *S.* Enteritidis in 72.1% of the cases from contaminated shell eggs mainly due to appropriate handling

conditions and integrity of yolk membrane were most likely to occur. Besides, growth was limited since in 83% of cases was lower than 1 log. The maintenance of refrigerated storage temperatures (10.73±3.29ºC) after egg processing reduced significantly the probability of growth of *S.* Enteritidis within contaminated eggs. In the sensitivity analysis performed, rank correlation values (r) were highest for storage temperature after processing (r = 0.643) and storage time (r = 0.365), thus, they were identified as the most relevant inputs on the log increase in shell eggs.

Using statistical methods described in van Schothorst *et al.* (2009) the log normal concentration distributions together with prevalence distributions of *S.* Enteritidis were used to determine POs and safety limits, respectively. By taking the 95th percentile of the prevalence distribution (safety limit of 8.2%) as a worst-case scenario, the developed MC in shell eggs was: lot mean = 1.13 log cfu/g; s.d. = 0.56; n = 35; m = absence in 25g; c = 0 and PO = 0.35 log cfu/g. With this new MC, *S.* Enteritidis did not grow in 88.8% of the cases, and the extreme values of the log increase distribution in shell eggs were reduced from 9.23 to 6.93 log cfu/g.

Table 1: Variables considered in the probabilistic model of *S.* Enteritidis in shell and liquid pasteurized eggs.

Parameters	Notation	Description
Prevalence shell egg	$P_{shell\ egg}$	Cumulative[(0.006, 0.08), (0.006, 0.01; 0.026, 0.06, 0.08),(0.11, 0.20, 0.29, 0.70, 0.99)]
Prevalence liquid egg	$P_{-liquid\ egg}$	0.639 x $P_{shell\ egg}$
Initial concentration egg (log cfu/g)	N_0	LogNormal(1.13,0.56)
Growth of *S.* Enteritidis	G_{-egg}	Baranyi primary model
Storage time/temperature farm (ºC)	t_{farm}/T_{farm}	Uniform (0,0.033)/Uniform(26.67,40.56)
Storage time processing (d)	t_{proc}	Triangle(0.04,0.25,1) + Triangle(0.004,0.1,0.25)
Storage temperature processing (ºC)	T_{proc}	Triangle(7.22,15.56,32.22)
Storage time/temperature after processing (ºC)	$t_{af\ proc}/T_{af\ proc}$	Triangle(0.04,2,3)/Triangle(5,7.22,32.22)
Loss of integrity of yolk membrane (h)	LI_{YM}	Eq 1.
Maximum growth rate (h^{-1})	μ_{max}	Gamma model: $\mu_{opt}\ \gamma(T)\ \gamma(pH)$
Lag time (h)	lag	$Ln[1+(1/0.03)/\mu_{max}]$
Maximum population density	N_{max}	Lognormal(9.64, 0.05)
Pasteurization treatment	T_{past}/t_{past}	61.5ºC-3 min
Log of decimal reductions (min)	LogD	Inactivation model (Jordan et al. 2010)
Inactivation rate (min^{-1})	k	$1/10^{logD}$
Final concentration in liquid pasteurized egg (log cfu/ml)	$C_{-liquid\ egg}$	N_0 - Log_{red} + G_{-egg}
Log Increase of *S.* Enteritidis in shell eggs (log cfu)	Log_{Inc}	N_0 + G_{-egg}

Pasteurization treatments in liquid eggs (3 minutes) have shown to be effective in the inhibition of *S.* Enteritidis. At 61.5ºC, the log reduction achieved was 3.43 log cfu/ml, while at temperatures above 62ºC, Salmonella is inactivated in more than 4.6 log cfu/ml.

Storage temperature after processing (r = 0.814) and time to yolk membrane disruption (r = -0.654) influenced the most on the final concentration of *S.* Enteritidis in liquid pasteurized eggs.

Besides, the impact of the application of the proposed PO (0.22 log cfu/ml) in liquid unpasteurized eggs (n = 56, c = 0) was high since a substantial reduction in the mean value of

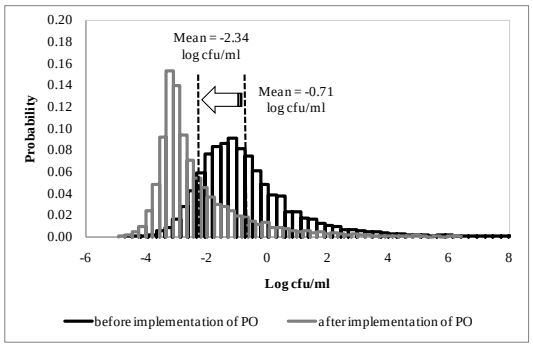

the distribution of the final concentration of *S.* Enteritidis was obtained, from -0.71 to -2.34 log cfu/ml (Figure 1).

Figure 2 shows the number of samples required as a function of different safety limits (percentiles of prevalence distributions) in shell and liquid unpasteurized eggs.
It can be seen that a higher number of samples is required if low percentiles of the prevalence distributions are taken.

Figure 1: Distributions of the final concentration of *S.* Enteritidis in liquid pasteurized eggs before and after the implementation of the proposed PO.

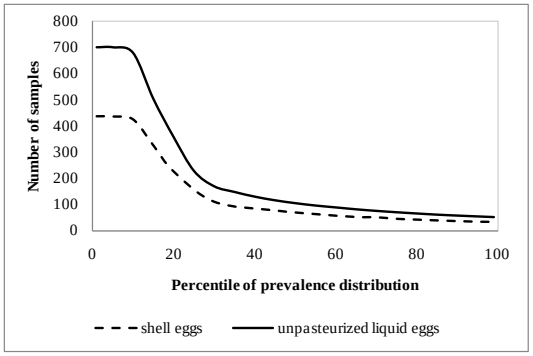

It is demonstrated that microbiological criteria is one of the potential control measures to reduce risk (van Schothorst *et al.* 2009).
Although log normal distributions were assumed in this study, other approaches should be evaluated especially when contamination is present at very low levels (Poisson-log normal or Poisson-Gamma).
These results are of great importance for risk managers in order to set risk-based control strategies in shell eggs and egg products.

Figure 2: Relation between the required number of samples in shell and unpasteurized liquid eggs and the percentile of the prevalence distributions.

Acknowledgements

This work was partly financed by the project FP7-KBBE-222738 (BASELINE) from the European Commission through the Seventh Framework Programme for Research and Development and the AGR 170 Research Group (HIBRO).

References

Chemaly M., Huneau-Salaün A., Labbe A., Houdayer C., Petetin I. and Fravalo P. (2009) Isolation of *Salmonella enterica* in laying-hen flocks and assessment of eggshell contamination in France. *Journal of Food Protection* 72 2071-2077.

European Food Safety Authority, European Centre for Disease Prevention and Control (EFSA/ECDC) (2011) The European Union Summary Report on Trends and Sources of Zoonoses, Zoonotic Agents and Food-borne Outbreaks in 2009. EFSA Journal 2011; 9(3):2090.

Jordan J.S., Gurtler J.B., Marks H.M., Jones D.R. and Shaw W.K. (2011) A mathematical model of inactivation kinetics for a four-strain composite of *Salmonella* Enteritidis and Oranienburg in commercial liquid egg yolk. *Food Microbiology* 28, 67-75.

Latimer H.K., Jaykus L.A., Roberta A., Morales A., Cowen P. and Crawford-Brown D. (2002) Sensitivity analysis of *Salmonella enteritidis* levels in contaminated shell eggs using a biphasic growth model. *International Journal of Food Microbiology* 75, 71-87.

Rivoal K., Protais J., Quéguiner S., Boscher E., Chidaine B., Rose V., Gautier M., Baron F., Grosset N., Ermel G. and Salvat G. (2009). Use of pulsed-field gel electrophoresis to characterize the heterogeneity and clonality of *Salmonella* serotype Enteritidis, Typhimurium and Infantis isolates obtained from whole liquid eggs. *International Journal of Food Microbiology* 129, 180-186.

U.S. Department of Agriculture/Food Safety and Inspection Service (USDA/FSIS) (2005) Risk assessments for *Salmonella* Enteritidis in shell eggs and *Salmonella* spp. in egg products.

van Schothorst M., Zwietering M.H., Ross T., Buchanan R.L., Cole M.B., and International Commission of Microbiological Specifications for Foods (ICMSF) (2009) Relating microbiological criteria to food safety objectives and performance objectives. *Food Control* 20, 967-979.

Meta-analysis for quantitative microbiological risk assessments and benchmarking data

H.M.W. den Besten, M.H. Zwietering

Wageningen University, Laboratory of Food Microbiology, Wageningen, The Netherlands
(heidy.denbesten@wur.nl, marcel.zwietering@wur.nl)

Abstract

Meta-analysis is an emerging approach in the food microbiology area to quantitatively integrate the findings of individual studies on kinetic parameters of interest. Meta-analyses provide global estimates of parameters with their variabilities, and give insight into the main influencing factors on microbiological kinetics. This paper discusses the opportunities of meta-analysis to generate sufficiently generic parameters – with their variability – for quantitative microbiological risk assessments, and demonstrates how the output of a meta-analysis can be used to benchmark future studies in order to position new data in perspective.

Keywords: *QMRA, kinetics, global parameter estimates, variability, benchmarking*

Introduction

Quantitative microbiological risk assessments (QMRAs) aim to quantify the risk related to the consumption of food products and include the assessment of the severity of a microbiological hazard (pathogens and/or toxins) and its likelihood of appearance (i.e. prevalence and concentration) (Lammerding, 1997). The four cornerstones of a QMRA are hazard identification, exposure assessment, hazard characterization, and risk characterization. During the exposure assessment a farm-to-fork approach can be applied, meaning that all steps of a food supply chain are quantitatively described in order to estimate the number of pathogens or the concentration of toxins at the moment of consumption. QMRAs are more and more used to set microbiological criteria and specifications in different steps of the food chain, to justify measures, to predict the effects of interventions, for food safety legislation, and to obtain insight into the most important phenomena responsible for the risks of foodborne diseases. One of the main practical difficulties of QMRAs is the need for an enormous amount of data for a wide range of kinetic parameters including their averages, variabilities and distributions.
An emerging approach to gather global estimates of kinetic parameters with their associated variability is meta-analysis. A meta-analysis is a systematic analysis of a large collection of data from individual studies aiming to integrate the findings and to produce a global estimate of the effect of a particular intervention or treatment (Gonzales-Barron and Butler, 2011). Because a meta-analysis provides a quantitative summary of results over a broad range of individual studies, it allows not only to produce a global estimate of a parameter, but it also gives information about its variability and the sources of heterogeneity among the data of the individual studies. Moreover, the output of a meta-analysis can be used to benchmark future studies in order to position new data in perspective.

Materials and Methods

The meta-analysis approach can be used to address various questions where a reasonable amount of data exists. For several parameters needed to describe microbial behaviour, a literature search was performed and freely accessible data bases were searched. All quantitative data was structurally organized in databases on the question or parameter of interest to include quantitative and qualitative information of the individual studies. The data were then analysed for main explanatory factors and clustered to obtain global parameters (with their variability) and more specific parameters (with their variability). Furthermore the data bases were used to compare newly gathered data under specific conditions, to investigate the relevance of the effect of these conditions (benchmarking).

Results and Discussion

From a global to a product-specific parameter estimate

Large data sets for irradiation parameter D_{10} (Van Gerwen *et al*. 1999), concentration of contaminants in air in factory environments (Den Aantrekker *et al*. 2003), sedimentation velocities of micro-organisms (Den Aantrekker *et al*. 2003), heat inactivation parameters (Van Asselt and Zwietering, 2006), and high hydrostatic pressure inactivation parameters (Santillana-Farakos and Zwietering, 2011) were successfully gathered previously in our laboratory and evaluated. Main influencing factors could be identified and global and more specific estimations of the parameters with their attendant variabilities were estimated. The quantitative evaluation of the collated heat inactivation data resulted in global estimations of *D*-values and *z*-values for various foodborne pathogens. Many effects of factors reported to affect the *D*-value, such as pH and water activity (a_w) of the food product, species and strain variability, were shown to be smaller in comparison with the variability of published *D*-values. Only a limited number of factors, including temperature, did have a significant effect on the *D*-values. For *Listeria monocytogenes* 967 *D*-values were extracted from 14 individual studies and only the presence of salt (10% w/v, or $a_w < 0.92$) resulted in a significantly higher heat resistance. The upper limit of the 95% prediction interval (PI) of the *D*-values, estimated by integrating the data of all products excluding those with a low water activity (940 *D*-values), was used as a conservative estimation of the *D*-value (Table 1).

Table 1: *D*-values (D_{ref}) at reference temperature (T_{ref}) for *Listeria monocytogenes* in a wide variety of products (all products), and for a more specific product group (dairy) and product type (milk)

Product group	D_{ref} (min) [a]	T_{ref} (ºC)	*z* (ºC)
All products	0.273 (0.045)	72	7
Dairy	0.104 (0.027)	72	6.4
Milk	0.091 (0.024)	72	6.2

[a] Raw data were derived from the data set published by Van Asselt and Zwietering (2006) and represent the upper 95% prediction interval *D*-values, and the mean *D*-values between brackets.

When a large data base is available for a specific product or product group, then one can progress to a less conservative estimate which is based on a still sufficiently generic data set. The data set of Van Asselt and Zwietering (2006) included 280 *D*-values obtained in dairy-related products including 226 from milk. These data were further analysed to derive global *D*-value estimates for dairy products and more specific also for milk (Table 1). The lower variability between individual studies resulted in smaller 95% prediction intervals. Segregation by product type requires ample data sets to include variability between individual studies that can be attributed to factors such as experimental design, strain, laboratory, etc. When these data sets are available, then global estimates of parameters (with their variability) can be obtained for specific product groups.

Benchmarking new data

Both for heat inactivation and high hydrostatic pressure inactivation data, new literature information could be easily benchmarked using the data in the databases, showing the relevance of the studied effects in these studies. Van Asselt and Zwietering (2006) showed that the heat resistance of *Salmonella* species was neither significantly affected by product types or media nor by stain variability, pH and a_w (1141 data extracted from literature). Only chocolate had a significant protective effect on *Salmonella* as inactivation in this product type resulted in remarkably high *D*-values and *z*-value (Figure 1).

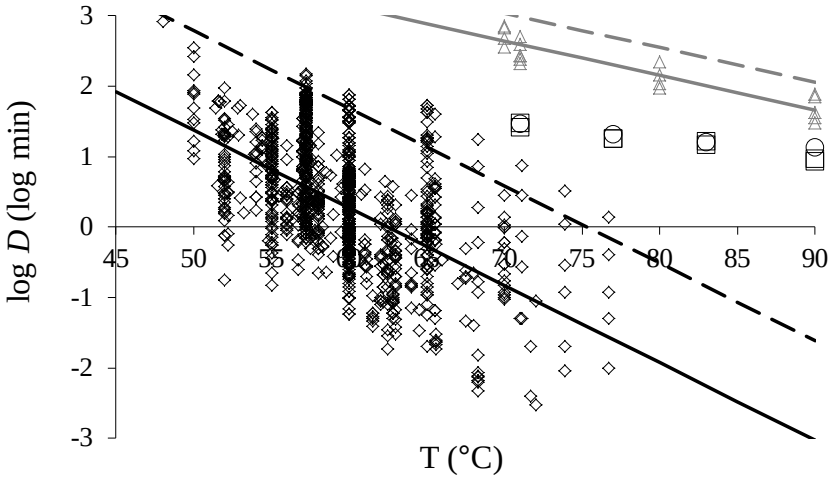

Figure 1: Heat resistance of *Salmonella* species in various food products and media (◇), and in chocolate (△) as published by Van Asselt and Zwietering (2006). The solid line represents the linear regression of log *D* on the temperature and the dotted line represents the upper 95% prediction level. And the heat resistance of outbreak-associated *Salmonella* strains (○) and *Salmonella* strains obtained from other sources (□) in peanut butter as published by Ma *et al*. (2009).

This knowledge can be used to benchmark new published information. A recent publication reported the heat resistance of three sets of *Salmonella* strains in peanut butter, including strains isolated from patients associated with a peanut butter outbreak, culture collection strains and clinical isolates from sporadic cases (Ma *et al*. 2009). The heat resistance of the outbreak-associated strains were found to be more heat resistant at 90ºC than the other *Salmonella* strains. However, when the *D*-values in peanut butter of the three different sets of strains were combined with the data set of Van Asselt and Zwietering (2006), then the heat resistance differences between the three sets of strains became – although significant – less obtrusive (Figure 1). The heat resistance of *Salmonella* in peanut butter was lower than those in chocolate as reported by Van Asselt and Zwietering (2006), but noticeably higher compared to inactivation in other product types. The product characteristics of peanut butter and chocolate – both high in fat content and low a_w – might have contributed to the protective effect during heat inactivation in these product types. Because inactivation of *Salmonella* in both peanut butter and chocolate resulted in remarkably high *D*-values, it strengthened the separation of these product types from others, although these separative conclusions were based on a rather limited number of data collected for peanut butter (12 *D*-values) and for chocolate (20 *D*-values). The integration of new published data in an existing database can put new data in perspective, and highlights the prospects of meta-analysis to evaluate new data.

Conclusions

Meta-analysis is an emerging methodology in the area of food microbiology to systematically and critically collate a large number of individual studies and to quantitatively integrate their findings. When compiling comprehensive microbiological data from individual studies of different laboratories, several issues will be encountered. The overlap between individual studies can be rather limited as many differences can occur in the experimental set ups of individual studies, such as the strain(s) of choice and the intrinsic and extrinsic factors of the experiments. Therefore, often more than one variable has been changed between different studies, which make it unfeasible to quantify the effect of a single variable and urging to firstly focus on global estimation of parameters. Meta-analysis allows to quantitatively synthesize information and translate this into global parameter estimates and their

corresponding variabilities. The differences between individual studies can contribute to rather high variabilities of parameter estimates, allowing to make conclusive separations of main effects. When ample data sets are available for a specific product types or effects, then progressing to a more detailed segregation level provides opportunities for less conservative estimations of parameters without forfeiting safety margins. The generation of sufficiently generic information, with its variability, is of importance to supply QMRAs with relevant data. Database building on the reviewed question or parameter reveals also a clear picture of the present knowledge, and can highlight areas where there is insufficient or an absence of information on factors that might affect the parameter of interest, and can therefore provide direction for future research. Moreover, systematically structured data bases on parameters give prospects to evaluate new published data, allowing to evaluate new findings and position them in perspective.

References

Den Aantrekker E.D., Beumer R.R., van Gerwen S.J.C., Zwietering M.H., van Schothorst M. and Boom R.M. (2003) Estimating the probability of recontamination via the air using Monte Carlo simulations. *International Journal of Food Microbiology* 87, 1-15.

Gonzales-Barron U. and Butler F. (2011) The use of meta-analytical tools in risk assessment for food safety. *Food Microbiology* 28, 823-827.

Lammerding A.M. (1997) An overview of microbial food safety risk assessment. *Journal of Food Protection* 60, 1420-1425.

Ma L., Zhang G., Gerner-Smidt P., Mantripragada V., Ezeoke I. and Doyle M.P. (2009) Thermal inactivation of *Salmonella* in peanut butter. *Journal of Food Protection* 72, 1596-1601.

Santillana-Farakos S.M. and Zwietering M.H. (2011) Data analysis of the inactivation of food-borne microorganisms under high hydrostatic pressure to establish global kinetic parameters and influencing factors. Submitted.

Van Asselt E.D. and Zwietering M.H. (2006) A systematic approach to determine global thermal inactivation parameters for various food pathogens. *International Journal of Food Microbiology* 107, 73-82.

Van Gerwen S.J.C., Rombouts F.M., van ‘t Riet K. and Zwietering M.H. (1999) A data analysis of the irradiation parameter D10 for bacteria and spores under various conditions. *Journal of Food Protection* 62, 1024-1032.

A preliminary risk assessment model of *Escherichia coli* O157:H7 in ground beef and beef cuts in Canada: Evaluating the effects of interventions using results of systematic review and meta-analysis

B. A. Smith, A. Fazil, A. M. Lammerding

Science to Policy Division, Laboratory for Foodborne Zoonoses, Public Health Agency of Canada, Guelph, Ontario, Canada. (ben.smith@phac-aspc.gc.ca)

Abstract

A stochastic risk assessment model was developed to evaluate the public health risks associated with consumption of ground beef and beef cuts contaminated with *Escherichia coli* O157:H7 in households in Canada. Rather than considering efficacy of all interventions at primary production and processing as default values, the model incorporated findings from critical systematic review and meta-analysis of published literature. The objectives of this work included the baseline estimation of the prevalence and concentration of *E. coli* O157:H7 in ground beef and beef cuts, the impact of specific interventions on public health outcomes, and development of a model in which the cost-effectiveness of various management options can be incorporated. Canadian *E. coli* O157:H7 data were used as primary inputs for the model. Pathogen prevalence and concentration transfer from faeces to hide, and hide to carcass, as well as behaviour were modelled, allowing for the evaluation of specific interventions targeted at cattle faeces, hides, and carcasses. Growth throughout retail and home storage modules was predicted using a modified Gompertz equation. Predictions from the exposure assessment were used as inputs for a Beta-Binomial dose-response model, assuming a non-threshold level of illness. The model was populated with intervention efficacy data obtained from the literature following data analysis by systematic review and/or meta-analysis. Public health risks, expressed as various metrics including probability of illness per serving, were reduced by up to two to three orders of magnitude depending on the intervention(s) evaluated. Combinations of interventions applied at the farm-level and throughout processing resulted in the greatest risk reduction. The use of systematic review methodology to critically assess the results of scientific studies before use of the data in risk modelling enhances the confidence in risk predictions, and provides a more evidenced-based model for subsequent public health and cost-effectiveness analyses.

Keywords: *VTEC, EHEC, risk model, probabilistic model, E. coli, beef*

Introduction

Escherichia coli O157:H7 is considered the most important of the verotoxigenic *E. coli* (VTEC) serotypes from a public health perspective in Canada. Ruminants are considered to be one of the main vehicles of the pathogen, and numerous outbreaks have been linked to the consumption of beef products. *E. coli* O157:H7 can cause serious illness when ingested by humans; children and the elderly are particularly susceptible to developing haemolytic ureamic syndrome (HUS), a life-threatening sequelae that usually requires blood transfusions and dialysis.

Canadian VTEC infections are captured through the National Notifiable Database (NND) by the Public Health Agency of Canada. An incidence rate of 4.0 cases/100,000 population per year was estimated following analysis of this database (Ruzante *et al.*, 2010); however, the true incidence rate is likely 10 to 47 times greater (Thomas *et al*. 2006) because the majority of cases of VTEC infections are not reported and therefore not identified in national databases. It is expected that a significant portion of VTEC infections are caused by *E. coli* O157:H7 in ground beef products, and, to a lesser extent, *E. coli* O157:H7 in beef cuts. Beef cuts can be classified as either non-intact or intact. Non-intact cuts are portions of beef subjected to blade or needle tenderization, a process where small blades or needles pierce the cuts to increase perceived tenderness. Blade or needle tenderization can internally

contaminate beef pieces; therefore it is expected that non-intact beef cuts pose a greater public health risk than intact beef cuts (i.e., non-tenderized).
A stochastic risk assessment model was developed to evaluate the public health risks associated with consumption of ground beef and beef cuts contaminated with *E. coli* O157:H7 in households in Canada. Rather than considering efficacy of all interventions at primary production and processing as default values, the model incorporated findings from critical systematic review and meta-analysis of published literature. Systematic review follows a structured research protocol to reduce sources of bias and evaluate study quality, and therefore differs from traditional narrative reviews to provide a clear picture of the state of knowledge (Sargeant *et al*. 2006). A description of considerations during model development, methodologies, and preliminary results of the relative efficacies of categories of interventions are presented herein.

Materials and Methods

A Monte Carlo simulation model using Latin Hypercube Sampling was constructed in Microsoft Excel 2003 with the add-on package @Risk (version 5.5.0, Palisade Corporation, New York, USA) to describe prevalence, concentration, and behaviour of *E. coli* O157:H7 through the agri-food beef chain and the public health risks from consumption of contaminated ground beef, non-intact beef cuts, and intact beef cuts. The conceptual model developed upon which the mathematical model was based is shown in Figure 1. Growth throughout retail and home storage modules was predicted using a modified Gompertz equation (Cassin *et al*. 1998), allowing for freezing of product. Predictions from the exposure assessment were used as inputs for a Beta-Binomial dose-response model, assuming a non-threshold level of illness (Cassin *et al*. 1998). Data obtained from the literature were used for the development of the model; Canadian data were used where possible. Simulations of the model representing different intervention application scenarios were run with 25,000 iterations each to generate the results presented herein.

Prevalence and Concentration in Faeces

Data describing the prevalence of *E. coli* O157:H7 in Canadian cattle faeces are available from several peer-reviewed sources for input into the model. Reported prevalence of *E. coli* O157:H7 in faeces of cattle after adjusting for test sensitivities ranged from 0% to 82% (Van Donkersgoed *et al*. 1999; Lejeune *et al*. 2004; Vidovic and Korber 2006; Stephens *et al*. 2009; Van Donkersgoed *et al*. 2009). A mean prevalence of 17.2% was derived from the beta distribution used to describe the prevalence of *E. coli* O157:H7.
A cumulative distribution of the concentration of *E. coli* O157:H7 in cattle faeces was constructed based on data reported by Stephens *et al*. (2009); these authors reported concentrations of *E. coli* O157:H7 in faeces of cattle of up to 9.29 log CFU/g (Figure 2). Therefore, the model accounted for a proportion of super-shedders, that is, cattle that for a period of time yield high levels of *E. coli* O157:H7 in faeces [i.e., greater than approximately 4 log CFU/g (Stephens *et al*. 2009)]. This is a central distinction from previous work for *E. coli* O157:H7 in ground beef because importance analysis demonstrated that probability of illness is highly dependent upon the concentration in faeces; however, the maximum faeces concentration used in that model was 5 log CFU/g, and a low proportion of cattle were considered super-shedders (Cassin *et al*. 1998).

Interventions

Data describing the efficacy of various on-farm interventions intended to decrease prevalence and/or concentrations of *E. coli* O157:H7 in faeces were applied during different simulations of the model. These data were obtained from systematic reviews and meta-analyses. Systematic reviews and meta-analyses considered all types of primary studies irrespective of study design (e.g., challenge trials, observational studies, *etc*.) and identified those that met or exceeded screening criteria for quality of methodology. Sargeant *et al*. (2007) performed a systematic review of the literature and summarized data for quantifying the impacts of on-farm interventions including: probiotics, sodium chlorate in feed and water, and vaccination.

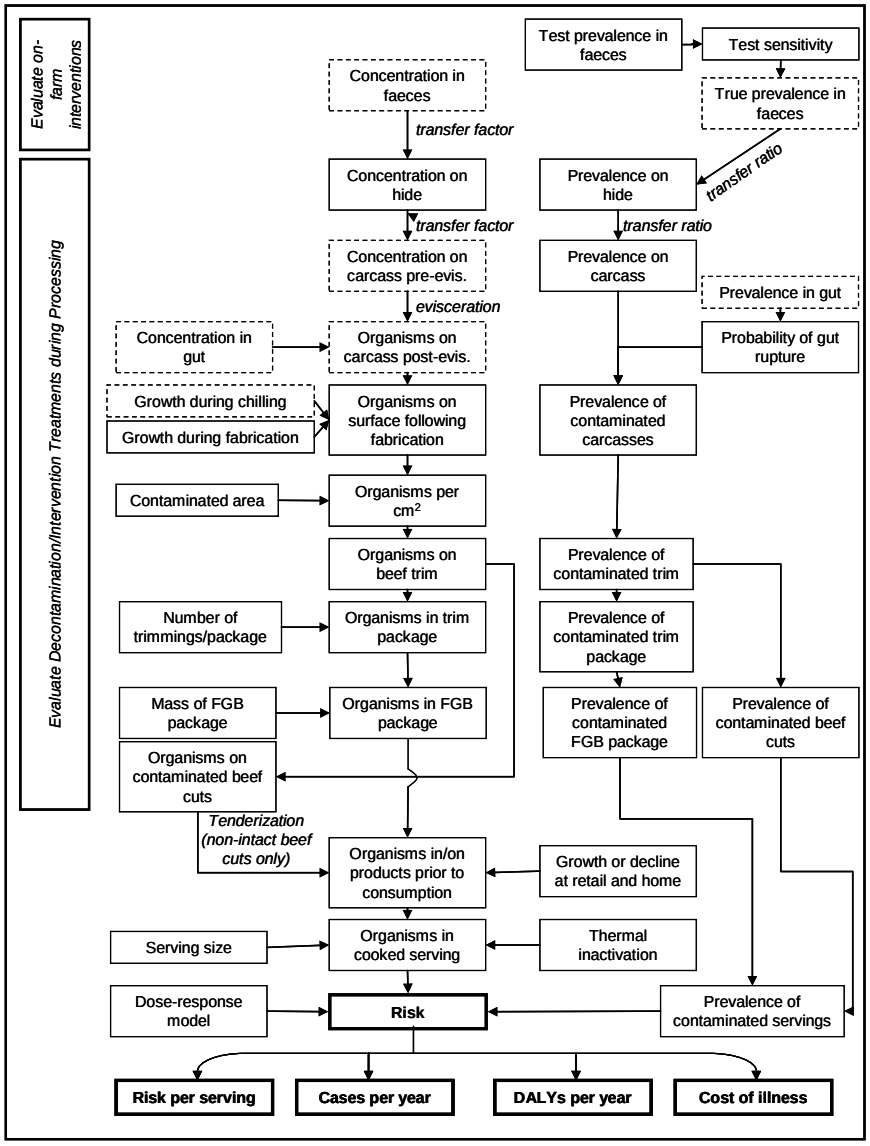

Figure 1: Flow diagram of the mathematical model for *E. coli* O157:H7 in ground beef and intact and non-intact beef cuts. Dashed boxes indicate points along the farm-to-fork continuum where interventions identified through systematic review and meta-analysis are evaluated in the model. Bolded boxes indicate key model outputs. FGB = fresh ground beef.

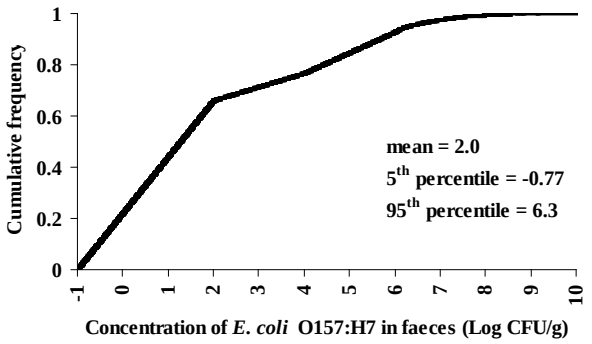

Figure 2: Distribution of *E. coli* O157:H7 in faeces of Canadian cattle (Stephens *et al*. 2009).

These data were used to construct distributions representing efficacies of the on- farm interventions. To quantify the impacts of various interventions applied at processing on concentrations of generic *E. coli* of cattle carcasses, data from a concurrent in-house systematic review and meta-analysis of published literature were used (Greig 2011, personal communications). The efficacies of washing, steam pasteurization, and spray chilling interventions were evaluated in the risk assessment model using triangular distributions defined by the parameters of the meta-analysis outputs.

The model allows for the quantification of impacts to public health from application of interventions targeted at reducing prevalence and/or concentrations of *E. coli* O157:H7 on hides of cattle. However, no systematic reviews of such interventions were identified and they were not evaluated herein.

Results and Discussion

Several intervention scenarios were applied to evaluate single on-farm or processing interventions, combinations of on-farm interventions and processing interventions, or multiple processing interventions. All interventions reduced the mean probability of illness from consumption of ground beef, non-intact beef cuts, or intact beef cuts contaminated with *E. coli* O157:H7, relative to the modelled probability of illness in a reference scenario where no interventions are applied throughout the entire farm-to-fork continuum. Note that this scenario is not a true representation of current practices in Canada (i.e., interventions are applied in Canadian processing facilities whereas this scenario assumes that no interventions are applied), but was used as a reference point for demonstrating relative risk reductions.

Mean probabilities of illness from consumption of ground beef, non-intact beef cuts, and intact beef cuts, following application of single on-farm interventions were reduced by average factors of 1.8-5.4, 1.9-3.9, and 1.8-2.8, respectively. Solitary processing interventions applied at a single point during processing decreased the mean probability of illness from consumption of ground beef, non-intact beef cuts, and intact beef cuts by average factors of 1.1-7.3, 1.1-5.9, and 1.1-4.4, respectively. Combinations of interventions had the greatest impacts, and reduced the mean probabilities of illness from consumption of ground beef, non-intact beef cuts, and intact beef cuts by factors of 2.7-478, 2.2-6,330, and 2.2-1,090, respectively.

Caution must be exercised when interpreting the results of each intervention scenario, because data were derived from multiple studies using different study designs. Data quantifying some on-farm interventions used in the model were based on challenge trials where cattle were exposed to high doses of *E. coli* O157:H7 in order to measure the decrease in levels following application of the intervention, as opposed to non-randomized or randomized controlled trials and observational studies. The results of challenge trials might not adequately represent real-world phenomena where expected levels of *E. coli* O157:H7 are generally lower than those artificially achieved in challenge trials, and may overestimate the efficacy of interventions; however, these were the only quality data identified in the extensive systematic reviews studies. In contrast, all data used to evaluate the effects of processing interventions were based on non-randomized and/or randomized controlled trials.

Conclusions

A systems model to determine the prevalence and concentration of *E. coli* O157:H7 on cattle through the farm-to-fork continuum can be used to determine the public health risks to a population, in this case residents of Canada, using country-specific data inputs from consumption of ground beef and non-intact and intact beef cuts. Results provide an indication of relative efficacies of different interventions applied at the farm and processing level. The use of systematic review methodology to critically assess the results of scientific studies before use of the data in risk modelling enhances the confidence in relative risk predictions. However, the use of challenge trials as sole predictors of intervention efficacy could be problematic, and future studies should compare the relative power of data derived from challenge trails versus other study designs. Nevertheless, the most effective strategy for

E. coli O157:H7 management appears to be one that includes interventions at several stages along the agri-food beef chain.

The next stage of this assessment, integration of economic modules, permits the calculation of cost-of-illness from *E. coli* O157:H7 infections in beef products, and the cost-utility of applying different on-farm and/or processing interventions in Canada. The use of systematic review data to quantify the impact of various interventions provides a more evidenced-based model for subsequent public health and cost-utility analysis.

References

Cassin M.H., Lammerding A.M., Todd E.C.D., Ross W. and McColl R.S. (1998) Quantitative risk assessment for Escherichia coli O157:H7 in ground beef hamburgers. *International Journal of Food Microbiology* 41 (1), 21-44.

Lejeune J.T., Besser T.E., Rice D.H., Berg J.L., Stilborn R.P. and Hancock D.D. (2004) Longitudinal study of fecal shedding of Escherichia coli O157:H7 in feedlot cattle: Predominance and persistence of specific clonal types despite massive cattle population turnover. *Applied and Environmental Microbiology* 70 (1), 377-384.

Ruzante J.M., Majowicz S.E., Fazil A and Davidson V.J. (2010) Hospitalization and deaths for select enteric illnesses and associated sequelae in Canada, 2001-2004. *Epidemiology and Infection*, DOI: 10.1017/S0950268810001883.

Sargeant J.M., Amezcua M.R., Rajic A. and Waddell L. (2007) Pre-harvest interventions to reduce the shedding of E. coli O157 in the faeces of weaned domestic ruminants: A systematic review. Zoonoses and Public Health 54 (6-7), 260-277.

Sargeant J.M., Rajic A., Read S. and Ohlsson A. (2006) The process of systematic review and its application in agri-food public-health. *Preventative Veterinary Medicine* 75 (3-4) 141-151.

Stephens T.P., McAllister T.A. and Stanford K. (2009) Perineal swabs reveal impact of super shedders on the transmission of Escherichia coli O157:H7 in commercial feedlots. *Journal of Animal Science* 87 (12), 4151-4160.

Thomas M.K., Majowicz S.E., MacDougall L., Sockett P.N., Kovacs S.J., Fyfe M., Edge V.L., Edge V.L., Doré K., Flint J.A., Henson S. and Jones A.G. (2006) Population distribution and burden of acute gastrointestinal illness in British Columbia, Canada. *BMC Public Health* 6 (1), 307-317.

Van Donkersgoed J., Bohaychuk V., Besser T., Song X., Wagner B., Hancock D., Renter D. and Dargatz D. (2009) Occurrence of foodborne bacteria in Alberta feedlots. *The Canadian Veterinary Journal* 50 (2), 166-172.

Van Donkersgoed J., Graham T. and Gannon V. (1999) The prevalence of verotoxins, Escherichia coli 0157:H7, and Salmonella in the feces and rumen of cattle at processing. *The Canadian Veterinary Journal* 40 (5), 332-338.

Vidovic S. and Korber D.R. (2006) Prevalence of Escherichia coli O157 in Saskatchewan cattle: Characterization of isolates by using random amplified polymorphic DNA PCR, antibiotic resistance profiles, and pathogenicity determinants. *Applied and Environmental Microbiology* 72 (6), 4347-4355.

Behaviour of individual spores of non proteolytic *C. botulinum* as an element in quantitative risk assessment

J.P. Smelt[1], S.C. Stringer[2], S. Brul[1]

[1] Department of Molecular Biology and Microbial Food Safety, University of Amsterdam, Science Park 904 1098 XH Amsterdam. (j.p.p.m.smelt@uva.nl)
[2] Institute of Food research, Norwich Research Park, Colney Norwich NR4 7UA. (Sandra.stringer@bbsrc.ac.uk)
[1] Department of Molecular Biology and Microbial Food Safety, University of Amsterdam, Science Park 904 1098 XH Amsterdam. (s.brul@uva.nl)

Abstract

Published data on distribution of germination (t_{germ}), outgrowth ($t_1 - t_{germ}$) and time to first doubling ($t_2 - t_1$) of spores of non proteolytic *Clostridium botulinum* were further analysed. Most distributions could be described as lognormal distributions. Also the total development times from phase bright spores to doubling cells could be fitted as lognormal distributions. The latter distributions could serve for development of a model that predicts the distributions at all temperatures within the range between 8 and 22 °C. Combined with a distribution of temperatures in domestic refrigerators the probability of outgrowing *C. botulinum* spores could be estimated with a Monte Carlo simulation. Apart from the development of this model, detailed observations were made on the distributions of the various stages. No significant correlation (P> 0.05) was observed between the time lengths of the various stages. When spores were severely heat damaged an entirely different germination pattern was observed.

Keywords: *Clostridium spores, lognormal, risk assessment, heat damage*

Introduction

To apply quantitative microbiological risk assessment (QMRA) growth and inactivation models of pathogens are badly needed. They are particularly valuable for assessing the risk of toxigenic bacterial spores. Most models are limited by the fact that they are based on observations of whole cell populations. Apart from infant botulism, *C. botulinum* spores are harmless as long as they cannot grow out. An important element is knowledge of the various stages of development of the bacterial spore to a growing population of vegetative cells. The acceptable stage of development depends on the type of microorganism. Strict criteria are necessary for *Clostridium botulinum* with respect to the development of the spore. Growth is certainly not allowed and it is even questionable whether full development of the spore to the first doubling of the emerging vegetative cells can be tolerated. Time to the first doubling was taken here as the limiting time. On the other extreme, a relatively high concentration of vegetative cells (e.g. 100/ml) can be tolerated for relatively harmless pathogens such as *Bacillus cereus* and *Clostridium perfringens.* Ideally, the development of each spore in a population should be known to estimate the probability of development to a certain stage. To this purpose published data have been selected (Stringer *et al.* 2009). Here we describe a model that describes the distributions of times to doubling combined with distributions of refrigerator temperatures to estimate the probability of a potentially hazardous situation. Besides the distributions of the separate stages was analysed and these data might be used in a later stage to a refine the risk assessment.

Materials and Methods

All distributions were fitted with the Excel solver and a final check was done in SPSS to establish more detailed data of the model. All distributions (distributions of germination, of subsequent outgrowth and of subsequent time to doubling and the sum of these 3 stages) were fitted as a normal, lognormal and a Weibull distribution. The correlation between all stages was calculated. A secondary model was developed by modelling the effect of temperature on the parameters of the individual distributions of ‘time to doubling’ at 8, 10, 15 and 20 C.

Finally a whole model was obtained that describes the effect of temperatures between 8 and 22 °C. To fit lower probabilities relatively better log probabilities were fitted instead of probabilities. Data on distribution of refrigerator temperatures (Laguerre *et al.* 2002) was combined with the model by a Monte Carlo simulation to establish the risk. Apart from this risk model spore populations were divided into two groups: those that could develop to doubling cells and those that could only germinate. Special attention was paid to heated spores.

Results and Discussion

Modelling total time to doubling

The distribution of transition times from phase bright to first doubling could be best fitted as lognormal fit. The relation between μ of the lognormal distributions at individual temperatures could be described as linear. There was not a clear correlation between temperature and the variances. Hence it was decided to pool the variances. A total model was obtained by fitting the two parameters of the linear relation generating the mean doubling time dependence on temperature.The following parameters were estimated:

$$T_d = 10^{(1.7637 - 0.0397*T)}$$

T_d = mean time (μ of lognormal distribution) to first doubling; T = temperature (°C)
pooled standard deviation (σ of lognormal distribution) = 0.10492
As shown in Fig. 1 a reasonable fit was obtained.

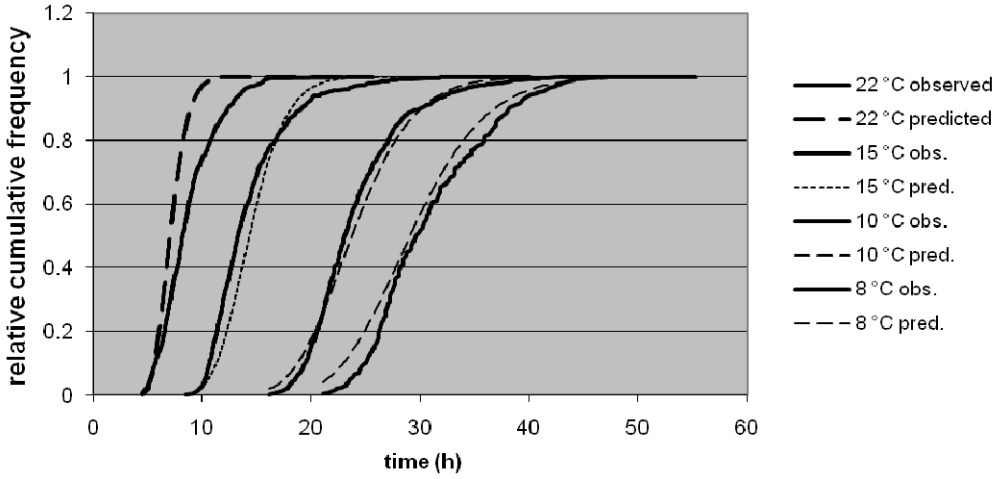

Figure 1: Distribution of 'total times to double' of non proteolytic *C. botulinum* spores at various temperatures (predictions are made by the general secondary model).

Non proteolytic *C. botulinum* can pose a particular problem at refrigerator temperatures. The temperature distribution in domestic refrigerators followed a normal distribution with a mean of 6.57ºC and a standard deviation of 2.23. The model developed here was combined with this temperature distribution and the final probability of development of a non proteolytic spore under refrigeration conditions was estimated by a Monte Carlo simulation resulting in a normal distribution with μ = 46.6 and σ = 8.42.

Distributions of various stages (germination, outgrowth and doubling)

No correlation was found between the time lengths of the various stages if the germinated spores could develop further. Fig. 2 shows an addition of randomised values of germination time (t_{germ}), outgrowth times ($t_1 - t_{germ}$) and doubling times (t_2-t_1), illustrated by comparing the observed 'total time to doubling (t_2). As no correlation was found it is to be expected that the

randomised data were quite similar to the observed data on complete development from phase bright spore to doubling cell. An example is shown in Fig 2 for 15 °C and similar fittings were obtained with the other temperatures (8, 10 and 22 °C). A small deviation was observed between random addition and t_2 when heated spores were incubated at 22 °C

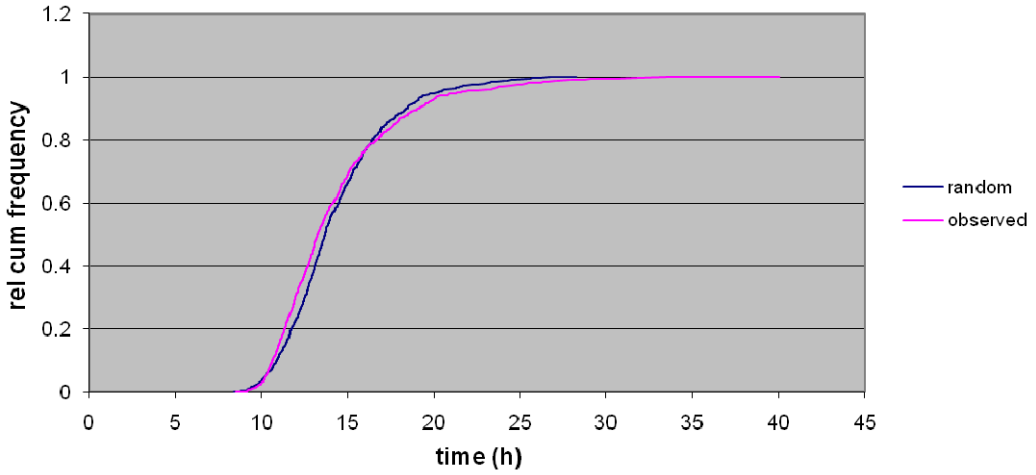

Figure 2: Comparison of observed total time to doubling at 15 °C and addition of randomised stages

In Figs 3 and 4 examples are given that show the transition from germination to the first doubling. Whereas the outgrowth time is always the longest in the process of development when spores were not heat damaged (results for 8, 10 and 15 °C not shown, but a similar pattern as for unheated spores incubated at 22 °C), the germination time was relatively long when cells were heat damaged.

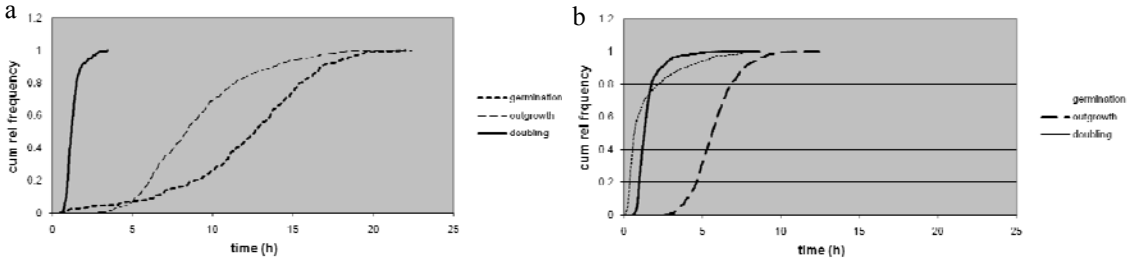

Figures 3a an 3b: Germination, outgrowth and doubling of heat damaged spores (a) and intact spores (b) both incubated at 22°C.

Spores could be divided into those that could develop further and those that could not. There was a significant ($P < 0.01$) difference between germination times of spores that could germinate and that could not. The distribution of germination times of spores that could not develop was always wider with a longer average generation time than those of spores that could develop further. A different pattern was observed when cells were heated. In Fig 4.the difference in germination pattern is illustrated. Whereas the cells that could develop were normally (but not log normally!) distributed, the germinated cells that could not develop further showed a bimodal distribution that could be fitted as a mixture of two distributions
The curves could be fitted as a normal distribution (outgrowing spores) or as mixed distribution consisting of a Weibull distribution and a normal distribution. (germinated spores that did not develop further). The parameters were $\mu = 12.89$ and $\sigma = 4.157679$ (spores that could develop to dividing cells) or $\mu = 19.2903$ and $\sigma = 4.0538 + \alpha = 0.783$ and $\beta = 2.4643$ and $\gamma = 0.336$. The parameters μ and σ are parameters of normal distributions and α and β are Weibull parameters a, whereas γ is the parameters representing the Weibull fraction and $1 - \gamma$ representing the normal fraction.

The germination of spores of non proteolytic *C. botulinum* was here described as log normal distribution, whereas there are several observations of *Bacilli* that showed that the germination pattern followed a the Weibull distribution (Collado *et al.* 2006, Smelt *et al.* 2008). It should be borne in mind that compared to *Bacillus* spores, intact spores of non proteolytic *C. botulinum* can easily germinate. That might have consequences for the shape of the distribution.
Particularly the germination pattern of heated cells is remarkable and should be further studied. Coleman *et al.* (2006) could separate heated spores of Bacillus by density centrifugation into two fractions one was hardly viable and lacked dipicolinic acid, whereas the other fraction was fully viable. It might be possible that the fast germinating fraction that could not develop further represents a similar fraction as was observed by Coleman *et al.* (2010)

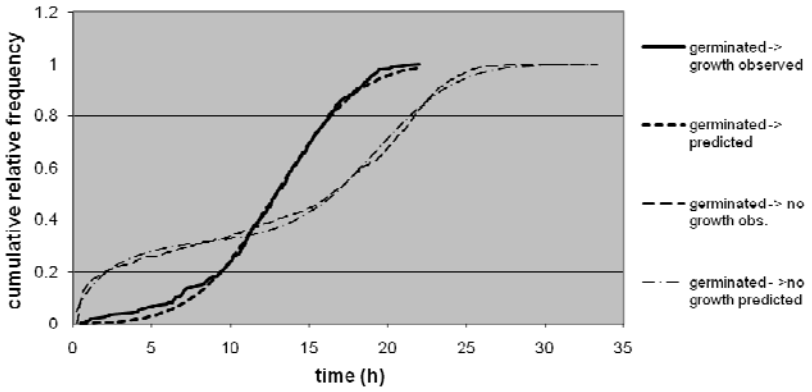

Figure 4: Distribution of germination times of heated damaged spores subsequently incubated at 22°C.

Conclusions

The analysis of the above mentioned data shows that these data cannot only serve as an input for quantitative risk assessment but also can lead to a better understanding of the mechanism of heat injury of bacterial spores.

References

Coleman W.H., Zhang P., Li Y.Q. and Setlow P. (2006) Mechanism of killing of spores of *Bacillus cereus* and *Bacillus megaterium* by wet heat. *Letters in Applied Microbiology* 50: 507-14.

Collado J, Fernández A, Rodrigo M. and Martínez A. (2006) Modelling the effect of a heat shock and germinant concentration on spore germination of a wild strain of Bacillus cereus. *International Journal of Food Microbiology* 106: 85-89.

Laguerre O., Derens E. and Palagos B. (2002) Study of domestic refrigerator temperature and analysis of factors affecting temperature: a French survey. *International Journal of Refrigeration* 25: 653-659.

Smelt J.P., Bos A.P., Kort R. and Brul S. (2008) Modelling the effect of sublethal heat treatment of Bacillus subtilis spores on germination rate and outgrowth to exponentially growing vegetative cells. *International Journal of Food Microbiology* 128(1) 34-40.

Stringer S.C., Webb M.D. and Peck M.W. (2009) Contrasting effects of heat treatment and incubation temperature on germination of and outgrowth of nonproteolytic *Clostridium botulinum* bacteria *Applied and Environmental microbiology* 75(9) 2712-2719.

Distribution of Cronobacter spp. in industrial batches of powdered infant formula and the impact of sampling approaches

I. Jongenburger[1], M.W. Reij[1], E.P.J. Boer[2], L.G.M. Gorris[1], M.H. Zwietering[1]

[1] Laboratory of Food Microbiology, Wageningen University, P.O. Box 8129, 6700 EV Wageningen, The Netherlands. (marcel.zwietering@wur.nl)
[2] Biometris, Wageningen University, P.O. Box 100, 6700 AC Wageningen, The Netherlands

Abstract

The spatial distribution of pathogenic microorganisms within a batch of food will influence the results of sampling for microbiological testing and will also influence the public health risk. However, knowledge about how microorganisms are actually spatially distributed in foods is scarce. This study investigates how *Cronobacter* spp. are distributed on batch-scale throughout a recalled batch of powdered infant formula (PIF) and it investigates on local-scale the occurrence of clusters of *Cronobacter* cells. Additionally, the performance of typical sampling plans and strategies are investigated. The concentration of *Cronobacter* spp. was assessed in the course of the filling time by taking samples of 333 g using the most probable number (MPN) enrichment technique. Since estimating concentrations by enrichment does not distinguish between a single cell or clusters of cells, the occurrence of clusters of *Cronobacter* spp. cells was investigated by plate counting 2290 samples of 1 g. In the recalled batch 415 MPN samples were drawn and in 58% the concentrations were estimated to be below the detection limit of -2.52 log CFU/g. *Cronobacter* spp. were heterogeneously distributed throughout the batch with parts with no detectable contamination and parts with concentrations between -2.52 and 2.75 log CFU/g. Clusters of cells occurred sporadically in 8 out of 2290 samples. The two largest clusters contained 123 (2.10 log CFU/g) and 560 (2.75 log CFU/g) cells. The concentration in the reference batch was -4.4 log CFU/g, 99% of the 93 samples were below the detection limit. Various sampling plans were evaluated for the contamination data from the recalled batch. Taking more and smaller samples and keeping the total sampling weight constant, improved the performance of the sampling plans to detect such a type of contaminated batch.

Keywords: *recalled batch, heterogeneity, probability, sampling plan, lot*

Introduction

There is little known about how microorganisms are actually spatially distributed in foods. In many cases, generalising or default assumptions are made regarding the spatial distribution and appropriate sampling strategies. According to Kilsby and Baird-Parker (1983), the total viable counts from batches including frozen meat, frozen vegetable, and frozen dairy products appeared to be lognormally distributed in 92% of the batches; in 8% of the batches the total viable count appeared to be not lognormally, with a maximum of 13% for powdered products. Based on studies including the findings of Kilsby and Baird-Parker, the International Commission on Microbiological Specification for Foods (ICMSF 2002) assumed a Lognormal distribution in order to evaluate the performance of attribute sampling plans. According to the ICMSF (2002), a standard deviation of 0.8 log CFU/g was chosen based on data derived from the meat industry (Greenberg *et al.* 1966) and similar observations in other food products. Assuming a lognormally distributed contamination, also the size of the standard deviation will affect the performance of a sampling plan (Legan et al. 2001). Habraken et al. (1986) established that substantial clustering of contamination occurs in dried milk products, with parts of the batch containing microorganisms and other parts containing no microorganisms at all. This clustering or heterogeneity will make the interpretation of the sampling results difficult. Besides heterogeneity on batch-scale, heterogeneity on local-scale is possible within the food product. One could speculate that bacteria may grow overnight to levels of 10^9 cells/mL in a droplet of water and powder. This may result in clusters of cells

with high concentrations, which may influence both risk assessments and public health. In order to investigate the spatial distribution of microorganisms in a batch of food and its impact on various sampling approaches, powdered infant formula (PIF) was chosen as product and *Cronobacter* spp. as target microorganism.

Powdered infant formulae (PIF) given to infants during the first months of life needs to be manufactured according to very stringent hygiene measures, since PIF has been linked to outbreaks related to the presence of *Cronobacter* spp. (FAO/WHO 2006; CAC 2008; Cordier 2008). Currently every batch of PIF has to be tested for *Cronobacter* spp. by drawing 30 samples of 10 g according direct sampling plans (CEC 2007). In a recent FAO/WHO risk assessment (FAO/WHO 2006) the mean concentration and standard deviation of *Cronobacter* spp. in batches of powdered infant formula have been estimated from prevalence data to be respectively, -3.8 log CFU/g and 0.7 log CFU/g.

This study investigated the distribution of *Cronobacter* spp. within a batch of PIF, that had been recalled after *Cronobacter* spp. had been detected. For comparison a reference batch produced in the same factory was investigated in detail as well. Estimating low microbial concentrations with the most probable number (MPN) technique by enrichment does not distinguish between a single cell or clusters of cells. Therefore, additionally on local-scale the occurrence of clusters of *Cronobacter* spp. cells was investigated by plate counting many small samples. Thereafter, the performances of various sampling plans were calculated.

Materials and Methods

Investigating batches of powdered infant formula

To assess the distribution of *Cronobacter* spp. in batches PIF, 415 samples of 333 g from the recalled batch and 93 samples from the reference batch were investigated. The concentration of *Cronobacter* spp. was estimated in samples of 333 g using the Most Probable Number (MPN) technique (3 x 100 g, 3 x 10 g , and 3 x 1 g) and the screening method as published by Iversen et al. (2008). To investigate the presence of local clusters of cells, 28 bags were chosen with high concentrations or concentrations below the detection limit of -2.52 log CFU/g (0.003 CFU/g). The remaining powder was divided in samples of 1 gram and all samples were diluted in 9 ml of PPS and 3 ml of the suspension was pour plated in Trypton Soy Agar with sodium pyruvate at a concentration of 0.1 % (wt/vol) (TSAP) and a top layer of TSAP. Sodium pyruvate was added in order to enhance the resuscitation of stressed *Cronobacter* spp. cells during plating (Gurtler and Beuchat 2005). Since 3 ml of the -1 dilution was plated, the lower detection limit was 3.3 CFU/g for a sample size of 1 g,

Random sampling

By randomly drawing a number of samples (*n*) with a specific sample size from the data set, the probability that the sampling scheme includes one or more positive samples $\Pr(n_+ > 0)$ can be calculated as follows:

$$\Pr_{rand}(n_+ > 0) = 1 - (1 - s_+)^n \qquad (1)$$

with: *n*: number of samples; n_+: number of positive samples; s_+: fraction of positive samples of a specific sample size. Since the data set contained information on triplicate samples of 100, 10, and 1 g, it was also possible to assess fractions of positive samples for sample sizes of 300, 30, and 3 g.

Results and Discussion

Distribution of Cronobacter *spp. in PIF*

On batch-scale, the distribution of *Cronobacter* spp. cells throughout a recalled and a reference batch was investigated by relating concentrations to the time that the bag is actually filled. Nearly 60 % of the MPNs had an MPN code of 0,0,0 and the concentration was estimated below the detection limit of -2.52 log CFU/g (0.003 CFU/g). Two samples had a concentration estimated above the upper detection limit of 0.041 log CFU/g (1.1 CFU/g) for

an MPN of 333 g. Figure 1 shows the empirical cumulative distribution function (ECDF) of the samples drawn from the recalled and reference batch.

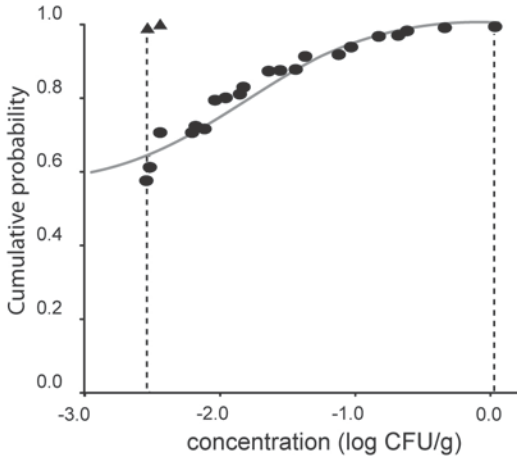

Figure 1 Empirical cumulative distribution functions of the concentrations of *Cronobacter* spp. (log CFU/g) in MPNs of 333 g drawn from the (▲) reference and (●) recalled batch. The grey curve represents a Normal distribution with a mean -1.779 log CFU/g and standard deviation 0.675 log CFU/g of the positive samples (y = 0.42 x Normal (-1.779, 0.675) + 0.58). The dotted vertical lines indicate the lower (-2.52 log CFU/g) and the upper (0.041 log CFU/g) detection limits.

On local-scale 2272 samples of 1 g were below the detection limit of 3.3CFU/g and 8 samples varied between 3.3 and 560 CFU/g and two concentrations peaked at 123.3 and 560 CFU/g.

The probability that the sampling scheme includes one or more positive samples by random ($\Pr_{rand}(n_+ > 0)$*) sampling*

Table 1 shows $\Pr_{rand}(n_+ > 0)$, the probability that the sampling scheme includes one or more positive samples, by drawing random samples from the recalled and reference batch. Eq. 1 and the fractions of positive samples were used to calculate $\Pr_{rand}(n_+ > 0)$. Table 1 shows that keeping the total sample weight constant at 300 g and increasing the number of samples from 1 to 30, increases $\Pr_{rand}(n_+ > 0)$ from 0.378 till 0.999.

Table 1: The probability ($\Pr_{rand}(n_+ > 0)$) that the entire sampling scheme contains one or more positive samples by sampling randomly with various numbers of samples and sample sizes from the recalled and the reference batch. $\Pr_{rand}(n_+ > 0)$ was calculated with Eq. 1

Total sample weight (g)	Number of samples	Sample size (g)	Recalled batch $\Pr(n_+ > 0)$	Reference batch $\Pr(n_+ > 0)$
300	1	300	0.378	0.0118
300	3	100	0.612	0.011
300	10	30	0.896	-[a]
300	30	10	0.969	-[a]
300	100	3	0.999	-[a]

[a] No positive sample available with this sample size

Conclusions

Thorough investigation of the recalled batch showed that *Cronobacter* spp. were heterogeneously distributed throughout the batch containing parts with no detectable contamination and parts with concentrations varying between -2.52 and 2.75 log CFU/g. Clusters of cells occurred sporadically in 8 out of 2290 samples of 1 g. The two largest clusters contained 123 (2.10 log CFU/g) and 560 (2.75 log CFU/g) cells. Taking more and smaller samples and keeping the total sampling weight constant, improved the performance of the sampling plans to detect such a type of contaminated batch.

Acknowledgements

The authors would like to thank Arie van Kan, Ingrid Maas, Karin Metselaar, and Judith Wolkers for assisting in the work at the laboratory of Food Microbiology in Wageningen.

References

CAC (Codex Alimentarius Commission) (2008). Code of hygienic practice for powdered formulae for infants and young children. *CAC/RCP 66*.

CEC (Commission of the European Communities) (2007). Commission regulation (EC) No 1441/2007 on microbiological criteria for foodstuffs. *Official Journal of the European Union 1441/2007*, L 322/312-L322/328.

Cordier J. L. (2008). Production of powdered infant formulae and microbiological control measures. In M. Farber & S. J. Forsythe (Eds.), *Enterobacter sakazakii, emerging issues in food safety*. Washington DC: ASM Press, USA

FAO/WHO (Food and Agriculture Organization/World Health Organization) (2006). *Enterobacter sakazakii* and *Salmonella* in powder infant formula. Meeting report. *Microbiological Risk Assessment Series 10*. ISBN 92 5 105574 2.

Greenberg R. A., Tompkin R. B., Bladel B., Kittaka R. S. and Anellis A. (1966) Incidence of mesophilic *Clostridium* spores in raw pork, beef, and chicken in processing plants in the United States and Canada. *Applied Microbiology 14*(5), 789-793.

Gurtler J. B. and Beuchat L. R. (2005) Performance of media for recovering stressed cells of *Enterobacter sakazakii* as determined using spiral plating and ecometric techniques. *Applied and Environmental Microbiology 71*(12), 7661-7669.

Habraken C. J. M., Mossel D. A. A. and van den Reek S. (1986) Management of *Salmonella* risk in the production of powdered milk products. *Netherlands Milk Dairy Journal 40*, 99-116.

ICMSF (International Commission on Microbiological Specification for Foods) (2002) Microorganisms in Foods 7. *Microbiological Testing in Food Safety Management.* New York: Kluwer Academic/Plenum Publishers, ISBN 0 306 47262 7.

Iversen C., Druggan P., Schumacher S., Lehner A., Feer C., Gschwend K., Joosten H. and Stephan R. (2008) Development of a novel screening method for the isolation of "*Cronobacter*" spp. (*Enterobacter sakazakii)*. *Applied and Environmental Microbiology 74*(8), 2550-2553.

Kilsby D.C., and Baird-Parker A.C. (1983) Sampling programmes for microbiological analysis of food. In *Food Microbiology: advances and prospects* (pp. 309-315). T. A. Roberts, & F.A. Skinner.(Eds.) Society for Applied Bacteriology Symposium Series No. 11. London: Academic Press.

Legan J. D., Vandeven M. H., Dahms S. and Cole M. B. (2001) Determining the concentration of microorganisms controlled by attributes sampling plans. *Food Control 12*(3), 137-147.

High number of servings reduces the coefficient of variation of food-borne burden-of-illness

F. Pérez-Rodríguez[1] and M.H. Zwietering[2]

[1] Department of Food Science and Technology, University of Córdoba, Campus de Rabanales, C-1, 14014 Córdoba, Spain
[2] Laboratory of Food Microbiology, Wageningen University, P.O. Box 8129, 6700 EV Wageningen, The Netherlands

Abstract

The Central Limit Theorem (CLT) is proposed as a means of understanding microbial risk in foods from a Public Health perspective. On the basis of the CLT, the hypothesis introduced by this paper states that the coefficient of variation (CV) of the annual number of foodborne illness cases decreases as result of larger number of exposures (or servings) (n). Second-order Monte-Carlo analysis and Classical statistic were used to prove the hypothesis, based on existing risk models on *L. monocytogenes* in deli meats products focused on elderly people in United States. Likewise, the hypothesis was tested on epidemiological data of annual incidence of Listeriosis in different countries (i.e. different n). Although different sources of error affected the accuracy of results, both the Monte-Carlo analysis (*in silico*) and epidemiological data (*in vivo*) demonstrated that the CV of the annual number of cases decreased as n increased as stated by the CLT. Furthermore, results from this work showed that classical statistical methods can be helpful to provide reliable risk estimations based on simple and well-established statistical principles.

Keywords: *quantitative risk analysis, predictive microbiology, Central Limit Theorem, Public Health, Monte-Carlo analysis, Food-borne diseases*

Introduction

Public Health Surveillance systems are intended to record the occurrence of diseases or intoxication as caused by pathogens and toxicants present in foods, to analyze epidemiological data and to disseminate information. The information provided by surveillance systems is crucial to design and implement strategies and/or interventions to minimize food-borne illness. However, burden-of-illness estimates often pose uncertainty due to several important limitations: test sensitivity, underreported cases, deficiencies in reporting systems, scarce human resources, etc. Despite these important sources of uncertainty, variations in the number of annual cases still remains small in comparison to the variation in pathogen doses which in most cases can span several orders of magnitude. In this work, we aimed to introduce the idea that although there may be considerable variation between individual risks, the annual variation of the total risk (number of cases) will be small as a result of the Central Limit Theorem (CLT) of probability theory. The CLT can be thought of as the cornerstone for understanding collective phenomena (Sornette *et al*. 2003). Based on the CLT and properties of variance and mean, it could be stated that the higher number of exposures (doses) to the pathogenic microorganism, the lower uncertainty on the number of attendant annual cases. From that, it could be expected that pathogenic microorganisms with high prevalence in foods such as *Listeria monocytogenes* showed a decreasing trend in the illness incidence variability as population size increases (related to number of exposures). This hypothesis was demonstrated on epidemiological data, analytical calculation and Monte-Carlo analysis.

Materials and Methods

Burden-of-illness explained by Central Limit Theorem

From a probabilistic view, the overall risk distribution can be seen as the sum of **n** individual risk distributions, being **n** the number of doses or exposures in a certain population. If **n** is

sufficiently great and none of those distributions (e.g., individual risk distributions) dominate the resultant distribution (e.g. the overall risk distribution), the CLT can be applied. The CLT states that as the number of variables increases (infinite), the sum of those variables approximates (asymptotically) to a normal distribution with parameters $\mathbf{n}^*\mu$ and $\sqrt{\mathbf{n}}^*\sigma$. The CLT applied to the sum of variables uses the properties of variance and mean to estimate μ and σ of the resultant normal distribution. It is important to note that although CLT conditions can not be reached exactly, a reasonable good approximation will be expected in a certain region around the mean whose accuracy will depend on how large the deviation from CLT is.

Based on the properties of variance and mean and CLT, it can be obtained that the coefficient of variance (CV) of the sum of variables follows the linear function:

$$\log_{10}(CV) = -0.5\log_{10}(n) + \log_{10}\left(\frac{\sigma_x}{\mu_x}\right) \quad (1)$$

Estimating Burden-of-illness by using Monte-Carlo Analysis (in silico)

Concentration at retail taken from Chen *et al*. (2003) was the initial input in the exposure assessment model previously developed by Perez-Rodriguez *et al*. (2007). After simulation, concentration at consumption in contaminated servings, i.e. doses, was obtained. The dose-response model modified by Perez-Rodriguez *et al*. (2007) was applied in the linear region ($r = 1.85\cdot10^{-14}$) and probability of getting ill (P_{ill}) was estimated by using concentration at consumption (doses) and a point-estimate value of serving size which corresponded to the mean value (64 g). To estimate the number of annual cases (i.e., overall risk), resultant distribution of individual probabilities of getting ill (individual risk) were summed **n** times by an iterative process (using Monte-Carlo analysis) being **n** the number of exposures corresponding with contaminated servings consumed by elderly population in the US which corresponded to $5.11\cdot10^7$ servings.

Estimating Burden-of-illness by applying the Central Limit Theorem

The initial input was the doses distribution taken from Monte-Carlo Analysis. Doses distribution ($\log_{10}$ cfu/serving) was described by a normal distribution with parameters σ_{logD} and μ_{logD}. The dose-response model was defined by a straight-line ($r = 1.85\ 10^{-14}$), therefore calculations of the probability of getting ill could be performed by applying the properties of variance and mean on the normal distribution of doses. If the logarithm is applied to dose-response model, then:

$$\log_{10}(P_{ill}) = \log_{10}(r) + \log_{10}(\text{Dose}) \quad (2)$$

Since variance does not change when a scalar value is summed, the distribution of $\log_{10}(P_{ill})$ denoted by $F(\text{Log}(P_{ill}))$ can be estimated according to the following expression:

$$F(\log_{10}(P_{ill})) = N(\mu_{logD} + \log_{10}(r), \sigma_{logD}) \quad (3)$$

Finally, based on CLT, the distribution of the number of cases of listeriosis can be approximated as the sum of **n** $N(\mu_D, \sigma_D)$, being **n**, the number of exposures (i.e. contaminated servings). The value for **n** was the same to that used by Monte-Carlo analysis ($\mathbf{n}=5.11\cdot10^7$):

$$F(\text{cases/year}) = N(\mathbf{n}\cdot\mu_D, \sqrt{\mathbf{n}}\cdot\sigma_D) \quad (4)$$

Epidemiological data analysis (in vivo)

Incidence data of food-borne diseases by *L. monocytogenes* in different countries around the world were collected from international and national surveillance system databases. The selection of countries was based on criteria of population size (~10^7-10^8) and reliability of the surveillance system. When possible, data were taken from the same source in order to avoid additional variation sources. Incidence data were expressed as confirmed number of cases per year. The CV was calculated for each country in the period 2002-2007 based the mean population in that same period.

Results and Discussion

Monte Carlo analysis resulted in a mean estimation of 29 annual cases of listeriosis with 95th percentile of 49 cases. On the other hand, analytical method based on the CLT obtained a lower number of cases with a mean and 95th percentile of 7 and 23 cases/year. Table 1 shows main statistics for the estimated number of listeriosis cases at a different number of exposures (**n**) for both approaches. Data revealed that both approaches converged to similar values as **n** increased. Mean values presented major similarity between both approaches at lower **n**. However, standard deviation and 95th values required a higher number of exposures (**n**) to converge. Results indicated that both approaches could be equivalent to estimate risk provided some requirements be met such as linearity in dose-response model and normality in the microbial concentration distribution as given in this example.

Table 1: Comparison between Monte-Carlo analysis and central Limit Theorem (CLT) for number of listeriosis cases at different number of contaminated servings or exposures (**n**)

n	Mean		Standard Deviation		95th		Coefficient of Variance	
	MC	CLT	MC	CLT	MC	CLT	MC	CLT
10	$4.59 \cdot 10^{-6}$	$1.47 \cdot 10^{-6}$	$2.39 \cdot 10^{-4}$	$4.13 \cdot 10^{-3}$	$1.68 \cdot 10^{-3}$	$6.80 \cdot 10^{-3}$	5.21·10	$2.80 \cdot 10^{3}$
10^2	$6.98 \cdot 10^{-5}$	$1.47 \cdot 10^{-5}$	$3.94 \cdot 10^{-3}$	$1.31 \cdot 10^{-2}$	$2.68 \cdot 10^{-4}$	$2.15 \cdot 10^{-2}$	5.65·10	$8.87 \cdot 10^{2}$
10^3	$4.72 \cdot 10^{-4}$	$1.47 \cdot 10^{-4}$	$8.71 \cdot 10^{-3}$	$4.13 \cdot 10^{-2}$	$2.23 \cdot 10^{-3}$	$6.81 \cdot 10^{-2}$	1.85·10	$2.80 \cdot 10^{2}$
10^4	$4.91 \cdot 10^{-3}$	$1.47 \cdot 10^{-3}$	$4.22 \cdot 10^{-2}$	$1.31 \cdot 10^{-1}$	$1.71 \cdot 10^{-1}$	$2.16 \cdot 10^{-1}$	8.58	8.87·10
10^5	$5.34 \cdot 10^{-2}$	$1.47 \cdot 10^{-2}$	$4.20 \cdot 10^{-1}$	$4.13 \cdot 10^{-1}$	$1.19 \cdot 10^{-1}$	$6.94 \cdot 10^{-1}$	7.86	2.80·10
10^6	$5.50 \cdot 10^{-1}$	$1.47 \cdot 10^{-1}$	1.66	1.31	1.11	2.30	3.02	8.87
10^7	5.66	1.47	8.27	4.13	9.64	8.27	1.46	2.80
*$5.11 \cdot 10^7$	2.83·10	7.53	4.22·10	9.34	4.92·10	2.29·10	1.66	1.24

*Due to computational restrictions, total number of cases for **n** = $5.11 \cdot 10^7$ were estimated by extrapolation based on the trend shown by each statistic parameter (e.g. the mean number of cases was estimated by multiplying by 5.11).

Overall, when different numbers of exposures (**n**) were studied by Monte-Carlo analysis, CV (log) reduced as **n** becomes higher (Figure 1) except for very low numbers of exposures (10-100) which did not show a clear decrease trend. Monte-Carlo analysis does not yield reliable estimations when low numbers of samples are simulated since standard deviation of the simulated distribution is not yet stabilized. Nevertheless, the discrepancies observed between CLT and Monte-Carlo analysis were progressively reduced as the number of exposures was increasing (**n** $\geq 10^6$). Convergence between both approaches is not a fact which can be observed at relatively low number of exposures because of, according to CLT, normality for sum of variables is met when **n** approximates to infinite, i.e. **n** becomes enormously high.

The regression analysis applied on Monte-Carlo analysis and Epidemiological data did not derive the exact mathematical equation given by the CLT (eq. 1). Nevertheless, regression analysis confidence intervals indicated a reasonable convergence to The Central Limit Theorem (Table 2). Probably, additional sources of uncertainty coming from the Random Number Generator seed variation and the high-dependency of Monte-Carlo analysis on the number of iterations together with the expected uncertainty derived from food-borne outbreaks reporting systems could be responsible for the lack of accuracy and precision in data.

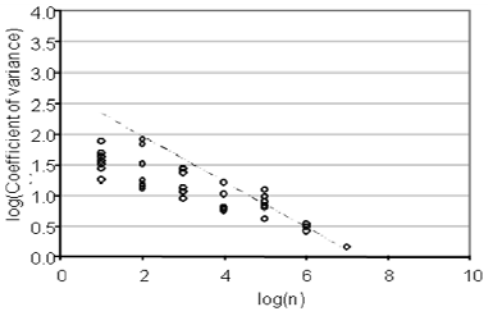

Figure 1: Representation on logarithmic scale of coefficient of variance (CV) of annual burden-of-illness obtained by Monte-Carlo analysis at different number of exposures (**n**). Solid line corresponded to the CV trend based on Central Limit Theorem (CLT) and dashed line represents the fitted eq. (1) to Monte-Carlo analysis data in range $\mathbf{n}=10^5$-10^7.

Table 2: Regression Parameters and statistics describing log-linear decrease of the coefficient of variance (eq. 1) fitted to data obtained from Monte-Carlo analysis and epidemiological data at different number of exposures (**n**).

Illness	*Data*	*m*	*Standard Error*	*p-value*	*Lower 95%*	*Upper 95%*	R^2	$R^2(m=-0.5)$
Listeriosis	Monte-Carlo	-0.37	0.06	<0.01	-0.51	-0.22	0.81	0.61
Listeriosis	Epidemiological	-0.20	0.07	0.11	-0.56	0.15	0.38	0.00

Conclusions

In many areas, the Central Limit Theorem is used as a first approach to understanding phenomena from a global perspective (e.g. economic sciences). Interpretation about reality is always complex and general rules can be helpful to extract basic and useful information. This was the main purpose in this work in which an attempt was made to study Microbiological Risk Assessment aspects from an angle of Public Health. The hypothesis suggested in this work was that "annual variation in number of food-borne illness cases is reduced as result of major exposure intensity (**n**)". Results did show a clear decreasing trend in the coefficient of variance of number of annual cases as **n** increases. Furthermore, the present study shows that classical statistical methods can be helpful to provide sound probabilistic risk estimation based on simple and well-established statistical principles.

Acknowledgements

This work was partly financed by MICINN AGL2008-03298/ALI, the Excellence Project AGR-01879 (Junta de Andalucía) and by the Research Group AGR-170 HIBRO of the "Plan Andaluz de Investigación, Desarrollo e Innovación" (PAIDI).

References

Chen Y., Ross W. H., Scott V. N. and Gombas D.E. (2003). Listeria monocytogenes: Low Levels Equal Low Risk. *Journal of Food Protection* 66, 570-577.

Pérez-Rodríguez F., van Asselt E. D., García-Gimeno R. M., Zurera G. and Zwietering M.H. (2007). Extracting additional risk managers information from a risk assessment of Listeria monocytogenes in deli meats. *Journal of Food Protection* 70, 1137–1152. 5.

Sornette, D. eds. Critical Phenomena in Natural Sciences. Chaos, Fractals, Selforganization and Disorder: Concepts and Tools. 2nd ed. New York, PA: Springer-Verlag Berlin Heidelberg; 2006.

Impact of microbial count distributions on human health risk estimates

A.S.R. Duarte, M.J. Nauta

Technical University of Denmark, National Food Institute (DTU Food), Division of Microbiology and Risk Assessment, Mørkhøj Bygade 19, 2860 Søborg, Denmark.(asrd@food.dtu.dk)

Abstract

In quantitative microbial risk assessment (QMRA), risk estimates are a function of the variability in concentrations of the bacterial pathogen in the food product concerned and the dose-response relationship. The choice of the probability distribution describing the pathogen variability may therefore be important. The lognormal distribution is a common choice, which is however complicated by the observation of relatively high proportions of zeros and low numbers in microbial counts. Discrete distributions have been indicated as alternatives to model counts with a considerable amount of low numbers, and their zero-inflations counterparts are considered appropriate to model counts with many zeros. In this study, we analysed the effect of the use of different distributions fitted to artificial data on the risk estimates in QMRA, using an existing QMRA model. A distribution of *Campylobacter jejuni* counts in chicken at retail was simulated and 9 data sets of 500 microbial counts were constructed, with 9 different proportions of zeros (10 to 90%). The outcome of fitting a negative binomial (NB), a zero-inflated NB (ziNB), a lognormal (LN) and a zero-inflated lognormal (ziLN) distribution to each of those samples was assessed, as well as the resulting estimates for the probability of illness (P_{ill}). The ziNB distribution showed a good fit to the data and P_{ill} estimates close to the expected P_{ill} in all cases. The NB overestimated the P_{ill} at high proportions of zero and the continuous distributions (LN and ziLN) underestimated the P_{ill} at low proportions of zero. These results showed that the choice of the distribution fitted through count data may have an important impact on the risk estimate.

Keywords: microbial counts, frequency distributions, risk estimates, QMRA

Introduction

Quantitative microbial risk assessment (QMRA) depends extensively on consistent descriptions of pathogen concentrations in food products (Busschaert *et al*. 2010). Numerous factors may have an impact on the collected data and on the frequency distribution used to describe it.

At the data assembly level, the existence of limits of quantification in the enumeration methods often leads to the gathering of semi-quantitative results (Busschaert *et al*. 2010). Recently, a maximum likelihood estimation (MLE) to represent censored results with parametric distributions has been proposed by many authors (Busschaert *et al*. 2010; Delignette-Muller *et al*. 2010; Lorimer and Kiermeier 2007). Microbial counts are often considered to follow a lognormal frequency distribution, which may be an acceptable assumption for high bacterial loads with negligible probability of zeros. However, the analysis of foodborne pathogen counts poses a challenge to this approach. The frequency distribution of pathogens in foods is characterized by a high probability of zero microorganisms and a high probability of low numbers. These characteristics complicate the fulfilment of log normality, as the lognormal distribution does not allow zero as an outcome and assigns probability to fractional numbers, which is not realistic at the low count level, where the difference between successive integers is high (ILSI 2010). Recently, many alternatives to the lognormal distribution have been discussed and proposed to represent bacterial data with low prevalence and low counts more appropriately (ILSI 2010; Gonzales-Barron *et al*. 2010). Discrete distributions, particularly generalizations of the Poisson distribution (negative binomial and Poisson-lognormal), have been indicated as better alternatives to model counts with a considerable amount of low numbers due to their ability to

model count data with over-dispersion (variance higher than the mean). Zero-inflated distributions were considered appropriate to model counts with a substantial amount of zeros as they are more adapted to extra zero-counts than the simple count distributions. However, there is little evidence available in the literature of the advantage of zero-inflated distributions over their non-zero-inflated counterparts. Recently, Gonzales-Barron *et al*. (2010) observed that for a data set with 42% zeros, the zero-inflated negative binomial distribution was comparable to the simpler negative binomial.

So far, most research on fitting distributions to microbial count data has focussed on the best statistical fits of the model to the data. In this study, we took it one step further and investigated the impact of the choice of the distribution fitted through bacterial count data on QMRA risk estimates. This was done by studying the effect of fitting artificially generated bacterial counts to either a discrete (negative binomial) or a continuous (lognormal) count distribution, or to their zero-inflated equivalents (zero-inflated negative binomial and zero-inflated lognormal), at different probabilities of zero counts. The effects were measured in terms of risk by using each distribution as the input for an existing QMRA model for *Campylobacter* in broiler meat.

Materials and Methods

Based on existing Danish retail data, a set of 500 count data of *Campylobacter jejuni* in poultry meat at retail was simulated, by sampling from a negative binomial (NB) distribution with mean concentration μ=8100 CFU/g and standard deviation σ=8100. Nine alternative sets of count data were constructed by randomly substituting 10% to 90% of the results by zeros.

Four types of frequency distributions were fit to each data set: a negative binomial (NB), a lognormal (LN) and their respective zero-inflated counterparts. The NB and the zero-inflated negative binomial (ziNB) were fit through null regression using STATA. The LN distribution was fit with a MLE method for censored data using the software R and the package "fitdistrplus" (Delignette-Muller *et al*. 2010). The zero counts were treated as being censored between $-\infty$ and -1 log CFU and the remaining results were treated as quantitative. The zero-inflated lognormal (ziLN) distribution was fit by MLE in Excel, with data arranged in semi-quantitative intervals.

To compare the impact of these different distributions on risk estimates, each frequency distribution was used as an input in an existing Consumer Phase Model (CPM) (Nauta *et al*. 2008) for broiler meat, combined with a dose response model (Nauta and Christensen 2011) to obtain estimates for the probability of illness (P_{ill}). A serving size of 100 g was assumed as standard in the model.

The different estimates of P_{ill} were visually compared with the expected P_{ill} for each data set. The expected P_{ill} was derived from the mean P_{ill} obtained with the initial NB distribution. Its value decreased in the same proportion as the probability of zeros present in the data set increased.

Results and Discussion

The estimates of the P_{ill} were obtained for each distribution and were compared with the expected P_{ill} (Fig. 1). The ziNB showed the best performance among all the candidate distributions, providing P_{ill} estimates that matched the expected values in all scenarios (different probabilities of zero CFU/g). This was not surprising, because the fitted count data were sampled from a ziNB distribution. For a data set without zeros, the expected P_{ill} was approximated by the P_{ill} estimates from the discrete NB and ziNB and underestimated with the use of the LN or ziLN as frequency distributions. When the probability of non-detects in the data increased, the two continuous distributions tended to approximate the expected P_{ill}, whereas the discrete NB increasingly overestimated it.

For increasing percentages of zeros, the difference between the non-zero-inflated distribution and its zero-inflated counterpart increased for the negative binomial distribution. Alternatively, the P_{ill} estimates showed smaller differences between LN and ziLN

distributions, where the LN provided even better estimates compared to its zero-inflated counterpart. The LN distribution has been indicated as appropriate to model high counts with a negligible probability of non-detects (ILSI, 2010). The poor fit that that distribution showed to a data set with 10% of zeros and its better fit to samples with higher probabilities may be related to the fact that the data in question was not made of high counts.

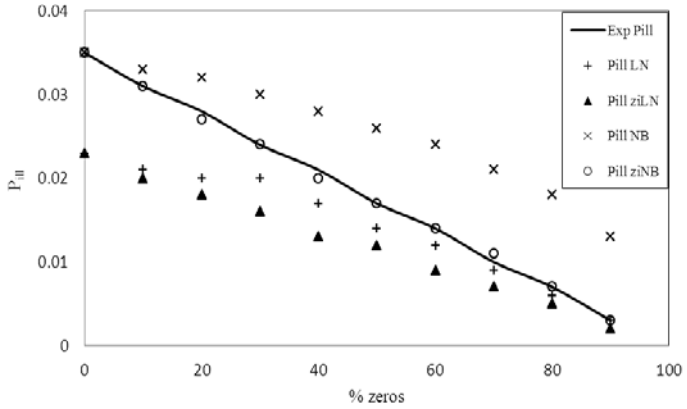

Figure 1: Expected probability of illness (P_{ill}) and estimates of P_{ill} obtained with four different frequency distributions, for data sets with various probabilities of zero CFU/g.

The difference between a P_{ill} estimate and the expected P_{ill} was apparently related to the fit of the frequency distribution to the data, especially at low count levels. Distributions that overestimated the probabilities of low counts, underestimated the P_{ill}. This was observed with the continuous distributions in data sets with low proportions of zeros (Fig. 2). Oppositely, when the probability of low counts was underestimated, as with the use of the NB with a 90% zero data set, the P_{ill} was overestimated. These results showed that the impact of a poor fit at low counts was higher than that of a poor fit at high count levels. The explanation for this fact lies in the dose-response curve. The slope of that curve is steeper for lower *Campylobacter* concentrations (Fig. 3), therefore, at that level of CFU counts, a misleading concentration frequency results in an amplified deviation from the expected P_{ill}.

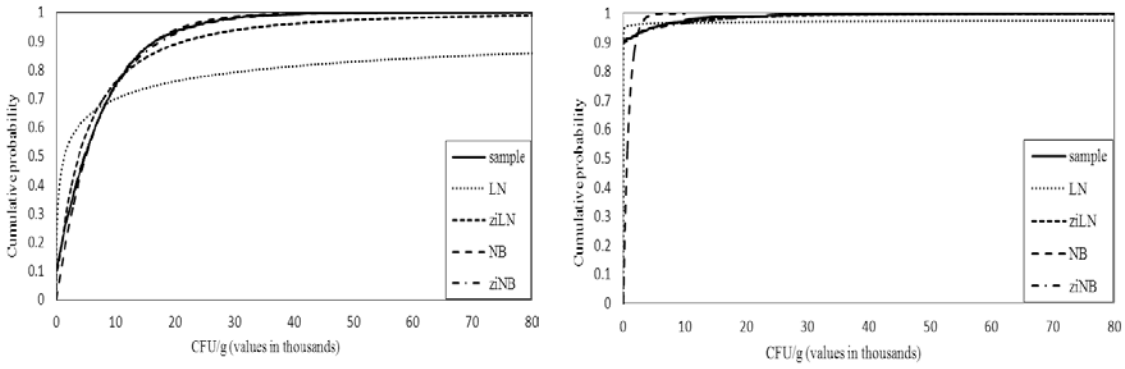

Figure 2: Cumulative density function of the data (sample) and the four fitted distributions, for a data set with 10% (left) and 90% probability of zero CFU/g (right).

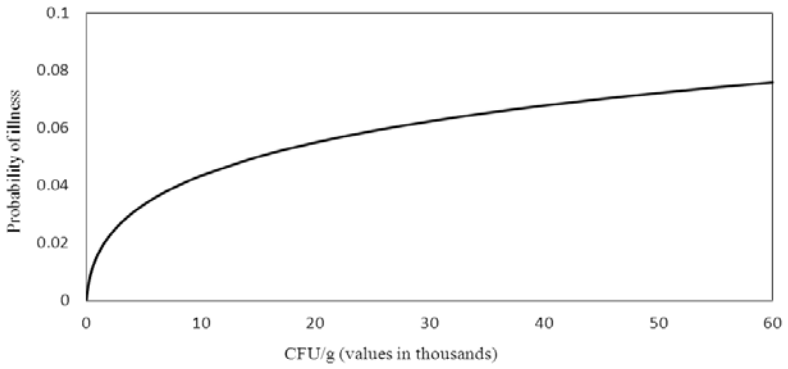

Figure 3: Dose-response relationship for *Campylobacter*.

Conclusions

We showed that the selection of the count distribution that describes the variability in the pathogen concentration has an impact in the risk estimate of a QMRA model.
Among the four distributions used in this study, the zero-inflated negative binomial showed a good fit and reliable P_{ill} estimates with all the data sets, independently of the proportion of non-detects. This result was expected due to the nature of the simulated data. The performance of the NB, LN and ziLN varied for data sets with different proportions of zero and, according to either an overestimation or underestimation of the probability of low counts they either underestimated or overestimated the P_{ill}, respectively. This effect was also associated with the specific dose-response curve used in the QMRA model.
The LN and ziLN distributions were not appropriate to model the data sets with low proportions of zero, contrarily to what was expected (ILSI 2010). This was probably due to the fact that the CFU numbers in the samples were not high enough to allow for the use of continuous distributions. However, further studies are needed to check this hypothesis. Specifically, it is important to investigate the reproducibility of the present results in a situation where data is generated from a continuous distribution.
We conclude that the estimated probability of illness can be highly influenced by the count distribution used to describe the pathogen concentration, in combination with the characteristics of the sample and the dose-response relationship. As fitting data with an inappropriate distribution may lead to an incorrect risk estimate, the choice of the distribution fitted through count data may be crucial in QMRA studies.

References

Busschaert P., Geeraerd A.H., Uyttendaele M. and Van Impe J.F. (2010) Estimating distributions out of qualitative and (semi)quantitative microbiological contamination data for use in risk assessment. *International Journal of Food Microbiology* 138 (3), 260-269.

Delignette-Muller M. L., Pouillot R., Denis J.-B. and Dutang C. (2010) Fitdistrplus: help to fit of a parametric distribution to non-censored or censored data. R package version 0.1-3. http://riskassessment.r-forge.r-project.org (accessed 30 January, 2011).

Gonzales-Barron U., Kerr M., Sheridan J.J. and Butler F. (2010) Count data distributions and their zero-modified equivalents as a framework for modeling microbial data with a relatively high occurrence of zero counts. *International Journal of Food Microbiology* 136, 268–277.

International Life Sciences Institute (ILSI) (2010) Impact of microbial distributions on food safety. http://www.ilsi.org/Europe/Publications/Microbial%20Distribution%202010.pdf (accessed 15 January, 2011).

Lorimer M.F. and Kiermeier A. (2007) Analysing microbiological data: Tobit or not Tobit? *International Journal of Food Microbiology*, 116, 313-318.

Nauta M.J., Fischer A.R.H., Van Asselt E.D., De Jong A.E.I., Frewer L.J. and De Jonge R. (2008) Food safety in the domestic environment: The effect of consumer risk information on human disease risks. *Risk Analysis* 28, 179–192.

Nauta M. and Christensen B. (2011) The impact of consumer phase models in microbial risk analysis. *Risk Analysis* 31, 255–265.

Quantitative Microbiological Risk assessment (QMRA) on foodborne zoonoses at European level

M. Hugas

European Food Safety Authority. Unit on Biological Hazards. Largo N.Palli 5/A. 43121 Parma .Italy.
marta.hugas@efsa.europa.eu

Introduction

EU Directive 178/2002 EC (General Food Law) requires food legislation to be based on "risk analysis" except where this is not appropriate for the circumstances or the nature of the measure. There is no specific requirement on the nature of the risk assessment and regulations can be based on qualitative as well as quantitative. EFSA is responsible for giving independent scientific advice for the European Community legislation and politics in all fields which have a direct or indirect impact on food and feed safety. EFSA's main attributes for this task are the Scientific Committee and the Scientific Panels. Questions from European risk managers are addressed in scientific opinions published by EFSA.

To provide scientific advice and risk assesments, EFSA has set up a structure existing of a Scientific Committee and Scientific Panels, involving scientists from all Member States. The Panel on Biological Hazards (BIOHAZ) provides independent scientific advice on biological hazards in relation to food safety and food-borne diseases. This covers: Food-borne zoonoses, Transmissible spongiform encephalopathies (BSE/TSEs), Food microbiology, Food hygiene and associated waste management issues. The BIOHAZ Panel carries out risk assessments in order to produce scientific opinions and advice for risk managers. This helps to provide a sound foundation for European policies and legislation and supports risk managers in taking effective and timely decisions.

The opinions of the BIOHAZ Panel are based on qualitative or quantitative assessments. The Panel aims to structure its opinions according to the established risk assessment framework with four stages: hazard identification, hazard characterization, exposure assessment and risk characterization. Due to the qualitative nature of some opinions, they can also be considered as risk profiles.

The application of Risk Assessment was promoted by the World Trade Organisation in 1995 with the ratification of the Agreement on the Application of Sanitary and Phyto-sanitary Measures (SPS Agreement). It requires that any measures applied to protect human, animal and plant health are developed using a scientific and transparent approach. The international developments on risk assessment and risk based management of microbial hazards have been coordinated mainly by the Codex Committee on Food Hygiene. The risk assessment framework as applied in food safety was initially defined by FAO, WHO and the Codex Alimentarius Commission (CAC, 1995) as a process consisting of three components: Risk assessment, Risk management and Risk communication. In the EU system risk assessment is the responsibility of EFSA, risk management is for the European commission, the Member States and/or the European Parliament, while risk communication is a shared responsibility between risk assessors and risk managers.

The risk analysis framework defined by FAO and WHO and adopted by CAC allows for the conduct of both qualitative and quantitative risk assessments. The decision which approach to take depends on the risk management issue, on the quality of the available data and on the available resources and time. CAC does not give specific guidance on the choice between qualitative and quantitative risk assessment although it is stated that "the use of quantitative information is encouraged to the extent possible, but the value of qualitative information should not be discounted" (CAC, 1999).

A study commissioned by EFSA in 2005 to Prof Havelaar (EFSA, 2005) identified many expected benefits from Quantitative Microbiological Risk Assessment (QMRA) at the European level: (i) a more solid basis for common and more objective, science-based criteria for food safety across Europe, (ii) the quantitative analyses would also support national food

safety risk management and help to evaluate the possibilities of different risk mitigation options that might be used by different Member States to reach common targets, (iii) the increased transparency of a quantitative approach was expected to improve risk communication between professionals and to help building trust among stakeholders, (iv) a European approach was also recommended because it enables the sharing and optimal use of available data and resources. This would be more efficient, and avoid duplication of work between Member States. Less experienced countries expected a European approach to be helpful in building up their capacities for risk based food safety management and stressed the need for the promotion and development of harmonised models and databases.
QMRA in the above report was also identified as to help to focus data collection efforts and identify key knowledge gaps, to provide more insight in complex processes and to integrate regulations across different stages of the food chain. It was also considered a useful tool to rank the relative contribution of different exposure pathways (food, water, person-to-person transmission, direct contact with animals etc.) resulting in better targeting of control options It has also been widely acknowledged that QMRA may lead to a more transparent, systematic and efficient risk management process including improved risk communication, resulting in reduced consumer exposure to microbial hazards.
Since the establishment of EFSA in 2002 and the appointment of the first mandate of the BIOHAZ Panel in 2003, the Panel has evolved in their scientific advice to the risk managers. The EU risk managers have also evolved in sending request for quantitative microbiological risk assessments to EFSA which have resulted in a full farm-to-fork microbiological risk assessment in the EU for the first time: *Salmonella* in slaughter and breeder pigs and *Campylobacter* in broilers apart form other quantitative studies on Salmonella in breeding hens, layers, broilers and turkey. In the results and discussion chapter, only the main results obtained from, the two first studies are mentioned.

Results and Discussion

Salmonella in pigs

Following a request from the European Commission, the Panel on Biological Hazards was asked to deliver a scientific opinion on a QMRA of *Salmonella*. The assessment was to provide the input for a future cost/benefit analysis of setting a target for reduction in slaughter pigs at EU level. EFSA commissioned a QMRA modelling the pig meat food chain from farm to fork. The QMRA model was based on input data from the baseline studies of *Salmonella* in breeder and slaughter pigs, and other relevant data.
The QMRA represents a major step forward in terms of modelling *Salmonella* in pigs from farm to consumption as it takes into account the variability between and within EU Member States (MSs). Around 10-20% of human *Salmonella* infections in EU may be attributable to the pig reservoir as a whole. From the QMRA analysis it appears that an 80% or 90% reduction of lymph node prevalence should result in a comparable reduction in the number of human cases attributable to pig meat products. Theoretically, according to the QMRA the following scenarios appear possible (a) by ensuring that breeder pigs are *Salmonella*-free a reduction of 70-80% in high prevalence MSs and 10-20% in low prevalence MSs can be foreseen; (b) by feeding only *Salmonella*-free feedstuffs, a reduction of 10-20% in high prevalence MSs and 60-70% in low prevalence MSs can be foreseen; and (c) by preventing infection from external sources of *Salmonella* (i.e. rodents and birds) a reduction of 10-20% in slaughter pig lymph node prevalence can be foreseen in both high and low prevalence MSs. A hierarchy of control measures is suggested - a high prevalence in breeder pigs needs to be addressed first, followed by control of feed and then control of environmental contamination. Also according to the QMRA, for each MS, a reduction of two logs (99%) of *Salmonella* numbers on contaminated carcasses would result in a 60-80% reduction of the number of human salmonellosis cases attributable to pig meat consumption.

Control of *Salmonella* in pig meat as a public health problem should be based on the individual MSs situations and include combinations of following interventions: Salmonella-

free (low risk) breeder pigs, Salmonella-free feed, cleaning-disinfection between batches both on-farm and during lairage, avoidance of faecal contamination during slaughter and decontamination of the carcasses. Efficient vaccination will also be useful to control Salmonella on farm, but might interfere with the interpretation of serological test results in monitoring/surveillance programmes. From the current evidence, it would appear that specific slaughterhouse interventions are, at present, more likely to produce greater and more reliable reductions in human illness, at least in a shorter timeframe than can be achieved at the farm in high prevalence MSs. However, the hypothetical reductions and multiple interventions investigated with the current risk assessment model suggest that MSs can achieve more effective reductions in human cases by targeting both farm and slaughterhouse. MSs should have the possibility to assess their national pig meat food chains using this QMRA model.
The slaughterhouse remains a critical step of the pig meat chain in respect to pig and carcass contamination and numerous aspects (e.g. airborne transmission of Salmonella in the abattoir) still remain unknown. Therefore studies need to be performed to properly assess the ways carcasses become contaminated.
The control of Salmonella in pig reservoir in the EU is a reasonable objective. The EU Salmonella control strategy in pigs should be continuously evaluated to identify possible improvements.

Campylobacter in broilers

Following a request from the European Commission, the Panel on Biological Hazards was asked to deliver a scientific opinion on Campylobacter in broiler meat production: control options and performance objectives and/or targets at different stages of the food chain. EFSA commissioned the development of a QMRA model which has been used to estimate the impact on human campylobacteriosis due to the presence of Campylobacter spp. in broiler meat. This QMRA was also used to rank/categorize selected intervention strategies in the farm to fork continuum, for which quantitative data, of sufficient quality on efficacy for Campylobacter reduction at the point of application, were available. The evaluation of microbiological criteria required the development of a specific model by the BIOHAZ Panel, using data from the EU baseline survey, as an input.
It is estimated that there are approximately nine million cases of human campylobacteriosis per year in the EU27. The disease burden of campylobacteriosis and its sequelae is 0.35 million disability-adjusted life years (DALYs) per year and total annual costs are 2.4 billion €. Broiler meat may account for 20% to 30% of these, while 50% to 80% may be attributed to the chicken reservoir as a whole (broilers as well as laying hens). The public health benefits of controlling *Campylobacter* in primary broiler production are expected to be greater than control later in the chain as the bacteria may also spread from farms to humans by other pathways than broiler meat. Strict implementation of biosecurity in primary production and GMP/HACCP during slaughter may reduce colonization of broilers with *Campylobacter*, and contamination of carcasses. The effects cannot be quantified because they depend on many interrelated local factors. In addition, the use of fly screens, restriction of slaughter age, or discontinued thinning may further reduce consumer risks but have not yet been tested widely. After slaughter, a 100% risk reduction can be reached by irradiation or cooking of broiler meat on an industrial scale. More than 90% risk reduction can be obtained by freezing carcasses for 2-3 weeks. A 50-90% risk reduction can be achieved by freezing for 2-3 days, hot water or chemical carcass decontamination. Achieving a target of 25% or 5% BFP in all other MS is estimated to result in 50% and 90% reduction of public health risk, respectively. A public health risk reduction > 50% or > 90% could be achieved if all batches would comply with microbiological criteria with a critical limit of 1000 or 500 CFU/gram of neck and breast skin, respectively, while 15% and 45% of all tested batches would not comply with these criteria.
Microbiological criteria could theoretically be implemented immediately but the ability to comply will also differ between MSs. They stimulate improved control of *Campylobacter* during slaughter.

The BIOHAZ Panel recommended that effective control options should be selected and verified under conditions where the application is intended to be used by industry to reduce Campylobacter and comply with potential targets and/or MC when established. Several data gaps were identified and generation of data in several areas was recommended.

Conclusions

QMRA of food borne pathogens at European level has been proved as a feasible and good tool to enable risk managers to undertake impact assessment studies so to evaluate the feasibility and the cost/benefit of introducing control measures and target to further protect public health of European consumers.
The BIOHAZ Panel after undertaking some major exercises n identifying quantitatively some microbiological risks in some animal populations and/or foodstuffs is now reflecting which were the lessons learnt and how improvements could be introduced in future exercises.

Acknowledgements

The author wishes to thanks the BIOHAZ Panel and its working groups on the preparation of the opinions reported above, particularly Prof. Ivar Vagsholm the WG chair for the *Salmonella* opinion in slaughter and breeding pigs and Prof. Arie Havelaar for the *Campylobacter* opinion. I feel also obliged to acknowledge the work and devotion of the EFSA staff in the BIOHAZ unit.

References

Principles and guidelines for the conduct of microbiological risk assessment, Codex Alimentarius Commission, Rome, 1999. CAC/GL30, p.4.

The Application of Risk Analysis to Food Standards Issues. Report of a joint FAO/WHO Expert Consultation. World Health Organization, Geneva, Switzerland. 1995.

EFSA Panel on Biological Hazards (BIOHAZ); Scientific Opinion on *Campylobacter* in broiler meat production: control options and performance objectives and/or targets at different stages of the food chain. *EFSA Journal 2011* ;9(4):2105. [7 pp.]. doi:10.2903/j.efsa.2011.2105. Available online: www.efsa.europa.eu/efsajournal

EFSA Panel on Biological Hazards; Scientific Opinion on a Quantitative Microbiological Risk Assessment of *Salmonella* in slaughter and breeder pigs. *EFSA Journal 2010*; 8(4):1547. [7 pp.]. doi:10.2903/j.efsa.2010.1547. Available online: www.efsa.europa.eu/efsajournal

An accept-and-reject algorithm to determine performance objectives that comply with a food safety objective

L. Guillier[1], J.-C. Augustin[1,2], J.-B. Denis[3], M.-L. Delignette-Muller[4]

[1] Agence nationale de sécurité sanitaire (Anses), Laboratoire de sécurité des aliments, 23 avenue du Général de Gaulle, F-94700 Maisons-Alfort, France (laurent.guillier@anses.fr)
[2] Université Paris-Est, Ecole Nationale Vétérinaire d'Alfort, Unité USC MASQ, 7 Avenue du Général de Gaulle, F-94704 Maisons-Alfort Cedex, France (jcaugustin@vet-alfort.fr)
[3] INRA, UR341 Mathématiques et informatique appliquées, F-78350 Jouy-en-Josas (Jean-Baptiste.Denis@jouy.inra.fr)
[4] Université de Lyon, CNRS UMR 5558, Laboratoire de Biométrie et Biologie Evolutive, VetAgro Sup, 1 avenue Bourgelat, 69280 Marcy l'Etoile, France (ml.delignette@vetagro-sup.fr)

Abstract

Quantitative risk assessment of microbiological hazards in foods (QMRA) can assess the impact of control measures on risk and can help to achieve food safety targets. Generally, the effect of a particular input variable of a QMRA model is assessed by comparing the results corresponding to the default situation to those obtained from scenarios modifying its behaviour. The purpose of this work is to handle and propose alternative methods to scenario testing for determining PO (performance objective) or process criterion from a given FSO (food safety objective). These methods were applied in the framework of a QMRA model that considered the fate of a hazard from raw material to the consumption stage. A second order Monte-Carlo simulation approach separately assessing the uncertainty and variability on the final exposure, we applied an accept-and-reject algorithm to measure the importance of each variable of the model and to determine, with its uncertainty, the probability of compliance with an FSO according to the range of values that these variables can take. Within a first order Monte-Carlo simulation approach, we applied the Saltelli sensitivity analysis method to select the most influential variables on the compliance with the FSO. Then, an accept-and-reject algorithm was applied for the most influential variables. With both approaches, we managed to identify influential variables and were able to determine which ranges of values should be met to respect the FSO. Complications originated from correlated variables or QMRA models with low probability to reach the FSO were also tackled. It is concluded that accept-and-reject algorithms are simple methods to apply and that they allow extrapolation of the classical point estimate scenario analysis to the entire range of values taken by input variables.

Keywords: *exposure assessment; performance objective; accept and reject algorithm*

Introduction

Quantitative risk assessment of microbiological hazards (QMRA) in foods is now a widely applied methodology. Originally founded to meet the needs of risk managers such as governments or international organizations, it assesses the impact of general measures on risk and can help to achieve food safety targets. These targets could be "the maximum frequency and/or concentration of a hazard in a food at the time of consumption" (food safety objective, FSO) or "at a specified step in the food chain before the time of consumption" (performance objective, PO) (Codex Alimentarius 2004). The use of QMRA is not limited to institutional organizations; today it is an integrated methodology for some industries or professional associations. QMRAs can provide assistance to move HACCP from a mostly "hazard based" approach to a "risk-based" quantitative modelling. POs and process criteria (PC) can then be calibrated to comply with FSO.

However, it is not straightforward to get back from a given objective (e.g. FSO) "up" to operational values (e.g. critical limits, process and product criteria) (Havelaar *et al.* 2004; Rieu *et al.* 2007). Generally a variable of a QMRA model is assessed by comparing the results corresponding to the default situation to those obtained from different scenarios (e.g.

Tuominen *et al.* 2007). The objective of this work was to handle and propose alternative methods to scenario testing for determining PO or PC from a given FSO.

Materials and Methods

Exposure assessment model

In order to handle and compare different methods for determining PO or PC from a given FSO, we proposed the use of an exposure assessment model. This theoretical model is not linked to a specified hazard or food process and was only built for the didactic reasoning. This model considered the fate of a hazard along three stages: growth in raw material, inactivation during cooking and growth during storage. Model parameters and relation between nodes are presented in Figure 1.

A second-order Monte Carlo simulation (MC2D) (Pouillot and Delignette-Muller 2010) was used in order to separately assess the uncertainty and variability on final exposure at the end of storage (N3). We also considered the same model without separating uncertainty and variability (MC1D). We focused on how to determine the levels of five variables (t_2, T_2, T_3, T_1, N_0), on which risk managers can act, that comply with the FSO. We chose for FSO a value of 5 $\log_{10}$ (cfu/g).

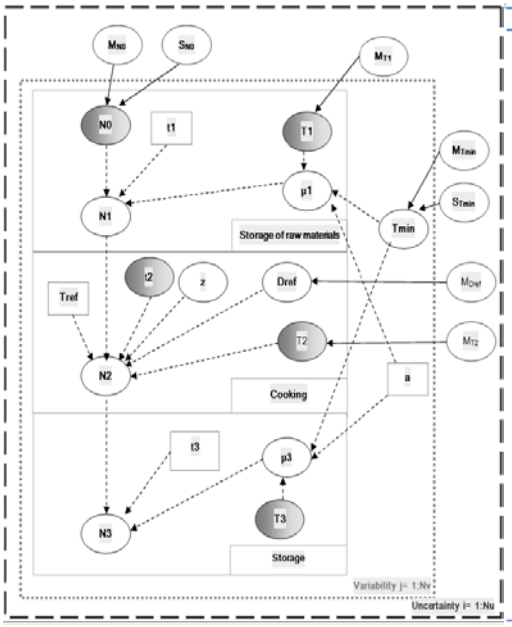

Parameter	Variability	Uncertainty	Abbreviation	Definition	Unit
Parent nodes					
Mean of initial concentration		X	M_{N0}	N(2.2,0.1)	$\log_{10}$(cfu/g)
Standard deviation of initial concentration		X	S_{N0}	Unif(0.05,0.15)	$\log_{10}$(cfu/g)
Mean of temperature of storage of raw materials		X	M_{T1}	N(4,0.1)	°C
Mean of cooking temperature		X	M_{T2}	N(63,0.2)	°C
Mean of minimal growth temperature		X	M_{Tmin}	N(-4,1)	°C
Standard deviation of minimal growth temperature		X	S_{Tmin}	Unif(0.2,0.3)	°C
Mean decimal reduction time at T_{ref}		X	M_{Dref}	Unif(0.5,0.7)	minutes
Duration of storage of raw materials			t_1	10	hours
Shelf life duration			t_3	140	hours
Cooking duration	X		t_2	N(5,0.5)	minutes
Classical thermal resistance constant	X		z	N(8,0.05)	°C
Temperature throughout shelf-life	X		T_3	N(6,1.5)	°C
Constant of the square-root model for growth rate			a	0.033	-
Reference temperature			T_{ref}	70	°C
Child nodes	X				
Initial contamination	X		N_0	$N(M_{N0},S_{N0})$	$\log_{10}$(cfu/g)
Contamination before cooking	X		N_1	$N_0+\log_{10}(\exp(\mu_1.t_1))$	$\log_{10}$(cfu/g)
Temperature of storage of raw materials	X		T_1	$N(M_{T1},1)$	°C
Growth rate during storage of raw materials	X		μ_1	$(a.(T-T_{min}))^2$	h^{-1}
Minimal growth temperature	X		T_{min}	$N(M_{Tmin},S_{Tmin})$	°C
Decimal reduction time at T_{ref}	X		D_{ref}	$N(M_{Dref},0.05)$	minutes
Cooking temperature	X		T_2	$N(M_{T2},0.5)$	°C
Contamination after cooking	X		N_2	$N_1-t2/10^{((Dref-(T2-Tref))/z)}$	$\log_{10}$(cfu/g)
Growth rate during storage	X		μ_3	$(a.(T_3-T_{min}))^2$	h^{-1}
Contamination at consumption	X		N_3	$Min(9,N_2+\log_{10}(\exp(\mu_3.t_3)))$	$\log_{10}$(cfu/g)

Figure 1: Directed acyclic graph of the exposure model and definition of the parameters of the model. Logical links between nodes are represented by dotted arrows whereas solid arrows indicate stochastic links. Ellipses represent uncertain and/or variable nodes while rectangles represent constants. Shaded ellipses correspond to variables of interest.

Accept-and-reject algorithm

In the MC2D framework, we proposed the following algorithm in order to check the importance of five considered variables :

1. Sample random values in the uncertainty distributions (index i from 1 to N_u):
    2. Sample random values in the variability distributions, conditionally to uncertainty (index j from 1 to N_v):
    - If $N3_{i,j}$<FSO accept $X_{i,j}$ and registered its value in X_A
    - Else registered $X_{i,j}$ in X_R

In the MC1D framework, steps 1 and 2 are combined in the same loop, with only one index.

Sensitivity analysis

Sensitivity analysis was only applied in the MC1D framework.The impact of variables (Table 1) on compliance with FSO was checked with sensitivity analysis (SA). The output of the

model N3, was here expressed in 0 and 1 (respectively lower or higher than 5 $\log_{10}$ cfu/g, the FSO). For sensitivity analysis we used the Saltelli method (2002). This SA method is based on variance decomposition and computes first order indices (S*i*) which represent the main effect contribution of each input factor to the variance of the output, and total effect indices (S*ti*) which account for the total contribution to the output variance due to the first order effects (Si) and to their non linear interactions.

Probability of compliance to the FSO

For each variable of interest we considered the range of possible values different variables can take. Each range was divided in *k* classes of equal size. Let nb_A and nb_R (A, R for Acceptance and Rejection) as the numbers of simulation runs (in the variability dimension for the MC2D framework) that allow compliance or non-compliance with a FSO, respectively. This was done for each class of the considered variable. We could then calculate the probability of compliance with the criterion for the class *k* by $P_k = \frac{nb_A}{nb_A + nb_R}$.

P_k ranges from 0 to 1. Variation of P_k through the different classes indicates that the order of magnitude of the variable is of importance for the compliance of the FSO. In the MC2D framework, N_u values of P_k were obtained (one for each value of index i), enabling the characterization of its uncertainty.

Results and Discussion

Sensitivity analysis

Table 1 summarises the results of SA of the model in MC1D framework. The variables influencing the compliance of the FSO were mainly D_{ref}, T_3 and T_2 and then T_{min}, t_2, z, T_1, N_0. Apart from T_3 which had a first order indice of importance, other variables influenced the compliance of the FSO interacting with other variables.

Table 1: Estimates of the first order (Si) and total effect (Sti) indices of the sensitivity analysis and their bootstrap confidence intervals.

Factor	Range	S*ti*	S*i*
N_0 ($\log_{10}$ cfu/g)	1.5, 2.85	0.05 [0.02,0.08]	0.00 [-0.01,0.00]
T_{min} (°C)	-5.4, -3.8	0.15 [0.12,0.18]	0.02 [0.01,0.03]
T_1 (°C)	2.5, 5.6	0.03 [0.00,0.05]	0.00 [0.00,0.00]
T_2 (°C)	60.5, 65.4	0.19 [0.16,0.21]	0.02 [0.02,0.03]
t_2 (min)	3.5, 6.5	0.14 [0.11,0.16]	0.01 [0.00,0.02]
D_{ref} (sec)	10, 20	0.18 [0.16,0.21]	0.02 [0.01,0.03]
Z (°C)	7.2, 10.4	0.15 [0.13,0.18]	0.01 [0.01,0.02]
T_3 (°C)	1.5, 10.5	0.92 [0.89,0.94]	0.65 [0.64,0.66]

Probability of compliance

Figure 2 shows the probabilities of compliance according to the values of the variables for the initial contamination level (N_0), the temperature of cooking (T_2) and the storage temperature (T3) in the MC2D framework. The mean, 5 and 95th percentiles of the probability of compliance to the FSO are shown. Uncertainty was very large for N_0 and T_2 and the probability of compliance was slightly affected by the values these variables can take. The same conclusion can be drawn for t_2 and T_1 (data not shown). T_3 greatly impacted the probability of compliance to the FSO. For example if T_3 is below 4°C the mean probability of compliance is higher than 95%.

Correlations between variables

Before applying accept-and-reject algorithm, parameters of the model were independent. Figure 3 shows examples of correlations between parameters induced by the algorithm. Theses correlations should be taken into account for setting PO or PC values that comply with FSO.

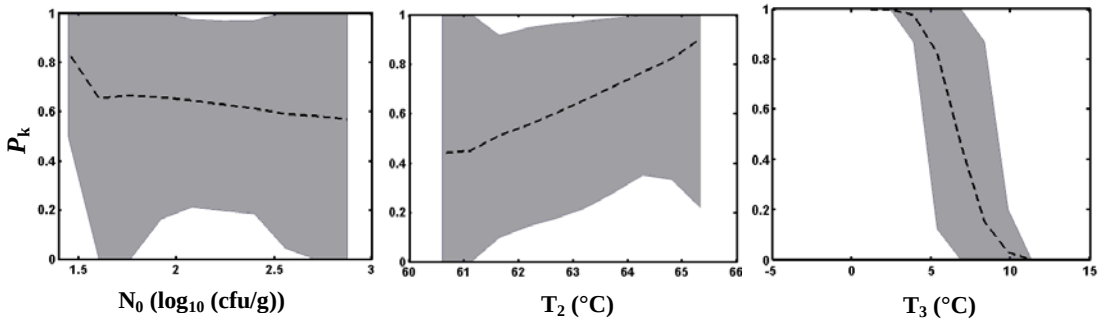

Figure 2. Probabilities of compliance to the FSO according to possible values of three variables of interest. Dotted lines represent mean P_k. Shaded areas characterize uncertainty : they comprise 90% of simulated P_k values (between 5th and 95th percentiles).

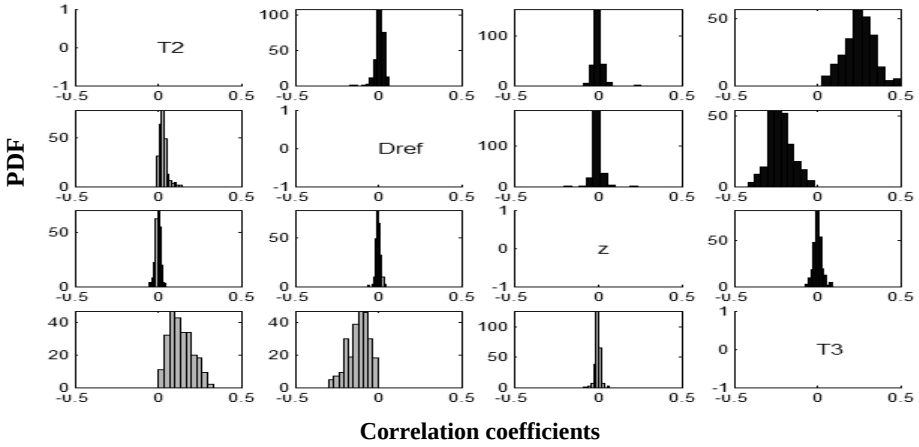

Figure 3. Distributions of N_u values of correlation coefficients between some variables of the model. In dark correlation coefficients for accepted set of parameters, in gray for rejected.

Conclusions

Sensitivity analysis methods are efficient in determing which variables of a model impact on the compliance with FSO. For the determination of PO or PC, accept-and-reject algorithms are simple tools to apply and are more powerful than classical point estimate scenario analysis as the entire space of values taken by input variables is considered.

Acknowledgements

This work was supported by a grant from the Agence Nationale de la Recherche (ANR) (France), as a part of the Quant'HACCP project.

References

Codex Alimentarius (2004) Commission, Procedural Manual, 14th Edition, Appendix IV, Working Principles for Risk Analysis for Application in the Framework of the Codex Alimentarius.

Havelaar A.H, Nauta M.J. and, Jansen J.T. (2004) Fine-tuning Food Safety Objectives and risk assessment. *International Journal of Food Microbiology* 93(1), 11-29.

Pouillot R. and Delignette-Muller M.-L (2010) Evaluating variability and uncertainty separately in microbial quantitative risk assessment using two R packages, *International Journal of Food Microbiology* 142, 330-340.

Rieu E., Duhem K., Vindel E. and Sanaa M. (2007) Food safety objectives should integrate the variability of the concentration of pathogen. *Risk Analysis* 27(2), 373-86.

Saltelli A. (2002). Making best use of model evaluations to compute sensitivity indices. *Computer Physics Communications* 145, 280-297.

Tuominen P., Ranta, J. and Maijala, R. (2007) Studying the effects of POs and MCs on the *Salmonella* ALOP with a quantitative risk assessment model for beef production. *International Journal of Food Microbiology* 118, 35-51.

The Application of the Appropriate Level of Protection (ALOP) and Food Safety Objective (FSO) concepts in food safety management, using *Listeria monocytogenes* in deli meats as a case study

E. Gkogka[1], M.W. Reij[1], L.G.M. Gorris[1,2], M.H. Zwietering[1]

[1] Laboratory of Food Microbiology, Wageningen University, Wageningen, The Netherlands. (elissavet.gkogka@wur.nl)
[2] Unilever R&D Shanghai, Shanghai 200335, China. (Leon.Gorris@unilever.com)

Abstract

To establish a link between governmental food safety control and operational food safety management, the concepts of the Appropriate Level of Protection (ALOP) and the Food Safety Objective (FSO) have been suggested by international bodies as a means of making food safety control transparent and quantifiable. The purpose of this study was to investigate how the concepts of ALOP and FSO could be applied in practice. As a case study, the risk of severe listeriosis due to consumption of deli meat products in the Netherlands was taken. The link between these concepts was explored for two situations following a "top-down" approach, using epidemiological country data as a starting point, and a "bottom-up" approach, using data on the prevalence and concentration of the pathogen at retail as a starting point. Models based on both approaches were able to describe the link between ALOP and FSO and our results showed that meaningful estimations are feasible, although interpretations need to be made with care. For the top-down approach, the mean estimated value derived for ALOP was 3.2 cases per million inhabitants per year (95% CrI: 1.1-6.6). For the bottom-up approach, ALOP values ranged considerably, 4.7-55 (with 95% CrI ranging from 2.9-162), depending on the input parameters selected. The level of detail considered in the stochastic models considerably influenced the ALOP and FSO estimates. As best practice it is recommended to develop both approaches, although depending on the application context one may appear more appropriate than the other.

Keywords: *risk assessment, stochastic modelling, foodborne disease, public health targets*

Introduction

Food safety is an issue of fundamental public health concern and providing guidance to the food industry on achieving a safe food supply poses major challenges for competent authorities who have the responsibility to articulate the level of control they expect the industry to achieve. To establish a link between governmental public health goals related to food safety and operational food safety management, the concepts of the Appropriate Level of Protection (ALOP) and the Food Safety Objective (FSO) have been suggested by respectively the World Trade Organization (WTO 1995) and Codex Alimentarius (2010) as a means of making food safety control transparent and quantifiable. A major difficulty related to the implementation of these concepts is that they are still evolving and there is no uniform agreement with regards to their use (Stringer 2005). A consistent approach is necessary from a legal point of view (WTO 2000). So far very few case-studies have been published on how these concepts might work in practice (Crouch *et al.* 2009; Membré *et al.* 2007; Rieu *et al.* 2007; Tuominen *et al.* 2007). Our aim was to investigate further how the ALOP and FSO concepts could be applied in a real life example, the risk of severe listeriosis due to the consumption of deli meat products (cooked ready-to-eat meat products) in the Netherlands. In this example, two likely approaches to establish a link between the concepts have been followed. One approach was based on analysis of public health data and epidemiological surveys (from now on referred to as the top-down approach). The second approach was based on data related to the level and/or frequency of *Listeria monocytogenes* in deli meat, from which through a risk characterization curve disease incidence estimates are derived (from

now on referred to as the bottom-up approach) (Codex Alimentarius 2007). Our aim is to compare both approaches.

Materials and Methods

For the two different approaches the estimation steps in either Figure 1 or 2 were followed. Stochastic models were built in Microsoft Excel using the @RISK 5.7 software (Palisade Corporation). The dose response model was the common element in both approaches (WHO/FAO, 2004) through the formula:

$$LOP = S \cdot 10^6 \cdot (1 - \exp(-r \cdot D)) \text{ or } LOP = S \cdot 10^6 \cdot (1 - \exp(-r \cdot M \cdot 10^{SO})) \quad (1)$$

where: LOP = the Level of Protection, defined as the currently achieved number of cases of severe listeriosis per million people per year in each risk group, being either the healthy or the susceptible population (Young-Old-Pregnant-Immunocompromised or YOPI)
S = the number of servings per person per year
r = the probability of a single microorganism causing listeriosis for each risk group
D = the dose consumed (log CFU)
M = the mass per serving (g)
SO = the Safety Objective, defined as the concentration of microorganisms at consumption (log CFU per g)

The FSO was considered to be the stricter of the two estimated SO in the top down approach. The ALOP was considered to be the sum of the LOPs for the healthy and the susceptible population after adjusting for the different percentages of each group in the general population in the bottom up approach. In their baseline version the models were built as simple as possible and alternative versions were included using different deterministic or stochastic input parameters for r, M and S and selecting r values based on different assumptions for the maximum dose at consumption (D_{max}).

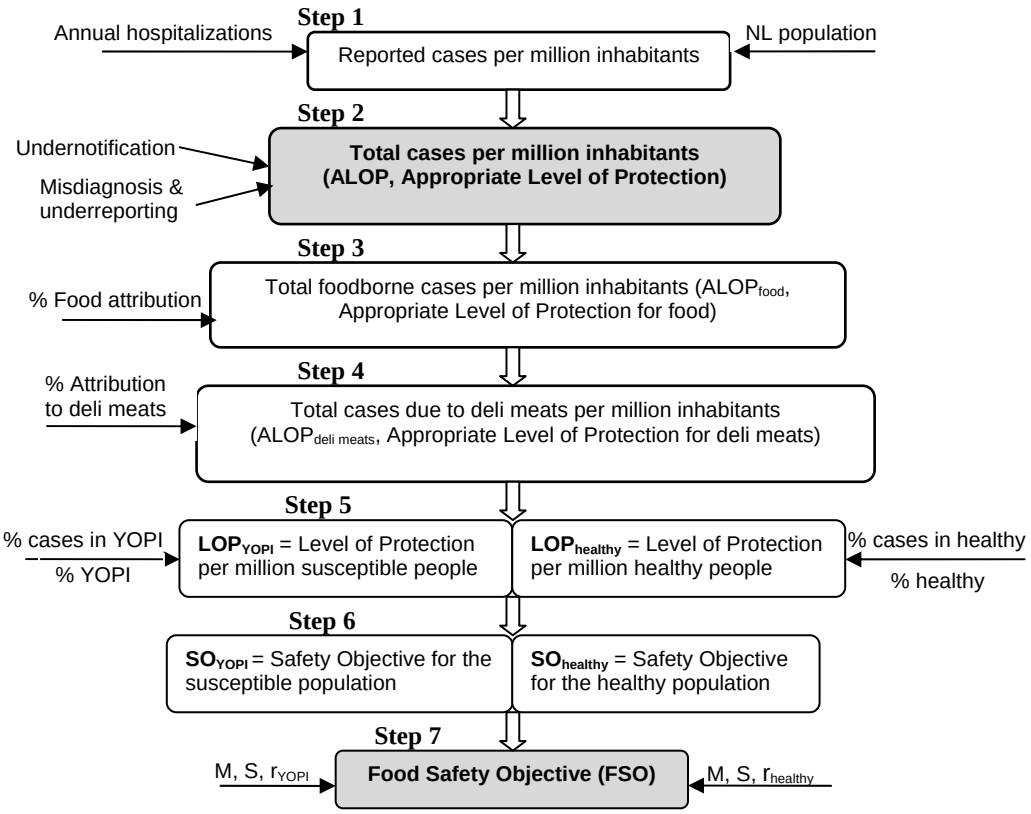

Figure 1: Outline of the estimation steps in the top down approach model.

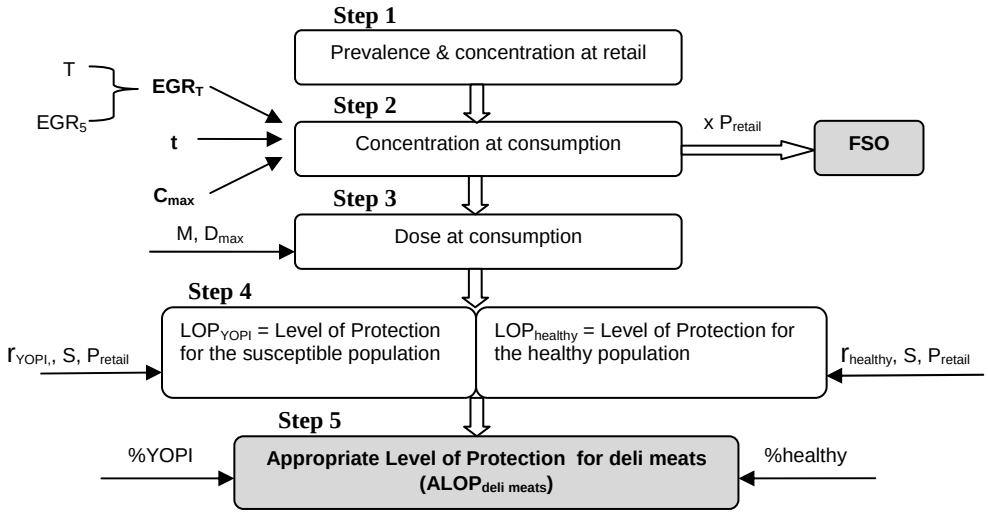

Figure 2: Outline of the estimation steps in the bottom up approach model.

Results and Discussion

The results for the different models used in the top down and bottom up approach to estimate the ALOP can be seen in Table 1. For the bottom up approach the estimated FSO was the same for the different combinations of input parameters tested with a mean of -0.82 log CFU per g (95% CrI: -3.2 to 5.6). For the top down approach mean estimates for the FSO varied from 2.3 to 3.9 log CFU per g with 95% CrI covering the range 1.6-4.4 log CFU per g (data not shown).

Table 1: ALOPs (cases of severe listeriosis due to the consumption of deli meat per million people per year) estimated with both the top down approach and bottom up approach for different combinations of input parameters.

Parameter	**Description**	**ALOP$_{deli\ meat}$ Top down approach**	**ALOP$_{deli\ meat}$ Bottom up approach**
		Mean (95% CrI)	Mean (95% CrI)
Baseline	r, M, S fixed		12 (8.8-15)
Alternative 1	r stochastic, M & S fixed		44 (5-118)
Alternative 2	r, M, S fixed, D_{max}=7.5 log CFU		4.7 (3.5-6.0)
Alternative 3	r, M, S fixed, D_{max}=8.5 log CFU		6.8 (5.1-8.8)
Alternative 4	r, M, S fixed, D_{max}=9.5 log CFU		12 (9.0-16)
Alternative 5	r, M, S fixed, D_{max}=10.5 log CFU		6.1 (4.5-7.9)
Alternative 6	r stochastic, M,S fixed, D_{max}=7.5 log CFU		4.8 (3.0-7.0)
Alternative 7	r stochastic, M,S fixed, D_{max}=8.5 log CFU		7.0 (4.3-10)
Alternative 8	r stochastic, M,S fixed, D_{max}=9.5 log CFU		13 (7.9-19)
Alternative 9	r stochastic, M,S fixed, D_{max}=10.5 log CFU	3.2 (1.1-6.6)	6.2 (3.9-9.1)
Alternative 10	r fixed, M,S stochastic		15 (8.1-25)
Alternative 11	r fixed, M,S stochastic, D_{max}=7.5 log CFU		5.9 (3.2-9.9)
Alternative 12	r fixed, M,S stochastic, D_{max}=8.5 log CFU		8.7 (4.7-15)
Alternative 13	r fixed, M,S stochastic, D_{max}=9.5 log CFU		16 (8.3-26)
Alternative 14	r fixed, M,S stochastic, D_{max}=10.5 log CFU		7.8 (4.2-13)
Alternative 15	r, M, S stochastic		55 (6.0-162)
Alternative 16	r, M, S stochastic, D_{max}=7.5 log CFU		6.1 (2.9-11)
Alternative 17	r, M, S stochastic, D_{max}=8.5 log CFU		8.9 (4.3-16)
Alternative 18	r, M, S stochastic, D_{max}=9.5 log CFU		16 (7.7-29)
Alternative 19	r, M, S stochastic, D_{max}=10.5 log CFU		7.9 (3.8-14)

The mean estimates of the ALOP and FSO were different for most of the combinations of input parameters used in the two approaches although considering the uncertainties involved they are not so far apart. Moreover, the interpretation of the concepts suggests that comparisons should be made taking into account the frequency of the hazard in the case of FSO (Codex Alimentarius Commission 2010) or the credible intervals in the case of the

ALOP (FAO/WHO 2002). Keeping this in mind, for several of the bottom up approach outcomes the 97.5th percentile of the ALOP estimates is well in agreement with the 97.5th percentile of the ALOP based on the top down approach, being different by a factor smaller than two. With regards to the FSO however this was less the case, with the 97.5th percentiles being 1 to 3 log CFU per gram different. Obviously, with comparisons based on other percentiles these differences might be smaller or greater depending on the input parameters selected. An important finding is that the level of detail encompassed in the risk assessment process (bottom up approach) influenced considerably the risk estimates with the introduction of additional stochastic parameters instead of point estimates leading to higher mean estimates for the ALOPs and larger credible intervals. Uncertainty related with the maximum dose at consumption was another parameter that also considerably influenced our risk estimates as observed by other authors (Pouillot and Lubran 2011). Although ideally the two approaches should yield comparable results (Whiting 2010), in reality a single approach should be used for consistency purposes (WTO 2000). Nevertheless, as a best practice we recommend that both approaches should be used to allow validation of the risk estimates, although depending on the application context one may appear more appropriate than the other.

Conclusions

It was found to be better practice to base decisions for ALOP and FSO values on both different approaches considering the level of detail encompassed in the base data.

Acknowledgements

We would like to thank Unilever for sponsoring this research.

References

Codex Alimentarius. (2007). Principles and guidelines for the conduct of microbiological risk management (MRM), CAC/GL 63-2007.

Codex Alimentarius Commission. (2010). Joint FAO/WHO Food Standards Programme. Codex Alimentarius Commission. Procedural Manual. Nineteenth Edition. World Health Organization/Food and Agriculture Organization of the United Nations. Geneva/Rome. Available from: ftp://ftp.fao.org/codex/Publications/ProcManuals/Manual_19e.pdf

Crouch, E. A., LaBarre, D., Golden, N. J., Kause, J. R. and Dearfield, K. L. (2009) Application of quantitative microbial risk assessments for estimation of risk management metrics: *Clostridium perfringens* in ready-to-eat and partially cooked meat and poultry products as an example. *Journal of Food Protection 72*(10), 2151-2161.

FAO/WHO. (2002) Principles and guidelines for incorporating microbiological risk assessment in the development of food safety standards, guidelines and related texts. Report of a Joint FAO/WHO Consultation. Food and Agriculture Organization of the United Nations/World Health Organization. Rome/Geneva. Available from: http://www.who.int/foodsafety/publications/micro/en/march2002.pdf

Membré, J. M., Bassett, J. and Gorris, G. M. L. (2007) Applying the food safety objective and related standards to thermal inactivation of *Salmonella* in poultry meat. *Journal of Food Protection, 70*(9), 2036-2044.

Pouillot, R., and Lubran M. B. (2011) Predictive microbiology models vs. modeling microbial growth within *Listeria monocytogenes* risk assessment: What parameters matter and why *Food Microbiology, 28*(4).

Rieu E., Duhem K., Vindel E. and Sanaa M. (2007) Food Safety Objectives should integrate the variability of the concentration of pathogen. *Risk Analysis 27*(2), 373-386.

Stringer M. (2005). Food safety objectives - role in microbiological food safety management. *Food Control 16*, 775-794.

Tuominen P., Ranta J. and Maijala R. (2007) Studying the effects of POs and MCs on the *Salmonella* ALOP with a quantitative risk assessment model for beef production. *International Journal of Food Microbiology* 118(1), 35-51.

Whiting R. C. (2011) What risk assessments can tell us about setting criteria. *Food Control* 22, 1525-1528.

WHO/FAO. (2004) Risk assessment of *Listeria monocytogenes* in ready-to-eat foods: technical report. World Health Organization/Food and Agriculture Organization of the United Nations. Geneva/Rome. Available from: http://www.who.int/foodsafety/publications/micro/mra_listeria/en/

World Trade Organization (WTO) (1995) Agreement on the application of sanitary and phytosanitary measures (SPS Agreement).

World Trade Organization (WTO) (2000) Committee on Sanitary and Phytosanitary Measures. Guidelines to further the practical implementation of Article 5.5, *G/SPS/15*.

Simulation modelling for the assessment of operating conditions: case study in the Colombian dairy industry

F. Garces, C. Aguilar, B. Klotz

Engineering Faculty, University of La Sabana, Bogota, Colombia (Bernadette.klotz@unisabana.edu.co)

Abstract

In this study, the microbial quality of milk from the collection centres through the operations of transport to the processor plant, reception and cold storage of raw milk, thermization and cold storage, were simulated in order to establish the suitability of milk towards UHT (ultra high temperature) processing in Colombian dairy industries. The growth and inactivation rates at different temperatures were determined based on experimental data of ComBase and published articles. The @Risk software (Palisade Corporation, Newfield, NY, USA) was used to simulate the distribution of microbial concentration in milk. The simulation included 10 000 iterations with Latin Hypercube sampling. The results obtained showed a non appropriate performance of the model with deviations of predictions of growth and of inactivation up to 2 log cycles when validated with real microbial concentration data at the different stages of the milk flow before entering the UHT equipment. Therefore, the simulation exercise was repeated but with the introduction of kinetic parameters from more psychrotolerant and thermoduric bacteria generating outputs close to the real system (0.3 – 0.6 log cycle deviation). In this instance, this simulation model shows the need to redesign supply and manufacturing conditions to meet microbial standard quality criteria for milk in the UHT milk production.

Keywords: *simulation, fluid milk quality*

Introduction

Milk is a highly perishable food and requires refrigeration and special handling; quality and shelf life depend on continuous and appropriate cooling. By virtue of the milk supply chain, milk is susceptible to contamination by a wide variety of bacteria. Microorganisms are naturally present in milk in a concentration range of 10^3 to 10^5 of aerobic mesophilic bacteria per ml when good hygienic practices have been applied. Cooling reduces the growth of bacteria and under refrigeration temperature the microbial quality of raw milk can be preserved for at least two days. Subsequent thermal processing renders fluid milk safe for consumption. Psychrotolerant endospore forming bacteria, such as *Bacillus* and *Paenibacillus* spp., are important spoilage microorganisms present in raw milk that can influence the quality and shelf life of pasteurized and UHT milk (Huck *et al.* 2007). These thermoduric bacteria can survive heat treatments and jeopardized further production processes. They are responsible for the production of heat resistant proteolytic enzymes that cause the sweet curdling of processed fluid milk (Griffiths and Phillips 1990).

The maintenance of an uninterrupted cool chain from the producer to the consumer is a challenge especially in underdeveloped and developing countries. In Colombia, the distances between milk collection centers and processing plants are long and time consuming and the storage of preprocessed milk is almost the rule. Therefore, in the UHT fluid milk production, a so called thermization and storage precede the UHT treatment. The purpose of this simulation exercise was to establish the microbial quality of the milk through different stages of the UHT fluid milk production in order to assess the quality of milk entering the UHT treatment; shelf life largely depends on microbial load and presence of proteolytic enzymes.

Materials and Methods

Experimental data

Aerobic mesophilic bacterial counts (plate count method) from different fluid milk processing industries at four stages of the production line were used in the analysis: (1) primary collection

centres, (2) plant reception, (3) after thermization, and (4) before UHT treatment. For each stage 50 data points were collected. The probability distribution of the data at each stage was established with @Risk (Palisade Corp., USA), using Anderson-Darling criteria. Other operation conditions were established as reported by the fluid milk processors (Table 1).

Table 1: Operation condition of the production line.

Stage	Parameter	Distribution	Descriptors
Transport	Time/Duration (h)	Uniform	(0.5;24)
	Temperature (°C)	Normal	(12;2)
Storage before thermization	Time/Duration (h)	Uniform	(0.5;48)
	Temperature (°C)	Uniform	(4;12)
Thermization	Temperature (°C)	RiskNormal	(74;1)
	Time/Duration (s)	RiskNormal	(15;0.5)
Storage after thermization	Temperature (°C)	Uniform	(0.5;8)
	Temperature (°C)	Uniform	(4;12)

Growth estimation

To predict the microbial growth the modified Gompertz equation was used. The parameters of the equation were set as follow: maximum population 9.0 $\log_{10}$CFU/ml, lag time 0 h, and μ was established by linear regression (eq. 1) of growth data of indigenous milk microflora obtained from ComBase (81 data sets, Australian Food Safety Centre of Excellence, University of Tasmania, Hobart, Australia).

$$\mu = 0.0131 \times T - 0.0447 \qquad R^2 = 0.86 \tag{1}$$

Inactivation estimation

The effect of the thermization on the microbial load was established based on the *D* and *z* parameters of the Bigelow model. The *D* - values at different temperatures were calculated according to the equation 2, considering a thermoresistant D_{63} of 22s (Verrips and van Rhee 1981) and a *z* - value of 10 (Xu *et al.* 2006).

$$D_1 = D_2 \times 10^{\frac{(T_2 - T_1)}{z}} \tag{2}$$

Simulation

The process was simulated using sequential steps for each of the stages. Variability of the operation parameters and microbial loads were simulated using @Risk (Palisade Corp., USA). The full simulation was done with 10 000 iterations and Latin Hypercube sampling.

Results and Discussion

Experimental data adjustment

The distributions of data from the four stages are shown in Table 2. The number of bacteria along the process varied in a wide range from 0.88 to7.39 $\log_{10}$CFU/ml. At the collection centres, the microbial loads were under the standard criteria for raw milk. During transportation (0.5 - 24h at 12 ± 2°C) the microbial load increased to values up to 7.39 $\log_{10}$ CFU/ml rendering milk of very poor quality. After the thermization process (15 - 0.5s at 74 - 1°C) and during the refrigerated storage (0.5 - 8h at 4 - 12°C) the concentration of bacteria increased between 1 and 3 log cycles. These results indicated low efficiency of the heat treatment on the inactivation of bacteria and a possible germination of bacterial spores (Hanson *et al.* 2005; Novak *et al.* 2005).

Table 2: Probability distributions of experimental data.

Stage	Probability distribution	Descriptors
Collection centre	BetaGeneral	(2.29;1.75;1.51;4.37)
Plant reception	Triang	(3.98;6.95;7.39)
After thermization	BetaGeneral	(1.26;0.88;2.45;5.03)
Before UHT treatment	Triang	(3.82;6.84;6.84)

Simulation results

The microbial load of the fluid milk was sequentially simulated during the production process according to the distribution of the original data and proposed equations for growth and inactivation (Table 2). The simulation results had great discrepancies with the experimental data (Figure 1) at the different production stages. Simulated growth was higher than the observed; 19.8% and 22.2% of the observed data fall below the 95% confidence interval of the model at the stages of plant reception and before the UHT process respectively. The simulated efficacy of the thermization was lower than the observed and 31.2% of the experimental data were above the 95% confidence interval of the model. These deviations showed the need to adjust the kinetic parameters: to reduce the growth rate and to increase the *z* – value.

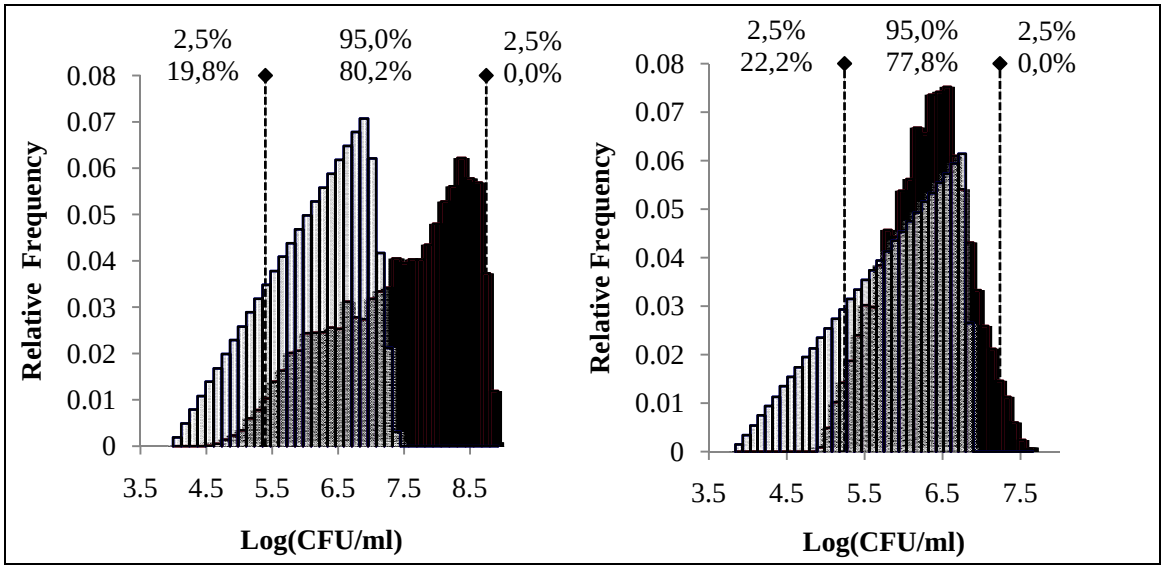

Figure 1: Results of simulation of microbial loads at the stages of plant reception (left) and before UHT processing (right). (Experimental data distribution ion white, simulation results in black).

Adjustment of the simulation

Bacterial diversity in milk is great due to the number and diverse possible sources of contamination (Coorevits *et al.* 2010). Bacterial population shifts and changes in the spoilage potential of milk contaminants due to process properties are also often observed (Jaspe *et al.* 1995). Growth and inactivation behaviour of the microorganisms in milk suggested the presence of more psychrotolerant and thermoduric bacteria. The growth rate was decreased by lowering the intercept value of the regression from -0.0447 to -0.14 in those stages that favour growth. The *k* value for the heat treatments was modified increasing the *z* value from 10 to 13 (Xu *et al.* 2006). The figure 2 shows the effect of the adjustments at the stages of plant reception and before the UHT process.

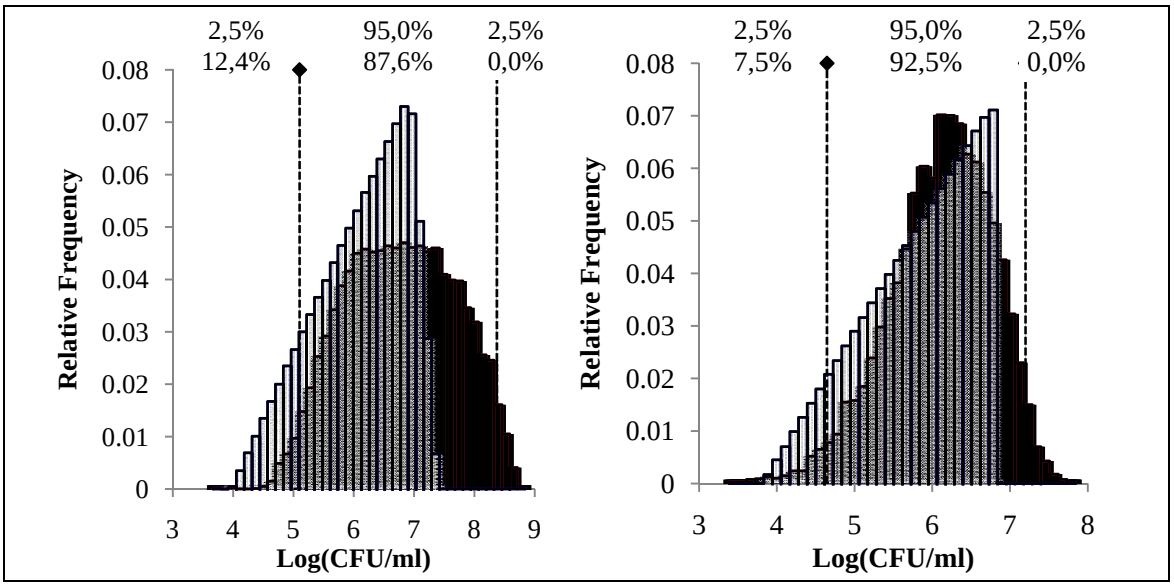

Figure 2: Simulation with the adjusted model. Results of simulation of microbial loads at the stages of plant reception (left) and before UHT processing (right). (Experimental data distribution on white, simulation results in black).

In this case the simulated growth decreased and only 12.4% and 7.5% of the observed data fall below the 95% confidence interval of the model during the stages of plant reception and before the UHT process. In the simulation, the distributions were wider; the upper limit values were higher than those observed experimentally. The relative frequencies of the simulated values in the stage of plant reception were higher than the experimental data (maximum 1.5 logarithmic units). If 5 $\log_{10}$ CFU/ml is considered as the upper limit that renders milk suitable for UHT treatment, 93.8% (simulation) and 84.7% (experimental data) of the milk will not complain for such preservation technology.

Conclusions

The simulation of a production process enables milk processors to better design their production processes in order to assure safe and quality products. The analysis of experimental data and the simulation results showed that during the fluid milk production system (1) the quality a milk deteriorated, (2) the thermization was not effective in reducing microbial load, (3) the quality of milk before the UHT was mostly of poor and will be reflected in UHT milk with reduced shelf life and high incidence of sweet curdling.

References

Coorevits A., De Jonghe V., Vandroemme J., Van Landschoot A., Heyndrickx M. and De Vos P. (2010) How can the type of dairy farming influence the bacterial flora in milk? In: Organic Farming and Peanut Crops. Ed. D. C. Grossman, T. L. Barrios, pp. 123-136. Nova Science Publishers, Inc. ISBN: 978-1-60876-187-6.

Griffiths M.W. and Phillips J.D. 1990. Incidence, source and some properties of psychrotrophic *Bacillus* spp. Found in raw and pasteurized milk. *Journal of the Society of Dairy Technology* 43: 62-66.

Hanson M.L., Wendorf W.L. and Houck K.B. (2005) Effect of heat treatment of milk on activation of *Bacillus* spores. *Journal of Food Protection* 68 (7): 1484-1486.

Huck J.R., Woodcock N.H., Ralyea R.D. and Boor K.J. (2007) Molecular subtyping and characterization of psychrotolerant endospore-forming bacteria in two New York State fluid milk processing systems. *Journal of Food Protection* 70 (10): 2354-2364.

Jaspe A., Oviedo P., Fernández L., Palacios P. and Sanjosé C. (1995) Cooling raw milk: Change in the spoilage potential of contaminating *Pseudomonas*. *Journal of Food Protection* 58 (8): 915-921.

Novak J.S., Call J., Tomasula P. and Luchansky J.B. (2005) An assessment of pasteurization treatment of water, media, and milk with respect to *Bacillus* spores. *Journal of Food Protection* 68 (4): 751-757.

Verrips C.T. and Van Rhee R. (1981) Heat inactivation of *Staphylococcus epidermidis* at various water activities. *Applied and Environmental Microbiology* 41 (5): 1128-1131.

Xu S., Labuza T.P. and Diez-González F. (2006) Thermal inactivation of *Bacillus anthracis* spores in cow´s milk. *Applied and Environmental Microbiology* 72 (6): 4479-4483.

Evaluation and recalibration of a risk-based protocol for optimization of Safety Inspections by Hellenic Food Authority

A. Vakalopoulos[1], M. Mataragas[2], D.B. Panagiotakos[3], E.H. Drosinos[2], P. Skandamis[2], G.-J.E. Nychas[1]

[1] Hellenic Food Safety Authority, 124 Kifisias Ave. and 2 Iatridou Str., Athens, GR-11526 (avakalopoulos@efet.gr and nychas@efet.gr)
[2] Laboratory of Food Quality Control and Hygiene, Department of Food Science and Technology, Agricultural University of Athens, Iera Odos 75, GR-118 55 Athens, Greece (mmat@aua.gr, pskan@aua.gr and ehd@aua.gr)
[3] Department of Science of Dietetics – Nutrition, Harokopio University, 70 El. Venizelou Ave., GR-17671, Greece (dbpanag@hua.gr)

Abstract

Risk-based inspection of food-producing plants is crucial for efficient monitoring of Food Safety by the National Authorities. Targeting certain food categories, based on the risk profile of specific food-hazard combinations, may save time and resources and ensure that insignificant risks will not be over-addressed, while significant risks will receive proper attention. A well-established nomogramm was adopted incorporated input variables regarding food-specific hazards, whereas the output was the frequency of the sampling. A regression model was developed to evaluate the nomogram. The recalibration procedure was based on the rationale of having close limits of agreement as well as on a modified regression calibration procedure. The present methodology suggests a risk-based tool for optimization of Food Inspection that could be adopted by Food Authorities that have not developed local tools. The proposed methodology will minimize time and resources waste and enable the development of a useful track-record for National Surveillance purposes.

Keywords: *risk-based inspection, nomogram, calibration, control frequency*

Introduction

In European Union, Member States (MS) has an obligation to submit a multiannual plan for controls in food businesses according to the Community legislation. The purpose is the control of foods to be equivalent in every MS. Hellenic Food Authority (EFET) has been considered to develop a risk-based tool for the determination of the frequency of control in the food businesses. This will help to improve the efficiency of EFET *via* his own resources. Nomogramm is a calculator designing to graphically interpret a set of related variables. In many nomogramms the variables are empirically and not functionally related. The outcome of the nomogramm is a figure of interest, e.g., in our case the number of controls in food businesses performed within a certain time interval. Nomogramms have been used in food inspections, but to the best of our knowledge none of them has been widely used.
Therefore the aim of this work was to propose a methodology for modeling and calibrating into local data a specific nomogramm that has already been developed to propose the frequency of sampling in food industries, based on local conditions and facts. This methodology could be applied by any other country.

Materials and Methods

The nomogramm

A well established nomogramm (Lenartowicz and Michie 2002a,b) was adopted that incorporated input variables regarding food-specific hazards, whereas the output was the frequency of the sampling in a specific food industry on a tri-annual basis. Specifically, variables such as the type of food product processed and the hazards potentially present, volume of production, history of laboratory results for food-related hazards, establishment practices including interventions that reduce food-related hazards contamination and testing programs that effectively detect food-related hazards, frequency of food product consumption

and hazard severity were taken into account. The nomogramm uses non-parallel axes enabling the non-linear relationships to be incorporated in the model. The variables requiring input after appropriate assessment are denoted by square boxes. The tool is divided into two parts. The pair of nomogramm at the top of the tool determines the probability of occurrence, and the availability, which are then incorporated in the bottom multistage nomogramm. In the bottom of the tool there are two extra lines, the so-called 'tie lines' for the transition between the stages of the nomogramm. The final parallel logarithmic scale is not nomogramm as such, but reading-off scale to translate the risk score (remote to extremely high) into a sampling frequency to address safety aspects. The nomogramm was based on that developed by the UK Public Analyst Service in conjunction with the UK Food Standards Agency for use as a tool to guide the appropriate frequency of sampling and analysis of food for official food control purposes, intended to be used to assess all potential problems with foods. The modification made was referred to the substitution of the original variable "Likelihood of defect recognition by consumer" with the variable "Occurrence of positive samples to a specific hazard" to include the history of laboratory results for food-related hazards. Until now the aforementioned nomogramm has not been modeled through a formal statistical procedure. Thus, in this work a Poisson regression model was applied to model the input variables of the nomogramm in relation to the number of inspections suggested by the tool. Discrete, ordered scores ranging from 0 to 5 were assigned to each factor Q_i of the nomogramm (Table 1). Based on these scores the frequency of inspections was derived on a tri-annual basis.

Table 1: Scoring of the factors (Q_i) included in the nomogramm.

Factor	**Score**
Q_1=level of hazards' presence	0 (very rare) to 5 (almost inevitable)
Q_2=control level within the company	0 (no control) to 4 (total control)
Q_3=frequency of food consumption	0 (rare) to 3 (daily)
Q_4=estimated level of population at risk	0 (hundreds or less) to 4 (millions)
Q_5=level of severity in the case of hazard	0 (minor) to 4 (extremely severe)
Q_6=history of positive inspections	0 (12 months) to 3 (1 month)

Application to national data

The database of the EFET was used to retrieve the inspections made in 64 group of companies during the years 2007 and 2009 (a total of 21.621 inspections).

Statistical methodology

The modeling of the nomogramm

Using the aforementioned nomogramm, a panel of experts that applied established criteria, evaluated companies' and food's related hazards. As mentioned above a random variable was derived, let *S*, denoting the suggested number of inspections based on a tri-annual basis for each company. *S* is considered to follow the Poisson distribution. Thus, the following model has been estimated:

$$\ln(S) = \hat{\theta}' \times Q \qquad (1)$$

where θ' is the vectors of parameters estimates of the Poisson regression model and Q is the vector of factors included in the nomogramm. The factors used in the aforementioned nomogramm, where: Q1=level of hazards' presence, Q2=control level within the company, Q3=frequency of food consumption, Q4=estimated level of population at risk, Q5=level of severity in the case of hazard, Q6=history of positive inspections, as well as their interactions as they have been proposed by the nomogramm, i.e., Q1XQ2, Q3XQ4, Q1XQ2XQ5 and Q1XQ2XQ5XQ6. The maximum likelihood method was used to estimate the vector of model's parameters. Factors Q_i with significant impact on estimating *S* were considered at type-I error level <0.05. The results are presented as b-coefficient, standard error, Wald test and the corresponding exact probability of type-I error (p-value).

The calibration method

At this point it should be underlined that the *S* could not be considered as the optimal number of inspections (i.e., the gold standard), since the nomogramm has never been evaluated in Greek population before, and does not take into account potential peculiarities of the existed conditions. To evaluate the performance of the nomogramm into the Greek data, a generalized linear regression model, with probit link, was applied. Let $p_i \in [0, 1]$ the probability of a true positive inspection for the *i*-th company. The *probit* regression for the suggested by the nomogramm numbers of inspections, S, takes the form:

$$\Phi^{-1}(p_i) = b_0^* + b_1^* \times S_i \quad (2)$$

The results are presented as b-coefficient, standard error, Wald test and the corresponding exact probability of type-I error (p-value); where a p-value <0.05 was considered as statistically significant. To evaluate the predictive ability of S, on true positive rate, *p*, various goodness-of-fit measures were calculated. In particular, Pearson chi-square and scaled Pearson chi-square, log-likelihood and Akaike's information criterion (AIC), are presented.

To calibrate the nomogramm a new methodology is proposed here based on the concept of regression calibration method (Brown 1994). At first model (2) is estimated. Based on the results obtained from model (1) a calibration of $\hat{\theta}$ is applied in order to obtain a new estimation of the suggested number of inspection *S*, let *S'*. Then, model (2) is re-estimated using S' instead of S (i.e., model (3)). The calibration of $\hat{\theta}$ is based on the effect size measures of each Q_i obtained in model (1) and the correlation between Q_i and p_i. In particular,

$$\hat{\theta}' = \frac{\hat{\theta}}{rho} \quad (3)$$

where rho is Spearman's correlation coefficient. If goodness-of-fit criteria (e.g., Pearson chi-square, log-likelihood and Akaike's information criterion (AIC)) of model (3) are better than of model (2) then parameter estimates of model (1) are replaced and the suggested number of inspections is now *S'*, alternatively, the initial modeling of the nomogramm is used, since the suggested number of inspections, i.e., S, predicts better true positive events. Moreover, by this approach, the best model leads also to less overdispersion, a common problem in Poisson regression.

Results and Discussion

The vector of parameter estimates of model (1) was θ = {5.95, -.86, 0.72, -.89, -2.39, -.20, .19, .60, .05, -.08, .03} (*P-value<.05). According to this model, the median number of inspections suggested by the nomogramm during a three year period was 2.17 inspections. The corresponding median number of inspections as estimated by the model (1) was *S*=1.47. Model's goodness of fit was poor (Pearson chi-square = .014, log-likelihood=-33.105, and AIC=88.210).

The evaluation of S on the probability of a true positive inspection revealed that S was not significantly associated with the investigated outcome (b±SE: $8 \times 10^{-3} \pm .02$, Wald chi-sq., = .09, p=.763); model's goodness-of-fit statistics were Pearson chi-square and scaled Pearson chi-square = 2976,123, log-likelihood = -238.251, and AIC = 584.502. Then, vector θ was calibrated and equation (1) was re-applied in order to calculate *S'*.

The calibration of the models' parameters was based on the observed relationships between Q_i and p_i, as they assessed using the individual effect of Q_i on p_i. Data analysis revealed that the calibrated equation and the corresponding calibrated number of inspections

S’(=2.39), performed better than the original (Pearson chi-square and scaled Pearson chi-square = 2918,844, log-likelihood = -237.691, and AIC = 583.382).

Conclusions

A new approach in deciding the number of regular food-related inspections was proposed in the current work by modeling and calibrating a previously designed nomogramm into local conditions. The application and use of tools and methodologies like the presented will minimize time and resources waste and enable the development of a useful track-record for National Surveillance purposes.

References

Brown P.J. (1994) Measurement, Regression and Calibration, OUP Pub., UK.

Lenartowicz P. and Michie N. (2002a). Risk-based sampling of food: A scientific approach to sampling for analysis, Volume 1: Risk Assessment for sampling. Public Analyst Service Ltd for Food Standards Agency. URL: http://www.publicanalyst.com/Risk_Based_Sampling_Vol_1.pdf

Lenartowicz P. and Michie N. (2002b). Risk-based sampling of food: A scientific approach to sampling for analysis, Volume 2: Background and support. Public Analyst Service Ltd for Food Standards Agency. URL: http://www.publicanalyst.com/Risk_Based_Sampling_Vol_2.pdf

Predictive models to support manufacturers of processed meat in their compliance with EU regulation 2073/2005

A. Vermeulen[1,2], A.M. Cappuyns[1,3], J. Beckers[2], A. De Loy-Hendrickx[2], H. Paelinck[4], M. Uyttendaele[2], J.F. Van Impe[1,3], F. Devlieghere[1,2]

[1] CPMF² - Flemish Cluster Predictive Microbiology in Foods – http://www.cpmf2.be/
[2] LFMFP – Laboratory of Food Microbiology and Preservation, Department of Food Safety and Food Quality, Ghent University, Belgium (Frank.Devlieghere@UGent.be)
[3] BioTeC - Chemical and Biochemical Process Technology and Control, Department of Chemical Engineering, Katholieke Universiteit Leuven, Belgium (Jan.VanImpe@cit.kuleuven.be)
[4] Laboratorium voor Levensmiddelenchemie en Vleeswarentechnologie, Katholieke Hogeschool Sint-Lieven, Belgium (Hubert.Paelinck@kahosl.be)

Abstract

This study, in cooperation with 30 Flemish companies of the processed meat industry, aims at implementation of predictive models in their production environment to support the compliance with the EU regulation 2073/2005, particularly regarding *L. monocytogenes.*
An inventory of the different processed meat products from the participating companies was made. Based on the intrinsic and extrinsic factors of these products on the one hand and the process characteristics on the other hand, different categories were defined. Extended challenge tests according to the EU technical guidance (15 data points) were performed on two different batches of cooked ham and aspic products. Also the physicochemical characteristics of these products were analyzed. Next to that, samples following a certain T-profile, were analyzed in threefold on day 0 and at the end of shelf-life to assess growth potential. Available predictive models were evaluated regarding their performance towards these meat products. These models could (*i*) support the companies in demonstrating their compliance with EU regulation 2073/2005 while reducing the amount of necessary challenge tests, (*ii*) stimulate their product innovation and (*iii*) determine the shelf-life of these products more precise.
Keywords: *L. monocytogenes, challenge testing, growth potential, predictive models*

Introduction

As part of the control measures for *L. monocytogenes,* Food Business Operators (FBO) should conduct studies to identify growth potential of *L. monocytogenes* in products put on the market. Next to the specifications of physicochemical characteristics and available scientific literature, predictive microbiology can be used. Therefore, it is important that existing predictive models are validated for a large category of products and that predictions are compared with results obtained from extensive challenge tests.
The objective of the study was the evaluation of the challenge test protocol described in the technical guidance document published by the EU Community Reference Laboratory (EU CRL, 2008) for *L. monocytogenes.* The concept of a simple challenge test to assess growth potential on actual data measurements at start and end of shelf life was compared to a modelling approach. Processed meat was chosen as a target food product. Based on the intrinsic and extrinsic characteristics of the products, obtained from 30 Flemish meat companies, several categories were defined and model products were made on lab scale.

Materials and Methods

Standardisation of the inoculum

All strains (LMG 23194, LMG 13305, LFMFP 392, LFMFP 491 and LFMFP 802) were taken from stock cultures stored at -80°C and were cultured in BHI at 37°C. In case of cold adaptation, a subculture was inoculated in fresh BHI broth and incubated at 7°C for 4 days (Vermeulen *et al.*, 2011). To determine growth rates two monoculture strains were used, while for the growth potential tests a mixture of three *L. monocytogenes* strains was used.

Inoculation and packaging

Cooked ham was prepared on lab scale while the aspic products were purchased from a local producer. The products were immediately after production sliced in the lab and randomised before packing. After portioning in test units (150 ± 5 g), blanks were inoculated with 100 µl PPS and the other samples with 100 µl of the diluted mixed culture (growth potential tests) or the monoculture (tests assessing growth rate). An inoculum of ca. 50 CFU/g was obtained. The aspic products were vacuum packed in high barrier packaging material using a gas packaging chamber machine. Cooked ham was MAP packed (30% CO_2 and 70% N_2) in a 1/1.8 G/P-ratio by using a traysealer. The concentration of O_2 and CO_2 in the packages were determined using a O_2 CO_2 gas analyser.

Storage conditions

In a first approach growth rates of two monocultures were determined for the meat products at constant temperature (7°C). In a second approach growth potential based on the actual measurements data of *L. monocytogenes* at the beginning and end of shelf-life was performed for different time-temperature profiles or for experiments that were inoculated with different cultures (Table 1).

Table 1: Overview of the different growth potential tests.

N°	Pre-inoculation conditions	T-profile
1	Cold adapted	7d@8°C+15d@12°C
2	Not adapted	14d@4°C+8d@7°C
3	Cold adapted	14d@4°C+8d@7°C
4	Cold adapted	24d@4°C+12d@7°C

Microbial and physico-chemical analyses

For each growth curve at constant temperature total aerobic count (TAC), lactic acid bacteria (LAB) and *L. monocytogenes* count were analysed at 15 time points. This was performed for the blanks and two *L. monocytogenes* strains in monoculture. For growth potential tests the same parameters were analysed on day 0 en end of shelf-life in threefold. Enumeration of *L. monocytogenes* was performed according to ISO 11290-2 using a reduced detection limit. The enumeration of TAC at 22°C was derived from ISO 6222 (4-5 days incubation of PCA at 22°C). LAB was determined according to ISO 15214 (4-5 days incubation of MRS at 22°C).
On day 0 and the end of shelf life, the pH, a_w, % dry matter, % salt, % lactate and % acetate were determined according to the methods described in Vermeulen *et al.* (2011). Also the nitrite concentration was determined by an external laboratory.

Predictive modelling

The data of the extensive challenge tests (15 data points) were used to compare the growth rates predicted by SSSP (http://sssp.dtuaqua.dk) (one model with and one model without interaction with background flora) with the obtained growth rates by linear regression. Besides, these tertiary models and the modelling process as recommended by the EU technical guidance (EU CRL, 2008) were used to predict the growth potential for the different studied temperature profiles (Eq. 1 and Eq. 2). As input factors for the SSSP model the mean values of the experimentally determined intrinsic factors at day 0 were used. The lag phase was ignored as the *L. monocytogenes* originated from an adapted culture, except for condition 2.

$$\mu_{max} = \mu_{max_{ref}} \cdot \frac{(T - T_{min})^2}{(T_{ref} - T_{min})^2} \quad (1)$$

with μ_{max} the maximum specific growth rate at temperature T, $\mu_{max,ref}$ the maximum specific growth rate at the reference temperature T_{ref} (i.e. 7°C), and T_{min} the minimum growth temperature of *L. monocytogenes* (-2 °C) (EU CRL 2008).

$$\Delta \log \mathrm{CFU/g} = \sum \mu_{max,\,i} \cdot d_i \qquad (2)$$

with Δ log CFU/g the logarithmic increase in cell count during the shelf-life, $\mu_{max,i}$ the maximum specific growth rate at a certain temperature (T_i) and d_i the time of incubation at temperature T_i.

Results and Discussion

Extensive challenge or growth potential tests were performed on two batches for the two monocultures, cocktails and for blank samples. These tests showed a large variability on microbial growth within a batch and between different batches, as it was also seen for smoked salmon (Vermeulen *et al*, 2011). From commercial software packages, only the SSSP model was used as this model allowed to combine most of the intrinsic factors. For cooked ham the model showed good correspondence with the observed growth rates (Table 2). The model including nitrite and acetic acid underestimated the growth rate while the other model predicted much faster growth.

Table 2: observed and predicted growth rates (log CFU/g . d).

			Growth rate		
			Observed	SSSP[a]	SSSP[b]
Cooked ham	Batch 1	LMG 13305	0.2140	0.1782	0.2950
		LFMFP 802	0.2085		
	Batch 2	LMG 13305	0.2218	0.1303	0.2752
		LFMFP 802	0.1953		
Aspic	Batch 1	LMG 13305	0.1602	0.0323[c]	0.2085[c]
		LFMFP 802	0.1337		
	Batch 2	LMG 13305	0.1187	0.0219[c]	0.1917[c]
		LFMFP 802	0.1294		

[a] model without interaction with background flora
[b] model considering background flora, without nitrite and acetic acid
[c] pH was set on 5.6 (lowest value in the model), while the measured pH was 5.5

Table 3: Observed and predicted growth potential (log CFU/g) for *L. monocytogenes* in cooked ham.

		Observed	Predicted		
N°			Linear	SSSP[a]	SSSP[b]
1	Batch 1	5.03	9.49	6.61	3.72
	Batch 2	5.86	11.00	6.70	3.50
2	Batch 1	2.12	3.40	1.18	1.89
	Batch 2	> 1.82	3.94	0.37	1.10
3	Batch 1	2.98	3.40	2.53	3.25
	Batch 2	2.34	3.94	1.73	2.76
4	Batch 1	2.46	5.38	3.92	2.95
	Batch 2	2.74	6.24	2.64	2.26

[a] model without interaction with background flora
[b] model considering background flora, without nitrite and acetic acid

The growth potential was in a few cases underestimated (fail-dangerous) (Table 3). For the model incorporating nitrite and acetic acid, this is caused by the slower growth rate while for the other model this is due to the overestimation of the background flora which suppresses the growth of *L. monocytogenes.* On the blank and inoculated samples, TAC and LAB count was initially very low (< 1 log CFU/g) and growth started only after six days (data not shown). It should be noted that this underestimation was still within the limits of microbial variability between the three replicates of the growth potential tests. Results also showed that growth

potential was higher for the cold adapted cultures due to the absence of lag phase. This illustrates the importance of a standardized inoculum preparation.
For the T-profile as suggested by the EU-protocol (condition 1), the prediction of growth potential was strongly deviating from the observed data. The linear model overestimated the growth potential far, even to unrealistic high levels, because it ignores the stationary phase of *L. monocytogenes*. The SSSP model, which takes into account the background flora underestimated the growth of *L. monocytogenes* due to the very low background flora in the samples. By consequence, the industrial trend towards food which is almost free from background flora (prolonged shelf-life) can compromise the food safety if *L. monocytogenes* is present in the food product.
The growth potential of *L. monocytogenes* in aspic products was in general relatively low (< 2.0 log CFU/g) (Table 4). This was mainly due to the low pH, the high acetic (0.1 %) and lactic acid (0.17 %) concentration and the fast growth of the background flora which reached the stationary phase after 10 days incubation at 7°C. For the aspic products the growth rate predicted by the SSSP model including nitrite and acetic acid underestimated far the growth of the two monocultures. Still the growth potential was not underestimated by this model as it does not consider the background flora.

Table 4: Observed and predicted growth potential (log CFU/g) for *L. monocytogenes* in aspic products.

N°		Observed	Predicted		
			Linear	SSSP[a]	SSSP[b]
1	Batch 1	1.35	6.60	6.57	3.56
	Batch 2	1.72	9.37	6.26	4.03
2	Batch 1	-0.34	2.37	0.00	2.15
	Batch 2	1.99	3.35	0.00	2.62
3	Batch 1	0.53	2.37	1.33	3.50
	Batch 2	1.15	3.35	1.23	3.97
4	Batch 1	1.35	3.74	2.02	3.48
	Batch 2	1.18	6.20	2.18	3.93

[a] model without interaction with background flora
[b] model considering background flora, without nitrite and acetic acid

Conclusions

This study proves that to fulfil the need from the industry to provide product specific, easy-to-use software models, more model validation is necessary. This is of utmost importance for the implementation of predictive models in assuring compliance with the EU-regulation and for the acceptance of this by the controlling agencies. Focus should be on (*i*) a better estimation of the background flora, (*ii*) the calculations of an adaptation factor to bridge the gap between challenge test and model prediction and (*iii*) the confidence interval on the predicted growth curves, to cover microbial variability. If the industry could use these models to prove compliance with the EU-regulation it can significantly reduce the costs of challenge tests and easily implement newly developed recipes or products.

Acknowledgements

This research is supported by the Agency for Innovation by Science and Technology (IWT) project n° 100206 and by and the Belgian Program on Interuniversity Poles of Attraction initiated by the Belgian Federal Science Policy Office. Jan Van Impe holds the chair Safety Engineering sponsored by the Belgian chemistry and life sciences federation essenscia.

References

EU CRL for *Listeria monocytogenes* (2008). Technical guidance document on shelf-life studies for *Listeria monocytogenes* in ready-to-eat foods.

Vermeulen A., Devlieghere F., De Loy-Hendrickx A. and Uyttendaele M. (2011) Critical evaluation of the EU-technical guidance on shelf-life studies for *L. monocytogenes* on RTE-foods: A case study for smoked salmon. *International Journal of Food Microbiology* 145, 176-185.

Suggestion for a decision support tool (DST) for corrective storage of sausages suspected of VTEC survival during fermentation and maturation

T.B. Hansen[1], A. Gunvig[2], H.D. Larsen[2], F. Hansen[2], S. Aabo[1]

[1] National Food Institute, Technical University of Denmark, Mørkhøj Bygade 19, DK-2860 Søborg, Denmark. (tibha@food.dtu.dk)
[2] DMRI – Danish Meat Research Institute, Danish Technological Institute, Maglegaardsvej 2, DK-4000 Roskilde, Denmark. (agg@teknologisk.dk)

Abstract

It is well documented that pH inactivation of verocytotoxin producing *Escherichia coli* (VTEC) in fermented sausages is higher when stored at ambient temperatures when compared to chilled temperatures. We investigated whether storage at ambient temperature could provide sufficient consumer protection from sausages where the processing (fermentation and drying) did not provide the required pathogen reduction. A decision support tool (DST) is suggested, which can predict a possible corrective action to be applied dependent on the sausage characteristics, such as pH, $NaNO_2$, salt levels and choice of starter culture. Sausages were produced according to 19 recipes with 3 % (w/w) salt, $NaNO_2$ (0 to 200 ppm) and starter cultures (Bactoferm T-SPX, F-1 and F-SC 111) used in the batter. Sausages were challenged with a 3-strain-cocktail of O26, O111 and O157 and survival was measured during storage of vacuum packaged fermented sausages at 5 °C for 4 weeks and 16 and 22 °C for 2 weeks. Decimal reduction times (D_T) were estimated for each recipe and storage temperature, T. The square root of D_{22} was modelled as a function of pH (4.3 – 5.3) and salt-in-water (8.9 – 16.0 %) in sausages with and without $NaNO_2$ separately. The influence of storage temperature on D was described by the classical z-concept, which primarily depended on salt and starter culture. For the starter cultures F-1 and F-SC 111, also the use of $NaNO_2$ affected the z-value. The combination of D- and z-models served as the DST suggesting time/temperature storage conditions capable of providing a one $\log_{10}$-reduction of VTEC.

Keywords: *CCP, corrective action, VTEC O26:H-, VTEC O111:H-, VTEC O157*

Introduction

Previous studies (*e.g.* Hwang *et al.* 2009) have shown that pH inactivation of VT *Escherichia coli* in fermented sausages is higher if combined with storage at ambient temperatures between 20 and 30 °C, when compared to chilled temperatures. We wanted to investigate whether this mechanism could be applied to ensure consumer safety from sausages where the processing (fermentation and drying) did not induce the required pathogen reduction. The aim of this work was to set up a decision support tool (DST), which could suggest storage conditions to be applied dependent on the sausage characteristics, such as pH, $NaNO_2$, salt level and starter culture. Such DST would provide the manufacturer a possibility to introduce an additional holding step at a specified temperature before release of the sausages to ensure that adequate inactivation of VTEC is achieved.

Materials and Methods

VTEC challenge study

Sausages consisting of meat from beef and pork were produced according to 19 recipes with 3 % (w/w) salt, 0 to 200 ppm $NaNO_2$ and the starter cultures T-SPX, F-1 and F-SC 111 used in the batter. A 3-strain-cocktail of *Escherichia coli* (VTEC) O26:H-, O111:H- and O157 (all being VT negative) was added during batter preparation to obtain a concentration of 10^5 - 10^6 cfu/g. The batter was stuffed in 60 mm fibre casings. Each sausage weighed *approx.* 600 g at the time of production. Fermentation was performed at 24 °C for 48 h followed by drying at

16 °C until 30 - 35% weight loss. Sausages were smoked twice in the beginning of the drying process. Three times during post-maturation storage of vacuum packaged fermented sausages at 5 °C for 4 weeks and at 16 and 22 °C for 2 weeks, survival was investigated. Samples were resuscitated for 2 h in Brain Heart Infusion broth, surface inoculated on Enteric Medium (SSI, Denmark) and incubated at 37 °C for 18 - 24 h.
Duplicate measurements of pH, salt, moisture and $NaNO_2$ contents in the batter were conducted. After fermentation and drying, pH and moisture was measured in two sausages from each recipe and salt% = 100 x %salt / %moisture was calculated.

Modelling and validation

All VTEC counts were $\log_{10}$-transformed. Linear regressions, using $\log_{10}$VTEC/g as response variable, were applied for estimating D_T for T = 5, 16 and 22 °C. Linear regressions using $\log_{10}D_T$ as response variable were applied for estimating z-values. Variants of the following secondary model were used for modelling the effect of sausage pH and salt on the square root of D_{22} and the z-values:

$$(D_{22}\text{-value})^{½} \text{ or z-value} = b \times (Salt - Salt_{min}) \times (Salt - Salt_{max}) \times (pH - pH_{min}) \times (pH - pH_{max})$$

The units of D_{22} and z are days and °C, respectively, *b* is a constant, Salt is Salt% in the fermented sausage, pH is pH of the fermented sausage, $Salt_{min}$ and $Salt_{max}$ represent minimum and maximum salt% where the models work, and pH_{min} and pH_{max} represent minimum and maximum pH where the models work. The goodness of fit of models to the observed data was evaluated by the root mean sum of squared errors, RMSE.
Data for reduction of VTEC in fermented sausages, which had been vacuum-packaged during post-maturation storage, were selected from the literature for validation of the predictive models defining the decision support tool. Reduction rates were converted to D-values and expressed in days. Performance was evaluated by bias (B_f) and accuracy (A_f) factors.

Results and Discussion

After fermentation and drying, sausages had a pH from 4.3 to 5.3 and salt% from 8.9 to 16.0 depending on the specific recipe used. For each recipe, results revealed a simple log-linear relationship between counts of VTEC and storage time at constant temperatures (results not shown). This is in agreement with previous published studies (Faith *et al.* 1997; Calicioglu *et al.* 2001; Calicioglu *et al.* 2002; Porto-Fett *et al.* 2008; Hwang *et al.* 2009) and D-values were, therefore, used for the description of reduction rates of VTEC during storage of the sausages.

Table 1: Comparison of observed D-values with D-values predicted from PMP's VTEC survival model for soudjouk-style sausages using bias factor (B_f) as performance criterion.

D-values used for comparison[a]	Storage temperature (°C)					
	5		16		22	
	N	B_f	n	B_f	n	B_f
All recipes	12	0.62	27	2.51	30	0.86
Recipes without added $NaNO_2$	6	0.56	11	2.51	14	0.81
Recipes with added $NaNO_2$	6	0.68	16	2.50	16	0.90
Recipes where F-1 was used	6	1.26	9	1.56	10	0.89
Recipes where F-SC 111 was used	6	0.30	8	0.90	8	0.63
Recipes where T-SPX was used	0	-[b]	10	8.73	12	1.02

[a] Only recipes that produced D-values below 120 days were included.
[b] – as sausage pH, after fermentation and drying, using T-SPX was ≥5.0, no reduction was predicted with the PMP model at this storage temperature.

When the observed D-values were compared to values predicted with the VTEC survival model published in PMP (Hwang *et al.* 2009) it was found that only D_{22} were within an acceptable prediction zone having a B_f close to 1.0 (Table 1). D_{16} were strongly overestimated whereas D_5 were underestimated (Table 1). Explanations for these deviations could be many, *e.g.* strain variation, presence of smoke components and concentration of $NaNO_2$ or use of different starter cultures. As illustrated in Table 1, exclusion of recipes without $NaNO_2$ improved B_f for D_{22} and D_5 with 5-10 %. Looking at the three starter cultures separately resulted in large difference in B_f (Table 1), which indicated that the type of starter culture significantly affected the VTEC reduction during post-maturation storage of fermented sausages. Therefore, a model distinguishing between starter cultures was developed.

As opposed to the PMP model (Hwang *et al*. 2009), we found that the influence of temperature on D could be described by the classical z-concept. It was observed that z-values primarily depended on salt and starter culture, whereas sausage pH appeared to have no influence. For the F-1 and F-SC 111 starter cultures, use of $NaNO_2$ also affected the z-value.

Table 2: Parameter estimates for the models used in the decision support tool.

Models	Parameter estimates					
	b	pH_{min}	pH_{max}	WPS_{min}	WPS_{max}	RMSE
z-value						
T-SPX	-12.52	-[a]	-	8.459	13.44	8.18
F-SC 111 without $NaNO_2$	-0.9038	-	-	4.363	18.02	1.35
F-SC 111 with $NaNO_2$	-1.854	-	-	-	23.37	0.43
F-1 without $NaNO_2$	-0.6351	-	-	6.649	19.57	3.65
F-1 with $NaNO_2$	-2.378	-	-	7.329	18.47	2.56
$(D_{22}\text{-value})^{½}$						
Without $NaNO_2$	0.1279	3.558	5.793	6.590	16.54	0.60
With $NaNO_2$	0.7020	1.569	-	-	-	0.13

[a] – indicates that the parameter in this column is not included in the model.

This may also be the case for T-SPX, but our data did not support that. As a result, the five models shown in Table 2 were developed and combined for prediction of z-values in fermented sausages made from various recipes. Figure 1A compares observed to predicted z-

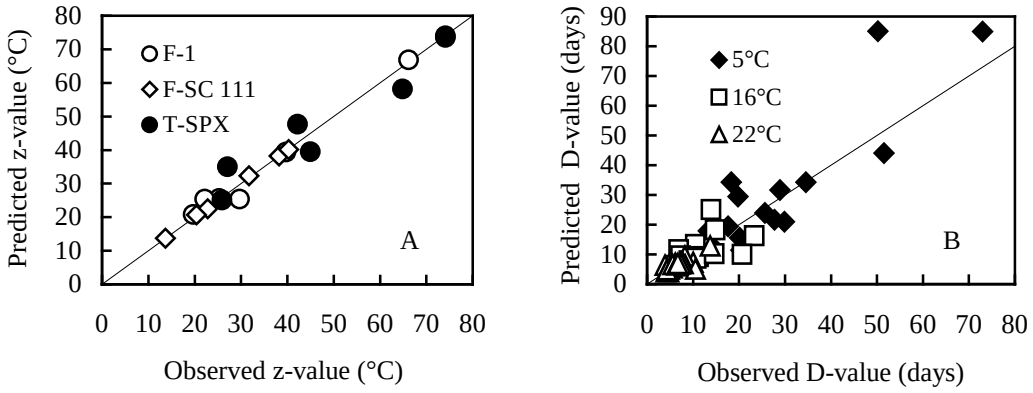

Figure 1: Comparison of observed and predicted values. A) z-values (°C); B) D-values (days).

values (RMSE = 3.53). Data from sausages, where T-SPX had been applied for fermentation, were the major contributor to the total error (Figure 1A). As the effect of storage temperature was described satisfactorily by the z-concept, it was only necessary to model D for one temperature and use this as a reference value for calculation of D for other temperatures. The D_{22}-value was chosen as reference value and for modelling purposes the square root transformation was applied in order to minimize variation. As shown in Table 2, two models were required for the prediction of the square root of D_{22}. Figure 1B compares observed to predicted D_T for T = 5, 16 and 22°C. RMSE was 6.91 when all three temperatures were included and decreased to 3.56 when D_5 were omitted.

The combination of the square root of D_{22}- and z-models represented our idea for a DST (Figure 2). Based on input of 1) whether or not $NaNO_2$ was added to the batter, 2) which starter culture was used, 3) sausage salt content and 4) sausage pH after maturation, time/temperature combinations resulting in 1 $\log_{10}$-reduction of VTEC will be suggested.

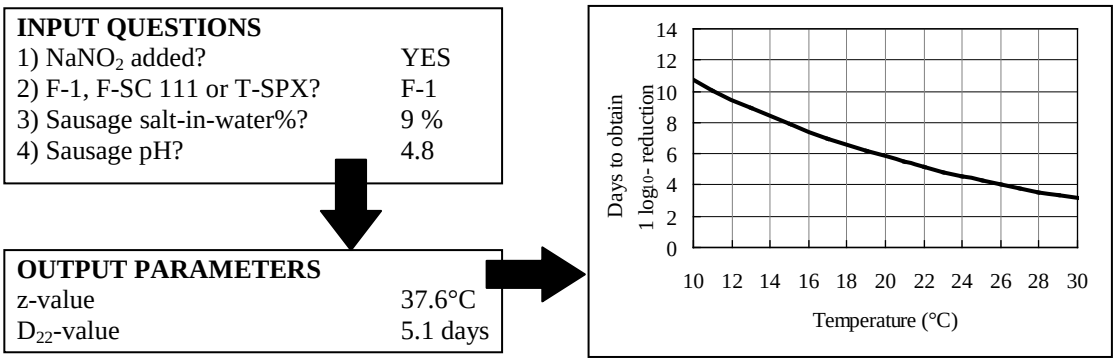

Figure 2: An example of output parameters and graph for the suggested decision support tool.

For validation of the DST, VTEC survival data were collected from five published studies (Faith *et al.* 1997; Calicioglu *et al.* 2001; Calicioglu *et al.* 2002; Porto-Fett *et al.* 2008; Hwang *et al.* 2009). All five studies used starter cultures different from the ones used in the present study and Hwang *et al.* (2009) did not include information on salt content. This complicated the validation as it was necessary to assume a starter culture and, in the case of Hwang *et al.* (2009), to convert a_w to salt% using the equation salt% = -93.958 x a_w + 95.939 (n = 67; R^2 = 0.946) derived from observation in the present study (results not shown). Evaluation of performance of the DST for temperatures from 4 to 30 °C resulted in B_f and A_f of 0.82 and 1.54, respectively. Narrowing the temperature interval to 10 – 30 °C improved the B_f to 0.85. When adopting acceptability limits used for growth models, the DST was evaluated acceptable on the borderline as B_f was between 0.85 – 1.3 and A_f was $\leq$ 1.5. However, the underestimation of D, observed when compared to literature values, stresses the importance of the specific starter culture for the obtainable reduction of VTEC during post-maturation storage. Therefore, application of the suggested DST should be limited to sausages where the starter cultures modelled in the present study are used.

Conclusions

Manufacturers of fermented sausages sometimes face the problem that processing does not provide the required pathogen reduction. Using VTEC as example, we have presented the idea for a DST that could help manufacturers choose a corrective storage in the form of introducing a holding step, between 10 and 30 °C, before release of the sausages for sale.

References

Calicioglu M., Faith N.G., Buege D.R. and Luchansky J.B. (2001) Validation of a manufacturing process for fermented, semidry Turkish soudjouk to control *Escherichia coli* O157:H7. *Journal of Food Protection* 64 (8), 1156-1161.

Calicioglu M., Faith N.G., Buege D.R. and Luchansky J.B. (2002) Viability of *Escherichia coli* O157:H7 during manufacturing and storage of a fermented, semidry soudjouk-style sausage. *Journal of Food Protection* 65 (10), 1541-1544.

Faith N.G., Parniere N., Larson T., Lorang T.D. and Luchansky J.B. (1997) Viability of *Escherichia coli* O157:H7 in pepperoni during the manufacture of sticks and the subsequent storage of slices at 21, 4 and -20°C under air, vacuum and CO_2. *International Journal of Food Microbiology* 37, 47-54.

Hwang C.-A., Porto-Fett A.C.S., Juneja V.K., Ingham S.C., Ingham B.H. and Luchansky J.B. (2009) Modeling the survival of *Escherichia coli* O157:H7, *Listeria monocytogenes*, and *Salmonella* Typhimurium during fermentation, drying, and storage of soudjouk-style fermented sausage. *International Journal of Food Microbiology* 129, 244-252.

Porto-Fett A.C.S., Hwang C.-A., Call J.E., Juneja V.K, S.C., Ingham B.H. and Luchansky J.B. (2008) Viability of multi-strain mixtures of *Listeria monocytogenes*, *Salmonella typhimurium*, or *Escherichia coli* O157:H7 inoculated into batter or onto the surface of a soudjouk-style fermented semi-dry sausage. *Food Microbiology* 25, 793-801.

A predictive shelf life model as a tool for the improvement of quality management in pork and poultry chains

S. Bruckner[1], B. Petersen[1], J. Kreyenschmidt[2]

[1] Institute of Animal Science, University of Bonn, Katzenburgweg 7-9, 53115 Bonn, Germany (bruckner@uni-bonn.de)
[2] Institute of Construction- and Functional Materials, University of Applied Science Münster, Stegerwaldstraße 39, 48565 Steinfurt, Germany (j.kreyenschmidt@fh-muenster.de)

Abstract

The aim of the present study was the development of a common shelf life model for fresh pork and fresh poultry meat. Overall, 42 time series were investigated at constant and dynamic temperature conditions to collect microbiological growth data of *Pseudomonas* sp. for the development as well as for the validation of the model. Additionally, the influence of several intrinsic factors (pH-value, a_w-value, Warner-Bratzler shear force, D-glucose, L-lactic acid, fat and protein content) on the microbiological growth was analysed during storage at 4°C. Based on the growth of *Pseudomonas* sp., the model was developed by combining the Gompertz model as primary and the Arrhenius model as secondary model. Since the investigated intrinsic factors had only minor or no influence on the growth of *Pseudomonas* sp. in both meat types, they were not considered in the predictive shelf life model. Temperature was identified as the main influencing factor. Relevant microbial growth parameters for fresh poultry were related to the corresponding parameters for fresh pork which enabled the development of a common shelf life model. Predictions of the growth of *Pseudomonas* sp. and the shelf life at dynamic temperature conditions were in good agreement with the observations for fresh pork and fresh poultry even if only short temperature abuses occurred. With the information provided by the model the handling of the product as well as the stock rotation can be optimised in companies in meat chains and thus economic losses and product waste due to early unexpected spoilage can be reduced.

Keywords: predictive microbiology, Gompertz model, Arrhenius model, Pseudomonas sp., spoilage

Introduction

Fresh meat with high moisture content, moderate pH-value and readily available sources of energy provides an ideal matrix for microbial growth (Lambert *et al.* 1991). The spoilage flora of aerobically packed meat is mainly dominated by the growth of *Pseudomonas* sp. (Kreyenschmidt 2003, Raab *et al.* 2008).

Unexpected spoilage of meat can lead to food waste and thereby economic losses as well as the loss of consumer confidence (Nychas *et al.* 2007). Thus an accurate definition of shelf life and remaining shelf life is of high relevance for companies at all stages of meat supply chains. A good estimation of the remaining shelf life allows to optimise the storage management and thus to reduce the waste of meat resulting from a lack of knowledge concerning the products real shelf life (Kreyenschmidt *et al.* 2008, 2010; Raab *et al.* 2010). An alternative to traditional microbiological challenge tests for shelf life definition is the concept of predictive microbiology which uses mathematical models to predict microbiological growth and thus shelf life (McMeekin *et al.* 1993). But until now only a few models were developed for fresh meat or meat products, which are also usable for dynamic temperature conditions. However, most of these models were just developed for one type of meat product. Predictive shelf life models that are usable for different types of fresh meat (e.g. fresh pork and poultry) are missing.

Therefore, the objective of the study was the development of a common predictive shelf life model for fresh pork and fresh poultry based on the growth of *Pseudomonas* sp. as specific spoilage organism (SSO).

Materials and Methods

Skinless chicken breast fillets (150 - 170 g) and sliced pork loins (150 - 200 g) were packed aerobically. Immediately after packaging, pork and poultry samples were stored in high precision low temperature incubators at five different isothermal temperatures (2, 4, 7, 10 and 15°C). At dedicated points of time, total viable counts, the numbers of *Pseudomonas* sp. and sensory changes of pork and poultry samples were analysed.

For the validation of the model, the growth of *Pseudomonas* sp. was also investigated under non-isothermal conditions with periodically changing temperatures. The temperature cycle was 4 h at 12°C, 8 h at 8°C and 12 h at 4°C. Furthermore, four trials with short temperature abuses were performed. These trials consisted of three scenarios each: one control scenario at a constant storage temperature of 4°C (scenario 0) as well as two dynamic temperature scenarios with a basic storage temperature at 4°C and short temperatures shifts to 7°C (scenario 1) and 15°C (scenario 2), respectively. The trials differed in the number and duration of temperature shifts in scenario 1 and 2. Additionally, several intrinsic factors (pH-value, a_w-value, Warner-Bratzler shear force, D-glucose, L-lactic acid, fat and protein content) were analysed during the storage at 4°C to investigate their influence on the growth of *Pseudomonas* sp. (and thus the shelf life). Overall, 638 pork samples and 600 poultry samples were investigated in 42 time series.

The Gompertz model (1) was used as the primary model to describe the growth of *Pseudomonas* sp. with time (Gibson *et al.* 1987) and the Arrhenius equation (2) as a secondary model to describe the growth rate *B* at time *M* as a function of temperature.

$$N(t) = A + C \cdot e^{-e^{-B\cdot(t-M)}} \quad (1)$$

N(t): microbial count [cfu/g] at time t
A: initial bacterial count [cfu/g]
C: difference between N_{max} (= maximum population level) and A [cfu/g]
B: relative growth rate at time M [1/h]
M: reversal point [h]
t: time [h]

$$\ln(B) = \ln F - \left(\frac{E_a}{R \cdot T} \right) \quad (2)$$

B: relative growth rate at time M [1/h]
F: pre-exponential factor [1/h]
E_a: activation energy for bacterial growth [kJ/mol]
R: gas constant = 8.314 J/mol K
T: absolute temperature [K]

The accuracy of the fits was evaluated with the adjusted coefficient of determination ($\overline{R^2}$). The variable $\overline{R^2}$ is written as R^2 in the following text. As described by Bruckner (2010) the primary and the secondary model were combined to predict the growth of *Pseudomonas* sp. under non-isothermal conditions. The combined model predicts the microbial growth within intervals. Therefore, the time-temperature history of the product was divided into several assumed time-temperature intervals with constant storage temperature. Microbial growth could then be predicted by using the Gompertz function.

In every interval except the first interval a new reversal point *M* had to be calculated as a function of *B* (calculated with the Arrhenius equation) and as a function of the initial microbial count of the respective interval which has to equal the final microbial count of the previous interval. The bacterial count at the end of each interval could than be computed with the so calculated *M* for the respective interval as well as *B* for the respective interval (calculated with the Arrhenius equation). For the first interval in the non-isothermal temperature scenarios a proper *M* was derived from the linear regression of *M* against temperature in the isothermal experiments (Bruckner 2010 for detailed description and formulas).

Results and Discussion

A comparison of the growth of *Pseudomonas* sp. on fresh pork and poultry revealed that the growth was faster on poultry than on pork resulting in shorter shelf lives for fresh poultry at all investigated constant storage temperatures. The investigated intrinsic factors had only minor or no influence on the growth of *Pseudomonas* sp. in both meat types. Therefore these factors were not considered in the predictive shelf life model.

The growth of *Pseudomonas* sp. was well described with the Gompertz function with $R^2 \geq 0.93$ for both meat types. Furthermore, the Arrhenius equation described the temperature dependency of the growth rates ($R^2 = 0.98$ for pork and $R^2 = 0.99$ for poultry).

The linear fits of M values (obtained at isothermal temperatures) against temperature showed a good linearity with $R^2 = 0.97$ for pork and $R^2 = 0.94$ for poultry. This enabled the calculation of an adequate *M* value for the first interval in non-isothermal storage scenarios. *B* and *M* values for poultry could be related to pork values by linear fitting. The fits were good with R^2 values of 0.98 (for *B*) and 0.998 (for *M*) which made it possible to predict the growth of *Pseudomonas* sp. for fresh poultry based on the kinetic of fresh pork.

Figure 1 shows the observed bacterial count as well as the model predictions for the trial with periodically changing temperature (cycle: 4 h at 12°C, 8 h at 8°C and 12 h at 4°) for fresh pork and poultry. The model predicted the growth of *Pseudomonas* sp. well for pork during the whole storage. For poultry, a slight underprediction became visible in the first 50 h. However, at the determined end of shelf life, when the count of *Pseudomonas* sp reached 7.5 $\log_{10}$ cfu/g (Bruckner 2010), the predictions for both meat types matched to the observations. Predicted shelf life was in good agreement with observed shelf life (difference < 8 h for both meat types).

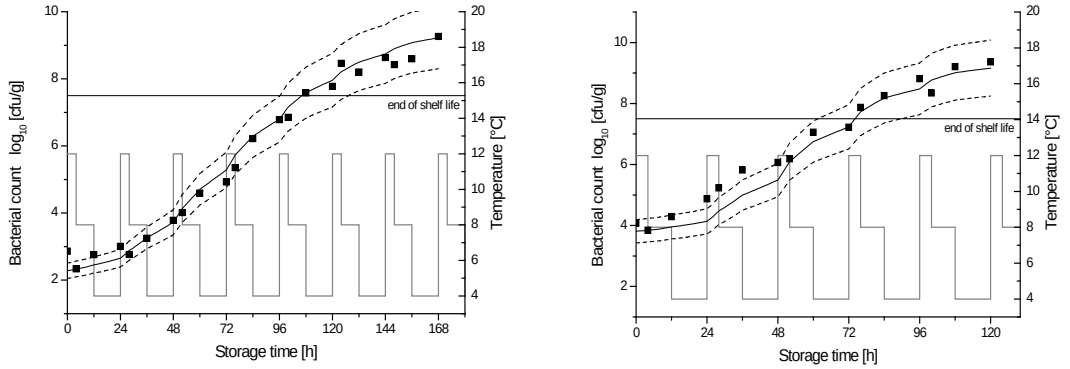

Figure 1: Observed and predicted growth of *Pseudomonas* sp. on fresh pork (left) and poultry (right) under periodically changing temperature conditions; (■) observed growth, (—) predicted growth; (---) ± 10 %, (grey line: temperature profile) (Bruckner 2010).

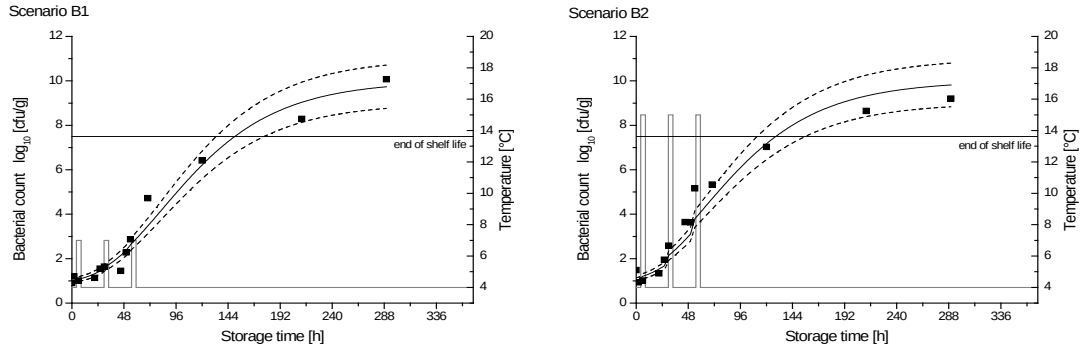

Figure 2: Observed and predicted growth of *Pseudomonas* sp. on fresh pork at two dynamic temperature scenarios with short temperature abuses; (■) observed growth data (—) predicted growth; (---) ± 10 %, (grey line: temperature profile) (Bruckner 2010).

In the dynamic temperature scenarios with only short temperature shifts of durations less than 5 % of the total storage time, the predictions for the growth of *Pseudomonas* sp. and the shelf lives were also in good agreement with the observations for both meat types. An example is shown in Figure 2. Whereas for poultry in general a slight underestimation of shelf life occurred (mean difference between observed and predicted shelf life: 11.1%), the shelf life times for pork were marginally overestimated (mean difference: 2.7 %).

Conclusions

A common predictive shelf life model was developed by combining the Gompertz and the Arrhenius model. The model delivered reliable shelf life prediction for fresh pork as well as poultry under dynamic temperature conditions even if short temperature shifts of less than 5 % of the total storage time occurred

With the information provided by the model the handling of the product as well as the stock rotation can be optimised in companies in meat chains and thus economic losses and product waste due to early unexpected spoilage can be reduced.

Acknowledgements

The study was partly financed by the EU project Chill-On (FP6-016333-2) and the InterregIIIC project PromSTAP. Thanks to all companies involved as well as to students and technical assistants for supporting the study.

References

Bruckner S. (2010) Predictive shelf life model for the improvement of quality management in meat chains. Doctoral thesis, Rheinische Friedrich-Wilhelms-Universiät Bonn, Germany.

Gibson A., Bratchell N. and Roberts T. (1987). The effect of sodium chloride and temperature on rate and extent of growth of Clostridium botulinum type A in pasteurized pork slurry. *Journal of Applied Bacteriology* 62(6), 479–490.

Kreyenschmidt J. (2003). Modellierung des Frischeverlustes von Fleisch sowie des Entfärbeprozesses von Temperatur-Zeit-Integratoren zur Festlegung von Anforderungsprofilen für die produktbegleitende Temperaturüberwachung. Doctoral thesis, Rheinische Friedrich-Wilhelms-Universität Bonn, AgriMedia GmbH, Bergen/Dumme, Germany.

Kreyenschmidt J., Hansen T. B., Kampmann Y., Christensen B. B., Aabo S., Lettmann T., Bruckner S., Kostov I., Van Beek P. and Petersen B. (2008). Innovative systems in the field of food quality and safety. In MUNLV and GIQS (eds.), Food quality and safety in international food chains – Technical reports of the Interreg IIIC Initiative PromSTAP, 152–165.

Kreyenschmidt J., Hübner A., Beierle E., Chonsch L., Scherer A. and Petersen B. (2010). Determination of the shelf life of sliced cooked ham based on the growth of lactic acid bacteria in different steps of the chain. *Journal of Applied Microbiology* 108(2):510–520.

Lambert A. D., Smith J. P. and Dodds K. L. (1991). Shelf life extension and microbiological safety of fresh meat – a review. *Food Microbiology* 8(4), 267–297.

McMeekin T. A., Olley J., Ross T. and Ratkowsky D. A. (1993). *Predictive Microbiology: theory and application. Innovation in Microbiology*. Research Studies Press and John Wiley and Sons, Taunton, UK, 360 pp. (ISBN 0471935452)

Nychas G.-J. E., Marshall D. L. and Sofos J. (2007). Meat, poultry and seafood, In: M.P. Doyle, L.R. Beuchat and T.J. Montville. (Eds.), *Food microbiology: fundamentals and frontiers*, 105–140, ASM Press, Washington, USA, 768 pp. (ISBN 1555811174).

Raab V., Bruckner S., Beierle E., Kampmann Y., Petersen B. and Kreyenschmidt J. (2008). Generic model for the prediction of remaining shelf life in support of cold chain management in pork and poultry supply chains. *Journal on Chain and Network Science* 8(1), 59–73.

Raab V., Petersen B. and Kreyenschmidt J. (2010). Temperature monitoring in meat supply chains. *British Food Journal*, in press.

Modelling the effect of the temperature and carbon dioxide on the growth of spoilage bacteria in packed fish products

B. Alfaro[1], I. Hernández[1], Y. Le Marc[2], C. Pin[2]

[1]AZTI-Tecnalia, Bizkaiako Teknologi Parkea. Asontodo Bidea, Edf.609, 48160 Derio, Bizkaia, Spain (balfaro@azti.es)
[2] Institute of Food Research, Norwich Research Park, Norwich NR4 7UA, UK

Abstract

The aim of this research was to evaluate the combined effect of the temperature and carbon dioxide on the growth of spoilage bacteria isolated from fish products under MAP. Isolates obtained from Atlantic horse mackerel (*Trachurus trachurus)* fillets packed in MAP at time of sensory rejection were genotypically characterized. Identified bacteria included *Carnobacterium maltaromaticum, Serratia proteamaculans, Yersinia intermedia, Shewanella baltica*. These bacteria were inoculated alone and in a mixed culture into modified Long and Hammer's broth. Cultures were incubated at several temperatures (0, 4, 6, 12 and 20ºC) under CO_2 enriched atmospheres (0, 25, 50, 75, 100% v/v, balance nitrogen) and under air (21% O_2). The growth kinetic parameters were estimated by fitting the model of Baranyi and Roberts (1994). The dependence of the maximum specific growth rate on temperature, CO_2 and O_2 was described by a cardinal model similar to that described by Mejlholm *et al.* (2010). The performance of the models was validated under constant temperature conditions. Models were implemented in a user-friendly computing program called "Fishmap". This program predicts the growth of spoilage bacteria in horse mackerel under MAP at constant and fluctuating temperature conditions.

Keywords: kinetic modelling, spoilage bacteria, fish products, software application

Introduction

Modified atmosphere packaging (MAP) with carbon dioxide (CO_2) as active gas is widely used, together with refrigeration, to delay spoilage and extend the shelf life of fresh fishery products. Modelling the behaviour of specific microflora and quantitatively correlating it with shelf life can provide an effective tool for predicting fish quality.
In previous work, a good correlation was found between sensory attributes and bacterial population in Atlantic horse mackerel fillets packed under MAP stored at different temperatures, however lipid oxidation was not observed at sensory rejection time.
The aim of this work was to develop mathematical models for studying the dependence of the maximum specific growth rate on temperature, CO_2 and O_2 of *Carnobacterium maltaromaticum, Serratia proteamaculans, Yersinia intermedia, Shewanella baltica* and a mixed culture isolated from Atlantic horse mackerel fillets packed in MAP at time of sensory rejection. The performance of the models was validated in different fish products.

Materials and Methods

Initial studies with naturally contaminated fish products

In a previous work samples of Atlantic horse mackerel (*Trachurus trachurus*) fillets packed in MAP were obtained directly from fish processing plant. Fillets of 400 ± 20g were packed with a gas ratio of 48% CO_2, 50%N_2 and 2% O_2. Isolates obtained at time of sensory rejection were genotypically characterized. Identified bacteria included *Carnobacterium maltaromaticum, Serratia proteamaculans, Yersinia intermedia and Shewanella baltica.*

Inoculum preparation and growth data

Identified bacteria alone *Carnobacterium maltaromaticum, Serratia proteamaculans, Yersinia intermedia and Shewanella baltica* and mixture of four species, was studied. These bacteria

and the mix were inoculated into modified Long and Hammer's broth (L&H) (Koutsoumanis *et al.* 2000). Cultures were incubated at several temperatures (0, 4, 6, 12 and 20ºC) under CO_2 enriched atmospheres (0, 25, 50, 75, 100% v/v, balance nitrogen) and under air (21% O_2). Total viable counts (TVC) were determined by spread plating on Long and Hammers medium and incubated for 7 days at 10ºC. The growth kinetic parameters, the lag phases, maximum specific growth rates (μ_{max}) and maximum cell numbers (N_{max}) were estimated by fitting the model of Baranyi and Roberts (1994).

Models development

The dependence of the maximum specific growth rate on temperature, CO_2 and O_2 was described by a cardinal model similar to that described by Mejlholm, *et al.* (2010):

$$\mu = \mu_{ref}\left(\frac{T-T_{\min}}{T_{ref}-T_{\min}}\right)^2\left(\frac{CO_{2\max}-CO_{2equilibrium}}{CO_{2\max}}\right)\left(\frac{O_2-O_{2K}}{O_{2ref}-O_{2k}}\right)\xi \qquad (1)$$

The concentration of CO_2 dissolved at equilibrium, $CO_{2equilibrium}$, was calculated according to the initial percentage of CO_2 in the headspace, to the temperature and to the initial gas product volume ratio as described by Mejlholm *et al.* (2010). The same terms as in Mejlholm, *et al.* (2010) were used for the effects of temperature and CO_2 . A new term was introduced in the model for the effect of O_2:

$$\phi(O_2) = \left(\frac{O_2-O_{2K}}{O_{2ref}-O_{2k}}\right) \qquad (2)$$

In Equation 2, O_2 is the concentration of O_2 (ppm) dissolved in the medium. O_2 was estimated according to the data of Lewis (2006). From this data the estimation of the amount of O_2 dissolved in water at 760 millimetres of mercury (sea level) is estimated as:

$$O_2 = \frac{(0.0045\,T^2 - 0.3628\,T + 14.486)\,O_{2percent}}{21.2} \qquad (3)$$

where $O_{2percent}$ is the percentage of oxygen in the atmosphere. According to our experimental design this percentage has only two values, either 21.2% for air or 0% for vacuum. In equation 2, O_{2ref} is the amount of O_2 dissolved in water at 760 mmHg (10.0565 ppm) and at the reference temperature used in equation 1, 15°C.

For organisms unable to grow at low concentrations of O_2, the parameter O_{2k} could be interpreted as the minimum amount of O_2 required for growth. However, since all bacteria studied in this work are able to grow in absence of O_2, O_{2k} takes negative values.

The smaller the values of O_{2k} are, the smaller the effect of the lack of oxygen on the growth rate. The proportional decrease of the growth rate as a consequence of vacuum packaging with respect to storage under air can be estimated from O_{2k} as follows:

$$\text{Proportional decrease} = \frac{-O_{2k}}{O_{ref}-O_{2k}} \qquad (4)$$

The model, in Equation 1, comprises an interaction term, ξ, described by (Le Marc, *et al.* 2002) but adding the correspondent term for the oxygen as follows:

$$\varphi_{O_2} = (1-\phi(O_2))^2 \qquad (5)$$

T_{ref} and O_{2ref} were fixed in the model to 15°C and 10.0565 ppm, respectively. The other parameters were estimated using the *nlin* procedure (SAS version 9.2, SAS Institute Inc., Cary, NC).

Product validation

Validation experiments were carried out with four batches of commercial products, Atlantic horse mackerel fillets packed under MAP (%50 $C0_2$). Each batch was stored at different temperatures (2, 4, 6 and 8ºC). Numbers of total viable counts were analysed at regular intervals during storage of each batch of fish product. In addition, observations of growth of Lactic Acid Bacteria (LAB) on fish product under MAP from fish naturally contaminated (data obtained from Combase) were compared to predictions of the model developed for *Carnobacterium*.

Results and Discussion

The population dynamics of total viable counts in Atlantic horse mackerel fillets packed under MAP (%50 $C0_2$) stored at 6ºC and the growth of the bacteria isolated from Atlantic horse mackerel in L&H growth liquid medium are presented in Figure 1. Similar growth parameters were obtained in mackerel and in L&H culture medium. For this reason, this medium was chosen to evaluate the combined effect of the temperature and carbon dioxide on the growth of spoilage bacteria isolated from Atlantic horse mackerel.

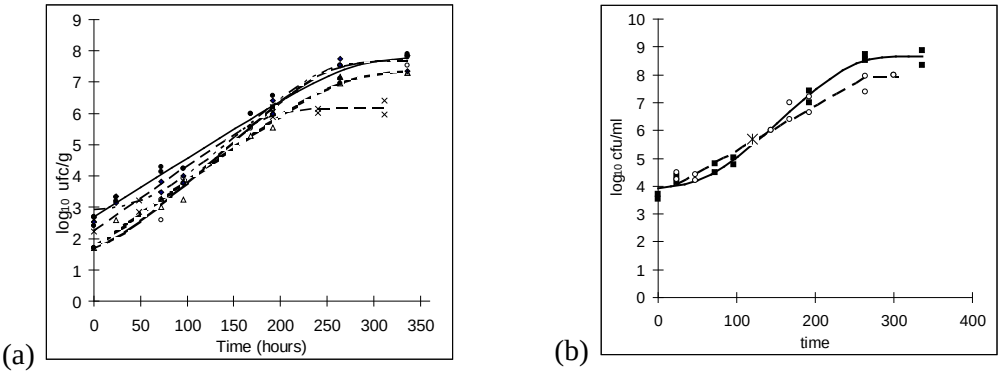

Figure 1: Growth curves (a) of *Carnobacterium maltaromaticum*(●), *Serratia proteamaculans*(x), *Yersinia intermedia*(○) and *Shewanella baltica*(Δ) in LH liquid medium stored at 6ºC with 50% of CO_2(b) of total bacteria counts in naturally contaminated Atlantic horse mackerel stored at 6ºC in an atmosphere with 50% CO_2(○) and growth of the mix (■) in LH liquid medium stored at 6ºC with 50%. Sensory rejection time (*) was 120 hours. Lines represent the fitted models.

Table 1 shows the parameters estimates and standard error of the model with and without interactions. The results showed that *Carnobacterium* had the slowest growth rate under air while it was the group with the greatest resistance to CO_2 and to the lack of O_2.The growth rate of *Carnobacterium* was reduced only by 9% under vacuum conditions. *Shewanella* showed also high resistant to CO_2. *Yersinia* was the least resistant isolate to CO_2 while *Serratia* was the most sensitive to the lack of O_2. Serratia growth rate was reduced 29% under 0% O_2 condition.

Table 1: Parameters estimates and standard error for the cardinal model with and without interactions for each group of bacteria.

Model for	Estimated model parameters				Effect of 0% O_2 *	Fixed model parameters		standard error	
	μ_{ref}	T_{min}	CO_{2max}	O_{2k}		O_{2ref}	T_{ref}	No interactions	With interactions
Carnobacterium	0.299	-6.58	5974	-102.7	0.09	10.06	15	0.0442	0.0446
Mixed bacteria	0.517	-7.19	5839	-16.8	0.37	10.06	15	0.0785	0.0786
Serratia	0.458	-5.39	4867	-24.2	0.29	10.06	15	0.0369	0.0364
Shewanella	0.398	-7.68	5112	-67.7	0.13	10.06	15	0.0487	0.0484
Yersinia	0.425	-6.01	3803	-47.7	0.17	10.06	15	0.069	0.0688

*Proportional decrease of the growth rate under 0% of O_2 with respect to storage under air condition.

Validation of the applicability of the predictive models

The model for "mixed bacteria" was validated by comparing predictions with independent observed growth rates in Atlantic horse mackerel fillets and in L&H growth medium (Figure 2a). For "mixed model" values of 1.12 and 1.29 were obtained for the bias factor B_f and the accuracy factor A_f, respectively. The model for *Carnobacterium maltaromaticum* was validated on ComBase data in fish products (sea bream and red mullet) under MAP (Figure 2b). For this model values of 0.96 and 1.67 were obtained for B_f and A_f, respectively.

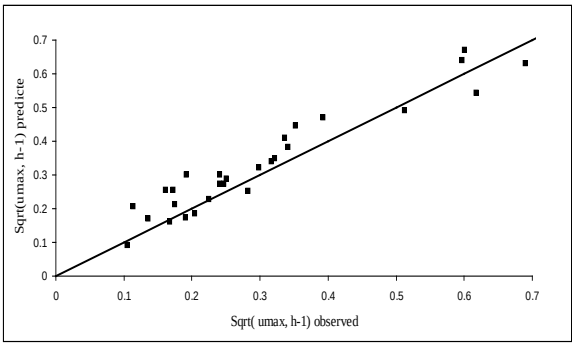

(a)

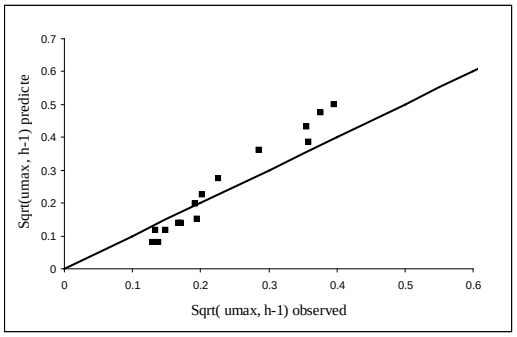

(b)

Figure 2: (a) Comparison of observed and predicted μ_{max} values for TVC in Atlantic horse mackerel fillets and in L&H growth medium stored at different temperatures and CO_2 concentrations (n=31) (b)Comparison of observed and predicted μ_{max} values for LAB in fish products under MAP (n=18). Predicted μ_{max} values were obtained by the model developed for *Carnobacterium maltaromaticum*. The solid line represents the perfect adequacy between observed and predicted values.

Conclusions

The validation study showed that μ_{max} values of spoilage microflora in fish products under MAP can be accurately predicted. The models have been implemented in a Visual Basic add-in for Excel called "Fishmap". This program predicts the growth of spoilage bacteria in fish products under MAP at constant and fluctuating temperature conditions.

Acknowledgements

This work was supported by the Basque Government (Department of the Environment, Regional Planning, Agriculture and Fisheries)

References

Baranyi J. and Roberts T.A. (1994) A dynamic approach to predicting bacterial growth in food. *International Journal of Food Microbiology* 23, 277-294.

Koutsoumanis K. and Nychas G.-J. E. (2000) Application of a systematic experimental procedure to develop a microbial model for rapid fish shelf life predictions. *International Journal of Food Microbiology* 60:171-184.

Mejlholm O., Gunvig A., Borggaard C., Blom-Hanssen J., Mellefont L., Ross T., Leroi F., Else T., Visser D. and Dalgaard P. (2010) Predicting growth rates and growth boundary of *Listeria monocytogenes* - An international validation study with focus on processed and ready-to-eat meat and seafood. *International Journal of Food Microbiology* 141, 137-150.

Lewis M.E. (2006) Correction factors for oxygen solubility and salinity: U.S. Geological Survey Techniques of Water-Resources Investigations, book 9, chap. A6., section 6.2, from http://pubs.water.usgs.gov/twri9A6/.

Le Marc Y., Huchet V., Bourgeois C.M., Guyonnet J.P., Mafart P. and Thuault D. (2002) Modelling the growth kinetics of *Listeria* as a function of temperature, pH and organic acid concentration. *International Journal of Food Microbiology* 73, 219-237.

Survival and growth of enteropathogenic *Escherichia coli* against temperature in iceberg lettuce exposed at short-term storage

M.Y. Rodríguez-Caturla[1], A. Valero[1], E. Carrasco[1], F. Pérez[1], G.D. Posada[1], A. Morales-Rueda[1], G. Zurera-Cosano[1]

[1]Department of Food Science and Technology, University of Cordoba, Campus Rabanales s/n Edif.Charles Darwin C1-14014 Córdoba (Spain). (myrcazul@hotmail.com)

Abstract

Minimally processed lettuce is a ready-to-eat (RTE) food commodity subjected to be contaminated by pathogenic microorganisms if processing and distribution conditions as well as handling practices are not efficient. In this study we evaluated the behaviour of a Enteropathogenic *Escherichia coli* strain (serotype O158:H23) in RTE iceberg lettuce by simulating different time/temperature (t/T) scenarios along the processing and distribution chain found in catering establishments. Different initial contamination levels (4, 3 and 2 log cfu/g) were used and lettuce samples were incubated at static (8, 12, 16, 20 and 24ºC) and dynamic temperatures (six representative t/T scenarios) during 6h. Observed log increase (Log_{inc}) was calculated at each studied condition. Statistical tests (ANOVA, t test, correlation coefficients) were implemented in Statistica for Windows v10. The results indicated that the maintenance of the lettuce at 8ºC reduced the *E. coli* population (reductions from -0.36 to -0.45 log cfu/g). However, if chill-chain is not maintained, *E. coli* can grow up to 1.13 log cfu/g at temperatures above 16ºC, even from the lowest contamination levels. Indeed, significant differences were obtained ($P<0.05$) in Log_{inc} at these conditions. Dynamic t/T profiles resulted in growth of *E. coli* excepting the storage between 8 and 16ºC. However, no significant differences were observed in *E. coli* behaviour between the simulated scenarios. The survival of *E. coli* in RTE iceberg lettuce samples depended on the contamination level, since from an inoculum of 4 log cfu/g, growth was observed at 12ºC while low initial concentrations (2 and 3 log cfu/g) led to a slight final reduction (-0.78 and -0.37 log cfu/g respectively). It can be concluded that time delays from processing to consumption of RTE lettuce salads together with inappropriate food temperatures would allow *E. coli* growth at unacceptable levels. These findings may serve to food safety managers to better define the control measures to be adopted in catering establishments in order to prevent foodborne infections.

Keywords: *Ready-to-eat lettuce salads, Enteropathogenic Escherichia coli, short-term storage, dynamic t/T profiles, predictive models*

Introduction

Verotoxigenic *Escherichia coli* is one of the most important emerging foodborne pathogen, affecting a large group of people, being the very young, elderly and inmunocompromised the most susceptible groups (Schneider *et al.* 2009). It is well known that non-O157 *E. coli* strains can be transmitted throughout contaminated foods such as meat, water and fresh or raw vegetables (Marzocca *et al.* 2006; Frias *et al.* 1996; Rowe *et al.* 1974).

Besides, cutting, shredding, packaging and shipping processes, together with the storage conditions of RTE lettuce salads between food preparation and consumption can to affect the food quality, allowing the growth and survival of pathogenic microorganisms (Luo *et al.* 2010). Given the number of meals served in catering establishments, storage and distribution conditions are not always well established, thus favouring microbial growth.

In order to provide quantitative data on the microbial behaviour in foods, growth and survival models are shown to be a basic tool to predict the safety of food and microbial spoilage in the food chain (Franz *et al*. 2010; McMeekin *et al*. 2005; Tamplin *et al*. 2005; Rodríguez *et al*. 2000).

The main objective of this study was to provide a more insight on the *E. coli* behaviour in RTE iceberg lettuce salads by evaluating the impact of storage and distribution conditions. This was done by simulating different time/temperature (t/T) scenarios (static and dynamic conditions) along the processing and distribution chain commonly found in catering establishments.

Materials and Methods

200g-packages of RTE iceberg lettuce were purchased in a local supermarket. A frozen stock culture of a Enteropathogenic *Escherichia coli* strain (serotype O158:H23, NCTC 10974), was re-suspended in Tryptone Soja Broth (TSB, Oxoid) and serial dilutions were made. RTE iceberg lettuce samples (10g) were inoculated at different initial contamination levels (2, 3 and 4 log cfu/g), and subsequently incubated at static (8, 12, 16, 20 and 24ºC) and dynamic temperatures (six representative t/T scenarios: 8-24ºC, 8-20ºC, 8-16-24ºC, 8-16-20, 8-12-20ºC and 8-16ºC) during 6h. Growth monitoring was performed at six storage periods (30, 60, 90, 120, 180, 360 min) in Tryptone-Bile-X Glucuronide agar (TBX, Oxoid), incubated at 42ºC during 24h. The dynamic t/T profiles studied corresponded to the most representative temperatures measured during preparation and distribution of RTE salads in Spanish catering establishments. The temperatures inside the RTE lettuce packages were measured by a Datalogger (MicrologPro EC700, Fourier Systems) together with the external temperature of the refrigerator. Subsequently, observed log increases (Log_{inc}) of *E. coli* population in RTE iceberg lettuce were obtained and the relationship between Log_{inc} and static temperatures was described by a linear regression for each inoculum level studied (Fig. 1). Regarding dynamic t/T profiles, the secondary Ratkowsky model proposed by Koseki and Isobe (2005) (Eq. 1) was used to estimate the growth of *E. coli*. The methodology of Carrasco *et al.* (2010) was applied to calculate the maximum growth rate and the "effective" static temperature that produced the same Log_{inc} (Eq. 2):

$$\sqrt{\mu_{\max}} = 0.033 \cdot (T - 4.54) \qquad \text{(Eq.1)}$$

where μ_{max} is the maximum growth rate (h^{-1}) and T is the storage temperature (ºC).

$$T_{eff} = \frac{\sqrt{\frac{\log_{inc}}{t}}}{0.033} + 4.54 \qquad \text{(Eq.2)}$$

where T_{eff} is the effective static temperature (ºC), t is the time during which the temperature was recorded (h), and Log_{inc} is the increase of *E. coli* at each temperature profile.

Results and Discussion

The results obtained in our study have shown the ability of *E. coli* to grow in RTE lettuce salads at temperatures above 16ºC. Fig. 1 shows the Log_{inc} of *E. coli* at static temperature conditions (8, 12, 16, 20 and 24ºC) and the fitted linear regression models. Results at 8ºC showed a slight decrease in *E. coli* population at the three contamination levels studied (2 log cfu/g: Log_{inc} = -0.36; 3 log cfu/g: Log_{inc} = -0.27 and 4 log cfu/g: Log_{inc} = -0.33). Other published studies performed at lower temperatures (2-5ºC) have shown that *E. coli* cannot grow and a decrease in the microbial population was observed at the end of the storage period (Koseki and Isobe 2005; Bharathi *et al.* 2001). We also observed that growth of *E. coli* was observed at temperatures above 12ºC corroborating what other related studies has found (Abdul-Raouf *et al.* 1993). At abuse temperature conditions (24ºC), the initial inoculum level resulted in a lower Log_{inc} at 2 log cfu/g than at 3-4 log cfu/g (0.89 and ~1.50 log cfu/g respectively).

Beside this, significant differences ($P<0.05$) in the Log_{inc} at the different storage temperatures were observed. At 4 log cfu/g, larger differences in Log_{inc} values were noted (from -0.33 to 1.52 log cfu/g). Therefore, if chill-chain is not maintained, *E. coli* can grow up to 1.13 log cfu/g at temperatures above 16ºC, even from the lowest contamination levels. Similar results were found by Bharathi *et al.* (2001) in minimally processed vegetables at 16ºC with a higher

inoculum level (6.3 $\log_{10}$ cfu/g). They detected an increase of *E. coli* up to 11 $\log_{10}$ cfu/g in 2 days.

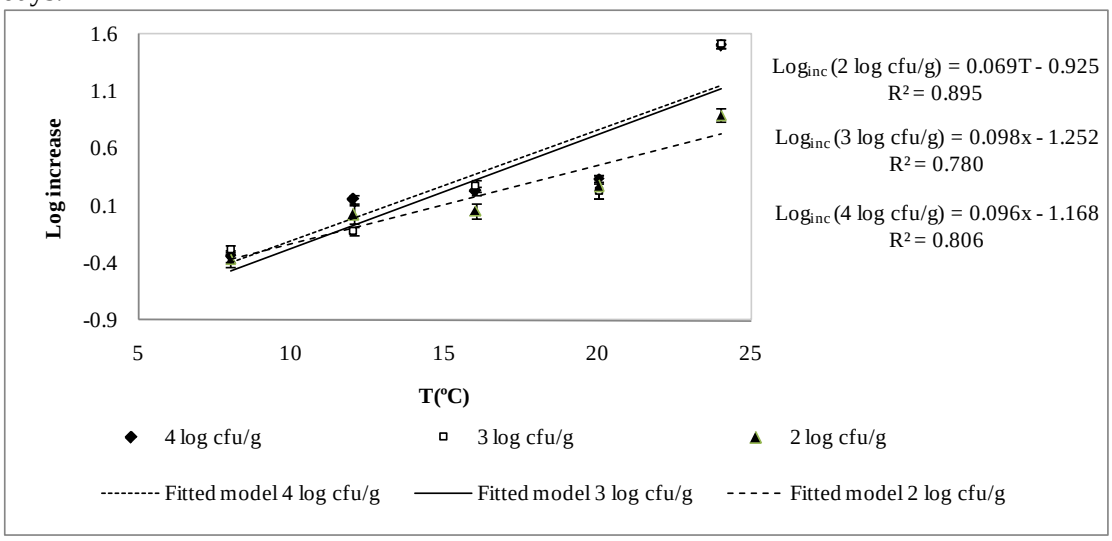

Figure 1: Logarithmic increase (Log_{inc}) of the *E. coli* population and linear regression models as a function of storage temperature at 2, 3 and 4 log cfu/g in RTE lettuce.

Regarding dynamic profiles, through the secondary model of Koseki and Isobe (2005), it was estimated maximum growth rate (μ_{max}) and the effective temperature (T_{eff}) that produced the same value of Log_{inc} for each t/T profile in *E. coli* population (Table 1).

No significant differences were observed between the six t/T profiles (P>0.05) in Log_{inc}, however, some difference was noted between the profile (8-16ºC) and the other scenarios. This was especially relevant at low inoculation levels, since when the initial contamination was equal to 2-3 log cfu/g, Log_{inc} were negative (-0.78 and -0.37 log cfu/g respectively, Table 1). In contrast, at 4 log cfu/g of inoculum level a slight increase of *E. coli* was observed at the end of the storage period. These results suggest the importance of good manufacturing practices of food, together with a more strict control of the temperature during preparation and distribution of RTE lettuce. Additionally, the importance of a good monitoring of microbial quality of raw material can lead to reduce the initial contamination of *E. coli*.

Table 1: Estimated maximum growth rate (μ_{max}, h^{-1}) and the effective temperature T_{eff} (ºC) that produced the same Log_{inc} of *E. coli* in RTE lettuce at each dynamic t/T profiles and contamination levels.

t/T Profiles		8-24º	8-20º	8-16-24º	8-16-20ºC	8-12-20ºC	8-16ºC
4 log cfu/g	Log_{inc}	0.39	0.20	0.31	0.24	0.22	0.27
	μ_{max} (h^{-1})	0.07	0.03	0.05	0.04	0.04	0.04
	T_{eff} (ºC)	12.29	10.10	11.38	10.60	10.39	10.96
3 log cfu/g	Log_{inc}	0.21	0.15	0.31	0.14	0.17	-0.37
	μ_{max} (h^{-1})	0.04	0.03	0.05	0.02	0.03	- *
	T_{eff} (ºC)	10.23	9.38	11.44	9.14	9.67	-
2 log cfu/g	Log_{inc}	0.13	0.21	0.13	0.03	0.09	-0.78
	μ_{max} (h^{-1})	0.02	0.04	0.02	0.01	0.01	-
	T_{eff} (ºC)	9.04	10.20	9.05	6.77	8.18	-

*T_{eff} and μ_{max} could not be estimated since a logarithmic decrease of *E. coli* population was observed.

Conclusions

This study demonstrated that *E. coli* can grow at temperatures above 12ºC, even at low contamination levels (2 log cfu/g). Likewise, dynamic storage conditions can result in growth of *E. coli* at short-term storage if lettuce is left at room temperatures (above 20ºC).
Estimating the growth and behaviour of *E. coli* in RTE lettuce salads will help to reduce the microbial risks associated with preparation and/or distribution of RTE lettuce. Also this data will serve as proof of the importance of cooling temperatures management. These findings may serve to food safety managers to better define the control measures to be adopted in catering establishments in order to prevent foodborne infections.

Acknowledgements

This work was partly financed by the AGR-01879 Excellence Project (Andalusia Government), AGL 2008-03298/ALI project (Spanish Ministry of Science and Innovation), European ERDF funding and by a grant awarded by the International Cooperation and Development Spanish Agency (AECID).

References

Abdul-Raouf U.M., Beuchat L.R. and Ammar M.S. (1993) Survival and growth of *Escherichia coli* O157:H7 on salad vegetables. *Applied and Environmental Microbiology* 59(7), 1999-2006.

Bharathi S., Ramesh M.N. and Varadaraj M.C. (2001) Predicting the behavioural pattern of *Escherichia coli* in minimally processed vegetables. *Food Control* 12(5), 257-284.

Carrasco E., Pérez-Rodríguez F., Valero A., García-Gimeno R.M. and Zurera G. (2010) Risk Assessment and Management of *Listeria Monocytogenes* in Ready-to-Eat Lettuce Salads. *Comprehensive Reviews in Food Science and Food Safety* 9, 498-512.

Franz E, Tromp S.O., Rijgersberg H. and Van Der Fels-Klerx H.J. (2010) Quantitative microbial risk assessment for *Escherichia coli* O157:H7, *Salmonella*, and *Listeria monocytogenes* in leafy green vegetables consumed at salad bars. *Journal of Food Protection* 73(2), 274–285.

Frias C. (1996) Study of the pathogenity factors of Enterohaemorrhagic *Escherichia coli*. Doctoral Thesis. Universidad Autónoma de Barcelona (Spain).

Koseki S. and Isobe S. (2005) Prediction of pathogen growth on iceberg lettuce under real temperature history during distribution from farm to table. *International Journal of Food Microbiology* 104(3), 239-248.

Luo Y., He Q. and McEvoy L. (2010) Effect of storage temperature and duration on the behaviour of *Escherichia coli* O157:H7 on packaged fresh-cut salad containing Romaine and Iceberg lettuce. *Journal of Food Science* 75(7), M390-M397.

Marzocca M.A., Marucci P.L., Sica M.G. and Álvarez E.E. (2006) Detection of *Escherichia coli* O157:H7 in raw minced meat and frozen hamburgers. *Argentine Microbiology Journal* 38(1), 38-40.

McMeekin T.A. and Ross T. (2005) Predictive Microbiology: providing a knowledge-based framework for change management. *International Journal of Food Microbiology* 78(1-2), 133-153.

Rodríguez A.M.C., Alcala E.B., Gimeno R.M.G. and Cosano G.Z. (2000) Growth modelling of *Listeria monocytogenes* in packaged fresh green asparagus. *Food Microbiology* 17(4), 421-427.

Rowe B., Gross R.J., Lindop R. and Baird R.B. (1974) A new *E. coli* O group O158 associated with an outbreak of infantile enteritis. *Journal of Clinical Pathology* 27, 832-833.

Schneider K.R., Schneider R.G., Hubbard M.A. and Chang A. (2009) Preventing Foodborne Illness: *Escherichia coli* O157:H7. University of Florida. IFAS Extension. FSHN031. http://edis.ifas.ufl.edu.

Tamplin M.L., Paoli G., Marmer B.S. and Phillips J. (2005) Models of the behaviour of *Escherichia coli* O157:H7 in raw sterile ground beef stored at 5 to 46º C. *International Journal of Food Microbiology* 100(1-3), 335-344.

Integrative mathematical modelling for packaging design of fresh produce

P. V. Mahajan, M.J. Sousa-Gallagher

Department of Process and Chemical Engineering, School of Engineering, College of Science Engineering and Food Science, University College, Cork, Ireland (p.mahajan@ucc.ie or m.desousagallagher@ucc.ie)

Abstract

Equilibrium Modified Atmosphere Packaging (EMAP) of fresh produce is a dynamic system and relies on the modification of the atmosphere inside the package, achieved by the natural interplay between two processes, the respiration of the product and the transfer of gases through the packaging film, which leads to an atmosphere richer in CO_2 and poorer in O_2. A real challenge is how to integrate the mathematical modelling depicting product respiration rate and package permeability on a packaging system. The "pack-and-pray" approach and in-house trial-and-error experiments are normally used to find a suitable packaging material, film area for gas/water vapour exchange, package size and the quantity of product to be packaged. This is both time and labour intensive and a potential risk to health. Mathematical models on product respiration rate and package permeability were integrated in order to determine the needs for packaging of fresh produce and predict gas composition EMAP during storage period. Further, it also provides the impact of temperature variation, and variability of product/package on gas composition providing a system which allows selection of suitable packaging materials for fresh produce. Pack-in-MAP® is a knowledge web-based system combining product and film databases and various mathematical models to test several packaging designs on a value-for-money basis while minimising costs and avoiding costly trial-and-error approaches.

Keywords: fresh produce, MAP, respiration, permeability, packaging simulation, Pack-in-MAP®

Introduction

The segment of ready-to-eat fresh-cut consumer products is one of the few that has shown consistent growth in the last few years. Trends for healthier eating increased consumption of fruits and vegetables, while trends for convenience stimulate ready-to-eat products. However, fresh produce are living commodities which respire even after harvest. Equilibrium modified atmosphere packaging (EMAP) is a well known technique for preserving fruit and vegetables for longer time. It relies on the modification of the atmosphere inside the package, achieved by the natural interplay between two processes, the respiration of the product and the transfer of gases through the packaging film, which leads to an atmosphere richer in CO_2 and poorer in O_2. In this system, atmosphere is generated naturally by product respiration rate (passive MAP). Low O_2 and high CO_2 are widely assumed to maintain quality and extend shelf life of fresh produce (Fig. 1).

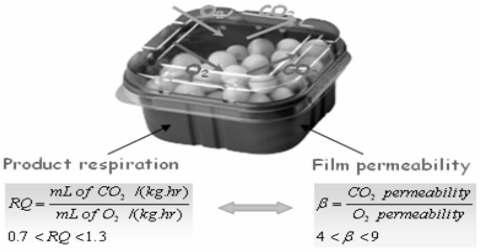

Figure 1: Principles of MAP

The major challenge faced by the fresh produce industry is "What packaging material do I use?" While it may be possible to find an appropriate packaging material through simply testing various packages ("pack & pray" approach), the optimal packages is likely to be found by taking an integrative mathematical modelling process. There is a wealth of published information on MAP, which could be used to find which polymeric films would be most suitable for a particular produce under a given set of processing and environmental conditions. Such analysis could provide an initial screening of films, point out their potential limitations/benefits and reduce the experimental testing.

The ultimate aim of this integrative mathematical modelling process is to contribute to the development of a knowledge-based system, in order to help design of an optimal package by selecting a suitable film for a given product, its area and thickness, filling weight, equilibrium time, and the equilibrium gas composition at constant and varying temperature conditions.

Materials and Methods

EMAP design entails consolidated knowledge of the i) fresh produce quantification, ii) polymer engineering and iii) converting technology, and a successful packaging needs the interaction of these three different disciplines (Brandenburg and Zagory 2009). EMAP design for fresh produce requires an integrated model considering:

1. Product respiration rate as a function of both gas composition and temperature,
2. Amount of product,
3. Permeability of packaging to O_2, CO_2, as a function of temperature and
4. Packaging geometry and size, among other product characteristics (Fig. 2) (Mahajan *et al.* 2006, 2009).

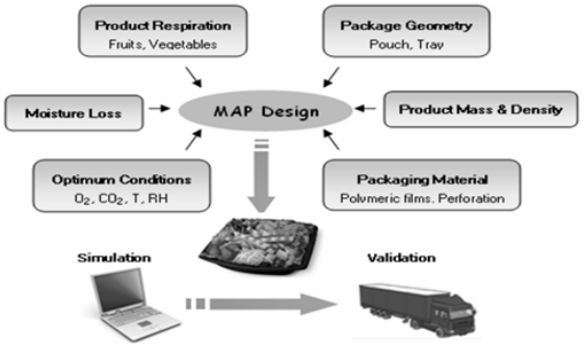

Figure 2: Factors affecting EMAP design

A real challenge is how to integrate the needs of the product to find an optimal package. The answer through an engineering approach involves the use of mathematical models depicting product respiration rate and package permeability to be integrated into the mass balance equation of a packaging system. The differential equations of mass balance for O_2 and CO_2 in MAP containing a respiring product in a permeable package can be generated (Fig. 3).

Package geometry & size — Film area — Respiration rate

$$V_f \times \frac{dy_{O_2}}{dt} = P_{O_2} \times A \times \left(y^e_{O_2} - y_{O_2}\right) - R_{O_2} \times M$$

Film permeability — Optimal atmosphere — Product type, size & mass

V_f	: Package free volume, ml	A	: Film area, m^2
P_{O2}	: O_2 permeability, $ml/m^2.hr.atm$	R_{O2}	: Respiration rate, ml/kg.hr
y_{O2}	: O_2 concentration, atm	M	: Product mass, kg
y^e_{O2}	: O_2 concentration at equilibrium, atm	t	: Storage time, hr

Figure 3: Integrative mathematical modelling of EMAP for packaging design of fresh produce

Ultimate result of this integrative mathematical modelling was a web-based packaging design software called Pack-In-MAP® (www.packinmap.com) (Mahajan *et al*. 2009)

Results and Discussion

Pack-in-MAP® is a knowledge based system containing databases on product characteristics, respiration rate, optimum temperature, optimum range of O_2 and CO_2 concentrations as well as permeability of different packaging materials, including micro-perforated films. Pack-in-MAP® is a web-based (www.packinmap.com) software developed by University College Cork, Ireland, that helps in designing EMAP for fresh and fresh-cut fruits and vegetables. The software determines the needs for packaging of fruits and vegetables in order to generate their optimal gas composition for maintaining quality and maximizing shelf-life (Mahajan *et al*. 2009).

Pack-in-MAP® software can be accessed online, the user defines the type of product, storage conditions, amount of product to be packed, and size and geometry of the package. The

software selects the optimum gas composition (O_2 and CO_2) and calculates the respiration rate for that product. The software then selects the best possible films in the given range of permeability ratio (Fig. 4). Pack-in-MAP® software then simulates how the package atmosphere (O_2 and CO_2) changes over storage time for the given time-temperature profile for the particular product, indicating the O_2 and CO_2 at equilibrium and the time required to reach it. It also has the capability of simulating the impact of product and package variability on internal package atmosphere (results not shown).

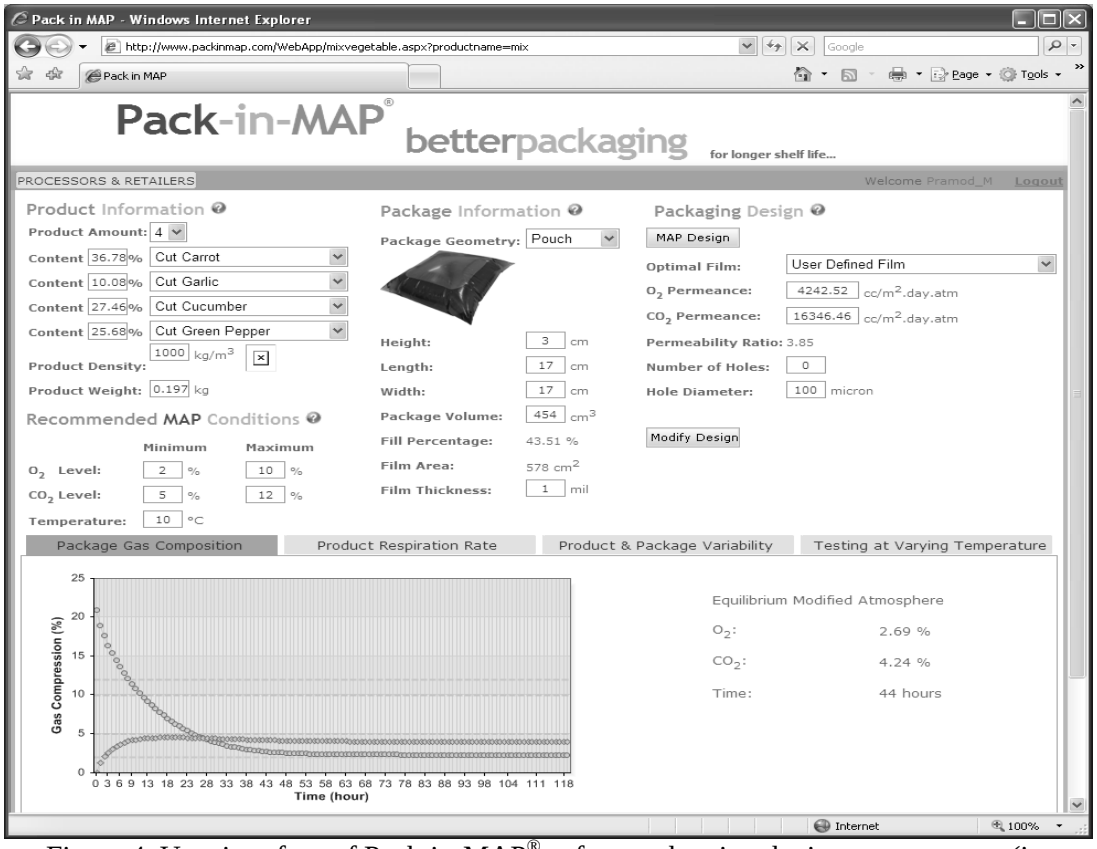

Figure 4. User interface of Pack-in-MAP® software showing the input parameters (i.e., product information, package geometry (e.g., tray) and dimensions), the recommended MAP conditions and temperature (e.g., 10 ºC) and the output parameters (recommended film, film permeability to O_2 and CO_2 and if necessary number of holes and its diameter.

Pack-in-MAP® has been successfully used to design EMAP of mushrooms, carrots, cheese, mango, blueberry, mixed vegetables, and onions and the results have been validated with the experimental data.

A validation test on a package containing a mixed vegetable salad at 10 ºC is reported in this study (Fig. 4). This package contained 75 g of cut carrot, 20 g of sliced garlic, 55 g of cut cucumber, and 50 g of green pepper. The target atmosphere for such vegetable mix was 3-4 % O_2 and 3-5% CO_2. Respiration rate characteristics were obtained from Lee *et al.* (1996) and incorporated into the software. Breathable film area and package volume were 0.06 m^2 and 313 ml, respectively.

The design protocol of Pack-in-MAP® software was then implemented and the results are shown in Fig 4. The results indicate that LDPE film (P_{O2} = 4242.42 and P_{CO2} = 16346.46 ml/m^2.day.atm) would be ideal for packaging mixed vegetable salad. This package would yield an equilibrium atmosphere of 2.69% O_2 and 4.24% CO_2 at equilibrium. This was validated experimentally and the results are shown in Fig 5. The experimental and predicted gas compositions during storage are closely matching (Table 1) and within optimal range for O_2 and CO_2, thereby showing the ability of Pack-in-MAP® software to determine the ideal packaging material and predict the gas composition inside the package during the storage period.

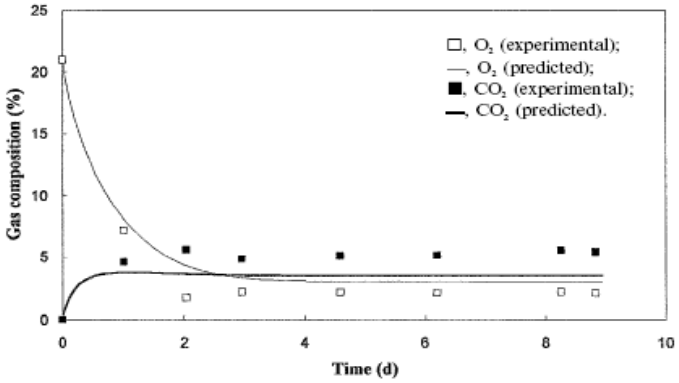

Figure 5: Experimental versus predicted gas composition as a function of time inside LDPE 27 ìm thick LDPE package of mixed prepared vegetable dish at 10ºC.

Table 1: Equilibrium modified atmosphere parameters

	O_2 (%)	CO_2 (%)	Time (hr)
Predicted	2.69	4.25	44
Experimental	2.7	4.8	48
R^2 (%)	97.4	65.7	

Overall, integration of product and package models in Pack-in-MAP® software enables the users to choose the best packaging material to achieve EMAP rapidly and within the optimal O_2 and CO_2 range. It can help the fresh produce industry to simulate "what- if" scenarios without any knowledge of mathematical models, package design and MAP itself.

Other features of Pack-in-MAP® software:

- Study the impact of product/package variability on package atmosphere
- Design a package considering varying temperature during a real life distribution chain
- Input users' own data to customize it further for their own requirements (e.g., product respiration rates or film permeabilities)

Conclusions

Integrative mathematical models for packaging design of fresh produce have been developed, validated and added to the Pack-in-MAP® software knowledge-based system, with the overall goal to design optimal packages, avoiding costly trial-and-error approaches with the added benefit of testing several solutions on a value-for-money basis. Potential users will be able to define a packaging solution to improve shelf life and prevent potential safety hazards.

Acknowledgments

The authors acknowledge financial support from FIRM (00/R&D/UL55 and 08/R&D/UL661), administered by the Department of Agriculture, Fisheries & Food, and from Enterprise Ireland (PC/2008/0118 and CP/2009/0205).

References

Brandenburg J.S. and Zagory D. (2009) Modified and controlled atmosphere packaging technology and applications. In: E.M. Yahia (Ed.) Modified and Controlled Atmospheres for the Storage, Transportation, and Packaging of Horticultural Commodities, Chapter 3, 74-91, CRC Press. (ISBN: 1420069578)

Lee K.S., Park I.S. and Lee D.S. (1996) Modified atmosphere packaging of a mixed prepared vegetable salad. International Journal of Food Science and Technology 31, 7-13.

Mahajan P.V., Oliveira F.A.R., Sousa M.J., Fonseca S.C. and Cunha L.M. (2006). An Interactive Design of MA-Packaging for Fresh Produce. In: Y. H. Hui (ed.), Handbook of Food Science, Technology, and Engineering, Volume 3, Chapter 119, 119-1 – 119-6, CRC Taylor & Francis, New York.

Mahajan P.V., Oliveira F.A.R., Montanez J.C. and Frias F. (2007). Development of user-friendly software for design of modified atmosphere packaging for fresh and fresh-cut produce. Innovative Food Science & Emerging Technologies 8, 84-92.

Mahajan P.V., Sousa-Gallagher M.J., Yuan B., Patel H.A. and Oliveira J.C. (2009). Development of web-based software for modified atmosphere packaging design, Oral presentation in 10th Controlled & Modified Atmosphere Packaging Conference (CAMA2009), 4-7th April 2009, Antalya, Turkey.

Modelling of in-mouth flavour release during eating dairy gels

I. Souchon[1,2], M. Doyennette[1,2], M. Panouillé[2,1], I. Déleris[1,2], A. Saint-Eve[2,1], I.C. Tréléa[2,1]

[1] INRA, UMR782 GMPA, F-78850 Thiverval Grignon, France
[2] AgroParisTech, UMR782 GMPA, F- 78850 Thiverval Grignon, France

Abstract

The flavor of food accounts for a large part in the choices and preferences of consumers. It is notably induced by odorant molecule that are released during food consumption due to intra oral processing and swallowing. The development of food products with high nutritional (such as salt and fat reduction) and sensory qualities is now a challenge for the food industry. Therefore, identifying mechanisms that lead to in-mouth flavor release could be a valuable help for the formulation of healthy foods. On the basis of an experimental and modeling study, the objective of this work is to better understand the relative importance of the individual, the product and of the product-person interaction leading to the release of odorous stimuli. The physicochemical parameters (air / product partition coefficient and mass transfer coefficient of aroma compounds) relating to the dairy matrices studied as well as relating to the bolus formed during food consumption (mixture of saliva and food product) were measured. Physiological data (oral and nasal volumes, masticatory efficiency test etc.) and in vivo aroma compound release data were obtained at UMR CSGA (Dijon, France) on a panel consisting of 50 individuals. A mechanistic model describing the release of aroma compounds during consumption of a solid food product by humans has been developed. This model is based on mass balances between the different compartments of the oro-naso-pharyngeal area during the different eating stages (product mastication and swallowing). These assessments are based on mass transfer phenomena and dissolution of the product into the saliva during chewing, resulting in the formation of bolus made of saliva and product. Simulations issued from the model were then compared to in vivo release data of two aroma compounds during the consumption of the cheeses obtained by atmospheric pressure chemical ionization mass spectrometry (APCI-MS). Ten panelists and four cheeses were selected for this step. Model assumptions and a discussion on their validity will be presented. This work has led to a better understanding of the mechanisms and parameters having a major impact on the release of aroma compounds during consumption of solid food. This work constitutes a step toward computer-aided product formulation by allowing calculation of retronasal aroma intensity as a function of transfer and volatility properties of aroma compounds in food matrices and anatomophysiological characteristics of consumers.

Keywords: mechanistic modeling, solid food product, chewing, flavor release, oral physiology

Introduction

Delivery of aroma compounds determines the aromatic quality of food products and plays also a role in food intake by affecting the perception of satiety (Ruijschop et *al.* 2008). During the consumption of a complex food product, flavour release depends both i) on the food properties (structure, rheology and composition) and ii) on the individual eating the product (breakdown efficiency, saliva flow, breath frequency…). Coupling nutrient criteria (such as salt and fat reduction) and organoleptic qualities is a challenge for the food industry. Therefore, identifying mechanisms that lead to in-mouth flavor release could be a precious help for the formulation of healthy foods. On the basis of an experimental and modeling approach, the objective of this work was to understand the relative importance of the individual, the product and of the product-individual interaction leading to the release of odorous stimuli.

Mathematical model for in vivo release

The current model is dedicated to solid food products. It is an extension of the model developed for liquid and semi-liquid food by Doyennette *et al.* (2011). This new model takes the mastication process into account. The global eating process involves several steps, including :

• the intra-oral manipulation of the product, which consists of several masticatory cycles;
• several swallowing events;
• the resting phase which occurs when there is no more product in the mouth.

Each swallowing leads to the deposit of a small part of the liquid part of the bolus present in mouth on the pharyngeal walls. A residual amount of the solid part of the bolus remains in the mouth and is chewed again in order to form a new food bolus suitable for swallowing.

A schematic representation of the four compartments involved in the model design, as well as their connections and the mechanisms responsible for flavor release, are given on Figure 1. The model structure is similar the one found in Doyennette *et al.* (2011). However, two main differences can be observed:

- the presence of three instead of two sub-compartment in the mouth (the non-dissolved food product, which is the solid part of the bolus, the liquid phase of the bolus, made of saliva and dissolved food product and the air phase);
- the opening of the velopharynx during the intra-oral manipulation phase, allowing exchanges of aroma compounds between the air phases of the mouth and of the pharynx.

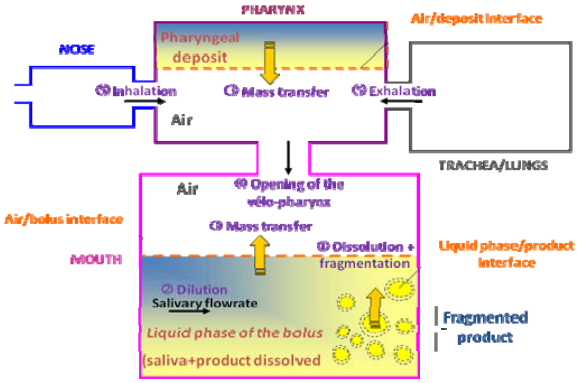

Figure 1: Schematic representation of the interconnected compartments and of the mechanisms involved in flavor release during the consumption of a solid food product.

When eaten, the solid food product placed in the mouth is destructed during intra-oral manipulation. Two concurrent phenomena can occur:

• the fragmentation of the product which increases the exchange surface between the solid food product and the bolus (mixture of saliva and dissolved product), and which promotes the transfer of aroma compounds from the food product to the bolus;
• the melting of the product into the bolus, which changes the volume of the product and of the liquid phase of the bolus.

In the following paragraphs, the main differences with the previously published model for liquid products are presented (Doyennette *et al.* 2011).

Air in the oral cavity

In addition to the exchange of aroma compound with the bolus, the air in the mouth can also exchange aroma compounds with the air of the pharynx when velopharynx opens due to the jaw and teeth movements during mastication.

The variation of aroma concentration in the air in the oral cavity C_{OA} is due to the volatile flux ϕ_{OAB} from the food bolus and from the air coming from the pharynx (Q_{OA}≥0 with velopharynx opening):

$$V_{OA}(t) \times \frac{dC_{OA}(t)}{dt} = \Phi_{OAB} + \begin{Bmatrix} Q_{OA}(t) \times \left(C_{FA}(t) - C_{OA}(t)\right) & if\ Q_{OA}(t) \geq 0 \\ 0 & if\ Q_{OA}(t) \leq 0 \end{Bmatrix} \quad (1)$$

with V_{OA} the volume of air in the oral cavity, and C_{FA} the aroma concentration in the air of the pharynx.
The masticatory movements create a cyclic variation of the air volume V_{OA} around a mean value:

$$V_{OA}(t) = V_{OA}mean + \Delta V_{OA} \times \sin(2 \times \pi \times fr_{masticatiory} \times t) \quad (2)$$

Where ΔV_{OA} corresponds to the opening variation of the mouth during mastication, and $fr_{masticatory}$ of the masticatory frequency of the individual. Little is known on the real evolution of the air flow coming from the mouth Q_{OA}. We hypothesized that it was coordinated with the masticatory cycles as it has been observed by Matsuo *et al.* (2005) :

$$Q_{OA}(t) = \frac{dV_{OA}(t)}{dt} = 2 \times \pi \times fr_{masticatory} \times t \times \Delta V_{OA} \times \cos(2 \times \pi \times fr_{masticatory} \times t) \quad (3)$$

Product in the oral cavity

Due to dissolution process, the volume of the food product decreases over time, while its exchange surface with the bolus rises to a certain point because of the fragmentation process and then decreases due to swallowing.
The dissolution of the product at a rate *v* gives the following equation:

$$\frac{dV_{OP}(t)}{dt} = -v \times A_{OBP}(\mathrm{t}) \quad (4)$$

with V_{OP} the volume of product in the oral cavity, and A_{OBP} the contact area in the oral cavity between the liquid part of the bolus and the product.
We assumed that the exchange surface evolved linearly over time, i.e.:

$$\frac{dA_{OBP}(t)}{dt} = \frac{A_{OBPdeg} - A_{OBPini}}{d_{deg} - t_{ini}} \quad if\ V_{OP}(t) \geq 0 \quad (5)$$

with the index "*deg*" meaning “at the deglutition moment”, and the index "*ini*" meaning “at the introduction of the food product in the mouth”.

Bolus in the oral cavity

The volume of the bolus V_{OB} can be divided into two parts:

$$V_{OB}(t) = V_{OS}(t) + V_{OPD}(t) \quad (6)$$

where V_{OS} is the volume of saliva in the bolus and V_{OPD} is the volume of product dissolved in the bolus.
The mass balance for aroma compounds in the bolus gives us the following equation:

$$\frac{dV_{OB}(t) \times C_{OB}(t)}{dt} = \Phi_{OBP} - \Phi_{OAB} \quad (7)$$

with the mass flux ϕ_{OBP} coming from the dissolution of the product

$$\Phi_{OBP} = v \times A_{OBP}(t) \times C_{OP} \quad (8)$$

The mass flux ϕ_{OAB} is given by the difference between the bolus concentration (C_{OB}) and the interfacial concentration (C^*_{OB}):

$$\Phi_{OAB} = k_{OB}(t) \times A_{OAB}(t) \times (C_{OB}(t) - C^*_{OAB}(t)) \quad (9)$$

As we have:

$$\frac{dV_{OB}(t) \times C_{OB}(t)}{dt} = C_{OB}(t) \times \frac{dV_{OB}(t)}{dt} + V_{OB}(t) \times \frac{dC_{OB}(t)}{dt} \quad (10)$$

Phenomena governing flavor release in the pharynx and in the nose are similar to the ones described in the liquid model.

Results and discussion

An analysis of model sensitivity was performed to evaluate the effect of some physiological or physicochemical parameters. For that, each simulated kinetic, expressed in arbitrary unit, was divided by its own maximum intensity. Only the flow of saliva incorporated to the bolus during food consumption, the duration of the period before the first swallowing as well as the velopharynx opening (amplitude and frequency) has a strong influence on the overall kinetics.

For example, an increase in the flow of saliva incorporated to the bolus during food consumption results in a decrease in the part of the curve after the first swallowing (renewal of liquid phases present in the mouth and pharynx by supply of fresh saliva).

Comparison of model predictions with experimental data for ethyl propanoate

To determine the unknown parameters of the model, simulations were fitted to experimental data as follows:

- the flow rate of saliva incorporated to the food bolus was adjusted so that the simulated release kinetic after the first deglutition fits the decay phase of the experimental curve;
- the air flow rate resulting from the opening of the velopharynx was adjusted to fit the simulated release kinetic before the first deglutition to experimental data.

All the simulations have been reproduced satisfactorily compared to *in vivo* release data. Figure 3 presents some comparisons of simulations and experimental data for one panelist and one cheese.

It is highly likely that for these specific cases, a modification of other parameters for which the value was approximately set due to a lack of knowledge (such as the amplitude of the opening of velopharynx) may improve the predictions.

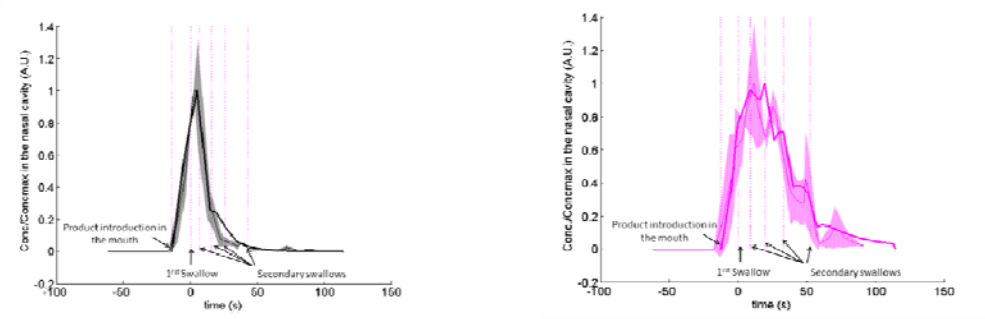

Figure 2: Comparison of model predictions (bold line) with in vivo ethyl propanoate release (thin line) for panelist S090, Cheese Sl (left) and S002, cheese Fh (right). Experimental standard deviation is represented by the colored envelopes. Vertical lines represent the various consumption events.

Conclusions

Comparison of model predictions with the experimental release of two aroma compounds during the consumption of cheeses by APCI-MS gave satisfactory results for the ten panelists and four cheeses. The adjusted parameters are in a range of variation that is in agreement with literature data. This work has led to a better understanding of the mechanisms and parameters having a major impact on the release of aroma compounds during consumption of solid food.

Acknowledgements

The authors gratefully acknowledge the French National Research Agency (ANR) project “SensInMouth” for financial support and the UMR CSGA (Dijon) for all the performed experiments on the panel.

References

Doyennette M., de Loubens C., Déléris I., Souchon I. and Trelea I. C. (2011) Mechanisms explaining the role of viscosity and post-deglutitive pharyngeal residue on in vivo aroma release: a combined experimental and modelling. *Food Chemistry* 128, 380–390.

Doyennette M., Déléris I., Saint Eve A., Gasiglia A., Souchon I. and Trelea I.C. The dynamics of aroma compound transfer properties in cheeses during simulated eating conditions. *Food Research International* (under submission).

Yven C., Patarin J., Magnin A., Labouré H., Repoux M., Feron G., and Guichard E. Consequences of indiviual chewing strategies on bolus rheological properties at the swallowing threshold. *Journal of Texture Studies* (under submission).

Matsuo C., Hiiemae K. and Palmer J. (2005) Cyclic motion of the soft palate in Feeding. *Journal of Dental Research* 84, 39-42.

Understanding how the structure of dairy matrices affects protein hydrolysis in the gastrointestinal tract

F. Barbé[1,2], S. Le Feunteun[3], I. Souchon[3], D. Rémond[4], O. Ménard[1], Y. Le Gouar[1], C.Gaudichon[5], B. Laroche[6], D. Dupont[1]

[1] INRA-Agrocampus Ouest UMR 1253, Science et Technologie du Lait et de l'œuf, 35000 Rennes, France (florence.barbe@rennes.inra.fr)
[2] Univ Paris Sud-CNRS-Supélec, UMR 8506, Laboratoire des Signaux et Systèmes (L2S)-Supélec, 91192 Gif-sur-Yvette, France (florence.barbe@rennes.inra.fr)
[3] INRA-AgroParisTech UMR 782 Génie et Microbiologie des Procédés Alimentaires, 78850 Thiverval-Grignon, France
[4] INRA, UMR 1019 Unité de Nutrition Humaine, 63122 St Genès Champanelle, France
[5]INRA-AgroParisTech UMR 914 Physiologie de la Nutrition et du Comportement Alimentaire, 75231 Paris, France
[6] INRA, UR314 Mathématiques et Informatique Appliquées, 78352 Jouy-en-Josas, France

Abstract

The objective of this study is to better understand and model the effect of dairy matrix structure on the hydrolysis and transit rates of milk proteins during digestion. 4 dairy matrices having a similar composition but differing by their internal structure were manufactured: 2 solutions, 1 acid gel and 1 stirred acid gel which all contained a small amount of Cr-EDTA complexes, a non-absorbable and non-hydrolysable water soluble marker. These 4 matrices were given to six adult mini-pigs and, for each experiment, 9 samples corresponding to 8 different times after the meal ingestion and 1 time before the meal were collected after the pylori, i.e. at the stomach exit. Effluents were analysed by ELISA to determine their residual concentration in β-lactoglobulin and caseins (intact proteins and large fragments) and by atomic absorption to measure the Cr^{2+} concentration. Statistical analyses performed on ELISA data for proteins are presented. They allow distinguishing the gelled from the liquid matrices, the stirred acid gel being equally distributed among the two groups. A first mathematical model describing the gastric emptying of Cr-EDTA is also presented. This model provides a good fitting of the Cr-EDTA concentrations and allows estimating several unknown digestion parameters (level of gastric juice flow and half-life of the chromium complex in the stomach) with a good accuracy.

Keywords: *caseins, food structure, gastrointestinal transit tract, modelling, in vivo digestion, whey proteins*

Introduction

Degradation of food proteins is a major source of biological signals (peptides and amino acids) which can have an effect on human health. It has been shown that the structure of the ingested food can affect the dynamics of the amino-acid appearance within the blood, in particular for dairy products (Lacroix *et al*. 2008). However, little is still known about the influence of food structure on their digestibility and nutritional properties. In this context, monitoring the behaviours of the dairy proteins within the gastro-intestinal tract is an important challenge in order to gain knowledge on the phenomena involved.

Materials and Methods

In vivo experiment

The dairy solution was reconstituted from skim Ultra Low Heat powder manufactured at INRA-STLO (Rennes) and Milli-Q pure water in order to obtain 14.5% dry matter. The reconstituted solution contained 40 g/L of caseins, 10 g/L of β-lactoglobulin and 95 g/L of lactose and minerals. 110.8 ppm (w/w) of Cr-EDTA was then added to the solution and 4 dairy matrices (1kg each) were prepared thereafter: raw skim milk (M1), skim milk heated 10

min at 90°C (M2), stirred (M3) and non-stirred (M4) acid gel made with 30g of gluconodeltalactone and 1 kg of heated skim milk. The acid induced gelation was performed at 20°C and launched 24h before the beginning of the *in vivo* experiment. When carried out, stirring was made with a Magimix mixer during 2 min. Each sample was given to six adult mini-pigs (U, V, W, X, Y and Z) according to a Latin-square experiment. Effluents were then taken 8mm after the pilori (at the end of stomach exit) at 1 time point before the meal and 8 time points during meal digestion (-30, 0, 20, 50, 105, 165, 225, 315, 405 min) and characterized by ELISA in order to monitor digestion dynamics. The concentration of Cr-EDTA was measured by atomic absorption spectrometry according to Siddons *et al*., 1985.

Software

The statistical analyses (Principal Component Analyses and Factorial Discriminant Analyses) were performed with R 2.12.1 on concentration data of whole caseins and β-lactoglobulin obtained from ELISA assays, which were normalized in order to limit analytical variability. For each subject, the 4 dairy matrices are submitted to statistics. A 24 lines×9 columns table was created for both groups of proteins when they are analysed separately: the lines are subjects×dairy matrices and the columns are the sampling times. When both groups of proteins were analysed together, a 48 lines×9 columns table was created: 24 lines for each protein. A method of clustering (kmeans) was also employed for the PCA analyses to underline similar or different behaviours between subjects and/or matrices. The AMIGO (Advanced Model Identification using Global Optimization) toolbox was used to estimate model parameters with MATLAB R2010a in the Cr-EDTA concentration model (Balsa-Canto *et al*., 2010).

Formulae used in the Cr-EDTA concentration model

Cr-EDTA is a non-absorbable and non-hydrolysable marker: a first model describing the transit of this matrix component in the case of liquid matrices was thus developed by taking into account the fluxes of ingestion (ϕ_{in} [1], Figure 1), gastric secretions (ϕ_g [2], Figure 1) and gastric emptying (ϕ_{sd} [3], Figure 1). The compartment s (volume V_s) represents the stomach (Figure 1). Cr-EDTA enters into the compartment s and is emptied according to a power exponential model ([4], Elashoff *et al*., 1982). The states of the model are: V_s (stomach volume [5]), mCr_s (Cr-EDTA mass in the stomach [6]) and cCr_s (Cr-EDTA concentration in the compartment s [7]). The parameters of the model are: $t_{1/2}$ (half-life time in the stomach), β (Elashoff exponent), t_g (time of transition between high and low levels of gastric secretions), fgh (high level of gastric secretions), fgl (low level of gastric secretions), t_{in} (time of ingestion), λ (parameter controlling the shape of gastric secretions), mCr_{tot} (Cr-EDTA mass in the matrix before ingestion), m_{tot} (matrix mass) and V_{basal} (fasted stomach volume).
Some parameters have known values: t_{in}=4 min ; $mCr_{tot}=110.8\times10^{-3}$ g ; m_{tot}=1000 g and some others were fixed according to the literature: β=1; fgl=2 mL/min; λ=5 ; V_{basal}=15 mL.
The remaining parameters were estimated: $t_{1/2}$; t_g and fgh (initial guess: 60 min; 40 min and 30 ml/min, respectively).

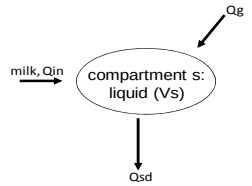

Figure 1: Cr-EDTA model

$$\Phi_{in} = \begin{cases} \dfrac{m_{tot}}{t_{in}} & if \;\; 0 < t \le t_{in} \\ 0 & if \;\; t_{in} < t \end{cases}, \qquad (1)$$

$$\Phi_g = \left(-\frac{2}{\pi}\arctan\left(\frac{t-t_g}{\lambda}\right)+1\right)\left(\frac{fgh-fgl}{2}\right)+fgl \qquad (2)$$

$$\Phi_{sd} = \begin{cases} 0 \ if \ \ t = 0 \\ \dfrac{mCr_{tot}}{cCr_s \times t_{in}}(1 - E(t)) \ \ if \ \ t \le t_{in} \\ \dfrac{mCr_{tot}}{cCr_s \times t_{in}}(E(t - t_{in}) - E(t)) \ \ if \ \ t_{in} < t \\ \Phi_g - (V_{basal} - V_s) \ if \ \ V_s < V_{basal} \end{cases} \quad (3)$$

$$E(t) = \begin{cases} 0 \quad if \ \ t \le 0, \\ 2^{-(t/t_{1/2})^{\beta}} \ \ if \ \ 0 < t \end{cases} \quad (4)$$

$$u_1(V_s) = \begin{cases} 1 \ if \ \ V_s \ge V_{basal} \\ 0 \ if \ \ V_s < V_{basal} \end{cases} \qquad u_2(V_s) = \begin{cases} 0 \ if \ \ V_s \ge V_{basal} \\ 1 \ if \ \ V_s < V_{basal} \end{cases}$$

$$\frac{dV_s}{dt} = \Phi_{in} + (\Phi_g - \Phi_{sd}) \times u_1(V_s) + (V_{basal} - V_s) \times u_2(V_s) \quad (5)$$

$$\frac{dmCr_s}{dt} = \frac{mCr_{tot}}{t_{in}}(E(t) - E(t - t_{in})) \quad (6)$$

$$\frac{dcCr_s}{dt} = \frac{\Phi_{in}}{V_s}(cCr_{ech} - cCr_s) - \frac{cCr_s}{V_s}\Phi_g \quad (7)$$

Results and Discussion

Statistical analyses: Principal Component Analyses (PCA)

Two approaches were used to analyse the proteins and Cr-EDTA data: in the first one, both groups of proteins were compared simultaneously for each matrix (Figures 2a, 2b for M1 and M2); in the second one, the four matrices were compared simultaneously for each group of proteins and for Cr-EDTA. For all PCA analyses, the first two principal components represented more than 70% of the variance.

The first approach gives information about digestion dynamics of both proteins for each matrix. For M1 (Figure 2a) the dynamics of both proteins are clearly different. For M3 the behaviours of the two proteins are less distinct and, for M2 (Figure 2b) and M4 (not shown), the behaviours of both proteins are very similar for each subject. This could be explained because M1 is the only meal which has not been subjected to thermal treatment, a process which induces aggregates of β-lactoglobulin, part of them being covalently bound to the surface of casein particles.

The second approach gives information about the influence of the matrix on digestion dynamics for each group of proteins and on transit for Cr-EDTA. Clustering allows discriminating between M3 points on one side and M1, M2 and M4 points on the other side. For Cr-EDTA, the clusters are even more discriminatory between M1-M2 and M3, M4 having an intermediate behaviour between the former 2 clusters (not shown). This shows that the viscoelastic properties of the meal have an effect on the digestion dynamics and could be explained because solutions are emptied more rapidly than the acid gel, the stirred acid gel having an intermediate transit between the liquid matrices and the gel.

Statistical analyses: Factorial Discriminant Analysis (FDA)

The FDA performed on both groups of proteins and on Cr-EDTA data for the 4 matrices allows to maximize the variance between groups: the FDA is a PCA carried out on barycenters of *a priori* groups (the 4 matrices). The FDA for caseins (Figures 3a) and Cr-EDTA (not shown) are quite similar, M3 being properly separated from the other matrices, M1 and M2 being joined and M4 having an intermediate behaviour. The FDA for β-lactoglobulin (Figure 3b) underlines the distinct behaviour of the raw skim milk (M1) and the similarity in the behaviours of gelled matrices, M3 and M4. The FDA results thus confirmed PCA analyses and reinforced the hypothesis of a significant influence of viscoelastic properties and thermal treatment of the dairy matrix on proteins digestion dynamics.

Gastrointestinal transit model: Cr-EDTA concentration

Below are shown the curve fitting of Cr-EDTA concentration (Figure 4), the simulations of the evolutions of gastric secretions and gastric emptying recovered from the fitting (Figure 5) and the parameter estimations (Table 1) after ingestion of skim milk heated 10 min at 90°C by subject U. The parameters are properly estimated (Table 1) and the curve fitting matches closely the experimental data (Figure 4).

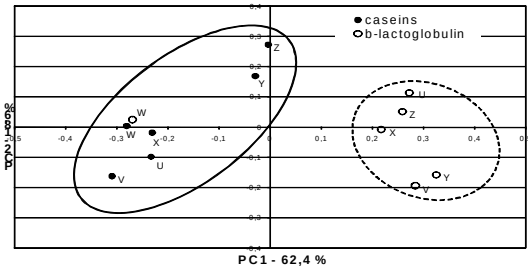

Figure 2a: PCA for raw skim milk (M1)

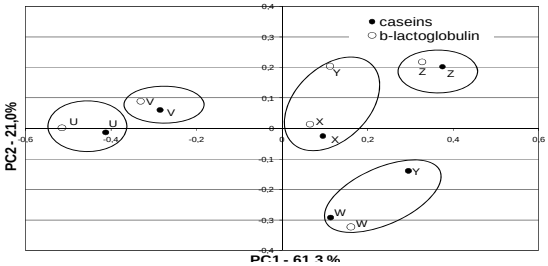

Figure 2b: PCA for heated skim milk

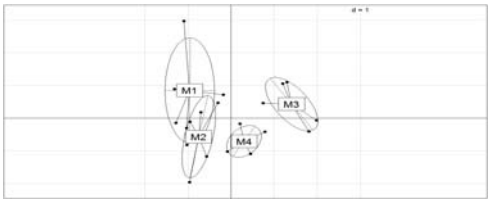

Figure 3a: FDA for caseins

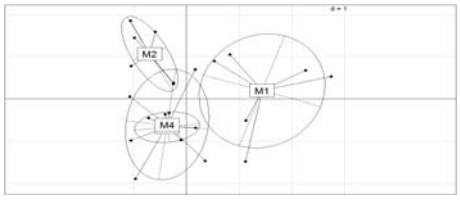

Figure 3b: FDA for β-lactoglobulin

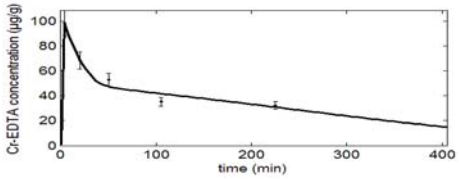

Figure 4: Curve fitting of Cr-EDTA concentrations

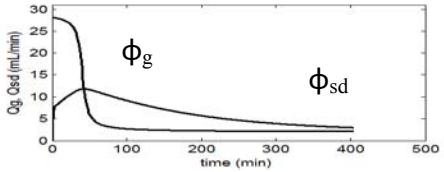

Figure 5: Simulations of gastric secretions (ϕ_g) and gastric emptying (ϕ_{sd}) evolutions

Table 1: Parameters estimations obtained with the Cr-EDTA model (local estimation)

parameter	parameter value
$t_{1/2}$	97.116 +- 19.583
t_g	40.395 +- 4.8355
fgh	29.274 +- 2.3006

Conclusions

By means of statistical analyses, the influence of matrix structure on proteins digestion dynamics and on Cr-EDTA transit was underlined. Furthermore the Cr-EDTA model presented offers a good pattern to implement hydrolysis mechanisms in a next step aimed at integrating ELISA data. Such a work is on progress.

References

Balsa-Canto E. and Banga J.R. (2010) AMIGO: A model identification toolbox based on global optimization. In *Computer Applications in Biotechnology, Leuven*.

Elashoff J.D., Reedy T.J. Meyer J.H. (1982) Analysis of gastric emptying data. *Gastroenterology* 83, 1306-1312.

Lacroix M., Bon C., Bos C., Léonil J., Benamouzig R., Luengo C., Fauquant J., Tomé D. and Gaudichon C. (2008) Ultra High Temperature treatment, but not pasteurization, affects the postprandial kinetics of milk proteins in humans. *The Journal of Nutrition* 138 (12), 2342-2347.

Siddons R.C., Paradine J., Beever D.E. and Cornell P.R. (1985) Ytterbium acetate as a particulate-phase digesta-flow marker. *British Journal of Nutrition* 54, 509-519.

The dynamics of the HS/SPME-GC/MS as a tool to assess the spoilage of beef stored under different packaging and temperature conditions

A.A. Argyri[1,2], A. Mallouchos[1], E. Z. Panagou[1], G.-J.E. Nychas[1]

[1]Laboratory of Microbiology and Biotechnology of Foods, Department of Food Science and Technology, Agricultural University of Athens, Iera Odos 75, Athens 11855, Greece (e-mail; gjn@aua.gr)
[2]Applied Mycology Group, Cranfield Health, Cranfield University, Bedford MK43 0AL, UK

Abstract

The shelf life of minced beef stored aerobically and under modified atmosphere packaging (MAP) at 0, 5, 10, and 15 ºC was assessed by monitoring the microbial association of meat and the changes of the volatile compounds occurring in the meat substrate. Microbiological analyses, concerning total viable counts (TVC), *Pseudomonas* spp., *Brochothrix thermosphacta*, lactic acid bacteria (LAB), *Enterobacteriaceae*, yeasts and moulds, were performed in parallel with sensory analysis, pH measurements and headspace SPME-GC/MS (solid phase microexraction-gas chromatography/mass spectrometry). In particular, a large number of volatile compounds, including aldehydes, alcohols, ketones, esters, hydrocarbons and terpenes, were identified at each storage condition, whilst more than 100 of them were further semi-quantitatively determined. Correlation of the volatile compounds with the spoilage sensory status of the samples and subsequent qualitative classification of the samples was performed with principal component and factorial discriminant analysis (PCA and FDA, respectively), whilst quantitative estimations of the different microbial groups was performed using the partial least squares-regression (PLS-R). Both temperature and packaging were found to have a great impact on the evolution of volatiles during storage that resulted in different chemical profiles. Through PCA, many of the identified compounds were correlated with the sensory scores, depicting possible spoilage indicators such as 2-Pentanone, 2-nonanone, 2-methyl-1-butanol, 3-methyl-1-butanol, ethyl hexanoate, ethyl propanoate, ethyl lactate, ethyl acetate, ethanol, 2-heptanone, 3-octanone, diacetyl, and acetoin. The FDA and PLS-R models indicated that the dynamic changes of the volatile metabolic compounds being present in the meat substrate during storage can provide estimations about the microbial populations and the sensory scores. The overall results the HS/SPME-GC/MS analysis of the volatile profile of meat combined with chemometrics, may be considered as a potential method to predict the spoilage of a meat sample regardless the storage conditions (e.g. packaging and temperature).

Keywords: GC/MS, SPME, spoilage indicators, chemometrics, PLS-R

Introduction

The correlation between microbial growth and chemical changes during spoilage has been continuously recognised as a means of revealing indicators that may be useful for quantifying muscle tissue quality as well as the degree of spoilage (Nychas *et al.* 2007). Different volatile microbial metabolites have been detected in naturally contaminated samples of meat with GC or GC-MS. Tsigarida and Nychas (2001) have investigated the profile of the volatile compounds as attributed from GC analysis of sterile beef fillets inoculated with meat spoilage bacteria and stored in air and in MAP. The volatile compounds using GC or GC/MS analysis have also been studied for inoculated and/ or naturally contaminated beef stored in air (Dainty *et al.* 1989) and in MAP and/ or VP (Stutz *et al.* 1991; Jackson *et al.* 1992; Insauti *et al.* 2002), for chicken stored in MAP (Eilamo *et al.* 1998) and for cooked ham stored in MAP (Leroy *et al.* 2009). Finally, the GC-GC/MS volatiles profile of different types of fresh or processed meat (chicken, beef or pork) has been studied, to assess their quality characteristics, without subsequent storage of the samples (Wettasinghe *et al.* 2001; Marco *et al.* 2004; Xie *et al.* 2008; Rivas-Cañedo *et al.* 2009). However, knowledge gaps related to GC or GC/MS analysis

need to be addressed since the above studies do not include combinations regarding numerous compounds, several storage conditions (i.e. temperature and packaging), microbiological and sensory evaluation.

Materials and Methods

The shelf life of minced beef stored aerobically and under Modified Atmosphere Packaging (MAP) at 0, 5, 10, and 15 ºC was assessed by monitoring the microbial association of meat and the changes of the volatile compounds occurring in the meat substrate. Microbiological analyses, concerning total viable counts (TVC), *Pseudomonas* spp., *Brochothrix thermosphacta*, lactic acid bacteria (LAB), *Enterobacteriaceae*, yeasts and moulds, were performed in parallel with sensory analysis, pH measurements and headspace SPME-GC/MS (solid phase microexraction-gas chromatography/mass spectrometry). Correlation of the volatile compounds with the spoilage sensory status of the samples and subsequent qualitative classification of the samples was performed with principal component and factorial discriminant analysis (PCA and FDA, respectively), whilst quantitative predictions of the different microbial groups was performed using the Partial Least Squares-Regression (PLS-R). The performance of the PLS-R models was evaluated using four different criteria, namely, the RMSE, the bias factor (B_f), the accuracy factor (A_f) and the percent relative error (% RE) between predictions and observations (Ross 1996).

Results and Discussion

Figure 1 shows indicatively the volatile metabolic profile of a fresh minced beef sample at the onset of storage (a) and a spoiled minced beef sample stored under MAP at 5 °C (b). A large number of volatile compounds, were identified from the analysis of the GC/MS ion chromatograms, that included aldehydes, alcohols, ketones, esters, hydrocarbons and terpenes, were identified at each storage condition, whilst more than 120 of them were further semi-quantitatively determined. Out of these compounds, 34 were selected for mathematical analysis. Both temperature and packaging had a great impact on the evolution of volatiles during storage that resulted in different chemical profiles.

According to the PCA, the derived loading plots and scores plot gave useful information about the possible correlations of the compounds used for the analysis in correlation with the sensory scores. 2-butanone was correlated with acceptable samples (fresh and semi-fresh) and showed a decrease during storage. Moreover, the most of the acceptable samples were correlated with 2-butanone, 2, 3-pentanedione, 2, 5-octanedione, pentanal, hexanal, trans-2-heptanal, trans-2-octenal that all showed a mixed, mostly decreasing trend during storage. 2-Pentanone, 2-nonanone, 2-methyl-1-butanol, 3-methyl-1-butanol, ethyl hexanoate, ethyl propanoate, ethyl lactate, ethyl acetate, ethanol, 2-heptanone, 3-octanone, diacetyl, acetoin were associated with spoiled samples which increased during storage at the most storage conditions.

The correct classification rate for the validation of the FDA model was 77.78% correct for the fresh samples, 62.50% for the semi-fresh and 89.66% for the spoiled ones, with an overall performance of 79.17% accuracy (Table 1). These results revealed a good correlation of the sensory estimates of the spoilage with the dynamic changes of the amounts of the volatiles compounds. The potential of PLS-R analysis to estimate the population of selected microbial groups of the indigenous microbiota of meat samples such as total viable counts (TVC), *Pseudomonas* spp, *Br. thermosphacta*, lactic acid bacteria, *Enterobacteriaceae*, and yeasts/moulds was also demonstrated in this study (Table 2). The values of B_f were generally close to unity, indicating good agreement between observations and estimations. The fact that in certain cases it is slightly above 1 indicates a slightly 'fail-dangerous' model (Ross, 1996). In addition, the values of the A_f indicated that the average deviation between estimations and observations of the various microbial groups ranged from 9.3 % (either above or below the line of equity) for TVC to 14.0% for *Br. thermosphacta* (Table 2). Regarding the estimations for TVC, the % RE values were distributed above and below 0, with 91.78 % of predicted microbial counts included within the ± 20% RE zone. However, a trend of over-prediction

was evident especially at lower population densities (counts less than 7 log cfu g^{-1}) and some times an under-prediction was observed at higher populations. As far as the models of the remaining microbial groups are concerned, the *Pseudomonas* spp., *Br. thermosphacta* and yeasts/moulds were generally under-estimated, whilst the LAB were slightly over-estimated at the lower populations densities. These results indicate that the HS/SPME- GC/MS analysis can provide useful information about the dynamic changes of the volatile metabolic compounds being present in the meat substrate during storage and provide estimations about the microbial populations and the sensory scores.

Conclusions

In this study, it was demonstrated that GC/MS analysis is a promising tool for monitoring the freshness of meat, whilst it provides numerous information about the progress of meat spoilage depending on the temperature and packaging storage conditions. The analysis of the GC/MS data depicted a well discrimination regarding the sensory classes of the samples, whilst sufficient estimations of the microbial counts were provided.

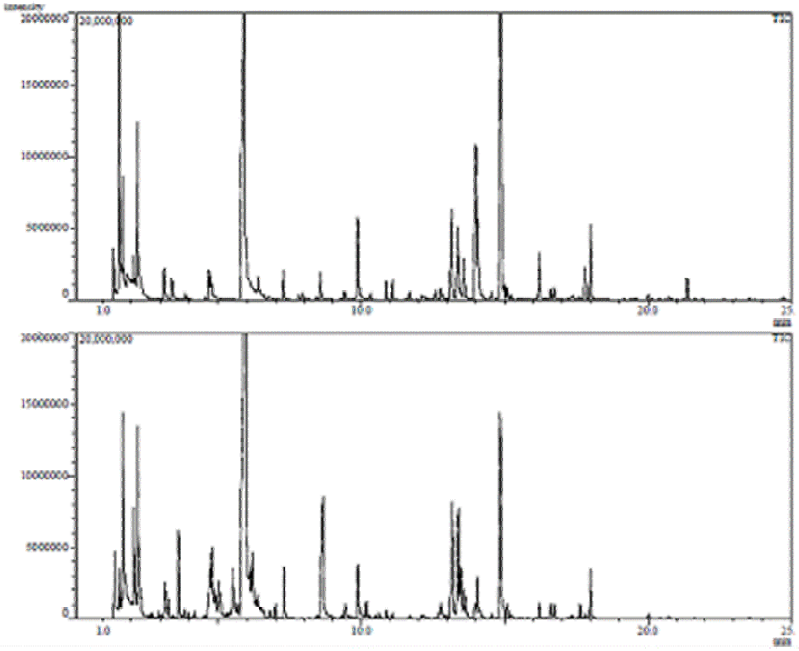

Figure 1: Typical GC/MS volatile metabolic profiles of minced beef at the onset of storage (a) and after 268h stored aerobically at 5ºC (b).

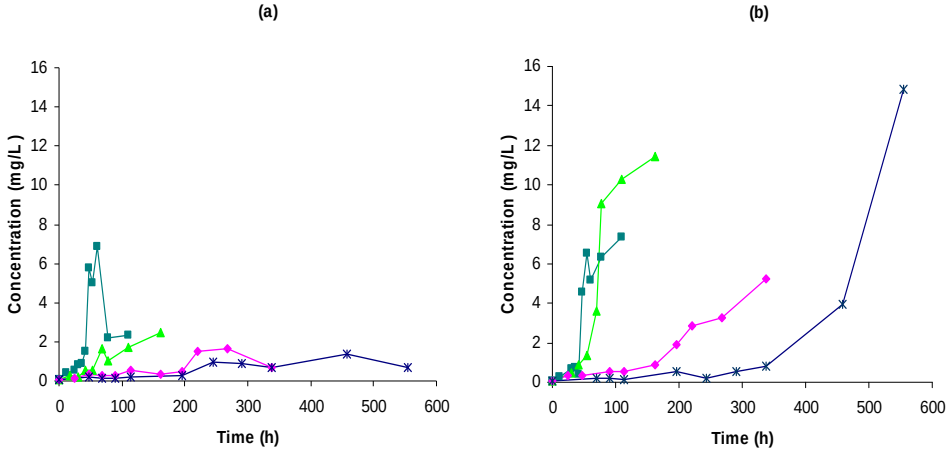

Figure 2: Changes of the concentration of hexanol in minced beef stored aerobically (a) and under MAP (b) at 0 °C (*), 5 °C (◆), 10 °C (▲) and 15 °C (■) for 110h.

Table 1: Confusion matrix according to the FDA for the validation of the sensory estimates.

True class	Estimated class			Correct Classification
	Fresh	Semi-fresh	Spoiled	(Sensitivity %)
Fresh (n = 27)	21	0	6	77.78
Semi-fresh (n=29)	1	10	5	62.50
Spoiled (n =16)	1	2	26	89.66
Total (n =72)	23	12	37	79.17
Specificity (%)	91.30	83.33	70.27	

Table 2: Comparison of calculated performance indices for the estimation of the microbial population in minced beef samples using the validation estimates from the PLS-R models.

Microbial group	No of latents	B_f [a]	A_f [b]	% of the samples in ± 20% RE [c] zone	% of the samples in ±10% RE zone	R^2	RMSE[d]
TVC	2	1.001	1.093	91.78	76.71	0.65	0.81
Pseudomonas spp	3	1.012	1.125	83.56	60.27	0.78	0.97
Br. thermosphacta	2	1.010	1.140	75.34	58.90	0.54	0.94
LAB	3	1.008	1.099	90.41	65.75	0.47	0.81
Enterobacteriaceae	2	1.008	1.112	80.82	65.75	0.71	0.84
Yeasts and moulds	3	1.009	1.111	84.93	78.08	0.74	0.78

[a] bias factor, [b] accuracy factor, [c] relative error, [d] root mean square error

Acknowledgements

This work financially supported from SYMBIOSIS-Eu project (7th FP).

References

Dainty R. H., Edwards R.A., Hibbard C.M. and Marnewick J. J. (1989) Volatile compound associated with microbial growth on normal and high pH beef stored at chill temperatures. *Journal of Applied Bacteriology* 66, 281-289.

Insausti H.K., Beriain M.J., Purroy A., Alberti P., Gorraiz C. and Alzueta M.J. (2001) Shelf life of beef from local Spanish cattle breeds stored under modified atmosphere. *Meat Science* 67, 1580-1589.

Jackson T.C., Acuff G. R. and Dickson, J. S. (1997) Meat, poultry, and seafood. In *Food microbiology: fundamentals and frontiers*, pp. 83–100. Edited by M. P. Doyle, L. R. Beuchat, & T. J. Montville. Washington DC: ASM Press.

Leroy F., Verluyten J. and De Vuyst, L. (2006). Functional meat starter cultures for improved sausage fermentation. *International Journal of Food Microbiology* 106, 94–102.

Marco, A., Navarro, JL, Flores, M. (2004). Volatile compounds of dry-fermented sausages as affected by solid-phase microextraction (SPME). *Food Chemistry* 84, 633–641.

Nychas, G.-J. E., Tassou, C. C. (1997). Spoilage process and proteolysis in chicken as noted by HPLC method. *Journal of Science of Food and Agriculture* 74, 199–208.

Nychas G-J. E., Marshall D. L. and Sofos J. N. (2007) Meat, Poultry, and Seafood. In M. P. Doyle, L. R. Beuchat (Eds.), *Food microbiology: fundamentals and frontiers,* 105-140. ASM Press Washington, D.C

Rivas-Cañedo A., Fernández-García E. and Nuñez M. (2009) Volatile compounds in fresh meats subjected to high pressure processing: Effect of the packaging material. *Meat Science* 81, 321-328.

Ross T. (1996) Indices for performance evaluation of predictive model in food microbiology. *Journal of Applied Microbiology* 81, 501-508.

Stutz H.K., Silverman G.J., Angelini P. and Levin, R.E. (1991) Bacteria and volatile compounds associated with ground beef spoilage. *Journal of Food Science* 56, 1147-1153.

Tsigarida, E., and Nychas, G.-J. E. (2001) Ecophysiological attributes of a *Lactobacillus* sp. and a *Pseudomonas* sp. on sterile beef fillets in relation to storage temperature and film permeability. *Journal of Applied Microbiology* 90, 696–705.

Xie J., Sun B., Zheng F. and Wang, S. (2008) Volatile flavor constituents in roasted pork of Mini-pig. *Food Chemistry* 109, 506–514.

Wettasinghe M., Vasanthan T., Temelli F., Swallow K. (2001) Volatile flavour composition of cooked by-product blends of chicken, beef and pork: a quantitative GC-MS investigation. *Food Research International* 34: 149-158.

Quality by design for packaging of granola breakfast product

I.S.M. Macedo, M.J. Sousa-Gallagher, J.C. Oliveira, P.V. Mahajan, E.P. Byrne

Department of Process and Chemical Engineering, School of Engineering, College of Science, Engineering and Food Science, University College Cork, Ireland (email: m.desousagallagher@ucc.ie)

Abstract

A quality by design approach considers both the critical product characteristics and process variables in order to design for optimum packaging. Mathematical modelling can be used to describe the effect of process variables (e.g. environmental conditions) on product characteristics and predict quality and shelf-life. The aim of this study was to i) determine the water-vapour-transmission-rate (WVTR) of different packaging materials, and ii) develop and validate a predictive model for the shelf-life of packed granola breakfast cereal using accelerated storage conditions. The WVTR for each film was measured according to an experimental design (3^2) with 2 factors (temperature and relative humidity) at 3 levels (10, 30, 40 °C; 32-33, 75-76, 89-96%). Granola breakfast cereal was packed using 3 commercial biodegradable materials (NK, NM, N913), biaxial-oriented-polypropylene (BOPP), commercial-packing-material (control) and stored using accelerated conditions (38 °C and 90% RH). Samples were assessed for moisture content (critical quality parameter), at regular intervals throughout 82 days of storage. The WVTR of BOPP and N913 films were not significantly affected by RH, whereas temperature had a significant effect on all types of materials studied; an Arrhenius relationship was found to describe the dependency of WVTR on temperature. A global model considering the dependency of temperature and RH was developed and was found to fit the experimental data well. Moisture uptake for packaged granola was found to be significantly affected by both storage time and packaging material. The BOPP film resulted in the lowest moisture gain for the granola, followed by the biodegradable film N913. The predicted shelf life for granola under accelerated conditions ranged from 13-2 days depending on the packaging film, and these results were in agreement with those obtained experimentally. The predicted shelf life for granola under normal storage conditions ranged from 283, 90, 33, 228 days in BOPP, NK, NM, N913 pouches, respectively.

Keywords: quality by design, mathematical modelling, packaging, shelf life, water vapour transmission rate

Introduction

Granola is a dry granulated cereal product which has a low water activity. During the distribution chain, granola can be exposed to a range of quite different environmental conditions, and if there is a differential between water activity inside and outside the package, this driving force allows the transfer of water molecules through the package leading to an increase of internal water activity, therefore causing an increase of moisture content and consequently a loss of granola quality (Macedo *et al*. 2009).

The shelf life of a moisture sensitive food product is typically estimated using mathematical models that describe and connect the equilibrium sorption isotherm of the product, the initial and the permissible final moisture content of the product, the permeance properties of the package and also the environmental relative humidity and temperature.

The aim of this work was to i) determine the water vapour transmission rate of different packaging materials (BOPP, NK, NM, and N913) at different environmental conditions, and ii) develop and validate a predictive model for the shelf-life of packed granola breakfast cereal using accelerated storage conditions.

Materials and Methods

WVTR Assessment: The biodegradable packaging films (NatureFlex 30 NK; NaturFlex 55 N913; NaturFlex 23 NM; and Propafilm RGP 30) were supplied by Innovia Films (Innovia Films Ltd, Cumbria, United Kingdom). The WVTR was calculated for each film using a full factorial experimental design at different RH (32-33, 75-76, and 89-96 %) and T (10, 30, 40 °C). WVTR was determined by gravimetric "cup" method described in ASTM E-96.

Shelf-life Assessment: Granola samples (30 g) were packed in pouches made from the different films, and closed by heat sealing. Care was taken to minimize the pouches head space and to ensure that the pouches were leak proof. Beside the four different films studied (BOPP, NK, NM and N913), a control film used in the packaging of a commercial brand was removed and designed similarly to the other film pouches (8.5 cm x 10 cm). Seven sample pouches of each film were hanged on top of a big airtight container, ensuring that pouches were not in contact with each other and that all were exposed to the same environmental conditions (38 °C and 90% RH). One pouch was taken out from each container at 7 or 14 days interval up to 82 storage days, and moisture content was assessed in triplicate.

Shelf-life Modelling: A shelf life model was developed describing the relationship of the food, packaging and environmental conditions. Granola is a moisture sensitive product, and moisture content was identified as its critical quality parameter (Macedo *et al.* 2009). Therefore its shelf-life was determined based on product response to moisture content. The different packaging materials considered were good moisture barriers and the shelf-life of the granola was assumed to be controlled by the film WVTR. The package headspace was neglected once WVTR was assumed to be accounted totally by the gain in moisture content of granola. The mass balance and permeation of the package system is described by Eq. 1:

$$W_s \frac{dM}{dt} = PA(p_{wout} - p_{win}) \quad (1)$$

where W_s is the product dry weight (g); M is the moisture content of granola (g H_2O/g dry solids); t is the time (days); P is the permeance (g/m^2.day.Pa); A is the packaging surface area (m^2); and p_{wout} and p_{win} are water vapour pressures outside and inside the package.

The p_{wout} and p_{win} could be described by Eq. 2 and 3, respectively:

$$p_{wout} = p_s \times RH \quad (2)$$

$$p_{win} = p_s \times a_w \quad (3)$$

where, p_s is the saturated water vapour pressure (Pa), RH is the environmental water activity and a_w the food water activity.

Combining the granola moisture sorption model (Eq. 4) (Macedo *et al.* 2011) with the mass balance and permeation of the packaging system (Eq. 1) to establish the interaction between the moisture gain by the granola and the internal environment, led to Eq. 5., and the shelf-life of granola was then calculated by numerical methods.

$$M = a + ba_w^{\ c} \quad (4)$$

$$W_s \frac{dM}{dt} = PAp_s \left[RH - \left(\frac{M-a}{b} \right)^{1/c} \right] \quad (5)$$

where W_s is product dry weight (28.17 g); A is pouch area (0.017 m^2); p_s (38 °C) is 6556 Pa; permeance (P) was determined based on the WVTR (38 °C) parameters a, b and c (modified Freundlich) which were 4.055, 43.72 and 3.718 respectively; MC_i is the initial moisture content (0.0650 gH_2O/gdry solids) and MC_c is the critical moisture content (0.0890 gH_2O/gdry solids).

Results and Discussion

Water vapour transmission rate

The WVTR of the films (BOPP, NK, NM and N913) was determined using a full factorial experimental design at different temperatures and RH (Table 1).

Table 1: Water vapour transmission rate (±the confidence intervals) of each film at different temperature (T°C) and relative humidity (RH %).

T (°C); RH (%)	Water vapour transmission rate ($g.m^{-2}.day^{-1}$)			
	BOPP	NK	NM	N913
10; 33	0.310 ± 0. 197	0.837 ± 0. 395	0.558 ± 0.0	0.837 ± 0.395
10; 76	0.420 ± 0.197	2.23 ± 0.790	4.47 ± 1.58	1.40 ± 0.395
10; 96	1.95 ± 1.18	9.21 ± 0.395	11.7 ± 1.58	2.23 ± 0.0
30; 32	1.67 ± 0.0	3.07 ± 0.395	1.95 ± 0.395	2.23 ± 0.0
30; 75	2.79 ± 0.0	7.54 ± 0.395	22.9 ± 5.53	4.19 ± 0.395
30; 92	3.63 ± 0. 395	21.8 ± 0.790	35.7 ± 0.0	6.14 ± 0.0
40; 32	7.54 ± 0.395	8.65 ± 2.76	6.70 ± 0.790	7.54 ± 0.395
40; 75	6.42 ± 2.76	15.1 ± 0.790	44.7 ± 13.4	11.4 ± 4.34
40; 89	9.49 ± 1.58	38.2 ± 1.97	47.4 ± 0.0	18.4 ± 0.790

The WVTR of BOPP and NatureFlex N913 films was independent of RH, but were shown to be T dependent, which was described well by the Arrhenius relationship. The NaturFlex NK and NM films showed that WVTR increased significantly with increasing T and RH. An Arrhenius relationship was used to describe the dependence between T and WVTR at constant RH. The activation energy (Ea) followed a linear relation with RH, Ea decreasing with the RH; an exponential function was used to fit the $WVTR_{ref}$ as a function of RH. A global model for WVTR as a function of T and RH is presented in Eq. 6.

$$WVTR = \left[a\exp(b * RH)\right]\exp\left[-\frac{Ea}{R}\left(\frac{1}{T}-\frac{1}{T_{ref}}\right)\right] \quad (6)$$

Assessment of shelf life of packed granulated product

An ANOVA analysis showed that the moisture uptake by granulated product was significantly affected ($p < 0.05$) by storage time and type of packaging material. Therefore, the water vapour permeability of the packaging film is crucial for control of the moisture uptake by granola and consequently its shelf life. The kinetics of moisture content of the granulated product packed in the different packaging materials under accelerated storage conditions, followed a first order reaction model (Figure 1). The model showed a suitable fitting and the coefficient of determination was higher than 0.803 and the mean relative deviation modulus was lower than 8.77.

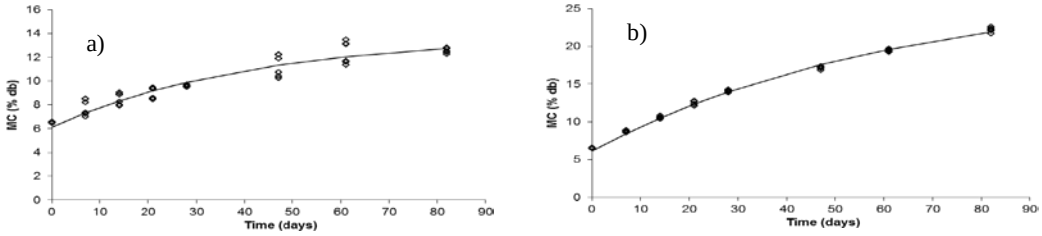

Figure 1: Example of kinetics of moisture content (MC) of granola under accelerated storage conditions (38°C and 90% RH) packed in a) BOPP, and b) N913 film. The markers correspond to the experimental values and the solid lines correspond to the predicted values by a first order reaction model.

As an example, the diagnosis plot between experimental values and predicted by a first order reaction model for N913 film is shown in Figure 2, and also the plot of frequency distribution of residuals and the plot of residuals vs. predicted values. A normal distribution of residuals was found and the trend was not biased showing a dispersed data points centred on zero.

The initial moisture content of granola was 6.50 ± 0.057 % (d.b.) and the critical limit for moisture gain was decided on the basis of the consumer's acceptability. The sensory cut-off point was determined based on the least significant differences and the threshold value was 2.4 p.p. of moisture gain i.e., the critical moisture content was 8.9 % (d.b.)

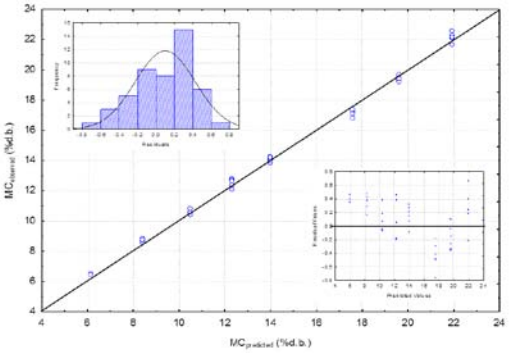

Figure 2: Diagnosis plot between experimental and predicted values of moisture content (MC) of N913 film. The upper left graph shows the frequency distribution of residuals and bottom right graph shows distribution of the residuals versus predicted values of WVTR.

The shelf life of packaged granola was predicted by solving Eq.5 numerically for each type of packaging film. For validation, accelerated tests were performed at 38 °C and 90% RH, as shown in Fig 1. The data of Fig. 1 were fitted by a first order reaction model to determine the time when critical moisture content was reached. Table 2 gives the predicted and experimental shelf-life for 38 °C and 90% RH, showing a good agreement always with a conservative estimate. The predicted shelf-life for normal storage conditions is also given.

Table 2: Shelf life of granola for the different packaging films at accelerated and normal storage conditions; permeance predicted by Eq.6, shelf-life predicted by Eq.5, experimentally for accelerated conditions Fig1.

Packaging film	38°C and 90% RH		Experimental Shelf life (days	20°C and 60% RH	
	Permeance (g/m^2.day.Pa)	Shelf life (days)		Permeance (g/m^2.day.Pa)	Shelf life (days)
control	---	---	21	---	---
BOPP	0.0012	13	19	0.00074	283
NK	0.0047	3	7	0.0023	90
NM	0.0074	2	3	0.0063	33
N913	0.0023	7	9	0.00093	228

Conclusions

The BOPP film was found to be the best barrier to water followed by the biodegradable N913, Moisture content gain during storage of granola product was less pronounced in BOPP packages compared to the others, and BOPP showed to be as effective as the control film. Among the biodegradable packages, the N913 was the most effective in controlling moisture gain of granulated product. Under accelerated conditions, the predicted shelf life of granola ranged from 13, 3, 2, and 7 days in BOPP, NK, NM and N913 pouches, respectively showing a good agreement with the experimental shelf-life. Under normal storage conditions the predicted shelf-life of granola ranged from 283, 90, 33, and 228 days in BOPP, NK, NM and N913 pouches, respectively.

Acknowledgements

Research funding was provided under the NDP, through FIRM (06/RDC/428), administered by the Department of Agriculture, Fisheries & Food, Ireland. A special thanks to Innovia Films Ltd (Cumbria, UK) for supplying the packaging materials.

References

ASTM E 96 (2006) Standard Test Methods for Water Vapour Transmission of Materials.

Macedo I.S.M, Sousa-Gallagher M.J. and Byrne E.P. (2009) Identification of critical quality parameters and most influential environment conditions of granola breakfast cereal during storage, Conference Proceedings, poster presentation, 344, NMPOS [8th World Congress of Chemical Engineering, Montreal (Canada) August 23-27th].

Macedo I. S. M., Sousa-Gallagher M. J. and Byrne E. P. (2011) Moisture Sorption Isotherms of Granola Breakfast Product, in Program & Abstracts [40th Annual UCC Food Research Conference, March31st-April 1st].

A comparison of Raman and FTIR Spectroscopy for the prediction of meat spoilage

A. A. Argyri[1,2], R. M. Jarvis[3], D. Wedge[3], Y. Xu[3], E. Panagou[1], R.Goodacre[3], G.-J. E. Nychas[1]

[1] Lab of Microbiology and Biotechnology of Foods, Dept of Food Science and Technology, Agricultural University of Athens, Iera Odos 75, Athens 11855, Greece (e-mail; gjn@aua.gr)
[2] Applied Mycology Group, Cranfield Health, Cranfield University, Bedford MK43 0AL, UK
[3] Lab of bioanalytical spectroscopy, School of Chemistry, University of Manchester,, PO Box 88, Sackville St, Manchester M60 1QD, UK

Abstract

The aim of this study was to investigate and compare the dynamics of FTIR and Raman spectroscopy in predicting the microbial spoilage of meat stored under different packaging conditions (aerobic and modified atmosphere packaging) at 5°C. Time series spectroscopic, microbiological and sensory analysis data were obtained from minced beef samples and analysed using machine learning and evolutionary computing methods, including partial least square regression (PLS-R), genetic programming (GP), genetic algorithm (GA), artificial neural networks (ANNs) and support vector machines regression (SVR) including different kernel functions [i.e. linear (SVR_L), polynomial (SVR_P), radial basis (RBF) (SVR_R) and sigmoid functions (SVR_S)]. Models predictive of the microbiological load and sensory assessment were calculated using these methods and the relative performance compared. In general, it was observed that for both FTIR and Raman calibration models, better predictions were obtained for TVC, LAB and *Enterobacteriaceae*, whilst the FTIR models performed in general slightly better in predicting the microbial counts compared to the Raman models. Additionally, regarding the predictions of the microbial counts the deterministic methods (SVM, PLS) that had similar performances gave better predictions compared to the evolutionary ones (GA-GP, GA-ANN, GP). This may arise from the fact that the stochastic nature of the later methods may make them unreliable for not big datasets like those used here, with GA-GP particularly prone to 'over-fit' the data. On the other hand, the GA-GP model performed better from the others in predicting the sensory scores using the FTIR data, whilst the GA-ANN model performed better in predicting the sensory scores using the Raman data. The results demonstrated that FTIR and Raman spectroscopy can be applied reliably and accurately separately or in combinations, to the assessment of meat spoilage.

Keywords: FTIR, Raman, meat spoilage, PLS-R, ANN, SVR

Introduction

Fourier transform infrared (FTIR) spectroscopy has attracted considerable interest since it is rapid and non-destructive and has been identified as having considerable potential for applications in food and related industries, with several reports on muscle food analysis. Studies correlating the microbial spoilage of meat with biochemical changes within the meat substrate have been conducted for chicken (Ellis *et al.* 2002) and beef (Ammor *et al*. 2009, Argyri *et al*. 2010; Ellis *et al*. 2004). Raman spectroscopy is a vibrational spectroscopy method that is complementary to absorbance and can be used in food analysis, since it is non-destructive, requires little pre-treatment of samples, provides information about different food compounds at the same time, offering quantitative analysis of food components with simultaneous information on molecular structure. Examples of this technique for muscle food analysis, include studies upon the authenticity of poultry species, the quality screening of beef (Beattie 2004) and the texture of pork muscle (Herrero *et al.* 2008). However, we know if no reported studies using Raman spectroscopy that have been conducted on the *spoilage* of muscle foods.

Materials and Methods

Minced beef samples were packaged under air and MAP (40% CO_2/ 30% O_2/ 30% N_2), and stored at 5˚C. Microbiological and sensory analyses, pH measurements, FTIR and Raman spectroscopy measurements were carried out in an attempt to correlate the total and individual microbial loads from these samples with the biochemical metabolites that fluctuate during the spoilage process. The data obtained from the above analyses were analysed using machine learning and evolutionary computing methods, including partial least square regression (PLS-R), genetic programming (GP), genetic algorithm (GA), artificial neural networks (ANNs) and support vector machines regression (SVR) including different kernel functions [i.e. linear (SVR_L), polynomial (SVR_P), radial basis (RBF) (SVR_R) and sigmoid functions (SVR_S)]. Models predictive of the counts of the different microbial groups (TVC, *Pseudomonas* spp., *Brochothrix thermosphacta*, lactic acid bacteria (LAB), *Enterobacteriaceae* and yeasts/moulds) and sensory scores were calculated using these methods and the relative performance was compared. The criteria for evaluating and comparing the models were the root mean square error (RMSE), the square of the correlation coefficient R^2 and the percentage of Prediction Error (% PE) (Oscar 2009) for the known values versus validation estimates. In addition, the confusion matrix was used to evaluate the correct classification of the estimated sensory scores.

Results and Discussion

Microbial association and shelf life

The minced beef samples were stored for 144 h aerobically and under MAP at 5 °C, until spoilage was very pronounced, whilst a total of 13 sampling points were collected for each condition with a sampling frequency of 12h. The microbiological analysis revealed that during the aerobic storage of minced beef, *Pseudomonas* spp. were the dominant microorganisms, followed by *Br. thermosphacta*, yeasts and moulds, LAB and *Enterobacteriaceae*. Packaging under MAP delayed the growth of the pseudomonads, yeasts/ moulds, and *Enterobacteriaceae* and suppressed the maximum level of the aerobic counts compared with the aerobic storage, whilst affected positively the growth of *Br. thermosphacta* and LAB. Similar results for meat have been described previously (Skandamis and Nychas 2001; Ercolini *et al*. 2006).

FTIR and Raman spectroscopy

Typical spectral data obtained from FTIR in the range of 1800 to 900 cm-1 and Raman in the range of 3400 to 200 cm-1 collected from minced beef stored aerobically and under MAP at 5 °C, as well as possible tentative assignments are shown in Figure 1 and Figure 2 respectively.

Calibration models

Tables 1 and 2 present the RMSE and the R^2 values for the models built for FTIR and Raman measurements. In general, it was observed that for both FTIR and Raman calibration models, better predictions were obtained for TVC, LAB and *Enterobacteriaceae*, whilst the FTIR models performed in general slightly better in predicting the microbial counts compared to the Raman models. Additionally, regarding the predictions of the microbial counts the deterministic methods (SVM, PLS) that had similar performances gave better predictions compared to the evolutionary ones (GA-GP, GA-ANN, GP). This may arise from the fact that the stochastic nature of the later methods may make them unreliable for not big datasets like those used here, with GA-GP particularly prone to 'over-fit' the data. The % PE values of the models (data not shown), indicates that for FTIR models, PLS, SVR_L and SVR_P gave for all the counts acceptable predictions (% PE > 70%), except from the counts of yeasts/ moulds. For Raman models, SVR_R and SVR_P gave for all the counts acceptable predictions (% PE > 70%). The classification accuracies of the sensory estimates regarding the FTIR and Raman models for each class and in total can be seen at Table 3. On the other hand, the GA-GP model performed better from the others in predicting the sensory scores using the FTIR data,

whilst the GA-ANN model performed better in predicting the sensory scores using the Raman data.

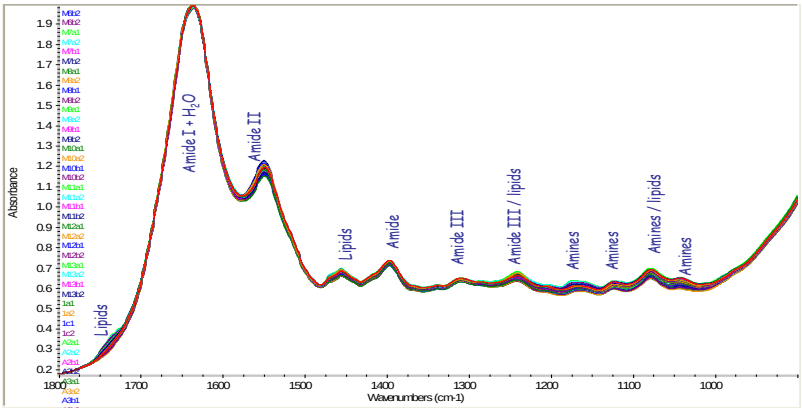

Figure 1: FTIR spectra collected from minced beef samples stored aerobically and under MAP at 5ºC.

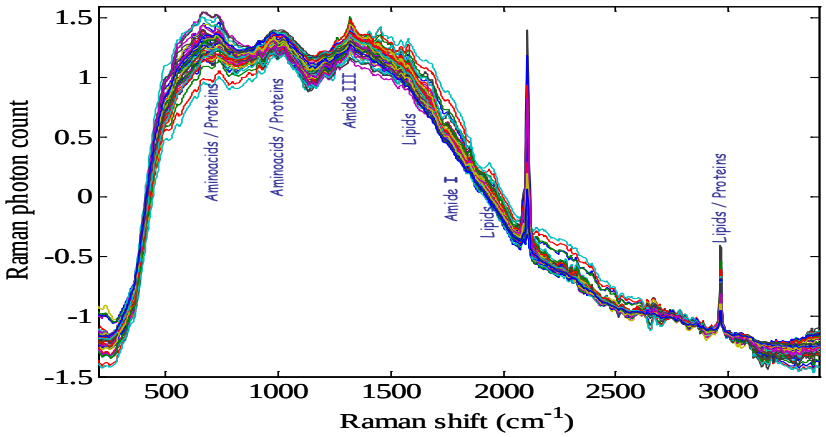

Figure 2: Raman spectra collected from minced beef samples stored aerobically and under MAP at 5ºC

Table 1: Root mean square errors for the validation estimates for each FTIR and Raman. model

	Model	TVC	Pseudomo-nads	LAB	*Br. thermo-sphacta*	Enterobact eria	Yeasts & Moulds	Sensory
FTIR	PLS	0.5472 (9*)	0.6007 (9)	0.4368 (9)	0.6886 (9)	0.4442(4)	0.5478(7)	0.3937(9)
	SVR_L	0.5040	0.5662	0.4162	0.7846	0.4345	0.5516	0.3932
	SVR_R	0.5109	0.5793	0.4111	0.6849	0.4382	0.5154	0.3941
	SVR_P	0.5098	0.5648	0.4153	0.6842	0.4394	0.5475	0.3908
	GA-ANN	0.7909	0.7845	0.5857	0.9914	0.4835	0.5683	0.6499
	GA-GP	43.8596	0.6375	0.5740	0.7635	0.4205	0.5807	0.3450
Raman	PLS	0.6301 (6)	0.8122 (3)	0.5513 (6)	0.7280 (6)	0.5245 (9)	0.6789 (5)	0.3228 (6)
	SVR_L	0.6777	0.8494	0.5328	0.8269	0.6502	0.3445	0.3932
	SVR_R	0.5629	0.7060	0.4626	0.7054	0.4961	0.6291	0.3277
	SVR_P	0.5713	0.7252	0.5107	0.7245	0.4345	0.5516	0.3932
	GA-ANN	0.9954	1.1708	0.6421	0.7905	0.7050	0.7907	0.3352
	GA-GP	1.0419	9.4335	0.6465	1.3131	0.8000	8.3899	0.7657

*Number of latent variables used to calculate the PLS model. SVR_L = linear. SVR_R = radial basis function. SVR_P = polynomial.

Table 2: R^2 for the validation estimates for each FTIR and Raman model.

	Model	TVC	Pseudomo-nads	LAB	*Br. thermo-sphacta*	Enteroba cteria	Yeasts & Moulds	Sensory
FTIR	PLS	0.8066	0.7885	0.8392	0.7269	0.7562	0.7172	0.6453
	SVR_L	0.8368	0.8129	0.8163	0.6693	0.7740	0.7240	0.6660
	SVR_R	0.8316	0.8036	0.8178	0.7329	0.7600	0.7629	0.6580
	SVR_P	0.8329	0.8147	0.8167	0.7347	0.7682	0.7201	0.6659
	GA-ANN	0.7086	0.6504	0.6920	0.5313	0.7466	0.7654	0.5533
	GA-GP	0.0086	0.7656	0.6730	0.6670	0.7902	0.7101	0.7346
Raman	PLS	0.7259	0.5183	0.7449	0.7142	0.7169	0.6169	0.7834
	SVR_L	0.7205	0.5940	0.7220	0.6856	0.6068	0.7531	0.6660
	SVR_R	0.7951	0.7003	0.7874	0.7317	0.7232	0.6254	0.7781
	SVR_P	0.7893	0.6835	0.7649	0.7333	0.7740	0.7240	0.6660
	GA-ANN	0.4779	0.2894	0.6206	0.7035	0.4774	0.4341	0.8246
	GA-GP	0.3457	0.0018	0.6218	0.2697	0.3191	0.0045	0.2766

Table 3: Percentage of the correct classification of the validation sensory estimates for the FTIR and Raman models

	Class	Correct Classification (%)					
		PLS	**SVR_L**	**SVR_R**	**SVR_P**	**GA-ANN**	**GA-GP**
FTIR	**Fresh** (*n* =6)	33.33	16.67	33.33	33.33	66.67	**66.67**
	Semi-fresh (*n*=12)	83.33	91.67	100.00	100.00	50.00	**91.67**
	Spoiled (*n* =30)	90.00	93.33	93.33	93.33	96.67	**90.00**
	Total (*n* =48)	81.25	83.33	87.50	87.50	81.25	**87.50**
Raman	**Fresh** (*n* = 26)	80.77	73.08	69.23	73.08	**96.15**	23.08
	Semi-fresh (*n*=30)	56.67	70.00	66.67	80.00	**76.67**	73.33
	Spoiled (*n* =74)	90.54	90.54	87.84	90.54	**81.08**	87.84
	Total (*n* =130)	80.77	82.31	79.23	84.62	**83.08**	71.54

Conclusions

The results of this study demonstrate that Raman spectroscopy as well as FTIR, in combination with the appropriate data analysis and model development can be applied reliably and accurately to the rapid assessment of meat spoilage. However, further studies are required to create data bases and apply the appropriate prediction models, so as these methods can be applied in meat industries.

Acknowledgements

This work financially supported from SYMBIOSIS-Eu project (7^{th} FP).

References

Ellis D. I., Broadhurst D., Kell D. B., Rowland J. J. and Goodacre R. (2002) Rapid and quantitative detection of the microbial spoilage of meat by Fourier transform infrared spectroscopy and machine learning. *Applied and Environmental Microbiology* 68, 2822-2828.

Ellis D. I., Broadhurst D., and Goodacre R. (2004) Rapid and quantitative detection of the microbial spoilage of beef by Fourier transform infrared spectroscopy and machine learning. *Analytica Chimica Acta*, 514, 193-201.

Ammor M., Argyri A. and Nychas G.-J. (2009) Rapid monitoring of the spoilage of minced beef stored under conventionally and active packaging conditions using fourier transform infrared spectroscopy in tandem with chemometrics. *Meat Science* 81, 507-515.

Argyri A.A., Panagou E.Z., Tarantilis P.A, Polysiou M. and Nychas G.-J.E. (2010) Rapid qualitative and quantitative detection of beef fillets spoilage based on Fourier transform infrared spectroscopy data and artificial neural networks, *Sensors and Actuators B: Chemical,* 145 (2), 146-154.

Beattie R. J., Bell S. J., Farmer L. J., Moss B. W. and Patterson, D. (2004) Preliminary investigation of the application of Raman spectroscopy to the prediction of the sensory quality of beef silverside. *Meat Science, 66*, 903–913.

Herrero A. M. (2008) Raman spectroscopy a promising technique for quality assessment of meat and fish: A review. *Food Chemistry* 107, 1642–1651.

Simulation of food products a_w: development of a modelling tool

T. De Broucker, Mohammed El Jabri, D. Thuault

ADRIA Développement, ZA Creac'h Gwen F29196 Quimper Cedex
(thibaud.debroucker@adria.tm.fr, mohammed.eljabri@adria.tm.fr, dominique.thuault@adria.tm.fr) ,

Abstract

The influence of water activity (aw) on microbiological and organoleptic properties of food is a well-known phenomenon. Several models have been described in order to calculate water activity of multicomponent solution. They are based on the hygroscopic properties of components. In this study we have compared the robustness of the main predictive models for aw solution (Grover, 1947, Norrish, 1966, Roa, 1998 and Roos, 1975). For insoluble macromolecules, sorption isotherms are used to calculate the a_w. Fitting accuracy of the two models was studied. The GAB model (Guggenheim-Anderson-deBoer, 1966) is robust for a_w values from 0 to 0.85 and Ferro-Fontan model (1982) is robust for a_w values from 0.5 to 0.98. In order to simulate the a_w of formulated food which contain solutes and insoluble compounds, it is necessary to combine models described for solution and descriptive models for sorption isotherms. We have developed a Matlab® based tool called awDesigner in order to simulate the a_w value of formulated foodstuff. Software modelling is based on Roa and Ferro-Fontan models and simulates the equilibrium aw of all the components. Validation of the mathematical model was done on different type of matrices with an a_w range from 0.7 to 1 (bakery products, meat products, syrup...). This tool shows great correlations between predictive values and aw values measured with Aqualab Aw-meter (R^2=0.94).

Keywords: *simulation, water activity, modelling, software*

Introduction

The influence of water activity (a_w) on microbiological and organoleptic properties of food is a well-known phenomenon. Several models have been developed in order to determine precisely the water activity value in high moisture range. All these mathematical models are based on the compositions of the solutions. The main models are empirical but give good accuracy (Roa, 1998; Teng and Seow, 1981, Chirife *et al.,* 1980). But all these models could only be used for binary and multicomponents solutions but not for foodstuff containing insoluble compounds. The objective of this work is to develop mathematical model in order to simulate water activity of foodstuff and develop awDesigner software to simulate water activity of complex foodstuff in a wide range of formulation and water activity.

Material and methods

Several models were used to simulate the aw values of various solutions.

Description of the main published models for simulation of water activity of multi components solutions

- Roa equation

For multi components solutions, Roa proposed a model based on the K constant which is the depressor coefficient of water activity of each solute. m represents the molality of the solutes, and K the Roa parameters (Rao and Tapia, 1998).

$$a_w = 1 - \sum K_j . m_j \qquad (1)$$

- Grover equation

The Grover equation (Barbosa *et al.*, 1986) presents the water activity value as a function of solute concentration (C_i, g / g water) and the coefficient of sucrose equivalence of the solute (S_i).

$$a_w = 1{,}04 - 0{,}1 \cdot (\sum_i C_i S_i) + 0{,}0045 \cdot (\sum_i C_i S_i)^2 \quad (2)$$

- Ross equation

The binary contributions (aw_i^0) for each solute, necessary for the application of the Ross equation were calculated using Teng and Lenzi model. The calculations were reported by Roa (Roa and Tapia, 1998).

$$a_w = \prod_i a_{wi}^0 \quad (3)$$

Table 1: Parameters for Roa, Grover and Norrish equations determined for various solutes.

solute	K (molal^{-1}) of Roa	Parameters of Grover	K AwDesigner (eq8)
Glucose	0.01959	1.3	0.01889
Glycerol	0.01723	4	0.01787
Sucrose	0.02395	1	0.02289
Mannitol	0.01806	4	0.01782
NaCl	0.03710	9	0.03591
KCl	0.03248	9[a]	0.03208
$MgCl_2$	0.05620	9[a]	0.08207

Model for fitting sorption isotherm

In order to describe the sorption isotherm, the two main models described are: Guggenheim Anderson deBoer (GAB, 1966) model and Ferro-Fontan model (1982). The Ferro-Fontan (eq 4) model is defined by the following equation (Chirife *et al.*, 1983). The parameters γ, α and C have no real physical meaning. The first advantage of this model is that it can account for the asymptotic character of sorption isotherms at high humidity. For each ingredient, the sorption isotherm was obtained using salt-saturated solution method. Then, the Ferro-Fontan parameters (eq 4) were determined by minimizing the differences between the modelled and experimental values.

$$X = \left[\left[\ln(\frac{\alpha}{a_w})\right].\left[\frac{1}{\beta}\right]\right]^C \quad (4)$$

Validation of the models for multicomponent aqueous solutions

For multicomponent aqueous solutions, the validation of the models was performed comparing experimental data with water activity simulations using reported models, ***i.e.*** Ross model, Roa model and Grover model (Teng and Seow, 1981; Chirife *et al.*, 1980).

To evaluate the accuracy of the predictions, two parameters were determined (i) delta values which represents the difference between estimated and experimental values (eq 6) and (ii) PE value representing the percentage error (PE, eq 5). The mean of PE was also calculated for each studied model.

$$PE = 100.\left[\left(a_{w\,predicted} - a_{w\,experimental}\right)/\left(1 - a_{w\,experimental}\right)\right] \quad (5)$$

$$\delta = a_{w\,predicted} - a_{w\,experimental} \quad (6)$$

Validation of the developed model on bakery products

The validations have been made on different bakery products with different formulations containing: flour meal (26.8% to 48.1%), rapeseed oil (0% to 19.2%), sucrose (20% to 36.4%), whole egg (10.4% to 29.2%), sorbitol (0% to 5.3%), water (5% to 20%), glucose syrup DE 60 (0% to 2.1%), fructose (0% to 26%), glucose (0% to 26%), black chocolate 60% cocoa (0 to 10%), salt (0;5%) and bakery yeast (0.4%). The cakes have been cooked in a bakery oven 11 minutes at 180°C using 25g cake molds.

The determination of water activities were performed for the dough and the cooked cake. Cooked cakes were cut and ground before a_w measurements. Calculations of cooked cakes aw took into account the dehydration of dough during the cooking step.

Results and Discussion

Model development for multi components systems

For binary solutions (water with one solute), the equation of Roa (eq 7) determines water activity as a function of solute mass (m_j), molar mass (M_j), depressor coefficient constant K_j and the volume of water (V). Equation 8 is similar to equation 6 with X_i representing the water content of the solute (expressed in dry basis). Constant K (table 1) was calculated using the Teng and Lenzi database (Teng and Lenzi, 1974).

$$a_w = 1 - \left(K_j . \frac{m_j}{M_j . V} \right) \quad (7) \qquad X_i = \frac{V}{m_j} = \frac{K_j}{M_j . (1 - a_w)} \quad (8)$$

We propose a model to describe the impact of water content on a multi components solution taking into account the global water content and the relative percentage of each component in the solution.

This model is a different expression of the model of Roa (eq 9). Roa model determines the water activity of multicomponents solutions as a function of molality of each components and their depressor coefficient constant K. While our model explains the water content as a function of water activity, K constant, molar mass of the components and mass ratio of the compound (γ_i) expressed as dry mass of the constituent divided by the total dry mass.

The model is based on the simulation of the repartition of water between all the components in order to equilibrate the a_w value of each component. This model presents the advantage to be usable in food industry by using only the concentration of each solute.

$$X = \sum_{i=1}^{n} \left(\frac{K_i}{(1 - a_w) . M_i} . \gamma_i \right) \quad (9)$$

The figure 1 shows comparison between the simulated aw value obtained with Ross model (x), Roa model (□), Grover model (○) and the model developed for AwDesigner software (▲). The experimental aw value and the a_w value obtain with Roa and Ross are reported by Roa, 1998, Grover simulation was calculated for this work. The formulations of the studied solutions are described by Roa (Roa, 1995) for different electrolytes and non-electrolytes: NaCl, KCl, MgCl2, CaCl2, Sucrose, Glycerol, glucose and mannitol.

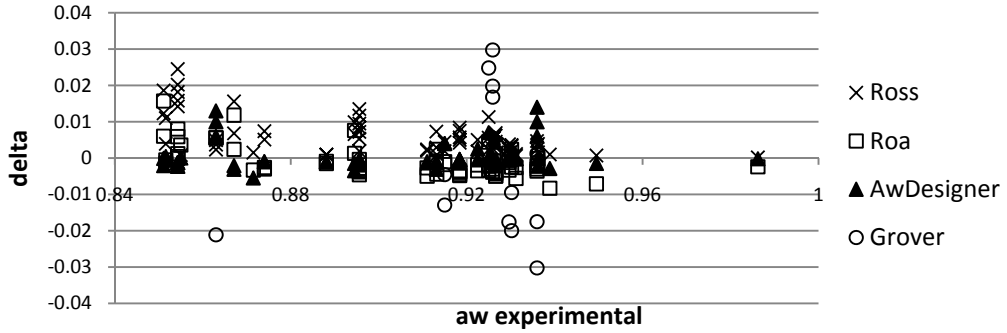

Figure 1: Differences delta obtained between experimental and simulated values obtained using Ross equation, Roa equation, Grover equation, and AwDesigner.

Figure 1 shows a general tendency of Roa's equation to underestimate aw value when the a_w is higher than 0.9, and to over-estimate aw value when aw value is lower than 0.9. Ross' equation over-estimates aw for all the solutions tested. The percentage error (PE) calculated using equation 6 for ternary and quaternary solution shows differences between the accuracies of the different models. AwDesigner gives the best accuracy of calculation. AwDesigner's PE is 2.21%, Roa's PE is 4.02%, Ross' PE is 5.84%. Grover's model gives the highest PE value: 18.85%.

Development of model for multi component system containing insoluble compounds

Assuming the equilibrium of all the water activity of all the components of the foodstuff, we can describe the following equation 11 including the solutes and the insoluble components. Where γ_i is the mass fraction of each solute (expressed by g/g total dry basis) and γ_i is the mass fraction of each unsoluble components described by sorption isotherm. X_i and X_j represent the repartition of water on all solutes and non-solutes compounds respectively. For solutes, X_i is expressed using eq. 8. For non-solutes compounds, previous works have shown that GAB model give good accuracy in sorption isotherm fitting from 0 to 0.85 a_w, Ferro-Fontan gives good accuracy from 0.5 to 0.98 a_w. For X_j values, in our work we used Ferro-Fontan model, eq 4.

$$X = \sum_{i=1}^{n}\left(X_i.\gamma_i\right)+\sum_{j=1}^{m}\left(X_j.\gamma_j\right) \quad (10)$$

This model has been programmed on Matlab in order to provide software with user friendly interface (AwDesigner®). Different comparison between simulated aw value and measured aw values have been done in order to validate the developed program. For these validation we have work on cereal based products, sauce and meat products. The simulations gave good fitting. Correlation between simulated values and predicted values is 0.947. The PE value is 7.5%.

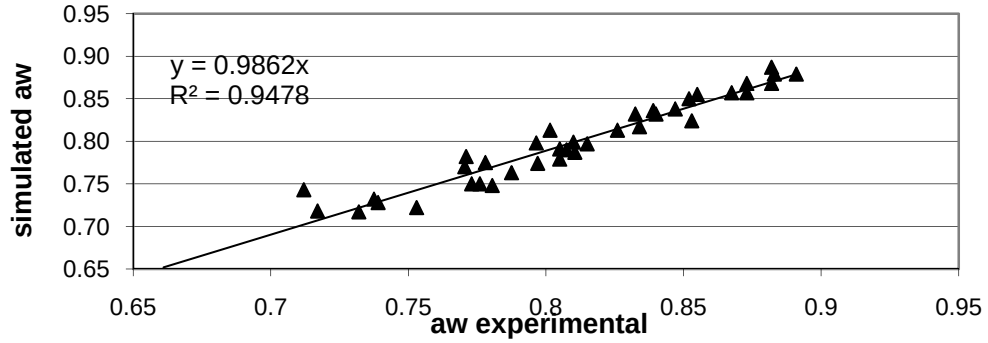

Figure 2: Comparison between experimental a_w and a_w simulated with AwDesigner for bakery products.

Conclusion

Simulation of a_w of formulated foodstuff is more complicated than a_w simulation of multicomponent solution. Previous developed models enabled to calculate with good accuracy, the a_w of multicomponent solution containing only solutes but does not take into account the solid phases. This work allowed to develop models and a software in order to determine the a_w of formulated foodstuff as a function of its formulation. The validations of the model give good accuracy: $R^2 = 0.94$ and the average error (PE value) is 7.5% for bakery products. The software has also been designed for other types of product (sauce, meat products...) and contains more than 230 different ingredients.

References

Chirife J., Ferro Fontán C. and Benmergui E.A. (1980) The prediction of water activity of aqueous solutions in connection with intermediate moisture foods. IV: aw prediction in aqueous nonelectrolyte solutions. *Journal of Food Technology*, 15, 59-70.

Teng T.T. and Lenzi F. (1974) Water activity data representation of aqueous solutions at 25ºC. *Canadian Journal of Chemical Engineering*. 52, 387-391.

Teng T.T. and Seow C.C. (1981) A comparative study of methods of prediction of water activity of multicomponent aqueous solutions. *Journal of Food Technology*, 16, 409-419.

Barbosa-Canovas G.V. and Vega-Mercado H. (1986) *Dehydration of foods*. Chapman & Hall, New-York, USA, 330pp. (ISBN 0-412-06421-9)

Roa V. and Tapia S. (1998) Estimating water activity in systems containing multiple solutes based on solute properties. *Journal of Food Science*. 63, 559-564.

Shelf life modelling of osmotically pre-treated gilthead seabream bream fillets with the addition of antimicrobial agents

T.N. Tsironi, P.S. Taoukis

National Technical University of Athens, School of Chemical Engineering, Laboratory of Food Chemistry and Technology, Iroon Polytechniou 5, 15780 Athens, Greece (ftsironi@chemeng.ntua.gr).

Abstract

The objective of the study was the kinetic modelling of temperature and osmotic pre-treatment with antimicrobial agents dependence on the shelf life of chilled fish fillets. Fresh gilthead seabream (*Sparus aurata*) fillets were osmotically treated with 50% maltodextrin (DE47) plus 5% NaCl for 45 min at 15°C. HDM/NaCl solutions with 0.5% carvacrol, 0.5% glucono-δ-lactone or 1% Citrox (commercial antimicrobial mix) were also used. Untreated and pre-treated slices were aerobically packed and stored isothermally (0-15°C). Quality assessment was based on microbial growth, total volatile basic nitrogen (TVB-N), trimethylamine nitrogen (TMA-N), lipid oxidation (TBARs) and sensory scoring. Quality indices were kinetically modelled and temperature dependence of quality loss rates was modelled by Arrhenius equation. The models developed from the isothermal experiments were validated at dynamic conditions (T_{eff}=8.8°C).

Microbial growth, change in chemical indices and sensory scoring were modelled at isothermal conditions and the temperature dependence of each index was expressed by the E_a value of the Arrhenius equation (ranging from 48 to 76 kJ/mol). End of shelf life determined by sensorial unacceptability was correlated to the respective values of the quality indices. Osmotic pre-treatment led to significant shelf life extension of fillets, in terms of microbial growth and organoleptic deterioration. The use of antimicrobial agents gave additional shelf life increase of pre-treated fillets. Based on microbial growth, the shelf life was 7 days for raw samples and 9 days for osmotically pre-treated fillets at 5°C. The addition of antimicrobials increased shelf life to 15, 17 and 12 days for carvacrol, glucono-δ-lactone and Citrox at 5°C, respectively. The non-isothermal experiments indicated the suitability of the models to predict the shelf life of fish at the different alternative treatments under non-isothermal conditions.

Keywords: *Osmotic dehydration, fish, carvacrol, glucono-δ-lactone, kinetic modelling*

Introduction

Spoilage of chilled fresh and minimally processed fish is attributed mainly to bacterial activity and it manifests itself as changes in the sensory characteristics (Gram and Huss 1996). Gilthead seabream (*Sparus aurata*) is a Mediterranean fish of high commercial value due to its desirable characteristics (aroma, taste, white flesh) and has high commercial potential if its shelf life can be extended through packaging or minimal processing. Gilthead seabream is one of the most cultured species in the Mediterranean area and its production in Greece was estimated at 52165 tons in 2008, with Greece being the leading world producer with the 40.5% of the total Mediterranean production (FAO 2010).

Osmotic dehydration (OD) is a technique used to reduce water activity (a_w) in order to improve nutritional, sensorial and functional properties of food. It consists of an immersion of the product into a concentrated solution (i.e. sugar, salt, sucralose etc.). Previous studies for osmotic treatment of fish products evaluate the effect of different solutes, mainly sucrose or salt, on the equilibrium and mass transfer into fish slices (Collignan and Raoult-Wack 1994; Medina-Vivanco *et al*. 2002; Tsironi *et al*. 2009).

Minimal processes offer the potential to further increase the shelf life of fish products. A wide range of antimicrobial systems have been examined for their potential use in food preservation. Carvacrol is the major component of the essential oil fraction of oregano and thyme, responsible for their antimicrobial activity (Mahmoud *et al*. 2004). Glucono-δ-lactone is hydrolyzed to form gluconic acid and is used mainly in acidified meat products, like salami and sausages, to reduce the risk of bacterial contamination (Barmpalia *et al*. 2005). Several

studies investigate the potential use of commercial antimicrobial mixes as shelf life extenders for meat products. Citrox Biocite AFA001 (ProVigoroTM, Citrox Limited, Middlesbrough, UK) is a nutritional food supplement, consisting of bioflavonoid complexes, vitamins and naturally occurring organic acids.
The objective of the study was the kinetic modelling of temperature and osmotic dehydration with antimicrobial agents dependence on the shelf life of chilled gilthead seabream fillets and the establishment of reliable kinetic equations validated in dynamic conditions.

Materials and Methods

Marine cultured gilthead seabream (*Sparus aurata*) fillets (weight: 90±10 g, capture zone: Aegean Sea, Greece), provided by a leading Greek aquaculture company, were cut into rectangular slices (3x3x1cm^3, 10±1g) in a laminar flow hood. Osmotic solution was prepared by dissolving high dextrose equivalent maltodextrin (DE 47, HDM, 50% ww), NaCl (5% ww) and distilled water. HDM/NaCl solutions with 0.5% carvacrol, 0.5% glucono-δ-lactone or 1% Citrox were also used (coded as HDM+carvacrol, HDM+g-δ-l and HDM+Citrox, respectively).
Sliced samples were osmoticaly treated at 15ºC for 0-360 min, as described by Tsironi *et al*. (2009). The solution to sample ratio was 5:1 (w/w) to avoid significant dilution of the medium by water removal. Moisture content, salt content, a_w, water loss and solid gain were calculated.
Untreated and pre-treated slices were aerobically packed and stored isothermally at 0, 5, 10 and 15°C. Quality assessment was based on microbial growth (total viable count, *Pseudomonas* spp., lactobacilli, *Brochothrix thermosphacta*, *Enterobacteriaceae* spp., *Shewanella putrefaciens*, yeasts and molds), total volatile basic nitrogen (TVB-N), trimethylamine nitrogen (TMA-N), lipid oxidation (TBARs) and sensory scoring (Tsironi and Taoukis, 2010). The microbial growth was modelled using the Baranyi Growth Model (Baranyi and Roberts, 1995). Quality indices were kinetically modelled and temperature dependence of quality loss rates was modelled by Arrhenius equation.
In order to validate the applicability of the models from the isothermal experiments to real conditions, a variable temperature experiment (Var) was applied, that consisted of three, repeated isothermal steps (2 h at 5°C, 2 h at 9°C and 2 h at 12°C), corresponding to an equivalent effective temperature (T_{eff}) of 8.8°C. The rates of the quality deterioration observed by the non-isothermal experiment were compared to the values determined by the models developed by the isothermal experiment.

Results and Discussion

The treatment with all osmotic solutions caused a significant moisture loss from fish flesh. The a_w value decreased with the osmotic pretreatment and the final values averaged 0.89. The decrease of a_w at these levels could lead to more stable products without significant quality and nutritional damage, observed with traditional drying methods. Processing time of 45 min was selected as the reference pre-treatment used in the shelf life study. At the selected pre-treatment conditions the fish flesh has 69% moisture, 2.5% solid gain and 0.95 water activity. The addition of the antimicrobial agents did not have any effect on the mass transfer into fish slices.
Pseudomonas spp. dominated spoilage in all samples, as also reported by Gram and Huss (1996) for aerobically packed fish. After the osmotic pretreatment the microbial population was lowered for 0.2-1.3 logcfu/g, depending on the bacteria species, due to decontamination induced by high solute concentrations at the product/solution interface (Collignan *et al*. 2001). The osmotic pre-treatment led to significantly lower microbial growth rates at all storage temperatures. The antimicrobial agents gave additional hurdles on microbial growth. Carvacrol and glucono-δ-lactone seem to have stronger antimicrobial action than Citrox, especially at the lower storage temperatures. Under this context, osmotic pre-treatment and antimicrobial agents can practically extend the shelf life of fish fillets. The untreated samples showed increased TBAR values (1.20 mg MDA/kg) after 13 days of storage at 5°C, while

osmotic pre-treated samples reached this level after 15 days. HDM+carvacrol samples showed significantly lower values than the respective ones for the other pre-treatments. A mild antioxidant effect was also observed for Citrox, mainly due to the presence of flavonoid compounds.

TVB-N values increased with storage time following apparent first order kinetics. Osmotically pre-treated samples showed lower TVB-N values than untreated fish slices. TVB-N values increased from initial values of 13.0±0.6 mg N/100 g and reached relatively high levels at the end of storage period (25-50 mg N/100 g, depending on storage conditions and treatment of samples). Samples pre-treated with osmotic solutions with the addition of antimicrobials led to significantly lower rates of TVB-N production, with carvacrol and glucono-δ-lactone showing the stronger effect.

The sensory scores of untreated and osmotically pre-treated slices were modelled by apparent zero order lines. Osmotic pre-treatment maintained the sensory attributes of fish slices, indicating freshness for longer times than the untreated samples. Osmotically pre-treated fish with the addition of antimicrobial agents exhibited the highest sensory scores in terms of odour, taste and overall acceptability, with glucono-δ-lactone showing the stronger preservative effect. Carvacrol affected significantly the taste of fish, while Citrox and glucono-δ-lactone did not show similar effect on the organoleptic parameters of fish.

The temperature dependence of the rates of microbiological deterioration, TNB-N changes and sensory deterioration was adequately described by Arrhenius kinetics in the temperature range 0-15ºC, with E_a values ranging from 48 to 76 kJ/mol. A score of 5 for overall impression was judged as the lower limit of acceptability coinciding with slight off odour and off taste development. At all storage temperatures, the time of sensory rejection coincided with an average TVB-N concentration of 22 mg N $100g^{-1}$, being in agreement with the limits reported by relevant studies (Koutsoumanis and Nychas 2000; Tsironi *et al*., 2009; Tsironi and Taoukis 2010). *Pseudomonas* spp. growth was a good quality index for shelf life evaluation. The limit of sensory shelf life coincided with a *Pseudomonas* spp. level of 6 logcfu/g at all storage temperatures. Based on the limits of acceptability for the selected quality indices (*Pseudomonas* spp. count, TVB-N, sensory scoring) and the temperature dependence of their rate constants expressed by the Arrhenius kinetics, the shelf life can be determined at any storage temperature (Equations 1-3)

$$t_{SL} = \frac{\log N_l - \log N_o}{k_{ref,LAB} \exp\left[\frac{-E_a}{R}\left(\frac{1}{T} - \frac{1}{T_{ref}}\right)\right]} \quad \text{based on } \textit{Pseudomonas} \text{ spp. growth} \quad (1)$$

$$t_{SL} = \frac{\ln C_{TVB-N,l} - \ln C_{TVB-N,o}}{k_{ref,TVB-N} \exp\left[\frac{-E_a}{R}\left(\frac{1}{T} - \frac{1}{T_{ref}}\right)\right]} \quad \text{based on TVB-N} \quad (2)$$

$$t_{SL} = \frac{s_o - s_l}{k_{ref,sens} \exp\left[\frac{-E_a}{R}\left(\frac{1}{T} - \frac{1}{T_{ref}}\right)\right]} \quad \text{based on sensory scoring} \quad (3)$$

where t_{SL} is the shelf life (d) of gilthead seabream slices, loN_l is the limit *Pseudomonas* spp. load (6 log cfu/g), $logN_o$ is the initial *Pseudomonas* spp. load, $C_{TVB\text{-}N,l}$ is the limit TVB-N concentration (22 mg N $100g^{-1}$), $C_{TVB\text{-}N,o}$ is the initial TVB-N concentration, s_l and s_o are the limit (s_l=5) and the initial sensory scores for overall acceptability, respectively, k_{ref} is the rate constant of change of each index, at a reference temperature T_{ref} (4°C), E_a is the activation energy of each index, R is the universal gas constant. The shelf life determined based on the different quality indices showed no significant differences, indicating high correlation between the organoleptic deterioration, TVB-N production and *Pseudomonas* spp. growth (Figure 1a).

The models developed from the isothermal experiments were validated at dynamic conditions. The growth rates of the spoilage microflora and the rates of change of the chemical indices and sensory parameters derived from the models were compared to the observed by the experiment under non-isothermal conditions (T_{eff}=8.8°C), as shown in Figure

1b. The model gave satisfactory results with the predictions, as the maximum relative error (RE) value (%RE=[($k_{observed}$-$k_{predicted}$)/$k_{observed}$]x100) was 18.5%, indicating the suitability of the models to predict the shelf life of fish under non-isothermal conditions (Gougouli *et al*. 2008).

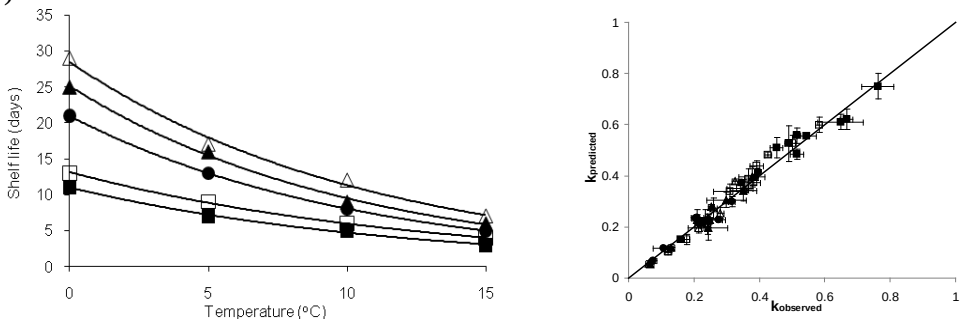

Figure 1. (a) Shelf life of gilthead seabream slices based on sensory scoring and (b) Specific growth rates (d^{-1}) of spoilage microflora and rate constants of TVB-N and sensory scoring calculated by the models from the isothermal experiments and determined by the non-isothermal experiments: ■ Control, □ HDM, ▲ HDM+carvacrol, △ HDM+g-δ-l and ● HDM+Citrox.

Conclusions

The results of the study show the potential of adding carvacrol, glucono-δ-lactone or Citrox in the osmotic solution to extend the shelf life and improve commercial value of fresh chilled osmotically pre-treated fish products. Pre-treated samples were found to have improved quality stability during subsequent refrigerated storage, in terms of microbial growth, TVB-N changes and organoleptic degradation, resulting in a significant shelf life extension at all storage temperatures. The non-isothermal experiments indicated the suitability of the models to predict the shelf life of fish at the different alternative treatments under non-isothermal conditions.

References

Baranyi J. and Roberts T.A. (1995). Mathematics of predictive food microbiology. *International Journal of Food Microbiology* 26, 199-218.

Barmpalia I.M., Koutsoumanis K.P., Geornaras I., Belk K.E., Scanga J.A., Kendall P.A., Smith G.C. and Sofos J.N., (2005). Effect of antimicrobials as ingredients of pork bologna for Listeria monocytogenes control during storage at 4 or 10°C. *Food Microbiology* 22(2), 205-211.

Collignan A. and Raoult-Wack A.L. (1994). Dewatering and salting of cod by immersion in concentrated sugar/salt solutions. *LWT-Food science and Technology* 27, 259-264.

Collignan A., Bohuon P., Deumier F. and Poligné I. (2001). Osmotic treatment of fish and meat products. Journal of Food Engineering 49, 153-162.

FAO (2010). FISHSTAT Plus: Universal Software for Fishery Statistical Time Series. FAO Fisheries Department, Fishery Information, Data and Statistics Unit, Version 2.3, 2000.

Gougouli M., Angelidis A.S. and Koutsoumanis K. (2008). A study on the kinetic behavior of Listeria monocytogenes in ice cream stored under static and dynamic chilling and freezing conditions. *Journal of Dairy Science* 97, 523-530.

Gram L. and Huss H.H. (1996). Microbiological spoilage of fish and fish products. *International Journal of Food Microbiology* 33, 121-137.

Koutsoumanis K. and Nychas G.J.E. (2000). Application of a systematic experimental procedure to develop a microbial model for rapid fish shelf life predictions. *International Journal of Food Microbiology* 60, 171-184.

Mahmoud B.S.M., Yamazaki K., Miyashita K., Shin I.S., Dong-Suk C. and Suzuki T. (2004). Bacterial microflora of carp (*Cyprinus carpio*) and its shelf-life extension by essential oil compounds. *Food Microbiology* 21, 657–666.

Medina-Vivanco M., Sobral P.J. and Hubinger M.D. (2002). Osmotic dehydration of tilapia fillets in limited volume of ternary solutions. *Chemical Engineering Journal* 86, 199-205.

Tsironi T., Salapa I. and Taoukis P. (2009). Shelf life modelling of osmotically treated chilled gilthead seabream fillets. *Innovative Food Science and Emerging Technologies* 10, 23-31.

Tsironi T.N. and Taoukis P.S. (2010). Modeling Microbial Spoilage and Quality of Gilthead Seabream Fillets: Combined Effect of Osmotic Pretreatment Modified Atmosphere Packaging and Nisin on Shelf Life. *Journal of Food Science* 75(4), 243-251.

Predictive models and tools for food processing

S. Koseki

National Food Research Institute, 2-1-12 Kannondai, Tsukuba, Japan (koseki@affrc.go.jp)

Abstract

Herein we describe an alternative predictive model for microbial inactivation and a novel web-tool for the application of predictive microbiology. The developed model enabled the identification of a minimum processing condition for a required log reduction, regardless of the underlying inactivation kinetics pattern. The developed new web-tool, MRV (Microbial responses viewer) provides information concerning growth/no growth boundary conditions and the specific growth rates of queried microorganisms. Using MRV, food processors can easily identify the appropriate food design and processing conditions.

Keywords: *food processing, inactivation model, web-tool, ComBase*

Introduction

Predictive microbiology is a well-established and recognised scientific discipline with a burgeoning literature. Quantitative evaluation of microbial responses in food environment allows us to set an appropriate processing condition and formulation of processed food. However, it seems that most of the outcomes of studies in predictive microbiology so far are not necessarily converted to practical use in real food processing. For example, although extremely complex mathematical models might be worth evolving basic understanding of microbial responses, their application would not be easy in practical. Thus, our research group has been conducted for developing predictive models and tools that are intended to contribute to practical use in a real food processing. This paper describes our main contributions to food industry.

1. An alternative approach to evaluate effects of microbial inactivation

Background and objective

The main concern for the food processor in ensuring microbiological safety is to set processing criteria for achieving a required log reduction of the microbial population. This point is also the focus of concepts such as the food safety objective (FSO), performance objective (PO), and performance criterion suggested by the International Commission on Microbiological Specifications for Foods and Codex Alimentarius. The performance criterion concept signifies the change required to reach a hazard level at each step of the food chain in order to meet a PO or FSO. The determination of the *D*-value and the *z*-value has been widely applied to thermal inactivation processes to assess the inactivation effect and set a processing condition for achieving a required log reduction. These concept values are calculated for inactivated microorganisms that follow log-linear kinetics. However, these values are not applicable to those microorganisms that display nonlinear inactivation kinetics. The calculation of a *D*-value from nonlinear inactivation kinetics results in an underestimation or overestimation of the log reduction, depending on the calculation method used. Furthermore, the evaluation of the inactivation effect on the basis of a survival curve is conducted by using the difference between the initial cell numbers (normally 6 to 8 $\log_{10}$ CFU) and reduced cell numbers induced by some treatments. When the inactivation curve follows log-linear kinetics, the same log reduction will be obtained regardless of the inoculum level. For example, 5-log reductions from 8 log to 3 log and 6 log to 1 log would show the same treatment time with log-linear kinetics. These reductions, however, would not always appear to require the same treatment time with nonlinear kinetics. In addition, these two 5-log reductions underlie different net reductions of microbial cell numbers. Therefore, we should examine the net log reduction to obtain an accurate treatment time for a required log reduction by taking into account the initial level.

Recently, we developed a survival/death interface model, which is a new predictive modeling procedure used to determine bacterial behavior after high pressure processing (HPP) inactivation as a probability of survival or death (Koseki and Yamamoto 2007). In this procedure, the probability of death after processing is modeled using logistic regression. The modeling procedure is used to predict a minimal processing condition to achieve a required log reduction, which represents a net log reduction that takes into account the inoculum level independent of the underlying inactivation kinetics. In addition, the certainty of the predicted inactivation effect under the predicted processing condition can be estimated simultaneously. Herein, a probabilistic model for predicting *Cronobacter sakazakii* inactivation in trypticase soy broth (TSB) and infant formula (IF) by high-pressure processing was introduced.

Highlights of the study

The developed survival/death interfaces model describes the effects of the applied pressure and pressure-holding time at different inoculum levels (3, 5, and 7 log10 CFU/ml) in different media (TSB and infant formula) at different temperatures (25 and 40°C). Overall, the survival/death interfaces are consistent with the observed data. All variable factors mentioned above greatly influenced the pressure-holding time required for *C. sakazakii* inactivation induced by HPP. *C. sakazakii* cells in infant formula showed higher resistance to pressure than those in TSB, demonstrating that the medium type significantly affects bacterial inactivation. The representation of this model prediction (Fig. 1) permits visual determination of a processing time for a required arbitrary log reduction with arbitrary probability. These survival/death interface models enable the identification of minimum processing criteria, along with the probability for achieving a required bacterial log reduction.

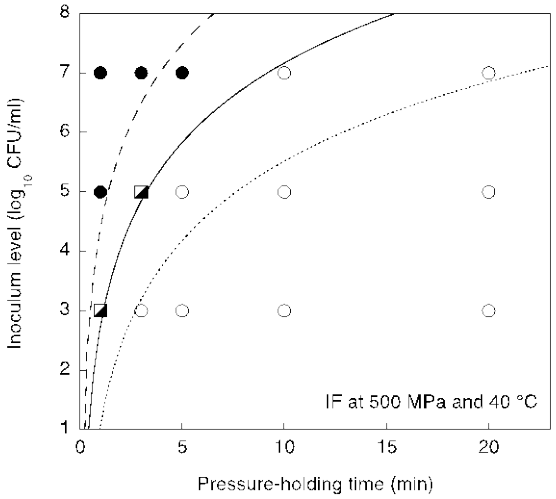

Figure 1: Representation of the survival/death interface with respect to the pressure-holding time at 500 MPa with the inoculum level predicted by model 1 for *C. sakazakii* in infant formula (IF) at 40°C. The black and white circles represent survival and death, respectively, in all three replicate experiments. The black and white squares represent responses that differed among the three replicate trials. The interface with *P* of 0.5 (50% probability of growth) is indicated by the solid lines. The dashed and dotted lines represent predictions at *P* of 0.1 (more conservative) and 0.9 (less conservative), respectively.

Since the developed model expresses the odds ratio of the survival of *C. sakazakii*, the probability of survival can be calculated with respect to the pressure-holding time under different pressure conditions and at different inoculum levels, as shown in Fig. 2. The results show that as the pressure-holding time is increased, the probability of inactivation increases. Figure 2 illustrates the effects of the medium type on the probability of inactivation.

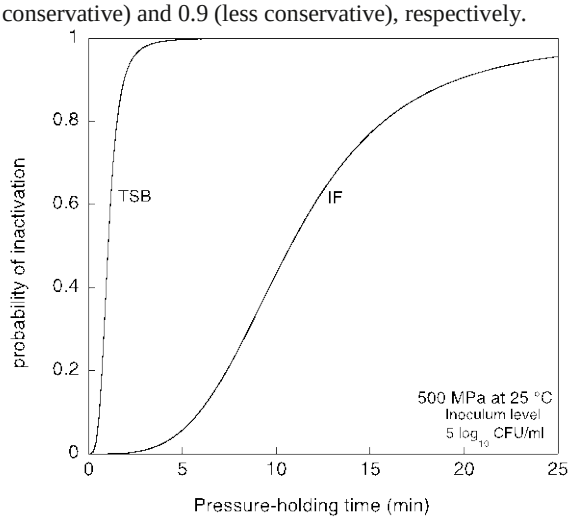

Figure 2: Representation of the changes in the probability of inactivation with respect to the pressure-holding time under different pressure conditions and at different inoculum levels. Effect of the medium type on HPP-induced *C. sakazakii* inactivation with an inoculum level of 5 $\log_{10}$ CFU/ml in TSB and infant formula (IF) treated at 500 MPa and 25°C.

Employment of the new model described in this study would be useful for food processing in terms of microbiological food safety requirements based on the concepts of FSO and PO, since microbial inactivation conditions that cause the required log reduction can be

determined, along with the achievement probability. The new model can also be employed to determine processing criteria that meet FSO or PO requirements.

In conclusion, the survival/death interface model enables the prediction and evaluation of HPP-induced *C. sakazakii* inactivation in reconstituted infant formula with a probability of achieving a required log reduction that takes into account the effect of plural factors. The model will contribute to setting processing criteria corresponding to FSO and/or PO guidelines. Furthermore, the modelling procedure would contribute to progress regarding predictive microbiology as a new and different trend for a microbial inactivation model.

2. Collaboration with ComBase: development of microbial responses viewer (MRV)

Background and objective

Predictive microbiology is used to ensure microbial food safety by facilitating the selection of appropriate processing and distribution conditions. Several predictive tools have been developed such as the Pathogen Modeling Program (PMP) (Buchanan 1993), Sym'Previus (Leporq *et al.* 2005) and ComBase (Baranyi and Tamplin, 2004) which provide microbial growth and/or inactivation kinetics. However, in order to establish food processing and distribution guidelines, food processors are required to employ processing conditions that prevent microbial growth. Exploring targeted bacterial growth or no growth conditions has been recognized as an important component in ensuring food safety (McMeekin *et al.* 2000, 2002).

We developed a web-based new database, MRV (Microbial Responses Viewer: http://mrv.nfri.affrc.go.jp) (Koseki 2009), consisting of bacterial growth/no growth data classified from ComBase using specific criteria. MRV can retrieve bacterial growth/no growth data defined under specified environmental conditions of temperature, pH, and a_w. In addition, MRV simultaneously retrieves growth rate data produced under specified environmental conditions. In the present initiative it was important to recognize data visually and intuitively, and the growth/no growth and growth rate data were therefore combined to make it easy to retrieve the required information. This innovative database facilitates the retrieval of growth/no growth data for various kinds of bacteria and will contribute to ensuring microbiological food safety.

Highlights of the study

We developed a new database, MRV, which enables the collection and retrieval of growth/no growth data for 17 kinds of microorganisms. The data in MRV were calculated on the basis of temperature, pH, and a_w data extracted from ComBase. In addition to growth/no growth data, MRV simultaneously provides information on specific growth rate (μ_{max}). The interface of the developed database is designed to easily and visually find the required data. Accordingly, we have developed a revolutionary predictive tool for determining bacterial growth/no growth under specified conditions.

The retrieval interface was designed to visually understand the effect of environmental conditions (Fig. 3). Users can easily find the environmental combination (temperature, pH, and a_w) that support bacterial growth or not. The change in specific growth rate (μ_{max}) is illustrated as a growth curves that follows the μ_{max} changes in real time. Furthermore, users can access the detail of the original data by clicking each data point. The growth/no growth data extracted from ComBase are derived from a large amount of bacterial growth/death kinetics data. The development of a database with the extracted data from ComBase allows us to retrieve comprehensively various bacterial growth/no growth data. MRV provides μ_{max} data that are modelled on ComBase data. MRV enables the retrieval of growth/no growth boundary conditions and μ_{max}, playing an important role in determining various food processing and distribution conditions.

Although the growth/no growth data in the present development were extracted from ComBase, modelling the growth/no growth interface has not been implemented. Since many

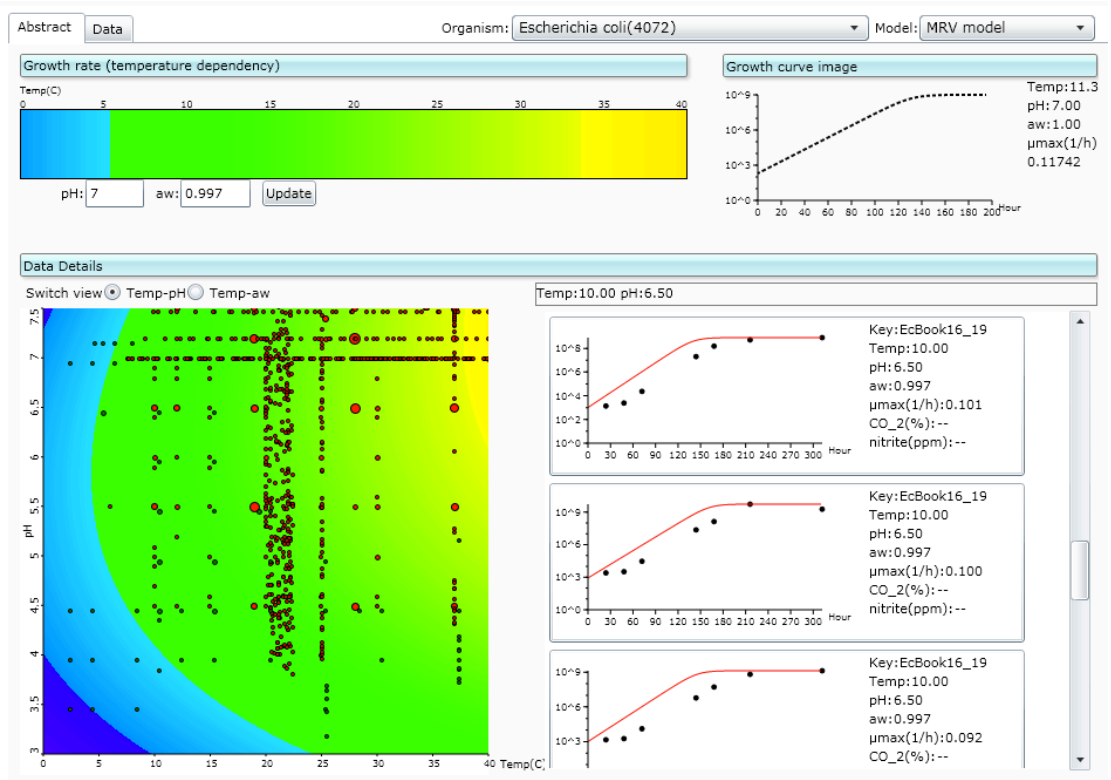

Figure 3: An example of retrieval of *E. coli* in broth conditions by MRV. Movement of mouse pointer on the contour graph of μ_{max} (blue: slow growth, yellow: fast growth) makes it possible to draw growth curve in real time. The detail of the data can be seen by clicking on each point on the graph (red and green means growth and no growth, respectively). The size of the point on the graph reflects the number of records. The larger the size of point, the more number of records indicate.

modelling procedures for the growth/no growth interface have been reported, the data in the present study facilitate the examination of various modelling approaches by the user. While the ComBase platform consists of microbial response kinetic data, MRV could be a platform focused on growth/no growth data that are expected to accumulate as the field evolves. Nevertheless, MRV data need to be updated on a continuous basis, incorporating data from both the published literature and future studies. In addition, modelling the growth/no growth interface would enhance the usability of MRV. Since ComBase contains an ample amount of microbial inactivation data, it would also be possible to develop a database of survival data in an effort to estimate inactivation effects. The development of MRV is expected to continue in the future.

References

Baranyi J. and Tamplin M.L. (2004) ComBase: a common database on microbial responses to food environments. *Journal of Food Protection* 67, 1967–1971.

Buchanan R.L. (1993) Developing and distributing user-friendly application software. *Journal of Industrial Microbiology* 12, 251–255.

Koseki S., and K. Yamamoto (2007) Modelling the bacterial survival/death interface induced by high pressure processing. *International Journal of Food Microbiology* 116, 136–143.

Koseki S. (2009) Microbial Responses Viewer (MRV): A new ComBase-derived database of microbial responses to food environments. *International Journal Food Microbiology* 134, 75-82.

Leporq B., Membre J.M., Dervin C., Buche P. and Guyonnet J.P. (2005). The “Sym'Previus” software, a tool to support decisions to the foodstuff safety. *International Journal of Food Microbiology* 100, 231–237.

McMeekin T.A., Presser K., Ratkowsky D., Ross T., Salter M. and Tienungoon S. (2000) Quantifying the hurdle concept by modelling the bacterial growth/no growth interface. *International Journal of Food Microbiology* 55, 93–98.

McMeekin T.A., Olley J., Ratkowsky D.A. and Ross T. (2002) Predictive microbiology: towards the interface and beyond. *International Journal of Food Microbiology* 73, 395–407.

A mathematical model for predicting growth/no growth of psychrotrophic *C. botulinum* in meat products with five variables

A. Gunvig[1], F. Hansen[1], C. Borggaard[1]

[1] Danish Technological Institute, DMRI, 2 Maglegaardsvej, DK 4000 Roskilde, Denmark (agg@dti.dk)

Abstract

The objective was to develop a mathematical model for predicting growth/no growth of psychrotrophic *C. botulinum* in pasteurised meat products packed in modified atmosphere (30% CO_2 and 70% N_2) for combinations of storage temperature, pH, NaCl, added nitrite and sodium lactate. Data for developing and training the ANN (artificial neural network) were generated in meat products. A total of 257 growth experiments were carried out in three different meat products with different combinations of storage temperature, pH, NaCl, nitrite and sodium lactate. The meat batter was inoculated with 10^4 - 10^6 spores/g using a 4-strain cocktail of gas-producing *C. botulinum*. The meat products were sliced, packed in modified atmosphere (30% CO_2 and 70% N_2) and stored at 4°C, 8°C and 12°C, respectively, for up to 8 weeks. The enumeration of *C. botulinum* was performed when the headspace volume of the package was increased by 10% or more, or at the end of the storage period. Each of the 257 combinations was made in 20 replicates, making it possible to estimate the probability of growth in each combination. These 257 estimates and the matching levels of the hurdles were used to train the ANN with network architecture of 5 input neurons and 3 hidden neurons. The model includes five variables: temperature (4 - 10°C), pH (5.4 - 6.4), NaCl (1.2 - 2.4%), nitrite (0 - 150 ppm) and sodium lactate (0 - 3%). On a separate validation data set (n = 60), a bias of 0.008 was obtained, indicating that the model is slightly fail-safe.

Keywords: *Psychrotrophic C. botulinum, predictive modelling, meat products*

Introduction

In mild pasteurised ready-to-eat (RTE) meat products packed in modified atmosphere (30% CO_2/70% N_2) and stored at temperatures below 10°C, there is a possibility of growth of non-proteolytic *C. botulinum* if the shelf-life is longer than 10 days. Non-proteolytic *C. botulinum* is a anaerobic and spore-forming bacterium that is capable of forming a neurotoxin even at temperatures down to 3.3°C. Thus, it is necessary to ensure that growth is prevented in RTE meat products during storage at temperatures below 10°C. EFSA (EFSA, 2005) and FSA (2008) recommend that RTE meat products with a shelf-life of more than 10 days are to be stored below 8°C, heat-treated at 90°C for 10 minutes, have pH < 5.0, minimum 3.5% WPS (water phase NaCl) or have a water activity < 0.97. Alternatively, a combination of heat-treatment and preservation preventing growth of non-proteolytic *C. botulinum* can be used. To ensure that the later alternative actually prevents growth of *C. botulinum*, documentation is needed i.e. by developing a mathematical model with relevant variables, as suggested by Peck (2006). A predictive model including relevant variables ensures that excessive processing and preservation are avoided and that the RTE meat product remains safe. The predictive model for growth of non-proteolytic *C. botulinum*, "Combase Predictor", only includes temperature, pH and WPS. In this study, the objective was to develop a mathematical model that predicts growth/no-growth of *C. botulinum* in relation to temperature, WPS, pH, added nitrite and sodium lactate.

Materials and Methods

Data: Data for developing and training the artificial neural network (ANN) were generated in meat products. A total of 257 growth experiments were carried out in three different meat products with different combinations of storage temperature, pH, WPS, nitrite and sodium lactate. The meat batter was inoculated with 10^4 - 10^6 spores/g using a 4-strain cocktail of gas-

producing *C. botulinum.* After heat treatment the meat products were sliced, packed in modified atmosphere (30% CO_2 and 70% N_2) and stored at 4°C, 8°C and 12°C, respectively, for up to 8 weeks, each combination having 20 replicates. The enumeration of *C. botulinum* was performed when the headspace volume of the package had increased by more than 10% or at the end of the storage period.

Model: Each of the 257 combinations was made in 20 replicates, making it possible to estimate a rough "probability of growth" in each combination. The estimated probabilities (numbers between 0 and 1) were logit-transformed (Berkson, 1944) in an attempt to linearise the regression task prior to training the neural network.

$$\rho = logit(P) = \log\left(\frac{P}{1-P}\right) \quad (1)$$

Prior to training, each input variable and the measured values for ρ are maximum/minimum scaled:

$$X \rightarrow (X - X_{min})/(X_{max} - X_{min}) \quad (2)$$

Equation 2 changes the scale of any input variable X to be between zero and one. An ANN based model was chosen as we have previously been successful in applying this type of model to the problem of modelling bacterial growth (Mejlholm et al. 2010). As a benchmark for its performance, the ANN was compared to standard chemometrics PCA/PLS-regression with non-linear interactions. The ANN proved to perform significantly better than the PCA/PLS based model.

The 257 "probability of growth" values and the matching input variables were used to train the ANN with network architecture of 5 input neurons, 3 hidden neurons (with sigmoidal response functions) and a single output neuron. An artificial neural network with 5 hidden neurons actually performed better on both calibration and monitoring data sets (Borggaard & Thodberg 1992). However, the smaller network with fewer resources was selected so that outputs are a monotonically decreasing function of the concentration of additives.
The weight parameters of the neural network were found by training the network using the back propagation of error algorithm.

Validation: In order to validate the model, data from 60 other experiments in meat products with different levels of WPS (1.9 – 4.2%), pH (5.8 – 6.4), nitrite (0, 60 or 150 ppm) and sodium lactate (0.0 - 3.0%), packed in 30% CO_2/70% N_2 or 20% CO_2/80% N_2 and stored mainly at 5, 8 and 10°C were used.

Before validation, the predicted probabilities of growth are compared to a set of thresholds set in such a way that the model displays a bias equal to zero for the calibration set. When considering the probability for growth in actual products, it should be kept in mind that the initial inoculum in the dataset is many orders of magnitude higher than any contamination that could be reasonably expected to occur in a true situation.

Table 1: Thresholds for the predicted probabilities of growth.

Estimated probability	Assignment	Meaning
$P < 0.0045$	0	Safe
$0.0045 \leq P \leq 0.018$	0.5	Uncertain
$P > 0.018$	1	Dangerous

It is the assigned values that are used for validating the model, as the validation set only contains the outcomes 0 (safe) or 1 (dangerous).

The bias of the model is defined as:

$$Bias = \sum_{i=1}^{n}(p_i^{pred} - P_i^{ref})/n \quad (5)$$

Here, p^{ref} and p^{pred} are the assigned values for the measured and predicted probabilities, respectively.

Results and Discussion

User-interface: A web based implementation makes the model accessible for QA workers in the Danish meat industry. The user enters the values of the input variables. The intervals for the five variables are:

temperature 4 - 10°C, added NaCl in the recipe 1.2% - 2.4%, pH 5.4 - 6.4, added sodium nitrite 0 - 150 ppm, added sodium lactate 0 - 3%, water content in the final product 53% - 78%.

The maximum temperature is limited to 10°C to avoid interference from mesophilic *C. botulinum* which is capable of growth above 10°C but markedly more resistant to NaCl and low pH. The "added NaCl in the recipe" and "added sodium lactate" are converted into the actual concentrations in the water phase before being entered into the neural network. Also, the "lactate in water" is further adjusted by adding the natural content of L-lactate present in meat. The model uses two pre-set values for L-lactate in meat: either 0.7% for recipes containing a large amount of meat (select "whole muscle product") or 0.35% for recipes containing a small amount of meat (select "emulsified product").

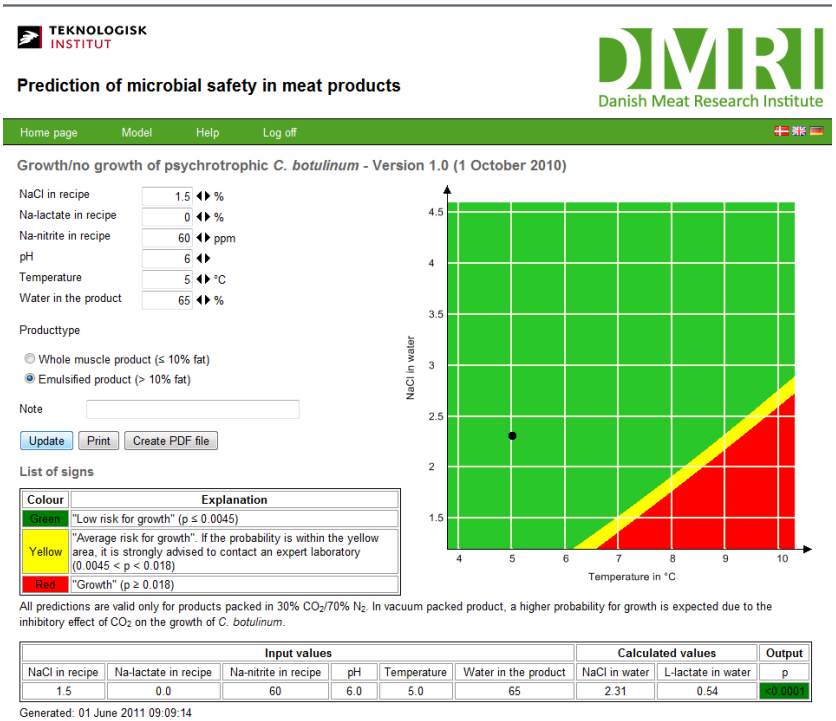

Figure 1: Contour plot of the user interface

The estimated "probability of growth" is presented in a contour plot (see Figure 1) over an area spanning the allowed values for temperature and WPS. The depicted area is divided into 3 regions, indicating different "probabilities of growth" (green area: P < 0.0045 = safe, yellow

area: 0.0045 ≤ P ≤ 0.018 = uncertain, red area: P > 0.018 = dangerous). A black dot in the contour plot represents the product being considered with a given combination of the input values. The calculated values of WPS, "lactate in water" and the predicted "probability of growth" are shown in a separate table on the web page.

Validation: The performance of the model was validated by comparing predicted and observed "probabilities of growth" from a separate validation data set (n=60), obtaining a bias of 0.008, indicating that the model is slightly fail-safe.
Out of the 60 observations, model and observations were in agreement in 52 cases.
The 8 remaining observations were distributed with 5 "uncertain" predictions and 3 failed predictions as shown in Table 2.

Table 2: 8 validation cases of disagreement between predicted and observed growth.

Observed	No growth (fail-safe)		Growth (fail-dangerous)	
Predicted	Growth	Uncertain	Uncertain	No growth
Number	2	2	3	1

The fail-dangerous prediction of "no growth" occurred in a product containing 2% WPS, 0 ppm nitrite, 3.6% "lactate in water" and pH 6.3 and stored at 8°C packed in 30% CO_2/70% N_2. The actual growth experiment showed weak growth indicated by gas formation, but no significant increase in *C. botulinum* count was found.
The two fail-safe predictions of "growth" occurred in products stored at 10°C, product 1 containing 2.14% WPS, 0 ppm nitrite, 3% "lactate in water" and pH 6.3 and product 2 containing 2.19% WPS, 60 ppm nitrite, 0.7% "lactate in water" and pH 6.4. In both experiments, no growth was detected after 8 weeks storage.

Conclusion

A model for predicting growth/no growth of psychrotrophic *C. botulinum* was developed based on an artificial neural network. The predictive model includes five variables: temperature (4 - 10°C), pH (5.4 - 6.4), added NaCl (1.2% - 2.4%), added nitrite (0 - 150 ppm) and added sodium lactate (0 - 3%). The model has a bias of 0.008, corresponding to the model being slightly fail-safe.

Acknowledgements

The project was funded by the Danish Directorate for Food, Fisheries and Agri Business (J. no. 3414-07-01993) and the Danish Pig Levy Fund.

References

Berkson J. (1944). Application of the Logistic Function to Bio-Assay. *Journal of the American Statistical Association*. Vol 39, No 227, September 1944.

Borggaard C., Thodberg H.H.. (1992) *Anal. Chem*., 1992, 64 (5), pp545-551.

Combase Predictor http://modelling.combase.cc/ComBase_Predictor.aspx (accessed 5 April 2011)

Food Standard Agency (2008). Food Standard Agency guidance on the safety and shelf-life of vacuum and modified atmosphere packed chilled foods with respect to non-proteolytic *Clostridium botulinum* http://www.food.gov.uk/multimedia/pdfs/publication/vacpacguide.pdf (accessed 5 April, 2011).

Mejlholm, O; Gunvig, A; Borggaard, C.; Blom-Hanssen, J.; Mellefort, L., Ross, T., Leroi, F.; Else, T.; Visser, D.; Dalgaard, P. (2010). Predicting growth rates and growth boundary of L. monocytogenes – An international validation study with focus on processed and rady-to-eat meat and seafood. *International Journal of Food Microbiology*, Vol 141, Issue. 3, p. 137-150..

Peck, M.W.(2006) *Clostridium botulinum* and the safety of minimally heated chilled foods. *Journal of Applied Microbiology* 101, 556-570

The EFSA Journal (2005). Opinion of the Scientific Panel on biological Hazards on a request from the commission related to *Clostridium* spp in foodstuffs, 199, 1-65

Growth/no-growth models for heat-treated spores of psychrotrophic *Bacillus cereus* strains.

J. Daelman[1], L. Jacxsens[1], A. Vermeulen[1], T. Willemyns[1], F. Devlieghere[1]

[1] Laboratory of Food Microbiology and Food Preservation, Department of Food Safety and Food Quality, Ghent University, Coupure Links 653, 9000 Ghent, Belgium. (jeff.daelman@ugent.be)

Abstract

Refrigerated processed foods of extended durability (REPFED) are a growing group of products. This research aims to minimize the heat treatment, to provide higher quality products, without compromising food safety. One of the microbial risks in REPFEDs are psychrotrophic *Bacillus cereus* strains due to their high thermal resistance and ability to grow under cold storage. Twenty-five psychrotrophic *B. cereus* strains, isolated from different REPFEDs were screened for their time to detection (TTD) under cold storage at three temperatures (8, 9, 10°C). The TTD was determined for vegetative cells, spores and heat-treated spores of these strains using Optical Density (OD) measurements. Results show a great inter- and intra-strain variability in TTD. At 8°C only 40.7% of the strains were able to grow, compared to 77.8% at 9 and 10°C. Based on these data two strains, exhibiting spore-growth at 8°C after heat treatment, were selected: a very heat resistant strain ($D_{90°C}$=90min) and a more heat sensitive strains ($D_{90°C}$=17min). For each strain a full factorial growth/no-growth model was created with 3 parameters (pH: 5.2–6,4; a_w: 0.97–0.99; P_{90}: 0–10 min). Results show that the presence of a heat treatment and the pH are the main factors preventing the growth of *B. cereus* under cold storage. The minimal pH for growth increases as the heat treatment increases.

Keywords: Bacillus cereus, growth/no growth, heat treatment, pasteurization, REPFED

Introduction (scope and objectives)

Refrigerated processed foods of extended durability (REPFED) are a growing group of products. Their food safety is assured using a combination of mild heat treatment (pasteurization) and cold storage. Because the pasteurization treatments affect the structure and the nutritional value of a food product, this research aims to minimize the heat treatment without compromising food safety. One of the main microbial risks in REPFEDs are psychrotrophic *Bacillus cereus* strains due to their high thermal resistance and ability for growth under cold storage. Most models that are currently available do not take the heat treatment prior to storage into account. The presented models assess the ability of *B. cereus* to grow under cold storage after heat treatment and provide information about the effect of product composition (a_w, pH) and pasteurization-value on this ability.

Materials and Methods

Screening of psychrotrophic capacity of vegetative cells, spores and heat-treated spores

Twenty-seven psychrotrophic *B. cereus* strains isolated from various REPFEDs or ingredients thereof were screened for their ability to grow under cold storage. This ability was tested for three physical states: vegetative cells (VC), spores (S) and heat-treated spores (HS). Six replicates for each strain and state were tested at three temperatures (8, 9 and 10°C). These temperatures were selected because previous testing of vegetative cells had shown that all isolates were able to grow at 8°C but not at 7°C. Growth was monitored using optical density (OD) measurement in 96-well polystyrene microplates (Eppendorf, Hamburg, DE). Time To Detection (TTD) was used as an approximation of the lag phase and determined as the moment when the OD exceeded the detection limit (average OD of six replicates at inoculation + three times the standard deviation at inoculation). Spores were harvested using

a method similar to that of Coroller *et al.* (2001). Strains were inoculated on sNA plates (i.e. Nutrient agar with $MnSO_4$ (40 mg l^{-1}) and $CaCl_2$ (100 mg l^{-1})) and incubated for five to seven days at 30°C. Spores were collected by suspending agar in a NaCl solution (8.5 g l^{-1}) and scraping the surface. The resulting spore solution was washed three times by centrifugation (10,000g for 15 minutes at 4°C, Sigma Laboratory centrifuges 4K15) and resuspension in 10mL NaCl solution. After the third washing, the pellet was resuspended in 10 mL of ethanol (50% (v/v)) and stored for one hour at 2°C to eliminate vegetative cells. Finally the suspension was washed three times by centrifugation and resuspended each time in sterile distilled water. Spore solutions were stored at 2°C for no more than 4 weeks.

Vegetative cells and spores were inoculated at $10^{4\text{-}5}$ CFU ml^{-1} in 200µL of Trypton Soy Broth (Oxoid, Basingstoke, UK), and the plates were sealed with a lid and parafilm. For heat-treated spores the decrease in concentration during heat treatment was determined in triplicate as 10^{X} CFU ml^{-1}. These plates were inoculated at $10^{4\text{-}5}$+10^{X} CFU ml^{-1}. This higher inoculum concentration was necessary because TTD depends on the inoculum concentration. Plates were sealed with a gastight transparent film (Viewseal nonpiercable, Greiner Bio-one, Frickenhausen, DE) to prevent evaporation during heat treatment and subsequently heated and cooled to obtain a P_{90} (pasteurization value at 90°C (Gaze 2006)) of 10 minutes using a Thermostat Plus with adaptor for microplates (Eppendorf). After heating the film was replaced by a lid and parafilm. Plates were stored at the desired temperature and the OD was measured every three days.

Growth/no-growth models for psychrotrophic heat-treated B. cereus spores.

Based on the screening, two *B. cereus* strains, able to grow at low temperatures after heat treatment were selected: FF140 ($D_{90°C}$: 90.9 min) isolated from béchamel sauce and FF355 ($D_{90°C}$: 17.9 min) isolated from carrots. For both strains a full-factorial growth/no-growth (G/NG) model was developed with 3 variables: water activity (0.973-0.980-0.987-0.995), pH (5.2-5.6-6.0-6.4) and P_{90}-value (0-4-7-10). This resulted in 64 combinations of a_w, pH and P_{90} per model. Each combination was tested eight-fold using the same methodology as the screening. Spores were inoculated at $10^{4\text{-}5}$+10^{X} CFU ml^{-1} (X depended on strain and the heat treatment) to reach a *B. cereus* concentration after heating of $10^{4\text{-}5}$ CFU ml^{-1}. After inoculation the procedure was identical to that of the screening: the microplates were heated, cooled and stored at 10°C. Data was processed using excel (excel 2007, Microsoft, Redmond WA, USA) and the logistic regression was performed in SPSS 17.0 (SPSS Inc., Chicago IL, USA). Graphic representations of the model were created using Matlab 7.11 (Mathworks, Natick MA, USA). All data sets were modeled using a type-I logistic regression model (Ross and Dalgaard 2004):

$$logit(p) = \ln\left(\frac{p}{1-p}\right)$$

$$logit(p) = b_0 + b_1 \cdot a_w + b_2 \cdot pH + b_3 \cdot P_{90} + b_4 \cdot a_w^2 + b_5 \cdot pH^2 + b_6 \cdot P_{90}^2 + b_7 \cdot a_w \cdot pH + b_8 \cdot a_w \cdot P_{90} + b_9 \cdot P_{90} \cdot pH$$

Results and Discussion

Screening of psychrotrophic capacity of vegetative cells, spores and heat-treated spores

The time to detection (TTD) data were gathered for 27 strains, at different temperatures and for different physiological states. The data, given in table 1, show a considerable effect of the heat treatment on the ability to grow at the lowest temperature (8°C) but not at the two other temperatures (9 and 10°C). Only 40.7% of the strains (11 of 27) were able to grow at 8°C after heat treatment. For higher temperatures or for not heat-treated spores or cells, the percentage of strains able to grow varied between 74.1 (20 of 27) and 92.6% (25/27). This result illustrates that the psychrotrophic characteristics of *B. cereus* may disappear during heat

treatment. Because the TTD was very variable between the six replicates no clear effect of physiological state, temperature or heat treatment of the TTD could be established.

Table 1: Number of *B. cereus* strains able to grow at specified temperatures. 27 strains were tested (V: Vegetative cells; S: Spores; HS: Heat-treated spores)

Storage Temperature	8°C			9°C			10°C		
Physiological state	V	S	HS	V	S	HS	V	S	HS
Number of strains able to grow	20	21	11	20	22	21	21	25	21

Growth/no-growth models for psychrotrophic heat-treated B. cereus spores

The developed growth/no-growth models for FF140 and FF355 after twelve days at 10°C had a high predictive power (98,8% and 95,1%), indicating a good fit of the data. Although the D-value of strain FF140 is more than five times larger than the D-value of strain FF355, the results after twelve days are similar. None of the strains were able to grow at a water activity of 0.973 or at a pH of 5.2 and at the highest water activities (0.987 and 0.995) and high pH (6.4) both strains were able to grow, even after the highest heat-treatment (P_{90}=10).

The main difference between both models is the size of the growth-zone. The growth zone for the more heat-resistant strain FF140 is larger than that of the more heat-sensitive strain FF355. This difference is most clear at the higher water activities. At a water activity of 0.987, nine of the sixteen tested conditions (56.3%) showed growth in all replicates for strain FF140, while this was only four of sixteen conditions (25%) for strain FF355. The width of the growth boundary, between 10% and 90% chance of growth, increased as water activity decreased, and was wider for FF355 than for FF140 at the same water activity

The models for both strains share two important features. Firstly, after 10 days the presence of a heat treatment has a greater effect than the actual duration of the heat treatment. This effect is shown for strain FF140 in figure 1, the growth zone observed for P_{90}-values of 4, 7 and 10 minutes are similar in size and smaller than the growth zone for a P_{90}-value of 0 (no heat treatment).

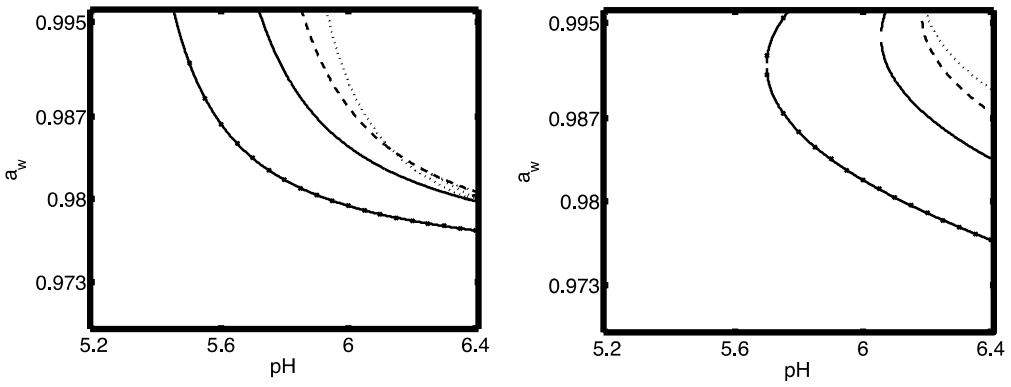

(a) (b)

Figure 1: growth/no-growth border for *B. cereus* FF 140 (a) and FF 355 (b) after 12 days at 10°C. Conditions allowing growth are situated to the right of the curves. Model predictions for p = 0.9: no heat treatment (–•–•); P_{90} = 4 min (—); P_{90} = 7 min (---); P_{90} = 10 min (...).

Secondly, the effect of pH increases with the intensity of the heat treatment. This effect is illustrated for strain FF140 in figure 2 (a and b). At a pH of 6.0 and a water activity of 0.987, growth of this strain is possible after all heat treatments. At the same water activity and a pH

of 5.6, growth was only possible without heat treatment. This pH-effect became more pronounced over time, after 21 days the growth border at pH 6.0 shifter further down (figure 2 b), while the growth boundary at pH 5.6 shifted very little.

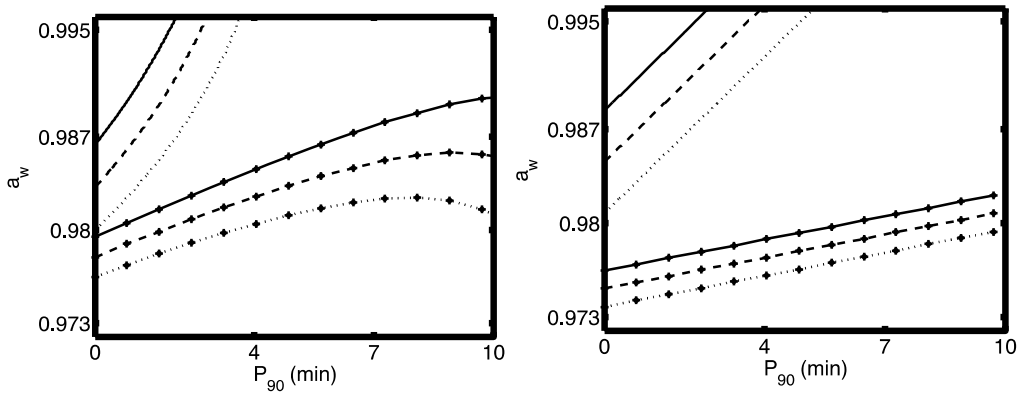

Figure 2: Growth/no-growth boundaries for *B. cereus* strains FF140 after (a) 12 days and (b) 21 days at 10°C. The growth zone is situated to the left of the curves. Model predictions: p = 0.9 (—), p = 0.5 (--), p=0.1 (…). Curves with markers represent pH 6; curves without markers represent pH 5.6.

Conclusions

This research shows that a heat treatment can alter the psychrotrophic characteristics of a *B. cereus* strains and that cold storage is be crucial to prevent outgrowth of *B. cereus* after pasteurization. The developed growth/no-growth models show that the length of the heat treatment has less effect than the presence of a heat treatment, and that a limited decrease in pH (0.4) greatly reduces the pasteurization value required (6 min) to prevent growth of *B. cereus.* In future models heat treatment should be taken into account as a variable that determines the growth of *B. cereus.*

Acknowledgements

This study was funded by the Federal Public Service of Health, Food Chain Safety and Environment (Contract RT 09/01 MICRORISK).

References

Coroller L., Leguerinel I. and Mafart P. (2001) Effect of water activities of heating and recovery media on apparent heat resistance of Bacillus cereus spores. *Applied and Environmental Microbiology* 67(1), 317-322.

Gaze J. E. (2006) *Pasteurisation: A Food Industry Practical Guide (Second Edition)*, Guideline No. 51. Chipping Camden: Campden & Chorleywoord Food Research Association.

Ross T., and Dalgaard P. (2004) Secondary models. In R. C. McKellar & X. Lu (Eds.), *Modeling microbial responses in food*. Boca Raton: CRC Press.

Modelling the high pressure inactivation of *Listeria monocytogenes* on cooked ham

A. Hereu[1], P. Dalgaard[2], M. Garriga[1], T. Aymerich[1], S. Bover-Cid[1]

[1]IRTA, Food Safety Programme, Finca Camps i Armet s/n, E-17121, Spain. (anna.hereu@irta.cat)
[2]Technical University of Denmark (DTU), National Food Institute, Soltofts Plads, Bygning 221, DK-2800, Kgs. Lyngby, Denmark. (pada@food.dtu.dk)

Abstract

High hydrostatic pressure (HHP) inactivation curves of *Listeria monocytogenes* CTC1034 inoculated (*ca*. 10^7 CFU/g) on sliced cooked ham were obtained at seven pressure levels (300, 373.2, 450, 550, 600, 726.8 and 800 MPa) for several treatment times (from 0.1 up to 900 s). Bacterial inactivation was assessed as the difference between *L. monocytogenes* counts after the treatments and the initial inoculum. Different modelling approaches were applied and the outputs compared: (i) a classical two-steps predictive microbiology approach with primary (log-linear with tail) and secondary (polynomial for both k_{max} and N_{res}) models. In addition, one-step global modelling was assessed with (ii) combined primary and secondary models and (iii) a polynomial model resulting from multivariate linear regression to all results obtained for each single pressure and time combination. According to the results, HHP-inactivation of *L. monocytogenes* on sliced cooked ham did not follow a log-linear kinetics and an obvious tailing shape occurred at pressures from 450 MPa. This behaviour was appropriately described using the Log-linear with tail model. The global regression procedure was more appropriate than the classical two-steps approach and also superior to the multivariate linear regression analysis of the entire dataset.

Keywords: *Listeria monocytogenes, high hydrostatic pressure inactivation, cooked ham, modelling*

Introduction

High hydrostatic pressure (HHP) processing can inactivate microorganisms, extend shelf-life and improve microbiological safety of food, while undesired changes in nutritional and sensory properties are limited. HHP processing can be applied to packaged food products, which is important to eliminate post-process contamination and interesting (e.g. as a listericidal) treatment for ready-to-eat foods, such as sliced cooked ham (FSIS 2006). HHP processed foods are commercially available, but further research is still required to identify optimal conditions for microbial inactivation (Rendueles *et al*. 2011). Importantly, the bactericidal effect of HHP largely depends on the physico-chemical characteristics of foods and a product-oriented approach seems most relevant to study microbial inactivation kinetics (Rendueles *et al*. 2011; Bover-Cid *et al*. in press). The aim of the present study was to quantify and model the effect of HHP on inactivation kinetics of *L. monocytogenes* inoculated on sliced cooked ham. Inactivation kinetics was quantified at pressures from 300 to 800 MPa and modeled by a classical two-steps predictive microbiology approach with primary and secondary models (approach i). In addition, one-step global modelling was evaluated with combined primary and secondary models (approach ii) and a multivariate linear regression model (approach iii).

Materials and Methods

Preparation and HHP processing of inoculated cooked ham samples

A frozen (-80 ºC) stock culture of *L. monocytogenes* CTC1034, previously grown at 37 ºC in Brain Heart Infusion (BHI) broth with 2.5% NaCl was used to inoculate (*ca*. 10^7 CFU/g) 25 g slices of cooked ham. The product had pH 6.09 and a_w of 0.983, 2.75% NaCl, 6400 mg/kg lactic acid, < 5 mg/kg sodium nitrite, 18.32% of protein and 4.55% lipid content. Inoculated

slices were vacuum-packed and HHP treated at 300, 373, 450, 550, 600, 726.8 and 800 MPa at different time intervals ranging from 0.1 to 900 seconds. HHP treatments were carried out at an initial fluid temperature of 15 ºC. A commercial (Wave6000, NC Hyperbaric, Burgos, Spain) and a pilot (Thiot ingenierie - NC Hyperbaric, Bretenoux, France) HHP units were used for pressure treatments up to and above 600 MPa, respectively. The average pressure come-up rate was 220 MPa/min whereas the pressure release was almost instant. For each pressure level, 12-36 samples were analysed at 6-12 time points, resulting in a total of 231 data points for the seven HHP treatments.

Microbiological analysis

Inoculated and HHP treated 25 g-samples were homogenised and 10-fold serially diluted in physiological saline (0.85% NaCl and 0.1% Bacto Peptone). *L. monocytogenes* was enumerated on Chromogenic Listeria Agar (CLA, 37ºC for 48 h). To achieve a quantification limit of 4 CFU/g, 2.5 ml of the 1/10 diluted homogenate was spread on CLA plates with a diameter of 14 cm. For samples with expected concentration of *L. monocytogenes* below this quantification limit, the presence/absence of the pathogen was investigated by enrichment of the 25 g-sample in 225 ml tryptic soy broth with 0.6% yeast extract (TSBYE) (37 ºC, 48 h). After enrichment *L. monocytogenes* was detected on CLA and colonies were confirmed by PCR (Aymerich *et al*. 2005). For modeling purposes, positive results below the quantification limit were recorded as 0 Log CFU/g while absence in 25g was computed as -1.4 Log CFU/g.

Primary modelling

Inactivation data (Log CFU/g *vs.* time) for each pressure level were fitted using the Log-linear, the Log-linear with tail, the biphasic and the Weibull models (Geeraerd *et al*. 2005). Curve fitting was carried out with the Solver Add-in of MS Excel and evaluated visually. The root mean squared error (RMSE) was calculated as a measure for goodness-of-fit. Fitted models were compared pair-wise through an F-test.

Secondary modelling

The effect of pressure (MPa) on the key kinetic parameters (k_{max} and N_{res}) of the selected primary inactivation model (i.e. Log-linear with tail) was described by simple secondary models, fitted using the MS Excel Solver Add-in.

One-step global modelling

The selected primary and secondary kinetic models were combined and fitted to the entire set of 231 data points in a one-step global regression procedure (Martino and Marks 2007). To eliminate small differences in initial inoculation concentrations between experiments, data for the global modelling were expressed as Log (N_t/N_0) with N_0 being the initial inoculum of *L. monocytogenes* and N_t the pathogen concentration after the HHP treatment. A second degree polynomial model was also obtained by multivariate linear regression (with Statistica v8; StatSoft) to describe the effect of time and pressure on *L. monocytogenes* inactivation.

Evaluation and product validation of the developed models

For each modeling approach, the residual sum of squares (RSS) and the RMSE of the fitting were calculated and compared. Observed *vs.* fitted data (in terms of Log N_t/N_0) were also compared graphically for the three approaches followed. In addition, data from the literature, including inactivation of different strains of *L. monocytogenes* in liquid laboratory media and in different foods, were compared with the predictions provided by the one-step global model (approach ii).

Results and Discussion

Inactivation kinetics and primary modelling

The HHP-inactivation kinetics of *L. monocytogenes* inoculated on sliced cooked ham were appropriately described by a Log-linear model with tail (Fig. 1, Eqn. 1). It is worth noting that HHP processing could not totally eliminate *L. monocytogenes*, which was detected even after

15 min at 800 MPa. The Log-linear and the Weibull models did not fitted inactivation curves appropriately, especially at HHP of 600 MPa and above. Moreover, F-tests showed the Log-linear with tail model (Eqn. 1) to be the most appropriate, being superior to the biphasic model with one more parameter ($P < 0.05$). For individual inactivation curves, RMSE values between 0.05 and 0.92 were obtained for Eqn. 1. The corresponding R^2-values were 0.94 and 0.80. Therefore, for estimation of the kinetic parameters k_{max} and N_{res}, Eqn. 1 was used, with a value of Log (N_0) fixed as equal to the average inoculation concentration in an experiment.

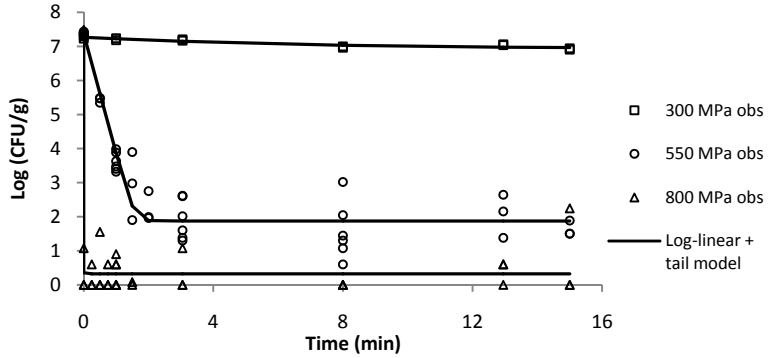

Figure 1: Inactivation of *L. monocytogenes* inoculated on sliced cooked ham during HHP treatments at 300 MPa (open squares), 550 MPa (open circles) and 800 MPa (open triangles). Lines show the fitted Log-linear with tail model (Eqn. 1).

$$Log(N) = Log\left[\left(10^{Log(N_0)} - 10^{Log(Nres)}\right) \cdot e^{-k_{max}t} + 10^{Log(N_{res})}\right] \quad (1)$$

Secondary modelling

For Log-transformed values of k_{max} and N_{res}, secondary models obtained using observed data showed a linear relationship with pressure ([P] in MPa, Eqn. 2 and 3).

$$Log(k_{max}) = -4.3544 + 0.0104 \cdot P \quad (2)$$

$$Log(N_{res}) = 5.4508 - 0.0071 \cdot P \quad (3)$$

One-step global modelling

When Eqn. 1, 2 and 3 where combined into one model with four parameters, the one-step global regression procedure resulted in RSS of 352 and RMSE of 1.246 for the entire set of 231 data. In comparison, the classical two-steps predictive modelling approach had RSS of 450 and RMSE of 1.407. The one-step global regression procedure (approach ii) resulted in a slightly better average datafit as also reported by Martino and Marks (2007) (See Fig. 2).

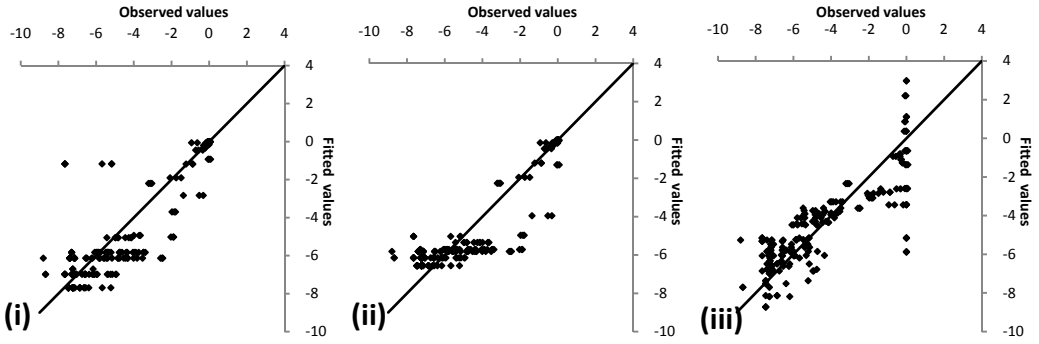

Figure 2: Plots of observed values *versus* fitted values corresponding to the: (i), two-steps procedure; (ii), global regression procedure and (iii), multivariate linear regression.

Multivariate linear regression (iii) resulted in a second-order polynomial model (Eqn. 4, where [P] is the pressure level in MPa and [t] is the treatment time in min). This six-

parameter model had RSS of 572 and RMSE of 1.574 and thus provided a fit inferior to the four parameter kinetic model (approach ii). A polynomial model with four parameters (resulting from a regression with the linear and interactive term but without the squared terms, equation not shown) had an RSS of 718 and RMSE 1.763 and did not seem appropriate.

$$Log(N/N_0) = 12.690 - 3.791 \cdot \frac{P}{100} + 0.184 \cdot \left(\frac{P}{100}\right)^2 - 0.894 \cdot t + 0.037 \cdot t^2 + 0.030 \cdot \frac{P}{100} \cdot \mathrm{t} \quad (4)$$

Validation of the developed model

Figure 3 shows the comparison between the predictions provided by the developed global model (approach ii) and the observed inactivation data from the literature (broth, milk, fruit juices and dry-cured ham) as well as data obtained in experiments with mortadella (unpublished results). The model performed well for mortadella and raw milk. Probably, the product characteristics (e.g low pH for fruit juice, low a_w for dry-cured ham) could be the reason for the discrepancy between predicted and observed HHP inactivation of *L. monocytogenes*.

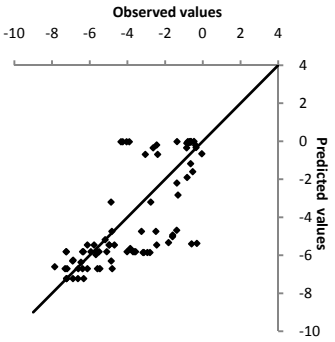

Figure 3: Evaluation of the developed model (one-step regression, approach ii) by comparison of observed data from the literature and the model predictions.

Conclusions

This works shows the Log-linear with tail model as the most appropriate primary model to fit HHP inactivation kinetics of *L. monocytogenes* on cooked ham, and reinforces the idea that the global modelling procedure combining primary and secondary models fits better than the two-steps procedure or multivariate linear regression. Furthermore, the product-oriented approach followed in the present study seemed justified.

Acknowledgements

The work was financially supported by the Spanish *Ministerio de Ciencia e Innovación* (RTA2007-00032 and CSD2007-00016). Anna Hereu thanks the *Instituto Nacional de Investigación y Tecnología Agraria y Alimentaria* (INIA) for the doctoral fellowship.

References

Aymerich M. T., Jofré A., Garriga M. and Hugas M. (2005) Inhibition of *Listeria monocytogenes* and *Salmonella* by natural antimicrobials and high hydrostatic pressure in sliced cooked ham. *Journal of Food Protection* 68 (1), 173-177.

Bover-Cid S., Belletti N., Garriga M. and Aymerich T. (in press) Model for *Listeria monocytogenes* inactivation on dry-cured ham by high hydrostatic pressure processing. *Food Microbiology*. doi:10.1016/j.fm.2010.05.005.

Food Safety and Inspection Service (FSIS) (2006). Compliance guidelines to control Listeria monocytogenes in post-lethality exposed ready-to-eat meat and poultry products. www.fsis.usda.gov/OPPDE/rdad/FRPubs/97-013F/Lm_Rule_Compliance_Guidelines_May_2006.pdf (accessed September 2010).

Geeraerd A. H., Valdramidis V. P., Van Impe J. F. (2005). GInaFiT, a freeware tool to assess non-log-linear microbial survivor curves. *International Journal of Food Microbiology* 102 (1), 95–105.

Martino K. G., Marks B. P. (2007) Comparing uncertainty resulting from two-step and global regression procedures applied to microbial growth models. *Journal of Food Protection* 70 (12), 2811-2818.

Rendueles E., Omer M. K., Alvseike O., Alonso-Calleja C., Capita R., Prieto M. (2011). Microbiological food safety assessment of high hydrostatic pressure Processing: a review. *LWT - Food Science and Technology* 44 (5), 1251-1260.

Variability of single cells of *Listeria monocytogenes* after high hydrostatic pressure treatments

M. Munoz-Cuevas[1], L. Guevara[1], A. Martínez[2], Paula M. Periago[1,3], P.S. Fernandez[1,3]

[1]Dpto. Ing. Alimentos y del Equipamiento Agrícola. Escuela Técnica Superior de Ingeniería Agronómica. Universidad Politécnica de Cartagena. Paseo Alfonso XIII, 48; 30203 Cartagena, Spain
[2]Instituto de Agroquímica y Tecnología de Alimentos, Apartado de Correos, 73, 46100 Burjassot, Valencia, Spain
[3]Instituto de Biotecnología Vegetal. Universidad Politécnica de Cartagena. Cartagena, Spain

Abstract

The use of non-thermal methods of food preservation is due to consumer demand for microbiological safe products, without changes in the sensory and nutritional qualities of the product. High pressure has emerged as an alternative to traditional thermal processing methods for foods. *Listeria monocytogenes* CECT 5672 was treated under high-hydrostatic pressures (HHPs) (350, 400 and 450MPa) for 3, 16 and 23 min. The effects of pH (5, 6 and 7) and sodium chloride concentration (0, 0.5 and 1.0) of the recovery medium were studied on single cells of *Listeria monocytogenes*. The kinetic parameters of the single-cell were estimated by the method described by Metris *et al*. (2006). From results obtained, histograms of the lag phase were generated and distributions were fitted. The duration of the lag phase of HHP damaged cells increased with the application of additional stresses. Histograms showed a shift to longer lag phases and an increase in variability with high stress levels in the recovery medium. Using a primary model together with Monte Carlo simulation, predictions of time to growth (100 cfu/g) of *L. monocytogenes* were established and they were compared with deterministic predictions. It was evident that deterministic predictions do not give a good indication of the probability of a certain level of growth.

Keywords: *Listeria*, high hydrostatic pressure, frequency distribution, Monte Carlo simulation

Introduction

Consumers have increased their demand for high-quality foods that are convenient and nutritious, that have fresh flavor, texture, and color and minimal or no chemical preservatives, and above all, that are safe. Although conventional thermal processing ensures food safety and extends the shelf life, it often leads to detrimental changes in the sensory and nutritional qualities of the product. With nonthermal processing technologies, more fresh-like products can be obtained. High hydrostatic pressure is considered to be a promising alternative to thermal pasteurization for fruit juices and other products when this process is used alone or in combination with traditional techniques.

The major benefit of pressure is its immediate and uniform effect throughout different media, avoiding difficulties such as nonstationary conditions typical for convection and conduction processes. HHP is an attractive nonthermal process because the pressure treatments required to inactivate bacterial cells, yeasts, and molds have a minimal effect on the sensory qualities associated with fresh-like attributes such as texture, color, and flavor. HHP involves the use of pressures of approximately 300 to 700 MPa for periods of approximately 30 s to a few minutes to destroy pathogenic bacteria such as *Listeria, Salmonella, Escherichia coli*, and *Vibrio* and other bacteria, yeasts, and molds that cause foods to spoil.

Monte Carlo analysis is a general method to deal with stochastic models. Monte Carlo simulation has been proposed as a tool to establish the probability of growth or inactivation of microorganisms under certain conditions (Ferrer *et al*. 2007; Poschet *et al*. 2003).

The aim of this study was to compare the effect of environmental conditions in the recovery medium on individual cells of *Listeria monocytogenes* previously treated under high hydrostatic pressure. Combinations of pH and NaCl in the recovery medium were used in our experiment and the variability of kinetic parameters were contrasted using frequency

distribution. The time to achieve a certain level of growth of *L. monocytogenes* was established using a Monte Carlo simulation.

Materials and Methods

Preparation of cell suspensions for pressurization

The strain used in the experiments was *Listeria monocytogenes* CECT 5672 (from Spanish Type Culture Collection, CECT, Valencia, Spain). *Listeria monocytogenes* was stored on tryptic soy agar (TSA) slopes at 6 ºC and subcultures were grown in tryptic soy broth with addition of 0.6 % yeast extract (TSYB).
Overnight cultures of *L. monocytogenes* were centrifuged at 3,000 x g for 15 min at 5 ºC and the pellets were resuspended in 100 mL of TSYB. Eppendorf tubes were filled with 1.5 mL of the cell suspensions (approximately 10^9 cfu/mL) and were placed in polyethylene bags.

High hydrostatic pressure treament

For each time and pressure condition, three of the Eppendorf vials were placed in polyethylene bags. The bags were filled with water and heat-sealed (MULTIVAC Thermosealer) before being placed in the high hydrostatic pressure unit (High Pressure Food Processor; EPSI, Belgium). The pressurization liquid was a mixture of water and glycol. The pressure level, pressurization time, and temperature were controlled automatically. The pressure increase rate was 300 MPa/min and the depressurization time was less than 1 min. The treatment time described in this study does not include come-up and comedown times. The cells were pressurized at 350, 400, and 450 MPa for specific times of 3, 16 and 23 min at a maximum temperature of 30 °C (initial temperature 25 °C). Immediately after pressurization the samples were transferred to an ice-water bath and used for enumeration of colony-forming units. The unpressurized cell suspension was enumerated as a control.

Recovery, growth curves and determination of the lag phase

Recovery of pressurized cells was carried out in TSYB at three different NaCl concentrations (0, 0.5 and 1%) combined with three different pH values (pH 5, 6 and 7). For each recovery medium, serial dilutions of bacterial cultures were made and, aliquots (400 µL) were added into the wells of a microwell plate. The plates were incubated in the Bioscreen C automatic reader (Labsystems, Helsinki, Finland) at 37 ºC and optical density (OD) was measured at 600 nm. The kinetic parameters of the single-cell lag times were estimated by the method described by Metris et al. (2006). The individual cell lag times (λ) were calculated from the following formula (Baranyi and Pin, 1999):

$$t_d = \lambda + (\ln(N_d) - \ln(N_o))/\mu \quad (1)$$

where Nd is the bacterial number at t_d obtained by means of calibration curves and N_0 the number of cells initiating growth in the considered well.

Statistical data processing and distribution fitting

Statistical data processing was performed and histograms were made from every set of conditions showing the distribution of the lag phases. From each histogram, the most common statistical parameters (mean value, standard deviation, etc.) were determined.
Distributions were fitted to time to growth and were ranked using the $\chi 2$ and the Anderson–Darling (A–D) goodness of fit statistics. Monte Carlo simulation was performed to predict the time to growth to a certain microbial concentration (10^2 cfu/mL, in this case). Equation (1) was used to analyse the dependence of N_0 and λ on the times to reach 100 cfu/mL. The individual cell lag times were assumed to follow a Gamma distribution of shape parameter β and scale parameter α. The parameters of the Gamma distribution and the growth rate, μ, in each environmental condition were calculated from the detection times. On the other hand, the initial number of cells in a well followed a Poisson distribution with an average of 1 cell per well according to Metris *et al*. (2006).

Results and Discussion

Recovery of cells treated under HHP

The effect of NaCl concentration (0, 0.5 and 1%) and pH (5, 6 and 7), single or in combination, in the recovery medium of cells of *L. monocytogenes* CECT 5672 previously treated by high hydrostatic pressure was studied.

The mean lag phase duration for the strain pre-treated under pressure increased when the environmental conditions became more severe, a trend that can be confirmed for both NaCl concentration and pH. Also the standard deviations were calculated and increases were found with the combination of both stresses. The duration of the lag phase of *L monocytogenes* CECT 5672 increased significantly with the decrease of the pH in the recovery medium e.g., after 3 min at 350 MPa, the mean individual cell lag phase was increasing from 1.78 h to 29.6 h when pH decreased from 7 to 5. The effect of increasing NaCl concentration was also significanted as the mean individual lag phase was increasing from 29.5 h to 42.5 h when the %NaCL was from 0 to 1.0% at a pH 5.

The largest increase of lag phase was found with combinations of acid pH (pH 5) and 1% NaCl in the recovery medium, reaching lag values of 102.5 and 232.7 h for *L monocytogenes* CECT 5672 treated at 450 Mpa for 3 and 16 min, respectively.

On the other hand, increased exposure to HHP resulted in a significantly increased level of injury, and subsequently a longer lag phase. Values of individual cell lag phase for cells of *L monocytogenes* CECT 5672 pre-treated at 450MPa for 3 min were significantly ($p \leq 0.05$) higher than the corresponding values for *L monocytogenes* treated at 350MPa for 3 min but the effect of the stress conditions were similar.

Histograms of the lag values for different treatments are shown in Figure 1

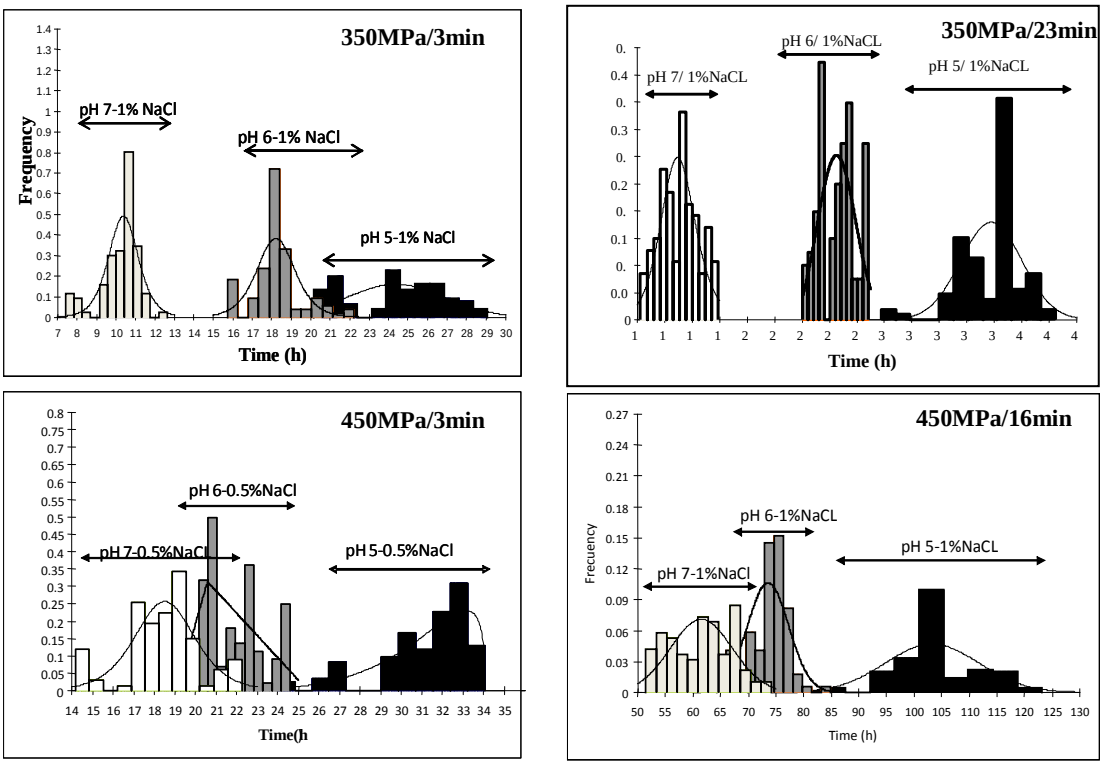

Figure 1: Histograms of distribution of lag phase of individual cells of *L. monocytogenes* exposed to HHP and recovered in the conditions indicated

Increases in the variability of histograms representing the lag phase of individual cells were observed and shifts of the histograms to the right were detected. It can also be observed that the variance of the lag time is generally higher with longer lag and the width of histograms

varied depending on the level of stress during the growth of the cells. There was less dispersion with optimal conditions than at lower pHs or higher salt concentrations or combinations of them. The shape of the histogram changed when stress levels increased. The highest density of the curve was situated at the left side for moderate stress levels, whereas it shifted to the right one for more severe conditions.

Effect on distribution fitting

Weibull, Gamma and Normal distributions were selected as they have been described in other studies and they covered the whole range of observed dataset and gave a good description of the experimental data. When the most severe stress conditions were applied, both Weibull and normal distribution fitted the data for lag times. Weibull has been used to fit high levels of stress conditions before (Francois *et al*. 2005, 2007) and also normal distribution (Delgado *et al*.,2004; Wu *et al*. 2000; Francois *et al*. 2005).

Prediction of the time to a certain growth

A simulation was performed to establish the time to growth to a concentration of 100 cfu/mL of *Listeria monocytogenes*. The mean value of time to a specific growth provided by the Monte Carlo simulation was very close to the deterministic values obtained in all cases (less than 10% variation) and the prediction limits (95% confidence interval) gave a good description of the experimental observations and the probability associated.
The Monte Carlo analysis gave information of the variability and distribution over the time of the predictions.

Conclusions

High pressure-treated *L. monocytogenes* showed evidence of damaged cells, with an increase in lag duration with stressful recovery conditions for both pH and NaCl stresses. The incidence of damaged cells increased at the higher pressure treatments tested and so did the spread of the time to recover of *L. monocytogenes* cells.

Acknowledgements

Marina Muñoz acknowledges Fundacion Cajamurcia for awarding her a post-doc grant. This project was funded by Spanish "Ministerio de Ciencia e Innovación", ref. AGL 2010-22206-C02-02/ALI and Fundación SENECA, CARM, Spain ref 08795/PI/08.

References

Baranyi J. and Pin C., (1999) Estimating growth parameters by means of detection times. *Applied and Environmental Microbiology* 65**,** 732–736.

Delgado B., Fernandez P.S., Palop A. and Periago P.M. (2004) Effect of thymol and cymene on Bacillus cereus vegetative cells evaluated through the use of frequency distributions. *Food Microbiology* 21 , 327-334.

Ferrer C., Rodrigo D., Pina M.C., Klein G., Rodrigo M. and Martínez A. (2007) The Monte Carlo simulation is used to establish the most influential parameters on the final load of pulsed electric fields *E. coli* cells. *Food Control* 18, 934–938.

Francois K., Devlieghere F., Smet K., Standaert A.R., Geeraerd A.H., Van Impe J.F. and Debevere J. (2005) Modeling the individual cell lag phase: effect of temperature and pH on the individual cell lag distribution of Listeria monocytogenes. *International Journal Food Microbiology*, 100, 41–53.

Francois K., Valero A., Geeraerd A.H., Van Impe J.F., Debevere J., García-Gimeno R.M., Zurera G. and Devlieghere F. (2007) Effect of preincubation temperature and pH on the individual cell lag phase of *Listeria monocytogenes*, cultured at refrigeration temperatures. *Food Microbiology*, 24, 32-43

Métris A., George S.M. and Baranyi J. (2006) Use of optical density detection times to assess the effect of acetic acid on single-cell kinetics. *Applied and Environmental Microbiology* 72, 6674–6679.

Poschet F., Geeraerd A.H, Scheerlinck N., Nicolai B.M. and Van Impe J.F. (2003) MonteCarlo analysis as tool to incorporate variation on experimental data in predictive microbiology. *Food Microbiology*, 20, 285-295.

Wu Y., Griffiths M. W. and McKellar R. C. (2000) A comparison of the Bioscreen method and microscopy for determination of lag times of individual cells of *Listeria monocytogenes*. *Letters in Applied Microbiology* 30, 468–472.

Growth of *Listeria monocytogenes, Salmonella* Typhimurium and *Escherichia coli* in the presence of sodium chloride following a mild thermal process

I. Mytilinaios[1], R. J.W. Lambert[2]

[1] Cranfield Health, Cranfield University, Cranfield, Bedforshire, MK43 0AL, UK (i.mytilinaios@cranfield.ac.uk)
[2] Cranfield Health, Cranfield University, Cranfield, Bedforshire, MK43 0AL, UK (rjwlambert@cranfield.ac.uk)

Abstract

There is significant interest in applying milder processing technologies in order to increase the shelf life and ensure the safety of foods. Thus, a major focus of predictive modelling has been on the models which accurately predict the effect of combining multiple processes or hurdles. Among the various processes used by the Food Industry to control microbial growth, heat treatment represents the most common. Obtaining data for the construction of a combined thermal injury model with a growth inhibition model, i.e. a stochastic with a deterministic, was a goal of this project.

Keywords: *predictive modelling, thermal injury, NaCl, TTD method*

Introduction

Foodborne disease is a common and serious threat to public health all over the world. There are several consumer trends that may have an impact on foodborne disease. Now days, there is a trend towards more natural, fresh, less preserved and processed foods (Newell *et al.* 2010). The aim of hurdle technology is the deliberate and intelligent combination of different hurdles in order to improve the microbial stability and the total quality of foods (Leistner 2000; Leistner and Gorris 1995). The food industry uses various processes to control microbial growth. Heat represents a common form of preservation (Gould 1989). Also, with predictive microbiology all the knowledge of microbial responses in different environmental conditions is summarized as equations or mathematical models (McMeekin *et al.* 1997). In this research, the effect of a mild thermal injury on the growth of *Listeria monocytogenes, Salmonella* Typhimurium and *Escherichia coli* in the presence of different salt (NaCl) concentrations using the method of time to detection (TTD) was studied.

Materials and Methods

All analyses were performed in a Bioscreen Microbiological analyser (Labsystems Helsinki, Finland). Two (10x10) microtitre plates were prepared identically: from a standardised culture tenfold serial dilutions were prepared which were subsequently half-fold diluted across the plates, giving up to 100 different initial inocula (range $1x10^9$ to less than 1organism per well) per plate. Both plates were initially incubated at either 30 or 37^{o}C together. After a given time (allowing up to 1/3rd of the wells to reach the detection limit), one plate was chosen and placed in a preheated oven at 60^{o}C for 25 minutes and then replaced back into the Bioscreen incubator for the remainder of the experiment. In some experiments specific wells were ‘sacrificed’ to enable the distribution of injury to be gauged from colony sizes on spread plates. The effect of the thermal treatment was studied in TSB with different concentrations of NaCl (0.5, 3, and 6%).
The time to detection (defined as the time to reach an optical density = 0.2 at 600nm in the Bioscreen) was obtained for each well. From the control plate (without thermal injury) the method of Cuppers and Smelt (1993) was used to obtain growth rates.

Results and Discussion

The effect of a mild thermal injury was studied using the Bioscreen, in conjunction with the methods developed for the analysis of the initial inoculum size on the TTD. *L. monocytogenes*

252(industrial isolate), *Salmonella* Typhimurium and *E.coli* were examined. Figure 1.1 shows the TTD in relation with the initial populations of *L.monocytogenes* 252 at 30^{o}C and 37^{o}C, *Salmonella* Typhimurium and *E.coli* at 30^{o}C in the presence of different NaCl concentrations, respectively.

The data obtained using the Bioscreen before the heat treatment showed that as the NaCl in the media increased, the gradient obtained increased, hence the growth rate decreased. Following the heat treatment, at the lowest salt concentrations used, for *L. monocytogenes* the gradient of the data was essentially the same as that before the treatment, but had a higher degree of variability. Further, a step in the TTD plot following the heat treatment was observed. The variability and the size of the step increased with increasing salt concentration and was more pronounced in the *E.coli* and *Salmonella* Typhimurium data than the *Listeria* (which is more salt tolerant). The observed discontinuity after a period of thermal injury was interpreted as a heat induced lag, before growth recommenced. Table 1.1 summarises the results obtained.

A major focus of the research was to obtain an understanding of the injury profile of a population following a mild thermal process. From the results obtained, a low level thermal injury (short time at a mild inhibitory temperature) gave little apparent lag, but an increase in the variance of the data was noted. One method to model the distribution of injury throughout the population is to assume that the injury process is a Poisson process. Lambert and Ouderaa (1999) considered the injury process following an injurious or inimical procedure to be a rate process with multiple injured states, populated by given rates. The model was therefore strictly deterministic, based on, essentially chemical kinetics. In the case of a thermal injury, the model of Lambert and Ouderaa could be used, but given the ubiquitous nature of the thermal energy applied, a process modelled by the simple Poisson birth process may be a more practicable method.

The Poisson birth process is governed by a factor, which regulates the proportion of a population changing from one state to another. The process itself is strictly random, and is known as a ‘no-history’ process, since events which have already occurred bear no relation on the probability of another event occurring. When the inimical process is stopped, we hypothesise that the injured population distribution is fixed, and it is from this distribution that recovery occurs. The Bioscreen data therefore describes the times taken for an injured population (or portions of the injured population) to recover the ability to reproduce. This must be dependent on the ratios of the sub-populations. If the inimical process is ‘low level’, then few sub-populations will have substantial members. As the process becomes more inhibitory, more sub-populations become populated and there are few or no members in the uninjured or least injured states. Thus it is predicted that the population within each well, after recovery, grows at a rate dictated to by the environment in which it is immersed (i.e. will grow at the rate dictated by the given temperature and salt concentration in these cases).

By half-fold diluting specific wells after the thermal process, we have shown that the gradient obtained is equivalent to that obtained from the controls and has a variability equivalent to the control.

Table 1: Parameters describing the relationship between TTD with the initial populations of *Listeria monocytogenes* No.252, *Salmonella* Typhimurium and *Escherichia coli* in different concentrations of NaCl, as estimated from the primary growth data at 30°C or/and 37°C, before and after heat treatment at 60°C for 25min.

Strain	NaCl (%)	T(°C)	Heat treatment	Gradient (hours)	Gradient - CI	Gradient +CI	Intercept (hours)	Intercept -CI	Intercept +CI
252	0.5	30°C	Before	-2.07	-2.18	-1.94	18.71	17.89	19.52
252	0.5	30°C	After	-2.29	-2.46	-2.12	21.66	21.18	22.14
252	3	30°C	Before	-2.62	-2.70	-2.54	23.43	22.86	23.99
252	3	30°C	After	-2.58	-2.73	-2.44	24.26	23.83	24.69
252	6	30°C	Before	-3.98	-4.15	-3.81	37.66	36.52	38.81
252	6	30°C	After	-3.94	-4.48	-3.41	39.94	38.34	41.54
252	0.5	37°C	Before	-1.80	-1.81	-1.78	16.00	15.90	16.10
252	0.5	37°C	After	-1.90	-2.15	-1.65	18.02	17.48	18.56
252	3	37°C	Before	-2.14	-2.16	-2.12	19.37	19.23	19.52
252	3	37°C	After	-2.18	-2.39	-1.96	22.05	21.35	22.75
252	6	37°C	Before	-3.44	-3.55	-3.34	30.47	29.79	31.15
252	6	37°C	After	-3.41	-3.79	-3.03	35.28	34.01	36.56
Salmonella T.	0.5	30°C	Before	-1.77	-1.80	-1.74	15.27	15.13	15.41
Salmonella T.	0.5	30°C	After	-1.59	-2.09	-1.08	21.43	20.24	22.62
Salmonella T.	3	30°C	Before	-2.66	-2.76	-2.55	22.76	22.06	23.47
Salmonella T.	3	30°C	After	-2.66	-2.39	-1.92	33.96	31.56	36.37
E.coli	0.5	30°C	Before	-1.66	-1.72	-1.60	13.45	13.09	13.82
E.coli	0.5	30°C	After	-1.57	-2.05	-1.08	17.07	15.90	18.24
E.coli	3	30°C	Before	-2.09	-2.12	-2.05	18.16	17.92	18.39
E.coli	3	30°C	After	-2.18	-2.90	-1.46	29.99	27.93	32.05

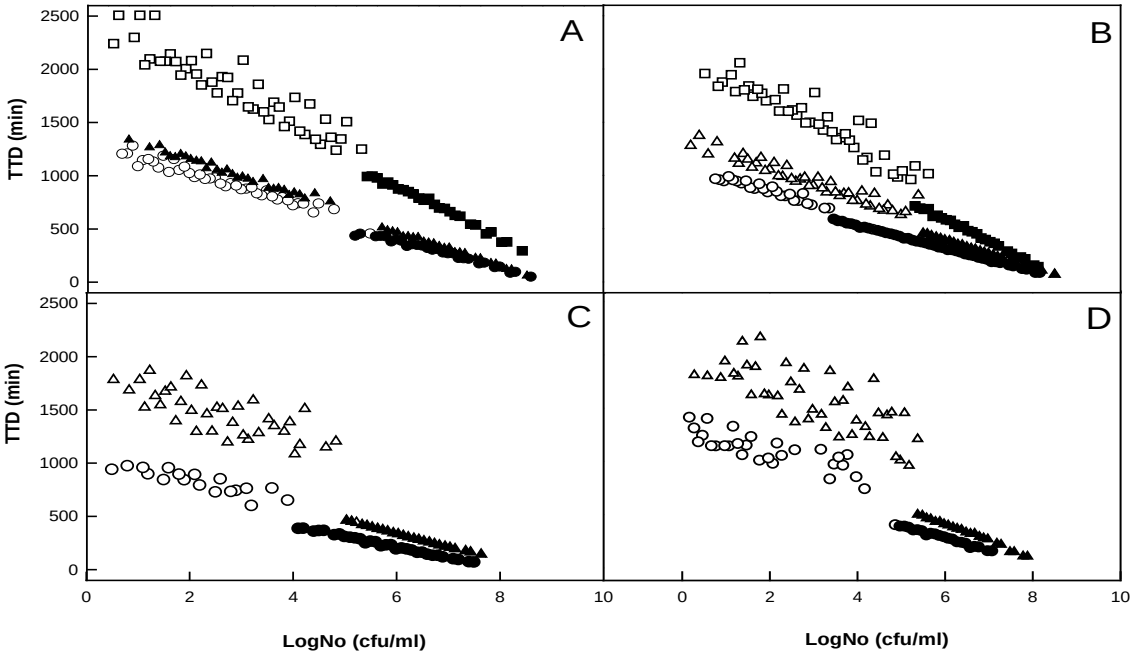

Figure 1: Relationship between TTD with the initial populations of A) and B) *Listeria monocytogenes No.252* at 30°C and 37°C respectively, C) *Escherichia coli* grown at 30°C and D) *Salmonella* Typhimurium at 30°C, grown in TSB with 0.5% NaCl (●,○), 3% NaCl (▲,△) and 6% NaCl (■, □). The closed symbols represent the observed data before the heat injury while the opened symbols represent the observed data after the heat injury in a preheated oven at 60°C for 25 min.

Conclusions

The mild thermal injury induced a lag before growth recommenced, with a distribution of injury dependent on the time of the thermal treatment. On recovery the population grew at a rate dictated by the environment present, i.e. at the same rate as observed for the control. The rate of recovery can be modelled by a Poisson 'Death process' – the opposite to the birth process. We can hypothesise that this process occurs in a similar manner to the Birth process – recovery occurs in stages governed by a rate constant (λ).

References

Cuppers H.G.A.M., Smelt J.P.P.M., (1993) Time to turbidity measurement as a tool for modelling spoilage by Lactobacillus. *Journal of Industrial Microbiology* 12, 168-171.

Gould G.W., Jones M.V., (1989) Combination and synergistic effects. In: Gould, G.W. (Ed.), *Mechanisms of Action of Food Preservation Procedures*. Elsevier Applied Science, London, 401–421.

Lambert R.J.W., van der Ouderaa M.-L.H., (1999) An investigation into the differences between the bioscreen and the traditional plate count disinfectant test methods. *Journal of Applied Microbiology* 86, 689–694.

Leistner L., (2000) Basic aspects of food preservation by hurdle technology. *International Journal of Food Microbiology* 55, 181–186.

Leistner L., Gorris L.G.M., (1995) Food preservation by hurdle technology. *Trends Food Science Technology* 6, 41–46.

McMeekin T.A., Brown J., Krist K., Miles D., Neumeyer K., Nichols D.S., Olley J., Presser K., Ratkowsky D.A., Ross T., Salter M., Soontranon S., (1997) Quantitative microbiology: a basis for food safety. *Emerging Infectious Disease* 3, 541–549.

Newell D.G., Koopmans M., Verhoef L., Duizer E., Aidara-Kane A., Sprong H., Opsteegh M., Langelaar M., Threfall J., Scheutz F., Der Giessen J.V. and Kruse H. (2010) Food-borne diseases — The challenges of 20 years ago still persist while new ones continue to emerge. *International Journal of Food Microbiology* 139, S3-S15.

Efficiency of a reheating step to inactivate *Clostridium perfringens* vegetative cells : how to measure it?

S. Jaloustre[123], L. Guillier[1], G. Poumeyrol[1], E. Morelli[1] and M.L. Delignette-Muller[34]

[1] Agence Nationale de Sécurité Sanitaire (Anses), LSA, 23 av. du Gal de Gaulle, F-94706, Maisons-Alfort Cedex, France. (Severine.SEVRIN-JALOUSTRE@anses.fr)
[2] AgroSup Dijon, F- 21079 Dijon, France
[3] Université de Lyon, F-69000, Lyon, Université Lyon 1, CNRS, UMR5558, Laboratoire de Biométrie et Biologie Evolutive, F-69622, Villeurbanne, France
[4] Université de Lyon, F-69000, Lyon, VetAgro Sup Campus Vétérinaire de Lyon, F-69280 Marcy l'Etoile, France

Abstract

Clostridium perfringens is responsible for foodborne diseases often associated with processed meats in institutions. This study investigated the behavior of *C. perfringens* in beef-in-sauce products in a French hospital. Before their distribution to patients, these products undergo a final linear reheating step making inactivation of vegetative form of *C. perfringens* possible. An inactivation of three $\log_{10}$ was targeted to obtain a final *C. perfringens* concentration in food low enough to reduce probability of food borne illness using published dose response models. The aim of this study was to combine microbial and thermal modeling to propose, for this reheating step, three control measures based on duration above 53°C (DA53), final temperature in food (FTF) and sum of temperatures-minutes above 53°C (ST53) required to achieve this target microbial inactivation. Temperature threshold for inactivation was fixed at 53°C, the estimated maximum temperature for *C. perfringens* growth, in order to prevent any residual growth.

In order to estimate acceptable values of DA53, FTF and ST53, two sources of variability were taken into account : variability on $\log_{10} D_{ref}$ (with D_{ref} the D value at $T_{ref} = 60°C$) and variability on temperature increase rates observed in hospital. Temperature increase rates and $\log_{10} D_{ref}$ –values were randomly selected from their estimated distributions in order to simulate *C. perfringens* inactivation under realistic dynamic linear temperature profiles from 53°C. Each simulation was stopped as soon as the microbial inactivation target was reached. These simulations provided distributions of acceptable values for the three control measures, making it possible to define thresholds from an upper percentile (in this study the 97.5th percentile) : 18 minutes for DA53, 68.7°C for FTF and 1082°C.min for ST53. The applicability of the three control measures, single and combined, was then compared by estimating the proportion of estimated inactivation below the target and the duration required to reach measure threshold. If their efficiency is quite equivalent, duration required differs significantly from a control measure to the other and the combination of FTF and DA53 appears as the less time-consuming one.

Keywords: *Clostridium perfringens*, *thermal inactivation*, *control measures*

Introduction

Clostridium perfringens is responsible for foodborne diseases often associated with processed meats in institutions (Crouch and Golden 2005). This study investigated the behavior of *C. perfringens* in beef-in-sauce products in a French hospital. Beef and other ingredients undergo first a cooking step before their cooling down. Products are then kept refrigerated at 4°C during two or three days. During the cooling, *C. perfringens* spores can germinate and grow. Immediately before their distribution to patients, these products undergo a final linear reheating step making inactivation of vegetative form of *C. perfringens* possible. French regulation prescribes a final temperature at 63°C or more and reheating from 10°C to 63°C within one hour or less. In the hospital, because of the difficulty in controlling the speed of temperature increase during reheating, some of the reheated meals did not comply with French regulation in terms of speed of temperature increase and could theoretically not be

distributed in the absence of other control measures. The aim of this study is to propose and compare other control measures, easier to apply than French regulation, taking into account potential sources of variability.

Materials and Methods

Inactivation model

Evolution of microbial concentration under dynamic thermal conditions was predicted using a linear model whose parameter D was described as a function of temperature by the Bigelow model (Bigelow, 1921) :

$$\log_{10} N(t) = \log_{10} N_0 - \frac{t}{D(T)} \qquad with \quad \log_{10} D(T) = \log_{10} D_{ref} - \frac{T - T_{ref}}{z}$$

Variability on $\log_{10} D_{ref}$ was estimated from the fit of a linear mixed-effects model on published data collected from various studies (Jaloustre *et al.* submitted). $\log_{10} D_{ref}$ variability distribution was described by a normal distribution $N(\log_{10} D_{ref,0}, \sigma_D)$ with σ_D resulting from random effects related to strains, vegetative cell culture conditions before inactivation and other uncontrolled experimental factors.

Thermal model

209 time temperature profiles of the final reheating step were registered in a French hospital. As they were linear from 20°C until the end of reheating step, these profiles were fitted by linear regression using the following model:

$$T = T_0 + k \times t$$

with T the temperature [units : °C] at time t [units : hours], T_0 the initial temperature and k the temperature increase rate [units : °C.hours^{-1}]. 209 k values were estimated and fitted by the normal distribution $N(75.8, 22.2)$ characterizing variability on temperature profiles. French regulation prescriptions, which correspond to a reheating from 10°C to 63°C within less than one hour, correspond to a k value above 53°C.h^{-1}. This k value is the 15.2th percentile of the fitted normal distribution, indicating that around 15% of observed temperature profiles could not respect French regulation because of a too low temperature increase rate.

Definition of control measures

In order to reduce probability of food borne illness, a low final *C. perfringens* concentration in food was targeted using published dose response models (Golden *et al.* 2009) and modelling portion size. Considering that potential growth during the first part of the process could induce a cell number increase at three $\log_{10}$ or more if cooling down step was delayed (Jaloustre *et al.* 2011), an inactivation of three $\log_{10}$ (performance criterion) was targeted to obtain this low final concentration. Three control measures were then proposed: duration above 53°C (DA53), final temperature in food (FTF) and sum of temperatures-minutes above 53°C (ST53) required to achieve the target performance criterion. Temperature threshold for inactivation was fixed at 53°C, the estimated maximum temperature for *C. perfringens* growth, in order to prevent any residual growth (Jaloustre *et al.* 2011). French regulation prescriptions, defined as a reheating from 10°C to 63°C within one hour, correspond to DA53 = 11.3 min, FTF = 63°C and ST53 = 694°C.min.

To define thresholds for each control measure that allow to comply the target performance criteria, temperature increase rates and $\log_{10} D_{ref}$ –values were randomly selected from their estimated distributions in order to simulate realistic dynamic linear temperature profiles starting from 53°C and *C. perfringens* corresponding inactivation kinetics. Each simulation was stopped as soon as the target performance criterion was reached. These simulations

provided distributions of acceptable values for the three control measures and thresholds for each control measure were defined from the 97.5th percentile of these distributions.

Comparison between control measures

The applicability of single or combined control measures was compared, as presented in Table 1. Efficiency and duration required to achieve each control measure threshold were compared. A set of 15000 temperature increase rates and $\log_{10} D_{ref}$ –values were randomly selected from their estimated distributions such as to simulate *C. perfringens* inactivation from 53°C until each control measure threshold was achieved (when two control measures were combined, simulations were stopped when one of the thresholds was achieved). As soon as each control measure threshold was achieved, both *C. perfringens* final concentration and duration required to reach this threshold were estimated. These simulations provided distributions of *C. perfringens* final inactivation and duration required to reach threshold for all the tested control measures.

Results and Discussion

Control measure thresholds

Table 1 synthesizes the control measure thresholds required to achieve the target performance criterion. 95% variability intervals of the three single control measures ([4,18] min for DA53, [58.3,68.7] °C for FTF and [226,1082] °C.min for ST53) are huge, both due to variability on $\log_{10} D_{ref}$ and temperature increase rates. From those distributions, it is possible to define a threshold, for the control measure, that must be reached to stop reheating. Such thresholds were defined for each control measure using the 97.5th percentile, as reported in Table 1.

Table 1: Comparison between control measures. Median duration required to reach threshold is reported with the 95% variability interval between brackets.

Control measure	Threshold	Percent of simulations below the target criterion	Duration required to reach threshold (min)
French regulation	63°C and k > 53°C.h^{-1}	60.89%	7.6[5,11]
DA53	18 min	2.37%	18
FTF	68.7 °C	2.35%	12.5 [7.9,28.8]
ST53	1082 °C.min	2.39%	18 [16,19]
DA53 & FTF	18 min or 68.7 °C	4.76%	12.5 [7.9,18]
DA53 & ST53	18 min or 1082 °C.min	2.80%	18 [16,18]
FTF & ST53	68.7 °C or 1082 °C.min	4.48%	12.5 [7.9,19]

Comparison between control measures

Efficiency of all the control measures and durations required to reach them are reported in Table 1. Simulations of inactivation along temperature profiles respecting French regulation, *i.e.* stopped when 63°C is reached and accepted if temperature increase rates is over 53°C.h^{-1}, lead to a very low efficiency as only 39.11% of accepted simulations reached the target performance criterion. If efficiency of DA53, FTF and ST53 appears equivalent as expected by construction of the threshold, durations required to reach their thresholds, reported in Fig.1, differ from a measure to the other. Variability on duration required to reach ST53 appears low, as all the estimated values are between 16 and 20 minutes. On the opposite, variability on duration required to reach FTF threshold clearly appears huge. If FTF threshold is often quickly reached, even before the ST53 and the DA53 ones in respectively 77% and 85% of the cases, for some temperature profiles FTF threshold is reached after a long time : in 4.5% of the cases, duration required to reach FTF threshold exceeds 25 minutes.

As reported in Table 1, while reducing required duration, combinations of control measures do not seem to excessively penalize efficiency insofar the estimated proportion of incomplete

inactivation stays below 5%. As the less time consuming one and the easiest one to apply, combination of FTF and DA53 appears particularly interesting. If caterers found it necessary to reach a higher efficiency of that combination, higher FTF and/or DA53 thresholds could be defined. With FTF fixed at 71°C and DA53 at 19 minutes, that combination becomes as efficient as each control measure taken alone for a median duration at 14.4 [8.8,19] minutes.

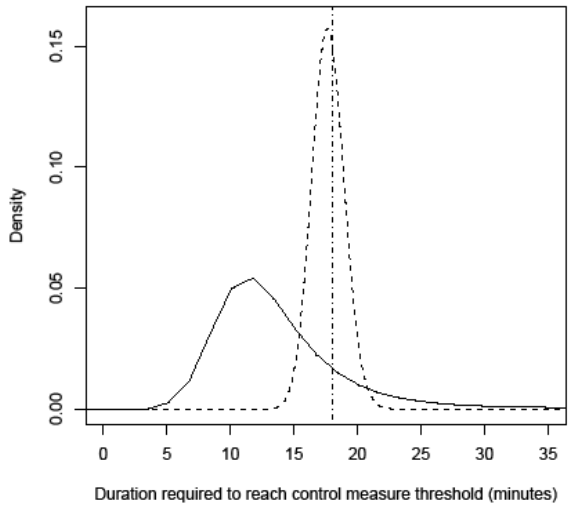

Figure 1: Distributions of durations required to reach DA53 (vertical dotted line), FTF (solid line) and ST53 (dashed line) thresholds.

Conclusions

As French regulation prescribes measures, which appear difficult to apply and sometimes inappropriate, three other alternative control measures were defined to reach a performance criterion of three $\log_{10}$ *C. perfringens* inactivation during the final reheating step of a beef-in-sauce product. For these control measures, distributions of acceptable values were estimated taking into account biological variability on $\log_{10} D_{ref}$ described in a mixed-effects model and observed variability on temperature increase rates. After estimating thresholds for the measures, the three single measures appear equally efficient but with very different durations required to reach their thresholds. With needle probe thermocouples able to perform real-time temperature measures, caterers could easily use any of these three control measures, more easily than French regulation as they do not depend on temperature increase rate. The combination of FTF and DA53, defined as the final temperature in food and the duration above 53°C, seems to be an interesting combination of control measures both efficient and far less time consuming than each control measure taken alone.

Acknowledgements

This work was supported by a grant from the Agence Nationale de la Recherche (ANR) (France), as a part of the Quant'HACCP project.

References

Bigelow W.D. (1921) The logarithmic nature of thermal death time curves. *Journal of Infectious Disease* 29, 528-536.

Crouch E.A. and Golden N.J. (2005) A Risk Assessment for *Clostridium perfringens* in Ready-To-Eat and Partially Cooked Meat and Poultry Products, USDA, Food Safety Inspection Service, September 2005.

Golden N.J., Crouch E.A., Latimer H., Kadry A.R. and Kause J. (2009) Risk assessment for *Clostridium perfringens* in ready-to-eat and partially cooked meat and poultry products. *Journal of Food Protection* 72, 1376-1384.

Jaloustre S., Cornu M., Morelli E., Noël V. and Delignette-Muller M.L. (2011) Bayesian modeling of *Clostridium perfringens* growth in beef-in-sauce products. *Food Microbiology* 28, 311-320.

Jaloustre S., Guillier L., Morelli E., Noël V and Delignette-Muller M.L. Modelling of *Clostridium perfringens* vegetative cell inactivation in beef-in-sauce products: a meta-analysis using mixed linear models. Submitted to *International Journal of Food Microbiology*.

Development of an integrated physical and microbiological probabilistic model for risk-based design and optimisation of aseptic processes for sterilisation of liquid foods

A. Amézquita[1], D. Kan-King-Yu[1]

[1] Unilever, Safety & Environmental Assurance Centre, Colworth Science Park, Sharnbrook, Befordshire, MK44 1LQ, United Kingdom. (alejandro.amezquita@unilever.com, denis.kan-king-yu@unilever.com)

Abstract

This study presents the development of a probabilistic simulation framework that integrates a combined energy-flow physical model with a microbiological inactivation model to estimate the minimum required heat treatment that would ensure microbiological safety and stability of aseptically processed soups. The framework accounts for the natural variability and uncertainty in processing and microbiological inputs to develop a risk-based sterilisation process design. The following inputs were used in the analysis: (1) concentration distribution of naturally occurring bacterial spores in ingredients, (2) heat-resistance distribution of these spores, and (3) product-temperature distribution during processing. Inputs (1) and (2) were obtained from an internal ingredient database. Input (3) was obtained from the energy-flow physical model, which in turn used probabilistic inputs to characterise parameter uncertainty and expected operational variability of key processing parameters. The model output was the concentration of surviving spores per pack. The main criterion used for decision-making was the probability of spore survival being less than 1×10^{-6} when benchmarked against a Performance Objective of < 1 spore/pack. Simulation results supported reductions of 4 and 5°C in the temperature set-points for a soup containing particulates and a creamy vegetable soup, respectively. Such processes were implemented in pilot plant conditions followed by microbiological analyses to support the validity of results.

Keywords: *risk-based design, integrated engineering-microbiological modelling, probabilistic modelling, thermal processing*

Introduction

Current regulations governing the safety of low-acid ambient-stable foods require “commercial sterility” of the product, but do not actually define a required safety level. As such, food companies have flexibility in designing their own processes to ensure “commercial sterility”, which in most cases rely on inactivation of microorganisms by heat as the only control measure. With that aim, companies have historically adopted ‘blanket’ process criteria (e.g. F_0 values ranging between 6-15 min) as design targets for thermal processes for this type of product. This approach has been convenient for industry because it allows for processes to be established without detailed knowledge of raw material contamination, variability in process, and variability in the heat resistance of microorganisms, it has a low risk of misinterpretation in operational settings, and it has proven to be effective. However, the approach is hazard- and not risk-based, and its apparent benefits are hindered by the negative impact that its practical implementation may have on product quality and environmental sustainability (i.e. it relies on worst-case assumptions about microbiological, product and process parameters, which often leads to over-designed processes). The aim of this study is to propose a risk-based approach to set the required heat-treatment for aseptically processed soups. This was achieved by: (i) using the ICMSF (i.e. International Commission on Microbiological Specifications for Food) conceptual equation (ICMSF 2002) as the main risk-based framework, (ii) developing an integrated physical and microbiological model (which underpins the ICMSF equation) to predict the total required reduction in the levels of microorganisms to meet a target Performance Objective (*PO*), and (iii) by setting relevant microbiological and process model inputs at their realistic distribution of levels rather than their worst-case levels.

Materials and Methods

Risk-based conceptual framework

To determine the operational design target for inactivation of microorganisms based on risk, we used the concept of Performance Objective (ICMSF 2002), which offers a conceptual framework for risk-based product/process design, and can be expressed by Eq. 1

$$H_0 - \sum R + \sum I < PO \tag{1}$$

The elements of Eq. 1 are described as follows:

H_0: initial level of spores before the heat treatment ($\log_{10}$ spore kg^{-1}). The quantity has been adjusted as function of the unit of finished product (i.e. 1 kg soup cartons). The value of H_0 was given by mesophilic aerobic spore counts (after a heat treatment of 80°C for 15 min), for each ingredient in the soup formulation. These were obtained from a database collected over 10 years in a soup factory, reflecting variability of naturally occurring spores. A prevalence of 100% was assumed (Membré and van Zuijlen 2011).

ΣR: total log-reduction, by heat inactivation, required to meet the *PO*. This was deduced from H_0, ΣI and *PO* (i.e. $\Sigma R \geq H_0 + \Sigma I - PO$). The mathematical calculation ΣR will be described later (see *Microbiological inactivation model* section).

ΣI: total increase in spore levels (expressed in $\log_{10}$ units) before heat treatment. It was assumed that $\Sigma I = 0$ since growth or recontamination before heat treatment is unlikely.

PO: Performance Objective after the heat-treatment ($\log_{10}$ spore kg^{-1}). In our context, we set the *PO* as the maximum concentration of spores which needs to be achieved to ensure a stable product, defined as absence of mesophilic aerobic spores per pack, i.e. $PO < 0$ $\log_{10}$ spore kg^{-1} (i.e. < 1 spore $pack^{-1}$).

Microbiological inactivation model

The calculation of the sterilisation value required to meet the *PO* was based on the classical Bigelow inactivation kinetics (Bigelow 1921), which describe death of spores by a log-linear relationship. This can be expressed by Eq. 2

$$\sum R = \frac{1}{D^i_{121}} \int_0^t 10^{\left(\frac{T-121}{z^i}\right)} \cdot dt \tag{2}$$

where T is the product temperature (°C), D^i_{121} is the decimal reduction time at 121°C (min) for ingredient i, and z^i is the so-called 'z-value' (C°) for ingredient i. The values of D^i_{121} and z^i were obtained from the same ingredient database used to define H_0, where the same ingredients were heat treated at 100 and 110°C for 15 min. The methodology for estimating D^i_{121} and z^i has been previously reported by our group (Membré and van Zuijlen 2011).

Physical model

The product (fluid + particulates) temperature, T, in Eq. 2, was predicted by means of an energy-flow model. For a multiphase food product sterilised in an aseptic processing line, assuming a radially well-mixed system, the energy balance on the fluid phase at any cross section along the tube can be expressed by Eq. 3 (Sastry and Cornelius 2002)

$$\rho_f C_{p,f} A_f \frac{dT_f}{dt} = h_{fw} l_f (T_e - T_f) + n_p h_{fp} A_p (T_p^{surf} - T_f) \tag{3}$$

where ρ_f is fluid density ($kg\ m^{-3}$), $C_{p,f}$ is fluid heat capacity ($J\ kg^{-1}\ °C^{-1}$), A_f is cross-section area through which the product flows (m^2), T_f is fluid temperature (°C), t is time (s), h_{fw} is overall heat transfer coefficient between heating/cooling medium and fluid ($W\ m^{-2}\ °C^{-1}$), l_f is perimeter of cross-section area (m), T_e is external heating/cooling medium temperature (°C), n_p is number of particulates per unit length of tube (m^{-1}), h_{fp} is fluid-particulate convective heat transfer

coefficient, A_p is surface area of a single particulate (m^2), and T_p^{surf} is temperature at surface of particulate (°C). To solve Eq. 3, each unit (e.g. a heat-exchanger) in the aseptic processing line was discretized into M small elements, and solved for the steady-sate temperature in each element. The solution was then moved on time (explicitly) by iterating over the entire length of each unit using the values of T_f, T_e, T_p^{surf} at the current element M (or time level) to update the solution at the next element M+1. With the exception of T_p^{surf}, all the inputs in Eq. 3 were obtained either from geometrical considerations or experimental data. The value of T_p^{surf} was calculated by solving numerically (i.e. finite differences) for unsteady-state heat conduction (with convective boundary conditions) within a particulate. The coefficient h_{fw} lumps the overall energy transfer between external media and fluid in a single parameter, and it is estimated as an average value for each unit of the aseptic processing line based on the measured inlet and outlet temperatures of the carrier fluid. The coefficient h_{fp} is defined as an uncertainty distribution (a uniform distribution – see next section), whose minimum and maximum values are defined from published data for similar products (Sastry and Cornelius 2002).

Simulation framework and decision rules

Since the *PO* is a single value, the output distribution of surviving spores (log$N$) was deemed to give an acceptable scenario when the probability of having a surviving spore was less than $1x10^{-6}$ compared against the *PO* (i.e. $\Pr\{\log N \geq PO\} < 1\times10^{-6}$). Additionally, for microbiological safety assurance, a minimum F_0 3 min in the holding tube was required for an acceptable scenario. Seven model inputs (i.e. H_0, z^i, h_{fp}, T_e, A_p, ratio of maximum to average fluid velocity, and product mass flow rate) were defined by probability distributions (from data, measurements or expert opinion). The complete model was solved by running Monte Carlo simulations implemented in Matlab R2009a (The Mathworks, Natick, MA, USA). A baseline simulation was run with standard process conditions. Optimisations were subsequently run with the aim of reducing controllable process parameters towards milder conditions, whilst still meeting the criteria for an acceptable scenario.

Results and Discussion

The proposed risk-based design framework was evaluated with two different types of soup: (i) a creamy vegetable soup (without particulates), and (ii) a clear bouillon containing large particulates. In both cases, the baseline model (i.e. simulating the process implemented currently) resulted in conservative distributions of surviving spores (log$N$) and F_0 values in the holding tube, thus providing sufficient opportunities for process optimisation. Simulations for optimised processes focussed on reducing the severity of the heat-treatment with a view to improve product quality and to reduce environmental impact (i.e. reduced energy usage). Optimisation options focussed on two main strategies: (a) a reduction of the temperature set-point for product at the inlet of the holding tube, and (b) a reduction of the total length (i.e. heat transfer area) in the main steriliser. Simulation outputs for the distribution of surviving spores (log$N$) and F_0 in the holding tube are illustrated in Table 1 for the two types of soup.

Table 1: Simulation results for two types of soup formulations evaluated

Simulation	Percentile	Creamy vegetable soup		Bouillon with particulates	
		log$N$ (log spore/kg)	F_0 (min)	log$N$ (log spore/kg)	F_0 (min)
Baseline	5th	-41.48	12.59	-28.89	13.34
	50th	-19.36	15.73	-16.67	17.09
	95th	-11.87	19.62	-11.44	21.75
Strategy (a)	5th	-10.32	4.11	-8.17	4.34
	50th	-6.27	5.19	-5.68	5.56
	95th	-3.96	6.54	-3.58	7.06
Strategy (b)	5th	-13.36	5.24	n.d.[a]	n.d.
	50th	-7.89	6.50	n.d.	n.d.
	95th	-5.14	8.05	n.d.	n.d.

[a] n.d. = not determined (see discussion below)

The recommended optimised processes were implemented in a pilot aseptic processing plant, followed by sensory evaluation and microbiological analyses. For the creamy vegetable soup, the simulation strategy (a) resulted in a reduction of 5°C in the product temperature (i.e. fluid temperature) set-point as compared to the baseline process, whilst strategy (b) resulted in a reduction of 20% in the total steriliser length. In the case of the bouillon with particulates, strategy (a) resulted in a reduction of 4°C in the product temperature (volume-averaged temperature for particulate phase) set-point; however, from a practical implementation viewpoint, it was not possible to implement any reductions in the steriliser length due to instability of product flow rate in pilot plant conditions. A representative simulation output is depicted in Figure 1 for the creamy vegetable soup.

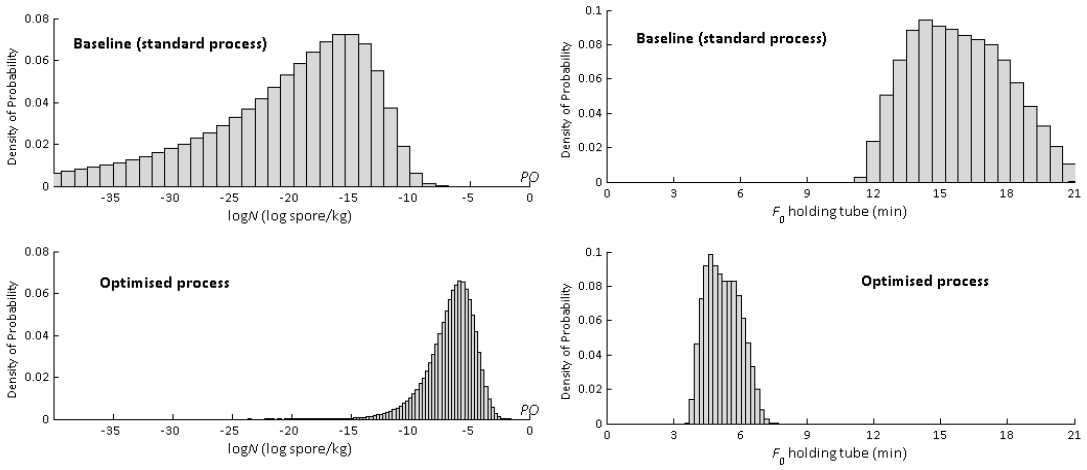

Figure 1: Output distributions of surviving spores (log$N$) –left plots– and F_0 value in the holding tube –right plots– obtained after Monte Carlo simulation procedure; illustration with the creamy vegetable soup (baseline and optimised, i.e. strategy (a), simulations).

For both formulations, microbiological analyses confirmed absence of mesophilic aerobic spores per pack of finished product, supporting the validity of the risk-based design approach. Sensory evaluation results, both at expert panel level and in consumer preference tests, indicated that the optimised processes resulted in better organoleptic quality products.

The proposed risk-based approach for process design and optimisation illustrates an extension of application of the ICMSF conceptual equation to spoilage microorganisms. As such, we propose a tiered decision criteria approach for setting design targets for aseptic processed soups as follows: (i) control of spoilage microorganisms decided by output of simulation so that $\Pr\{\log N \geq PO\} < 1\times10^{-6}$, and (ii) assurance of food safety (i.e. control of pathogens) by constraining the process setting to $F_0 \geq 3$ min in the holding tube.

Conclusions

The proposed risk-based approach is promising to support the design of milder thermal processes, moving away from worst-case scenarios without compromising microbiological stability and safety. The main benefits for industry are increased product quality (due to milder processing) whilst reducing the environmental impact (green house gas profile).

References

Bigelow W.D. (1921) The logarithmic nature of thermal death curves. *The Journal of Infectious Diseases* 29 (5), 528-536.

International Commission on Microbiological Specifications for Foods (ICMSF) (2002) *Microorganisms in Foods 7, Microbiological Testing and Food Safety Management*, Kluwer Academic/Plenum Publishers, New York, USA, 362 pp. (ISBN 0-306-47262-7).

Membré J.-M. and van Zuijlen A. (2011) A probabilistic approach to determine thermal process setting parameters: Application for commercial sterility of products. *International Journal of Food Microbiology* 144, 413-420.

Sastry S.K. and Cornelius B.D. (2002) *Aseptic Processing of Foods Containing Solid Particulates*, Wiley-Interscience, New York, USA, 250 pp. (ISBN 0-471-36359-6).

Multivariate regression model of thermal inactivation of *Listeria monocytogenes* in liquid food products

J.H.M. van Lieverloo[1], M. de Roode[1], M. B. Fox[1], M. H. Zwietering[2], M. H.J. Wells-Bennik[1]

[1] NIZO food research, Kerhemseweg 2, 6718 ZB Ede, The Netherlands (Hein.van.Lieverloo@nizo.nl; Matthew.deRoode@nizo.nl; Martijn.Fox@nizo.nl; Marjon.Wells-Bennik@nizo.nl)
[2] Wageningen University & Research centre, Bomenweg 2, 6703 HD Wageningen, The Netherlands (Marcel.Zwietering@wur.nl)

Abstract

A model was constructed from literature data for thermal inactivation of *Listeria monocytogenes* in liquid food products based on 735 sets of literature data. Significant variables were pH, sugar and fat content and the time and temperature of growth or storage before inactivation, as well as a heat shock. The model reduces the variability in the dataset due to these variables (known or controllable in practice), while keeping the variability of heat resistance of the 58 strains (unknown and not controllable in practice).

Keywords: pasteurisation, food matrix, processing, Monte Carlo analysis

Introduction

The variability of the efficacy of thermal inactivation of *L. monocytogenes* (e.g. during pasteurisation) can be estimated by a model that is based on literature data. Differences in food composition, process conditions and other variables can influence thermal inactivation. When calculating inactivation of *L. monocytogenes* for a specific food and process using Monte Carlo simulations, there is likely an overestimation of the variability of the thermal inactivation efficacy. On the other hand, using inactivation data in a certain food based on a limited number of *L. monocytogenes* strains may lead to underestimation of the variability of strain resistance to heat. The objective of this research was to generate a multivariate regression model to predict (variability of) thermal inactivation from literature data while accounting for effects of food composition and processing conditions. As specific data on food composition is lacking in most literature on heat inactivation in solids (fish, sea food, meat, vegetables), the model was limited to fluids.

Materials and Methods

Inactivation data and some condition variables were present in a database constructed from literature as described by Van Asselt & Zwietering (2006). Data on more variables were collected from the original papers they cited and from the cited reviews of ICMSF (1996) and Doyle *et al*. (2001). The database was further supplemented with other, mostly more recent literature (Edelson-Mammel *et al*. (2005), Hassani *et al*. (2005a, 2005b, 2007), Huang (2004), Ignatova *et al*. (2007), Juneja & Eblen (1999), Maisnier-Patin *et al*. (1995), Van der Veen *et al*. (2007)). Missing data on pH and concentrations of fat, salt and sugars in growth media, dairy, juices and egg (parts) were estimated from other literature or the internet. Data sets (26) with antimicrobials (peroxide, lactoperoxidase, nisin and ethanol) were not included. In total, the 801 data sets from 53 papers included 58 *L. monocytogenes* strains or cocktails (7).
Statistical analysis was performed using GenStat 13.2 (VSN International Ltd.). Concentrations of fat (0 – 83%), sodium chloride (0 – 20%) and sugars (0 – 58%) were 10-logarithmically transformed to approach a normal distribution, as was the duration of the last temperature phase (0 – 336 h, culturing or storage, excluding heat shock). Zero values were transformed to -5 (% sodium chloride), and -4 (% fat and sugar). The highest, acceptable, colinearity found was between ^{10}log(sodium chloride) and ^{10}log (fat), with a correlation coefficient of 0.24 (-0.06 when zero values were excluded). The 'all-subsets regression' procedure was used to attain the basic linear model without interaction terms.

Results and Discussion

Preliminary multivariate modelling could not reduce unequal variance over the temperature range, the variance at 60 – 70 °C remained too high. High ^{10}logD (D = time to 10-fold reduction) was linked to 5-20% sugar and/or sodium chloride added to liquid egg products. Low ^{10}logD was linked to long cold storage in chicken gravy. As inclusion of ^{10}log(sodium chloride), ^{10}log(sugars) and ^{10}log(duration of last temperature phase) in the model could not reduce this high variance at mid temperatures, chicken gravy data (40 data sets) were removed from the data set, as were liquid egg products with added sugar or sodium chloride (26 sets). This limited the concentration range of sodium chloride to a maximum of 8.8% (initially 20%), but stabilised the variance. Figure 1 shows the variability of all ^{10}logD values, not corrected for food or process variables. The univariate model of 735 datasets (logD = 9.07 – T / 6.74) had an R^2 of 0.77 and a standard error of 0.409.

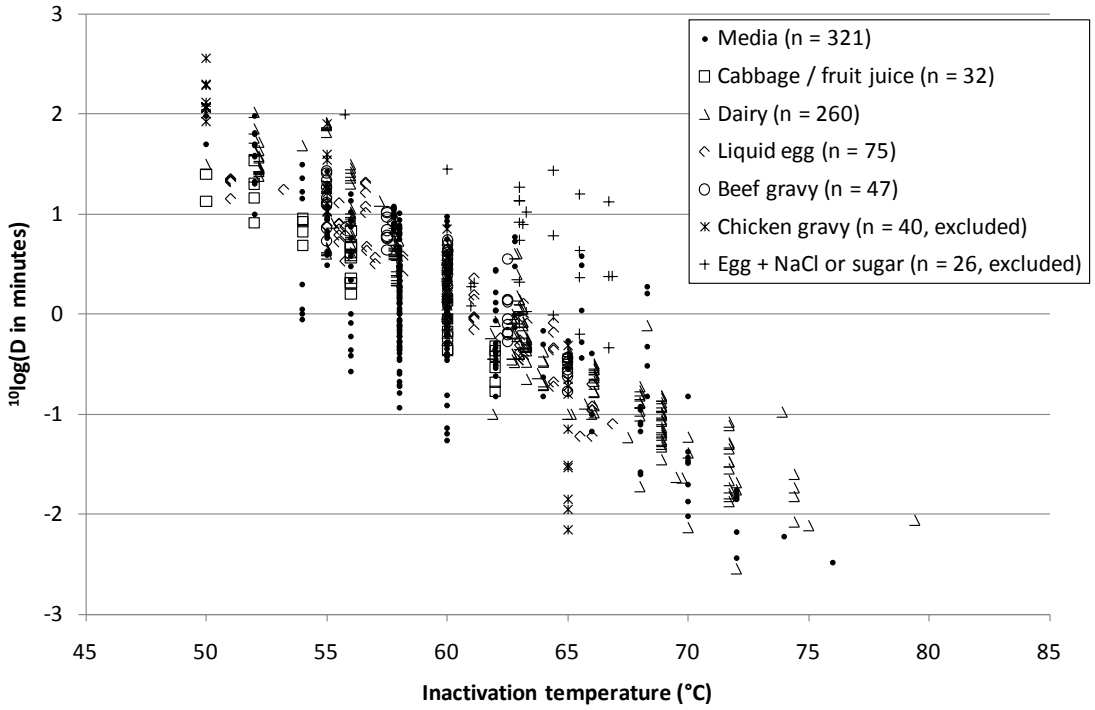

Figure 1: Variability of inactivation times (D = time to 10-fold reduction) of Listeria monocytogenes per heating menstruum as a function of the heating temperature. Inactivation times are not corrected for effects of other variables. Total number of data sets is 801 and 66 of these were excluded for further modelling (chicken gravy and liquid eggs with added sugar or sodium chloride). Fruit juices are apple, orange and white grape. Dairy includes milk, cream, butter and ice-cream. Liquid eggs are separated in whole, white and yolk. Media include deionised water, physiological saline, phosphate buffer, brain heart infusion, tryptose phosphate broth and trypticase soy broth (with or without yeast extract).

To select variables for the basic multivariate model including processing conditions and menstruum composition, all possible combinations of variables were tested, including leaving out one or more variables. To limit the complexity of the initial model, individual menstrua (17 groups) were not included at first. The selected best model had an R^2 of 88.3% and a standard error or 0.292 and is presented as model A in Table 1. Allowing for interaction between heating temperature and menstruum groups, i.e. allowing different slopes per menstruum group, did not change R^2 or standard error, and consequently interaction terms were not included. ^{10}log(sodiumchloride) was not significant (p = 0.055), had little effect on R^2 (88.4%) and the standard error (0.292) and was not included in model A.

Table 1: Coefficients (and standard error) of models of the effect of heat and other variables on 10log D (D = time in minutes for 10-fold inactivation). Significance levels are $p < 0.001$ unless indicated otherwise: ** $p < 0.01$, * $p < 0.05$, # $p < 0.1$, & $p > 0.1$.

Variable	Model A	Model B
Intercept	**9.33** (0.189)	**9.01** (0.170)
Heating temperature (°C)	**-0.161** (0.0025), z = 6.21	**-0.157** (0.0023), z = 6,37
pH	**0.165** (0.011)	**0.167** (0.011)
^{10}log(sugars % wt/vol)	**0.081** (0.018)	**0.090** (0.017)
^{10}log(fat % wt/vol)	**0.063** (0.014)	**0.060** (0.014)
Last temperature phase (°C) [a]	**0.0053** (0.009)	**0.0060** (0.009)
^{10}log (last temp. phase (h)) [a]	**-0.220** (0.028)	**-0.249** (0.027)
Heat shock difference (°C) [b]	**0.0153** (0.018)	**0.0138** (0.018)
Heating method 2 [c]	**-0.189** (0.047)	
Heating method 3 [c]	**-0.078** (0.037)*	
Heating method 4 [c]	0.078 (0.049)&	
Liquid egg [d]	**-0.142** (0.064)*	-0.074 (0.060)&
Beef gravy [d]	**0.516** (0.073)	**0.414** (0.073)
Cabbage / fruit juice [d]	**0.216** (0.077)**	0.116 (0.071)&
Media [d]	0.071 (0.051)&	0.069 (0.050)&
Estimated standard error	**0.292**	**0.298**
R^2	**88.3%**	**87.8%**
Number of data sets	735	735

[a] Duration and temperature of last temperature phase, either during culturing or storage, not heat shock.
[b] Heat shock (54 sets) temperature difference with the last temperature phase (culturing or storage).
[c] Heating method 1 = lab scale pasteuriser with flow (n = 93), 2 = low culture volume in large volume pre-heated menstruum (n = 211), 3 = low volume in submerged glass capillary tube or coil (n = 350), 4 = large volume in glass vial in water bath (n=81). Reference method is heating method 1.
[d] Reference menstruum is dairy

When all 17 individual menstrua were included in model A (instead of menstruum groups), milk, cream and some media were significantly different from other menstrua, R^2 was 89.9% and standard error 0.271. Whereas there could be merits in considering all menstrua separately, doing so would result in considerable increase of model complexity and general applicability, which is undesirable. Allowing polynomial effects of variables and interaction between variables in model A, the model would improve slightly (R^2 = 89.4, s.e. = 0.278), the polynome of ^{10}log(sodium chloride) would be included, as would the product of ^{10}log(sodium chloride) and ^{10}log(sugars). In this model, however, an increase of the ^{10}log(sodium chloride) terms would have a lowering effect on logD and this is contradictory to results in individual papers (Jorgensen *et al.* (1995), Juneja & Eblen (1999) and Edelson-Mammel *et al.* 2005). Furthermore, these changes would result in a lower and more uncertain intercept, only a low increase of R^2 and low decrease of the estimated standard error, as well as in increased complexity. Therefore, this change is suboptimal and model A is preferred. An even simpler model with a relatively high R^2 and low standard error also excludes the effect of the heating method from model A, resulting in model B (Table 1). This model is overall preferred, as the effect of heating method does not seem to follow logic; the best heating and cooling method (1: lab scale pasteuriser with flow) gives results that are not significantly different from the worst heating and cooling method (4: large volume in water bath). Model B is applied for inactivation of *L. monocytogenes* in raw milk (without pre-heating, i.e. no heat shock), described in Formula 1 (standard errors are given in Table 1).

$$^{10}\log D_{\text{raw milk}} = 9.01 - 0.157 \text{ heating temperature (76 °C)} + 0.167 \text{ pH (6.5 - 6.7)} + 0.090\ ^{10}\log(\text{sugar (4.5 - 4.7\%)}) + 0.060\ ^{10}\log(\text{fat (3.8 - 4.2\%)}) + 0.0060 \text{ temperature last storage phase (5-7 °C)} - 0.249\ ^{10}\log(\text{time last storage phase (16 – 80 h)}) \pm 0.298 \quad (1)$$

Sanaa *et al.* (2004) estimated mean concentrations of *L. monocytogenes* in raw milk from two areas in France at 0.3 and 0.8 cells/l, with their mean being 0.55 cells/l. Assuming a distribution of the concentration of Poission(Gamma (1;0.55)) cells/l, the P99.9999 in raw milk is 13 cells/l (10 million iterations). With the univariate model of 735 data sets, uncorrected for the effect of food composition and processing conditions, there is a calculated probability of 5.10^{-5} of the presence of a surviving *L. monocytogenes* cell in a litre of milk pasteurised at 76 °C for 20 s (assuming equal variance at all temperatures). Using the preferred model B, and assuming uniform distributions of variables with ranges described in Formula 1, the calculated probability is reduced to less than 1.10^{-7}, due to the lower variability resulting from the inclusion of the effect of product and process variables.

Conclusion

A practical multivariate regression model from literature data can be used to predict heat inactivation of *L. monocytogenes* in fluids like dairy (milk, cream, butter), fruit and vegetable juices and liquid eggs without additives. The model includes variability of strain tolerance to heat and limits the variability for specific processing conditions and food composition.

References

***Literature used as cited by* Doyle *et al.* (2001):** Bartlett & Hawke (1995), Beuchat *et al.* (1986), Bradshaw *et al.* (1991), Bunning *et al.* (1988), Bunning *et al.* (1990), Donnely & Briggs (1986), El-Shenawy *et al.* (1989), Fairchild & Foegeding (1993), Farber & Fagotto (1992), Foegeding & Stanley (1990), Foegeding & Stanley (1991), Golden *et al.* (1988), Jorgensen *et al.* (1995), Jorgensen *et al.* (1999), Juneja *et al.* (1998), Kamau *et al.* (1990), Knabel *et al.* (1990), Knight *et al.* (1999), Linton *et al.* (1990), Linton *et al.* (1992), Lou & Youssef (1996), Michalski *et al.* (2000), Muriana *et al.* (1996), Palumbo *et al.* (1995), Patchett *et al.* (1996), Quintavalla & Campanini (1991), Rowan & Anderson (1998), Schuman & Sheldon (1997), Sörqvist (1993), Sörqvist (1994), Sumner *et al.* (1991).

***Literature used as cited by* ICMSF (1996):** Boyle *et al.* (1990), Bradshaw *et al.* (1985), Bradshaw *et al.* (1987), Bunning *et al.* (1986), Huang *et al.* (1992).

***Literature used as cited by* Van Asselt & Zwietering (2006):** Casadei *et al.* (1998), Chhabra *et al.*(1999), Holsinger *et al.* (1992), Mazotta (2001).

Doyle M.E., Mazotta S.A., Wang T., Wiseman D,W, and Scott V.N. (2001) Heat resistance of *Listeria monocytogenes*. *Journal of Food Protection* 86 (3) 410-429.

Edelson-Mammel S.G., Whiting R.C., Joseph S.W. and Buchanan R.L. (2005) Effect of prior growth conditions on the thermal inactivation of 13 strains of *Listeria monocytogenes* in two heating menstrua. *Journal of Food Protection* 68 (1) 168-172.

Hassani M., Álvarez I., Raso J., Condón S. and Pagán R. (2005a) Comparing predicting models for heat inactivation of *Listeria monocytogenes* and *Pseudomonas aeruginosa* at different pH. *International Journal of Food Microbiology* 100: 213 - 222

Hassani M., Manas P., Raso J., Condón S. and Pagán R. (2005b) Predicting heat inactivation of *Listeria monocytogenes* under nonisothermal treatments. *Journal of Food Protection* 68 (4) 736-743

Hassani M., Manas P., Pagán R. and Condón S. (2007). Effect of a previous heat shock on the thermal resistance of *Listeria monocytogenes* and *Pseudomonas aeruginosa* at different pHs. *International Journal of Food Microbiology* 116: 228-38

Huang L. (2004) Thermal resistance of *Listeria monoeytogenes*, *Salmonella* Heidelberg, and *Escherichia coli* 0157:H7 at elevated temperatures. *Journal of Food Protection* 67 (8) 1666-1670

ICMSF (1996) Microorganisms in Foods 5. Characteristics of Microbial Pathogens. Blackie Academic & Professional London (ISBN 0412 47350 X)

Ignatova M., Leguerinel I. Guilbot M., Prévost H. and Guillou S. (2007) Modelling the effect of the redox potential and pH of heating media on *Listeria monocytogenes* heat resistance. *Journal of Applied Microbiology* 105: 875-883

Juneja V.K. and Eblen B.S. (1999) Predictive thermal inactivation model for *Listeria monocytogenes* with temperature, pH, NaCI, and sodium pyrophosphate as controlling factors. *Journal of Food Protection* 62 (9) 986-993

Maisnier-Patin S., Tatini S.R., and Richard J. (1995) Combined effect of nisin and moderate heat on destruction of *Listeria monocytogenes* in milk. Lalt 75: 81-91

Sanaa M, Corroler L and Cerf. O (2004) Risk Assessment of listeriosis linked to the consumption of two soft cheeses made from raw milk: Camembert of Normandy and Brie of Meaux. *Risk Analysis* 24: 389-399.

Van Asselt E.D. and Zwietering M.H. (2006) A systematic approach to determine global thermal inactivation parameters for various food pathogens. *International Journal of Food Microbiology* 107: 73-82

Van der Veen, S., Wagendorp A., Abee T. and Wells-Bennik M.J.H. (2009) Diversity assessment of heat resistance of *Listeria monocytogenes* strains in a continuous-flow heating system. *Journal of Food Protection* 72 (5) 999-1004(6)

Parameter estimation for dynamic microbial inactivation; which model, which precision?

K. D. Dolan[1,2], V.P. Valdramidis[3], D.K. Mishra[4]

[1] Department of Biosystems & Agricultural Engineering, Michigan State University, East Lansing, MI 48824 USA (dolank@msu.edu)
[2] Department of Food Science & Human Nutrition, Michigan State University, East Lansing, MI 48824
[3] UCD Biosystems Engineering, School of Agriculture, Food Science & Veterinary Medicine, University College Dublin, Dublin 4, Ireland (vvaldram@gmail.com)
[4] Néstle Nutrition, Fremont, MI (Dharmendra.Mishra@rd.nestle.com)

Abstract

One-step regression was used to estimate the dynamic microbial inactivation parameters of *E. coli* K12 using the differential form of three different models. Previously published microbial data were used in which samples of 100 μl with initial microbial concentration ~10^9 cfu/mL were heated at three different rates (1.64, 0.43, or 0.15°C/min), in duplicate, from 49.5 °C to 60°C over a total experimental time from 11 to 60 min. The best-performing models based on their statistical assessment were, in order: Geeraerd *et al.* (6 parameters), Weibull (6 parameters), and the first-order model (5 parameters). The statistics used to evaluate the models were: minimum root mean square error (RMSE); distribution of residuals; asymptotic standard errors of parameters; scaled sensitivity coefficients; and sequential estimation. RMSE for first-order model was nearly twice that for Geeraerd *et al*., showing that the first-order model was inappropriate for these data. The optimum reference temperature (T_{ref}) for the secondary model (Bigelow type) was interpolated by estimating all the other parameters for different fixed T_{ref} values, and choosing T_{ref} that minimized the correlation coefficient between AsymD_{ref} and z. The advantage of finding optimum T_{ref} was that it minimized the confidence interval for AsymD_{ref}. Scaled sensitivity coefficients of the Geeraerd al. model revealed that a) none of the parameters was linearly correlated with others, and b) that the most easily estimated parameters were the three initial microbial concentrations log$N(0)$, followed by z, AsymD_{ref} and log$C(0)$. Sequential estimation was also applied which derived parameter values after successively adding each data point. Sequential results showed that a) each parameter except from one of the log$N(0)$s nearly reached a constant half-way through the experiment, and b) parameter values were affected by heating rate. These results show that dynamic microbial inactivation parameters can be estimated accurately and precisely, directly from few experiments, potentially eliminating the need to apply isothermal parameters to dynamic industrial processes.

Keywords: Microbial inactivation modeling, parameter estimation, non-isothermal, optimum reference temperature

Introduction

Transposition of results obtained from static to dynamic conditions has shown that adjustment of the initial mathematical structure is required (Valdramidis *et al.* 2007; Bernaerts *et al.* 2002). Dolan (2003) and Valdramidis *et al.* (2008) have also shown that even if the results are excellent by the use of isothermal inactivation parameters one does not know the actual values of non-isothermal estimates. This highlights the importance of further studying parameter identification techniques under dynamic conditions representative of a realistic (processing) environment.

The objectives of this work were: 1) to demonstrate that non-isothermal microbial inactivation kinetic model parameters could be accurately and precisely estimated using one-step nonlinear regression following an ordinary least squares and a sequential approach; and 2) to determine based on statistical indices the best-performing out of three differential models.

Materials and Methods

Experimental

Previously published data (Valdramidis *et al*. 2008) were used. Briefly, samples of 100 μl with initial microbial concentration ~10^9 cfu/mL were heated at three different rates (1.64, 0.43, or 0.15°C/min), in duplicate, from 49.5 °C to 60°C over a total experimental time from 11 to 60 min.

Data Analysis

Three different types of models were used for this study: a log-linear, a Weibull (refer to its differential form) and the reduced model of Geeraerd *et al*. (2000) not incorporating the so called tailing effect. The latter reads as follow:

$$\frac{dN(t)}{dt} = k \cdot N(t) \Rightarrow \frac{d\log N(t)}{dt} = -\frac{1}{\ln 10} \cdot k \tag{1}$$

$$\frac{d\log C_c(t)}{dt} = -\frac{1}{\ln 10} \cdot k_{\max} \tag{2}$$

where k is

$$k = k_{\max}\left(\frac{1}{1+10^{\log C_c}}\right) \tag{3}$$

and k_{max} is given by the Bigelow model

$$k_{\max} = \frac{\ln 10}{\mathrm{Asym}D_{ref}} \exp\left(\frac{\ln 10}{z}(T - T_{ref})\right) \tag{4}$$

N is the microbial cell density cfu/mL, C_c is related to the physiological state of cells [-], k_{max} is the specific inactivation rate [1/min], $AsymD_{ref}$ is the asymptotic decimal reduction time at reference temperature T_{ref}, and z is the degrees Celsius temperature change causing a 10-fold change in AsymD_{ref}. Parameters were estimated both for all the heating rates simultaneously and for each heating rate alone using Ordinary Least Squares (OLS) minimization in Matlab (Version 2010a), nlinfit or lsqnonlin (statistical and optimization toolbox, respectively), and ode45 for the differential equations for each of the three models. Sequential estimation was performed in Matlab using the algorithm presented by Beck and Arnold (1977).

Results and Discussion

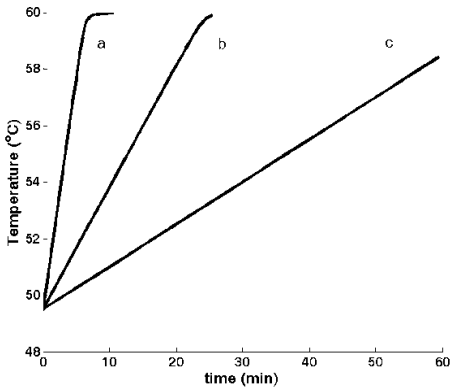

Figure 1: Temperature histories, performed in duplicate.

The temperature histories were approximated with nearly-linear curve fits (Figure 1).The optimum reference temperature T_{ref} was dependent on the model, even though the data were exactly the same. T_{ref} = 57.98, 58.68, and 58.1°C, in the Bigelow secondary model for the first-order, Weibull, and Geeaerad *et al.* models, respectively. T_{ref} was determined by minimizing the correlation coefficient between AsymD_{ref} and z by using all the experimental data sets (Figure 2).

Parameter estimation by OLS

The model fit of the Geeraerd et al. model is given in Figure 3. The RMSE= 0.435, 0.291, and 0.221 for the first-order, Weibull, and Geeaerd *et al*. models, respectively. The two 6-parameter models, with 3 representing the log$N(0)$s (Weibull and Geeaerd *et al*. with integrated Bigelow model) gave significantly better fits than the 5-parameter model (first-

order integrated with Bigelow model), as assessed by the reduced RMSE and verified by AIC_c. The parameter estimates and other statistical results for the Geeaerd *et al*. model are shown in Table 1. The condition number of the Jacobian = 9.3, a desirable low value indicating a very stable system for parameter estimation. The residuals (Figure 4) indicate that the errors met the following standard statistical assumptions: additive errors, zero mean, constant variance, uncorrelated (except for the slowest heating rate, Figure 1), and normal distribution (data not shown). The correlation coefficient between the two Bigelow parameters was nearly zero, due to choice of the optimum T_{ref}. The other parameters were not highly correlated. The relative standard errors for all parameters were small, under 7% (Table 1), giving desirable small confidence intervals. The scaled sensitivity coefficients were estimated as follows:

$$X'_{\beta_i} = \beta_i \frac{\partial \log N(t)}{\partial \beta_i} \tag{5}$$

where β_i is the ith parameter, are shown in Figure 5. None of the X' was linearly dependent, thereby allowing each parameter to be separately estimated. All of the X' were large, except log$C(0)$, which correspondingly had the largest relative standard error = 7% (Table 1). X' for parameters AsymD_{ref} and z were significantly larger for the slowest heating rate (Figure 5), showing that it was these data that most influenced their estimation. The parameter estimates for individual heating rates b and c were significantly worse than those for all the data. Parameters would not converge for heating rate a.

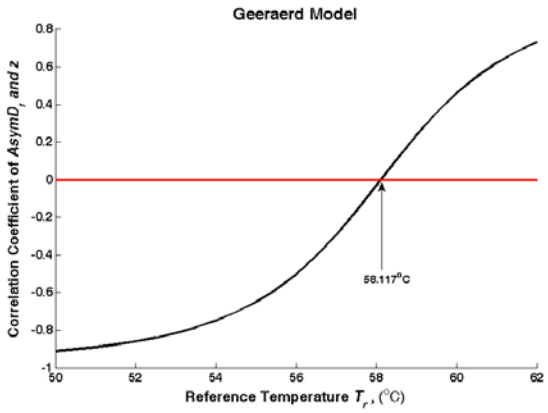

Figure 2: Correlation coefficient of AsymD_{ref} and z vs. reference temperature for Geeaerd et al. model.

Table 1: Parameter estimates for Geeaerd *et al*. model.

RMSE (log (cfu/mL))	0.221				
			95% conf		
parameters	estimate	std error	interval		cov (%)
Asym$D_{58.117\,C}$ (min)	2.20	0.05	2.09	2.30	2.5%
z (^{o}C)	5.14	0.08	4.98	5.31	1.6%
log$C(0)$	1.83	0.13	1.57	2.08	7.1%
log$N(0)_1$ (log (cfu/mL))	9.42	0.05	9.33	9.52	0.5%
log$N(0)_2$ (log (cfu/mL))	9.23	0.05	9.14	9.32	0.5%
log$N(0)_3$ (log (cfu/mL))	9.38	0.05	9.28	9.48	0.5%

Sequential estimation

Sequential results were plotted vs. –log$N(t)$ to determine how the parameters were continually updated with each datum addition as the log reductions increased. The results were favorable (Figure 6 is an example), in that they all reached a constant by half-way through the

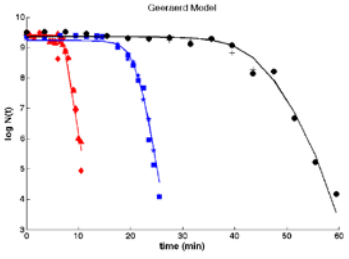

Figure 3: log(microbial concentration) vs. time. Observed (markers) and estimated (lines) for Geeaerd et al. model.

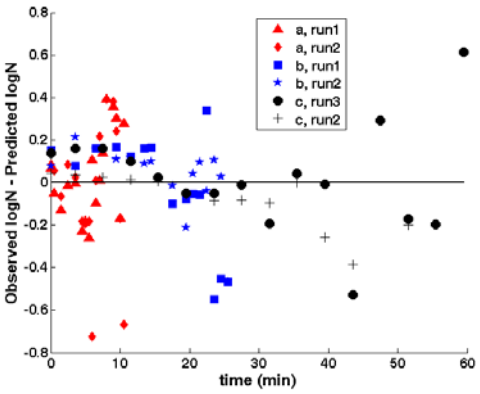

Figure 4: Residuals for Geeaerd *et al*. model.

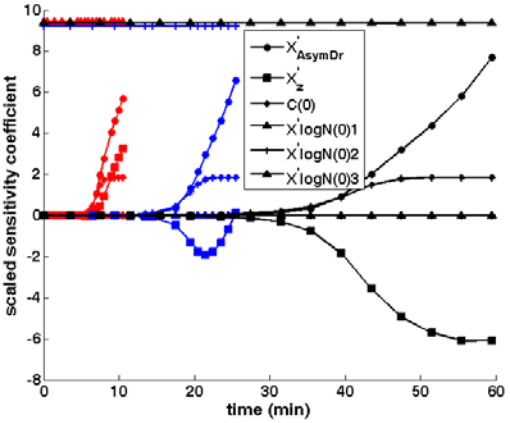

Figure 5: Scaled sensitivity coefficients for Geeaerd *et al*. model.

experiment, except for one of the log$N(0)$. Therefore, the experiment could be stopped when log$N(t)$ was approximately 7 (i.e., following 2.5 log reduction) with minimal loss of accuracy in the parameters. The final sequential estimates were very similar to those from OLS.

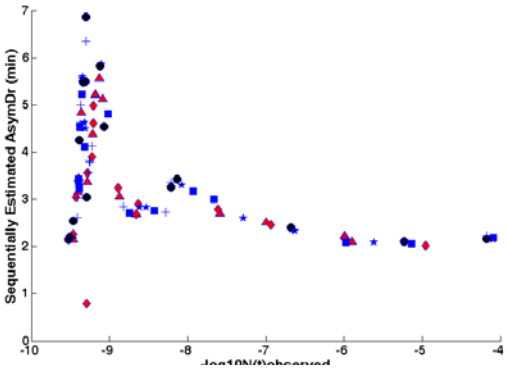

Figure 6: Sequential estimates of AsymD_{ref} vs –logN(t).

Conclusions

This work demonstrates that non-isothermal microbial inactivation parameters can be estimated accurately and precisely with a minimum of experiments and nonlinear regression. The slower heating rate allowed for more accurate estimates, while the faster heating rate would not allow convergence alone. The larger value of the scaled sensitivity coefficients also confirmed that slower heating rates give more accurate estimates, especially for the *z* parameter, because the temperature was still changing while microbe survivor numbers were decreasing. These methods (OLS and sequential estimation) can be used as alternatives to numerous isothermal experiments and multiple-step linear regression, which typically have too few degrees of freedom to attain desirable small standard error for the Bigelow *z* parameter. Additionally, the performance of three different inactivation models widely used in the literature was compared based on statistical indices. Further studies will focus on assessing the specific structural properties of these models (e.g., parameter interpretation, time dependency).

References

Beck J. V. and Arnold K. J. (1977) Parameter Estimation in Engineering and Science. John Wiley & Sons, Inc., New York.

Dolan K. (2003) Estimation of kinetic parameters for nonisothermal food processes. *Journal of Food Science* 68, 728–741.

Geeraerd A.H., Herremans C.H. and Van Impe J.F. (2000) Structural model requirements to describe microbial inactivation during a mild heat treatment. *International Journal of Food Microbiology* 59, 185–209.

Valdramidis V. P., Geeraerd A. H., Bernaerts K. and Van Impe J. F. M. (2008) Identification of non-linear microbial inactivation kinetics under dynamic conditions. *International Journal of Food Microbiology* 128, 146-152, doi:DOI 10.1016/j.ijfoodmicro.2008.06.036.

Valdramidis P., Geeraerd A. and Van Impe J. (2007) Stress adaptive responses by heat under the microscope of predictive microbiology. *Journal of Applied Microbiology* 103, 1922–1930.

Predictive model for bioactive stability during non-isothermal heat treatment and storage in beverages: Case study of acidified feverfew beverages.

J.-C. Jacquier, N. Harbourne, E. Marete, D. O'Riordan

Institute of Food and Health, School of Agriculture, Food Science and Veterinary Medicine, University College Dublin, Belfield, Dublin 4, Ireland. (jean.jacquier@ucd.ie)

Abstract

Recently, phytochemical constituents have attracted a lot of interest as potential sources of bioactive ingredients in food product formulations. However, before being incorporated into foods or beverages, the stability of these bioactive constituents during both processing and storage must be considered. This presentation will focus on recent work in our laboratory concerned with developing a non isothermal model to accurately predict the effects of both storage and thermal processing conditions on the stability of phytochemical bioactives, in particular to the case of pH-catalysed degradation of parthenolide in acidified feverfew beverages. It will be shown that this mathematical model for non-isothermal bioactive degradation has many advantages as it mimics well the industrial heat-treatment processes while minimising the number of experiments necessary to its validation. Also, its implementation leads to a full understanding of the complex influences of time, temperature and pH on bioactive stability, thereby allowing the accurate prediction of bioactive shelf-life.

Keywords: *non-isothermal degradation, bioactive, shelf-life, prediction model*

Introduction

The incorporation of bioactive compounds into functional foods is a rapidly growing market (Bech-Larsen and Scholderer 2007) matched by an increased consumer interest in traditional products has lead recent studies to focus on the potential of phytochemicals as natural sources of health promoting ingredients for functional foods and beverages (Gruenwald 2009). Despite these promising opportunities, one of the main issues associated with the incorporation of natural phytochemicals in beverages is related to the inherent thermal instability of these bioactive molecules, and their potential degradation during either the traditional heat treatments necessary to inactivate food-borne pathogens or during the typically long non-refrigerated shelf-lives of these food products.

The use of a non-isothermal model based on the works of Dolan (2003) has been found to allow rapid access to all kinetic parameters of the degradation processes, while helping to mimic the heat processes encountered in the food industries (Harbourne, Jacquier, Morgan and Lyng 2008). Here, this model is presented in the case study of acidified beverages fortified with feverfew (Tanacetum parthenium), a medicinal herb used traditionally to treat various conditions including prophylaxis of migraine headaches, relief of pain and inflammation from arthritis. Pharmacological studies indicate that a sesquiterpene lactone, parthenolide is responsible for the biological activity of feverfew preparations (Kang, Chung and Kim 2001), but this bioactive is known for its lability in acidic media (Fonseca, Rushing, Thomas, Riley and Rajapakse 2006). In addition, feverfew contains phenolic compounds which have been reported to possess anti-inflammatory activity (Williams, Harborne, Geiger, and Hoult 1999), but due to latent Polyphenol Oxidase (PPO) activity, these phenols have been shown to degrade quite rapidly in pH neutral solutions and lead to substantial browning of the beverages upon storage.

Therefore, the objectives of this study were first to determine the thermal degradation kinetics of parthenolide using a non-isothermal method in feverfew infusions, at pH levels representative of those that are commonly encountered in beverage products. Secondly to establish a model unifying the combined influence of time, temperature and pH on parthenolide degradation in order to predict the loss associated with heat processing in

acidified beverages. Lastly, to use the model to predict the loss of the parthenolide bioactive upon storage and to optimise the acidification level of the beverage in order not only to minimise bioactive degradation, but also to minimise browning, leading to an acceptable shelf-life of the final beverage.

Materials and Methods

Beverage preparation and analysis.

Organically grown feverfew was harvested in Roscommon, Ireland. The aerial parts were frozen at -20 ºC and subsequently freeze-dried and then ground into a moderately fine powder before being extracted in water at 100 ºC for 10 mins as described in detail by Marete *et al*. (2009). The pH of the infusions was then adjusted using various concentrations of citric acid and sodium citrate to achieve a pH of 2.9, 3.7, 4.6 and 6.0 with a final citric/citrate concentration of 0.06 M to mimic the citric content in fruit beverages. 1.5 ml aliquots were then filtered using 0.2 µm GHP membrane into small HPLC vials closed with a Teflon septum thus preventing any liquid loss even at high temperature. After heat treatment or storage, with temperature recordings inside the sample vials using fast response type K thermocouples, HPLC analysis of parthenolide content was carried out as described in detail in Marete *et al*. (2009).

Results and Discussion

The non-isothermal method is based on a single experiment in which the temperature is recorded as a function of time. Thus the kinetic parameters can be determined from this single experiment that covers the desired temperature range (Dolan 2003). For this case study, the samples were submitted to non-isothermal heat treatments such as those presented in figure 1.

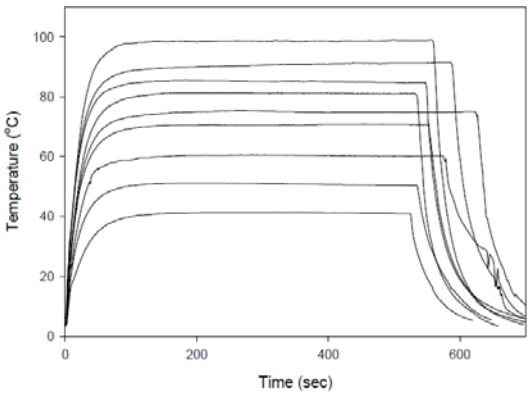

Figure 1: Examples of the temperature profiles of the heat treatments subjected to the samples.

These heat-treatments clearly show the temperature profiles achieved by the samples which allowed for a fast heating rate (up to 80 °C/min) to the desired temperature, followed by the required holding time. The temperature of the sample then dropped sharply due to the fast cooling of the samples in ice to stop further thermal degradation.

From these curves, the independent variables time (t) and sample temperature (T) were combined into one variable, the thermal history (β), according to Eq. (1):

$$\beta = \int_0^t \exp\left[-\frac{E_a}{R}\left(\frac{1}{T(t)} - \frac{1}{T_{ref}}\right)\right] \mathrm{dt} \qquad (1)$$

where T_{ref} is the arbitrary reference temperature and T(t) is the temperature T at time t.

The measured C/C_0 values indicating the ratio of bioactive left in the sample after heat treatment could then be plotted as a function of β as shown in figure 2.

In view of the exponential decay of the parthenolide concentration ratio with thermal history (figure 2), first-order kinetic rate constants (k) were calculated according to equation 2:

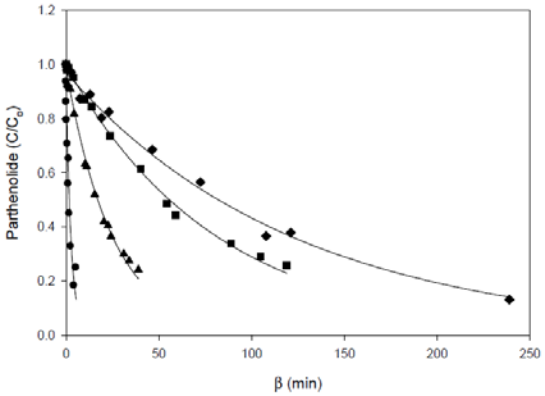

Figure 2: Parthenolide degradation in beverages at pH 2.9 (●), 3.7 (▲), 4.6(■) and 6.0 (♦) against thermal history (β) at a reference temperature of 100°C. The lines are non-linear fits calculated according to equation 2.

$$\frac{C}{C_0} = \exp(-k\beta) \tag{2}$$

The experimental and calculated values showed a good fit as evidenced by good correlation coefficients ($r^2 > 0.98$). Infusions at pH 6.0 exhibited a slow degradation rate constant of (8.0 ± 0.4) x 10^{-3} min^{-1} increasing to (259 ± 39) x 10^{-3} min^{-1} at pH 2.9. The time required to cause a 10 % degradation of parthenolide at pH 6.0, 4.6, 3.7 and 2.9 were 13.2, 8.6, 2.6 and 0.3 minutes respectively, indicating low degradation during heat treatment except for the most acidic beverages. There was no major effect on the calculated activation energies (Ea) with pH (88.5 to 89.6 kJ/mol) indicating a similar reaction mechanism in the chemical reactions involved at all the pH levels studied. The evolution in acidic media (pH ≤ 7) of the rate of degradation of parthenolide k with pH was then modelled according to equation 3

$$k_{pH} = k^0 + A\left[H_3O^+\right] \tag{3}$$

where k^0 is the first order rate constant for parthenolide degradation at neutral pH and A is a constant which indicates the pH dependency of the degradation rate.

By combining the degradation at a reference temperature (equation 1) and reference pH (equation 3), the kinetic parameters of parthenolide degradation as a function of combined pH and temperature can therefore be estimated according to equation 4:

$$k(T, pH) = (k^0_{Tref} + A\left[H_3O^+\right]) \times \exp\left[-\frac{E_a}{R}\left(\frac{1}{T(t)} - \frac{1}{T_{ref}}\right)\right] \tag{4}$$

where k^0_{Tref} is the degradation rate at the reference Temperature T_{ref} and neutral pH.

This equation enabled the drawing of a "master curve" of parthenolide degradation at pH 4.5 and a reference temperature of 100 °C as shown in figure 3a. Together with all experimental points at various pH, temperature and time treatments, this figure also shows the predicted residual parthenolide concentrations according to equation 4 at these reference temperature and pH values (represented by the line). Considering the extent of experimental variations in terms of pH, time and temperature encompassed in this figure, the goodness of fit of the model is excellent ($r^2 > 0.99$ and Standard Error of Estimates 0.03 on all 47 independent samples) and can readily be used to predict the optimum pH and time-temperature profile required for retaining the parthenolide content during heat processing e.g. pasteurisation processes. For example, a mild acidic (~pH 4.5) beverage can be processed at 100 °C for up to 2 mins holding time and retain parthenolide content of more than 95%.

Despite this apparent stability of parthenolide to the classic heat treatment processes (pasteurisation, sterilisation), excessive degradation can be predicted at room temperature (figure 3b). For example, one can estimate the storage time required to degrade 10%

parthenolide at pH 4 (5.4 ± 0.4 d) or the minimum pH to ensure less than 20% degradation over 30 days (pH > 4.74). In order to protect bioactive stability for a reasonable shelf-life, refrigeration is shown to be necessary (figure 3b). For example, refrigerated storage of acidified feverfew beverages to a pH value of 4.5 will retain 90% of parthenolide for approximately 3 months while room temperature storage for the same period will result in a 65% loss in bioactive.

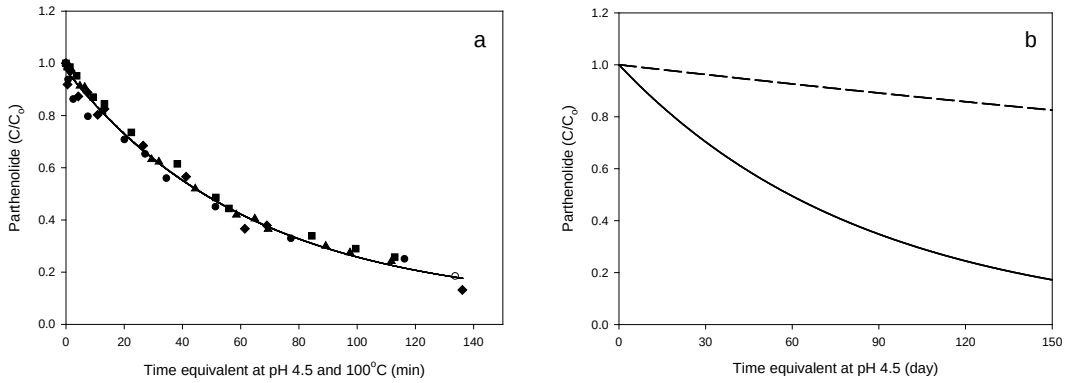

Figure 3: (a) Parthenolide degradation in feverfew infusions at pH 2.9 (●), 3.7 (▲), 4.6 (■) and 6.0 (♦) at various temperatures (5-100 °C) and reported at a reference pH of 4.5 and a reference temperature of 100°C. The line is the estimated degradation loss calculated from equation 4. (b) Prediction of parthenolide degradation upon storage at 5 °C (hatched line) and 22°C (solid line) in pH 4.5 beverages.

Conclusions

These results provide very important information for the development of functional beverages. The development of a unified degradation model combining pH, time and temperature is likely to be a useful tool not only to estimate the impact of traditional heat treatment processing on the degradation of bioactives, but also to assess the bioactive loss during storage.

This model can therefore predict the need for alternative heat treatment protocols and for refrigerated storage at an early stage in the development of functional beverages in order to ensure maximum retention of bioactive compounds is delivered to the consumer.

Acknowledgements

This work was funded by the Food Institutional Research Measure (FIRM) administered by the Department of Agriculture, Fisheries and Food, Republic of Ireland.

References

Bech-Larsen T. and Scholderer J. (2007) Functional foods in Europe: Consumer research, market experiences and regulatory aspects. *Trends in Food Science and Technology* 18, 231–234.

Dola, K. D. (2003) Estimation of kinetic parameters for non-isothermal food processes. *Journal of Food Science* 68 (3), 728-741.

Fonseca J. M., Rushing J. W., Thomas R. L., Riley M. B. and Rajapakse N. C. (2006) Post-production stability of parthenolide in feverfew. *Journal of Herbs, Spices and Medicinal Plants* 12, 139–152.

Gruenwald J. (2009) Novel botanical ingredients for beverages. *Clinics in Dermatology* 27, 210–216.

Harbourne N., Jacquier J.C., Morgan D. J. and Lyng J. G. (2008) Determination of the degradation kinetics of anthocyanins in a model juice system using isothermal and non-isothermal methods. *Food Chemistry* 111 (1), 204-208.

Kang B. Y., Chung S. W. and Kim T. S. (2001) Inhibition of interleukin-12 production in lipopolysaccharide-activated mouse macrophages by parthenolide a predominant sesquiterpene in Tanacetum parthenium: Involvement of nuclear factor. *Immunology Letters* 77, 159–163.

Marete E. N., Jacquier J. C. and O'Riordan D. (2009) Effects of extraction temperature on the phenolic and parthenolide contents, and colour of aqueous feverfew extracts. *Food Chemistry* 117(2), 226-231

Williams C. A., Harborne J. A., Geiger H. and Hoult J. B. S. (1999) The flavonoids of Tanacetum parthenium and T. vulgare and their anti-inflammatory properties. *Phytochemistry* 51(2), 417-423

Effect of water activity and storage conditions on shelf life of packaged bakery product

T. De Broucker, M. El Jabri, D. Thuault

ADRIA Développement, ZA Creac'h Gwen F29196 Quimper Cedex
(thibaud.debroucker@adria.tm.fr, mohammed.eljabri@adria.tm.fr, dominique.thuault@adria.tm.fr)

Abstract

The formulation of foodstuff and the storage condition have great influences on water activity (a_w) value and its evolution during its shelf life. The aim of this work is to study the effect of food composition and storage conditions on the a_w and moulds development (growth rate) on bakery products. Firstly, the impact of the formulation of foodstuff on the a_w was studied using AwDesigner ® computer program for a_w simulation integrating the vaporization during baking. Secondly, we modeled the influence of storage conditions (relative humidity of storage, temperature, time) and water permeability of the packaging on the evolution of the water activity in bakery products. Nine different packaging, different temperature conditions (for 10 to 40°C) and different relative humidity (from 40 to 85%) were studied. Packaging water permeability and a_w evolution are greatly influenced by storage conditions (temperature and relative humidity). Storage conditions on textural properties were also studied. The impact of a_w on the development of five moulds species was studied: *Aspergillus flavus*, *Cladosporium cladosporoïdes, Eurotium herbariorum, Penicillium chrysogenum*, and *Wallemia sebi*. Potato Dextrose Agar was adjusted with glycerol in order to obtain a wide range of a_w. In addition, temperature was studied in the range of 10 to 40°C. Fungal development shows two parameters: the growth rate (which is expressed as the increase of colony diameter per day) and the lag time (or moulds apparition time). Rosso model (1993) was used to describe the influence of temperature and a_w on growth rate. This model allows to evaluate the cardinal values of water activity (a_{wmin}, a_{wopt} and a_{wmax}) and temperature (T_{min}, T_{opt}, T_{max}) for each studied moulds. Such models allow to predict the shelf life of the products integrating formulation, baking, packaging permeability and environmental storage conditions.

Keywords: *water activity, shelf life, bakery*

Introduction

Food shelf life is directly influenced by the a_w of the product. The shelf life can be defined either by microbiological criteria or by sensory criteria. During its lifetime, transfers of water take place between the baked products and the surrounding air. And the physical properties may change. Initially, we have determined the impact of storage conditions (temperature, relative humidity and type of packaging) on the evolution of the a_w of the product. Then we modeled organoleptic shelf life by evaluating critical organoleptic a_w value. We have also modeled the impact of water activity on moulds development.

Material and methods

Formulation of the bakery products

The formulation of the studied cake is composed of flour meal (29%), rapeseed oil (18%), sucrose (24%), whole egg (18%), sorbitol (3%), water (6%), glucose syrup DE 60 (2.1%), salt (0;5%) and baking yeast (0.4%). The cakes have been cooked in a bakery oven 11 minutes at 180°C, using a 25g cake mold. Cooked cakes were ground before a_w measurements.

The sorption isotherm of the cake was realized using salt concentrated solutions method, using 7 saturated salt solutions in a range for a_w from 0.113 to 0.900. Then we have used the Ferro-Fontan model to fit the sorption isotherm. The Ferro-Fontan parameters for the sorption

isotherm are: α=1,0882; β=0,07627; C=-1,0983 (Chirife *et al.* 1980). The accuracy of the model were evaluated using eq 2 is 6.1%.

$$X = \left[\left[\ln\left(\frac{\alpha}{a_w}\right)\right].\left[\frac{1}{\beta}\right]\right]^{C} \quad (1)$$

Permeability of packaging

9 different packaging were studied during this work, most of the packaging was bi-oriented polypropylene base with different induction (PVDC, EVOH, aluminum). Equation 2 gives the permeability of the packaging (K) as a function of the flux of water across the packaging (dm/dt), the gradient of water activity (da_w) and the total area of the packaging (A).

$$K = \frac{dm}{dt}\frac{1}{\Delta a_w.A} \quad (2)$$

The accuracy of the model is calculated using Root Mean Square Value (RMS, eq 3).

$$\boldsymbol{RMS^2} = \sum_{\boldsymbol{i=1}}^{\boldsymbol{n}} \frac{\left(\frac{K_{predicted}-K_{exp}}{K_{exp}}\right)^2}{n} \quad (3)$$

Texture Measurement

The textural properties was measured on different cakes stored at different conditions using a texturometer TAXT2 in compression test (speed: 1mm/s, cylinder of 2.5mm diameter).

Growth simulation of moulds

The impact of a_w on the development of five moulds species was studied: *Aspergillus flavus*, *Cladosporium cladosporoïdes, Eurotium herbariorum, Penicillium chrysogenum*, and *Wallemia sebi*. Potato Dextrose Agar was adjusted with glycerol in order to obtain a wide range of a_w (from 0.78 to 0.998). Otherwise, temperature was studied in the range of 10 to 40°C. The temperature and a_w cardinal values for growth has been defined by using Rosso model (Sautour *et al.* 2001, eq 4).

$$\gamma(aw) = \begin{cases} aw < aw_{\min}, & 0 \\ aw_{\min} < aw, & \dfrac{(aw - aw_{\min})^2 (aw - 1)}{(aw_{opt} - aw_{\min})\left[(aw_{opt} - aw_{\min})(aw - aw_{opt}) - (aw_{opt} - 1)(aw_{opt} + aw_{\min} - 2aw)\right]} \end{cases} \quad (4)$$

Results and discussion

Development of models for the simulation of the packaging permeability

The normalized method to evaluate permeability of the packaging requires calculating the permeability of packaging at 38 ° C and 90% relative humidity. This value is not useful in industry because the storage of pastry products is generally carried out at 15 to 22°C.

$$K = K_F.0{,}9.1{,}9^{\left(\frac{T-38}{10}\right)} \quad (5)$$

We have evaluated the permeability of each studied packaging in several conditions of temperature and relative humidity. The results show that the permeability of the packaging is strongly influenced by temperature and gradient of relative humidity across the packaging. Equation 5 shows the influence of temperature (T) on permeability of packaging (K). K_F is the permeability value from providers. The parameter (1.9) is obtained by fitting experimental

value with the model. Because of the very weak value of water permeability at 8°C, the RMS is 59%. At 40°C, the RMS of the fitting is 19.8%. At 20°C, the RMS is 27.7%.

Evolution of the water activity of the cake during the shelf life

During the storage and independently of the storage temperature, cakes a_w and cakes water content changes on the sorption isotherm (fig. 1).

The evaluation of the water content of the cake during the storage is given by eq 6. This equation is obtained from eq 1 where X_i is the initial water content and X_t is the water content at t time and take into account the storage conditions. Using eq 5 and sorption isotherm (eq 1) of the cake, we can evaluate the a_w of the cake during the storage. We have developed a program on Matlab® in order to simulate aw during the shelf life of the cake.

$$X_t = \frac{(X_i.MS - K.A.\Delta a_w.t)}{MS} \quad (6)$$

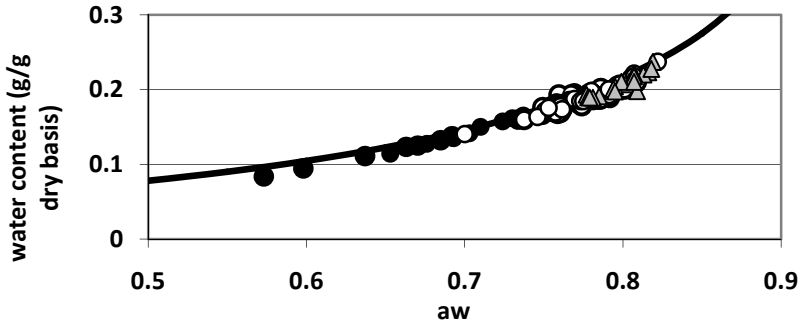

Figure 1: superposition of sorption isotherm (---) and evolution of the aw and water content of the cake during storage (Δ: at 8°C, ○ at 20°C, ● at 40°C).

Evolution of texture as a function of aw

Figure 2 shows the impact of water activity on textural properties of the cake. Sensory analysis shows that the critical value for textural properties is 1000 g/mm, the critical value for a_w is 0.71. Under this value, the cake is not smooth enough. By modeling the evolution of water activity, we can determine the storage time needed to obtain this value.

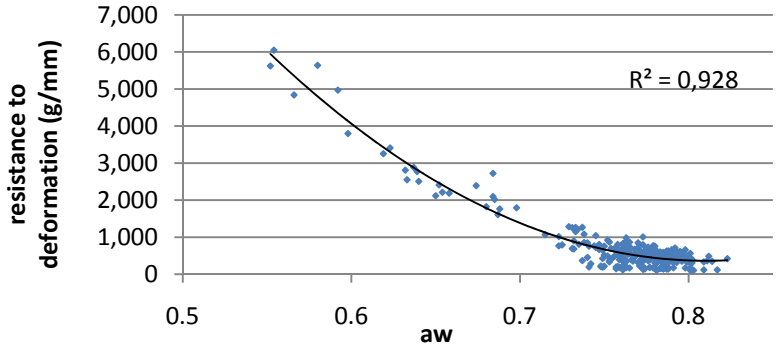

Figure 2: Impact of water activity on textural properties of the cake

Modeling moulds development

In order to define the impact of water activity on microbiological shelf life, we have studied the growth of five species of molds, using Zwietering (Zwietering *et al.* 1991) and Rosso (Sautour *et al.* 2001) models. This work has identified the cardinal values for temperature

(T_{opt}, T_{max} and T_{min}) and a_w (a_{wmin}, $a_{w\ opt}$). Figure 3 shows the impact of temperature and a_w on appearance time of the molds. The microbiological shelf-life of pastry product is generally regarded as the time of appearance of mold on the surface of the products. This work shows that a_w and storage temperature have a great impact on microbiological shelf life of food products.

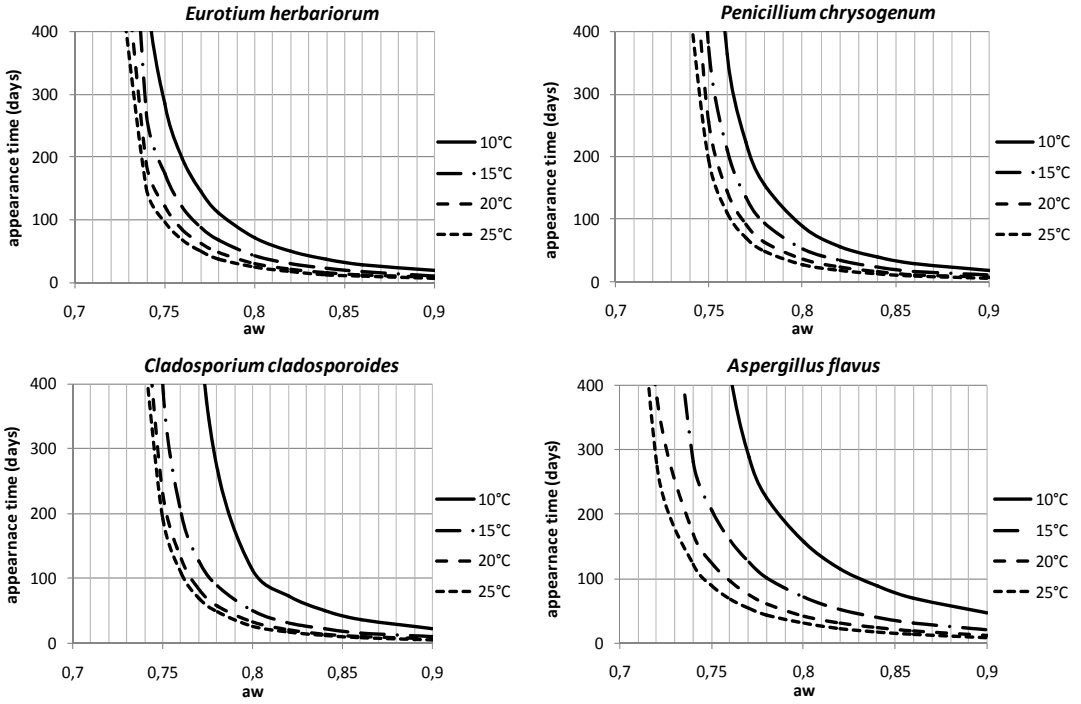

Figure 3: Appearance time of molds as a function of aw and temperature.

Conclusion

The shelf life of bakery products depends on two main factors: moulds development and textural properties. We can evaluate critical a_w for each of these two factors.

To ensure food safety and organoleptic properties, producers have to find the intermediate a_w values and keep it at a stable value. The science of formulation and use of several ingredients (like polyol) with strong ability to depress water activity is a great way to reduce water activity and molds development. The use of packaging with low water permeability is a solution to increase the life of pastry products. This work also enables the development of a software designed to simulate the evolution of a_w depending on storage conditions.

References

Rosso L., Lobry J.R., Bajard S. and Flandrois J.P. (1995) Convenient model to describe the combined effects of temperature and pH on microbial growth. *Applied Environmental Microbiology* 61, 610-616.

Zwieterring J.T., Koos J.T., Hasenack B.E. Wit J.C. and Van't Riet K. (1991) Modelling of bacterial growth as a function of temperature. *Applied Environmental Microbiology* 57, 1094-1101.

Chirife J., Ferro Fontán C. and Benmergui E.A. (1980) Prediction of water activity of aqueous solutions in connection with intermediate moisture foods. IV: aw prediction in aqueous nonelectrolyte solutions. *Journal Food Technol*ogy 15, 59-70.

Sautour M., Dantigny P., Divies C. and Benssoussan M. (2001) A temperature type model for describing the relationship between fungal growth and water activity. *International Journal of Food Microbiology* 67, 63-69.

Inhibition of growth of *Penicillium expansum* and *Botrytis cinerea* by copper sulphate

D. Judet-Correia[1], M. Bensoussan[2], C. Charpentier[3], P. Dantigny[2]

[1] Laboratoire Eau, Molécules actives, Macromolécules, Activité, AgroSup Dijon, Université de Bourgogne, France. (correiadaniela@hotmail.fr)
[2] Laboratoire de Génie des Procédés Microbiologiques et Alimentaires, AgroSup Dijon, Université de Bourgogne, France. (bensouss@u-bourgogne.fr, phdant@u-bourgogne.fr)
[3] Institut Universitaire de la Vigne et du Vin, UMR INRA 1131. (claudinecharpentier@neuf.fr)

Abstract

Copper sulphate is the active component of Bordeaux and Burgundy mixtures, fungicides used for vineyard treatments. This study aimed to investigate the effect of copper sulphate (from 0 to 8 mM) on radial growth rate and lag time of two moulds responsible for vine grapes spoilage: *Penicillium expansum* strain 25.03 and *Botrytis cinerea*, strains BC1 and BC2. By modeling the effect of copper on the radial growth rate, the concentrations at which $\mu = \mu_{opt}/2$, (Cu_{50}), were in the range of 2.2 to 2.6 mM. *P. expansum* exhibited a linear correlation (r = 0.84) between the radial growth rate and the reciprocal of the lag time. In contrast, in the range 0-4 mM, the radial growth rate of *B. cinerea* decreased whereas the lag time was constant. In the range 4-8 mM, the radial growth rate of *B. cinerea* was almost constant (c.a. 1 mm d^{-1}) while the lag time was increased. Therefore, the minimum inhibitory concentration, MIC, was not defined as the concentration at which no growth was observed, but as the concentration at which the lag time was infinite. The MIC values that depended significantly on the moulds were 4.7 mM for *P. expansum*, 8.2 and 7.3 mM for *B. cinerea* strain BC1 and BC2 respectively.

Keywords: *Penicillium expansum, Botrytis cinerea, inhibition, growth, copper*

Introduction

Penicillium expansum and *Botrytis cinerea* are fungi which commonly infect grape berries (Laforgue *et al.* 2009). Bordeaux and Burgundy mixtures are fungicides based on copper sulphate that are necessary to prevent from the growth of these moulds in vineyards. However, due to regular treatments with these fungicides, copper can be accumulated in the soils up to 250 mg/kg (Pietrzak and McPhail 2004). In order to ensure the sustainability of vineyards, it is necessary to limit the quantities of copper applied to these cultures. Little information is available on the inhibitory effect of copper sulphate on these two grape rot fungi. The aim of this study was to assess the influence of copper sulphate on radial growth rate and lag time of one strain of *P. expansum* and two strains of *B. cinerea*. The minimum inhibitory concentration, MIC, for copper sulphate, was determined for these fungi by means of predictive models.

Materials and Methods

Penicillium expansum (strain 25.03) and *Botrytis cinerea* (strain BC1 and BC2) were isolated from cv. Pinot grapes in September 2007 (Burgundy, France). Moulds were maintained on Potato Dextrose Agar medium (PDA) at room temperature, from 17 to 25°C.

Fungi were inoculated on PDA medium and incubated at 25°C for 7 days. Sporulating cultures were flood with 4.5 ml of a saline solution (NaCl, 9 $g.l^{-1}$) that contained Tween 80 (0.1 % vol/vol). Suspension counts were determined by a Malassez cell and standardised to 10^6 spores ml^{-1}. 10 µl of the spore suspensions were used to inoculate the centre of the dishes.

The PDA medium, pH 5.7, 0.99 a_w, was used for assessing the influence of copper sulphate on radial growth rate and lag time. Copper sulphate was added to PDA medium as a solid salt ($CuSO_4 \cdot 5\ H_2O$) to final concentrations from 0 (control cultures) to 8 mM of copper (II) ions with a 1 mM increment. The incubation temperature was 25°C.

Growth was evaluated daily by measurement of the diameter of the fungal colony along two perpendicular diameters. The mean radius was plotted against time and radial growth rates, μ, (mm day^{-1}) were evaluated from the slopes by linear regression. The lag time, λ (h), was determined from the intercept of the straight line with the initial radius of the inoculated droplet (ca 4.5 mm). All experiments were carried out in triplicate at least for a maximum period of 8 weeks. Prior to fitting a square-root (Dantigny and Bensoussan, 2008) logarithmic (Zwietering *et al.* 1994) transformations were used to stabilise the variance of μ and λ, respectively.

Models

The influence of copper sulphate on the radial growth rate was assessed by the following:

$$\sqrt{\mu} = \sqrt{\frac{\mu_{opt}}{1+\left(\frac{Cu}{Cu50}\right)^{p}}} \quad (1)$$

where μ_{opt} (mm d^{-1}) is the radial growth rate at Cu = 0 mM; Cu_{50} (mM) is the copper sulphate concentration at which $\mu = \mu_{opt}/2$ and p, a design parameter.

The influence of copper sulphate on lag time was determined by the reciprocal of a re-parameterized Monod-type equation :

$$\ln(\lambda) = \ln\left(\lambda_{opt}\frac{Cu_{200}\cdot MIC - 2Cu_{200}\cdot Cu + Cu\cdot MIC}{Cu_{200}\cdot(MIC - Cu)}\right) \quad (2)$$

where λ_{opt} (h) is the lag time at Cu = 0 mM; Cu_{200} (mM) is the copper sulphate concentration at which $\lambda = 2\lambda_{opt}$ and MIC (mM) is the minimum inhibitory concentration of copper sulphate at which the lag time is infinite.

Results and Discussion

Effect of copper sulphate on growth

The optimum growth rates, μ_{opt}, were determined at 0mM copper. The copper sulphate concentrations at which the growth rate was equal to $\mu_{opt}/2$, Cu_{50} were estimated by the growth inhibition model. The optimum radial growth rate of *P. expansum* strain 25.03 was equal to 2 mm d^{-1} (Table 1) and characterized by a narrow confidence interval (ca. 10 % error). At Cu_{50} = 2.41 mM, the radial growth rate was equal to half the optimum growth rate, 1 mm d^{-1}. The design parameter was significantly greater than 1. The low RMSE value showed the suitability of the model for describing the effect of copper sulphate on the radial growth rate of *P. expansum* 25.03.

At 0 mM copper *B. cinerea* strains BC1 and BC2 exhibited μ_{opt} values equal to 15.9 and 14.3 mm d^{-1} respectively, Table 1. The confidence intervals overlapped, therefore the μ_{opt} values of the strains BC1 and BC2 did not differ significantly. The model provided a good estimation of this parameter, (less than 10 % and 7 % error for BC1 and BC2 respectively). The p values were 3.04 and 3.59 respectively.

The optimum radial growth rates of *B. cinerea* strains BC1 and BC2 were greater than that for *P. expansum* 25.03. But, the Cu_{50} values were no significantly different between the studied strains (ca. 2.4 mM). The Cu_{50} did not depend on the radial growth rate. *B. cinerea* strains were characterized by smaller p values than *P. expansum* although the differences were not significant. Model proved less accurate for *B. cinerea* than for *P. expansum* (see Table 1).

Usually the decrease of the growth rate with increasing the concentration of the inhibitor can be represented by a model exhibiting an upward or a downward concave shape (Dantigny *et al.* 2005). In such a case the minimum inhibitory concentration, MIC, can be determined as the concentration of the inhibitor at which no growth occurs. In contrast S-shape curves exhibiting an inflection point were observed for the influence of copper sulphate

on the radial growth rate of *B. cinerea*. Accordingly, a new model equation was developed to fit the experimental data. However, the MIC, could not be determined by this model, because the growth rate was almost constant for copper sulphate in the range 4-7mM or 4-8mM for the strains BC1 and BC2 respectively.

Table 1: Parameter estimates and RMSE values for modelling the influence of copper on growth**,** 95 % confidence intervals in brackets.

Mould	μ_{opt} (mm day^{-1})	Cu_{50} (mM)	p (-)	RMSE
P. expansum 25.03	1.99 [1.79; 2.19]	2.41 [2.19; 2.63]	4.43 [3.39; 5.48]	0.070
B. cinerea BC1	15.9 [14.4; 17.4]	2.21 [1.92; 2.50]	3.04 [1.79; 3.04]	0.254
B. cinerea BC2	14.3 [13.3; 15.2]	2.60 [2.39; 2.82]	3.59 [1.79; 3.59]	0.181

Effect of copper sulphate on lag time for growth

Because an infinite lag time results in an absence of growth, the MIC was defined as the copper sulphate concentration at which the lag time for growth was infinite. The second model was therefore developed to fit the lag time as a function of copper sulphate concentration and to estimate the MIC. *P. expansum* strain 25.03 was characterized by λ_{opt} equal to 13.6 h at 0 mM of copper, Table 2. The Cu_{200} value was less than the Cu_{50} estimated. Accordingly, at 0.8 mM the lag time was twice that at 0 mM copper, whereas the effect of copper sulphate on the growth rate was not detectable (Figure 1). At 4.65 mM the estimation of the lag time of *P. expansum* strain 25.03 was infinite, therefore no growth could occurred. Accordingly this value was defined as the minimum inhibitory concentration.

The optimum lag time estimated for *B. cinerea*, strains BC1 and BC1 was about 30 h. The Cu_{200} values, 3.31 and 3.42 mM for BC1 and BC2, respectively, were not significantly different. These values were greater than the respective Cu_{50} values, although not significant. The MIC value for *B. cinerea* was greater than the MIC value for *P. expansum*. In addition, the MIC value for the strain BC1 was less than that estimated for the strain BC2 (Table 2).

B. cinerea strains exhibited λ_{opt} values greater than that of *P. expansum*. However, the confidence intervals for λ_{opt} did overlap between *P. expansum* and *B. cinerea* strain BC1 due to a wide confidence interval for the latter strain (Table 2). The estimated Cu_{200} values were greater for *B. cinerea* strains BC1 and BC2 than for *P. expansum*. The estimated MIC values were also greater for *B. cinerea* than for *P. expansum* thus suggesting that the latter fungus was more sensitive to copper sulphate than *B. cinerea*.

Table 2: Parameter estimates and RMSE values for modelling the influence of copper on the lag time for growth**,** 95 % confidence intervals in brackets.

Mould	λ_{opt} (mm day^{-1})	Cu_{200} (mM)	MIC (mM)	RMSE
P. expansum 25.03	13.6 [8.59; 18.7]	0.809 [0.422; 1.19]	4.65 [4.26; 5.05]	0.244
B. cinerea BC1	29.6 [17.9; 41.3]	3.31 [1.84; 4.79]	8.22 [7.99; 8.44]	0.532
B. cinerea BC2	32.0 [26.1; 37.9]	3.42 [2.67; 4.17]	7.28 [7.14; 7.42]	0.257

The model was fit to the experimental data for *P. expansum* 25.03, Figure 1. A correlation (r = 0.84) was observed between the radial growth rate and the reciprocal of the lag time. In contrast, for *B. cinerea* strains BC1 and BC2, in the range 0-4 mM, the radial growth rate decreased whereas the lag time was constant. Beyond 4 mM of copper until their respective MIC concentrations, the radial growth rate was constant whereas the lag time was increased (Figure 1).

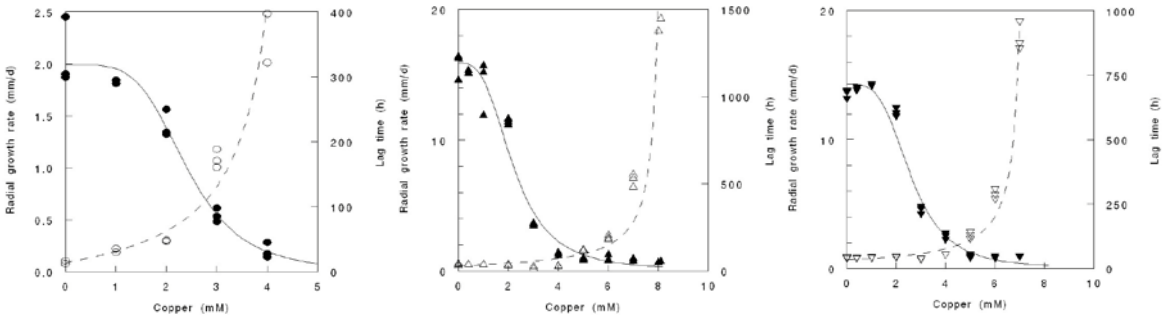

Figure 1: Effect of copper on radial growth rate and lag time of *Penicillium expansum* strain 25.03, *Botrytis cinerea* strains BC1 and BC2 (from left to right).

Conclusions

Copper tolerant fungi were defined as being capable of growth at approximately 100 mg/kg, 1.6 mM (Wainwright and Gadd 1997). The moulds examined in this study showed a great tolerance at high copper concentrations added in the PDA medium. However, comparisons of our data with MIC values from the literature are difficult because the methods and the experimental conditions may be different. The tolerance of the species to copper should be assessed both in the ability to germinate and hyphal extension after germination (Phelan *et al.* 1990). These biological responses can be evaluated from the lag time for growth, because germination occurred during that time, and from the growth rate respectively. The radial growth rate and the lag time are though important indicators of metal tolerance.

P. expansum exhibited an increase in the lag time for growth with increasing copper concentration. This indicated that germination was affected by copper.

The lag time for growth of *B. cinerea* was not affected by copper concentrations from 0 to 4 mM. It is suggested that, in contrast to growth, the germination did not depend on these copper concentrations. In contrast, at greater concentrations (i.e., above 4 mM) copper delayed germination of *B. cinerea* spores. Copper may bind on the surface of the spores during germination so some time is necessary for a detoxification process and a selection of surviving spores. More time was required for detoxification of the medium by binding copper at the surface of some spores, thus preventing them from germination. However, it is suggested that this mechanism allow the other spores to germinate once the medium is sufficiently detoxified.

Acknowledgements

This work was supported by the National Program on earthy/musty taste of wine (AGRIMER, Paris, France) project N° 01 04 21 08 0004 21**.**

References

Dantigny P., Guilmart A., Radoi F., Bensoussan M.and Zwietering M. (2005) Modelling the effect of ethanol on growth rate of food spoilage moulds. *International Journal of Food Microbiology*, 98, 261-269.

Dantigny P.and Bensoussan M. (2008) The logarithmic transformation should be avoided for stabilising the variance of mould growth rate. *International Journal of Food Microbiology* 121, 225-228.

Laforgue R., Guérin L., Pernelle J. J., Monnet C., Dupont J.and Bouix M. (2009) Evaluation of PCR-DGGE methodology to monitor fungal communities on grapes. *Journal of Applied Microbiology* 107, 1208-1218.

Phelan A., Thurman D.A. and Tomsett A.B. (1990) The isolation and characterization of copper-resistant mutants of *Aspergillus nidulans*. *Current Microbiology* 21, 255-260.

Pietrzak U. and McPhail D.C. (2004) Copper accumulation, distribution and fractionation in vineyard soils of Victoria, Australia. *Geoderma* 122, 151-166.

Wainwright M. and Gadd G.M. (1997) Fungi and industrial pollutants. In: D.T. Wicklow and B. Söderström (Eds.) *The Mycota IV, Environmental and Microbial Relationships*. 85-97, Springer Verlag, Berlin, Germany, 373 pp. (ISBN 3-540-58005-0).

Zwietering M. H., Cuppers H. G. A.M., de Wit J. C. and van't Riet K. (1994) Evaluation of data transformation and validation of a model for the effect of temperature on bacterial growth. *Applied and Environmental Microbiology* 60, 195-203.

Effectiveness of the process hygiene criterion of *Enterobacteriaceae* on Irish sheep carcasses using a Poisson-gamma regression model and derivation of a variables sampling plan

U. Gonzales-Barron, F. Butler

UCD Biosystems Engineering, School of Agriculture, Food Science and Veterinary Medicine, University College Dublin, Belfield, Dublin 4, Ireland. (ursula.gonzalesbarron@ucd.ie)

Abstract

An assessment of the performance of an EC 1441/2007 microbiological criterion (MC) was conducted based for the first time on the new Poisson-gamma modelling framework used to characterise within-batch and between-batch variability in *Enterobacteriaceae* counts on pre-chill sheep carcasses. Since the model does not assume within-batch constant variance but instead represents an association between within-batch means and dispersion measures, the operating characteristic (OC) curves could be constructed with confidence intervals arising from the uncertainty in the within-batch spread conditional to the within-batch mean. The model predicted that in Ireland the MC would categorise the hygiene of sheep processing as 'satisfactory' (below m_T=1.5 log CFU/cm^2) and 'acceptable' (between m_T and M_T=2.5 log CFU/cm^2) on average 98.6% (95% CI: 84.6 – 100%) and 1.4% (95% CI: 0 – 14.8%) of the times a batch is tested. Batches produced beyond 3120 CFU/cm^2 of mean *Enterobacteriaceae* concentration would have at least 95% confidence of being spotted by the 'unsatisfactory' criterion (>M_T), although under the existing contamination levels virtually no tested batch will prompt the revision of hygiene procedures in the Irish sheep abattoirs. Most importantly, this work proposes the definition of microbiological limits in *arithmetic means*, as by simulation this approach was found to lead to sampling plans that are both *more effective* (i.e., reduced uncertainty around the acceptance probabilities as a result of the between-batch variability) and with *more discriminatory power* than those based on the common *mean log scale*.

Keywords: *Microbiological criteria, Enterobacteriaceae, Poisson-gamma, sampling plan, operating characteristic curve*

Introduction

Historically, in the development or evaluation of acceptance sampling plans by attributes (van Schothorst *et al.* 2009; Whiting *et al.* 2006; Legan *et al.* 2001) and by variables (Smelt and Quadt 1990; Malcolm 1984), two simplifying assumptions have been always made: that the true concentration of microorganisms is log-normally distributed, and that the variance of the samples is the same for a low or highly contaminated lot. Gonzales-Barron and Butler (2011a,b) showed however that these assumptions do not necessarily hold and that the Poisson-gamma model has the ability to overcome these two simplifying assumptions, and as a result the capacity to incorporate the quantification of between-batch variability. On the other hand, procedures to assess the performance of MC are more documented for attributes sampling plans than for variables sampling plans, albeit EC No 1441/2007 also implies the use of the latter. Thus, this study aimed to present a methodology to assess the performance of a MC based on a *variables sampling plan* (*Enterobacteriaceae* on sheep carcasses) by the construction of operating characteristic (OC) curves that for the first time bring together the Poisson-gamma assumption and the dependence of the within-batch variance (dispersion) on the within-batch mean. Finally, a procedure for establishing a variable sampling plan based on the a-priori knowledge of the overall contamination of the process is illustrated.

Materials and Methods

Plate count data was available in duplicate for twenty pre-chill sheep carcasses swabbed on each of the four sampling visits to five large Irish abattoirs (n=400, j=20 batches). The

between-batch and within-batch variability in *Enterobacteriaceae* was modelled by a Poisson-gamma regression with correlated random effects of the within-batch mean (m_j) and the within-batch dispersion parameter (k_j) using the procedure (and notation) described in Gonzales-Barron and Butler (2011b). OC curves for the variables sampling plan for *Enterobacteriaceae* on sheep carcasses (mean of the samples, n=5; m_T=1.5 log CFU/cm^2, M_T=2.5 log CFU/cm^2) were constructed calculating the probability of 'accepting' a batch (P_a) or probability that a samples' mean is below a microbiological limit (m_T) for a given batch of mean microbial concentration *m*. However, in the Poisson-gamma model, the within-batch dispersion factor *k* is allowed to vary for a fixed within-batch mean *m* (Fig. 1). Therefore, the uncertainty in *k* given *m* will produce uncertainty in P_a given *m*, and hence the resulting OC curve may be displayed with confidence intervals. For a given within-batch mean *m*, the family of within-batch dispersion factors ($k|m$) conditional to that mean was computed using the conditional distribution of the bivariate normal distribution for the random effects of the dispersion *v* given the random effects of the mean *u*, as follows,

$$u_m = \log(m) - Int_0$$

$$v \mid m = v \mid (u = u_m) \sim Normal\left(\frac{\sigma_v}{\sigma_u}\rho\, u_m, \sigma_v\sqrt{(1-\rho^2)}\right)$$

$$k \mid m = \exp(Int_1 + v \mid m)$$

To estimate P_a as P($\overline{\lambda}$ <m_T/M_T), it is necessary to translate the within-batch true distribution (λ) to a distribution of the samples' mean ($\overline{\lambda}$). From this point, two approaches were used: the first approach, solved by simulation, mimics the common practice of taking the average of the logs of the individual samples while imputing the limit of quantification (LoQ) of the microbiological analysis to the zero counts. The second approach utilises the property that the arithmetic mean of the samples taken from a gamma population distribution follows another gamma distribution, and was therefore solved by calculation. These methods will be respectively referred to as the common *approach of the mean log* (or geometric mean) and the *approach of the arithmetic mean*. At a producer's α risk and consumer's β risk of 5%, the mean acceptable quality level (*AQL*) and 95% confidence intervals, and the mean limiting quality level (*LQL*) and 95% confidence intervals, respectively, were extracted from the OC curves.

Results and Discussion

The five parameters of the Poisson-gamma model turned out to be significant with the Pearson's correlation coefficient ρ of the random effects for log(m) and log(k) of -0.62. Thus, the two parameters of the within-batch true distributions (gamma) appeared to be moderately correlated: the higher the contamination level within a batch, the lower the dispersion (and the proportion of zero counts) (Fig. 1). Assuming that this model is representative for all Irish sheep abattoirs (Fig. 1), the performance of the MC was assessed. Under the current hygiene conditions in the production of sheep carcasses in Ireland, the EC MC for *Enterobacteriaceae* would categorise a process as 'satisfactory' (below m_T=1.5 log CFU/cm^2) on average 98.6% (95% CI: 84.6 – 100%; Table 1) of the times a batch is tested, and 'acceptable' (between m_T and M_T=2.5 log CFU/cm^2) with a probability of 1.4% (95% CI: 0 – 14.8%), when the average of the results of five samples is computed in mean logs. If instead, arithmetic means of the samples were taken and compared against the 'rescaled' arithmetic microbiological limits m_T'=82 CFU/cm^2 and M_T'=820 CFU/cm^2 (Table 1), the probability of labelling the hygiene of a process as 'satisfactory' and as 'acceptable' will be 99.05% and 0.95%, respectively, and the sampling plan will be *more effective* as evidenced by their narrower 95% confidence intervals (95.03-100% and 0-4.47%, respectively). Both approaches however predicted that virtually no tested batch would prompt revision of the production process and hygiene standards as no simulated batch fell within the 'unsatisfactory' process (>M_T). Furthermore, in terms of batch quality levels, under the EC *mean log* microbiological criterion, Irish sheep batches of mean *Enterobacteriaceae* concentration higher than 538 CFU/cm^2 and 3123

CFU/cm^2 will have at least 95% confidence of being spotted by the lower and upper microbiological limits, respectively, while from the producer's side, batches of mean concentrations up to 22 CFU/cm^2 and 224 CFU/cm^2 have at least 95% probability of leading to a 'satisfactory' and an 'acceptable' process result, respectively.

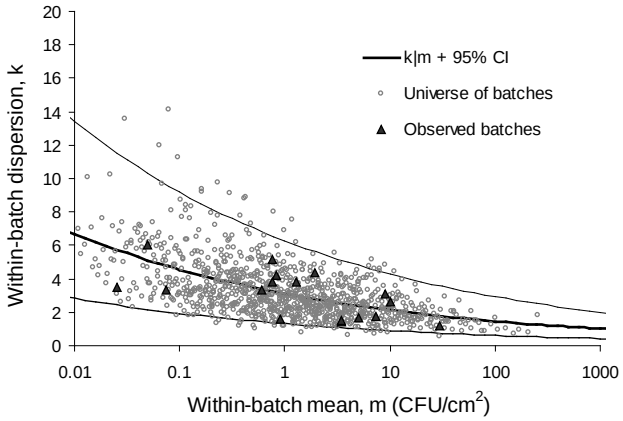

Figure 1: Universe of sheep carcass batches contaminated with *Enterobacteriaceae* generated by simulation from the correlated Poisson-gamma model, along with mean and 95% confidence intervals of the within-batch dispersion values conditional to a within-batch mean.

Table 1: Performance of the EC microbiological criterion of *Enterobacteriaceae* on pre-chill sheep carcasses operating under the actual level of contamination in Irish abattoirs.

Samples' arithmetic mean			Samples' mean log		
Probabilities and QLs (CFU/cm^2)	Mean	95% CI	Probabilities and QLs (CFU/cm^2)	Mean	95% CI
P (satisfactory) = P($\overline{\lambda} \leq m'_T$)	0.9905	[0.9503 – 1.0]	P(satisfactory)= P($\overline{\log Y} \leq m_T$)	0.9859	[0.8465 – 1.0]
P(acceptable) = P($m'_T < \overline{\lambda} \leq M'_T$)	0.0095	[0.0 – 0.0447]	P(acceptable)= ($m_T < \overline{\log Y} \leq M_T$)	0.0141	[0.0 – 0.1485]
P(unsatisfactory) = P($\overline{\lambda} > M'_T$)	0.0000	-	P(unsatisfactory)= P($\overline{\log Y} > M_T$)	0.0000	-
AQL, m'_T	38	[30 - 51]	AQL, m_T	26	[22 – 30]
LQL, m'_T	245	[158 - 422]	LQL, m_T	258	[105 – 538]
AQL, M'_T	429	[347 – 519]	AQL, M_T	247	[224 – 280]
LQL, M'_T	1973	[1456 – 3054]	LQL, M_T	1655	[780 – 3123]

In comparison to the samples' arithmetic mean approach, the samples' mean log approach generates greater uncertainty in acceptance probabilities (see 95% CI in Fig. 2), and hence causes a given sampling plan to be less effective. For instance, for a batch whose mean concentration is 100 CFU/cm^2, the probability that the arithmetic mean of the five samples' results is below the (arithmetically) 'rescaled' microbiological limit m_T' of 82 CFU/cm^2 ranges between 0.37 to 0.52 (95% CI) depending on the 'uncertain' within-batch dispersion value. However, for the same batch, the probability that the mean log (or geometric mean) of the five samples is below the microbiological limit of 1.5 log CFU/cm^2 is much broader and lies between 0.05 to 0.68 (95% CI). One should bear in mind that the heterogeneity in the dispersion factor (i.e., a consequence of the between-batch variability) reduces per se the effectiveness of a sampling plan, and yet, the samples' mean log approach appears to *further undermine* the sampling plan's effectiveness, by producing even greater uncertainty in the acceptance probabilities. Another attribute in favour of the samples' arithmetic mean approach is that their OC curves are steeper than those produced using the mean log scale (Fig. 2). The steeper the curve, the higher the discriminatory power of the sampling plan.

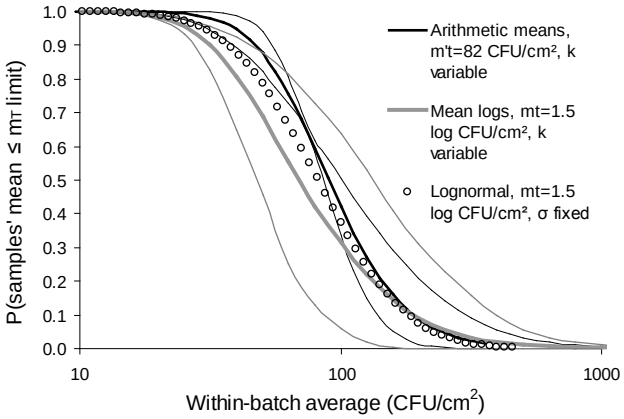

Figure 2: OC curves of the lower microbiological limit for *Enterobacteriaceae* on sheep carcasses (n=5) as modelled under the lognormal assumption with fixed σ and the two variants of the Poisson-gamma assumption to approximate the samples' mean distribution.

Considering that the counts of *Enterobacteriaceae* on Irish sheep carcasses are relatively low (overall within-batch mean of 4.5 CFU/cm^2) (Fig. 1), it can be deemed from the producer's perspective that batches of concentration up to the 95th percentile (22 CFU/cm^2) of the within-batch means are produced *under control* in terms of process hygiene. With the premises that batches up to that AQL should have at least 95% probability of producing a 'satisfactory' result, the more *discriminatory* and *effective* arithmetic means approach led to a *warning* limit of m'$_T$=60 CFU/cm^2, which is more conservative that the m'$_T$ of 82 CFU/cm^2 (i.e., value rescaled from m$_T$=1.5 log CFU/cm^2). The probability that a batch exceeds this newly defined warning limit with the arithmetic mean of the five samples is expected to be 1.5% (95% CI: 0 – 16.3%). The use of the lognormal assumption with fixed within-batch standard deviation would have led to the derivation of a less conservative sampling plan (Fig. 2).

Conclusions

Setting microbiological limits in *arithmetic scale* lead to *more efficient* and *discriminatory* sampling plans than those based on the common mean logs. Furthermore, OC curves with confidence intervals representing the uncertainty in the within-batch dispersion constitute a better tool to assess the effectiveness of sampling plans. They are equally important when establishing MC, as it is *more conservative* to derive a sampling plan based on a more cautious *upper percentile* of a limiting quality level for a given α or β risk than on its mean.

Acknowledgment

Food Institutional Research Measure (FIRM) administered by the Irish Department of Agriculture, Fisheries and Food

References

EC No. 1441/2007, Regulation. Official Journal of the European Communities L322/12-29.

Gonzales-Barron U. and Butler F. (2011a) A comparison between the discrete Poisson-Gamma and Poisson-Lognormal distributions to characterise microbial counts in foods. *Food Control* 11, 1279-1286.

Gonzales-Barron U. and Butler F. (2011b) Characterisation of within-batch and between-batch variability in microbial counts in foods using Poisson-gamma and Poisson-lognormal regression models. *Food Control* 11, 1268-1278.

Legan J.D., Vandeven M.H., Dahms S. and Cole M.B. (2001) Determining the concentration of microorganisms controlled by attributes sampling plans. *Food Control* 12, 137-147.

Malcolm S. (1984). A note on the use of the non-central t-distribution in setting numerical microbiological specifications for foods. *Journal of Applied Bacteriology* 57, 175-177.

Smelt J.P., and Quadt J.F. (1990) A proposal for using previous experience in designing microbiological sampling plans based on variables. *Journal of Applied Bacteriology* 69, 504-511.

Van Schothorst M., Zwietering M.H., Ross T., Buchanan R.L. and Cole M.B. (2009) Relating microbiological criteria to food safety objectives and performance objectives. *Food Control* 20, 967-979.

Whiting R.C., Rainosek A., Buchanan R.L., Miliotis M., LaBarre D., Long W., Ruple A. and Schaub S. (2006) Determining the microbiological criteria for lot rejection from the performance objective or food safety objective. *International Journal of Food Microbiology* 110, 263-267.

Estimating distributions out of microbiological MPN data for use in risk assessment.

R. Pouillot[1], K. Hoelzer[2], Y. Chen[3]

[1] Risk Assessment Coordination Team, Center for Food Safety and Applied Nutrition, Food and Drug Administration. 5100 Paint Branch Parkway, College Park, MD 20740. USA (Regis.Pouillot@fda.hhs.gov) [2] (Karin.Hoeltzer@fda.hhs.gov) [3] (Yuhuan.Chen@fda.hhs.gov)

Abstract

Estimating the distribution of microbiological concentrations in products is a key element of quantitative risk assessments. The classical bacteriological protocol applies a detection test to a set of samples and, for positive results, uses a quantification method such as dilution series assays. The most probable number (MPN) of bacteria is then estimated from these assays. Recently, Busschaert *et al.* (2010a) proposed a maximum likelihood approach considering censored data to estimate a distribution of bacterial concentration from this kind of protocol.

Through the use of simulation results we show that this proposed estimation of parameters of a contamination distribution from a set of MPN results leads to biased estimates, notably when the concentration of bacteria is low. As an alternative, we propose a complete likelihood maximization method that integrates in a single pass the MPN evaluation and the specification of the parameters of the underlying product-to-product distribution of bacteria, and show that this method leads to unbiased estimates.

The censored data method and our complete likelihood method were applied on a set of bacteriological results issued from a survey of *Listeria monocytogenes* in the US. The censored data method led to a bias of *ca*. 1 $\log_{10}$ in the estimation of the mean concentration.

The pattern of positive tubes for each dilution of the series assays is needed for the method proposed here. Indeed, the MPN is not a sufficient statistic, as considerable information is lost compared to the pattern of positive tubes. Reporting of individual tube patterns, or MPN values with a sufficient number of decimal points, should be encouraged to facilitate a more robust derivation of contamination distributions for risk assessments.

Keywords: *MPN, contamination distribution, risk assessment*

Introduction

In Quantitative Microbial Risk Assessment, exposure assessment models for foodborne pathogens usually consider a specified distribution of pathogens in the food at a given step of the food supply system. This distribution is frequently derived from a set of bacteriological results obtained on a representative set of samples. The classical bacteriological protocol applies a detection test to the sample set and, for samples that are positive in the detection test, applies an enumeration method. A popular enumeration method is the tube serial dilution assay, frequently denoted as Most Probable Number (MPN) method.

This protocol leads to left censored data (negative detection test), interval censored data (positive detection test, no positive tube in the dilution assay), non censored data (positive detection test with finite MPN estimates), and right censored data (positive detection test, all tubes positive). A maximum likelihood approach has been derived to estimate the parameters of a pre-specified parametric distribution from such a dataset (Busschaert *et al.* 2010a). However, a formal statistical evaluation of the properties of the proposed estimators has so far been missing.

Here we show through simulation studies that the estimators from this method (hereinafter denoted as CDM for "Censored Data Method") are biased. As an alternative, we derive a complete likelihood maximization method. In this latter method, the likelihood considers in a single pass the sample-to-sample distribution of bacteria as well as the intra-sample distribution of bacteria. The CDM and the Complete Likelihood Method (CLM) are

subsequently applied to a set of bacteriological results issued from a survey of *Listeria monocytogenes* in retail foods in the US (Gombas *et al.* 2003).

Materials and Methods

Following others (e.g. Busschaert *et al.* 2010a; Gonzales-Barron *et al.* 2010), assume that the sample-to-sample variability of the $\log_{10}$ concentration of a given pathogen in a given food follows a normal distribution, *i.e.* $\log_{10}(\lambda) \sim N(\theta = (\mu, \sigma))$. Let $f(x) = \phi\left(\frac{\log_{10}(x)-\mu}{\sigma}\right)$ and $F(x) = \Phi\left(\frac{\log_{10}(x)-\mu}{\sigma}\right)$ where $\phi(x)$ and $\Phi(x)$ are the probability density function and the cumulative density function of a standard normal, respectively.

Bacteriological method and results.

A detection test using v_d grams of sample is applied to a set of I representative samples of the considered food. If the detection test is positive, an MPN method is applied: dilutions 1 through r, each with n_r tubes, are inoculated with v_r grams of sample. A bacteriological procedure (assumed to be 100% specific and sensitive) will generate a positive result if at least one bacterial cell is present in a given tube.
In the following simulation and the real-world data, let v_d = 25 g , r = 3, $\boldsymbol{v}$ = {1, 0.1, 0.01} and $\boldsymbol{n}$ = {3, 3, 3},

Likelihood estimation

MPN estimation: Under the assumption of a Poisson distribution of the bacteria at each dilution and independence among dilutions and replicates, the likelihood with which a random vector $P = \langle p_1, \ldots, p_r \rangle$ of positive tube is observed is

$$L_{\mathrm{i}}(\lambda) = \prod_{d=1}^{r} \binom{n_d}{p_d} \left(e^{-\lambda v_d}\right)^{n_d - p_d} \left(1 - e^{-\lambda v_d}\right)^{p_d}$$

The most probable number (MPN) is the maximum likelihood estimator (MLE) of the likelihood function.
CDM: Let M_{min} and M_{max} equal the minimal and maximal finite MPN value achievable with the MPN protocol. In the CDM (Busschaert *et al.* 2010a), a set of four likelihood functions describes the set of possible outcomes: *i*) for left-censored results $L_i(\theta) = F\left(v_d^{-1}\right)$; *ii*) for interval-censored results, $L_i(\theta) = F(M_{min}) - F\left(v_d^{-1}\right)$; *iii*) for right-censored results $L_i(\theta) = 1 - F(M_{max})$; *iv*) for finite MPN results M, $L_i(\theta) = f(M)$. Maximization of the overall likelihood function yields the MLEs $\hat{\mu}$ and $\hat{\sigma}$.
For our simulation example and in the real-world data, v_d^{-1} = 0.04 cfu/g, M_{min} = 0.30 MPN/g and M_{max} = 110 MPN/g
CLM: Clearly,

$$L_i(\theta) = \int_{x=0}^{\infty} e^{-x v_d} f(x) dx$$

is the likelihood function for samples negative in detection, and

$$L_i(\theta) = \int_{x=0}^{\infty} (1 - e^{-x v_d}) \prod_{d=1}^{r} \binom{n_d}{p_d} \left(e^{-\lambda v_d}\right)^{n_d - p_d} \left(1 - e^{-\lambda v_d}\right)^{p_d} f(x) dx$$

is the likelihood function of all other samples. $\hat{\mu}$ and $\hat{\sigma}$ can again be estimated by maximization of the overall likelihood function.

Simulations to evaluate the behavior of the tests

To evaluate and compare bacterial concentration estimates generated using the CDM and the CLM, one thousand sets of I = 2 000 samples were simulated. Two different contamination levels were compared, with $\lambda \sim N(\mu = -5, \sigma = 2)$ or $\lambda \sim N(\mu = -7, \sigma = 3)$. To evaluate the

asymptotic behavior of the estimators, the tests were also applied to one set of I = 500 000 samples.

Test on real-world data

The dataset consists of *Listeria monocytogenes* detection and MPN results from a market basket sampling of ready-to-eat foods (RTE) performed in the US. Sampling protocol, bacteriological testing protocol and results have been described previously (Gombas *et al.* 2003), and the raw data for five food categories are available on the FoodRisk.org website. Mean and standard deviation of the assumed underlying log normal distributions of *L. monocytogenes* concentrations were evaluated separately for each category of RTE (Table 2). Two tests were used to evaluate the goodness-of-fit of the models: *i*) a chi-square test using three categories (no detection, detection with negative MPN, detection with positive MPN) with *p*-values computed using a Monte-Carlo procedure; *ii*) a chi-square test using all possible categories (i.e., each of the 65 possible outcomes of the experiment) with *p*-values computed using a Monte-Carlo procedure.

R (© The R foundation for Statistical Computing) codes are available from the authors on request.

Results and Discussion

Table 1 shows the simulation results for both methods. The CDM provides clearly biased estimates, with the bias tending to overestimate μ by approx. 1 $\log_{10}$ for the values tested and underestimating σ by approx. 0.3 $\log_{10}$ for the values tested. Importantly, these estimators for μ and σ are not asymptotically unbiased, and the bias does not appear to decrease as sample size increases. On the contrary, the complete likelihood method is unbiased.

Table 1: Simulation results.

			Censored Data Method		Complete Likelihood Method	
(μ, σ)	*n* tests		$\hat{\mu}$	$\hat{\sigma}$	$\hat{\mu}$	$\hat{\sigma}$
(-5; 2)	500 000		-4.1	1.7	-5.0	2.0
	1 000 sets	Mean	-4.2	1.7	-5.0	2.0
	of 2 000	Median	-4.2	1.7	-5.0	2.0
	samples	[Q0.025 ; Q0.975]	[-4.8 ; -3.7]	[1.4 ; 2.1]	[-5.7 ; -4.7]	[1.7 ; 2.4]
(-7; 3)	500 000		-6.0	2.6	-7.0	3.0
	1 000 sets	Mean	-6.0	2.6	-7.0	3.0
	of 2 000	Median	-6.0	2.6	-7.0	3.0
	samples	[Q0.025 ; Q0.975]	[-7.2 ; -5.1]	[2.1 ; 3.2]	[-8.2 ; -6]	[2.4 ; 3.6]

Table 2: Actual data sets

Product category	Number of observed samples (expected using the complete likelihood method)			Censored data method ($\hat{\mu}$; $\hat{\sigma}$)	Complete likelihood method ($\hat{\mu}$; $\hat{\sigma}$)	χ^2 test, 3 cat. (*p*-value)	χ^2 test, all cat. (*p*-value)
	Detection Neg.	Detection Pos. MPN Neg.	Detection Pos. MPN Pos.				
Bagged salad	2 944 (2 944)	17 (13)	5 (8)	(-8.1; 2.7)	(-9.2; 3.0)	NS (0.27)	NS (0.29)
Fresh soft cheese	2 926 (2 926)	2 (2)	3 (3)	(-21; 6.7)	(-23; 7.3)	NS (1.0)	NS (0.10)
Soft cheeses	2 933 (2 933)	30 (27)	7 (10)	(-5.4; 1.8)	(-6.5; 2.1)	NS (0.58)	NS (0.21)
Smoked seafood	2 530 (2 531)	67 (52)	47 (61)	(-6.6; 3.1)	(-7.6; 3.4)	0.03	0.002
Seafood salads	2 331 (2 332)	82 (75)	33 (39)	(-4.4; 1.8)	(-5.2; 2.0)	NS (0.47)	0.021

As expected from the simulation results, the MLE $\hat{\mu}$ obtained when applying the CDM on real-world data is always greater than the one obtained using the CLM (Table 2), and $\hat{\sigma}$ is always lower.

A significant Chi-square test using three categories indicates a higher than expected number of samples positive in the detection test while negative in the MPN method. This observation may indicate that the Poisson distribution between detection sample and MPN samples does not hold. Results (Table 2) shows that the number of detected samples with a negative MPN is always higher than expected under the parametric model, suggesting a possible departure from the Poisson assumption; nevertheless, the Chi-square test rejects goodness of fit only for

one category (smoked seafood). Two RTE foods out of five did not pass the chi-square test using all categories. Looking to the raw data in more details, it seems that this lack-of-fit is linked to the observation of few improbable combinations of positive tubes in the MPN test. As an example, an MPN outcome $\boldsymbol{P}$ = (1,3,0) is obtained for one smoked seafood sample: the "improb" (*i.e*. the sum of the probabilities of all outcomes as likely as or less likely than the observed one (Blodgett 2010)) for this pattern is 0.0018 at its MPN value, and 0.00017 in the log normal-Poisson model at its MLEs. These significant Chi-square test results might therefore rather indicate a larger number of improbable MPN outcomes than an overall lack-of-fit.

Our study suggests that the use of aggregated data (*i.e*. enumeration results) could lead to a bias and that the use of raw data (*i.e*., number of positive tubes in a MPN experiment) should be preferred, even for a simple parametric model. Indeed, the MPN is not a sufficient statistic, as some information is lost compared to the complete pattern of positive tubes. The pattern of positive tubes for each dilution of the series assays is needed for the method proposed here. These patterns, or individual MPN values with a number of decimal points sufficient to uniquely deduce the pattern, should be made available to risk assessors for a more robust derivation of contamination distribution. The transfer of raw data on dedicated website, such as FoodRisk.org should be encouraged.

More complete and complex Bayesian models have been described for the analysis of similar contamination data for risk assessment (*e.g*. Crepet *et al.* 2007; Busschaert *et al.* 2010b; Gonzales-Barron *et al.* 2010). However, the method proposed here may be easier to implement. Further studies are clearly needed to better describe the goodness-of-fit of the model proposed here, to evaluate test power, and to test alternative parametric models (*e.g*., gamma-Poisson, zero-inflated models). Nevertheless, our study suggests a 1 $\log_{10}$ bias in the mean of the log normal distribution estimated using the CDM compared to the CLM. In a risk assessment framework, this bias could lead to significant differences in the final risk, notably if the average pathogen concentration is low.

Conclusions

Our study shows that, whenever the raw data is available, the Complete Likelihood Method should be preferred over the Censored Data Method when applied to MPN results, because the latter leads to biased estimates.

Acknowledgements

The authors acknowledge Robert J. Blodgett for his help. This work was supported in part by an appointment to the Research Participation Program at the Center for Food Safety and Applied Nutrition administered by the Oak Ridge Institute for Science and Education through an interagency agreement between the U.S. Department of Energy and the U.S. Food and Drug Administration.

References

Blodgett R. J. (2010) Does a serial dilution experiment's model agree with its outcome? *Model Assisted Statistics and Applications* 5, 209-215.

Busschaert P., Geeraerd A.H., Uyttendaele M. and Van Impe J.F. (2010a) Estimating distributions out of qualitative and (semi)quantitative microbiological contamination data for use in risk assessment. *International Journal of Food Microbiology* 138 (3), 260-269.

Busschaert P., Geeraerd A.H., Uyttendaele M. and Van Impe J.F. (2010b) Hierarchical Bayesian analysis of censored microbiological contamination data for use in risk assessment and mitigation. *Food Microbiology* In Press.

Crepet A., Albert I., Dervin C. and Carlin F. (2007) Estimation of microbial contamination of food from prevalence and concentration data: application to *Listeria monocytogenes* in fresh vegetables. *Applied and Environmental Microbiology* 73(1): 250-8.

Gombas, D. E., Chen Y., Clavero R.S. and Scott V.N. (2003) Survey of *Listeria monocytogenes* in ready-to-eat foods. *Journal of Food Protection* 66 (4): 559-69.

Gonzales-Barron U., Redmond G. and Butler F. (2010) Modeling prevalence and counts from most probable number in a Bayesian framework: An application to *Salmonella* Typhimurium in fresh pork sausages. *Journal of Food Protection* 73: 1416-1422.

FILTREX: A New Software for identification and optimal sampling of experiments for complex microbiological dynamic systems by nonlinear filtering

J.-P. Gauchi[1], J.-P. Vila[2], C. Bidot[1], E. Atlijani[1], L. Coroller[3], J.-C. Augustin[4], P. Del Moral[5]

[1] Institut National de la Recherche Agronomique (INRA), département Mathématiques et Informatique Appliquées (UR3141), Jouy-en-Josas, France. (jean-pierre.gauchi@jouy.inra.fr).
[2] Institut National de la Recherche Agronomique (INRA), département Mathématiques et Informatique Appliquées, Montpellier, France. (jean-pierre.vila@supagro.inra.fr)
[3] Université Européenne de Bretagne, France. Université de Brest, EA3882 Laboratoire Universitaire de Biodiversité et Ecologie Microbienne, UMT 08.3 Physi'opt, IFR148 ScInBioS, Quimper, France. (louis.coroller@univ-brest.fr)
[4] Université Paris-Est, Ecole Nationale Vétérinaire d'Alfort, Unité MASQ, Maisons-Alfort, France. (jcaugustin@vet-alfort.fr)
[5] Institut National de Recherche en Informatique et Automatique (INRIA), Equipe ALEA, Bordeaux, France. (pierre.del-moral@inria.fr)

Abstract

At the 6th ICPMF Gauchi *et al.* (2009) considered the issue of the identification of complex microbiological dynamic systems and the possibility offered by particle nonlinear filtering to tackle this problem. As the computations involved in this identification approach are rather sophisticated, it is crucial for microbiologists to have access to a user-friendly software for managing them. We present in this 7th ICPMF the FILTREX software, based on Matlab language (Bidot *et al.* 2009) for reaching several objectives in the predictive microbiology context.

Keywords: *FILTREX software, particle nonlinear filtering, Bayes factors, sequential optimal designs, predictive modeling, microbiology*

Introduction

In the present release of the software are proposed: (i) parametric identification by particle filtering of microbiological dynamic systems, based on primary models (growth or thermal inactivation models); (ii) statistical model comparison and selection among several primary or inactivation models through particle estimation of Bayes factors (e.g. primary Baranyi and Roberts (1994), here referred to as the BR model, and the delay-logistic model (Rosso *et al*. 1996), here referred to as the DL model; (iii) computation of sequential optimal sampling designs (counting of cells on Petri plates, or counting of bacteria by means of flow cytometry). These three functionalities are based on a well established theory published elsewhere (see references in the next sections). Hereafter, only the main principles of these functionalities are recalled and screen outputs of the FILTREX software are displayed.

Materials and Methods

Parametric identification

This FILTREX identification functionality is based on the implementation of a new nonlinear particle technique using a convolution kernel approach (Rossi and Vila 2005, 2006). Let us just recall here that for this efficient particle filtering procedure, the only *a priori* information needed for the parameters is their respective possible variation ranges. The coding of this functionality in FILTREX has been developped from an open source code of the convolution particle filter (Choquet and Rossi 2005).

Model comparison and selection

This second functionality computes the so called Bayes Factor, for deciding which of two models better fits a given set of data (see Vila and Saley 2009, for details). This Bayes Factor

is the ratio of the respective marginal likelihood functions of the two competing models. It is not a genuine statistical test but it has been proved to be one of the best indices for comparing two nonlinear models. Its particle estimation in FILTREX does not need the knowledge of the model likelihoods as required by the usual statistical selection procedures (*e.g.* Akaïke criterion).

Optimal sequential designs

Several approachs were proposed to tackle this difficult question, where the difficulty is due to both the nonlinearity and dynamic aspects of the involved microbiological models. We propose in his Conference a poster where a new method is detailed (Gauchi and Vila 2011b).

Results and Discussion

The following FILTREX outputs are based on the BR model and on both the BR and the DL models for the model comparison subsection. For these computations a growth kinetic was used (given in Gauchi *et al.* 2009).

Parametric identification

In this subsection an example of estimation of seven parameters of the dynamic system is given: not only the four usual parameters ($N0$, μmax, λ , $N max$) are estimated, but also the three Coefficients of Variation (CV) characterizing the weighting errors, the pipette errors, and the diluting errors. These CV cannot be estimated with the usual nonlinear regression tools. At the initial step of the filtering process prior parameter probability distributions are simulated as uniforms laws on *a priori* membership intervals for these parameters. All other needed procedural informations are introduced as shown in the left panels of Figure 1.

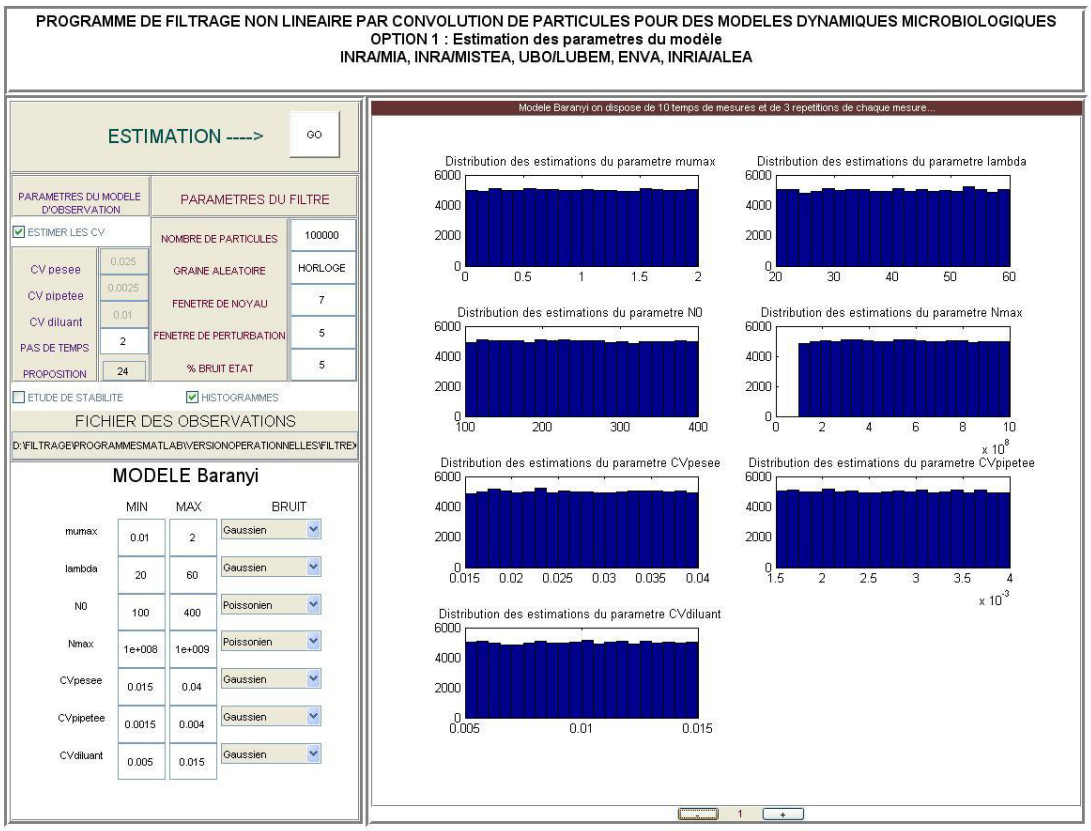

Figure 1: Parameter Identification Option, initial step.

Figure 2 displays the estimated posterior densities for the seven parameters – from which means and confidence intervals can be computed – at the final 10^{th} step (ten sampling times were considered, as given in the first line of Table 1).

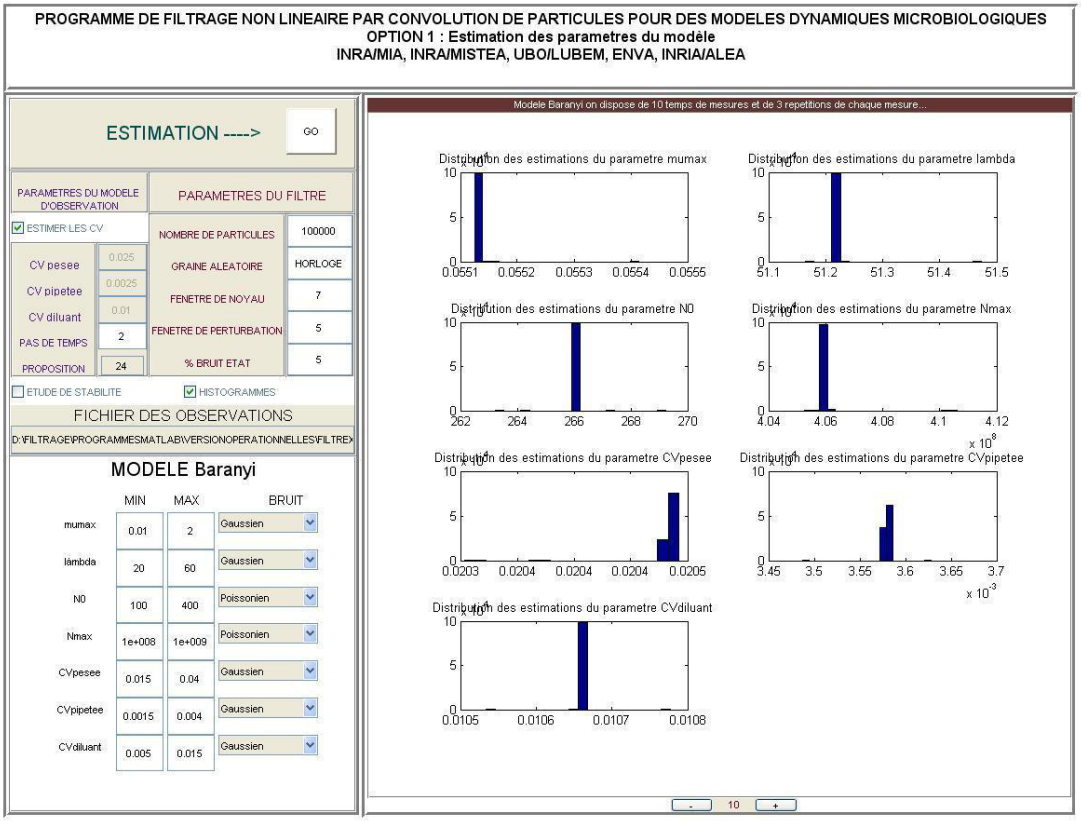

Figure 2: Parameter Identification Option, last step.

We also show in Figure 3 an example of estimated inactivation dynamics for the Weibull model obtained with FILTREX (more details during the talk).

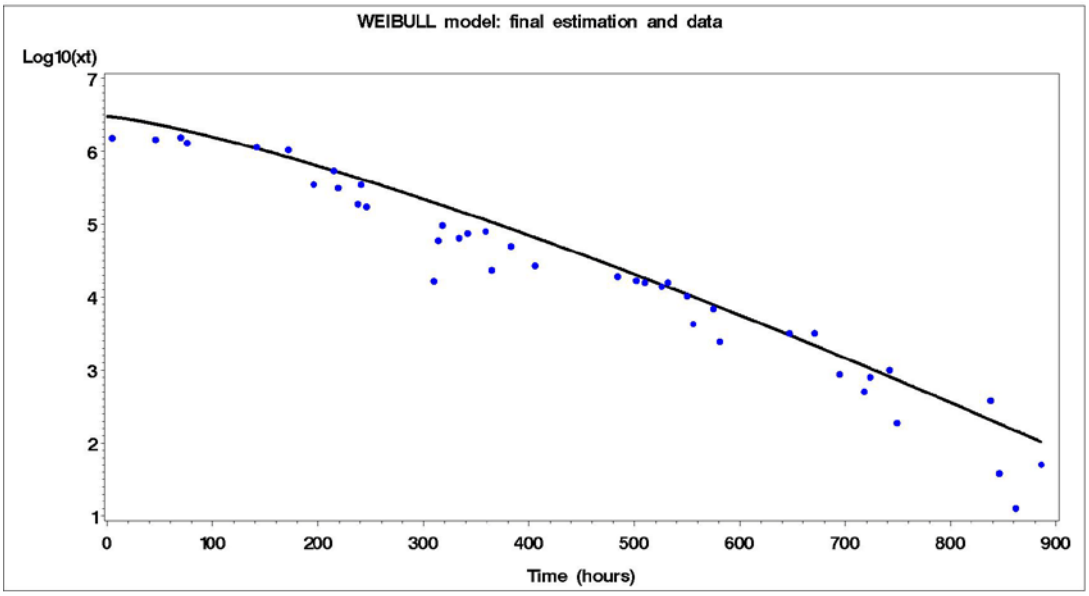

Figure 3: Estimated Weibull cinetics with data.

Model comparison and selection

The BR and DL models were compared. The following results have already been given in Gauchi and Vila (2011a). The estimated marginal likelihood of the DL model was put in the numerator of this Bayes Factor ratio and that of the BR model in the denominator. The FILTREX software provided the results of Table 1 for a chosen number of 10^5 particles.

Table 1. Bayes factor estimates at successive sampling time (hour).

t	0	72	120	168	240	264	288	336	408	504
BF(t)	1.07	1.07	1.06	1.06	1.06	1.08	1.12	1.08	1.7	1.22

One can notice the relative stability of the successive Bayes Factor estimates as time goes on. However as the numerator and denominator values become smaller with the successive introductions of the sampling times, the BF, as a tendency, fluctuates slightly for numerical reasons. To interpret the BF, Kass and Raftery (1995) proposed the following rule of thumb: from 1 to 3 the competing models are not really discriminitable, from 3 to 20 the model in the numerator sensibly fits the data better, and above 20 it is strongly better. It can be concluded here that the successive BF estimates, all close to one, confirm the equivalence of the two models, rather than a clear-cut superiority of the DL model over the BR's one, on this kinetic.

Optimal sequential designs

For details on this topics see Gauchi and Vila (2011b) in the same congress proceedings.

Conclusions

Some of the present features of the FILTREX software have been discussed. The next release (by the end of 2011) will propose an extension of the available functionalities to the hierarchical models (i.e. secondary models nested in the primary models) and new prediction facilities for the bacterial evolution. In the long term, dynamic regulation and control facilities (for example by means of temperature) of microbiological systems are planed to be introduced in FILTREX.

References

Barany J. and Roberts T.A. (1994) A dynamic approach to predicting bacterial growth in food. *International Journal of Food Microbiology* 23, 277-294.

Bidot C., Gauchi J.P. and Vila J.P. (2009) Programmation Matlab du filtrage non linéaire par convolution de particules pour l'identification et l'estimation d'un système dynamique microbiologique. Rapport technique INRA/Jouy-en-Josas/MIA/ n°2009-1.

Choquet R. and Rossi V. (2005) Routines pour le filtrage particulaire. Rapport CEFE-CNRS.

Gauchi J.-P., Bidot C., Augustin J.-C. and Vila J.-P. (2009) Identification of complex microbiological dynamic systems by nonlinear filtering. 6th International Conference "Predictive Modelling in Foods", Septembre 2009, Washington, USA.

Gauchi J.-P. and Vila J.-P. (2011a) Nonparametric filtering approaches for identification and inference in nonlinear dynamic systems. *Statistics and Computing*. Submitted.

Gauchi J.P. and Vila J.P. (2011b) Optimal sequential sampling design for improving parametric identification of complex microbiological dynamic systems by nonlinear filtering. Poster at the 7th International Conference "Predictive Modelling in Foods", September 2011, Dublin, Ireland.

Kass R.E and Raftery A.E. (1995) Bayes factors. J. Amer. Statist. Assoc., 90, 773-795.

Rossi V. and Vila J.P. (2005) Approche non paramétrique du filtrage de système non linéaire à temps discret et à paramètres inconnus. C.R. Acad. Sci. Paris. Ser I 340, 759-764.

Rossi V. and Vila J.P. (2006) Nonlinear filtering in discrete time: a particle convolution approach. Inst. Stat. Univ. Paris, 3, 71-102.

Rosso L., Bajard S., Flandrois J.P., Lahellec C., Fournaud J. and Veit P. (1996) Differential growth of *Listeria monocytogenes* at 4 and 8°C: Consequences for the shelf life of chilled products. *Journal of Food Protection* 59, 944-949.

Vila J.P. and Saley I. (2009) *Bayes Factor estimation for nonlinear dynamic state space models.* C.R. Acad. Sci., Paris, Ser. I 347, 429-434.

Evaluating the effect of experimental design schemes on parameter estimates of secondary square-root-type models

L. Mertens, E. Van Derlinden, J.F. Van Impe

CPMF2 – Flemish Cluster Predictive Microbiology in Foods – http://www.cpmf2.be/
BioTeC, Chemical and Biochemical Process Technology and Control, Dept. of Chemical Engineering, Katholieke Universiteit Leuven, W. de Croylaan 46, 3001 Leuven, Belgium (jan.vanimpe@cit.kuleuven.be)

Abstract

In predictive food microbiology, full factorial designs are still more the rule than the exception, despite the huge experimental workload and cost related to this method. This work evaluates the performance of different experimental designs with respect to three criteria: *(i)* number of experiments, *(ii)* goodness-of-fit statistics with respect to the original model structure, and *(iii)* accuracy and uncertainty of the parameter estimates. Full factorial, fractional factorial, central composite, Latin-square and Box-Behnken designs are evaluated and compared to randomly selected datasets. As a guideline, a full factorial design should be preferred for rather simple model structures and a limited number of levels per environmental factor. For more complex cases, a Latin-square design is an attractive alternative as it does not require a priori model knowledge and provides relatively accurate and reliable parameter estimates while keeping the experimental efforts to a minimum.

Keywords: *experimental design, secondary square-root-type model, parameter estimation*

Introduction

In predictive microbiology, as with other scientific disciplines, the collection of high-quality data forms the basis of scientific exploration. Both the selection of an appropriate model structure and the identification of accurate model parameters are data-driven processes, i.e., the efficiency and accuracy of these procedures are determined by the quality of the experimental data. When the impact of several environmental factors on the microbial response is investigated, as is the case in the development of secondary models and (probabilistic) growth/no growth models, the experimenter is confronted with a huge experimental workload. With respect to the experimental design, *full factorial designs* are still mostly used. This approach considers all combinations of the different explanatory variables, is very simple and easy to handle statistically, but also very labor-intensive and costly, certainly when a high number of variables and/or an extended range of levels are considered. Avoiding such excessive experimental work can be achieved through careful selection of the experimental conditions, i.e., by adopting a well-founded design-of-experiment (DOE) strategy. Based on certain statistical principles, various *fractional factorial designs* have been developed, e.g., Box-Behnken design, central composite design, Latin-square design.
Despite the significant reduction in the number of experiments obtained through these specific designs, full factorial designs are still more the rule than the exception in predictive microbiology and this observation forms the rationale for the present study. As such, this study aims at investigating the impact of different types of experimental designs on the reliability of secondary model parameter estimates. More specifically, a simulation-based approach was adopted to evaluate the performance of different designs with respect to two square-root-type secondary models, i.e., the model of Wijtzes *et al.* (2001) (developed for *Lactobacillus curvatus*) and the model of Ross *et al.* (2003) (developed for *Escherichia coli*).

Materials and Methods

Selection of secondary models and experimental conditions

<u>*Case study 1*</u>: the general form of the model of Wijtzes *et al.* (2001) is:

$$\mu_{\max} = b \cdot (a_w - a_{w\min}) \cdot (pH - pH_{\min}) \cdot (pH - pH_{\max}) \cdot (T - T_{\min})^2 \quad (1)$$

with μ_{max} the maximum specific growth rate [1/h], $a_{w\ min}$ the theoretical minimum a_w for growth, pH_{min} and pH_{max} the theoretical minimum and maximum pH for growth, and T_{min} the theoretical minimum temperature for growth. This model was originally developed for an overall range of environmental conditions: pH 4.6 - 9.0, a_w 0.932 - 0.990, and T 1 – 30 °C. For the present study, the ranges considered were: pH 5.0 - 8.0, a_w 0.937 - 0.985, and T 7 -27 °C.

<u>*Case study 2*</u>: the general form of the model of *Ross et al.* (2003) is:

$$\begin{aligned}\sqrt{\mu_{\max}} &= c\cdot(T-T_{\min})\cdot\left(1-\exp\left(d(T-T_{\max})\right)\right)\\ &\cdot\sqrt{a_w-a_{w\min}}\\ &\cdot\sqrt{1-10^{pH_{\min}-pH}}\cdot\sqrt{1-10^{pH-pH_{\max}}}\\ &\cdot\sqrt{1-\frac{LAC}{U_{\min}\cdot\left(1+10^{pH-pK_a}\right)}}\cdot\sqrt{1-\frac{LAC}{D_{\min}\cdot\left(1+10^{pK_a-pH}\right)}}\end{aligned} \quad (2)$$

with T_{max} the theoretical maximum temperature for growth. *LAC* is the total lactic acid concentration [mM], U_{min} and D_{min} [mM] respectively the minimum concentration of undissociated and dissociated lactic acid that prevent growth when all other factors are optimal, and pK_a the pH for which concentrations of undissociated and dissociated lactic acid are equal, i.e., 3.86. The model is based on data in the ranges: pH 4.02 - 8.28, a_w 0.951 - 0.999, temperature 7.6 - 47.4 °C, and lactic acid 0-500 mM. For the present study, the selected ranges were: pH 5.2 - 7.6, a_w 0.969 - 0.997, temperature 10 - 42 °C, and lactic acid 0-120 mM.

Selection of experimental designs

For each environmental factor included in the models, a maximum of five levels was considered for the present study. The different types of experimental designs considered included the following: full factorial (FF), fractional factorial (FRF), central composite (CC), Latin-square (LS) and Box-Behnken (BB). Based on the FF-design, the fractional factorial design (FRF) was developed such that the selection of sets of conditions was based on the underlying model structure. More specifically, the design included five levels for temperature, three levels for pH, two levels for a_w, and, for the Ross-model, three levels for lactic acid concentration. All designs were also compared to random sets of combinations of conditions (RA), selected by MatLab Version 7.9 (The MathWorks, Inc., Natick).

Simulation strategy

For both case studies, the simulation strategy consisted of the following steps.

1. Calculation of μ_{max} from model equations (1) and (2), by using the original parameter estimates and the environmental conditions and experimental designs as stated above.
2. Based on obtained μ_{max} values, simulation of growth curves with the primary model of Baranyi and Roberts (1994). For this, fixed values for n_0 (natural logarithm of initial cell count), n_{max} (natural logarithm of maximum cell number) and λ (lag time) were used. Simulation of growth curves resulted in a data set n(t) for each combination of conditions.
3. Based on n(t), creation of new fictitious data set n'(t) with the addition of noise at each sampling time t: $n' = n + noise = n + \sqrt{3.27\cdot10^{-2}}\cdot r$ with r pseudorandom values drawn from the standard normal distribution with variance taken equal to $3.27\cdot10^{-2}$ [CFU/mL] (determined in the lab as the experimental error related to plate count measurements). For each set of conditions, two data sets n'(t) were generated.
4. Determination of a new value for the maximum specific growth rate $\mu_{max'}$ by fitting n'(t) data sets with the model of Baranyi and Roberts (1994).
5. Estimation of new secondary model parameters by fitting $\mu_{max'}$ values with equations (1) or (2). To homogenize variance, the square root transformation of μ_{max} was used.

Model fits were performed in MatLab using the lsqnonlin routine of the Optimization Toolbox Version 3.0.2 (The MathWorks, Inc., Natick) to minimize the sum of squared errors (SSE). The RMSE was used to evaluate the performance of the secondary models.

Results and Discussion

In order to select a suitable experimental design, a trade-off should be made between the three different criteria considered in this study.

(i) Number of experiments. As shown in Tables 1 & 2, all the specific designs yield a similar reduction in workload compared to a 5-level FF-design, with exception of the BB-design for the Wijtzes-model (larger reduction in experimental workload) and the FRF-design for the Ross-model (smaller reduction in experimental workload). Evidently, the benefit of choosing a reduced design is larger when more environmental factors are involved.

(ii) Goodness-of-fit statistics. The RMSE was chosen as the criterion because it can be considered as the most simple and informative goodness-of-fit measurement for (non)linear models. However, as shown in Tables 1 & 2, for both models, discrimination between the different experimental designs is not possible on the basis of this value, since all designs performed equally well.

Table 1: Experimental designs considered for the model of Wijtzes *et al.* (2001)

Experimental design	FF5	FRF	CC	LS	FF3	BB	RA
# levels per factor	5	max. 5	5	5	3	3	5
# experiments	125	30	24	25	27	15	24
RMSE	0.0036	0.0041	0.0041	0.0040	0.0039	0.0033	0.0031

Table 2: Experimental designs considered for the model of Ross *et al.* (2003)

Experimental design	FF	FRF	CC	LS	RA
# levels per factor	5	max. 5	5	5	5
# experiments	625	90	36	25	36
RMSE	0.0091	0.0088	0.0099	0.0059	0.0056

(iii) Reliability of parameter estimates. Contrary to the previous criteria, large differences occurred between the designs when considering the accuracy and uncertainty of the parameter estimates. All experimental designs performed well with respect to $a_{w\,min}$, for which an almost perfect fit was obtained, and the parameters related to the pH-effect (results not shown). The most difficult parameters to estimate, i.e., the parameters with the lowest accuracy and the highest degree of uncertainty on the estimated value, were the ones related to the temperature effect and, for the Ross-model, also the lactic acid concentration (as illustrated in Figure 1).

Overall, the 5-level *FF-design* performed best for both case studies, as was expected from the high number of necessary experiments involved. At the other end of the spectrum, the *CC-design* proved to be inadequate, not particularly with respect to the accuracy of the parameter estimations in comparison to the original values, but more importantly, because of the high levels of uncertainty involved with this method (as illustrated in Figure 1 for some parameters of the Ross-model). Despite the occasional use of this design in predictive microbiology, the present results clearly indicate that it is certainly not a reliable method. In the same context, it can be stated that a random selection of conditions is clearly not advisable either. Although random designs yield realistic parameter values with acceptable estimation errors for some cases, this approach can not guarantee a good outcome. In general, the performance of the other 5-level designs (i.e., LS and FRF) with respect to the parameter estimates was acceptable (Figure 1). As the *FRF-design* relies on a priori knowledge of the underlying model structure, it can be stated that the *LS-design*, with its highly reduced number of experiments and overall good performance, is a good competitor for the FF-design. Particularly for the Ross-model, the experimental benefit is enormous, i.e., the number of experiments decreases from 625 to 25 when going from a FF- to a LS-design. For the Wijtzes-model, which has a model structure with a significantly lower degree of complexity,

the 3-level FF- and BB-designs appeared to be only slightly less suitable than the 5-level LS-design (results not shown). In this case, it is worth mentioning that the very low number of experiments (i.e., 15) for the *BB-design* resulted in relatively good parameter estimates.

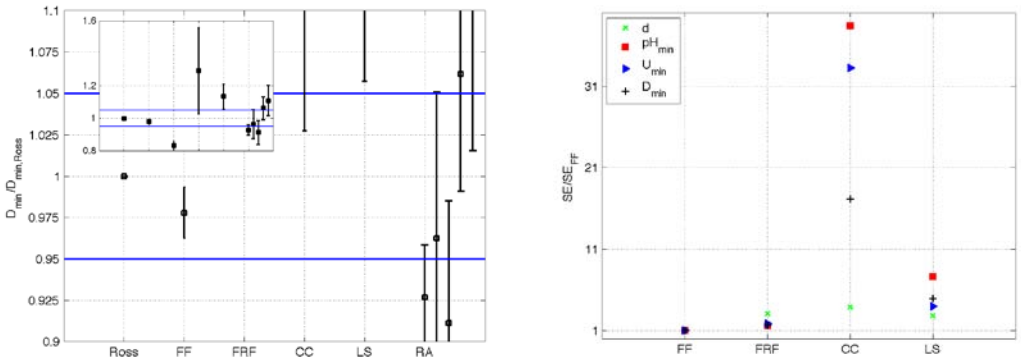

Figure 1: Ross-model parameter estimates. (Left) D_{min} estimates and standard error bars, expressed relative to the values of the original model. (Right) Uncertainty of parameter estimates, expressed relatively to the 5-level full factorial design (right).

The previous considerations were based on the deviation of individual parameter estimates from the originally published values and their degree of uncertainty. It is also important to keep in mind that differences exist between interpolation regions of models developed from different experimental designs and thus, comparison is often not possible at all investigated combinations of conditions, particularly near the edges of the design space. As such, the selection of a specific design may have consequences for the final use of the model.

Conclusions

The following general conclusions and guidelines can be drawn for square-root-type models:
(1) For rather simple model structures and a limited number of levels per environmental factor, full factorial designs are preferable because these designs guarantee accurate and reliable model parameters. (2) However, for more complex cases, a Latin-square design can be considered as an attractive alternative, as it does not require a priori knowledge on the model structure (as is the case for a typical fractional factorial design), and provides relatively accurate and reliable parameter estimates while keeping the experimental workload and cost to a minimum. In contrast, central composite designs should be avoided due to the high degree of uncertainty on the parameter estimates.
In addition, it would be of interest to explore the applicability of these guidelines towards other types of models, e.g., polynomial-type models.

Acknowledgements

This work was supported by project PFV/10/002 (Center of Excellence OPTEC-Optimization in Engineering) of the Research Council of the K.U.Leuven, project KP/09/005 (www.scores4chem.be) of the Industrial Research Fund, and the Belgian Program on Interuniversity Poles of Attraction, initiated by the Belgian Federal Science Policy Office. E. Van Derlinden is supported by postdoctoral grant PDMK/10/122 of the K.U.Leuven Research Fund. J. Van Impe holds the chair Safety Engineering sponsored by the Belgian chemistry and life sciences federation essenscia.

References

Baranyi J. and Roberts T.A. (1994) A dynamic approach to predicting bacterial growth in food. *International Journal of Food Microbiology* 23, 277–294.

Ross T., Ratkowsky D.A., Mellefont L.A. and McMeekin T.A. (2003) Modelling the effects of temperature, water activity, pH and lactic acid concentration on the growth rate of *Escherichia coli*. *International Journal of Food Microbiology* 82, 33-43.

Wijtzes T., Rombouts F.M., Kant-Muermans M.L.T., van't Riet K. and Zwietering M.H. (2001) Development and validation of a combined temperature, water activity, pH model for bacterial growth rate of *Lactobacillus curvatus*. *International Journal of Food Microbiology* 63, 57-64.

Modelling the effects of osmoprotectants in the medium on growth of *E. coli* during osmotic stress

A. Métris, S.M. George, J. Baranyi

Institute of Food Research, Norwich Research Park, Norwich, NR4 7UA, U.K. (aline.metris@bbsrc.ac.uk, susie.george@bbsrc.ac.uk, jozsef.baranyi@bbsrc.ac.uk)

Abstract

In predictive microbiology, secondary models, for example the Gamma model or cardinal models, evaluate the detrimental effect of food conditions (pH, water activity, etc.) on the growth rate of bacteria, compared to optimal conditions. The purpose of this study is to link such models with cell physiology in case of osmotic stress, using systems biology approaches. Bacteria adapt to osmotic stress by accumulating osmoprotectants in their cytoplasm. The effect of NaCl on the growth rate of *E. coli* depends on the presence and nature of osmoprotectants in the medium. We measured, by optical density, the growth yield and the growth rates during exponential growth of *E. coli* in glucose minimal medium with a range of NaCl concentrations and different osmoprotectants. In the absence of osmoprotectant, the growth yield decreased because some of the glucose was used to metabolise trehalose. The growth yield, in the presence of glycine betaine or choline, did not vary with NaCl concentration up to close to the growth/no growth boundary. With proline in the medium, the growth yield also decreased because some trehalose was metabolised. The specific growth rates depended strongly on the nature of the osmoprotectant. An analysis of the fluxes of the metabolic network model of *E. coli* was carried out to evaluate the metabolic state of the bacteria under osmotic stress in relation to its optimum. The method provides a link between empirical secondary models and the physiology of the bacteria during osmotic stress.

Keywords: *osmotic stress, growth rate, Escherichia coli, metabolic network, convex space*

Introduction

In predictive microbiology, secondary models evaluate the effect of environmental conditions on kinetics parameters, such as growth rate, of the primary models. Apart from polynomial response surface models which are purely empirical, most modelling approaches compare the growth rate obtained under a given set of conditions, to an optimum. This is explicit in the formulation of the Gamma concept (Zwietering *et al.* 1992) where the γ functions are factors representing the inhibition of each environmental factor on the growth rate, assuming that they are independent, compared to its optimum. For the effect of water activity, the proposed γ function (Zwietering *et al.* 1992) is a normalisation of the square root approach at suboptimal water activity (McMeekin *et al.* 1987). The cardinal parameter models (CPM) are based on the same idea except that the cardinal functions are more complex than the initial gamma functions and include model parameters that have a biological or graphical interpretation such as a_{wopt}, and a_{wmin} and a_{wmax}, the minimum and maximum values at which no growth occurs (Rosso *et al.* 1993). These modelling approaches remain empirical and it would be desirable to link them to the physiology of the cell (McMeekin *et al.* 2008). In this study, we propose to link these modelling approaches to the metabolic network of *Escherichia coli* under osmotic stress, with NaCl as the humectant.

Constraint-based analysis of the metabolic network assumes that in balanced growth (the exponential phase in batch culture), the cells reach a steady-state governed by mass balance and physicochemical constraints (Kauffman *et al.* 2003). The mass balance constraint is determined by the stoichiometry of the metabolic reactions taking place in the cell. These reactions are usually derived from the genome annotation and biochemical studies. A flux, ν, the concentration of the chemicals weighed by their stoichiometric coefficient per time unit, is defined for each reaction. If we call the stoichiometric matrix for the system, S, then, at steady state, $S.\nu=0$. The system is underdetermined (there is more than one solution) because

there are more fluxes than metabolites. However, each flux is bounded further by the physicochemical constraints, so S.ν=0, with $\nu_{min}<\nu_i<\nu_{max}$ (i=1 … n), defines a convex domain in the space of solutions (Kauffman *et al.* 2003). Because of the convexity of the space of solution, the optima lie on the vertices of the convex domain (Palsson 2006). It has been shown that *E. coli* optimises its biomass production in chemostat and that by optimising the biomass (the objective function), the growth rate, as well as the distribution of fluxes in the central metabolism, can be predicted from the uptake of nutrients (Feist *et al.* 2007).
In the case of osmotic stress, bacteria accumulate osmoprotectants to increase their cytoplasmic water activity. If there is no osmoprotectant in the medium, they convert glucose into trehalose by activation of the ostA and ostB genes (Giaever *et al.* 1988). This is regulated by the general stationary phase stress response σ^s factor encoded by rpoS (Hengge-Aronis 1991). Some osmoprotectants, such as glycine betaine or proline can be directly imported into the cell. The transport for these two osmoprotectants is through the proP and proU channels (Wood 2006). Alternatively, the cell can metabolise some precursors such as choline into osmoprotectant, for example, glycine betaine. The two-step-conversion is catalysed by betA and betB and is regulated by a specific system which is sensitive to oxygen, osmotic stress and temperature (Lamark *et al.* 1996, Landfald and Strøm 1986). In the case of osmotic stress, the metabolic network of the bacteria is modified to accommodate these changes and we have shown that additional constraints have to be sought and that biomass optimisation may not be achieved (Metris *et al.* submitted). In this study, similar to secondary modelling, we compare the fluxes during osmotic stress and when the cells optimise their biomass without stress.

Materials and Methods

Culture: *Escherichia coli* K12, strain MG1655, was maintained in Tryptone Soya Broth (TSB, Oxoid CM0129) with 40% glycerol stored at -80°C. The culture was resuscitated in TSB at 37°C for 7 hours then subcultured to Basic Minimal Medium, BMM (Zhou *et al.* 2011) with 0.05% glucose instead of 4% glucose. Subsequent subcultures were incubated at 37° for 7 or 17 hours.
Determination of the biomass yield, glucose uptake and growth rates: Four batches of BMM were prepared with no glucose. To three batches 150mM of the osmoprotectants glycine betaine, proline, or choline was added. The fourth batch with no added osmoprotectant was the control. Each of the four batches was divided into smaller volumes and glucose added to give a range of concentrations. Each of these solutions was further divided and NaCl added to give a range of water activities. Finally the solutions were made up to volume and filter sterilised. Wells of a Bioscreen plate were inoculated with 25µl of cell suspensions of different concentrations and filled with 375µl of the above solutions. Plates were incubated without shaking for 4 days at 37°C.
The glucose uptake and biomass yield were determined by plotting the slope of the maximum OD as a function of glucose concentration for each condition (Krist *et al.* 1998). The calibration OD/dry weight biomass was linear in the range of ODs studied (up to 0.7). The rates of growth in cell number were determined as the inverse of the slope of the detection times (for OD(600nm)=0.1) as a function of the cell concentrations in the different conditions (Cuppers and Smelt 1993). The growth rates in terms of biomass were obtained by fitting the logarithm of OD as a function of time with the Baranyi model (Baranyi and Robert 1994). The rates were adjusted to cell numbers in control conditions by multiplying them by a factor 1.91 (Dalgaard *et al.* 1994).
Analysis of the fluxes of the metabolic network:
The metabolic network of *E. coli* chosen for this study was that of Feist *et al.* (2007). For the optimum condition, the glucose uptake was adjusted to obtain the specific growth rate, µ, found in the control conditions (-7.7 mmol/g dry weight/h, µ=0.71 /h) and the biomass objective function optimised. At 3.5% NaCl, the concentration of osmoprotectants in the biomass equation was assumed as measured by Cayley *et al.* (1992). The rate of glucose

uptake as well as growth rate was deduced from experiments with the Bioscreen. The uptake of oxygen was set to its minimum to obtain the measured growth rate.
The calculations were carried out with the COBRA toolbox (Becker *et al.* 2007) in Matlab (R2010b, Mathworks, Inc.) equipped with the glpk package (http://www.gnu.org/software/glpk/glpk.html). The optimum solutions were obtained by linear programming. For non-optimum solutions, the space of solution was sampled randomly. The minimum and maximum for each flux were determined by flux variability (Reed and Palsson 2004).

Results and Discussion

Glucose/biomass yield

The biomass yield (g of biomass produced per g of glucose used) did not vary with osmotic stress when choline or glycine betaine was present in the medium (Figure 1).

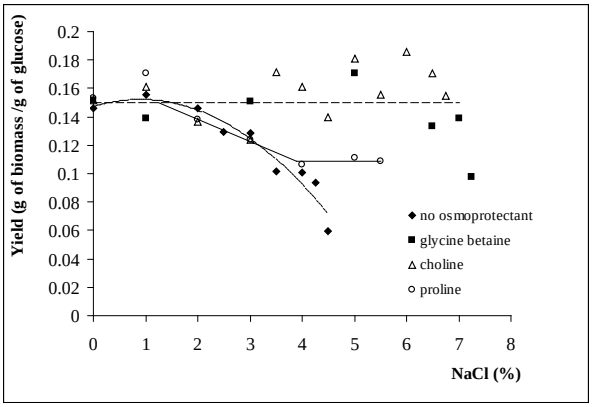

Figure 1: Yield of *E coli* in Bioscreen wells as a function of NaCl concentration.

This shows that energetic demands are not significantly increased by osmotic stress. When there was no osmoprotectant in the medium, additional glucose was needed to synthesise trehalose (Giaever *et al.* 1988) so the yield decreased markedly. When proline is present, the bacteria use it as an osmoprotectant but also synthesise some trehalose (Cayley *et al.* 1992) which explains why the yield decreases with increasing NaCl concentration. Altogether these results are in agreement with the measurements of osmoprotectant accumulated in the cells at high concentration of NaCl (Cayley *et al.* 1992). In this study the yield in the control conditions, Y=0.15, was low (0.3 in a batch culture, Fisher and Sauer 2003) perhaps because oxygen uptake is limited by the low exchange surface in the wells of the Bioscreen.

The effect of osmoprotectant and water activity on the growth rate

Figure 2 shows the effect of the water activity (modelled by $b_w = \sqrt{1-a_w}$ on the x axis) on the growth rate, measuring the rate of increase in both cell number and biomass.
They are the same for glycine betaine and proline, whereas, with choline or no osmoprotectant in the medium, they are different, showing that the cell size changes depending on the nature of the osmoprotectant. These different cell strategies may be linked to the different types of regulation of osmotic stress responses.

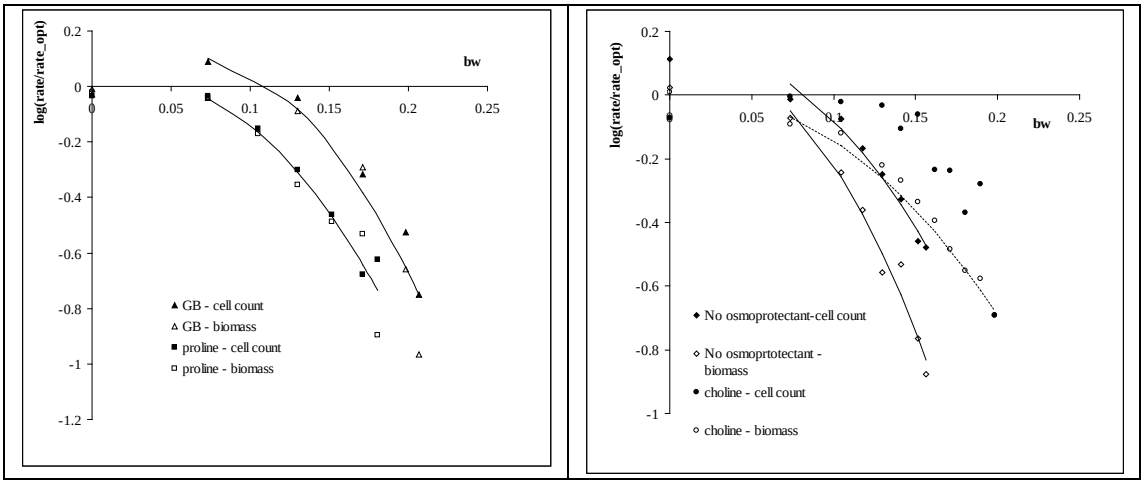

Figure 2: Effects of osmoprotectant on the growth rates as a function of water activity.

"Metabolic" distance

The minimum and maximum fluxes obtained by flux variability analysis were normalised to the fluxes going through the biomass (the specific growth rates) and the example with no osmoprotectant is shown in Figure 3. By convention, the 0 fluxes were set to -20 on the log scale. Some fluxes were the same in stress as in optimum conditions, some changed in the stress conditions compared to optimum but the normalised fluxes were the same in all stress conditions, typically fermentative pathways not used when aeration is good (optimum). Some were specific for each stress (pathways specific to the stress response but also general metabolism since the different osmoprotectants have different efficiencies).

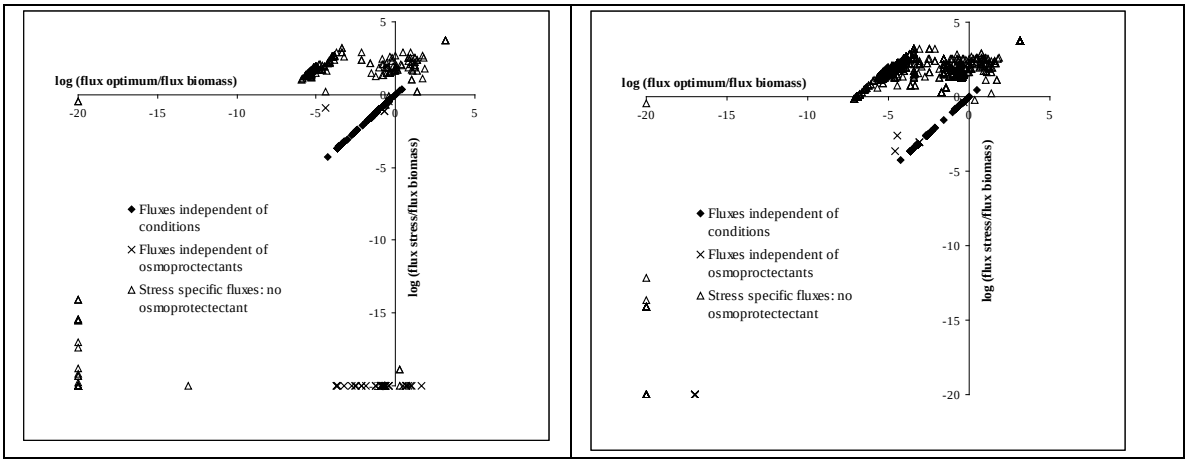

Figure 3: Logarithm of the minimum (left panel) and maximum (right panel) fluxes obtained by flux variability analysis of the convex space formed by *E. coli* at steady state in MBM with 3.5% NaCl compared to the optimum control conditions.

To compare the effect of the different osmoprotectants in the medium, the fluxes of pathways of interest can be compared to obtain Z-scores, Z_i, for each flux i, quantifying the significance of the change in fluxes (Bordel *et al.* 2010):

$$Z_i = \frac{E_{\%NaCl,osmoprot.}(v_i) - E_{optimum}(v_i)}{\sqrt{Var_{\%NaCl,osmoprot.}(v_i) + Var_{optimum}(v_i)}}$$

where the expected values and variances of the fluxes are obtained by random sampling of the space of solutions obtained under the different conditions for each flux, i.

Conclusions

The metabolic network of *E. coli*, constrained by mass balances and physicochemical properties at steady-state, results in a convex domain of solutions. This mathematical property means that the fluxes can be sampled, and if a suitable objective function is found, the physiological state of the cell can be determined (Schuetz *et al.* 2007). It has been demonstrated that the fluxes obtained by minimizing the total reaction flux with the growth rate as a constraint, similarly to this study, are in agreement with ^{13}C-metabolic flux analysis for Arabidopsis under osmotic stress (Williams *et al.* 2010). We anticipate that this kind of approach can provide a link between empirical predictive models and the cell physiology.

References

Baranyi J. and Roberts T.A. (1994) A dynamic approach to predicting bacterial growth in food. *International Journal of Food Microbiology* 23, 277-294.

Becker S.A., Feist A.M., Mo M. L., Hannum G., Palsson B.O. and Herrgard M.J. (2007) Quantitative prediction of cellular metabolism with constraint-based models: The COBRA Toolbox. *Nature Protocols* 2, 727-738.

Bordel S., Agren R., and Nielsen J. (2010) Sampling the Solutions Space in Genome-Scale Metabolic Networks Reveals Transcriptional Regulation in Key Enzymes. *Plos Computational Microbiology* 6, 7, e1000589.

Cayley S. Lewis B.A. and Record Jr. M.T. (1992) Origins of the osmoprotective properties of betaine and proline in *Escherichia coli* K-12. *Journal of Bacteriology* 74(5) 1586-1595.

Cuppers H.G.A.M. and Smelt J.P.P.M. (1993) Time to turbidity measurement as a tool for modeling spoilage by Lactobacillus. *Journal of Industrial Microbiology Biotechnology* 12, 168–171.

Dalgaard P., Ross P., Kamperman L., Neumeyer K. and McMeekin T.A. (1994) Estimation of bacterial growth rates from turbidimetric and viable count data. *International Journal of Food Microbiology* 23, 391–404.

Feist A.M., Henry C.S, Reed J.L., Krummenacker M., Joyce A.R., Karp P.D., Broadbelt L.J., Hatzimanikatis V. and Palsson B.O. (2007) A genome-scale metabolic reconstruction for *Escherichia coli* K-12 MG1655 that accounts for 1260 ORFs and thermodynamic information. *Molecular Systems Biology* 3, 121.

Fischer E. and Sauer U. (2003) A Novel Metabolic Cycle Catalyzes Glucose Oxidation and Anaplerosis in Hungry *Escherichia coli*. *The Journal of Biological Chemistry* 278, 46446-46451.

Giaever H.M., Styrvold O.B., Kaasen I. and Strom, A.R. (1988) Biochemical and genetic characterization of osmoregulatory trehalose synthesis in *Escherichia coli*. *Journal of Bacteriology* 70(6), 2841-2849.

Hengge-Aronis R., Klein W., Lange,R., Rimmele M. and Boos W. (1991) Trehalose synthesis genes are controlled by the putative sigma factor encoded by RpoS and are involved in stationary phase thermotolerance in *Escherichia coli*. *Journal of Bacteriology* 173, 7918–7924.

Kauffman K.J., Prakash P. and Edwards J.S. (2003) Advances in flux balance analysis. *Current Opinion in Biotechnology* 14, 491–496.

Krist K.A., Ross T. and McMeekin T.A. (1998) Final optical density and growth rates; effects of temperature and NaCl differ from acidity. *International Journal of Food Microbiology* 46, 195-203.

Lamark T., Rokenes T.P., McDougall J. and Strom A.R. (1996) The complex bet promoters of *Escherichia coli*: regulation by oxygen (ArcA), choline (BetI), and osmotic stress. *Journal of Bacteriology* 178(6), 1655-1662.

Landfald, B. and Strøm A.R. (1986) Choline-glycine betaine pathway confers a high level of osmotic tolerance in *Escherichia coli*. *Journal of Bacteriology* 165, 849–855.

McMeekin T.A., Bowman J., McQuestin O., Mellefont L., Ross T. and Tamplin M. (2008) The future of predictive microbiology: Strategic research, innovative applications and great expectations. *International Journal of Food Microbiology*, 128 (1), 2-9.

McMeekin T.A., Chandler R.E., Doe P.E., Garland C.D., Olley J., Putro S., and Ratkowsky D.A. (1987) Model for combined effect of temperature and salt concentration/water activity on the growth rate of *Staphylococcus xylosus*. *Journal of Applied Bacteriology* 62(6), 543-550.

Palsson, B. Ø. (2006) The (right) null space of S, In: Palsson, B. Ø., Systems Biology, Chapter 10, 136-153. Cambridge University Press.

Reed J.L. and Palsson B.Ø. (2004) Genome-Scale *In Silico* Models of *E. coli* Have Multiple Equivalent Phenotypic States: Assessment of Correlated Reaction Subsets That Comprise Network States. *Genome Research* 14(9), 1797-1805.

Rosso L., Lobry R. and Flandrois J.P. (1993) An unexpected correlation between cardinal temperatures of microbial growth highlighted by a new model. *Journal of Theoretical Biology* 162(4), 447-463.

Schuetz R., Kuepfer L. and Sauer U. (2007) Systematic evaluation of objective functions for predicting intracellular fluxes in *Escherichia coli*. *Molecular System Biolology* 3,119.

Williams T.C.R., Mark G.P., Howden A.J.M., Schwarzlander M., Fell D.A., Ratcliffe R.G. and Sweetlove L.J. (2010) A Genome-Scale Metabolic Model Accurately Predicts Fluxes in Central Carbon Metabolism under Stress Conditions. *Plant Physiology* 154, 311-323.

Wood J. M. (2006) Osmosensing by bacteria. Sciences STKE 2006, pe43.

Zhou K., George S.M., Metris A and Baranyi J. (2011) Lag phase of *Salmonella* under osmotic stress. *Applied and Environmental Microbiology* 77, 5, 1758-1762.

Zwietering M.H., Wijtzes T., De Wit J.C. and Van't Riet K. (1992) A decision support system for prediction of the microbial spoilage in foods. *Journal of Food Protection* 55, 973-979.

Omics as a basis to model the effect of competitiveness-enhancing factors on the growth and metabolism of the meat starter culture Lactobacillus sakei CTC 494

T. Rimaux, A. Rivière, L. De Vuyst, F. Leroy

Research group of Industrial Microbiology and Food Biotechnology, Vrije Universiteit Brussel, Pleinlaan 2, B-1050 Brussels, Belgium (fleroy@vub.ac.be)

Abstract

The genome sequence of *Lactobacillus sakei* 23K indicates that the species *L. sakei* has evolved to close adaptation to (fermented) meat environments. Several genes involved in the catabolism of non-glucose energy sources present in meat, such as arginine, nucleosides, and glycerol have been annotated. Therefore, the effective survival of *L. sakei* in meat seems to be mediated through a versatile use of energy sources other than glucose present in meat. Based on these insights, the metabolic potential of *L. sakei* CTC 494, a meat starter culture, to grow on non-glucose energy sources was quantified through modelling, including the use of the arginine deiminase pathway and the catabolism of nucleosides. Consumption of glycerol did not occur, despite the presence of glycerol-catabolising enzymes and a specific glycerol transporter in the genome. A detailed kinetic analysis of the catabolism of inosine and adenosine, and its interaction with the conversion of glucose or arginine, was performed and expressed as a function of different pH values. Metabolomic analysis revealed that inosine and adenosine were converted by *L. sakei* CTC 494 into a mixture of acetic acid, formic acid, and ethanol, suggesting a shift to mixed-acid fermentation when the strain was grown on nucleosides. The nucleobases (adenine and hypoxanthine) were excreted into the medium stoechiometrically. This indicates that the pentose moiety of adenosine and inosine was utilized to sustain cell energy requirements. Real time-PCR was applied to link the obtained data to gene expression, indicating a link with the growth phase and the external pH. In conclusion, the combined use of genomic, transcriptomic, and metabolomic approaches opens perspectives for the quantitative analysis and modelling of the competitive behaviour and metabolic traits of bacteria in view of food applications. These data may help the selection of appropriate starter cultures for food (meat) fermentations.

Keywords: Lactobacillus sakei, *meat*, *competitiveness*, *gene expression*, *metabolite analysis*

Introduction

Lactobacillus sakei is the most prevalent lactic acid bacterium (LAB) species encountered in spontaneously fermented sausages, which demonstrates its competitiveness in and adaptation to the meat environment (Leroy *et al.* 2006). For this reason its use as a starter culture for meat fermentation is widespread. The variety of carbohydrates in fresh meat is relatively restricted and their amounts are limited, with ribose and glucose being the main fermentable carbohydrates (Rimaux *et al.* 2011). Therefore, a flexible use of all available nutrients and energy sources present in meat is of importance. Genes involved in the catabolism of arginine, nucleosides, and glycerol (all present in meat) have been annotated in the genome of *L. sakei* 23K (Chaillou *et al.* 2004). Therefore, it has been suggested that the effective survival of *L. sakei* in meat is mediated through a versatile use of energy sources, other than glucose, present in meat. Up to now, no attempt was made to investigate the catabolism of these potential energy sources by *L. sakei*. Therefore, the aim of the present study was to investigate the impact these alternative energy sources on the competitiveness and survival of *L. sakei*. A detailed kinetic analysis of the metabolites resulting from the conversion of arginine, inosine, and adenosine by *L. sakei* CTC 494 was performed as a function of environmental pH. In addition, a direct link between estimated model parameters and gene expression data of the arginine deiminase (ADI) pathway as a function of environmental pH was set-up as a validation of the proposed model.

Materials and Methods

Microorganisms, media, and fermentation experiments

Fermentations were carried out in 10 L customized MRS medium, without glucose and supplemented with 3 g/L of arginine, glycerol, inosine, or adenosine in a 15-L Biostat®C fermentor (Sartorius AG/B. Braun Biotech). The fermentation temperature was kept at 30°C; the pH was kept constant through automatic addition of 10 M NaOH and 10 M HCl. Cell counts were obtained by plating on MRS agar (MRS medium plus 1.5 % agar, w/v). All measurements were performed on three independent samples.

Modelling

Following the lag phase λ (in h), the biomass concentration [X] (in CFU mL^{-1}) as a function of time t (in h) was modelled with the logistic growth equation (Rimaux *et al.* 2011):

$$d[X]/dt = \mu_{max} [X] (1 - [X]/[X]_{max}) \quad \text{if } t > \lambda \qquad [1]$$

with X_{max} the maximum obtained biomass (in CFU mL^{-1}) and μ_{max} the maximum specific growth rate (in h^{-1}).

Arginine [Arg] (in mM) conversion into ornithine [Orn] (in mM), via citrulline [Cit] (in mM), was modelled as (Rimaux *et al.* 2011):

$$d[Arg]/dt = -(k_1+k_2) [X] \qquad [3]$$

$$d[Cit]/dt = k_1 [X] - k_3 [Cit][X] \qquad [4]$$

$$d[Arg]/dt + d[Cit]/dt + d[Orn]/dt = 0 \qquad [5]$$

with k_1 and k_2 [mM (CFU mL^{-1} $h)^{-1}$], and k_3 [(CFU mL^{-1} $h)^{-1}$] as biokinetic model parameters.

Nucleoside [N] (in mM; inosine or adenosine) conversion into organic acids [O] (in mM), and nucleobase [Nb] (in mM; hypoxanthine or adenine) excretion were modelled as:

$$d[N]/dt = -k_N [X] \qquad [6]$$

$$d[O]/dt = -Y_{O/N} d[N]/dt \qquad [7]$$

$$d[Nb]/dt = -Y_{N/Nb} d[N]/dt \qquad [8]$$

with k_N the specific rate constant for nucleoside catabolism [mM (CFU mL^{-1} $h)^{-1}$], $Y_{O/N}$ the yield coefficient for the production of organic acids from nucleoside catabolism [mM organic acid (mM nucleoside)$^{-1}$], and $Y_{N/Nb}$ the yield coefficient for the excretion of nucleobase resulting from nucleoside catabolism [mM nucleoside (mM nucleobase)$^{-1}$].

The equations were fitted to the experimental data with Athena Visual Studio (www.athenavisual.com) using a multiresponse approach (Rimaux *et al.* 2011).

Metabolic analysis

Concentrations of arginine, citrulline, and ornithine were determined using LC-MS/MS (Waters Corp.) Inosine, adenosine, hypoxanthine, and adenine were quantified using HPLC with UV detection (Waters Corp.). Glycerol concentrations were determined using HPAEC-PAD (Dionex). Concentrations of lactic acid, acetic acid, and formic acid were determined using HPAEC-CIS (Dionex). Finally, concentrations of ethanol in end samples were determined with GC-FID (CompactGC, Interscience).

Gene expression analysis

Several samples (at different time points) were withdrawn from a growing culture of *L. sakei* CTC 494, grown in MRS supplemented with 3 g/L of arginine at constant pH 5.0, 6.0, and 7.0, for extraction of total RNA. After conversion of total extracted RNA into cDNA, quantitative real time PCR (RT-q-PCR) (ABI 7300, Applied Biosystems) was applied to determine relative gene expression of the genes coding for the ADI pathway in *L. sakei* CTC 494.

Results and Discussion

Genomic analysis

Several catabolic pathways, involved in the conversion of non-glucose energy sources present in meat, have been predicted based on the genome sequence of *L. sakei* 23K. For example, two operons responsible for the conversion of arginine through the ADI pathway have been annotated. Furthermore, other energy sources, such as glycerol and nucleosides could be effective energy sources, as several transporters and catabolic genes were detected in the genome sequence. This indicates that the species *L. sakei* is perfectly adapted to the meat environment, which may explain its dominance throughout the fermentation and drying process of fermented dry sausages. However, phenotypic evidence for these potential pathways, as well as its contribution to the dominance or survival of *L. sakei* was lacking.

Metabolic analysis

No glycerol conversion was found for *L. sakei* CTC 494. Arginine conversion was influenced by environmental pH. At optimal pH values, arginine was converted into both citrulline and ornithine, whereas at low pH values a higher ornithine-to-citrulline ratio was found. Inosine and adenosine were both used as energy source by *L. sakei* CTC 494. Metabolite analysis showed that inosine and adenosine were converted into a mixture of acetic acid, formic acid, and ethanol (Fig. 1). Only at low pH values production of lactic acid was found as well. This suggests a mixed-acid fermentation of the ribose moiety of inosine and adenosine by *L. sakei* CTC 494. For all pH values, adenine and hypoxanthine were not used by the cells and were stoechiometrically excreted into the medium. Finally, addition of glucose to the fermentation medium showed a delay in the catabolism of nucleosides by *L. sakei* CTC 494, indicating carbon catabolite respression as a regulatory mechanism involved in the catabolism of nucleosides. All metabolic profiles were successfully modelled (Fig. 1).

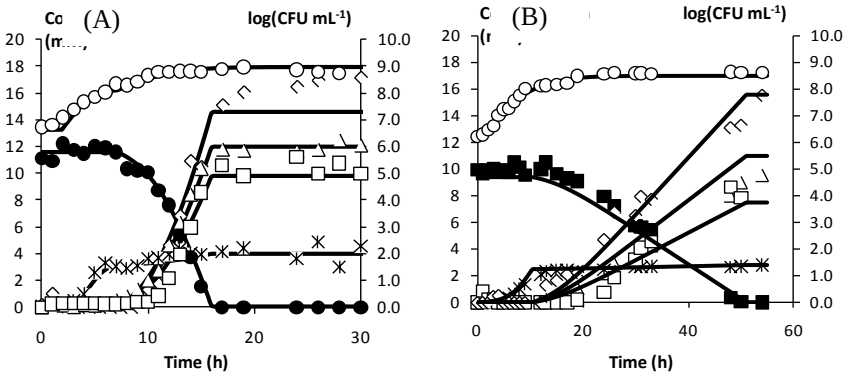

Figure 1: *Lactobacillus sakei* CTC 494 in customized MRS medium supplemented with 3 g/L of (A) inosine or (B) adenosine at 30°C and pH 6.5. (A) Cell counts (○), inosine (●), lactic acid (x), acetic acid (◊), formic acid (□), and hypoxanthine (Δ). (B) Cell counts (○), adenosine (■), lactic acid (x), acetic acid (◊), formic acid (□), and adenine (Δ). Lines are according to the model.

Gene expression

RT-q-PCR was applied to link the obtained kinetic data (modelled biokinetic parameters) as a function of pH to data on gene expression of the ADI pathway. In this way, the proposed model for the ADI pathway (Rimaux *et al.* 2011) could be validated using a more fundamental (molecular) methodology. It was found that the expression of the genes of the ADI pathway was highest in the middle of the exponential growth phase. Furthermore, the influence of the pH had a similar pattern on the level of gene expression as was proposed by the model (Fig. 2), with highest gene expression (Fig. 2A, example of *arcA*) and highest arginine-into-citrulline conversion (Fig. 2B, example of k_{AC}) at optimal pH, with a decreasing trend towards high and low pH. Finally, a putative transporter was co-expressed with the other genes of the ADI pathway, suggesting a role as a citrulline-ornithine antiporter, which

was proposed in the model for arginine conversion in *L. sakei* CTC 494 (the biokinetic parameter k_{CO}; Rimaux *et al.* 2011).

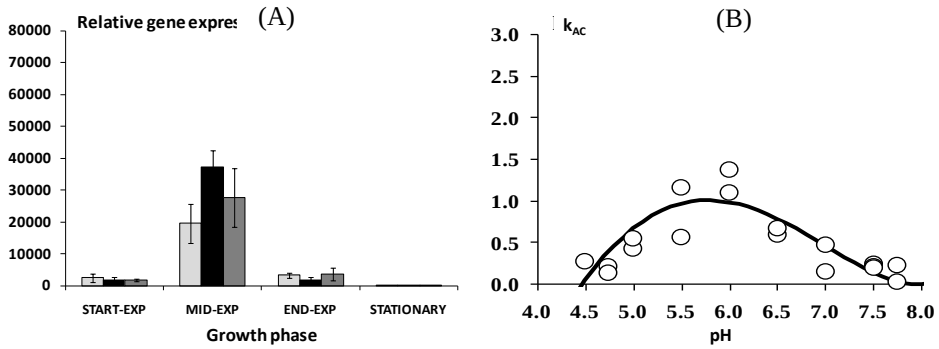

Figure 2: (A) Relative gene expression of the arginine deiminase gene (*arcA*) as a function of pH (5.0, 6.0, and 7.0) and growth phase. (B) Evolution of the biokinetic parameter k_{AC} corresponding with the conversion of arginine-into-citrulline as a function of pH.

Conclusions

In this study, the catabolism of arginine, glycerol, inosine, and adenosine by *L. sakei* CTC 494 was performed. It was shown that inosine and adenosine were perceived as an additional carbohydrate source for *L. sakei* 494, resulting in the production of a mixture of acetic acid, formic acid, lactic acid, and ethanol. Also, the kinetics of arginine catabolism through the ADI pathway revealed a similar response to environmental pH as predicted by the kinetic model. In conclusion, the combined use of genomic, metabolomic, and transcriptomic approaches opens perspectives for the quantitative analysis and modelling of the competitive behaviour and metabolic traits of bacteria in view of food applications. These data may help the selection of appropriate starter cultures for food (meat) fermentations.

Acknowledgements

The authors acknowledge their financial support of the Research Council of the Vrije Universiteit Brussel, the Fund for Scientific Research-Flanders, and the IWT-Flanders. TR is supported by a predoctoral fellowship of the FWO-Flanders.

References

Chaillou S., Champomier-Vergès M.C., Cornet M., Crutz-Le Coq A.M., Dudez A.M., Martin V., Beaufils S., Darbon-Rongère E., Bossy R., Loux V. and Zagorec M. (2005) The complete genome sequence of the meat-borne lactic acid bacterium *Lactobacillus sakei* 23K. *Nature Biotechnology* 23, 1527-1533.

Leroy F., Verluyten J. and De Vuyst L. (2006) Functional meat starter cultures for improved sausage fermentation. *International Journal of Food Microbiology* 106, 270-285.

Rimaux, T., Vrancken, G., Pothakos, V., Maes, D., De Vuyst, L. and Leroy, F. (2011) The kinetics of the arginine deiminase pathway in the meat starter culture *Lactobacillus sakei* CTC 494 are pH-dependent. *Food Microbiology* 28, 597-604.

Flux balance analysis of *E. coli* K12 growth dynamics: a balance between model complexity and flux measurements

D. Vercammen, E. Van Derlinden, J.F. Van Impe

BioTeC - Chemical and Biochemical Process Technology and Control, Department of Chemical Engineering, Katholieke Universiteit Leuven, Leuven, Belgium
{dominique.vercammen, eva.vanderlinden, jan.vanimpe}@cit.kuleuven.be

Abstract

To assure applicability of predictive models in general conditions, it is necessary to move from the black box methodology to more mechanistically-inspired models. The objective of this work is the incorporation of mechanistic, intra-cellular knowledge into a dynamic, macroscopic model structure. This will be accomplished through the use of a metabolic reaction network, which defines an underdetermined linear system of the intracellular reaction rates or fluxes. Flux balance analysis (FBA) uses an objective function to derive, through optimization over the solution space of this underdetermined linear system, an intracellular flux distribution. The classical FBA technique is, however, not directly applicable in this context. To be able to use flux predictions by FBA for a dynamic model, all degrees of freedom of the underdetermined linear system need to be removed. In most cases, not all degrees of freedom can be fixed through optimization and multiple flux solutions are found. Extra information is required to identify the remaining degrees of freedom. A procedure to identify a reduced parameter set which can remove all degrees of freedom is described. The procedure is illustrated on a small-scale metabolic network for *E. coli*. The size of the reduced parameter set varies for different experimental data sets. These parameter sets guarantee a unique identification of the fluxes. A study of the effect of measurement noise on predictions is carried out to evaluate the usefulness of these parameter sets, together with the objective function, as control variable sets in a dynamic flux balance model.

Keywords: *flux balance analysis, metabolic flux analysis, modelling of microbial dynamics*

Introduction

To assure applicability of predictive models in general conditions, it is necessary to move from the black box methodology to more mechanistically-inspired models (McMeekin *et al.* 2008). The objective of this work is the incorporation of intracellular knowledge into a dynamic, macroscopic model structure. This will be accomplished by using a metabolic reaction network. Metabolic network analysis starts from a simple algebraic equation,

$$\mathbf{S} \cdot \mathbf{v} = 0$$

with $\mathbf{S}$ the $(m \times n)$ stoichiometric matrix for the metabolic reaction network, with m the number of intracellular metabolites and n the number of intracellular and transport reactions, and $\mathbf{v}$ the $(n \times 1)$ vector of intracellular reaction rates or fluxes. This equation describes a subspace of $\mathbb{R}^n$ of dimension $n - \text{rank}(\mathbf{S})$ which is the null space of the stoichiometric matrix $\mathbf{S}$. All points inside this flux space satisfy the stoichiometric constraints imposed by the metabolic network and are thus possible metabolic flux states of the cell.
To characterise one flux vector inside this space, it is necessary to fix $n - \text{rank}(\mathbf{S})$ fluxes, in specific combinations which are found by performing calculability analysis (Klamt *et al.* 2002). These combinations effectively are parameterizations of the metabolic network model. In the remainder of this text, a possible combination will be referred to as a MFA parameter set. *Metabolic flux analysis* (MFA) estimates these parameters by measuring transport fluxes and/or intracellular isotopic mass distributions and minimizing the least squares residual between these measurements and the simulated values by varying the parameter values (Wiechert 2001). Simulations are carried out by solving a square system of linear equations:

$$\begin{cases} \mathbf{S} \cdot \mathbf{v} = 0 \\ v_i = p_i \quad \forall\, i \in MFA\ parameter\ set \end{cases}$$

with p_i the estimated parameter values.
Another technique to identify solutions inside the flux space is *flux balance analysis* (FBA), which uses linear optimization and an objective function, often chosen *"maximize growth rate"* (Varma and Palsson 1994). This choice can be motivated from an evolutionary point of view. FBA simulations are carried out by optimizing the objective function, which is a linear function of the fluxes with coefficients **c**.

$$\begin{aligned} &\max_{\mathbf{v}} \mathbf{c}^T \mathbf{v} \\ &s.t. \quad \mathbf{S} \cdot \mathbf{v} = 0 \\ &\qquad v_{lb,i} \le v_i \le v_{ub,i} \quad , i = 1 \dots n \end{aligned}$$

Whereas MFA always identifies one unique flux solution, this is not true for FBA. In some cases, all degrees of freedom are removed and a unique flux solution is found. However, in other cases, the flux space is only brought down to a space of lower dimension. Flux vectors in this space of lower dimension can be uniquely described by fewer parameters. The objective of this work is to assess the minimality of the parameterization used by MFA, and to identify other parameterizations based on the use of an objective function in combination with fewer parameters. These parameterizations can generally be described by the following optimization problem (*constrained flux balance analysis*, cFBA):

$$\begin{aligned} &\max_{v} c^T v \\ &s.t. \quad \mathbf{S} \cdot v = 0 \\ &\qquad v_i = p_i \quad \forall\, i \in reduced\ parameter\ set \\ &\qquad v_{lb,i} \le v_i \le v_{ub,i} \quad , i = 1 \dots n \end{aligned}$$

effectively combining the MFA and FBA approaches. In future work, these parameterizations will be used in a dynamic flux balance model.

Materials and Methods

Metabolic reaction network and flux data

The metabolic reaction network used to illustrate the procedure is taken from Ishii *et al.* (2007). It consists of 17 metabolites and 25 reactions. As such, the dimension of the flux space is $8\ (25 - 17)$, meaning there are 8 degrees of freedom for the regular MFA. Flux 1, the glucose uptake flux, was fixed at the experimental value, leaving 7 degrees of freedom and a MFA parameter set of size 7. The network is accompanied by four sets of flux data for all 25 fluxes, measured with ^{13}C-MFA at four different growth rates (data set 1-4).

Identification of reduced sets of parameters

Starting from a MFA parameter set, reduced sets of parameters were identified. Starting from a MFA parameter set, an iterative search is carried out by making combinations of the parameters. Starting from combination sets with 1 parameter (which are unlikely to give good predictions), the size of the combination sets is systematically increased until a set size is found for which there exists at least one parameter combination which gives unique and correct simulations. Correctness is checked by comparing the least squares distance between the simulation data based on the smaller size parameter set with the original experimental data for the MFA parameter set. Uniqueness is checked by comparing simulation data for the smaller size parameter set based on two LP-algorithms: (*i*), the simplex algorithm, and (*ii*), an interior point method. The simplex algorithm always finds an optimal basic feasible solution, meaning the solution is always on a vertex of the flux space. If there are multiple solutions, the simplex algorithm gives one vertex of the optimal face. Interior point methods, on the

other hand, approximate the optimal solution following a central path through the interior of the flux space. If there are multiple solutions possible, interior point methods converge to the centre of the optimal face, meaning that if both solutions are equal, the solution is unique.

Parameter estimation for constrained FBA

Estimation of the parameters in constrained FBA is difficult due to the optimization problem in the cFBA simulation itself. With addition of the upper-level objective of minimizing the least-squares residuals, a bilevel optimization problem arises. This problem was solved by employing a multi-parametric programming approach for bilevel programs (Faísca *et al.* 2007). To estimate the confidence intervals on the estimated parameters, a Monte-Carlo sampling approach was used.

Numerical computations

All simulations and optimizations were carried out in Matlab R2010b. For the simplex optimizations, IBM ILOG CPLEX 12.2 was used. The interior-point algorithm used was IPOPT (Wächter and Biegler 2006).

Results and Discussion

Identification of reduced parameter sets

By employing the described procedure, reduced sets of parameters were found for each of the four experimental flux data sets. An example of the results of the identification for flux data set 1 and 3 is shown in Figure 1. The size of the reduced parameter set depends on the experimental data set and, in some cases, also on the MFA parameter set started from. For data set 3, e.g., in some cases five parameters sufficed to predict unique and correct fluxes, whereas in other cases six parameters were needed.

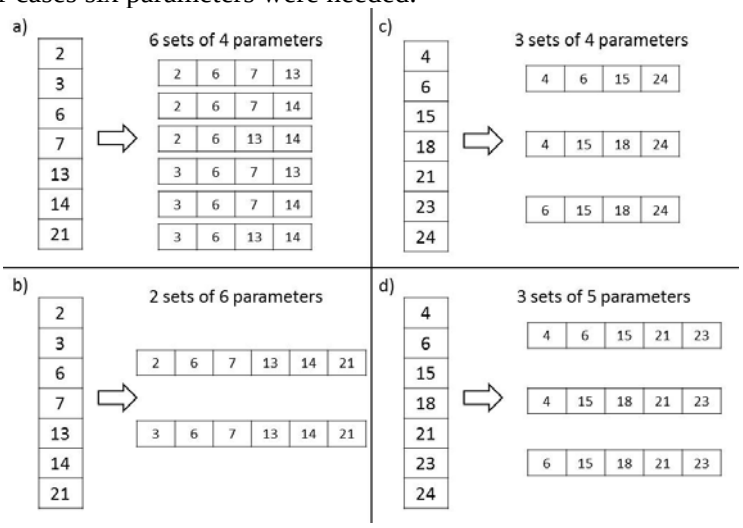

Figure 1: Reduced parameter set identification. Starting from a first MFA parameter set: (a) for data set 1, (b) for data set 3. Starting from a second MFA parameter set: (c) for data set 1, (d) for data set 3.

Evaluation of confidence levels of predictions

The benefit of this procedure lies in the fact that, with fewer parameters needed to estimate, fewer measurements are needed to get the same level of confidence on the estimated parameters and also on the simulated fluxes from these parameters. The other way around, with the same number of measurements, the variance on estimated parameters is lower as well as the variance on the simulated fluxes. To illustrate this, a Monte-Carlo parameter estimation was done for the first set of 4 parameters in Figure 1a with data from data set 1, which was assumed to be normal distributed with a standard deviation of 5% of the average values. Based on the estimated parameters and their variances, fluxes were simulated, both starting

from the MFA parameter set of size 7 and the reduced parameter set consisting of 4 parameters. The results are shown in Figure 2. The variance is considerably reduced by reducing the number of parameters. The sum of all confidence ranges is reduced by 75%.

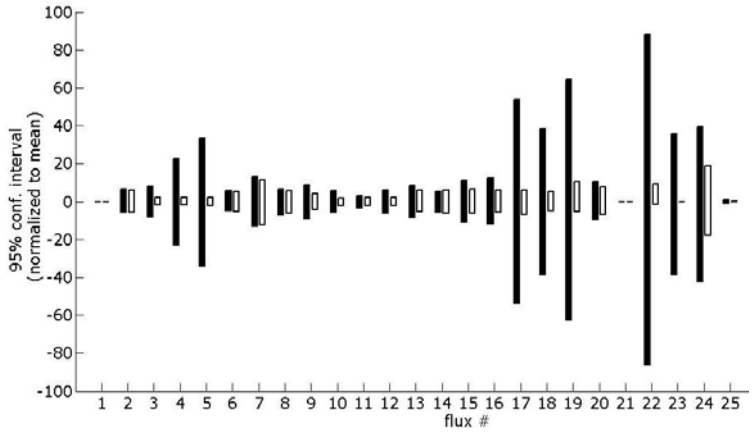

Figure 2: Confidence intervals for simulations based on the MFA parameter set (black bars) and the first reduced parameter set of Figure 1a (white bars) for data set 1. Confidence intervals were normalized to the mean of the flux predictions.

Conclusions

A procedure to reduce the number of parameters needed to fully describe a flux solution by means of optimization of an objective function is presented. The procedure is illustrated for a small-scale metabolic network. By simulating flux predictions based on the reduced parameter set, significant reductions in prediction variances are accomplished. In further research, these parameterizations will be implemented in a macroscopic model structure to be able to predict macroscopic dynamics of micro-organisms.

Acknowledgements

This work was supported by project PFV/10/006 (Center of Excellence OPTEC-Optimization in Engineering) of the Research Council of the K.U.Leuven, project KP/09/005 (www.scores4chem.be) of the Industrial Research Fund, and the Belgian Program on Interuniversity Poles of Attraction, initiated by the Belgian Federal Science Policy Office. E. Van Derlinden is supported by postdoctoral grant PDMK/10/122 of the K.U.Leuven Research Fund. J. Van Impe holds the chair Safety Engineering sponsored by the Belgian chemistry and life sciences federation essenscia. D. Vercammen is supported by a doctoral research grant of the Institute for the Promotion of Innovation by Science and Technology in Flanders (IWT).

References

Faísca N.P., Dua V., Rustem B., Saraiva P.M. and Pistikopoulos E.N. (2007) Parametric global optimization for bilevel programming. *Journal of Global Optimisation* 38, 609-623.

Ishii N. et al. (2007) Multiple high-throughput analyses monitor the response of *E. coli* to perturbations. *Science* 316, 593-597.

Klamt S., Schuster S. and Gilles E.D. (2002) Calculability analysis in underdetermined metabolic networks illustrated by a model of the central metabolism in purple nonsulfur bacteria. *Biotechnology and Bioengineering* 77 (7), 734-751.

McMeekin T., Bowman J., McQuestin O., Mellefont L., Ross T. and Tamplin M. (2008) The future of predictive microbiology: strategic research, innovative applications and great expectations. *International Journal of Food Microbiology* 128 (1), 2-9.

Varma A. and Palsson O. (1994) Metabolic flux balancing: basic concepts, scientific and practical use. *Nature Biotechnology* 12, 994-998.

Wächter A. and Biegler L.T. (2006) On the implementation of an interior-point filter line-search algorithm for large-scale nonlinear programming. *Mathematical Programming* 106 (1), 25-57.

Wiechert W. (2001) ^{13}C Metabolic Flux Analysis. *Metabolic Engineering* 3 (3), 195-206.

Determination of acid-stress bacterial resistance and viability biomarkers of *Bacillus weihenstephanensis* KBAB4

N.Desriac[1,2,3], F. Postollec[1], D. Sohier[1] and L. Coroller[2,3]

[1] ADRIA Développement, UMT 08.3 PHYSI'Opt , Z.A. de Creac'h Gwen, F-29196 Quimper cedex, France(noemie.desriac@adria.tm.fr); (florence.postollec@adria.tm.fr) (Daniele.sohier@adria.tm.fr)
[2] Université Européenne de Bretagne, France
[3] Université de Brest, EA3882, Laboratoire Universitaire de Biodiversité et Ecologie Microbienne, UMT 08.3 PHYSI'Opt , IFR148 ScInBioS, 6 rue de l'Université, F-29334 Quimper, France (louis.coroller@univ-brest.fr)

Abstract

The *Bacillus cereus* group that contains six closely related species among which *B. weihenstephanensis*, is ubiquitously encountered in soil and may either cause emetic or diarrheal types of food-borne illnesses. To prevent bacterial development, food industries use preservation techniques such as low pH and cold temperature storage. In this study, the acid resistance of the psychrotrophic *B. weihenstephanensis* KBAB4 strain is investigated using microbiological and transcriptomic methods. Standardized protocols were used to determine bacterial inactivation during an acid stress with a pH of 4.6. Population evolution was followed by CFU enumeration and kinetics were fitted using a mixed Weibull model. In parallel, the expression of twelve genes, selected as potential biomarkers, was performed using RT-qPCR. Quantification of each gene transcription was relative to three housekeeping reporter genes (*tuf, gyrA* and *sigA*) which showed stable expression (M value of respectively 0.414, 0.445 and 0.445).In optimal conditions, exponentially growing cells submitted to an acid shock could be divided in two populations, *i.e.* one sensitive (first decimal decrease after 1hour of inactivation) and one resistant (first decimal decrease after 3 hours of inactivation). In these conditions, gene expression showed up-regulation (4 genes) or down-regulation for 2 genes (*narL* and *napA*). Furthermore for individual genes, the expression profile during the inactivation treatment may vary extensively. For instance, *sigB* encoding general stress sigma factor, is up-regulated at the beginning of the inactivation with a peak after 2h (4.9 fold ± 1.3) whereas *katB*, encoding for a major catalase, is up-regulated at the beginning of the kinetic and stays constant (around 20 fold) between 3h and 4h of inactivation. Studies on gene expression along inactivation kinetics are being carried out under various physiological states. These results will allow us to develop a predictive tool that will correlate gene expression to the bacterial resistance. The prediction of bacterial history-dependent behavior using gene expression will offer a decision making tool adapted to food products.

Keywords: Food-borne pathogen, Acid stress, Modelling, Resistance, Weibull, Biomarkers, RT-qPCR

Introduction

Bacillus cereus, a gram-positive rod shaped spore-forming bacteria, is the etiological agent of two types of food-borne poisoning, caused by the production of emetic or diarrheal toxinsFood poisoning outbreaks are mostly due to the consumption of contaminated food such as RTE (ready to eat), vegetables, dairy, rice and pasta. Most of the time the contaminated products have been subjected to temperature abuse, yielding to the germination and multiplication of toxigenic strains in food. *B. cereus* is also known for its ability to cause food spoilage. Industrial issues therefore mainly concern the presence of spores and their survival to heat processes or cleaning procedures which lead to their persistence in the industrial environment. Nowadays, thermal processes need to ensure food organoleptic properties, food safety as well as the prevention of food spoilage. Minimal thermal processes are now used in combination with preservatives. For instance, weak organic acids and cold temperature storage are widely used to control microbial growth. In this study, the acid resistance of psychrotrophic *B. weihenstephanensis* KBAB4, that belongs to the *B. cereus* group, was investigated using microbiological and transcriptomic analysis for mid-

exponential phase cells submitted to an acid stress. Quantification of the expression of several genes by RT-qPCR will allow to identify biomarkers of bacterial viability and stress resistance for further implementation of predictive models.

Materials and methods

B. weihenstephanensis KBAB4, a psychrotrophic strain isolated from the soil of the forest of Versailles was kindly provided by INRA Avignon and used in this study. As previously described by Coroller *et al.* (2006), two pre-cultures of Brain heart Infusion BHI (BIOKAR DIAGNOSTIC, Beauvais, France) were used to ensure reproducible bacterial physiological states (30°C, 100 rpm). The bacterial inactivation was performed by transferring 5 ml of bacterial culture at a given physiological states in BHI supplemented with HCl 10N to obtain a final pH of 4.6. Survivors were enumerated on Nutrient Agar (BIOKAR DIAGNOSTIC, Beauvais, France) immediately after inoculation and at appropriate time intervals by surface plating cultures using Spiral Plater (AES laboratoire, Combourg, France). In parallel of bacterial enumeration, RNA extraction was performed using the RNeasy® Mini kit (QIAGEN, Courtaboeuf, France) according to manufacturers' recommendations. RNA quantity and quality from three independent cultures were reproducible, as shown by NanoDrop (Thermo Fisher Scientific, Wilmington, USA) and microfluidic analysis (Experion, BIORAD, Mitry Mory,France) performed according to MIQE guidelines. As described by the manufacturer, cDNA synthesis was performed using iScript cDNA synthesis kit (BIORAD, Mitry Mory,France). Nine genes were quantified using CFX 96^{TM} (BIORAD, Mitry Mory, France) and standardized by using three reference genes (*tuf*, *gyrA* and *sigA*) which showed stable expression (M value of respectively 0.414, 0.445 and 0.445). As mentioned by Postollec *et al.* (2011), some other controls have been performed, such as the evaluation of DNA contamination, non-template control or the use of reference sample. All Reverse Transcription qPCR were performed from three independent cultures, for each tested conditions.

Results and discussion

Physiological response to acid stress

It is well known that physiological state can be related to culture conditions. In tested conditions, the growth of *B. weihenstephanensis* KBAB4 reaches a population of 10^7 CFU.ml^{-1} after four hours incubation corresponding to the middle of the exponential phase (Figure 1, A).

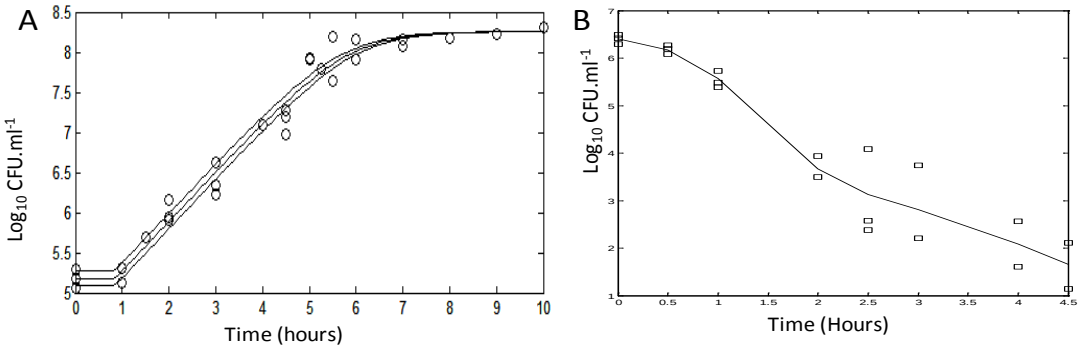

Figure 1 : A- B.weihenstephanensis KBAB4 (BHI, pH7.2, 30°C, 100 rpm). Open symbols represent independent experimental data during bacterial growth while solid line represents the fitting using Rosso model (1995). B- *B. weihenstephanensis* KBAB4 (BHI, pH4.6, 30°C, 100 rpm). Open symbols represent independent experimental data during the acid inactivation step while the solid line represents the fitting using mixed Weibull model (Coroller *et al.*, 2006).

Preliminary results are obtained for growing cells sampled from the middle of exponentially phase and submitted to an acid stress at pH 4.6. Bacterial enumeration was fitted using a mixed Weibull model (Coroller *et al.*,2006). A biphasic non linear shape is obtained, with a shape parameter (p) estimated at 1.8 (Figure1, B). This biphasic shape underlines the presence of two sub-populations, *i.e.* one sensitive (first decimal decrease obtained after one hour of inactivation) and one more resistant (first decimal decrease obtained after 3 hours of inactivation). Nevertheless, the more resistant population represents approximately 1/1000 (α=2.6) of the starting population. Because bacterial resistance varies depending on the transcription of a specific set of genes, a selection of thirty genes was performed as potential biomarkers for bacterial acid resistance. In parallel of bacterial inactivation counts, samples were extracted to quantify gene expression by optimized RT-qPCR protocol to define potential biomarkers to target during acid inactivation kinetics.

Gene expression during acid inactivation

Transcription quantification of each gene was related to three housekeeping reporter genes (*tuf, gyrA* and *sigA*) which showed stable expression. Preliminary results concern the quantification of the expression of nine genes of *B. weihenstephanensis* KBAB4 by RT-qPCR, during acid inactivation. Inactivation was performed by after a few minutes (T0), 1 hour, 2 hours, 3 hours and 4 hours incubation in acid conditions (pH 4.6). Throughout inactivation, gene expression quantification showed up-regulation (4 genes), down-regulation for 2 genes (*narL* and *napA*) or no significant variation (3 genes). As an example, Figure 3 presents the expression quantification of *sigB*, a gene encoding for a general stress transcription factor, *narL*, encoding for a nitrate sensing regulator and *katB*, encoding for hydrogen peroxide-inducible catalase.

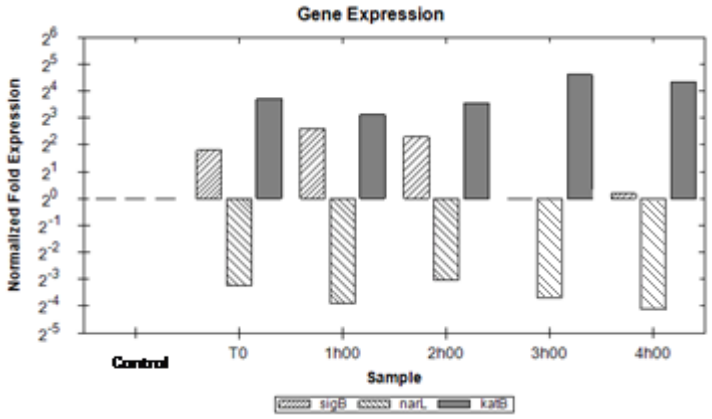

Figure 3 : *B. weihenstephanensis* KBAB4 gene expression quantification performed by RT-qPCR targeting *sigB, narL, katB* genes. The evolution of targeted genes expression is quantified after a few minutes (T0), 1h, 2h, 3h and 4h in acid conditions (pH 4,6) and can be compared to the expression of the unstress cells (control). Gene expression is standardized using three housekeeping genes.

Besides the expression of targeted genes during acid inactivation exposure, a control condition representing exponentially growing cells tested before inoculation in pH 4.6, was systematically performed. Gene expression of *sigB, katB* and *narL* was preliminary normalized using *tuf, gyrA, sigA* as reference genes. The *sigB* gene exhibited up-regulation during the first part of the inactivation kinetic, with a peak of expression at 2 hours (4.9 fold ± 1.3 compared to the unstress control). The *katB* gene of *B. weihenstephanensis* KBAB4 was up-regulated from the beginning to the end of acid inactivation, with a maximal up-regulation at 3h (24.3 fold ± 2.6 compared to the unstress control). The *narL* geneknown to be involved in nitrogen metabolismand may serve as an alternative to aerobic respiration, was down-regulated throughout acid inactivation. Besides up- or down-regulation, gene variation profile may vary as well during inactivation kinetic. For instance, *sigB*, was up-regulated at the

beginning of inactivation with a peak after 2h whereas *katB*, was up-regulated throughout the kinetic with a maximal up-regulation at 3h.These promising preliminary results emphasize the use of gene expression quantification, for the elucidation of *B. weihenstephanensis* KBAB4 physiology under exposure to a lethal acid stress. Indeed, *sodA*, which encodes for superoxide dismutase, is up-regulated throughout the inactivation kinetic. This up-regulation may indicate the formation O_2- radicals. The induction of *katB* also corroborates to the formation of oxidative compounds. Similarly to what is observed for *B. cereus* ATCC 14579 (Mols *et al.*, 2010), the formation of oxidative compounds may be due to perturbation of the aerobic Electron Transfer Chain (ETC). Nevertheless, the acid response of *B. weihenstephanensis* KBAB4 is not exactly the same for *B. cereus* ATCC 14579, as Mols *et al.* (2010) showed an over-expression of the nitrate and nitrite reductases. This up-regulation was correlated to the formation of Nitric Oxide (NO), formed from arginine by nitric oxide synthase, Mols and co-workers also demonstrated the up-regulation of nitric oxide dioxygenase, which catalyses the reaction of NO with oxygen to form nitrate, thus explaining the up-regulation of nitrate and nitric reductases. In *B. weihenstephanensis* KBAB4, the nitrate reductase (*narL*) is down-regulated throughout the acid inactivation kinetic, showing different pattern compared to *B. cereus* ATCC 14579 acid stress response. Whereas implementation of a secondary oxidative stress response upon lethal acid stress occurs both in *B. cereus* ATCC 14579 and *B. weihenstephanensis* KBAB4, the difference between these two species in the expression of some genes remains to be elucidated.

Conclusion

Research employing genomic technologies is helpful to elucidate microbial spoilage and pathogen behavior at the molecular level and to develop better detection and characterization systems. The selection and quantification of universal biomarkers by RT-qPCR enable the exploration of complex biological processes in a quantitative and integrative manner via a systems biology approach. These methods of analysis help to identify genes of interest, *i.e.* genes involved in cell injury and generic biomarkers of cell activity. Since cell history strongly impacts on bacterial resistance, this study will provide data on the simulation of the impact of salt, cold or acid conditions on exponentially growing cells. Comparison between genes expression of adapted and non adapted cells submitted to an acid stress will allow the identification of resistance and viability biomarkers. From the wide range of targeted genes involved in metabolic activity and stress response, the definition and quantification of universal biomarkers to track the behavior of *B. cereus* during inactivation will enable mathematical modeling. Prediction of bacterial behavior and physiology during inactivation will be implemented in a decision making tool, in order to provide help in food formulation and stability.

Acknowledgements

This research is part of national UMT08.3 PHYSI'Opt national network and has received funding from the European Community's Seventh Framework Programme (FP7/2007-2013) under the grant agreement n°FP7-222 654 within DREAM Project.

References

Bustin S.A., Benes V., Garson J.A., Hellemans J., Huggett J., Kubista M., Mueller R., Nolan T., Pfaffl M.W., Shipley G.L., Vandesompele J. and Wittwer C. (2009) The MIQE Guidelines: Minimum Information for publication of Quantitative real-time PCR Experiments. Clinical Chemistry 55 (4), 611-622.

Coroller L., Leguerinel I., Mettler E, Savy N. and Mafart P. (2006) General model based on two mixed Weibull distributions of bacterial resistance for describing various shapes of inactivation curves. Applied and Environmental Microbiology 72 (10), 6493-6502.

Mols M., van Kranenburg R., van MelisC.C.J.,Moezelaar R. and Abee T. (2010) Analysis of acid-stressed Bacillus cereus reveals a major oxidative response and inactivation-associated radical formation. Environmental Microbiology 12 (4), 873-885.

Postollec F., Falentin H., Pavan S., Combrisson J. and Sohier D. (2011) Recent advances in quantitative PCR (qPCR) applications in food microbiology. Food Microbiology In press: doi:10.1016/j.fm.2011.02.008

Optimizing the use of peracetic acid for sporicidal activity

A. Camarero[1,2], A.-G. Mathot[1,2], I. Leguérinel[1,2], F. Postollec[3] and L. Coroller[1,2]

[1] Université Européenne de Bretagne, France
[2] Université de Brest, EA3882, Laboratoire Universitaire de Biodiversité et Ecologie Microbienne, IFR148 ScInBioS, UMT 08.3 PHYSI'Opt, 6 rue de l'Université, F-29334 Quimper, France
[3] ADRIA Développement, UMT 08.3 PHYSI'Opt, Z.A. de Créac'h Gwen, F-29196 Quimper cedex, France

Abstract

Peracetic acid presents a bactericidal and sporicidal activity at room temperature and it is widely used as sanitizer for surfaces as well as disinfectant for fruits and vegetables in the food industry. The aim of this study was to quantify the impact of peracetic acid on spores of *Bacillus* as a function of environmental conditions.

The spores of a psychrotolerant *Bacillus weihenstephanensis* strain were inactivated by a peracetic acid solution. The treatment was done at four peracetic acid concentrations and four temperatures; ranging respectively from 0.25 g/L to 1.05 g/L and from 5 to 20°C. The surviving spores were enumerated using spiral plate count on Nutrient Agar. The survival curves were fitted by the Weibull model.

The bacterial resistance decreases with increasing peracetic acid concentration and storage temperature. A model was proposed to quantify the treatment efficiency at a given peracetic acid concentration and temperature of use. Even though the synergy between the temperature and the concentration on the bacterial resistance is neglected, this model has a good quality of fit (RMSE = 0. 04). But its main advantage remains simplicity and practical interpretation of parameters. For instance, the inactivation of bacterial spores with 1.48g/L peracetic acid is ten fold higher with an increase of 17.1°C (z_T values), for the conditions tested. The model allows the estimation of bacterial population decrease for given concentration of peracetic acid, time and temperature of treatment. But, it might be used also to optimize the process parameters (time, temperature and acid concentration) knowing a targeted value of bacterial decrease.

Keywords: *disinfection, biocide, resistance, modelling, Weibull*

Introduction

Peracetic acid is used mainly in food industry and in medicine for disinfection or sterilization of surface and equipment. It is also used for residual and process water treatment because it has the advantage of no residual toxic products (Kitis 2004). Its spectrum of activity is broad with a bactericidal, fungicidal, virucidal and sporicidal effect. Indeed, it has a strong oxidizing power through the production of reactive oxygen species that will oxidize proteins, enzymes and metabolites and led to the denaturation or unfold of membrane proteins. The sporicidal activity of peracetic acid is enhanced for acidic pH and increasing temperature. This biocide is highly volatile and its sporicidal activity may decrease over time (Sagripanti *et al.* 1996). It is often presented in a combined form with acetic acid (CH_3CO_2H) and hydrogen peroxide (H_2O_2).

The aim of this study is to quantify the impact of peracetic acid on the survival of *Bacillus cereus* group spores depending on the exposure time, concentration and temperature conditions.

Materials and Methods

Biological materials and experiments

Spores of *B. weihenstephanensis* KBAB4 were produced using a sporulation mineral buffer (Baril *et al.* 2011). The exposure of spores with 100 ml of peracetic acid solution (Oxyanios 5, Anios Laboratories, Lille, France) was done in an Erlenmeyer flask under agitation (100 rpm). The initial spore concentration used for inactivation assay was 10^6 CFU/mL. The inactivation kinetics were followed by spreading 0.5 mL suspension which was previously

neutralized by 0.5 mL of sodium thiosulfate (Na2S2O3, final concentration: 25 g / L (Sigma, St. Louis, USA)) on nutrient agar (Biokar, Beauvais, France) using a spiral plater (WASP1, Don Withley Scientific Ltd, Shipley, England). The enumeration of the colonies forming unit was performed after 20 hours incubation at 30 °C.
The influence of the peracetic acid concentration and the storage temperature were studied for four levels of peracetic concentration (0.25 g/L to 1.05 g/L) and for four temperature ranging from 5°C to 20° C. Triplicates were performed at 10 and 20 ° C for both 0.45 g/L and 0.85 g/L concentrations.

Inactivation modeling

The Weibull primary model (Mafart *et al.* 2002) was used to fit the spore inactivation kinetics. It could be written as follow:

$$\log N(t) = \log N_0 - \left(\frac{t}{\delta}\right)^p \qquad (1)$$

Where N is the number of survivors at time t, N_0 is the initial cell number, t is the time of exposure to a stress, δ is the time leading to the first reduction by 10 of the treated population and p is the shape parameter of the curve, it reflects the distribution of resistance within the spore suspension.
To model the influence of the peracetic acid concentration and temperature on the bacterial resistance, a Bigelow type model was used:

$$\log(\delta) = \log(\delta^*) - \frac{T - T^*}{Z_T} - \frac{C - C^*}{Z_c} \qquad (2)$$

Herein δ is the first decimal decrease at the temperature T (°C) and peracetic acid concentration C (g/L). The z value reflects the sensitivity of the spores to a temperature variation (z_T) or a concentration variation (z_C). An increase of z value will yield a ten fold increase of δ values. The star symbol indicates the reference resistance and reference conditions of treatment.
These models were fitted by minimizing the sum of squared errors (lsqcurvefit, Optimization Toolbox, MATLAB 7.9.0, The Math-works, Natick, USA).

Results and Discussion

All inactivation kinetics obtained were concave, showing a little decline of the population at the beginning of the peracetic acid exposure followed by an important inactivation for longer time exposure (figure 1). This observation was confirmed by the fact that no significant dependence of the shape parameter (p) was observed as a function of the temperature or the acid concentration (α=0.05). A unique p parameter of 2.52±0.09 was estimated from all the inactivation kinetics. The advantage of such a simplification was to have only the δ parameter to model as a function of the temperature and the acid concentration.
The estimated values of δ decrease log-linearly according to an increase of the storage temperature or an increase of peracetic acid concentration (figure 2). At 5, 10, 15 and 20°C, the estimated z_C values are 1.23±0.92, 1.82±0.50, 1.28±0.70, and 1.57±0.91 g/L, respectively. The estimated z_T were also slightly influenced by the peracetic concentration. A two-way ANOVA indicated a weak interaction between temperature and concentration (1.5%), which was neglected. The estimation of the common value for z_T and z_C were, respectively 1.48±0.21 g/L and 17.10±0.51°C. The time for the first decimal decrease was estimated at 47.7 min ($\log(\delta^*)$ estimated at -0.099 ±0.019) for a treatment at 20°C (T*), 1.25 g/L (C*). The reference conditions were chosen to be as close as the conditions recommended for the industrial use. Figure 2 shows the experimental data and their fitting according to the equation (2). The root mean square error on the log δ was as low as 0.04. However, as it can be noticed, at low concentration our model seems to underestimate the bacterial resistance. Note that a non-linear model was tested but it used could not be justified on our dataset.

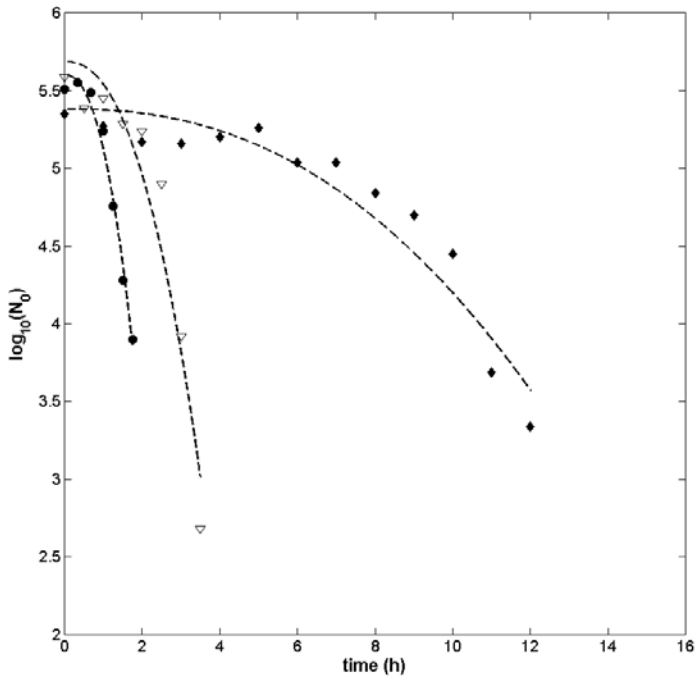

Figure 1: Survival kinetics of *B. weihenstephanensis* spores during an exposure to a peracetic acid solution at 0.85g/L and 20°C (●), at 0.45g/L and 20°C (Δ) and at 0.45g/L and 10°C (♦). The fitted curves are represented by the dashed lines.

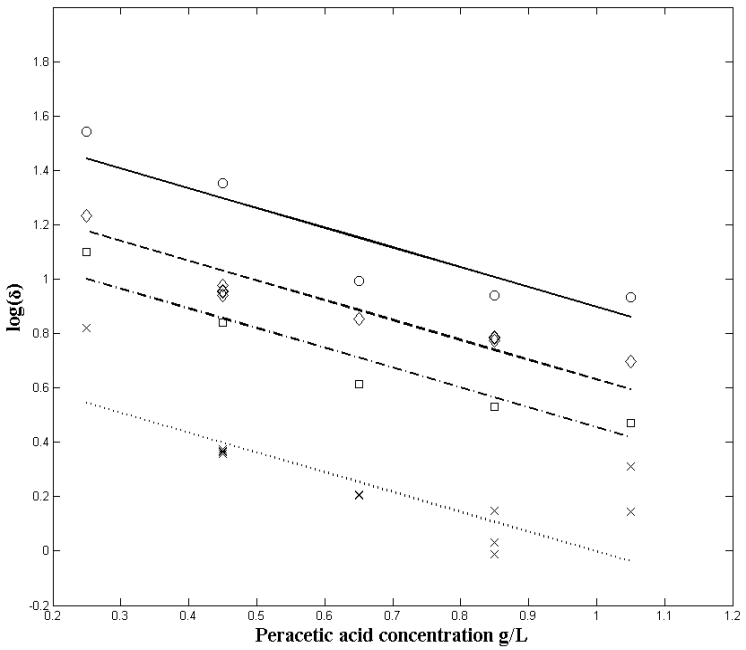

Figure 2: Resistance (log δ h) of *B. weihenstephanensis* spores as a function of peracetic acid concentration (g/L) at 5°C (x), 10°C (□), 15°C (◊) and 20°C (○). The fitted values are shown with the black or dotted lines.

The used of a log-linear relation between the resistance and the concentration or the temperature could be extrapolated to the results obtained in the literature with *B. cereus, B. subtilis* and *B. atropheus* (Mohan *et al.* 2009, Yamazaki *et al.* 2009). The spores produced in this study were four times more resistant compared to those of *B. subtilis* for a treatment at 20°C and 0.5 g/L.
The model allows the optimization of the disinfection or sterilization process using peracetic acid. For example, the objective of a spore population reduction of 3 log is reached after an inactivation treatment of 1h15 at reference conditions (20°C and 1.25 g/L). If the sanitation process is made at 4°C, we can choose to increase either the treatment time up to 10h30 or the concentration of peracetic acid up to 2.64 g/L to reach a similar 3 log reduction.
The developed model shows a high accuracy in simplified conditions used. Nevertheless, the presence of interfering agents such as proteins, sugars may decrease the action of peracetic acid on surface. Indeed, Xu *et al.* (2008) observed that, due to possible reaction with amino groups of proteins, the presence of organic material may decrease the effectiveness of the peracetic acid. Moreover, microorganisms adhering to surfaces may form biofilm yielding to the emergence of cells with acquired characteristics such as greater resistance to biocides. Nevertheless, the temperature has a great impact on the spore resistance. The importance of the storage temperature was already mentioned for *Listeria* and *Escherichia* in the case of acid or osmotic stress by Zhang *et al.* (2010).

Conclusions

The model allows the optimization of the processing conditions of sanitation by modifying and combining different parameters in simplified conditions: peracetic acid concentration, temperature and time of exposure. Nevertheless, the use of peracetic acid with different formulations or in combination with other compounds may have different impact. These combinations and the presence of inhibitory substances such as protein or sugar still have to be quantified.

References

Baril E., Coroller L., Postollec F., Leguerinel I., Boulais C., Carlin F. and Mafart P. (2011) The wet-heat resistance of *Bacillus weihenstephanensis* KBAB4 spores produced in a two-step sporulation process depends on sporulation temperature but not on previous cell history. *International Journal of Food Microbiology* 146, 57-62.

Kitis M. (2004) Disinfection of wastewater with peracetic acid : a review. *Environment International* 30, 47-55.

Mafart, P., Couvert, O., Gaillard, S. & Leguerinel, I. (2002) On calculating sterility in thermal preservation methods: application of the Weibull frequency distribution model. *International Journal of Food Microbiology* 72, 107-113.

Mohan A., Dunn J., Hunt M. C. and Sizer C. E. (2009) Inactivation of *Bacillus atrophaeus* spores with surface-active peracids and characterization of formed free radicals using electron spin resonance spectroscopy. *Journal of food science* 74, 411-417.

Russel A.D. (2001) Chemical sporicidal and sporostatic agents, p. 529-541. *In* Disinfection, sterilization and preservation. Seymour S.Block. Lippincott W&W, USA.

Sagripanti J.L. and Bonifacio A. (1996) Comparative Sporicidal Effects of Liquid Chemical Agents. *Applied and environnemental microbiology* 62. 545-551.

Xu S., Labuza T. P. and Diez-Gonzalez, F. (2008) Inactivation of *Bacillus anthracis* spores by a combination of biocides and heating under high-temperature short-time pasteurization conditions. *Applied and environnemental microbiology* 74, 3336-3341.

Yamazaki S., Sakamoto J.J., Okano T., Tamura S. and Tsuchido T. (2009) Sporicidal activity of a novel preparation of peracetic acid and the influence of coexisting hydrogen peroxide. In: S. Sohier and I. Leguérinel (Eds.), *Spore forming bacteria in food- Conference proceedings*, p 182-185. [Spore forming bacteria in food, Quimper (France), 15-17 June 2009].

Zhang D., McQuestin O.J., Mellefont L.A. and Ross T. (2010) The influence of non-lethal temperature on the rate of inactivation of vegetative bacteria in inimical environments may be independent of bacterial species. *Food Microbiology* 27, 453-459.

Effect of temperature and pH on sporulation kinetics and sporulation boundaries of *Bacillus weihenstephanensis* and *Bacillus licheniformis*

E. Baril[1,2,3], L. Coroller[1,2], O. Couvert[1,2], M. El Jabri[3], I. Leguerinel[1,2], F. Postollec[3], C. Boulais[4], F. Carlin[5,6], P. Mafart[1,2]

[1] Université Européenne de Bretagne
[2] Université de Brest, EA3882, Laboratoire Universitaire de Biodiversité et Ecologie Microbienne, IFR148 ScInBioS, UMT 08.3 PHYSI'Opt, 6 rue de l'Université, F-29334 Quimper, France. (Eugenie.baril@univ-brest.fr)
[3] ADRIA Développement, UMT 08.3 PHYSI'Opt, Z.A. de Creac'h Gwen, F-29196 Quimper Cedex, France.
[4] Danone Research, Avenue de la Vauve, RD128, F-91767 Palaiseau Cedex, France.
[5] INRA, UMR408, Sécurité et Qualité des Produits d'Origine Végétale, F-84000 Avignon, France.
[6] Université d'Avignon et des Pays de Vaucluse, UMR408, Sécurité et Qualité des Produits d'Origine Végétale, F-84000 Avignon, France.

Abstract

The resistance properties of *Bacillus sp.* spores are strongly influenced by the sporulation physicochemical environment. Many steps of the food chain may be suitable for sporulation depending on nutrient availability and other environmental factors, and provided that incubation time is sufficient for the completion of the sporulation process. Assessing quantitatively the sporulation yields and rates allows the identification of sporulation niches and where to focus control measures throughout the food chain. The sporulation of psychrotrophic *B. weihenstephanensis* and mesophilic *B. licheniformis* was studied from 5°C to 50°C (every 5°C) and from pH 5.2 to 8.5 (every 0.3 pH unit) in a sporulation mineral buffer.

B. weihenstephanensis was able to form spores from 5°C to 35°C and from pH 5.2 to 8.5. When sporulation occurred at 30°C, the time to achieve one spore per ml was the shortest (6.7 h) and the sporulation rate and final spore concentration were the highest (0.60 h^{-1} and 7.4 logCFU/ml). At 10°C, the time to achieve one spore/ml was lengthened and estimated at 148.0 h, the sporulation rate was lower (0.05 h^{-1}) as well as the sporulation yield (6.5 logCFU/ml). Similarly, at pH lower than 7.0 – 8.5, the sporulation process was lower and resulted in a lower sporulation yield. Similar results were observed with *B. licheniformis* at temperatures ranging from 20°C to 50°C and pH ranging from 6.0 to 8.5. Interestingly, the range of temperature and pH allowing sporulation were close to those allowing growth. Moreover, the temperature and pH appear to affect the sporulation kinetics in the same way than the growth kinetics.

Keywords: sporulation environment, *Bacillus weihenstephanensis*, *Bacillus licheniformis*

Introduction

The sporulation environment is known to affect the spore heat resistance (Mazas *et al.* 1997; Palop *et al.* 1999). Spore formation is mainly induced by nutrient depletion and corresponds to the acquirement of a high cell resistance (Sonenshein 1999). However numerous authors pointed out a clear effect of some environmental factors such as temperature and pH on the spore formation. At low temperatures and pHs, the sporulation time is lengthened and spore concentration decreases (Gonzalez *et al.* 1999; Mazas *et al.* 1997). Spores are found in many steps of the food chain and as the condition of sporulation impacts on the spore concentration and resistance, it is important to better characterize the spore formation which would contribute to the identification of sporulation niches. Thus sporulation boundaries and kinetics were studied on *B. weihenstephanensis* KBAB4 and *B. licheniformis* AD978 at different temperature and pH environments.

Materials and Methods

Sporulation kinetics

B. weihenstephanensis KBAB4 strain and *B. licheniformis* AD978 strain were studied. The sporulation was performed in the sporulation mineral buffer (SMB) (Baril *et al.* 2011) at temperatures ranging from 5°C to 50°C (every 5°C) and at pHs ranging from pH 5.2 to 8.5 (every 0.3 pH unit). At the end of the sporulation process, total count and spore count were enumerated. Spores were defined as heat resistant cells to a heat treatment at 70°C for 5 min.
Sporulation boundaries were studied through the observation of spore concentration on a wide range of temperatures and pH. In order to assess the sporulation time and rate, sporulation kinetics were performed in triplicates at two temperature levels and at two pH levels for each bacterial strain: 30°C, 10°C, pH 7.2 and 5.9 for *B. weihenstephanensis* KBAB4 and 45°C, 20°C, pH 7.2 and 6.3 for *B. licheniformis* AD978. Total count and spore count were enumerated throughout the sporulation process. The detection threshold corresponded to 2.6 log(CFU/ml).

Estimation of kinetic parameters

The following sporulation kinetic model which is a particular form of a logistic function (hyperbolic tangent) was proposed to fit sporulation curves:

$$\log(N_S)_t = \frac{\log(N_S)\left[1-\exp\left[-\mu_s\left(t-t_{1s}\right)\right]\right]}{1+\exp\left[-\mu_s\left(t-t_{1s}\right)\right]} \quad ,t > t_{1s} \qquad (1)$$

where $\log(N_S)_t$ (logCFU/mL) is the spore concentration at the t time (h), $\log(N_S)$ (logCFU/mL) is the maximal spore concentration obtained at the studied sporulation temperature and pH, μ_s (h^{-1}) is the sporulation rate and t_{1s} (h) is the time to achieve one spore per ml.
This model was fitted by minimizing the sum of square error (lsqcurvefit, Optimization Toolbox, MATLAB 7.9.0, The Math-works, Natick, USA). The 95% confidence intervals were computed using nlparci function (Statistical Toolbox, MATLAB 7.9.0, The Math-works, Natick, USA).

Results and Discussion

B. weihenstephanensis KBAB4 was able to sporulate at temperatures ranging from 5°C to 35°C and at pH higher than 5.2. *B. licheniformis* AD978 was able to form spores at temperatures ranging from 20°C to 50°C and at pH higher than 5.7. Inside these sporulation boundaries, spore concentrations were quite stable, while they dropped near the sporulation boundaries. These sporulation boundaries were close to growth limits, in agreement with published data (De Pieri & Ludlow 1992; Mazas *et al.* 1997).

Table 1: Estimated sporulation kinetic parameters of *B. weihenstephanensis* KBAB4 and of *B. licheniformis* AD978 (Equation 1).

	T	pH	t_{1S} (h)	μ_S (h^{-1})	Log(N_S) (logUFC/mL)	RMSE
B. weihenstephanensis KBAB4	30°C*	7.2*	6.66 (± 0.36)	0.60 (± 0.10)	7.45 (± 0.17)	0.371
	30°C	5.9	14.47 (± 0.87)	0.50 (± 0.14)	7.68 (± 0.29)	0.380
	10°C	7.2	148.00 (± 7.30)	0.05 (± 0.01)	6.54 (± 0.20)	0.373
B. licheniformis AD978	45°C*	7.2*	1.63 (± 0.44)	0.37 (± 0.05)	7.10 (± 0.17)	0.549
	45°C	6.3	4.19 (± 0.12)	0.55 (± 0.10)	5.46 (± 0.12)	0.328
	20°C	7.2	45.86 (± 11.67)	0.02 (± 0.00)	6.85 (± 0.27)	0.226

*: reference conditions

As shown in table 1 and figure 1A, the sporulation kinetics parameters of *B. weihenstephanensis* KBAB4 were affected by the sporulation temperature. When sporulation occurred at 30°C, the time to achieve one spore per ml was shorter (6.7 h) and the sporulation

rate and the maximal spore concentration were higher (0.60 h^{-1} and 7.45 logCFU/ml). At 10°C, the time to achieve one spore per ml was 148.0 h, the sporulation rate was 0.05 h^{-1} and the sporulation yield was 6.54 logCFU/ml. Sporulation kinetic parameters were also affected, but to a lower extent, by the pH.

In the same way, as shown in figure 1B and table 1, sporulation kinetics parameters of *B. licheniformis* AD978 was faster with higher maximal spore concentration at 45°C and pH 7.2. In such conditions, the time to achieve one spore per ml (t_{1S}) was less than 2 h, the sporulation rate was estimated at 0.33 h^{-1} and the final spore concentration reached 7.10 logCFU/ml. As observed for *B. weihenstephanensis*, a lower sporulation pH or temperature led to lower sporulation rate of *B. licheniformis* AD978.

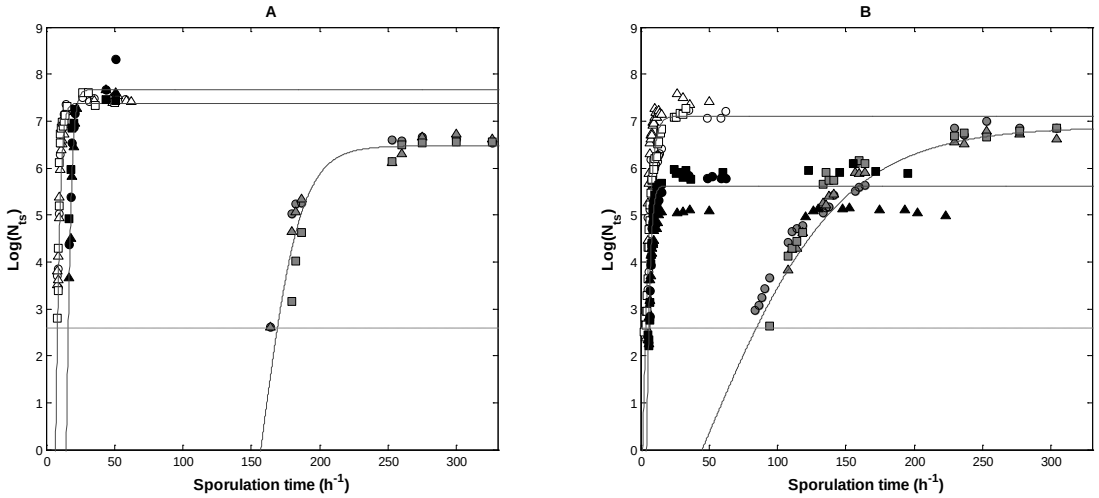

Figure 1: Influence of the sporulation temperature and pH on sporulation kinetics of *Bacillus* strains. (A) Sporulation of *B. weihenstephanensis* KBAB4 at 30°C pH 7.2 (white filled symbols) at 30°C pH 5.9 (black filled symbols) and at 10°C pH 7.2 (gray filled symbols). (B) Sporulation of *B. licheniformis* AD978 at 45°C pH 7.2 (white filled symbols), at 45°C pH 6.3 (black filled symbols) and at 20°C pH 7.2 (gray filled symbols). Each symbol (triangles, squares and circles) represents one of the independent triplicates. Lines correspond to the estimated spore concentrations from the sporulation kinetic model (Equation 1).

Inspired by the relative effect of environmental factors (Ross & Dalgaard 2004), for *B. weihenstephanensis* KBAB4, the ratio between the maximum sporulation rates at 10°C and 30°C ($\mu_{S10°C}/\mu_{S30°C}$) was calculated using the equation 1. The ratio between the specific growth rates at the same temperatures ($\mu_{G10°C}/\mu_{G30°C}$) were calculated by using the growth cardinal model (Rosso *et al.* 1995). These sporulation and growth ratios were both equal to 0.08 (Table 2). Similarly, for sporulation pH of 5.9 and 7.2, the growth and sporulation ratios were close, respectively 0.78 and 0.83. For *B. licheniformis* AD978, the effect of temperature on growth and sporulation ratios (20°C and 45°C) were calculated and reached respectively 0.07 and 0.05. However, the effect of pH on these ratios (pH 6.3 and 7.2) was less comparable between growth and sporulation, with values calculated at 0.89 and 1.49, respectively.

Table 2: Comparison of the growth and sporulation ratios.

	B. weihenstephanensis KBAB4		*B. licheniformis* AD978	
	$\mu_{10°C}/\mu_{30°C}$	$\mu_{pH5.9}/\mu_{pH7.2}$	$\mu_{20°C}/\mu_{45°C}$	$\mu_{pH6.3}/\mu_{pH7.2}$
Growth	0.08	0.78	0.07	0.89
Sporulation	0.08	0.83	0.05	1.49

Conclusions

The range of temperature and pH allowing spore formation were close to those allowing growth. Spore formation was strongly lengthened when sporulation occurred at suboptimal temperature and pH. Furthermore, the effect of temperature and pH on growth ratios on the one hand, and on sporulation ratios on the other hand, were similar. Thus, a parallel might be drawn between the effect of temperature and pH on growth and sporulation processes. In addition, the sporulation kinetic model can be useful in HACCP procedures aimed at identifying steps where there is an unacceptable risk of highly heat resistant spore formation in food chain. This study aims at defining process parameters, and in particularly temperature, pH and time on spore formation to reduce that risk.

Acknowledgements

This work is supported by the Agence Nationale de la Recherche (ANR) (France) as part of an ANR-07-PNRA-027-07 MEMOSPORE contract, by the industrial association Bretagne Biotechnologies Alimentaires (BBA) and the French National Association of the Technical Research (ANRT).

References

Baril E., Coroller L., Postollec F., Leguerinel I., Boulais C., Carlin F. and Mafart P. (2011) The wet-heat resistance of *Bacillus weihenstephanensis* KBAB4 spores produced in a two-step sporulation process depends on sporulation temperature but not on previous cell history. *International Journal of Food Microbiology* 146, 57-62.

De Pieri L. A. and Ludlow I. K. (1992) Relationship between *Bacillus sphaericus* spore heat resistance and sporulation temperature. *Letters in Applied Microbiology* 14, 121-124.

Gonzalez I., Lopez M., Martinez S., Bernardo A. and Gonzalez J. (1999) Thermal inactivation of Bacillus cereus spores formed at different temperatures. *International Journal of Food Microbiology* 51, 81-84.

Mazas M., Lopez M., Gonzalez I., Bernardo A. and Martin R. (1997) Effects of sporulation pH on the heat resistance and the sporulation of *Bacillus cereus*. *Letters in Applied Microbiology* 25, 331-334.

Palop A., Manas P. and Condon S. (1999) Sporulation temperature and heat resistance of *Bacillus spores*: a review. *Journal of Food Safety* 19, 57-72.

Ross R. and Dalgaard P. (2004) Secondary models. In Modeling microbial responses in food, pp. 63-150. Edited by R. C. Mc Kellar & X. Lu. Washington D. C.: CRC Press.

Rosso L., Lobry J. R., Bajard S. and Flandrois J. P. (1995) Convenient model to describe the combined effects of temperature and pH on microbial growth. *Applied and Environmental Microbiology* 61, 610-616.

Sonenshein A. L. (1999). Endospore-forming bacteria: an overview. In *Procaryotic developement*, pp. 133-150. Edited by A. Press. Washington, D.C.: Y. V. Brun and L. J. Shimkets.

Lag time and growth rate at different storage temperatures of psychrotrophic *Clostridia* isolated from meat and abattoir samples

A.R. Silva[1], R.D. Chaves[1], P.R. Massaguer[2]

[1]Department of Food Science, Faculty of Food Engineering (FEA), University of Campinas (UNICAMP), Campinas, SP – Brazil (alers.marques@gmail.com; chaves@fea.unicamp.br);
[2]Department of Chemical Processes, Faculty of Chemical Engineering, University of Campinas, Campinas, SP – Brazil (pilar.rodriguez@terra.com.br)

Abstract

No reports are available on growth parameters for psychrotrophic clostridia so this research aimed to investigate the effect of different temperatures (from -1.5°C to 30°C) on lag time (λ; h) and growth rate(μ; h^{-1}) of 12 psychrotrophic *Clostridium* strains isolated from spoiled and unspoiled meat samples and abattoir (10 *C.gasigenes* and 2 *C.algidicarnis*). For this, 1mL of each strain suspension (~10^4CFU/mL), was inoculated in 9mL of pre-reduced Reinforced Clostridial Broth (RCM, Oxoid) and incubated at -1.5, 2, 15, 20, 30°C, at anaerobic conditions. Growth was measured by increase of optical density (OD-600nm) at: 0, 6, 12, 24, 48, 72, 168 and 336h or until the stationary phase was reached. For each temperature growth data was fit to Baranyi and Roberts and modified Gompertz models (DMFit, v.2.0), obtaining λ, μ and ODmax. All the isolates grew at all tested temperatures, with exception of *C.gasigenes* strain C1I11EEXPKP no capable of growth at -1.5°C. Most of the isolates (58.3%) showed short lag time (2-4h) at -1.5 and 2°C (psychrotrophic profile). 25% of isolates demonstrated mesophilic character, with short adaptation periods (2-3.5h) at 30°C. Fifty % of the isolates did not show a good adaptation at 20°C (~40h of lag time), but when this barrier was overcome, growth was similar to the other conditions, while at 30°C lag time was shorter. *C.algidicarnis* (C2I5EXCHPKP), previously reported as the isolate with best blown ability, showed psychrotrophic profile, with short λ(1.74h), higher μ ($0.16h^{-1}$) and maximum OD (0.71) at 2°C but slow growth at 30ºC, μ ($0,03h^{-1}$). Nine from ten strains of *C.gasigenes* showed superior μ at 30°C and superior ODmax at 30 or 20°C. Baranyi & Roberts model showed Best performance (r^2 from 0.92 to 0.999). Abusive temperatures can accelerated growth of *C.gasigenes* strains, reducing lag time, however for *C.algidicarnis* 2°C was the best growth temperature. Effective barriers, other than temperature, are still needed for proper control.

Keywords: *psychrotrophic Clostridium, storage temperature, growth parameters*

Introduction

"Blown pack" spoilage occurs in vacuum-packed meat through the generation of large amounts of CO_2 and H_2, after one month of storage. Until 2009, occasional episodes of 'blown pack' in meat industry were associated with temperature abuse and due microorganisms such as *Enterobacteriaceae* and Lactic Acid Bacteria that caused economic losses for producers (Broda *et al.* 2009). Nowadays, psychrophilic Clostridia spp. such as *C.estertheticum, C.gasigenes, C.algidicarnis, C.algidixylanolyticum* and *C.frigidicarnis* (Adam *et al*. 2010), have been reported to cause "blown pack" spoilage of vacuum-packed meat stored at chilled temperature. So, it is too important the knowledge about variables or environmental conditions to inhibit the meat spoilage by psychrotrophic *Clostridium*. The growth of *Clostridium* strains could be affected by many factors, including storage temperature, heat shrinking and pH (Dong *et al*. 2007; Bell *et al*. 2001), but for Mckellar and Lu (2004), temperature is the most important parameter to be tested. However, there are no reports about growth parameters for psychrotrophic clostridia.

For this purpose, Predictive Microbiology is a powerful tool that has been used through the last 30 years to predict microorganisms' behavior (Nakashima *et al*. 2000). Primary parameters dependence on environment such as temperature, pH and water activity can be adjusted in secondary models to describe its dependence.

This research aimed to predict the effect of different temperatures on growth parameters of 12 psychrotrophic *Clostridium* strains (10 *C.gasigenes* and 2 *C.algidicarnis*) isolated from spoiled and unspoiled meat samples and abattoir (Silva *et al*. 2011).

Materials and Methods

Test organisms and vegetative suspensions production

Ten psychrotrophic *Clostridium* strains isolated from spoiled and unspoiled samples, genetically identified as *C.gasigenes* (8 isolates) and *C.algidicarnis* (2 isolates) and two from abattoir (*C.agasigenes)* (Silva *et al*., 2011), were inoculated in pre-reduced Reinforced Clostridial Broth (RCM, Oxoid) and incubated at 15°C/3 weeks in anaerobic conditions. For vegetative suspensions production, after incubation period, 1 mL of each strain suspension (~10^4UFC/mL, adjusted by Densimat, bioMérieux) was inoculated in 9 mL of pre-reduced RCM (triplicate) and incubated at each tested temperature.

Curve fitting and growth parameters observation

In order to measure the temperature effects, each triplicate of each strain was incubated at -1.5; 2; 15; 20 and 30ºC, at anaerobic conditions. Growth was measured by increase of optical density (OD-600nm) at 0, 6, 12, 24, 48, 72, 168 and 336h or until microorganism had reached the stationary phase of the growth. Baranyi and Roberts model (Equations 1 and 2) and modified Gompertz (Equation 3 and 4), by DMFit v.2.0 program (Institute of Food Research, Norwich, UK) were used to fit the OD data for each temperature, obtaining λ(h); μ(h^{-1}) and ODmax.

$$y(t) = y_0 + \mu_{\max} A(t) - \frac{1}{m}\ln\left[1 + \frac{e^{\mu_{\max} A(t)} - 1}{e^{(y_{\max} - y_0)}}\right] \quad (1) \qquad A(t) = t + \frac{1}{v}\ln\left[\frac{e^{-vt} + q_0}{1 + q_0}\right] \quad (2)$$

where: y(t) = maximum population (LogN/No), y_0 = initial population (Log No), y_{max} = final population (Log N), μ_{max} = maximum specific growth rate (h^{-1}) and v is the rate of increase of the limiting substrate, generally assumed to be equal to μ_{max}, q_0 = a measure of physiological state of cell at t=0.

$$y = A.e^{-e^{\left\{\left[\frac{\mu m^e}{A}.(\lambda - t)\right]+1\right\}}} \quad (3) \qquad \lambda = \frac{\ln\left(1 + \frac{1}{q_0}\right)}{\mu_{mas}} \quad (4)$$

where: y = maximum population (log (N/N_0); A = adjustment function; μm = maximum growth rate (h^{-1}); λ = adaptation time (h), q_0 = a measure of physiological state of cell at t=0 and to μ_{max} = maximum growth rate (h^{-1}).

Results and Discussion

All the isolates grew at all tested temperatures, with exception of *C.gasigenes*, strain C1I11EEXPKP no capable of growth at -1.5°C (Figure 1a) and LMI13CA/EC, isolated from abattoir, that showed a mesophilic profile (Figure 1b). After OD measurement for each combination, a total of 60 growth curves of 12 psychrotrophic *Clostridium* strains were obtained. Baranyi model provided a good description of the data, and Baranyi function had better predictive capabilities (R^2>0.92) than modified Gompertz (Table 1). This fact suggests that Gompertz function is a purely empirical function, used to predict both longer lag and shorter generation times compared with Baranyi function (Dong *et al*. 2007).

Growth parameters change according to incubation temperature: most of the isolates (58.3%) showed short lag time (2-4h) at -1.5 and 2°C (psychrotrophic profile) (Table 1). On the other side, 25% of isolates demonstrated mesophilic character, with short adaptation periods (2-3.5h) at 30°C.

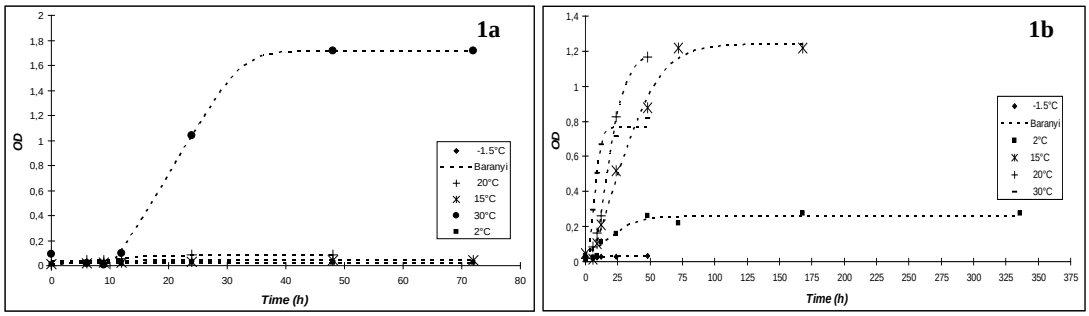

Figure 1: Temperature effects on growth of *C.gasigenes:* a. isolated from exudate spoiled samples (C1I11EEXPKP) and b. isolated from abattoir - stuning room corridor, beef package conveyor belt (LMI13CA/EC).

Table 1: Comparison between growth parameters for spoiled samples isolates and abattoir isolates, obtained by Baranyi and Gompertz models.

Microorganisms	□ (h^1)		□ (h)		Initial OD		Final OD		R^2	
	B*	**G****	**B**	**G**	**B**	**G**	**B**	**G**	**B**	**G**
C.algidicarnis (C2I5EXCHPKP) –isolated from spoiled sample exudate										
- 1.5°C	0.0031	0.0039	2.9334	3.6264	0.0037	0.0037	0.0318	0.0316	*0.9960*	0.9907
2°C	**0.1558**	**0.1095**	**1.7367**	**1.6100**	**0.1368**	**0.1357**	**0.7088**	**0.7088**	***0.9922***	**0.9919**
15°C	0.0004	0.0005	n.d.m.	2.4076	0.0234	0.0235	0.0277	0.0279	*0.9698*	0.8667
20°C	0.0065	0.0352	40.0652	46.468	0.0361	0.0363	0.2218	0.2214	*0.9406*	0.9405
30°C	0.0320	0.0135	3.8391	n.d.m.	0.0327	0.0046	0.3492	0.3487	*0.9354*	0.9151
C.gasigenes (C2I8EXCHPC) isolated from spoiled sample exudate										
- 1,5°C	0.0054	0.0059	5.8540	5.9671	0.0065	0.0069	0.0494	0.0496	*0.9889*	0.9841
2°C	0.0006	0.0007	**2.9956**	2.9837	0.0166	0.0163	0.0292	0.0297	*0.9565*	0.9078
15°C	0.0050	0.0049	10.2864	0.3518	0.0196	-0.017	0.4615	0.4689	*0.9852*	*0.9832*
20°C	0.0145	0.0163	13.9259	14.672	0.0139	0.0186	0.6759	0.6849	*0.9943*	0.9912
30°C	0.3692	0.1816	8.4294	8.4395	0.1035	0.1032	1.1282	1.1253	*0.9894*	0.9889
Abattoir isolate from Hide										
C.gasigenes (LMI1C4°C)										
- 1.5°C	0.0135	0.0108	5.8075	5.9672	0.0061	0.0048	0.0872	0.0868	*0.9999*	0.9945
2°C	0.0043	0.0050	**2.1195**	2.7598	0.0081	0.0077	0.0864	0.0890	*0.9851*	0.9694
15°C	0.0088	0.0136	8.3447	8.5368	0.0106	0.0106	0.044	0.044	*0.9921*	0.9912
20°C	0.0914	0.2917	24.7932	24.149	0.0292	0.0292	0.8091	0.8091	*0.9987*	0.9987
30°C	0.1460	0.0964	8.5268	9.0167	0.0314	0.0294	0.7262	0.7041	*0.9918*	0.9828

Where: ndm = no determined by models; *B: Baranyi model; **G: Gompertz model

Fifty percent of the isolates did not show a good adaptation at 20°C(~40h of lag time), but when this barrier was overcome, growth was similar to the other conditions, and at 30°C these isolates showed shorter lag time. There are no reports available at literature that could explain the maximum lag time at 20°C for psychrotrophic *Clostridium.*

C.algidicarnis (C2I5EXCHPKP), previously reported as the isolate with best blown ability (Silva *et al*., 2010), showed psychrotrophic profile, with short λ(1.74h), higher μ($0.16h^{-1}$) and maximum OD(0.71) at 2°C but slow growth at 30ºC, μ ($0.03h^{-1}$), however at -1.5°C growth was minimum (Figure 2). This fact suggests a strain completely adapted to lower temperatures and capable to promote 'blown pack' spoilage if present in meat stored at these temperatures for long periods of time.

Nine from ten strains of *C.gasigenes* showed superior μ at 30°C and superior ODmax at 30 or 20°C and both isolates obtained from abattoir (*C.gasigenes)* could growth at lower temperatures but the growth rate was reduced and the lag time, increased. This fact is so important because the abattoir could act as a source of psychrotrophic *Clostridium* strains, which could promote the 'blown pack' spoilage at meat storage at these conditions, however

for these isolates, the reduced temperature effects were more effective for lag time extension and growth rate reduction.

It is important to emphasize that temperature is the major factor determining the specific growth rate or lag time of microorganisms in chilled foods, however, in this research we observed that, for inhibition of psychrotrophic *Clostridium* growth, the use of temperature as the only barrier was not efficient, because these microorganisms are able to growth at <0ºC conditions and still cause 'blown pack' spoilage.

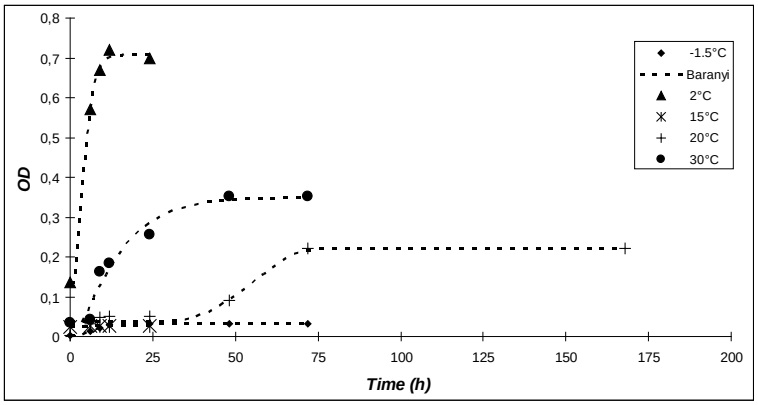

Figure 2: Temperature effects on growth of *C.algidicarnis* (C2I5EXCHPKP).

Conclusions

The temperature conditions tested in this paper just increased the lag time, but did not inhibit growth during the entire shelf life period. This research it is the first one to calculate growth parameters (λ and μ) under different temperature conditions for psychrotrophic clostridia, it provides an import tool for discussion on this subject. As temperature is not an effective barrier for control, there is a clear need for other factors such as heat shrink temperature and/or vacuum level increase, presence of growth inhibitors and improvement of hygienic conditions in abattoirs as well as combinations of these factors, to attain the microbiological stability of vacuum packed meat.

Acknowledgements

The authors would like to thank FAPESP and CNPq by financial support.

References

Adam K.H., Flint S.H. and Brightwell G. (2010) Psychrophilic and psychrotrophic clostridia: sporulation and germination processes and their role in the spoilage of chilled, vacuum-packaged beef, lamb and venison. *International Journal of Food Science & Technology* 45, 1539–1544.

Bell R.G., Moorhead S.M. and Broda D.M. (2001) Influence of heat shrink treatments on the onset of clostridial blown pack' spoilage of vacuum packed chilled meat. *Food Research International* 34, 271-275.

Broda D.M., Boerema J.A., Brightwell G. (2009) Sources of psychrophilic and psychrotolerant clostridia causing spoilage of vacuum-packed chilled meats, as determined by PCR amplification procedure. *Journal of Applied Microbiology* 107, 178-186.

Dong Q., Tu K., Guo L., Li H and Zhao Y. (2007) Response surface model for prediction of growth parameters from spores of *Clostridium sporogenes* under different experimental conditions. *Food Microbiology* 24, 624-632.

McKellar R.C. and Lu X. (2004) Modelling microbial responses in food. Ed.: Boca Raton, CRC Press.

Nakashima S.M.K., Andre C.D.S. and Franco B.D.G.M. (2000) Revisão: Aspectos básicos da Microbiologia Preditiva. *Brasilian Journal of Food Technology* 3. 41-51.

Silva A.R., Tsai S.M. and Massaguer P.R. (2010) Psychrotrophic clostridia identification and blowing ability in vacuum package meats. In: Food Micro 2010, Copenhagen.

Silva A.R., Paulo E.N., Sant'ana A.S., Chaves R.D. and Massaguer P.R. (2011) Involvement of *Clostridium gasigenes* and *C. algidicarnis* in 'blown pack' spoilage of Brazilian vacuum-packed beef. Article submitted at *International Journal of Food Microbiology*, status: under review.

Fate of *Listeria monocytogenes* in (semi) hard cheese made from starter-induced curds in a microcheese model

E. Wemmenhove[1,2,3], I. Stampelou[1], M.H. Zwietering[2], A.C.M. van Hooijdonk[3], M.H.J. Wells-Bennik[1]

[1] NIZO food research, Ede, The Netherlands
[2] Wageningen University, Laboratory of Food Microbiology, Wageningen, The Netherlands
[3] Wageningen University, Product Design and Quality Management, Wageningen, The Netherlands

Abstract

Current models for predictions the development of *Listeria monocytogenes* in cheese use growth rates from mainly (semi) soft cheeses. In previous cheese challenge studies (Colby, Swiss-type, Cheddar and Feta and young Gouda cheeses) growth of *L. monocytogenes* was not observed, and moreover, gradual inactivation after extended ripening times was observed. At NIZO, a microcheese model has been developed that allows for semi-automatic production of 500 semi-hard cheeses of 0.17 g from starter-induced curds per day. This system was used to study the fate of *L. monocytogenes* in semi-hard Gouda cheese. Viable numbers of four individual *L. monocytogenes* strains that were inoculated into cheese milk were determined during curd formation and ripening up to 1 year at 12°C. In addition, pH, organic acid concentrations, NaCl concentrations and moisture content were monitored in time. The outcome of this study was compared with previous (semi)hard cheese studies and cheese model predictions. Upon whey separation, *L. monocytogenes* bacteria were retained in the curd, causing a concentration increase in the curd. No growth was observed in Gouda during the first 6 weeks and a decline in viable numbers was observed afterwards, which is in line with results of previous semi-hard cheese studies. Findings from the microcheese study (*i.e.* no growth of *L. monocytogenes* and data on pH, organic acid concentrations, NaCl concentrations and moisture content) corresponded very well with the outcomes of a previous 4.5 kg Gouda cheese study and with previous semi-hard cheese studies. The microcheese model proved to be a very suitable challenge test system for the fate of pathogens in (semi)hard cheese and very useful to establish inactivation rates for semi-hard cheeses and validate quantitative microbiological risk models.

The interaction of multivariate factors (nitrite, pH, salt, temprature and time storage) on growth and toxigenesis of *Clostridium botulinum* in B.H.I model

Z. Mashak[1], K. Ghanati[2], Y. Saadati[3], A. Saadati[4]

[1] Department of food hygiene. Faculty of veterinary medicine. Islamic Azad university, Karaj Branch , Karaj , Iran. (mashak@kiau.ac.ir),(zohreh_mashak@yahoo.com)
[2] The International branch of shahid beheshti university of medical sciences, Tehran, Iran. (Kian.Ghanati@gmail.com)
[3] Camputer college of shahid beheshti university, Tehran , Iran. (yasaman_1300_s@yahoo.com)
[4] Tehran university of medical sciences, Tehran, Iran. (Amirreza_saadati2000@yahoo.com)

Abstract

In this study, the interference in interaction between intrinsic and extrinsic parameters including nitrite, pH, salt, temperature and storage time on growth and toxigenesis of *Clostridium botulinum* type A, has been examined during three steps. In the first step, sporogenesis of *Clostridium botulinum* type A was plated on Egg yolk Agar and spore count in one millilitre of suspension was obtained. In the second step, the turbidity time with inoculum level of 4×10^4 spore in each millilitre of BHI broth was examined within 32 days of storage (2,4,8,16,32) considering two level of pH(5.5,6.5), three different salt concentration (0.5,3,6)%, three different temperature (15,25,35)°C and finally usage of sodium nitrite treatment of 80ppm (or not using that, i.e. control treatment). In the third step toxigenesis was performed according to the USDA instruction and mouse bioassay. The results evaluated with completely randomized ANOVA, using SAS system, version 9, and indicated a significant statistical differences among different concentrations of salt, pH, temperature and sodium nitrite within turbidity times ($p<0.0001$). Usage of 6% salt, pH:5.5, temperature of 15°C and sodium nitrite(80ppm) and control treatment within 32 days of storage inhibit growth and toxigenesis of *Clostridium botulinum* type A with inoculum size level of 4×10^4 cfu/ml in contrast with salt (0.5,3)%, pH:6.5 and temperature (25,35)°C , pH 6.5, %3 salt, temperature 25°C and sodium nitrite treatment had more inhibitory effect in comparison with pH:6.5, 0.5% salt, temperature 35°C and control treatment. And finally in growth and toxigenesis of bacteria observed a substitute effect between 0.5% salt and sodium nitrite treatment compared to % 3 salt and control treatment.

Key words: Clostridium botulinum type A, time to turbidity, time to toxicity

Introduction

Clostridium botulinum is an anaerobic, gram positive, and spore forming rod. Four phenotypic groups exist in this species and type A of bacteria is located in group I (proteolytic). Based on antigenic specificity of the toxin production, seven types (A–G) of botulism recognized. Foodborne botulism is Fatal illness that caused by the consumption of contaminated foods containing neurotoxin. Its production is usually followed through germination, out growth of spores and vegetative forms and cell autolysis.

Some outbreaks of this intoxication (type A) have been reported in all of the world by ingestion of various food. So using special tools controlling the growth and toxigenesis of bacteria in food seems necessary. In recent years, some challenge studies using inoculum pack studies initially used culture media, then in different food system, due to importance of food safety in public health. So, in this study, growth (visible turbidity) and toxigenesis of *Clostridium botulinum* type A was surveyed under independent and interference effect of intrinsic and extrinsic parameters such as salt, pH, sodium nitrite, temperature and storage time with the inoculum size level 4×10^4 cfu/ml in Brain Heart Infusion Broth media.

Material and methods

The study was performed in three steps. In the first step sporogenesis of bacteria was determined, after three consecutive passages of lyophilized bacterium under anaerobic condition in BHI tubes, then surface cultured to Egg Yolk Agar plate was done. Sporogenesis started from 4^{th} till 15^{th} day, the maximum free spores were observed (more than %90) daily using of wet lam and malaschite green staining through video microscope. Then colonies in plates washed aseptically by sweeping method, and gathered with phosphate buffer gel dilutor and cold centrifuge 5000 – 10000 rpm/15'/4°C. At last spore count got in one mililiter of suspension. In the second step the multifactorial combination effect such as pH (5.5 and 6.5); salt (0.5 , 3 , 6)% , temperature (15, 25, 35)°C, sodium nitrate (80 ppm) and storage time (2,4,8,16,32) days under anaerobic condition (usage of vaspar and Gaspack A in anaerobic Jar) with inoculum size level 4×10^4 cfu/ml were cultured into the BHI broth tubes and 144 different biocondition (repeating twice) for the time of turbidity and toxigenesis were examined. In the third step; after centrifuging of the content of turbid tubes at 7000 rpm/15'/4°C; their supernatants were transferred in two tubes. For one of them performed thermal treatment (100 ºC/10') and theother didn't. Toxigenesis was done with United State Department of Agriculture (USDA) instruction and mouse bioassay. The mice that had received unheated samples, died within 6–24 hr after injection with sign of botulism. Statistical analysis with completely Randomized was done, ANOVA, In SAS, ver: 9.

Result and discussion

Growth and toxigenesis of *Clostridium botulinum* type A with inoculum size level 4×10^4 cfu/ml, observed at different temperatures (25, 35)°C, salt concentrations (0.5, 3, 6)%, pH:6.5, sodium nitrite (80 ppm) and without sodium nitrite (control) within 32 days 2, 4, 8, 16, 32, ($p<0.0001$) (table 1, Fig1). Growth and toxigenesis in Fig1-a occurred in a shorter period of time in 35°C, 0.5% salt in comparison with 25°C and 3% salt. whereas no growth was observed in 15°C and 6% salt. It seems use of 6% salt leads to plasmolysis and a series metabolic events in bacterium, damage to cell membrane and reduction of its permeability that sensitize it to other medium condition and finally stopped the growth. Kiss *et al.* (1978) also observed the same result in different strains of *Clostridium botulinum* type A. Also the interference effect of pH and temperature indicated that the growth and toxigenesis in 35°C and pH:6.5 occurred in a shorter time in comparison with 25°C and definite reduction of growth all temperatures at pH:5.5 was observed (Fig1-b). It seems that pH:5.5 has resulted in disturbing nutrient transportation in to the bacterium cell and reduction of enzyme reaction and consequently limited bacterial growth. In Whiting, (1993) study, temperature<20°C and pH<5.5 has considerably delayed the growth of bacterium. Also as the same as our study, Schaffner *et al*. (1998) found that the toxin formation decreased at lower temperature (15°C) and at pH further from the optimum. In Fig1-c the interaction of temperature (25, 35) °C with sodium nitrit (80ppm) and without it (control) has delayed growth and toxigenesis of bacterium. Also the interaction of salt and pH indicates definite effect of pH:5.5 on absence of growth in all concentration of salt, but in pH:6.5 growth and toxigenesis occurred in a shorter time with decreasing of salt from 3% to 0.5% (Fig 1-d). In Zhao *et al*. (2004), the best and the worst condition for growth and toxigenesis was reported in pH:6.5, salt 0.5% and pH:5.5, salt 4%, respectively. In Fig 1-e interaction effect of pH:6.5, sodium nitrite and without it on growth and toxigenesis of *Clostridium botulinum* occurred, but the growth inhibitory effect of sodium nitrite in comparison with control group was better. Sodium nitrite has a protection against clostridial foodborne poisoning. Commack *et al.* (1999) reported that salt form of nitrite for commercial properties is more effective. In Fig 1-f and Fig1-g observed the same effect between sodium nitrite 80 ppm, 0.5% salt, and the control group with 3% salt. Also usage of sodium nitrite 80 ppm under different temperatures (25, 35)°C, salt (0.5, 3)%, pH:6.5 on inhibition growth and toxigenesis of *Clostridium botulinum* is better more than control group. In pH:6.5, 3% salt, 25°C and sodium nitrite 80 ppm had more inhibitory effect in contrast with other groups ($p<0.0001$). In a number of studies it has been observed combinations inhibitory effect of preservatives like sodium nitrite, salt, acid and temperature

on growth and toxigenesis of *Clostridium botulinum*. Finally the time of storage on growth is effective in food safety and shelf life of food. In this study the interaction between time of storage and temperature was observed, and with rise of temperature from 25°C to 35°C, this duration was decreased.

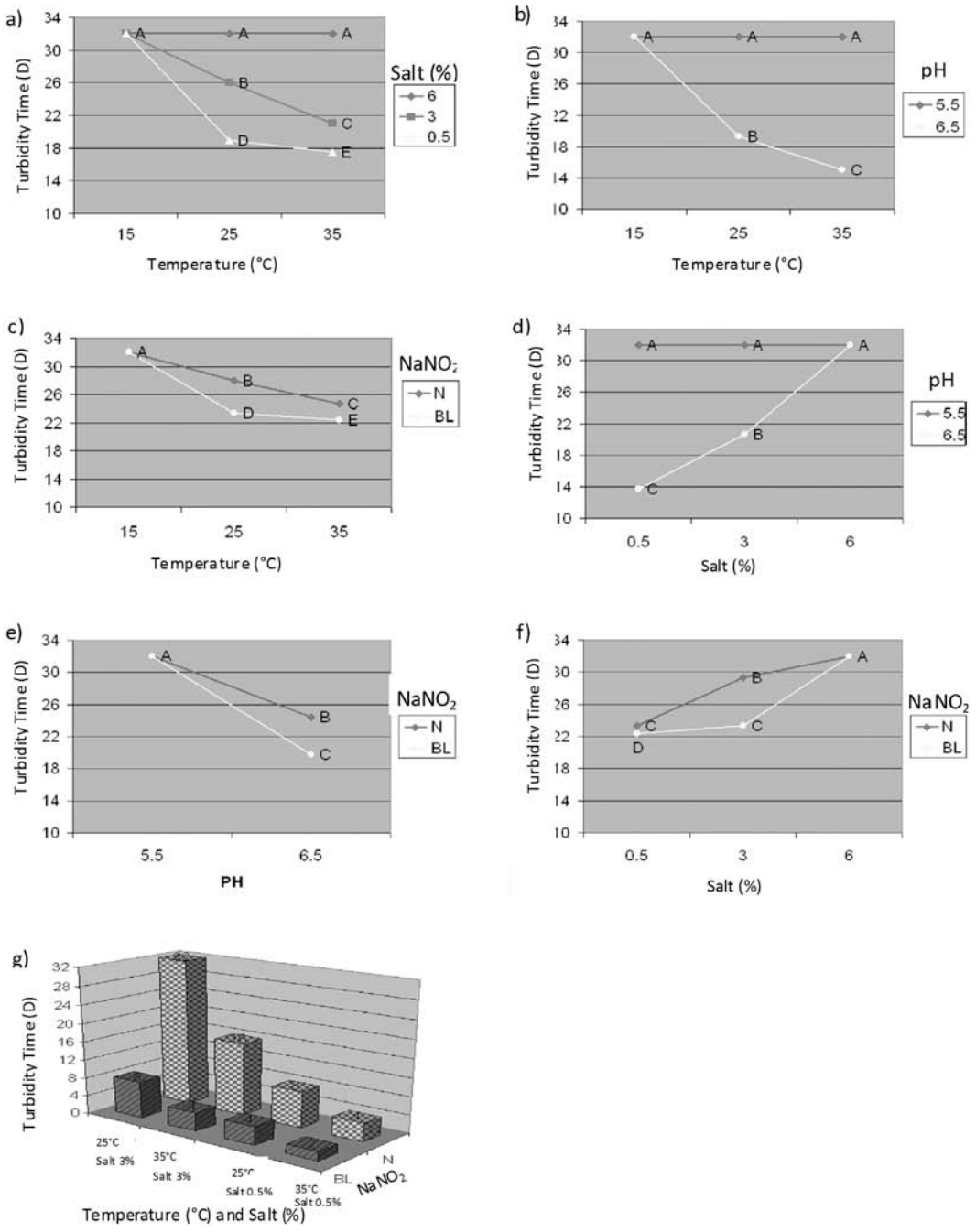

Fig 1. The interaction of temperature (D), Salt (%) and pH on growth and toxigenesis of *Clostridium botulinum* Type A in 32 days with inoculums size of 4×10^4 CFU/ml; a. Interaction of temperature (15, 25 and 30°C) and salt (0.5, 3 and 6%); b. Interaction of temperature (15, 25 and 30°C) and pH (5.5 and 6.5); c. Interaction of temperature (15, 25 and 30°C) and Sodium Nitrite (80ppm "N" and Control "BL"); d. interaction of salt (0.5, 3 and 6%) and pH (5.5 and 6.5%); e. Interaction of pH (5.5 and 6.5) and Sodium Nitrite (80ppm "N" and Control "BL"); f. Interaction of salt (0.5, 3 and 6%) and Sodium Nitrite (80ppm "N" and Control "BL"); g. Interaction of temperature (25 and 35°C), salt (0.5 and 3%) and Sodium Nitrite (80ppm "N" and Control "BL").

Table 1: Variance analysis of turbidty time, affected by salt, pH, sodium nitrite, temperature within 32 days with inoculum size 4×10^4 *Clostridium botulinum*. type A with ANOVA.

Source	DF	Squares	Mean Squares
Temp	2	1872.88	936.44
Salt	2	2054.22	1027.11
PH	1	3520.44	3520.44
Temp × salt	4	1132.44	283.11
Temp × PH	2	1872.88	936.44
Temp × sodium nitrite	2	130.66	65.32
salt × PH	2	2054.22	1027.11
salt × sodium nitrite	2	24.70	124.00
PH × sodium nitrite	1	196.00	196.00
Temp × salt × PH	4	1132.44	283.11
Temp × salt × sodium nitrite	4	165.33	41.23
Temp × PH × sodium nitrite	2	130.66	65.33
Salt × PH × sodium nitrite	2	248.00	124.00
Temp× salt × PH × sodium nitrite	4	165.33	41.33
Error	108	0	0
Corrected total	143	15119.55	-

Conclusion

In this study environmental conditions required to inhibit the growth of *Clostridium botulinum* need to be optimized. So salt 6%, 15°C, pH:5.5, with sodium nitrite 50 ppm have inhibited the growth and toxigenesis of bacteria. The longest turbidity time was achieved in 25°C, pH:6.5, salt 3%, sodium nitrite 80 ppm and the shortest turbidity time was achieved at 35°C, pH:6.5, salt 0.5%, and without use of sodium nitrite.

References

Bell Ch. and Kyriatides A. (2000) Practical Food Microbiology Series, Clostridium Bbotulinum. A practical to the organism and it's control in Foods. Black-Well Science.

Cammack R., Joannou C.L., Cui X.Y., Martinez C.T., Maraj Sh.R. and Hughes M.N. (1999) *Biochemica et Biophysica Acta* 1411, 475-488

Doyle M.E. (2001) Clostriduim botulimun. Fact sheet. Food research institute, university of wisconsin-Madison.

International commission on Microbiological specification for Foods. (1996) Microorganisms of Foods.5. Microbiological specifications of Food Pathogens. Blackie Academic and proffessional. London, UK.

Jay J.M. (2000) Modern of Food Microbiology. 6th ed. Gaithersburg (MD): Aspen.

Kiss I., Rhee C.O., Grecz N., Roberts T.A. and Frankas J. (1978) Relation between radiation and salt sensivity of spores of five strains of *Clostridium botulinum* type A,B and E. *Applied and Environmental Microbiology* 35, 533-539.

Mcmeekin T.A., Brown J.. Krist K., Miles D., Neumeyer K., Nichols D.S., Olley J., presser K., Ratkowsky D.A., Ross T., Salter M., and Soontranon S. (2002) Quantative microbiology; Abasis for Food safety. 3(4): 1-12.

Opinion of the scientific panel on Biological hazards on the request from the commission related to the effects on Nitrites/ Nitrates on the microbiological safety of meat products the (2004) EFSA Journal. (14) 1-31

Schaffner D.W., Ross W.H. and Montville T. J. (1998) Analysis of the influence of Environmental Parameters on clostridium botulinum time to toxicity by using three modeling Approchest. *Applied and Environmental Microbiology*, 46(11): 4416-4422.

Vanderzant C. and Splittstoesser D.F. (1992) Compendium of Methods for the Microbiological Examination of Foods. *Clostridium botulinum* and it's toxins. Chapter 6: 605-621.

Zhao L., Montville T.J., Schaffner D.W. (2004) Effect of inoculom size on maximum growth rate, lag time and maximum percent growth of *Clostridium botulinum* at varying pH and salt concentration. Food Science, Rutgers University, 65. Dudly Road, New Brunswick, NJ 901

Whiting R.C. and Strobaugh T.P. (1993) Expansion of the time to turbidity model for proteolytic *C. botulinum* include spore numbers. *Food Microbiology* 15, 449-453.

Sublethal heating of *Cronobacter* spp. followed by determination of individual lag times during recovery

Y. Xu, JP Sutherland

Microbiology Research Unit, School of Human Sciences, Faculty of Life Sciences, London Metropolitan University, 166-220 Holloway Road, London N7 8DB, UK

Abstract

Cronobacter spp. are increasingly regarded as emerging opportunistic pathogens and can infect all age groups. They are ubiquitous in nature and, apart from their association with powdered infant formula, have been isolated from various foods, including salad, confectionery, cheese, water and cooked meat. The ability of some strains of *Cronobacter* to grow at 5.5^{o}C makes these microorganisms particularly important in chilled foods. Heat treatment is a widely used preservation process to prolong lag phase of microorganisms in order to maintain safety and control spoilage. However, consumers nowadays prefer milder heat processes and minimal use of preservatives, since such foods are perceived as more "healthy". These demands may lead to a situation where ready-to-eat foods become potentially unsafe, as even a few pathogenic bacteria may initiate illness if they multiply in food to an infective level. In order to model the potential for *Cronobacter* spp. to recover from mild heating during the shelf life, the thermal inactivation of *Cronobacter* spp. after sublethal heating (resulting in injury but not death) has been investigated. Three strains (*Cr.sakazakii* NCIMB5920, *Cr. turicensis* 1211 and *Cr.turicensis* 57) were heated at 48, 49 and 50^{o}C in nutrient broth using the method of Métris et al. (2008). The sublethal phases of the heat treatments were, for *Cr. sakazakii* NCIMB5920: 40 min at 48^{o}C, 20 min at 49^{o}C, 5 min at 50^{o}C; for *Cr. turicensis* 1211: 40 min at 48^{o}C, 7 min at 49^{o}C and for *Cr.turicensis* 57:10 min at 48^{o}C, 3.5min at 49^{o}C. The 50^{o}C temperature was lethal for *Cr. turicensis*. Compared with *Cr.turicensis strains*, *Cr. sakazakii* NCIMB5920 was more thermotolerant. Current research is using this information for studies to determine lag phase of individual cells of *Cronobacter* spp. using optical density measurements after the sublethal heating process.

Key words: Cronobacter spp., sublethal heating, Individual lag times

Modelling the effect of sublethal injury on variability of individual lag times of *Cronobacter turicensis* cells compared with undamaged cells

Y. Xu[1], D. Stasinopoulos[2], J.P. Sutherland[1]

[1]Microbiology Research Unit, Faculty of Life and Sciences; London Metropolitan University, 166-220 Holloway Road, London N7 8DB, UK
[2]Operational Research and Mathematics Research Centre, Faculty of Computing; London Metropolitan University, 166-220 Holloway Road, London N7 8DB, UK

Abstract

Research on lag is of considerable importance to the food industry. Traditional lag phase models are generally developed using a relatively high initial inoculum of bacteria. However, in reality, foods are usually contaminated with low concentrations of pathogens. Moreover, besides the previous history of the cells and current environment, lag phase depends also on inoculum size. Therefore, an approach based on individual cells is required to quantify variability of the lag phase. *Cronobacter* spp. are increasingly regarded as emerging opportunistic pathogens and are associated with illness among infants following consumption of powdered infant formula (PIF). Immuno-compromised adults and the elderly are also at risk. Apart from PIF, *Cronobacter* spp. can be recovered from foods such as cheese, vegetables and bread. Mildly-heated foods without preservatives are likely to gain popularity due to organoleptic superiority; however this may have implications for food safety, even in chilled products. This study aims to determine how sublethal heat stress affects subsequent duration of lag time of individual cells of *Cronobacter turicensis* using optical density (OD) measurements. Single cells of *Cr.turicensis* were obtained by serial dilution in microtitre plates and the assumption made that there was only one cell in each well that could potentially grow after incubation. A calibration curve will be prepared to determine cell concentration at the OD corresponding to the detection time. The growth rate at 22^{o}C under optimal conditions of pH and water activity was estimated using viable counts, followed by fitting data with DMFit software (J. Baranyi). The distribution of individual lag times of heat damaged and healthy cells can thus be compared using detection times, indicating the shift of the distribution caused by heating. Work is in progress to obtain data which will be analysed using R for Windows to produce a predictive capability.

Key words: Sublethal injury, individual lag times, Cronobacter turicensis

Effect of low inoculum size on the *Listeria innocua* lag phase at refrigeration temperatures.

J. Aguirre, M. R. Rodríguez, M. Gañán, A. González, G. García De Fernando

Depto. Nutrición, Bromatología y Tecnología de los Alimentos, Facultad de Veterinaria, UCM, Madrid 28040, Spain

Abstract

Microbial growth models usually give reliable information on specific growth rate; however, results for lag phase are less accurate probably due to our poor understanding of the physiological events taking place during adaptation of cells to new environments and other factors as stress kind, cell variability and the effect of the population size. The objective of this study was to determine the effect of low inoculum size on the *Listeria innocua* lag phase variability at refrigeration temperatures. This effect was investigated using Bioscreen C equipment. Detection times (time to reach 0.2 $A_{480\text{-}520}$ units, around 10^7 cfu/ml) of different inoculum sizes (1-200 cells/well) in tryptic soy broth were estimated at 7ºC and 16ºC. Lag phases at 7ºC were much longer than at 16ºC. The inoculum size did affect the mean lag phases. Growth curves initiated with few cells showed longer lag times than those initiated with more cells. Nevertheless, the incubation temperature magnifies the inoculum size effect. At 16ºC, the effect was lost from 40 cells per sample, while the effect was still appreciable at ca. 100 cells per sample at 7ºC. Lag phase variability was more noticeable at the lowest temperature. Furthermore, the lower the inoculum was, the higher the standard deviation. On the other hand, the standard deviation continued decreasing, even when the average lag phase became stabilized. These facts indicate that variability depends on the inoculum size and the growth conditions. The more stressing growth conditions and the lower the inoculum are, the higher the variability. These results are relevant to predict lag times and calculate growth probability from low cell numbers, especially in quantitative microbiological risk assessment of food-borne pathogenic, which become dangerous at very low level.

Acknowledgements

Authors acknowledge the support of the Ministerio de Educación y Ciencia (Spain), Program Consolider CARNISENUSA CSD2007-0016 and AGL-2010-16598.

Modelling the inhibitory effects of ZnCl2 on *Saccharomyces cerevisiae* TOMC Y4

J. Bautista-Gallego, V. Romero-Gil, A. Garrido-Fernández, F.N. Arroyo-López

Departamento de Biotecnología de Alimentos. Instituto de la Grasa (CSIC). Avda\ Padre García Tejero nº 4. 41012, Seville, Spain. (fnarroyo@cica.es)

Abstract

This survey examines the inhibitory effects of zinc chloride on *Saccharomyces cerevisiae* TOMC Y4, a yeast strain isolated from table olive packaging. For this purpose, yeast was first incubated in laboratory medium supplemented with different $ZnCl_2$ concentrations (from 0 up to 200 mg/L) and monitored by means of optical density measurements in a Bioscreen C spectrophotometer. Fractional areas were used to obtain the NIC (susceptibility) and MIC (resistance) values of this microorganism to $ZnCl_2$, which were 90±10 and 110±10 mg/L, respectively. Then, yeast was incubated in laboratory medium supplemented with four $ZnCl_2$ concentrations above MIC value (125, 250, 500 and 1000 mg/L) to determine if this compound only retained yeast growth, or, on the contrary, had killer effect. The four concentrations decreased the initial cell number (~10^6 cells/mL), but reduction was significantly different according to inhibition parameters obtained from a Weibull fit. In this way, the time for the first decimal reduction (D_β) was 17.28±2.20, 13.36±1.74, 10.34±1.14 and 6.14±0.25 hours for 125, 250, 500 and 1000 mg/L of $ZnCl_2$, respectively. Thus, results obtained in this work open new alternatives to the application of $ZnCl_2$ as a yeast preservative agent in diverse fermented vegetable packing (olives, cucumber, capers, etc.) where this microorganism is present.

Keywords: *Zinc chloride, Weibull model, fractional areas, table olives, preservative*

Introduction

The use of zinc salts have been recently patented for its proved antifungal activity (Bautista Gallego *et al.* 2010). Zinc can be accumulated, mainly in aerobic conditions, in *Saccharomyces cerevisiae* cells and markedly influence its physiological status (Stehlik-Tomas *et al.* 2004). Its presence in the continuous alcoholic fermentation reduced the size of flocks, increased the tolerance to alcohol and temperature, decreased the production of glycerol, and accumulated in the yeast dry matter (Zhao *et al.* 2009). Zinc addition (~ 4 mg/L) was convenient to produce maximum alcohol yield with *S. cerevisiae* 251 TP strain (Tosun and Ergun, 2007). Zinc oxide has also shown antimicrobial activity against pathogen microorganism such as *Listeria monocytogenes*, *Salmonella enteriditis* and *Escherichia coli* O157:H7 (Jin *et al.* 2009).

Zinc is also used in food technology because forms green color complexes with chlorophyll derivatives, particularly at moderate high temperature. It has recently been applied to preserve the green color of pears, but the process required the application of heat to stabilize the final product colour (Ngo and Zhao, 2007). Moreover, zinc salts are currently included in the strategy designed by the UNICEF to combat the diarrhea in children in developing countries. The doses recommend ranges from 10 to 20 mg Zn per day (United Nations Childrens' Fund, 2004). The use of zinc acetate, chloride, citrate, gluconate, lactate, oxide, carbonate and sulphate is authorized in the European Union to fortify foods according to Directive 2002/46/CE of the European Union. In the USA the same compounds are authorized for the same purpose and are considered as GRASS (Office of Dietary Supplements, 2011).

The aim of this work was to study the inhibitory effects of $ZnCl_2$ on *S. cerevisiae* TOMC Y4, a spoilage microorganism usually found in olive and other fermented vegetable packaging, to be used as a preservative agent during olive processing.

Materials and Methods

The basal growth medium selected in this work for all experiments was Yeast-Malt-peptone-glucose broth medium (YM, Difco™, Becton and Dickinson Company, Sparks, USA) supplemented with different $ZnCl_2$ concentrations (from 0 up to 200 mg/L). Yeast growth was monitored by means of optical density measurements in a Bioscreen C automated spectrophotometer at 30ºC for 7 days, with an initial inoculums level of ~10^6 cells/mL.

The basis of the technique used for estimating the non-inhibitory concentration (NIC) and minimum inhibitory concentration (MIC) of this strain to $ZnCl_2$ was the comparison of the area under the OD/time curve of a positive control (absence of compound, optimal conditions) with the areas of the tests (presence of $ZnCl_2$, increasing inhibitory conditions). As the amount of inhibitor in the well increases, the effect on the growth of the organism also increases. This effect on the growth is manifested by a reduction in the area under the OD/time curve relative to the positive control at any specified time. The areas under the OD/time curves were calculated by integration using OriginPro 7.5 software (OriginLab Corporation, Northampton, USA). The relative amount of growth for each $ZnCl_2$ concentration, denoted as the fractional area (*fa*), was obtained using the ratios of the test area ($area_{test}$) to that of the positive control ($area_{cont}$), according to the following formula:

$$fa = (area_{test})/(area_{cont}) \quad (1)$$

The plot of the *fa* versus $ZnCl_2$ concentration produced a sigmoid-shape curve that could be well-fitted with the modified Gompertz function for decay (Lambert and Pearson, 2000), which has the following expression:

$$fa=A+C*\exp[-\exp(B(x-M)] \quad (2)$$

where, A is the lowest asymptote of *fa* (approximately zero), B is a slope parameter, C is the distance between the upper and lower asymptote (approximately 1) and M is the $ZnCl_2$ concentration of the inflexion point. These parameters were obtained by a non-linear regression procedure, minimizing the sum of squares of the difference between the experimental data and the fitted model, i.e., loss function $(observed-predicted)^2$. The NIC and MIC values were later estimated as (Lambert and Pearson 2000):

$$NIC= M – (1.718/B) \qquad MIC= M + (1/B) \quad (3)$$

Then, in a second step, to determine if this compound only retained yeast growth or, on the contrary, had killer effect, four $ZnCl_2$ concentrations above MIC value (125, 250, 500 and 1000 mg/L) were assayed. In this case, the evolution of the initial population (~10^6 cells/mL) was followed by plate count on YM agar. A Weibull model (Van Booekel, 2002) was used to fit the reduction of the yeast population over time for the four $ZnCl_2$ levels, which has the following expression:

$$Log_{10} N_t/N_0= -(t/D_\beta)^\beta \quad (4)$$

where N_t is the number of cells at time (t), N_0 is the initial inoculums level, D_β is the time (hours) for the first decimal reduction and β is the shape of the inhibition curve. As in the previous case, both parameters were obtained by a non-linear regression procedure.

Results and Discussion

Figure 1 shows the fit of the *fa* of *S. cerevisiae* TOMC Y4 to increasing concentrations of $ZnCl_2$. The plot gave a typical sigmoid decay function. Clearly, the whole sigmoid-shaped curve could be divided into three sections: i) points corresponding to concentrations from zero up to the NIC (concentrations at which no effect of the inhibitor was observed and *fa* was around 1), ii) concentrations between NIC and MIC (within which growth inhibition progressively occurred and the *fa* decreased), and iii) a third section above MIC (where no growth relative to the control was recorded and *fa* was around 0).

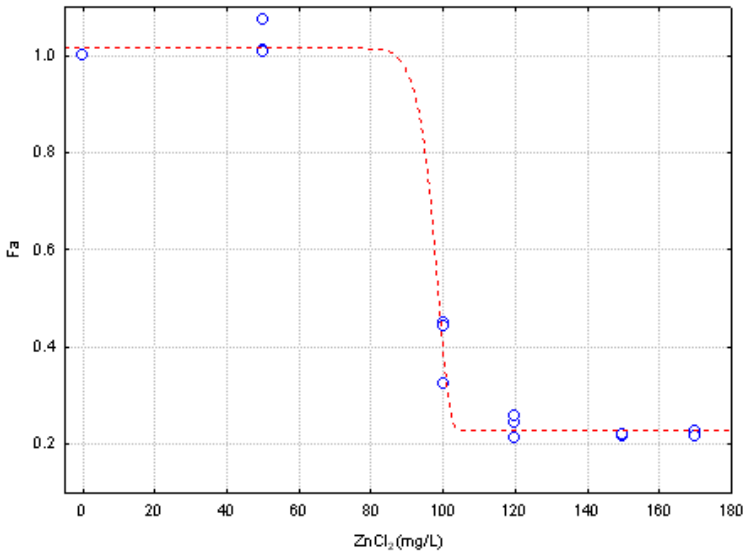

Figure 1: Fractional areas (*fa*) of *S. cerevisiae* TOMC Y4 as a function of $ZnCl_2$ concentration.

NIC value, which shows the susceptibility of this yeast strain to $ZnCl_2$, was 90±10 mg/L, while the MIC value, related to the resistance, was 110±10 mg/L. Thus, the range where this compound showed its inhibitory effect was very narrow (only 20 mg/L). Above, MIC value, and as it can be easily deduced from Figure 2, this chloride salt reduced the number of viable cells of *S. cerevisiae* TOMC Y4. However, the death rate was different according to $ZnCl_2$ concentration.

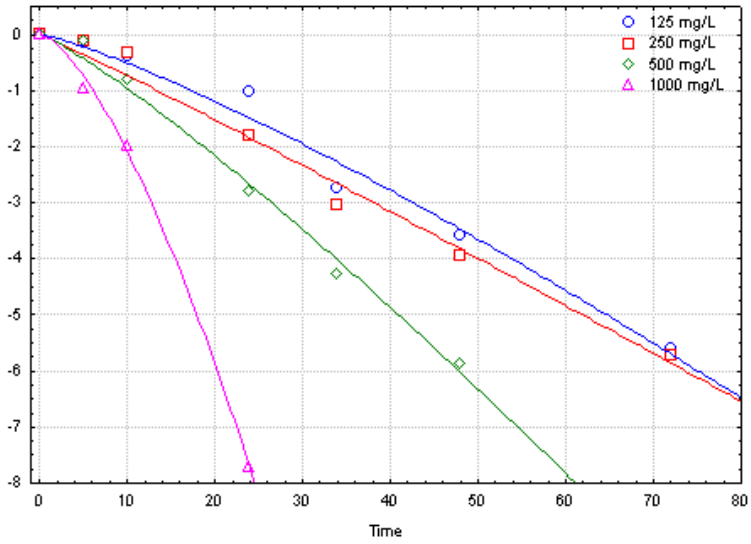

Figure *2*: Weibull's fit for the four $ZnCl_2$ concentration assayed in this work above MIC value.

In this way, the time for the first decimal reduction (90% of death cells with respect to the initial inoculums) were 17.28±2.20 h, 13.36±1.74, 10.34±1.14 and 6.14±0.25 hours for 125, 250, 500 and 1000 mg/L of $ZnCl_2$, respectively. According to these data, when the concentration of $ZnCl_2$ increased, cells were killed faster.

Conclusions

Results obtained in this work open new alternatives to the application of $ZnCl_2$ as an anti-fungi preservative agent in diverse fermented vegetable packaging where these microorganisms can produce spoilage.

Acknowledgements

This work was supported by the European Union (Probiolives, contract 243471), Spanish Government (projects AGL-2006-03540/ALI, AGL2009-07436/ALI and AGL2010-15494/ALI, partially financed by European regional development funds, ERDF), CSIC project 201070E058), and Junta de Andalucía (through financial support to group AGR-125). J. Bautista-Gallego and F.N. Arroyo-López want to thank CSIC for their JAE predoctoral fellowship and JAE-DOC postdoctoral research contract, respectively.

References

Bautista-Gallego J., Arroyo-López F.N., Garrido-Fernández A., García-García P., López-López A. and Rodríguez-Gómez F. (2010) Composiciones conservantes de aceitunas con actividad antifúngica. P201030491. Ref. ES1641.387.

Jin T., Su D., Zhang H. and Sue H. (2009) Antimicrobial efficacy of zinc oxide quantum dots against *Listeria monocytogenes, Samonella enteriditis, Samonella enteriditis* y *Escherichia coli* O157:H. *Journal of Food Science* 74, M46-M52.

Lambert R.J.W. and Pearson J. **(**2000) Susceptibility testing: accurate and reproducible minimum inhibitory concentration (MIC) and non-inhibitory concentration (NIC) values. *Journal of Applied Microbiology* 88, 784-790.

Ngo T. and Zhao Y. (2007) Formation of zinc-chlorofill derivative complexes in thermally processed green peas (*Pyrus communis* L.). *Journal of Food Science.*72, C397-C404.

Office of Dietary Supplements (National Institute of Health). (2011). Dietary Supplement Facts Sheet. Zinc. http://ods.od.nih.gov/ . Last access January 2011.

Stehlik-Tomas V., Gulan Zetić V., Stanzer D., Grba S. and Vahčić N. (2004) Zinc, copper and manganese enrichment in yeast *Saccharomyces oleaginosus*. *Food Technology and Biotechnology* 42, 115-120.

Tosun A. and Ergun M. (2007) Use of experimental design method to investigate metal ion effects in yeast fermentations. *Journal of Chemical Technology and Biotechnology* 82, 11-15.

United Nations Childrens' Found. (2004) WHO/UNICEF joint statement. Clinical management of acute diarrhea. World Health Organization and Unicef. Switzerland and New York.

Van Boekel M.A.J.S. (2002) On the use of the Weibull model to describe the thermal inactivation of microbial vegetative cells. *International Journal of Food Microbiology* 74, 139-159.

Zhao X.Q., Xue C., Ge X.M., Yuan W.J. and Bai F.W. (2009) Impact of zinc supplementation on the improvement of ethanol tolerance and yield of self-flocculating yeast in continuous ethanol fermentation. *Journal of Biotechnology* 139, 55-60.

Impact of texture on *Listeria monocytogenes* growth in gel models

T. De Broucker, M. El Jabri, F. Postollec, D. Thuault

ADRIA Développement, ZA Creac'h Gwen F29196 Quimper Cedex (thibaud.debroucker@adria.tm.fr, mohammed.eljabri@adria.tm.fr, florence.postollec@adria.tm.fr, dominique.thuault@adria.tm.fr)

Abstract

Listeria monocytogenes is a well known foodborne pathogenic bacteria which has the ability to grow on a wide range of environmental conditions enabling its persistence in food processing industry despite the use of cold chain procedures. Predictive microbiology approaches enable microbial behaviour simulation as a function of physico-chemical environmental parameters which, via already existing tools, allows *L. monocytogenes* growth simulation in food. The aim of this study was to define a gamma function parameter (based on Zwietering model) taking into account the impact of food texture on *L. monocytogenes* growth. *L. monocytogenes* growth has been evaluated in continuous fibrous gels (enriched BHI with k-carrageenan) and globular gels (enriched BHI with caseinate) at 8, 15 and 25°. To study the impact of textural properties, mass inoculation of 4 CFU/g was performed. Gel texture, determined by elastic modulus measurements (G'), was ranging between 0,01 Pa (liquid gels) and 40.000 Pa (solid gels). For each condition, maximal population (N_{max}), and maximal growth rate (μ_{max}) were determined. Maximal population and growth rates highly depend on incubation temperature and textural properties. Evaluation of the optimal growth rate (μ_{opt}) was determined with the use of Sym'Previus software which allows comparison of the impact of different texturing agents on bacterial growth without considering the impact of temperature incubation on gel texture. Similarly to Minimal Inhibitory Concentration estimated by inhibitory models (Rosso, 1995), this work proposes the determination of minimal inhibitory gel texture (MIG) and gamma functions related to each studied texturing agents. Various impacts of texture were observed and simulated between continuous carrageenan-based network and globular gel matrix related to growth inhibition of *L. monocytogenes* in food models.

Keywords: *Listeria monocytogenes, texture, growth rate, growth inhibition*

Assessing the effect of a gelified environment on the heterogeneous heat response of *E. coli* K12 at temperatures close to T_{max}

K. Boons, E. Van Derlinden, L. Mertens, J.F. Van Impe

CPMF2 – Flemish Cluster Predictive Microbiology in Foods – www.cpmf2.be
Chemical and Biochemical Process Technology and Control (BioTeC), Department of Chemical Engineering, Katholieke Universiteit Leuven, Leuven, Belgium, [kathleen.boons, jan.vanimpe]@cit.kuleuven.be

Abstract

Microbial growth is influenced by the structure of the environment. Contrary to liquid, movement in structured media is confined and transport of substrates to and metabolites away from the cell is limited. Literature suggests that (1) the growth domain of bacteria is confined by this structure-induced stress (Antwi *et al.* 2006, Brocklehurst *et al.* 1997 and Wilson *et al.* 2002), or (2) a solid(like) environment can enhance survival/growth (Mertens *et al.* 2010).
In this research, the effect of a solid (like) environment on the dynamics of *Escherichia coli* K12 at temperatures close to T_{max} is studied. Previous research revealed that the dynamics of *E. coli* at these temperatures was disturbed which could be explained by the co-existence of two subpopulations (Van Derlinden *et al.* 2010). To elucidate the effect of structure on the dynamics of *E. coli* at super optimal conditions, static experiments were performed in BHI, structured with xanthan gum, in parallel with experiments in liquid BHI. Hereto, spectrophotometer tubes, filled with liquid or structured medium were simultaneously placed in a temperature controlled water bath. At regular times, a tube was removed and cell density was determined via plate counting. Temperature was put at 45, 45.7, 46 and 46.5°C.
For all temperatures, sigmoid growth curves are observed. In comparison to Van Derlinden *et al.* (2010) however, the growth curves do not indicate the presence of subpopulations. A first feasible explanation is the possibly lower oxygen concentration in spectrophotometer tubes versus test tubes (as used in Van Derlinden *et al.* 2010). At super optimal temperatures, oxygen generates reactive oxygen species (ROS) which have a negative effect on growth kinetics. Possibly, the reduction in stress, i.e., reduced ROS, results in continuous growth instead of the stress-induced behaviour as seen in Van Derlinden *et al.* (2010). Another or additional factor that can explain the difference in the observed growth behaviour is a change in the composition of the BHI-medium. The BHI used for the current experiments uses porcine brain instead of bovine brain for the BHI used in the experiments of Van Derlinden *et al.* (2010).
The results show a minimal difference between growth in liquid and in structured medium. As there is less oxygen in the headspace of the spectrophotometer tubes, the oxygen concentration of the liquid might resemble the concentration in the diffusion-limited structured medium. Equally low concentrations of ROS in liquid and in structured media may lead to a similar stress response and consequently similar growth behaviour.

Keywords: *structured food model system, T_{max}, oxygen stress, heat stress, subpopulations*

Introduction

Next to the chemical and physical composition of food, the behaviour of microorganisms is also affected by the food structure. Effects of food structure are mostly related to the reduced mobility of the microorganisms and the distribution of water, nutrients and metabolites (Wilson *et al.* 2002). In structured media, cells do not grow planktonically but as colonies on or in the medium. As the colony grows, the cells in the inner part of the colony experience a reduced supply of substrates and oxygen and an increased local concentration of metabolites. In contrary, the cells at the outside of the colony have free access to substrate and can dispose their metabolites faster. As a result, a metabolite and nutrient gradient exists over the cell, causing stress to the cells at the inner of the colony (Wimpenny 1992). In literature some suggest that structure stress results in a lower growth rate or a smaller growth domain (e.g.,

Antwi *et al.* 2006, Brocklehurst *et al.* 1997 and Wilson *et al.* 2002). On the other hand, growth promoting effects of structure were observed by Mertens *et al.* (2010).
When investigating the dynamics of *E. coli* K12 MG 1655 at temperatures close to T_{max} (45-46.5ºC), Van Derlinden *et al.* (2010) observed non-sigmoid growth curves, i.e., a sequence of growth, inactivation and re-growth. A possible explanation for this behaviour is the co-existence of two subpopulations: a heat sensitive subpopulation that inactivates after a short growth period co-exists with a heat resistant subpopulation that keeps growing (Van Derlinden *et al.* 2010).
The objective of this research is to investigate whether the same disturbed growth behaviour as seen in Van Derlinden *et al.* (2010) is observed in structured systems at temperatures close to T_{max}. The differences in growth behaviour in liquid and structured media are studied by the use of a xanthan-based food model system.

Materials and Methods

Experiments are performed with an *E. coli* K12 MG 1655 stock culture obtained from the Genetic Stock Centrum, University of Yale. In a first culture step, a loop of the stock culture was transferred in an Erlenmeyer containing 20mL of BHI medium (Oxoid, Basingstoke, UK). After 9h at 37ºC, 20µL was transferred to a second Erlenmeyer with 20mL BHI medium which was placed for 15h at 37ºC.
Structured medium was obtained by adding 1.5g xanthan gum per 100mL of BHI. The structured medium was stirred for 30min and afterwards centrifuged for 30min at 4000rpm.
Spectrophotometer tubes were filled with 1mL of inoculated medium and placed in a temperature controlled water bath (GR 150 S12; Grant, Shepreth, UK). At regular times, one tube with structured and one with liquid medium were removed. After making the proper dilution in liquid BHI medium, samples were plated on agar plates (BHI and 14g/L agar (Oxoid, Basingstoke, UK)). Plates were kept for at least 18h at 37ºC before counting.

Results and Discussion

The difference in dynamics of *E. coli* when cultured in liquid BHI versus structured BHI was studied at 45ºC; 45.7ºC; 46ºC and 46.5ºC. Generally, sigmoidal curves are observed for all temperatures and for both liquid and structured systems. Figure 1 shows the data of all experiments. It is clear that the overall growth rate is similar for liquid and structured systems. As can be expected, the growth rate decreases with increasing temperature.

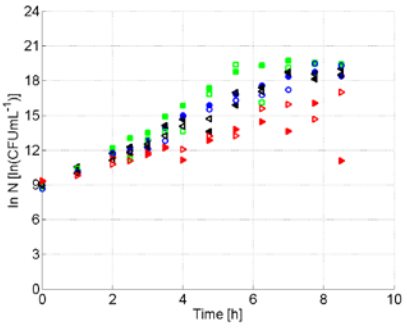

Figure 1: Dynamics of *E. coli* K12 MG 1655 in liquid (open symbols) and solid (filled symbols) BHI medium at 45ºC (□), 45.7ºC (○), 46ºC (<) and 46.5ºC (>).

Liquid systems: sigmoid growth curve

As the experiments are performed at super optimal temperatures, for liquid systems, growth behaviour similar to that observed in Van Derlinden *et al.* (2010) is expected. However, the presented data show a sigmoidal growth curve. The growth rate decreases with increasing temperature. As time proceeds, the experimental variability increases, i.e., data are more scattered near the end of the experiment. In addition, data points collected at later times

(>10h, data shown in Figure 2), indicate that at all temperatures a stationary phase of about 18 to 20ln (CFU/ml) is reached.
A possible explanation for this unexpected difference in behaviour is the effect of oxygen. In literature (Bai *et al.* 2003, Steels *et al.* 1994), it is suggested that heat stress is accompanied by oxidative stress under aerobic conditions. Oxidative stress is the result of an imbalance between generation and elimination of reactive oxygen species (ROS) which are toxic to micro-organisms (Scandalios 2002). In the present study, experiments are performed in spectrophotometer tubes (sealed tubes with screw) for which the oxygen to medium ratio is smaller than in test tubes as the headspace in test tubes is approximately four times bigger than that in spectrophotometer tubes. During growth, *E. coli* consumes oxygen, such that the concentration above the medium decreases. Possibly, this will lead to oxygen depletion being faster in the spectrophotometer tubes than in the test tubes. As the oxygen in the headspace and the oxygen in the medium are in equilibrium (via diffusion mechanisms), it is possible that the oxygen concentration in the spectrophotometer tubes is lower than in the test tubes. As such, a lower concentration of oxygen will reduce the reactive oxygen concentration and so the total stress level, resulting in growth dynamics more similar to dynamics observed at lower, less stressing temperatures.
Alternatively, small changes in BHI composition might explain for the differences in dynamics. In a personal communication, Oxoid, the supplier of the BHI, reported a change in BHI product since May 2009 (*calfe brain infusion solids* were replaced by *porc brain infusion solids*). Experiments at non-stressing temperatures do not reveal any influence of the change in components on the growth behaviour (data not shown). However, throughout literature, studies can be found that report on the effect of small medium composition differences under stress conditions (De Spiegeleer *et al.* 2004, Oteiza *et al.* 2003). As such, the change in composition might evoke a different stress response, leading to a sigmoidal growth curve instead of the disturbed growth behaviour.

Liquid versus solid

Figure 2 shows that experimental data obtained from liquid and solid systems coincide, indicating that the influence of the structure of the environment on the growth of *E. coli* is limited. Although the structured medium causes the bacteria to grow in colonies, diffusion limitations are not restricting the growth rate of *E. coli*. This can be explained by the fact that xanthan gum is a weak gel. In this structured medium, it is possible that the diffusion of nutrients and oxygen is fast enough to fulfil the needs of the growing bacteria. As such, conditions in liquid and solid might be very similar. The removal of metabolites seems to go sufficiently fast so no negative effect of accumulation of metabolites in the centre of the colonies is observed.

Conclusions

The objective of this research is to further elucidate the growth behaviour in structured media at super optimal temperatures. For liquid media the experimental data show a sigmoid growth curve for *E. coli* K12 grown at temperatures close to $T_{max,}$ which is in contrast to the disturbed growth behaviour observed by Van Derlinden *et al.* (2010). Possible explanations are the change in oxygen in the headspace and the composition of the BHI-medium. Contrary to what is mentioned in literature for structured media, the presented data show that growth in structured food model systems is similar to that in liquid systems. To further evaluate this hypothesis, it would be of interest to compare the behaviour in liquid and in gelified systems at more severe conditions, e.g., low pH. In parallel, a profound study on the influence of medium composition can reveal if this can explain for the differences with experiments performed in 2010. In addition, a quantitative analysis of the data will be performed.

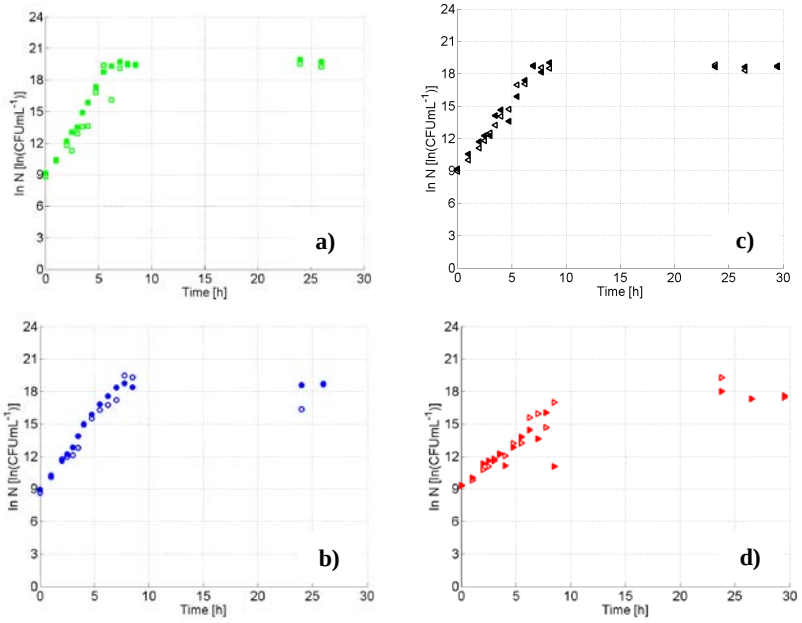

Figure 2: Dynamics of *E. coli* K12 MG 1655 in liquid (open symbols) and solid (filled symbols) BHI medium at a) 45ºC, b) 45.7ºC, c) 46ºC and d) 46.5ºC.

Acknowledgements

This work was supported by project PFV/10/002 (Center of Excellence OPTEC-Optimization in Engineering) of the Research Council of the K.U. Leuven, Knowledge Platform KP/09/005 (www.scores4chem.be) of the Industrial Research Fund, and the Belgian Program on Interuniversity Poles of Attraction, initiated by the Belgian Federal Science Policy Office. E. Van Derlinden is supported by postdoctoral grant PDMK/10/122 of the K.U. Leuven Research Fund. J. Van Impe holds the chair Safety Engineering sponsored by the Belgian chemistry and life sciences federation essenscia. K. Boons is supported by a research grant of the Institute for the Promotion of Innovation by Science and Technology in Flanders (IWT).

References

Antwi M., Geeraerd A.H., Vereecken K.M., Jenné R., Bernaerts K. and Van Impe J.F. (2006) Influence of a gel microstructure as modified by gelatin concentration on *Listeria innocua* growth. *Innovative Food Science and Emerging Technologies* 7, 124-131.

Bai Z., Harvey L.M. and McNeil B. (2003) Elevated temperature effects on the oxidant/antioxidant balance in submerged batch cultures of the filamentous *Aspergillus niger* B1-D. *Biotechnol Bioeng* 83 (7), 772-779.

Brocklehurst T.F., Mithcell G.A., and Smith A.C. (1997) A model experimental gel surface for the growth of bacteria on foods. *Food Microbiology* 14, 303-311.

De Spiegeleer P., Sermon J., Lietaert A., Aertsen A. and Michiels C.W. (2004) Source of tryptone in growth medium affects oxidative stress resistance in *Escherichia coli*. *Journal of Applied Microbiology* 97, 124-133.

Mertens L., Van Derlinden E., Dang T.D.T., Cappuyns A.M., Vermeulen A., Debevere J., Moldenaers P., Devlieghere F., Geeraerd A.H. and Van Impe J.F. (2010) On the critical evaluation of growth/no growth assessment of *Zygosaccharomyces bailii* with optical density measurements: Liquid versus structured media. *Food Microbiology* 28(4), 736-45.

Oteiza J., Giannuzzi L., Califano A.(2003) Thermal inactivation of *Escherichia coli* O157:H7 and *Escherichia coli* isolated from morcilla as affected by composition of the product. *Food Research International* 36, 703-712.

Scandalios J. G. (2002) Oxidative stress responses – What have genome scale studies taught us? *Genome Biology* 3(7), reviews1019.1–1019.6.

Steels E.L., Learmonth R.P. and Watson K. (1994) Stress tolerance and membrane lipid unsaturation in *Saccharomyces cerevisiae* grown aerobically or anaerobically. *Microbiology* 140, 569-576.

Van Derlinden E., Boons K. and Van Impe J.F. (2010) *Escherichia coli* population heterogeneity: Subpopulation dynamics at super-optimal temperatures. *Food microbiology* 28(4), 667-77.

Wilson P., Brocklehurst T., Arino S., Thuault D., Jakobsen M., Lange M., Farkas J., Wimpenny J. and Van Impe J.F. (2002) Modelling microbial growth in structured foods: Towards a unified approach. *International Journal of Food microbiology* 73, 275-289.

Wimpenny J.W.T. (1992) Microbial systems: Patterns in time and space. In: K.C. Marshall (Ed.), *Advances in Microbial Ecology, Volume 12*, Plenum Publishing Corporation, New York, USA, 534 pp. (ISBN: 0306442663).

Modelling the growth of *E.coli* under the effect of *Rhus coriaria L.* essential oil, temperature and pH

G. Karim[1], B. Radmehr[2], R. Khaksar[3], M. Sadatmosavi[1]

[1]Department of Food Hygiene, School of Veterinary Medicine, University of Tehran, Iran. (gkarim@ut.ac.ir)
[2]Department of Food Hygiene and Quality Control, School of Veterinary Medicine, Islamic Azad University-Karaj Branch, Iran. (radmehr@kiau.ac.ir)
[3]Department of Food Technology, National Nutrition and Food Technology Research Institute, Faculty of Nutrition Science and Food Technology, Shaheed Beheshti University, M.C. Iran. (r.khaksar@sbmu.ac.ir)

Abstract

Regarding to increasing interest in use of natural preservatives, in this study effects of *Rhus coriaria L.* essential oil, pH and temperature on the probability of growth of *E.coli,* that is important pathogen in food safety, were evaluated. So combined effects of four different concentration of *Rhus coriaria L.* essential oil , (0 , 0.0062 , 0.0125 , 0.025 , 0.05%) with three level of pH (5.5 , 6 , 7) and three incubation temperature (20 , 25 , 35 C) on the probability of *E.coli* growth in Brain Heart Infusion broth model were evaluated. Based on turbidity in broth model , growth of bacteria was recorded up to 48 hours by BioscreenC® and probability of growth was calculated. Then effects of different factors were studied and mathematical model was developed. According to the results, different values of essential oil had significant effects on the probability of growth ($P<0.05$). As the concentration of essential oil increased the probability of growth of bacteria was decreased. Also other growth factors like pH , temperature and storage time had significant effects on the probability of growth ($P<0.05$). So that by increasing them growth probability was increased. Stepwise multiple regressions were used for selection of a predictive mathematical model. In the obtained mathematical model, determination coefficient (R^2) was 0.842 which shows good correlation between predicted and expected values in the study. So we can use this model to predict growth probability of *E.coli* under the effects of these factors.

Keywords: Modelling, Rhus coriaria L., essential oil, E.coli

Introduction

In recent years, developments of mathematical models to predict the growth of bacteria in food systems have been expanded. Predictive microbiology is an essential element of modern food microbiology and offers to provide a scientific foundation to meet the ongoing needs of food safety (Mc MeMeekin and Ross 2002). However there are few works for modelling the effects of plant extracts and essential oils in combination with other factors on the growth kinetics of bacteria.

Because of negative consumer reactions to traditional preservatives, substitution of chemical and artificial food preservatives by natural ones is a growing interest in food safety (Tassou *et al.* 2000). One of these natural preservative is plant essential oils. Plant essential oils are aromatic oily liquid obtained from plant material (Valero and Salmeron, 2003; Burt, 2004).

Rhus coriaria L. that called Sumac in Iran is a plant that wildly grows in Iran. The name is derived from ‘‘sumaga’’, meaning red. In folk medicine, it is used for treatment of indigestion, anorexia, diarrhea, hemorrhagia and hyperglycemia. This plant has been used traditionally as flavor agent in variety of food in Iran. Few studies have been done which shows the antimicrobial effect of this plant. It seems that more studies are needed to establish such an effect (Nasar-Abbas and Kadir Halkman 2004).

To establish the usefulness of natural antimicrobial preservatives, they must be evaluated alone and in combination with other preservation to determine whether there are synergistic effects (Lopez-Malo *et al*. 1998).

E. coli is the important member of *Enterobacteriaceae* family, which are facultative anaerobic Gram-negative rods that live in the intestinal tracts of animals and can easily contaminate food. *E. coli* are among the most important bacteria in medicine and food hygiene.
Therefore, the present study was done to evaluate the effects of *Rhus coriaria L.* essential oil, temperature and pH on the growth of *E.coli* that is an important pathogen in food safety, in Brain Heart Infusion broth. We also attempted to generate predictive models for the growth of *E.coli* under the effects of these factors.

Materials and Methods

Rhus coriaria L. purchased from Tehran city local markets and essential oil was extracted by steam distillation method. Lyophilized cultures of *E.coli* obtained from scientific and industrial organization of Iran were used in this study. The lyophilized cultures were grown in tubes containing of Brain Heart Infusion (BHI) broth at least twice at $35^{\circ C}$ for 18 hours and used for experiments. *E.coli* inocula were prepared by transferring cells from second cultures to tubes of BHI broth for each experiment. After incubation at $35^{\circ C}$ for 18 hours and preparing serial dilutions of *E.coli* broth cultures, optical density (OD) of each tube were measured by BioscreenC®. Then, the number of cells in the each tube was estimated by duplicate plating from the serial dilutions on BHI agar and counting the colonies after 24 hours incubation at $35^{\circ C}$ and the tube contains 10^7 cfu ml^{-1} bacteria used to preparing 10^5cfu ml^{-1} concentration of bacteria for the experiments (Basti and Razivilar 2004).
BHI powder (3.7 g) was dissolved in 90 ml distilled water in a 250 ml screw capped flask by mild heating. Then, different concentration of *Rhus coriaria L.* essential oil, (0 , 0.0062 , 0.0125 , 0.025 , 0.05%) was added in different amounts to satisfy the experimental design. Three levels of pH (5.5 , 6 , 7) for all different concentration of *Rhus coriaria L.* essential oil, were adjusted by adding acetic acid (Basti *et al.* 2007).
Different combinations of essential oil and pH were prepared by adding 50µlit of 10^5 cfu ml^{-1} concentration of bacteria to 350µlit of different essential oil and pH adjusted media in BioscreenC® microplates. After that, microplates were incubated in three incubation temperature (20 , 25 , 35°C) for 48 hours and the ODs of each microwell were measured every 30 minutes by BioscreenC®. Growth of bacteria was recorded based on turbidity in broth. Stepwise multiple regressions with data transformations were used for selection of a predictive mathematical model.

Results and Discussion

According to the results of ANOVAs, the ODs were affected significantly ($P<0.05$) by essential oil, pH, temperature and their two and three way interactions. That means different concentration of *Rhus coriaria L.* essential oil had significant effects on the growth of bacteria. As the concentration of essential oil increased, the probability of growth of bacteria was decreased.
Also other growth factors like pH , temperature and storage time had significant effects on the probability of growth ($p<0.05$). So that by increasing them growth probability was increased.
The regression equation for the effects of essential oil (EO), temperature (T), pH and time (M) was obtained as:

$$OD = 1.097 + (0.0001\ T\ \ pH\ \ M) + (0.0001\ \ T\ \ M) - (0.0001\ \ EO\ \ T) + (0.0001\ \ pH\ T) - (0.001\ \ M) + (5.691\ \ EO) - (0.187\ \ T\ \ EO) - (26.231/T) - 0.899\ T^{1/2} - 0.004\ M^{1/2} - 0.155\ EO^{1/2} + (0.007\ EO\ \ pH\ \ M) - (0.122\ pH^2) + (1.29\ \ pH) + (0.009\ \ T\ \ pH) \quad (1)$$

In this mathematical model, determination coefficient (R^2) was 0.842 which shows good correlation between predicted and expected values in the study. According to our results the inhibitory action of the *Rhus coriaria L.* essential oil on the organism growth was enhanced

by decreasing the pH value at each defined temperature. This can be attributed either to the direct effect of pH or to the better dissolving of the essential oil in the lipid phase of the bacterial membrane at the low pH (Koutsoumanis *et al*. 1999). The amount of essential oil needed to exert antimicrobial activity is often higher than the amount usually used as flavoring and is associated with adverse sensorial effects (Bagamboula *et al*. 2004). It is recommended to apply essential oils as part of a hurdle system and to use them as antimicrobial components along with other preservation techniques e.g. in combination with reduced temperature and pH (Tassou *et al*. 2000), thus enabling to decrease their concentrations and minimizing adverse sensorial effects. Evidently more studies are needed on the antimicrobial properties of essential oils, before they can be used as food preservatives (Bagamboula *et al*. 2004).

It is evident, from the magnitude of the values of obtained (R^2), as well as the good agreement between the predicted and observed values of OD, that the model, provide a high degree of accuracy of prediction against observed data (Davey and Daughtry, 1995; Oscar, 1999). From these models the values of predicted ODs can be calculated from any combinations of essential oil, pH and incubation time within the limits studied. Such models offer a cost-effective approach to understanding and controlling microbial growth response in foods (Basti and Razavilar 2004). So we can use this model to predict growth probability of *E.coli* under the effects of these factors in broth.

Mathematical models for predicting the growth of pathogens in food are usually developed in broth because enumeration of pathogens in food is difficult (McClure *et al*. 1994). However, models developed in laboratory media do not provide reliable predictions of bacterial growth in real food environment. The effect of *Rhus coriaria L.*essential oil may be reduced in foods as compared with pure cultures. The fat, protein, water and salt contents of food improve microbial resistance as it has been observed that higher levels of spices are necessary to inhibit growth in food than in culture media (Nasar-Abbas and Kadir Halkman 2004). Thus, we need to develop this type of models for the growth of pathogenic bacteria in real food.

Conclusions

The results obtained in this study showed significant effects of *Rhus coriaria L.* essential oil, pH, temperature and a number of interactions including on the growth of *E.coli.*

The (R^2) values of the models obtained in our study showed a high degree of goodness-of-fit between the models and data. These become obvious also from the comparisons of predicted and observed.

Considering the importance of *E.coli* in food safety and the power of predicting models, we suggest that this kind of models can be used as a prediction tool in food safety.

Acknowledgements

The authors express their appreciation and thanks for the supports received from Food Microbiology Laboratory of National Nutrition and Food Technology Research Institute, Shaheed Beheshti University.

References

Bagamboula C.F., Uyttendaele M. and Debevere J. (2004) Inhibitory effect of thyme and basil essential oils, carvacrol, thymol, estragol, linalool and p-cymene towards Shigella sonnei and S. flexneri. *Food Microbiology* 21, 33-42.

Basti A.A., Misaghi A. and Khaschabi D. (2007) Growth response and modelling of the effects of Zataria multiflora Boiss. essential oil, pH and temperature on Salmonella Typhimurium and Staphylococcus aureus. *LWT-Food Science and Technology* 40,973-981.

Basti A.A. and Razavilar V. (2004) Growth response and modelling of the effects of selected factors on the time-to-detection and probability of growth initiation of Salmonella typhimurium. *Food Microbiology* 21, 431–438.

Burt S. (2004) Essential oils: their antibacterial properties and potential application in foods-a review. International *Journal of Food Microbiology* 94, 223-253.

Davey K.R. and Daughtry B.J. (1995) Validation of a model for predicting the combined effect of three environmental factors on both exponential and lag phases of bacterial growth: Temperature, salt concentration and pH. *Food Research International* 28, 233–237.

Lopez-Malo A., Alzamora S.A. and Argaiz A. (1998) Vanillin and pH synergistic effects on mold growth. *Journal of Food Science* 63, 143-146.

McClure P.J., Blackburn C.D., Cole M.B., Curtis P.S., Jones J.E., Legan J.D., Ogden I.D., Peck M.W., Roberts T.A., Sutherland J.P. and Walker S.J. (1994) Modeling the growth, survival and death of microorganisms in foods - the uk food micromodel approach. International *Journal of Food Microbiology* 23, 265–275.

McMeekin T. A. and Ross T. (2002) Predictive microbiology: providing a knowledge-based framework for change management. *International Journal of Food Microbiology* 78, 133-153.

Nasar-Abbas S.M. and Kadir Halkman A. (2004) Antimicrobial effect of water extract of sumac (Rhus coriaria L.) on the growth of some food borne bacteria including pathogens. *International Journal of Food Microbiology* 97, 63– 69

Oscar T.P. (1999) Response surface model for effect of temperature. pH, and previous growth pH on growth kinetics of Salmonella typhimurium in brain heart infusion broth. Journal of Food Protection 62, 106–111.

Tassou C., Koutsoumanis K. and Nychas G.J.E. (2000) Inhibition of Salmmonella enteritidis and Staphylococcus aureus in nutrient broth by mint essential oil. *Food Research International* 33, 273–280.

Valero M. and Salmeron M.C. (2003) Antibacterial activity of 11 essential oils against Bacillus cereus in tyndallized carrot broth. *International Journal of Food Microbiology* 85, 73–81.

Modelling growth of *Escherichia coli* O157:H7 in extract of different leafy vegetables.

G. Posada-Izquierdo[1], S. Del Rosal[1], F. Perez-Rodriguez[1], M. Rodríguez[1], A. Morales[1], E. Todd [2], A. Valero[1], E. Carrasco[1], G. Zurera[1].

[1]Deparment of Food Science and Technology Ed. Darwin-Anexo. Campus Rabanales. University of Cordoba Cordoba, 14014. Spain. (bt2poizg@uco.es)
[2]Advertising, Public Relations and Retailing, Michigan State University, East Lansing, MI, USA

Abstract

Microbial risk derived from consumption of minimally processed vegetables is a serious concern for industry and governments. *Escherichia coli* O157:H7 is a food-borne pathogen which has been recently linked to several outbreaks associated with the consumptions of minimally processed vegetables. This pathogen can contaminate produces at harvest, and then, survive and/or grow during manufacturing, distribution, and storage, reaching the end consumer. The present work aims to study and model the potential growth of *E. coli* O157:H7 in extract of different leafy vegetables at different storage temperatures. A cocktail including five *E. coli* O157:H7 strains resistant to nalidixic acid (NalR+) was built. Sterile extract from different leafy vegetables (iceberg lettuce, chard, spinach, parsley and romaine lettuce) was supplemented with nalidixic acid (50 μg/mL) and inoculated by the NalR+ pathogen cocktail (≈ 10^6 cfu/mL) in micro-plates (10x10 wells) and then incubated at different temperatures (4, 8, 10, 13, 16, and 20°C). The growth was monitored by absorbance measurement (8 replicates) by using Bioscreen C. Based on the observed absorbance data in the growth exponential phase, maximum growth rates and secondary models were estimated by using Excel Microsoft ®. Results indicated that the pathogen was able to grow in all assayed vegetable extracts. However, at 8°C, growth was only observed for parsley and chard. The fastest growth was obtained in chard extract (e.g. 0.26 h^{-1} at 20 °C), followed by spinach (e.g. 0.12 h^{-1} at 20 °C). The slowest growth was obtained in parsley extract (e.g., 0.012 h^{-1} at 20°C), although, in this extract, the microorganisms was able to grow at 8 °C (0.001 h^{-1}). Finally, estimated maximum grow rates were used to derive a secondary model describing maximum growth rate as a function of temperature. The Ratkowsky´s model showed better convergence to observed data. The best fitting was obtained for spinach and chard extracts (R^2>0.85). Furthermore, the study provides evidence that compounds contained in vegetable tissues can result in a distinct growth niche producing different response in various types of vegetables.

Keywords: v*egetables, Escherichia coli O157:H7, growth modeling, chard, parsley, spinach*

Introduction

In recent years, consumer trends have shifted focus to healthier diets, increasing demand for natural products (or processed, that at least appear, such as salads RTE), especially leafy raw vegetables. This type of product can become contaminated by foodborne pathogens such as *Escherichia coli* O157:H7 and *Listeria monocytogenes* (Gleeson and O`Beirne 2005) at various stages of the food chain from “farm to table”. However, no heat treatment or other inactivation method is applied which can guarantee a complete elimination of pathogenic microorganisms when presented in products. Hence, the incidence of illnesses transmitted by vegetables has been increasing as a result of these changes in consumption habits.

E. coli O157:H7 has been linked to outbreaks of various leafy vegetables such as lettuce, spinach, parsley, etc. (EFSA 2009). Therefore, the aim of this study was to study and model the potential growth of *E. coli* O157: H7 in different leafy vegetables, which have not been studied extensively by the scientific literature so far. In addition, the work looks to give more information based on predictive microbiology and expanding the tools available that will

enable us to assess the microbiological risks more effectively and to implement corrective action from the knowledge of the behavior of this pathogen.

Materials and Methods

Growth medium

Sterile vegetable extracts were used to simulate growth of the pathogen in leafy vegetable matrices. To obtain the extract, first different vegetables (chard, spinach, parsley, iceberg and romaine lettuce) were homogenized in distilled water with a proportion 1:3 (vegetable/water) by using Stomacher. Then, generated extracts were sterilized by filtration through a step-by-0.22 micron membrane (Millipore filter unit-Express Plus PES). Extracts of each vegetable were plated to confirm sterility.

Bacterial strains and inoculum preparation

A cocktail of five strains of *Escherichia coli* O157: H7 (CECT 4076, 4267, 4782, 4783 and 5947) was used in this study. Cocktail trains were previously made resistant at 50 μg/mL of Nalidixic acid (NaL) (Merck, Darmstadt, Germany) (Allende *et al*. 2008). Prior to growth experiments, cultures were grown in Tryptic Soy Broth (TSB) at 37 ° C for 18-20 h in three incubation loops, and then mixed at equal volumes of cell suspensions to give approximately equal populations of each culture. Then, the cocktail was washed three times by centrifugation (4100 g) and suspended in phosphate buffer (PBS) obtaining an inoculum level of 10^8 cfu/mL, approximately. Counts were obtained by growth on McConkey-Sorbitol, MCS agar and on Tryptone Bile X-Glucuronide Medium, TBX agar (Oxoid, UK) supplemented with Nal (50 μg/mL).

Inoculation procedure and assessment of growth

The Bioscreen C (Labsystems, Finland) was used to monitor bacterial growth based on absorbance measures at 420-580 nm. A cocktail of *E. coli* O157: H7 previously washed and resuspended in PBS was diluted 1:100 in vegetable extracts supplemented with NaL (50 μg/mL) obtaining a concentration of 10^6 cfu/mL, approximately. Micro-plates (10x10 wells) belonging to Bioscreen C were utilized to perform the growth experiment. Each well was filled with 300 μl of inoculated vegetable extracts with a total of eight replicates and two blanks per extract. The plates were incubated at different temperatures (4, 8, 10, 13, 16 and 20 °C) during a period of 21 days. At high temperatures (13, 16 and 20 °C), growth was monitored continuously by Bioscreen C, while at lower temperatures, absorbance measurements were made at specific time points during experiments (8 and 10 °C). Growth observed in wells was confirmed by plating an extract aliquot on MCS agar supplemented with NaL.

Growth modelling

Maximum growth rates were estimated based on the observed absorbance data (log) in the growth exponential phase by using Excel Microsoft ®. Secondary models were fitted to maximum rates using the DMFit program (Excel Add-In) (Baranyi and Roberts 1994).

Results and Discussion

Growth was not detected in romaine and iceberg vegetable extracts at all temperatures. However, parsley, spinach and chard presented a significant increase of absorbance for all temperatures except for 4 ºC at which no growth was detected in all extracts. Chard extract did not support *E. coli* O157: H7 growth at 8 ºC. Likewise for assays at 10 ºC in the same extract, only few replicates presented a significant increase of absorbance, within the linearity range (>0.074); although growth data was not enough to appropriately estimate the maximum growth rate. *E. coli* O157:H7 in spinach at 8 ºC showed a digenetic behavior, in which 8 out

of 4 wells presented a significant growth. To model growth in chard extract, temperatures 8 and 10 ºC were discarded, while for spinach only positive replicates at 8 ºC were considered.

Overall, the pathogen presented different growth patterns in the different vegetable extracts. The fastest growth was obtained in chard extract (0.26 h^{-1} at 20 °C), followed by spinach (0.12 h^{-1} at 20 °C). In turn, the slowest growth was observed in parsley extract (0.012 h^{-1} at 20 °C); although in this extract the microorganism was able to grow at 8 °C (0.001 h^{-1}). There are few studies in scientific literature dealing with these food matrices and *E. coli* O157:H7 growth. Growth rates observed, in our study, at refrigeration temperatures (8-13 °C) were low when compared to other studies (Valero *et al*. 2010). For instance, Koseki and Isobe (2005) reported a growth rate of 0.03 (h^{-1}) for *E. coli* O157:H7 in lettuce at 10 ºC, while in our study, at this temperature, the growth rate oscillated between 0.002 and 0.004 h^{-1}. Similarly, Rowaida and Josepth (2010) found higher growth of *E. coli* O157:H7 in damaged spinach stored for 3 days at 8 and 12ºC with increases of 1.18 and 2.08 log cfu/g, respectively. By contrary, at high temperatures (20 ºC), growth rates were quite similar to those reported by other studies. For instance, the study by Koseki and Isobe (2005) showed a maximum growth rate of 0.26 h^{-1} in lettuce leaves stored at 20 ºC which was equal to the value obtained in our study for chard extract at the same temperature (i.e. 0.26 h^{-1}).

Surprisingly, romaine and iceberg lettuce did not present any growth during 21 days. This result is not in concordance with that reported by most studies which demonstrate a significant growth in the temperature range 10-25 ºC (Koseki and Isobe 2002). However, these studies were mostly performed on inoculated vegetable surfaces, and not in aqueous extracts of vegetable, which contain a complex and concentrated mixture of substances released from vegetable tissues (peptides, phenols, fiber, enzymes, etc.). Regarding this, the study Rowaida and Josepth (2010) found that *E. coli* 057:H7 was not able to grow on damaged leaves of romaine lettuce at 8 and 12 ºC, but growth was observed at 15 ºC. This study hypothesized that the inhibition at low temperatures could be caused by oxidation reactions associated with tissue damaged. In fact, it is known that some vegetable species can present substances with antimicrobial activity (Hashem and Saleh 1999). Besides that, it cannot be discarded that both samples of romaine and iceberg lettuce were contaminated with pesticides with antimicrobial activity.

Finally, estimated maximum grow rates were used to derive a secondary model describing maximum growth rate as a function of temperature. The Ratkowsky´s model (Ratkowsky *et al*. 1982*)* showed better convergence to observed data in all extracts. For spinach and parsley, the best fitting was obtained when square root was applied to maximum growth rate, while for chard extract the best fitting was attained when no mathematical transformation was used. Regression parameters (*b* and T_{min}) and Standard Error of the Ratkowsky´s model for the *E. coli* O157:H7 growths in the three extracts are showed in Table 1.

Table 1: Estimated regression parameters of the Ratkowsky´s model based on *E. coli* O157:H7 growth in different vegetable extracts.

Vegetable Extract	Temperature range (ºC)	*b*	T_{min}	SE*
Chard	13-20	5.00 x10^{-03}	13.0	3.4x10^{-02}
Parsley	8-20	4.64 x10^{-05}	2.9	5.6 x10^{-03}
Spinach	8-20	9.97 x10^{-04}	8.7	4.8 x10^{-02}

SE : Standard Error

Conclusions

Results indicated that *E. coli* O157:H7 was able to grow in different aqueous extracts of vegetables in a broad range of temperatures, although growth patterns varied depending on the type of extract. Use of vegetable extracts can help to better simulate conditions given in vegetable tissues where bacteria can reside (internalization or injury), survive and growth thereby allowing the pathogen transmission through the food chain. Further, results suggest that unknown compounds present in vegetable extracts could exert an inhibition effect on *E. coli* O157:H7 growth at low temperatures. However, further study will be needed to confirm the existence of potential antimicrobial substance in these types of vegetable.

Acknowledgements

The research has received funding from (project AGL2008-03298), the AGR-170Research Group, HIBRO and the MCINN with a predoctoral scholarship for Guiomar Posada-Izquierdo.

References

Allende A., Selma V., Lopez-Galvez F., Villaescusa R. and Gil M.I. (2008) Impact of wash wáter quality on sensory and microbial quality, including *Escherichia coli* cross-contamination, of fresh-cut escarole .*Journal of Food Protection* 71, 2514-2518.

Baranyi J. and Roberts T.A. (1994). A dynamic approach to predicting bacterial-growth in food. *International Journal of Food Microbiology* 23, 277– 294.

EFSA(2009). The Community Summary Report on Trends and Sources of Zoonoses and Zoonotic Agents in the European Union in 2007. *The EFSA Journal*, 223.

Gleeson E. and O`Beirne D. (2005) Effects of process severity on survival and growth of *Escherichia coli* and Listeria innocua on minimally processed vegetables. *Food Control* 16, 677-685.

Hashem and Saleh M. (1999) Antimicrobial components of some cruciferae plants (*Diplotaxis harra Forsk.* and *Erucaria microcarpa* Boiss). *Phytotherapy Research* 13 , 329–332.

Koseki S and Isobe S. (2005). Prediction of pathogen growth on iceberg lettuce under real temperature history during distribution from farm to table. *International Journal of Food Microbiology* 104, 239–48.

Ratkowsky D., Olley J., McMeekin. T. and Ball A. (1982) Relationship between temperature and growth rate of bacterial cultures. *Journal of Bacteriology* 149, 1-5.

Rowaida K. and Joseph F. (2010) Behaviour of *Escherichia coli* o157:H7 on damaged leaves of spinach, letture, cilantro and parsley stored at abusive temperature. *Journal of Food Protection* 72, 2038-2045.

Valero A., Rodríguez M., Carrasco E., Pérez-Rodríguez F., García-Gimeno R. and Zurera G. (2010) Studying the growth boundary and subsequent time to growth of pathogenic *Escherichia coli* serotypes by turbidity measurements. *Food Microbiology* 27, 819-828.

Modeling the effect of an abrupt temperature shift on the lag phase and the growth curve

W.S. Robazza[1], J.T. Teleken[2], G.A. Gomes[1]

[1]Food Engineering Department, Santa Catarina State University, Pinhalzinho, Santa Catarina, Brazil. (wrobazzi@yahoo.com.br;gilmargomess@yahoo.com.br)
[2]Food Engineering Department, Santa Catarina Federal University, Florianópolis, Santa Catarina, Brazil. (jhony_tt@yahoo.com.br)

Abstract

The main concept of predictive microbiology is that a detailed knowledge of the behavior of micro organisms in food products, condensed into mathematical models, enables an objective evaluation of the microbial safety and quality of foods. During the growth process, a phenomenon widely studied, but not yet clearly understood is the lag phase. Some studies showed that an abrupt temperature shift may induce an intermediate lag phase, which depends on the magnitude and the direction of the shift (Swinnen *et al*. 2005). In this study, a mathematical model that investigates the influence of an abrupt temperature shift on the lag phase was proposed. The model consists of the solution of a system of two differential equations and encompasses the Gompertz modified model as a special case. The secondary model employed to describe the temperature dependence is the extended square-root model and the lag phase duration is estimated according to the definition proposed by Buchanan and Cygnarowicz (1990). The duration and magnitude of the temperature rise were modeled by using an arctan function. Calculation of the second derivative of the growth curve, allows one to observe two local maxima indicating the occurrence of an intermediate lag phase. Quantification of this phenomenon can provide useful insights into new aspects of the lag/no lag interface and its influence on microbial growth.

Keywords: *lag phase, abrupt temperature shift, mathematical model, predictive microbiology*

Introduction

The growth of micro organisms in food systems usually exhibits a characteristic pattern constituted by different phases under isothermal conditions. The lag phase is not considered as being completely understood and is typically described as being a period of adjustment to the new environment (Baranyi and Roberts 1995). In general, the phase following the inoculation in a laboratory medium is known as the initial lag phase. However, sudden environmental variations during growth can also result in an intermediate lag phase (Swinnen *et al*. 2004). In this context, Ng *et al*. (1962) and Shaw (1966) observed that sudden temperature shifts resulted in an immediate lag in growth and Swinnen *et al*. (2005) studied the intermediate lag phase for a range of temperatures. Buchanan and Cygnarowicz (1990) proposed that the end of the lag phase can be estimated based on the calculation of the second derivative of the growth curve. According to these authors, the end of the lag phase corresponds to the maximum and the end of the exponential phase corresponds to the minimum of this curve. Although this procedure is not largely employed in the literature, it is directly associated with a physical plausible interpretation of the lag phase, i.e., the point in which the velocity of growth increases more rapidly. The aim of the study presented in this paper is to propose a mathematical model describing the growth of micro organisms in isothermal and fluctuating temperature conditions and to derive mathematically the initial and the intermediate lag phase. The secondary model employed is the Ratkowsky extended square-root model (Ratkowsky *et al*. 1982, 1983) and the abrupt shift on temperature was modeled with an arctan function.

Materials and Methods

In this paper, the following model of microbial growth is considered:

$$\frac{dN(t)}{dt} = \mu(N) \cdot N(t) \quad (1)$$

$$\frac{d\mu(N)}{dN} = -\alpha(t) \cdot N^m \quad (2)$$

where N is the population density (log cfu), μ is the specific growth rate (1/h), α is a positive variable related to environmental conditions, and m is a shape parameter with no microbiological meaning.

Equation 1 is a fundamental law used in population growth modeling and Equation 2 stresses the fact that the specific growth rate is a decreasing function of the population density. It is assumed that this decrease obeys a power law and α changes if the environmental conditions are non stationary. As a secondary model, it was employed a modified version of Ratkowsky´s extended square-root model (1982, 1983) which is given by Equation 3:

$$\sqrt{\alpha(t)} \cong b \cdot [(T(t) - T_{\min}) \cdot (1 - \exp(c \cdot (T(t) - T_{\max})))]^{-1} \quad (3)$$

where T is the temperature, $T_{\min}$ and $T_{\max}$ are the minimum and maximum temperature for which the growth can be observed and *b* and *c* are parameters.

In order to estimate the time of occurrence of the lag phase and the duration of the exponential phase, it was employed the procedure proposed by Buchanan and Cygnarowicz (1990). These authors suggested that the lag time can be considered as being the time in which the velocity of growth increases more rapidly, i.e., the maximum of the acceleration growth curve. The usage of this procedure can be used to accurately define and calculate the duration of the lag phase and can be easily extended to include situations in which temperature is not kept constant as will be apparent later.

Results and Discussion

Isothermal environment

To study growth in an isothermal environment, the mathematical model expressed in Equations 1, 2, and 3 was used with $T(t)$ (and $\alpha(t)$) kept constant. In the following simulations, the values employed for the parameters were: $N_0 = 1$, $\mu_0 = 0.08$, $b = 0.002$, $c = 0.02$, $T_{\min} = 0$, $m = 4$, and $T_{\max} = 50$. As result of the calculations, Figure 1A shows the growth curves for different values of the temperature with the other parameters kept constant. The curves exhibit the usual sigmoidal shape.

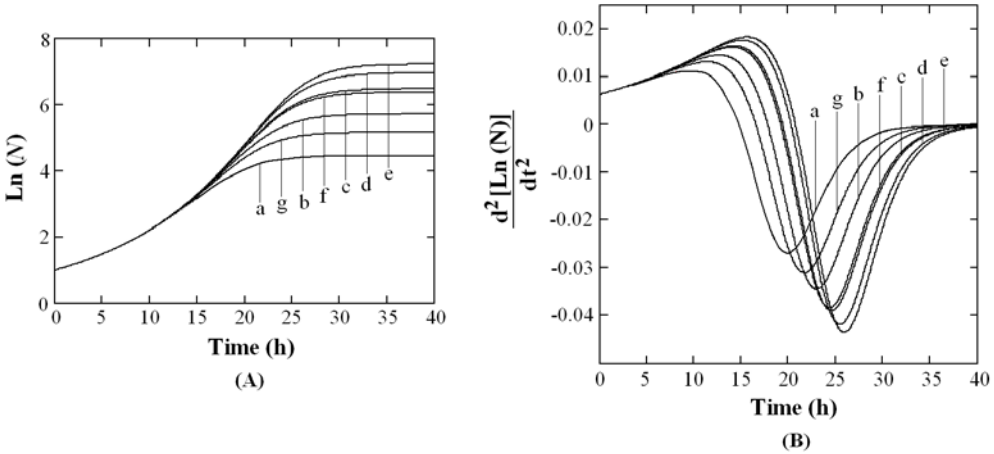

Figure 1: A) Growth curves for an isothermal environment B) Growth acceleration curves: a) $T = 5$ ºC, b) $T = 10$ ºC, c) $T = 15$ ºC, d) $T = 20$ ºC, e) $T = 30$ ºC, f) $T = 40$ ºC, g) $T = 45$ ºC.

Curves of the acceleration growth (second derivative of $N(t)$) for the same temperatures used to obtain the curves of Figure 1A are presented in the Figure 1B. As can be seen, all the curves exhibit the same pattern with a maximum corresponding to the end of the lag phase and a minimum, which corresponds to the end of the exponential phase.

Non-Isothermal environment

In order to account for a dynamical profile of temperature, the following equation was used to model the temperature:

$$T(t) = \left(\frac{T_2 - T_1}{\pi}\right)\arctan(a \cdot t - t_1) + \left(\frac{T_2 + T_1}{2}\right) \quad (4)$$

where T_1 and T_2 are the inferior and superior asymptotes and a is a parameter related to the abruptness of the temperature change.

In this paper the following temperature profiles were employed:

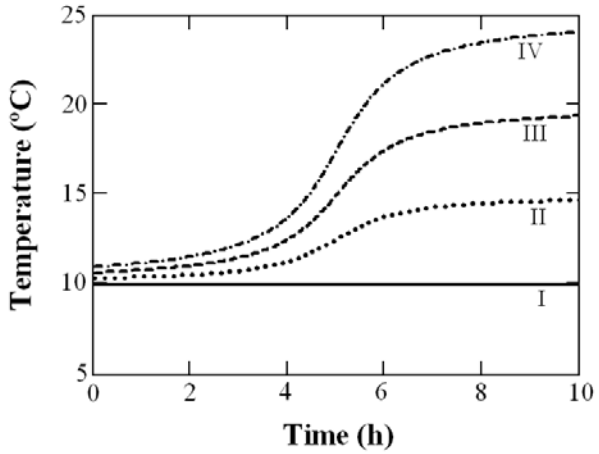

Figure 2: Temperature profiles used in this study.

The growth curves associated with the temperature profiles showed in Figure 2 are presented in Figure 3. It can be seen that for profiles II, III and IV, it is observed an additional lag phase and, as shown in Figure 4, this second lag phase can be estimated through usage of the acceleration growth curves, which shows an additional maximum that can be associated to the intermediate lag phase.

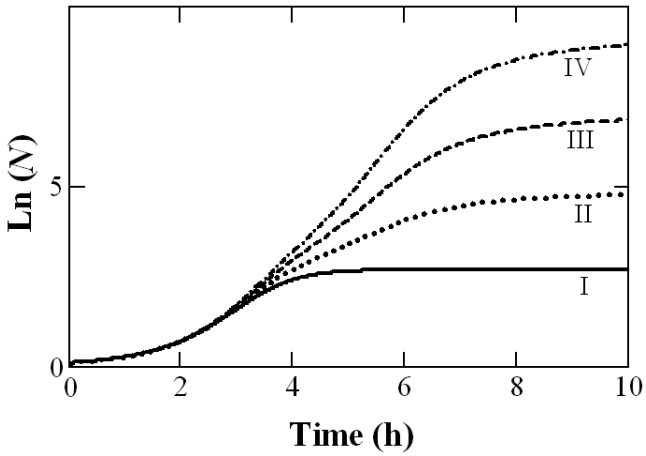

Figure 3: Growth curves associated to the temperature profiles presented in Figure 2.

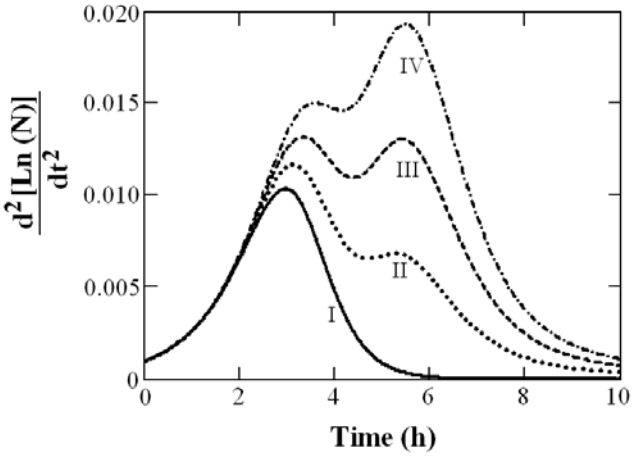

Figure 4: Acceleration growth curves associated to the growth curves of the Figure 3.

In addition to the profiles of temperature showed in Figure 2, other profiles with the same initial and final temperatures but with different "abruptnesses" were used. Results (not presented in this study) showed that, depending on the abruptness, the additional or absence of the lag phase can be observed. A systematic study of the conditions necessary for the occurrence of an additional lag phase can provide useful theoretical insights of the influence exerted by the temperature profile on the microbial growth.

It should be mentioned that the model accounts for a lag phase even if there is no explicit mention for this stage of growth in the equations. This behaviour is observed because the model describes the average behaviour of the population and not of its individuals. As the end of the lag phase does not occur simultaneously for all individuals, it can be considered that, on average, the model reproduces the global behaviour of the population predicting a lag phase which is not sharply defined but can be mathematically defined and calculated.

Conclusions

The mathematical model predicts an intermediate lag phase in both the growth and acceleration of growth curves. An important point lies in the fact that this lag phase is not explicitly included in the equations, appearing as a natural consequence of the hypothesis used in the derivation of the model. This is a crucial point in adopting the procedure proposed by Buchanan and Cygnarowicz (1990), which is independent of the mathematical model used, because it allows an explicit evaluation of the behaviour of the microbial growth curve under different environmental conditions.

References

Baranyi J. and Roberts T.A. (1995). Mathematics of predictive food microbiology. *International Journal of Food Microbiology* 26, 199-218.

Buchanan R.L. and Cygnarowicz M.L. (1990). A mathematical approach toward defining and calculating the duration of the lag phase. *Food Microbiology* 7, 237-240.

Ng H., Ingraham J.L. and Marr A.G. (1962). Damage and depression in *Escherichia coli* resulting from growth at low temperatures. *Journal of Bacteriology* 84, 331-339.

Ratkowsky D.A., Olley J., McMeekin T.A. and Ball A. (1982). Relationship between temperature and growth rate of bacterial cultures. *Journal of Bacteriology* 149 (1), 1-5.

Ratkowsky D.A., Lowry R.K., McMeekin T.A., Stokes A.N. and Chandler R.E. (1983) Model for bacterial culture growth rate through the entire biokinetic temperature range. *Journal of Bacteriology* 154 (3), 1222-1226.

Shaw M.K. Effect of abrupt temperature shift on the growth of mesophilic and psychrophilic yeasts. (1967). *Journal of Bacteriology* 93 (4), 1332-1336.

Swinnen I.A.M., Bernaerts K., Dens E.J.J., Geeraerd A.H. and Van Impe J.F. (2004). Predictive modelling of the microbial lag phase: a review. *International Journal of Food Microbiology* 94, 137-159.

Swinnen I.A.M., Bernaerts K., Gysemans K. and Van Impe J.F. (2005). Quantifying microbial lag phenomena due to a sudden rise in temperature: a systematic macroscopic study. *International Journal of Food Microbiology* 100, 85-96.

Modelling the effects of temperature and osmotic shifts on the growth kinetics of *Bacillus weihenstephanensis* in broth and food products

V. Antolinos[1,2], M. Muñoz-Cuevas[3], M. Ros-Chumillas[2], P.M. Periago[1,2], P. S. Fernández[1,2]*, Y. Le Marc[3]

[1]Instituto de Biotecnología Vegetal. Edificio I+D+i, Plaza del Hospital s/n, Campus Muralla del Mar. 30202. Cartagena, España.
[2]Dpto. Ing.Alimentos y del Equipamiento Agrícola. Escuela técnica Superior de Ingeniería Agronómica. Unversidad Politécnica de Cartagena. Paseo Alfonso XIII, 48, 30203, España. (*pablo.fernandez@upct.es)
[3]Institute of Food Research, Norwich NR4 7UA, United Kingdom

Abstract

This study aims to model the effects of temperature and a_w downshifts on the lag time of *Bacillus weihenstephanensis* and the dependence of μ_{max} on the growth conditions (temperature and a_w). Effects of temperature shifts were studied on 30 conditions (shifts magnitude ranging from 2 to 20 °C, temperature after shift from 10 to 20 °C and a_w ranging from 0.977 to 0.997). Osmotic shifts were studied for 10 conditions (shift magnitude ranging from 0.008 to 0.020 units of a_w, temperature from 10 to 30 °C, a_w after shift from 0.977 to 0.997). The effects of shifts were modelled through the dependence of the parameter h_0 ("work to be done" prior to growth) induced on the magnitude of the shift and the stringency of the new environmental conditions. The predictive ability of the combined model (h_0 and μ_{max}) was assessed in carrot soup and ready meal products. The inclusion of the effects of shifts in the model improves the accuracy of predictions in dynamic conditions.

Keywords: *Bacillus Weihenstephanensis, lag time, osmotic stress, temperature shift*

Introduction

Bacillus weihenstephanensis is a psychrotolerant bacterium belonging to the *Bacillus cereus* group. Some strains may be cytotoxic although they have not been described as food-poisoning agents so far. The objective of this work is to model the effects of temperature and a_w downshifts on the lag time of *B. weihenstephanensis* and the dependence of μ_{max} on the growth conditions (temperature and a_w).

Materials and Methods

Bacterial strain and inoculum preparation

The strain used in this study was *Bacillus weihenstephanensis* KBAB4, kindly provided by the National Institute of Agronomy Research (INRA, Avignon, France). This microorganism was sporulated in Fortified Nutrient agar at 30ºC (Mazas *et al.* 1995) and stored at -20°C until use. Before experiments, to ensure that vegetative cells grown from spores would have the same physiological state, spores were heated at 80 °C for 10 min. Two successive subcultures were grown overnight in Brain Heart Infusion broth (BHI; Scharlau, Barcelona, Spain) at 30 °C for 18 hours. After incubation time, cells were at their stationary phase of growth.

Temperature and a_w downshifts

The effects of downshift magnitude and current conditions on the parameters h_0 and μ_{max} were studied in BHI by using viable count measurements (VCM) and optical density (OD). For viable count measurements, growth rates and lag times were calculated by fitting the growth curves obtained after shifts with the model of Baranyi and Roberts (1994). For OD experiments, growth rates and lag times were calculated as described by Muñoz-Cuevas *et al.* (2010). For temperature downshifts, 30 experimental conditions (shifts magnitude ranging from 2 to 20 °C, temperature after shift from 10 to 20 °C and a_w ranging from 0.977 to 0.997).

Effects of osmotic shifts were studied for 10 conditions (shift magnitude ranging from 0.008 to 0.020 units of a_w, temperature from 10 to 30°C, a_w after shift from 0.977 to 0.997).

Growth rate model

To describe the dependence of μ_{max} on the specific growth rate, we used the square root model proposed by Muñoz-Cuevas *et al.* (2010):

$$\sqrt{\mu_{\max}} = b_0\left(T - T_{\min}\right)\sqrt{bw_{\max} - bw} \quad (1)$$

where $b_w = 100\sqrt{1 - a_w}$ T_{min} is the minimum temperature for growth, bw_{max} is the maximum b_w value supporting growth and b_0 a parameter without biological meaning.

Model for h_0

The effects of shifts magnitude and current conditions were modelled with the equations 2 (temperature shifts) and 3 (osmotic shifts).

$$\sqrt{h_0} = \left(T_p - T_c\right)^{a_1}\left(T - T_{\min}\right)^{a_2} bw^{a_3} \quad (2)$$

where T_p and T_c are the temperature conditions before and after shift, respectively. T_{min}, a_1, a_2 and a_3 are the model parameters identified by non linear regression.

$$\sqrt{h_0} = \left(bw_p - bw_c\right)^{c_1}\left(T\right)^{c_2}\left(bw_{\max} - bw\right)^{c_3} \quad (3)$$

where bw_p and bw_c are the b_w values before and after shift, respectively. bw_{max}, c_1, c_2 and c_3 are the model parameters.

Food products preparation

Carrot soup and creamed pasta were elaborated for validation experiments. To prepare the soup, carrots were washed and peeled before being homogenized and partially sieved. Creamed pasta was made in our laboratory using olive oil, bacon, cream, cheese, water and macaroni. NaCl was added to the homogenized food products until reaching a concentration of 0.5% or 2% and pH was adjusted to 6.5. Samples were heated at 100 ºC for 10 min during three consecutive days to inactivate background microflora before inoculation studies.

Model validation

The predictive ability of the combined model (h_0 and μ_{max}) was assessed by comparing model predictions and observed growth curves of *B. weihenstephanensis* in broth, carrot soup and creamed pasta under changing conditions of temperature and a_w. References curves were obtained in the studied food products to calculate the ratio $(\mu_{max})_{food/}$ $(\mu_{max})_{broth}$. This ratio was used to correct predictions of Equation 1 for predictions of μ_{max} in food. Predictions were performed by solving the system consisting of the model of Baranyi and Roberts (1994) and equations 1 to 3.

Results and Discussion

Effects of shift on the growth parameters

F-tests (p = 0.05) performed did not highlight significant differences between growth rates obtained at the same experimental conditions but after different pre-incubatory conditions. This confirms that the maximum growth rate depends only on the current conditions of growth. *B. weihenstephanensis* was found to be more sensitive to temperature shifts than other microorganisms, such as *L. monocytogenes*. Whereas the values for h_0 observed Muñoz-Cuevas *et al.* (2010) for *L. monocytogenes*, did not exceeded ca 3.0, the maximum h_0 values observed in this study reached a level of ca 20. The effects of temperature downshifts are

more pronounced when they occur near growth limiting conditions (i.e. low temperatures and high concentrations of NaCl). For example, shifting temperature from 16 to 10 °C in the presence of 4% NaCl induced a workload of h_0 = 18 (corresponding to a lag time of 530 h).
In comparison with temperature, osmotic shifts within the range studied have less significant effects on the lag time of *B. weihenstephanensis*.

Model fitting

Table 1 shows estimates and standard deviations of the model parameters for growth rates and h_0 models respectively.

Table 1: Estimates of the model parameters and their 95% confidence intervals

Model	Parameter	Estimate	95% Inf	95% Sup	R^2
Sqrt(μ_{max})	b_0	0.0148	0.012	0.016	0.98
	T_{min}	6.10	5.65	6.56	
	bw_{max}	25.3	22.5	28.0	
Sqrt(h_0)(temperature)	a_1	0.13	0.03	0.24	0.76
	a_2	-0.55	-0.74	-0.36	
	a_3	0.66	0.53	0.80	
Sqrt(h_0) (NaCl)	c_1	0.39	0.10	0.69	0.61
	c_2	-0.41	-0.69	-0.14	
	c_3	0.40	0.11	0.68	

Comparison between the square root of observed and fitted growth rates is shown in Figure 1. The good concordance between the observed lag times and predicted (using the models for h_0 and μ_{max} models) is shown on Figure 2.

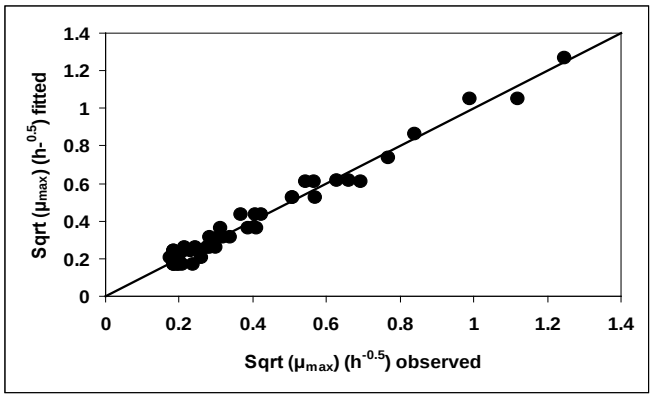

Figure 1: Square root of the observed and fitted specific growth rates of *B. weihenstephanensis*.

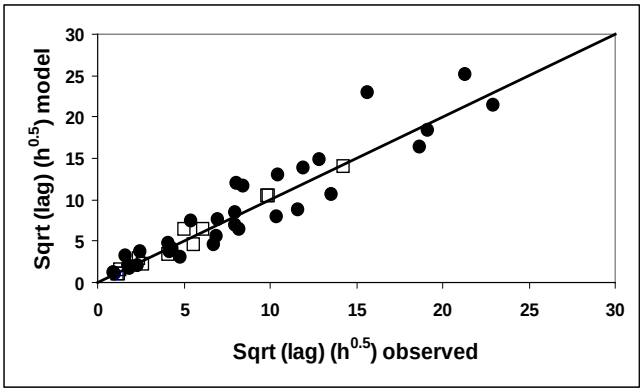

Figure 2: Comparison between lag times observed and predicted by the model developed (combination of equations 1, 2 and 3); (●) Temperature shifts (□) A_w shifts.

Model validation

The overall results show that inclusion of the lag time in the model improves the quality of predictions. An example of comparison between observed growth of *B. weihenstephanensis* and model predictions is given in Figure 3.

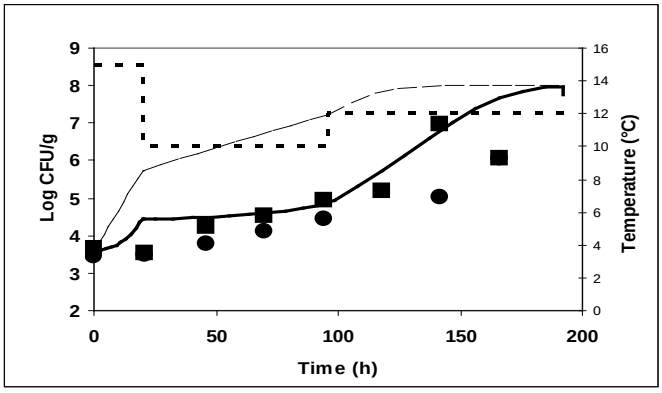

Figure 3: Growth of *B. weihenstephanensis* (■: replicate a, ●: replicate b) in cream pasta in changing temperature conditions (dotted line). Shown is a comparison between the model prediction with (straight line) and without (dashed line) considering the lag time.

Conclusions

Our results support the findings of other studies (Muñoz-Cuevas *et al.* 2010; Le Marc *et al.* 2010) which show that: i) the "work to be done" h_0 depends not only on magnitude of shifts but also on the current growth conditions after shifts and ii) that shifts occurring near the growth limits induce significant higher h_0 values. This model can be used to improve predictions of growth of *B. weihenstephanensis* in dynamic conditions, which can be useful for HACCP and microbial risk assessment purposes.

Acknowledgements

Vera Antolinos acknowledges "Ministerio de Ciencia e Innovación" for awarding her fellowship. This project was funded by Spanish "Ministerio de Ciencia e Innovación", ref. AGL 2010-22206-C02-02/ALI and Fundación SENECA, CARM, Spain ref 08795/PI/08.

References

Baranyi J. and Roberts T. A. (1994) A dynamic approach to predicting bacterial growth in food. *International Journal of Food Microbiology* 23, 277-294.

Le Marc Y., Skandamis P. N., Beles C. I. A., Merkouri S. I., George S. M., Gounadaki A. S., Schvartzma S., Jordan K., Drosinos E. H. and Baranyi. J. (2010) Modelling the effect of abrupt acid and osmotic shifts within the growth region and across the growth boundaries on the adaptation and growth of *Listeria monocytogenes*. *Applied and Environmental Microbiology* 76, 6555-6563.

Mazas M., González I., López M., González J. and Martín-Sarmiento R. (1995) Effects of sporulation media and strain on thermal resistance of *Bacillus cereus* spores. *International Journal of Food Science Technology* 30, 71-78.

Muñoz-Cuevas M., Fernández P. S., George S. and Pin C. (2010) Modeling the lag period and exponential growth of *Listeria monocytogenes* under conditions of fluctuating temperature and water activity values. *Applied and Environmental Microbiology* 76, 2908-2915.

Modeling the growth of *Escherichia coli* under the effects of *Carum copticum* essential oil, pH, temperature, and NaCl using response surface methodology

M. Shahnia[1], A. Khanlarkhani[2], F. Shahraz[1], B. Radmehr[3], R. Khaksar[1]

[1] Food Science and Technology Department, Shahid Beheshti Medical University, Tehran, Iran (maryamshahnia@yahoo.com)
[2] Department of Nanotechnology and Advanced Material, Material and Energy Research Center, Tehran, Iran
[3] Food Hygiene Dept., Islamic Azad University-karaj branch, Karaj, Iran

Abstract

The effects of temperature (20–42 C), pH value (4.5–8.5), concentration of sodium chloride (0–5%) and concentration of essential oil (0-750 ppm) on the growth parameters of *E.coli* were investigated. The growth curves generated within different conditions were fitted using the Baranyi function. To achieve much more useful results in the context of hazard analysis and critical control points and risk analysis studies, probability density functions for (i) the model parameters and (ii) the predictions as a function of time were obtained by using Monte Carlo analysis. A normal distribution over the experimental data was considered. Two parameters (growth rate, GR; lag-time, LT) of the growth curves under the combined effects of temperature, pH, sodium chloride and essential oil were modelled using a quadratic polynomial equation of response surface (RS) model. Mathematical evaluation demonstrated that the standard error of prediction (%SEP) and RMSE obtained by RS model were 74% and 0.061 for GR and 3.544% and 0.687 for LT for model establishing. The results show that RS model provides a useful and accurate method for predicting the growth parameters of *E. coli*, and could be applied to ensure food safety with respect to *E. coli* control.

Keywords: *E. coli, growth model, Monte Carlo, response surface*

Introduction

Clearly, over the past few decades, much effort has been conducted towards predictive models describing the combined effects of the environmental factors on the growth of pathogens in foods (Devlieghere *et al.* 1998). One of the most prevalent pathogens which are of great concern is *Escherichia coli*. The aims of the present study were to (a) generate a model for the combined effects of temperature, pH, salt and *Carum copticum* essential oil on the growth rate and lag-time of *E. coli* (b) to investigate the effects of these factors in controlling the growth of this bacteria (c) to examine the single and combined effects of *Carum copticum* essential oil with pH, temperature, and sodium chloride on the growth of *E. coli* (ATCC 8739).

Materials and Methods

Bacterial strain

Lyophilized stock culture of *E. coli* (ATCC 8739) was grown in TSB broth at least twice at 37°C for 24 h followed by streaking on a TSB agar (Difco) slants, then incubated at 37°C for 24 h and the cultures subculture weekly. The optical density of the culture was adjusted to 0.2 by diluting in TSB in order to reach a population of approximately 10^6cfu ml^{-1}.

Experimental design

To estimate the effects of pH, sodium chloride, temperature, and *Carum copticum* essential oil on maximum growth rate and lag-time of *E. coli*, a central composite design (CCD) was

employed using Design-Expert software 7.1.5 (Stat-Ease, Inc., Minneapolis, Minnesota, USA). The design included five levels of pH (4.5, 5.5, 6.5, 7.5 and 8.5), five levels of sodium chloride(0%, 1.25%, 2.5%, 3.75% and 5%), five levels of temperature(20°C, 25.5°C, 31°C, 36.5°C and 42°C), and five levels of *Carum copticum* essential oil (0, 187.5, 375,562, 750 ppm). The procedure was carried out using the Bioscreen C analyser.

Plant material and preparation of the essential oil

Carum copticum (zenyan in Persian) is an aromatic plant grown in different parts of some countries such as Iran, India, and Egypt. 100 g of the dried seeds was powdered and subjected to steam distillation in a Clevenger-type apparatus for 4 h in order to obtain the essential oil.

Curve fitting and growth parameters observation

The DMFit 2.0 program (Institute of Food Research, Norwich, UK) was used for the OD values by fitting of 30 media combinations applying the Baranyi function (Baranyi and Roberts 1995).

Establishment of response surface models

RS models were established on the basis of the Design Expert software. The stepwise regression equations, with independent variables entered at alpha = 0.05 and eliminated at alpha = 0.10

Model validation and mathematical evaluation

After the establishment of RS models, additional 10 conditions for model validation were selected randomly within the range of experimental design. Both predicted values (GR and LT) with the 30 conditions for model establishment and those with 10 conditions for model validation were mathematically evaluated.

Monte Carlo Analysis

In this paper, the Monte Carlo analysis was used to incorporate experimental variation on OD data. The Monte Carlo analysis results in a probability density distribution for each of the four model parameters and also in a probability distribution for the microbial load prediction at a certain time instant.

Results and Discussion

Curve fitting and growth parameters observed

After OD measurement of each combination, total 90 growth curves of *E. coli* were obtained by DMFit software, which applies Baranyi function. The mean of growth parameters (GR and LT) calculated can be seen in Table 1. It indicated that the model provided a good description of those data, and Baranyi function had good predictive capabilities for the growth of *E.Coli* (R^2>0.92).

Establishment and validation of response surface models

According to growth parameters of *E. coli*, both GR and LT were made to natural logarithm transformation in order to yield higher correlation coefficients (R^2). The RS models were established by stepwise regression as follows:

$$\begin{aligned}\ln(GR) = {} & -53.08670 + 2.65193 * T + 2.23013 * pH + 0.30303 * NaCl \\ & -1.84060E\text{-}003 * E.O - 0.040048 * T * pH \\ & -5.66956E\text{-}004 * NaCl * E.O - 0.038406 * T^2 \quad (R^2=0.9271) \qquad (1)\end{aligned}$$

$$\begin{aligned}\ln(LT) = {} & 12.36533 - 0.47216 * T - 0.44128 * pH + 0.19692 * NaCl \\ & -0.010620 * E.O - 2.45658E\text{-}003 * T * NaCl \\ & +1.01405E\text{-}003 * pH * E.O - 1.19882E\text{-}004 * NaCl * E.O \\ & +7.41660E\text{-}003 * T^2 + 6.52652E\text{-}006 * E.O^2 \quad (R^2=0.9978) \qquad (2)\end{aligned}$$

The ANOVA of RS models indicated that both Eqs. (1) and (2) were significant ($p<0.05$), and the test of lack-of-fit showed that equation (1) was not significant ($p>0.05$) but equation (2)

was. Based on this, Eq. (1) and (2) were used to estimate the predicted values of GR and LT under different conditions.

Table 1: Observed and predicted growth rate (GR) and lag-time (LT) of *E.Coli* by RS models under different combined conditions.

	T(ºC)	pH	NaCl%	E.O(ppm)	GR(h^{-1})		LT(h)	
					Obs	Pred	Obs	Pred
1	20.00	4.50	0.00	0.00	4.50E-05	1.26E-04	NC*	49.55
2	20.00	8.50	0.00	0.00	7.41E-02	3.83E-02	8.70	8.48
3	20.00	4.50	5.00	0.00	5.15E-03	5.73E-04	106.59	103.75
4	20.00	8.50	5.00	0.00	8.18E-02	1.74E-01	17.73	17.76
5	20.00	4.50	0.00	750.00	5.29E-05	3.17E-05	NC	20.73
6	20.00	8.50	0.00	750.00	1.16E-02	9.63E-03	74.22	74.34
7	20.00	4.50	5.00	750.00	2.47E-06	1.72E-05	NC	27.69
8	20.00	8.50	5.00	750.00	NC	5.23E-03	97.09	99.29
9	25.50	6.50	2.50	375.00	1.01E-01	4.77E-02	6.36	6.75
10	31.00	5.50	2.50	375.00	9.19E-02	6.01E-02	5.44	5.18
11	31.00	7.50	2.50	375.00	1.62E-01	4.34E-01	5.30	4.59
12	31.00	6.50	1.25	375.00	1.23E-01	1.44E-01	4.05	4.43
13	31.00	6.50	3.75	375.00	1.44E-01	1.81E-01	5.32	5.36
14	31.00	6.50	2.50	187.50	1.74E-01	2.98E-01	5.16	5.51
15	31.00	6.50	2.50	562.50	1.16E-01	8.77E-02	7.11	6.81
16	31.00	6.50	2.50	375.00	1.62E-01	1.62E-01	4.84	4.87
17	31.00	6.50	2.50	375.00	1.54E-01	1.62E-01	4.81	4.87
18	31.00	6.50	2.50	375.00	1.56E-01	1.62E-01	4.78	4.87
19	31.00	6.50	2.50	375.00	1.67E-01	1.62E-01	4.97	4.87
20	31.00	6.50	2.50	375.00	1.65E-01	1.62E-01	4.85	4.87
21	31.00	6.50	2.50	375.00	1.61E-01	1.62E-01	4.74	4.87
22	36.50	6.50	2.50	375.00	1.30E-01	5.35E-02	5.71	5.51
23	42.00	4.50	0.00	0.00	1.10E-03	9.24E-04	NC	37.78
24	42.00	8.50	0.00	0.00	9.94E-03	8.27E-03	NC	6.47
25	42.00	4.50	5.00	0.00	1.14E-03	4.20E-03	NC	60.37
26	42.00	8.50	5.00	0.00	3.31E-02	3.76E-02	10.12	10.33
27	42.00	4.50	0.00	750.00	9.32E-05	2.32E-04	NC	15.80
28	42.00	8.50	0.00	750.00	NC	2.08E-03	NC	56.68
29	42.00	4.50	5.00	750.00	7.21E-04	1.26E-04	NC	16.11
30	42.00	8.50	5.00	750.00	NC	1.13E-03	NC	57.77

NC: DMFit could not find value for this.

Effects of different experimental conditions on the growth of E.Coli

On the basis of quadratic polynomial equation of RS models obtained (Eqs. (1) and (2)), the effects of independent variables (temperature, pH, NaCl concentration and essential oil concentration) on the parameters (GR and LT) were analyzed. First, pH was the most important factor ($p<0.0001$) affecting GR. It was found that pH had a positive linear effect on GR in Eq. (1), which means the GR tends to increase when temperature increases. Next important factor affecting GR was the square of temperature ($p<0.0001$). Essential oil concentration significantly affects GR ($p=0.0008$). The essential oil concentration had a negative linear effect as we expect. In the case of LT, the main affecting factors are essential oil concentration ($p=0.0133$), temperature ($p=0.0162$) and NaCl($p=0.0231$). Again the essential oil concentration had a negative linear effect on LT.

Mathematical evaluation of the RS models

Tables 2 and 3 revealed that RMSE of internal or external evaluation were below 0.1 for GR and below 0.8 for LT, especially for prediction of GR values (0.061 and 0.086, respectively).

This suggested the RS models fitted well with the observed data. B_f is a measure of the extent of under- or over-prediction by the model of the GR or LT observed.

Table 2: Mathematical internal evaluation based on growth rate (GR) and lag-time (LT).

	%SEP	RMSE	B_f	A_f
GR	74.000	0.061	1.001	1.817
LT	3.544	0.687	1.000	1.035

%SEP, %standard error of prediction, RMSE, root-mean-squares error, B_f, bias factor, A_f, accuracy factor.

Table 3: Mathematical internal evaluation based on growth rate (GR) and lag-time (LT).

	%SEP	RMSE	B_f	A_f
GR	51.000	0.086	1.009	1.513
LT	3.257	0.249	1.010	1.034

Conclusions

In summary, Baranyi function showed goodness-of-fit to describe the growth of *E. coli* under different laboratory conditions (R^2>0.92). The experiments also established RS models to predict the curve parameters of *E. coli* growth influenced by different combinations of temperature (20–42C), pH value (4.5–8.5) , concentration of sodium chloride (0.0–5.0%) and concentration of essential oil (0-750 ppm). Different combinations of temperature, pH, NaCl and essential oil were found to have significant effects on the growth of *E. coli*. From the model validation and mathematical evaluation, RS model proved to be a useful and accurate method of predicting the growth parameters of *E. coli* within certain laboratory conditions, for its lower standard errors and lower RMSEs of predictions as well as acceptable ranges of bias and accuracy factors. These models need validation in the actual food environment before applied in practice, and could be considered as references in controlling the propagation of *E. coli*.

References

Baranyi J. and Roberts T.A. (1995) Mathematics of predictive food microbiology. *International Journal of Food Microbiology* 26, 199–218.

Devlieghere F., Geeraerd A. H., Versyck K. J., Van De Waetere B., Van Impe J. and Debevere J. (1998) Growth of Listeria monocytogenes in modified atmosphere packed cooked meat products: a predictive model. *Food Microbiology* 18, 53–66.

Performance evaluation of models describing the growth rate as a function of temperature: focus on the suboptimal temperature range

E. Van Derlinden, B. Herckens and J.F. Van Impe

CPMF2 – Flemish Cluster Predictive Microbiology in Foods – www.cpmf2.be
BioTeC - Chemical and Biochemical Process Technology and Control, Department of Chemical Engineering, Katholieke Universiteit Leuven, W. de Croylaan 46, B-3001 Leuven, Belgium
[eva.vanderlinden, jan.vanimpe]@cit.kuleuven.be

Abstract

Secondary models, describing the microbial growth rate as a function of temperature, are evaluated with focus on model performance in the suboptimal temperature region. *Escherichia coli* K12 MG1655 and *Salmonella* Typhimurium are considered as a case study. A large set of $\mu_{max}(T)$-estimates is fitted with (1) the cardinal temperature model with inflection (CTMI, Rosso *et al*. 1993), (2) the square root model (SQRT, Ratkowsky *et al*. 1983), and (3) the CTMI adapted to describe the particular behavior of *Listeria* at suboptimal temperatures (aCTMI, Le Marc *et al*. 2002). Compared to the CTMI and the SQRT, a more accurate description of the $\mu_{max}(T)$-relation is obtained with the aCTMI, certainly at temperatures below 30 ºC. Also, the T_{min} estimate is far more realistic considering the experimental data. Use of the aCTMI improved $\mu_{max}(T)$-data description significantly which indicates the existence of two phases in the suboptimal temperature region. These results point at a possible shortcoming of commonly used secondary models describing the temperature effect on the microbial growth rate.

Keywords: predictive microbiology, secondary model, temperature, E. coli, Salmonella

Introduction

In general, each microorganism is characterized by its own intrinsic temperature region for growth, outlined by the minimum and maximum temperature for growth (T_{min} and T_{max}, respectively). At and below T_{min}, growth is not possible and slightly above the minimum temperature for growth, the growth rate is very low. As temperature increases, the rate of key intracellular processes increases and microorganisms grow faster. This relation is only valid up to a certain temperature, i.e., T_{opt}, the temperature at which the growth rate is maximal. Further increase of the temperature negatively affects the cellular metabolism and the growth rate decreases fast until T_{max} is reached. At and beyond this temperature, growth is no longer sustained.

Within the domain of predictive microbiology, a series of secondary models exists that describe the influence of temperature on the microbial growth rate. Most currently used secondary models can be subdivided in four classes: (*i*) square root models, (*ii*) cardinal parameter models, (*iii*) neural networks, and (*iv*) response surface models. All of the above models are data-driven black box models as no information on the underlying mechanism of the temperature effect on the microbial metabolism is included.

The validity of the square root model (SQRT) developed by Ratkowsky *et al*. (1983) and the cardinal temperature model with inflection (CTMI) (Rosso *et al*. 1993) to describe the effect of temperature on the microbial growth rate is widely accepted. Together with the SQRT, the CTMI is among the most frequently used in (predictive) microbiology. Up until now, exceptions have only been reported for *Listeria*, i.e., *Listeria monocytogenes* (Bajard *et al*. 1996) and *Listeria innocua* (Le Marc *et al*. 2002). In the suboptimal temperature region of *Listeria*, the $\sqrt{\mu_{max}(T)}$-curve displays two linear phases. Inspired by the work of Bajard *et al*. (1996), Le Marc *et al*. (2002) added two parameters to the existing CTMI to model this deviating behavior, i.e., the change temperature T_c (previously introduced by Bajard *et al*. (1996)), and the temperature T_1 which is the intersection between the first linear part of the model and the temperature axis.

Also, in most cases validity of the CTMI and the SQRT has only been evaluated (*i*) for a limited number of experimental data, or (*ii*) at temperatures around the optimum growth temperature and temperatures close to the growth boundaries are not included.
The aim of this work is to evaluate the CTMI, SQRT and aCTMI model for *Escherichia coli* K12 MG1655 and *Salmonella* Typhimurium, with the focus on the behavior at the suboptimal temperature region and near the minimum temperature for growth. Especially for *E. coli*, an extended experimental data set was used to examine the relationship between temperature and the maximum specific growth rate.

Materials and methods

Experiments

Experimental data were acquired for (1) *Escherichia coli* K12 MG1655 (CGSC#6300) and (2) *Salmonella Typhimurium* SL1344. $\mu_{max}(T)$-data were extracted from experiments performed in: (*i*) test tubes and/or (*ii*) bioreactors and/or (*iii*) Erlenmeyers. Maximum specific growth rates were obtained by fitting the experimental data with the model of Baranyi and Roberts (1994).

Mathematical modeling

Three models, used to describe the influence of temperature on the microbial growth rate, are discussed.

(*i*) The square root model (Ratkowksy *et al*. 1983)

$$\sqrt{\mu_{max}} = b \cdot (T - T_{min}) \cdot (1 - \exp(c \cdot (T - T_{max}))) \quad (1)$$

with b [1/(°C·√h] and c [1/°C] constants, and T_{min} [°C] and T_{max} [°C] the notional minimum and maximum growth temperature.

(*ii*) The Cardinal Temperature Model with Inflection (Rosso *et al*. 1993).

$$\mu_{max} = \gamma \cdot \mu_{opt} \quad (2)$$

with

$$\begin{aligned} T \le T_{min} \quad & \gamma = 0 \\ T_{min} < T < T_{max} \quad & \gamma = \frac{(T - T_{min})^2 (T - T_{max})}{(T_{opt} - T_{min})((T_{opt} - T_{min})(T - T_{opt}) - (T_{opt} - T_{max})(T_{min} + T_{opt} - 2T))} \\ T \ge T_{max} \quad & \gamma = 0 \end{aligned} \quad (3)$$

Parameters included in this model are the three cardinal temperatures T_{min} [°C], T_{opt} [°C], and T_{max} [°C] (i.e., the minimum, optimum and maximum temperature for growth, respectively) and μ_{opt} [1/h] (i.e., the maximum specific growth rate at T_{opt}).

(*iii*) The structural adaptation of the CTMI by Le Marc *et al*. (2002). As a response to the observation of a nonlinear relation between $\sqrt{\mu_{max}}(T)$ and temperature for *Listeria* strains by Bajard *et al*. (1996), the original structure of the CTMI was adapted.

$$\begin{aligned} T \ge T_c \quad & \gamma = \frac{(T - T_l)^2 (T - T_{max})}{(T_{opt} - T_l)((T_{opt} - T_l)(T - T_{opt}) - (T_{opt} - T_{max})(T_l + T_{opt} - 2T))} \\ T < T_c \quad & \gamma = \frac{(T_c - T_{min})^2 (T_c - T_{max})}{(T_{opt} - T_{min})((T_{opt} - T_{min})(T_c - T_{opt}) - (T_{opt} - T_{max})(T_{min} + T_{opt} - 2T_c))} \left(\frac{T - T_{min}}{T_c - T_{min}} \right)^2 \end{aligned} \quad (4)$$

Next to the three cardinal temperatures and μ_{opt}, two additional parameters define the model, i.e., T_c and T_l. T_c [°C] is the so-called change temperature and T_l [°C] is the point of intersection between the first linear part and the temperature axis.

Data processing

Model parameters and standard deviations are obtained by minimizing the sum of squared errors (SSE) using *lsqnonlin* of the optimization toolbox of Matlab (The Mathworks Inc.).

Results and discussion

Evaluation of the secondary models

For *E. coli* and *Salmonella*, all $\mu_{max}(T)$-estimates are fitted with the cardinal temperature model with inflection (CTMI) (Rosso *et al*. 1993) and the square root model (SQRT) developed by Ratkowsky *et al*. (1983) (Figure 1). It has been reported that the fitting quality of the CTMI and the SQRT are comparable, but that the CTMI has the advantage that all parameters have a biological interpretation. Furthermore, the CTMI parameters are less characterized by structural correlation and easier to estimate (Rosso *et al*. 1993).

Little difference was observed between the CTMI and SQRT model fits. A closer look at the temperature range between 8 and 25 ºC for *E. coli* reveals that growth rates are estimated significantly lower and that both models overestimate T_{min}, i.e., T_{min} is estimated at 10-11 ºC while growth is still observed at 8 ºC. For *Salmonella*, growth rates between 8 and 25 ºC are overestimated and T_{min} is underestimated.

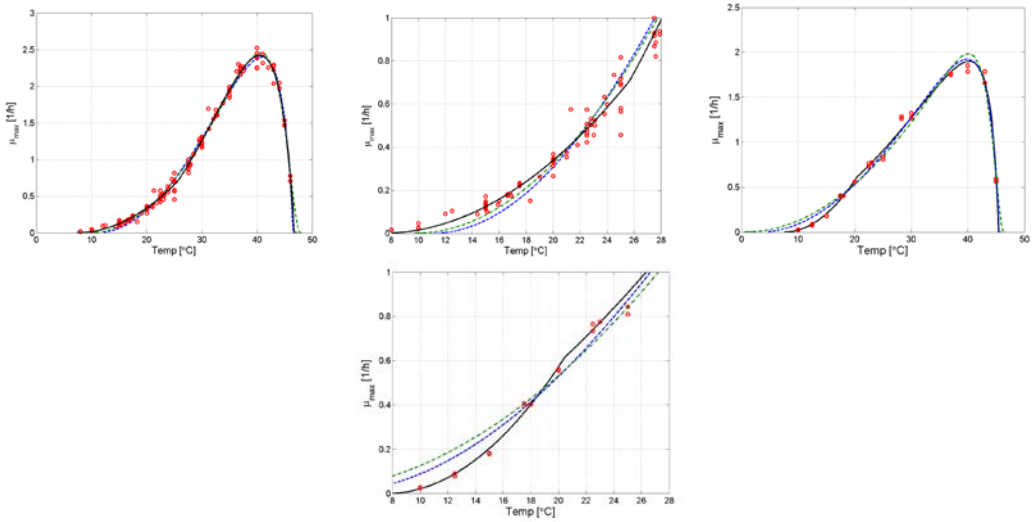

Figure 1: Modeling the effect of temperature on the growth rate of *E. coli* K12 (upper plots) and *Salmonella* Typhimurium (lower plots): (*i*) square root model (-.), (*ii*) model of Rosso (--), and (*iii*) model of Le Marc (-).

The lack of model fit is related to the structure of the CTMI and SQRT model. Both models use a second order polynominial to describe the temperature effect in the neighborhood of T_{min} (i.e., $x \cdot (T-T_{min})^2$). This corresponds with the assumption that, at suboptimal temperatures, the relation $\sqrt{\mu_{max}(T)}$ is linear. Generally, it is assumed that this relation is valid for all microorganisms and exceptions have only been discovered for *Listeria* strains (Bajard *et al*. 1996, Le Marc *et al*. 2002), i.e., in their suboptimal temperature region, the $\sqrt{\mu_{max}(T)}$-curve displays two linear phases. To be able to describe this deviating behavior, Le Marc *et al*. (2002) adapted the CTMI structure by adding two parameters, i.e., T_c, the change temperature, and T_1, the intersection between the first linear phase and the temperature axis.

In a next step, this adapted CTMI structure (aCTMI) is also fitted to the $\mu_{max}(T)$-data set (see Figure 1). A more accurate description of the $\mu_{max}(T)$-relation at temperatures below 25 ºC is obtained. For *E. coli*, T_{min} is estimated at 7.3 ºC, which corresponds with experimental observations and the change temperature (T_c) was estimated ≈at 25 ºC. Below this temperature, the $\mu_{max}(T)$-relation changes. Use of the aCTMI improved the data description significantly which confirms the existence of two phases in the $\mu_{max}(T)$-relation the suboptimal temperature region.

At first sight, fitting the aCTMI also improves data description for *Salmonella*, and a more realistic T_{min} estimate is obtained. The followed trend, however, is opposite to the model description of *E. coli*. Growth rates as a function of temperature decrease faster after the changing temperature T_c (≈ 20 ºC). The data available so far are rather limited and additional information will be collected to reveal the true $\mu_{max}(T)$-relation.

Discussion of the E. coli change temperature

At the change temperature T_c, the relation between temperature and the maximum specific growth rate alters. As the growth rate is a translation of the net microbial metabolism, a change in the $\mu_{max}(T)$-relation suggest a metabolic change. A possible explanation can be found in the cold shock response.

The effect of temperature on μ_{max} of *E. coli* has been related to the concept of the normal physiological temperature range (NPTR). This temperature region is defined as the linear part of the Arrhenius plot ($\ln(\mu_{max}(T))$ versus 1/T). At higher and lower temperatures, μ_{max} decreases more rapidly, reaching zero at T_{min} and T_{max}. Swinnen *et al*. (2005) identified the lower boundary of the NPTR for *E. coli* K12 as a transition zone situated between 22.78 °C and 23.86 °C. Within the NPTR, steady state levels of proteins are approximately constant (Herendeen *et al*. 1979). However, when the temperature is outside the NPTR, microorganisms encounter a temperature shock and protein levels change significantly. As the lower boundary estimates of the NPTR for *E. coli* are similar to the switching temperature T_c, the presence of the cold shock proteins possibly decreases protein denaturation and inactivation, and increases protein stability, which results in a slower decline of the growth rate with decreasing temperature.

Conclusions

Implementation of the adapted CTMI model improved the description of the $\mu_{max}(T)$-relation significantly. This possibly indicates that two phases exist in the suboptimal temperature region. These results reveal a possible shortcoming of commonly used models describing the temperature effect on the microbial growth rate.

Acknowledgements

This work was supported by project PFV/10/002 (Center of Excellence OPTEC-Optimization in Engineering) of the Research Council of the K.U.Leuven, knowledge platform KP/09/005 (www.scores4chem.be) of the Industrial Research Fund, and the Belgian Program on Interuniversity Poles of Attraction, initiated by the Belgian Federal Science Policy Office. E. Van Derlinden is supported by postdoctoral grant PDMK/10/122 of the K.U.Leuven Research Fund. J. Van Impe holds the chair Safety Engineering sponsored by the Belgian chemistry and life sciences federation essenscia.

References

Bajard S., Rosso L., Fardel G. and Flandrois J. (1996) The particular behaviour of *Listeria monocytogenes* under sub-optimal conditions. *International Journal of Food Microbiology* 29, 201-211.

Baranyi J. and Roberts T.A. (1994) A dynamic approach to predicting bacterial growth in food. *International Journal of Food Microbiology* 23, 277-294.

Herendeen S.L., VanBogelen R.A. and Neidhardt F.C. (1979) Levels of major proteins of *Escherichia coli* during growth at different temperatures. *Journal of Bacteriology* 139, 185-194.

Le Marc Y., Huchet V., Bourgeois C., Guyonnet J., Mafart P. and Thuault, D. (2002) Modelling the growth kinetics of *Listeria* as a function of temperature, pH and organic acid concentration. *International Journal of Food Microbiology* 73, 219-237.

Ratkowksy D.A., Lowry R.K., McMeekin T.A., Stokes A.N. and Chandler, R.E. (1983) Model for bacterial culture growth rate throughout the entire biokinetic temperature range. *Journal of Bacteriology* 154, 1222-1226.

Rosso L., Lobry J.R. and Flandrois J.P. (1993) An unexpected correlation between cardinal temperatures of microbial growth highlighted by a new model. *Journal of Theoritical Biology* 162, 447-463.

Swinnen I.A.M., Bernaerts K., Gysemans K. and Van Impe, J.F. (2005) Quantifying microbial lag phenomena due to a sudden rise in temperature: a systematic macroscopic study. *International Journal of Food Microbiology* 100, 85-96.

Growth response and modeling the effects of Carum copticum essential oil, pH, temperature, and NaCl on *Escherichia coli*, *Listeria monocytogenes* and *Staphylococcus aureus* by an optimized computational neural networks (OCNN)

M. Shahnia[1], A. Khanlarkhani[2], S. Shojaee[1], F. Shahraz[1], R. Khaksar[1], H. Hosseini[1]

[1]Food Science and Technology Department, Shaheed Beheshti Medical University, Tehran, Iran (ramin.khaksar@gmail.com)
[2]Department of Nanotechnology and Advanced Material, Material and Energy Research Center, Tehran, Iran

Abstract

Growth predictive models are currently accepted as informative tools that assist to predict the growth of forborne pathogens. In the present study the computational neural networks (CNN) were used to investigate the effects of temperature (20 to 42 C), pH value (4.5 to 8.5), concentration of sodium chloride (0 to 5%) and concentration of Carum copticum essential oil (0 to 750 ppm) on the growth parameters . We used Central Composite Design (CCD) for the design of the experiment. The architecture of OCNN was designed to contain three input parameters in the input layer and one output parameter in the output layer. The training set consisted of growth responses data from a combination of *Listeria monocytogenes* and *Staphylococcus aureus* in a laboratory medium as affected by pH level, sodium chloride concentration, essential oil concentration and temperature. Trained OCNN then used to predict the growth parameters as well as growth curve of *E. coli*. The standard error of prediction (%SEP) obtained was under 5%, and the results clearly show the ability of OCNN trained on appropriate data to predict growth curves for new microbial growth cases without the need to conduct any experimental investigation.

Effect of temperature and inoculum level on the maximum population (Rg) of *Lactobacillus fermentum* grown in co-culture with *Saccharomyces cerevisiae* using sugar cane must as substrate

V.O. Alvarenga[1], P.R. Massaguer[2]

[1]Rondônia Federal University , Food Engineering Department (ortiz@unir.br)
[2]Campinas State University – Chemical Engineering Faculty

Abstract

Sugar cane must is obtained by triturating sugar cane with water in mills, producing a substrate rich in sucrose and reducer sugars. Further, this substrate is diluted to undergo fermentation. The microbial contamination of sugar cane must is formed by contaminants originated from both the field and factory. The objective of this study was to develop a secondary model to describe the effects of temperature and initial load of lactobacilli on maximum population of lactobacilli cultivated in co-culture with *Saccharomyces cerevisiae*. The Davey and Ratwosky model was tested and did not show good fitness to the maximum population. Thus, a second order polynomial model was built using codified values (temperature and inoculum level), and presented inoculum level (linear and quadratic) and temperature and inoculum level interaction as significant coefficients ($p < 0.10$). This model was shown to have high coefficient of determination (0.975), Bias (1) and accuracy factors (1.02). Our results indicate that the most significant variable in our model is the inoculum level of lactobacilli (L) (p value 0.000045). The model developed for maximum population of lactobacilli can be applied in the fermentation sugar cane industry, to predict the maximum population of lactobacilli during fermentation process.

Key-words: predictive microbiology, secondary model, Saccharomyces cerevisiae, Lactobacillus fermentum

Introduction

Bacterial contamination of sugar cane must is the major cause of reduction in yield during ethanol production by *S. cerevisiase.* The growth of *Lactobacillus* spp. is stimulated when growing in co-culture with yeasts due to excretion of several nutrients such as adenine, guanine, aspartic acid and nicotinic acid, tryptophan, glycine, alanine and lysine, biotin and vitamin B12 by the later (Narendranath *et al*. 1997, Chin and Ingledew 1994). The consumption of sucrose by microbial contaminants during ethanol fermentation process, results in the release of lactic and acetic acids and in losses for industries (Nobre 2005). As the metabolism of each molecule of sugar by bacterial contaminants results in two less molecules of ethanol being produced (Nobre 2005), any correlation between the level of contaminants and reduction in yielding during ethanol fermentation is needed. Secondary model takes into account not only the effect of each individual factor of a model on its outputs, but also how different factors interact and affect the outputs (McMeekin *et al*. 2002). The physiological state of the microorganism under consideration (stress in the environment *versus* stress during preparation of inoculum) should be considered because they might affect lag time much more than growth rate (Miconnet *et al.* 2005). In spite of the importance of ethanol production from sugar cane must for Brazil, there are no data on the influence of co-culturing of yeasts with lactobacilli on the growth kinetic parameters such as lag time and maximum population of the former. Thus, the objective of this study was to develop a secondary model to describe the effect of temperature and initial load of lactobacilli co-cultured with *Saccharomyces cerevisiae* on maximum population of the yeast.

Material and Methods

A central rotational composite design (CRCD), with two variables, three central points and four axial points, totaling 11 essays ($2^k+2*k+n_o$) was used in this study. An Erlenmeyer flask containing sterilized must (121 ºC/40 min), adjusted to 21.5ºBrix (Nolasco Jr, 2005) was inoculated with the yeast (10^6 CFU/mL) and lactobacilli ($10^1 – 10^8$ CFU/mL). The inoculum was adjusted with the aid of a Neubauer chamber and Densimat (BioMérieux, S.a., France). For each assay carried out two others tests with pure culture were done for comparison of growth parameters. The assays were conducted in an incubator with continuous agitation (120 rpm) and controlled temperature (Essia Ngang, 1989) during 100 hours (New Brunswick Scientific, Model G-27, U.S.A.). The yeasts and lactobacilli were enumerated by pour-plating malt extract agar (MEA) supplemented with tetracycline and chloramphenicol (100 mg/L, each) and MRS agar supplemented with Natamax® (50 mg/L) with pH 5.5, respectively. Secondary modeling and response surface plots were performed in Statistica 7.0. The bias and accuracy factors were estimated as described by Ross (1996).

Results and Discussion

Davey and Square root (Ratwosky) models did not fit the data for maximum population (table 1). Thus, a second order polynomial model was generated using variables coded values (temperature and inoculum level). Inoculum level (linear and quadratic) and interaction between temperature and inoculum level were significant ($p < 0.10$) (Table 2). This model showed a high coefficient of determination (0.97). Regarding the indices of performance of the model, bias showed that 100% of the data are in the region of safe prediction. The accuracy factor indicated that only 2% of the data are in disagreement with the data predicted by the model.

Table 1: Performance indices of secondary models for maximum population of lactobacilli (Rg) co-cultured with *S. cerevisiae*.

Model								
Ratwosky			Square Root			Polynomial Secondary order		
R^2	Bias	Accuracy	R^2	Bias	Accuracy	R^2	Bias	Accuracy
-	-	-	-	-	-	0.975	1.0	1.02

(-) Non-significant variables obtained.

Among the variables defined in this model, inoculum level (L) presented the greatest significance ($p = 0.000045$) (Table 2), demonstrating that maximum population of lactobacillus influenced by the initial population of this microorganism (Equation 1).
This equation allows one to calculate the lactobacilli maximum population reached at the end of ethanol fermentation process, based on a known initial population of Lactobacillus. The response surface plot (Figure 1) demonstrates the quadratic and linear effects of lactobacillus inoculum level and temperature, respectively.

$$Log(Rg) = 11.68645 + 1.80619 \times L - 0.58622 \times L^2 - 0.43887 \times T \times L \quad (1)$$

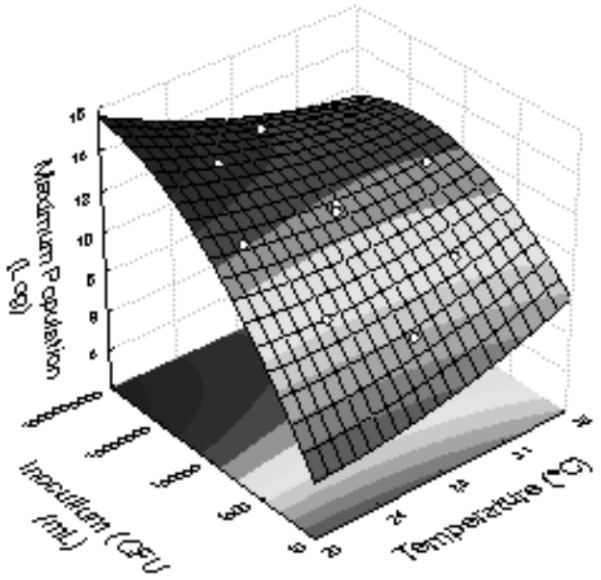

Figure 1: Effect of temperature and *Lactobacillus fermentum* inoculum level on the maximum population of this microorganism when co-cultured with *S. cerevisiase.*

Table 2: ANOVA for the effect of temperature and inoculum level on lactobacilli maximum population in co-culture with *S. cerevisiae*.

	SS	df	MS	F	p
(1)Temperature(L)	0,16278	1	0,16278	1,0819	0,345934
Temperature(Q)	0,13450	1	0,13450	0,8939	0,387825
(2)Inoculum (L)	26,09866	1	26,09866	173,4599	0,000045
Inoculum (Q)	1,94064	1	1,94064	12,8981	0,015685
1L by 2L	0,77042	1	0,77042	5,1205	0,073091
Error	0,75230	5	0,15046		
Total SS	30,38480	10			

Conclusions

- The model developed in this study can be applied during the ethanol fermentation process to predict the maximum population of *Lactobacillus.*
- The model showed no significant difference ($p > 0.90$) for growth rate and lag time of *Lactobacillus* growing in sugar cane must. However, maximum population of this microorganism was significantly different ($p < 0.90$) when grown in pure and co-culture with yeast.

Acknowledgements

The authors acknowledge financial support from *Fapesp* (Fundação de Amparo à pesquisa do Estado de São Paulo) and *Danisco Cultor do Brasil.*

References

Chin P.M. and Ingledew W.M. (1994) Effect of lactic acid bactéria on wheat mash fermentation prepared with laboratory backset. Enzyme *Microbiology and Technology* 16(4), 311-317.

Crueger W. and Crueger A. (1993) Biotecnología: Manual de Microbiologia Industrial. Zaragoza (España). Editora Acribia. 1993. 3ª edição.

Essia Ngang J.J.E., Letourneau F. and Villa P. (1989) Alcoholic fermentation of beet molasses: effect of lactic acid on yeast fermentation parameters. *Applied Microbiology and Biotechnology* 31, 125-128.

McMeekin T.A., Olley J.N., Ratkoswsky D.A. and Roos T. (2002) Predictive micorbiology: towards the interface and beyond. *International Journal of Food Microbiology* 73, 395-407.

Miconnet N., Geeraerd A.H., Van Impe J.F., Rosso L. and Cornu. M. (2005) Reflections on the use of robust and least-squares non-linear regression to model challenge tests conducted in/on food products. *International Journal of Food Microbiology* 104, 161-177.

Narendranath N.V., Hynwa S.H., Thomas K.C. and Ingledew W.M. (1997) Effects of lactobacilli on yeast-catalyzed ethanol fermentation. *Applied and Environmental Microbiology* 63(11), 4158-4163.

Nobre T. P. (2006) Viabilidade celular de Saccharomyces cerevisiae cultivada em associação com bactérias contaminantes da fermentação alcoólica. Piracicaba, 90p. Dissertação (Mestrado) – Escola Superior de Agricultura "Luiz de Queiroz", Universidade de São Paulo.

Nolasco J.J. (2005) Desenvolvimento de processo térmico otimizado para mosto de caldo de cana na fermentação alcoólica. Campinas, 2005, 155p. Dissertação (Mestrado) – Faculdade de Engenharia de Alimentos, UNICAMP.

Ross T. (1996) Indices for performance evaluation of predictive models in food microbiology. *Journal Applied Bacteriology* 81, 501-508.

Microbial individual-based models and sensitivity analyses: local and global methods

M. Ginovart[1], C. Prats[2], X. Portell[3]

[1] Department of Applied Mathematics III, Escola Superior d'Agricultura de Barcelona, Universitat Politècnica de Catalunya, Esteve Terradas 8, 08860 Castelldefels (Barcelona), Spain. (marta.ginovart@upc.edu)
[2] Department of Physics and Nuclear Engineering, Escola Superior d'Agricultura de Barcelona, Universitat Politècnica de Catalunya, Esteve Terradas 8, 08860 Castelldefels (Barcelona), Spain. (clara.prats@upc.edu)
[3] Department of Agri-Food Engineering and Biotechnology, Escola Superior d'Agricultura de Barcelona, Universitat Politècnica de Catalunya, Esteve Terradas 8, 08860 Castelldefels (Barcelona), Spain. (xavier.portell@upc.edu)

Abstract

A microbial Individual-based Model (IbM) to deal with yeast populations growing in liquid batch cultures has been designed and implemented in a simulator called INDISIM-YEAST. Interesting qualitative results have already been achieved with its use in the study of fermentation profiles, small inocula dynamics and lag phase, among others. Nevertheless, in order to improve its predictive capabilities and further development, a deeper comprehension of how the variation of the output of the model can be apportioned to different sources of variation must be investigated. One way to consider a sensitivity analysis for this IbM, providing an understanding of how the model response variables react to changes in the inputs, is the statistical study of well-designed computer experiments. The aim of this contribution is to show how the insights into nine individual cell parameters of INDISIM-YEAST, mainly related to uptake and reproduction sub-models, can be obtained by combining local and global sensitivity analyses using simple and classic methods. From data obtained with an extensive set of computer experiments, a study of the variability observed in the evolution of two outputs of this model, ethanol production and mean biomass of the population, was performed. In addition, mono-factorial (one-at-a-time) analyses and ANOVA-based global analyses were also carried out on these two outputs. The model is clearly less sensitive to some parameters than others, depending on the output controlled. Moreover, this study allows identification of the parameters which have the greatest impact on the corresponding outputs and their significant first-order interactions. This work must be understood as an exercise to set up the procedure to be used in a sensitivity analysis study involving microbial IbMs. The knowledge gained will facilitate future parameterization and calibration of different parameters and outputs depending on the purpose of any study.

Keywords: *sensitivity analysis, computer experiments, individual-based model, yeast population*

Introduction

Microbial modelling deals with complex spatio-temporal systems, involving the building and use of increasingly intricate models. Individual-based Models (IbMs) are being applied to the study of microbial systems nowadays (Ferrer *et al.* 2009, Hellweger and Bucci 2009). The only way to assess the behaviour of these models, including sensitivity, uncertainty, stability and error propagation, is the statistical study of well-designed computer experiments (Saltelli *et al*. 2000, Ginot *et al.* 2006). Sensitivity analysis is the study of how the variation in the output of a model can be apportioned, qualitatively or quantitatively, to different sources of variation, and of how the given model depends upon the information fed into it. It is used to increase confidence in the model and its predictions by providing an understanding of how the model response variables react to changes in the inputs (Saltelli *et al.* 2000). Such analysis can be employed prior to a calibration process to assess the importance of each parameter, especially useful in the calibration of an IbM which can control a great number of processes and, hence, the number of parameters to be estimated is high. This kind of study may allow a dimensionality reduction of the parameter space where the calibration and/or optimization is

carried out. Since IbMs are non-linear models, the sensitivity of an output to a given parameter depends on the value of that parameter, the values of the other parameters (interactions), time and the output itself. Thus, it is essential to combine local and global methods that explore the entire parameter space and allow for quantifying interactions between parameters. In this contribution, we suggest combining the use of different sensitivity analysis methods on diverse model outputs of a microbial IbM in order to gain knowledge of their inherent variability throughout the time evolution of the virtual system. The chosen IbM is INDISIM-YEAST, a simulator that deals with yeast populations growing in liquid batch cultures. The aim of this work is to show how insights into the individual cell parameters of INDISIM-YEAST can be obtained by combining local and global sensitivity methods using classic and well-proven techniques, and to illustrate that they provide, when applicable, a good and effective alternative to more sophisticated methods.

Materials and Methods

INDISIM-YEAST is an adaptation of the IbM INDISIM (Ginovart *et al.* 2002) for the study of yeast batch cultures. A detailed description of this stochastic model can be found in the pertinent bibliography (Ginovart and Cañadas 2008, Ginovart *et al.* 2011a, b). All the simulations run started from the same inoculum, made up of a unique yeast cell, growing in a spatial domain with a fixed number of glucose particles distributed uniformly in the beginning. We explored the influence of nine input parameters on two outputs. The selected parameters are shown in Table 1, as well as their reference values and explored ranges. The outputs assessed were the ethanol production and the mean biomass of the yeast population.

Table 1: Input parameters considered in this study, together with their symbols, reference values, explored ranges and ANOVA levels.

Parameter (simulation units)	Reference value	Range	ANOVA levels
U_{max}: maximum number of glucose particles that may be consumed per unit time and per unit of cellular surface	0.20	0.18 - 0.45	0.2475 0.3150
K_1: constant that represents the effect of the cellular surface scars on the uptake	0.10	0.075 - 0.20	0.10625 0.13750
E: prescribed amount of translocated glucose per unit of biomass that a yeast cell needs to remain viable	0.001	0.00005 - 0.003	0.00079 0.00153
Y: metabolic efficiency that accounts for the synthesised biomass units per metabolised glucose particle	0.60	0.5 - 1.5	0.75 1.00
m_C: critical mass, the minimum mass of a yeast cell required to move to the budding phase	140	75 - 225	112.5 150.0
Δm_{B1}: minimum growth of the cell biomass during unbudding phase required to move to the budding phase	50	25 - 80	38.75 52.50
Δm_{B2}: minimum growth of biomass required for the initiation of cell bud separation	70	40 - 110	57.5 75.0
ΔT_2: minimum number of time steps that a yeast cell must remain in the budding phase	4	1 - 40	10.75 20.50
q: proportion that allows determination of the mass that the daughter cell will have	0.80	0.56 - 0.95	0.6575 0.7550

Some simple and classic methods are used in order to combine local and global sensitivity analyses of this simulator INDISIM-YEAST. A local mono-factorial (one-at-a-time) analysis consists of plotting the model outcome at a given time (often the last one of evolution or at specific times) versus a fairly wide range of values of the input parameter. When running the simulations, all the parameters are fixed to their referenced values except the one being explored. A “curve” or trend is obtained for each parameter and for each model outcome, and the slope at any point of this curve (hence for a given value of the parameter) actually represents the local sensitivity coefficient with respect to that parameter value. A well-known

global method that is seldom employed for sensitivity analysis purposes is the analysis of variance (ANOVA) (Saltelli *et al*. 2000, Ginot *et al*. 2006). It is a natural method for variance decomposition combined with a factorial simulation design, which tests the contribution of the parameters and of their interactions to the variability of the outcome of the model. In standard ANOVA the effect of input factors is assessed globally, testing only whether at least one of the levels of the factor has an effect on the output, and thus ignoring "how" this effect specifically occurs. A few well-chosen levels may account for the general pattern of the model response. The ANOVA-based Total Sensitivity Index (TSI) for each parameter (and for each output) accounts for the percentage of variance explained by both the main effect of this parameter and the interactions involving it. This index can be defined as the ratio of the sum of squares explained by the main effect and the sum of squares explained by the interactions involving that parameter to the total sum of the squares of the corresponding output.

Results and Discussion

Since we are using a stochastic model, a preliminary analysis of the random seed effects on both outcomes, ethanol production and mean biomass of the yeast population, was carried out. In this analysis, all the parameters were kept constant and equal to their reference values, and 100 replications were performed. The set of data obtained for the two outputs every 100 time steps was assessed with statistical tools. The highest variability was observed in mean biomass during the initial stages, when the population size is still small and developing, while ethanol production is less sensitive to the random seeds throughout the temporal evolution. Figure 1 shows the mono-factorial (one-at-a-time) analyses of the nine chosen parameters on the two outcomes. A linear pattern would indicate that the sensitivity of the model outcome to this parameter is constant, whatever the parameter's value. It is shown that U_{max}, Y, K_1 and q have great influence on ethanol production but small or inexistent effect on mean biomass. In contrast, mean biomass reflects the changes of m_C and ΔT_2, while ethanol production does not. Sensitivity of both parameters to Δm_{B2} is similar, and the analysis of Δm_{B1} and E show only slight (or none) influence on them.

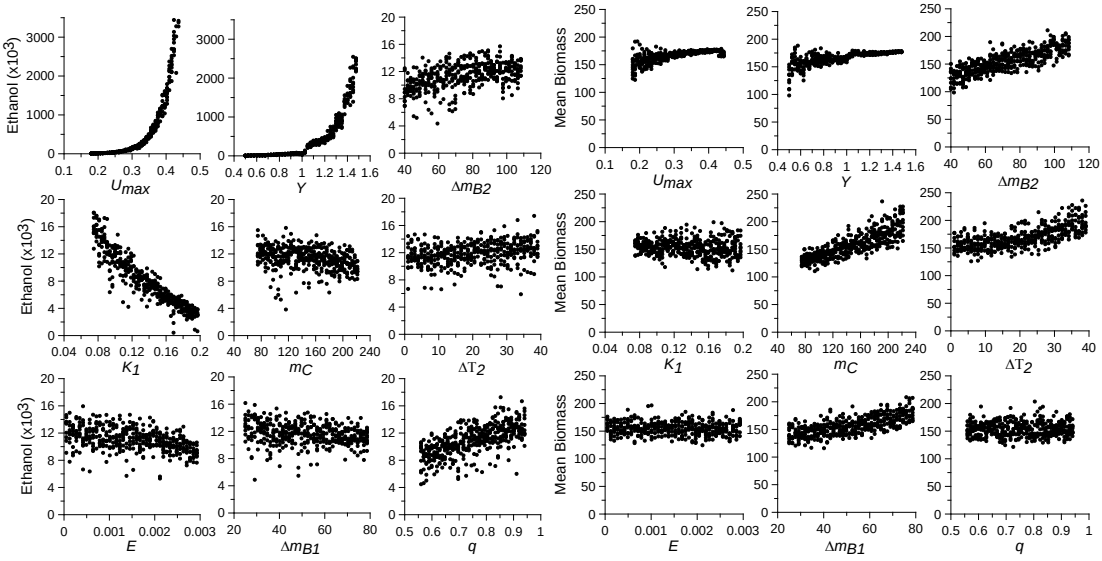

Figure 1: One-at-a-time analyses of the sensitivity of ethanol (left) and mean biomass (right) of the nine chosen parameters.

Figure 2 shows the results of the ANOVA-based TSI corresponding to the logarithm of ethanol production. These results were obtained with equireplicate factorial design with the main effects and first order interactions, indicating a well-balanced design with good statistical properties after the logarithm transformation. The explained variance was 98.4%, a good result for an ANOVA model that included first-order interactions only. The significance

of the main effects and the two-way (first-order) interactions are provided by the ANOVA table, together with the p-values pointing out the importance of each effect on the outcome. Some interactions are not always absent, which means that the parameters do not have an independent additive effect on the output.

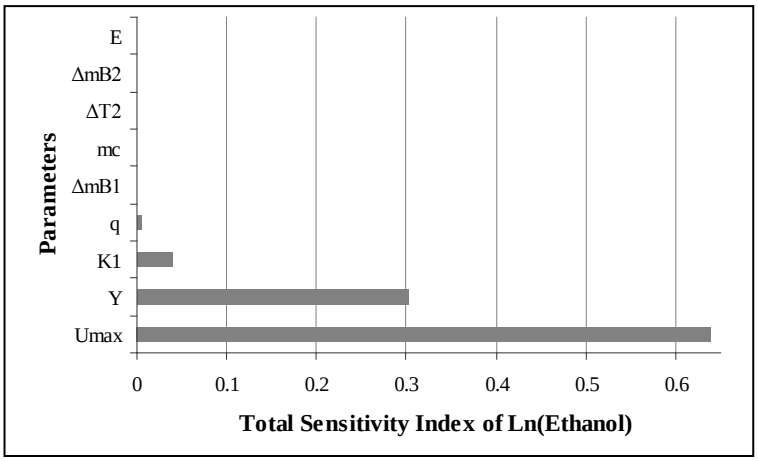

Figure 2: TSIs for the logarithm of ethanol production from the results of the ANOVA table obtained for the nine selected input parameters.

Conclusions

The sensitivity of outputs to the input parameters strongly depends on the kind of variables selected. Ethanol production is a global variable, and we have seen that it strongly depends on U_{max} and Y, and less on K_1. On the contrary, mean biomass is a feature of the individuals of the population and is related with its structure. Thus, its dependence on some of the parameters related with the reproduction sub-model is greater. ANOVA, a statistical method widely used in experimental research, has proven useful in the field of virtual (simulation) experiments with IbMs, in particular in the analysis of first-order interactions between input parameters. These results are useful for two purposes: to evaluate the consequences of sub-model formulations on the output dynamics, and to delimit the calibration to be performed. This is still a methodological work by which we are trying to set the best sensitivity analysis methods to be used in IbMs in general and, in INDISIM-YEAST in particular.

Acknowledgements

The financial support of the Spanish Government (MICINN, CGL2010-20160) and the Universitat Politècnica de Catalunya (BarcelonaTech).

References

Ferrer J., Prats C., López D. and Vives-Rego J. (2009) Mathematical modelling methodologies in predictive food microbiology: A SWOT analysis. *International Journal of Food Microbiology* 134, 2-8.

Ginot V., Gaba S., Beaudouin R., Aries F. and Monod H. (2006) Combined use of local and ANOVA-based global sensitivity analyses for the investigation of a stochastic dynamic model: Application to the case study of an individual-based model of a fish population. *Ecological Modelling* 193, 479-491.

Ginovart M. and Cañadas J.C. (2008) INDISIM-YEAST: an individual-based simulator on a website for experimenting and investigating diverse dynamics of yeast populations in liquid media. *Journal of Industrial Microbiology and Biotechnology* 35, 1359-1366.

Ginovart M., Prats C., Portell X. and Silbert M. (2011a) Analysis of the effect of inoculum characteristics on the first stages of a growing yeast population in beer fermentations by means of an Individual-based Model. *Journal of Industrial Microbiology and Biotechnology* 38, 153-165.

Ginovart M., Prats C., Portell X. and Silbert M. (2011b) Exploring the lag phase and growth initiation of a yeast culture by means of an Individual-based Model. *Food Microbiology* (In Press).

Hellweger F.L. and Bucci V. (2009) A bunch of tiny individuals-Individual-based modeling for microbes. *Ecological Modelling* 220, 8-22.

Saltelli A., Chan K. and Scott M. (2000) *Sensitivity Analysis*. *Wiley Series in Probability and Statistics*. John Wiley and Sons, New York, 475 pp. (ISBN 9780470743829).

Upgrading the uptake and metabolism sub-models of the Individual-based Model INDISIM-YEAST to tackle the behaviour of *Saccharomyces cerevisiae* in different culture conditions

X. Portell[1], A. Gras[1], R. Carbó[1], M. Ginovart[2]

[1]Department of Agri-Food Engineering and Biotechnology, Escola Superior d'Agricultura de Barcelona, Universitat Politècnica de Catalunya, Campus Baix Llobregat, Esteve Terradas 8, 08860 Castelldefels, Barcelona, Spain. (xavier.portell@upc.edu; anna.gras@upc.edu; rosa.carbo@upc.edu)
[2] Department of Applied Mathematics III, Escola Superior d'Agricultura de Barcelona, Universitat Politècnica de Catalunya, Campus Baix Llobregat, Esteve Terradas 8, 08860 Castelldefels, Barcelona, Spain. (marta.ginovart@upc.edu)

Abstract

INDISIM-YEAST is an Individual-based Model (IbM) that has been already used to qualitatively investigate different features of yeast populations evolving in liquid batch cultures such as, among others, fermentation profiles, small inocula dynamics and lag phase. Previous INDISIM-YEAST versions did not take into account that yeasts under industrial processes face different oxygen availability through the course of the target process. The introduction of new variables in this model would facilitate its use in industrially oriented processes. The aim of the study is to enhance the uptake and metabolism sub-models of INDISIM-YEAST in order to be able to mimic experiments without a fixed oxygen availability. Two main substrates were taken into account on previous INDISIM-YEAST versions, i.e. glucose as carbon and energy source, and ethanol as metabolite. In the present version of this model, nitrogen metabolism has been added with the introduction of the organic nitrogen and ammonium. The addition of the oxygen and carbon dioxide as substrates permits both the aerobical respiration and fermentation metabolic pathways to be taken into account. When possible, the individual parameter values assigned were chosen from the literature to be consistent with the yeast *Saccharomyces cerevisiae*. The values for the individual parameters which cannot be inferred from the literature will need to be calibrated. This work is a valuable step forward to using this IbM in industrially relevant processes where *S. cerevisiae* plays a distinguished role as, for example, in the productions of beer and wine.

Keywords: *Individual-based Model, yeast cell, yeast metabolism, oxygen*

Introduction

INDISIM-YEAST is an Individual-based Model (IbM) designed to study the behaviour of yeast cells based on the INDISIM model (Ferrer *et al.* 2008). It has already been used to qualitatively investigate different features of yeast populations evolving in liquid batch cultures such as, among others, fermentation profiles, small inocula dynamics and lag phase (Ginovart and Cañadas 2008, Ginovart *et al.* 2011a, b).When it comes to yeast metabolism, these published works were built on taking into account that glucose was the only carbon and energy source, the catabolism of which resulted in ethanol production. This entails the assumption that glucose can simply be metabolized, at first, via the Embden-Meyerhof pathway (Glycolysis) leading to the production of two molecules of ethanol and metabolic energy.

S. cerevisiae is a budding yeast widely used both in industrial processes and as a microorganism model for understanding the eukaryotic cell cycle. This microorganism is a Crabtree-positive yeast; therefore, even in aerobic conditions, when growing in high glucose concentration, *S. cerevisiae* catabolizes most of the glucose via fermentative (respirofermentative metabolism) (Walker 1998). Accordingly, it seems reasonable that a model aiming to reproduce *S. cerevisiae* experimental results should include this behaviour, or its validity must be kept in at a narrow set of conditions. In the present version of this

model, nitrogen metabolism has been added with the introduction of the organic nitrogen and ammonium. The addition of the oxygen and carbon dioxide as substrates permits the aerobical respiration and fermentation metabolic pathways to be taken into account. Therefore, this study aims to enhance the uptake and metabolism sub-models of INDISIM-YEAST in order to be able to mimic experiments without a fixed oxygen availability.

Materials and Methods

A reduced overview of the created model according the updated Overview, Design concepts, and Details protocol by Grimm *et al.* (2010) is shown in this section.

Purpose

The model aims to analyse *S. cerevisiae* population dynamics in experimental batch cultures with glucose as a sole carbon source and taking into account oxygen and nitrogen dynamics.

Entities, state variables, and scales

Three entities are considered: *S. cerevisiae* cells, spatial cells and the environment. A yeast cell (E_i) is defined by the variables: $e_1(t)$, $e_2(t)$ and $e_3(t)$, identifying its position in the spatial domain; $e_4(t)$, its biomass (pmol); $e_5(t)$, its genealogical age (bud scars); $e_6(t)$, the reproduction phase in the cellular cycle in which the cell is currently (unbudded or budding); $e_7(t)$, its "start mass" (pmol), the mass required to change from the unbudded to the budding phase; $e_8(t)$, the minimum biomass increase (pmol) to enter the budding phase; $e_9(t)$, the minimum time required to complete the budding phase (time steps); and $e_{10}(t)$, the amount of carbon (pmol) stored in the cell as reserve carbohydrates. Letting N = N(t) denote the number of individuals at time t, and identifying an individual by i, the population's state at t is:

$$P_N(t) = \{E_i[e_1^i(t), e_2^i(t), \dots, e_{10}^i(t)]\}_{i=1,2,\dots N}$$

The simulated space is a cube which holds a liquid medium and yeast, and is divided into spatial cubic cells (S_{xyz}) described by a vector that is represented by the variables: $s_1(t)$, the amount of glucose (pmol); $s_2(t)$, the amount of organic nitrogen (pmol); $s_3(t)$, the amount of ammonium (pmol); $s_4(t)$, the amount of oxygen (pmol); $s_5(t)$, the amount of ethanol (pmol); and $s_6(t)$, the amount of carbon dioxide (pmol). The whole three dimensional grid is then described by:

$$D(t) = \left\{S_{xyz}\left[s_1^{xyz}(t), s_2^{xyz}(t), \dots, s_6^{xyz}(t)\right]\right\}_{x=1,\dots,6;y=1,\dots,6;z=1,\dots,6}$$

The environment is a closed and stirred medium so there is no ingress or egress either of organic or of inorganic elements.

The temporal evolution of the system emerges after the simulation runs a number of time steps. Each time step corresponds to 6 minutes and the simulated volume is set to 1 mm^3. The simulation shown in this contribution lasts for 14 days.

Submodels

The actions of the individual are: movement, uptake, metabolism, reproduction and death checking.

Uptake submodel

Four substrates are taken into account: glucose, organic N, ammonium and oxygen (j=1,…,4). The maximum uptake of C and N sources are controlled by the internal C to N ratio, a value lower than r_C to uptake C sources and greater than r_N to uptake nitrogen sources. The yeast cells always uptake oxygen. The final substrate j uptake (pmol) at a given time step [$U_j(t)$] is then defined by:

$$U_j(t) = MIN\left(A_j(t), (U_{MAX})_j(t)\right)$$

$$A_j(t) = s_{(j)}^{xyz}(t) \cdot \frac{\mathrm{A_j}}{N_{XYZ}(t)}$$

$$(U_{MAX})_j(t) = u_j(t) \cdot e_4(t)^{\frac{2}{3}} \cdot (1 - P_s\, e_5(t))$$

where, $A_j(t)$ is the maximum amount of substrate j available for an individual, $(U_{MAX})_j(t)$ the maximum substrate j uptake capacity of the individual, A_j is the uptake coefficient for substrate j to cells, N_{XYZ} is the number of individuals within the cell, $u_i(t)$ is the uptake coefficient for a substrate j (pmols per unit of cell surface), which is taken from a normal distribution and P_s is a penalization per cell scar.

Metabolism submodel

Yeasts can obtain energy from glucose by two catabolic pathways: respiration (glycolysis and Krebs's cycle) and fermentation (Glycolysis and alcoholic fermentation). The model assumes that, because of the Crabtree effect, individuals evolving into a spatial cell without oxygen or with glucose content over a given limit will use a fermentative pathway, otherwise they will respire. Maintenance energy requirements (pmol of glucose) for a respiring individual are:

$$M_R(t) = \mathrm{E_R} \cdot e_4(t) \cdot \left(1 + P_e(t) \cdot s_5^{xyz}(t)\right)$$

where E_R is the maintenance rate (pmol of glucose/pmol of CN_{MIC}), $P_e(t)$ a penalization due to ethanol content (pmol of ethanol^{-1}) obtained from a normal distribution and with x, y, z values being the coordinates of the acting individual. Maintenance energy requirements under fermentative conditions [$M_F(t)$] are obtained from a relation between the energy obtained from both metabolic pathways (mol fermented/mol respired). In order to cover its maintenance needs, glucose cell uptake is used. If a cell does not have enough glucose uptake for maintenance it can use its carbon reserves without being able to create further biomass in the current time step (if it is under respirative metabolism it needs oxygen uptake in addition). If the carbon reserve is not enough (or there is not oxygen enough to respire) then it lyses.

After maintenance, the remaining glucose uptake is used to create new biomass or to create new carbon reserves. Carbon reserves are created when glucose content in the spatial cell is under a given amount, otherwise new biomass [$\Delta e_4(t)$] can be created, as follows:

$$\Delta \mathrm{e}_4(t) = MIN(R_O, R_G, R_N)$$

where R_O, R_G and R_N are moles of biomass that can be created with, respectively, the remaining amounts of oxygen, glucose and N inside the cell (R_O not necessary when fermenting). Ammonium uptake is taken into account first and organic N later.

Parameters and constants used in the simulation shown below are presented in table 1.

Table 1: Values of parameter and constants used in the simulation shown.

Parameter description	Units	Value
Yeast C/N molar ratio	mol C/mol N	7
C/N to uptake carbon sources	mol C/mol N	12
C/N to uptake nitrogen sources	mol C/mol N	4
Average biomass at reproduction	pmol of CN_{MIC}	20
Min mass increase to start bud formation	pmol of CN_{MIC}	1
Min mass increase for budding	pmol of CN_{MIC}	3
Minimum time for budding	H	0.5
Mass fraction from the mother released to the bud	dimensionless	0.8
Energy penalization due to ethanol	pmol of ethanol^{-1}	$1x10^{-7}$
Uptake penalty per cell scar	Cell scar^{-1}	$1x10^{-2}$
Maintenance energy	g C/gC_{MIC}	$5x10^{-5}$
Respiration to fermentation energy from glucose	mol F./mol R.	19
Biomass yield production following respiration	g C_{MIC}/g C	0.9
Biomass yield production following fermentation	g C_{MIC}/g C	0.2
Glucose conc. to accumulate carbon reserves	mg/ml	$2x10^{-3}$
Glucose conc. to start Crabtree effect	mg/ml	$5x10^{-3}$
Maximum growth rate	h^{-1}	$1x10^{-1}$
Availability of glucose	h^{-1}	0.1
Availability of organic nitrogen	h^{-1}	0.22
Availability of ammonium	h^{-1}	0.1
Availability of oxygen	h^{-1}	0.5

Results and Discussion

Once the model is built up, values need to be assigned to the individual model constants (parameterization process). When those data are described in the specialized literature and they are consistent with *S cerevisiae* biology, then it is possible to assume the referred data. Other constant values can be inferred from the literature and more will be found after calibration of the model. Before finishing this process it is good to trial the model to check if performance and qualitative behaviour agree with the experimental tests. This in turn is useful for improving knowledge about modelled system behaviour. One of the simulations already done can be seen, jointly with experimental data points, in Figure 1. Although the general behaviour of the system is well reproduced, it is necessary to keep in mind that exploration of the biologically relevant values is still to be completed.

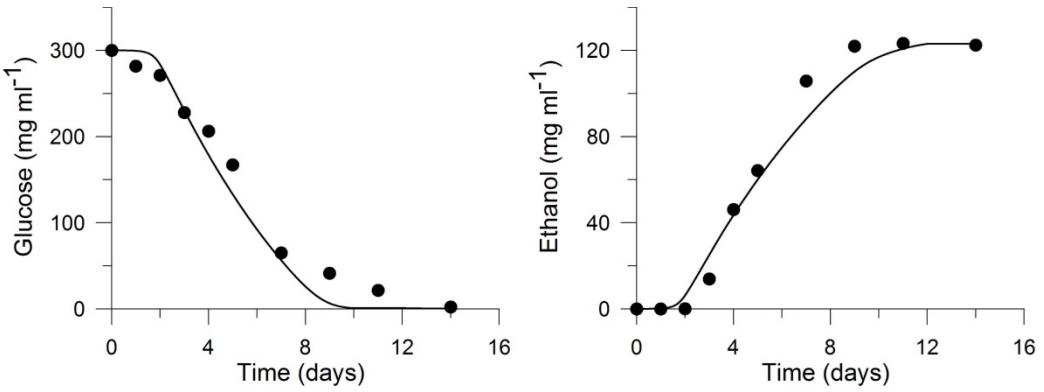

Figure 1: Simulated against experimental glucose and ethanol evolutions. Simulation (lines) was conducted using preliminary parameters values (Table 1). Experiments using *S. cerevisiae* yeast cells (dots) were conducted, in triplicate, at 27ºC under aerobical conditions with 300 mg ml^{-1} as initial glucose content and with proximally $1x10^4$ CFU ml^{-1}.

Conclusions

In the present work, new uptake and metabolism submodels have been successfully implemented within the previous INDISIM-YEAST simulator to deal with the yeast *S. cerevisiae*. First results from this new version reproduce glucose consumption and ethanol production with an acceptably close concordance with experimental data. This is a valuable step and one which justifies further research to develop the simulator in order to gain better understanding of the behaviour of this yeast under industrial processes.

References

Ferrer J., Prats C. and López D. (2008) Individual-based Modelling: an essential tool for microbiology. *Journal of Biological Physics* 34, 19-37.

Ginovart M. and Cañadas J.C. (2008) INDISIM-YEAST: an individual-based simulator on a website for experimenting and investigating diverse dynamics of yeast populations in liquid media. *Journal of Industrial Microbiology and Biotechnology* 35, 1359-1366.

Ginovart M., Prats C., Portell X. and Silbert M. (2011a) Analysis of the effect of inoculum characteristics on the first stages of a growing yeast population in beer fermentations by means of an Individual-based Model. *Journal of Industrial Microbiology and Biotechnology* 38, 153-165.

Ginovart M., Prats C., Portell X. and Silbert M. (2011b) Exploring the lag phase and growth initiation of a yeast culture by means of an Individual-based Model. *Food Microbiology* (In Press).

Grimm V., Berger U., DeAngelis D.L., Polhill J.G., Giskee J. and Railsback S.F. (2010) The ODD protocol: A review and first update. *Ecological modelling* 216, 2760-2768.

Walker G.M. (1998). *Yeast physiology and biotechnology*, John Wiley & sons, Chichester, UK. (ISBN 0-471-96446-8).

How does the average number of cells per sample influence the lag phase distribution of single cells?

J. Aguirre, M. Ganan, M. R. Rodriguez, A. Gonzalez, G. D. Garcia de Fernando

Depto. Nutrición, Bromatologia y Tecnologia de los Alimentos, Facultad de Veterinaria, UCM, Madrid, 28040 SPAIN

Abstract

The assumption that growth comes from one cell in homogeneous samples, when growth is not detected in a certain percentage of them contradicts the Poisson distribution function. Knowing the percentage of samples with microbial development, the Poisson function allows ascribing higher inocula to the samples with shorter lag phases. A gamma distribution lag phase simulation was generated considering different average number of cells per sample. Three scenarios were considered: scenario I assumes that all samples contain one cell. In scenario II, the sample with the shortest lag phase contains the highest number of cells, the sample with the second shortest contains the second one, and so on, according to the Poisson predictions. Scenario III is calculated like scenario II, but all samples with more than one cell are ignored.
The higher the average number of cells per sample is, the longer the lag phase and the smaller the variances in both scenarios, II and III, in comparison with scenario I. A permutation test was used to compare the variances among the three scenarios. The higher the average number of cells per sample is, the bigger and more significant the differences. To check how well our simulations model reality, the three scenarios were applied to experimental data. Considering Poisson-based predictions of the number of cells per sample, instead of considering that all samples contain one cell improves the accuracy of lag phase determinations of micropopulations. In fact, the more samples there are that contain more than one cell, the greater the improvement is. This improvement is likely to be statistically significant mainly in cases where both the average number of cells per sample and the specific growth rate are relatively high.

Acknowledgements

Authors acknowledge the support of the Ministerio de Educación y Ciencia (Spain), Program Consolider CARNISENUSA CSD2007-0016 and AGL-2010-16598.

Live-cell imaging of aerobic bacteria; a tool to assess and model heterogeneous germination & outgrowth of *Bacillus subtilis* spores

R. Pandey[1], A. Ter Beek[1], N. O. Vischer[2], E. M.M. Manders[2], S. Brul[1]

[1]Molecular Biology & Microbial Food Safety, Swammerdam Institute for Life Sciences, University of Amsterdam, Science Park 904, 1098 XH Amsterdam, The Netherlands (r.pandey@uva.nl)
[2]Centre for Advanced Microscopy, Section of Molecular Cytology, Swammerdam Institute for Life Sciences, University of Amsterdam, Science Park 904, 1098 XH Amsterdam, The Netherlands

Abstract

Spores of various *Bacillus spp.* can remain in a dormant, stress resistant state for long periods. Their return to vegetative cells involves a rapid germination followed by a more extended outgrowth phase. Spore-forming bacteria are a special problem for the food industries as some of them are able to survive preservation processes. Spore germination & outgrowth progression are often very heterogeneous and therefore makes predictions of microbial stability of food products exceedingly difficult. Mechanistic details of the cause of this heterogeneity are necessary. In order to examine heterogeneity we made a novel cast for live imaging which allows the growth, germination & outgrowth of *Bacillus subtilis* cells and spores, respectively. In order to check the efficiency of the setup, growth and division of *B. subtilis* 1A700 vegetative cells were monitored at different concentrations of rich, undefined media (TSB, LB) as well as a defined medium (MOPS). Phase-contrast images were recorded every 30s for 4 hours and doubling times were calculated. We were able to monitor nine areas in one slide per time-point using a routine that steers the lens appropriately. Thus, maximally ~100 starting cells (or spores) could be examined per experiment. The calculated generation times in our system were comparable to generation times obtained in well-aerated shake flask cultures. Hence, the setup is suitable for heterogeneity measurements at the single cell/spore level. Preliminary results show that also proper germination & outgrowth of spores is observed in our setup. To monitor where most heterogeneity ensues, recording of germination (phase bright to phase dark transition) and outgrowth times (formation of two cells) of individual spores is in progress. Current challenges are to extend the observation time frame from 4 to 24 hours such that monitoring outgrowth of damaged spores as well as of spores under adverse conditions can be started.

Keywords: *B. subtilis spores, heterogeneity, germination and out growth, live cell imaging*

Introduction

Spores from Gram-positive bacterial genera e.g. *Bacillus* and *Clostridium* can cause food spoilage and food born diseases (S. Ghosh *et al.* 2009). The Spores are metabolically dormant and very resistant to environmental stresses. Such spores can remain in the dormant, stress resistant state for long periods but can return to life rapidly through the process of germination and outgrowth (Fig.1) (Peter Setlow, 2003). During this period the spore's dormancy and extreme resistance properties are lost. Spore-forming bacteria are a special problem for the food industries as some of them can survive preservation processes commonly used in the food industries. Such spores which escape the processing treatment can germinate, grow out, and may cause food spoilage and food safety hazards. Spore germination and outgrowth is often quite heterogeneous. Some super dormant spores' progress extremely slowly through these stages and potentially come back to life, long after preservation treatments were applied (Sonali Ghosh *et al*. 2008).

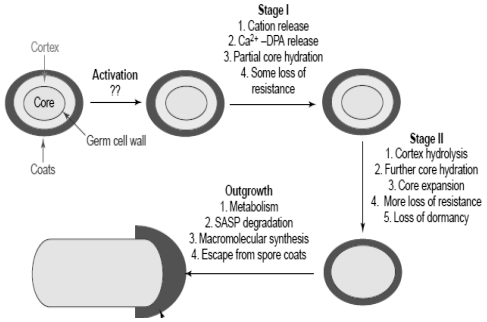

Figure 1: Different stages of germination and outgrowth.

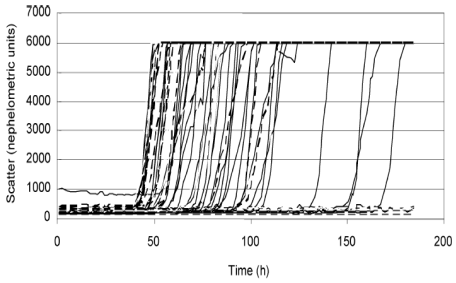

Figure 2: Growth behaviour of thermally stressed single bacterial spores in individual wells of a microtitreplate (Smelt and Brul 2007).

To check the heterogeneity in *B. subtilis*spores experiment was done in micro titer plate and shown that spores germinated after 150 hrs. of incubation in TSB medium (Smelt and Brul, 2007). Heterogeneity and super dormancy make predictions of microbial stability of food products exceedingly difficult. Since outgrowing spores or vegetative cells are much easier to kill than dormant spores, it would be advantageous to rapidly and completely trigger germination of spores in foods and then inactivate all at the outgrowth stage with heat or other physical treatments. To do so with appropriate robustness one should have mechanistic details of the cause of heterogeneity in spore germination and outgrowth. A study has been done on *Clostridium botulinum* for spores' germination and out growth (Sandra .Stringer, 2009, 2011). In order to study the heterogeneity in spore germination and outgrowth we made a cast. The cast allows growing aerobic bacteria and germination and outgrowth of spores and hence analysis of vegetative cell/spore at single cell level. To check the efficiency of the setup the *B. subtilis 1A700* vegetative cells were grown in different concentrations of rich, undefined media (TSB, LB) as well as a defined medium (MOPS). Rich, undefined media (TSB, LB) are routinely used in laboratory; moreover TSB is used for spore germination and outgrowth experiments and also to confirm the previous results which were done on TSB medium. Defined medium (MOPS) was used to check the growth and division of vegetative cells. These media were also used for spore germination and outgrowth experiments. Preliminary results showed proper germination & outgrowth of spores of *B. subtilis* 1A700.

Materials and Methods

Strain, media, and growth conditions

B.subtilis 1A700 cells were inoculated in 10 ml of TSB (pH 7.5) medium and incubated overnight at 200 rpm at 37^{o}C. Overnight grown culture of *B. subtilis* 1A700 was reinoculated in to fresh 10 ml TSB/ LB medium for respective experiments and grown for 3 hrs. at 37^{o}C to get an exponentially growing culture. Exponentially grown *B. subtilis* 1A700 cells were reinoculated into fresh 10 ml TSB/LB or MOPS medium and grown for 3 hrs. till $O.D._{600nm}$ reaches to ~ 0.2

Growth Measurement

The overnight grown culture was used to inoculate experimental flasks containing TSB / LB / MOPS medium at an $O.D._{600nm}$ between 0.01 and 0.02 units and was allowed to grow till the $O.D._{600nm}$ reached ~ 0.4. Data obtained only between $O.D._{600nm}$ of ~0.1 and ~0.4 was used to calculate the growth rates. Growth was followed by periodic sampling of the culture and Growth rate was expressed as the specific first-order rate constant (k) in dimensions of h^{-1}: ln2 doubling time. The first-order rate constant, k, was obtained as the plot of the natural log of $O.D._{600nm}$ as a function of time in hours.

Sporulation conditions

Cells from a single colony were inoculated in Tryptic Soy Broth (TSB; pH 7.5), cultivated until early exponential phase, and transferred into a defined minimal medium, buffered with

3-(N-Morpholino) propanesulfonic acid (MOPS) to pH 7.4 as described previously (Kort *et al*., 2007). As carbon- and nitrogen- sources, 10 mM glucose and 10 mM NH_4Cl were used. Cells were grown until early exponential phase and diluted into 20 ml of fresh MOPS buffered medium. When early exponential phase was reached again, 1% of this final pre-culture was used to inoculate 500 ml MOPS buffered medium. Sporulation was initiated by growing the culture into stationary phase, induced by glucose exhaustion. Sporulation was allowed for 96 hours during which its efficiency was followed using phase contrast microscopy.

Slide preparation

A cast was prepared by attaching a 65µl capacity (1.5 X 1.6 cm) Gene Frame (Thermo Scientific) to a standard microscope slide. A thin small square semisolid matrix pad with different concentrations of TSB, LB or MOPS medium and supplemented with 1% agarose (Sigma-Aldrich) was made by using plane and Siliconized glass cover slip (24 X 32 mm, Thermo Scientific Exponentially growing *B. subtilis* 1A700 cells ($O.D._{600nm}$ ~ 0.2) or spores were spotted onto the pad and the pad was transferred upside down on the cast having the gene frame and sealed with a cover slip (18 X 18 mm, Thermo Scientific).This cast was used for Time-Lapse Microscopy.

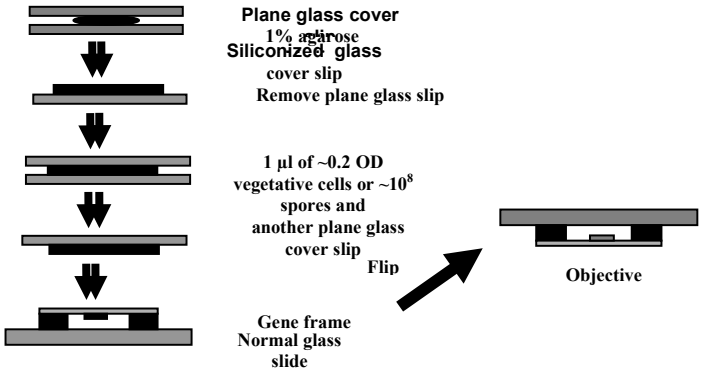

Figure 3: A cast of a silicon coated cover slip, containing a few mm thin layers of agarose and bacterial vegetative cells or spores was made.

Time-Lapse Microscopy

The cast was kept on a stage in a temperature-controlled (Box incubation system; Life Imaging Services) automated microscope (Zeiss cell observer) at 37°C. Images were obtained at a magnification of 100X. Growth and cell division of *B. subtilis* 1A700 vegetative cells were checked at different concentrations of TSB, LB and MOPS medium. Phase-contrast images were recorded at every 30 sec. for 4hrs. Minimum of two and maximum of nine different areas were selected from the slide per experiment per concentration of TSB, LB, and MOPS medium. One to fourteen cells i.e. maximally ~100 starting cells per area were manually identified and cell length was measured. The length measurement of cells per area was done at every 10 min for 30- 60 min. Doubling time of individual cell was calculated and average doubling time, for all the cells from all the areas, was calculated and plotted as the cell number vs. doubling time for respective concentrations.

Results and Discussion

In order to check the efficiency of the setup, growth and division of *B. subtilis* 1A700 vegetative cells was checked at different concentrations of rich, undefined media (TSB, LB), as well as a defined medium (MOPS). Three biological replicates were carried out at 50%, 10%, 5%, 2.5% TSB medium, 10%, 5%, 2.5% LB medium and 100% and 50% MOPS medium with *B. subtilis* 1A700 vegetative cells. Three biological replicates and four to nine technical replicates (area in slide) were done in almost all experiment except at 50% TSB medium as it induced a filamentous growth of cells and at 100% MOPS medium. Four to nine

areas per experiment were selected. Table 1. shows a comparison of generation times of *B. subtilis* 1A700 vegetative cells for all the concentrations of TSB, LB and MOPS medium. Generation times of 1A700 vegetative cells on TSB, LB and MOPS medium were compared to the measured generation times of 22.15+/-1.12 min., 21.55+/- 0.9 and 54.37+/- 0.6 min. for the same strain in shake flask cultures.

Table 1: Calculated Generation time of 1A700 vegetative cells in different medium. Concentration on slide and in shake flask

S.No	Medium	Conc.	Total Cell	Experiment -1	Experiment -2	Experiment -3	Average	Shake flask
	TSB			-	-	-	-	22.15+/-1.12
				-	-	-	-	
				-	-	-	-	
				-	-	-	-	
	LB			-	-	-	-	-
				-	-	-	-	
				-	-	-	-	
	MOPS			-	-	-	-	-
				-	-	-	-	

Table1. shows that the measured generation times of 1A700 vegetative cells on 50%, 10%, 5% and 2.5% TSB medium were 20.11 +/- 0.49 min, 23.11 +/- 2.84 min, 23.12+/-2.57 min, and 22.59+/-1.45 respectively. Figure 4. shows that 2.5% concentration of TSB medium supports good growth with generation time of 22.59+/-1.45 min. and clear division of *B. subtilis* 1A700 vegetative cells on the other hand 50% concentration of TSB showed filamentous growth. These results are comparable to generation time of 22.15+/-1.12 min. for *B. subtilis* 1A700 vegetative cells in shake flask i.e. 22.15+/-1.12

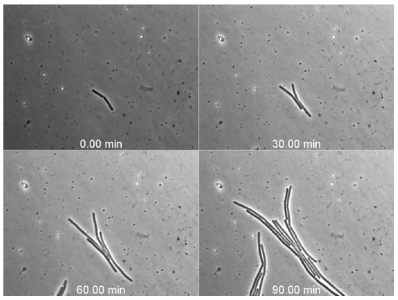

Figure 4: A time-resolved series of still images at 0, 30, 60, 90 min of growing *B. subtilis* vegetative cells

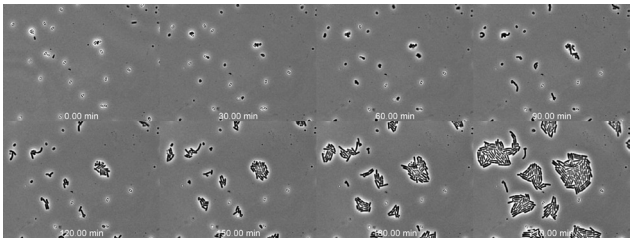

Figure 5: A time-resolved series of still images of germinating and outgrowing *B. subtilis* 1A700 spores.

50% LB also induced a filamentous growth and hence was not considered in the experiments. Generation times of 1A700 vegetative cells on 10%, 5% and 2.5% TSB medium were 25.87+/-3.235 min., 23.57+/-6.97min., 23.15+/-3.10 min. as seen in Table 1 2.5% TSB gave good growth with generation time of 23.15+/-3.10 min and clear division of *B. subtilis* strain 1A700 vegetative cells. For MOPS medium 100% and 50% concentration were checked. The generation times of 1A700 vegetative cells at these concentrations were 56.68+/-8.528 min. and 65.78+/-7.58 min. respectively. Both the concentrations gave good cell division but generation times in all biological replicates showed lager standard deviation. *B .subtilis* 1A700 spores were checked for germination and outgrowth. Preliminary results showed that proper germination & outgrowth of spores can be followed in our setup. To monitor where most heterogeneity ensues, recording of germination (phase bright to phase dark transition) and outgrowth times (formation of two cells) of individual spores was done and analysis is in progress. Also to account for the super-dormant spores, the current challenge is to extend the time frame in the method from 4 hrs. to 24 hrs. such that monitoring outgrowth of damaged spores as well as of spores under adverse conditions becomes feasible.

Conclusions

Heterogeneity of outgrowth of *B. subtilis* spores and growth of vegetative cells can be studied with our single-cell analysis techniques. Our technique enables us to analyze individual spores for investigating the physiological basis of observed heterogeneity in germination, outgrowth and resulting vegetative growth. We optimised the acquisition of live images by microscopy and ensured the oxygen availability in the cast used for microscopy. With the use of single-cell analysis techniques we can enhance the understanding of the mechanistic basis of food preservation and design possible spoilage models for targeting bacterial spores.

Acknowledgements

R.P. acknowledges the Erasmus Mundus program (EMECW 15) for funding of her PhD project. A.T.B. is supported by a grant from the Dutch Foundation for Applied Sciences (STW 10431). We thank Norbet for providing with a macro suitable for image analysis by Image J tool.

References

Setlow P. (2003) Spore germination. *Current Opinion in Microbiology* 6, 550–556.

Kort R., O'Brien A.C., van Stokkum I.H.M., Oomes S.J.C.M., Crielaard W., Hellingwerf K.J. and Stanley Brul (2005) Assessment of Heat Resistance of Bacterial Spores from Food Product Isolates by Fluorescence Monitoring of Dipicolinic Acid Release. *Applied and Environmental Microbiology* 71(7) 3556-3564.

Smelt J.P.P.M. and Brul, S. (2007) Modelling lag-time in predictive microbiology with special reference to lag phase of bacterial spores. In: *modelling microorganisms in food*. 67–81.

Ghosh S. and Setlow P. (2008) Isolation and Characterization of Superdormant Spores of Bacillus Species. *Journal of Bacteriology* 191 (6) 1787–1797.

Ghosh S. and Setlow P. (2009) The preparation, germination properties and stability of superdormant spores of *Bacillus cereus*. *Journal of Applied Microbiology* ISSN 1364-5072.

Stringer S.C., Webb M.D. and Peck M.W. (2009) Contrasting effects of heat treatment and incubation temperature on germination and outgrowth of individual spores of nonproteolytic *Clostridium botulinum* bacteria. *Applied and Environmental Microbiology* 75 (9) 2712–2719.

S.C. Stringer, M.D. Webb, M.W. Peck (2011) Lag time variability in individual spores of *Clostridium botulinum. Food Microbiology*, 28, 228-235.

Quantitative risk assessment of *Listeria monocytogenes* in cold-smoked salmon in the Republic of Ireland

S. Chitlapilly Dass[1], N. Abu-Ghannam[1], E. J. Cummins[2]

[1]School of Food Science and Environmental Health, College of Sciences and Health, Dublin Institute of Technology, Cathal Brugha St., Dublin 1, Ireland
[2]Biosystems Engineering, UCD school of Agriculture, Food science and Veterinary medicine, University College Dublin, Belfield, Dublin 4, Ireland

Abstract

Smoked-salmon is a ready-to-eat food which undergoes no thermal treatment before consumption, thus making it a 'high-risk' food product. In the event of pre or post process contamination with *Listeria monocytogenes*, even with low levels of contamination; this microorganism has the potential to reach unacceptable levels at the time of consumption. In this study, a quantitative Monte Carlo risk assessment model was developed to assess likely human exposure and the probability of human illness by L. monocytogenes on cold-smoked salmon in Ireland. The mean simulated prevalence of *L. monocytogenes* in cold-smoked salmon after the retail storage was 22.1 % and the simulated mean count on contaminated cold-smoked salmon was 2.60 log10 CFU/g (95 % confidence interval 0.00 – 4.53 log10 CFU/g). The model predictions were validated by a parallel surveillance study. The model predicted the log probability of illness annually by consuming contaminated cold-smoked salmon in a low risk and high risk population, with mean values – 8.02 and – 3.08, respectively. The model sensitivity analysis highlights the importance of reducing the initial contamination levels of *L. monocytogenes* on raw fish and the maintenance of proper storage conditions. Various 'what-if' scenarios were studied to assess the likely impact on the log probability of illness. Careful control of consumer storage temperature and time were identified as the best strategies to decrease the probability of illness. The quantitative risk assessment developed in this paper may help risk managers to make informed decisions with regard to possible control measures for *L. monocytogenes* in cold smoked salmon and therefore improve food safety.

Keywords: L. monocytogenes, smoked salmon, risk assessment, exposure assessment

Probabilistic exposure assessment of coagulase + staphylococci, *Clostridium perfringens* and *Listeria monocytogenes* in large wild game meats in Europe

J.-M. Membré [1,2], M. Laroche [1,2], C. Magras [2,1]

[1]INRA, UMR 1014 Secalim, Oniris, Rue de la Géraudière, BP 82225, 44322 Nantes Cédex 3, France
[2] LUNAM Université, Oniris, Atlanpole-La Chantrerie, F-44307, France
(jeanne-marie.membre@oniris-nantes.fr, michel.laroche@oniris-nantes.fr, catherine.magras@oniris-nantes.fr)

Abstract

In a previous study, the variations in prevalence and levels of coagulase + staphylococci, *Clostridium perfringens* and *Listeria monocytogenes* in large wild game meat such as red deer, roe deer, and wild boar were studied (Membré *et al*. 2011).
The objective of the current study was to incorporate these results in a probabilistic exposure assessment model to determine the level of consumer exposure once the meat is ready-to-eat. The inputs were the probability distribution of log count of bacteria on raw meat (from the previous study), the storage (time and temperature profiles) at retail and consumers home combined with the microbial ability to grow at refrigerated conditions, and finally the heating regime at home combined with the microbial thermal inactivation characteristics. Scenarios of consumer exposure were built in Excel, Monte Carlo simulations were run with the Excel Add-in @Risk.
The consumer exposure to the microbial hazards associated with the wild game meat is low and acceptable if the meat dishes (stewing meat or roasting meat) are properly cooked and eaten just after cooking. However, if the consumer cooking/eating habits change, the risk for the consumer will be highly frequent: with roasting meat consumed rare or prepared as a carpaccio-type dish, *L. monocytogenes* will not be controlled; with stewing meat maintained at room temperature for several hours after cooking, the risk associated with *C. perfringens* will be high.

Keywords: *risk assessment, Monte Carlo simulation, food safety, foodborne pathogens*

Introduction

For the meat industry, several risk assessment have already been done for various pathogens and types of meat, however, to the best of our knowledge, there is no risk assessment carried out specifically for large wild game meat, nor specific microbiological criterion within the European legislation. The consumption of game meat in EU is estimated to 0.37 kg per year and per capita (Reinken 1998), it varies among the countries from 0.06 kg to 2.6 kg (0.62 kg in France). Although low, the consumption of large game meat is increasing in Europe (Bertolini *et al*. 2005). Moreover, the global trading activity is important.
In a previous study, the microbial contamination level of raw wild game meat in France (native or imported animals) was assessed (Membré *et al.* 2011). A total of 1549 roasting and stewing meat samples from three species (red deer, roe deer, wild boar) were collected at French game meat traders' facilities. The samples were analyzed for detection and enumeration of coagulase + staphylococci, *Listeria monocytogenes* and *Clostridium perfringens*. The levels of bacterial contamination of the raw meat were determined by performing statistical analysis involving Bayesian inference. *C. perfringens* was found in the highest numbers, with means of contamination estimated to be in a range of -0.35 to 2.78 log cfu/g depending on game species, storage condition before commercialization and type of meat.
The objective of the present study is to combine the level of contamination of raw meat with an exposure assessment scenario (time and refrigeration temperature at retail and domestically, heating conditions during consumer preparation) to calculate the level of consumer exposure once the meat is cooked and then ready-to-eat.

Materials and Methods

Building the scenario of consumer exposure

Four scenarios of consumer exposure to ready-to-eat game meals were built. The scenarios were based on consumer choice when buying the meat at retail level: type of meat preparation (roasting and stewing meat) and game species (red and roe deer, wild boar). The exposure assessment was built considering one kg of meat designed to serve five consumers.

The probability distributions of microbial contamination of raw meat were derived from the statistical analysis carried out in a previous study (Membré *et al.* 2011).

The shelf-life of both roasting and stewing meats was 21 days (information provided by the industrial partners). In France, meat products are generally bought when 33 % of their shelf-life has lapsed and consumed at 44 % of their shelf-life (Derens *et al.* 2004); the durations of storage of the raw meat at retailer and consumer stages were assumed to be 7 and 3 days, respectively. The temperature of refrigerated cabinets in retail and domestic refrigerators were described with Normal probability distribution functions, N(3.2, 2.0) and N(5.9, 2.9), respectively (Derens *et al.* 2006).

The ability of growth of the three hazards were calculated by determining the growth rates (no lag time assumed) as a function of the storage temperature and the pH of raw meat (Uniform function, U(5.5, 7.0)), defined by expert opinion according to high variation of *ante-mortem* conditions (notably hunting practices) that may induce animal stress. At these chilled temperatures, it was assumed that the growth of *C. perfringens* was null and the toxin production of coagulase + staphylococci was negligible. The growth rates of *L. monocytogenes* on meat as a function of temperature and pH was modelled using data from ComBase (http://www.combase.cc/) based on the following query: beef + *L. monocytogenes* / *inocua* + temperature [0 – 40 °C] + pH [4 – 7.5] +aw [0.99 – 1.0] + no additional factors. This query corresponded to 258 matches, 137 of which related to kinetics and 121 related to growth rate datasets. Only experimental data obtained in raw meat and kinetics with more than five points were kept in the analysis. Finally, a set of 108 data points was generated; the temperature was in the range of 0 to 40°C and the value of pH in the range of 5.3 to 7.0. A Gamma model (Zwietering *et al.* 1992) was used to fit the square root of growth rates as a function of temperature and pH (Figure 1).

To determine the heating regime of consumers, information from cuisine practice, literature and from industrial partners was used. The piece of meat was considered as contaminated only on its surface since the sterility of the muscle is a widely accepted assumption (Gill and Penney 1977). For cooking, red and roe deer meat was assimilated to beef, wild boar to pork. Roast was assimilated to a cylinder, with a temperature (°C) at the surface of the meat described by a Pert probability distribution function, Pert(80, 90, 100). The cooking times (min) of a 1 kg-roast were described by Uniform functions: U(30, 60) and U(60, 120) for red/roe deer and wild boar, respectively (Obuz *et al.* 2002). For stewing meat, 1 kg meat was assimilated to 20 small cylinders, with a temperature (°C) at the surface of the meat described by a Uniform function, U(90, 100), for both red/roe deer and wild boar (Laroche 1988) and a cooking time (min) described by a Uniform function, U(60, 240).

The microbial thermal reduction was estimated using a log linear thermal inactivation model, in which D and Z values were picked from a literature review (van Asselt and Zwietering 2006) (Table 1).

Monte Carlo simulation and software.

The four scenarios of consumer exposure were built in Excel (version 2003, Microsoft). The Monte Carlo simulation was carried out with the Add-in @Risk (version 5.5.1 Professional Edition, Palisade Corporation). For each scenario, 100 000 iterations were run.

Table 1: Thermal inactivation parameters utilized in the exposure assessment model.

Thermal inactivation parameter	**Coagulase + staphylococci**	***C. perfringens*, vegetative cell**	***C. perfringens*, spores**	***L. monocytogenes***
Z value (°C)	8.8	10.3	16.8	7
log D*	0.33	0.32	0.43	0.78
T_{ref}	70	70	120	70

* upper limit of 95% confidence interval

Results and Discussion

The exposure assessment model was run for three hazards and four scenarios. The output was the probability distribution of the quantity of hazards in a 200g-consumer portion, once the meat is cooked. In Figure 2, this output is illustrated with the spores of *C. perfringens* in red/roe deer stewing meat. The mean of the distribution was assessed to 1.09 log per 200 g-consumer portion, the 95 th percentile to 4.31 log per portion.

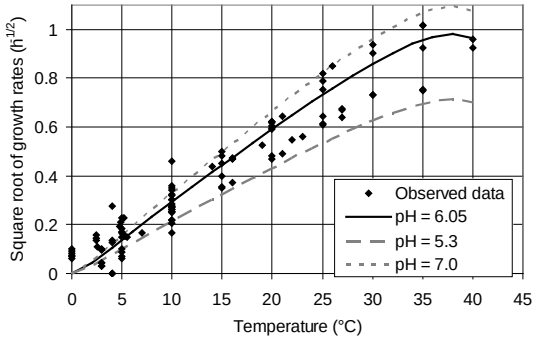

Figure 1: Growth rates of *L. monocytogenes* in raw beef vs temperature. Observed data (symbols) and model at mean, min and max pH values (lines).

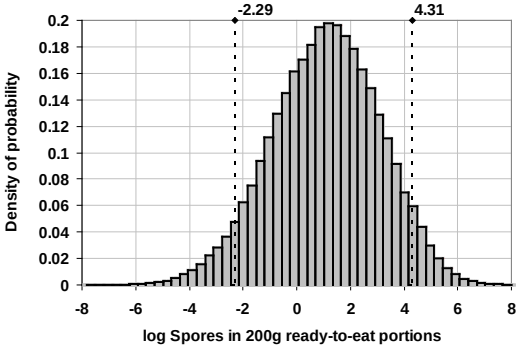

Figure 2: Predicted amount of spores of *C. perfringens* in a ready-to-eat 200 g- portion of red/roe deer stewing meat. The 5 th and 95 th quantiles are depicted with dotted lines

Whatever the type of meat, the probability of having one bacteria in a 200 g-portion was estimated to be null ($Pr(\log \text{bacteria} \geq 0) \leq 0.00\ \%$) for coagulase + staphylococci and *L. monocytogenes*. For the latest microorganism, even if the growth in refrigerated cabinets and domestic refrigerators was assessed to be important (mean increase of 4.48 log cfu/g), the pathogen was eradicated from the meat at the cooking step. However, if the consumer preparation / cooking habit moves to rare meat, or even worse, to carpaccio-type dishes, as encouraged by the modern cuisine, this current assessment will be different ; the consumer exposure to *L. monocytogenes* will not be negligible.

For *C. perfringens*, the exposure assessment model was run for both vegetative cells and spores. Indeed, in the animal digestive track, the *C. perfringens* hazard is present as spores which contaminate the meat during the evisceration. Some of these spores may germinate and outgrow during the meat cutting, conditioning and distribution.

The model output indicated that the vegetative cells were eliminated during the cooking step whatever the game species and type of meal, i.e. the probability of having one vegetative cell in a 200 g-portion was estimated to be null ($Pr(\log \text{vegetative cells} \geq 0) \leq 0.00\ \%$).

However, it is likely to have mostly spores of *C. perfringens* contaminating the raw meat. In this case, it was established that these spores survived the cooking step to end up in the consumer portion (Table 2 and Figure 2). Particularly with roasting meat (less cooked than stewing meat), the probability of exceeding 10^5 spores / g was not negligible: 0.32 % and 0.98 % in red/roe and wild boar meat, respectively. This level of contamination is important to bear in mind since $\geq 10^5$ cells of *C. perfringens* per g can cause foodborne illness (Golden *et al.* 2009).

Table 2: Probability of obtaining spores of C. *perfringens* in a 200 g - portion of cooked meat.

	Roasting meat		Stewing meat	
X value in the Pr(log spores ≥ X) formula	Red and roe deer	Wild Boar	Red and roe deer	Wild Boar
X = 1 spore	99.45%	99.71%	70.83%	73.67%
X = 10^4 spores	36.71 %	49.86 %	7.05 %	16.17 %
X = **Infectious dose** = 200×10^5 (10^5 spores / g)	**0.32%**	**0.98%**	**0.03%**	**0.24%**

Consequently, the risk of having the consumer exposed to *C. perfringens* depends on his/her eating habits. Indeed, if the meat is eaten quickly after the cooking, the exposure is still low because the spores surviving the heat treatment have no time to germinate. Inversely, if the meat dish once cooked, is not eaten quickly but kept at room temperature for several hours, spores of *C. perfringens* may germinate and outgrow to become vegetative cells able to produce toxin. In the exposure assessment, the value 10^5 cells of *C. perfringens* per g has been considered as an infectious dose (Golden *et al.* 2009), however this value might be revisited if more data becomes available.

To enhance public health, reduction of the prevalence of *C. perfringens* in raw meat is needed. That might be achieved by improving better hunting practices across European countries and encouraging good hygienic practice in large wild game meat.

Conclusion

An exposure assessment of large wild game meat distributed in France was conducted. It indicated that consumers were not significantly exposed to coagulase + staphylococci and *L. monocytogenes*, once the meat is properly cooked. On the other hand, with *C. perfingens*, a consumer may be exposed if the meat, once cooked is cooled down at room temperature and eaten after several hours. Performing a consumer exposure assessment brings an added value in terms of evaluating public health. Even with simple scenarios, the impact of a high raw meat contamination level is weighted in term of actual consequences for the consumer.

Acknowledgements

The DGAl (French Ministry of Food and Agriculture), Dr. Béatrice Poignet and the five industrial partners are gratefully acknowledged for their financial and technical support.

References

Bertolini R., Zgrablic G. and Cuffolo E. (2005) Wild Game Meat: Products, Market, Legislation and Processing Controls. *Veterinary Research Communications* 29, 97-100.

Derens E., Guilpart J., Palagos B. and Prosen E. (2004) Données chiffrées sur la chaîne du froid des produits réfrigérés. *Revue Générale du Froid* 1045, 27-32.

Derens E., Palagos B. and Guilpart J. (2006) The cold chain of chilled products under supervision in France, p. 51-64, IUFoST World Congress. http://dx.doi.org/10.1051/IUFoST:20060823 (Accessed on 12/04/2011).

Gill C.O. and Penney N. (1977) Penetration of bacteria into meat. *Applied and Environmental Microbiology* 33, 1284-1286.

Golden N.J., Crouch E.A., Latimer H., Kadry A.R. and Kause J. (2009) Risk assessment for *Clostridium perfringens* in ready-to-eat and partially cooked meat and poultry products. *Journal of Food Protection* 72, 1376-1384.

Laroche M. (1988) La Cuisson. In: Girard, J. P. (Ed.), *Technologie de la Viande et des Produits Carnés*. Chapter 2, 33-82. Technique et Documentation - Lavoisier, Paris, France, 280 pp. (ISBN 2-85206-439-1)

Membré J.M., Laroche M. and Magras C. (2011) Assessment of levels of bacterial contamination of large wild game meat in Europe. *Food Microbiology* 28, 1072-1079.

Obuz E., Powell T.H. and Dikeman M.E. (2002) Simulation of cooking cylindrical beef roasts. *Lebensmittel-Wissenschaft und-Technologie* 35, 637-644.

Reinken G. (1998) Erzeugung und Handel von Wild- und Hirschfleisch in Europa. *Zeitschrift für Jagdwissenschaft* 44, 167-177.

van Asselt E.D. and Zwietering M.H. (2006) A systematic approach to determine global thermal inactivation parameters for various food pathogens. *International Journal of Food Microbiology* 107, 73-82.

Zwietering M.H., Wijtzes T., de Wit J.C. and Van't Riet K. (1992) A decision support system for prediction of the microbial spoilage in foods. *Journal of Food Protection* 55, 973-979.

Development of a quantitative risk assessment for cheese made from raw goat milk contaminated by *Listeria monocytogenes*

L. Delhalle[1], M. Ellouze[2]; A. Clinquart[1], G. Daube[1], M. Yde[3], N. Korsak[1]

[1] University of Liège, Faculty of Veterinary Medicine, Department of Food Science, Sart-Tilman, B43bis, 4000 Liège, Belgium (l.delhalle@ulg.ac.be)
[2] IFIP, French Institute for Pig and Pork Products, Fresh and Processed Meats Department, 7, Avenue du Général de Gaulle, 94 704 Maisons Alfort, France. (mariem.ellouze@ifip.asso.fr)
[3] Scientific Institute of Public Health, Bacteriology section, Rue Juliette Wytsmanstraat 14 - 1050 Brussels, Belgium (Marc.Yde@wiv-isp.be)

Abstract

A retrospective study was performed to assess the potential risk of human listeriosis following a contamination by *L. monocytogenes* of cheeses made from goat raw milk reported by the Belgian Federal Agency for the Safety of the Food Chain in 2005. The source of the contamination was related to a shedder goat, excreting 2.6 log cfu (colonies forming units) *L. monocytogenes* / ml without any clinical symptom. On the basis of the collected data, a quantitative microbial risk assessment model was developed covering the production chain from the milking of goats until the consumed products. Predictive microbiology models were used to simulate the growth of *L. monocytogenes* during the process of cheeses made from goat raw milk. The modular exposure assessment model showed a significant growth of *L. monocytogenes* during chilling and storage of the milk collected the day before the cheese production (increase of 1.7 log cfu/ml for the median) and during the step of starter and rennet adjunction to milk (increase of 0.8 log cfu/ml for the median). The median estimated final result (in the fresh cheese) was equal to 3.5 log cfu/g. The model estimates (expressed as median final result issued from the exposure assessment) were realistic compared to the number of *L. monocytogenes* measured in the fresh cheese (3.6 log cfu/g) reported during the cheese contamination period. The average number of expected cases of human listeriosis was between 0 and 1 for a high-risk sub-population and 0 for a low-risk healthy sub-population. Scenario analysis was finally performed to identify the most significant factors and aid in developing priorities for risk mitigation. Thus, by using quantitative risk assessment and predictive microbiology models, this study provided valuable information to identify and to control critical steps in a local production chain of goat cheese made from raw milk.

Keywords: quantitative risk assessment, predictive microbiology, goat, cheese, L. monocytogenes, raw milk

Introduction

The model presented in this paper assesses potential health risks associated with a case of contamination by *L. monocytogenes* of goat cheese made from raw milk, due to the presence in the herd of an asymptomatic "milk-shedder" goat. Using field and laboratory collected data, a modular quantitative microbial risk assessment (QMRA) model was built to simulate the food production pathway from milking of goats until the consumption of cheeses made from raw milk. The model was established in accordance with guidelines published by the *Codex Alimentarius* Commission. This QMRA uses dynamic predictive microbial models to simulate *L. monocytogenes* growth during the food processing and storage. Options of risk mitigations are finally evaluated with scenario analysis.

Materials and Methods

Monte Carlo (MC) simulations were used to obtain stochastic estimates of the output variables. The principles of the Modular Process Risk Model (MPRM) methodology were used to represent the food chain into modules and to follow the bacteriological concentration of the pathogen in function of unit size (Nauta 2001). The fresh cheeses with no ripening are

the most sold cheese in farm this and were chosen for the exposure assessment model. The model simulated the main events involved in the cheese processing: growth of microorganisms, mixing of milk and partitioning of curd.

Exposure assessment

The exposure assessment model comprised the following eight modules: (1) storage of the evening milk, (2) storage of the morning milk, (3) mixing of the morning and evening milk (4) adjunction of ferment to milk, (5) adjunction of rennet to milk, (6) draining off of curds, (7) storage and salting at ambient temperature and (8) cooled storage and wrapping. The input values were implemented as estimated distributions of probability, which described the natural variability (Delhalle *et al.* 2011). Each module generated an output that was used as an input for the next module. The effect of temperature, pH and water activity on the maximum growth rate of *L. monocytogenes* was modelled by the gamma concept with the square root model without interactions (Augustin et *al.* 2005; Pouillot and Lubran 2011). The primary growth model used was the three phase linear model without lag (Buchanan et *al.* 1997). The starting point of the model is the initial concentration of *L. monocytogenes* in the milk from the right part of the mammary gland of the contaminated goat measured by the Belgian Food Agency (2.6 log cfu). The final output of the exposure assessment model is the number of *L. monocytogenes* per cheese serving. This result was compared for validation purposes with data collected during the characterization of the contaminated cheeses by the Belgian Food Agency.

Hazard and risk characterization

The exponential dose-response model for *L. monocytogenes* was chosen (FAO/WHO 2004). The outputs from the exposure assessment were fed into the dose-response model to develop the risk characterization in order to estimate the potential number of human listeriosis cases. It was assumed that the number of contaminated servings corresponds to the number of exposed people. Based on the official statistics of the Belgian population, (proportions of normal and susceptible population are 74 % and 26%, respectively), the final output was expressed as the number of human listeriosis cases for normal and susceptible population.

Scenario analysis

The effect of some variables was assessed using simulation scenarios to provide valuable possibilities to reduce the final risk of human listeriosis cases after consumption of contaminated cheese. The scenarios are described in Table 2.

Results and Discussion

The results indicate that the growth of *L. monocytogenes* was decreased when the pH was around the pH_{min}. In the model, the pH of the product decreases after adjunction of ferment and rennet to 4.4 at the end of these steps. After that, *L. monocytogenes* could grow slowly. Table 1 gives the base line results of the exposure assessment model and the risk characterization modules.

The modular exposure assessment model shows a significant growth of *L. monocytogenes* during chilling and storage of the milk collected the day before the cheese production (increase of 1.7 log cfu/ml for the median) and during adjunction of starter and rennet to milk (increase of 0.8 log cfu/ml for the median).

Figure 1 gives the evolution of *L. monocytogenes* concentration during the process under environmental dynamic conditions. During the storage of the evening milking over night, the milk is slowly chilled from 39.5 to 10°C (Figure 1a). The pH decrease when the ferment is added to the milk and the growth of *L. monocytogenes* is slowed (Figure 1b).

The estimated median final result in the fresh cheese was equal to 3.5 log cfu/g . The model estimates issued from the exposure assessment were realistic compared to the number of *L. monocytogenes* reported in the fresh cheese by the Belgian food agency (3.6 log cfu/g).

Table 1: Baseline results of the exposure assessment and the risk characterization modules along the cheese production chain.

Modules	Item	Percentiles			Unit
		5th	50th	95th	
Milking	Concentration of *L. monocytogenes* in the tank	-5	0	0.47	log cfu/ml
Storage of the evening milk	Concentration in milk in the tank after night storage	-3.6	1.7	2.4	log cfu/ml
Adjunction of ferment and rennet	Concentration before draining off the curds	-2.9	2.5	3.6	log cfu/ml
Draining off the curds	Number of *L. monocytogenes* per cheese	-0.91	4.5	5.6	log cfu/cheese
	Concentration of *L. monocytogenes* in a cheese	-2.9	2.5	3.6	log cfu/g
Cooled storage and wrapping	Concentration of *L. monocytogenes* in a cheese	-2.0	3.5	5.9	log cfu/g
	Number of *L. monocytogenes* per cheese serving	-0.4	5.2	7.5	log cfu/serving
Human effect	Risk of human listeriosis (normal population)	0	0	0	
	Risk of human listeriosis (susceptible population)	0	0	0.00002	
	Total number of human listeriosis	0	0	1	people

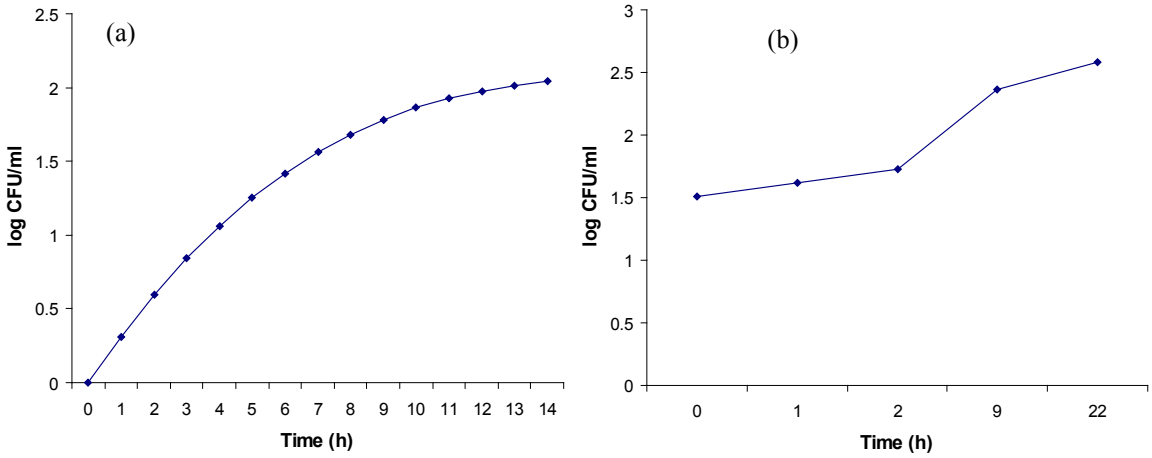

Figure 1: Evolution of *L. monocytogenes* concentration during (a) the storage of the evening milk and (b) the adjunction of rennet to milk steps.

In this episode of contamination, the potential number of expected cases of listeriosis due to the consumption of goat cheese made with raw milk was estimated between 0 and 1 case for the high-risk sub-population and 0 for the low-risk healthy sub-population. The results of the scenario analysis are displayed in Table 2. The outputs are the number of *L. monocytogenes* per cheese serving. The results obtained for the first scenario show that, the installation of a heat exchanger after milking could reduce the median concentration by 1.1 log cfu/g compared with the baseline results and could be a good alternative for risk mitigation. The results obtained for the second scenario prove that a reduction of 0.5 pH units at the start of

the adjunction of ferment and rennet could only reduce by 0.1 log cfu/g the median concentration compared with the baseline results. The results obtained for the last scenario, which combines scenario 1 and 2 show a reduction of 1.3 log cfu/g of the median concentration compared with the baseline results.

Table 2: Results of scenarios analysis displayed *L. monocytogenes* concentration in a cheese serving.

Scenarios	**Percentiles**		
	5th	**50th**	**95th**
Baseline results : Concentration of *L. monocytogenes* in a cheese	-2.0	3.5	5.9
Scenario 1: installation of a heat exchanger plate to obtain a temperature of 7 °C directly after milking and maintain a constant temperature during the overnight storage.	-3.2	2.4	4.4
Scenario 2: pH reduction of 0.5 units at the start of adjunction of ferment and rennet. This could be achieved, for example, by adjunction of lactic acid.	-2.2	3.4	5.6
Scenario 3: Increase efforts along the production by combining previous scenarios	-3.3	2.2	4.2

Conclusions

In this paper, the modular process risk model (MPRM) was used as a QMRA modelling framework. Bacterial growth was modelled with dynamic predictive microbiology models to give an useful tool to understand and control the contamination trough the production chain. Scenario analysis gave managing options to effectively reduce the risk of human listeriosis by consumption of chesses made from goat raw milk. This study thus shows a practical case of the use of QMRA and predictive modelling as efficient tools to increase food safety, especially at local level.

References

Augustin J. C., Zuliani V., Cornu M. and Guillier L. (2005) Growth rate and growth probability of *Listeria monocytogenes* in dairy, meat and seafood products in suboptimal conditions. *Journal of Applied Microbiology* 99(5), 1019-1042.

Buchanan R. L., Whiting R. C. and Damert W. C. (1997) When is simple good enough: a comparison of the Gompertz, Baranyi, and three-phase linear models for fitting bacterial growth curves. *Food Microbiology* 14(4), 313-326.

Delhalle L., Ellouze M., Yde M., Clinquart A., Daube G. and Korsak N. (2011) Retrospective analysis using quantitative microbial risk assessment of a *Listeria monocytogenes* contamination episode of cheese made from raw goat's milk. *International Journal of Food Microbiology* (submitted).

FAO/WHO (2004). Risk assessment of *Listeria monocytogenes* in ready to eat foods. Geneva: Food and Agriculture Organization of the United Nations/World Health Organization.

Nauta M. J. (2001) A modular process risk model structure for quantitative microbiological risk assessment and its application in an exposure assessment of Bacillus cereus in a REPFED, National Institute of Public Health and the Environment, Bilthoven, The Netherlands, 100 pp

Pouillot R. and Lubran M. B. (2011) Predictive microbiology models vs. modeling microbial growth within Listeria monocytogenes risk assessment: What parameters matter and why. *Food Microbiology* (in press).

The paradox of validating a Monte Carlo model that predicts non-testable microbial contamination risks

B.M. de Roode, J. Meeuwisse, E. Wemmenhove, M.H.J. Wells Bennik

NIZO food research, Ede, The Netherlands

Abstract

Improved process quality control in most food processes have resulted in non-testable small risks with respect to microbial contamination. We applied Monte Carlo simulation to evaluate the risk of *Listeria monocytogenes* contamination for the complete production and consumer cycle of fresh consumer milk. To validate the results of this model, the first five steps of the model were recreated on a laboratory scale.

A comparison between the outcome of the model simulations and experimental data showed that the experimental results fitted the model reasonably well. However, in case of inactivation the experiments were often outside the predicted confidence intervals. The differences between the model and experimental data were biased; therefore the following actions will be executed before introducing fit parameters in the model: a) using a broader range of inactivation data and b) repeat the current laboratory scale experiment.

Keywords: Listeria monocytogenes, milk, Monte Carlo simulation, contamination risk

Introduction

Improved process quality control in most food processes have resulted in non-testable small risks with respect to microbial contamination. Efforts to find the contaminated product in the total production would lead to sampling regimes that are impossible in practice. Therefore, Monte Carlo simulation is a powerful tool to evaluate this non-testable small microbiological contamination risk in food products. More specifically, we applied this tool to evaluate the risk of *Listeria monocytogenes* inactivation and/or outgrowth for the complete production and consumer cycle of fresh consumer milk upon introduction of a given contamination. Although these simulations are powerful in giving an insight in the magnitude and variability of the risk of contamination, the paradox is that it is not possible to validate the outcome of the model with experiments. Ways to circumvent this paradox is the introduction of response-dose data to retrofit the results of the risk characterization (for example Barron *et al*. 2010). However, data are scarce making the link more difficult. Therefore, we propose to test the robustness of our model by the introduction of inactivation and growth data of selected micro-organisms and mimicking the process on laboratory scale. In the current study the results are presented from a validation on laboratory scale of the first five steps of the consumer milk process.

Materials and Methods

Software

The Monte Carlo model was created in Microsoft Excel with the @Risk add in for Excel (Version 5.5.0, Palisade Corporation, New York, USA).

Model of the consumer milk cycle

A full production and consumer cycle of the consumer milk of 12 subsequent steps was created. However, to show the proof of principle of the current validation method only the first 5 steps of the full cycle were used. The description of all input and output variables per process step are described in Table 1.

Table 1: General model of the first five steps of the consumer milk process with the input variables, the distribution and outputs per process step. C_{in}: initial microbial contamination in CFU/kg, T_x: temperature in the process step (^oC) , t_x: residence time in the process step (hrs or sec.), pH_x: pH in the process step (-), aw_x: water in activity in the process step (-), C_x: microbial contamination after each process step (CFU/kg).

Step	Process	Input variables	Model/distribution*	Output
1	Initial contamination	C_{in}	Normal	-
2	Initial storage	C_{in}	Gamma	C_2
		T_2	Pert (4.9, 5.0, 5.1)	
		t_2 (h)	Pert (1.9, 2.0, 2.1)	
		pH_2	Fixed value	
		aw_2	Fixed value	
3	Secondary storage	C_2	Gamma	C_3
		T_3	Pert (3.9, 4.0, 4.1)	
		t_3 (h)	Pert (17.9, 18.0, 18.1)	
		pH_3	Fixed value	
		aw_3	Fixed value	
4	Thermisation	C_3	Arrhenius	C_4
		T_4	Pert (61.9, 62.0, 62.1)	
		t_4 (sec)	Pert (30, 33, 45)	
5	Pasteurisation	C_4	Arrhenius	C_5
		T_5	Pert (74.9, 75.0, 75.1)	
		t_5 (sec)	Pert (15, 18, 33)	

* Although most temperatures and residence times in the well controlled and monitored laboratory equipment showed a balanced behaviour around an average value, the pert distribution was chosen for its natural truncation and a higher probability density between the most likely value and both limits.

After an initial Monte Carlo simulation the variance in the results converged after ca. 10.000 iterations. Hence, all following simulations were based on this number of iterations.

Inactivation and growth models

Inactivation of *L. monocytogenes* was modeled by using publically available inactivation data (van Asselt and Zwietering 2006, Combase) in liquid products and fitting the data to first order kinetics according to Arrhenius. The fitted values for lnk_0 and E_a are -3.77 and 333,433 respectively. The variance based on the linear fit to the data was added to the model with a normal distribution.

Growth of *L. monocytogenes* was modeled by using the Gamma model (te Giffel and Zwietering 1999) with the following minimum and optimum values (see Table 2):

Table 2: Minimum and optimum values that where used in the Gamma model.

Variable	X_{min}	X_{opt}
T (^oC)	0	37
pH (-)	4.32	6.70
Aw (-)	0.92	-

Initially, the values in the gamma model where not varied in the Monte Carlo simulation.

Cultivation of L. monocytogenes *strains*

Three strains of *L. monocytogenes* (Scott A, L4 and 1E, all milk isolates from the NIZO culture collection) were cultivated overnight in BHI at 30^{o}C. Subsequently, the cultures were mixed with 20 ml of glycerol and 100 ml of BHI and stored in 1 ml vials at -20^{o}C. After 1 week the concentration of viable cells was measured. Aliquots of these stocks were used to artificially contaminate milk (see details below).

Consumer milk cycle on laboratory scale

Cooling and heating cycles were performed in a GeneAmp PCS system 9700 in order to control and monitor temperature and residence time accurately.
Triplicates of each of the three frozen strains were diluted to result in an estimated final concentration of 10^3 CFU/ml in sterile skimmed milk (Milzani). The contaminated milk was then stored at 2°C. Per strain 15 vials were filled with 0.1 ml of contaminated milk and placed in a temperature controlled system. The viable numbers per strain were assessed by plating on BHI agar plates and incubation was performed at 30°C for 48h.
The process settings are given in Table 3.

Table 3: Process setting in the PCR system for four subsequent steps.

Step (conform table 1)	Process	Temperature (°C)	Time*
2	Initial storage	5 ± 0.05	2 h
3	Secondary storage	4 ± 0.05	18 h
4	Thermisation	62 ± 0.05	30 sec
5	Pasteurisation	75 ± 0.05	17 sec

* The cooling time in step 2 and 3 were 30 and 7 sec. respectively. After step 5 a cooling step of 36 sec was introduced to a temperature of 1°C. These additional residence times are reflected in the distribution of the residence time in table 1.

Results and Discussion

Validation of the Monte Carlo model with laboratory experiments

Since the initial contamination levels of milk differed slightly between the three strains, the validation was performed individually for each strain. A typical result of the simulation and the laboratory validation is given in Figure 1.

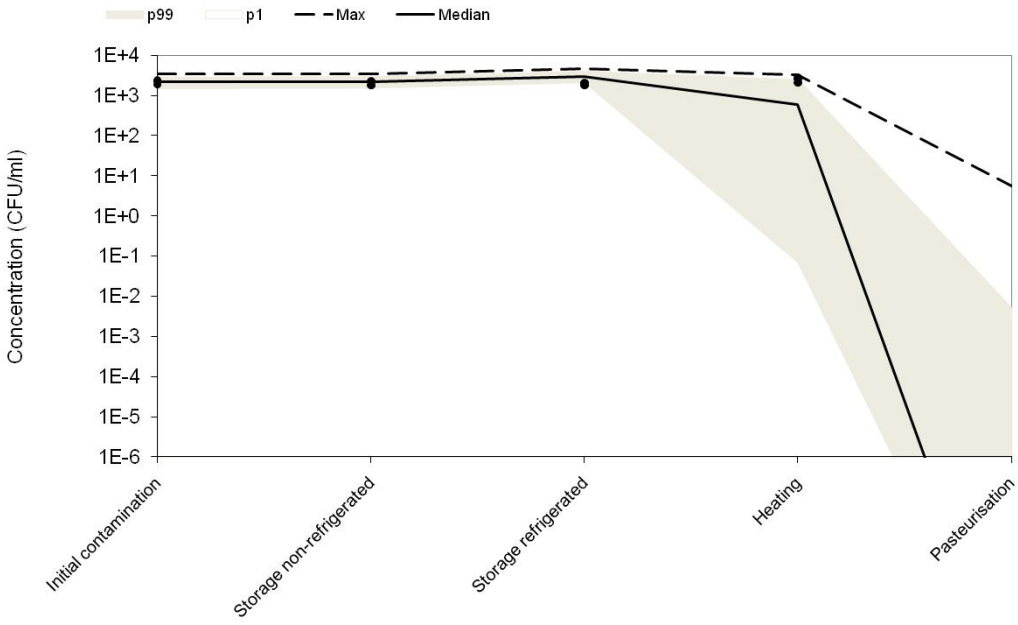

Figure 1: Experimental results (black dots) and Monte Carlo simulation (black line) of *L. monocytogenes* Scott A contamination in milk for the first five steps of the consumer milk process after 10.000 iterations. Dotted black line: maximum contamination, grey area: 99% probability area. Results after the pasteurization step are not shown.

From Figure 1 it can be concluded that the experimental results are in line with the simulation results. In all cases it appears that the experimental values fit in the 90% probability area of the simulation. Inactivation was established at a level of $\geq 10^{2}$ after the pasteurization step. From the model an inactivation of $\geq 10^{12}$ was calculated (not shown in Figure 1). Based on the current dilution factor, no full validation of this result can be established. Therefore, the results after the pasteurization step will not be included in the validation.
If we compare the experimental viable counts with the median viable count from the simulation the differences between simulation and experiment appear larger than shown in Figure 1. Especially in the case of the thermisation step, the experimental results show a broad variability even outside the predicted confidence intervals. In case of the two storage steps the experiments fit the model data reasonably well.

Possible causes for non-fitting

Regarding the large deviation between inactivation data and model, the current kinetics are based on single step inactivation experiments without consideration of the effect of subsequent cooling and heating steps. In addition, a selection was made for inactivation data from liquid products. Expanding the dataset would introduce more (undesired) variance but would also make the model more robust.
Finally, although the variability in the experiment was safeguarded by using three different strains and measuring triplicates for every single step, the results are based on one experiment. Therefore, the experiment will be repeated. Hopefully, using more independent experiments will have an effect on the current unbalanced correlation between model and experiments.

Conclusions

Currently, the Monte Carlo model does fit the experimental data reasonably well. Optimisation routes were identified and can be categorized into: a) using a broader range of inactivation data and b) repeat the current laboratory scale experiment. Both routes will be evaluated and included in the presentation.

Acknowledgements

The current research was commisioned by the Dutch organisation for dairy research.

References

van Asselt E.D., Zwietering M.H. (2006) A systematic approach to determine global thermal inactivation parameters for various food pathogens. *International Journal of Food Microbiology* 107, 73-82.

Barron U.G., Redmond G. and Butler F. (2010), Risk characterization of Salmonella typhimurium from consumption of irish fresh prok sausages. *Proceedings of the 6th international conference on simulation and modeling in the food and bio-industry 2010* 147-153.

Combase (2003), http://www.combase.cc/default.html (accessed between March 2009 and December 2010).

te Giffel, M.C. and Zwietering, M.H. (1999) Validation of predictive models describing the growth of *Listeria* monocytogenes. *International Journal of Food Microbiology* 46 135-149.

Risk assessments of *Listeria monocytogenes* in Dutch-type semihard cheese: incorporating variability in both product parameters and microbial growth parameters

E. Wemmenhove[1,2,3], M.H. Zwietering[2], A.C.M. van Hooijdonk[3], M.H.J. Wells-Bennik[1]

[1] NIZO food research, Ede, The Netherlands
[2] Wageningen University, Laboratory of Food Microbiology, Wageningen, The Netherlands
[3] Wageningen University, Product Design and Quality Management, Wageningen, The Netherlands

Abstract

Dutch-type Gouda cheeses made from pasteurized milk have not been associated with growth of *Listeria monocytogenes*, the causative agent of listeriosis. To further validate the microbiological safety of these cheeses, compounds with potential bacteriostatic or bactericidal action against *L. monocytogenes* were identified and the natural variation in concentrations was evaluated (experimentally and through literature review). In addition, the sensitivity of *L. monocytogenes* for these compounds was experimentally determined using a variety of strains and by literature review. The variability of compounds present in Gouda cheese and sensitivity amongst *L. monocytogenes* strains were subsequently incorporated in a risk assessment model to predict the fate of *L. monocytogenes* in Gouda cheese.

Compounds that potentially inhibit *L. monocytogenes* in semi-hard cheese were identified as lactic, acetic, propionic and citric acid, diacetyl, lactoferrin, nitrate, nitrite and nisin and the enzyme lactoperoxidase. Of the potential inhibiting compounds in cheese, undissociated lactic acid has the largest inhibiting effects on *L. monocytogenes*. Additional experiments were performed to assess the efficacy of undissociated lactic acid to inhibit 6 different strains of *L. monocytogenes* at pHs relevant to cheese (pH 4.2-6.0). By taking the variation of both product parameters and microbiological growth parameters into account, critical factors for growth inhibition of *L. monocytogenes* in Gouda cheese were identified. The approach followed is applicable to all bacteria in all kinds of liquid, soft or (semi)hard foods.

Together with pH, temperature and water activity, undissociated lactic acid has a prominent role in inhibition of *L. monocytogenes* in Gouda cheese. Undissociated lactic acid has therefore been incorporated into a predictive model on the fate of *L. monocytogenes* in Gouda cheese in time.

Keywords: *Listeria monocytogenes, Gouda cheese, lactic acid, microbial sensitivity, inhibiting compounds, MIC, critical factors*

Introduction

Listeria monocytogenes is a severe food-borne pathogen as it can cause listeriosis, which is a rare *food*-borne infection with a high case-fatality rate (20%). Listeriosis is mainly a risk for immune-compromised people, but *L. monocytogenes* is ubiquitous and difficult to ban from the food processing environment. Therefore predictive models for the pathogen during food production are necessary. To predict whether *L. monocytogenes* is unable to grow in a food product, simple and more complex predictive models are used. Simple models for growth of *L. monocytogenes* in food incorporate pH, temperature and water activity. More complex models are extended with factors like organic acids, CO_2 and nitrite concentration. Such predictive models do not always incorporate the right critical parameters for growth, as the critical factors differ largely for specific foods. It is essential to determine the right critical growth parameters, as incorporation of the wrong parameters can lead to strong over- or underestimation of risks. This work presents a systematic way to determine the critical factors for growth of *L. monocytogenes* in Gouda cheese in addition to pH, temperature and water activity. Gouda cheese is a semi-hard cheese made from pasteurized milk. Semi-hard cheese is a highly complex product for food modelers, as it is a solid fermented product, made from starter-induced curds. Previous challenge tests show that growth of *L. monocytogenes* is not

promoted in Gouda cheese. The critical parameters for this growth inhibition need to be determined in Gouda cheese in order to build a good predictive model for *L. monocytogenes*. The presented approach is applicable for all pathogens in fluid and (semi)solid food products and reduces the chance of over- or underestimation of growth.

Materials and methods

Identification of critical factors for growth of L. monocytogenes in Gouda cheese

A literature research was performed for growth-inhibiting factors that inhibit growth of *L. monocytogenes* in Gouda cheese. First, the components were listed that are present in Gouda cheese which can cause growth inhibition of Gram-positive bacteria. The concentration of these compounds needed for growth inhibition of *L. monocytogenes* was reviewed, and the concentration at which these components are present in cheese was determined as well. A compound was evaluated as critical for growth when the concentrations of the compound present in Gouda were higher or in the same range as the concentration needed for suppression of growth of *L. monocytogenes*, as observed in culture medium. Undissociated lactic acid was evaluated as critical for growth of *L. monocytogenes* and the existing lactic acid data set was limited. Therefore, additional experiments have been performed to determine the undissociated lactic acid concentration needed for growth inhibition of *L. monocytogenes* (MIC) at different pHs.

Determination of MIC of undissociated lactic acid for growth inhibition of L. monocytogenes.

L. monocytogenes strains Scott A (4b, milk isolate), EGDe (1/2a, rabbit isolate), 1F (1/2a, cheese isolate), 2F (1/2a, cheese isolate), 6E (1/2a, cheese equipment isolate) and L4 (1/2b, milk isolate) were used (NIZO culture collection). The strains were cultivated overnight (18 hours) in BHI. The cells in the overnight culture were harvested and resuspended in BHI of the desired pH and added to 96 wells plates with BHI and lactic acid at set pHs, with final *L. monocytogenes* concentrations of $1.8*10^6$ cfu/ml. *L. monocytogenes* strains were exposed to lactic acid independently and in three-fold and experiments were reproduced in an independent experiment.

The minimal undissociated lactic acid concentration needed for growth inhibition (MIC) was determined in BHI in triplicate in 2 independent experiments for 6 *L. monocytogenes* strains at small increments of lactic acid (0-1.67 M) and pH (4.2-6.0) (Table 1) and 12 and 30°C. The MIC was evaluated by optical density measurements and enumeration of viable numbers (comparison of optical density and viable numbers after 30 days incubation at 30°C to inoculum). The MIC values were calculated by the Henderson-Hasselbalch equation:

$$Undissociated\ acid = \frac{Total\ acid\ concentration}{1+10^{pH-pKa}} \quad (1)$$

Lactic acid was set at the target pH by use of predetermined molarities of lactic acid and potassium lactate (experiment 1). In addition, the interaction in growth inhibition of lactic and acetic acid was studied at 30°C by a combination of 0, 5 and 10 mM undissociated lactic and acetic acid (experiment 2).

MIC values of *L. monocytogenes*, as determined in BHI at pH 5.0-5.6 were compared with literature MICs in broth with cumulative frequency distributions based on Monte Carlo simulations (Microsoft Excel with the @Risk add in for Excel, Version 5.5.0, Palisade Corporation, New York, USA).

Table 1: Intervals of total lactic and acetic acid concentrations and pH chosen in experiment 1 (lactic acid), experiment 2 (lactic & acetic acid).

Experiment	pH	Lactic acid concentration (M)	Acetic acid (mM) concentration
1	4.2-4.4-4.6-4.8-5.0-5.2-5.6-5.8-6.0	0-0.02-0.03-0.04-0.06-0.08-0.1-0.12-0.15-0.19-0.24-0.37-0.43-0.67-1.06-1.67	-
2	5.2-5.6	0-0.11-0.23	0-0.02-0.04

Results and discussion

Determination of critical factors for growth of L. monocytogenes in Gouda cheese

Compounds that potentially inhibit *L. monocytogenes* in semi-hard cheese were identified as lactic, acetic, propionic and citric acid (Table 2), diacetyl, lactoferrin, nitrate, nitrite and nisin and the enzyme lactoperoxidase (Table 3). The concentrations of the compounds as found in Gouda were divided by the concentration at which growth was inhibited by the compound. When this resulted in values larger than 1, the compound was evaluated as critical for growth of *L. monocytogenes*. In Table 3 it is shown that diacetyl, nitrate and nitrite do not have an inhibitory effect on *L. monocytogenes*. Nisin is not present in Gouda, but could have an inhibitory effect of *L. monocytogenes* in other types of semi-hard cheeses that contain nisin-producing starter cultures. At the concentration present in cheese, lactoferrin could inhibit growth of *L. monocytogenes* based on broth experiments, but in milk higher concentrations lactoferrin were needed for growth inhibition, so lactoferrin is not expected to inhibit growth of *L. monocytogenes* in Gouda cheese; Calcium could possibly counteract the inhibiting activity of lactoferrin. Lactoperoxidase is not completely inactivated after pasteurisation, but as it is known to only increase the lag time of *L. monocytogenes* in milk, lactoperoxidase will not prevent growth of *L. monocytogenes* in semi-hard cheese. As concentrations of diacetyl, lactoferrin, nitrate, nitrite, nisin and lactoperoxidase present in Gouda are much lower than the concentration needed for inhibition, no further study on the variation of the concentrations present and the sensitivity of *L. monocytogenes* has been performed.

Table 2 Identification of critical parameters for growth of L. monocytogenes by dividing the present concentrations of organic acids in Gouda cheese at pH 5.0-5.6 by the MIC (minimal concentration of the compound needed for inhibition of growth of *L. monocytogenes*).

Compound	Concentration present in Gouda cheese (mM) at pH 5.0-5.2-5.4-5.6 / Inhibiting concentration (MIC)	Critical parameter for growth?
Lactic acid	0.6 – 13.8	Yes
Acetic acid	0.07-0.7	No
Propionic acid	0	No
Citric acid	0	No

Table 3 Identification of critical parameters for growth of *L. monocytogenes*, next to organic acids, by dividing the present concentrations in Gouda cheese at pH 5.0-5.6 by the MIC (minimal concentration of the compound needed for inhibition of growth of *L. monocytogenes*).

Compound	Concentration present in Gouda cheese (mM) at pH 5.0-5.2-5.4-5.6 / Inhibiting concentration (MIC)	Critical parameter for growth?
Diacetyl	0.012	No
Lactoferrin	<0.6 with decrease in time	No
Nitrate	<0.2	No
Nitrite	<0.01	No
Nisin	0 in Gouda (0.01-280 in semi-hard cheeses with nisin-producing starters, but decrease of effect in time)	No

Lactic acid was evaluated as critical for growth of *L. monocytogenes* in Gouda cheese (Table 2), as the concentration undissociated lactic acid present in Gouda cheese was larger or in the same range as the concentration needed for inhibition of growth of *L. monocytogenes*, as was observed in experiments with culture medium. Experimental MIC values were lower than literature data, probably due to our experimental setup in which the stepwise intervals of pH and lactic acid were smaller (Figure 1). The variability between our strains, however, was larger. Additional experiments show no synergistic effects with acetic acid and no influence of temperature (although at 12°C the lag time is increased, the MIC values were the same at 12 and 30°C).

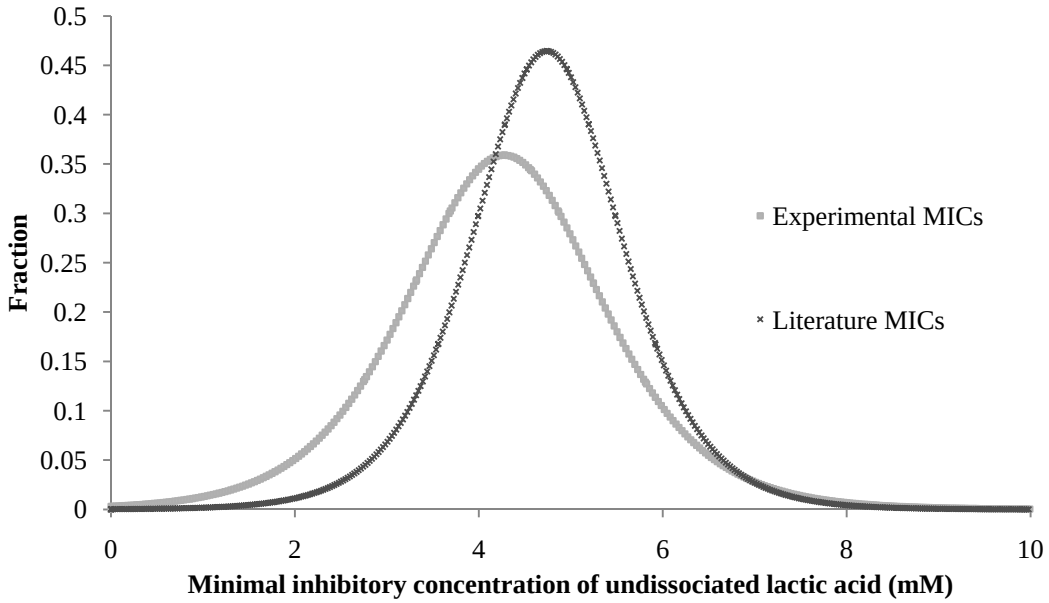

Figure 1: Comparison of minimal inhibitory concentration of lactic acid needed for inhibition of growth of *L. monocytogenes*, with a Monte Carlo simulation of the experimental and literature data.

Conclusion

Literature and experimental data on concentrations needed for growth inhibition have been compared to concentrations that are present in Gouda cheese to determine which compounds in Gouda cheese are critical for growth of *L. monocytogenes* in Gouda. Of all parameters reviewed, lactic acid was identified as the most critical growth factor and for that reason this factor was included into a *L. monocytogenes* model for Gouda cheese that incorporates variation, together with water activity, temperature and pH. Growth-inhibiting effects of calcium and sodium have not been taken into account yet. Preliminary experiments show a slight increase in MIC values when calcium and sodium are added to lactic acid at relevant concentrations for Gouda cheese, which could lower the growth-inhibiting capacity of lactic acid. The influence of calcium and sodium will be further explored.

Listeria monocytogenes – process risk modelling of lightly preserved and ready-to-eat seafood

A.C.J. Grønlund, O.Mejlholm, P.Dalgaard

Seafood & Predictive Microbiology, Division of Industrial Food Research, National Food Institute, Technical University of Denmark, Søltofts Plads, Building 221, DK-2800, Kgs.Lyngby, Denmark

Abstract

Chilled RTE seafood are of increasing economic importance in Europe but requests for mild preservation, including low sodium content, represent shelf-life and safety challenges. A range of environmental parameters influence microbial responses in these products and complex predictive models are required to predict how growth and survival of pathogenic and spoilage microorganisms can be managed. The objectives of the present study were to relate processing and storage conditions for cold-smoked Greenland Halibut and marinated cold-water shrimp with concentrations of *Listeria monocytogenes* and lactic acid bacteria (LAB) at the time of consumption and the risk of listeriosis in Denmark. Our previously validated predictive model for *L. monocytogenes* was used in combination with a newly developed and expanded version of our LAB model to predict growth of the respective microorganisms as well as microbial interaction between them. The effect of (a) a series of specific product/storage scenarios and (b) distributions of relevant environmental conditions were studied. An exponential dose-response model was used to evaluate the risk of listeriosis for consumer groups with different relative susceptibility. Cold-smoked Greenland Halibut with a high product pH close to 7 represented a significant risk for growth of *L. monocytogenes*. By adding acetic and lactic acids and thereby reducing pH close to 6 this risk was reduced to an acceptable level. Also for chilled and marinated shrimp, the combined effect of pH and different combinations of organic acids allowed growth *L. monocytogenes* and the risk of listeriosis to be managed. Growth of LAB significantly reduced the risk of listeriosis whereas typical concentrations of water phase salt (of ~3.5% or lower) had relatively little effect on the risk of listeriosis.

Keywords: *listeria, fish, RTE*

A quantitative microbial risk assessment model for Campylobacter and *Listeria monocytogenes* contamination of boxed beef trimmings from Irish abattoirs

C. Shanahan[1], G. Duffy[2], F. Butler[1]

[1]Biosystems Engineering, UCD school of Agriculture, Food science and Veterinary medicine, University College Dublin, Belfield, Dublin 4, Ireland
[2]Teagasc Food Research Centre, Ashtown, Dublin 15, Ireland.

Abstract

A quantitative microbial risk assessment using Monte Carlo simulation was developed for contamination of boxed beef trimmings in Irish abattoirs. Microbiological survey data from an Irish abattoir was used as model inputs. The prevalence and concentration of Campylobacter and *Listeria Monocytogenes* was recorded from the hide of the animal, the animals were tracked and the prevalence and concentration was also noted from the carcass post de-hiding. The model returned hide prevalence of Campylobacter as 48.5% with a concentration of 0.799 $\log_{10}$ CFU/100 cm^2, and carcass prevalence as 14.3% with a concentration of 0.455 $\log_{10}$ CFU/100 cm^2. The prevalence and concentration of *Listeria Monocytogenes* on the hide was 26.3% and 1.76 $\log_{10}$ CFU/100 cm^2, respectively and the carcass prevalence was 14.6% with a concentration of 0.855 $\log_{10}$ CFU/100 cm^2. The effect of gut rupture during evisceration was included in the model, faecal contamination data from European studies were using to indicate if the faeces were positive for Campylobacter or *Listeria Monocytogenes*. The refrigeration step for Campylobacter was modelled using three separate triangular distributions (representing log reductions of high, medium and low) this is a major source of uncertainty in the model. The results post chilling are, low reduction; prevalence 10.9% concentration 0.239 $\log_{10}$ CFU/100 cm^2, medium reduction; prevalence 10.3% concentration 0.214 $\log_{10}$ CFU/100 cm^2 and high reduction prevalence 8.6% concentration 0.138 $\log_{10}$ CFU/100 cm^2. The refrigeration step for *Listeria Monocytogenes* was modelling using data from an Irish abattoir study, giving post chilling results with a prevalence of 11.1% and concentration of 0.694 $\log_{10}$ CFU/100 cm^2. The production of 70% visual lean beef trimmings was modelled in order to predict the prevalence and concentration of the pathogens in boxed beef.

Quantitative risk assessment of chemical decontamination on *Campylobacter* on chicken skin

H. Meredith[1,3], E. Cummins[2], D. McDowell[3], D. Bolton[1]

[1]Teagasc Food Research Centre, Ashtown, Dublin, Ireland.
[2]Biosystems Engineering, School of Agricultural and Veterinary Medicine, University College Dublin, Ireland.
[3]Food Microbiology Research Unit, School of Health and Life Sciences, University of Ulster, Jordanstown, Newtownabbey, Co. Antrim, Northern Ireland, UK.

Abstract

Campylobacter is a foodborne pathogen which is excreted by warm blooded animals, mainly poultry, and has a low infectious dose. In Ireland, in 2010, there were 1,808 cases of campylobacteriosis. The objective of this study was to modify an existing Quantitative Risk Analysis (QRA) model for Campylobacter in a poultry slaughterhouse, incorporating a chemical decontamination step. The QRA used Monte Carlo simulation techniques to model various stages, including: scalding, defeathering, evisceration, chemical decontamination and human consumption. The outputs suggest that carcass washing with 14% tri-sodium phosphate (TSP) or 5% citric acid (CA) would achieve a lower mean probability of illness of 0.001 compared with the untreated carcasses with a probability of 0.02. In the poultry slaughterhouse, a sensitivity analysis identified the initial level of bacteria on the exterior of the carcass to be the most critical determinant of Campylobacter infection (correlation coefficient of 0.75). This highlights the importance of biosecurity measures on the farm in minimising the ultimate risk to the consumer. Chemical decontamination with TSP and CA are also important factors in the reduction of Campylobacter (correlation coefficient of -0.35). Leaking of feces during the slaughtering process (correlation coefficient of 0.25) and cross-contamination via the chopping board in the food preparation environment (correlation coefficient of 0.17) were also important determinants of consumer risk.

A predictive model for *Escherichia coli* O157:H7 in Salami: quantitative risk assessment

E. Cosciani Cunico[1], J. Baranyi[2], G. Maccabiani[1], G. Finazzi[1], P. Boni[1]

[1]Istituto Zooprofilattico Sperimentale della Lombardia e dell'Emilia Romagna, Italy
(elena.coscianicunico@izsler.it)
[2]Institute of Food Research, United Kingdom

Abstract

The main objective of this study is to analyse the microbial safety of some typical Italian food products by predictive microbiology tools. The data studied here have been generated at the "Istituto Zooprofilattico Sperimentale della Lombardia e dell'Emilia Romagna" (IZSLER), where the processes and the microbiological, physical, chemical variables of Italian meat products are regularly tested. A predictive model was developed from relevant data available from the ComBase database (www.combase.cc) to describe the effects of a_w and pH on the D-value of *E.coli* O157:H7. Challenge tests were carried out to validate the model, by determining the log reduction of *E.coli* O157:H7 in fermented meat product during storage. The log reduction of this foodborne pathogen during process is one of the safety requests for the trading of fermented meats. A correction factor (cf) was established to compensate for the bias between the food matrix and the culture medium in which the data used to create the predictions were generated. The corrected predictions were compared with observations in fermented meat. The validation indicators of the model were calculated with the formulae suggested by Baranyi et al. (1999). Predictive models can save cost and time compared to the traditional challenge tests. They can help to make decisions in risk assessment quickly, in order to guarantee the safety of the food. However, predictive models are just one set of tools in decision support and they should not be used without prejudice. The correct interpretation of the results needs food microbiology and technology expertise.

Probabilistic modelling of dioxins and dioxin-like PCBs consumed in dairy products

A.O. Adekunte[1], B.K.Tiwari[2], C.P. O'Donnell[1]

[1]Biosystems Engineering, School of Agriculture, Food Science and Veterinary Medicine, University College Dublin, Belfield, Dublin 4, Ireland (adefunke.adekunte@ucd.ie; colm.odonnell@ucd.ie).
[2]Manchester Food Research Centre, Manchester Metropolitan University, Manchester, United Kingdom (b.tiwari@mmu.ac.uk).

Abstract

Dairy products play an essential function in the human diet, especially for infants and children, thus their potential contamination with dioxins and DL-PCBs is of public health concern. This present study reports the dietary exposure of dioxins and DL-PCBs in infants (0-1 year), through consumption of reconstituted powdered infant formula (PIF) in addition to intake of butter, cheese, pasteurised bovine milk and yogurt by children (5-12 years) and adults (18-64 years) using probabilistic modelling. Probabilistic exposure models of dioxins and DL-PCBs in dairy products were developed using Monte Carlo simulation techniques and probabilistic distributions were used to account for uncertainty and variability in the models. The mean dioxins and DL-PCBs concentration in the dairy products were estimated as (0.72, 0.61 pg WHO-TEQ/g fat), (0.92, 0.78 pg WHO-TEQ/g fat), (0.73, 0.62 pg WHO-TEQ/g fat), (0.50, 0.17 pg WHO-TEQ/g fat) and (1.16, 0.64 pg WHO-TEQ/g fat) for butter, cheese, pasteurised bovine milk, PIF and yogurt, respectively. The simulated mean exposure of dioxins and DL-PCBs for all age groups due to consumption of dairy products were below the Provisional Tolerable Weekly Intake (PTWI) of 14 pg WHO-TEQ/kg bw/week recommended by Scientific Committee on Food (SCF) nor Provisional Tolerable Monthly Intake (PTMI) of 70 pg WHO-TEQ/kg bw/month recommended by Joint FAO/WHO Expert Committee on Food Additives (JECFA).

Keywords: *Dioxins, DL-PCBS, dairy products, exposure assessment, stochastic models*

Introduction

Dioxins (PCDD/Fs) and polychlorinated biphenyls (PCBs) are very toxic environmental pollutants that are widely distributed around the world (Wang *et al*. 2009). PCDD/Fs have been classified by International Agency for Research on Cancer (IARC) as class 1 carcinogens that are potential risks to human and animal health (Loufty *et al*. 2006). Dioxin-like PCBs (DL-PCBs) have also been considered as toxic chemicals based on their structural and toxicological behaviour, which is similar to dioxins (Van den Berg *et al*. 1998). Exposure to dioxins and DL-PCBs is associated with carcinogenic effects, developmental effects, thyroid hormone changes, immunotoxicity and delayed psychomotor functions (Tsutsumi *et al*. 2001). As a result of the toxicity of these chemicals, regulatory authorities have implemented legislative limits to minimise human exposure on daily, weekly or monthly basis.

Various sources have been identified as the pathways of dioxins and DL-PCBs in the environment, including combustion and industrial processes. Contamination of foods occurs through deposition of these compounds on plants and soils, subsequently ingested by dairy cattles. Incidences of dioxins and DL-PCBs in dairy products has been linked to contaminated animal feed (Adekunte *et al*. 2010), but the consumption of these products is considered to be an important source of human exposure

Dairy products play an essential function in the human diet, especially for infants and children. Several studies have been carried out to assess human dietary intake of dioxins and DL-PCBs from dairy products (Wang *et al*. 2009) while other studies attributed 30 % of dioxins and DL-PCBs in the total diet to dairy products (Fürst *et al*. 1992). This present study reports the dietary exposure assessment of dioxins and DL-PCBs in infants (0– 1 year)

through the consumption of reconstituted PIF in addition to intake of butter, cheese, pasteurised bovine milk and yogurt by children (5 12 years) and adults (18 − 64 years). Hence, the objective of this study was to estimate the daily dietary exposure of dioxins and DL-PCBs in the general population through the consumption of butter, cheese, pasteurised bovine milk, PIF and yogurt using probabilistic modelling approach.

Materials and Methods

Infants' consumption data were obtained from Euro-Growth study while children and adults' consumption data were from North/South Ireland food consumption database (IUNA 2001). Dioxins and DL-PCBs concentration data was extracted from available research studies. The @RISK software package, version 4.0 (Palisade Software, Newfield, USA) was used to run the simulations at 10,000 iterations using Latin Hypercube sampling, a Monte Carlo type simulation. Considering the opinion of EFSA (2006) on dealing with uncertainties in exposure assessment, uncertainty analysis was used to estimate the magnitude of concentration and consumption data on the model output.

Results and Discussion

The mean dietary exposure of infants, children and adults to dioxins and DL-PCBs through the intake of dairy products are presented in Table 1. Several studies have estimated daily dietary exposure of dioxins and DL-PCBs by multiplying concentrations data by consumption data (Loutfy *et al*. 2006). However, in this present study, dioxins and DL-PCBs exposure in dairy products was obtained employing Monte Carlo analysis to simulate a number of possible combinations of uncertainties, thus resulting in output distributions that accounts for variability.

Table 1: Mean daily exposure of infants, children and adults to dioxins and DL-PCBs.

	Daily exposure (pg WHO-TEQ/kg bw/day)											
	Dioxins						DL-PCBs					
	Infants (0 – 1 y)		Children (5 –12 y)		Adults (18 – 65 y)		Infants (0 – 1 y)		Children (5 – 12 y)		Adults (18 – 65 y)	
Dairy product	Boys	Girls	Boys	Girls	Men	Women	Boys	Girls	Boys	Girls	Men	Women
Butter	-	-	0.04	0.02	0.06	0.03	-	-	0.03	0.02	0.05	0.03
Cheese	-	-	0.11	0.01	0.05	0.02	-	-	0.09	0.01	0.06	0.04
Pasteurised bovine milk	-	-	0.23	0.18	0.06	0.04	-	-	0.20	0.15	0.05	0.04
Powdered infant formula	1.76	1.91	-	-	-	-	0.60	0.64	-	-	-	-
Yogurt	-	-	0.25	0.21	0.009	0.02	-	-	0.14	0.12	0.005	0.01

As shown in Table 1, mean daily exposure to dioxins and DL-PCBs is higher in infants than children and adults. This result is comparable to a previous study, which reported that infants may have relatively high intake of dioxins and DL-PCBs than adolescents or adults, due to high consumption per kilogram body weight (Weijs *et al*. 2006). Similarly, DEWHA (2004) reported that high dietary intake relative to body weight results in higher mean intakes in infants and toddlers than other age groups. Bergkvist *et al*. (2008) also reported that the exposure to dioxins and DL-PCBs is higher among the young consumers, both girls and boys than among adults. Men are slightly more exposed to dioxins and DL-PCBs through butter, cheese and pasteurised bovine milk intakes than women. On the contrary, women are more exposed through yogurt than men. Higher butter, cheese and pasteurised bovine milk consumption by men justifies the estimated higher exposure in men than their female counterpart (Figure 1). Llobet *et al*. (2003) reported that dioxins exposure was mostly higher in men than women as a result of lower food consumption by women.

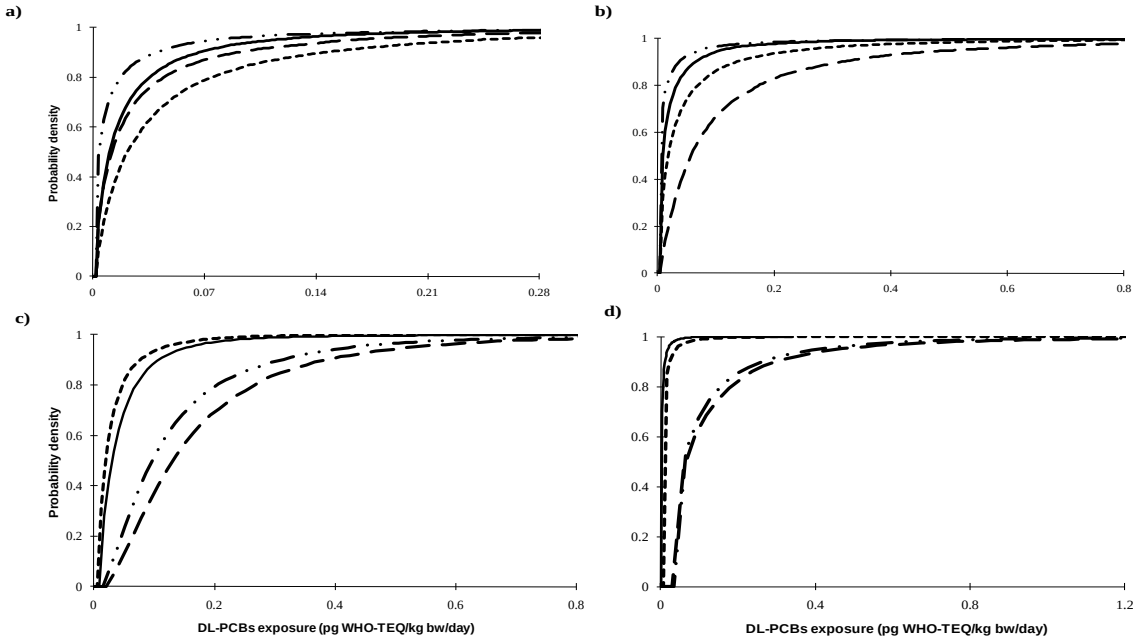

Figure 1: Daily DL-PCBs exposure of boys (--), girls (-¨), men (-) and women (- - -) from the consumption of a) butter, b) cheese, c) pasteurised bovine milk and d) yogurt simulated at 10,000 iterations using Monte Carlo analysis

The simulated mean exposure for boys and girls from ages 4-12 years was between 0.01-0.25 pg WHO-TEQ/kg bw/day for dioxins and 0.01 – 0.20 pg WHO-TEQ/kg bw/day for DL-PCBs in butter, cheese, pasteurised bovine milk and yogurt. Higher exposure was estimated for children is due to higher pasteurised bovine milk consumption (boys; 267 ± 200 g/day) and (girls; 209 ± 170 g/day) than men (195 ± 220 g/day) and women (110 ± 141 g/day) resulting into higher exposure in the range of 0.15 – 0.23 pg WHO-TEQ/kg bw/day for children than 0.04 – 0.06 pg WHO-TEQ/kg bw/day for adults. Figure 2 show the probabilistic models of infants' dioxins and DL-PCBs exposure estimated in this study. Results showed that female infants (girls) are slightly more exposed to dioxins (1.91 ± 0.75 pg WHO-TEQ/kg bw/day) and DL-PCBs (0.64 ± 0.73 pg WHO-TEQ/kg bw/day) than male infants (boys) with dioxins exposure of 1.76 ± 0.67 pg WHO-TEQ/kg bw/day and DL-PCBs exposure of 0.60 ± 0.74 pg WHO-TEQ/kg bw/day for DL-PCBs). Higher exposure in girls is as a result of lower body weights in comparison to boy's weight reported in the Euro-Growth study (Haschke et al., 2000).

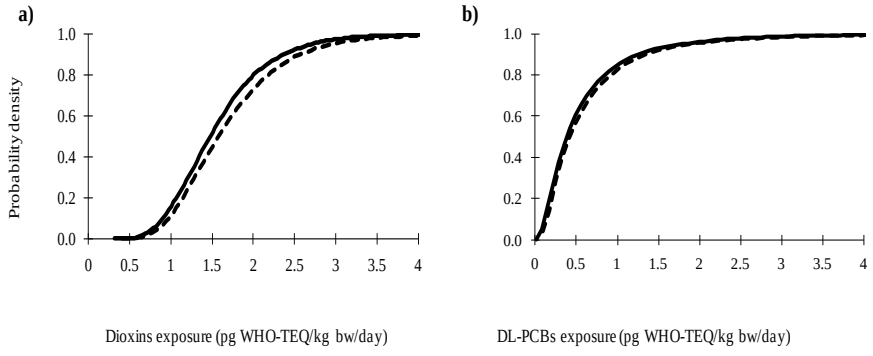

Figure 2: Daily exposure of boys (—) and girls (----) to a) dioxins and b) DL-PCBs through the consumption of reconstituted PIF. Horizontal dot lines show the TDI of 2 pg WHO-TEQ/kg bw/day (SCF, 2001).

In general, dioxins and DL-PCBs exposure through consumption of dairy products is higher in infants than children and adults. This fact is comparable to previous studies (Schecter *et al*. 2001; Bocio and Domingo 2005), which reported that daily exposure to dioxins and DL-PCBs decreases at 12 months of age throughout childhood and adolescence until adulthood. The utmost finding of this present study is that all age groups (infants, children and adults) are below the recommended regulatory limits. However, it is important to specify that the uncertainties in the model outputs may occur from the use of upper bound concentrations which assumed that all individual dioxins and DL-PCBs that are present at concentrations below the detection limit are present at the detection limit, and therefore could be an overestimation of exposure. Additionally, the use of Euro-Growth study due to unavailability of infant dietary consumption survey in Ireland may under or overestimate food consumption patterns of infants. Thus, the estimated outputs in this study are likely to cause slight under/over-estimation of infants, children and adults exposures to dioxins and DL-PCBs through the consumption of dairy products.

Conclusions

This study assessed the daily dietary exposure of infants, children and adults to dioxins and DL-PCBs from the consumption of pasteurised bovine milk and dairy products using probabilistic modelling. Results showed that the mean exposure of dioxins and DL-PCBs for different age groups did not exceed the PTWI of 14 pg WHO-TEQ/kg bw/week (equivalent of 2 pg WHO-TEQ/kg bw/day) recommended by the Scientific Committee on Food (SCF, 2001) nor the PTMI of 70 pg WHO-TEQ/kg bw/month (equivalent of 2.3 pg WHO-TEQ/kg bw/day) recommended by Joint FAO/WHO Expert Committee on Food Additives (JECFA, 2002).

References

Adekunte A., Tiwari B.K. and O'Donnell C. (2010) Exposure assessment of dioxins in pasteurised bovine milk. *Chemosphere* 81(4), 509-516.

Bergkvist C., Öberg M., Appelgren M., Becker W., Aune M., Ankarberg E.H., Berglund M. and Håkansson H. (2008) Exposure to dioxin-like pollutants via different food commodities in Swedish children and young adults. *Food and Chemical Toxicology* 46, 3360-3367.

European Food Safety Authority (EFSA) (2006) Guidance of the scientific committee on a request from EFSA related to uncertainties in dietary exposure assessment. *EFSA Journal* 438, 1-54.

Fürst P., Fürst Chr. and Wilmers K. (1992) Survey of dairy products for PCDDs, PCDFs, PCBs and HCB. *Chemosphere* 25(7-10), 1039-1048.

Haschke F., van't Hof M., Euro-Growth Study Group. (2000) Euro-growth references for length, weight, and body circumferences. *Journal of Pediatric Gastroenterology and Nutrition* 31, S14-S38.

Irish Universities Nutrition Alliance (IUNA) (2001) North/South Ireland Food Consumption Survey. http://www.safefood.eu/Global/Publications/Research/reports (accessed 22 September, 2010).

Llobet J.M., Domingo J.L., Bocio A., Casas C., Teixidó A. and Müller L. (2003) Human exposure to dioxins through the diet in Catalonia, Spain: carcinogenic and non-carcinogenic risk. *Chemosphere* 50(9), 1193-1200.

Loutfy N., Fuerhacker M., Tundo P., Raccanelli S. M. and Ahmed M.T. (2007) Monitoring of polychlorinated dibenzo-p-dioxins and dibenzofurans, dioxin-like PCBs and polycyclic aromatic hydrocarbons in food and feed samples from Ismailia city, Egypt. *Chemosphere* 66(10), 1962-1970.

Van den Berg M., Birnbaum L.S., Bosveld A.T.C., Brunström B., Cook P., Feeley M., Giesy J.P., Hanberg A., Hasegawa R., Kennedy S.W., Kubiak T., Larsen J.C., van Leeuwen F.X.R., Liem A.K.D., Nolt C., Peterson R.E., Poellinger L., Safe S.H., Schrenk D., Rillitt D., Tysklind M., Younes M., Waern F. and Zachrewski T. (1998) Toxic equivalency factors (TEFs) for PCBs, PCDDs, PCDFs for humans and wildlife. *Environmental Health Perspectives* 106, 775-792.

Wang I.C., Wu Y.L., Lin L.F. and Chang-Chien G.P. (2009) Human dietary exposure to polychlorinated dibenzo-p-dioxins and polychlorinated dibenzofurans in Taiwan. *Journal of Hazardous Materials* 164, 621-626.

Weijs P.J.M., Bakker M.I., Korver K.R., van Goor Ghanaviztchi K. and van Wijnen J.H. (2006). Dioxins and dioxin-like PCB exposure of non-breastfed Dutch infants. *Chemosphere* 64(9), 1521-1525.

A semi-quantitative risk assessment methodology to prioritise microbial hazards in reconstituted powdered infant formula

A.O. Adekunte[1], B.K. Tiwari[2], C.P. O'Donnell[1], A.G.M. Scannell[3]

[1]Biosystems Engineering, School of Agriculture, Food Science and Veterinary Medicine, University College Dublin, Belfield, Dublin 4, Ireland (adefunke.adekunte@ucd.ie; colm.odonnell@ucd.ie).
[2]Manchester Food Research Centre, Manchester Metropolitan University, Manchester, United Kingdom (b.tiwari@mmu.ac.uk).
[3]Food Science, School of Agriculture, Food Science and Veterinary Medicine, University College Dublin, Belfield, Dublin 4, Ireland (amalia.scannell@ucd.ie).

Abstract

Commercial powdered infant formula (PIF) is commonly used for feeding infants as an alternative to human breast milk. The occurrence of pathogenic microbial hazards in PIF represents a safety concern and may pose health risks to infants, especially preterm, underweight and the immunocompromised. The risk ranking of the 5 most industrially relevant microbial hazards in PIF was carried out using a semi-quantitative risk assessment tool known as Risk Ranger. Risk Ranger provided information relating to hazard severity and population susceptibility, probability of infants' exposure to contaminated reconstituted PIF (likelihood of occurrence) and the probability that reconstituted PIF contains an infectious dose. From this study, numerical estimates in form of risk scores and the numbers of illnesses per annum were obtained. The microbial risk scores were 61, 56, 41, 36 and 21 for *Cronobacter sakazakii*, *Salmonella species*, *Clostridium botulinum*, *Staphylococcus aureus* and Bacillus cereus, respectively. The predicted cases per annum were 2.96, 42.1, 0.098, 0.0049 and 0.14 for *C. sakazakii*, *Salmonella spp*., *C. botulinum*, *S. aureus* and *B. cereus* respectively. Results showed that *C. sakazakii* and *Salmonella spp*. had the highest risk scores, which signify the need for novel risk reduction strategies or measures to minimise or eliminate the risk of infants' exposure

Keywords: *risk ranking, microorganisms, Risk Ranger, food safety, risk assessment*

Introduction

Powdered infant formula (PIF) is a human breast milk substitute for infants, and a main source of nutrition for some infants, especially infants under the age of 6 months. The microbiological safety of PIF is of public health concern due to infants' vulnerability to enteric pathogens. Studies have demonstrated that contamination of PIF with microbial contaminants may cause infections and illnesses in infants, which can severely impact their development and health; in severe cases it can cause death (Coignard *et al*. 2006). However, PIF containing low levels of microbial contaminants may not cause illnesses in healthy infants and young children, but, the ability of these organisms to multiply during and after preparation of reconstituted PIF poses significant food safety risk (EFSA 2004).

C. sakazakii and *Salmonella spp.*, both in the family Enterobacteriaceae have been reported to be occasionally present in PIF (Cawthorn *et al*. 2008). *C. sakazakii* has been reported to cause illness in neonates, low birth weight infants and immunocompromised (Iversen and Forsythe 2003). Several studies have reported *C. sakazakii* infections and outbreaks in neonates and infants (Coignard *et al*. 2006). Apart from the reported outbreaks of *C. sakazakii*, *Salmonella spp.* infections have also been studied. Jourdan *et al*. (2008) reported a case of Salmonellosis in exclusively bottle-fed infants that developed symptoms of febrile diarrhoea due to the consumption of PIF. Other microorganisms such as *C. botulinum*, *B. cereus* and *S. aureus* have been recognised as sources of food-borne infections in infants. Brett *et al*. (2005) carried out a study on a case of infant botulism which was linked to PIF. Moreover, Redmond *et al*. (2009) reported that staphylococcal contaminations usually arise from mishandling of cleaned ready to re-use infant bottles by preparers, thus leading to cross-contamination. In the case of *B. Cereus*, Becker *et al*. (1994) studied the distribution of PIF in 17 countries and reported

that 54 % of 261 samples were contaminated with this organism with levels ranging from 0.3 to 600 cells/g. Based on the vulnerability of infants to these microbial contaminants, there is a need to rank and provide information required for further risk management. Microbial risk ranking provides information on hazard severity, exposure, likelihood of occurrence and other information relevant to risk management decision-making. The objective of this study was to compare and prioritise the 5 most industrially relevant microbial contaminants in PIF using the Risk Ranger software application.

Materials and Methods

C. sakazakii, *Salmonella spp.*, *C. botulinum*, *S. aureus* and *B. cereus* were considered the 5 most industrially relevant contaminants implicated in food-borne outbreaks associated with the consumption of reconstituted PIF based on reported research studies. To compare and prioritise the risks of these microbial contaminants, a semi-quantitative spreadsheet software (Risk Ranger), developed by Ross and Sumner (2002) was employed. Qualitative data used in this study was obtained from existing research studies. Using Risk Ranger (Figure 1), a risk rating was assigned to each microbial contaminant based on the susceptibility and severity of the hazard, probability of exposure to food and the probability of food containing an infectious dose.

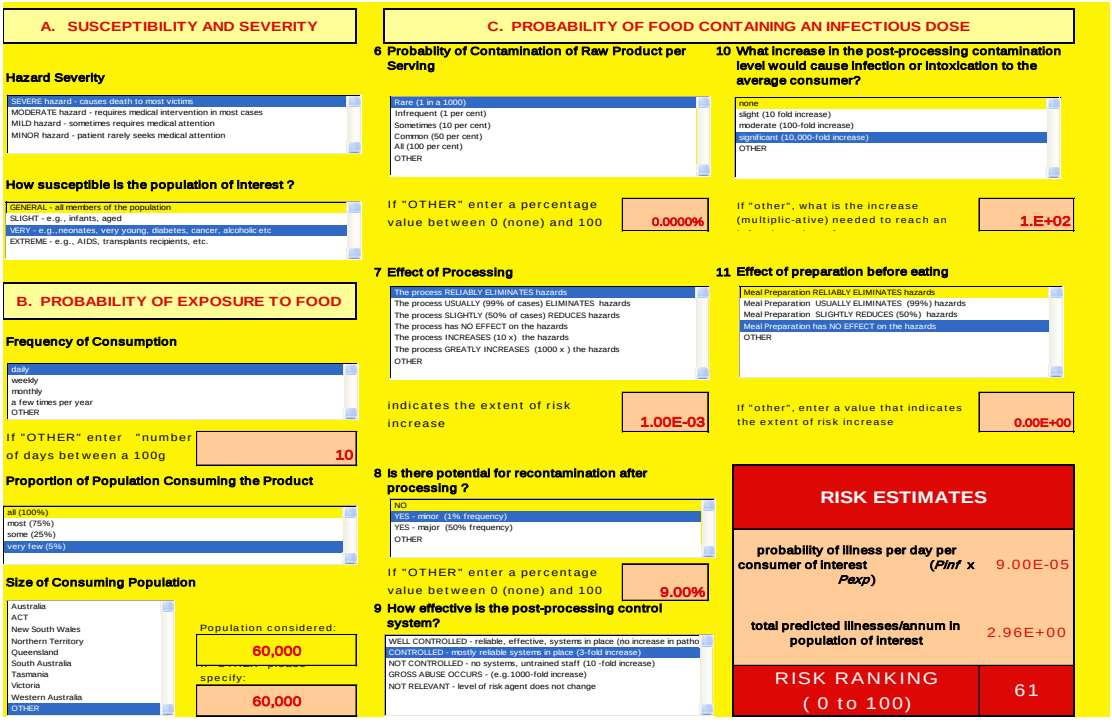

Figure 1: Risk ranking and estimation of possible infection of *C. sakazakii* in infants using Risk Ranger.

Results and Discussion

The Risk Ranger tool was used to convert qualitative statements to numerical values using a series of mathematical steps with risk ratings on a scale of 0 – 100. Zero represented no risk and 100 represented the consumption of PIF by infants containing a lethal dose of microbial contaminant. Risk Ranger combines qualitative statements to produce three risk estimates; risk ranking, predicted annual illnesses and probability of illness per day in a selected population (Ross and Sumner 2002). The result of risk estimation made by Risk Ranger tool per pathogen in PIF is shown in Table 1. Risk Ranger predicted 2.96 outbreaks of *C. sakazakii* per annum (0.0049 % of the consuming population). Stoll *et al*. (2004) estimated an

annual incidence of *C. sakazakii* infections to be 9.4 per 100,000 infants (0.000094 %) for very low birth weight. An outbreak of C. sakazakii infections in infants occurred in France in 2004 (Coignard *et al*. 2006) with a total of nine cases (including two deaths), which was at a higher level than the outbreaks predicted in this study. Moreover, there have been a number of recalls linked to the French outbreak that occurred in countries around the world such as, Brazil, Hong Kong, Ireland, the Gambia, Gabon and the United Kingdom (FAO/WHO 2006). In case of Salmonella spp., a number of outbreaks have been reported in the literature. CDC (2004) reported 139.4 cases per 100 000 (0.139 % of consuming population) of salmonellosis incidence among infants to be more than eight times greater than the incidence across all age groups. In 2005, 104 infants developed Salmonella infections in France (InVS 2005) and PIF was reported to be the cause of illness. Thus, 42.1 outbreaks predicted for *Salmonella spp*. (0.07 % of the consuming population) in this present study was lower in comparison to CDC report.

Table 1: Risk ranking of selected microbial contaminants in powdered infant formula.

Qualitative questions	***Cronobacter sakazakii***	***Salmonella species***	***Clostridium botulinum***	***Staphylococcus aureus***	***Bacillus cereus***
1. Hazard severity	Severe hazard	Moderate hazard	Moderate hazard	Mild hazard	Mild hazard
2. Population susceptibility	Very susceptible	Very susceptible	Very susceptible	Very susceptible	Very susceptible
3. Frequency of consumption	Daily	Daily	Daily	Daily	Daily
4. Proportion consumption (%)	Very few (1.5 %)	Very few (1.5 %)	Very few (1.5 %)	Very few (1.5 %)	Very few (1.5 %)
5. Size of consuming population[a]	60,000	60,000	60,000	60,000	60,000
6. Proportion of raw product contaminated (%)	Nil	Nil	Nil	Nil	Nil
7. Effect of processing	100 % reduction	100 % reduction	99 % reduction	99 % reduction	99 % reduction
8. Post processing contamination rate (%)	Minor (1 %)	Minor (1 %)	None	Minor (1 %)	1 %
9. Post processing control	Controlled	Controlled	Controlled	Controlled	Controlled
10. Increase required to cause infection/intoxication	Moderate,100 fold	Moderate, 100 fold	Slight, 10 fold	Slight, 10 fold	Slight, 10 fold
11. Effects of preparation on contaminant	Not applicable to PIF	Not applicable to PIF	Not applicable to PIF	Not applicable to PIF	Not applicable to PIF
Predicted cases per annum	2.96	42.1	0.098	0.14	0.0030
Risk ranking	61	56	41	36	21

In most infant botulism cases, the source of *C. botulinum* is not known (Jones *et al*. 1990), nevertheless, honey and corn syrup have been identified as sources of the organism in a small number of cases (Midura 1996). Recently, few studies have identified association between infant botulism and infant formula milk feeding. A clinical diagnosis of infant botulism linked to the consumption of PIF in United Kingdom was reported as the sixth case since 2001 (Brett *et al*. 2005). This shows that 0.098 (0.00016 % of consuming population) cases/per annum predicted in our study is comparable to similar studies based on the fact that outbreaks of this organism in PIF is minimal. The Risk Ranger predicted 0.14 cases per annum (0.00023 % of consuming population) for *S. aureus* due to consumption of PIF. Though, PIF cannot be linked directly to staphylococcal infections and poisoning in infants as contamination occurs during preparation and handling. Studies have shown that infants usually get infected with staphylococcal poisoning through human carriers preparing their foods (Redmond *et al*. 2009). A study carried out by AIFST (2003) showed that the predicted number of cases for *B. cereus* in France, Germany and the USA was less than 0.1 cases per 10,000,000 (0.000001 % of consuming population) per annum while Finland, Scotland, England/Wales, Hungary and Cuba all report more than 4.0 cases per 10,000,000 (0.00004 % of consuming population) per annum were lower. This shows that the predicted number of

cases estimated for B. cereus (0.000008 % of consuming population) using the Risk Ranger were within the range reported in similar studies.

Conclusions

The use of Risk Ranger for ranking microbial contaminants in PIF was described in this study. Risk Ranger provided an estimation of the total number of illnesses per annum in Irish infants and identified 2 high risk microbial contaminants, which have been implicated in PIF outbreaks. From the ranking, *C. sakazakii* and *Salmonella spp*. are the microorganisms of greatest concern in PIF. Results from this study are comparable to those reported by the European Food Safety Authority (EFSA) Scientific Panel on Biological Hazards (BIOHAZ Panel) as well as the FAO/WHO (2006). In conclusion there is a high need for novel risk reduction strategies or measures to minimise or eliminate *C. sakazakii* outbreaks among infants.

References

Australian Institute of Food Science and Technology (AIFST) (2003) *Food-borne microorganisms of public health significance* (6th edition), Food microbiology group, Southwood Press Pty Ltd., Australia.

Becker H., Schaller G., von Wiese W. and Terplan G. (1994) Bacillus cereus in infant foods and dried milk products. International *Journal of Food Microbiology* 23(1), 1-15.

Brett M. M., McLauchlin J.A., Harris A., O'Brien S., Black N., Forsyth R. J., Roberts D. and Bolton F.J. (2005) A case of infant botulism with a possible link to infant formula milk powder: evidence for the presence of more than one strain of Clostridium botulinum in clinical specimens and food. *Journal of Medical Microbiology* 54, 769-776.

Cawthorn D., Both S. and Witthuhn, C.R. (2008) Evaluation of different methods for the detection and identification of Enterobacter sakazakii isolated from South African infant formula milks and the processing environment. *International Journal of Food Microbiology* 127, 129-138.

Centers for Disease Control and Prevention (CDC) (2004) FoodNet Annual Report. http://www.cdc.gov/foodnet/annual/2002/2002AnnualReport_tables&graphs.pdf (accessed April 15, 2010).

Coignard B., Vaillant V., Vincent J-P, Leflèche A., Mariani-Kurkdjian P., Bernet C., L'Hériteau F., Sénéchal H., Grimont P., Bingen E. and Desenclos J-C. (2006) Infections sévères à Enterobacter sakazakii chez des nouveau-nés ayant consommé une préparation en poudre pour nourrissons, France, octobre-décembre 2004. *Bulletin Epidémiologique Hebdomadaire* (BEH) 2-3, 10-13.

European Food Safety Authority (EFSA) (2004) Opinion of the Scientific Panel on Biological Hazards on a request from the commission related to the microbiological risks in infant formulae and follow-on formulae. *The EFSA Journal* 113, 1-34.

Food and Agriculture Organisation/World Health Organisation (FAO/WHO) (2006) Enterobacter sakazakii and Salmonella in powdered infant formula. Meeting report, Rome, Italy. Microbiological Risk Assessment series No. 10. ftp://ftp.fao.org/ag/agn/jemra/e_sakakazii_salmonella.pdf (accessed March 23, 2009).

Institut de Veille Sanitaire (InVS) (2006) Infections à Enterobacter sakazakii associées à la consummation d'une préparation en poudre pour nourrissons. Rapport d'investigation. http://www.invs.sante.fr/display/?doc=publications/2006/infections_e_sakazakii/index.html (accessed September 2009).

Iversen C. and Forsythe S. (2003) Risk profile of Enterobacter sakazakii, an emergent pathogen associated with infant milk formula. *Trends Food Science and Technology* 14, 443-454.

Jones S., Huma Z., Haugh C., Young Y., Starer F. and Sinclair L. (1990) Central nervous system involvement in infantile botulism. *Lancet* 335, 228.

Jourdan N, Le Hello S, Delmas G, Clouzeau J, Manteau C, Désaubliaux B, Chagnon V., Thierry-Bled F., Demare N., Weill F.X. and de Valk H. (2008) Nationwide outbreak of Salmonella enterica serotype give infections in infants in France, linked to infant milk formula, September 2008. *Euro Surveillance* 13(39), 1 – 2.

Midura T. F. (1996). Update: Infant botulism. *Clinical Microbiology Reviews* 9, 119-125.

Redmond E.C. and Griffith C.J. (2009) The importance of hygiene in the domestic kitchen: Implications for preparation and storage of food and infant formula. *Perspectives in Public Health* 129(2), 69 – 76.

Ross T. and Sumner J. (2002) A simple, spreadsheet-based, food safety risk assessment tool. *International Journal Food Microbiology* 77, 39 – 53.

Stoll B., Hansen N., Fanaroff A., Lemons A. (2004) Enterobacter sakazakii is a rare cause of septicemia or meningitis in VLBW infants. *The Journal of Pediatrics* 144(6), 821 – 823.

Dynamic modelling of *L. monocytogenes* growth in vacuum packed cold-smoked salmon under typical retail and consumer storage conditions

S. Chitlapilly Dass[1], N. Abu-Ghannam[1], E. J. Cummins[2]

[1]School of Food Science and Environmental Health, College of Sciences and Health, Dublin Institute of Technology, Cathal Brugha St., Dublin 1, Ireland
[2]Biosystems Engineering, UCD school of Agriculture, Food science and Veterinary medicine, University College Dublin, Belfield, Dublin 4, Ireland

Abstract

Vacuum packed cold-smoked salmon contaminated with *Listeria monocytogenes* has been implicated in food-borne listeriosis. The bacterium has the ability to grow under a wide range of temperatures (1 – 45 ˚C), thus possessing the ability to grow throughout the temperature fluctuation encountered during food storage and distribution. Modelling *L. monocytogenes*' dynamic behaviour under fluctuating temperatures is critical for an accurate evaluation of food safety. In this study, a product specific model for cold-smoked salmon was constructed that covers the retail and consumer phase of the food pathways. The variability in time and temperature during retail storage, consumer transport and consumer storage was included in the model. Vacuum packed cold-smoked salmon were inoculated with 3-cocktail strains of *L. monocytogenes*, with an initial concentration of 101 CFU/g and stored at 4, 8, 12 and 16 °C for 18 days. The primary growth kinetics parameters at each temperature were obtained by fitting the observed data in the DMFit Excel add-in. The maximum specific growth rate was further modelled as a function of temperature by the square root model. The model was validated under two scenarios of dynamic temperature conditions incorporating the fluctuations occurring during the various stages of the food pathways (post-production, retail and consumer phase). The model predictions were based on the square root model and the differential equation of Baranyi and Roberts (1994). The model performance was based on the measures of bias factor Bf, accuracy factor Af and goodness of fit GoF. The values of Bf and Af of the model were close to unity, indicating good agreement between observations and predictions of the model. The model was compared to two growth predictors; Combase and Seafood Spoilage and Safety Predictor (SSSP) and the predictions obtained gave an overestimation of *L. monocytogenes* growth. This study illustrates the potential of dynamic modelling of *L. monocytogenes* growth for cold-smoked salmon from retailer to consumer as a means of evaluating the product safety at different stages of the food pathways.

Keywords: L. monocytogenes, *smoked salmon, product specific modelling, food-pathways*

Predictive modelling as a tool for Performance Objectives (PO) achievement and Performance Criteria (PC) and Process/Product Criteria (PcC/PdC) calculation for the mycotoxin hazard

D. García, A.J. Ramos, V. Sanchis, S. Marín

Food Technology Department, Lleida University, XaRTA-TPV, Lleida, 25198, Spain (smarin@tecal.udl.cat)

Abstract

In this work the processing of maize to cornflakes was considered. The starting point was the maximum levels in commission regulation 1881/2006 for total aflatoxins. Having these values in mind, the process steps were individually considered and PCs determined when required. Moreover, according to these PCs, possible PcC and PdC were calculated, using previously published results. The present study demonstrates the usefulness of predictive modelling in management and prevention of the mycotoxin hazard. It highlights the need for predictive model development for mycotoxigenic fungi at the boundaries of growth and for the kinetics of inactivation of mycotoxins in food substrates. Finally, uncertainty is a key point to be addressed; compliance with maximum levels, as in this example, may depend on the magnitude of this parameter.

Keywords: *food safety objectives, performance objectives, performance criteria, mycotoxins, maize*

Introduction

A Food Safety Objective (FSO) is the maximum frequency and/or concentration of the hazard in a food at the time of consumption that provides the appropriate level of protection and is preceded by the Performance Objective (PO), which is the maximum frequency and/or concentration of a hazard in a food at a specified step in the food chain before the time of consumption. In practice, FSOs are met through the establishment and implementation of performance and process criteria. In the food chain it is necessary to know the effect of every step and treatment, Performance Criteria (PC), as well as the process parameters, Process Criteria (PcC) (t, T, pH, a_w) which can be applied in any level, and Product Criteria (PdC) (pH, a_w, gaseous atmosphere). PdC assure that the hazard level never overtakes safety levels before being cooked or consumed (Codex Alimentarius 2007). While Codex considers FSOs only for microbial hazards, the concept could apply to other types of hazards as well. Mycotoxins are chemical hazards with a microbiological origin.

Maize is a very important cereal for the human and animal diet; however, it can be contaminated by mycotoxins. *Aspergillus* is a mould genus which can contaminate maize and produce mycotoxins. *Aspergillus flavus* and *A. parasiticus* can contaminate maize and their by-products and synthesize aflatoxins (AFs), causing damage to human and animal health. Processing of maize to by products involves a series of steps in which AFs content might either increase or decrease.

Commission regulation 1881/2006 sets the maximum levels of aflatoxin B_1 and total aflatoxins (B_1+B_2+G_1+G_2) for maize to be subjected to sorting or other physical treatment before human consumption or use as an ingredient in foodstuffs at 5 and 10 µg/kg, respectively, and for all products derived from cereals at 2 and 4 µg/kg, respectively.

Materials and Methods

In this work the processing of maize to cornflakes was considered. The process involved traditional grits cooking (non extruded), flaking and toasting as main steps (Figure 1). The starting point was the maximum levels in commission regulation 1881/2006 for total AFs. The FSO was set at 4 µg/kg, and the level 10 µg/kg was used as a guideline PO along the processing chain. Having these values in mind, the process steps were individually considered

(Table 1) and PCs determined when required. Moreover, according to these PCs, possible PcC and PdC were calculated, using previously published results. This process can either be done forward, starting from the PO guideline in the raw material, or backward, starting from the FSO to be accomplished in the final product.

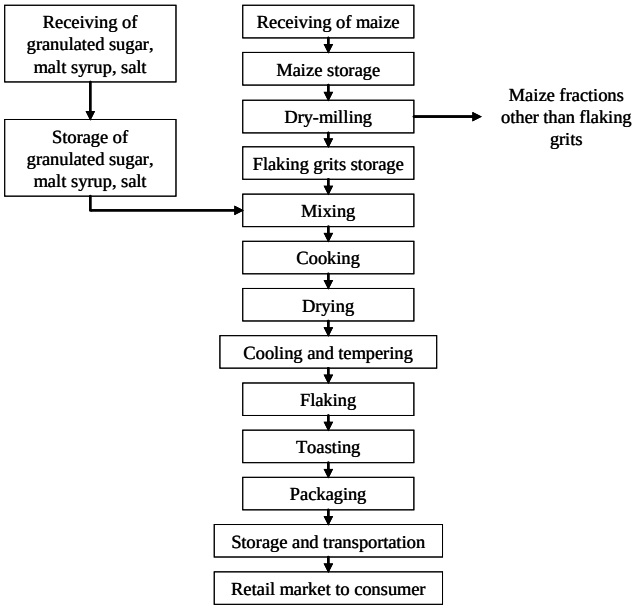

Figure 1. Flow chart for corn flakes production from raw maize.

Results and Discussion

For the particular case of cornflakes production, relevant steps regarding AFs hazard were grouped:

- Storage steps: maize storage, grits storage, final product storage, in these steps a 'zero increase' PC was stated to be achieved by proper storage conditions in terms of temperature and humidity (water activity, a_w). Predictive models can be applied at this point.
- Dry-milling: It is known to be the most important critical control point in maize processing, as it allows for separation of the most contaminated outer fractions of the maize grain.
- Thermal treatments: cooking, drying, toasting. Although thermostability of AFs is well-known, inactivation may occur to some extent. There is a lack of predictive models describing AFs destruction as a function of temperature and time in food matrices, and the impact of moisture content.

Storage steps

In the storage cases, in order to prevent mycotoxin production, control of mycotoxigenic mould growth is required. Despite the absence of direct correlation between mould growth and mycotoxins production, prevention of fungal growth effectively conduces to prevention of mycotoxin accumulation. In general, a_w and temperature are regarded as the main controlling factors determining the potential for mould growth during storage. Although in the past many studies dealt with temperature and a_w effects on mould growth and AFs production, only a few sought for the conditions limiting growth and toxin production. Thus at this point PcC were calculated from the kinetic models given in Samapundo *et al.* (2007) and Garcia *et al.* (2011), and from the probability model in Garcia *et al.* (2011) to guarantee a zero increase in AFs through temperature/a_w control (Table 1).

For kinetic models a growth rate <0.05 mm/d was considered the no-growth boundary, while the probability model $p<0.1$ was considered indicative of no-growth. Similar PcC were calculated for a given isolate from both kinetic and probability models, e.g. for guaranteeing no growth of an *A. parasiticus* isolate a a_w under 0.81 would be enough, or a combination of

a_w bellow 0.85 with a temperature under 15ºC (Garcia *et al.* 2011). On the other hand, the *A. flavus* isolate studied by Samapundo *et al.* (2007) showed better adaptation to low a_w, leading to calculated PcC of, for example: < 0.76 a_w, < 11ºC, or <0.80 a_w together with a temperature under 21ºC (Table 1). There is a need for ecophysiological studies involving a higher number of isolates under limiting growth conditions.

Dry milling

Dry milling is a crucial step in post-production of grains. Its basic objective is to remove the surface parts of the grain with minimum breakage of the endosperm by a physical process to produce an edible kernel. By means of removing the outer parts of the corn kernel such as hull and bran, the main products obtained include grits, germ, meals and flours. Coarse grits are the target fraction for corn flakes production. Taking into account the effect of dry-milling in AFs distribution in lots with initial concentration <10 µg/kg, the levels of AFs reduction vary from 7% (Castells *et al.* 2008) to 49-56% (Brera *et al.* 2006; Pietri *et al.* 2009). The dry-milling process may vary in the number of steps involved, leading to different reduction levels. A tentative level of PC=50% reduction was chosen in this work as an example.

Thermal processes

The application of heat to cook and preserve products is the basis of all thermal processes. These processes include cooking, roasting and heat drying. Although the stability of several mycotoxins, mainly fumonisins, in various methods of thermal processing has been reported, studies with AFs are scarce, except for roasting of nuts. In particular, studies of the kinetics of AFs, and other mycotoxin reduction as a function of temperature would be of interest to be applied in PcC calculation. The stability of AFs is, among other things, crucially determined by the availability of H_2O in the medium. Heating an AFs solution containing carbohydrates for 30 min led to a decrease in AFs of 50 and 75%, at 150 and 180ºC, respectively (Raters and Mattisek 2008).

Cooking of grits involves steam-heating over 100ºC. Cooking wheat (100ºC, 30min) with 10% moisture content led to 40-47% AFs reduction (Hwang and Lee 2006). The loss of AFs was considerably higher when using a pressure cooker at 160 °C for 20 min (78-88% loss) than the ordinary cooker without pressure under similar conditions (31-36% loss) (Je and Kim 2006). In another study, boiling corn grits gave an average reduction of AFs of 28%. Castells *et al.* (2008) did not find a significant reduction. Thus for a pressure cooking, PC might be around 80% reduction (Table 1).

Drying is usually done at <121ºC until 10-14% humidity is achieved (Arvanitoyannis and Traikou 2005). Heating wheat or maize at 100ºC or lower did not lead to any marked reduction in AFs (Hawkins *et al.* 2005; Hwang and Lee 2006). No more data were found in AFs reduction through maize drying, thus this point was not considered to clearly contribute to food safety.

Toasting of flakes involves high temperatures (274-329ºC) for seconds (90 s) (Arvanitoyannis and Traikou 2005). In a study of corn muffins made from cornmeal naturally contaminated with AFs, 87% of the initial amount of aflatoxin B_1 in the cornmeal was found in the baked muffins (Stoloff and Trucksess 1981). Moreover, Castells *et al.* (2008) did not find a significant reduction. Roasting of nuts has been reported as a crucial step for reducing AFs, however, the residence times involved are usually longer than 20 min. Considering the existing information, toasting was not considered to clearly contribute to food safety.

Analytical uncertainty

For the particular case of mycotoxins, the maximum level as set in the EC Regulation 1881/2006 (FSO) must be over the final product PO. EC Regulation (401/2006) states as criterion for acceptance of a lot or sublot that the laboratory sample conforms to the maximum limit, taking into account the correction for recovery and measurement uncertainty (U). According to the performance criteria for AFs analysis (EC 401/2006, recommended RSD_r=24% for a concentration of 4 µg/kg), calculated measurement uncertainty would take a value of 1.94 µg/kg. Thus in this case PO for the final product should take a value of 4-1.94~2

µg/kg. Thus, in the example, given a recommended value of U, either the PO at the reception of the maize should be lower than 10 µg/kg or the PrC might need to be redesigned to comply with the maximum level.

Table 1: Food safety metrics applied to total AFs in cornflakes production from maize.

Process step	PC	PrC	PdC	PO
Receiving of maize	-	-	-	≤10 µg/kg (1881/2006)
Maize storage	Zero increase	< 0.76 a_w, or < 11ºC, or <0.80 a_w and <21ºC	-	≤10 µg/kg
Dry-milling	50% reduction	-	-	≤5 µg/kg
Flaking grits storage	Zero increase	< 0.76 a_w, or < 11ºC, or <0.80 a_w and <21ºC	-	≤5 µg/kg
Cooking	80% reduction 20% reduction	160ºC 20 min 100ºC (30-120 min)	-	≤1 µg/kg ≤4 µg/kg
Storage, transportation and retail market	Zero increase	-	< 0.76 a_w	≤1 µg/kg ≤4 µg/kg
Consumer	-	-	< 0.76 a_w	FSO≤4-U µg/kg (1881/2006)

U=measurement uncertainty

Conclusions

The present study demonstrates the usefulness of predictive modelling in management and prevention of the mycotoxin hazard. It highlights the need for predictive models development for mycotoxigenic fungi at the boundaries of growth and for the kinetics of inactivation of mycotoxins in food substrates.

Acknowledgements

The authors are grateful to Spanish government (project AGL2010-22182-C04-04) and EC, KBBE - Food, Agriculture and Fisheries and Biotechnology (project 222738- Selection and improving of fit-for-purpose sampling procedures for specific foods and risks) and Comissionat per a Universitats i Recerca d'Innovació, Universitats i Empresa de la Generalitat de Catalunya (AGAUR) and European Social Fund for the financial support.

References

Arvanitoyannis I.S. and Traikou, A. (2005) A comprehensive review of the implementation of Hazard Analysis Critical Control Point [HACCP] to the production of flour and flour-based products. *Critical Reviews in Food Science and Nutrition* 45 (5), 327-370.

Brera C., Catano C., De Santis B., Debegnach F., De Giacomo M., Pannunzi E. and Miraglia M. (2006) Effect of industrial processing on the distribution of aflatoxins and zearalenone in corn-milling fractions. *Journal of Agricultural and Food Chemistry* 54 (14), 5014-5019.

Castells M., Marín S., Sanchis V. and Ramos A.J. (2008) Distribution of fumonisins and aflatoxins in corn fractions during industrial cornflake processing. *International Journal of Food Microbiology* 123 (1-2), 81-87.

Codex Alimentarius. (2006) Principles and guidelines for the conduct of microbiological risk management (MRM), CAC/GL63-2007.

European Commission. (2006). Commission Regulation (EC) No 1881/2006 of 19 December 2006. Official Journal of European Union L364, 5-24.

European Commission. (2006). Commission Regulation (EC) No 401/2006 of 23 February 2006. Official Journal of European Union L70, 12-34.

Garcia D., Ramos A.J., Sanchis V. and Marín S. (2011) Modelling the effect of temperature and water activity in the growth boundaries of *Aspergillus ochraceus* and *Aspergillus parasiticus*. *Food Microbiology* 28 (3), 406-417.

Hawkins L.K., Windham G.L. and Williams W.P. (2005) Effect of different postharvest drying temperatures on *Aspergillus flavus* survival and aflatoxin content in five maize hybrids. *Journal of Food Protection* 68 (7), 1521-1524.

Hwang J.-H. and Lee K.-G. (2006) Reduction of aflatoxin B1 contamination in wheat by various cooking treatments. *Food Chemistry* 98 (1), 71-75.

Je W.P. and Kim Y.-B. (2006) Effect of pressure cooking on aflatoxin B1 in rice. *Journal of Agricultural and Food Chemistry* 54 (6), 2431-2435.

Pietri A., Zanetti M. and Bertuzzi T. (2009) Distribution of aflatoxins and fumonisins in dry-milled maize fractions. *Food Additives and Contaminants - Part A Chemistry, Analysis, Control, Exposure and Risk Assessment* 26 (3), 372-380.

Raters M. and Matissek R. (2008) Thermal stability of aflatoxin B1 and ochratoxin A. Mycotoxin Research 24 (3), 130-134.

Samapundo S., Devlieghere F., Geeraerd A.H., De Meulenaer B., Van Impe J.F. and Debevere, J. (2007) Modelling of the individual and combined effects of water activity and temperature on the radial growth of *Aspergillus flavus* and *A. parasiticus* on corn. *Food Microbiology* 24 (5), 517-529.

Stoloff L. and Trucksess M.W. (1981) Effect of boiling, frying, and baking on recovery of aflatoxin from naturally contaminated corn grits or cornmeal. *Journal of the Association of Official Analytical Chemists* 64 (3), 678-680.

Development of predictive model to predict the outgrowth of *Listeria monocytogenes* in Ready-To-Eat food products

S. Kumar[1], T. Wijtzes[2], G. Lommerse[1], D. Visser[1], E. Bontenbal[1]

[1]PURAC, Arkelsedijk 46, Gorinchem, 4206AC, The Netherlands (s.kumar@purac.com)
[2]WFC-Food Safety

Abstract

EU regulations state that the food industry, within the framework of good hygiene practices and hazard analysis of critical control point programmes, can make use of predictive models to comply with the directives of controlling *Listeria monocytogenes* outgrowth in food products (EC 2073/2005). Hence, it is important to develop validated models, based on challenge studies in food products. The objectives of this study are to: (1) Develop a mathematical model for *Listeria monocytogenes* that predicts its potential for growth in food products as a function of temperature, pH, water activity and the concentration of organic acids and their salts. (2) Demonstrate the significance of lactic acid, acetic acid and their salts against *Listeria monocytogenes* in food products. The model shows that the intervention of lactic acid, acetic acid or their salts addition to food products significantly impedes the outgrowth of *Listeria monocytogenes* in a food product. Addition of 0.75 % PURASAL Powder S98 to a food product (pH 5.9, moisture 80%, aw 0.988) was simulated at 95 % confidence level. At 4 °C, for the treated sample, the time for 2 log growth for *Listeria monocytogenes* was increased from 11 days to 17 days compared to that of control. The developed model describes the growth kinetics very well, including independent challenge studies, and in general gives fail safe predictions. The developed model gives reliable predictions of the potential for outgrowth of *Listeria monocytogenes* in RTE foods. This modeling tool can be utilized by food industry to assess how they can control the growth of *Listeria monocytogenes* by addition of lactic acid, acetic acid or their salts to their product formulations, and by sufficient temperature control.

Keywords: Listeria monocytogenes, predictive model, lactic acid, acetic acid

Application of predictive microbiology in food and drink SMEs: assessment based on 20 years of experience

M. El Jabri, F. Postollec, D. Sohier, C. Travaille, D. Thuault

ADRIA Développement, ZA Creac'h Gwen, F-29196 QUIMPER Cedex

Abstract

Food industry in the European Union is characterized by a large percentage of Small and Medium Enterprises (SMEs, 99%) with 308000 enterprises representing 63% of the direct employees and 48% of the turnover of this sector. Consumers and society ask for safe, healthy and tasty food. Models which can help the food operators to predict and control food quality, are needed and the access of SMEs to these models must be optimized. The development of software like Sym'Previus is the best way for SMEs to use these models. Predictive microbiology may be useful for the following applications:

- Support for training course,
- Help to identify Critical Control Point in a process and formalize an HACCP plan,
- Classify products according to their safety and to focus more attention on more sensitive products,
- Ensure food shelf-life with the understanding of factors influencing bacterial growth in food and reduce laborious challenge studies saving time and money,
- Optimize the formulation (pH, water activity, additives) in order to assure the best stability and reduce time-to-market,
- Optimize new process conditions (temperature and heat treatment time).

Examples of research transfer in predictive microbiology in SMEs will be given. The provision of this information to food companies (particularly SMEs) requires the presence of an expert unavailable in SMEs. Financial supports are needed and can be brought by trade associations, programs for research transfer or by regional support.

Keywords: predictive microbiology, HACCP, shelf-life, decision making tool

Accurate assessment of microbial safety in food industry: adapting predictive models for specific food products

A.M. Cappuyns[1,2], A. Vermeulen[1,3], H. Paelinck[4], F. Devlieghere[1,3], J.F. Van Impe[1,2]

[1]CPMF² - Flemish Cluster Predictive Microbiology in Foods – http://www.cpmf2.be
[2]BioTeC - Chemical and Biochemical Process Technology and Control, Department of Chemical Engineering, Katholieke Universiteit Leuven, Belgium (Jan.VanImpe@cit.kuleuven.be)
[3]LFMFP – Laboratory of Food Microbiology and Preservation, Department of Food Safety and Food Quality, Ghent University, Belgium (Frank.Devlieghere@UGent.be)
[4]Laboratorium voor Levensmiddelenchemie en Vleeswarentechnologie, Katholieke Hogeschool Sint-Lieven, Belgium (Hubert.Paelinck@kahosl.be)

Abstract

In this study available predictive models are evaluated and adapted with respect to their potential use in predicting outgrowth of *Listeria monocytogenes* in two types of meat products, i.e., cooked meat products and aspic products. Major criteria for selecting models were the ranges of physico-chemical parameters covered by the model, together with the type of broth or type of product used during model development. Challenge test data and simulation results of the selected models were compared. Based on this comparison, the existing models were evaluated and adapted to take into account the observed differences. The adapted predictive models can be a very useful tool for the food industry. It could assist companies during product development and in the accurate assessment of microbial food safety during shelf life.

Keywords: *growth, Listeria monocytogenes, predictive modelling, meat, food safety*

Introduction

Although the EU regulation specifically indicate predictive models as a tool to document the growth of *L. monocytogenes* in RTE foods, predictive models are until now only being applied in a limited extent by companies. The aim of this research is to develop/adapt and validate predicting models for specific categories of meat products, i.e., meat products with similar intrinsic and extrinsic characteristics. Two categories of meat products are considered in this paper, i.e., cooked meat products and aspic products. The resulting models are promising tools for assessing shelf life and for product development in the food industry.

Materials and Methods

Data collection

For the category of cooked meat products, cooked ham was prepared on a lab scale; for the category of aspic products, a commercial product was purchased from a local producer.
For each batch of meat products challenge tests (7 °C, 25/30 days) were performed according to the EU technical guidance. The meat products were sliced, inoculated with *L. monocytogene*s, and MAP (for the cooked ham) or vacuum (for the aspic product) packed. Microbial analyses were performed at regular time intervals to quantify the evolution of *L. monocytogenes* and lactic acid bacteria (background flora). At day 0, the pH, water activity (a_w), % dry matter, % NaCl, % lactate, % acetate and nitrite were determined.

Computational environment

Simulations are performed in Matlab (The Mathworks Inc., Natick), numerial integration is performed with the ode23s routine in Matlab.

Results and Discussion

In the first step, an inventory was made of available predictive models with respect to their applicability to predict growth of *L. monocytogenes* for different types of meat products.

Major criteria for selecting models were the ranges of temperature, pH, a_w/salt and acid concentrations covered by the model, together with the type of broth or type of food product used during model development.
Based on a study on smoked salmon, Vermeulen *et al*. (2011) concluded that an appropriate predictive model should also include the interaction with background flora. In this work, the growth of background flora (lactic acid bacteria) and their effect on the growth of *L. monocytogenes* is modelled as described by Mejlholm and Dalgaard (2007). The interaction is modelled by the Jameson effect, i.e., the assumption that all microorganisms are suppressed when the total microbial population achieves the maximum population density.

Cooked meat products

Based on the screening of models available in the literature, the cardinal parameter model of Mejlholm and Dalgaard (2009) was chosen as a starting point. This model was developed for seafood, but was also evaluated for predicting growth in meat products (Mejlholm *et al*. 2010). Besides temperature, pH and a_w/NaCl, this model also takes CO_2, nitrite and acid levels and the interaction between all these parameters into account:

$$\mu_{\max,Lm} = 0.419 \cdot \left(\frac{T+2.83}{25+2.83}\right)^2 \cdot \left(\frac{a_w - .923}{1-.923}\right) \cdot \left(1-10^{(4.97-pH)}\right) \cdot \frac{3140 - CO_{2,eq}}{3140} \cdot \left(\frac{350 - NIT}{350}\right)^2 \cdot \left(\frac{1-LACu}{3.79}\right) \cdot \left(1-\sqrt{\frac{AACu}{10.3}}\right) \cdot \xi \quad (1)$$

with $\mu_{max,Lm}$ the maximum specific growth rate of *L. monocytogenes*, T (°C) temperature, a_w water activity, $CO_{2,eq}$ (ppm) the concentration of dissolved CO_2 at equilibrium, NIT (ppm) the nitrite concentration, and LACu (mM) and AACu (mM) the concentration of undissociated lactate and acetate, respectively. ξ describes the relative effect of the interactions between environmental parameters on μ_{max}. The measured values of physico-chemical parameters of the meat products were used as input for model simulations.
Experimental data for the growth of *Listeria* in cooked ham together with the corresponding model simulations (with and without taking interaction with lactic acid bacteria (LAB) into account) are presented in Figure 1 (only the results of batch 1 are shown).

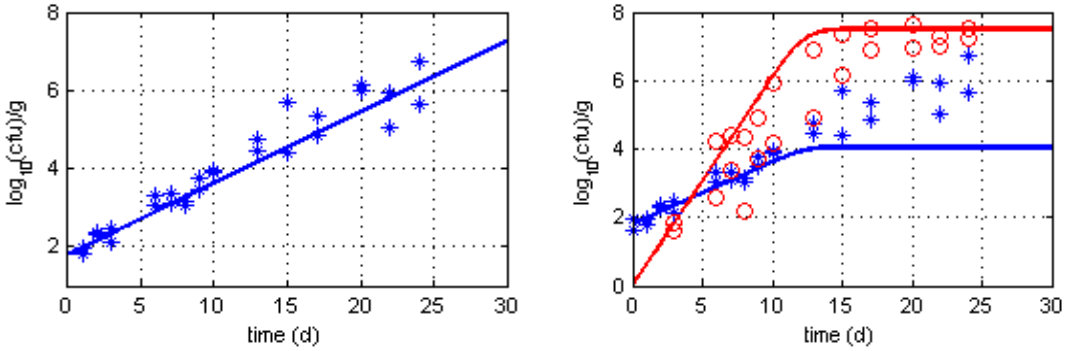

Figure 1: Experimental data (∗,o) and model simulations (-) (equation (1)) for cooked ham. Right plot: no interaction with LAB; left plot: interaction with LAB (Jameson effect)

For both batches of cooked ham, the model of Mejlholm and Dalgaard (2009) provides a good estimate of $\mu_{max,Lm}$. Taking interaction between *L. monocytogenes* and lactic acid bacteria into account, however, results in an underestimation of the growth curve (Figure 1, right plot). *L. monocytogenes* continues to grow even when lactic acid bacteria have reached the stationary phase and thus the assumption of the Jameson effect does not hold for this case.

Aspic products

The pH-values for the aspic products (5.47 and 5.41 for batch 1 and 2, respectively) were lower than the lower pH limit (5.6) of the model of Mejlholm and Dalgaard (2009). Extrapolation of the model to these lower pH values give rises to an underestimation of the growth rate of *L. monocytogenes*. For batch 2, e.g., a $\mu_{max,Lm}$ of 0 was calculated, while an increase of more than 2 $\log_{10}$(cfu)/g was observed.

Lebert *et al*. (1998) published surface response models for the growth rate of 2 strains of *L. monocytogenenes* as a function of temperature (4 °C - 30 °C), pH (5.4 - 7.0), and water activity (0.96 - 1.00). The measured values of the aspic products are within the range of model validity. Simulations with these models gave rise to an overestimation of the growth rate of *L. monocytogenes* (results not shown). This is not unexpected since only temperature, pH, and water activity are taken into account, while the products also contain significant amounts of nitrite, acetic acid and lactic acid.

To obtain a more accurate estimation of the growth rate for aspic products, the model of Lebert, i.e., which can cope with lower pH values, and the model of Mejlholm, i.e., which takes the effect of nitrite and acids into account, were combined. The following equation was used for simulations

$$\mu_{\max,Lm} = \mu_{Lebert} \cdot \frac{3140 - CO_{2,eq}}{3140} \cdot \left(\frac{350 - NIT}{350}\right)^2 \cdot \left(\frac{1 - LACu}{3.79}\right) \cdot \left(1 - \sqrt{\frac{AACu}{10.3}}\right) \cdot \xi \qquad (2)$$

with μ_{Lebert} the maximum specific growth rate according to the model of Lebert for the fast growing strain of *L. monocytogenes*. Simulation results and experimental data are presented in Figure 2.

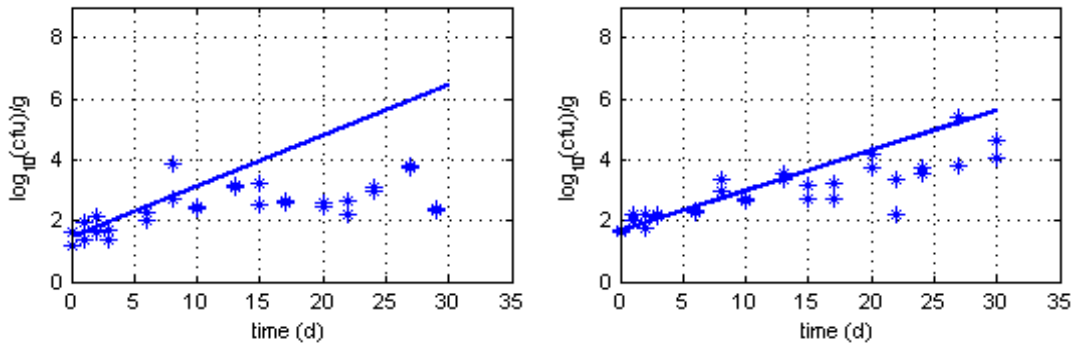

Figure 2: Experimental data (∗) and simulations with the adapted model (equation (2)) for batch 1 (left plot) and batch 2 (right plot) of aspic products

The adapted model provides a good estimate of the specific growth rate for both batches of aspic products during the first half of the storage period. Towards the end of the storage period the model simulation deviates from the observed growth. The stationary phase is reached, but this is not yet included in the model. Therefore the model is further adapted. Equation (2) is combined with the model for lactic acid bacteria published by Mejlholm and Dalgaard (2007) and interaction between *L. monocytogenes* and lactic acid bacteria is taken into account. Results are presented in Figure 3.

Taking interaction with background flora into account improves the prediction of the growth rate for *L. monocytogenes.* The deviation between prediction and data for batch 2 are mainly due to the poor description of the growth of lactic acid bacteria, resulting in an underestimation of the growth curve of *L. monocytogenes*. For this category, an accurate description of background flora is needed to get an accurate estimation of the growth rate of *L*. monocytogenes

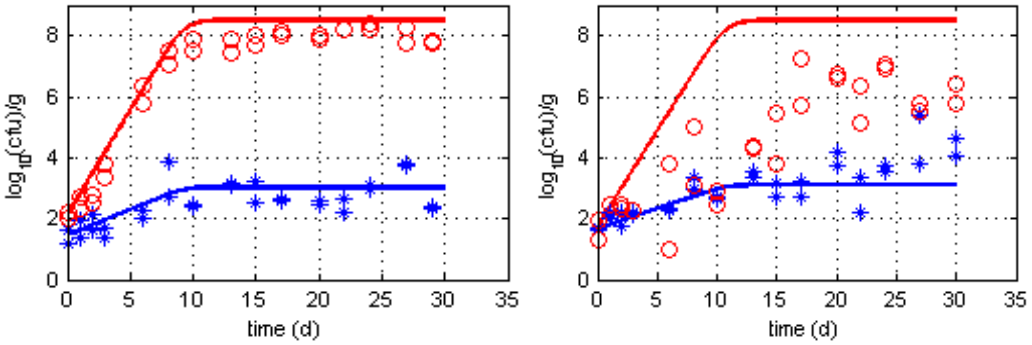

Figure 3: Experimental data (∗,o) and simulations with the adapted model (including the interaction with LAB) for batch 1 (left plot) and batch 2 (right plot) for aspic products

Conclusions

For the cooked meat products, the model of Mejlholm and Dalgaard (2009) provides a good estimate of the growth of *L. monocytogenes*, but only if interaction with lactic acid bacteria is not taken into account. For this category, the initial level of back ground flora was very low and did not seem to have much effect on the growth of *L. monocytogenes*.

For the aspic products, the pH was out of the validity range of the Mejlholm and Dalgaard model and extrapolation of the model resulted in an underestimation of the growth rate. Therefore this model was adapted by combining it with the model of Lebert. This way a model was obtained which can cope with the low pH of aspic products and which takes the effect of nitrite and acid concentrations into account.

In a next stage, the models will be further analysed and compared with data obtained at different temperatures or under a time varying temperature profile. This will result in adapted models which are valid for specific categories of meat products and which can be used by companies as a supporting tool in product development and as a tool for accurate shelf life estimation.

Acknowledgements

This work was supported by project 100206 of the Agency for Innovation by Science and Technology (IWT), project KP/09/005 (www.scores4chem.be) of the Industrial Research Fund and by the Belgian Program on Interuniversity Poles of Attraction initiated by the Belgian Federal Science Policy Office. Jan Van Impe holds the chair Safety Engineering sponsored by the Belgian chemistry and life sciences federation essenscia.

References

Lebert I., Begot C. and Lebert A. (1998) Development of two Listeria monocytogenes growth models in a meat broth and their application to beef meal. *Food Microbiology* 15(5), 499-509

Mejlholm O. and Dalgaard P. (2007) Modeling and predicting the growth of lactic acid bacteria in lightly preserved seafood and their inhibiting effect on *Listeria monocytogenes. Journal of Food Protection* 70(11), 2485-2497

Mejlholm O. and Dalgaard P. (2009) Development and Validation of an Extensive Growth and Growth Boundary Model for Listeria monocytogenes in Lightly Preserved and Ready-to-Eat Shrimp. *Journal of Food Protection* 72(10), 2132-2143

Mejlholm O., Gunvig A., Borggaard C., Blom-Hanssen C., Mellefont L., Ross, T., Leroi, F., Else, T., Visser D. and Dalgaard P. (2010) Predicting growth rates and growth boundary of *Listeria monocytogenes* — An international validation study with focus on processed and ready-to-eat meat and seafood. *International Journal of Food Microbiology* 141(3), 137–150

Vermeulen A., Devlieghere F., De Loy-Hendrickx A. and Uyttendaele M. (2011) Critical evaluation of the EU-technical guidance on shelf-life studies for *L. monocytogenes* on RTE-foods: A case study for smoked salmon. *International Journal of Food Microbiology* 145(1), 176-185

The integration of compliance and economic outcomes through the application of enhanced traceability and verification systems in food production

P. C. Pond, A. R. Wilson

Safe Food Production Queensland, Newstead, Queensland, Australia. (ppond@safefood.qld.gov.au)

Abstract

Traditionally, food safety regulation has been based upon a system of prescriptive legislation employing a system of active auditing and subsequent enforcement and prosecution activities for non-compliance. Safe Food Production Queensland (SFPQ) is the regulatory authority in the state of Queensland, Australia, responsible for the promotion and protection of food safety across a span of primary production and processing, to ensure the reliability and safety of the food chain. This agency has progressed away from traditional systems of prescription towards implementing outcome-based, industry food safety schemes that outline food safety requirements without defining the method by which they are to be achieved. This is accomplished through a philosophy of responsive regulation and active engagement, to assist industry in making better business decisions that concurrently deliver better food safety outcomes.

In synergy with these objectives, SFPQ has evaluated and developed decision-making tools to primarily optimise economic efficiencies for primary production and processing. These tools aim to assist businesses in identifying critical food safety points within a production chain to allow the judicial allocation of resources to maximise efficacy across the chain. As a result, enterprises are driven by economics to achieve improvements in food safety and the objectives of monitoring and compliance can be readily integrated as a secondary outcome. Most recently, systems to enhance monitoring and verification along with the mathematical modelling of food safety risks through-chain of primary production systems have been developed. These initiatives encompass measures to identify critical food safety points within a supply chain, improve monitoring at these points and integrate automatic reporting technology in an effort to mitigate risks posed by events that compromise food safety.

Overall, these systems are designed to support business management decisions and introduce economic efficiencies within primary production and processing industries, whilst concurrently satisfying regulatory requirements and delivering improved food safety outcomes to enable industry to move towards partial self-regulation.

Keywords: Regulation, verification, monitoring, risk management

Introduction

The safety and suitability of food for human consumption is globally managed by governments who recognise that they have a primary duty of care to ensure that suitable measures are taken to ensure that the health and wellbeing of their citizens is not compromised (Jouve 1998). However, both government and food production industries share a common goal in ensuring food safety and each fulfil a distinctly separate yet complementary role. Industry holds the primary responsibility in the safe production of food, whilst government is required to verify that industry is fulfilling this responsibility (Tompkin 2001).

In order to achieve this, governments have enacted food safety legislation that embodies requirements and procedures intended to minimise the risk to public health. Traditionally, this regulation has been based upon a system of rigid, detailed prescriptive legislation enforced through active auditing of constituents and subsequent enforcement and prosecution activities for reported non-compliance. Government policy has focussed upon industrial management practices and was most often reactive in response to immediate or perceived food safety

hazards, resulting in *ad hoc*, fragmented legislation as opposed to providing comprehensive coverage of all hazards through a supply-chain. The challenge remains to compel all sectors of the food production industry to adopt scientifically validated safe food-handling practises as standard operating procedures (Hoffmann 2010, Jouve 1998, Powell *et al.* 2011).

In an attempt to combat these issues, major efforts have been made to move food safety legislation away from the traditional systems of prescription to preventative, outcome-based legislation that provides complete and integrated management of foodborne hazards through the entire supply chain. Underpinning this outcome-based legislative approach is a policy based on "responsive regulation" which reflects the shared common goal philosophy. Traditional regulatory models are principally developed from and based upon achieving a scientific risk assessment outcome, whereas the proposed model is based upon a combination of science and economics to develop risk management tools that efficiently target critical points throughout the production process and allows for flexibility in achieving public health goals.

The purpose of this paper is to examine this concept and its practical application in the regulation of food safety in the state of Queensland, Australia, and how management tools in combination with the integration of traceability and verification systems may be utilised to achieve food safety outcomes, whilst concurrently providing economic incentives for industry compliance.

Materials and Methods

Safe Food Production Queensland (SFPQ) is the regulatory authority in the state of Queensland, Australia, responsible for developing and implementing risk-based food safety management schemes to ensure that the primary production and processing of food is carried out in a way that ensures it is fit for human consumption. This agency was established as part of a national food safety regulatory system to replace former prescriptive legislation that had been independently developed and implemented in each separate jurisdiction (Martin *et al.* 2003). SFPQ has progressed away from the traditional systems of prescription by developing and implementing outcome-driven, industry based food safety schemes that outline regulatory requirements without defining the method by which they are to be achieved. In line with this strategy, the agency has evaluated and developed a suite of decision-making tools and systems that utilise a combination of economic and science-based risk management approaches to assist businesses in identifying critical food safety points allow the judicious allocation of monitoring resources through the supply chain. As a result, enterprises are primarily driven by economic savings and/or increased income to achieve improvements in food safety and the objectives of monitoring and compliance are readily achieved as a secondary outcome.

To facilitate this and assist in its regulatory role, SFPQ has undertaken two major projects to enhance food safety management in Queensland in this method: firstly, a computer-based model has been developed to examine food safety risks in food supply chains and, secondly, information collection systems have been introduced to enhance traceability and verification of food safety in primary production and processing. In conjunction with collaborators in CSIRO and industry, SFPQ undertook a study to develop a prototype stochastic model based upon the pathogen *Listeria monocytogenes* in the fresh-cut lettuce supply chain. This model utilised a microbial food safety risk assessment to estimate the prevalence and concentration of *L. monocytogenes* at each step in the supply chain as a way to identify the most effective strategies or actions to reduce food safety risk. These methodologies were converted into mathematical equations and incorporated into a computer-based model to predict the growth of this pathogen along the entire supply chain from production to retail and identify the points of greatest risk within the chain. The prototype model was then applied in conjunction with a database application to support a traditional risk assessment approach to analyse, recognise and respond to potential risks.

With the development of computer-based models to identify critical food safety control points, such as the one mentioned above, information collection can be applied judiciously to maximise the efficiency of these activities through the production chain from farm to factory. Data collected from these points can be analysed to provide baseline data and key performance indicators for a given primary production and processing supply chain. Such indicators can be utilised to monitor individual performances through-chain and their individual contribution to pathogen control. SFPQ developed an information database in conjunction with the Queensland dairy industry to assist in the monitoring of critical food safety parameters within the supply of milk from farm to processing facility.

Results and Discussion

Modelling Food Safety Risks within a Supply Chain

The identification of food safety risks within a supply chain is traditionally difficult due to the size and complexity of primary production and processing networks. There are large numbers of primary producers in numerous regions supplying a range of processing facilities, distribution centres and retail sale through various transport networks and there is a considerable lack of knowledge as to the impact of post-harvest handling and transport operations in some food production industries. Validation studies to assess the fit of the predictions of the model to historical real world data demonstrated that the model in its initial form was inconclusive, with modelling data reflecting observations in some, but not all, scenarios. Historical observation data relating to *Listeria monocytogenes* growth after use-by dates demonstrated a degree of similarity to those predicted by the model. However results at the processing stage were very different, with the model showing larger amounts of growth than were recorded in the data. Additionally, the amount of data available to validate this model was a major limitation within this analysis and the availability and application of such will demonstrate more conclusive results.

This model was an initial step towards developing new tools to assist in measuring uncertainty and indicating risks during transport, packing, processing and distribution, subject to available data and research studies. Moreover, this model can indicate to government and industry where appropriate intervention can be applied within a supply chain to maximise benefit whilst minimising regulatory cost. The modelling philosophy has been founded upon the prevalence and concentration of a food safety risk at each stage being represented by a probabilistic distribution, allowing for the model to be adapted to a range of new parameters (e.g. new pathogens, new temperature distributions) and also be able to support a range of perishable products and their relevant supply chains. This initial modelling project has provided a sound basis for the further development of computer-based models to monitor food safety risks in supply chains and future improvements are currently planned to extend the model to encompass other pathogens and food products.

Monitoring Identified Control Points

Another facet of responsive regulation involves the replacement of the active enforcement of prescriptive requirements with continuous monitoring, traceability and verification via information collection. The historical collection of information allows data to be organised and analysed in such way so as to not only demonstrate trends of compliance over a period of time, but also recognise indicators of food safety hazards and their associated risks.

In Queensland, technology has been developed in conjunction with the dairy industry to collect and record information pertaining to identified food safety critical control points such as the temperature of milk, somatic cell counts, pathogen detections and antibiotic residue data from production on farm to delivery at a retailer or distributor. This raw data is collected by milk processors and independently uploaded to a central on-line database to allow monitoring and traceability of product and provide key performance indicators at these critical control points. These indicators are established from previously collected data and allow industry to detect inefficiencies or failures within the food production chain to enable

corrective action and reduce costs associated with product losses and logistics. This allows processors to identify individual producers who do not meet the designated performance standards and may require assistance with retraining or monitoring, whilst providing evidence of compliance to food safety legislation. Furthermore, individual businesses can readily trace and monitor product through-chain to ensure that it meets quality requirements and customer demands in the most efficient and timely way possible, as well as enabling them to improve efficiencies and obtain premiums for higher quality production. Additionally, through the co-operation of producers and processors, SFPQ as government regulators are also able to remotely access, analyse and monitor these production chains, providing instant verification and an economic saving to stakeholders in reduced auditing costs. Automatic advice can be issued when requirements are breached to trigger a co-ordinated and timely response to potential food safety incidents, providing the opportunity to arrest the situation before effects are seen in the marketplace and recover product to alternative product streams. Auditing resources can then be focussed upon verification of individuals who demonstrate consistently lower performance and in-turn drive industry-wide improvements.

Conclusion

The development and implementation of these systems in Queensland has allowed SFPQ to begin to shift the primary reason for compliance within the food production industry from the consequences of enforcement (i.e. financial penalty or suspension of accreditation) to an economic driver for compliance. By providing verification systems that support business management decisions, it can be demonstrated that improvements in food safety at identified critical food safety control points (i.e. reduction in pathogens, time and temperature monitoring) create further efficiencies through reductions in cost and increase in production quality. Thus, controlling members of primary production supply chains, such as processing establishments, are able to provide direct feedback to suppliers and demand high quality, safe supply from producers. Food production businesses are able to respond to these demands for improvements in the safety and quality of product and in-turn control their individual inputs and on-farm hygiene to improve overall quality in an effort to gain market share or increase the price obtained for production. Overall, these systems drive industry improvement by aligning an improvement in food safety with greater economic efficiencies, concurrently removing the emphasis on regulatory intervention and allowing industry partial self-regulation.

Acknowledgements

We would like to acknowledge the work conducted by Dr Andrew Higgins and Mrs Di Prestwidge, CSIRO Ecosystem Sciences and Dr Silvia Estrada, Food Chain Intelligence, for their work in developing the fresh-cut lettuce model referred to in this paper

References

Hoffmann S. (2010) Food Safety Policy and Economics: A Review of the Literature. *Resources for the Future: Discussion Paper* July 2010, 36pp. http://www.rff.org/RFF/Documents/RFF-DP-10-36.pdf (accessed 11 March 2011).

Jouve J.L. (1998) Principles of food safety legislation. *Food Control* 9, 75-81.

Martin T., Dean E., Hardy B., Johnson T., Jolly F., Matthews F., McKay I., Souness R. and Williams J. (2003) A new era for food safety regulation in Australia. *Food Control* 14, 429-438.

Powell D.A., Jacob C.J. and Chapman B.J. (2011) Enhancing food safety culture to reduce rates of foodborne illness. *Food Control* 22, 817-822

Tompkin R.B. (2001) Interactions between government and industry food safety activities. *Food Control* 12, 203-207.

Pasta Salad Predictor – development of a new tool to support shelf-life and safety management

N. B. Østergaard[1,2], J. J. Leisner[2], P. Dalgaard[1]

[1] Seafood & Predictive Microbiology, Division of Industrial Food Research, National Food Institute, Technical University of Denmark, Søltofts Plads, Building 221, DK-2800, Kgs. Lyngby, Denmark
[2] Section of Microbiology, Department of Veterinary Disease Biology, Faculty of Life Sciences, University of Copenhagen, Grønnegårdsvej 15, DK-1870, Frederiksberg C, Denmark

Abstract

Ready-to-eat (RTE) pasta salads from small food outlets are popular but they have short shelf-life due to growth of spoilage microorganisms. Importantly, RTE pasta salads have resulted in several major outbreaks of food-borne disease *e.g.* due to *Salmonella*. We studied oil based pasta salads with the objective of developing a new predictive tool to support shelf-life and safety management. High concentrations (6-8 Log CFU/g) of *Enterobacteriaceae*, lactic acid bacteria (LAB) and *Pseudomonas* spp. were detected in different commercial products based on cooked pasta, raw vegetables, pesto and fermented cheese and olives. Storage trials, challenge tests and experiments with liquid laboratory media (Bioscreen C) at 5, 10, 15 and 20°C allowed growth of *Enterobacteriaceae*, LAB, *Listeria monocytogenes*, *Pseudomonas* and *Salmonella* to be quantified. The effect of temperature on growth rates (μ_{max}) was appropriately described by the simple square root model. Growth responses in pasta salads were compared to our new secondary temperature models as well as available models. The most appropriate models were then included in a spreadsheet-based Pasta Salad Predictor. Growth of psychrotolerant *Pseudomonas*, originating from raw vegetables and initially present in concentrations as high as 6 Log CFU/g, limited shelf-life of the pasta salads included in this study. The developed Pasta Salad Predictor allowed shelf-life and safety of the product to be evaluated based on both initial microbial contamination (hygiene), storage time and storage temperatures (constant or variable). This new predictive tool seems useful to help food outlets and authorities reach a common understanding of reasonable hygiene requirements and storage conditions for pasta salads.

Development of response surface model to describe the effect of temperature and relative humidity on *Staphylococcus aureus* on cabbage

T. Ding, J. Wang, N.J. Choi, H.N. Kim, S.M.E. Rahman, J.H. Park, D.H. Oh

Department of Food Science and Biotechnology and Institute of Bioscience and Biotechnology, Kangwon National University, Chuncheon, Gangwon, Korea. (deoghwa@kangwon.ac.kr)

Abstract

In this study, different temperature (15, 25, and 35 ºC) and relative humidity (60, 70, and 80%) values were simulated as environmental factors of climate changes in a closed environmental chamber, and the combined effects of temperature and relative humidity on the growth or survival of *Staphylococcus aureus* were determined on cabbage. Also, a response surface methodology (RSM) was developed for modelling the growth of *S. aureus* on cabbage as a function of temperature (15-35 ºC) and relative humidity (60% - 80%). The growth data were collected under different conditions, and were then fitted into the modified Gompertz model to estimate the growth rate (GR) at each condition with high determination of coefficients (R^2 > 0.98). Then, the secondary models were developed for the GRs obtained from the modified Gompertz model using the RSM quadratic polynomial equation. The established model was significant (P < 0.01), and the predicted values of the growth parameters obtained using the model equations were in close agreement with experimental values (R^2 = 0.995). Furthermore, several statistic characteristics such as root mean square error (*RMSE*), bias factor (B_f), accuracy factor (A_f) and %standard error of prediction (*%SEP*) were employed to validate the developed models using the additional experimental data. The results showed that the overall predictions had slight deviation with the observations, indicating success at providing reliable predictions of *S. aureus* growth on cabbage. Through this study, the impact of the climatic factors such as temperature and relative humidity on growth or survival of *S. aureus* on cabbage was obviously observed, while the predictive growth model was also established which could supply sufficient information to HACCP or MRA programs in the future.

Keywords: Staphylococcus aureus, cabbage, temperature, relative humidity, response surface methodology

Introduction

Climate change, affected by temperature, relative humidity, composition of air etc., has implications on food production, food security and food safety (FAO 2008). Also, it can influence all foodborne pathogens and their associated diseases potentially (ECDC 2007). In the last decades, outbreaks of foodborne diseases have become an increasingly important public health issue all over the world. Foodborne illnesses caused by *Staphylococcus aureus* have been associated with leafy vegetables (Beuchat 1996; Seo *et al.* 2010; Sokari 1991). Although, numerous literature studies have studied the single or combined effects of temperature, high pressure, and radiation on the population dynamics of *S. aureus* (Gao, *et al.* 2006; Lee *et al.* 2006), there are still few research projects investigated the impact of simulated temperature and relative humidity (RH).

The objectives of this study were to investigate the combined effect of temperature (15-35 °C) and RH (60%-80%) on the growth kinetics of *S. aureus* on cabbage under simulated environmental conditions using response surface methodology (RSM).

Materials and Methods

Operation and design of the experiment

A mixed culture of *S. aureus* strains (ATCC12598, ATCC13565, and ATCC12480) was inoculated on the surface of cabbage samples purchased from a local supermarket in Chunchon, Korea. The initial pathogen level was approximately 3.0 log CFU/g. Inoculated samples were transferred into a closed environmental chamber which was used to simulate the storage temperature and relative humidity. Then, tested samples were exposed on sterile aluminum foil and were stored at 15, 25 and 35 °C for 4 days, 2 days and 1 day, respectively. At each temperature, experiments were conducted with three RH levels (60%, 70%, and 80%). All trials were carried out according to the central composite design (CCD) method. The population of *S. aureus* was enumerated by plating on Baird-Parker Agar Base (Difco) supplemented with Egg Yolk Tellurite Solution before 24 h incubation at 37 °C.

Development and validation of predictive models

The collected growth data at each combined condition were fitted into the modified Gompertz model to estimate the growth rate (GR: h^{-1}), and a secondary model was established for obtained GRs using the response surface methodology. Then, a validation step was carried out through external validation using independent data sets for selected conditions, which were not used for model development. Root mean square error (*RMSE*), bias factor (B_f), accuracy factor (A_f), and %standard error of prediction (*%SEP*) were employed to assess the performance of the developed model.

Results and Discussion

The effect of temperature and relative humidity on the growth kinetics of S. aureus on cabbage

Experimental data obtained during the storage period at each simulated combined condition showed that temperature and relative humidity have a strong influence on the growth or survival behaviour of *S. aureus* (Figure 1). Low temperature or relative humidity was able to inhibit the growth of *S. aureus*, while increasing temperature or RH could lead to a higher maximum population density (MPD). Similar result has been published in a previous study that a higher MPD of *Salmonella enterica serovar* Typhimurium DT104 in beef at 10 °C and 96% RH was observed compared with that at 5 °C and 76% RH after 72 h storage (Kinsella *et al.* 2009). Moreover, it can be obviously observed that the growth or survival curve emerged with a sharper decline at lower RH in the later storage period at 15 and 25 °C after a certain holding time.

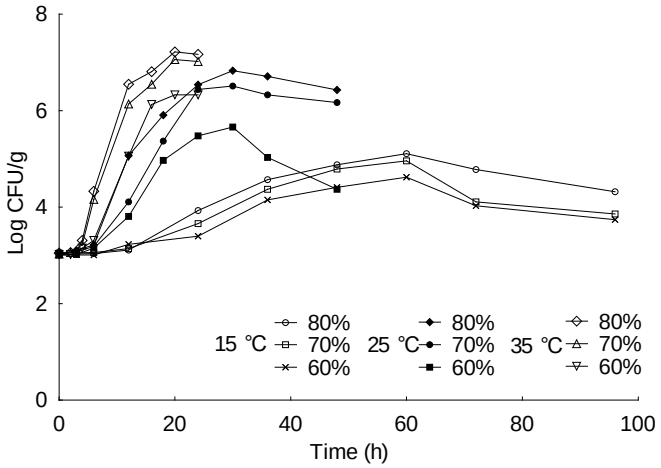

Figure 1: The effect of temperature and relative humidity on the growth or survival of *S. aureus* on cabbage at different combined conditions.

Development of predictive models

The primary predictive model was developed based on the growth portion data with high determination of coefficients ($R^2 > 0.98$). GR values of *S. aureus* on cabbage (Table 1) generated from the modified Gompertz model were used to develop the secondary model using a quadratic polynomial equation. Figure 2 illustrated the GR values of *S. aureus* in response to changes in temperature and relative humidity via three-dimensional surface diagrams and showed that shifts of temperature and relative humidity could influence the growth rates significantly. The statistical test for the significance and adequacy of the model was evaluated using analysis of variance (ANOVA). The *P* values ($P < 0.0001$) show that the developed model was highly significant, while the lack-of-fit test was not significant ($P > 0.05$). The established response surface quadratic polynomial equation was obtained with a high R^2 (0.995) as follows (Eq. 1):

$$Y = 0.24 + 0.18x_1 + 0.039x_2 + 0.032x_1x_2 + 0.0011x_1^2 - 0.0079x_2^2 \quad (1)$$

Table 1: CCD arrangement and growth rate (GR) of *S. aureus* on cabbage estimated from the modified Gompertz model.

Temperature (°C)	Relative humidity (%)	GR (log CFU/h)
15	60	0.057
35	60	0.369
15	80	0.071
35	80	0.512
15	70	0.063
35	70	0.412
25	60	0.209
25	80	0.284
25	70	0.246
25	70	0.255
25	70	0.227
25	70	0.238
25	70	0.259

Validation of predictive models

External validation was conducted using additional experimental data sets for selected conditions within the developed model boundaries presented in Table 2. The predicted values were calculated by the developed model and were compared with the observations graphically (Figure 3) to illustrate the goodness of the proposed model. As shown in Figure 3, most of the points fell close to the regression line within the confidence intervals which indicated a high line-linear relationship between the observed and predicted values. *RMSE*, B_f, A_f and *%SEP* were employed to evaluate the fit quality of the obtained model. The results (*RMSE* = 0.034, B_f = 1.132, A_f = 1.181 and *%SEP* = 13.043) indicated that the secondary model exhibited a good performance for describing the experimental data and was also expected to provide the reliable predictions in practice.

Table 2: Observed and predicted growth rates of *S. aureus* for model validation.

Temperature (°C)	Relative humidity (%)	Growth rate (log CFU/h)	
		observed	predicted
15	75	0.090	0.060
18	70	0.127	0.110
20	75	0.207	0.159
27	70	0.238	0.274
30	65	0.334	0.304
33	65	0.351	0.353
35	70	0.467	0.419

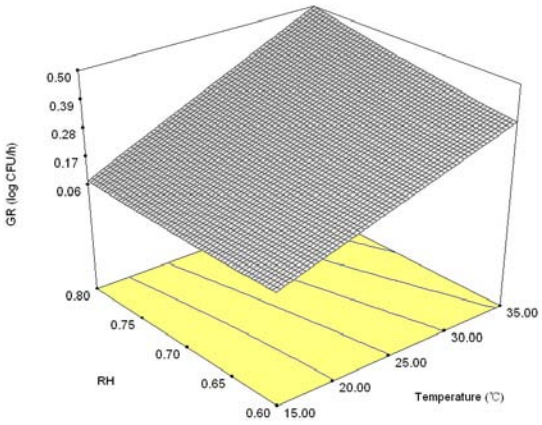

Figure 2: Response surface plot of the obtained growth rate of *S. aureus* in response to changes in temperature and relative humidity.

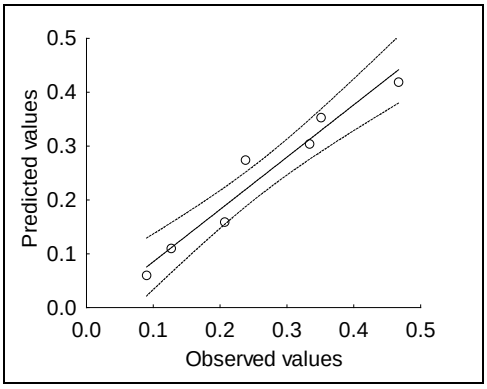

Figure 3: Observed growth rates (GRs) of *S. aureus* versus predicted GRs. Dotted lines are the linear regression lines, and the dashed lines indicate a 95% confidence interval.

Conclusions

A secondary predicted model developed using a response surface methodology was used to estimate the effect of simulated combined conditions of temperature and relative humidity on the growth kinetics on cabbage. The results demonstrated that temperature and relative humidity, two important factors among various climatic factors, were capable of affecting the growth or survival of *S. aureus*. The validation step indicated that the developed predictive model showed good performance in describing the experimental data and is able to provide credible predictions. It will be useful for conducting HACCP or MRA programs in the future.

Acknowledgements

This research was supported by a grant (10162KFDA995) from Korea Food and Drug Administration in 2010.

References

Beuchat L.R. (1996) Pathogenic microorganisms associated with fresh produce. *Journal of Food Protection* 59 (2), 204-216.

European Centre for Disease Prevention and Control (ECDC) (2007) Environmental change and infectious disease workshop. Meeting report. Stockholm, Sweden. http://www.ecdc.europa.eu/en/publications/Publications/0703_MER_Environmental_Change_and_Infectious_Disease.pdf (accessed 25 March, 2011).

Food and Agriculture Organization (FAO) (2008) Food safety and climate change. FAO conference on food security and the challenges of climate change and bioenergy. http://www.fao.org/ag/agn/agns/files/HLC1_Climate_Change_and_Food_Safety.pdf (accessed 25 March, 2011).

Gao Y.L., Ju X.R. and Jiang H.H. (2006) Use of response surface methodology to investigate the effect of food constituents on *Staphylococcus aureus* inactivation by high pressure and mild heat. *Process Biochemistry* 41 (2), 362–369.

Kinsella K.J., Prendergast D.M., McCann M.S., Blair I.S., McDowell D.A. and Sheridan J.J. (2009) The survival of *Salmonella enterica* serovar Typhimurium DT104 and total viable counts on beef surfaces at different relative humidities and temperatures. *Journal of Applied Microbiology* 106 (1), 171–180.

Lee N.Y., Jo C., Shin D.H., Kim W.G. and Byun M.W. (2006) Effect of γ-irradiation on pathogens inoculated into ready-to-use vegetables. *Food Microbiology* 23 (7), 649–656.

Seo Y.H., Jang J.H. and Moon K.D. (2010) Occurrence and characterization of enterotoxigenic *Staphylococcus aureus* isolated from minimally processed vegetables and sprouts in Korea. *Food Science and Biotechnology* 19 (2), 313-319.

Sokari T. (1991) Distribution of enterotoxigenic *Staphylococcus aureus* in ready-to-eat foods in eastern Nigeria. *International Journal of Food Microbiology* 12 (2-3), 275-280.

Development of an all-Ireland food microbial database and its implications for food chain integrity

F. Tansey[1], F. Butler[1]

[1] UCD School of Biosystems Engineering, Agriculture and Food Science Centre, University College Dublin, Belfield, Dublin 4, Ireland. (fergal.tansey@ucd.ie)

Abstract

The main objective of the FIRM funded Safe and Healthy Foods project is to develop and maintain a state-of-the-art all-Ireland Food Microbial Database (FMD). The project partners are University College Dublin (UCD), Department of Agriculture, Fisheries and Food (DAFF), Food Safety Authority of Ireland (FSAI), Marine Institute (MI), Teagasc Ashtown Food Research Centre (AFRC), Teagasc Moorepark Food Research Centre (MFRC), and University of Ulster (UU). UCD is working with Open Sky (database provider), in conjunction with the other project partners (data providers), to develop a web-based database. The database will be populated with up to 4 years validated pathogenic data from the data providers by the end of 2012. Project partners and other key stakeholders will have full access to the database and the general public will have limited access. The database will provide relevant, reliable, and timely data on both microbial pathogens (*Campylobacter* spp., *Escherichia coli* O157, *Listeria* spp., and *Salmonella* spp.) and noroviruses, covering 28 food and environmental categories. It is envisaged that the database will strengthen links between existing all-island institutional surveillance systems (veterinary, food and clinical), improve data quality, identify data gaps, and foster international links.

Keywords: *database, pathogens, food, surveillance, web-based*

Introduction

The EU Zoonoses Directive (2003/99/EEC) mandates that all EU member states must provide data on zoonoses and zoonotic agents (EFSA 2006). This information is passed to the European Centre for Disease Prevention & Control (ECDPC) and the European Food Safety Authority (EFSA), where it is collated into the EU Zoonoses Reports. Ireland is a major food exporting country, and the quality and comprehensiveness of the information provided from Ireland should be the best in the EU. However, delivering effective surveillance is difficult in Ireland, as currently there are no established links between veterinary, food, and public health laboratories. This project brings together established experts in food safety research and regulation, to develop and implement a comprehensive programme designed to capture and analyse foodborne pathogenic data (Singer *et al*. 2007; Tebbutt 2007; Younus *et al*. 2006).

The main objectives are: (1) to develop and maintain a state-of-the-art all-Ireland Food Microbial Database (FMD) and to populate it with validated data from Irish data providers to provide relevant, reliable, and up-to-date data in a format that allows timely decision-making, risk assessment and management; (2) to develop an inaugural standardised molecular sub-typing database to include, initially, three food-related zoonotic microbial pathogens; and (3) to investigate the feasibility of linking Northern Ireland foodborne pathogen data, methods, and reporting systems, to the database so as to provide an accurate all-island overview underpinning effective and efficient responses to challenges posed by foodborne pathogens.

This project is part of a Food Institutional Research Measure (FIRM) funded project, involving several major food research institutes in Ireland: University College Dublin (UCD); Department of Agriculture, Fisheries and Food (DAFF); Food Safety Authority of Ireland (FSAI); Marine Institute (MI); Teagasc Ashtown Food Research Centre (AFRC); Teagasc Moorepark Food Research Centre (MFRC); and University of Ulster, Jordanstown (UU).

Materials and Methods

UCD is currently working with the other project partners (data providers) to develop a web-based database (Figure 1), which is expected to be operational for use between the project partners by the end of May 2011. The database will be populated with up to 4 years validated pathogenic data from the data providers by the end of 2012. Project partners and other key stakeholders will have full access to the database and will be able to download data for their own use via Microsoft Excel. The general public will have limited access via Adobe PDF information sheets.

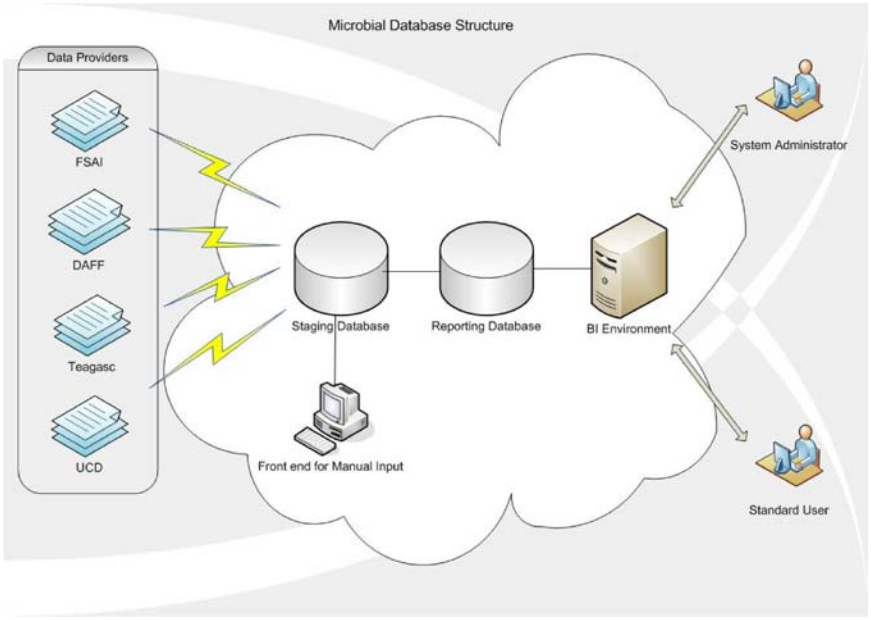

Figure 1: Overview diagram of the web-based Food Microbial Database (FMD).

Results and Discussion

The database will provide relevant, reliable, and timely data on both microbial pathogens (*Campylobacter* spp., *Escherichia coli* O157, *Listeria* spp., and *Salmonella* spp.) and viruses, covering 22 food and environmental categories (Figure 2). It is envisaged that the database will strengthen links between existing all-island institutional surveillance systems (veterinary, food and clinical), improve data quality, identify data gaps, and foster international links.

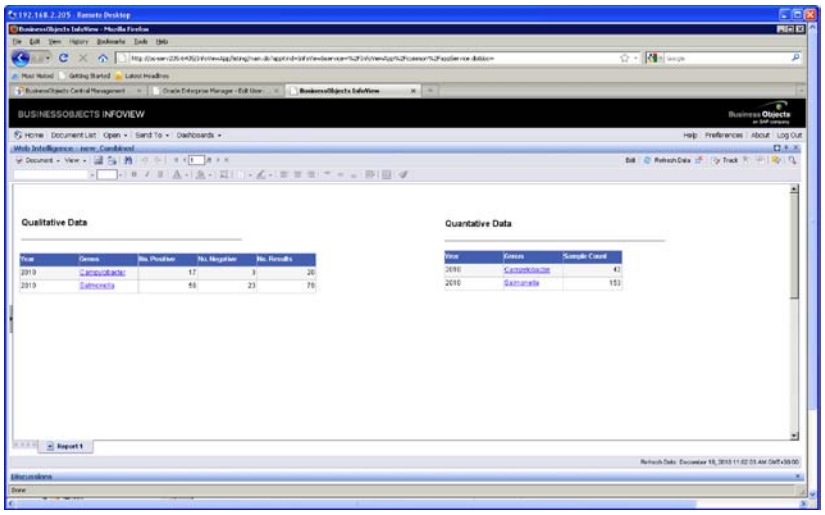

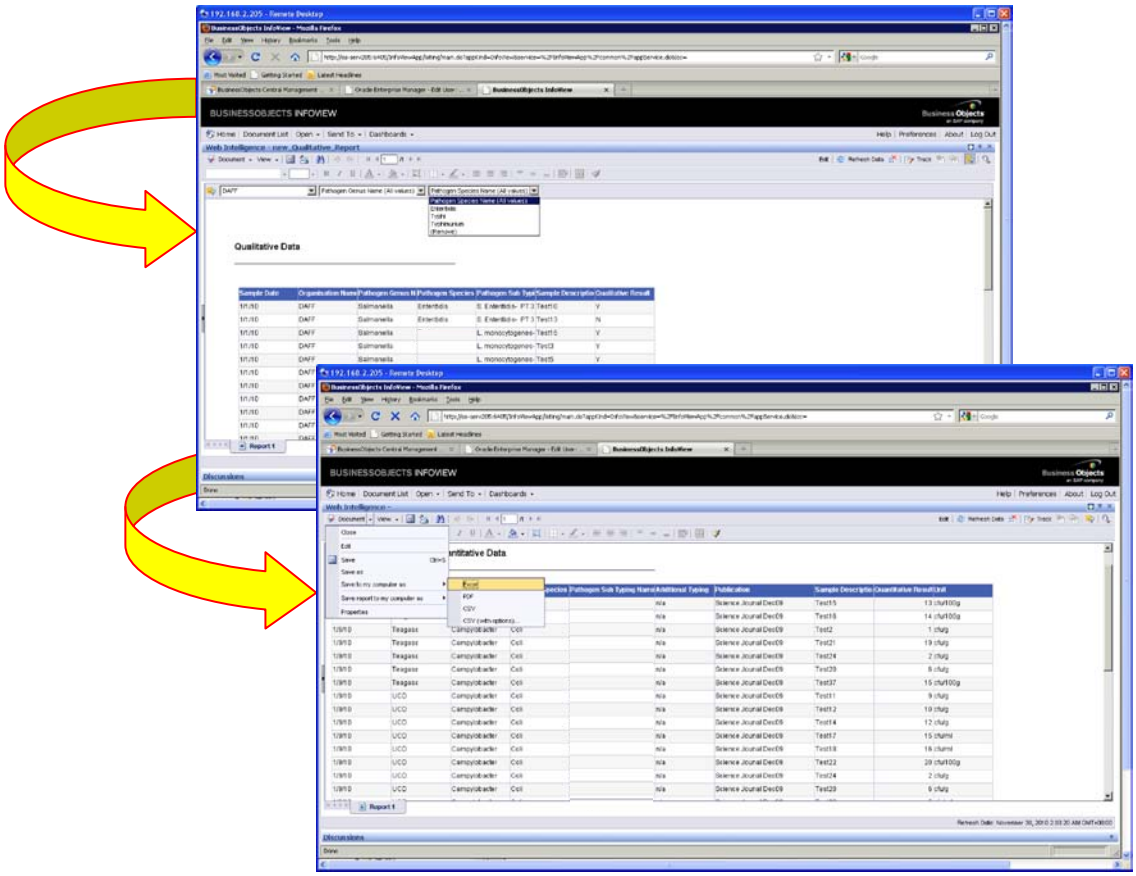

Figure 2: Web-based screenshots of draft microbial data from the FMD using Microsoft Business Objects software.

Conclusions

This database will allow, for the first time, researchers and regulators access to Irish foodborne pathogenic data from veterinary, food and clinical surveillance systems, spanning a wide spectrum of products from farm to fork.

Acknowledgements

This research is funded by the Food Institutional Research Measure (FIRM) as part of the Irish National Development Plan.

References

European Food Safety Authority (EFSA) (2006) Zoonoses Report. Trends and sources of zoonoses, zoonotic agents and antimicrobial resistance in the EU in 2004.

Singer R.S., Cox L.A. and Dickson J.S. (2007). Modelling the relationship between food animal health and human foodborne illness. *Preventive Veterinary Medicine* 79, 186-203.

Tebbutt G.M. (2007) Does microbiological testing of foods and the food environment have a role in the control of foodborne disease in England and Wales. *Journal of Applied Microbiology* 102, 883-891.

Younus M., Wilkins M.J. and Arshad M.M. (2006) Demographic risk factors and incidence of Salmonella enteritidis infection in Michigan. *Foodborne Pathogenic Diseases* 3, 266-273.

Modeling pathogens of foodborne infections at the pre-harvest level of the food production chain

I. Soumpasis[1,2], F. Butler[1]

[1]Biosystems Engineering, School of Agriculture, Food Science and Veterinary Medicine, University College Dublin, Belfield, Dublin 4, Ireland.
[2]New address of correspondence: Safety and Environmental Assurance Centre, Colworth Park, Sharnbrook, MK44 1LQ, United Kingdom, (ilias.soumpasis@unilever.com)

Abstract

During previous work elaborated models were developed to describe the infection of pigs with *S.* Typhimurium in modern industrialized pig farms and to evaluate the effect of risk mitigation strategies, including vaccination. During this work, a number of challenges were identified, given the specific characteristics of farms. The objective of this work was to disseminate this knowledge and to propose ways to cope with these challenges. Infectious disease modeling in farms has a clear distinction from modeling in human and wildlife disease modeling and need extra effort to adapt models to specific situations, type of farms and adapted pathogens. In order to build a valid model, a number of infection and host population characteristics should be taken into account. Models incorporating non-dynamic factors can add value towards the optimization of intervention strategies.

Keywords: foodborne infections, modelling, pathogens, pre-harvest, food production chain

Introduction

In the last five years there has been an increasing interest in mathematical modelling of infectious diseases for food production animals at the farm level towards developing more holistic models that will serve from a farm to fork food safety strategy. However, and in order to model successfully infectious diseases in pig farms some special characteristics of this extraordinary and artificial way of life must be considered. Indeed, food production pigs in modern pig farming have a short and generally similar in duration life expectancy. Prolonged serological historical data is usually unavailable in contrast to the cases of human or wild life animal diseases, since the infection usually has not enough time in order for its dynamics to arrive at equilibrium. Moreover, food production animals are usually gathered in farms, either in compartmental or free range states, limiting or increasing the probability of an effective contact, respectively. In some cases, as with finisher pigs or broiler chicken, all-in-all-out farming systems are applied breaking the continuity of the system. The aim of this work was to identify these differentiating characteristics and discuss way that could be addressed.

Materials and Methods

In order to achieve our aim we have used the finding from primary and secondary sources, forming a data triangulation, which increases the validity of the research. Regarding the primary sources, data from our previous work on *Salmonella* infections in pig farms was used. *S.* Typhimurium is a major source of human foodborne salmonellosis with limited effects on the health of the pigs themselves. We have used these models as a case study to demonstrate the deterministic and stochastic dynamics of the pathogen in a farm (*Soumpasis and Butler* 2009; 2011) and to serve as a base for comparison with other types of farms as well with the models developed for human and wildlife animal communities.

Regarding the secondary data a number of papers were reviewed and selected on the basis of the modelling followed (infectious disease modelling), the pathogen (to cause to foodborne infection) and the type of farm (major farmed food production animals i.e. pigs, cattle, broilers).

Results and Discussion

A number of issues were identified that would need special attention when modelling the transmission of a pathogen in a farm. These issues along with some actions that could be taken are analysed in the following paragraphs.

Commonalities among Farms

Current intensive farming of food production animals is much industrialised. Farms generally follow specific standards and are organised into a limited number of husbandry systems. In contrast the "open" or "green" type of farming, where animals have a greater interaction with the environment, animals in industrialised farms are living in building with controlled micro-clima that it is optimised for their growth. This micro-clima is usually common in countries with the same characteristics, e.g. European countries, allowing for generalisation of the models and use in wider areas, assuming that similar systems are followed.

Definition of the Community

Although in wildlife and human epidemiology the definition of the community may be sometimes clear (i.e. a city, a country, an isolated animal population in an island), in farms may not always be as straight forward. In the case of pig or broiler farms, the animals may live isolated in rooms, while at the same time being affected from external factors, replacement of animals, wind transfer of pathogens and more. It has to be thought carefully, what would be the community, where the individuals actually can have contact with each other, and if and how the imports of the pathogen through other routes in the isolated system should be modeled.

Frequency or Density Dependent Transmission

Once the community has been defined, the type of transmission should be thought of. In case the individuals can have unrestricted access and contact to any other individual within the community, the density dependent approach should be followed to ensure the rate of transmission is analogous to the probability of contacts. Examples of this case, can be the "open" or "green" type of farms, where animals are free to move and have contacts with any other individual, or the case of broilers, where again in the house they have unlimited contacts with all the other individuals. On the other hand, when the number of contacts with other individuals is limited, such as in the case of fattening pigs, dividing a room with fences into pens, a frequency dependent approach may be more appropriate.

Probabilistic Nature

As it was shown from previous work when the community size is small, then the infection may have stochastic fluctuations and may suffer of stochastic extinctions (*Soumpasis and Butler*, 2009). Once the community is defined, the size of the community would guide the researcher to the decision of using (or not) demographic stochasticity.

Host Adaptation and Infection Characteristics

Salmonella is a very good example of host adaptation and infection characteristics (*Kingsley and Baumler*, 2000). There is a large number of subspecies and serotypes of the pathogen, which are adapted to a different extent to different hosts and this has effect also to the infection characteristics. E.g. from previous studies it is clear that *S.* Typhimurium has very different characteristics (shedding period, sero-reaction) compared to all the other major sero-types of *Salmonella*, that can be isolated from pigs. This can and should have an effect on the transmission of the pathogen and should be captured when the infection is modeled.

Levels of Transmission

In contrast to the traditional one level of transmission for homogenous populations (i.e. all the individuals share the same characteristics and have the same probability of transmitting the infection), a new approach is developing for a number of infectious diseases, where more than one level of transmission may occur. This idea has been used in modeling infectious diseases with a carrier state, such as hepatitis B (Keeling and Rohani 2007) and in more modern cases

modeling influenza and influenza A (Coelho and Codeco 2009). In the cases of modeling the transmission in farms of pathogens responsible for foodborne diseases, the transmission of at least *S.* Typhimurium and *E. coli* seem to be able to be described in such way (Soumpasis and Butler 2009; 2011). Although, in the first approache this was modeled using a percentage of individuals that will follow one or other path (of low or high infection), in case of farms, where the population is small, the decision of which syndrome will occur can be modeled using indirectly a dose-response and following the number of animals that are infected in the host community (Soumpasis and Butler 2009; 2011); thus the higher the proportion of infectious animals, the higher dose that a susceptible animal will receive. Higher doses in this way lead to highly infectious individuals and lower doses low infectious individuals.

Births and Mortality

Answering the question of defining a community, some more issues may arise on the births and mortality. Many times, the term of replacement is used instead of births, because the animals that are removed from a closed farm system are being replaced by some already born and being already at the appropriate age. This gives rise to the concept of "pulsed" births or replacement, where a number of animals are introduced altogether into a farm. On the other hand, naturally occurring deaths are rare in a farm, except in the case of chronic diseases being present. Mortality occurs either as harvesting again like a "pulse" or because of the disease if there is any morbidity. In any case, the research should be very careful modeling births and mortality and always these two terms should be equal, in order for the farm to be sustainable.

Immunity

Immunity against the infection may be active, i.e. following after natural infection or passive such as the one passed from the mother to the offspring through the colostrum and the milk. The latter can protect the young individuals until they will start developing their own immunity system. Active immunity may be for life or may be waning, leading to a vicious circle of re-infections.

Indirect Transmission

Some pathogens may have a clear and distinct stage out of the host, where they can survive for a significant amount of time while still being infectious. Questions such as the survival time, the ability to travel in the medium, etc should be thought before deciding to model this stage explicitly. In other cases, the concept of imports of the pathogen in the community would suffice to describe the situation.

Host Heterogeneities

In some cases, such as the fattening pigs and the broilers, the individuals are all of the same age, usually of the same breed, with no distinct differentiation and homogenous mixing is assumed. However, in other cases, such as the case of dairy farms, there can be a clear differentiation of the susceptibility of the individuals, which should be taken into account (Turner *et al*. 2006; 2008).

Intervention Strategies

The intervention strategies in farms can be divided into two major categories, management and pharmaceutical, including vaccination (Soumpasis *et al.* 2010). The management strategies are geared towards altering the management practices towards reducing the susceptibility and the overall transmission rate. Pharmaceutical can have two aims, either response using antibiotics in order to reduce the number of infectious individuals or proactive reducing the susceptibility of the individuals, either using antibiotics or vaccinating the individuals. In either case, the effect of the strategy should be clear and should be modeled explicitly. Combining more than one strategies in one framework model, could have better results because the strategies are not tested in isolation and a combination of strategies can lead to more efficient results (Soumpasis *et al.* 2010).

Conclusions

Infectious disease modeling in farms has a clear distinction from modeling in human and wildlife disease modeling and need extra effort to adapt models to specific situations, type of farms and adapted pathogens. In order to build a model that reflects the situations in the farm as realistically as possible, a number of infection and host population characteristics, that depend on the type of both the pathogen and the farm, should be taken into account. Models incorporating non-dynamic factors can add value towards the optimization of intervention strategies.

Acknowledgements

We acknowledge the 6th EU framework Integrated Project QPorkchains that has been the major source of information for this paper. The content of the paper reflects only the view of the authors; the community is not liable for any use that may be made of the information contained in this paper.

References

Andrews JR. and Basu S. (2011) Transmission dynamics and control of cholera in Haiti: an epidemic model. *The Lancet* 377(9773), 1248 - 1255

Coelho F.C. and Codeco C.T. (2009) A Bayesian framework for parameter estimation in dynamical models with applications to forecasting, Nature Precedings http://precedings.nature.com/documents/4044/version/1 (accessed 11 March, 2011).

Keeling M. J. and Rohani P. (2007) Modeling Infectious Diseases, Princeton: Princeton University Press. 408pp. (ISBN**:** 0691116172)

Kingsley R. A. and Baumler A. J. (2000) Host adaptation and the emergence of infectious disease: the Salmonella paradigm. *Molecular Microbiology* 36(5), 1006–1014.

Soumpasis I., Alban L. and Butler F. (2010) Controlling Salmonella infections in pig farms: A framework modelling approach, *Food Research International* In Press, –.

Soumpasis I. and Butler F. (2009) Development and application of a stochastic epidemic model for the transmission of Salmonella Typhimurium at the farm level of the pork production chain. *Risk Analysis* 29(11), 1521–1533.

Soumpasis I. and Butler F. (2011) Development of a Self-Regulated Dynamic Model for the Propagation of Salmonella Typhimurium in Pig Farms. *Risk Analysis* 31(1), 1521–1533.

Turner J., Begon M., Bowers R.G. and French N.P. (2003) A model appropriate to the transmission of a human food-borne pathogen in a multigroup managed herd. *Preventive Veterinary Medicine* 57(4), 175–198.

Turner J., Bowers R. G., Begon M., Robinson S. E. and French N. P. (2006) A semi-stochastic model of the transmission of *Escherichia coli* O157 in a typical UK dairy herd: dynamics, sensitivity analysis and intervention/prevention strategies. *Journal of Theoretical Biology* 241(4), 806–822.

Turner J., Bowers R. G., Clancy D., Behnke M. C. and Christley R. M. (2008) A network model of *E. coli* O157 transmission within a typical UK dairy herd: the effect of heterogeneity and clustering on the prevalence of infection. *Journal of Theoritical Biology* 254(1), 45-54.

Temperature Integrators as tools to validate thermal processes in food manufacturing

P.J. Fryer, M.J.H. Simmons, K. Mehauden, S. Hansriwijit, F. Challou, S. Bakalis

School of Chemical Engineering, University of Birmingham, B15 2TT, Birmingham, United Kingdom
(p.j.fryer@bham.ac.uk)

Abstract

Characterisation of thermal processes remains a challenge as it involves rotating parts and reasonably high temperatures, thus making use of measurement techniques such as thermocouples unusable. Time Temperature Integrators (TTIs) has been suggested as an alternative that would provide information that would allow process design and validation. In this work we aim to validate the use of TTIs as measurement tools to validate both the effect and also the uncertainty of thermal processes in conditions relevant to industrial processing. P values estimated using TTIs compared favourably with those obtained from thermocouple measurements for a range of temperature profiles relevant to food processing. Efficiency of large mixing vessels has been quantified in a pilot scale vessel. Factors such as fluid viscosity; fill level and heating options were examined. The results show that the free TTIs show higher P values than the thermocouple situated in the centre of the vessel (but similar to the thermocouple positioned on the wall of the vessel) while the TTIs fitted in balls correlate well with the centre thermocouple. The results indicate that the mixing performance is dependent on the fluid viscosity, the fill level and the heating options. As the free TTIs follow the fluid path they gave a more accurate representation of the real thermal impact on the food product. This work demonstrates that TTIs can be successfully used as a tool for validation of efficiency and uncertainty of industrial processes.

Multi spectral imaging analysis for meat spoilage discrimination

A.N. Christiansen[1], J.M. Carstensen[1], O. Papadopoulou[2,3], N. Chorianopoulos[4], E.Z. Panagou[2], G.-J.E. Nychas[2]

[1]Department of Informatics and Mathematical Modelling, Technical University of Denmark, Richard Petersens Plads 321, DK-2800 Kgs, Denmark
[2]Laboratory of Microbiology and Biotechnology of Foods, Department of Food Science and Technology, Agricultural University of Athens, Iera Odos 75, Athens, Greece, GR-11855, (e-mail: gjn@aua.gr)
[3]National Agricultural Research Foundation, Institute of Technology of Agricultural Products, Sofokli Venizelou 1, Lycovrissi, Greece, GR-14123
[4]National Agricultural Research Foundation, Institute of Veterinary Research, Neapoleos 25, Athens, Greece, GR-15310

Abstract

Beef fillets were stored aerobically and in modified atmosphere packaging (MAP, CO_2 40%/O_2 30%/N_2 30%) at six different storage temperatures (0, 4, 8, 12, 16 and 20°C). Microbiological analysis in terms of total viable counts (TVC) was performed in parallel with multispectral image snapshots and sensory analysis. Odour and colour characteristics of meat were determined by a taste panel and attributed into three pre-characterized quality classes, namely Fresh (F), Semi-fresh (SF) and Spoiled (S) during the days of its shelf life. The obtained images were converted into values that were comparable to the corresponding data, using the Minimum Noise Fraction (MNF) transformation and simple thresholding. Association of image data with sensory data was undergone using three different classification methods: Naive Bayes Classifier as a reference model, Canonical Discriminant Analysis (CDA) and Support Vector Classification (SVC). Results showed that image analysis provided good discrimination of meat samples regarding their spoilage status as evaluated from sensory as well as from microbiological data. The support vector classification (SVC) model outperformed other models. Specifically, the misclassification error rate (MER), derived from odour characteristics, was 18% for both aerobic and MAP meat samples. In the case where all data were taken together the misclassification error amounted to 16%. When spoilage status was based on visual sensory data, the model produced a MER of 22% for the combined dataset. The obtained results illustrated that it was feasible to employ a multi spectral image for the quantitative determination of meat spoilage status during storage in different conditions.

Keywords: image analysis, beef fillets, spoilage, Videometer, chemometrics, Support Vector Machines

Introduction

Today, different microbiological and (bio)chemical methods are employed to assess meat spoilage and microbiological counts, the majority of which are slow, time-consuming and expensive procedures (Nychas *et al.* 2008). It would be preferred to replace these established methods by faster and directly applicable methods, such as multi spectral imaging. Multispectral imaging techniques are a natural extension to normal colour cameras. Colour is among the most important factors playing a significant role in the evaluation of meat quality. Specifically, muscle colour at the point of purchase is an indicator of freshness and anticipated palatability for the consumer (Livingston *et al.* 2004; Singh *et al.* 2011). Whereas normal colour cameras integrate electromagnetic radiation over three broad banded areas in the visual area, multispectral cameras are able to record electromagnetic information in more narrow banded areas. Consequently, multispectral cameras are able to record spectral reflection properties in narrow bands, which thereby make it possible to assess the composition of surface chemistry of the object of interest. Such recordings may thus be used to extract intrinsic chemical and molecular information such as water, fat, protein or other hydrogen-bonded constituents. Sometimes multispectral images are also referred to as surface

chemistry maps or hypercubes (Carstensen *et al.* 2006). In short, multispectral images can provide not only spatial information, as regular imaging systems, but also spectral information for each pixel in an image. Thus, using hyper-spectral images, it is possible to assess physical and geometric characteristics such as colour, size, shape, and texture. Several publications have been written on the subject of using multispectral imaging for food control (Gowen *et al.* 2007; Daugaard *et al.* 2010; Taghizadeh *et al.* 2010). In the present study, the potential of multispectral imaging techniques was exploited for the rapid assessment of spoilage degree in beef fillets stored at different temperatures and packaging conditions.

Materials and Methods

Beef fillets from different carcasses were purchased from a local meat retail outlet and stored aerobically and under modified atmospheres (40%CO_2/30%O_2/30%N_2) at six different temperatures (0, 4, 8, 12, 16 and 20°C) for an overall period of 626 hours, depending on storage temperature, until spoilage was pronounced. Microbiological analyses in terms of total viable counts (TVC) were performed in parallel with videometer image snapshots and sensory analysis. Odour and colour characteristics of meat were assessed by a five-member sensory panel at the same time intervals as for microbiological analysis and attributed into three pre-selected quality classes as fresh (F), semi-fresh (SF) and spoiled (S). Each sensory attribute was scored on a ten-point hedonic scale corresponding to: 1-2 (fresh), 3-5 (marginal) and 6-10 (spoiled). A score of 3 was assigned to semi-fresh indicating the beginning of spoilage. Multi spectral images of meat samples consisted of 18 bands ranging from ultraviolet (395 nm) to near-infrared (970 nm). To convert images into usable values, segmentation into meat and non-meat was performed using Minimum Noise Fraction (MNF) transformation and thresholding. Subsequently, models for predicting the spoilage status of beef fillets were generated using the classification methods of Naive Bayes Classifier as a reference model, Canonical Discriminant Analysis (CDA) and Support Vector Classification (SVC). As a final step, generalization of the models was performed using k-fold validation. Model performance was evaluated with the determination of the corresponding confusion matrix and calculation of the misclassification error rate (MER) which is the percentage of meat samples that were misclassified by the model. Two more indices were calculated: (i) the false positive rate (FPR), which is the percent of meat samples that were classified as more fresh than really were, and (ii) false negative rate (FNR) which is the percent of meat samples that were classified as more spoiled than really were. Data from all temperatures were used in the analysis divided in the following four data sets: (i) data from meat stored in air, (ii) data from meat stored in MAP, (iii) the whole data set for aerobic and MAP data, and (iv) the whole data set with an additional dummy variable discriminating air from MAP data.

Results and Discussion

The segmentation using the orthogonal transformation MNF and afterwards thresholding using a fixed threshold was a robust and effective method for segmentation into meat and non-meat (Figure 1). From the obtained results (Table 1) it was evident that data from aerobic storage of beef fillets presented the lowest misclassification error compared to MAP data. In addition the use of a dummy variable to discriminate between the two packaging types did not produce better results. The model that produced the better classification was SVC (Table 2). The majority of misclassification errors in this model were predicting fresh samples as semi-fresh which falls in the safe side of erroneous predictions. The performance of using SVC for both colour and odour spoilage prediction was satisfactory, although colour predictions produced better results, which is not surprising as images were used in the analysis. A MER of 17.3% and 22.6% for colour and odour spoilage prediction respectively suggests that it is possible to make a precise prediction model that can categorize a piece of meat into quality classes. It is also worth noting that the fail-dangerous misclassifications for both color and odor spoilage prediction were low and that very few spoiled samples were classified as fresh

and vise versa. From Figure 2 it is evident that misclassifications were mainly close to the boundaries between classes, where the sensory panel was in doubt how to classify the sample.

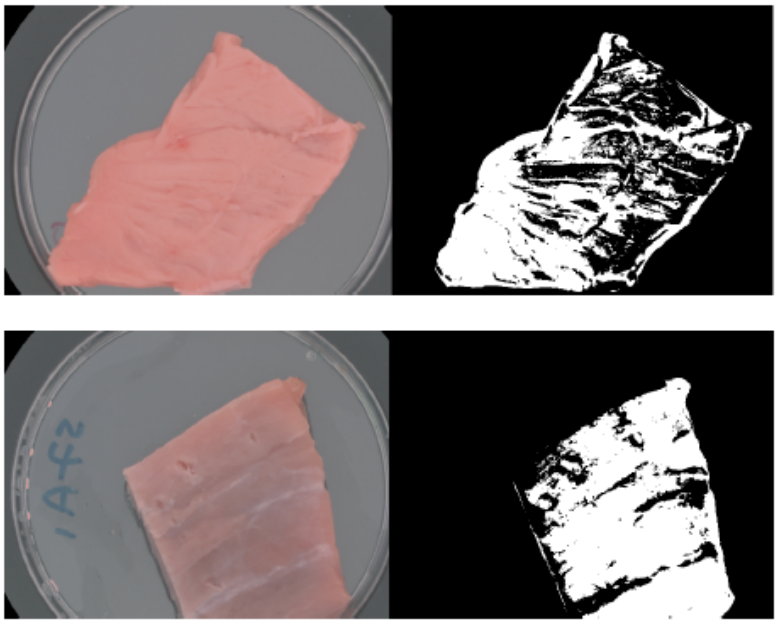

Figure 1: Pseudo RGB images created from multi spectral images of the meat samples (left) and the corresponding segmentations (right) into meat (white) and non-meat (black).

	MER	FNR	FPR
Air	17.7 %	11.7 %	6.1 %
MAP	19.1 %	11.7 %	7.4 %
All + dummy	17.9 %	11.4 %	6.5 %
All	17.3 %	10.3 %	7.0 %

Table 1: Error measure results for Support Vector Machines predicting the colour of meat samples using the four data sets (MER: Misclassification Error Rate, FNR: False Negative Rate, FPR: False Positive Rate).

	MER	FNR	FPR
NBC	24.7 %	7.0 %	17.7 %
CDA	20.9 %	8.6 %	12.3 %
SVC	17.3 %	10.3 %	7.0 %

Table 2: Error measure results for the three models predicting the colour of meat samples (MER: Misclassification Error Rate, FNR: False Negative Rate, FPR: False Positive Rate).

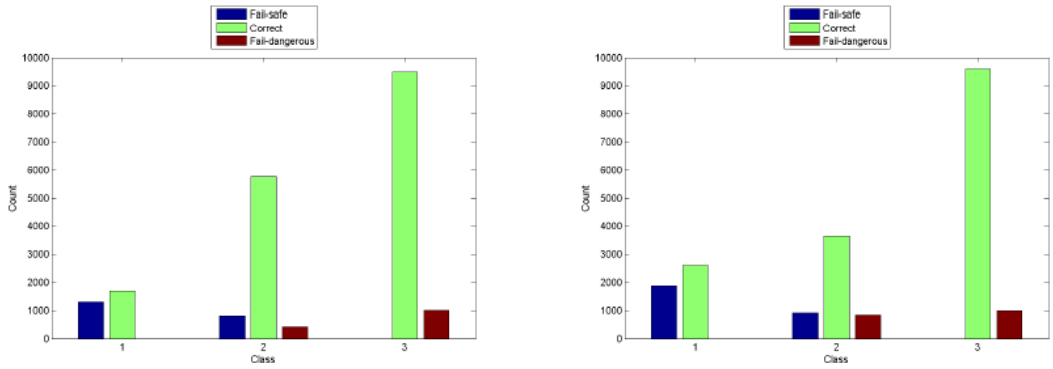

(a) Color prediction (b) Odor prediction

Figure 2: Classification results of beef fillets quality in three sensory classes using SVC.

Acknowledgements

This study was funded by SYMBIOSIS - EU (www.symbiosis-eu.net) project within the 7th Framework Programme of the EU.

References

Carstensen J.M., Hansen M.E., Lassen N.K., Hansen P.W. and Bjarne Ersbøll T.M.J. (2006) Creating surface chemistry maps using multispectral vision technology *9th MICCAI - Workshop on Biophotonics Imaging for Diagnostics and Treatment, IMM Technical Report* 2006-17.

Daugaard S.B., Adler-Nissen J. and Carstensen J.M. (2010) New vision technology for multidimensional quality monitoring of continuous frying of meat *Food Control* 21, 626-632.

Gowen A., O'Donnell C., Cullen P., Downey G. and Frias J. (2007) Hyperspectral imaging - an emerging process analytical tool for food quality and safety control *Trends in Food Science and Technology* 18, 590-598.

Livingston M., Brewer M.S., Killifer J., Bidner B. and McKeith F. (2004) Shelf life characteristics of enhanced modified atmosphere packaged pork *Meat Science* 68, 115-122.

Nychas G.-J.E., Skandamis P.N., Tassou C.C. and Koutsoumanis K.P. (2008) Meat spoilage during distribution *Meat Science* 78, 77-89.

Singh P., Wani A.A., Saengerlaub S. and Langowski H.C. (2011) Understanding critical factors for the quality and shelf-life of MAP fresh meat: a review *Critical Reviews in Food Science and Nutrition* 51, 146-177.

Taghizadeh M., Gowen A., Ward P. and O'Donnell C.P. (2010) Use of hyperspectral imaging for evaluation of shelf-life of fresh white button mushrooms (*Agaricus bisporus*) stored in different packaging films *Innovative Food Science and Emerging Technologies* 11, 423-431.

Development of spoilage classification models using support vector machines and combined analytical methods

F. Mohareb[1], A. Grauslys[1], A. Argyri[2], E. Panagou[2], B. Conrad[1], G.-J. Nychas[2]

[1]Cranfield University, United Kingdom
[2]Laboratory of Microbiology and Biotechnology of Foods, Department of Food Science and Technology, Agricultural University of Athens, Iera Odos 75, Athens 11855, Greece (e-mail; gjn@aua.gr)

Abstract

The shelf life of minced beef stored (i) aerobically, (ii) under modified atmosphere packaging (MAP), and (iii) under MAP with oregano essential oil (MAP/OEO) at 0, 5, 10, and 15 ºC was investigated. The microbial associations of meat and the temporal biochemical changes were monitored. Microbiological analyses, including total viable counts (TVC), *Pseudomonas spp.*, *Brochothrix thermosphacta*, lactic acid bacteria, Enterobacteriaceae, yeasts/moulds, were quantified, while in parallel sensory assessment, pH measurement, HPLC analysis of the organic acid profiles, FT-IR, and eNose measurements were recorded.

The aim of this work was to develop classification models for accessing freshness (e.g. microbiological and organoleptic parameters) in beef fillet samples using support vector machines (SVMs). Data analysed in this work was obtained from FT-IR, eNose and HPLC experiments. Additionally to the individual data sets, combined data sets were constructed by pairing the individual data sets in order to assess the affect of combined data to analysis results. The data was used for training and testing support vector machine models. The models were optimised to achieve the best classification accuracy for specific data types or data type combinations. The analysis models were implemented into a web-based analysis tool - SVM.ist. This tool allows through a simple web page interface an easy way to upload data files, perform SVM-based classification according to specified parameters and view or download the results of the analysis. This work was performed as part of the Symbiosis-EU project.

Keywords: spoilage, HPLC, Support vector machine, FTIR, converging

The potential of Raman spectroscopy in evaluating spoilage and safety of beef

A. Argyri[1], O. Papdopoulou[1], Y. Xu[2], A. Grounta[1], E. Panagou[1], R. Goodacre[2], G.-J. Nychas[1]

[1]Laboratory of Microbiology and Biotechnology of Foods, Department of Food Science and Technology, Agricultural University of Athens, Iera Odos 75, Athens 11855, Greece (e-mail; gjn@aua.gr)
[2]Lab of bioanalytical spectroscopy, School of Chemistry, University of Manchester,, PO Box 88, Sackville St, Manchester M60 1QD, UK

Abstract

In this study, minced beef samples inoculated with *Salmonella Enteritidis* and stored aerobically and under modified atmosphere (MAP-40%CO2/ 30% O2/ 30%N2) with and without an oregano essential oil (OEO) (2% v/w) slow releasing system and at four temperatures (0, 5, 10 and 15°C), were analysed with Raman spectroscopy. The data derived from the microbiological analysis (Total Viable Counts, *Pseudomonas* sp., *Brochothrix thermosphacta*, lactic acid bacteria (LAB), *Salmonella Enteritidis*) were correlated with the Raman spectra. The raman spectra were preprocessed using standard normal variate (SNV) and robust PCA was applied to identify the outliers and remove all the saturated spectra. Kernel PLS models were subsequently used to build a regression model between the Raman spectra and the cell counts of the bacteria, including TVC, *pseudomonads*, *Br. thermosphacta*, LAB, and *S. Enteridis*. The factors root-mean-square error of cross-validation (RMSECV), cross-validated correlation coefficient (Q2), and percentage of prediction error (% PE) were used to evaluate the performance of the models. It was observed that developed models regarding the predictions of *Br. thermosphacta*, LAB and *S. Enteridis* viable counts showed better performance than the rest microbial groups, whereas the models regarding storage under MAP and MAP/OEO showed better performance than the models for aerobic storage for all the microorganisms tested. In general the results were found promising, suggesting Raman spectroscopy as a rapid potential method to evaluate the spoilage and safety of meat.

Keywords: Raman, spoilage, safety, salmonella

Acknowledgements

This work financial supported from SYMBIOSIS-Eu project (7th FP).

Rapid assessment of beef fillet quality by means of an electronic nose and support vector machines

O.S. Papadopoulou[1,2], M. Vlachou[1], C.C. Tassou[2], E.Z. Panagou[1], G.-J.E. Nychas[1]

[1]Laboratory of Microbiology and Biotechnology of Foods, Department of Food Science and Technology, Agricultural University of Athens, Iera Odos 75, Athens, Greece, GR-11855, (e-mail: gjn@aua.gr)
[2]National Agricultural Research Foundation, Institute of Technology of Agricultural Products, Sofokli Venizelou 1, Lycovrissi, Greece, GR-14233

Abstract

Odour is a major olfactory parameter determining the sensory quality of food commodities and it would be therefore of interest to investigate whether volatile compounds could be considered as potential indicators of quality assessment. In the present study, beef fillets were stored aerobically and in modified atmospheres at three different temperatures (0, 4, and 8°C) and microbiological analysis in terms of total viable counts (TVC) was performed in parallel with e-nose measurements and sensory analysis for a total period of 434 hours until spoilage was pronounced. The acquired volatile fingerprints were used in order to discriminate the sensory quality of a meat sample during storage at chill temperatures. Correlation of the obtained volatile profiles with the spoilage status of beef fillets was performed with Support Vector Machines analysis (SVM) in order to classify meat samples in three pre-characterized classes, namely fresh (F), semi-fresh (SF), and spoiled (S). Results showed that SVM analysis provided good discrimination of beef fillet samples regarding their spoilage status at both packaging conditions. Specifically, the overall correct classification for the three sensory classes for the aerobically packaged meat samples was 87%, while classification for fresh, semi-fresh, and spoiled samples was 58, 92, and 90%, respectively. Results for MAP packaging were quite similar. The overall correct classification amounted to 83% while classification for fresh, semi-fresh, and spoiled samples was 82, 87, and 76%, respectively. The use of e-nose technique in combination with chemometrics could be employed satisfactorily to acquire volatile fingerprints of aroma profile and predict the sensory group of a sample of beef fillet during storage at various temperatures. E-nose has a considerable potential for application in the food industry as a rapid and non-invasive method.

Keywords: beef fillets, spoilage, electronic nose, chemometrics, Support Vector Machines

Introduction

It is generally accepted that detectable organoleptic spoilage is a result of decomposition and formation of metabolites caused by the growth of microorganisms. Especially changes in colour and odour could be regarded as the first indication of spoilage (Ellis *et al*. 2002, Nychas *et al*. 2008). Odour is a major olfactory parameter determining the sensory quality of food commodities and it is therefore of interest to investigate whether volatile compounds could be considered as indicators of quality assessment (Balasubramanian *et al.* 2009). During the last decade, electronic nose sensor array systems have been employed extensively for quality control of meat and meat products (Hansen *et al.* 2005; Rajamaki *et al.* 2006; Vestergaard *et al.* 2007; Zhang *et al.* 2008). Signal processing and pattern recognition in particular, is a fundamental part of data mining of any sensor array system. Developing e-nose systems to detect changes in active biological systems such as meat is a complex task due to the higher uncertainties and nonlinear sensor response involved. For this reason, advanced data processing techniques including artificial neural networks and support vector machines have been employed to process spectral e-nose data (Zhang *et al.* 2003; Brudzewski *et al.* 2004). The aim of the present study was to investigate the potential use of volatile fingerprints (snapshots) of meat, acquired by an electronic nose, in combination with chemometrics in quality discrimination of beef fillets stored at different temperatures and packaging conditions.

Materials and Methods

Beef fillets were stored aerobically and under modified atmospheres ($40\%CO_2/30\%O_2/30\%N_2$) at three different temperatures (0, 4, and 8°C) and microbiological analyses in terms of total viable counts (TVC) were performed in parallel with e-nose measurements and sensory analysis. An electronic gas sensor array system (Libra Nose, TechnoBioChip, Italy) implemented with an array of 8 quartz crystal microbalance (QCM) non-selective sensors coated with different poly-pyrrole derivatives, synthesized at Technobiochip and covered by a European patent [EP1505095], was used to generate a chemical fingerprint of volatile compounds of beef fillet samples during storage. Specifically, 5 g of beef fillet were introduced inside a 100 ml volume glass jar and left at room temperature (20°C) for 60 min to enhance desorption of volatile compounds from the meat into the headspace. Subsequently, the headspace was pumped over the sensors of the electronic nose and the generated signal was continuously and in real time recorded to a PC (Figure 1). The acquired volatile fingerprints of aroma profile were used in order to predict the sensory group of the sample of beef fillet during storage at the three selected temperatures. The volatile patterns collected from e-nose were initially subjected to Principal Component Analysis (PCA) to reduce multi-collinearity (e.g. sensors with overlapping sensitivities) and allow the information to be displayed in a smaller dimension. Subsequently, the scores of the first five principal components accounting for 99% of total variance observed in the experiment were further used as input in Support Vector Machines (SVM) analysis using linear, polynomial and radial basis function (RBF) kernels, in order to predict the quality of a meat sample that was pre-characterized as fresh (F), semi-fresh (SF) or spoiled (S) from a taste panel. The resulting database was randomly partitioned into training and testing subsets representing approximately 80% and 20% of the data, respectively. Test data were not employed in any step of model development, but they were used exclusively to determine its performance (i.e., its ability to predict cases for which there was no previous training). In each modelling approach, 3 independent runs with different training/testing data were performed, randomizing in each run the initial data set. The classification accuracy of the SVM model was determined as the number of correctly classified samples in each sensory class divided by the total number of samples in the class.

Results and Discussion

In this study, e-nose was used to obtain volatile fingerprints of beef fillets during storage at different temperatures and packaging systems in an attempt to monitor spoilage. The eight sensors had different responses to the samples analysed as illustrated in Figure 1. This could be attributed to the intrinsic selectivity of the molecular sensing mechanism and to the mass of the molecules that are bounded at the coated surface of the sensors (Di Natale *et al*, 1997). The volatile patterns collected from the eight sensors were initially subjected to Principal Component Analysis (PCA) for dimensionality reduction prior to SVM analysis. Results showed that SVM with RBF kernels provided good discrimination of beef fillet samples regarding their spoilage status at both packaging conditions. Specifically, the overall correct classification for the three sensory classes in the aerobically packaged meat samples was 87%, while classification for fresh, semi-fresh and spoiled samples was 58, 92, and 90%, respectively. Results for MAP packaging were quite similar. The overall correct classification was 83% while classification for fresh, semi-fresh and spoiled samples was 82, 87, and 76%, respectively. For the aerobically stored meat samples, the percentage of erroneous predictions in the safe side was 6.48% corresponding to 7 cases out of 108 meat samples, while the misclassified cases in the dangerous side were 5.56% corresponding to 6 cases out of 108 meat samples. Moreover for MAP samples, the percentage of erroneous predictions in both safe and dangerous sides was 8.33% corresponding to 9 cases out of 108 meat samples (Table 1 and 2).

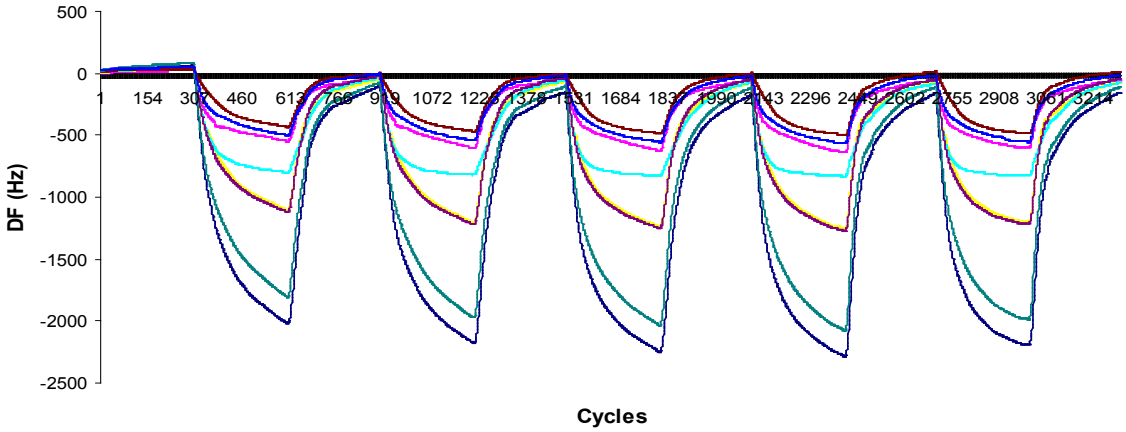

Figure 1: Response of the eight sensors of Libra e-nose during sampling.

Table 1: Confusion matrix for Support Vector Machines using RBF kernel performing the task of classification of the test samples of beef fillets in sensory classes (Fresh, Semi-fresh, Spoiled) during aerobic storage.

	True class	**Predicted class**			**Total**	**Correct (%)**
		Fresh	Semi-fresh	Spoiled		
SVM	Fresh	8	5	0	14	57%
	Semi-fresh	1	37	2	40	92%
	Spoiled	0	5	49	54	91%
		Overall correct classification (accuracy): 87%				

Table 2: Confusion matrix for Support Vector Machines using RBF kernel performing the task of classification of the test samples of beef fillets in sensory classes (Fresh, Semi-fresh, Spoiled) during storage in modified atmospheres.

	True class	**Predicted class**			**Total**	**Correct (%)**
		Fresh	Semi-fresh	Spoiled		
SVM	Fresh	14	3	0	17	82%
	Semi-fresh	2	54	6	62	87%
	Spoiled	0	7	22	29	76%
		Overall correct classification (accuracy): 83%				

Conclusions

The results obtained in this study demonstrated that volatile fingerprints collected from e-nose analysis combined with an appropriate machine learning strategy, such as Support Vector Machines, could become a promising tool to monitor beef fillet spoilage through monitoring of biochemical changes occurring in meat substrate. The collected aroma profile could be considered as biochemical fingerprint containing valuable information for the discrimination of meat samples in quality classes corresponding to different spoilage levels. However,

further studies are required for the method to be eligible and able to be updated with the novel packaging and preservation techniques, which character of spoilage.

Acknowledgements

This study was funded by SYMBIOSIS - EU (www.symbiosis-eu.net) project within the 7th Framework Programme of the EU.

References

Balasubramanian S., Panigrahi S., Logue C.M., Gu H. and Marchello M. (2009) Neural networks-integrated metal oxide-based artificial olfactory system for meat spoilage identification. *Journal of Food Engineering* 91, 91-98.

Brudzewski K., Osowski S. and Markiewicz T. (2004) Classification of milk by means of an electronic nose and SVM neural network *Sensors and Actuators B: Chemical* 98, 291-298.

Di Natale C., Macagnano A., Davide F., D'Amico A., Paolesse R., Boschi T., Faccio M. and Ferri G. (1997) An electronic nose for food analysis. *Sensors and Actuators B: Chemical* 44, 521–526.

Ellis D.I., Broadhurst D., Kell D.B., Rowland J.J. and Goodacre R. (2002) Rapid and quantitative detection of the microbial spoilage of meat by Fourier transform infrared spectroscopy and machine learning *Applied and Environmental Microbiology* 68, 2822-2828.

Hansen T., Petersen M.A. and Byrne D.V. (2005) Sensory based quality control utilizing an electronic nose and GC-MS analyses to predict end-product quality from raw materials. *Meat Science* 69(4), 621-634.

Nychas G.-J.E., Skandamis P.N., Tassou C.C. and Koutsoumanis K.P. (2008) Meat spoilage during distribution *Meat Science* 78, 77-89.

Rajamaki T., Alakomi H.L., Ritvanen T., Skytta E., Smolander M. and Ahvenainen R. (2006) Application of an electronic nose for quality assessment of modified atmosphere packaged poultry meat *Food Control* 17(1), 5-13.

Vestergaard J.S., Martens M. and Turkii P. (2007) Application of an electronic nose system for prediction of sensory quality changes of a meat product (pizza topping) during storage *LWT Food Science and Technology* 40(6), 1095-1101.

Zhang Z., Tong J., Chen D. and Lan Y. (2008) Electronic nose with an air sensor matrix for detecting beef freshness *Journal of Bionic Engineering* 5(1), 67-73.

Zhang H., Balaban M.O. and Principe J.C. (2003) Improving pattern recognition of electronic nose data with time-delay neural networks *Sensors and Actuators B: Chemical* 96, 385-389.

Mathematical modelling of migration from packaging into solid foods and Tenax®

I. Reinas[1], J. Oliveira[2,3], J. Pereira[1], F. Machado[2], F. Poças[1]

[1] CBQF/Escola Superior de Biotecnologia – Universidade Católica Portuguesa, Portugal (mfpocas@esb.ucp.pt;ireinas@gmail.com)
[2] Ernesto Morgado, S.A, Portugal (fmachado@emorgado.pt)
[3] Department of Process Engineering – University College Cork, Ireland (jmfcoliveira@gmail.com)

Abstract

The migration of chemicals from packaging materials into foods is an important issue in food safety and quality. The objective of this work was to develop and validate a mathematical model to describe the migration of two antioxidants (Irgafos 168 and Irganox 1076) from polyethylene into a food simulant - Tenax®. The migration behaviour into the simulant was compared to the migration into an actual food matrix, rice. The parameters of the models based on the Fick's law were estimated at three temperatures: 23, 40 and 70°C. Diffusion coefficients ranged between $4.80E^{-13}$ and $1.95E^{-11}$ cm^2/s for the migration into Tenax® and between $6.90E^{-18}$ and $4.33E^{-17}$ cm^2/s for the migration into rice. The partition coefficients ranged between 6 and 29 for Tenax® and were over 1000 for rice. The activation energy for the migration into rice was half of that for Tenax®. The models described relatively well the experimental data (ε < 12% and < 30% for rice and Tenax®, respectively). Results also indicate that Tenax® can be safely used as food simulant for these migrants because it overestimates the results as compared to results of migration into actual rice matrix.

Keywords: *migration, packaging, mathematical modelling, antioxidants, rice, Tenax®*

Introduction

Packaging plays an essential role in the food supply protecting and containing food from processing and manufacturing, through distribution, handling and storage to the final consumer. However, packaging and other food-contact materials are also a source of chemicals hazards in food products and beverages through migration and other mass transfer processes. Some of these chemicals are additives to prevent the plastic material degradation during processing and to enhance its performance during its lifetime (Dopico-García *et al*. 2003 and 2007). The direct contact between the material and the food yields the migration of low molecular weight compounds in generally low levels but still chronically ingested by consumers. European legislation sets specific migration limits depending on the toxicity of the migrant and on the potential exposure of the consumer to the migrant (Regulation UE 10/2011).

The assessment of materials safety and compliance with regulations includes monitoring the specific migration of many chemicals. These specific migration data may be obtained from monitoring levels of chemicals in real food systems. However, to overcome analytical difficulties migration data are commonly obtained through experiments carried out under controlled conditions of time and temperature of contact between the materials and a food simulant instead of the food itself. Such simulants include water, ethanol solutions, acetic acid solutions and olive oil (Directives EEC 85/572, 82/711, 97/48). Recently, the new Regulation UE 10/2011 included a new simulant – the Modified polyphenylene oxide (Tenax®) for solid foods.

Mathematical models describing the mass transfer of migrants from packaging materials to foods represent invaluable tools for industry professionals and regulators alike (Poças *et al*., 2008). Such models can at least partially, substitute expensive and time-consuming migration experiments. Diffusion models for estimation of the migration from plastic materials have been allowed for compliance assessment with regulations (Directive 2002 72/EC). These models have been used in a considerable extent to simulate migration into liquid foods or

liquid simulants. However, models to describe and simulate the migration from packaging into solid foods or simulant such as Tenax® are scarce or inexistent (Poças *et al*. 2011).
The objective of this work was to develop and validate a mathematical model to describe and simulate the migration of two antioxidants commonly used in polyethylene films: Irgafos 168 and Irganox 1076. The migration behaviour into the simulant was compared to the migration into an actual food matrix, rice, in a range of temperature from 23°C to 70 °C. The application of two different solutions of the 2nd Fick's law, described in the literature - Baner *et al.* (1996); Limm and Hollifield (1996) – to the present systems, was studied.

Materials and Methods

3.1 Packaging material, Migrants, Food and Simulant

Plastic packaging material: Low density polyethylene (LDPE), 60µm (Ernesto Morgado, Portugal).
Migrants: Irgafos 168 (CAS No. 31570-04-4) and Irganox 1076 (CAS 2082-79-3) with a concentration on the LDPE of 103 µg/g and 351 µg/g, respectively (Sigma-Aldrich).
The concentrations of migrants in the materials were determined previously by extraction with isooctane and determination by GC-MS.
Food: Japonica precooked medium white Rice Grains (Ernesto Morgado, Portugal).
Simulant: Tenax® 60/80 mesh, 0.29 g/cm3 of density (Quadrex Corporation, Woodridge, UK). It was cleaned up prior to use by extraction with isooctane.

3.2 Migration Tests

The food sample or simulant was sandwiched between two circular pieces of plastic, with the contact layer facing the sample. The rice (3 ± 0.0020 g) or Tenax® (0.63 ± 0.0010 g) was in contact with a total of 0.5652 dm^2 of plastic surface area. The set was placed in a petri dish 6 cm diameter which was then wrapped in aluminium foil and packed in a bag under vacuum conditions to promote good contact between the solids and the material. Samples were stored at three different temperatures: 23ºC - corresponding to room temperature; 40ºC - the testing temperature for the foreseen use conditions; and 70ºC - the temperature for accelerated tests. Samples were removed in triplicate at regular time intervals for preparation and analysis.

3.4 Quantification of Irgafos 168 and Irganox 1076 after migration

Quantification was carried out by GC-MS after extraction of the migrants from the rice or simulant matrix. Extractions were performed with 5 ml isooctane for 2 h. Chromatographic conditions: Chromatograph (Varian CP3800, Quad Mass Spectrometer 1200L, COMBIPAL autosampler). Column VF5MS (30m x 0.25mm, 0.25µm). Ionization mode: electronic impact 70eV; Scan mode: SIM: m/z 235+250 ion – IS; m/z 441 ion – Irgafos 168; m/z 647+662 ion – Irgafos oxidized; m/z 515+530 - Irganox 1076. Injector temperature: 320ºC. Oven temperature: 80ºC for 1min; 15ºC/min up to 320ºC for 10min. Injection volume: 1µl. Extracts were injected in duplicate.

3.5 Statistics and estimation of model parameters

Statistical Analysis: Statistica 6 (Statsoft, Inc.) and Excel (Microsoft, Inc) were used in data analyses. All statistical analyses were performed at a confidence level of 95%.

3.6 Mathematical models

Mass transfer process is commonly assumed to be a diffusion process that can be described by the Fick's second law (1):

$$\frac{\partial C_A^P}{\partial t} = D_A^P \frac{\partial^2 C_A^P}{\partial x^2} \quad (1)$$

Where C^P_A represents the concentration of the migrant species A in the packaging material P, t represents the time, x the linear dimension and D^P_A is the diffusivity of A in the material. It was considered that at the beginning of the mass transfer the migrant is homogeneously

distributed in the packaging and that there is no boundary resistance for the transfer between packaging and food. It is also considered that the migrant is homogeneously distributed in the food, and the total amount of the migrant in the system (packaging plus food) remains constant during the migration process. For these assumptions, two solutions can be derived from equation (1), according to Baner *et al.* (1996) and Limm and Hollifield (1996), respectively:

$$\frac{M_A^F}{M_A^F(\infty)} = 1 - \sum_{n=1}^{\infty} \frac{2\alpha(1+\alpha)}{1+\alpha+\alpha^2 q_n^2} \exp\left(-D_A^P t \frac{q_n^2}{L^2}\right) \quad (2)$$

Where: M^F_A is the concentration of A in the food/simulant over time and ($M^F_A(\infty)$) at equilibrium; L is the packaging thickness; q_n are the non-zero positive roots of: $\tan(q_n) = -\alpha q_n$; α is the quotient between the food volume and the product of the packaging volume and the partition coefficient of A in the system packaging/food.

$$\frac{M_A^F}{M_A^P(0)} = \frac{2}{L\sqrt{\pi}} \sqrt{D_A^P t} \quad (3)$$

Results and Discussion

Migration is represented as the quantity of migrated additive per gram of Tenax® or rice over the time in Figure 1. Migration curves of Tenax® and rice present the same pattern. However, migration into Tenax® is faster and occurs at higher values as compare to the migration into rice. Equilibrium of both antioxidants in Tenax® at 70ºC is achieved after 15 days, at 40ºC after 20 days for Irgafos 168 and after 10 days for Irganox 1076. The antioxidants do not achieve the equilibrium in rice at any temperature during the study duration. These different behaviours may be explained by the properties of Tenax®, particularly its high porosity and adsorption capacity.

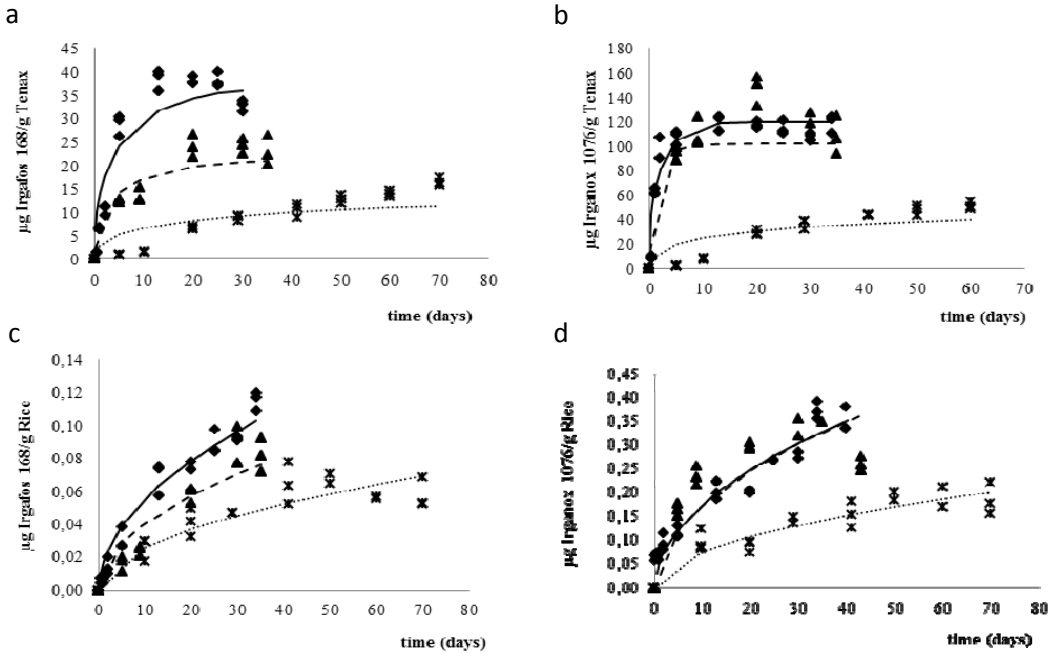

Figure 1: Migration experimental data (markers) and model (lines): a) Irgafos 168/Tenax®; b) Irganox1076/Tenax®; c) Irgafos 168/Rice; d) Irganox1076/Rice; ♦ -70ºC; ▲ -40ºC; ∗ -23ºC.

The experimental data was fitted to equations 2 and 3 using a non-linear regression analysis at a level of confidence of 95%. Equation 2 fitted well to the experimental data of the migration into Tenax® but not to the rice data, where equation (3) gave better fits. Nevertheless

Equation 2 does not describe well the migration at very early times at lower temperatures. Similar results were obtained in other studies of migration into Tenax® (Poças *et al.,* 2011). The diffusion (*D*) and partition (*K*) coefficients of the models were estimated and are summarized in Table 1. The error (ε) of the model is also presented.

Table 1: Diffusion, partition coefficients and error of the model for Tenax® and rice.

Antioxidant/ Temperature		D_{tenax} (cm^2/s)	ε tenax (%)	D_{rice} (cm^2/s)	ε rice (%)	K_{tenax}	K_{rice}
Irgafos	23ºC	$4.80E^{-13}$	30.0	$9.57E^{-18}$	8.8	28.7	1886
	40ºC	$5.78E^{-12}$	25.3	$2.31E^{-17}$	8.5	14.9	1443
	70ºC	$7.27E^{-12}$	20.5	$4.33E^{-17}$	4.5	6.2	1095
Irganox	23ºC	$8.34E^{-13}$	26.8	$6.90E^{-18}$	7.4	22.8	2194
	40ºC	$2.84E^{-11}$	80.3	$3.68E^{-17}$	12.2	8.4	1175
	70ºC	$1.95E^{-11}$	19.4	$3.71E^{-17}$	5.3	6.9	1229

The error of the model was higher for the Tenax® than for rice. This is probably related with the higher adsorptive capacity of Tenax® and with handling operations because this powder tends to stick to the packaging material after long periods of contact time yielding higher standard deviation between replicates for each sampling time. The diffusivity values in Tenax® are several orders of magnitude higher than in rice. Results also indicate that the diffusion coefficient is dependent of the temperature following an Arrhenius-type relationship (plot not shown). The impact of the temperature in the migration has the same magnitude for both antioxidants. However, temperature has a twice higher impact in the diffusivity of Tenax® as compared to rice.

Conclusions

Migration into Tenax® is faster and presents higher values than into rice. The influence of temperature on the migration rate follows an Arrhenius-type relationship. The temperature has similar impact on the migration of both Irganox and Irfgafos when migrating into the same matrix. However, the impact of temperature is much higher on the migration into Tenax® than into rice regardless of the migrant. The mathematical models described relatively well the experimental data (ε < 12% and < 30% for rice and Tenax®, respectively). Results indicate that the food simulant tends to overestimate migration values and thus can be safely used to assess materials compliance when materials are intended to contact with rice.

References

Baner A., Brandsch J., Franz R. and Piringer O. (1996) The Application of a predictive migration model for evaluating the compliance of plastic materials with European food regulations. *Food Additives and Contaminants* 13 (5), 587-601.

Commission Directive 2002/72/EC, of 6 August 2002 relating to plastic materials and articles intended to come into contact with foodstuffs

Commission Regulation (EU) Nº 10/2011, of 14 January 2011 on plastic materials and articles intended to come into contact with food

Dopico-García M.S, López-Vilariño J.M. and González-Rodríguez M.V. (2003) Determination of antioxidant migration levels from low-density polyethylene films into food simulants. *Journal of Chromatography A* 1018, 53–62.

Dopico-García M.S, López-Vilariño J.M. and González-Rodríguez M.V. (2007) Antioxidant Content of and Migration from Commercial Polyethylene, Polypropylene, and Polyvinyl Chloride Packages, *J. Agric. Food Chem.*, 2007, *55* (8), 3225–3231.

Limm, W. and Hollifield, H.(1996) Modeling additive diffusion in polyolefins. *Food Additives and Contaminants* 13 (8), 949-967.

Poças M.F.F., Oliveira J. Oliveira F.A.R. and Hogg T. (2008) A Critical Survey of Predictive Mathematical Models for Migration from Packaging. *Critical Reviews in Food Science and Nutrition* 48 (10), 913-928.

Poças M.F, Oliveira J.C, Pereira J.R, Brandsch R. and Hogg, T. (2011) Modeling migration from paper into food simulant. *Food Control* 22, 303-312.

Modelling the Kinetics of Galacto-oligosaccharides synthesis in organic solvents using β-galactosidase

F. Manucci[1], G.T.H Henehan[1], J.M. Frías[1]

[1] School of Food Science and Environmental Health, Dublin Institute of Technology, Cathal Brugha street, Dublin 1, Ireland (Jesus.Frias@dit.ie)

Abstract

Galactooligosaccharides (GOS) are prebiotics that have a beneficial effect on human health by promoting the growth of probiotic bacteria in the gut. GOS are commonly produced from lactose in a reaction catalysed by β-galactosidase, termed transglycosylation. In the present work the synthesis of GOS from Whey Permeate (WP) using commercially available β-galactosidases from *Kluyveromyces lactis* (Maxilact® L2000) was studied. The influence of low amounts of organic solvents (acetonitrile, ethanol, diethyl ether, dioxane, and acetone in 10% (v/v)) on GOS synthesis was examined, with the objective of obtaining valuable information on the reaction kinetics. Modelling of GOS synthesis profiles using a full reaction mechanism (Kim et al., 2004) fitted the experimental data. However, high correlation between kinetic parameters and high standard errors in parameter estimates were found. A reduced GOS synthesis mechanism based on simplifying assumptions previously identified in literature was devised. This reduced model fitted data appropriately and parameter estimation and associated uncertainty was improved. The use of organic solvents was found to modify the reaction kinetics, with promising applications to increase GOS yield.

Keywords: Galactooligosaccharides, β-galactosidase, whey permeate, organic solvents

Introduction

Galactooligosaccharides produced by the action of β-galactosidase on lactose were identified for the first time in the early 1950s. Four species of GOS were formed using *Kluyveromyces lactis* β-galactosidase (Aronson, 1952; Pazur, 1954), and three using *E. coli* β-galactosidase (Aronson, 1952). Experiments conducted with high lactose concentrations detected eleven species of GOS (Roberts *et al*., 1957). Since then, there have been several studies of the enzymatic synthesis of GOS by β-galactosidase.

Reduced water activity (a_w) may enhance the enzymatic synthesis of GOS (Goulas *et al*., 2007) and help to understand better how to improve the yields of this process. Moreover, many enzymes have altered specificity in the presence of organic solvents.

The objective of this work was to study the effect of the addition of small concentrations of organic solvents in the kinetics of enzymatic synthesis of GOS.

Materials and Methods

The effect of adding solvents in a 10% (v/v) to the GOS synthesis reaction mixture assay was investigated. The solvents were used in relatively low concentrations, to avoid inhibiting enzyme activity. The solvents used were ethanol, acetonitrile, acetone, diethyl ether and dioxane. All reagents were purchased from Sigma-Aldrich (Dublin, Ireland) except for the β-galactosidase Maxilact L2000 (Carbon Group (Ringaskiddy, Co. Cork, Ireland).

Laboratory scale reactions for GOS synthesis were carried out by dissolving demineralised Whey Permeate in phosphate buffer (0.1 M, pH: 6.8) to which Maxilact 0.4% (w/v) was added. The lactose concentration used was 200 g/L.

High Performance Liquid Chromatography (HPLC) analysis was used to quantify GOS synthesis products. HPLC was carried out using a SUPELCOGEL Ca^{2+} column (product no. 5930-U), 30 cm x 7.8 mm I.D., and a flow rate of 0.5 ml/min. A column heater (Waters Temperature Control Module I and II) was used to maintain the column temperature at 80ºC. The mobile phase used was ultrapure water. The detector used was a Refractive Index (RI)

Detector (Waters 410), with an internal temperature of 34ºC. The samples for HPLC analysis were diluted 1:100 or 1:500 and filtered (SUPELCO, 25 mm x 0.45µm) before injection.
Model building and parameter estimation using data from each of the experiments were performed using JSim version 1.6.82 (Physiom Project, Washington) (Bassingthwaighte 2005).

Reaction mechanism model

Previous studies (Iwasaki *et al*., 1996 and Kim *et al*., 2004) have investigated the modelling of GOS formation using the full feature mechanism model of reaction. Generally, this has resulted in an ill-conditioned system, where strong correlation between parameters and variables has resulted in no statistically meaningful results. The main approach to avoid this obstacle in this study focused on simplifying the reaction mechanism and tried to explain GOS synthesis with a reduced set of reaction steps (Boon *et al*. 1999 and 2000; Zhou *et al*. 2003; Neri *et al*. 2009).
In this work, the GOS synthesis mechanism has been simplified on the basis of the following considerations based on previous studies by Boon *et al*. (1999 and 2000) and Zhou *et al*. (2003):

- Enzymatic hydrolysis is assumed to be rapidly equilibrated, lumping therefore the whole process into a first order process.
- There is no GOS synthesis inhibition process due to glucose, therefore the step of allolactose formation is considered of negligible influence.

From these hypotheses the following system of ordinary differential equations (ODE) was constructed (equations 1-6).

$$\frac{dE}{dt} = -k_1 \cdot E \cdot Lac + k_3 \cdot E:Gal - k_{r3} \cdot E \cdot Gal + k_5 \cdot E:Gal \cdot Lac - k_{r5} \cdot E \cdot GOS \quad (1)$$

$$\frac{dE:Gal}{dt} = k_1 \cdot E \cdot Lac + k_{r3} \cdot E \cdot Gal - k_3 \cdot E:Gal + k_{r5} \cdot E \cdot GOS - k_5 \cdot E \cdot GOS - k_5 \cdot E:Gal \cdot Lac \quad (2)$$

$$\frac{dGal}{dt} = k_3 \cdot E:Gal - k_{r3} \cdot E \cdot Gal \quad (3)$$

$$\frac{dGlc}{dt} = k_1 \cdot E \cdot Lac \quad (4)$$

$$\frac{dLac}{dt} = -k_1 \cdot E \cdot Lac + k_{r5} \cdot E \cdot GOS - k_5 \cdot E:Gal \cdot Lac \quad (5)$$

$$\frac{dGOS}{dt} = -k_{r5} \cdot E \cdot GOS + k_5 \cdot E:Gal \cdot Lac \quad (6)$$

Where E, Lac, E:Gal, Gal, GOS stand for the enzyme, lactose, Enzyme:galactose complex, galactose, and galacto-oligosaccharide molar concentrations. The kinetic parameters k_1, k_{r3}, k_5 and k_{r5} are expressed in $M^{-1}min^{-1}$ and k_3 is expressed in min^{-1}.

Results and Discussion

It was noticed that some solvents, such as acetonitrile and dioxane, inhibited β-galactosidase activity. Some other solvents, such as acetone and diethyl ether, permitted β-galactosidase reaction. However, the yield of GOS synthesized in comparison to the control was not affected (Figure 1).

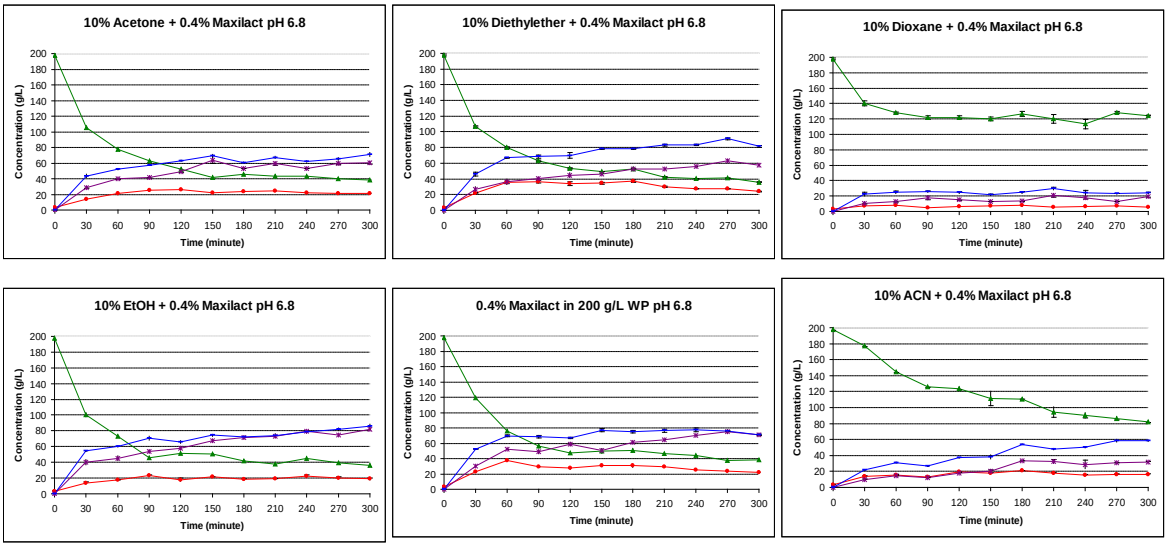

Figure 1: GOS synthesis in presence of different solvents. Average values of three replicates are reported with relative error bars. Assays were carried out in phosphate buffer (0.1 M, pH 6.8) with Whey Permeate (200 g/l), solvent (10%) and 0.4% Maxilact, at 40ºC, for 300 minutes reaction. Solvent added were: acetone, acetonitrile, diethyl ether, dioxane and ethanol. (Where ▲: Lac, ▬: Glc, : Gal, and ●: GOS)

Figure 2 shows the kinetic parameters of the enzymatic assays estimated from the data in Figure 1. the changing of $\ln(k_1)$ between the assays carried out with solvents. All the solvents, within experimental error, allowed for the formation of E:Gal complex at the same rate. E:Gal is the precursor to GOS formation. However acetonitrile and dioxane had slower kinetics, which is consisted with the initial lactose depletion observed in these assays. It can be seen that the introduction of small concentrations of acetonitrile and dioxane affected significantly ($p<0.05$) the initial step of precursor formation in the reaction.

The comparison of the kinetic parameter $\ln(k_3)$ and $\ln(k_{r3})$ between the different solvents can be seen in Figure 2 as well. The use of organic solvents resulted generally in a reduction of both $\ln(k_3)$ and $\ln(k_{r3})$ compared to the control. This is expected to result in slower degradation of the E:Gal complex towards the formation of free Galactose. This might have the interesting result of displacing the reaction towards the formation of GOS, which is characterised by $\ln(k_5)$ and $\ln(k_{r5})$. The ratio between $\ln(k_3)/\ln(k_{r3})$ showed that the use of dioxane and diethyl ether reduced this ratio ($p<0.05$). Therefore the use of solvents had an observable effect in the balance of the reaction mechanism. The kinetic parameter $\ln(k_5)$ did not change between the experiments taken into consideration, with no statistically significant difference between the different solvents. Finally, for the kinetic parameter $\ln(k_{r5})$, The assay carried out with dioxane addition showed a higher value then the other assays ($p<0.05$). Hence, in the presence of this solvent, the transglycosylation reaction is shifted towards the degradation of GOS rather than its synthesis. This is consistent with the kinetics shown in Figure 1.

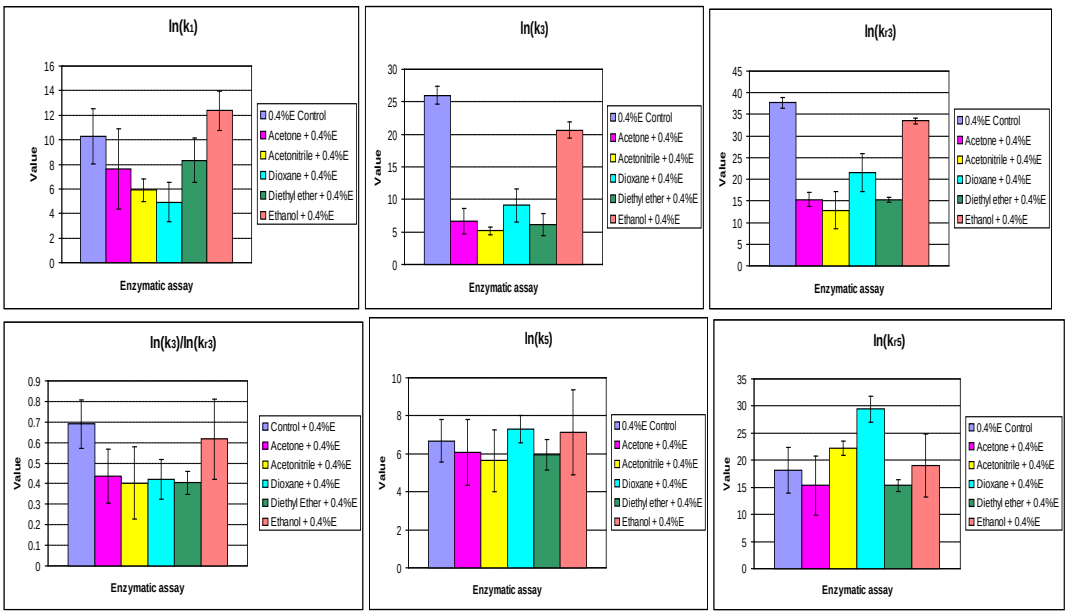

Figure 2: Comparison of estimated GOS formation kinetics parameters for enzymatic assays carried out with the addition of solvents. Error bars show the propagated 95% CI for the estimated parameters from individual experiments.

Conclusions

The kinetics of GOS enzymatic synthesis were affected by the addition of small concentraitons of solvents. Using 10% of acetone, diethyl ether and ethanol influenced the profile of the GOS reaction progress, possibly shifting the kinetics towards faster GOS production and slower inhibition by hydrolysis.

Acknowledgements

This material is based upon works supported by the DIT Strand III Research Project (2007-2010).

References

Aronson M. (1952) Transgalactosylation during lactose hydrolysis. *Archives of Biochemistry and Biophysics*, 39, 370-378

Pazur, J. H. (1954) The mechanism of enzymatic synthesis of galactosyl oligosaccharides. *The Journal of Biological Chemistry* 208, 439-444.

Bassingthwaighte J. B. (2005) Strategies for the Physiome Project. *Ann Biomed. Eng*., 28, pp. 1043-1058;

Boon M. A., Janssen A. E. M. and Padt A.V.D. (1999) Modeling and parameter estimation of the enzymatic synthesis of oligosaccharides by β-galactosidase from *Bacillus circulans*. *Biotechnology and Bioengineering* 64, 558-567.

Boon M. A., Janssen A.E.M. and Riet, K.V. (2000) Effect of temperature and enzyme origin on the enzymatic synthesis of oligosaccharides. *Enzyme and Microbial Technology* 26, 271-281.

Goulas A., Tzortzis G. and Gibson, G. R. (2007) Development of a process for the production and purification of α- and β-galactooligosaccharides from *Bifidobacterium bifidum* NCIMB 41171. *International Dairy Journal*, 17, 648-656.

Roberts H. R. and Pettinati J.D. (1957) Oligosaccharide Production, Concentration Effects in the Enzymatic Conversion of Lactose to Oligosaccharides. *Journal of Agricultural Food Chemistry* 5, 130

Iwasaki K., Nakajima M. and Nakao S. (1996) Galactooligosaccharides production from lactose by an enzyme batch reaction using β-galactosidase. *Process Biochemistry*, 31, 69-76;

Kim J.H., Lee D.H. and Lee, J.S. (2001) Production of Galactooligosaccharide by β-Galactosidase from *Kluyveromyces maxianus* var *lactis* OE-20. *Biotechnology Bioprocess* 6, 337-340

Neri D.F.M., Balcão V.M., Costa R.S., Rocha I.C.A.P., Ferreira E.M.F.C., Torres D.P.M., Rodrigues L.R.M., Carvalho Jr.L.B. and Teixeira J.A. (2009) Galacto-oligosaccharides production during lactose hydrolysis by free *Aspergillus oryzae* β-galactosidase and immobilized on magnetic polysiloxane-polyvinyl alcohol. *Food Chemistry* 115, 92-99.

Zhou Q.Z., Dong Chen X. and Li, X. (2003) Kinetics of Lactose Hydrolysis by β-Galactosidase of *Kluyveromyces lactis* Immobilized on Cotton Fabric. *Biotechnology and Bioengineering*, 81, 127-133.

Kinetic modelling of quality decay of granulated breakfast cereal during storage

I.S.M. Macedo, M.J. Sousa-Gallagher, P.V. Mahajan, E.P. Byrne

Department of Process and Chemical Engineering, School of Engineering, College of Science, Engineering and Food Science, University College Cork, Ireland (email: m.desousagallagher@ucc.ie)

Abstract

Granola is a dried granulated breakfast cereal product susceptible to moisture uptake. Therefore, being a moisture sensitive product it is dependent on the environmental conditions of storage, which can lead to undesirable product changes. The kinetics of moisture adsorption is an important tool to model product quality deterioration considering varying storage conditions. The aim of this study was to investigate the moisture adsorption kinetics and loss of firmness of granola under different environmental conditions (temperature and relative humidity), and develop a mathematical model describing the kinetics of quality decay of granola as a function of temperature and relative humidity. Samples of granola were stored in airtight containers at different relative humidities (32-33, 53-57 and 75-76%) and temperatures (10, 20, 30 and 40 °C). Moisture uptake and firmness loss showed an exponential growth and decay, respectively, which could be described by a first order reaction model. The effect of temperature and relative humidity on the reaction rate constant of firmness was not significant. The first order reaction model was shown to be a suitable model to describe the firmness loss as a function of time. The reaction rate for the moisture gain showed a temperature dependency, which was described by the Arrhenius equation. Therefore, an overall kinetic model was developed to described the quality decay in granola during storage as a function of temperature, and a good fit ($R^2 = 0.968$) was found.

Keywords: quality decay, kinetic modelling, lumped capacity model, moisture content, water activity

Introduction

Knowledge of the mechanism of food deterioration reactions that influence food quality, such as the rate at which these reactions occur, the effect of temperature, and water allows to counteracting the effect of these reactions minimizing undesirable changes in quality.

Granola breakfast cereals are products whose crispness/ firmness are considered a primary textural attribute. Undesirable changes in texture may occur when the product is exposed to high conditions of water vapour. The effect of environmental relative humidity can have a negative impact when the driving force is too high, the product will absorb moisture until reaches the equilibrium, which led to an increase of moisture content and consecutively a decrease of crispness. Because water affects the texture of dry food products, as moisture content increases above the monolayer value there is a gradual crispness loss, which is a function of water activity (Katz and Labuza 1981).

To minimize the loss in quality of a food product during storage, kinetic models describing deterioration rates and their relationship with temperature and water activity must be determined. The usefulness of any mathematical model that expresses the effect of intrinsic and extrinsic factors on the deterioration rate greatly depends on the accuracy of the model parameter estimates.

The aim of this study were to i) investigate the moisture uptake and the loss of firmness in granola breakfast product; ii) investigate the relationship between environmental relative humidity, temperature and absorption reaction rate of granola; iii) determine the kinetics of water activity and the kinetics of firmness of granola under different environmental conditions; and iv) develop a mathematical model describing the kinetics of quality decay of granola during storage.

Materials and Methods

Granola breakfast product was stored in airtight containers at different environmental conditions (32-33, 53-57 and 75-76% of relative humidity and temperatures 10, 20, 30 and 40 °C). Appropriate sampling was performed in triplicate to assess the moisture content and firmness of granola throughout 15 days of storage.

The quality decay for most foods can be represented by a first order degradation reaction and by integrating and normalising the quality characteristics, an appropriate model can be based on the changes occurring between the initial and an equilibrium value, by application of the concept of fractional conversion for an irreversible first order reaction (Ochoa *et al.* 2001):

$$C = C_e + (C_i - C_e)\exp(-kt) \quad (1)$$

where, C is the measured quality factor measured; C_i and C_e are the quality parameters initially and at equilibrium, respectively, t represents time; and k is the reaction rate constant.

Results and Discussion

Kinetics of water activity

The kinetics of moisture content gain in granola during storage, under different environmental conditions, was shown to follow a first order reaction model (Eq. 1), and the results obtained show clearly that the model fits the experimental data very well ($0.842 < R^2 < 0.988$) (results not shown). Moisture content by itself is not always the best parameter to follow the effects of water on reaction rates; it is preferable to use water activity instead (Saguy and Karel 1980). Therefore, water activity was determined from moisture content using the sorption isotherms of granola (Eq. 2) (Macedo *et al.* 2011):

$$MC = 4.055 + 43.72 a_w^{3.718} \quad (2)$$

where, MC is moisture content in dry basis and a_w is the water activity.

The kinetics of water activity gain in granola during storage were detemined as a function of temperature, time and environmental relative humidity and a first order reaction model was fitted (Eq. 3).

$$\frac{(a_w - a_{we})}{(a_{wi} - a_{we})} = \exp(-k_{aw} t) \quad (3)$$

where, a_w, a_{wi} and a_{we} are the water activity of granola at time t, at initial time and at the final equilibrium, respectively; and k_{aw} is the reaction rate constant (day^{-1}). As an example, Figure 1 shows the kinetics of water activity of granola at 40 °C.

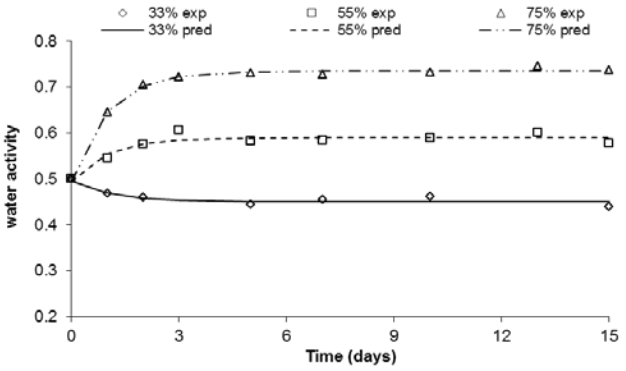

Figure 1: Kinetics of water activity of granola over time at 40 °C and at different conditions of relative humidity (%). The markers correspond to the experimental values and the lines correspond to the predicted values by a first order reaction model.

The reaction rate constant (k_{aw}) (day^{-1}) was determined by a non-linear regression method. Estimated values, standard errors and the goodness of the fit of the model are shown in Table 1.

The coefficient of determination (R^2) for all conditions was higher than 0.852 and the mean relative deviation modulus (E) was less than 3.24. Moreover, *p*-levels of all the constants estimated were less than 0.05. Therefore, the first order reaction model is suitable for fitting the experimental data at each condition.

Table 1: Reaction rate constants (ka_w) of water activity (± is the confidence intervals), coefficient of determination (R^2) and mean relative deviation modulus (E) of the first order reaction model of granola at different temperatures and relative humidities.

Temperature (°C)	RH (%)	Ka_w (day^{-1})	R^2	E
10	33	0.266±0.0773	0.929	1.82
	57	0.252±0.0334	0.978	1.29
	76	0.503±0.0921	0.940	3.24
20	33	0.344±0.0804	0.954	1.50
	54	0.355±0.0508	0.968	1.60
	75	0.628±0.105	0.951	2.61
30	32	0.484±0.106	0.970	0.948
	56	0.665±0.131	0.937	1.35
	75	0.964±0.136	0.972	2.08
40	32	0.882±0.401	0.852	1.30
	53	0.965±0.279	0.889	1.41
	75	1.00±0.0600	0.995	0.627

The reaction rate constant for water activity increased with an increase in temperature according to an Arrhenius relationship, whereby it was not significantly affected by relative humidity ($p < 0.05$). The increase of the rate constant with temperature can be explained by the fact that higher temperature promotes the mass transfer of water vapour from the environment to the surface of the product and from the surface to the centre (Zhengyong *et al.* 2008). The temperature dependence of the reaction rate constant for water activity gain in granola at constant environmental relative humidity is shown in Figure 2. The activation energies (Ea) and k_{ref} values were determined at each relative humidity, with Ea values obtained ranging between 17.1±4 and 34.5±3 KJ/mol, and k_{ref} from 0.441±0.039 to 0.760±0.051 day^{-1}. The activation energy decreased with an increase in environmental relative humidity.

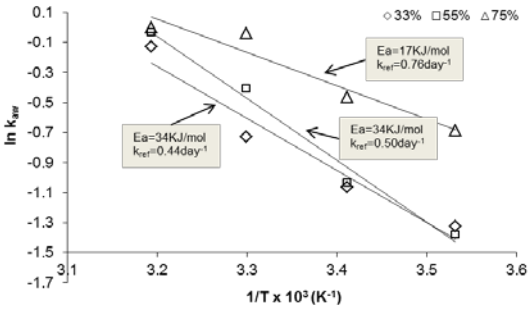

Figure 2: Water activity Arrhenius plot for granola at different RH (33, 55, and 75%).

The overall mathematical model describing water activity a function of both time and temperature (Eq. 4) is given combining the first order reaction model (Eq. 3) with the Arrhenius equation:

$$a_w = a_{we} + (a_{wi} - a_{we})\exp\left[-k_{ref}\exp\left(-\frac{Ea}{R}\left(\frac{1}{T}-\frac{1}{T_{ref}}\right)\right)t\right] \quad (4)$$

The overall model was fitted using a non-linear regression procedure, least squares, to all the water activity data, covering a range of temperature from 10 to 40 °C and environmental RH from 33 to 75%. The diagnosis plot is shown in Figure 3, as well as the plot of frequency distribution of residuals and the plot of residuals vs. predicted values.

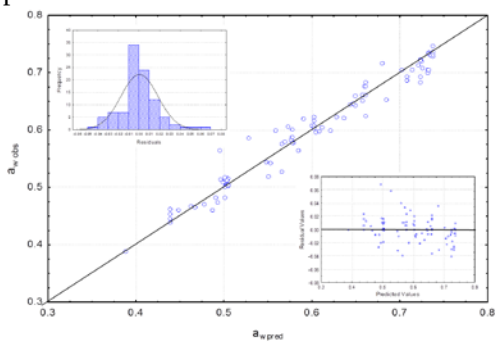

Figure 3: Diagnosis plot between water activity (a_w) experimental values obtained by sorption isotherm and predicted by the first order model. The upper left graph shows the frequency distribution of residuals and bottom right graph shows distribution of the residuals versus predicted values of water activity.

The Ea and k_{ref} values were estimated to be 23.4±3.2 KJ/mol and 0.612±0.029 day^{-1}, respectively, *p*-levels of all the constants estimated were less than 0.1, the coefficient of determination was 0.968 and the mean relative deviation modulus between experimental and predicted values was 2.02. From this can be concluded that the first order model can describe the relationship between water activity and time with accuracy.

Kinetics of firmness

Firmness decreased throughout time, the decrease being more pronounced at high relative humidity (RH). At low RH (32-33%) there was no kinetic trend, as there was not a significant change in firmness. The kinetics of firmness loss in granola during storage under different environmental conditions were modelled using a first order reaction and the results obtained showed a good fit ($0.953< R^2 <0.999$ and $8.67< E <19.2$).

Temperature and relative humidity did not show any significant influence ($p < 0.05$) on the reaction rate constant (k_F). The diagnosis plot between experimental values and predicted by the first order model is shown in Figure 4, as well as the plot of frequency distribution of residuals and the plot of residuals vs. predicted values. The k_F value was 0.697±0.076 day^{-1} and F_e 15.3±2.5 N and *p*-levels of all the constants were less than 0.1. The coefficient of determination was 0.836 and the mean relative deviation modulus was 65. Despite the deviation value, the first order reaction model was accepted to describe the relationship between firmness and time, considering the inherent firmness variability of the product.

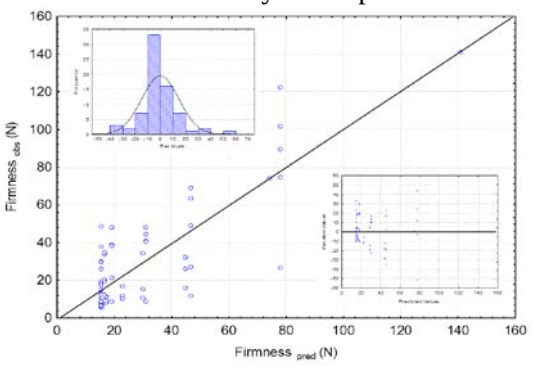

Figure 4: Diagnosis plot between experimental and predicted values of firmness. The upper left graph shows the frequency distribution of residuals and bottom right graph shows distribution of the residuals versus predicted values of firmness.

Conclusions

Moisture uptake and firmness loss showed exponential growth and decay respectively, which was described by a first order reaction model. The reaction rate for moisture gain was greatly influenced by the temperature during storage, which was described by the Arrhenius relationship, whereas relative humidity had no significant effect. An overall model was developed to described the quality decay in granola during storage as a function of temperature, and a good fit ($R^2 = 0.968$) was found.

Acknowledgements

Funding was provided under the NDP, through the FIRM (06/RDC/428), administered by the Department of Agriculture, Fisheries & Food, Ireland, Ireland. A special thanks to Stable Diet (Co. Wexford, Ireland) for providing the Granola products.

References

Katz E. E. and Labuza T. P. (1981) Effect of water activity on the sensory crispness and mechanical deformation of snacks food products. Caps. *Journal of Food Science* 46, 403-409.

Macedo I. S. M., Sousa-Gallagher M. J. and Byrne E. P. (2011) Moisture Sorption Isotherms of Granola Breakfast Product, in Program & Abstracts, [40th Annual UCC Food research Conference, March31st-April 1st].

Machado M. F., Oliveira F. A. R., Gekas V. and Singh R.P. (1998) Kinetics of moisture uptake and soluble-solids loss by puffed breakfast cereals immersed in water. Caps. *Journal of Food Science and Technology* 33, 225-237.

Ochoa M. R., Kesseler A. G., De Michelis A., Mugridge A. and Chaves A.R. (2001) Kinetics of colour change of raspberry, sweet (Prunus avium) and sour (Prunus cerasus) cherries preserves packed in glass containers: light and room temperature effects. Caps. *Journal of Food Engineering* 49, 55-62.

Saguy, I. and Karel M. (1980) Modelling of quality deterioration during food processing and storage. Caps. *Journal of Food Technology* 34 (2), 78-85.

Zhengyong Y., Sousa-Gallagher M. J. and Oliveira F.A.R. (2008) Mathematical modelling of the kinetics of quality deterioration of intermediate moisture content banana during storage. Caps. *Journal of Food Engineering* 84, 359-367.

A methodology to predict the pre-harvest and post-harvest level of polyacetylenes in carrots

A. Rawson[1], U. Tiwari[2], N. Brunton[1], Juan Valverde[1], Maria Tuohy[3], E. Cummins[2]

[1]Teagasc Food Research Centre, Ashtown, Dublin, Ireland (ashishrawson@gmail.com)
[2]Biosystems Engineering, UCD school of Agriculture, Food science and Veterinary medicine, University College Dublin, Belfield, Dublin 4, Ireland
[3]NUIGalway, Ireland

Abstract

Carrots (*Daucus carota* L.) are root vegetables of the Apiaceae family and are sometimes consumed raw or following cursory processing. However, carrots are also thermally processed as canned and frozen foods, ingredients in dehydrated soups, baby foods and food mixes. Nutritionally, carrots are known for their phytochemical content, including three biologically active C17-polyacetylenes (falcarinol, falcarindiol and falcarindiol-3-acetate) that may posses several human health benefits. Thermal processing and post harvest treatments have been shown to affect the level of some bioactive compounds including polyacetylenes in both fruit and vegetables. The objective of this study was to evaluate the change in level of polyacetylenes during both pre-and post-harvest stages, including both domestic and industrial processing. The model was developed using Monte Carlo simulation techniques to simulate the factors influencing polyacetylene levels in carrot cultivars. Probability density functions were fitted to relevant data sets collated from scientific literature and experimental data. A sensitivity analysis for the baseline model indicated that the cultivar selection had a positive influence (~0.20 correlation coefficient) followed by plant growth stage with a negative effect of harvest delay (-0.62 correlation coefficient). The mean simulated level of polyacetylenes, from initial cultivars to domestic processing (boiling), decreased by 76% (530 to 129 µg/g dry weight (DW)) and 58% (352 to 147 µg/g DW) for falcarinol and falcarindiol, respectively, whereas an increase of 2% (564 to 575 µg/g DW) was noted for falcarindiol-3-acetate. The model shows an overall decrease in both falcarinol and falcarindiol compounds, indicating the thermal degradation during domestic processing. Three industrial processing methods, (blanching, water immersion cooking and sous vide processing) were also considered in this model. A similar decrease during industrial processing for both the farcarinol and falcarindiol with a corresponding increase in falcarindiol-3- acetate was observed. This model will assist in optimising procedures to maximise polyacetylenes in processed carrots.

Development of shelf life predictive model for fresh-cut produce

F. Oliveira[12], M. J. Sousa-Gallagher[1]*, P. V. Mahajan[1], J. C. Teixeira[2]

[1]Department of Process & Chemical Engineering, School of Engineering, College of Science, Engineering and Food Science, University College Cork, Ireland
[2]Institute for Biotechnology and Bioengineering (IBB), Centre of Biological Engineering, University of Minho, Braga, Portugal
*email: m.desousagallagher@ucc.ie

Abstract

Modified atmosphere packaging (MAP) relies on the interplay between the product respiration and the package film permeability with the aim of maintaining initial quality and extending shelf-life of fresh produce. The aim of this work was to evaluate the effect of temperature and number of perforations on quality and the shelf life of sliced button mushrooms. Sliced mushrooms were packed in a tray, covered with biobased film, and stored at 4 levels of temperature (0, 5, 10 and 15 ºC) and 3 levels of perforations for each temperature (ranged from 1 to 6) for 7 days. Headspace gas composition and quality parameters of sliced mushrooms (weight loss, pH, firmness and colour) were measured throughout the storage period. Increasing the storage temperature resulted in the need to increase the number of perforations in order to obtain the optimum MAP conditions. Temperature had a significant effect ($p < 0.05$) on weight loss and firmness of sliced mushrooms. Firmness was identified as a critical quality parameter therefore a model was developed to describe the influence of temperature and time on shelf life of sliced mushrooms. The shelf life of sliced mushrooms packed in an optimum package with 1 perforation was 7.5 and 4 days when stored at 0 and 5 °C, respectively.

Keywords: mushrooms, MAP, fresh produce, optimal gas composition, shelf life

Introduction

MAP of fresh produce relies on modifying of the atmosphere inside the package, achieved by the natural interplay between two processes, the respiration of the product and the transfer of gases through the packaging, which leads to an atmosphere richer in CO_2 and poorer in O_2. MAP design depends of the characteristics of the product, its recommended gas composition and its respiration rate as affected by temperature and headspace gas composition; and the permeability of the packaging materials (perforated or non-perforated polymeric film) and its dependence on temperature (Fonseca *et al.* 2002).

Temperature is the most important environmental factor in the postharvest life of fresh produce, and decreasing storage temperature causes a reduction in the biochemical reaction rates (e.g., respiration) (Robertson 2006).

Shelf-life extension can also be obtained by a good modified atmosphere package (MAP) design, which can be attributed to low O_2 and high CO_2 concentrations in the atmosphere that surrounds the product, decreasing the respiration rate of the product and inhibiting microbial growth (Antmann *et al*. 2008).

Optimum mushrooms MAP conditions are 3-5 % O_2 concentration to reduce the respiration rate, but not lower than 3 % to avoid anaerobic respiration, and CO_2 concentrations should not be higher than 12 % to avoid physiological injuries (Parentelli *et al.* 2007).

The aim of this study were to study the effect of temperature and number of perforations on headspace gas composition of sliced mushrooms, the effect of time and temperature on quality and shelf life of sliced mushrooms.

Materials and Methods

Experimental setup

Button mushrooms (*Agaricus bisporus*) were sliced (0.5 cm of thickness) placed 110 g in each tray (11.1 x 15.5 x 3.4 cm^3) and covered with cellophane™ 335 PS film (Innovia Films Ltd., UK), 23.3 μm of thickness. The film was perforated with a needle of diameter 0.33 mm. A label of 10 x 5 cm^2 area was placed on the film, similar to the labels found in the supermarket packaging.
An experimental design was used for studying temperature and number of perforations on headspace gas composition of sliced mushrooms.

Table 1: Temperature and number of perforations used

Factors	Levels												
Temperature (ºC)	0			5			10			15			
Number of perforations	0	1	2	0	1	2	2	3	4	4	5	6	

After determining the number of perforations at each temperature to keep the desired atmosphere inside the packaging, a new experimental design was performed and quality parameters were studied with time and temperature, during 7 days, at 4 different temperatures (7 packages for each temperature), giving a total of 28 runs.

Analysis of quality parameters

The quality parameters, weight loss, pH, firmness and colour (L, a, b and Browning Index (BI)), were determined once a day, during 7 days.

Mathematical modelling

The Weibull model was used to describe kinetic degradation of quality parameters as a function of time and Arrhenius equation was used for the influence of temperature on that.

$$\frac{X - X_e}{X_0 - X_e} = \exp\left[-\left[\frac{t}{\alpha}\right]\right]^{\beta} \quad (1)$$

where, X_0 is the initial quality parameter, X is the quality parameter at time t, X_e is the equilibrium quality parameter, t is the time (d), α is the scale parameter (d^{-1}), and β is the shape parameter.

$$k = k_f \exp\left[\frac{-E_a}{R_c T}\right] \quad (2)$$

where, k is the parameter, k_f is the frequency factor, Ea is the activation energy (J mol^{-1}), Rc is the gas constant (8.314 J $mol^{-1}K^{-1}$) and T is the Temperature (K).
Statistical analysis and determination of parameters was carried out by using Anova and Solver tool from Microsoft Excel 2007.

Results and Discussion

Effect of Temperature and Perforations on Gas Composition

Increasing the storage temperature resulted in the need to increase exponentially the number of perforations, in order to obtain the optimum MAP conditions. Table 2 shows the number of perforations necessary to obtain that condition.

Table 2: Number of perforations in the film of the package, at determined temperature, to obtain optimum MAP conditions.

Factors	Levels			
Temperature (ºC)	0	5	10	15
Number of perforations	1	1	3	6

A new experimental design was carried out with conditions from Table 2 to study the effect of time and temperature on quality of sliced mushrooms, in an optimum MAP design.

Effect of Time and Temperature on Quality

Time and temperature had significant effect ($p < 0.05$) on quality of sliced mushrooms.

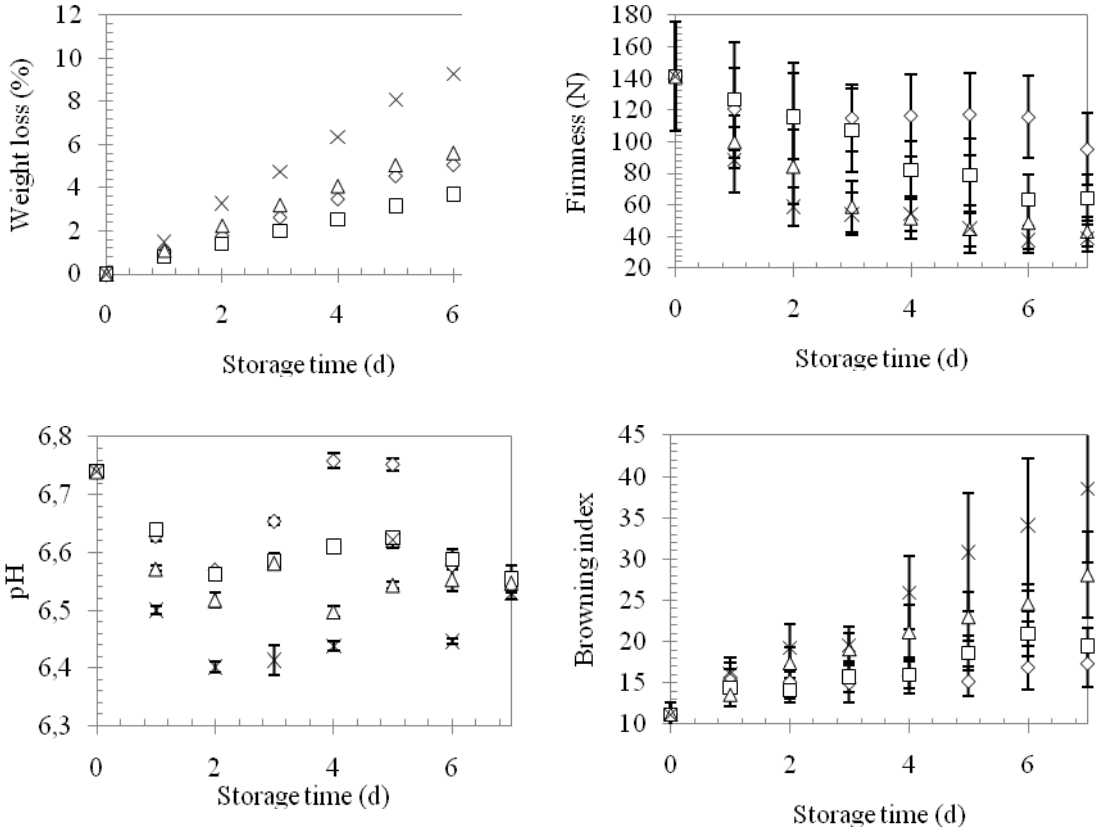

Figure 1: Quality parameters profiles of sliced mushrooms with time, at 0 ºC (◇); 5 ºC (□); 10 ºC (△); 15 ºC (×), in packages with 1, 1, 3 and 6 perforations, respectively.

Mathematical Modelling and Shelf life Prediction

Firmness was identified as a critical parameter, since presented highest effect produced by time and temperature (based on its *p*-value) and presented higher coefficient of determination from the global Weibull model fitted to data (equation 3).

$$\frac{F-\left[1.00T+325.32\right]}{141.14-\left[1.00T+325.32\right]}=\exp\left[-\left[\frac{t}{\left[\frac{1}{1.90E^{-14}}\exp\left[-\frac{7.64E^{4}}{R_cT}\right]\right]^{-1}}\right]^{\left[\frac{1}{6.16E^{-8}}\exp\left[-\frac{3.92E^{4}}{R_cT}\right]\right]^{-1}}\right] \quad (3)$$

A limit of acceptance was established (60% of loss of initial firmness (F_0)), therefore the global Weibul model was used to calculate the time (t, days) as a function of its firmness (F, N) and temperature (T, K), in order to predict the shelf life of sliced mushrooms.

$$t = \left[\frac{1}{1.90E^{-14}}\exp\left[-\frac{7.64E4}{R_cT}\right]\right]^{-1} \times \left[-\ln\left[\frac{F-[1.00T+325.32]}{141.14-[1.00T+325.32]}\right]\right]^{\left[\frac{1}{6.16E^{-8}}\exp\left[-\frac{3.92E^4}{R_cT}\right]\right]} \quad (4)$$

Shelf life was obtained by difference of the time which led to reduce to 0.6 of the initial firmness and the time which leaded to reduce to 1, 0.95, and 0.9 until 0.6 of the initial firmness.

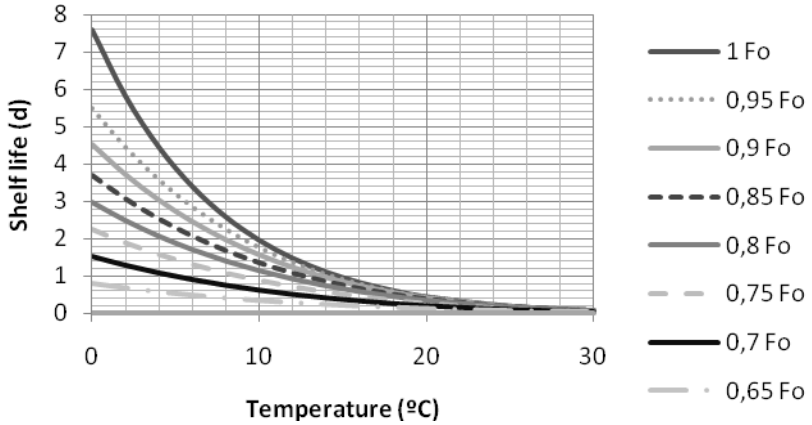

Figure 2: Shelf life prediction of sliced mushrooms based on firmness at different temperatures.

Fresh sliced mushrooms (1 F_0) showed 1 day of shelf life, at 15 ºC; 2 days at 10 ºC; 4 days at 5 ºC and 7.5 days at 0 ºC (Figure 2).
Sliced mushrooms presented 80 % of initial firmness (0.8 F_0), therefore the shelf life would be reduced by half, i.e., 0.5 day at 15 ºC, 1 day at 10 ºC, 2 days at 5 ºC and 3 days at 0 ºC.

Conclusions

Increasing the storage temperature the number of perforations had to increase in order to obtain the optimum MAP conditions. Time and temperature had significant effect on quality parameters of sliced mushrooms. The shelf life of fresh sliced mushrooms in an optimum package was 7.5 days and 4 days stored at 0 and 5 ºC, respectively.

Acknowledgements

The first author acknowledge financial support from the Erasmus Programme (2009) and research funding was provided under the NDP, through FIRM (08/R&D-UL/661), administered by the Department of Agriculture, Fisheries & Food, Ireland. Authors would also like to acknowledge Innovia Films Ltd (UK) for supplying the packaging materials.

References

Antmann G., Ares G., Lema P., Lareo C. (2008) Influence of modified atmosphere packaging on sensory quality of shiitake mushrooms. *Postharvest Biology and Technology 49*, 164-170.

Fonseca S. C., Oliveira F. A., Brecht J. K. (2002) Modeling respiration rate of fresh fruits and vegetables for modified atmosphere packages: a review. *Journal of Food Engineering 52*, 99-119.

Parentelli C., Ares G., Corona M., Lareo C., Gámbaro A., Soubes M. (2007) Sensory and microbiological quality of shiitake mushrooms in modified-atmosphere packages. *Journal of the Science of Food and Agriculture 87*, 1645-1652.

Robertson G. L. (2006) Packaging of horticultural products. In *Food Packaging: Principles and Practice* (pp. 360-380). CRC Press.

Modelling of antibacterial effect of spice extracts on growth of spoilage flora in VP and MAP cooked lamb product on chilled storage

S. AL-Kutby, J. Beal, V. Kuri

School of Biomedical and Biological Sciences, University of Plymouth, Plymouth, PL4 8AA, United Kingdom.

Abstract

Technologies such as vacuum packing (VP) and modified atmosphere packing (MAP) allow extended storage of ready to eat (RTE) meats, but issues with chemical and microbial deterioration remain. This work aimed to describe the effect of natural spice extracts on the growth kinetics of spoilage indicators, including total viable and lactic acid bacteria counts. Samples were prepared to resemble a RTE meat product prepared with minced lamb and a cereal ingredient following a doner kebab formulation in a pilot plan setting with conventional hygiene controls, which allow post-pasteurisation of the product before packaging in VP and MAP30% CO_2. Factors on the design included the storage atmosphere, type of added spice extract (rosemary-R, cinnamon-C, sumac-S and a combination of R, C and S) at high (0.2%) and low (0.05 %) levels, with a control without spices, and storage time (12 weeks). Weekly bacterial levels (log_{10} cfu/g) were determined and data was fitted to a Baranyi and Roberts model with DMfit v2.0; generally all growth data were satisfactorily fitted to growth curves for all the treatments with high R^2 values and low standard errors. For TVC, no significant differences on model parameters were found between VP and MAP samples. The use of cinnamon or rosemary significantly reduced the lag phase of TVC by about 2 weeks, and reduces the maximum final growth by 2 log cycles. All spices decreased LAB counts over time ($P>0.05$), with negative growth rate values between 0.11 to 0.78 for VP, but just to 0.3 for MAP. The high level of cinnamon addition controlled LAB levels below detection limit from the time of addition. The use of spices offers viable alternatives for spoilage control and modelling aids the prediction of the shelf life and allows better targeting of formulation strategies.

Modelling the effect of a_w and fat content on the high pressure resistance of *Listeria monocytogenes*

S. Bover-Cid[1], N. Belletti[1], M. Garriga[1], T. Aymerich[1]

[1] IRTA. Food Safety Programme. Finca Camps i Armet, E-17121 Monells, Spain (sara.bovercid@irta.cat).

Abstract

The inactivation of *Listeria monocytogenes* CTC1034, inoculated in a dry-cured ham system, was modelled as a function of pressure (347 MPa-852 MPa, 5 min/15ºC), water activity (a_w, 0.86 - 0.96) and fat content (10% - 50%) according to a central composite design. The response surface methodology through stepwise multivariate linear regression was applied to describe the relationship between bacteria inactivation and the studied variables.

According to the best fitting polynomial equation, besides pressure intensity, both a_w and fat content exerted a significant influence on the *L. monocytogenes* inactivation. A clear linear baroprotection trend was found lowering the a_w of the substrate. Fat content was included in the model through the quadratic term and its interaction with pressure, resulting in a particular behaviour. A protective effect due to the presence of high fat content was seen for pressure treatments above *ca.* 700 MPa. At lower pressures, higher inactivation of *L. monocytogenes* occurred by increasing the fat content above 30%. The results highlight the relevant influence of intrinsic factors on the pathogen inactivation by HP, which make necessary to assess and validate the effectiveness of HP on specific food products.

Keywords: Listeria monocytogenes, *high hydrostatic pressure, modelling, inactivation, food characteristics*

Introduction

The use in food processing of High Pressure (HP) has captured significant interest as an alternative to heat treatment, thanks to its ability to inactivate bacteria with minimal consequences for sensorial and nutritional properties of food (Rastogi *et al.* 2007).

The different sensitivity of microorganisms to pressure treatment is reported in scientific literature. The resistance of microorganisms to pressure in food depends on the HP processing conditions (pressure, time and temperature), and intrinsic factors of food. The presence of proteins and fat has been reported to act as a protective agent on microbial cells (Black *et al.* 2007). Similarly, a low water activity (a_w) values have been proved to decrease the efficiency of HP treatments (Moussa *et al.* 2006). Despite the recognised influence of food characteristics on the lethality of HP, modelling studies to quantify it are still scarce.

In this frame, the aim of the present work was to model the influence of the combined effect of three selected variables (pressure treatment, fat content, a_w) on the inactivation of *L. monocytogenes* inoculated in a dry-cured ham system.

Materials and Methods

Experimental design

A Central Composite Design (CCD) for three independent variables (a_w, fat content and pressure) was followed as indicated in Table 1; in parenthesis the measured a_w values are also reported, which were actually used in the mathematical modelling.

Sample preparation

The dry-cured ham system was prepared by adding water in different volumes to different aliquots of minced lean dry-cured ham (a_w = 0.85) to attain the required final a_w in the range on 0.860 – 0.960. Then different quantities of minced fat (from dry-cured ham) were added till final target concentration (10% - 50%) was reached.

L. monocytogenes *inoculation*

L. monocytogenes CTC1034 was previously cultured twice in BHI at 37ºC (for 7 and 18 hours, respectively). Samples were inoculated, to a final level of $2.38 \cdot 10^6$ CFU/g on average, adding the culture to the sterile water used for sample preparation.

High-pressure treatment

Inoculated samples were vacuum packaged in plastic bags PET/PE and submitted to HP according to the CCD (Table 1, 347 MPa-852 MPa, 5 min/15ºC). The Wave6000 NC Hyperbaric (Burgos, Spain) and the Thiot ingenierie – NC Hyperbaric (Bretenoux, France – Burgos, Spain) HP units were used for pressures up to and above 600MPa, respectively.

Enumeration of L. monocytogenes

Samples for each run of the CCD were sampled at least in duplicate. Inactivation of *L. monocytogenes* was measured in terms of logarithmic reductions as Log (N/N_0), i.e. difference between counts after the treatments (N) and the initial inocula (N_0). *L. monocytogenes* was enumerated on Chromogenic Listeria Agar (CLA, 37ºC for 48 h) and, for expected concentration below the quantification limit (<4CFU/g), the presence/absence of the pathogen was investigates by molecular techniques after 25g-sample enrichment in TSBYE (Aymerich *et al.* 2005). For modelling purposes, positive results below the quantification limit were recorded as 0 Log CFU/g while absence in 25g was computed as -1.18 Log CFU/g.

Mathematical modelling

To make the magnitude of the experimental variables similar, their values were rescaled (i.e. a_w*10, pressure/100, fat content/10) before the statistical modelling. Multivariate linear regression (Statistica, Statsoft, ver. 8.0) using the stepwise backward procedure was applied, which allowed only statistical significant terms (P<0.05) to be included in the final equation.

Results and Discussion

Inactivation results

Table 1 shows the HP-inactivation of *L. monocytogenes* in the dry-cured ham system, expressed as logarithmic viability reduction (Log N/N_0), achieved for each combination of a_w, fat content and pressure of the CCD. A relative low inactivation degree was obtained at pressure levels up to 450 MPa (runs 1. 3, 5, 7, 19), varying from 0.92 to 3.92 logs depending on the different fat content and a_w. These results were not surprising and are in agreement with those previously found for *L. monocytogenes* on sliced dry-cured ham (a_w = 0.88; 33.3 % fat) for the same pressure levels (Bover-Cid *et al.* 2010). The absence of the pathogen in 25g-sample was achieved only in runs 20, at the highest level of pressure applied (852 MPa) and 6, which combines relatively high pressure level (750 MPa) and moderate a_w (0.948).

Modelling of inactivation results

A multivariate regression analysis was performed on the inactivation data (response variable) to obtain the best fitting polynomial equation (Eq.1) describing the relationship between HP inactivation of *L. monocytogenes* and the independent variables a_w, fat content and pressure.

$$Log\left(\frac{N}{N_o}\right) = 38.653 - 3.429 \cdot [a_w \cdot 10] - 2.370 \cdot \left(\frac{P}{100}\right) - 0.349 \cdot \left(\frac{F}{10}\right)^2 + 0.334 \cdot \left(\frac{P}{100}\right) \cdot \left(\frac{F}{10}\right) \qquad \text{Eq. 1}$$

where Log(N/N_0) represents the logarithmic reduction of *L. monocytogenes;* a_w, the measured water activity of the food matrix; F, fat content (%) of the food matrix; and P, the pressure levels (MPa) of the HP treatment (for 5 min at 15 ºC).

The performance of the polynomial model obtained, was supported by the satisfactory value of adjusted R^2 (0.84). The significance of the model in terms of p (<0.0001) and F (26.40) was also good.

A clear representation of the influence of all the three independent variables in the *L. monocytogenes* inactivation is facilitated by the response surface plots presented in Figure 1. This graphics are constructed on the basis of the equation obtained and keeping the variable not represented in the plot at the central value of the CCD.

Table 1: Central Composite Design including the combinations of experimental variables for each run and *L. monocytogenes* inactivation result for each run.

Run	a_w	Fat (%)	Pressure (MPa)	Inactivation Log (N/N_0)
1	0.880 (0.883) *	18.18	450	-0.92
2	0.880 (0.883)	18.18	750	-5.26
3	0.880 (0.890)	42.18	450	-1.05
4	0.880 (0.890)	42.18	750	-5.75
5	0.940 (0.945)	18.18	450	-1.16
6	0.940 (0.948)	18.18	750	-7.96
7	0.940 (0.939)	42.18	450	-3.92
8	0.940 (0.939)	42.18	750	-6.07
9	0.920 (0.919)	30.18	600	-4.38
10	0.920 (0.919)	30.18	600	-4.12
11	0.920 (0.915)	30.18	600	-4.88
12	0.920 (0.915)	30.18	600	-4.64
13	0.920 (0.922)	30.18	600	-4.18
14	0.920 (0.922)	30.18	600	-4.71
15	0.860 (0.857)	30.18	600	-2.24
16	0.960 (0.961)	30.18	600	-6.82
17	0.920 (0.920)	10.00	600	-6.58
18	0.920 (0.911)	50.36	600	-6.28
19	0.920 (0.919)	30.18	347	-0.99
20	0.920 (0.922)	30.18	852	-7.04

* The column of a_w reports target theoretical a_w values according to a central composite design and the actual measured values are reported in parenthesis.

The influence of pressure and a_w was described by the corresponding linear terms. The increment of pressure had the most important contribution on the inactivation degree of *L. monocytogenes*, and the extent of its influence remained similar within the range of the assayed a_w values. The efficacy of HP processing was notably reduced by lowering the a_w values in agreement with the other studies (Hereu *et al.* 2011). The baroprotective effect of a_w has been related to the stabilisation of proteins (particularly enzymes), reducing its pressure-induced denaturation (Moussa *et al.* 2006). According to our results, the baroprotective effect of a_w would follow a linear trend, irrespective of the pressure level.

The factor fat content (%) was present as second order term. Additionally, its interaction with pressure was statistically significant and thus included in the model. The role of fat and its contribution as baroprotective agent remains unresolved but its influence seems dependent upon the pressure level (Figure 1B). A slight protective effect due to the presence of high fat content was seen for pressure treatments above *ca*. 700 MPa. At lower pressures, higher inactivation of *L. monocytogenes* occurred by increasing the fat content above 30%. The influence of fat content on the HP inactivation of bacteria has been scarcely studied and the available published results are controversial. A baroprotective action of fat has been occasionally found (Gervilla *et al.* 2000), though the particular mechanisms has not been established. Non significant influence of fat on the HP-inactivation of bacteria has also been reported (Escriu and Mor-Mur 2009). Additionally, as fat experiences higher compression heating (up to 8ºC/100MPa) than aqueous media (about 3ºC/100MPa), a slight thermal inactivation effect synergistically with the non-thermal HP lethal effects could also be hypothesised (Rasanayagam *et al.* 2003).

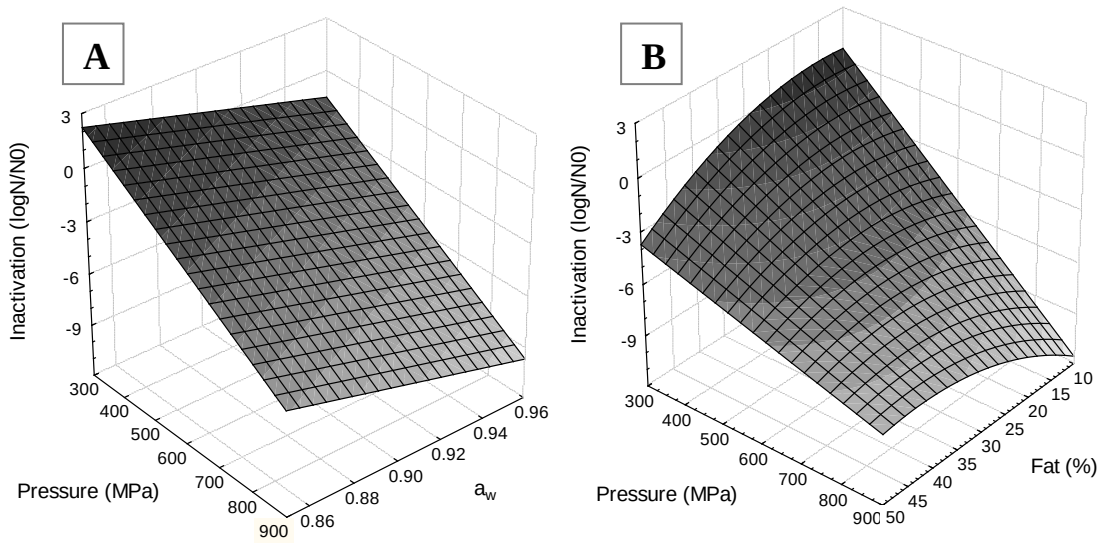

Figure 1: predicted inactivation in dry-cured ham system inoculated with *L. monocytogenes* evidenced by the combination of: (A) a_w and pressure and (B) fat content and pressure.

Conclusions

The HP inactivation of *L. monocytogenes* is strongly dependent on the physico-chemical characteristics of the media or food. The product-oriented modelling approach presented here has shown a protective effect of a_w against HP treatments following a linear trend, irrespectively of the pressure level. The role of fat and its contribution as baroprotective agent is still uncertain, but its influence seems dependent upon the pressure level. The results highlight the relevant influence of intrinsic factors on the pathogen inactivation by HP, which make necessary to assess and validate the effectiveness of HP on specific food products.

Acknowledgments

This work has been funded by the Spanish *Ministerio de Ciencia e Innovación* (RTA2007-00032).

References

Aymerich M.T., Jofré A., Garriga M. and Hugas M. (2005) Inhibition of *Listeria monocytogenes* and *Salmonella* by natural antimicrobials and high hydrostatic pressure in sliced cooked ham. *Journal of Food Protection* 68(1), 173-177.

Black E.P., Huppertz T., Fitzgerald G.F. and Kelly A.L. (2007) Baroprotection of vegetative bacteria by milk constituents: A study of *Listeria innocua*. *International Dairy Journal* 17(2), 104-110.

Bover-Cid S., Belletti N., Garriga M. and Aymerich T. (2010) Model for *Listeria monocytogenes* inactivation on dry-cured ham by high hydrostatic pressure processing. *Food Microbiology* in press (doi:10.1016/j.fm.2010.05.005).

Escriu R. and Mor-Mur M. (2009) Role of quantity and quality of fat in meat models inoculated with *Listeria innocua* or *Salmonella Typhimurium* treated by high pressure and refrigerated stored. *Food Microbiology* 26(8), 834-840.

Gervilla R., Ferragut V. and Guamis B. (2000) High pressure inactivation of microorganisms inoculated into ovine milk of different fat contents. *Journal of Dairy Science* 83(4), 674-682.

Hereu A., Bover-Cid S., Garriga M. and Aymerich T. (2011) High hydrostatic pressure and biopreservation of dry-cured ham to meet the Food Safety Objectives for *Listeria monocytogenes*. *International Journal of Food Microbiology* In Press, Corrected Proof.

Moussa M., Perrier-Cornet J.-M. and Gervais P. (2006) Synergistic and antagonistic effects of combined subzero tempearture and high pressure on inactivation of *Escherichia coli*. *Applied and Environmental Microbiology* 72(1), 150-156.

Rasanayagam V., Balasubramaniam V.M., Ting E., Sizer C.E., Bush C. and Anderson C. (2003) Compression heating of selected fatty food materials during high-pressure processing. *Journal of Food Science* 68(1), 254-259.

Rastogi N.K., Raghavarao K.S.M.S., Balasubramaniam V.M., Niranjan K. and Knorr D. (2007) Opportunities and challenges in high pressure processing of foods. *Critical Reviews in Food Science and Nutrition* 47(1), 69-112.

Effect of nisin and citral on the heat resistance and recovery of *Alicyclobacillus acidoterrestris* spores

J.P. Huertas[1], M.D Esteban[1], A. Palop[1]

[1] Deparment of Food Engeeniering & Aglicultural Machinery, Technical University of Cartagena, Paseo Alfonso XIII 48, Cartagena, Spain (alfredo.palop@upct.es)

Abstract

Alicyclobacillus acidoterrestris is a Gram-positive, acidophilic, thermophilic, spore-forming and spoiling bacterium. Commercial fruit juices are currently pasteurized at temperatures between 85ºC and 95ºC for a few minutes or seconds and *A. acidoterrestris* can survive these thermal treatments. These reasons make it an important threat for the fruit juice industry. The combination of mild heat treatments with natural antimicrobials (nisin and citral) can be an alternative for the control of *A. acidoterrestris*. Heat resistance determinations of *A. acidoterrestris* in pH 3.5 McIlvaine buffer at 95ºC with or without the addition of different antimicrobials (alone or combined) at the heating or recovery medium were assayed. None of the antimicrobials reduced the heat resistance of *A. acidoterrestris* spores when applied to the heating medium. However, nisin alone was able to decrease the viable counts of this microorganism in more than two log cycles when applied in the recovery medium at a concentration of 1.5 mM. The data on the effect of nisin in the recovery medium and on the reduction of viable counts were used to build a predictive model. The addition of natural antimicrobials such as nisin or citral, which would not affect the flavour or taste of citrus juices, alone or even combined, can help to the control of *A. acidoterrestris*.

Keywords: n*isin, citral, Alicyclobacillus acidoterrestris, antimicrobial, synergism, combined processes.*

Introduction

Alicyclobacillus acidoterrestris is a Gram-positive, acidophilic, thermophilic, spore-forming, spoiling and non pathogenic bacterium, containing ω-cyclohexyl fatty acids, which contribute to its survival at low pH and high temperature. Commercial fruit juices are currently pasteurized at temperatures between 85ºC and 95ºC for a few minutes or seconds (Silva and Gibbs 2001) and *A. acidoterrestris* can survive these thermal treatments. These reasons make it an important threat for the fruit juice industry (Bevilacqua *et al.* 2009). Some authors have proposed to increase the time or the temperature of treatment of the thermal processes to achieve the inactivation of this microorganism. However, thermal treatments cause important losses in sensorial and nutritional properties, making such alternative unviable to preserve natural fresh-like juices (Bevilacqua *et al.* 2009). The combination of mild heat treatments with natural antimicrobials (nisin, citral, etc.) can be an alternative for the control of *A. acidoterrestris* and respond to the demands of the consumers of fresh and natural products. The aim of this research was to evaluate the effect of the combination of a thermal treatment with the natural antimicrobial compounds nisin and citral on the survival and recovery of *A. acidoterrestris* spores. The data on the outgrowth of spores in the recovery medium and on the reduction of viable counts would permit to build a mathematical model that can predict the effect of antimicrobial concentration.

Materials and Methods

A. acidoterrestris DSM 3922 was provided by the German collection of micro-organism and cell cultures (DSMZ). Sporulation was carried out as described by Palop *et al.* (2000). The concentration of the spores was adjusted to 10^9 spores mL^{-1} with sterile bi-distilled water. The spore suspension was stored at 0-5ºC until used. The natural antimicrobials nisin and citral used in this research were provided by Sigma Aldrich Chemie (Steinheim, Germany) and stored at 4ºC until used.

Heat resistance determinations were carried out in a thermorresitometer Mastia as described by Conesa *et al.* (2009), with pH 3.5 McIlvaine buffer as heating medium. Samples were then appropriately diluted and immediately plated in PDA and incubated for 24h at 43ºC. Survival curves were obtained by plotting the log of the survivors against time, and D values were calculated by linear regression. The data on the effect of nisin on the reduction of viable counts were used to build a predictive model, based on the Weibull distribution.

Results and Discussion

The spores of *A. acidoterrestris* showed a $D_{95ºC}$ value of 2.26 min in a medium of pH 3.5 (table 1). Hence, they are able to survive thermal treatments currently applied to fruit juices, which even would provide the heat shock treatment necessary to stimulate spore germination and outgrowth (Walker and Phillips 2008). The D_{95} values obtained in our research are similar to those reported in the literature (Smit et *al.* 2011).

Table 1. D95-values, 95% confidence limits (CL), correlations coefficients (r0), initial log number (N0) and log number after 5 minutes of treatment (N5min), in pH 3.5 McIlvaine buffer under isothermal conditions with the antimicrobials at the recovery media for Alicyclobacillus acidoterrestris.

	Concentration of antimicrobial	D_{95} (min)	-95% CL	+95%CL	r_o	N_0 (log CFU/mL)	N_{5min} (log CFU/mL)
	0	2.26	2.09	2.46	0.996	5.16	3.03
Nisin (mM)	0.1	2.11	1.82	2.51	0.984	4.16	1.82
	0.3	3.38	2.97	3.94	0.988	3.06	1.48
	1.5	4.37	3.48	5.89	0.961	2.66	1.39
Citral (mM)	0.055	2.09	1.92	2.29	0.995	5.15	2.82
	0.11	1.69	1.51	1.91	0.992	5.16	2.30

When 0.1, 0.3 and 1.5 mM nisin was added to the plating medium without application of any previous thermal treatment, significant reductions in the counts were shown, as depicted in Fig. 1. Average log reductions were of 0.7 log cycles with 0.1 mM nisin, 1 log cycle with 0.3 mM nisin and 2.2 log cycles with 1.5 mM nisin.

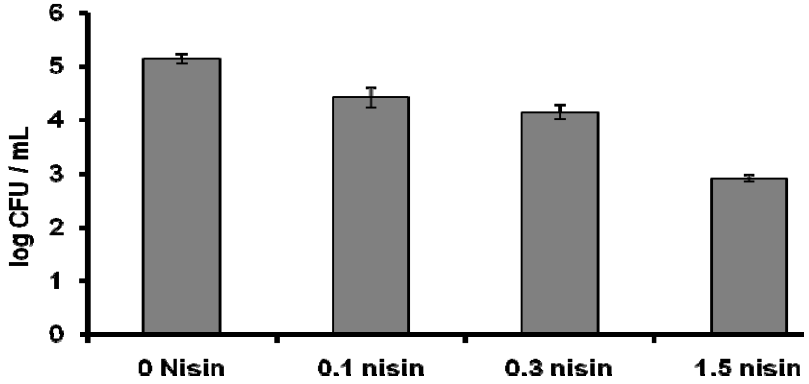

Figure 1: Influence of nisin concentration (mM) in the plating medium on the log viable *Alicyclobacillus acidoterrestris* spores not exposed to any previous heat treatment.

When nisin was applied to the recovery medium after a thermal treatment, similar log reductions were reached, even for the samples taken after only three seconds of heating (Table 1 and figure 2).

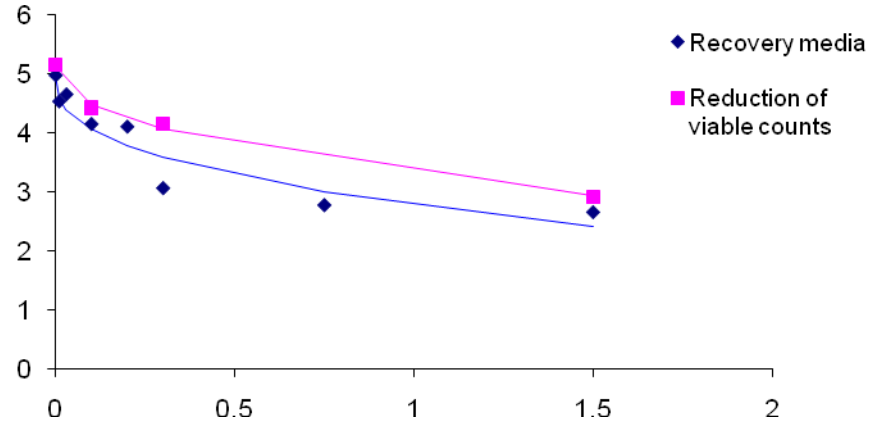

Figure 2: Curves obtained when plotting the reduction of viable counts of *A. acidoterrestris* spores against the concentration of nisin in the plating medium (before and after a short thermal treatment).

The addition of nisin led to a further decrease in the initial number of surviving microorganisms when the thermal treatment was applied. Since the first sample of the survival curves was taken 3 seconds after inoculation (in order to allow for the distribution of the inoculum into the heating medium), it means that even a very short thermal treatment, which did not lead to any heat inactivation, has significant synergistic effects on the reduction of viable spores of *A. acidoterrestris*. However, D_{95^oC} values increased with concentrations of nisin of 0.3 and 1.5 mM in the recovery media, which could mean that spores able to germinate in presence of nisin correspond also to the most heat resistant ones. The synergism of nisin and heat has already been postulated (Komitopoulou *et al.* 1999; Yamazaki *et al.* 2000).
The data on figure 2 were used to build models based on the survival function derived from Weibull distribution. The mathematical model for the data on the reduction of viable counts is depicted in Eq. 1. These data, obtained when nisin was applied without a previous heat treatment, generated a good fit of the experimental data (r=0.99).

$$Log\ N = Log\ N_0 - \left(\frac{[nisin]}{0.26}\right)^{0.45} \quad \text{(Eq.1)}$$

The mathematical model for the data on the survivors to the thermal treatment is depicted in Eq. 2. Also a good fit of the experimental data was achieved (r=0.95).

$$Log\ N = Log\ N_0 - \left(\frac{[nisin]}{0.12}\right)^{0.38} \quad \text{(Eq.2)}$$

Citral also showed an antimicrobial effect on *A. acidoterrestris* spores when applied to the recovery medium, but only at the highest concentration tested (0.11 mM citral; table 1). Additionally, the effect was different than that of nisin: there was no reduction in the initial number of surviving microorganism, but there was a decrease in the D value.
The addition of nisin or citral would not affect the flavour or taste of citrus juices and can help to inhibit the germination or outgrowth of *A. acidoterrestris* spores, reducing the risk of spoilage by this microorganism.

Conclusions

None of the antimicrobials reduced the heat resistance of *A. acidoterrestris* spores when applied to the heating medium. However, both nisin and citral, affected the recovery of the survivors. Nisin reduced the viable counts of non heat treated microorganisms and also of those exposed to a very short thermal treatment. A combination of nisin in the fruit juice with a thermal treatment

would help to reduce the spoilage by this microorganism. The best combination is probably 2.5 minutes at 95ºC with 0.3 mM nisin, since lower amounts of nisin is used, leading to almost the same inhibitory effect than much higher amounts.

Acknowledgements

The financial support of this research was provided by the Ministry of Science and Technology of the Spanish Government and Fondo Europeo de Desarrollo Regional (FEDER) through Project AGL-2006-10280. Juan Pablo Huertas is grateful to Technical University of Cartagena for his fellowship.

References

Bevilacqua A., Sinigaglia M. and Corbo M. (2009) Effects of pH, cinnamaldehyde and heat-treatment time on spore viability of Aliciclobacillus acidoterrestris. *International Journal of Food Science and Technology* 44, 340-385.

Conesa R., Andreu S., Fernández P.S., Esnoz A. and Palop A. (2009) Nonisothermal heat resistance determinations with the thermoresistometer Mastia. *Journal of Applied Microbiology* 107, 506-513.

Palop A., Alvarez I., Raso J. and Condon S. (2000) Heat resistance of Alicyclobacillus acidoterrestris in wáter, various buffers and orange juice. *Journal of Food Protection* 63, 353-380.

Silva F. and Gibbs P. (2001) Alicyclobacillus acidoterrestris spores in fruit products and design of pasteurization processes. *Trends in Food Science & Tecchnology* 12, 68-74.

Smit Y., Cameron M., Venter P. and Witthuhn R.C. (2011) *Alicyclobacillus* spoilage and isolation – A review. *Food Microbiology* 28, 331-349.

Komitopoulou E., Boziaris I., Davies E., Delves-Broughton J. and Adams M. (1999) Alicyclobacillus acidoterrestris in fruit juices and its control by nisin. *International Journal of Food Science and Technology* 34, 81-85.

Walker M. and Phillips C. (2008) Alicyclobacillus acidoterrestris: an increasing threat to the fruit juice industry?. *International Journal of Food Science and Technology* 43, 250-260.

Yamakazi K., Murakami Y., Kawai N., Inoue N. and Matsuda T. (2000) Use of nisin for inhibition of Alicyclobacillus acidoterrestris in acidic drinks. *Food Microbiology* 17, 315-320.

Antimicrobial activity of melt blended and Layer by Layer (LBL) self assembled Low Density Polyethylene (LDPE) – silver nanocomposite

M. Jokar[1], R.A. Rahman[2]

[1]Damghan Branch, Islamic Azad University, Damghan, Iran
[2] Food Science and Technology Faculty, University Putra Malaysia (UPM), Malaysia

Abstract

Developing nanocomposites is one of the emerging research activities in the field of active food packaging. Colloidal silver nanoparticles with a size of about 5 nm were prepared by chemical reduction using polyethylene glycol (PEG) as reducing agent as well as stabilizer and characterized by transmission electron microscopy (TEM). Silver nanoparticles were incorporated into low density polyethylene (LDPE) film by two procedures. One method is melt blending of LDPE pellets and silver nanoparticles as filler and subsequent hot pressing and the another method is layer by layer deposition of silver nanoparticles and chitosan onto LDPE film. Morphology of silver nanocomposite films were characterized by atomic force microscopy (AFM). Antimicrobial activity of silver nanocomposites against *Escherichia coli* ATCC 13706, *Staphylococcus aureus* ATCC12600 was evaluated by quantitative dynamic shake flask test. Growth kinetic parameters of *E.coli* and *S.aureus* affected by silver nanocomposites were calculated by modeling of absorbance data at 600 nm according to Gomperz equation. LDPE-silver nanocomposite produced by both melt blending or LBL coating, resulted in increasing lag time and reducing maximum bacterial concentration significantly ($p<0.05$). Layer by layer self assembly method is more effective to inhibit bacterial growth especially in reducing of specific growth rate (μ) of examined bacteria which may be attributed to easier release of silver ions from surface of LDPE nanocomposite film.

Introduction

In recent decades, antimicrobial active packaging is one of the emerging research activities in order to prolong shelf life of food products by inhibiting, reducing or retarding of microorganisms in foods. An antimicrobial agent can be incorporated into packaging polymer or coated onto polymer surface or associated with the packaging by using sachets or pads (Appendini and Hotchkiss 2002). Various synthetic and natural antimicrobial agents incorporated to packaging materials such as organic acids, enzymes, chelating agents, metal particles and plant extracted essential oils.

Among all of antimicrobials incorporated to packaging polymers, silver nanoparticles deserve special attention due to high thermal stability, long-term activity and their individual physicochemical properties. Silver nanoparticles represent one of the most interesting and developing area in recent nano-responding studies which can related to their unique physicochemical characteristics such as catalytic activity, optical and electronic properties ,and especially strong antimicrobial activity and broad spectrum toxicity to microorganism (Kim *et al.* 2007).Silver nanocomposites are polymer composites containing silver nanoparticles and deserve special attention in fields of medical industry and active packaging. Silver nanocomposites produced by several methods such as plasma depositing (Nobile *et al*. 2004), ion implantation (Li *et al*. 2007), melt processing on (Damm *et al*. 2008), impregnation using supercritical carbon dioxide (Furno *et al.* 2004), solution casting (Shameli, Ahmad *et al*., 2010) organic-inorganic hybrid coating (Marini *et al.* 2007). Antimicrobial efficiency of silver nanocomposite is strongly depended on silver ion release from nanocomposites. Silver ion release occurs on the surface of particles and only in the presence of water and oxygen (Damm and Munstedt 2008).

Materials and Methods

Silver nanoparticles produced by dissolving of silver nitrate in polyethylene glycol 200 at room temperature (25ºC) and. The transparent solution converted to gray-black colloid, which

indicated the formation of silver nanoparticles. The size and morphology of colloidal silver nanoparticles were characterized by TEM using Philips HMG 400 transmission electron microscope operating at 400 kV and by placing a drop of the colloidal dispersion. LDPE-silver nanocomposites produced by two methods: (i)melt blending as an industrially thermal processing and (ii) layer by layer (LBL) self assembly deposition. In melt processing, silver nanoparticles were added into low density polyethylene (LDPE) pellets by melt blending and subsequent hot pressing at 140°C in order to produce nanocomposite film by average thickness of 0.7mm. In LBL deposition method, nanocomposite films were built by sequential dipping of a LDPE film in either anionic silver colloid dispersion or cationic chitosan with the thickness of 2, 4, 8, 12, 16 and 20 layers. The surface morphology of melt blended and LBL deposited nanocomposites was investigated using atomic force microscope (AFM) operating with a Q-Scope 250 in contact mode.

Antimicrobial activity of silver nanocomposites investigated by dynamic shake flask test. Eight specimens (2×1.5 cm) of the nanocomposite films were immersed in Tripton Soy Broth (TSB). A 200 ml flask containing TSB and 0.4 g of Tween 80 inoculated with 1mL of *E. coli* (41.03×10^5) and *S. aureus* (19.55×10^6) and then incubated at 37 °C with 150 rpm agitation. Evidence of microbial growth was acquired by reading the absorbance changes at 600 nm (Han, Castell-Perez et al. 2007) by using a spectrophotometer at regular intervals (2 hours). The absorbance data were modeled according to Gompertz equation as modified by Zwietering *et al.* (1990) to estimate microbial growth kinetic parameters:

$$X(t) = X_0 + A\left\{exp\left[\frac{\mu_{max}\times 2.7182}{A}(\lambda - t) + 1\right]\right\} \quad (1)$$

where X(t) is the cell concentration of inoculated microorganism in the medium (absorbance at λ=600 nm), X_0 is initial value of absorbance, A maximum bacterial concentration attained at the stationary phase and its initial value, μ_{max} is maximum specific growth rate (h^{-1}), λ is lag phase and t is time (h). Growth kinetic parameters of bacteria determined using nonlinear regression estimation by using STATISTICA7.0 for windows (StatSoft, Inc, Tulsa, OK, USA)

Results and discussion

Atomic force micrographs of melt blended and LBL deposited nanocomposites illustrated that silver particles are homogeneously distributed on the surface and relatively uniform in size. Growth profile of *E.coli* and *S.aureus* were curved by plotting absorbance (600nm) of inculcated solutions as a function of time in contact with LDPE film (control) and nanocomposite films and fitting according to modified Gomertz equation (Eq.1). The results indicated that a modified Gompertz equation (Eq.4) was fitted to all experimental absorbance data. The R^2(adj.) values ranged from 0.9766 to 0.9972 were obtained for predicted values to experimental values and the lack of fit (p value = 0.000) which measure the fitness of the model for all samples, indicating the proposed model was sufficiently accurate and significant ($p<0.05$) for describing the examining data.

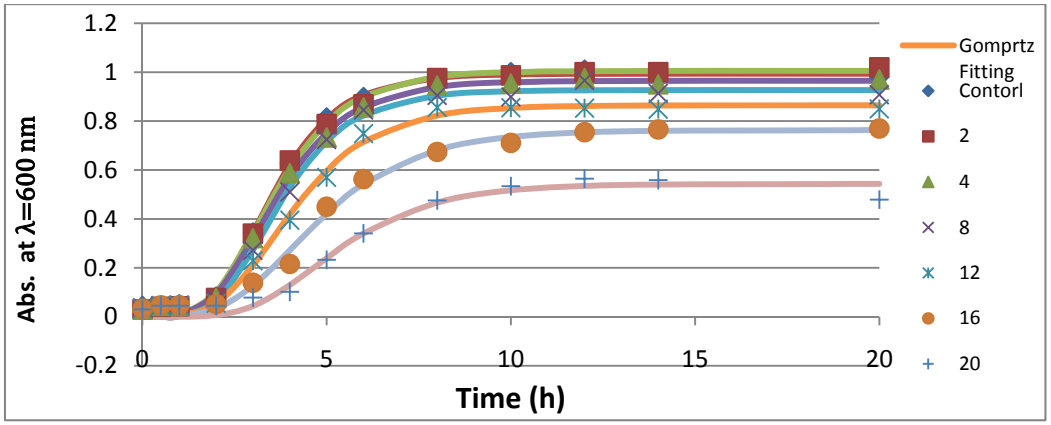

Figure 1: The growth curves result from fitting the Equation (1) to the experimental data of 20 layer by layer deposited nanocomposite for *E. coli*

20 layers LBL nanocomposite could extend lag time 52% , 12% and decrease specific growth arte 62% , 79% and reduce maximum growth rate 45%, 35% for *E. coli* and *S. aureus* respectively. More antibacterial activity for LBL deposited nanocomposite than melt blended silver nanocomposites was observed.

Conclusion

LDPE-silver nanocomposite films influenced growth parameters of *E. coli* and *S. aureus* significantly. LBL deposited nanocomposite films are more effective to inhibit growth of examined bacteria than melt blended nanocomposites. Antimicrobial efficiency of silver nanocomposites related to silver ion release from nanocomposites. LDPE-silver nanocomposites based on these findings may lead to valuable antimicrobial active packaging.

References

Appendini P. and Hotchkiss J.H. (2002) Review of antimicrobial food packaging. *Innovative Food Science & Emerging Technologies* 3, 113-126.

Damm, C. and Munstedt H. (2008) Kinetic aspects of the silver ion release from antimicrobial polyamide/silver nanocomposites. *Applied Physics* A 91, 479-486.

Damm C., Munstedt H. and Rosch A. (2008) The antimicrobial efficacy of polyamide 6/silver-nano- and microcomposites. *Materials Chemistry and Physics* 108: 61-66.

Furno F., Morley K. and Morley K.S. (2004) Silver nanoparticles and polymeric medical devices: a new approach to prevention of infection. *Journal of Antimicrobial Chemotherapy* 54, 1019-1024.

Han J., Castell-Perez M.E. and Moreira R.G. (2007) The influence of electron beam irradiation of antimicrobial-coated LDPE/polyamide films on antimicrobial activity and film properties. *LWT-Food Science and Technology* 40: 1545-1554.

Kim J. S., Kuk E., et al. (2007). Antimicrobial effects of silver nanoparticles. *Nanomedicine* 3: 95-101.

Li, J. X., Wang J., Shen L.R., Xu Z.J. Li P., Wan G.J. and Huang N. (2007) The influence of polyethylene terephthalate surfaces modified by silver ion implantation on bacterial adhesion behavior. *Surface & Coating Technology* 201, 8155-8159.

Marini M., De Niederhausern S., Iseppi R., Bondi M., Sabia C., Toselli M. and Pilati F. (2007) Antibacterial activity of plastics coated with silver-doped organic-inorganic hybrid coatings prepared by sol-gel processes. *Biomacromolecules* 8, 1246- 1254.

Nobile M.A.D., Cannarsi M., Altieri C., Sinigaglia M., Favia P., Iacoviello G. and D'Agostino R. (2004) Effect of Ag-containing Nano-composite Active Packaging System on Survival of *Alicyclobacillus acidoterrestris. Journal of Food Science* 9, 379-383.

Shameli K., Bin Ahmad M., Yunus W.M.Z.W., Ibrahim N.A., Rahman R.A., Jokar M. and Darroudi M. (2010) Silver/poly (lactic acid) nanocomposites: preparation, characterization, and antibacterial activity. *International Journal of Nanomedicine* 5, 573 -579.

Zwietering M., Jongenberger I., Rombouts F.M. and Vantriet K. (1990). Modelling of bacterial growth curve. *Applied and Enviromental Microbiology* 56, 1875-1881.

Comparison of the kinetic data of spores obtained in different heating systems

Z. Atamer, S. Bachmann, M. Witthuhn, J. Hinrichs

Institute of Food Science and Biotechnology, Department of Dairy Science and Technology, University of Hohenheim, 70599 Stuttgart, Germany (zeynep.atamer@uni-hohenheim.de)

Abstract

Different heating systems are used in the industry for the inactivation of bacterial endospores. However, the data used for industrial processes, such as ultra high temperature heating and pasteurization, are commonly obtained from studies conducted using batch-heating systems. The aim of this study was to investigate whether there are differences in the inactivation rates of spores treated in batch-heating systems and continuous-heating systems. In order to determine the effect of the heating system on the kinetic parameters of the spores, inactivation experiments for a thermophilic strain, *Geobacillus stearothermophilus* DSM 5934, were conducted on a batch-heating system as well as on two different continuous-heating systems. As medium, in which spores were suspended during the heating process, ultrafiltration permeate (minerals and lactose) was used. In the batch-heating system, the samples were kept in small tubes (1.5 mL) that were heated with steam. Two tubular heat exchanger systems with different capacities were used as continuous-heating systems. One of these was a laboratory scale continuous-heating system, which enables high temperature short time heating up to the temperature of 132 °C (7-60 L/h), whereas the other one was a pilot scale continuous-heating system, in which temperatures up to 150 °C can be applied (100-200 L/h). In a temperature range of 115 to 135 °C, the kinetic parameters were determined. The inactivation curves of the *G. stearothermophilus* spores were obtained for each system. Lines of equal effects for a 9 log reduction were plotted using the determined kinetic parameters. Comparison of the heating systems showed that there were differences in the inactivation rates. Inactivation was found to be the slowest in the batch-heating system. The results will be discussed concerning the applied kinetic model as well as regarding limitations in applying the kinetic data obtained from one type of heating system in another type of heating system.

Keywords: *heating systems, spores, Geobacillus stearothermophilus, kinetic parameters*

Introduction

Microbiological spoilage of milk and dairy products is often linked with the detection of endospores from genera *Bacillus* and *Geobacillus*. The resistance of bacterial endospores against heat, chemicals and dryness is very high. To manufacture “commercially sterile” products, meanwhile UHT (ultra high temperature) treatment of the food is commonly used in dairy industry. In 1995, heat resistant spores (HRS) were found for the first time in UHT treated milk from Italy and Austria (Hammer *et al.* 1995). Thermophilic sporulating bacteria present in the spoiled milk were detected in silage feed of milk cows. Although they are not dangerous for health, under appropriate nutrient conditions they may germinate, which activates enzyme production and acid formation. This leads to “off-flavour” in food (Chen *et al.* 2004). To prevent acute defects and to avoid prospective spoilage of UHT milk, better understanding of the inactivation of thermophilic spores is necessary.

Thermal inactivation of spores has been investigated using different heating systems. Lab scale batch-heating systems are often used for determining kinetic data. Most of the available data were determined on this convenient way (e.g., Behringer 1989; Horak 1980; Iciek *et al*, 2006). However, in practice often continuous systems for heating of milk are used (e.g., direct or indirect UHT heating). The kinetic data obtained from batch systems are directly applied in continuous processes, although various investigations reported differences between the inactivation of spores by means of batch- and continuous-heating systems (Burton *et al.* 1977; Dogan *et al.* 2009; Fairchild *et al.* 1994; Wescott *et al.* 1995).

In this work, the kinetic parameters, the activation energy (E_a) and the reaction rate constant (k) of *Geobacillus stearothermophilus* spores for a reaction order of 1 using three different heating systems were determined. One batch-heating system, which is assembled in the Dairy for Research and Training at the University of Hohenheim, and two continuous-heating systems, one located at Tetra Holdings GmbH in Stuttgart and the other is in the Dairy for Research and Training at the University of Hohenheim, were used. The obtained kinetic data from each heating system were compared to each other and the inactivation effect by means of batch- and continuous-heating system was discussed.

Materials and Methods

Suspension medium for the heat treatments

Sweet whey ultrafiltration (UF) permeate powder (Bayolan PT, Bayerische Milchindustrie eG, Landshut, Germany) was solved in water and used as heating medium.

Preparation of spore suspension

Freeze-dried cells of *G. stearothermophilus* were purchased at DSMZ (Braunschweig, Germany). Cells were revitalized in St-I-NB (Standard Nutrient Broth 1, Merck KGaA, Darmstadt, Germany) at 55°C. Petri dishes (Ø 140 mm) were filled with sporulation medium (5.0 g L^{-1} peptone from casein, 3.0 g L^{-1} meat extract, 20.0 g L^{-1} agar-agar, 1.0 g L^{-1} KCl, 0.12 g L^{-1} $MgSO_4*H_2O$, 1.0 mL L^{-1} 1 M $Ca(NO_3)_2*4H_2O$, 1.0 mL L^{-1} 0.01 M $MnCl_2*4H_2O$, 1.0 mL L^{-1}, 1 mM $FeSO_4*7H_2O$ were added). The agar plates were inoculated with 0.5 mL of overnight bacterial suspension and then incubated at 55°C for one week. After sporulation of about 80% of the vegetative cells, the petri dishes were harvested with sterile, cold water (4°C). Washing of the spores was performed four times while keeping the temperature at 4°C. For elimination of vegetative cells, the spore suspension was pasteurized at 80°C for 20 min. The prepared spores were suspended in 70% ethanol and stored at 4°C. The concentration of the spore suspension was approximately 10^7 cfu mL^{-1}.

Heating systems

Batch system: The batch heating system is built up based upon the system described by Behringer (1989). For the experiments small stainless steel tubes were filled with 1.4 mL of UF permeate and 0.1 mL of spore suspension. The initial spore concentration (C_0 in cfu mL^{-1}) was log C_0 = 7.3. Saturated steam for the heating of the medium and ice-water for the cooling were used. Continuous system in Tetra Pak: For determination of kinetic parameters under small-scale conditions, a continuous-heating system at Tetra Holdings GmbH in Stuttgart was used. This system (7 – 60 L h^{-1}) is built up with KERSYS Mediker modules (hde Metallwerke Menden GmbH, Germany). In the modules the liquid is transferred through several coiled capillary tubes. Secondary flow in the coiled tubes leads to Dean-swirls, which increase the heat transfer and mixing. The heating medium used was saturated steam up to 3 bars, and the cooling medium was cold water. Holding times varying from 1 to 30 s and temperatures up to 130 °C were used. On each day of testing, the cooled UF permeate was inoculated with spore suspension (log C_0 = 5.2). Continuous system in the Dairy for Research and Training (Hohenheim): A second continuous-heating system (Asepto GmbH, Germany) located at the Dairy for Research and Training in Hohenheim was used for this study. Heating temperatures up to 150 °C and holding times of 2 to 256 s can be performed. The trials were carried out with a flow rate of 150 L/h. UF permeate was inoculated with *G. stearothermophilus* spores having a final concentration of log C_0 = 5.1.

Determination of colony count

The colony count of the samples was assessed before and after heating. The samples were diluted in Ringer's solution and then dilutions were inoculated on Nutrient Agar using spread plate technique (Bast 2001).

Calculation of kinetic parameters

The colony counts determined in the experiments were used for the calculation of the kinetic parameters E_a, k_{ref} for a reaction order of 1 according to Eq. (1) (Dogan *et al.* 2009).

$$\frac{C_t}{C_0} = \exp\left(-k_{ref} \cdot \exp\left[-\frac{E_a}{R} \cdot \left(\frac{1}{T} - \frac{1}{T_{ref}}\right) \cdot t\right]\right) \quad \text{for n = 1} \qquad (1)$$

C_t: spore concentration at time t [cfu mL^{-1}]; C_0: initial spore concentration [cfu mL^{-1}]; k_{ref}: reaction rate constant at reference temperature 394 K [s^{-1}]; E_a: activation energy [J mol^{-1}]; R: universal gas constant (= 8.314 J mol^{-1} K^{-1}); t: holding time [s]; T: absolute temperature [K]; T_{ref}: reference temperature = 394 K

Results and Discussion

In total, 22 experiments with *G. stearothermophilus* spores were performed in the batch-heating system at 120, 125 and 130 °C. The initial spore concentration was log C_0 = 7.3±0.05. The curves of inactivation of the spores are shown in Fig. 1.

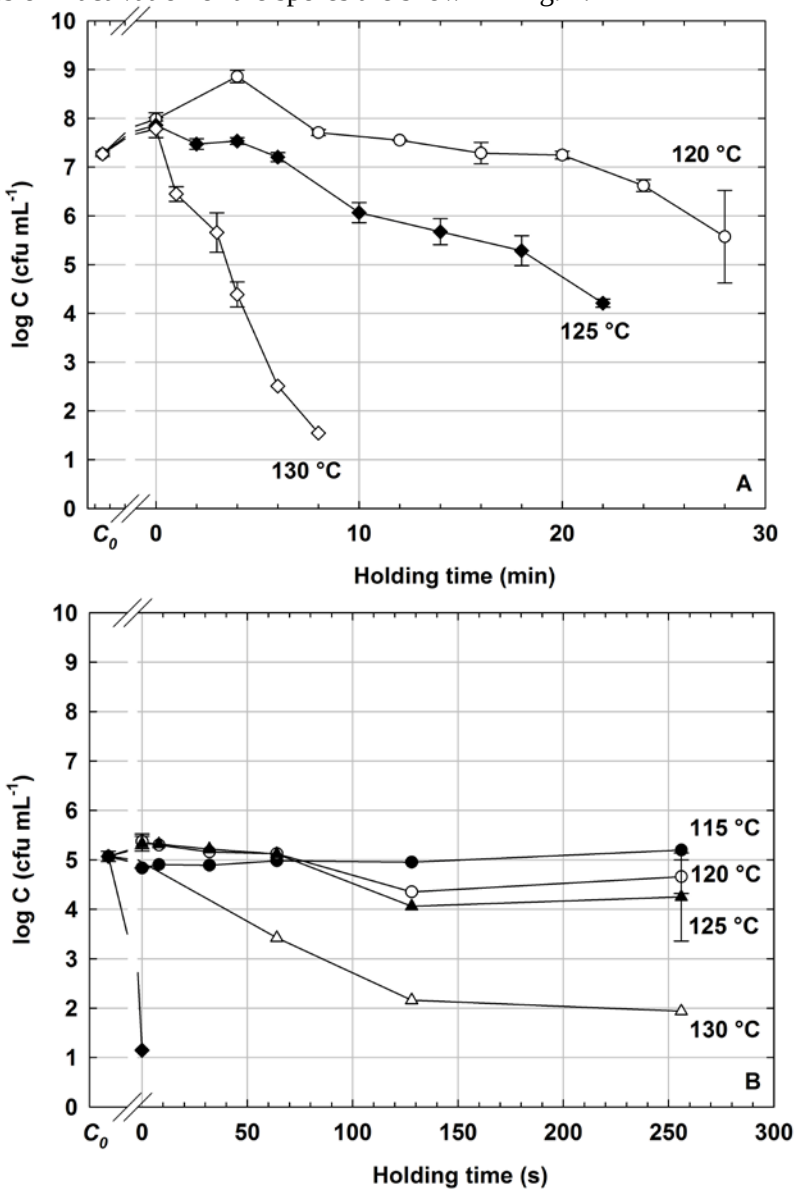

Figure 1: Thermal inactivation of *G. stearothermophilus* spores in batch-heating (A) and continuous-heating (B) system (in the Dairy for Research and Training in Hohenheim).

The inactivation of the spores runs nearly linear except the one at 120 °C, where the inactivation was preceded with a clear increase of the spore concentration (shoulder behaviour). The inactivation of spores of *G. stearothermophilus* in the continuous-heating system in Tetra Pak was performed at 120, 125 and 130 °C (data not shown). The initial spore concentration was log C_0 = 5.2±0.12. Temperatures at 115, 120, 125, 130 and 135 °C were applied for the experiments in the continuous system in the Dairy for Research and Training. In both batch and continuous system, 9-log inactivation lines of *G. stearothermophilus* at 121 °C were calculated using the obtained kinetic data, in order to compare the systems. According to the calculated values, application of a UHT process would not provide a 9-log reduction of spores.

Conclusions

In this study, the heat resistance of *G. stearothermophilus* spores was investigated. The heat resistance was characterized by the activation energy (E_a) and the reaction rate constant (k). Heating experiments were performed in a batch-heating system and two continuous-heating systems having different capacities. A slower inactivation of the spores was found in the batch-heating system. However, the fastest inactivation of the spores was observed at the continuous lab-scale system in Tetra Pak. Activation of spores at the beginning of the inactivation (shoulder effect) was observed.

Collection of the temperature data during heating and cooling stages has to be improved in the continuous-heating systems. The heat transfer of the double-pipe heat exchanger and the capillary tube heat exchanger in the two continuous-heating systems is affected through the mass flow of heating medium (e.g., water, saturated water). The determination of this mass flow may help to gain the actual temperature profiles in the systems. Using the actual temperature profiles during the heating process, the observed difference between the systems can be explained.

Acknowledgements

This work was supported by Tetra Holding GmbH, Stuttgart-Vaihingen (Germany).

References

Bast E. (2001) Mikrobiologische Methoden. Spektrum Akademischer Verlag GmbH, Heidelberg.

Behringer R. (1989) *Über das Absterbeverhalten von Bacillus-Sporen in Milch und Milchkonzentraten*, Dissertation, Technische Universität München.

Burton H., Perkin A., Davies F. and Underwood H. (1977) Thermal death kinetics of *Bacillus stearothermophilus* spores at ultra high temperatures *Journal of Food Technology* 12, 149-161.

Chen L., Coolbear T. and Daniel R. (2004) Characteristics of proteinases and lipases produced by seven *Bacillus sp*. isolated from milk powder production lines. *International Dairy Journal* 14, 495-504.

Dogan Z., Weidendorfer K., Müller-Merbach M., Lembke F.,and Hinrichs J. (2009) Inactivation kinetics of *Bacillus* spores in batch- and continuous-heating systems *LWT – Food Science and Technology* 42, 81-86.

Fairchild T., Swartzel K., and Foegeding P. (1994) Inactivation kinetics of *Listeria inocua* in skim milk in a continuous flow processing system *Journal of Food Science* 59 (5), 960-963.

Hammer P., Lembke F., Suhren G. and Heeschen W. (1995) Characterization of a heat resistant mesophilic *Bacillus* species affecting quality of UHT-milk – a preliminary report *Kieler Milchwirtschaftliche Forschungsberichte* 47 (4), 303-311.

Horak F. (1980) *Über die Reaktionskinetik der Sporenabtötung und chemischer Veränderungen bei der thermischen Haltbarmachung von Milch zur Optimierung von Erhitzungsverfahren*, Dissertation, Technische Universität München.

Iciek J., Papiewska A. and Molska M. (2006) Inactivation of *Bacillus stearothermophilus* spores during thermal processing *Journal of Food Engineering* 77 (3), 406-410.

Wescott G., Fairchild T. and Foegeding P. (1995) *Bacillus cereus* and *Bacillus stearothermophilus* spore inactivation in batch and continuous flow systems *Journal of Food Science* 60 (3), 446-450.

From laboratory inactivation experiments in static conditions to spore reduction at ultra-high temperature processing

M. Witthuhn[1], O. Couvert[2,3], Z. Atamer[1], J. Hinrichs[1], L. Coroller[2,3]

[1]Universität Hohenheim, Institute of Food Science and Biotechnology, Department of Dairy Science and Technology, Garbenstr. 21, D-70599 Stuttgart, Germany (Marina.Witthuhn@uni-hohenheim.de)
[2]Université Européenne de Bretagne, France
[3] Université de Brest, EA3882, Laboratoire Universitaire de Biodiversité et Ecologie Microbienne, IFR148 ScInBioS, UMT 08.3 PHYSI'Opt, 6 rue de l'Université, F-29334 Quimper, France (Louis.Coroller@univ-brest.fr)

Abstract

When dairy products are processed at ultra-high temperatures, a sufficient log reduction of the bacterial spore flora has to be achieved to ensure product quality during shelf-life. However, prediction of the inactivation behavior of the spores at the applied high temperatures is difficult. There is a need for a tool that describes the inactivation effects correctly at continuous ultra-high temperature processing for an industrial scale. Therefore, the objective of this study was to provide a model which is able to predict the inactivation at ultra-high temperatures based on laboratory experiments in static conditions.
Two data sets for the inactivation of a *Bacillus amyloliquefaciens*-strain isolated from a dairy product using the capillary method (static temperature conditions) and a batch method (dynamic temperature conditions) were acquired. The static and dynamic conditions were studied from 95 to 125 °C and 105 to 140 °C, respectively. Eight different primary models (influence of time) covering linear or non-linear shapes, and their corresponding secondary models (influence of temperature), were adjusted to the data from static conditions. The fit of the models was evaluated. The models were then used to simulate the inactivation of the spores at the dynamic temperature conditions.
Primary models covering sigmoidal shapes of the inactivation curves provided the best fit in static conditions (capillary system). At the secondary level, it was observed that models having only a few adjustable parameters at the primary level showed a better fit. The simulations for three of the eight models at the studied dynamic temperature conditions revealed that the models were able to describe the inactivation at low temperatures. Above 130°C, the three models failed to predict the inactivation. Changes in the shapes of the inactivation curves and an over-estimation of the temperature effect at high temperature ranges can be the reasons for the loss of accuracy.

Keywords: Bacillus spores, ultra-high temperature processing, microbial inactivation models, dairy products

Introduction

Bacterial spores are present in raw milk and they are able to survive the ultra-high temperature treatment of milk. For this reason, it is important to choose the correct temperature-time conditions for the UHT treatment in order to obtain a safe product with the least deterioration of the nutritional value. The challenge in predicting the inactivation behavior at ultra-high temperatures is mainly due to the difficulties in acquiring the inactivation kinetics. Thus, inactivation kinetics are usually determined at low temperatures and extrapolated into the desired temperature range. The usage of a heating system which allows the continuous determination of the temperature could help here. Nonetheless, the available data for the inactivation of spores of importance for dairies were often acquired at static temperature conditions (e.g., Iciek *et al.* 2006). The applied methods are easy to handle and do not require a lot of equipment, but, on the other hand, they do not include the examination of ultra-high temperatures. Therefore, there is a need to verify that inactivation parameters determined with the help of data from static temperature experiments predict the inactivation at continuous ultra-high temperature processes correctly.

An important aspect of modeling the thermal inactivation in UHT regions is that the applied model describes the inactivation kinetics for a wide temperature range. In this study, eight different primary models (effect of time) and their corresponding secondary models (effect of temperature) were investigated. The aim of this study was to find a model which predicts the inactivation of spores at ultra-high temperature processing (dynamic temperature conditions) based on the data from static conditions.

Materials and Methods

Test strain, spore production and thermal inactivation experiments

A *Bacillus amyloliquefaciens*-strain, previously isolated from a dairy product, was obtained from the Department of Food Microbiology (Technical University of Munich). For the spore production, *B. amyloliquefaciens* was incubated at 30 °C in Brain Heart Infusion (BHI) broth supplemented with vitamin B_{12}, streak-plated on BHI agar and incubated in broth (always for 24 h). From the cell suspension, 0.5 mL were plated on sporulation agar (composition: Dogan *et al.* (2009); 1 mL of 0.1 mol L^{-1} $MnCl_2$ were added) and incubated at 30 °C for 4 days. After harvesting the spore crop with phosphate buffer (0.01 mol L^{-1}; pH 7.2), the cells were centrifuged 4 times at 2218 x g for 7 min (2 °C), pasteurized (80 °C, 10 min), and washed. Ethanol was added (final concentration: 35 %). After 2 days, the ethanol was removed by washing. Two heating systems were used. For static temperature conditions, a capillary method (volume: 0.1 mL) described by Couvert *et al.* (2005) was applied. For dynamic temperature conditions, a batch-heating system (volume: 1.5 mL) described by Dogan *et al.* (2009) was utilized. Very short holding times with important come-up and cooling times were also realized. The spores were heated in ultrafiltration permeate of bovine milk as a model solution for milk. The initial spore count was app. 10^8 cfu mL^{-1}. Ringer solution for dilutions and CASO agar as recovery medium (4 days, 30 °C) were used.

Microbial inactivation models, model fitting and model selection

The evaluated inactivation models are listed in Table 1. The models were fitted to the data by minimizing the sum of squared errors (nlinfit function, MATLAB R2010a, The Mathworks, Natick, USA). Either overall (one parameter for all kinetics) or variable parameters (one parameter per kinetic) were calculated. The fit of the different primary models was evaluated by calculating the Akaike information criterion (AIC; Akaike 1973), the residual sum of squares (RSS), the root mean square error (RSME), and by performing an analysis of the residuals using hypothesis tests on the normality (lillietest hypothesis test, MATLAB), the homoscedasticity (archtest hypothesis test, MATLAB) and the autocorrelation (lbqtest hypothesis test, MATLAB). The fit of the secondary models was evaluated with the aid of the AIC and the hypothesis tests.

Table 1: Microbial inactivation models

Model	Primary	Secondary	Source	Remarks
1	First-order: *D*-value	*z*-value	e.g., Mafart *et al.* 2010	Log-linear
2	First-order reaction	Arrhenius	e.g., Mafart *et al.* 2010	Log-linear
3	n-order reaction	Arrhenius	Müller-M. *et al.* 2005	Overall[b] n
4	Weibull	Log-logistic	Peleg *et al.* 2008	Overall[b] n^a
5	Weibull	*z*-value	Mafart *et al.* 2002	Overall[b] p^a
6	Weibull	*z*-value	Mafart *et al.* 2002	Variable[c] p^a
7	Geeraerd	*z*-value	Geeraerd *et al.* 2000	Variable[c] parameters
8	Mixed Weibull	*z*-value	Coroller *et al.* 2006	Overall[b] p^a, N_0, α

[a]same shape factor; [b]one parameter for all kinetics; [c]one parameter per kinetic

Simulation of the inactivation at dynamic temperature conditions

Three selected models (1, 5 and 8) were used to simulate the inactivation for the dynamic temperature profiles recorded during the inactivation experiments with the batch-heating system. Predicted inactivation curves were compared to experimentally observed spore counts.

Results and Discussion

Thermal inactivation experiments

At static temperature conditions, the *B. amyloliquefaciens*-spores were inactivated for 5 log in 480 min at 95 °C, whereas at 125 °C, a reduction of 6 log was achieved in less than 1 min. At temperatures up to 105 °C, the inactivation curves showed a shoulder which did not appear at higher temperatures. At dynamic temperature conditions, a shoulder was also apparent at 105 °C (Figure 1). Above 110 °C, the shape of the inactivation curve changed. A tail was observed. At 140 °C, after a holding time of 5 s, the spores were inactivated for 7.5 log.

Assessment of model adequacy and model selection

The primary models were fitted to the data from the capillary method. The results for the primary model fit are shown in Table 2. With the results for the primary model, the secondary models were fitted. The results for the evaluation of the fit are shown in Table 3. The best fit to the data was obtained with the models covering sigmoidal shapes of the survival curves (models 7 and 8; Table 2). Concerning the simpler models, the Weibull model with a variable parameter *p* yielded the best result. For the secondary models, the models having only few variable parameters at the primary level showed a better fit (Table 2). Based on these results, model 8 was selected. Model 7 was not chosen for the simulations because this model assumes that a level N_{res} of resistant spores exists. The inactivation curve approaches this level only asymptotically. Thus, the extrapolation to higher temperatures is critical. Additionally, models 1 and 5 were chosen to cover a linear and a simple Weibull model.

Table 2: Fit of the primary models to the data obtained with the capillary method

	Model (no. of variable/overall estimated parameters)							
	1 (2/0)	2 (2/0)	3 (2/1)	4 (2/1)	5 (2/1)	6 (3/0)	7 (4/0)	8 (2/3)
AIC	176.24	176.24	176.88	170.72	170.72	175.38	151.97	**124.78**
RSS	29.19	29.19	28.31	24.67	24.67	16.74	**5.80**	8.08
RSME	0.53	0.53	0.52	0.49	0.49	0.40	**0.24**	0.28
Hypothesis tests[a]	10/13	10/13	**11/13**	10/13	9/13	**11/13**	10/13	9/13

[a]0/13 indicates that the model was accepted for none of the temperatures and 13/13 indicates that is was accepted for all the examined temperatures. Bold values indicate the best results.

Table 3: Fit of the secondary models to the data obtained with the capillary method

	Model (no. of parameters)								
	1 (2)	2 (2)	3 (2)	4 (2)	5 (2)	6 (2)	7 (2)	8[a] (2)	8[b](2)
AIC	45.10	41.51	54.69	58.53	42.69	50.65	75.02	40.99	42.78
Hypothesis tests[c]	acc.	acc.	rej.	rej.	acc.	acc.	rej.	acc.	acc.

[a]Fit for δ_1. [b]Fit for δ_2. [c]acc.: Model was accepted, rej.: Model was rejected.

Prediction of inactivation at ultra-high temperatures

The inactivation at dynamic temperature conditions was simulated with selected models (1, 5 and 8). The used temperatures profiles were recorded during the experiments conducted with the batch-heating system. The results for the comparison of the survival curves are shown in Figure 1. For the temperature range (105 – 125 °C) examined in both systems, the models mostly underestimated the inactivation. At temperatures ≥ 130 °C, they overestimated the inactivation. The model that predicted spore counts closest to the observed spore counts at high temperatures was model 1 (first-order). In this study, irrespective the model, the extrapolation of the inactivation to experimentally non-examined temperature ranges resulted in an underestimation of the survivor counts. The best result was obtained with a log-linear model.

Conclusions

With the chosen method, it was possible to assess the model adequacy and therefore to select the models for the simulations. Two conclusions can be drawn from the simulations for

dynamic temperature profiles: (1) Ultra-high temperatures have to be examined to design safe processes and (2) a simple model that does not describe well the inactivation curves can nevertheless provide the most robust predictions for industrial processing. Changes in the shapes of the inactivation curves with increasing temperature and an over-estimation of the temperature effect at high temperature ranges can be the reasons for the loss of accuracy. Studies need to be continued to improve the predictions at ultra-high temperatures.

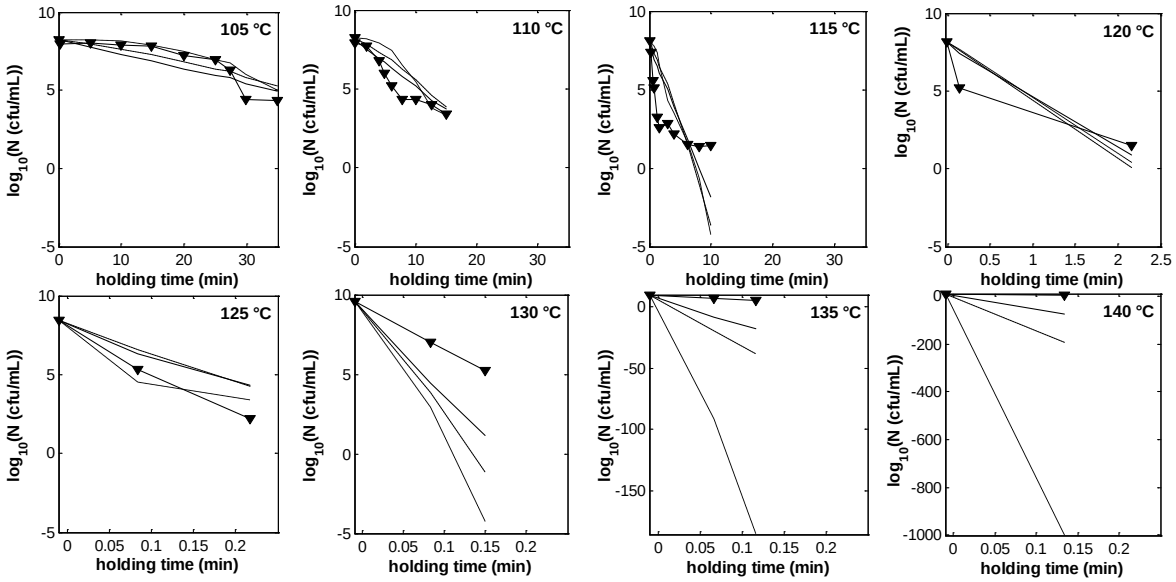

Figure 1: Predicted and observed survival curves for the dynamic temperature conditions. ▼: observed spore count, ─: model 1, ---: model 5, ···: model 8.

Acknowledgements

This research project is supported by the FEI (Forschungskreis der Ernährungsindustrie e.V., Bonn), the AiF and the Ministry of Economics and Technology (Project No.: AiF 16012 N).

References

Akaike H. (1973) Information theory and extension of the maximum likelihood principle. In: B.N. Petrov and F. Czáki (Eds.), *Proceedings of the 2nd International Symposium of Information Theory*, p. 267–281, Akadémiai Kiadó, Budapest, Hungary, 451 pp.

Coroller L., Leguerinel I., Mettler E., Savy N. and Mafart P. (2006) General model, based on two mixed weibull distributions of bacterial resistance, for describing various shapes of inactivation curves. *Applied and Environmental Microbiology* 72 (10), 6493-6502.

Couvert O., Gaillard S., Savy N., Mafart P. and Leguérinel I. (2005) Survival curves of heated bacterial spores: effect of environmental factors on Weibull parameters. *International Journal of Food Microbiology* 101 (1), 73-81.

Dogan Z., Weidendorfer K., Müller-Merbach M., Lembke F. and Hinrichs J. (2009) Inactivation kinetics of *Bacillus* spores in batch- and continuous-heating systems. *LWT - Food Science and Technology* 42 (1), 81-86.

Geeraerd A.H., Herremans C.H. and Van Impe J.F. (2000) Structural model requirements to describe microbial inactivation during a mild heat treatment. *International Journal of Food Microbiology* 59 (3), 185-209.

Iciek J., Papiewska A. and Molska M. (2006) Inactivation of *Bacillus stearothermophilus* spores during thermal processing. *Journal of Food Engineering* 77 (3), 406-410.

Mafart P., Couvert O., Gaillard S. and Leguerinel I. (2002) On calculating sterility in thermal preservation methods: Application of the Weibull frequency distribution model. *International Journal of Food Microbiology* 72 (1-2), 107-113.

Mafart P., Leguérinel I., Couvert O. and Coroller L. (2010) Quantification of spore resistance for assessment and optimization of heating processes: A never-ending story. *Food Microbiology* 27 (5), 568-572.

Müller-Merbach M., Neve H. and Hinrichs J. (2005) Kinetics of the thermal inactivation of the *Lactococcus lactis* bacteriophage P008. Journal of Dairy Research 72 (3), 281-286.

Peleg M., Normand M.D., Corradini M.G., Van Asselt A.J., De Jong P. and Ter Steeg P.F. (2008) Estimating the heat resistance parameters of bacterial spores from their survival ratios at the end of UHT and other heat treatments. *Critical Reviews in Food Science and Nutrition* 48 (7), 634-648.

Effect of heat treatment and recovery conditions on the inactivation of *Salmonella* Enteritidis

M. Munoz-Cuevas, A. Metris, J. Baranyi

Institute of Food Research, Norwich Research Park, Norwich, United Kingdom (jozsef.baranyi@bbsrc.ac.uk

Abstract

We evaluated the effect of NaCl concentrations of the heating and recovery media on the probability of post-treatment growth of *Salmonella* Enteritidis. A stationary phase culture was treated at 60°C in broth with NaCl concentrations ranging from 0 to 9%. The surviving cells were subsequently grown in media with concentrations between 0 and 9% of NaCl. The addition of NaCl to the heating medium had no significant effect on the D value, while at higher salt concentrations, its addition to the recovery medium reduced the number of recoverable cells.

We developed a model for the probability of regrowth as a function of the heating time and the recovery medium. The results were tested using the model of Koutsoumanis et al., 2004 (*Journal of Food Protection*, 67, (1), 53–59).

Keywords: *Salmonella, heat treatment, salt, recovery, probability of growth*

Introduction

Salmonella enterica serovar Enteritidis is the cause of a worldwide increase in human salmonellosis. During the last three decades *Salmonella* Enteritidis was involved in a number of food poisoning outbreaks mainly associated with the consumption of meats and egg products. In recent years there has been an increase in consumer demand for fresh, minimally processed foods, but foodborne disease linked to ready-to-eat food has also increased. Several recent studies have described outbreaks of *S. enterica*, associated with ready-to-eat products in EU and USA (Nygard *et al*. 2008; Pakalniskiene *et al*. 2006; Gupta *et al*. 2007; Crook *et al*. 2003; Pezzoli *et al*. 2007). The Commission Regulation (EC) No. 2073/2005 and No. 1441/2007 on microbiological criteria for foodstuffs has established a series of food safety rules for ready to eat products. An increased interest in "hurdle technology" has been observed because of the increased market demand for minimally processed foods. Hurdle technology employs the combinations of various antibacterial treatments to limit the growth of spoilage bacteria, improving the microbial safety and maintaining the sensory and nutritional quality of food. Among these hurdles, mild heat treatment, low temperature, water activity, acidity, etc have been used for centuries. However, these treatments could leave cells damaged, but not inactivated, so they may be able to grow in favourable environmental conditions. Factors such as temperature of incubation and culture medium influence the capacity of cells to repair heat damage.

The objective of this study was to assess the effects and interactions of temperature (60°C) and NaCl (from 0 to 9%) in the heating medium, on the probability of recovery of heat-injured *Salmonella* enteritidis in a culture medium supplemented with NaCl concentrations from 0 to 9 %.

Materials and Methods

Bacterial strain

The strain used in the experiments was *Salmonella enterica* subs. *enterica* serovar Enteritidis phage type 4. It was stored on tryptone soya agar (TSA) at 6 ºC. Subcultures were prepared by inoculating 5 ml of tryptone soya broth plus 0.3% yeast extract (TSYB) with a single colony. Cultures were incubated at 37°C for 24 h.

Thermal inactivation curves

Stationary phase cultures were centrifuged (3100 x g for 20 min at 4°C), and the pellets were combined and resuspended in 2 ml TSYB. Tubes, sealed with a rubber septum, and containing 10 ml of TSYB with NaCl concentrations from 0 to 9% (w/w), were used as heating media. The heat treatments were carried out in a water bath at 60°C. Tubes were submerged in the water bath to preheat, vented with a sterile needle to release pressure and then injected with 100 µl cell suspension directly into the liquid using a precision syringe fitted with a long sterile needle. After the appropriate heating time, the tubes were removed from the bath and cooled rapidly in ice water. Cooled tubes were refrigerated until ready to enumerate survivors. Appropriate dilutions of heated samples were inoculated into five tubes of each recovery medium. Recovery media consisted of TSYB containing NaCl concentrations from 0 to 9% (w/w). Tubes were incubated at 37°C, and Most Probable Number (MPN) technique was used to estimate the number of survivors. The probability of growth was calculated for various combinations of temperature of the heat treatment and salt concentration of the medium. The estimated numbers of survivors were modelled as a function of heating time and the NaCl concentrations of both the heating and recovery media.

Results and Discussion

The MPN values were collected as shown in Table 1. The effect of NaCl concentration in the heating medium was not noticeable below ca 6% level, so we abandoned the initial factorial design and concentrated on the salt concentration of the recovery medium only. We were especially interested in whether recovery is possible above 8% NaCl, if the heat treatment was also at this high NaCl concentration.

Because of the high nonlinearity of the effect of salt, we also refined the step and produced MPN estimates when both the heating and the recovery medium contained 8, 8.25, 8.5 and 8.75% NaCl.

Assuming linear kinetics and that all survivor cells are able to regrow in the optimal recovery medium (0.5 % NaCl) the difference between the log concentrations at identical time points are:

$$\log y(s) - \log y(0.5) = \log (y(s) / y(0.5)) = \log P \qquad (1)$$

where P is the fraction of cells that were able to grow at s salt concentration. In other words, the difference between the respective points of the curves in Figure 1 is the probability of regrowth for a single cell after the heat treatment considered. According to our assumption, the log P value must be 0 at the time zero, and then should decrease.

Table 1: MPN estimates of cell concentrations as a function of the heating time and NaCl concentration of recovery medium, after heating the cells at 60 °C, with 4% NaCl. See also Figure 1

Heating time at 60 °C (min)	**NaCl(%) of recovery medium**				
	0.5	**4**	**5**	**6**	**7**
0	9.52	9.89	9.69	9.23	9.11
1.5	8.69	8.52	7.52	7.11	7.11
3	7.89	7.69	7.34	6.52	5.41

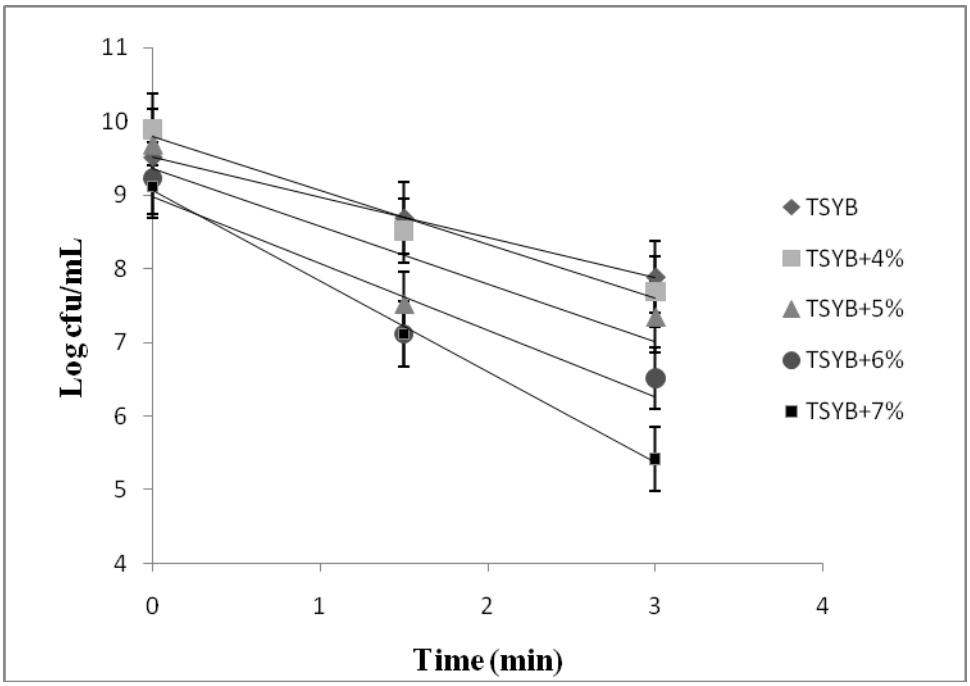

Figure 1: Effect of NaCl (%) in the recovery medium of cells treated at 60°C in TSYB with 4% NaCl.

We ran an ANOVA procedure on the log *P* values, which showed that the effect of the NaCl concentration in the heating medium was not significant ($p<0.01$). Therefore, we created a model for the log *P* values as affected by the heating time (t) and the NaCl concentration (s) of the recovery medium. Based on the features above, the form of the model is chosen as

$$\log P = -a \cdot t - (e^{b \cdot s} - 1)^n \quad (2)$$

where a and b are scaling parameters, n controls the abruptness of the curve for higher s values.

This model expresses that for small s values, the probability of growth depends only on the heating time, and then as s increases, its effect on log *P* is dramatic.

Using least squares method, the above model was fitted to all data combined and the parameter estimates were a=0.3, b=9.4, n=6.

Conclusions

The results suggest that ca 10 in a million salmonella cells are able to recover at as high as 8.75% NaCl, if the heating medium had similar level of NaCl. This demonstrates a noticeable history effect given that Koutsumanis et al (2008) found that the probability of growth for this organism was the same order of magnitude at 8% salt, where we predict recovery of more than one in a 1000 cells,

The results show that the more similar the heating and the recovery environments, the higher the chance for a cell to recover from sub-lethal heat treatments.

Acknowledgements

Marina Munoz-Cuevas was supported by Marie Curie Actions (Intra-European Fellowships, LAGSAL grant under FP7). A. Metris and J. Baranyi were funded by the Biological and

Biotechnological Research Council. We acknowledge S. George for her help with the manuscript.

References

Nygard K, Lassen J, Vold L, Andersson Y, Fisher I, Lofdahl S Threlfall, J., Luzzi, I., Peters, T., Hampton, M., Torpdahl, M., Kapperud, G., Aavitsland P. (2008) Outbreak of *Salmonella* Thompson infections linked to imported rucola lettuce. *Foodborne Pathogens and Disease* 5, 165–173.

Pakalniskiene J, Falkenhorst G, Lisby M, Madsen SB, Olsen KE, Nielsen EM, Mygh A, Boel J, Mølbak K (2006) A foodborne outbreak of enterotoxigenic *E.coli* and *Salmonella* Anatum infection after a high-school dinner in Denmark, November 2004. *Epidemiology and Infection* 6, 1–6.

Crook PD, Aguilera JF, Threlfall EJ, O'Brien SJ, Sigmundsdottir G, Wilson D. et al. (2003) A European outbreak of *Salmonella enterica* serotype Typhimurium definitive phage type 204b in 2000. Clinical Microbiology and Infection 9, 839–845.

Gupta SK, Nalluswami K, Snider C, Perch M, Balasegaram M, Burmeister D et al. (2007) Outbreak of *Salmonella* Braenderup infections associated with Roma tomatoes, northeastern United States, 2004: a useful method for subtyping exposures in field investigations. *Epidemiology and Infection* 135, 1165–1173.

Pezzoli L, Elson R, Little C, Fisher I, Yip H, Peters T et al. (2007) International outbreak of *Salmonella* Senftenberg. Euro Surveill 12: E070613–E070614

Koutsoumanis, K. P., Kendall P. A. and Sofos J. N. (2004) Modeling the boundaries of growth of *Salmonella* Typhimurium in broth as a function of temperature, water activity, and pH. *Journal of Food Protection*. 67, (1), 53–59

Koutsoumanis K. (2008) A study on the variability in the growth limits of individual cells and its effect on the behavior of microbial populations. *International Journal of Food Microbiology* 128, 116–121.

Modeling the thermochemical non-isothermal *Bacillus coagulans* spores inactivation in nutrient broth added with oregano essential oil

L.U. Haberbeck[1], C. Dannenhauer[2], B.C. Salomão[3], G.M.F. Aragão[4]

[1] Food Engineering, Department of Chemical and Food Engineering, Technological Center, UFSC, 88040-900 Florianópolis, Santa Catarina, Brazil. (lehaberbeck@gmail.com)
[2] Food Engineering, Department of Chemical and Food Engineering, Technological Center, UFSC, 88040-900 Florianópolis, Santa Catarina, Brazil. (dannenhauer@gmail.com)
[3] Food Engineering, Núcleo Tecnológico, Federal University of Rio Grande do Norte – UFRN, Lagoa Nova Natal/RN, Brazil (beatriz@eq.ufrn.br)
[4] Food Engineering, Department of Chemical and Food Engineering, Technological Center, UFSC, 88040-900 Florianópolis, Santa Catarina, Brazil. (glaucia@enq.ufsc.br)

Abstract

The objective of this work was to study a thermochemical non-isothermal inactivation of *Bacillus coagulans* spores in nutrient broth (NB) added with 400 ppm of oregano essential oil (OEO). Sealed TDT tubes were used for isothermal, with 0 and 400 ppm of OEO, and non-isothermal, with 400 ppm of OEO, resistance studies. GInaFiT (Geeraerd and Van Impe Inactivation Model Fitting Tool) was used to fit the Weibull model to the isothermal survivors curves. The program Matlab® (The MathWorks Inc, Natick, USA) was used to solve the dynamic Weibull model, proposed by Peleg (2006), by means of an ode15s solver. Temperatures profiles applied for non-isothermal studies were (1) 90/95 °C during 1 min each, up to 14 min, and (2) 95/90°C during 5 min each, up to 10 min. Weibull model presented a good fit to the isothermal inactivation data of *B. coagulans* in NB with 0 and 400 ppm of OEO. For the non-isothermal treatment, a slight overestimation of experimental data by the model was observed. The results lead to conclude that the dynamic model, based on Weibull primary model, can be used to estimate the inactivation patterns of *B. coagulans* spores under thermochemical non-isothermal heating treatments.

Keywords: *thermochemical non-isothermal inactivation, Bacillus coagulans, oregano essential oil*

Introduction

Most of the industrial heat treatment include non-isothermal heating up phases and temperature fluctuations during the process. Microbial responses under isothermal conditions may differ from the ones observed under dynamic conditions, compromising, thus, the process safety (Peleg, 2006). Traditionally, to develop a non-isothermal predictive model, for either inactivation or growth, two steps are required. First, kinetic parameters of a model describing the inactivation of microorganisms according to time, the primary model, are estimated. Afterwards, the influence of temperature on the inactivation primary parameters is described by secondary models. Finally, primary and secondary models are used to simulate microorganism inactivation under dynamic temperature conditions. To validate the dynamic model obtained, experimental data are compared to model prediction (Valdramidis *et al*. 2008).

Bacillus coagulans is an important food spoilage microorganism. This thermotolerant spore-forming bacteria is able to germinate at pH values as low as 4, so it is often isolated from acid canned vegetables (Lucas *et al*. 2006).

OEO has had its antimicrobial activities tested against a wide range of microorganisms inoculated in food products (Juneja *et al*. 2010). No studies describing the antimicrobial action of OEO against *B. coagulans* were found in the consulted literature.

The main objective of this work was to validate the prediction of the thermochemical inactivation of *B. coagulans* spores in NB with 400 ppm of OEO under variable temperature, using the dynamic model proposed by Peleg (2006). To achieve this goal, the inactivation curves of *B. coagulans* spores in nutrient broth with 0 and 400 ppm of OEO under different

temperatures were fitted with the Weibull model and a secondary model was used to represent the temperature dependence of inactivation parameters.

Materials and Methods

The *B. coagulans* sporulation was performed in Petri dishes containing Nutrient Agar supplemented with 5 ppm of manganese sulfate incubated over 10 days at 37 °C. The heating medium was NB adjusted to 4 °Brix and pH 4.2. The OEO was emulsified with soy lecithin. The heating medium, containing 0 ppm or 400 ppm of homogenized OEO emulsion, was inoculated with spores of *B. coagulans* with an initial concentration equal to 10^6 CFU/mL. TDT were filled with the inoculated heat medium, sealed, and then submerged into a thermostatic bath. TDT were individually removed in predetermined times and immediately cooled in an ice bath. The come-up-time for the temperature in the TDT tubes has been estimated to be 2 min. For the non-isothermal inactivation, two water baths were used; each bath at a temperature. Population density was determined by serial dilutions in 0.1% peptone water, and dilutions were pour plated in TDA. The plates were incubated at 37 °C for 48 h to determine the number of bacterial spores expressed in CFU/mL.

The isothermal inactivation, with 0 ppm were performed at 95, 97 and 100 ºC, and with 400 ppm of OEO at 90, 95, 97 and 100 °C. For the non-isothermal inactivation with 400 ppm of OEO, two different temperature profiles were studied. In profile 1 the temperature ranged from 90-95 °C every 1 minute for 13.5 minutes, and in profile 2 from 90-95 °C for 5 minutes at each temperature in a total of 10 minutes. During the experiments, temperatures were recorded every 5 seconds by thermocouples attached to a data acquisition system (Agilent System Acquisition 34970a). Weibull model (Equation 1) was fitted to experimental isothermal inactivation curves through GInaFit (Geeraerd *et al*. 2005).

$$\log\left(S(t)\right) = -bt^{\alpha} \tag{1}$$

where *S(t)* is the momentary survival ratio, *b* and α are parameters of the model and *t* is the time (min). An exponential type equation was adjusted to the experimental data of parameter *b(T)* values related to the temperature, through the software Excel (Microsoft®). The temperature profiles during non-isothermal inactivation, obtained with the data acquisition system, were described by a sinusoidal equation, as given by Equation 2, through the program Matlab® (The MathWorks Inc, Natick, USA).

$$T(t) = a_1.\sin(b_1.t + c_1) + a_2.\sin(b_2.t + c_2) + \ldots + a_8.\sin(b_8.t + c_8) \tag{2}$$

where *T(t)* is the temperature profile (°C) at time *t*, and a_i, b_i and c_i are the model parameters. The expressions *b(T)* and *T(t)*, then calculated, were combined to produce the *b[T(t)]* term for each non-isothermal profile. The program Matlab® (The MathWorks Inc, Natick, USA) was used to solve the dynamic Weibull-type model (Equation 3), proposed by Peleg (2006), by means of an ode15s solver.

$$\frac{d\log S(t)}{dt} = -b[T(t)]\alpha\left\{\frac{-\log S(t)}{b[T(t)]}\right\}^{\frac{\alpha-1}{\alpha}} \tag{3}$$

Results and Discussion

Figure 1 shows the isothermal inactivation curves of *B. coagulans* with 0 and 400 ppm of OEO, fitted by the Weibull model with a fixed α (2.98). The value of 2.98 is the mean value of α for the Weibull model with varying α, according to previous research. In Figure 1 is possible to observe that at any temperature, spore inactivation is faster with 400 ppm of OEO than without OEO (0 ppm). The temperature dependence of parameter b (b(T)) is shown in Figure 2, including the fit of the exponential equation to experimental data. The exponential equation, Equation 4 had a good fit to the experimental values of *b* as can be seen both visually and through the R^2 value next to 1.

$$b(T) = 2.10^{-29}\exp(-0.61T) \qquad R^2 = 0.972 \tag{4}$$

From the secondary and primary models, the non-isothermal model pointed by Peleg (2006) was established and validated to predict the *B. coagulans* spore thermochemical inactivation

in NB with 400 ppm of OEO under variable temperature conditions. Figure 3a shows results for the non-isothermal profile 1, and Figure 4a for profile 2. Figures 3b and 4b show the experimental temperature values and the fit of Equation 2 to them.

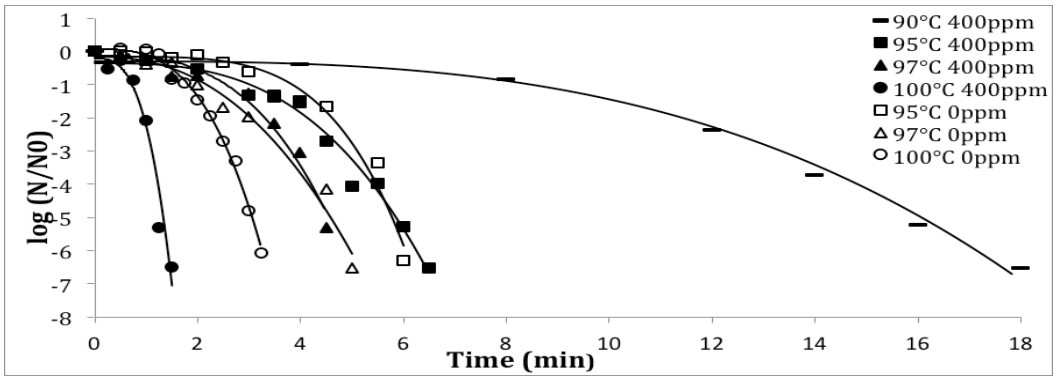

Figure 1: Experimental inactivation isothermal curves of *B. coagulans* in NB with 0 and 400 ppm of OEO at different temperatures. The continuous line represents the fit of the Weibull model with a fixed parameter α to the experimental data.

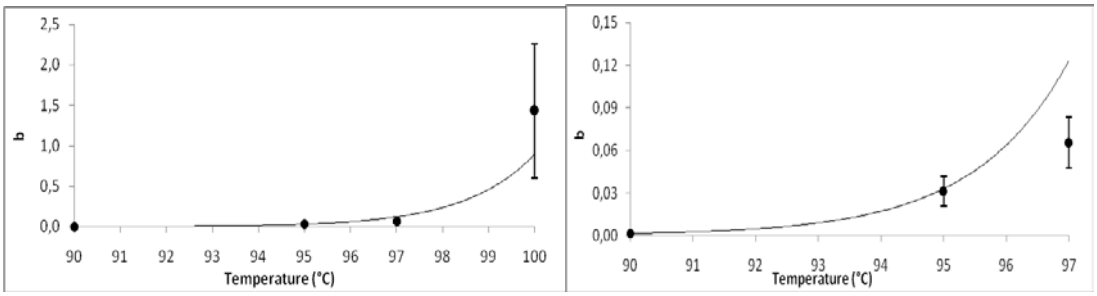

(a) (b)

Figure 2: The temperature dependence of the parameter (a) b(T) of *B. coagulans* with 400 ppm described by Equation 2; (b) re-scaled graphic (a) from temperature 90 to 97 °C.

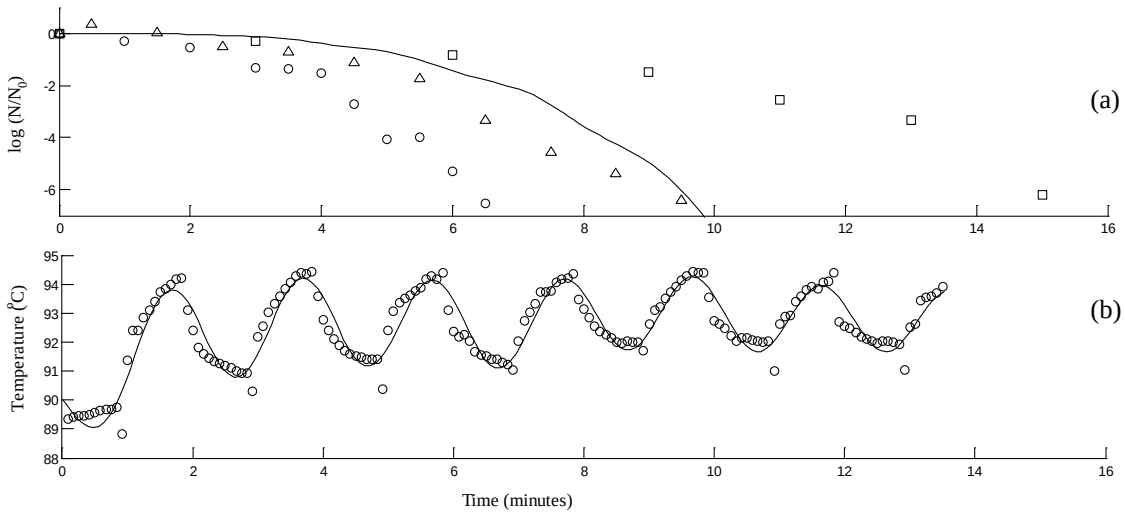

Figure 3: (a) Experimental data for isothermal inactivation at (□) 90 °C and (○) 95 °C, and for (Δ) non-isothermal inactivation of profile 1 (90-95°C/1 min). The continuous line represents the predictions of Weibull non-isothermal model to non-isothermal data. (b) Temperature profile. The continuous line represents the predictions of Equation 2, and (○) represent the experimental data.

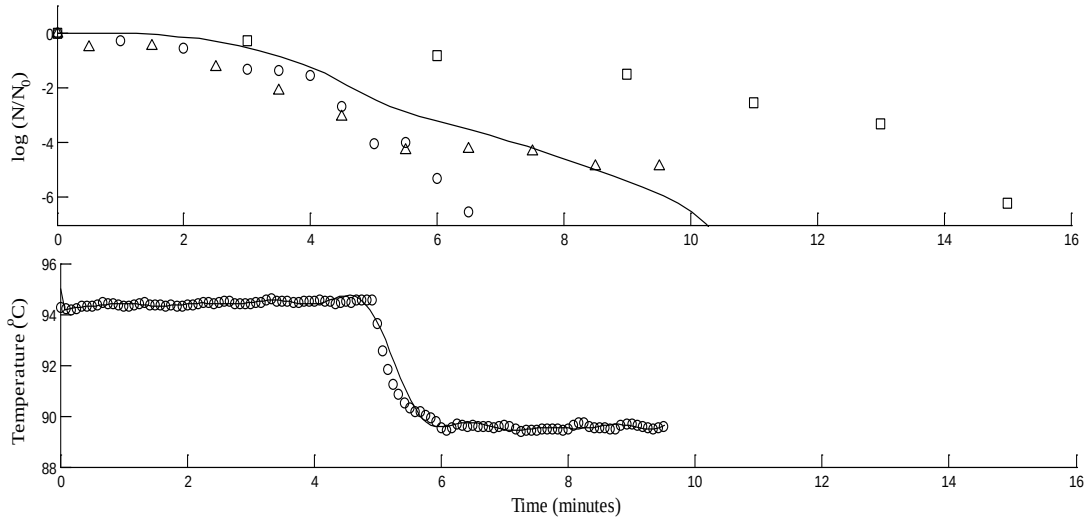

Figure 4: (a) Experimental data for isothermal inactivation at (□) 90 °C and (○) 95 °C, and for (Δ) non-isothermal inactivation of profile 2 (90-95°C/5 min). The continuous line represents the predictions of Weibull non-isothermal model to non-isothermal data. (b) Temperature profile. The continuous line represents the predictions of Equation 2, and (○) represent the experimental data.

The difference between predicted and observed inactivation values can be attributed mainly to the secondary model fit that does not describe the temperature influence on primary parameter accurately. However, Equation 4 showed a good fit to the experimental values of the parameter *b*, mainly between the temperatures used for the non-isothermal inactivation, 90 and 95 °C, as can be seen is Figure 2(b).

Conclusions

The experimental isothermal inactivation curves in Figure 1 showed that OEO enhances the sensitivity of *B. coagulans* to heat treatment, since heat treatments with 400 ppm of OEO were faster than without OEO for the tested temperatures. Although only a limited experimental database was employed for the analyses and the predicted values overestimated the observed values, the survival parameters can be used to estimate the inactivation patterns of the spores under non-isothermal heating treatments.

Acknowledgements

We would like to thanks CAPES and UFSC for the financial support.

References

Geeraerd A.H., Valdramidis V.P. and Van Impe J.F. (2005) GInaFiT, a freeware tool to assess non-log-linear microbial survivor curves. *International Journal of Food Microbiology* 102 (1), 95-105.

Juneja V.K., Hwang C.A. and Friedman M. (2010) Thermal Inactivation and Postthermal Treatment Growth during Storage of Multiple Salmonella Serotypes in Ground Beef as Affected by Sodium Lactate and Oregano Oil. *Journal of Food Science* 75 (1), M1-M6.

Lucas R., Grande M.J., Abriouel H., Maqueda M., Ben Omar N., Valdivia E., Martínez-Cañamero M. and Gálvez A. (2006) Application of the broad-spectrum bacteriocin enterocin AS-48 to inhibit *Bacillus coagulans* in canned fruit and vegetable foods. *Food and Chemical Toxicology* 44 (10), 1774-1781.

Peleg M. (2006). Advanced quantitative microbiology for foods and biosystems: models for predicting growth and inactivation. CRC Press, Boca Raton, USA, 417 pp. (ISBN : 0849336457).

Valdramidis V.P., Geeraerd A.H., Bernaerts K. and Van Impe J.F.M. (2008) Identification of non-linear microbial inactivation kinetics under dynamic conditions. *5th International Conference on Predictive Modelling in Foods* 128 (1), 146-152.

Kinetic characterisation of *Bacillus sporothermodurans* in liquid food under static and dynamic heating regimes

F. Cattani[1], S. D. Oliveira[1], C. A. S. Ferreira[1], P. M. Periago[2], M. Muñoz[2], V.P. Valdramidis[3], P. S. Fernandez[2]

[1]Laboratório de Imunologia e Microbiologia, Faculdade de Biociências, PUCRS, Brazil (fernandacattani@yahoo.com.br)
[2] Department of Food Engineering and Agricultural Machinery, Institute of Vegetable Biotechnology, Technical University of Cartagena (UPCT), P. Alfonso XIII, No. 48, 30203 Cartagena, Spain (pablo.fernandez@upct.es)
[3]UCD Biosystems Engineering, School of Agriculture, Food Science and Veterinary Medicine, University College Dublin, Dublin; Ireland (vasilis.valdramidis@ucd.ie, vvaldram@gmail.com)

Abstract

Thermal technologies have been one of the most extended processes used in commercial food manufacturing. However, its use may imply losses in the sensory and nutritional quality of the final product. Therefore it is necessary to optimize the heat treatments, so that they can ensure safe, stable foods while maintaining high standards of quality. High heat resistant, sporeforming bacteria are one of the main threats for the stability of shelf-stable, low-acid heat processed foods. At the same time they are the best indicators to establish the minimum requirements for heat processes, but in order to reduce existing heat treatments it is necessary to have precise scientific knowledge of the factors involved in their inactivation and good modelling tools.

The aim of the present work was to establish inactivation kinetics in static conditions (isothermal) in a food substrate (vegetable soup) and to perform dynamic heating profiles simulating processing conditions in the food industry collecting data at different times during processing. A thermoresistometer Mastia and spores of *Bacillus sporothermodurans* as sensor element have been used for this study. This equipment can perform non isothermal processing of foods under controlled conditions and samples can be taken at different time intervals. Results from these experiments have been modelled using a regression analysis under static and dynamic conditions similarly to the approach applied by Valdramidis *et al.* (2008). Inactivation parameters were estimated accurately and precisely by using profiles heating rates of 1.5 and 2.5^{o}C/min.

Keywords: *Thermal technologies, high heat resistant, Bacillus sporothermodurans, sporeforming*

Introduction

Bacillus spotothermodurans is characterized by the production of highly heat-resistant spores (HRS), which may survive in food processed by industrial sterilization (Hammer et al. 1995; Pettersson et al. 1996). These spores germinate during storage in UHT products causing instability due to their proteolytic activities thereby reducing the shelf life and consumer acceptability. Thermal technologies have long been at the heart of food processing. The application of heat is both an important method of preserving foods and a means of developing texture, flavour and colour. An essential issue for food manufacturers is the effective application of thermal technologies to achieve these objectives without damaging other desirable sensory and nutritional qualities in a food product (Richardson,2004).

Thermal treatments applied in the food industry have usually been calculated using microbial heat resistance data obtained under isothermal heating. Nevertheless, recent studies have shown that implementation of modelling in which parameter estimates are obtained under dynamic environments is preferable. This kind of estimated parameters give the actual values of non-isothermal estimates (Dolan 2003; Valdramidis *et al*. 2008)

The thermoresistometer Mastia enables to estimate heat resistance under isothermal and non-isothermal heating conditions as well as more complex heating profiles, like those usually applied in the food industry. Its design allows working with liquid heating media such as

buffers, liquid foods or foods containing small particles. It also allows to inoculate microorganisms or compounds and to obtain samples in order to study the changes on the quantity or the quality of these substances along with the thermal treatment. In this way, the intensity of the thermal treatments applied can be calculated and, as a consequence, the microbiological safety and nutritional quality of the food produces obtained can be estimated.
The objective of the present study was to characterize the microbial resistance of *B. sporothermodurans* spores in vegetable soup under static and dynamic temperature conditions and assess parameter accuracy and precision for designing optimal thermal process that ensure the food stability and safety.

Materials and Methods

Microorganism and spore crop preparation

B. sporothermodurans IC4 (Unilever Netherlands Sourcing Unit Oss), was isolated from Indian curry soup and was able to survive high heat treatments. The spore preparation was based on the method described by Zuijlen *et al.* (2009).
The heat resistance of the spores was determined using a thermoresistometer Mastia. The temperatures selected for isothermal experiments were 118, 121, 124, and 127 °C. Experiments were performed in triplicate for each temperature. For non-isothermal treatments, the procedure was similar, but the thermoresistometer was programmed to perform the corresponding temperature profile, and the surviving microorganisms were enumerated using Brain Heart Infusion (BHI) Media. The non-isothermal treatments for vegetable soup were run in a temperature range from 80 to a targeted 121°C at a rate of 1.5°C/min and from 75 to a targeted 121°C at a rate of 2.6 °C/min. Colonies were counted after incubation for 48 h at 37°C.

Data analysis

A global identification technique was performed for both the isothermal and the dynamic data. Based on preliminary assessment of the isothermal data the appropriate primary model appeared to be the classical log-linear. After integration of the Bigelow model in the log-linear model the following equation is obtained:

$$\frac{d\log_{10} N(t)}{dt} = -\frac{1}{D_{ref}} \cdot \exp\left(\frac{\ln 10}{z} \cdot (T - T_{ref})\right) \quad (1)$$

Herein, $\log_{10}N(t)$ represents the microbial cell density [log (cfu/ml)], D_{ref} is the decimal reduction time and z the thermal resistance constant . In the case of the dynamic temperature profiles temperature evolution T which was recorded every 5 seconds was plugged into equation 1. Linear interpolation was performed for estimating temperatures in between the recorded values.
Three different types of parameter identification approaches were applied during the regression analysis of Equation 1: (i) all isothermal data were treated at once (ii) the two dynamic experiments were studied separately (iii) the two dynamic profiles were studied together. All regression analyses were implemented by the MatLab Optimisation Toolbox (The Mathworks Inc., Natick, MA, USA). Statistical analysis included the estimation of Sum of Squared Error (SSE), Mean Squared Error (MSE), Root Mean Squared Error (RMSE), estimation of the parameters standard error and the 95% confidence interval of the estimated parameters.

Results and Discussion

Heat resistance *of B. sporothermodurans* was characterized over a wide range of temperatures (isothermal and non-isothermal treatments) in vegetable soup. Figure 1 shows survival curves of *B. sporothermodurans* IC4 under isothermal and dynamic conditions in vegetable soup for the different temperatures tested. Table 2 and Figure 1 show the results of the regression analysis.

Table 2: Parameter estimates and statistical indices of the performed parameter identification techniques

	D_{121}	SE	z	SE	SSE	MSE	RMSE
All static data	5.58	0.34	10.37	0.69	2.28	0.07	0.26
Ramp1	6.14	0.64	6.00	0.26	0.50	0.04	0.20
Ramp2	9.21	0.53	21.91	0.75	0.10	0.01	0.10
Ramp1 and 2	5.11	0.36	8.23	0.15	0.73	0.03	0.18

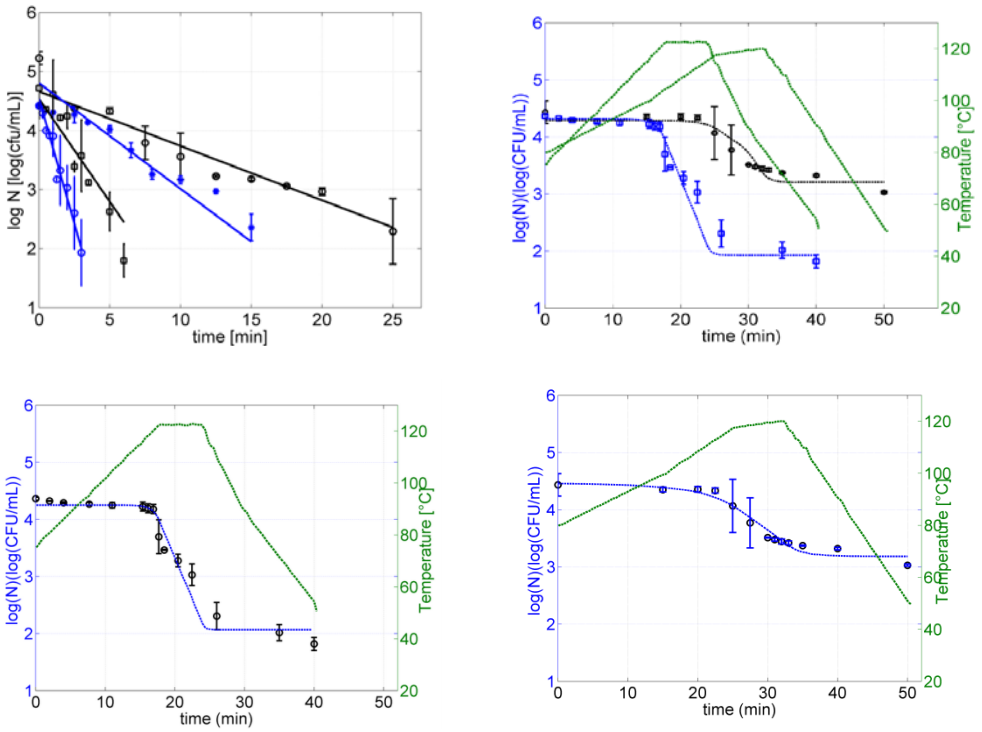

Figure 1: Example of the regression analysis of all the static data (top left), the dynamic data of ramp 1 and 2 (top right), ramp 1 (bottom left) and ramp 2 (bottom right).

Results show that accurate parameters (low SE values) and models with high statistical performance can be obtained by using dynamic profiles that are generated at realistic temperature conditions in a liquid food products. The values of the thermal resistance constant z deviated depending on the selected temperature profile. The most accurate estimates where derived when all dynamic data (ramp1 and ramp2) were used for parameter identification. Other studies have also shown that the more the microbial system is excited (in this case by temperature variations) the more the obtained information related to the microbiological responses (Valdramidis *et al.* 2008). Finally, this type of microbiological results can be generated more easily saving time and resources compared to the traditional methodology.

Conclusions

Estimated parameters varied with respect to the temperature profiles. The reason of this variation could be linked to an evolution of the thermal sensibility of bacterial spore depending on the time of the temperature profile (e.g., compare estimated parameters when

data of ramp1 or ramp2 are used) and the amount of the data (refer to the accuracy of the estimates in case that data from both ramp1 and ramp2 are used). Estimation of parameters under dynamic conditions is closer to the real processing conditions and generates a good description of the experimental results. Therefore this approach is preferable as it should produce more accurate predictions and smaller uncertainty than the traditional one-step or two step isothermal approaches.

Acknowledgements

Fernanda Cattani acknowledges Programa Capes/Fundação Carolina (Brazil) for finantial support. This project was funded by Spanish "Ministerio de Ciencia e Innovación", ref. AGL 2010-22206-C02-02/ALI and Fundación SENECA, CARM, Spain ref 08795/PI/08.

References

Dolan K. (2003). Estimation of kinetic parameters for nonisothermal food processes *Journal of Food Science* 68, 728–741

Hammer P., Lembke F., Suhren G. and Heeschen W. (1995) Characterization of a heat resistant mesophilic *Bacillus* species affecting quality of UHT-milk – a preliminary report. *Kiel Milchwirt Forschungsber* 47, 297-305.

Pettersson B., Lembke F., Hammer P., Stackebrandt E. and Priest F.G. (1996) *Bacillus sporothermodurans*, a new species producing highly heat-resistant endospores. *International Journal of Systematic Bacteriology* 46, 759-764.

Richardson S. P. (2004) Improving the thermal processing of foods. CRC Press. USA, 507 pp.

Valdramidis, V., Geeraerd, A., Bernaerts, K. and Van Impe, J. (2008) Identification of nonlinear microbial inactivation kinetics under dynamic conditions *International Journal of Food Microbiology* 128, 146-152.

van Zuijlen A., Periago, P.M., Amézquita, A., Palop, A., Brul, S. and Fernández, P.S. . (2010).Characterization of *Bacillus sporothermodurans* IC4 spores; putative indicator microorganism for optimisation of thermal processes in food sterilisation *Food Research International* b43: 1895-1901.

Modelling the survival and growth of *Salmonella* spp. in vacuum-packaged slices of RTE stuffed chicken breast as a function of temperature

A. Morales-Rueda, E. Carrasco, A. Valero, F. Pérez-Rodríguez, M.Y Rodríguez-Caturla, G.D Posadas-Izquierdo, R.M García-Gimeno and G. Zurera

Department of Bromatology and Food Technology, University of Córdoba, Córdoba, Spain (v22morua@uco.es)

Abstract

Ready-to-Eat (RTE) meat products constitute an expanding food commodity nowadays. *Salmonella* has been involved in large well-documented foodborne diseases originated by RTE meat consumption. In 2008, salmonellosis was ranked as the second foodborne illness mostly reported, accounting for 131,468 confirmed human cases in the EU. The aim of this work was to model the growth/survival of *Salmonella* spp. in vacuum-packaged slices of stuffed chicken breast stored at temperatures of 7, 11, 15 and 19ºC. A cocktail of four *Salmonella enterica subsp. enterica* strains (ATCC 13076/25928, 4391, 14028 and 13311) was inoculated in packages of vacuum-packaged slices of stuffed chicken breast at a level of ≈3 $\log_{10}$ cfu/g. Samples were stored at different temperatures (7, 11, 15 and 19ºC), and samples were periodically withdrawn for enumeration of *Salmonella* spp. For this, appropriate dilutions were spiral plated on XLD following the ISO 6579 standard method. The maximum growth rate (μ_{max}) of *Salmonella* was 0.021, 0.022, 0.059 and 0.073 $\log_{10}$ cfu/h at 7ºC, 11ºC, 15ºC and 19ºC, respectively. Maximum population densities were 5.3±0.1, 7.1±0.0, 8.8±1.1 and 8.3±0.8 $\log_{10}$ cfu/g at 7, 11, 15, and 19ºC respectively. After an initial growth, a decay of *Salmonella* was observed at each temperature studied. When *Salmonella* reached the maximum population density, the concentrations of aerobic mesophilic bacteria (AEM) were 5.4±2.8, 7.1±0.3, 8.7±0.1, and 9.5±0.4 $\log_{10}$ cfu/g at 7, 11, 15 and 19ºC, respectively. The pH values of samples varied from 6.34 to 4.87, the latter found towards the end of the experiment. The growth kinetic parameters were consistent with published data on *Salmonella* growth in poultry, and ComBase data based on growth of *Salmonella* on cooked ham and bologna. These findings underline the facultative anaerobe character of *Salmonella*, being capable of growing in vacuum conditions even at 7ºC. *Salmonella* reached high levels, being the product still acceptable from a sensorial perspective.

Keywords: *Salmonella, survival, growth, modelling, ready-to-eat meat products*

Introduction

Nowadays, supermarkets provide a wide variety of specialist foods, usually known as ready-to-eat (RTE) products. Examples of these commodities include sliced RTE meat products such as cooked stuffed chicken breast. Operations linked to slicing of RTE meat products slicing may pose a human health risk since these foods may come into contact with bacterial contaminated surfaces if proper hygiene practices are not applied. Often, these RTE products are packaged under vacuum or modified atmospheres and must be kept refrigerated before consumption in order to increase the shelf life. As this type of product does not require further treatment such as cooking, before consumption, contamination events during processing plays a major role in food-borne human diseases, including salmonellosis and other conditions linked to meat attribution. According to outbreak data (EFSA 2008), salmonellosis represents the second most reported zoonotic disease in humans in the European Union (EU), accounting for 131,468 confirmed human cases. Salmonella spp. has been responsible for causing well-documented illnesses linked to RTE meat consumption around the world (Luzzy *et al*. 2007). Kinetic processes such as growth, survival and inactivation of Salmonella have been deeply investigated in order to understand the behaviour of the pathogen under different conditions. In this sense, mathematical models of Salmonella have been developed to describe these

processes under established circumstances such as temperature during storage. The objective of this work was to model the growth/survival of Salmonella spp. in vacuum-packaged slices of stuffed chicken breast stored at temperatures of 7, 11, 15 and 19ºC.

Materials and Methods

Inoculum preparation

Four strains of *Salmonella enterica subsp. enterica* (ATCC 13076/25928, 4391, 14028 and 13311) were obtained from the Spanish Type Culture Collection (CECT, Valencia, Spain) in order to elaborate a cocktail of strains intended to be inoculated in packages of vacuum-packages slices of stuffed chicken breast. Freezed beads of the four strains were maintained at -20ºC in cryovials (Microbank™ Cryo beads; Pro-Lab Diagnostics, Canada) and then transferred to tubes containing 10 mL of Tryptone Soya Broth (TSB, Oxoid, UK) and incubated at 37ºC for 24 h. Subcultures were carried out by transferring 0.1 mL of the previous cultures to 10 mL of TSB tubes which were incubated at 37ºC for 24 h. These subcultures were performed twice and the last one was kept at 37ºC until the early stationary phase of *Salmonella* population was reached. A tube of 10 mL compounded of grown cells from the four strains was made up. Subsequently, appropriate decimal dilutions were carried out in sterile saline solution in order to obtain the desired inoculation level (≈3 $\log_{10}$ cfu/g).

Sampling microbiological analysis

Packages of RTE sliced stuffed chicken breast were collected from the industry in order to be inoculated with 0.1 mL of the cocktail above. A number of control samples packages were not inoculated in order to study the evolution natural microbial population until the end of shelf-life and to investigate the presence of *Salmonella* spp. Just after inoculation, at time 0, a control and an inoculated package of product were analyzed for the level of *Salmonella* and aerobic mesophilic bacteria. Also, pH values were measured. All samples were randomly assigned to different storage temperatures (7, 11, 15 and 19ºC) until the end of the analysis period, between 27-47 days. Periodically, samples were withdrawn and each slice (≈25 g) of product was homogenized in 225 mL of peptone water. Inoculated samples of *Salmonella* were then serially diluted and spiral plated (Eddy Jet, Barcelone, Spain) for enumeration of *Salmonella* on Xylose Lysine Deoxycholate agar (XLD) by following the ISO 6579 standard method and for enumeration of aerobic mesophilic bacteria on Plate Count Agar (PCA). Control samples were analyzed in order to investigate the presence of *Salmonella* spp.

Data modelling and model comparisons

Data growth (time *vs* concentration) for each temperature were introduced in Excel spreadsheet (Microsoft, Redmond, WA), and the growth model of Baranyi and Roberts (1994) was fitted to data with the aid of DMFit add-in (Institute of Food Research, Norwich Research Park, Norwich, UK). Maximum growth rate (μ_{max}) parameters were estimated by the model. *Salmonella* growth data in different foodstuffs taken from ComBase database (Baranyi and Tamplin 2003) and other study (Langstron *et al*. 1993), were used to compare our results.

Results and Discussion

Initial *Salmonella* concentration (at time 0, i.e. just after inoculation) on RTE sliced stuffed chicken breast was approximately 10^3 cfu/g. *Salmonella* population increased at all temperatures studied (7, 11, 15 and 19ºC). In most cases, short or no lag time evident. Maximum growth rates (μ_{max}) of *Salmonella* were 0.021, 0.022, 0.059 and 0.073 $\log_{10}$ cfu/h at 7ºC, 11ºC, 15ºC and 19ºC, respectively. Maximum population densities of *Salmonella* were 5.3±0.1, 7.1±0.0, 8.8±1.1 and 8.3±0.8 $\log_{10}$ cfu/g at 7, 11, 15, and 19ºC respectively. After growth was completed, decay was observed at all temperatures tested. When *Salmonella* reached the maximum population density, the concentrations of aerobic mesophilic bacteria (AEM) were 5.4±2.8, 7.1±0.3, 8.7±0.1 and 9.5±0.4 $\log_{10}$ cfu/g at 7, 11, 15 and 19ºC, respectively. In control samples, *Salmonella* was not detected The pH values of slices of RTE

stuffed chicken breast varied from 6.34 to 4.87, the latter found towards the end of the experiment.

Performance of microbial predictive models is commonly conducted by comparing predictions with microbial growth kinetic parameters published or obtained experimentally in different food matrices. The maximum growth rate (μ_{max}) predicted for *Salmonella* in our study was consistent when compared to others found in literature. Langston *et al*. (1993) quantified the variation of the growth rate of *Salmonella* Enteritidis within and between samples on raw chicken stored in air and modified atmosphere at abusive storage temperatures. When modelled data from Lanston *et al*. (1993) with the aid of DMFit, a μ_{max} of 0.029 at 13ºC was estimated, which represents an intermediate value between those found in our study at 11ºC (0.022) and 15ºC (0.059) being therefore consistent.

The parameter estimates of our study were also favourable when compared to ComBase growth data on vacuum-packed cooked ham sausages of pork and bologna sausages (Gill and Holey 2000; Nielsen and Zeuthen 1985). ComBase growth records of *Salmonella* Typhimurium at 8ºC showed a μ_{max} of 0.022 when inoculated on vacuum-packed cooked ham sausages and bologna sausages, very close to the estimate of our study at 7ºC (0.021). Otherwise, ComBase records presented faster maximum growth rates of *Salmonella* Typhimurium at 12ºC and 15ºC (0.046 and 0.087) in cooked bologna-type sausages than those observed in our study at the same temperatures (0.022 and 0.059). These variations may be due to differences in strains and environmental conditions. Growth data found in ComBase were referred to *Salmonella* Typhimurium, whereas in our study the serovars Enteritidis and Typhimurium were used in a cocktail. Also, in the records selected of ComBase, environmental conditions like presence of lysozime, nisin and ethylenenediaminetetraacetic acid (EDTA) in the food matrices could have inhibited the growth of natural flora, favouring the growth of *Salmonella* on ham and bologna in.

Overall, it is assumed that most *Salmonella* serotypes are able to grow over the temperature range 7-48ºC, although growth is quite reduced at temperatures below 10ºC (Bell and Kyriakides 2002). Literature data suggest that some serotypes may grow at temperatures as low as 4ºC, but this is not universally accepted (Bell and Kyriakides 2002). According to our study, *Salmonella* was able to grow in vacuum conditions even at 7ºC. Growth capability during extended incubation of *Salmonella* at low temperatures has been reported (Matches and Liston 1968). When Airoldi and Zottola (1988) assessed the behaviour of two strains of *Salmonella* Typhimurium in nutrient-deficient media, they observed that the bacteria were able to survive and grow at 7ºC. Even if presumed that most *Salmonella* serovars are not capable of growing at refrigeration temperatures, the pathogen is still able to survive for extended periods at chill temperatures. This phenomenon can become significantly relevant from a food safety perspective in RTE meat products intended to be stored for long periods of time at temperatures above 5ºC. In addition, the product in our study was still acceptable from a sensorial perspective at lower temperatures when *Salmonella* reached high levels.

Conclusions

The mathematical model used was capable of predicting the growth of *Salmonella* on slices of RTE stuffed chicken breast as a function of storage temperature. At the temperatures studied (7, 11, 15 and 19ºC), significant growth of *Salmonella* was observed before the product was rejected for consumption (at the lower temperatures) on the basis of odour and appearance. This may indicate that safety, rather than spoilage, may be the shelf-life limiting factor of sliced vacuum-packaged RTE stuffed chicken breast at foreseeable storage conditions.

Acknowledgements

This work was funded by the Project of Excellence CTS-3620 from the Andalusia Government and European Regional Development Fund (ERDF). Authors fully acknowledge the associated pre-doctoral grant associated to the project. This work has been performed by the Research Group AGR-170 (HIBRO) of the Research Andalusian Plan.

References

Airoldi A.A. and Zottola E.A. (1988) Growth and survival of *Salmonella typhimurium* at low temperature in nutrient deficient media. *Journal of Food Science* 53, 1511-1513.

Baranyi J. and Tamplin M. (2003) ComBase: A Common Database on Microbial Responses to Food Environments. *Journal of Food Protection* 67, 1834-1840.

Baranyi J. and Roberts T.A. (1994) A dynamics approach to predicting bacterial growth in food. *International Journal of Food Microbiology* 23, 277-294.

Bell, C. and Kyriakides, A. (2002) *Salmonella* in Foodborne pathogens: Hazard, Risk Analysis and Control. Eds Blackburn C de W., McClure P.J. Cambridge. Woodhead Publishing Ltd, 307-5.

Gill, A. and Holley R.A. (2000) Surface application of lysozyme, nisin, and EDTA to inhibit spoilage and pathogenic bacteria on ham and bologna. *Journal Food Protection* 63, 1338-1346

Langston S.W., Altman N.S. and Hotchkiss J.H. (1993) Within and between sample comparisons of Gompertz parameters for *Salmonella enteritidis* and aerobic plate counts in chicken stored in air and modified atmosphere. *International Journal of Food Microbiology* 18, 43-52.

Luzzi I., Galetta P., Massari M., Rizzo C., Dionisi A.M., Filetici E., Cawthorne A., Tozzi A., Argentieri M., Bilei S., Busani L., Gnesivo C., Pendenza A., Piccoli A., Napoli P., Loffredo R., Trinito M.O., Santarelli E. and Ciofi degli Atti M.L. (2007) An easter outbreak of *Salmonella* typhimurium DT 104a associated with traditional pork salami in Italy. *Eurosurveillance*, 12-3

Matches J.R. and Liston J. (1968) Low temperature growth of salmonella. *Journal of Food Science* 33, 641-645.

Nielsen, H.J.S and Zeuthen, P. (1985) Influence of lactic acid bacteria and the overall flora on development of pathogenic bacteria in vacuum-packed, cooked emulsion-style sausage. *Journal of Food Protection* 48, 28-34

Modeling the influence of the starter culture on proto-cooperation

W.S. Robazza[1], D.A. Longhi[2], G.A. Gomes[1], D.O. Stolf[3]

[1]Food Engineering Department, Santa Catarina State University, Pinhalzinho, Santa Catarina, Brazil. (wrobazzi@yahoo.com.br; gilmargomess@yahoo.com.br)
[2]Food Engineering Department, Santa Catarina Federal University, Florianópolis, Santa Catarina, Brazil. (ealdaniel@hotmail.com)
[3]Physics Department, Santa Catarina Federal University, Florianópolis, Santa Catarina, Brazil (denise_stolf@yahoo.com.br)

Abstract

Fermented milks are considered a very important group of functional foods. In this group, yogurt is the most popular product and its healthy image supports the dynamic development of a vast array of products. The interactions between two thermophilic lactic acid bacteria, *Streptococcus thermophilus* and *Lactobacillus delbrueckii subsp. Bulgaricus* are critical to the successful manufacture of yogurt. This interaction is described by the ecological term proto-cooperation. In such a relationship, each provides something the other needs and both organisms grow better as a result of the association. In this study, the influence of different proportions of the starter culture on physicochemical and microbiological properties of yogurt was evaluated. The influence of the proportions on the dynamical profiles of pH and acidity was analyzed. Results showed that different initial proportions of *Streptococcus thermophilus* and *Lactobacillus bulgaricus* strongly affect all properties studied and microbiological properties such as the duration of the lag and exponential phases. A mathematical model was proposed in order to explain and estimate the best proportion of the starter culture to the studied properties.

Keywords: *proto-cooperation, starter culture, mathematical model, lag phase*

Introduction

Yogurt is commercially produced through fermentation by lactic acid bacteria. The success of milk fermentation relies upon the synergy between *Streptococcus thermophilus and Lactobacillus bulgaricus*, which is known as proto-cooperation. This positive relationship often has a beneficial effect on bacterial growth and on the production of lactic acid and aroma compounds (Angelov *et al.* 2009). Due to its beneficial attributes to human health, there are increased interest to the fermented milks and their nutritional characteristics (Elli *et al.* 2006). An important trend on the investigation of these products is the study of the characteristics of *Streptococcus thermophilus* and *Lactobacillus bulgaricus*, as independent and associated cultures. The aim of this paper is to study the influence of the starter culture on physicochemical characteristics of yogurt. Curves of pH and conductivity profiles are presented for different proportions of the starter culture and mathematical modeling of microbiological properties is employed as a tool to describe the properties of the system. Such a study can provide useful insights about the proto-cooperation phenomenon.

Materials and Methods

Raw Material

Pasteurized milk from the region of Pinhalzinho, Santa Catarina, Brazil, was used in all experiments. The following commercial formulations were used: a formulation from Danisco Cultures (TA 40, LYO 100 DCU) for *Streptococcus thermophilus* and another formulation from Danisco Cultures (LB 340, LYO 100 DCU) for *Lactobacillus bulgaricus*.

Preparation of Yogurt

The milk was heated, by means of a circulating water bath, to 90 ^{0}C for 5 minutes. Then, the product was cooled to incubation temperature, inoculated with different proportions of the starter culture (0:1, 1:3, 1:1, 3:2, 11:9, 2:1, 3:1, 4:1, and 1:0 of *Streptococcus thermophilus* and *Lactobacillus bulgaricus*, respectively), where the proportions of 0:1 and 1:0 represent pure culture of *Lactobacillus bulgaricus* and pure culture of *Streptococcus thermophilus* respectively, poured into 300-mL plastic containers and incubated at 42 ^{0}C. The coagulation of milk was monitored for pH during the incubation period until a pH of 4,7 was attained.

Measurements of pH and acidity

pH was measured using a pH meter (Quimis Q-400MT). Acidity was determined by titration with 0.11N NaOH using phenolphthalein as indicator. Profiles of pH and acidity were used to monitor and study fermentation process.

Statistical analysis

All of the statistical and regression analyses were performed using Origin v.7.0 (OriginLab).

Results and Discussion

Figure 1 shows curves of pH versus time for several proportions of the starter culture (*Streptococcus thermophilus* and *Lactobacillus bulgaricus*, respectively) and Figure 2 shows evolution of acidity with time for the same proportions of the starter culture. As can be seen, 3 phases described the entire fermentation process agreeing with other studies (Soukoulis *et al.* 2007). The first is a lag phase (slow pH decline or acidity increase), then it was observed an exponential phase (rapid pH decrease or acidity increase) and a slow down of acidification rate. All of the curves were fitted using the Boltzmann Equation (Eq. 1) and the results of the duration of the lag phase and the duration of the exponential phase were calculated according to the procedure proposed by Buchanan and Cygnarowicz (1990).

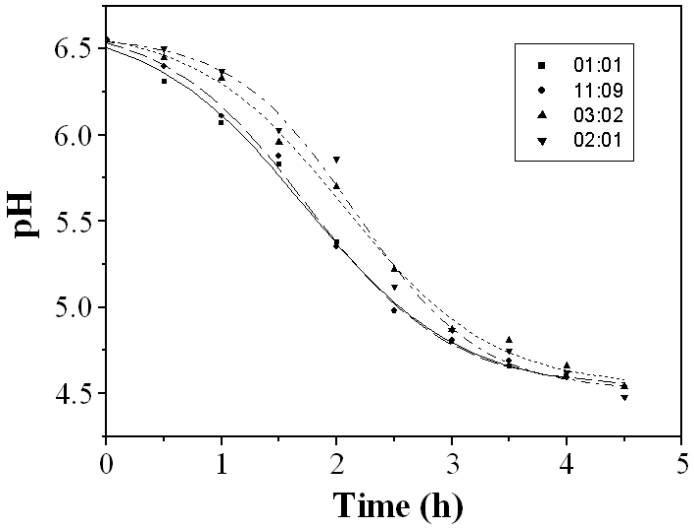

Figure 1: Evolution of pH with time during yogurt elaboration under different proportions of the starter culture.

$$y = B + \frac{A - B}{1 + \exp[(x - x0)/C]} \quad (1)$$

where *A*, *B*, *C*, and x_0 are parameters with no microbiological meaning.

Boltzmann´s equation was employed because it describes a sigmoid and the procedure proposed by Buchanan and Cygnorowicz (1990) is applicable to any sigmoid. According to these authors the duration of the lag phase and the duration of the exponential phase can be

estimated through computation of the maximum and minimum of the second derivative of the growth (pH or acidity) curves.

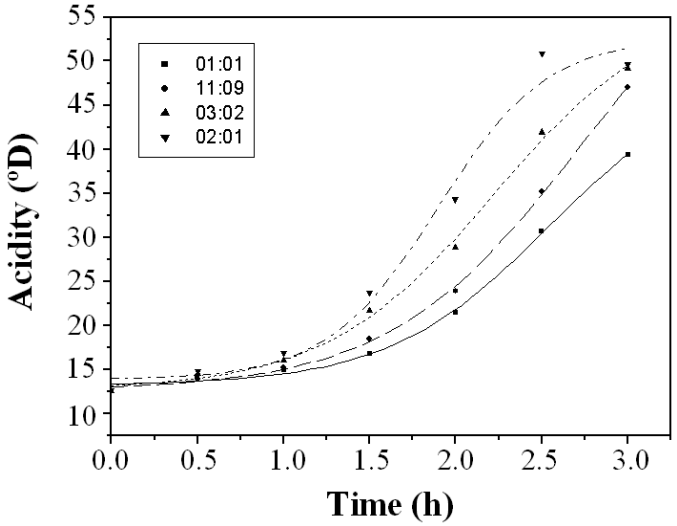

Figure 2: Evolution of acidity with time during yogurt elaboration under different proportions of the starter culture.

Figure 3 shows results obtained for the duration of the lag and exponential phases for different proportions of the starter culture which were obtained using the above mentioned procedure with the parameters of Eq.1 obtained after regression analysis.

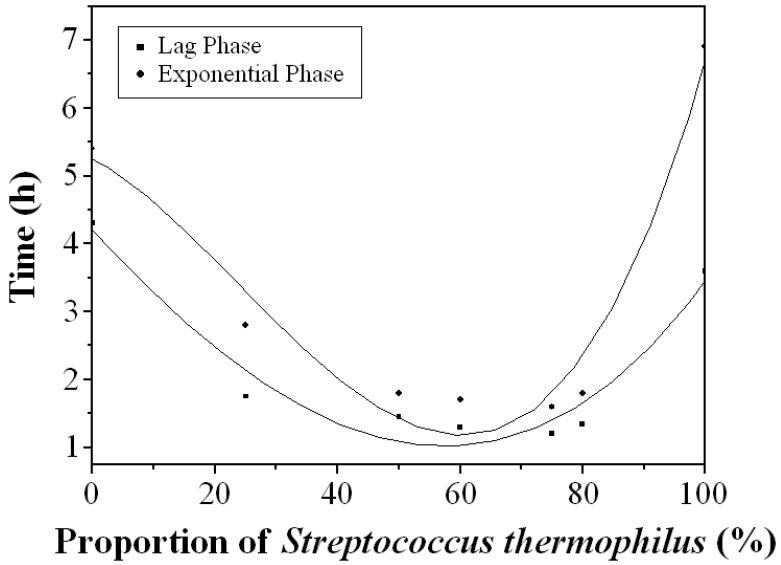

Figure 3: Duration of the lag and exponential phases for different proportions of the starter culture.

Both curves were fitted to a third degree polynomial and results for the duration of the lag and the exponential phases are presented as Equations 2 and 3, respectively:

$$t_{lag}(\%S) = 5{,}13449 - 0{,}08822 \cdot \%S - 0{,}00071 \cdot (\%S)^2 + 0{,}00002 \cdot (\%S)^3 \quad (2)$$

$$t_{\exp}(\%S) = 4{,}20103 - 0{,}03013 \cdot \%S - 0{,}00135 \cdot (\%S)^2 + 0{,}00002 \cdot (\%S)^3 \quad (3)$$

where t_{lag} and $t_{\exp}$ are the duration (h) of the lag and exponential phases respectively, and $\%S$ is the proportion (%) of *Streptococcus thermophilus*.

Visualization of Figure 3 makes apparent the interaction between the two bacteria. The association of both decreases markedly the duration of both the lag and the exponential phases of the pH and acidity curves. This behaviour reveals the favourable characteristics of the proto-cooperation, because there is a decrease in the time of adaptation of the culture (duration of the lag phase) when both micro-organisms were present in the culture in relation to the pure cultures. The minimum of the curves was observed for about 53% of *Streptococcus thermophilus* which may indicate that this is the most favourable proportion of the starter culture.

Conclusions

The fermentation process during yogurt manufacture can be studied by monitoring the pH and acidity. These methods are simple and require low-cost equipment. In the evaluation of the influence exerted by different proportions of the starter culture on pH and acidity profiles, the use of about 53% of *Streptococcus thermophilus* was found to result in the lower lag phase duration indicating that this proportion may be more favourable to the culture growth. Further studies are necessary in order to evaluate the influence of environmental parameters (e.g. temperature) on the pH and acidity profiles.

References

Aguirre-Ezkauriatza E.J., Galarza-González M.G., Uribe-Bujanda A.I., Ríos-Licela M., López-Pacheco F., Hernández-Brenes C.M. and Alvarez M.M. (2008) Effect of mixing during fermentation in yogurt manufacturing. *Journal of Dairy Science* 91, 4454-4465.

Angelov M., Kostov G., Simova E., Beshkova D. and Koprinkova-Hristova R. (2009) Proto-cooperation factors in yogurt starter cultures. *Revue de génie industriel* 3, 4-12.

Buchanan R.L. and Cygnarowicz M.L. (1990) A mathematical approach toward defining and calculating the duration of the lag phase. *Food Microbiology* 7, 237-240.

Elli M., Callegari M.L., Ferrari S., Bessi E., Cattivelli D., Soldi S., Morelli L., Goupil Feuillerat M. and Antoine J.-M. (2006) Survival of yogurt bacteria in the human gut. *Applied and Environmental Microbiology* 72, 5113-5117.

Soukoulis C., Panagiotidis P., Koureli R. and Tzia C. (2007) Industrial yogurt manufacture: monitoring of fermentation process and improvement of final product quality. *Journal of Dairy Science* 90, 2641-2654.

Modeling the effect of high pressure on the activity of orange limonoid glucosultransferase and limonin degradation

E. Gogou, M. Strofyllas, L. Goga, P. S. Taoukis

School of Chemical Engineering, National Technical University of Athens, Greece

Abstract

Juices from certain citrus fruits may face commercial problems due to delayed bitterness caused by the production of limonin. Limonin production rate depends on processing conditions and is accelerated by the enzyme limonin D-ring-lactonehydrolase. On the other hand, bitterness can be reduced by the enzymatic conversion of limonin to the nonbitter limonoid glucoside. The key enzyme in this conversion is limonoid glucosyltransferase (LGTase). The objective of this study was to investigate the effect of high pressure (HP) on LGTase activity and mathematically correlate the enzyme activity with the observed limonin degradation in citrus juice. LGTase was extracted from navel orange albedo tissue. The crude enzyme extract was purified, concentrated and subjected to HP treatments in the pressure range of 100-800 MPa. After HP treatment the enzyme activity was assayed by HPLC. The HP treated enzyme was further added to citrus juice and after incubation, in selected conditions, limonin content was determined. HP processing in the pressure range of 200-300 MPa led to the enhancement of LGTases activity, while treatments with pressures exceeding 300 MPa led to the inactivation of LGTases. Both enzyme inactivation and activation were mathematically modeled as a function of pressure at the respective ranges. Enhanced enzyme activity led to limonin degradation in juice samples and LGTase activity and was mathematically correlated with limonin. The data obtained from this work could be used for the determination of the appropriate HP conditions for the processing of citrus juices, for HP to be applied as an alternative to the conventional resin based debittering process in citrus juices. Furthermore, the developed mathematical model can be used as an effective tool to predict limonin in processed orange juice based on LGTase activity.

Monte Carlo simulation to predict the shelf-life of high pressure and thermally processed orange juice

B. Tiwari[1], T. Norton[2], C.Brennan[3], PJ Cullen[4], C. O'Donnell[1]

[1]Biosystems Engineering, UCD school of Agriculture, Food science and Veterinary medicine, University College Dublin, Belfield, Dublin 4, Ireland
[2]Harper-Adams University College, United Kingdom
[3]Manchester Metropolitan University, United Kingdom
[4]School of Food Science and Environmental Health, College of Sciences and Health, Dublin Institute of Technology, Cathal Brugha St., Dublin 1, Ireland

Abstract

Orange juice is known for its high vitamin C content. Thermal processing continues to be the most widely used method of preserving and extending the shelf-life of juices. However, high pressure processing (HPP) of orange juice has been shown to result in higher retention of ascorbic acid relative to thermally processed juice. Monte Carlo simulation techniques were employed to investigate the effect of processing factors on the stability of vitamin C (OVC) in high pressure processed orange juice. A model was developed which considered the variability which is typically encountered in processing operations. Processing factors influencing the level of Ovc in orange juice reported in the literature include; initial level of Ovc, storage conditions (i.e. time and temperature), juice extraction, high pressure processing and subsequent storage. The model resulted in a number of output distributions which were used to predict the likely Ovc content in high pressure processed orange juice and the impact of various processing stages on Ovc content of the juice. The predicted mean value for Ovc was 47.24 mg $100mL^{-1}$ (5th and 95th percentile being 22.9 and 79.38 mg $100mL^{-1}$, respectively). Sensitivity analysis showed that the initial level of Ovc content of the orange cultivar showed a positive correlation ($r = 0.82$) whereas storage time showed a negative impact ($r = -0.50$) on the vitamin C content of high pressure processed orange juice. A shelf-life of both HHP and thermally processed juice samples was calculated based on concentration of ascorbic acid in orange juice ($\geq$ 25 mg/100 mL) at the expiration date. Mean HHP processed juice samples had an extended shelf-life compared to thermally processed juice. The model output of shelf-life studies were validated with the experimental findings and were found to be within the confidence interval. This study models the effect of processing factors on the shelf-life of high pressure processed orange juice.

Modelling the heat resistance of *Bacillus* spores as a function of sporulation temperature and pH

E. Baril[1,2,3], L. Coroller[1,2], O. Couvert[1,2], I. Leguerinel[1,2], F. Postollec[3], C. Boulais[4], F. Carlin[5,6], P. Mafart[1,2]

[1] Université Européenne de Bretagne
[2] Université de Brest, EA3882, Laboratoire Universitaire de Biodiversité et Ecologie Microbienne, IFR148 ScInBioS, UMT 08.3 PHYSI'Opt, 6 rue de l'Université, F-29334 Quimper, France. (Eugenie.baril@univ-brest.fr)
[3] ADRIA Développement, UMT 08.3 PHYSI'Opt, Z.A. de Creac'h Gwen, F-29196 Quimper Cedex, France.
[4] Danone Research, Avenue de la Vauve, RD128, F-91767 Palaiseau Cedex, France.
[5] INRA, UMR408, Sécurité et Qualité des Produits d'Origine Végétale, F-84000 Avignon, France.
[6] Université d'Avignon et des Pays de Vaucluse, UMR408, Sécurité et Qualité des Produits d'Origine Végétale, F-84000 Avignon, France.

Abstract

Bacillus cereus and *Bacillus licheniformis* spores are able to resist heat treatments applied in minimal food processing. During the food shelf-life, spores germinate and vegetative cell multiplication can be the cause of foodborne poisoning and/or food spoilage. The capacity of spores to resist heat treatments is highly influenced by conditions encountered during the sporulation process. The aim of this study was to propose a model describing the heat resistance of spores depending on sporulation temperature and pH. The heat resistance of psychrotrophic *B. weihenstephanensis* and mesophilic *B. licheniformis* were characterized for spores produced at various temperatures ranging from 5°C to 50°C and pHs ranging from 5.2 to 8.5.

The highest spore heat resistance was estimated when spores were produced at temperatures of 24.4°C, pH 8.0 and 49.9°C, pH 8.5 respectively for both strains. Outside these optimal conditions, at lower and higher sporulation temperature and at more acidic sporulation pH, the spore heat resistance decreased significantly. Heat resistance data were fitted from a model combining a temperature and a pH cardinal parameter model according to the "gamma-concept". The model parameters were the maximum heat resistance, the optimal sporulation temperature and pH, and the minimal and maximal sporulation temperature and pH defined by vertical asymptotes. Furthermore, the model was validated by the characterization of spores produced at different temperatures in soil-based medium and in whey. The observed heat resistance values were consistent with those predicted by the model.

Optimal temperature and pH parameters resulting in the highest heat resistance were estimated at values close to those for optimal growth. This suggests that the highest spore heat resistance could be acquired when sporulation occurred at optimal growth temperature and pH. This study shows that growth cardinal values could represent valuable parameters for determining the conditions at which maximal heat resistant spores occurs.

Keywords: *modelling, spore, heat resistance, Bacillus, sporulation environment*

Introduction

Since *Bacillus* spores are able to resist harsh environmental conditions, optimized heating processes are necessary to ensure food safety. The increase in sporulation temperature has been extensively reported to increase the spore heat resistance (Baril *et al.* 2011; Palop *et al.* 1999; Planchon *et al.* 2011). However, at high sporulation temperatures spore resistance were stable or even decreased (Gonzalez *et al.* 1999; Lindsay *et al.* 1990). Regarding the effect of sporulation pH, an increase of pH from 6.0 to 8.1 in buffered sporulation media also caused a significant increase in *B. cereus* spore heat resistance (Mazas *et al.* 1997).

Sporulation environment induces obvious variations of spore heat resistance, but is not taken into account in heat process calculations. The aim of this study was to propose a model describing the spore heat resistance as a function of the two main sporulation environmental factors. Therefore, the influence of sporulation temperature and pH on the spore heat

resistance of the psychrotrophic species *Bacillus weihenstephanensis* and the mesophilic species *Bacillus licheniformis* was investigated.

Materials and Methods

Spore production and heat resistance determination

B. weihenstephanensis KBAB4 strain and *B. licheniformis* AD978 strain were studied. Spores were produced in a sporulation mineral buffer (Baril *et al.* 2011), at temperatures ranging from 5°C to 50°C and at pH ranging from 5.2 to 8.5. In addition, spores were produced in whey and in soil-based medium, at two temperature levels and one pH level for each bacterium and sporulation medium. Spore heat resistance was determined by the capillary method (Baril *et al.* 2011) at heating temperatures ranging from 80°C to 105°C.

Heat resistance models

Survival curves were fitted from the Weibull model modified by Mafart et *al.* (2002) as follows:

$$\log(N) = \log(N_0) - \left(\frac{t}{\delta}\right)^p \qquad (1)$$

where N (CFU/ml) is the population concentration at time t, N_0 (CFU/ml) is the initial population concentration, δ (min) is the time to the first decimal reduction and p is a shape parameter.

The modelling of the influence of sporulation temperature and pH on the spore heat resistance was inspired by the gamma-concept (Zwietering *et al.* 1992) and by the cardinal growth model (Rosso, 1995). To consider both the influence of sporulation environment (sporulation temperature and pH) and the heating environment (heating temperature) on spore heat resistance, this model was associated to the Bigelow log-linear model (Mafart *et al.* 2002), as follows:

$$\delta = \delta^*_{\max}\, \gamma_2(T_{spo})\gamma_1(pH_{spo})10^{-\left(\frac{T_{HT}-T^*_{HT}}{z}\right)} \qquad (2)$$

where δ^*_{max} is the δ value acquired by spores produced at the optimal sporulation temperature and pH for a treatment at the reference heating temperature (T^*_{HT}); $\gamma_2(T_{spo})$ and $\gamma_1(pH_{spo})$ correspond respectively to the influence of the sporulation temperature or pH; T_{HT} is the heating temperature; z is the increase of the heating temperature resulting in a decimal reduction of δ values.

The influence of the temperature and pH on spore heat resistance was described as follows:

$$\gamma_n(X_{spo}) = \begin{cases} 0.0 & X \le X_{\min(R)} \\ \dfrac{(X - X_{\max(R)})(X - X_{\min(R)})^n}{(X_{opt(R)} - X_{\min(R)})^{(n-1)}\left[(X_{opt(R)} - X_{\min(R)})(X - X_{opt(R)}) - (X_{opt(R)} - X_{\max(R)})((n-1)X_{opt(R)} + X_{\min(R)} - nX)\right]} & X_{\min(R)} < X < X_{\max(R)} \\ 0.0 & X \ge X_{\max(R)} \end{cases} \qquad (3)$$

where $X_{opt(R)}$ is the optimal sporulation temperature or pH and $X_{min(R)}$ and $X_{max(R)}$ are the theoretical minimal and maximal sporulation temperature or pH within which the spore heat resistance (δ) is higher than zero.

Model fits

In order to reduce the variances of the studied responses (N and δ), models were fitted by minimizing the sum of squared errors of the decimal logarithm of the spore concentration ($\log N$) and the decimal logarithm of the spore heat resistance ($\log\delta$) (lsqcurvefit, Optimization Toolbox, MATLAB 7.9.0, The Math-works, Natick, USA). The 95% confidence intervals were estimated using nlparci function (Statistical Toolbox; MATLAB 7.9.0; The Math-works, Natick, USA). The goodness of fit was assessed by the root mean square error (RMSE). The literature available data set of *B. cereus* ATCC7004 (Gonzalez *et al.* 1999) was also fitted from the equation 2 to test the robustness of the model.

Results and Discussion

Influence of sporulation temperature and pH on spore heat resistance

As shown on figure 1, the highest spore heat resistance was estimated when spores were produced at temperature of 24.4°C (±1.9) ($\log\delta_{90°C}$=0.90, p=1.3) and 49.9°C (±1.9) ($\log\delta_{100°C}$=0.78, p=1.0) for *B. weihenstephanensis* KBAB4 and *B. licheniformis* AD978, respectively. For lower and higher sporulation temperatures, a decrease in the spore heat resistance was observed. Following the same trend, the highest spore heat resistance was estimated for sporulation at pH 8.0 (±0.6) and pH 8.5 (±0.7) for both strains, respectively. For lower sporulation pHs, a decrease of spore heat resistance was observed. In addition, the z parameters were not significantly dependent on the sporulation temperature or pH and were estimated at 9.0°C (±0.7) and 7.3°C (±0.5) for both strains respectively.

The model was also fitted with a set of published data regarding *B. cereus* ATCC7004 (Gonzalez *et al.* 1999). The sporulation temperature resulting in maximal heat resistance was estimated at 37.7°C (±2.5) ($\log\delta_{100°C}$=-0.70, p=1.0) and the z parameter at 7.8°C (±1.2).

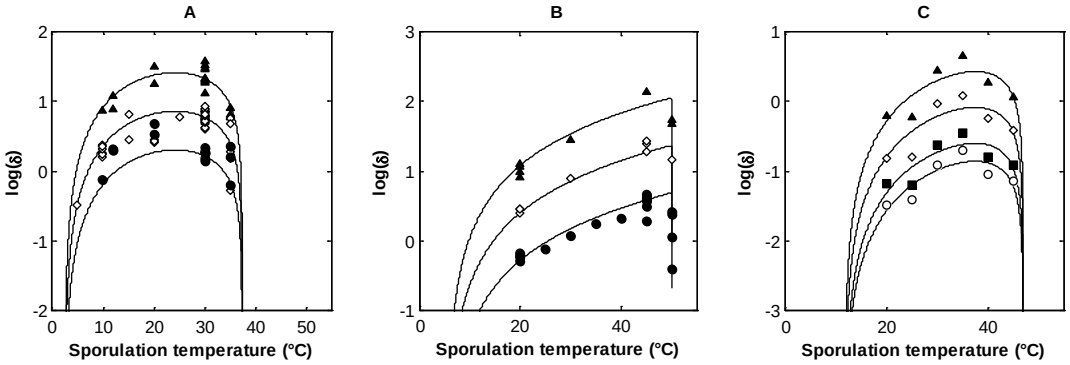

Figure 1: Modelling the influence of sporulation temperature on *Bacillus* spore heat resistance at different heating temperatures. (A) *B. weihenstephanensis* KBAB4 spores, treated at 95°C (circles), 90°C (diamonds) and 85°C (triangles). (B) *B. licheniformis* AD978 spores, treated at 100°C (circles), 95°C (diamonds) and 90°C (triangles). (C) *B. cereus* ATCC7004 spores (Gonzalez *et al.* 1999), treated at 102°C (circles), 100°C (squares), 96°C (diamonds) and 92°C (triangles). Symbols correspond to independent experimental data. Black lines correspond to estimated values from the equation 2.

Robustness of the model

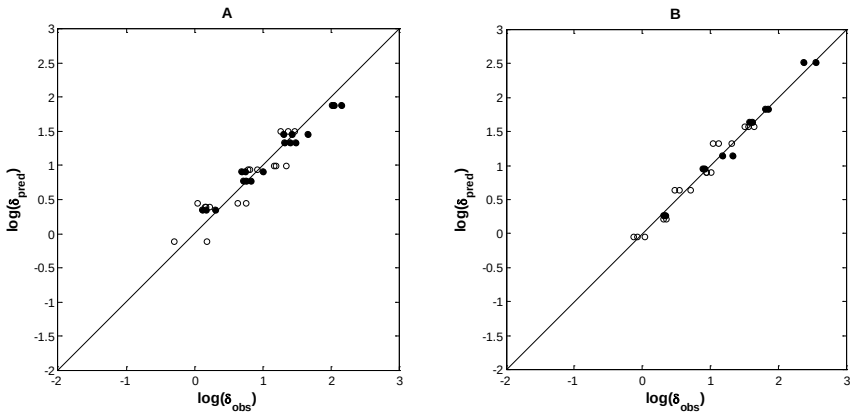

Figure 2: Predicted values of spore heat resistance ($\log\delta_{pred}$) versus observed values of spore heat resistance ($\log\delta_{obs}$). *B. weihenstephanensis* KBAB4 (A) and *B. licheniformis* AD978 (B) spores produced in whey (white filled symbols) and in soil-based medium (black filled symbols).

The heat resistance of *B. weihenstephanensis* KBAB4 and *B. licheniformis* AD978 spores produced at different temperatures in whey and soil-based medium were estimated from the model (sporulation temperature parameters were fixed at previous estimated values). Whatever the strain and the sporulation medium, the model provided an accurate prediction of the spore heat resistance as a function of sporulation temperature and heating temperatures (Figure 2). The mean error was evaluated between 0.08 and 0.23.

Conclusions

The predictive model we propose in this study enables the quantitative assessment of spore heat resistance as a function of temperature and pH for one sporulation environment. Estimated optimal temperature and pH resulting in maximal heat resistance are close to temperature and pH values determined for optimal growth. This suggests that the highest spore heat resistance could be acquired when sporulation occurred at optimal growth temperature and pH. This study shows that growth cardinal values could represent valuable parameters for determining the conditions at which maximal heat resistant spores occurs. Moreover, the environmental conditions of sporulation and subsequent recovery may act synergistically on the probability of survival and outgrowth. For instance, the decrease of spore heat resistance is favoured by acidic sporulation conditions as well as acidic recovery conditions decrease the outgrowth (Mafart *et al.* 2001). Estimating the sporulation temperature and pH at which spore heat resistance is maximal is useful for the food industry in their efforts to design appropriate process parameters given the presence of a particular spore population. Further research is needed to extend this study to anaerobic spore forming bacteria.

Acknowledgements

This work is supported by the Agence Nationale de la Recherche (ANR) (France) as part of an ANR-07-PNRA-027-07 MEMOSPORE contract, by the industrial association Bretagne Biotechnologies Alimentaires (BBA) and the French National Association of the Technical Research (ANRT).

References

Baril E., Coroller L., Postollec F., Leguerinel I., Boulais C., Carlin F. and Mafart P. (2011) The wet-heat resistance of Bacillus weihenstephanensis KBAB4 spores produced in a two-step sporulation process depends on sporulation temperature but not on previous cell history. *International Journal of Food Microbiology* 146, 57-62.

Garcia D., Voort V.D.M. and Abee T. (2010) Comparative analysis of Bacillus weihenstephanensis KBAB4 spores obtained at different temperatures. *International Journal of Food Microbiology* 140, 146-153.

Gonzalez I., Lopez M., Martinez S., Bernardo A. and Gonzalez J. (1999) Thermal inactivation of Bacillus cereus spores formed at different temperatures. *International Journal of Food Microbiology* 51, 81-84.

Lindsay J. A., Barton L. E., Leinart A. S. and Pankratz H. S. (1990) The effect of sporulation temperature on sporal characteristics of *Bacillus subtilis* A. *Current microbiology* 21, 75-79.

Mafart P., Couvert O. and Leguérinel I. (2001) Effect of pH on the heat resistance of spores: Comparison of two models. *International Journal of Food Microbiology* 63, 51-56.

Mafart P., Couvert O., Gaillard S. and Leguerinel I. (2002) On calculating sterility in thermal preservation methods: application of the Weibull frequency distribution model. *International Journal of Food Microbiology* 72, 107-113.

Mazas M., Lopez M., Gonzalez I., Bernardo A. and Martin R. (1997) Effects of sporulation pH on the heat resistance and the sporulation of *Bacillus cereus*. *Letters in Applied Microbiology* 25, 331-334.

Palop A., Manas P. and Condon S. (1999) Sporulation temperature and heat resistance of Bacillus spores : a review. *Journal of Food Safety* 19, 57-72.

Planchon S., Dargaignaratz C., Levy C., Ginies C., Broussolle V. and Carlin F. (2011) Spores of *Bacillus cereus* strain KBAB4 produced at 10 °C and 30 °C display variations in their properties. *Food Microbiology* 28, 291-297.

Rosso L. (1995) Modélisation et microbiologie prévisionnelle : élaboration d'un nouvel outil pour l'agro-alimentaire.: Thèse de doctorat, Université Claude Bernard Lyon I, n° 95-197.

Zwietering M. H., Wijtzes T., De Wit J. C. and van't Riet K. (1992). A decision support system for prediction of the microbial spoilage in foods. *Journal of Food Protection* 55, 973-979.

Effect of thymol in heating and recovery media on the heat resistance of *Bacillus* species

M.D. Esteban, J.P. Huertas, A. Palop

Department of Food Engineering and Agricultural Machinery,Technical University of Cartagena, Paseo Alfonso XIII 48, ES-30203 Cartagena, Murcia, Spain (alfredo.palop@upct.es)

Abstract

Bacillus spores are the main targets in most of the thermal treatments of canned foods. Essential oils are natural products extracted from herbs and spices, which can be used as natural preservatives in many foods because of their antibacterial, antifungal, antioxidant and anti-carcinogenic properties. Recently, some studies have recorded the antimicrobial efficacy of essential oils, alone or in combination with other preservation methods, against spoilage and food-borne pathogens. The aim of this study was to evaluate the influence of different concentrations of thymol in the heating and in the recovery media on the heat resistance of spores of *B. subtilis, B. licheniformis* and *B. sporothermodurans*. Heat resistance determinations were carried out in a thermoresistometer Mastia. The treatment temperatures were 100ºC and 110ºC. Different concentrations of thymol (from 0.1 to 0.6 mM) were added to the heating and to the recovery medium. The effect of thymol in the heating medium was rather small and no differences were found between the different microorganisms. When the thymol was added to the recovery medium significant differences were found between the control and the different concentration tested. The data on the effect of thymol in the recovery medium were used to build a predictive model. In view of their effects in lowering the heat resistance, together with their antimicrobial and sensorial properties, essential oils like thymol, could be used in combination with heat in order to reduce the intensity of the thermal treatments applied to some products like soups or vegetable dishes.

Keywords: *Bacillus, thymol, recovery medium, heating medium*

Introduction

Bacillus spores are the main problem in most of the food industries due to its capacity to survive to the industrial sterilisation processes. In the last years, high heat resistant spore-forming bacteria have increased challenges in industrial sterilisation processes to assure food safety and prevent spoilage. A large amount of over-processing is often applied to the products that have a prolonged shelf life. This is unfavourable for the product quality, so combined processes are needed in order to ensure microbial safety without affecting the sensorial and nutritional properties. The addition of thymol to the foods that are going to be heat treated could reduce process times and temperatures considerably.

Essential oils are natural products extracted from herbs and spices used as flavourings in the food industry. Nowadays their use as natural preservatives in many foods is gaining interest because of their antibacterial, antifungal, antioxidant and anti-carcinogenic properties. Recently, some studies have recorded the antimicrobial efficacy of essential oils, alone or in combination with other preservation methods, against spoilage and food-borne pathogens (Esteban and Palop 2011). Thymol is a phenolic compound present in the essential oil fraction of Oreganum and Thymus plants. Essential oil has been shown to exhibit antibacterial and antifungal activity including food pathogens (Ultee *et al.* 2000). The aim of this study was to evaluate the influence of different concentrations of thymol in the heating and in the recovery media on the heat resistance of spores of *B. subtilis, B. licheniformis* and *B. sporothermodurans*.

Materials and Methods

Bacterial strains and culture conditions

The strains used in this study were *Bacillus subtilis* CECT 4071, *Bacillus licheniformis* CECT 4525 (both supplied by the Spanish Type Culture Collection), and *Bacillus sporothermodurans* IC4 (supplied by Unilever Netherlands Sourcing Unit Oss). The spore suspensions were stored in sterilized distillate water at 4ºC until used.

Chemicals

Thymol (Sigma-Aldrich Chemie, Steinheim, Germany) stock solution 0.5 M was made in 95 % ethanol and stored at 4 °C.

Heat treatment

Heat resistance determinations were carried out in a thermoresistometer Mastia (Conesa *et al.* 2009). The D values were determined in Brain Heat Infusion (BHI) (Scharlau Chemie, Barcelona, Spain) at temperatures of 100 and 110ºC. Different concentrations of thymol were added to heating medium and recovery medium, Brain Heat agar (BHIA) (Scharlau Chemie, Barcelona, Spain).

Results and Discussion

The effect of the concentration of thymol in the heating medium on the heat resistance was rather small for all microorganisms under study and no dose dependent effect was found. No differences were found on the effect of thymol in the heating medium among the different microorganisms.

When thymol was added to the recovery medium after the thermal treatment at 100ºC applied to *B. subtilis* spores, significant differences were found between the D_{100} value of the control (without thymol added) and the different concentrations tested (Table 1). A dose dependent effect was found up to concentrations of 0.3 mM. Higher concentrations did not lead to further decreases in the D_{100} values. A similar effect was found at 110ºC for this microorganism.

Table 1: D-values (minutes) for *Bacillus subtilis* CECT 4071 heated to 100ºC and recovery media with thymol.

	Concentration mM	Thymol	
		D (min)	SD
Bacillus subtilis	0	2.84	0.27
CECT 4071	0.1	2.33	0.22
Heating TºC:100ºC	0.2	1.55	0.15
	0.3	0.95	0.1
	0.4	0.95	0.28
	0.5	0.88	0.33
	0.6	0.95	0.48

Similar results were obtained with *B. licheniformis* at 100ºC (Fig 1). However, *B. sporothermodurans* spores were not affected by the addition of thymol to the recovery medium (data not shown). Conesa *et al.* (2009) showed that the heat resistance of *Bacillus cereus* spores was also affected by the addition of thymol to the recovery medium up to concentrations of 0.3 mM. The heat resistance of this microorganism was neither affected by the presence of thymol in the heating medium.

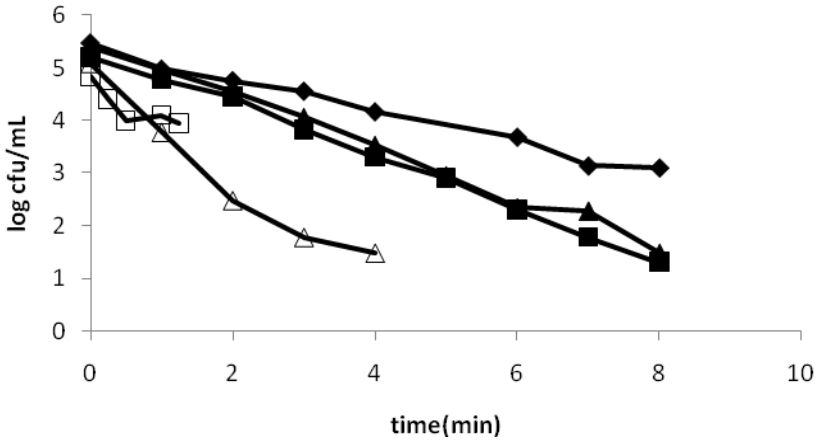

Figure 1: Indication of the paragraph format list box in the MS Word user interface.

The data on the effect of antimicrobials in the recovery medium were used to build a predictive model. This predictive model was based on the model of Mafart and Leguerinel (1998) (Eq. 1)

- —— (1)

In our case, the z_{thymol} value was 0.69 mM for *B. subitlis* at 100ºC, which means that a concentration of 0.69 mM thymol in the recovery medium is necessary to reduce the D_{100} value to one tenth. However, as stated before, the effect was only kept for concentrations up to 0.3 mM, since higher concentrations did not lead to further decrease in the D values. Lekogo *et al.* (2010) also found a relationship based on the same model, which enabled them to describe the effect on the heat resistance of *B. cereus* and *Clostridium sporogenes* of the addition of different fatty acids to the recovery medium. These authors also did not find any effect of these fatty acids when added to the heating medium. In view of their effects in lowering the heat resistance and hampering the recovery of the survivors to the thermal treatment, together with their antimicrobial and sensorial properties, essential oils like thymol, could be used in combination with heat in order to reduce the intensity of the thermal treatments applied to some products like soups or vegetable dishes.

Conclusions

The effect of the addition of thymol was different in the heating and in the recovery media. Thymol had a stronger effect on the recovery medium. A progressive decrease in heat resistance was observed when increasing thymol concentration in the recovery medium up to 0.3 mM. The addition of thymol to the heating medium did not significantly decrease the heat resistance of these microorganisms at concentrations up to 0.6 mM. *B. sporothermodurans* spores were not affected by the presence of thymol in the heating and in the recovery media.
A mathematical model was built to predict the D_{values} of *B. subtilis* and *B. licheniformis* at concentrations of thymol up to 0.3mM.

Acknowledgements

This research was financially supported by the Ministry of Science and Technology of the Spanish Government and European Regional Development Fund (ERDF) through Projects AGL-2006-10280 and AGL-2010-19775. M.D. Esteban is grateful to the Ministry of Science and Technology for offering her the fellowship BES 2007–15471.

References

Conesa R., Andreu S., Fernández P.S., Esnoz A. and Palop A. (2009) Nonisothermal heat resistance determinations with the thermoresistometer Mastia. *Journal of Applied Microbiology* 107, 506–513.

Conesa R., Leguerinel I. and Palop A. (2009) Effect of thymol in heating and recovery media on the heat resistance of *Bacillus cereus*. In: D. Sohier, A. Développement, I. Leguerinel (Eds.) [Symposium on Spore Forming bacteria in Food, Quimper (France),15-17 June, 2009].

Esteban M.D. and Palop A. (2011) Nisin, Carvacrol and Their Combinations Against the Growth of Heat-Treated *Listeria monocytogenes* Cells.*Food technology and biotechnology* 49(1), 89-95.

Lekogo B.M., Coroller L., Mathot A.G., Mafart P. and Leguerinel I. (2010) Modelling the influence of palmitic, palmitoleic, stearic and oleic acids on apparent heat resistance of spores of *Bacillus cereus* NTCC 11145 and *Clostridium sporogenes* Pasteur 79.3. International Journal of Food Microbiology 141, 242-247.

Mafart P.,and Leguerinel I. (1998) Modeling Combined Effects of Tempeature and pH on Heat Resistance of Spores by Linear-Bigelow Equiation. *Journal of Food Science* 63 (1), 6-8.

Ultee A., Kets EPW., Alberda M., Hoekstra F.A. and Smid E.J. (2000) Adaptation of the food-borne pathogen Bacillus cereus to carvacrol. *Archives of Microbiology* 174(4), 233-238.

Modeling inactivation of *Leuconostoc mesenteroides* in dextran added to dairy ingredients

C.P. Pacheco[1], A.R. Silva[2], P.R. Massaguer[3]

[1]FAJ, Jaguariuna Faculty, Food Engineering, Jaguariúna, SP, Brazil;
[2]Dept. of Food Science, FEA, University of Campinas (UNICAMP), Campinas, SP – Brazil;
[3]Dept. of Chemical Processes, Chemical Engineering, University of Campinas, Campinas, SP – Brazil

Abstract

Leuconostoc mesenteroides are especially important in the sugar and dairy industry due to its ability to produce CO_2, flavor compounds as a function of heterofermentative consumption of lactose and citrate, and dextran gum from sucrose. The dextran produced by *Leuconostoc* in sugary ingredients, can render a final product of lower sensorial and/or microbiological quality due to the physical barrier of dextran which could affect the efficiency of pasteurization. The objective was to determine the thermal inactivation of *L. mesenteroides*, by sealed TDT method, between 60-121ºC, in a solution of dextran 100ppm, and when it was added to liquid sugar 40% (v/v), whole milk or cream 40% (v/v). The survival data were adjusted by the GInaFiT program for kinetic parameters estimation. After obtaining adjusted models, it was determined the time required to promote five (5) decimals log reductions of *L. mesenteroides* population in these ingredients. The results showed that, in the four substrates the target microbial, *Leuconostoc mesenteroides*, in the presence of 100ppm dextran, is heat sensitive, however presents a non-linear kinetics with "tailing" in the final heat treatments that would enable their survival in higher content lipids ingredients. When comparing the time for five reductions t(5), for whole milk with dextran (R^2*=0.979 and* $t(5)_{75C}$*=24.40 sec*) with only dextran 100ppm solution (R^2*=0.984 and* $t(5)_{75C}$*=8.73 sec*), both complying with the Mafart Model, the thermal resistance was higher in milk with dextran and, when comparing the resistance of the microorganism in cream (R^2*=0.998 and* $t(5)_{60C}$*=574.85 sec*) and liquid sugar 40% (R^2*=0.993 and* $t(5)_{60C}$*=478.20 sec*), both containing 100ppm dextran and obeying the Cerf Biphasic Model, the thermal resistance was higher in the cream, delineated by K_{max1}*=5.53min*$^{-1}$ *and* K_{max2}*=0.49min*$^{-1}$.

Keywords: *thermal inactivation, cream, liquid sugar*

Introduction

Leuconostoc mesenteroides are defined as Gram positive cocci in pairs and chains, facultative with optimum growth temperature at 28°C, but no growth at 45°C (Mossel *et al.* 1995) it is an aciduric microorganism (Nickerson and Sinskey 1978). Metabolically, are defined as heterofermentative organisms, which converts one mol of glucose producing lactic acid to small parts of ethanol, acetic and fumaric acids and CO_2, using of glucose was aerogenic fermentative dissimilation (Mossel *et al*, 1995). The mainly sources of this bacteria first is sugar cane where the count normally range between 10^5 and 10^7CFU/mL for normal cane juices and 10^8CFU/mL for juices obtained from sour cane (ICMSF 2005), and second, the lactic products. This bacteria produce, frequently, dextran, a polysaccharide that causes significant processing problems for both raw sugar factories and refineries. Dextran increases the viscosity of process liquid sugar. Besides that, dextran damage pumps and increase the need and frequency of cleaning of equipments (ICMSF 2005).

For food industries, that use liquid sugar as an ingredient, recontamination with *Leuconostoc* is observed during inadequate storage conditions, before use, where insufficient attention is given to hygiene. When *Leuconostoc mesenteroides* growths in foods, it could promote spoilage by production of flavor compounds (diacetil due to fermentation of citric acid), lactic acid and CO_2 that causes in a pack a springer condition. Moreover, the viscosity of food was changed because dextran was also produced by *L.mesenteroides.* The microorganism heat resistance was lower but these values could be increased with dextran presence. The effect of the presence of dextran on the thermal resistance has not been reported in literature.

This research aimed to determine the thermal inactivation of *L.mesenteroides*, in a solution of 100ppm dextran and when it was added to liquid sugar 40% (v/v), whole milk and cream 40% (v/v).

Materials and Methods

Test organism and vegetative suspension production

For this study *Leuconostoc mesenteroides* strain recognized as a dextran producer was isolated from lactic ingredients. The cells suspension was produced by inoculation of *L.mesenteroides*, in Lactobacilli MRS Medium (Difco, 288130) plus 2% of Agar (Difco), incubated at 28°C/24h. After, growth the bacterial cells were collected using sterile water and the suspension was adjusted for $2.1x10^8$CFU/mL, by Densimat (bioMérieux). 1mL of this suspension was added to 99mL of dextran solution at 1000ppm (Sigma), previously sterilized at 115°C/30minuts.

Heat resistance determination

For heat resistance determination was applied the TDT (Time Death Time) tube Method (Stumbo 1965). For this, 1.8mL of each substrate with 100ppm dextran, previously sterilized, was dispensed in a Pyrex TDT tube, 0.2mL of vegetative suspension in dextran were added. The tests suspensions and the temperature x time applied were: dextran 100ppm (75°C; 3, 5, 16, 20 and 25s); liquid sugar 40% (v/v) (60°C; 1, 2, 3, 4 and 5min); whole milk (75°C; 3, 5, 16, 25 and 35s) and cream 40% (v/v) (60°C; 1, 2, 3, 4 e 5min). For all the tests suspensions, inside the TDT tube, the dextran concentration was 100ppm, in order to test the influence of dextran on microorganism heat resistance and the lag time of the suspension in the TDT tube was measured. The subculture was prepared in formulated Vancomycin Agar Medium, added with 20μg/L of vancomycin. The incubation was carried out for 5 days at 28°C, according to Mathot *et al.* (1994).

Treatment of thermal resistance data

Using obtained data (log of survivors x time) at each constant temperature, for each tested substrate was constructed a survivor curve adjusting the data by GInaFiT program (Geeraerd and Van Impe Inactivation Model, v.1.4.2), for kinetic parameters estimation. Two models were used for the destruction curves with best determination coefficient: Cerf (1977) – equation 1 and Weibull as proposed by Mafart *et al.* (2002) – equation 2. By Cerf model were obtained the parameters: *kmax1* (more sensitive fraction death constant), *kmax2* (more resistant fraction death constant), *f* (more sensitive fraction of the bacteria population) and *LOG10N0* (initial population log). This biphasic model is capable of describing survivor curves of shapes linear, linear with tailing and biphasic, and can, if being used for time-varying conditions, be written under the form of two first-order differential equations, one for *N1* (the major subpopulation) and one for *N2* (the minor subpopulation) (Geeraerd *et al.*, 2005).

$$\log10(N) = \log10(No) + \log10(f.e^{-k\max 1-t} + (1-f).e^{-k\max 2.t}) \quad (1)$$

where: *f* is the fraction of the initial population in a major subpopulation, *(1-f)* is the fraction of the initial population in a minor subpopulation (which is more heat resistant than the previous one), and *kmax1* and *kmax2* [1/time unit] are the specific inactivation rates of the two populations, respectively.

$$LOG10(N) = LOG10(N0) - \left(\frac{t}{\delta}\right)^p \quad (2)$$

where: δ [time unit] is a scale parameter and can be denoted as the time for the first decimal reduction if p=1, and *p* [–] is a shape parameter. For *p>1*, convex curves are obtained, while for *p<1*, concave curves are described.

After obtained adjusted models, it was determined the time required to promote five (5) decimal log reductions of *L.mesenteroides* population in each tested suspension, using the equations defined by models (equations 1 and 2) applying Excel Solver tool.

Results and Discussion

The results showed that, in the four substrates the target microbial, *Leuconostoc mesenteroides*, in the presence of 100ppm dextran, is heat sensitive, however presents a non-linear kinetics behavior with tailing at the finals heat treatments that would enable their survival in higher content lipids ingredients such as cream (Figure 1B). Figure 1A shows a survivor curve for *L.mesenteroides* in liquid sugar solution 40% with 100ppm of dextran, at 60°C.

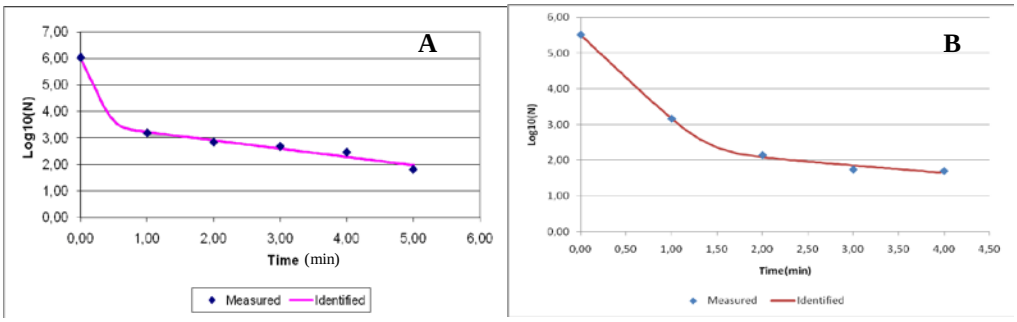

Figure 1: Survivor curve of *Leuconostoc mesenteroides* at 60ºC: A - in liquid sugar solution 40% with 100ppm of dextran and B: in cream 40% with 100ppm of dextran.

The microorganism destruction curve showed a non-linear biphasic behavior by Figures 1A and B, in liquid sugar solution and cream both with 100ppm dextran. At the first minute a quick destruction occurred (about 3 log cycles) but, after, the destruction was slower, and after 5 minutes, there is still a remaining population ($6.5x10^1$CFU/mL), a typical tailing effect probably due to the presence of dextran that at higher times has increased its viscosity. For this situation, the biphasic model Cerf (1977), adjusted very well by GInaFiT program, with R^2*0.9936*, equivalent $D_{60ºC}$ *191.4 sec*, calculated from 2.303/kmax2 (Table 1). Concerning the time for 5 log cycles reductions, *t(5)*, obtained by equation 1, it is necessary 478.20s to accomplished this target. The parameters obtained by the model were: *kmax1=12.56min*$^{-1}$*; kmax2=0.72min*$^{-1}$*; f=0.9968 and LOG10No=6.04*. So, it is possible to affirm that the more sensitive population is ~99.7% but the residual population (0.3%), corresponds to a population fraction with slow death, represented by a tailing.

Comparing the results obtained for sugar liquid solution 40% and cream (Figure 1B), both containing 100ppm of dextran, the thermal resistance was higher in cream with equivalent $D_{60ºC}$ *281.88s, kmax1=5.53min*$^{-1}$*, kmax2=0.49min*$^{-1}$*; f=0.9990* and R^2*0.9980* (Table 1). All the results for both ingredients were obtained by Cerf Biphasic Model, using GInaFiT Program. For this case, the more sensitive population is ~99.9% and the residual population (0.1%) corresponds to a population fraction with slow death, represented by a tailing. The high resistance shown in cream is probably due to protection given by the lipids and the gum.

For whole milk with 100ppm dextran and 100ppm dextran solution a concave survivor curve was observed, both complying with the Weibull Model (Mafart, 2002), with p<1. When comparing the time for five reductions t(5), for whole milk with dextran on Figure 3A (R^2*=0.979;* δ*=0.069min, p=0.27 and* $t(5)_{75C}$*=24.40 sec*) against only dextran 100ppm solution on Figure 2B (R^2*=0.984;* δ*=0.055min, p=0.32 and* $t(5)_{75C}$*=8.73 sec*), the thermal resistance was higher in milk with dextran, 0.069min for the first log cycle reduction (Table 1). It is important to emphasize that for whole milk (Figure 2A), after the first five seconds, the population was not reduced over 3 log cycles and for t>30sec, there were no more survivors. It is possible to affirm that the linearity deviation is a function of dextran presence, which provides a protection for cells.

Concerning the dextran 100ppm solution, there were no additional substrates besides dextran, so, it is possible to affirm that the presence of dextran it is the main responsible for linearity deviation.

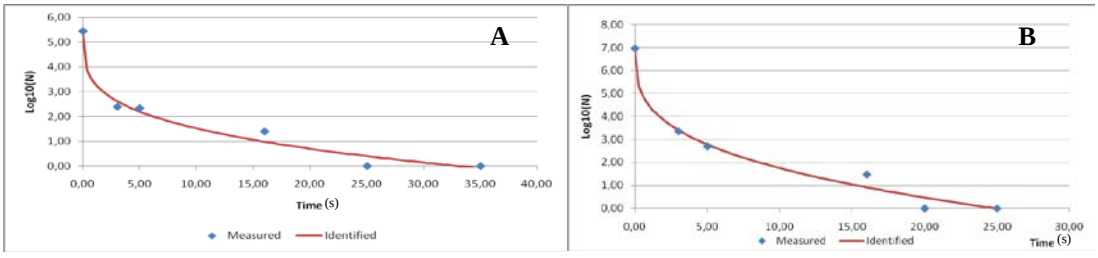

Figure 2: Survivor curve of *Leuconostoc mesenteroides* at 75ºC: A. in sterile whole milk with 100ppm of dextran and B. in dextran solution 100ppm.

Table 1: Kinetic parameters for *Leuconostoc mesenteroides* in different ingredients, added of 100ppm of dextran.

Ingredients	*t1**	*t5(s)***	*T(°C)*	*D (s)*	R^2	*Applied Model*
Liquid Sugar Solution 40%	12.29	478.20	60	191.4	0.9936	Cerf (1977) Biphasic non-linear model
Cream 40%	25.06	574.85	60	281.88	0.9980	Cerf (1977) Biphasic non-linear model
Whole Milk	0.069	24.40	75	0.069	0.979	Mafart *et al.* (2002) Non linear model
Dextran solution	0.055	8.73	75	0.055	0.9841	Mafart *et al.* (2002) Non linear model

Where: *t(1): time for the first log cycle reduction; t(5): time for 5 log cycle reductions

When the D values, obtained here are compared with literature, it is possible to observe that for liquid sugar, the D values is 2 times higher than the ones reported by Franchi *et al.* (2003) for sugar cane juice 14°Brix, pH 6.5, with no dextran added. These authors reported a linear destruction curve for *L.mesenteroides*. This confirms the fact the presence of dextran causes non linear behavior. Stumbo (1973), reported a D value for *Leuconostoc* and other lactic acid bacteria, from 0.5 to 1 min at 65°C, with z from 4.4 to 5.6°C. So, according to these values, it is possible to conclude that for liquid sugar, $D_{75°C}$ estimated was <4.78s (using Stumbo z value), was lower than the heat resistance for dextran solution and whole milk added of dextran, obtained by this research. Besides that, the time for 5 reductions, at 60°C, for cream was the highest, 281.88s, probably because of milk proteins, fats and gum promoting protection for *L.mesenteroides* cells.

Conclusions

The survivors curves for *Leuconostc mesenteroides* were non-linear and affect by the presence of dextran. The *Leuconostc mesenteroides* heat resistance was higher in cream 40% than liquid sugar, at 60°C, and in whole milk compared with dextran solution 100ppm, at 75°C; all added of 100ppm of dextran. For all the tested substrates, the microorganism showed a heat sensitive behaviour. The parameters calculated in this research are important to help design adequate pasteurization process when this organism is present as a contaminant.

Acknowledgements

The authors would like to thank Fundação Tropical de Pesquisas André Tosello and Rafael Guedes for the mathematical and statistical support.

References

Cerf O. (1977) A review: Tailing of survival curves of bacterial spores. *Journal of Applied Microbiology* 42, 1-19.

Franchi M.A., Serra G.E., Svilosen J. and Cristianni M. (2003) Thermal death kinetic of bacterial contaminants during cane sugar and alcohol production. *International Sugar Journal* v.105, 1259, 527-530.

Geereard A.H., Valdramidis V.P. and Van Impe J.F. (2005) GinaFit, a freeware tool to asses non-log-linear microbial survivor curves. *International Journal of Food Microbiology* 59, 185-209.

ICMSF (2005) Microorganisms in Foods 6: Microbioal Ecology of Food Commodities, ed. Kluwer Academic/Plenum Publishers, New York, p.522-527.

Mafart P., Couvert O., Gaillard S. and Leguerinel I. (2002) On calculating sterility in thermal preservation methods: application of the Weibul frequency distribution model. *International Journal of Food Microbiology* 72, 107-113.

Mathot A.G., Kihal M., Prevort H. and Divies C. (1994) Selective enumeration of *Leuconostoc* on vancomycin agar media. *International Dairy Journal* 4, 459-469.

Mossel D.A.A., Corry J.E.L., Struijkand C.B. and Baird R.M. (1995) Essentials of the Microbiology of Foods: A textbook for advanced studies, ed. John Wiley & Sons, New York, 699p.

Stumbo C.R. (1965) Thermobacteriology in food processing, ed. Academic Press, New York and London, 236p.

Calorimetric assessment of *Listeria innocua* relevant to thermal processes

T. Skåra[1,2], A. M Cappuyns[2], D. Skipnes[1], E. Van Derlinden[2], J. T. Rosnes[1], J. FM Van Impe[2], V. P Valdramidis[3]

[1] Nofima PO Box 8034, N-4068 Stavanger Norway (Torstein.Skara@nofima.no)
[2]Katholieke Universiteit Leuven, Department of Chemical Engineering, BioTeC - Chemical and Biochemical Process Technology and Control, Leuven, Belgium (Jan.vanImpe@cit.kuleuven.be)
CPMF2 – Flemish Cluster Predictive Microbiology in Foods – http://www.cpmf2.be/
[3]UCD Biosystems Engineering, School of Agriculture, Food Science and Veterinary Medicine, University College Dublin, Dublin 4, Ireland (vasilis.valdramidis@ucd.ie)

Abstract

Denaturation of the ribosome is an important inactivation mechanism of Gram-positive bacteria which can be evaluated by the use of Differential Scanning Calorimetry (DSC), in which bacterial cells concentrated by centrifugation are heated while their energy flow is recorded. Hence the microbial cell dynamics are studied in an experimental set-up different than usually chosen for inactivation studies. The validity of the results depends on factors that can affect the thermally induced changes in the DSC and the microbial inactivation kinetics in pellet form, as compared to static microbial inactivation of planktonic cells.
In this study *Listeria innocua* ATCC 33090 was preheated from 20ºC to 66-80ºC (5ºC/min), rapidly cooled to 20ºC and scanned from 20 to 120ºC. The thermograms were integrated between 60-90ºC to obtain the residual enthalpy corresponding to ribosome denaturation, showing a linear decrease with increasing dynamic pre-heating temperature. Ribosome denaturation could not be detected with preheating to 66ºC. The aspects of using DSC to elucidate inactivation mechanisms rely on the assumption of similar inactivation kinetics in the DSC samples as those used to determine thermal resistance. Based on this assumption, our results show that dynamic preheating to 66ºC should lead to an approximate log 3 reduction when linked to static inactivation experiments performed with planktonic cells (57ºC to 63ºC). Isothermal heating of pellets (62ºC and 68ºC) resulted in a log reduction of about 2-3 within one minute, but subsequent heating did not further reduce the total viable count (TVC).

Keywords: *Differential Scanning Calorimetry, Inactivation, Listeria, Ribosome denaturation*

Introduction

Listeria monocytogenes has been recommended as a target organism for thermal processing of refrigerated ready-to-eat foods. A six log reduction (e.g., 70ºC/2 min) is generally advised, also for seafood products (Rocourt *et al.* 2000). *L. innocua* is more heat resistant than *L. monocytogenes* and a well suited surrogate organism for thermal inactivation processes (Fairchild and Foegeding 1993). The thermal resistance of *L. monocytogenes* has been investigated in different foods and the environmental conditions during heating can have significant effect on the inactivation (Doyle *et al.* 2001). The prime cause of cell death related to heat exposure may vary with the severity of the stress, e.g., mild heat has been observed to cause membrane damage, and leakage of solutes to correlate with loss of viability (Lambert and Hammond 1973). At higher temperature, protein denaturation may play a major role. Ribosome denaturation is recognised as one of the inactivation mechanisms of Gram-positive bacteria. (Anderson *et al.* 1991; Bayles *et al.* 2000; Mackey *et al.* 1991). The objective of this study is to assess the inactivation of *L. innocua* ATCC 33090 by the use of both DSC and static microbial inactivation experiments.

Materials and Methods

Cultures of *L. innocua* ATCC 33090, stored frozen at -80ºC in cryovials (Microbank, Pro-Lab Diagnostics, CA), were recovered in Tryptic Soy Broth (Oxoid, Basingstoke, UK) with 0.6%

yeast extract (Merck, Darmstadt, DE) (TSBYE, 10 ml) at 37ºC over night prior to each experiment. Inoculum was prepared in TSBYE and grown to early stationary phase (12h/37ºC/150 rpm). Pellets were prepared by centrifuging the inoculum (10 mL, 8000 x g , 15 min) and resuspension in an equal volume of a cold buffer (10mM Tris-HCl, pH 7.5; 6 mM $MgCl_2$; 30 mM NH_4Cl). The cells were repelleted and the supernatant was removed.

Static inactivation of planktonic cells. Experiments were carried out with sterile glass capillary tubes containing re-suspended inoculum (100 µL, 10^9 CFU/ml) placed in a water bath (Lauda E300, Dr. R. Wobser GmbH & Co. KG, Lauda-Königshofen, DE) at static temperatures from 57ºC to 63ºC. At regular times one capillary was removed from the water bath, placed in an ice-water bath and analysed within ca. 45 minutes. Decimal serial dilutions of the samples were prepared in a TSBYE solution in order to reduce stress related to changing of medium, and surface plated on Tryptic Soy Agar (Oxoid, Basingstoke, UK) with 0.6% yeast extract (Merck, Darmstadt, DE). Plates were incubated at 30ºC for 48 hrs and colony forming units were enumerated, plates were checked after 96 hrs to ensure that all culturable cells were counted.Plates were incubated at 30ºC and colony forming units were enumerated at 48 hrs, and checked at 96 hrs to ensure that all culturable cells were counted. Each experiment was performed in duplicate.

Static inactivation of pellet. Pellet (± 70 mg) was transferred to glass tubes (Ø=4 mm) and heated (62 and 68ºC) in a water bath (GR150-S12, Grant Instruments Ltd, Shepreth, UK). At appropriate time intervals samples were removed and analysed as described above. Each experiment was performed in triplicate.

Dynamic heating in Differential Scanning Calorimetry. Pellet (± 70 mg) was transferred into a stainless steel DSC crucible (Medium pressure - 120 µL, Mettler-Toledo GmbH Analytical, Schwerzenbach, CH) and hermetically sealed. Preheating was carried out in a DSC (DSC 1 system, Mettler-Toledo GmbH Analytical, CH) from 20ºC to end temperature 66-80ºC at a rate of 5ºC/min. After preheating, the samples were immediately cooled to 20ºC (300ºC/min) and scanned from 20 to 120ºC (5ºC/min). The area below the thermogram was integrated between 60-90ºC, using the instrument's software (Star^e Excellence Software, Mettler-Toledo GmbH Analytical, Schwerzenbach, CH).

Results and Discussion

The inactivation of planktonic cells in capillary glass tubes showed a log-linear decrease. The *D*-value was calculated for each experiment. Based on the calculated D-values at different temperatures the *z*-value was estimated to 4.7°C. Inactivation kinetic studies of a similar pellet as used for DSC were performed in glass tubes.

The pellet showed very different kinetics compared to inactivation of the planktonic cells. From an initial TVC of approximately 10^{11} CFU the isothermal treatments of pellets resulted in a reduction of about 2-3 log within the first minute at the temperatures investigated (62 and 68ºC), as shown in Figure 1.

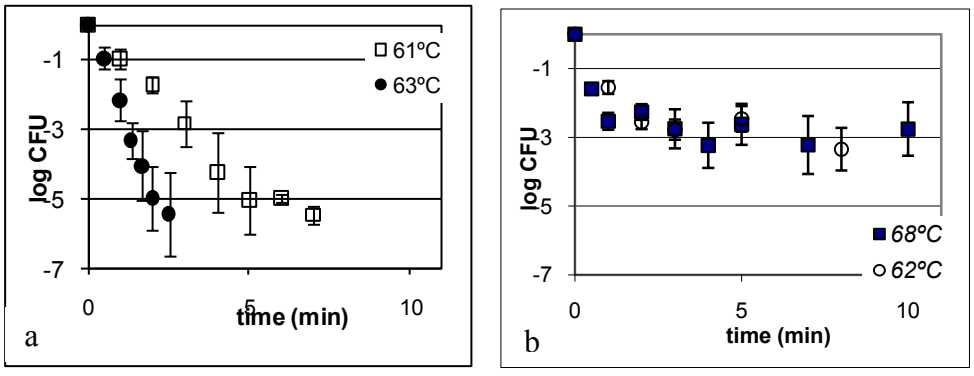

Figure 1: Inactivation (log reduction in function of time) of *Listeria innocua* for (a) plaktonic cell in capillary tubes (b) pellet in glass tubes.

Subsequent heating beyond 1 minute did not further significantly reduce the TVC. In a study with pellets of *Escherichia coli* cells in polypropylene tubes, log-linear inactivation was observed for isothermal heating of pellet (Lee and Kaletunc 2002). This may be related to the water content (83% of the *E. coli* pellet, 79% for our *L. innocua* pellet) or the species.
In our experiment, pellets were also analysed in the DSC and thermograms were obtained during heating from 20ºC to 120ºC, after dynamic pre-heating to 66, 68, 70, 72, 74, 76 and 78ºC at 5ºC/min. Examples are shown in Figure 2. The most prominent changes in the thermograms due to preheating took place between 60 and 90ºC, with a peak around 76ºC which could be associated to the denaturation temperature of the 50S subunit and the 70S particle of the ribosome (Bayles *et al.* 2000).

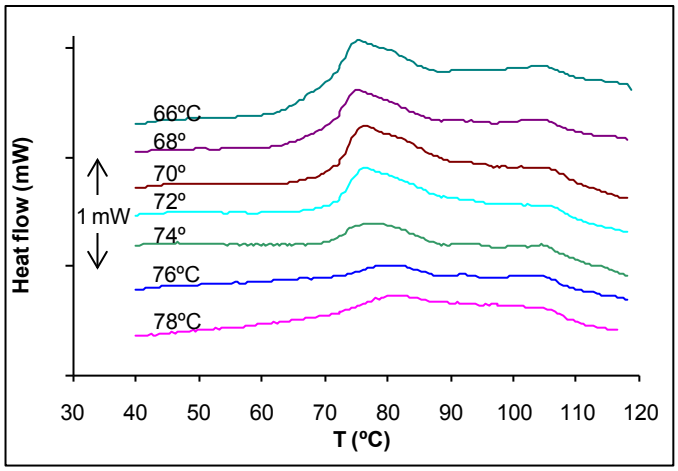

Figure 2: Typical thermograms obtained with preheating temperatures from 66 to 78ºC.

By integration of the thermogram in this temperature region the remaining enthalpy, ΔH [mJ/mg], could be determined for each dynamic profile; indicating to what degree the sample has absorbed energy, non reversibly, during the pre-heating. The remaining enthalpy showed a linearly decreasing trend with increasing pre-heating temperature. Preheating performed to temperatures below 66ºC did not show any increase in energy uptake during the subsequent scan to 120ºC, as compared to 66ºC. Hence it appears that the first ribosome denaturation takes place during treatment to temperatures higher than 66ºC. It should be noted, however, that it is not the total denaturation of the ribosome or other active molecules that is determining inactivation of microorganisms, but the enthalpy difference between the active and inactive states of the system.
Based on the inactivation kinetics (*D* and *z* values) of planktonic cells in capillary tubes, the microbial inactivation can be simulated by using the dynamic form of the linear model:

$$\frac{d\log_{10} N(t)}{dt} = -\frac{1}{D(T)} \qquad (1)$$

with $d\log_{10}N/dt$ being the change in surviving organisms per unit time. The relation between the value of the decimal reduction $D(T)$ at the actual temperature T was derived based on the inactivation experiments of planktonic cells:

$$\mathrm{Log}_{10}D(T) = -0.2121\ T + 13.055 \qquad (2)$$

The temperature evolution during the dynamic pre-treatment of the DSC experiments is described by:

$$T = 20 + 5\ t \qquad (3)$$

The inactivation caused by the dynamic heating profile could be calculated and used to estimate an isothermal heating temperature giving rise to the same inactivation as the dynamic heating profile within the same time span. Calculated this way, a dynamic heating from 20 to 66ºC at 5ºC/min will correspond to 59.6ºC for 9.2 minutes, although this calculation is solely related to inactivation, and not to ribosome denaturation. Although the DSC results indicate no enthalpy change during dynamic preheating to 66ºC, the available data cannot support to suggest that this is also the case at the equivalent isothermal temperature (59.6ºC for 9.2 minutes). Collection of isothermal calorimetric data might contribute to further interpreting this specific mechanism. Furthermore, very high cell densities of nonsporing micro-organisms, like the pellet samples used in this study, are associated with increased heat resistance (Hansen and Riemann 1963), as is also shown in Figure 1.
If independent of the specific form of the cells (pellet or planktonic form) then no denaturation of the ribosome would be expected during the studied heating process, which is in accordance with previous findings indicating that mild heat treatment primarily cause inactivation due to cell membrane damage (Lambert and Hammond 1973).

Conclusions

Our results indicate that in order to estimate the effects of the denaturation of the ribosomes, measured by the energy uptake during dynamic heating (5ºC/min), on thermal inactivation of *L. innocua* ATCC 33090, attention should be given to the specific form of the cells used in the analyses. The relationship between thermal death of planktonic cells and thermograms obtained from dynamic heating of pellet between 60-90ºC are of interest to further understand a major inactivation mechanism of *Listeria* species. Thermograms from isothermally pre-heated pellets would, however, further strengthen the relationship and the links between thermodynamic and microbial kinetic data obtained from isothermal inactivation studies.

Acknowledgements

This work was supported by The Research Council of Norway (project no. 186905), by project PFV/10/002 (Center of Excellence OPTEC-Optimization in Engineering) of the Research Council of the K.U.Leuven, project KP/09/005 (www.scores4chem.be) of the Industrial Research Fund, and the Belgian Program on Interuniversity Poles of Attraction, initiated by the Belgian Federal Science Policy Office. E. Van Derlinden is supported by postdoctoral grant PDMK/10/122 of the K.U.Leuven Research Fund. J. Van Impe holds the chair Safety Engineering sponsored by the Belgian chemistry and life sciences federation essenscia.

References

Anderson W.A., Hedges N.D., Jones M.V. and Cole M.B. (1991) Thermal inactivation of *Listeria monocytogenes* studied by differential scanning calorimetry. *Journal of General Microbiology* 137, 1419-1424.

Bayles D.O., Tunick M.H., Foglia T.A. and Miller A.J. (2000) Cold shock and its effect on ribosomes and thermal tolerance in *Listeria monocytogenes*. *Applied and Environmental Microbiology* 66(10), 4351-4355.

Doyle M.E., Mazzotta A.S., Wang T., Wiseman D.W. and Scott V.N. (2001) Heat resistance of *Listeria monocytogenes*. *Journal of Food Protection* 64(3),410-429.

Fairchild T.M. and Foegeding P.M. (1993) A proposed nonpathogenic biological indicator for thermal inactivation of *Listeria monocytogenes*. *Applied and Environmental Microbiology* 59(4), 1247-1250.

Hansen N.H. and Riemann H. (1963) Factors affecting the heat resistance of nonsporing organisms. *Journal of Applied Bacteriology* 26(3),314-333

Lambert P.A. and Hammond S.M. (1973) Potassium fluxes - First indications of membrane damage in microorganisms. *Biochemical and Biophysical Research Communications* 54(2), 796-799.

Lee J. and Kaletunc G. (2002) Calorimetric determination of inactivation parameters of micro-organisms. *Journal of Applied Microbiology* 93(1), 178-189.

Mackey B.M., Miles C.A., Parsons S.E. and Seymour D.A. (1991) Thermal denaturation of whole cells and cell components of *Escherichia coli* examined by differential scanning calorimetry. *Journal of General Microbiology* 137, 2361-2374.

Effect of a gelified matrix on the heat inactivation of *E. coli* and *Salmonella* Typhimurium

E.G. Velliou [1,2], E. Van Derlinden[1,2], L. Mertens[1,2], A. Cappuyns[1,2], A.H. Geeraerd[1,3], F. Devlieghere[1,4], J.F.M. Van Impe[1,2]

[1]CPMF2-Flemish Cluster Predictive Microbiology in Foods –http://www.cpmf2.be/
[2]BioTeC-Chemical and Biochemical Process Technology and Control, Department of Chemical Engineering, Katholieke Universiteit Leuven, W. de Croylaan 46, B-3001, Leuven, Belgium.
[3]Division of Mechatronics, Biostatistics and Sensors (MeBioS), Department of Biosystems, Katholieke Universiteit Leuven, W. de Croylaan 42, B-3001, Leuven, Belgium.
[4]Laboratory of Food Microbiology and Food Preservation, Department of Food Technology and Nutrition, Ghent University, Coupure Links 653, B-9000 Ghent, Belgium.

Abstract

The objective of this work is to investigate and further understand the effect of a solid(like) environment on the heat tolerance of bacteria, i.e., *Escherichia coli* K12 and *Salmonella* Typhimurium. Stationary phase bacterial cultures were gained after growth at 37^{o}C in laboratory medium which contained 1.5% (w/v) or 2.5% (w/v) xanthan gum. Afterwards, heat inactivation experiments took place at 54^{o}C. Generally, increased heat tolerance, i.e., slower inactivation, and higher viability, was observed in the solid matrix compared to the liquid system. Similar heat resistance was observed for 1.5% (w/v) and 2.5% (w/v) xanthan gum. The structure seems to protect the bacterial cells from heat stress, leading to an increased survival compared to the liquid systems. Results indicate that there is no clear effect of the concentration of the gelling agent on the microbial heat tolerance.

Key-words: heat inactivation, E. coli, Salmonella, colony formation, solid(like) matrix

Introduction

Generally, food products can be either *liquid* or *solid(like)*. In a liquid system microorganisms grow planktonically whereas bacteria are immobilized and grow as colonies in a *solid* environment. Due to the colony formation, diffusion of nutritional components into the colony and of cellular metabolites out of the colony is mainly based on (limited) diffusion. Therefore, microbial behaviour in a solid(like) matrix differs from the one in a liquid system.

The majority of predictive models, which describe growth, survival and/or inactivation of microorganisms as a function of environmental conditions, are based on studies in liquid systems. These models can efficiently predict the microbial behaviour in liquid foods or oil in water emulsions (Wilson *et al*. 2002). However, an accurate prediction in a solid(like) matrix is not guaranteed.

As opposed to the increasing research conducted on the effect of a solid(like) matrix on microbial growth, limited research has taken place with respect to thermal inactivation in a solid(like) system. This work studies the effect of a solid(like) environment on the heat tolerance of *Escherichia coli* K12 and *Salmonella* Typhimurium.

Materials and Methods

Inoculum preparation

E. coli K12 MG1655 and *Salmonella* Typhimurium stock cultures were stored at -80 ^{o}C in Brain Heart Infusion (BHI) and Tryptic Soy Broth (TSB), respectively (Oxoid Limited, Basingstoke, UK) with 25% (v/v) glycerol (Acros Organics, NJ, USA). For the preparation of the inoculum, a loopful of the stock culture was transferred in 20 mL of BHI/TSB and was incubated at 37 ^{o}C on a rotary shaker (175 rpm) for 9.5 h. Next, 20 μL of this cell suspension was transferred to 20 mL of fresh BHI/TSB and incubated 15 h under the same conditions, until the stationary phase (10^{9} CFU/mL) was reached.

Preparation of gelified matrix

Xanthan gum, chosen as the gelling agent, was added in BHI/TSB at a concentration of 1.5% or 2.5% (w/v) and vigorously stirred for at least 30 min (OST 20 basic, IKA Werke GmbH & Co). This mixture was autoclaved at 121 ^{o}C for 15 min and entrapped air bubbles were removed by centrifugation, before as well as after autoclaving.

Inoculation and growth in the gelified matrix

The (liquid) inoculum –prepared as described above– was diluted in order to obtain an initial inoculum level of 10^4 CFU/mL and added in tubes with 10 mL of gelified medium. Next, these tubes were centrifuged for homogenization and removal of entrapped bubbles. Afterwards, they were incubated at 37 ^{o}C for 24 h until the population reached stationary phase.

Microbial thermal inactivation

Static inactivation experiments took place in sterile glass tubes in which a volume of 2 mL (prepared as described above for the liquid and the gelified matrix) was pipetted. Tubes were immersed in a water bath (GR150-S12, Grant Instruments Ltd, Shepreth, UK) at 54 ^{o}C. The time needed for the internal temperature of the tube to reach 54 ^{o}C was tested with the use of a thermosensor (Keithley 2700 multimeter) and was approximately 30 seconds and 3 minutes for the liquid broth and the gelified matrix, respectively. Inactivation experiments started at this time instance. At regular times, tubes were removed from the water bath, placed in an ice-water bath and analyzed within approximately 45 min. Decimal serial dilutions of the samples were prepared in a BHI/TSB solution and surface plated on BHI/TSB agar (1.2% (w/v)) using a Spiral Plater (Eddy Jet IUL Instruments, Barcelona, Spain). The samples were pipetted approximately from the centre of the tube with special pipettes for viscous media (MICROMAN, Gilson, Middleton, WI, USA). Plates were incubated for 24 h at 37^{o}C and colony forming units (CFU) were enumerated. The detection limit was 3 log CFU/mL - because of the solid(like) nature of the samples, it is not possible to plate without diluting, therefore the detection limit is rather high-. All experiments were performed at least in duplicate.

Mathematical analysis

The experimental data (cell density data) were *log*-transformed and plotted as a function of time. The inactivation model of Geeraerd *et al.* (2000) was fitted to the data (Equation 1)

$$N = N_0 \cdot \exp\left(-k_{\max} \cdot t\right) \cdot \frac{\exp\left(k_{\max} \cdot S_\iota\right)}{1 + \left(\exp\left(k_{\max} \cdot S\iota\right) - 1\right) \cdot \exp\left(-k_{\max} \cdot t\right)}$$

with N [CFU/mL] the cell population, $N(0)$ [CFU/mL] the initial cell population, k_{max} [1/min] the maximum specific inactivation rate, $S\iota$ [min] the shoulder period and t [min] the time.
For data analysis MatLab® Version 7.4 (The Mathworks, Inc., Natick, USA) was used. The mathematical model was fitted globally to all data sets obtained under the same experimental conditions,, i.e., one k_{max} value was determined to describe all data starting from the same initial cell level. The SSE was minimized using the *lsqnonlin* routine of the Matlab Optimization Toolbox Version 3.0.2.

Results and discussion

The experimental data followed a log-linear trend with a preceding shoulder and/or a preceding tail, depending on the conditions. Experimental data were described after parameter identification using the inactivation model of Geeraerd *et al.* (2000). Changes in

thermotolerance are defined as a prolongation of the shoulder and/or a reduction of the inactivation rate and/or the formation of a tail.
In order to check whether bacterial heat stress adaptation takes place in the gelled matrix during the temperature adjustment time, 3 min in the solid(like) medium compared to 0.5 min in the liquid, a stationary phase liquid culture was added in the solid(like) medium medium right before inactivation at 54 °C. In this case, there were no colonies in the solid(like) matrix, but individual cells –since growth took place panktonically in liquid BHI broth-. Inactivation kinetics were identical to the ones obtained for a liquid system, indicating that no stress adaptation occurs at the beginning of the inactivation in the gelled matrix (data not shown).

Escherichia coli K12

The survival of *E. coli* at 54 °C in a gelled medium is significantly higher compared to the liquid system, i.e., inactivation curves from the xanthan system are in almost all cases situated above the inactivation curve in plain BHI. This is reflected in a lower inactivation rate, i.e., a slower inactivation, compared to the liquid BHI broth (Figure 1 – left plot). No difference in the heat tolerance was observed in the xanthan system when increasing the concentration of xanthan from 1.5 % (w/v) to 2.5 % (w/v), as can be seen in Figure 1 (right plot).

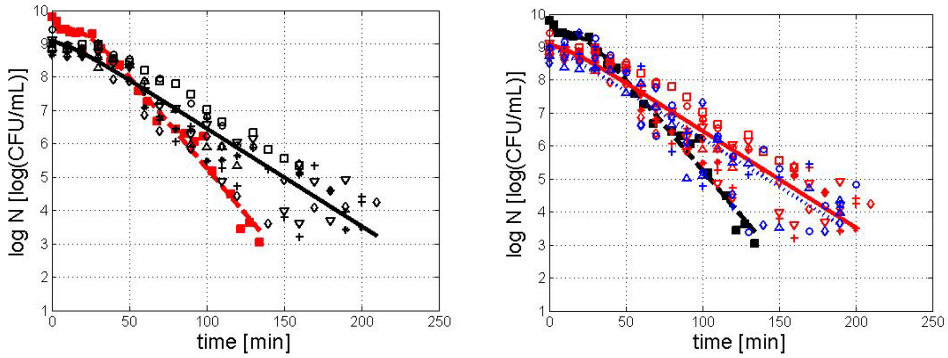

Figure 1: Thermal inactivation curves of *E. coli* and global fits of Geeraerd et al. (2000) inactivation model at 54°C. (Left) **(■, --)** normal BHI broth and (o, Δ, ◊ , +, □, v, *, -) gelified matrix (1.5 % (w/v)). (Right) (■, -,-) normal BHI broth, (o, Δ, ◊, +, □, v, *, -) gelified matrix (1.5 % (w/v)) and (o, Δ, +, ◊, ···) gelified matrix (2.5 % (w/v)).

Salmonella Typhimurium

Similar results were obtained for *Salmonella* Typhimurium. More specifically, when *Salmonella* was inactivated in a gelified matrix (xanthan gum in TSB), a higher heat tolerance was observed at 54 °C, i.e., a lower heat inactivation rate, compared to liquid TSB. No significant difference was observed in the inactivation kinetics for an increase of the concentration of the gelling agent from 1.5 to 2.5 % (w/v) (Figure 2, right plot).

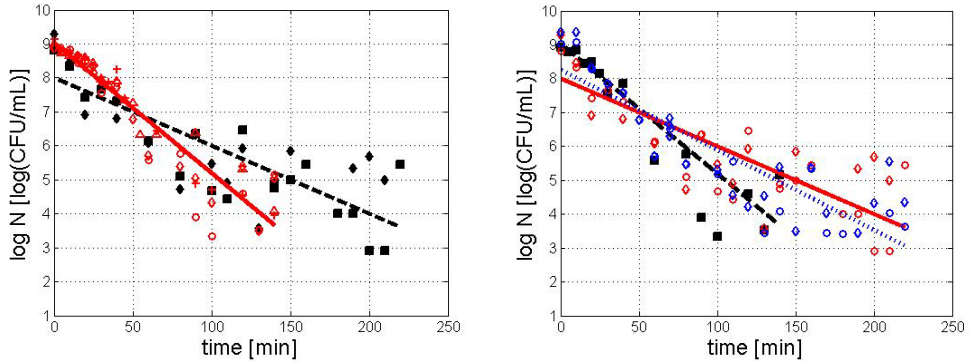

Figure 2: Thermal inactivation curves of *Salmonella* Typhimirum and global fits of Geeraerd et al. (2000) inactivation model at 54°C. (Left) **(*, -)** normal BHI broth and (o, Δ, ◊ , +, □, v, *, --) gelified matrix (1.5 % (w/v)). (Right) (■, --,) normal BHI broth, (o, Δ, ◊, +, □, v, *, -) gelified matrix (1.5 % (w/v)) and (o, Δ, +, ◊, ···) gelified matrix (2.5 % (w/v)).

Generally, our findings indicate that the microbial heat tolerance in the selected solid(like) environment is higher compared to the liquid system. This observation indicates that cells within a colony are better protected against heat stress than planktonically growing cells. Possibly, the higher heat stress resistance is related to a self induced *acid stress response*. The solid character of the environment not only results in the formation of colonies, but also in accumulation of the produced (acetic) acid in and around the colony. The high acid concentration results in a suboptimal pH, which is lower in the inner part of the colony, compared to the outer part due to limited diffusion (Malakar *et al.* 1999). The lower, suboptimal, pH most likely triggers the acid tolerance response (Davis *et al*. 1996). A myriad of studies has already proven that (pre-)exposure to acid can increase the general microbial stress resistance, see, e.g., Leyer and Johnson (1993), Tetteh and Beuchat (2003), Velliou *et al*. (2010). This phenomenon is defined as *cross protection* (Juneja *et al*. 2003) and its occurrence in a (complex) food system is of significant importance for microbiological safety issues.

Conclusions

As a general conclusion, it is observed that the gelified environment protects the *E. coli* and *Salmonella* Typhimurium cells from heat stress, leading to an increased survival compared to the liquid system. Results indicate that there is no clear effect of the concentration of the gelling agent on the microbial heat tolerance.
This work is a first step towards more detailed studies that investigate the effect of immobilization on microbial inactivation dynamics. Investigating and understanding this effect is of great importance for microbial safety issues in the food industry, as most food systems are solid(like).

Acknowledgements

This work was supported by project PFV/10/002 (Center of Excellence OPTEC-Optimization in Engineering) of the Research Council of the K.U.Leuven, Knowledge Platform KP/09/005 (www.scores4chem.be) of the Industrial Research Fund, and the Belgian Program on Interuniversity Poles of Attraction, initiated by the Belgian Federal Science Policy Office. E. Van Derlinden is supported by postdoctoral grant PDMK/10/122 of the K.U.Leuven Research Fund. J. Van Impe holds the chair Safety Engineering sponsored by the Belgian chemistry and life sciences federation essenscia.

References

Davis M.J., Coote P.J. and O' Byrne P. (1996) Acid tolerance in *Listeria monocytogenes*: the adaptive acid tolerance response (ATR) and growth-phase-dependent acid resistance. *Microbiology* 142, 2975-2982.

Geeraerd A.H., Herremans C.H. and Van Impe J.F. (2000) Structural model requirements to describe microbial inactivation during a mild heat treatment. *International. Journal of Food Microbiology* 59, 185-209.

Juneja V.K. and Novak J.S. (2003) Adaptation of Foodborne Pathogens to Stress from Exposure to Physical Intervention Strategies. In: Yousef, A.E. and Juneja, V.K. (eds.) *Microbial Stress Adaptation and Food Safety*, p.159-211, CRC Press, Boca Raton.

Leyer G.J. and Johnson E.A. (1993) Acid adaptation induces cross-protection against environmental stresses in *Salmonella typhimurium*. *Applied & Environmental Microbiology* 59, 1842-1847.

Malakar P.K., Brocklehurst T.F., Mackie A.R., Wilson P.D.G., Zwietering M.H. and van't Riet K. (2000) Microgradients in bacterial colonies: use of fluorescence ratio imaging, a non-invasive technique *International Journal of Food Microbiology* 56, 71-80.

Tetteth G.L. and Beuchat R. (2003) Exposure of *Shigella flexneri* to acid stress and heat shock enhances acid tolerance. *Food Microbiology* 20, 179-185.

Velliou E., Van Derlinden E., Cappuyns A., Nikolaidou A., Geeraerd A., Devlieghere F. and Van Impe J. (2011). Towards the quantification of the effect of acid treatment on the heat tolerance of Escherichia coli K12 at lethal temperatures. *Food Microbiology* (accepted).

Wilson P.D.G., Brocklehurst T.F., Arino S., Thuault D., Jakobsen M., Lange M., Farkas J., Wimpenny J.W.T. and Van Impe J.F., (2002) Modelling microbial growth in solid(like) foods: towards a unified approach. *International Journal of Food Microbiology* 73, 275-289.

A theoretical assessment of microbial inactivation in thermally processed fruits in syrup in still cans

A. Dimou, N.G. Stoforos, S. Yanniotis

Department of Food Science and Technology, Agricultural University of Athens, Greece

Abstract

Thermal processing is a widely used and an extensively studied method for food preservation. Destruction of spoilage agents (e.g., microbial spores) during thermal processing of foods is inevitably accompanied by quality degradation. Thus, for optimum product quality retention, there is a need for accurate design of a thermal process. Modeling and simulation of food processes is an effective tool for process optimization. The objective of this work was to apply Computational Fluid Dynamics in studying the flow field and the temperature profile, as well as microbial inactivation, in thermally processed still cans filled with peaches halves in sugar syrup. The software FLUENT 6.3.26, 2006© with 3-D, double precision, pressure – based, laminar flow, natural convection was used to solve numerically the system of governing equations for mass, momentum and energy conservation, applied in finite volumes for the system under investigation, coupled with first order microbial inactivation kinetics. The slowest heating zone during the heating cycle and the slowest cooling zone during the cooling cycle of a thermal process were investigated. The location of the critical zone, that is the region in the product receiving the least effects of the process, in terms of microbial destruction, was identified. For example, for the case of a metal can (7.6 cm in diameter, 10.9 cm in height) filled with 20% sugar syrup and five peach halves, symmetrically located on the can's central axis, the critical point, as far as the destruction of microorganisms (characterized by a z value of 10 °C) is concerned, was located at the center of the second peach half from the can bottom. It was assumed that the can was initially at 25 °C and thereafter heated for 30 min in boiling water at 100 °C followed by cooling in water at 25 °C with an infinite heat transfer coefficient being used for both heating and cooling cycles.

An asymmetric model dedicated to germination of fungi

P. Dantigny

Laboratoire de Génie des Procédés Microbiologiques et Alimentaires, Agro-Sup Dijon, Université de Bourgogne, France. (phdant@u-bourgogne.fr)

Abstract

All models used in the field of predictive mycology were previously developed for bacteria. This study presents a new model dedicated to germination of fungi. Attention was focused on the capability of the model to provide an accurate estimation of the germination time. This parameter was defined as the time at which half of the viable spores had germinated. The percentage of germinated spores, P(%), depended on the maximum percentage of germination P_{max} (%), the germination time, τ (h) and a design parameter, d (-) according to : $P = P_{max}\left[1 - \frac{1}{1+\left(\frac{t}{\tau}\right)^d}\right]$. In contrast to the logistic model, the new model is by essence asymmetric. Therefore, its use is consistent with skewed distributions of the individual germination times that were observed experimentally in many cases. In contrast to the Gompertz equation, the germination time is one of the parameters of the asymmetric model. Thus the germination time can be accurately determined by the new model. A dimensionless analysis showed that different shapes of the curves (P/P_{max}) *versus* (t/τ) can be obtained depended on the design parameter, d. A new data set for *Aspergillus niger*, percentage of germination *vs* time was used to compare the models (i.e., asymmetric, Gompertz and logistic) based on goodness of fit. It was shown that the design parameter was in the range 3-45. Greater this parameter is, less is the variance of the germination time among a population around the mean.

Keywords: *germination, model, fungi, mould, Aspergillus niger*

Introduction

For fungi germination can be considered as the main step to focus on, because a product is spoiled as soon as visible hyphae can be observed. A spore is considered to have germinated when the length of the longest germ tube is greater than or equal to the greatest dimension of the swollen spore (Dantigny *et al.* 2006). But since spores do not germinate at the same time, the distribution of the germination time amongst a population of spores should be considered. From the cumulative frequencies distributions, germination curves can be drawn (Nguyen *et al*. 2010). The shape of the germination curves, percentage of germinated spores *versus* time, would therefore depend on these distributions. Right skewed distributions were observed experimentally, thus leading to asymmetric germination curves (Judet *et al*. 2008).

Even assuming that the maximum percentage of viable spores equals 100%, the probability of examining the population of spores when exactly 50% of the spores had germinated is close to zero. Therefore the percentage of germinated spores, P(%), is plotted against time and kinetic models are used to estimate t_g. Many mycologists agreed to define the germination time, t_g (h), of a population of spores as the time required to obtain a percentage of germinated spores equal to 50% of the viable spores (Huang *et al.* 2001). A practical interest of the definition is whatever the percentage of viable spores, the germination time can be determined. For example, if the germination time is defined as the time required to have 50% of the inoculated spores, this time cannot be determined if the percentage of viable spores is 40% only. In contrast, 50% of the viable spores is synonymous to 20% of the inoculated spores.

The logistic model and the Gompertz equation that were used previously for fitting germination curves for fungi, were tested against many data sets available in the literature (Dantigny *et al*. 2007). Based on RMSE values, it was impossible to determine which one of the models performed better than the other one. The Gompertz model is asymmetrical but the

germination time cannot be determined directly thus leading to inaccuracy of this parameter. In contrast, the logistic equation provided accurate estimations of P_{max} and t_g, but concerns were raised because attempting to fit the symmetrical logistic function to actual asymmetrical data sets seemed inappropriate. Recently, a new asymmetric model based on the maximum percentage of germination and the germination time was described (Dantigny *et al.* 2011).

The objective of this presentation was to highlight the advantages of the new model. Firstly, the characteristics of the asymmetric model were detailed. Secondly, the goodness of fit of the model was tested against the Gompertz and the logistic equations. Thirdly, the model was fit to germination data for *Aspergillus niger* (Gougouli and Koutsoumanis 2010).

Materials and Methods

Logistic model

The logistic function is: $$P = \frac{P\max}{1+\exp[k(\tau - t)]} \quad (1)$$

where P_{max} (%) is the asymptotic P value at $t \to +\infty$, τ (h) is the inflection point where P equals half of the P_{max}, t is the time (h) and k (h^{-1}) is related to the slope of the tangent line through the inflection point. The slope of the tangent line at τ, is equal to $k.P_{max}/4$. The germination time t_g is equal to τ.

Gompertz model

The modified Gompertz equation is: $$P = A.\exp.(-\exp\left[\frac{\mu_m.e(1)}{A}(\delta - t) + 1\right]) \quad (2)$$

where A (%) is the asymptotic P value at $t \to +\infty$, μ_m (% h^{-1}) is the slope term of the tangent line through the inflection point (t_i) as defined further, δ (h) is the t-axis intercept of the tangent through the inflection point and t is the time (h).

The inflection point is: $t_i = \delta + A/(\mu_m\, e(1))$.

The germination time t_g (h) can be determined for P = A/2 as: $$t_g = \delta - \frac{[\ln(-\ln(0.5)) - 1]A}{\mu_m e(1)} \quad (3)$$

Asymmetric model

The asymmetric model : $$P = P_{max}\left[1 - \frac{1}{1+\left(\frac{t}{\tau}\right)^d}\right] \quad (4)$$

is derived from the non competitive inhibition model described by Yano and Koya (1973). P_{max} is the asymptotic P value at $t \to +\infty$, τ(h) the point where P equals half of the P_{max}. The germination time t_g is equal to τ. It was shown that whatever the value of d, the model was asymmetric (Dantigny *et al.* 2011). In practice, only values of d greater than 3 can represent the shape of germination curves.

Results and Discussion

Goodness of fit

Overall the logistic model performed better than the Gompertz and the asymmetric model, respectively, Table 1. The asymmetric model was characterized by smaller RMSE values in only 2 cases out of 10. But, in all the other cases, the asymmetric was consistently ranked second, with RMSE values very close (less than 17%) to that of the best model. These results indicate that the asymmetric model is a good trade-off between the other models and suggest its capability to adjust to either apparent symmetric and asymmetric germination curves (Figure 1).

Table 1: Determination of RMSE values by fitting the germination data of *A. niger* (data from Gougouli and Koutsoumanis 2010) to different models (bold values indicated the best goodness of fit).

Temperature	Model		
(°C)	Logistic	Gompertz	Asymmetric
10.5	4.51	**3.77**	3.80
12.5	1.57	**1.39**	1.54
15	**8.50**	9.85	8.60
19.5	**5.18**	5.84	5.25
25.5	**8.81**	9.69	8.95
30	2.57	2.70	**2.41**
35	**2.04**	3.46	2.09
37	**5.97**	7.13	6.14
40.1	5.70	**4.60**	5.35
41.4	1.17	1.29	**0.646**

Estimation of the parameter values

In all cases, the asymmetric model provided estimations of the maximum percentage of germinated spores that did not exceed 100% significantly. This was also observed for the other models (not shown). The estimation of the germination τ, was very accurate. With the notable exception of 10.5°C, the standard error was less than equal to 0.15h. This result is very important because a good accuracy of the germination time would allow to demonstrate significant effect of experimental conditions on the germination of fungi. The values of d were greater than 15, except at 10.5°C. The germination curves were very sharp thus suggesting that the conidia of *A. niger* did germinate at almost the same time.

Table 2: Parameter estimates obtained by fitting the germination data of *A. niger* (data from Gougoulis and Koutsoumanis 2010) to the asymmetric model.

Temperature	Parameter estimates : value (se)		
(°C)	P_{max} (%)	τ (h)	d (-)
10.5	102 (3.12)	207 (4.98)	3.96 (0.321)
12.5	98.6 (0.690)	73.9 (0.103)	30.5 (2.17)
15	100 (4.39)	32.1 (0.150)	43.1 (7.49)
19.5	100 (2.15)	17.9 (0.101)	22.9 (2.55)
25.5	101 (5.09)	11.2 (0.130)	17.8 (2.81)
30	98.8 (1.02)	7.88 (0.0214)	23.6 (1.18)
35	99.4 (0.928)	6.85 (0.0183)	20.3 (0.874)
37	100 (2.34)	7.06 (0.0502)	19.1 (2.05)
40.1	101 (3.08)	8.00 (0.106)	13.7 (2.50)
41.4	100 (0.395)	9.95 (0.0144)	16.3 (0.347)

Conclusions

Based on RMSE values, it was impossible to determine which model performed better, because this was dependent on the experimental conditions. It should be reminded that one of the major roles of a model is to provide accurate estimations of a parameter that cannot be determined easily. The asymmetric model can be used easily by mycologists because it is based on biological parameters. For germination of a population of spores, the widely accepted parameter amongst mycologists is the germination time. The asymmetric model gave accurate estimations of this parameter, in addition to the percentage of viable spores, P_{max}. The new model proved also versatile, as it can be adjusted to either apparent symmetric or asymmetric germination data. This versatility was obtained through the design parameter d. Depending on temperature, the values of d varied in the range 3-45. The value of d did not depend on the other parameters and can be related to the variance of the germination time

among a population of spores. The greater the parameter d, the less was the variance of the germination time.

In the present study, only one example of the potential applications of the equation was shown. There are many possibilities that the equation can be used, maybe after some transformations, to model inhibition or inactivation kinetics observed not only in fungi but also in bacteria or other organisms.

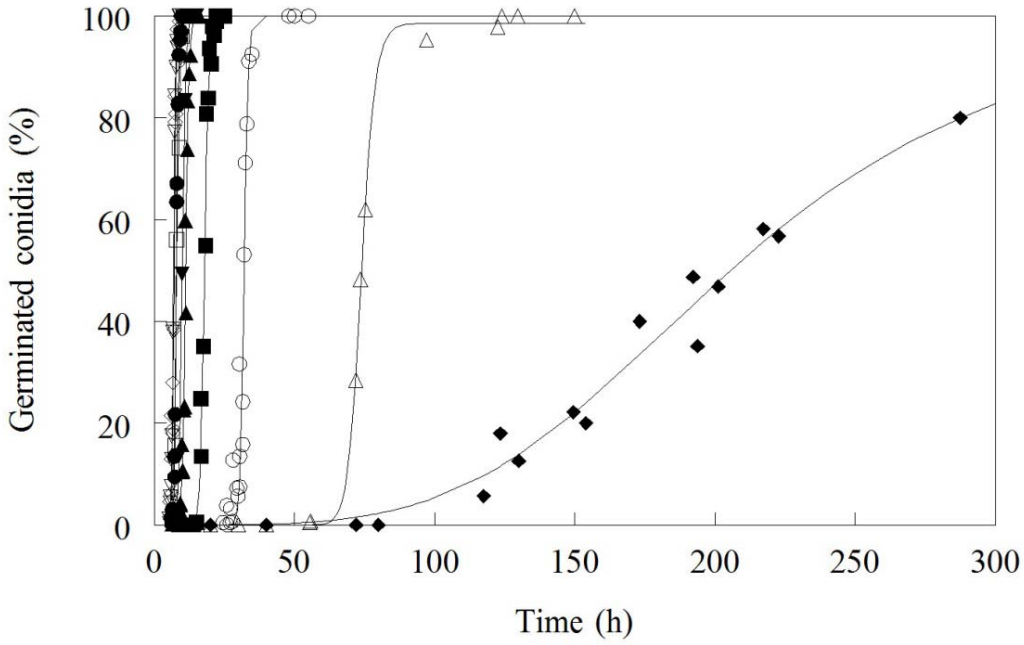

Figure 1: Germination curves obtained for *A. niger* at ◆ 10.5°C, △ 12.5°C, ○ 15°C, ■ 19.5°C, ▲ 25.5°C, ● 30°C, ▽ 35°C, ◇ 37°C, □ 40.1°C and ▼ 41.4°C by the asymmetric model (data from Gougouli and Koutsoumanis 2010)

Acknowledgements

Kostas Koutsoumanis is gratefully acknowledged for providing the experimental data.

References

Dantigny P., Bensoussan M., Vasseur V., Lebrihi A., Buchet C. Ismaili-Alaoui M., Devlieghere F. and Rousssos S. (2006) Standardisation of methods for assessing mould germination: a workshop report. *International Journal of Food Microbiology* 108, 286-291.

Dantigny P., Marín S., Beyer M. and Magan N. (2007) Mould germination: data treatment and modelling. *International Journal of Food Microbiology* 114, 17-24.

Dantigny P., Nanguy S., P-M., Judet-Correia D. and Bensoussan M. (2011) A new model for germination. *International Journal of Food Microbiology* 146, 176-181.

Gougouli M. and Koutsoumanis K. (2010) Modelling fungal spores germination at constant and dynamic temperature conditions. 22nd International ICFMH Symposium Food Micro 2010, Copenhagen 30th August-3rd September 2010, Denmark,, p. 121

Huang Y.J., Toscano-Underwood C., Fitt, B.D.L., Todd A.D., West J.S., Koopmann B. and Balesdent M.H., (2001) Effects of temperature on germination and hyphal growth from ascospores of A-group and B-group *Leptospaeria maculans* (phoma stem cancer of oilseed rape). *Annals of Applied Biology* 139, 193-207.

Judet D., Bensoussan M., Perrier-Cornet J-M. and Dantigny P. (2008) Distributions of the growth rate of the germ tubes and germination time of *Penicillium chrysogenum* conidia depend on water activity. *Food Microbiology* 25, 902-907.

Nguyen L., Bodiroga D., Kelemen R., Joo J. and Gwinn K.D. (2010) Modeling the effects of cymene on the distribution of germination and growth of *Beauvaria bassiana*. http://arxiv.org/PS_cache/arxiv/pdf/1010/1010.0919v1.pdf. (accessed 18 November, 2011).

Yano T. and Koya S. (1973) Dynamic behaviour of the chemostat subject to product inhibition. *Journal of General Applied Microbiology* 19, 97-114.

Influence of humidity, time of storage and temperature on the germination time of *Penicillium chrysogenum*

S. Nanguy, P. Dantigny

Laboratoire de Génie des Procédés Microbiologiques et Alimentaires, Agro-Sup Dijon, Université de Bourgogne, France. (snanguy@yahoo.fr and phdant@u-bourgogne.fr)

Abstract

In most of the studies dedicated to fungi, germination experiments were carried out immediately after spores were produced and harvested. Very few studies were concerned with the effect of storage conditions on the germination of fungal spores. After spores are disseminated there is a period of time, usually called storage, where the environmental conditions are not favorable enough to allow germination. This period of time may increase the germination time τ.

The effects of relative humidity, RH, time of storage, t and temperature, T on τ were assessed according to a Doehlert design in the range, 20-100%, 2-28 days and 5-25°C, respectively. In the experimental domain, the main factors that affected the germination time were by decreasing order of importance, RH, t and T. An increase of the germination time was shown for *P. chrysogenum* at reduced RH's, for increased periods of time and at lower temperatures. The key factor was relative humidity, but time may be also of paramount importance for storage periods that exceed many weeks.

Keywords: *germination fungi, mould, Penicillium chrysogenum, storage, humidity, temperature*

Introduction

The physiological state is an important factor for explaining biological responses, such as fungal spore germination and viability (Nanguy and Dantigny 2009). The physiological state is affected by environmental conditions during the production of spores and also during storage. In general, temperature, conidial moisture content, and the humidity of the storage atmosphere are the major factors that influence spore viability (Hong *et al.* 1997). For most fungi, their ability to germinate decreases as temperature, conidial moisture content, or relative humidity (RH) increase (Smilanick and Mansour 2007). At a fixed RH, increasing temperature (but below that which kills spores) generally decreases the viability of fungal spores, whereas lower temperatures (above freezing) increase viability. The relationship between RH and viability of fungal spores does not appear to be as simple; most persist longer at lower humidity, conversely, some species die more rapidly at lower humidity. An isolate of *Aspergillus flavus* was reported to lose viability rapidly at 75% RH while persisting much longer at lower or higher RH (Teitell 1958).

The effect of the period of time after discharge of ascospores of *Gibberella zeae* from perithecia on germination was also studied (Beyer and Verreet 2005). It was shown that freshly discharged ascospores germinated within 4h at 20°C and 100% RH, but the rate of germination and the percentage of viable ascospores decreased over time. Humidity during storage was a key factor in germination of *G. zeae*. By incubating ascospores at 53% RH, the percentage of viable spores decreased from 93 to 6% within 10 min. To our knowledge there are no studies that focused on the effect of the storage conditions on the germination time of fungal spores.

In laboratory studies, freshly harvested conidia are used to study the effect of environmental factors on germination time. In contrast, conidia that are disseminated into the environment can spend a period of time under unfavourable conditions prior to germination. The objective of this study was to assess the effects of RH, time of storage and temperature on the germination time of *Penicillium chrysogenum* by means of a Doehlert design, in the range 20-100%, 2-28 days and 5-25°C, respectively.

Materials and Methods

Mould

Penicillium chrysogenum was isolated from a spoiled pastry product and identified according to the descriptions of Samson *et al*. (1995).

Production of dry harvested conidia

Potato Dextrose Agar (PDA) medium, 0.99 a_w was central point inoculated and incubated at 25°C for 7 days. Conidia were collected by turning the plates upside-down then gently tapping the bottom of the dishes. Dry-harvested conidia were collected on the lid of the dishes, the bottom parts were substituted for sterile ones. Conidia were stored into closed boxes that contained glycerol solutions to control RH and placed into incubators at various temperatures for different periods of time according to the experimental design.

Germination assessment

The stored conidia were re-suspended into sterile saline solution (NaCl, 9g/l of water) containing Tween 80, 0.05% (vol/vol). After counting the conidia on a Malassez cell, the suspensions were standardized to $1x10^6$ conidia ml^{-1}. 10µl of the suspension was poured at the surface of a thin layer of PDA medium to allow automatic monitoring of the germination without opening the devices (Sautour *et al*. 2001). At least 100 spores (20-25 per microscopic field) were examined through the Petri dish lid every hour. Experiments were carried out in triplicate. The length of the germ tubes was measured by means of a Leica DMLB (x200) (Leica, Rueil-Malmaison, France) connected to a IXC 800 (I2S, Pessac, France) camera. Pictures were analyzed using Matrox Inspector 2.2 (Matrox Electronics Systems Ltd, Dorval, Canada). Spores were considered germinated when the length of the germ tubes was equal to the greatest dimension of the swollen spore (Dantigny *et al*. 2006).

Germination model

The asymmetric model (Dantigny *et al.* 2011): $P = P_{max}\left[1 - \frac{1}{1+\left(\frac{t}{\tau}\right)^d}\right]$ (1)

was used to determine the percentage of viable spores, P_{max}, the asymptotic P value at $t \to +\infty$ and the germination time τ(h), the point where P equals half of the P_{max}.

Experimental design

An experimental domain was defined over 20-100%, 2-28 days and 5-25°C. The Doehlert design allows the description of a region around an optimal response and contains k^2+k+1 points for k variables. For 3 variables, a set of 13 experiments was required. In this study, the germination time τ (h) was the experimental response. The influence of three environmental factors (*i.e.* variables): RH (X1), time (X2), and temperature (X3) on τ was assessed. The experimental values of these three factors are listed in Table 1. The coded values in the range (0-1) are used for the determination of the model coefficients.

Analysis and interpretation of the results

Multiple regression analysis based on the least square method was performed by using Nemrod software (LPRAI, Marseille, France). The analysis concerned the linear and quadratic effects of the three factors and their interactions. Thus, the equation giving T_{90} was a second-order polynomial model with 10 coefficients (b_0, b_1, b_{12}...b_{23}):

$Y = b_0 + b_1X_1 + b_2 X_2 + b_3 X_3 + b_{11} X_1^2 + b_{22}X_2^2 + b_{33} X_3^2 + b_{12} X_1X_2 + b_{13}X_1X_3 + b_{23}X_2X_3$

where X_1, X_2 and X_3 = coded factors studied.

The significance of the coefficients was evaluated by multiple regression analysis based upon the F-test with unequal variance.

Results and Discussion

All replicates were characterized by the same values or values that did not differ from more than 0.1h. Therefore the statistical analysis was performed on the mean germination time, otherwise all parameters coefficients of the model would be significant. The mean germination times, τ (h) were reported in Table 1.

Table 1: Experimental values obtained by applying the Doehlert matrix to assess the effect of relative humidity, time and temperature (factors) on the germination time of *Penicillium chrysogenum* (response).

Experiment	Experimental values			Germination time (h)
	RH (%)	Time (day)	Temperature (°C)	
1	100	15	15	17.5
2	20	15	15	21.4
3	80	28	15	19.8
4	40	2	15	19.0
5	80	2	15	17.7
6	40	28	15	21.0
7	80	19.3	25	19.0
8	40	10.7	5	20.1
9	80	10.7	5	18.0
10	60	23.7	5	19.6
11	40	19.3	25	20.2
12	60	6.3	25	17.5
13	60	15	15	19.6

Depending on the storage conditions, τ varied in the range 17.5-21.4 h. The average germination time for the central point of the experimental design, RH 60%, 15 days, 15°C, was equal to 19.6h (experiment 13). This value is in accordance with the response means, b_0, estimated by the polynomial model (Table 2). The suitability of the polynomial model to fit the experimental data is strengthened by a value of the determination coefficient, $r^2 = 0.979$.
All the coefficients for the main effects, b_1, b_2 and b_3 were significant with p-values less than 0.01. The relative effect of the factors can be ranked according to the absolute value of these coefficients. By a decreasing order of significance, the most important factors were RH, time and temperature. As compared to the response means and regardless of the other factors, the germination time decreased for positive values of X_1 because b_1 negative lead to $b_1.X_1$ also negative. The decrease of the germination time with increasing RH was shown on Figure 1. At 15°C, τ was equal to about 20h after a storage of 15 days at 20% RH, as compared to about 17h at 100% RH. This result can be explained by an initiation of the germination process (i.e., swelling) during storage at high relative humidity, thus decreasing τ.

In contrast, b_2 was positive, thus an increase of time, X_2, delayed germination. At 15°C, the germination time of the conidia of *P. chrysogenum* was equal to about 18h and 20.5h after being stored for 0 and 30 days respectively, Figure 1.

Table 2: Parameter estimates obtained by fitting the germination time of *P. chrysogenum* to a second-order polynomial model.

Coefficient	b_0	b_1	b_2	b_3	b_{11}	b_{22}	b_{33}	b_{12}	b_{13}	b_{23}
Factor	Mean	RH	t	T	RH^2	t^2	T^2	RH.t	RH.T	t.T
Value	19.6	-1.71	1.27	-0.20	-0.15	-0.25	-0.72	0.06	0.053	1.04
p-value	<0.01	<0.01	<0.01	0.206	31.8	10.1	<0.01	68.2	0.194	<0.01

The effect of temperature on the germination time was less clear than that of RH and time because the coefficient of the major effect b_3 was not as significant as b_1 and b_2. The quadratic

effect of temperature, b_{33} should be also be taken into account as highly significant, in addition to the interactive effect between time and temperature, b_{23}. Assuming, $b_2.X_2$ positive (for $X_2>0$) and $b_3.X_3$ also positive (for $X_3<0$), the interactive effect is negative ($b_{23}.X_2.X_3<0$) thus antagonistic. The contour plot (Figure 1, right) showed that for a short period of storage, the germination time decreased at increased temperatures. Conversely, for long period of storage, the germination time increased at increased temperatures.

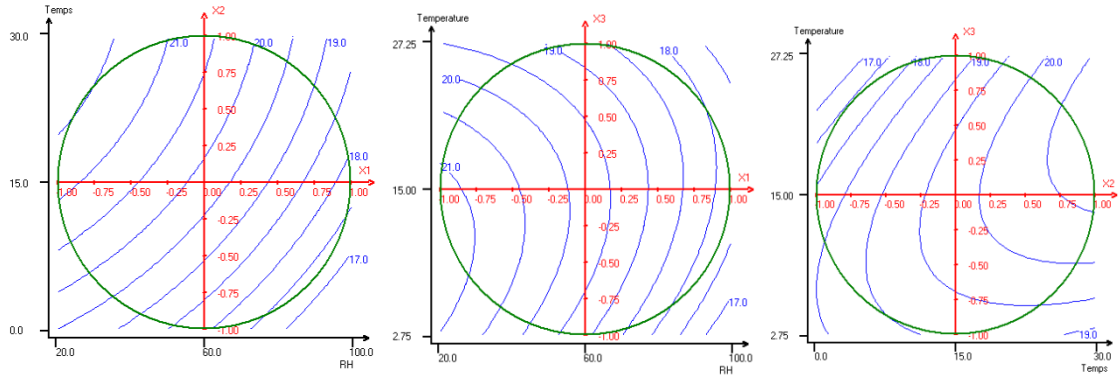

Figure 1: Contour plots of the influence of time and RH at 15°C (left), T and RH at 15 days (centre), T and time at 60% RH (right) on the germination time of *Penicillium chrysogenum* on Potato Dextrose Agar.

Conclusions

In the present study the effects of 3 factors, RH, time and temperature were assessed at 5, 7 and 3 levels, respectively. For this kind of study, full factorial designs are usually applied. In such a case, all the experiments are carried out, thus leading to 5x7x3=105 experiments as compared to only 13 with the Doehlert design. Concerning the present study, the paramount influence of the relative humidity during storage on the germination time of the conidia of *Penicillium chrysogenum* was highlighted. Obviously, longer period of storage should be examined as this could affect the germination time but also the viability of the conidia. Finally, it is very difficult to draw conclusions based on one mould only, because a great variability on the experimental responses was shown depending on the mould species. The present study is currently extended to other fungi.

References

Beyer M. and Verreet J-A. (2005) Germination of *Gibberella zeae* ascopores as affected by age of spores after discharge and environmental factors. *European Journal of Plant Pathology* 111, 381-389.

Dantigny P., Bensoussan M., Vasseur V., Lebrihi A., Buchet C. Ismaili-Alaoui M., Devlieghere F. and Rousssos S. (2006) Standardisation of methods for assessing mould germination: a workshop report. *International Journal of Food Microbiology* 108, 286-291.

Dantigny P., Nanguy S., P-M., Judet-Correia D. and Bensoussan M. (2011) A new model for germination. *International Journal of Food Microbiology* 146, 176-181.

Hong T.D., Ellis R.H. and Moore D. (1997) Development of a model to predict the effect of temperature and moisture on the longevity of conidia of *Beauvaria bassiana*. *Annals of Botany* 79, 121-128.

Nanguy S., P-M. and Dantigny P. (2009) Significance of the physiological state of fungal spores. *International Journal of Food Microbiology* 134, 16-20.

Samson R., Hoeckstra E.S., Frisvad J.C. and Filtenborg O. (1995) *Introduction to food-borne fungi*. 4th edition. CBS Baarn, the Netherlands, 322p. (ISBN: 90-70351-27-7).

Sautour M., Rouget A., Dantigny P., Divies C. and Bensoussan M. (2001) Prediction of conidial germination of *Penicillium chrysogenum* as influenced by temperature, water activity and pH. *Letters in Appied Microbiology* 32, 131-134.

Smilanick J.L. and Mansour M.F. (2007) Influence of temperature and humidity on survival of *Penicillium digitatum* and *Geotrichum citri-aurantii*. *Plant Disease* 91, 990-996.

Teitell L. (1958) Effects of relative humidity on viability of conidia of *Aspergilli*. *American Journ al of Botany* 45, 748-753.

Modelling the effect of temperature on the germination and mycelium formation dynamics of fungal spores

M. Gougouli, K.P. Koutsoumanis

Department of Food Science and Technology, School of Agriculture, Aristotle University of Thessaloniki, Thessaloniki Greece. (gougouli@agro.auth.gr, kkoutsou@agro.auth.gr)

Abstract

In an attempt to evaluate the life cycle of spoilage moulds in foods as affected by storage temperature, the germination time and mycelium growth kinetics of *Penicillium expansum* spores were modelled at isothermal conditions. Additionally, a time lapse microscopy method was developed for monitoring the kinetic behavior of the spore after germination. The applicability of the derived models in predicting the level of germination at fluctuating temperatures was evaluated by comparing predictions with the respective responses under dynamic conditions.

Keywords: *fungi, modelling, germination, mycelium formation, temperature*

Introduction

After the contamination of foods with fungal spores and if the conditions are suitable, the appearance of visible mycelia depends on the spore germination time and the mycelium growth rate (Gougouli and Koutsoumanis 2010). In real situations, the contamination of foods with fungal spores usually occurs at very low numbers (Dantigny *et al*. 2007), and the probability that their germination will result in a spoiled product or the production of mycotoxins at the time of the consumption depends greatly on the germination time of the contaminated spores and the mycelium growth kinetics. Therefore, the development of mathematical models, which are able to predict spore germination and fungal growth, is of great importance (Dantigny *et al*. 2002; Gougouli and Koutsoumanis 2010).

In the objective of assessing the germination of fungal spores, microscopic observations are required (Dantigny *et al*. 2002). Research data indicate that the germination time of a spore is not a fixed value and can be characterized better by a probability distribution (Dantigny *et al*. 2006). Thus, the primary germination models that are frequently used, quantify the percentage of germination of a population of spores in relation to time. On the contrary, fungal growth on solid substrates requires direct measurement of the colony diameter over time. The linear model is the most widely used for describing the mycelium fungal growth, while the mycelium's growth rate and the apparent lag time can be determined easily.

All the available models on spore germination and fungal growth have been developed and validated based on data from constant conditions. Environmental factor, such as temperature, can fluctuate during distribution, retail and domestic storage of foods. If such fluctuations are not taken into account during validation of a model, its use in a quality assurance system may lead to wrong decisions. Thus, there is a need for studying and modelling spore germination and fungal growth in real situations such as dynamic temperature conditions (Gougouli and Koutsoumanis 2010).

Given the above and that fungal behavior has been less studied compared to bacteria, the current study was conducted to evaluate the relationship between germination time and lag time of individual spores, and to assess the effect of temperature (static and dynamic) on the kinetics of germination time.

Materials and Methods

The growth and germination of *Penicillium expansum* was investigated on malt extract agar (LAB M, United Kingdom) (a_w 0.997, pH 4.2) under isothermal conditions (0.1-33°C). For the germination study and mycelium growth kinetics of single spores, portions (100-μL) of the inoculum, containing approximately 10^6 spores and 10 spores, respectively, were surface

plated aseptically on Petri dishes containing the solidified medium with a diameter of 90mm in the first case and 145mm in the last one.

For the germination study, at regular time intervals during storage, depending on the incubation temperature, the germination of spores was examined microscopically. Spores were considered to have germinated when the length of the germ tubes were equal with the greatest dimension of the swollen spores (Dantigny *et al*. 2006). In total, about 450 spores were observed in every trial. The percentage of germinated spores was calculated (P(%)), and data of P(%) over time were fitted to the modified Gompertz equation (Eq. (1)) for the estimation of the germination kinetic parameters (μ_g and λ_g):

$$P_t = P_{\max} \exp\left(-\exp\left[\frac{\mu_g e(1)}{P_{\max}} (\lambda_g - t) + 1 \right] \right) \quad (1)$$

where t (h) is the time, P_t (%) is the percentage of germinated spores at time t, $P_{\max}$ (%) is the asymptotic P_t value at $t \rightarrow +\infty$, μ_g (1/h) is the slope term of tangent line through the inflection point, and λ_g (h), the lag time for germination, is the t-axis intercept of the tangent through the inflection point.

For the growth study, perpendicular diameters (mm) of each mycelium were measured macroscopically and the average diameter of the colony was plotted against time and fitted to a linear model (Eq. (2)) for the estimation of the growth rate μ (mm/h) and the lag time λ (h).

$$D_{(t)} = \mu(t - \lambda) \quad (2)$$

where t is the time (h) and $D_{(t)}$ is the diameter at time t. Based on the above inoculation procedure, each mycelium that appeared was assumed to originate from a single spore. The growth of approximately 200 mycelia was examined and the cumulative frequencies of the estimated λ were fitted to Eq.(1) with the difference that the parameters μ_m and λ_m, were used instead of μ_g and λ_g.

The effect of temperature on x ($x = \mu_g$, $1/\lambda_g$, μ_m, $1/\lambda_m$) was modeled using the Cardinal Model with Inflection (CMI) originally developed by Rosso *et al*. (1993):

$$x = \frac{x_{\text{opt}} (T - T_{\max})(T - T_{\min})^2}{(T_{\text{opt}} - T_{\min})[(T_{\text{opt}} - T_{\min})(T - T_{\text{opt}}) - (T_{\text{opt}} - T_{\max})(T_{\text{opt}} + T_{\min} - 2T)]} \quad (3)$$

where T_{opt}, $T_{\min}$ and $T_{\max}$ are the theoretical optimum, minimum and maximum temperature (°C) for germination or growth depending on the case.

Under dynamic conditions, the prediction of the P_t when the temperature shift occurred (i) before the appearance of germ tubes ($t_s \leq \lambda_{gI}$) was made using Eq. (1), with the predicted λ_g being derived from Eq. (4) as λ_{gT}, or (ii) during germination ($\lambda_{gI} < t_s < t_{\max}$, $t_{\max}$ = time that all the spores have germinated) was made using Eq. (5).

$$\lambda_{g_T} = t_s + \lambda_{g_F} \left(1 - \frac{t_s}{\lambda_{g_I}} \right) \quad (4)$$

$$P_t = \begin{cases} 100 \exp\left(-\exp\left[\dfrac{\mu_{g_I} e(1)}{100} (\lambda_{g_I} - t) + 1 \right] \right) & \text{if} \quad t \leq t_s \\ P_s + (100 - P_s) \exp\left(-\exp\left[\dfrac{\mu_{g_F} e(1)}{100 - P_s} \right] (t_s - t) + 1 \right) & \text{if} \quad t > t_s \end{cases} \quad (5)$$

where μ_{gI} and μ_{gF} is the μ_g at the temperature before (T_I) and after (T_F) the shift, respectively, as predicted from the CMI (Eq. (2)) and P_s the percentage of germination at the time of the shift.

Additionally, a time lapse microscopy method was developed for monitoring spores' behavior after germination at 25°C.

Results and Discussion

A total of 200 growth curves were plotted for the *P. expansum* mycelia at each tested temperature and the frequency distributions of the estimated lag times from Eq. (2) were generated (Fig. 1). The mean values (±st.dev) were 800±71.2, 182.1±25.9, 91.4±11.1, 55.5±6.4, 37.7±4.2, 30.1±2.7, 35.9±3.9 and 89.1±18.8 h at 0.1, 5.2, 10.5, 15.0, 19.5, 25.5, 27.5 and 30.5 °C, respectively. As expected, the distributions of single spores' lag were shifted to higher values and became more spread when the temperature shifted to higher or lower values from the optimum, indicating that temperature contributes to both the extent and variability of the lag of a population of spores.

The cumulative frequencies of the single spores' lag, as well the germination data were fitted to Eq. (1). The relationship between germination time and lag time of a population of single spores is shown in Figure 2. The relative difference $\%(\lambda_m-\lambda_g)/\lambda_m$ was found to be constant for all temperatures tested (72.5±5.1, mean±st.dev).

When the effects of temperature on μ_g and $1/\lambda_g$ were modelled with the aid of CMI (Eq. (3)), the estimated values of the cardinal parameters for μ_g were found to be close to the respective values for $1/\lambda_g$, indicating similar temperature dependence between them (Fig. 3). The same trend was also observed for μ_m and $1/\lambda_m$. On the contrary, the germination region (T_{min}-T_{max}) was found to be slightly wider compared to mycelium growth region (Fig. 3). This can be attributed to the fact that at conditions close to the germination boundaries the spores can germinate but are not able to form a mycelium.

For the trials under dynamic conditions, germination time and mycelium growth was predicted with a model based on a cumulative approach for lag and the assumption that the rate is adopted instantaneously to the new temperature conditions. An agreement between the observed and the predicted plotted germination curves was revealed for all temperature scenarios with single temperature shifts before the λ_g. The same results were observed for scenarios with single temperature shifts inside the germination region after λ_g (Fig. 4). It needs to be noted that similar was the effect of temperature shifts on the growth rate of *P. expansum* mycelia (Fig. 5) as reported before (Gougouli and Koutsoumanis 2010). The assumption of the model about the rate, however, did not confirmed at scenarios which included an abrupt transition from a temperature optimum to a temperature close to minimum for germination.

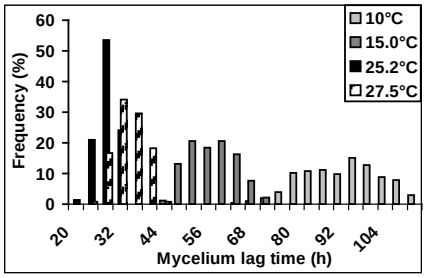

Figure 1: Frequency distributions of lag times of 200 *P.expansum* mycelia of different temperatures.

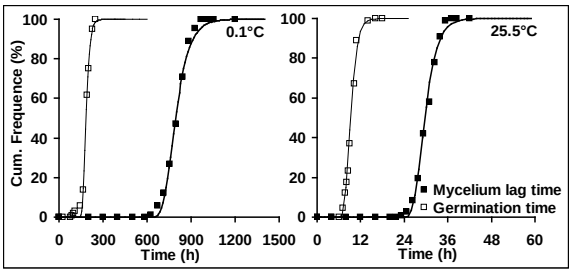

Figure 2: Germination kinetics and cumulative frequencies of the lag time of *P.expansum* spores (lines: fitting of Gompertz model).

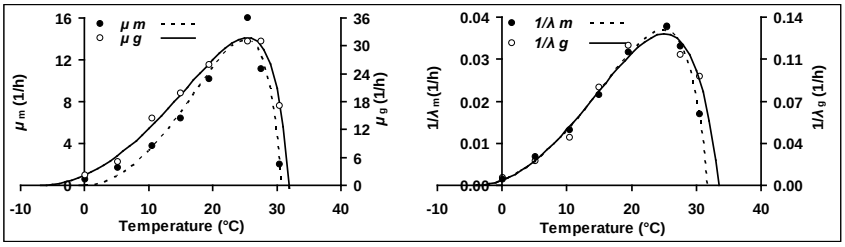

Figure 3: Effect of temperature on the parameters of the Gompertz model for germination (μ_g, λ_g) and mycelium lag times (μ_m, λ_m) fitted with the CMI (lines).

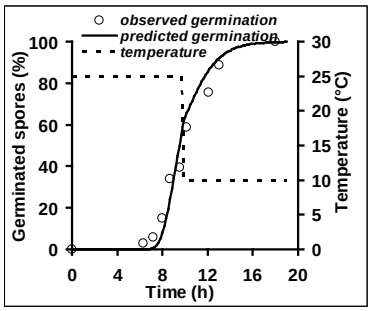

Figure 4: Comparison between observed and predicted germination of *P. expansum* spores incubated for 9.7h at 25°C and then at 10°C.

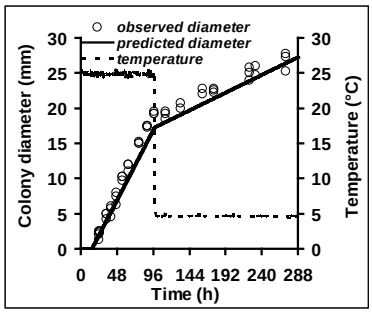

Figure 5: Comparison between observed and predicted growth of *P. expansum* incubated for 97h at 25 °C and then 191h at 5 °C (Gougouli and Koutsoumanis, 2010).

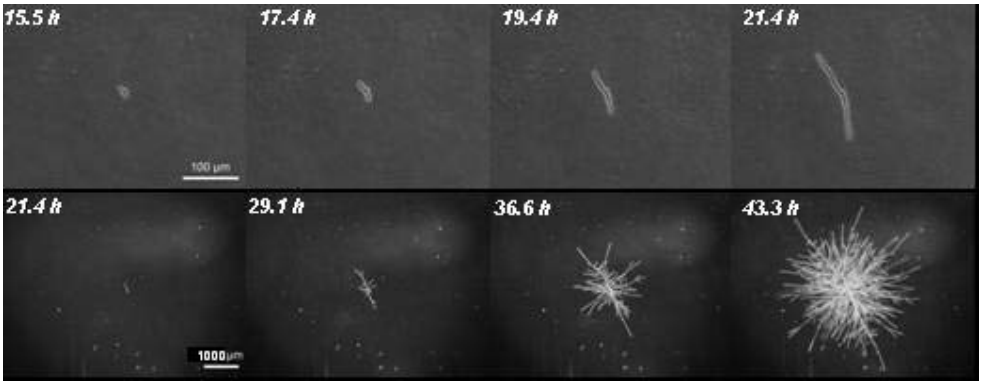

Figure 6: Representative kinetic behavior of a *P. expansum* single spore after germination.

Figure 6 illustrates a representative kinetic behaviour of single spore after germination at 25°C. After measuring the spanning of the peripheral zone, four growth curves were made for the four perpendicular radius of growth vs time. After a certain time of exponential growth of the tube's length, the growth for all the surface directions was linear and equal with the estimated growth rate from the subsequent macroscopic observation.

Conclusions

The data generated and the models developed in this work are useful in understanding and predicting the germination and mycelium growth behavior. Additionally, the results on the variability of the germination and lag time of *P. expansum* single spores and the observed relationship between spore germination kinetics and lag time for growth can be used for the development of stochastic models and the risk assessment of mould spoilage.

References

Gougouli M. and Koutsoumanis K.P. (2010) Modelling growth of *Penicillium expansum* and *Aspergillus niger* at constant and fluctuating temperature conditions. *International Journal of Food Microbiology* 140, 254-262.

Dantigny P., Soares Mansur C., Sautour M., Tchobanov I. and Bensoussan, M. (2002) Relationship between spore germination kinetics and lag time during growth of *Mucor racemosus*. *Letters in Applied Microbiology* 35, 395-398.

Dantigny P., Bensoussan M., Vasseur V., Lebrihi A., Buchet C., Ismaili-Alaoui M., Devlieghere F. and Roussos S. (2006). Standardisation of methods for assessing mould germination: A workshop report. *International Journal of Food Microbiology* 108, 286–291.

Dantigny P., Marín S., Beyer M. and Magan N. (2007) Mould germination: Data treatment and modelling. *International Journal of Food Microbiology* 114, 17-24.

Rosso L., Lobry J.R. and Flandrois J.P. (1993) An unexpected correlation between cardinal temperatures of microbial growth highlighted by a new model. *Journal of Theoretical Biology* 162, 447-463.

From single spores to mycelium: variability of *Aspergillus westerdijkiae, Aspergillus carbonarius* and *Penicillium verrucosum* growth and ochratoxin A production

A. E. Kapetanakou, E. H. Drosinos, M. Mataragas, P. N. Skandamis

[1] Laboratory of Food Quality Control & Hygiene, Department of Food Science & Technology, Agricultural University of Athens (pskan@aua.gr)

Abstract

We evaluated the growth and ochratoxin A (OTA)-production kinetics of single spores of *Aspergillus westerdijkiae*, *A. carbonarius* and *Penicillium verrucosum* on Malt Extract Agar at a pH 3.5 or 5.5 and a_w 0.99 or 0.94, at 10-30 ^oC. Individual spores were obtained with 2-fold dilutions in microtiter plates. Fungal growth was determined by measuring the radial growth rate (*RGR*) and time-to-visible growth (*TTVG*) of colonies from 80-100 spores, while 6-8 colonies were tested at each sampling time for OTA production (HPLC). The variance of *TTVG* and OTA production by colonies from single spores significantly increased at growth limiting conditions (a_w 0.94, pH 3.5 and 15 ^oC or 10 ^oC for *A. westerdijkiae* or *P. verrucosum,* respectively). OTA levels ranged from below to above the legislation limits (2-10 μg/L). At a_w 0.99/20 ^oC/pH 5.5, no toxin was detected by *P. verrucosum*. Fitted distributions showed marked symmetry regardless of experimental conditions. Given that *RGR* distributions were narrower than those of *TTVG*, the variability of the latter is likely associated with variability in germination times (GT) and growth rates of single germ tubes. GT is the time until the length of a germ tube equalled to the diameter of the original spore (~10 μm). We microscopically evaluated spore germination on gel 'cassettes', by monitoring changes of certain spores and % of germinated spores over time, in 10 optical fields per observation. Germination data were used to simulate the increase from spore to a mycelium of detectable size (1 mm). Monte Carlo simulations (10000 iterations) were used to model spore germination, increase in mycelium diameter and time for OTA detection from various spore populations (1-100 spores), assuming that spores behave independently. Simulations agreed well with validation data, suggesting that these findings may be used for risk assessment of OTA production based on the variability in responses of individual spores.

Keywords: *germination, mycotoxins, predictive mycology, stochastic, germ tubes, spores*

Introduction

The variability in the germination time and individual growth rate of germ tube of fungal spores has been reflected on the lag time (i.e., the time to visible growth) and radial increase of *Aspergillus*, and *Fusarium* mycelia grown on corn solid media (Samapundo *et al*. 2007). Experimental protocols involving microscopic observations can be used to monitor the kinetics of single fungal spores in response to a_w and % ethanol (Dantigny *et al.* 2005; Judet *et al.* 2008). Individual fungal spore kinetics may serve as a basis in stochastic modelling for predicting the time until spoilage occurs, in the form of visible mycellium. A similar concept is presented here for assessment of time to toxin production by ochratoxin producing fungi based on the variability of single spores in response to temperature, pH and a_w. Variability in macroscopic data was confirmed by microscopic measurements.

Materials and Methods

Isolation of individual fungal spores and macroscopic data collection

Aspergillus westerdijkiae (ochraceus), *A. carbonarius* and *Penicillium verrucosum* were grown on Malt Extract Agar (MEA) for 7 days to obtain sporulating cultures and then spores suspensions were harvested in sterile water with 0.01% Tween 80. Individual spores of all three fungi were isolated using a 1/2 serial dilution protocol in microtiter plates based on

calibration curves relating optical density (600 nm) to spores density (Francois *et al.* 2003). Following dilutions, the contents of the aforementioned columns were spread aseptically on MEA plates (pH 3.5 or 5.5 and a_w 0.99 or 0.94) and were incubated at 10, 15, 20, 25, and 30°C. Fungal growth was determined by measuring the radial growth rate (*RGR*) and time-to-visible growth (*TTVG*) of mycelia from 80-100 spores, while 6-8 mycelia were tested for ochratoxin A (OTA) production (HPLC) at each sampling.

Microscopic determination of spore kinetics

Individual germination rate (*GR*) of germ tubes and germination time (*GT*) were evaluated in cassettes containing solidified MEA between sheets of PVC film. An appropriate volume (0.6 mL) of MEA at pH 3.5 or 5.5 and a_w 0.99 or 0.94 was transferred into the cassettes through special holes located on the frame. Fungi were inoculated into the cassettes by injecting a total volume of 10 μL of spores suspension through the same holes. Cassettes were incubated at 10, 15, 20, 25, and 30 °C. Approximately 200 single spores per cassette were examined microscopically. Spores were considered to be germinated when the germ-tube was equal to or greater than the diameter of the spore.

Data analysis

The kinetic parameters of the single spore experiments were calculated using the Baranyi model. The diameter at which ochratoxin levels were detected was also determined. Gamma, Normal, Logistic and Weibull distributions were fitted to the kinetic parameters (time-to-visible-growth, *TTVG* and radial-growth-rate, *RGR*) using @Risk 4.5 software (Palisade Corp., New York, USA). Distributions were ranked using the Chi-squared (χ^2) and the Anderson-Darling (*A-D*) statistical tests. The type error I (a) of 0.05 was used as the cut off confidence limit. Monte Carlo simulations (10000 iterations) were used to model spore germination, increase in mycelium diameter and time for OTA detection (TTO) from various spore populations (1-100 spores), assuming that spores behave independently.

Results and Discussion

Level of detection and level of quantification for the ochratoxin A was 0.4-0.5 and 0.9-1.0 ppb, respectively. The variance of *TTVG* and OTA production by colonies from single spores significantly increased at growth limiting conditions (a_w 0.94, pH 3.5 and 15 °C or 10 °C for *A. westerdijkiae* or *P. verrucosum,* respectively). OTA levels ranged from below to above the legislation limits (2-10 μg/L; Fig. 1a). Monte Carlo simulation was performed to predict the time-to-ochratoxin detection ($t_{det\,OTA}$) using the following equation (Métris *et al*. 2003):

$$t_{\det OTA} = TTVG + \frac{d_{\det OTA} - d_o}{RGB} \qquad (1)$$

where, *TTVG* (d) and *RGR* (cm per day) are the distributions that best fitted the data from the single spore experiments, d_0 (cm) is the initial diameter described by a Poisson distribution of the length of a germ tube after spore germination with average equal to the diameter of the original spore (ca. 10 μm or 0.001 cm) and $d_{det\ OTA}$ (cm) is the diameter at which the OTA detection levels were experimentally determined. The distribution of the latter parameter was assumed to be uniform. The above equation was used to analyze the dependence of the distribution of the $t_{det\ OTA}$ parameter on the four variables, *RGR*, d_0 and $d_{det\ OTA}$ and *TTVG* (distribution of which depends on the initial number of spores, N_0). When there is more than one spore and considering that the different spores behave independently, the *TTVG* was estimated by the formula (Métris *et al.* 2003):

$$TTVG_{No} = -\frac{1}{RGB} x \ln\left(\frac{\Sigma e^{-RGRxTTVG}}{N_o}\right) \qquad (2)$$

The term inside the parenthesis is linked with the concept of the physiological state (Métris *et al.* 2006). For a population consisting of N_0 spores, the physiological state is defined as:

$$h(No) = e^{-RGRxTTVG(No)} \qquad (3)$$

The $TTVG(N_0)$ indicates that the time-to-visible-growth depends on the initial number of the spores, N_0. The physiological state of the population N_0 is equal to the arithmetic mean of the individual physiological states:

$$h(No) = \sum_{i=1}^{No} a_i / No \quad (4)$$

The term inside the parenthesis in the equation (2) was experimentally determined from the single spore experiments using the equations (3) and (4). After calculating the $TTVG_{N0}$, the equation (1) was used to determine the new $t_{det\ OTA}$ ($t_{det\ OTA/N0}$) for spore population N_0 (e.g. 1-100 spores) by substituting *TTVG* with $TTVG_{N0}$ and assuming that spores behave independently. Given that *RGR* distributions were narrower than those of *TTVG*, the variability of the latter is likely associated with variability in germination times (GT) and growth rates of single germ tubes. Thus, the % of germinated spores over time reflects the expected variance of *TTVG* (Fig. 1b).

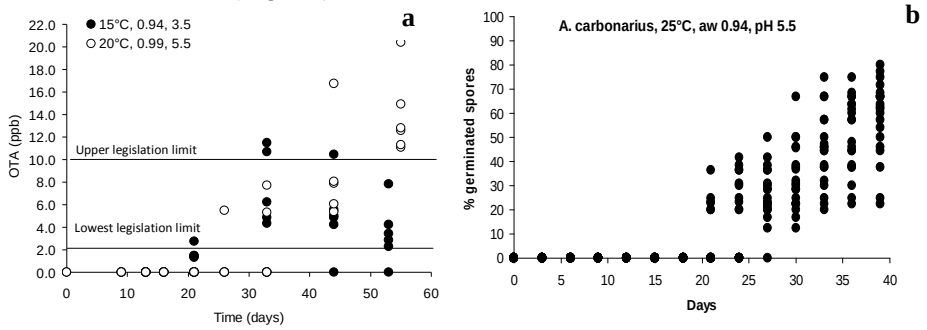

Figure 1: Variability in OTA production by A. *westerdijkiae* (a**)** and in % of germinated *A. carbonarius* spores (b), in various optical microscopic fields containing 10 spores.

Table 1: Representative predicted $t_{det\ OTA}$ (days) obtained by Monte Carlo simulation for individual spores.

Microorganism	Temperature (^{0}C)	Growth conditions		Observed and predicted by distribution			
		a_w	pH	Mean		5% percentile	95% percentile
				Observed	Predicted		
Aspergillus westerdijkiae	15	0.99	3.5	20-22	15.5	11.3	20
			5.5	24-26	19.2	16.1	22.4
		0.94	3.5	20-21	19.7	15.1	24.8
			5.5	22-24	19.9	17.3	22.8
	20	0.94	3.5	19-21	14.1	12.2	16.0
			5.5	25-28	17.9	15.6	20.5
	25	0.94	3.5	10-12	8.1	6.4	10
			5.5	19-20	10.9	9.7	12.3
	30	0.99	3.5	26-28	15.8	11.4	21.2
			5.5	9-10	7.9	6.3	9.8
		0.94	3.5	8-11	8.4	6.6	10.5
			5.5	10-17	5.9	5.1	6.7
Penicillium verrucosum	10	0.99	3.5	16-22	16.3	12.3	20.8
	15	0.99	5.5	8-11	8.7	6.5	11.1
		0.94	3.5	25-30	22.5	16.5	29.2
	20	0.99	3.5	18-21	20.5	17.8	23.4
		0.94	3.5	27-31	29.6	22.3	38.4
	25	0.99	5.5	16-18	18.6	13.4	26.5

Regarding the distribution fitting for *TTVG* and *RGR* parameters, the statistical test showed that Gamma distribution was not suitable for fitting in any experimental case. Weibull was suitable for fitting in most of the cases but the Normal and Logistic distributions were able to fit all the experimental datasets (100%). The logistic distribution displayed a high percentage of probability values (*p*-value) above 0.05 and low percentage with low significance, i.e., *p*-value < 0.05, in comparison with the Normal distribution. Therefore, the Logistic distribution was further selected to describe the variability of the individual spores relative to the *TTVG* and *RGR*. Regarding h_0, the Gamma distribution was able to fit only a fraction of the experimental datasets and Weibull was the most suitable distribution. Under stress conditions,

only Logistic and Normal distributions could adequately fit all experimental datasets. This could be due to distributions getting broader by the increased variability under stress. The times-to-OTA production predicted by Monte Carlo simulation of germination and growth of individual spores agreed well with the experimentally determined $t_{det\ OTA}$ production on MEA plates almost for all conditions tested (Table 1). Simulations for initial fungal spore populations of 100 spores, taking into account the variability in growth kinetics of individual spores and based on the assumption that spores behave independently showed that $t_{det\ OTA}$ were markedly shorter than those required by an individual spore (Table 2; Fig. 2). This was also confirmed by microscopic measurements. Therefore, the description of individual spore variability may be used to assess the risk of toxigenesis of potentially higher fungal populations.

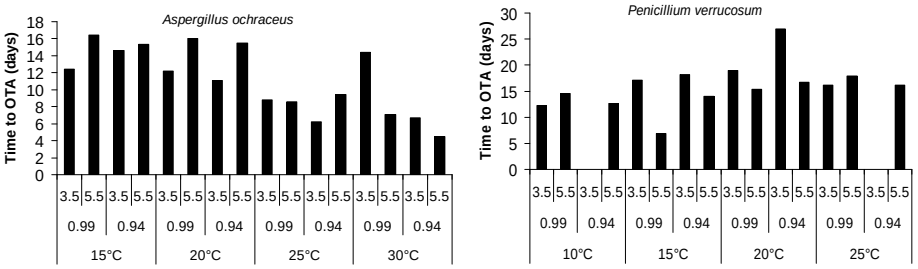

Figure 2: Representative differences between the mean predicted times-to-OTA detection of single (TTO_{single}) and 100 spores (TTO_{100}) inocula, obtained by Monte Carlo simulation.

Table 2: Detection of single (TTO_{single}) and 100 spores (TTO_{100}) inocula

Microorganism	Temperature (^{0}C)	Growth conditions		TTO_{single}-TTO_{100}	TTO_{100}	
		a_w	pH		5% percentile	95% percentile
Aspergillus westerdijkiae	15	0.99	3.5	3.1	8.2	17.1
			5.5	2.8	13.3	19.5
	20	0.94	3.5	3.0	9.2	13.1
	25	0.94	3.5	1.9	4.5	8.4
	30	0.94	5.5	1.4	3.8	5.4
Penicillium verrucosum	10	0.99	3.5	3.0	8.1	17.0
	15	0.94	3.5	3.4	11.8	25.0
	20	0.99	3.5	1.5	16.3	22.1
		0.94	3.5	2.7	19.5	36.0
	25	0.99	5.5	0.7	12.5	26

Conclusions

OTA production varies with the physiological state of spores. *TTVG* and $t_{det\ OTA}$ by any fungal population can be predicted through the stochastic behaviour of individual spores.

References

Dantigny P., Tchobanov I., Bensoussan M. and Zwietering M.H. (2005) Modeling the effect of ethanol vapour on the germination time of *Penicillium chrysogenum*. *Journal of Food Protection* 68, 1203-1207.

Francois K., Devlieghere F., Stadaert A.R., Geeraerd A.H., Van Impe, J.F. and Debevere, J. (2003) Modelling the individual cell lag phase. Isolating single cells: protocol development. *Letters in Applied Microbiology* 37, 26-30.

Judet D., Bensoussan M., Perrier-Cornet, J.-M. and Dantigny, P. (2008) Distributions of the growth rate of the germ tubes and germination time of *Penicillium chrysogenum* conidia depend on water activity. *Food Microbiology* 25, 902-907.

Métris A., George S.M., Peck M.W. and Baranyi J. (2003) Distribution of turbidity detection times produced by single cell-generated bacterial populations. *Journal of Microbiological Methods* 55, 821-827.

Métris A., George S.M. and Baranyi J. (2006) Use of optical density detection times to assess the effect of acetic acid on single-cell kinetics. *Applied and Environmental Microbiology* 72, 6674-6679.

Samapundo S., Devlieghere F., De Meulenaer B. and Debevere J. (2007) Growth kinetics of cultures from single spores of *Aspergillus flavus* and *Fusarium verticillioides* on yellow dent corn meal. *Food Microbiology* 24, 336-345.

Predictive modeling to describe the effect of water activity and temperature on the radial growth of heat resistant molds

A. Tremarin[1], B.C.M. Salomão[2], S. Zandonai[1], G.M.F. Aragao[1]

[1]Federal University of Santa Catarina - UFSC, Campus Universitário, Trindade, Florianópolis/SC, Brazil. (andreiatremarin@gmail.com, glaucia@enq.ufsc.br)
[2]Federal University of Rio Grande do Norte – UFRN, Núcleo Tecnológico, Lagoa Nova Natal/RN, Brazil (beatriz@eq.ufrn.br)

Abstract

Apples used for the production of juice in Brazil are those that do not reach the standard for *in natura* consumption, therefore there is a risk factor regarding contamination by molds, which can produce mycotoxins. The ascospores of heat resistant fungi as *Byssochlamys fulva* and *Neosartorya fischeri* can be activated by the heat process, being able to germinate and grow into the package during storage. The aim of this work was to study the influence of incubation temperature and water activity (a_w) of the medium on *B. fulva* and *N. fischeri* growth on apple juice. Agar added apple juices (1.5 g agar per 100 mL) adjusted to different a_w levels (0.88, 0.90, 0.93, 0.97 and 0.99) were put into Petri dishes. Both mold species were grown in plates and incubated at different temperatures (10, 20 and 30 ºC) for a period of 3 months. Growth responses were evaluated over time in terms of colony diameter changes. Gompertz and Logistic models were fitted to experimental data and the result growth rates (μ_{max}) and lag phase duration (λ) were further modeled as a function of temperature and water activity. The Gompertz model presented a slightly better performance than the Logistic model, so the former model was used to determine the growth parameters. The results showed that the growth of both molds was affected by temperatures and water activity. The elevation of a_w from 0.93 to 0.99 led to a decrease in λ and an increase in μ_{max}. How the ready to drink juices are usually stored at room temperature, these results are useful to establish the shelf life of these products.

Keywords: predictive modeling, heat resistant fungi, growth colony diameter, apple juice

Introduction

Heat preservation is the method usually employed for fruit juice. However, heat resistant molds can be activated during this process and germinate during juice storage causing deterioration of the product, mycotoxin production and economic losses (Engel and Teuber 1991, Zimmermann *et al*. 2011).

Some mold species show characteristics that make them more heat resistant due to the capacity of ascospore production. Species like *Byssochlamys* sp. and *N. fischeri* are reported as mycotoxin producers (Sant'Ana, Rosenthal and Massaguer 2009).

Mathematical modeling is an efficient tool for assessing how individual or combined environmental factors affect microorganisms that degrade processed foods. Various models have been developed in predictive microbiology for fitting growth curves and estimating biological parameters of food-borne pathogens (McMeekin *et al*. 2002; Lahlali *et al*. 2007).

Materials and Methods

In this study, the growth of *N. fischeri* and *B. fulva* IOC 4518 was analyzed. *N. fischeri* was isolated and identified in Biochemical Engineering laboratory in Federal University of Santa Catarina by Salomão (2002) in samples collected from the processing line of apple nectar. *B. fulva* strain was isolated from concentrate apple juice (Salomão *et al*. 2008).

The apple juice was prepared from clarified concentrate apple juice by dilution. The aw (determined by Aqualab - Models Series 3TE) was adjusted to 0.75, 0.88, 0.93, 0.97 and 0.99 and the pH to 3.8. The juice was added with 1.5 g of agar per 100 mL of juice and the samples were pasteurized at 115 °C/1 min and filled on duplicated Petri dishes of 150 x

15 mm. The plates containing the juice were individually inoculated by depositing a loop of microorganism in the center of each plate. The colonies growth was analyzed at different incubation temperatures (10, 20 and 30 °C) by measuring every 12 hours, approximately.
The primary models, Gompertz (Equation 1) and Logistic (Equation 2) were fitted to experimental growth curves and statistically compared by applying the following indexes: root mean square error (MSE) and correlation coefficient (R^2) between predicted values and observed values. After selection, the best model was used to obtain microbial growth parameters: maximum specific growth (μmax (mm/h)) and lag phase duration (λ (h)) for each temperature and soluble solids content, using Matlab® software.

$$\ln y = A.\exp\{-\exp[-B.(t-M)]\} \quad (1)$$

$$\ln y = \frac{A}{[1+\exp(M - B.t)]} \quad (2)$$

The diameter of the colony is y (mm) at a given time t (h), λ is the length of adaptation phase (h); A is the logarithmic increase of population (mm); M is a dimensionless parameter and B is the relative growth in half of the time of the exponential phase (h^{-1}). M and B are used to determine the microbiological parameters of growth λ and μmax. Secondary models may be used with empirical exponential equations, polynomials, logarithmic or other that best describe the influence of temperature on the primary parameters of growth (Corradini and Peleg 2005). General secondary models (exponential model presented on Equation (3), and linear model presented on Equation (4)) were used to describe the influence of the statistical significant factors on the growth parameters, using Excel software.

$$y = a.\exp(b.T) \quad (3)$$

$$y = aT + b \quad (4)$$

Results and Discussion

Gompertz and Logistic models were fitted and the results are shown in Figures 1 and 2. At water activity of 0.88 and 0.75 no growth was observed, even after 4200 hours incubation for the three studied temperatures to both microorganisms. At 10 °C, only after 960 hours of incubation the growth was observed (data not shown).

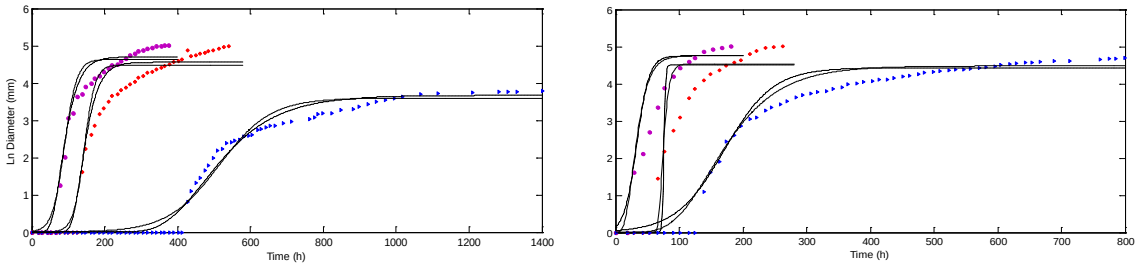

(a) (b)

Figure 1:.Growth curves of *B. fulva* in apple juice at temperatures of 20 °C and 30 °C (b) and water activity conditions of 0.99 (●), 0.97 (♦) and 0.93 (►).The continuous line (−) represents the fit of Gompertz model (G) and the dotted line (--) represents the fit of Logistic model to the experimental data.

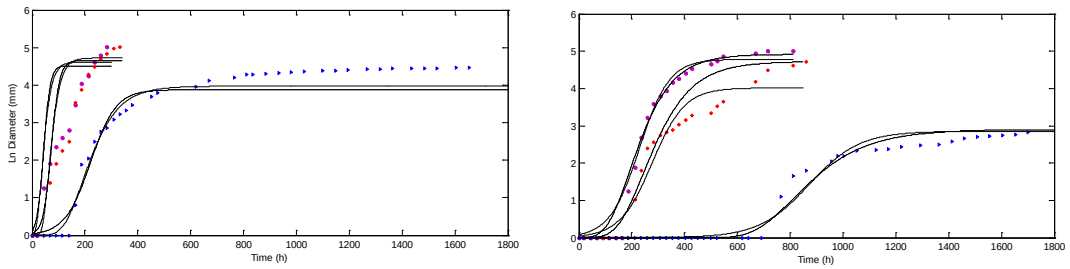

Figure 2: Growth curves of *N. fischeri* in apple juice at temperatures of of 20 °C (a) and 30 °C (b) and water activity conditions of 0.99 (●), 0.97 (♦) and 0.93 (▶).The continuous line (−) represents the fit of Gompertz model (G) and the dotted line (--) represents the fit of Logistic model to the experimental data.

The Gompertz and Logistic models fitted very well to the experimental data for both microorganisms, since the R^2 values were higher than 0.95. However, the Gompertz model fitted better for most temperatures and a_w. Analyzing Figures 1 and 2 can be observed that a_w and temperatures affected *B. fulva* and *N. fischeri* growth in apple juice. The highest length of lag phase (λ) for *B. fulva* was 362.1 h to a_w 0.93 at 20 °C and the lowest w (a) ı for a_w 0.99 to 30 ºC. For *N. fischeri*, the lag phase was higher at 20ºC and a_w 0.93, rea (b) 5.0 h and lowest was 17.3 h for a_w 0.99 to 30 °C. According to Marin *et al*. (2008), plotting diameters of a mould colony against time a lag phase is observed followed by a linear phase, but in most of the cases no decrease in growth rate is observed before the edge of the Petri plate is reached. The same was observed in the present results, as shown in Figure 1. These results showed that is very difficult to discuss A parameter (maximum colony diameter).
Considering the end of shelf life of juice is the time when the colony of the fungus becomes visible, the parameter λ is determinant to define the shelf life of the product.
Figure 3 presents the average values *B. fulva* and *N. fischeri* in apple juice in function of a_w, for different temperatures.

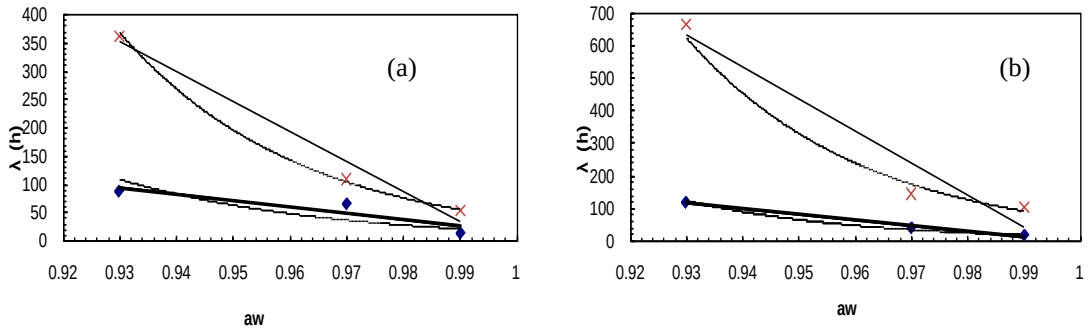

Figure 3: Influence of a_w of the media on the values of *B. fulva* (a) at 30 °C (♦) and 20 °C (x) and *N. fischeri* (b) at 30 °C (♦) and 20 °C (x) in apple juice. The continuous line (−) represents the fit of secondary model (Linear) and the dotted line (--) represents the fit of secondary model (Exponential) to the experimental data.

The secondary models for the two microorganisms are shown in Table 1.

Table 1: Secondary models for *B. fulva* and *N. fischeri* growth parameters.

Parameters	Equation	R^2
B. fulva 30 °C	$\lambda = 9E12.\exp(-27aw)$	0.84
λ (h)	$\lambda = -1148.6aw + 1163.4$	0.71
B. fulva 20 °C	$\lambda = 2E15.\exp(-31.5aw)$	0.99
λ (h)	$\lambda = -5304.6aw + 5285.4$	0.97
N. fischeri 30 °C	$\lambda = 6E14.\exp(-31.4aw)$	0.98
λ (h)	$\lambda = -1728.6aw + 1724$	0.98
N. fischeri 20 °C	$\lambda = 4E15.\exp(-31.8aw)$	0.97
λ (h)	$\lambda = -9855.7aw + 9799.3$	0.93

The mathematical relation between a_w and λ obtained by fitting the Exponential and Linear Model for *B. fulva* and *N. fischeri* at 20 and 30°C show that for the higher temperature a_w medium presents less influence on λ than that observed at lower temperature, for both moulds. . The influence of a_w and temperature on the growth parameter λ was clearly demonstrated through mathematical models that can be employees for both species analyzed, within the range of a_w studied.The empirical secondary models (Corradini and Peleg 2005) showed good prediction (Table 1), once the correlation coefficients (R^2) are close to one.

Conclusions

It is possible to conclude that the storage temperature of the juice and its soluble solids concentration directly influence the growth of the molds *B. fulva* and *N. fischeri* and the temperature elevation from 20 to 30 °C led to an increase six times in the duration of adaptation phase and about two times in the maximum specific growth.

Acknowledgements

Financial support provided by CAPES-Brazil is gratefully acknowledged.

References

Corradini M. G. and Peleg M. (2005) Estimating non-isothermal bacterial growth in foods from isothermal experimental data. *Journal of Applied Microbiology* 99 (1), 187-200.

Engel G. and Teuber M. (1991) Heat resistance of Byssochlamys nivea in milk and cream. *International Journal of Food Microbiology* 12, 225-234.

Lahlali R., Serrhini M. N. Friel D., Jijakli M. H. (2007) Predictive modelling of temperature and water activity (solutes) on the in vitro radial growth of Botrytis cinerea Pers. *International Journal of Food Microbiology* 114 1–9

McMeekin T.A., Olley J.N., Ratkowsky D.A., Ross T. (2002) Predictive microbiology: towards the interface and beyond. *International Journal of Food Microbiology* 73, 395–407.

Salomão B. C. M. (2002) Isolation, identification and study of the thermal resistance of heat resistant fungi in fruit products. MS thesis. Florianópolis. Brazil. Federal University of Santa Catarina. Department Food Engineering

Salomão B. C. M., Massaguer, P. R., Aragão, G. M. (2008) Isolation and selection of heat resistant fungi in the production process of apple nectar. Ciência e Tecnologia de Alimentos 28(1), 116-121.

Sant'Ana A.S., Rosenthal A., Massaguer P.R. (2009) Heat resistance and effects of continuous pasteurization on the inactivation of Byssochlamys fulva ascospores in clarified apple juice. *Journal of Applied Microbiology* 107, 197-209.

Zimmermann M., Miorelli S., Massaguer P. R., Aragão G. M. F. (2011) Modeling the influence of water activity and ascospore age on the growth of Neosartorya fischeri in pineapple juice. *Food Science and Technology* 44, 239-243.

Optimal sequential sampling design for improving parametric identification of complex microbiological dynamic systems by nonlinear filtering

J.-P. Gauchi[1], J.-P. Vila[2]

[1] Institut National de la Recherche Agronomique (INRA), département Mathématiques et Informatique Appliquées (UR3141), Jouy-en-Josas, France. (jean-pierre.gauchi@jouy.inra.fr).
[2] Institut National de la Recherche Agronomique (INRA), département Mathématiques et Informatique Appliquées, Montpellier, France. (jean-pierre.vila@supagro.inra.fr)

Abstract

The context of this work is the parametric identification of complex microbiological dynamic systems by particle nonlinear filtering. It is well known that the successive sampling times at which corresponding data are recorded (counts of UFC on Petri plates, or counts of bacteria by means of flux cytometry) have a strong influence on the quality of the estimation of the *p* parameters of the considered system model. In Gauchi and Vila (2011a) an innovative statistical approach was proposed to sequentially estimate the optimal sampling times. The aim of this poster is to give a practical synthesis of this approach, and show an illustration based on the Baranyi and Roberts (1994) model (BR model). This innovative approach can be put into practice through the FILTREX software (Bidot *et al.* 2009) presented in a talk of this Congress (Gauchi and Vila 2011b).

Keywords: particle nonlinear filtering, sequential optimal designs, predictive modeling, microbiology

Introduction

Several approaches were proposed to tackle the difficult question of optimal sequential (or not sequential) sampling design, where the difficulty is due to both the nonlinearity and dynamic aspects of the involved microbiological models. We can cite here, not exhaustively, the relevant works of Versyck *et al*. (1997), Grijspeerdt and Vanrolleghem (1999), Vassiliadis *et al*. (1999), Balsa-Canto and Banga (2000, 2001), Banga *et al*. (2002), Smets *et al*. (2004), Banga and Balsa-Canto (2005), and also the recent book of Ucinsky (2005). We propose in this conference the present work where a new method is summarized from Gauchi and Vila (2011a). Indeed, in the particle filtering context it is still an open issue to sequentially find the optimal sampling times while minimizing the costly data acquisition. One of the difficulties is to use a sampling criterion allowing relatively fast computations, in order to have the next optimal sampling time to be computed before the corresponding actual time occurrence.

Materials and Methods

The proposed innovative approach is based on a new type of model parameter sensitivity indices called *SI* for brevity's sake in this communication (see Gauchi *et al.* 2010, for technical details). The main idea of our procedure is threefold: (i) the *p SI* indices are computed and plotted versus time, leading to *p* sensitivity index curves (*SIC*), from the initial time t_0 to the final time t_{max} of the experiment, *a priori* chosen; (ii) the first occurring maximum among all of these *SI* curves is determined: it corresponds to the first optimal sampling time t_1^*; (iii) new counts corresponding to samples at this optimal time t_1^* are performed. Then, a new bundle of *p SI* curves are computed and plotted from t_1^*. This procedure is repeated for finding t_2^*, etc..., and goes on until the *a priori* chosen number of optimal sampling times is reached or the final time t_{max}. An important point to emphasize is that the successive new *SI* curves do not forget the previous parameter estimate values, when they are computed.

Results and Discussion

Simulation conditions

In this subsection simulation results obtained with the BR model are displayed: Data (counts of bacteria by means of flux cytometry) were simulated by means of the BR model, with the following *a priori* parameter values: N_0 = 200 UFC/ml, N_{max} = 5×10^8 UFC/ml, μ_{max} = 0.05/h, λ = 50 h. The *a priori* parameter intervals required by the particle filtering process (based on 10^5 particles) were assumed as: N_0 = [140 ; 260], N_{max} = [0.5×10^8 ; 10^9], μ_{max} = [0.01 ; 0.09], λ = [10 ; 110]. t_{max} was chosen as 504 hours. All these values are realistic because they are based on real microbiological studies.

Bundle of SI curves

A first curve bundle was computed for the BR model and is displayed on left panel of Figure 1 from t_0 to t_{max}. One can observe that the first optimal time will be $t_1^* = 2$, corresponding to the first occuring maximum (on the *SI* curve corresponding to the N_0 parameter).

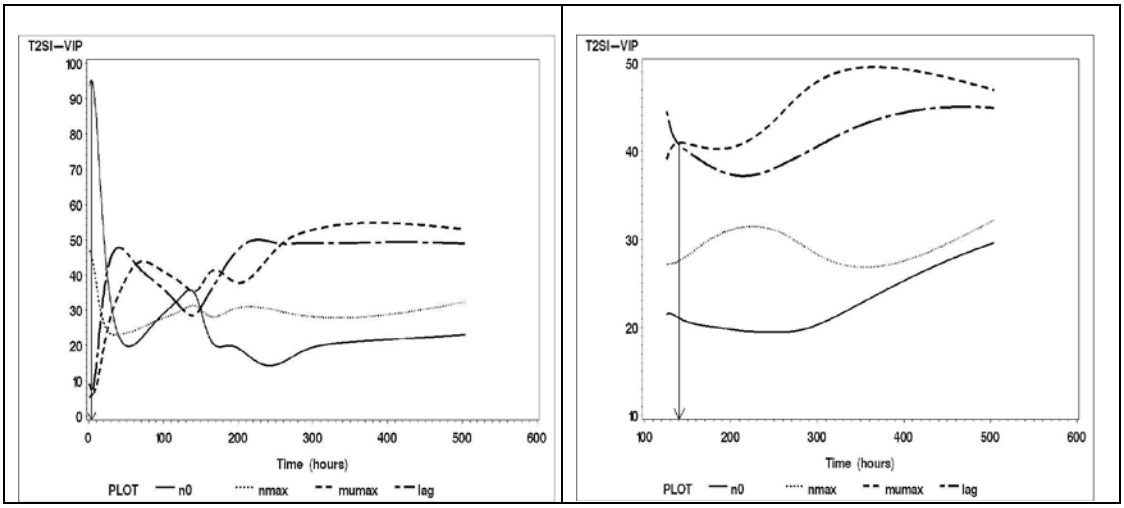

Figure 1: Left panel: bundle of the *p SI* curves from t_0 to the final time t_{max}; Right panel: bundle of the *p SI* curves from the optimal time $t_4^* = 125$ to the final time t_{max}.

On the right panel of Figure 1 a new bundle of *SI* curves from the optimal time $t_4^* = 125$ to t_{max}, is displayed: it can be seen that the next optimal time is $t_5^* = 140$, corresponding to a maximum of the μ_{max} *SI* curve.

Sequential optimal time design

The procedure found successively the ten optimal times t^*= {2; 69; 97; 125; 140; 160; 176; 263; 384; 504} where samplings must be collected. They are displayed on Figure 2 together with the simulated sampling data. One can notice the accumulation of the optimal sampling times in the first half of the evolution process, which is the most sensitive to the parameters N_0, μ_{max} and λ. Moreover the extreme right last sampling time has been judiciously positioned for the estimation of the fourth parameter N_{max}. The maximum sampling time number can be automatically determined by the procedure. Here the maximum time number of 13 was found. However, as it will be shown in the next subsection, the first ten optimal times were sufficient enough for providing correct (anticipated) estimated parameter confidence intervals (*ECI*). Indeed, it will be seen that these *ECI* are statistically better than those obtained from usual sampling time designs.

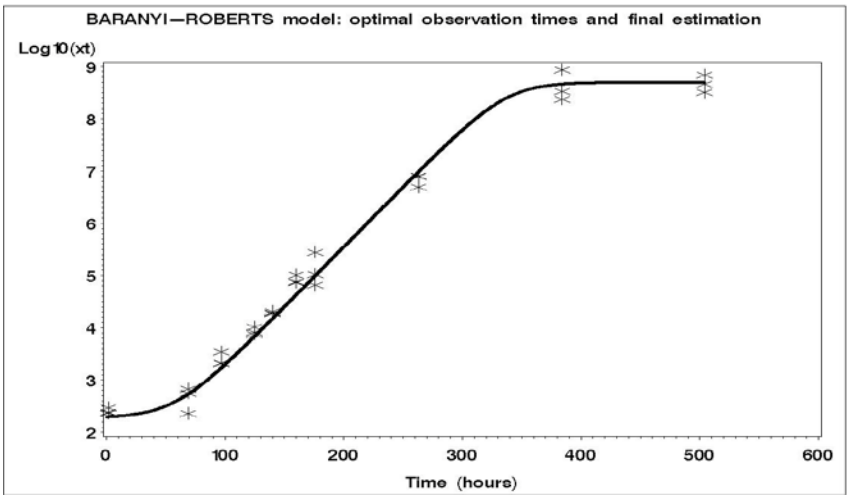

Figure 2: The first ten optimal sampling times and observed data ("*").

Comparison of Estimated Confidence Intervals (ECI)

From the 10 optimal sampling times, the particle filtering process provided the following parameter estimates with their estimated 95%-*ECI* given in Table 1.

Table 1: 95%-*ECI's* with the optimal time design.

Parameter	Lower bound	Estimation	Upper bound
N_0	193	198	204
λ	48.6	51.6	54.6
μ_{max}	0.049	0.051	0.053
N_{max}	5.3×10^8	5.6×10^8	5.8×10^8

Table 1 shows that the parameter estimates are very close to the true parameter values. They are globally better than those obtained from the design t_{usual} = {0; 72; 120; 168; 240; 264; 288; 336; 408; 504} already used by the microbiologists, given in Table 2.

Table 2: 95%-*ECI's* with a usual time design.

Parameter	Lower bound	Estimation	Upper bound
N_0	191	196	200
λ	61.7	65.1	68.5
μ_{max}	0.053	0.054	0.055
N_{max}	5.7×10^8	5.85×10^8	6.0×10^8

Results of table 1 are also better than those obtained from the naive 10-time equidistributed design between t_0 and t_{max}, given in Table 3.

Table 3: 95%-*ECI's* with a naive time design.

Parameter	Lower bound	Estimation	Upper bound
N_0	191	195	199
λ	59.6	64.0	68.4
μ_{max}	0.053	0.055	0.056
N_{max}	5.11×10^8	5.29×10^8	5.47×10^8

In Tables 2 and 3 it can be observed that the true parameters values for the crucial μ_{max} and λ parameters (0.05 for μ_{max} and 50 for λ) do not lie in the corresponding estimated 95%-*ECI's*.

On the contrary, thanks to the optimal design, one can see in Table 1 that the true parameter values lie in these 95%-*ECI's*, which confirms the better quality of the filtering process.

Comparison with other methods on the same optimal sampling problem

It is relevant to notice that our optimal time design - based on the ten optimal times shown on Figure 2 - is different from those of Grijspeerdt and Vanrolleghem (1999) where the design was based on four optimal times. Of course, the reason is that our criterion is different from the D-optimality criterion used by these authors. Moreover, the construction of their D-optimal design was not undertaken in an optimal sequential way. But the crucial point we want to recall here is that the D-optimality criterion was invented for linear models, and it is only an approximate criterion for nonlinear models such as the BR model. In this mind our optimal time design takes into account the nonlinearity of the model thanks to the particle filtering context detailed in Gauchi and Vila (2011a). At last, we want to emphasize a strong advantage: for determining the D-optimal design in the nonlinear case it is necessary to provide parameter guesses, whereas with our approach only parameter intervals guesses (even broad) are necessary.

Conclusions

This optimal sampling time computation procedure will be soon available in the FILTREX software. In the near future a real on-line version will be implanted: the experimenter will have the possibility to enter real observational data (counts) at each optimal sampling time computed by the procedure. In a further work this sequential optimal design procedure will be extended to hierarchical models.

Acknowledgements

We thank J.C. Augustin and L. Coroller for sharing with us their microbiological experience.

References

Banga J.R., Balsa-Canto E, Moles C.G. and Alonso A.A. (2005) Dynamic optimization of bioprocesses: Efficient and numerical strategies. *Journal of Biotechnology* 117, 407-419.

Banga J.R, Versyck K. J. and Van Impe J. F. (2002) Computation of Optimal Identification Experiments for Nonlinear Dynamic Process Models: a Stochastic Global Optimization Approach. Ind. Eng. Chem. Res., 41, 2425-2430.

Balsa-Canto E., Banga J.R., Alonso A.A. and Vassiliadis V.S. (2000) Efficient Optimal Control of Bioprocesses Using Second-Order Information. *Industrial & Engineering Chemistry Research* 39, 4287-4295.

Balsa-Canto E., Banga J.R., Alonso A.A. and Vassiliadis V.S. (2001) Dynamic optimization of chemical and biochemical processes using restricted second-order information. *Computers and Chemical Engineering* 25, 539-546.

Barany J. and Roberts T.A. (1994) A dynamic approach to predicting bacterial growth in food. *International Journal of Food Microbiology* 23, 277-294.

Bidot C., Gauchi J.P. and Vila J.P. (2009) Programmation Matlab du filtrage non linéaire par convolution de particules pour l'identification et l'estimation d'un système dynamique microbiologique. Rapport technique INRA/Jouy-en-Josas/MIA/ n°2009-1.

Gauchi J.-P. and Vila J.-P. (2011a) Nonparametric filtering approaches for identification and inference in nonlinear dynamic systems. *Statistics and Computing.* Submitted.

Gauchi J.-P. and Vila J.-P. (2011b) FILTREX: A New Software for Identification and Optimal Sampling of Experiments for Complex Microbiological Dynamic Systems by Nonlinear Filtering. Proceedings 7th International Conference "Predictive Modelling in Foods", Septembre 2011, Dublin, Ireland.

Gauchi J.P., Lehuta S. and Mahévas S. (2010) Optimal Sensitivity Analysis under Constraints : Application to Fisheries. *Reliability Engineering & System Safety*. Submitted.

Grijspeerdt K. and Vanrolleghem P. (1999) Estimating the parameters of the Baranyi model for bacterial growth. *Food Microbiology* 16, 593-605.

Smets I.Y., Claes J.E., November E.J., Bastin G.P. and Van Impe J.F. (2004) Optimal adaptive control of (bio)chemical reactors: past, present and future. *Journal of Process Control* 14, 795-805.

Ucinsky D. (2005) Optimal Measurement Methods for Distributed Parameter System Identification. CRC Press, Boca Raton, London.

Vassiliadis V.S., Balsa-Canto E. and Banga J.R. (1999) Second-order sensitivities of general dynamic systems with application to optimal control problems. *Chemical Engineering Science* 54, 3851-3860.

Versyck K.J., Claes J.E. and Van Impe J.F. (1997) Practical Identification of Unstructured Growth Kinetics by Application of Optimal Experimental Design. *Biotechnology Progress* 13, 524-531.

A novel class of statistical process control for microbial counts in foods

U. Gonzales-Barron, F. Butler

UCD Biosystems Engineering, School of Agriculture, Food Science and Veterinary Medicine, University College Dublin, Belfield, Dublin 4, Ireland. (ursula.gonzalesbarron@ucd.ie)

Abstract

Statistical process control (SPC) for microbial counts in foods has been little investigated, yet in all cases the assumptions of normality of microbial concentrations and constant within-batch standard deviation has been maintained. Previous research, however, has shown that the variance in contaminated food units cannot be assumed constant batch to batch, and furthermore that the within-batch spread measure correlates with the within-batch mean concentration. Additionally, for microorganisms present in low concentrations such as pathogens, the gamma distribution, assumed as the true within-batch distribution, has represented the observed plate count data by far better than the lognormal distribution. These latest findings posed the question as to whether the fundamentals of classical SPC – whereby the production process is assumed to be in control with a fixed process quality of μ (a long run mean concentration CFU/g) – could be applied for microbial counts considering the evident variability that occurs batch to batch. A novel SPC methodology for microorganisms of low counts is proposed that takes elements from variables sampling plan theory but it is based on the sample units created by the process itself. The 'observed' quality of a lot (j) is assumed to vary at random according to a Poisson-gamma (kj,mj) model with correlated random effects for the within-batch mean mj and the within-batch dispersion kj. On a two-dimensional space, a contour of tolerance criterion or critical level is established with basis on previous history of unsafe production lots, so that sampling inspection should distinguish unsatisfactory from satisfactory. Samples distributions for each of the lots, simulated from the lots' universe, are used to estimate the α (probability of misclassifying a satisfactory lot as unsatisfactory) and β (probability of misclassifying an unsatisfactory lot as satisfactory) risks at different upper control limits (UCL, samples' mean), so as to find an appropriate UCL. This methodology has been tested for the establishment of SPC for Enterobacteriaceae on pre-chill beef carcasses using Irish abattoirs' data. For a critical level of a maximum of 10% of the carcasses within a batch exceeding 60 CFU/cm2, a UCL of 12 CFU/cm2 that minimises the 'mean' conditional α and β risks at 6.6% is recommended for a sample size of 5 carcasses while for a sample size of 10, a UCL of 15.5 CFU/cm2 will minimise both mean risks at 3.4%. This novel procedure for SPC can be utilised in the development of both food safety criteria and process hygiene criteria based on the availability of multiple bacterial counts from production.

Keywords: statistical process control, microbial counts, poisson-gamma

Proposal for operating characteristic curves developed for Cronobacter in powder infant formula

A. Moussida, F. Butler

Biosystems Engineering, UCD School of Agriculture, Food Science and Veterinary Medicine, University College Dublin, Belfield, Dublin 4, Ireland.

Abstract

The microbiological criteria established in the EC 2073/2005 for Cronobacter in powder infant formula (PIF) are based on two-class attribute sampling plans, where the sample results are qualitative (sample indicates presence or absence) and the lot is rejected if any sample is positive. The performance of a sampling plan is revealed by its OC curve which plots the probability of acceptance against possible values of proportion defective. The objective of this study was to generate several OC curves assuming different statistical distributions of Cronobacter in PIF in order to determine and compare the probabilities of rejecting/accepting the lot and the respective level of contamination. The microbial distribution of Cronobacter in PIF was described by assuming a Poisson-lognormal (PLN), Poisson-gamma (PG), Zero-inflated Poisson (ZIP) and Zero-inflated Poisson-gamma (ZIPG). For each distribution the proportion defective of the population was estimated in order to determine the probability of acceptance. Furthermore, the effect of clustering of the bacteria on the probability of acceptance of the lot was assessed through a Poisson-logarithmic (PLOG) and a PLogn distribution. Probabilities of accepting the lot at a given level of contamination change drastically according to the statistical distribution assumed and by changing the values of its own parameters. The best case scenario was described by the PLN where we are 95% confident of rejecting a lot with mean level of contamination of 0.083 or 0.202 CFU/g (assuming standard deviation 10 and 100 CFU, respectively). Furthermore, results show that the size of the clusters does not have any effect on the proportion acceptable of the sample, which is affected only by the distribution of the clusters in the powder. The statistical distribution of Cronobacter in PIF and the sampling plan implemented play a crucial role in determining the confidence level of rejecting a contaminated lot.

Tracing the contamination levels of acid curd cheese implicated in an outbreak of listeriosis in Austria, 2009/2010

P. Skandamis[1], M. Wagner[2], D. Schoder[2]

[1]Agricultural University of Athens, Greece,
[2]Institute for Milk Hygiene, Milk Technology and Food Science, Department for Farm Animals and Veterinary Public Health, Veterinaerplatz 1, 1210 Vienna, Austria.

Abstract

As a result of an outbreak investigation on a cluster of 34 cases of listeriosis, with 8 fatalities mainly occurring in elderly, sour-milk cheese was identified as the source of infection. The company launched a recall action from Austrian and German supermarket chains and cheese of eighteen incriminated lots was shipped to the Institute for Milk Hygiene, Milk Technology and Food Science. All recalled cheese lots were investigated with challenge tests (storage at 4 °C, 15 °C, 20 °C), cultural methods (ISO 11290:1&2) and culture-independent quantification (qPCR). The lots were tested after delivery, at the end of shelflife (that is up to 50 days post production), and to mimic a worst case scenario, at timepoints beyond the shelf-life. Sixteen out of eighteen (16/18) lots were positive for *L. monocytogenes* at each timepoint whereas levels of *L. monocytogenes* increased dramatically during storage. The highest population enumerated in cheese was 2.8×10^8 CFU/g; however, intralot variability was crucial. Data collected througout this particular cheese chain included a_w and pH changes during ripening and storage of cheese and temperature during ripening and retail display and were fitted by proper distributions. Monte Carlo simulations were applied to describe the variability in early stages of potential contamination scenarios and predict the potential increase *of L. monocytogenes* with time. Predicted pathogen levels were plotted against the limit of quantification of the enumeration method. This approach is capable of showing the theoretical "at-line window of response" since, by using actual sampling schemes, a cheese lot could be contaminated but still remain undetected (due to the low contamination level being present). Such simulations may be used for re-assessment of the shelf life of this product under the constraint of *L. moncytogenes* growth and for establishing realistic performance objectives for *L. monocytogenes* before the product leaves the processing establishment.

Authors Index